

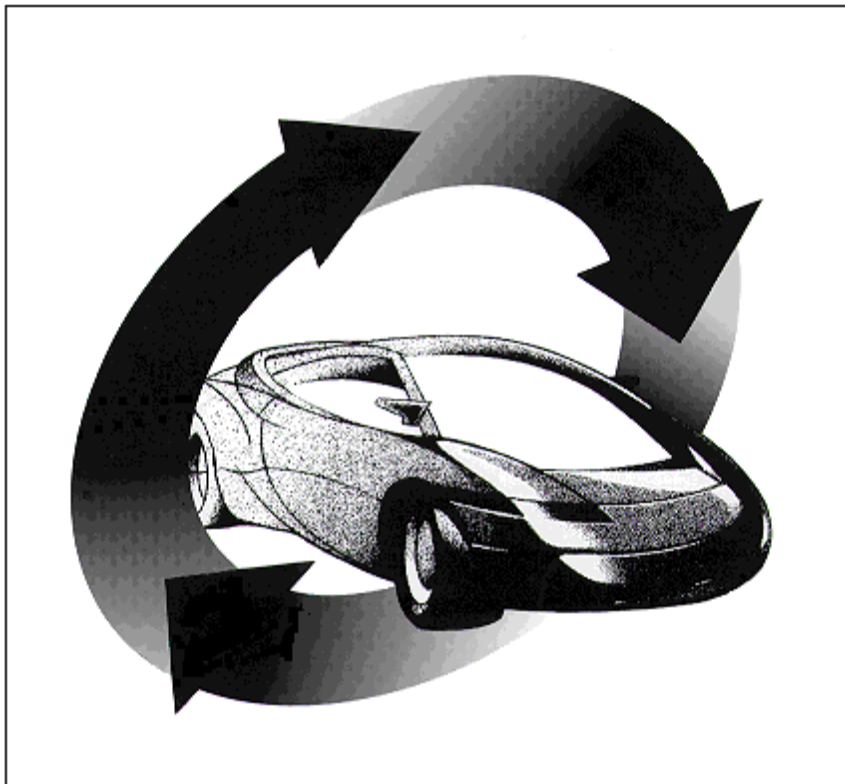
Automotive Steel Design Manual



American Iron
and Steel Institute



Revision 6.1
August 2002



American Iron and Steel Institute &
Auto/Steel Partnership

2000 Town Center • Suite 320 • Southfield, Michigan 48075-1123
Tel: (248) 945-4779 • Fax: (248) 356-8511

PREFACE

The Automotive Steel Design Manual (ASDM) is a living document, with periodic revisions and expansions as dictated by breadth of coverage, experience in application, and the needs of the automotive and steel industries. The first edition was issued in October 1986. This edition is the ninth in a series of updates.

The ASDM brings together materials properties, product design information and manufacturing information to make the most effective use of steel as an engineering material. It has been prepared and updated for the particular interests and needs of the product designer and design engineer. The major emphasis is on structural design, fatigue, crash energy management and corrosion protection. The primary applications are the body-in-white, attached frame members, and attached assemblies such as hoods, deck lids, doors and fenders. Information on materials and manufacturing processes is provided to enable the product design members of the engineering team to function more effectively.

The Computerized Application and Reference System (AISI/CARS) is an updated software program, with revisions and expansions that reflect the needs of the automotive and steel industries. The current version is CARS 2002. Based on the ASDM, it brings together the materials, design and manufacturing information in the ASDM for ready reference or automatic application of the design process by using database and equation solving techniques.

AISI/CARS automates the design process for the designer and engineer by:

- Eliminating the time-consuming search for design equations and criteria,
- Performing required calculations while eliminating potential errors, and
- Permitting unlimited, effortless parametric studies.

Users of the ASDM and AISI/CARS are encouraged to offer their comments and suggestions as an invaluable part of keeping these tools useful and up-to-date for the product designer and design engineer.

Development of the ASDM and AISI/CARS was sponsored by the American Iron and Steel Institute, Washington D.C., in cooperation with the Auto/Steel Partnership. The A/SP consists of DaimlerChrysler AG, Ford Motor Company, General Motors Corporation and the Automotive Applications Committee of the AISI. For further information, contact automotive applications engineers at any of the companies represented on the Automotive Applications Committee of the American Iron and Steel Institute.

Automotive Applications Committee
American Iron and Steel Institute
2000 Town Center Suite 320
Southfield, MI 48075-1123

Bethlehem Steel Corporation
Dofasco Inc.
Ispat Inland Inc.

National Steel Corporation
Rouge Steel Company
United States Steel Corporation

AISI/CARS was developed and is supported and distributed by Desktop Engineering Int'l Inc. Woodcliff Lake, New Jersey. For further information or technical support, contact:

AISI/CARS
Desktop Engineering Int'l Inc.
172 Broadway
Woodcliff Lake, NJ 07677

Hotline: (800) 888-8680
Tel: (201) 505-9200
Fax: (201) 505-1566
e-mail: techsupport@deiusa.com
web: www.deiusa.com

Engineering consultation will also be available upon request to assist in solving complex problems and to develop customized user-defined modules.

ACKNOWLEDGMENTS

AUTOMOTIVE STEEL DESIGN MANUAL and AISI/CARS

These editions of the Automotive Steel design manual and AISI/CARS have been guided by the Auto/Steel Partnership Automotive Design Task Force, which is composed of individuals from both the automotive and steel industries. Their efforts are hereby acknowledged.

B. K. Anderson	DaimlerChrysler Corporation
G. Chen	National Steel Corporation
T.E. Diewald	Auto/Steel Partnership
S.J. Errera	American Iron and Steel Institute, retired
R.L. Hughes	Rouge Steel Company
W.D. Jaeger	General Motors Corporation, retired
A.L. Kresse	General Motors Corporation
R.P. Krupitzer	American Iron and Steel Institute
D.S. Lee	Ford Motor Company
S.D. Liu	National Steel Corporation
D.C. Martin	American Iron and Steel Institute, retired
R. Mohan	Rouge Steel Company
D.G. Prince	United States Steel Corporation
N. Schillaci	Dofasco, Inc.
V.C. Shah	DaimlerChrysler Corporation
B.L. Thompson	Bethlehem Steel Corporation, retired

The original Task Force planned, guided and reviewed the drafts of portions of the ASDM prepared by a group of distinguished consultants:

K. Arning	S. P. Keeler
D. W. Dickinson	L. A. Lutz
J. A. Gilligan	A. K. Shoemaker
G.T. Hallos	

The contributions of J.J. Walters and the staff of Desktop Engineering Int'l Inc. are acknowledged for the verification and editing of the ASDM content.

Editing was performed in an insightful and efficient manner by G. O. Cowie, a consultant to the Auto/Steel Partnership.

AISI/CARS

AISI/CARS was designed and developed by the engineering and programming specialists from Desktop Engineering Int'l Inc. The contributions of the AISI/CARS development team are hereby acknowledged:

Daniel V. Schiavello
Jeffrey J. Walters
Dr. S. J. Wang
Dr. Soundar Rajan
Tymish P. Hankewycz

The contributions of other members of the AISI/CARS project staff are also acknowledged.

Auto/Steel Partnership &
American Iron and Steel Institute
August 2002

1. INTRODUCTION

The Automotive Steel Design Manual (ASDM) is offered to the automotive design community as a comprehensive guide for designing vehicle body components and assemblies in sheet steel. The ASDM recognizes the current practice in the automotive industry of mutually involving material, design and manufacturing engineers into a simultaneous engineering team, which functions throughout the design process, beginning at the concept stage. The major portion of the ASDM is contained in [Sections 2, 3](#) and [4](#), which deal with materials, design and manufacturing processes, respectively.

[Section 2, Materials](#), is intended to familiarize the design engineer with the fundamental characteristics of the many grades of available sheet steels. It emphasizes the influence of material properties on the design and manufacturing processes, and on the ultimate performance of the part. The scope of information is sufficient to make the designer conversant with material grades and properties, help him recognize the role of the materials engineer in the simultaneous engineering team, and enable him to interact with his materials counterpart.

[Section 3, Design](#), is specific to thin-wall sheet steel members. It recognizes that often the design of major body assemblies is subsequently analyzed by computer-aided processes, and that the performance is ultimately verified at the proving grounds. This section provides information that will guide the body designer to the first order analysis, help interpret the results generated by the computer, and suggest appropriate design modifications to be plugged into the next iteration.

The designer can be greatly assisted, particularly in the use of [Sections 3.1, 3.2, 3.3, 3.4](#) and [3.5](#), by using the AISI/CARS software. The AISI/CARS user can access the entire contents of the ASDM and perform word searches to gather information on a given subject. Moreover, this program allows the designer to perform tasks quickly, such as:

- Solve the equations contained in [Sections 3.1, 3.2, 3.3, 3.4](#) and [3.5](#).
- Execute the design processes described in the design procedures for those sections, which are presented in Section 5.
- Perform "What-If" calculations.
- Perform keyword searches.

The intent of [Section 4, Manufacturing Processes](#), is similar to that of [Section 2](#). It recognizes that the design of a part proceeds more efficiently when the designer is able to visualize the manufacturing process that will be employed to fabricate it. The scope of information is sufficient to make the designer conversant with manufacturing operations, help him recognize the role of the manufacturing engineer on the simultaneous engineering team, and enable him to interact with his manufacturing counterpart.

[Section 5, Procedures](#), contains the design procedures for [Sections 3.1](#) through [3.4](#). The flowchart formats give the designer a schematic view of the design procedure, systematically guiding the user and prompting for additional input or decisions at appropriate places. They are grouped into one section for the convenience of the user. As mentioned previously, the procedures can be executed quickly and accurately with the AISI/CARS program.

[Section 6, Applications](#), presents case studies and example problems. The case studies illustrate the application of the principles in [Sections 2, 3](#) and [4](#) to vehicle components. They are extracted

from actual design programs, simplified to focus on the principles that are being illustrated, and sometimes modified to emphasize those principles. The example problems are now grouped into one section for the convenience of the user.

[Section 7, AISI/CARS](#), contains the AISI/CARS User's Manual and tutorials. The AISI/CARS User's Manual is reproduced herein for the convenience of those who hold copies of the AISI/CARS software.

1.1 INFORMATION ON UPDATE 6.1

This update of the ASDM, issued August 2002, is the latest in a series of updates since the original publication in 1986. It contains major revisions to the following sections:

- [Section 2.4.3, Dent Resistant, High Strength and Advanced High Strength Steels](#)
This section has been revised to reflect the latest information
- [Section 3.1.3.1.3, Inelastic Stress Redistribution](#)
This section has been revised to reflect the latest information.
- [Section 3.6.8, Determining The Mean Crush Load of Stub Columns](#)
This section has been revised to reflect the latest information.
- [Section 3.11, AISI/CARS Geometric Analysis Of Sections \(Gas\) Theory](#)
This section has been revised to reflect the new analysis capability in CARS 2002, the latest release of AISI/CARS.
- [Section 7.1, AISI/CARS User's Manual](#)
This section has been revised to reflect the changes associated with CARS 2002, the latest release of AISI/CARS.

This update has new sections including:

- [Section 2.5, Steel Company Provided Stress-Strain Curves](#)
This section provides sample stress strain curves provided by steel companies.
- [Section 2.14, Strength Increase From Cold Work of Forming](#)
This section provides a procedure to evaluate numerically the increased yield strength due to cold work of forming.

2. MATERIALS

2.1 INTRODUCTION

Flat rolled steels are versatile materials. They provide strength and stiffness with favorable mass to cost ratios, and they allow high speed fabrication. In addition, they exhibit excellent corrosion resistance when coated, high energy absorption capacity, good fatigue properties, high work hardening rates, aging capability, and excellent paintability, which are required by automotive applications. These characteristics, plus the availability of high strength low alloy (HSLA) and alloy steels in a wide variety of sizes, strength levels, chemical compositions, surface finishes, with and without various organic and inorganic coatings, have made sheet steel the material of choice for the automotive industry.

In more recent times, stainless steels have found wide use in many applications where a combination of formability and excellent resistance to corrosion and oxidation at elevated temperatures is needed. Stainless steels are also available in a variety of sizes, shapes, strengths, chemical compositions, and surface finishes.

User fabrication methods applicable to sheet products include roll, brake and press forming, shearing, slitting, punching, welding, adhesive bonding, etc. Corrosion resistance is attained primarily by the application of coatings, either sacrificial or barrier, to flat rolled steels in continuous zinc or zinc alloy coating operations. Stainless steels possess their corrosion and oxidation resistance properties because of their chemical compositions and do not require additional protective coatings.

This section describes the sheet steel materials available to the automotive industry, by way of steelmaking practice, rolling practice, chemistries, definition of grades, and coatings. Mechanical properties and testing procedures also will be covered.

2.2 STEEL MAKING

Figure 2.2-1 is a block diagram of the steel making process from iron making through cold reduction. Most of the steel for automotive applications is produced in basic oxygen furnaces (BOFs), deoxidized, and continuously cast into slabs. These slabs are reheated and hot rolled into coils that can be used in heavier gage (≥ 1.83 mm [0.072"]) automotive structural applications or processed into lighter gage (0.4 – 1.5 mm [0.015 to 0.060"]) cold rolled coils for use in auto body applications.

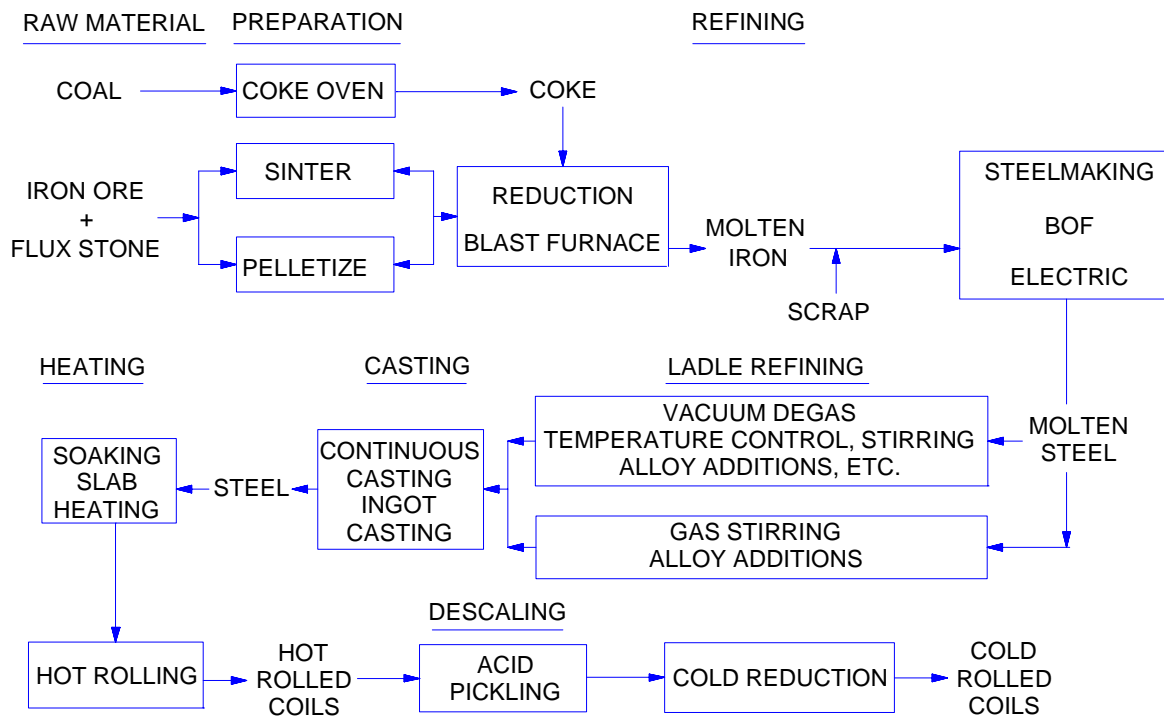


Figure 2.2-1 Steel making flowline

2.2.1 DEOXIDATION PRACTICES

Currently all of the steel for automotive applications is deoxidized. Deoxidation with aluminum is performed during and after pouring of the steel from the BOF into a ladle. Other alloying elements can be added to the ladle to produce compositions necessary to attain specified properties in a flat rolled sheet such as higher strength and improved corrosion resistance. Ladle treatments are available to further modify the steel characteristics, such as calcium treatment to reduce sulfur and modify sulfides, gas stirring to improve uniformity of the alloy additions, or vacuum degassing to lower carbon levels <0.01%. Additions of titanium and/or columbium in a vacuum degassed heat are used to produce interstitial free (IF) stabilized steels.

2.2.2 STEEL CHEMISTRY

Sheet steels used in the automotive industry are available in the following types:

- Commercial Quality
- Low Carbon –Drawing quality
- IF stabilized – Deep drawing quality
- Dent Resistant
- Bake Hardenable
- Non-Bake Hardenable
- High Strength Low Alloy
- High Strength Solution Strengthened
- Ultra High Strength
 - * Dual Phase
 - * Martensitic
- Laminated Steels
- Stainless Steels

The low carbon steels are generally less than 0.13% carbon, 0.60% manganese, 0.030% phosphorus, 0.030% sulfur, and greater than 0.02% aluminum. The drawing quality steels have carbon level in the 0.02 to 0.04% range. The Interstitial free (IF) steels are stabilized with Ti, Cb, or Cb + Ti, and are normally ultra low carbon (0.005% max). While most IF steels are produced as drawing quality, solid solution strengthening with P, Mn, and Si can be utilized to produce a higher strength formable steel (with higher **n** values and **r** values). (See [Section 2.5](#))

Bake hardenable steels utilize carbon in solution to provide an increase in strength during the paint bake cycle due to carbon strain aging. Therefore these steels can be produced in a relatively low strength condition and easily formed into parts. However, after forming and paint baking, a significantly stronger part is produced.

The dent resistant steels contain increased levels of phosphorus (up to 0.10%), and possibly manganese and silicon to low carbon steels and IF steels. The high strength solution strengthened steels contain increased levels of carbon and manganese with the addition of phosphorous and/or silicon.

The high strength low alloy steels (HSLA) contain the addition of the carbide forming elements Cb, V, or Ti singularly or in combination to a low carbon steel, providing strength through precipitation of fine carbides or carbonitrides of Cb, Ti, and/or V. Microalloying to these grades does reduce the ductility.

The dual phase, ultra high strength steels rely on a microstructure of ferrite and Martensite to provide a unique combination of low yield strength and high tensile strength as well as a high **n** value. This combination results in a high level of formability in the initial material and high strength due to work hardening in the finished part. The unique combination of properties is achieved by alloy additions of C, Mn, and Si, and possibly Cb, V, Mo, and/or Cr, coupled with continuous annealing for cold rolled steels. It is possible to produce a hot rolled product with a combination of alloying and a selected thermal practice on the Hot Mill.

The martensitic, ultra high strength steels are produced by alloying and continuous annealing followed with a rapid cool to produce a low carbon, martensitic structure.

Stainless steels are classified into austenitic, martensitic or ferritic steels. The major divisions are the 300 series steels, with nickel stabilized austenite, and the 400 series, which are nickel free but contain 10% or more chromium. Some of these are hardenable by quenching and tempering. The 200 series are special austenitic steels where portions of the nickel are replaced with manganese and nitrogen. The 500 series are low chromium steels (4-6%) but with small additions of molybdenum.

2.3 CLASSIFICATION AND PROPERTIES

In the past, steels were supplied to make the part where the steel representative determined the required grade that would perform well in the stamping operation. In a cooperative effort by SAE, AISI, and representatives of the auto industry and North American steel industry, specifications were established based on mechanical properties that affect manufacturing.

The Society of Automotive Engineers (SAE) has reclassified formable and high strength sheet steels for automotive use in recent years. Instead of the former system, which was based on commercial description and deoxidation practice, the new system is based on formability and strength levels as used in the automotive industry. The SAE recommended practice furnishes a categorization procedure to aid in the selection of low carbon sheet steels for identified parts and fabrication processes.

The new SAE specifications J2329 and J2340 identify the properties that the steel company can produce in controlling formability. These are the new guidelines that automotive companies want to use, thereby identifying the strengths and formability of the materials from which parts are produced.

There are two new SAE specifications covering automotive sheet steels:

- SAE J2329 Categorization and Properties of Low Carbon Automotive Sheet Steels
- SAE J2340 Categorization and Properties of Dent Resistant, High Strength, and Ultra High Strength Automotive Sheet Steel.

Following is an approximate comparison of the former commercial description, based on deoxidation practice, with the new SAE classification:

Table 2.3-1 SAE J2329 categorization and properties of low carbon automotive sheet steels

Old AISI Description	New SAE Classification	Property
Hot Rolled Steels		
CQ Commercial Quality	SAE J2329 Grade 1	N/A
DQ Drawing Quality	SAE J2329 Grade 2	Yield: 180-290 MPa n value: 0.16 min.
DDQ Deep Drawing Quality	SAE J2339 Grade 3	Yield: 180-240 MPa n value: 0.18 min.
Cold Rolled Steels		
CQ Commercial Quality	SAE J2329 Grade 1	N/A
DQ Drawing Quality	SAE J2329 Grade 2	Yield: 140-260 MPa n value: 0.16 min.
DQ Drawing Quality	SAE J-2329 Grade 3	Yield: 140-205 MPa n value: 0.18 min.
DDQ Deep Drawing Quality	SAE J-2329 Grade 4	Yield: 140-185 MPa n value 0.20 min.
EDDQ Extra Deep Drawing Quality	SAE J2329 Grade 5	Yield: 110-170 MPa n value 0.22 min

Table 2.3-2 SAE J2340 categorization and properties of dent resistant, high strength, and ultra high strength automotive sheet steel

Old AISI Description	New SAE Classification
Cold Rolled Steels	
Dent Resistant (DR)	SAE J2340 Grades 180A, 210A, 250A, 280A Dent Resistant Non Bake Hardenable
Bake Hardenable (BH)	SAE J2340 Grades 180B, 210B, 250B, 280B Dent Resistant Bake Hardenable
High Strength Solution Strengthened	SAE J2340 Grades 300S, 340S High Strength Solution Strengthened
High Strength Low Alloy (HSLA)	SAE J2340 Grades 300X,Y; 340X,Y;380X,Y High strength low alloy 20X,Y;490X,Y;550X,Y
High Strength Recovery Annealed	SAE J2340 Grades 490R, 550R, 700R, 830R High Strength Recovery Annealed
Dual Phase (DP) (HSS)	SAE J2340 Grades DH/DL 500-1000 MPa Tensile Ultra High Strength Dual Phase
Martensitic Grade M, HSS	SAE J2340 Grade M 800-1500 MPa Tensile Ultra High Strength Low Carbon Martensite

These are approximate comparisons, as steelmaking practice varies from producer to producer to make a specific grade. The old AISI classifications are based on deoxidation practice and yield strength level, whereas the new classifications are based on formability. The formable high strength steels are listed with minimum yield and n values, whereas the ultra high strength steels are listed with minimum tensile values. Specification details can be found in SAE J2329 for formable steels, and SAE J2340 for high strength steels.

2.4 HOT ROLLED AND COLD ROLLED STEELS

2.4.1 INTRODUCTION

Steels are classified initially as Hot Rolled or Cold Rolled. Hot Rolled steels, finished on the Hot Mill are the most economical sheet products and are generally used in thicknesses greater than 1.83 mm (0.72") for unexposed surfaces. Cold rolled steels are usually hot rolled to approximately 4.0 mm and then finished cold to 2.0 mm (0.080") or less. Class 1 is for exposed surfaces where surface appearance is of primary importance, and Class 2 is generally for unexposed applications. The mechanical properties of cold rolled and hot rolled steels are discussed in the following sections.

Hot rolled carbon steels were formerly produced in four principal categories: commercial quality (CQ), drawing quality (DQ), drawing quality special killed (DQSK), and structural quality (SQ). The formability of DQ is better than that of CQ, and the formability of DQSK is better than that of DQ. Formability decreases with increasing strength and hardness.

Cold rolled carbon steels were formerly in four principal categories:

- Commercial quality (CQ)
- Drawing quality (DQ)
- Deep drawing quality (DDQ)
- Extra deep drawing quality (EDDQ)

Formability increases in the following order: CQ, DQ, DDQ, and EDDQ. The EDDQ steels are usually produced from interstitial free (IF) or stabilized steels. They have very high values of n and r that give them the best formability. However, dent resistance is lower than other grades of steel because of their lower yield strength.

Cold rolled sheet steels are available in several surface finishes: that is, surface smoothness or luster. Matte finish is a dull finish, without luster. Commercial bright is a relatively bright finish having a surface texture intermediate between that of matte and luster finish. Luster finish is a smooth, bright finish. Normally these finishes are furnished to specified surface roughness values.

Cold reduced uncoated and metallic coated sheet steels are produced in three surface conditions:

- Exposed (E) is intended for the most critical exposed applications where painted surface appearance is of primary importance. This surface condition will meet requirements for controlled surface texture, surface quality, and flatness.
- Unexposed (U) is intended for unexposed applications and may also have special use where improved ductility over a temper rolled product is desired. Unexposed can be produced without temper rolling. This surface condition may be susceptible to exhibit coil breaks, fluting, and stretcher straining. Standard tolerances for flatness and surface texture are not applicable. In addition, surface imperfections can be more prevalent and severe than with exposed.
- Semi-exposed (Z) is intended for non-critical exposed applications. This is typically a hot dip galvanized temper rolled product.

2.4.2 LOW CARBON FORMABLE STEEL (SAE J-2329)

Increased demands of formability and uniformity on steel properties from the automotive industry has led the Society of Automotive Engineers to re-classify the properties of the DQ, DDQ, and EDDQ low carbon, formable steels into property classifications.

There is a wide variety of parts within the automotive industry, and different levels of specific mechanical properties (for example r value, n value, yield strength, and total elongation) may be required for specific applications. In the past yield strength has been chosen as a major discriminator of the categorization system since this property has meaning to both automotive and steel engineers. In the SAE J2329 document, low carbon sheet steel is classified by 3 grade levels of hot rolled and 5 levels of cold rolled with yield strength, tensile strength, elongation, and n value requirements.

[Table 2.4.2-1](#) illustrates the minimum mechanical property requirements for 3 grades of Hot Rolled formable steel, and [Table 2.4.2-2](#) illustrates minimum mechanical properties for 5 Grades of Cold Rolled Formable steels as described in the SAE Specification J2329. Note the inclusion of the formability properties of n value, r value and elongation.

Table 2.4.2-1 Minimum properties of hot rolled formable steels

SAE J2329 Designation	Yield Strength (MPa) @.2% offset	Tensile Strength (MPa) Minimum	Total % Elongation in 50mm Minimum	n Value Min.
Grade 1	N/R	N/R	N/R	N/R
Grade 2	180-290	270	34	0.16
Grade 3	180-240	270	38	0.18

© 1999 Society of Automotive Engineers, Inc. Used with permission.

Table 2.4.2-2 Minimum properties of cold rolled formable steels

SAE J2329 Designation	Yield Strength (MPa) @ 0.2% offset	Tensile Strength (MPa) Minimum	Total % Elongation in 50mm Minimum	r Value Min.	n Value Min.
Grade 1	N/R	N/R	N/R	N/R	N/R
Grade 2	140-260	270	34	N/R	0.16
Grade 3	140-205	270	38	1.5	0.18
Grade 4	140-185	270	40	1.6	0.20
Grade 5	110-170	270	42	1.7	0.22

© 1999 Society of Automotive Engineers, Inc. Used with permission.

[Table 2.4.2-3](#) illustrates the required chemical compositions as described in SAE J2329 for materials in the hot and cold rolled formable low carbon steel classifications.

Table 2.4.2-3 Required chemical compositions of hot rolled and cold rolled formable steels

SAE J2329 Designation	Carbon max. %	Manganese max. %	Phosphorus max. %	Sulfur max. %	Aluminum min. %
Grade 1	0.13	0.60	0.035	0.035	---
Grade 2	0.10	0.50	0.035	0.030	0.020
Grade 3	0.10	0.50	0.030	0.030	0.020
Grade 4	0.08	0.40	0.025	0.025	0.020
Grade 5	0.02	0.30	0.025	0.025	0.020

© 1999 Society of Automotive Engineers, Inc. Used with permission.

2.4.3 DENT RESISTANT, HIGH STRENGTH AND ADVANCED HIGH STRENGTH STEELS

High Strength sheet steels cover a broad spectrum of steels designed and used for higher yield and tensile strength applications than the low carbon formable steels. Many different high strength steels have been developed by the various steel producers and are available in hot rolled, cold rolled, and coated products. As indicated in an earlier section, high strength steels are specified in SAE J2340; these are listed in [Table 2.4.3-1](#) below. Advanced high strength steels are defined in the Ultra-light Steel Automotive Body – Advanced Vehicle Concept (ULSAB-AVC) and are discussed in [Section 2.4.3.3](#). Descriptions are listed below:

- Dent Resistant (DR)
 - * Bake Hardenable (BH)
 - * Non-Bake Hardenable
- High Strength Solution Strengthened
- High Strength Low Alloy (HSLA)
- High Strength Recovery Annealed
- Advanced High Strength
 - * Dual Phase (DP)
 - * Complex Phase (CP)
 - * Transformation-Induced Plasticity (TRIP)
 - * Martensitic

Higher strength steels are desirable for dent resistance, increased load bearing capacity, better crash management, and /or for mass reduction through decrease in sheet metal thickness.

Strength in these steels is achieved through chemical composition (alloying) and special processing. Special processing could include mechanical rolling techniques, percent cold reduction, temperature control in hot rolling, and time and temperature in annealing of cold reduced sheet. Each of these major groups of steel is discussed below.

Table 2.4.3-1 High and advanced high strength steel grades as described in SAE J2340 and ULSAB-AVC

Steel Description	Grade Type	Available Strength Grade MPa
Dent Resistant Non-Bake Hardenable	A	180, 210, 250, 280
Dent Resistant Bake Hardenable	B	180, 210, 250, 280
High Strength Solution Strengthened	S	300, 340
High Strength Low Alloy	X&Y	300, 340, 380, 420, 490, 550
High Strength Recovery Annealed	R	490, 550, 700, 830
Advanced High Strength	See Figure 2.4.3-1	See Figure 2.4.3-1

© 1999 Society of Automotive Engineers, Inc. Used with permission.

[Figure 2.4.3-1](#) shows a graphic comparison of the strengths and percent elongation for various grades of automotive sheet steels.

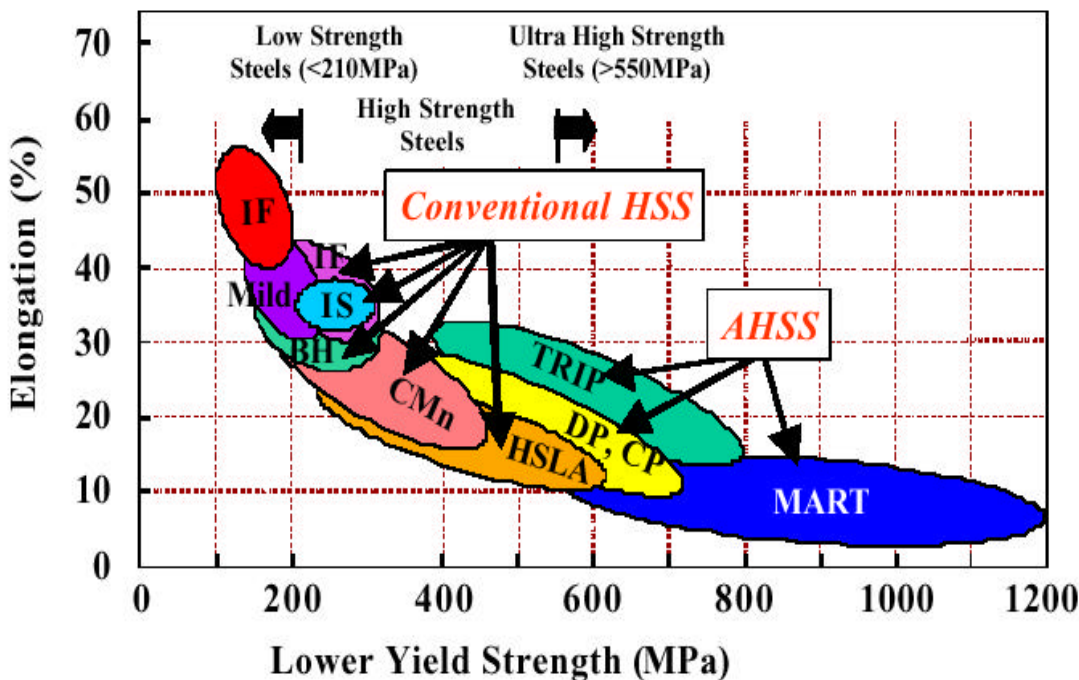


Figure 2.4.3-1 A comparison of lower (or initial) yield strength and % elongation for various grades of steels¹

2.4.3.1 Dent Resistant, Bake Hardenable and Non-Bake Hardenable Sheet Steel

There are two types of dent resistant steels: non bake-hardenable and bake-hardenable. SAE has classified them as Type A and Type B, both of which are available in grades with minimum yield strengths from 180 MPa and higher. Dent resistant steels are cold reduced low carbon (0.01%-0.08%), typically deoxidized and continuous cast steel made by basic oxygen, electric furnace, or other processes that will produce a material that satisfies the requirements for the specific grade. The chemical composition is capable of achieving the desired mechanical and formability properties for the specified grade and type. For grades 180 and 210 using an interstitial free (IF) base metal having a carbon content less than 0.01%, an effective boron addition of <0.001% may be required to minimize secondary work embrittlement (SWE) and to control grain growth during welding.

Dent Resistant Type A steel is a non-bake hardenable, dent resistant steel achieving the final strength in the part through a combination of the initial yield strength and the work hardening imparted during forming. Solid solution strengthening elements such as phosphorus, manganese and/or silicon are added to increase strength. Work hardenability depends upon the amount of carbon remaining in solution, which is controlled through chemistry and thermo-mechanical processing. Small amounts of columbium or vanadium are sometimes used, but are limited because they reduce ductility.

Dent Resistant Type B steel is a bake hardenable dent resistant steel that makes up a relatively new class of sheet steel products. They offer a combination of formability in the incoming steel and high yield strength in the application that is not attained in conventional high strength steels. They can be potentially substituted for drawing quality sheet at the stamping plant without

requiring major die modifications. The combination of formability and strength makes bake hardenable steels good options for drawn or stretched applications where resistance to dents and palm printing is important in applications such as hoods, doors, fenders, and deck lids. Bake hardenable steels may also assist in vehicle mass reduction through downgaging.

The forming operation imparts some degree of strain hardening, which increases yield strength. The paint baking cycle, typically about 175°C (350°F) for 20 to 30 minutes, provides another increase due to moderate “carbon strain aging”. Material properties are generally stable, depending on the process. [Figure 2.4.3.1-1](#) illustrates the hardening process with bake hardening steels.

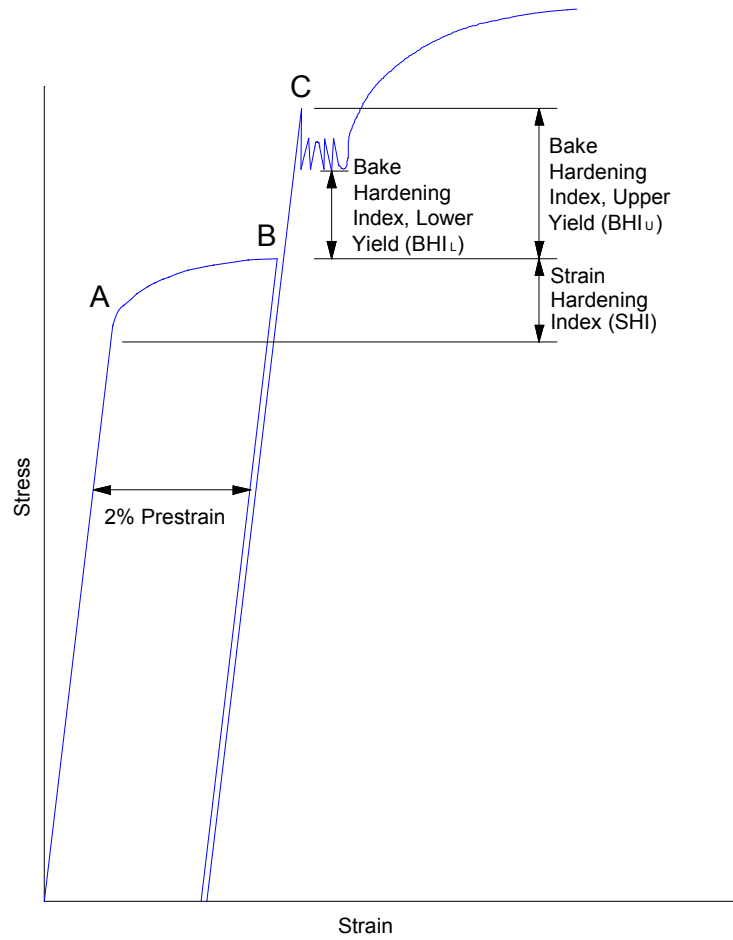


[Figure 2.4.3.1-1](#) Schematic illustration showing strain hardening and bake hardening index and the increase in yield strength that occurs during the bake cycle

[Table 2.4.3.1-1](#) shows the required mechanical properties for the Type A and Type B bake hardenable and non-bake hardenable dent resistance steels as described in the SAE J2340 specification.

Mechanical property requirements of dent resistant cold reduced uncoated and coated sheet steel grades are based on the minimum values of as received yield strength (180, 210, 250, and 280 MPa) and n Value of the sheet steel, the minimum yield strength after strain and bake, and tensile strength.

Table 2.4.3.1-1 Required minimum mechanical properties of Type A and Type B dent resistant cold reduced sheet steel as described in J2340

SAE J2340 Grade Designation and Type	As Received Yield Strength MPa	As Received Tensile Strength MPa	As Received n Value	Yield Strength After 2% Strain MPa	Yield Strength After Strain and Bake MPa
180 A	180	310	0.20	215	
180 B	180	300	0.19		245
210 A	210	330	0.19	245	
210 B	210	320	0.17		275
250 A	250	355	0.18	285	
250 B	250	345	0.16		315
280 A	280	375	0.16	315	
280 B	280	365	0.15		345

© 1999 Society of Automotive Engineers, Inc. Used with permission.

2.4.3.2 High Strength Solution Strengthened, High Strength Low Alloy (HSLA), and High Strength Recovery Annealed Hot Rolled and Cold Reduced Sheet Steel

High strength solution strengthened, HSLA, and high strength recovery annealed categories include steel grades with minimum yield strengths in the range of 300 to 830 MPa. Steel made for these grades is low carbon, deoxidized and continuous cast steel made by basic oxygen, electric furnace, or other processes that will produce a material that satisfies the requirements for the specific grade. The chemical composition is capable of achieving the desired mechanical and formability properties for the specified grade and type.

Several different types of high strength steel based on chemistry can fall under this category. Solution strengthened high strength steels are those that contain additions of phosphorus, manganese, or silicon to conventional low carbon (0.02-0.13% carbon) steels. HSLA steels have additions of carbide formers, such as, titanium, niobium (columbium), or vanadium made to conventional low carbon steels. High strength recovery annealed steels have chemistries similar to the above varieties of steel, but special annealing practices prevent recrystallization in the cold rolled steel.

Classification is based on the minimum yield strength: 300 to 830 MPa. Several categories at each strength level are defined as follows:

Type S: High strength solution strengthened steels use carbon and manganese in combination with phosphorus or silicon (as solution strengtheners) to meet the minimum for improved formability and weldability. Phosphorus is restricted to a maximum of 0.100%. Sulfur is restricted to a maximum of 0.020%.

Type X: High Strength Low Alloy steels (typically referred to as HSLA), are alloyed with carbide and nitride forming elements, commonly niobium (columbium), titanium, and vanadium either singularly or in combination. These elements are used with carbon, manganese, phosphorus, and silicon to achieve the specified minimum yield strength. Carbon content is restricted to 0.13% maximum for improved formability and weldability. Phosphorus is restricted to a maximum of 0.060%. The specified minimum for niobium (columbium), titanium, or vanadium is 0.005%. Sulfur is restricted to a maximum of 0.015%. A spread of 70 MPa is specified between tensile strengths and the required minimum of the yield strength.

Type Y: Same as Type X, except that a 100 MPa spread is specified between the required minimum of the yield and tensile strengths.

Type R: High strength recovery annealed or stress-relief annealed steels achieve strengthening primarily through the presence of cold work. Alloying elements mentioned under Type S and X may also be added. Carbon is restricted to 0.13% maximum for improved formability and weldability. Phosphorus is restricted to a maximum of 0.100%. Sulfur is restricted to a maximum of 0.015%. These steels are best suited for bending and roll-forming applications since their mechanical properties are highly directional and ductility and formability are limited.

Table 2.4.3.2-1 shows the required mechanical properties for the Type S, Type X, and Type Y of the High Strength Low alloy steels. The SAE specification of these properties are described in SAE J2340.

Table 2.4.3.2-1 Required mechanical properties of high strength and HSLA hot rolled and cold reduced, uncoated and coated sheet steel²

SAE J2340 Grade Designation and Type	Yield Strength Mpa		Tensile Strength MPa	% Total Elongation Minimum	
	Minimum	Maximum	Minimum	Cold Rolled	Hot Rolled
300 S	300	400	390	24	26
300 X	300	400	370	24	28
300 Y	300	400	400	21	25
340 S	340	440	440	22	24
340 X	340	440	410	22	25
340 Y	340	440	440	20	24
380 X	380	480	450	20	23
380 Y	380	480	480	18	22
420 X	420	520	490	18	22
420 Y	420	520	520	16	19
490 X	490	590	560	14	20
490 Y	490	590	590	12	19
550 X	550	680	620	12	18
550 Y	550	680	650	12	18

© 1999 Society of Automotive Engineers, Inc. Used with permission.

Table 2.4.3.2-2 shows the required mechanical properties for the Type R, Recovery Annealed steels. The SAE specification of these properties are described in SAE J2340.

Table 2.4.3.2-2 Required mechanical properties of Type R, high strength recovery annealed cold reduced sheet steel

SAE J2340 Grade Designation and Type	Yield Strength MPa		Tensile Strength MPa	% Total Elongation
	Minimum	Maximum	Minimum	Minimum
490 R	490	590	500	13
550 R	550	650	560	10
700 R	700	800	710	8
830 R	830	960	860	2

© 1999 Society of Automotive Engineers, Inc. Used with permission.

2.4.3.3 Advanced High Strength Steels; Dual Phase, TRIP and Low Carbon Martensite

New challenges of unprecedented requirements for passenger safety, vehicle performance and fuel economy targets in North America, Europe, and Asia, have forced the automotive industry into advances in material utilization and processing that would have been considered impossible less than a decade ago. The recent drive towards lightweighting in the transportation industry has led to strong competition between steel and low density metal industries. The steel industry's response to the increasing use of lower density materials such as aluminum and magnesium is to develop increasingly higher strength materials while maintaining, or even improving formability, thereby making it possible simultaneously to improve the strength characteristics of the parts and reduce the weight through reduction of the steel sheet thickness. In response, the steel industry has recently produced a number of advanced high strength steels (AHSS) that are highly formable, yet possess an excellent combination of strength, durability, strain rate sensitivity and strain hardening. These characteristics may enable automotive designers to achieve both weight reduction and improved crash safety.

2.4.3.3.1 AHSS Nomenclature

Classification of AHSS differs from conventional high strength steels (HSS). Since AHSS are relatively new to the Automotive Industry, a consistent nomenclature was not available until the Ultra-Light Steel Automotive Body – Advanced Vehicle Concept (ULSAB-AVC) Consortium adopted a standard practice. The practice specifies both yield strength (YS) and ultimate tensile strength (UTS)³. In this system, steels are identified as:

XX aaa/bbb where, XX = Type of Steel
 aaa = minimum YS in MPa, and
 bbb = minimum UTS in MPa.

The types of steels are defined as:

DP = Dual Phase
CP = Complex Phase
TRIP = Transformation-Induced Plasticity
Mart = Martensitic

For example, DP 500/800 designates dual phase steel with 500 MPa minimum yield strength and 800 MPa minimum ultimate tensile strength.

Table 2.4.3.3.1-1 shows some generalized mechanical properties of several advanced high strength steels, which are the grades used in the ULSAB-AVC body structure. The differences between conventional high strength steels and advanced high strength steels arise from the microstructure, which is determined by controlling the cooling rate during processing.

Table 2.4.3.3.1-1 Typical Mechanical Properties of AHSS

Product	YS (MPa)	UTS (MPa)	Total EL (%)	n-value ^a (5-15%)	r-bar	k-value ^b (MPa)
DP 280/600	280	600	30-34	0.21	1.0	1082
DP 300/500	300	500	30-34	0.16	1.0	762
DP 350/600	350	600	24-30	0.14	1.0	976
DP 400/700	400	700	19-25	0.14	1.0	1028
TRIP 450/800	450	800	26-32	0.24	0.9	1690
DP 500/800	500	800	14-20	0.14	1.0	1303
CP 700/800	700	800	10-15	0.13	1.0	1380
DP 700/1000	700	1000	12-17	0.09	0.9	1521
Mart 950/1200	950	1200	5-7	0.07	0.9	1678
Mart 1250/1520	1250	1520	4-6	0.065	0.9	2021

© 1999 Society of Automotive Engineers, Inc. Used with permission.

Where: YS and UTS are minimum values, others are typical values.

Total EL % - Flat sheet (A50 or A80).

^a n-value is calculated in the range of 5 to 15% true strain, if applicable.

^b k-value is the magnitude of true stress extrapolated to a true strain of 1.0. It is a material property parameter frequently used by one-step forming simulation codes.

2.4.3.3.2 Work Hardening and Plasticity of AHSS

The work hardening characteristics of a material and its behavior in the plastic range affect both formability and crash performance.

Dual Phase (DP) Steels¹

Dual Phase steels have a high initial work hardening rate (n-value), which better distributes plastic strain and improves uniform elongation. This work hardening rate will produce a much higher ultimate tensile strength than that of conventional high strength steels with similar initial yield strengths. DP steels also exhibit a high uniform and total elongation and a lower YS/TS ratio when compared with conventional high strength steels. These characteristics provide improvements in both formability and structural performance in automotive components.

TRIP Steels¹

During the first stages of strain, from 0 to 7%, TRIP steels have a similar, yet higher, work hardening rate than conventional HSS. But after 7% strain, the unique microstructure of TRIP locally stabilizes plastic deformation and increases strength. Material stretching is then distributed to adjacent material. The progression delays the onset of localized thinning and necking that often leads to stamping failure. This characteristic of sustained high n-value between 5% and 20% strain is different from that of conventional HSS and dual phase steels, whose n-values tend to diminish in this range. As a result, complex automotive components that cannot be made with dual phase can often be made with TRIP steels. Properties of several materials are compared in [Figure 2.4.3.3.2-1](#) ⁴ ⁵ ⁶

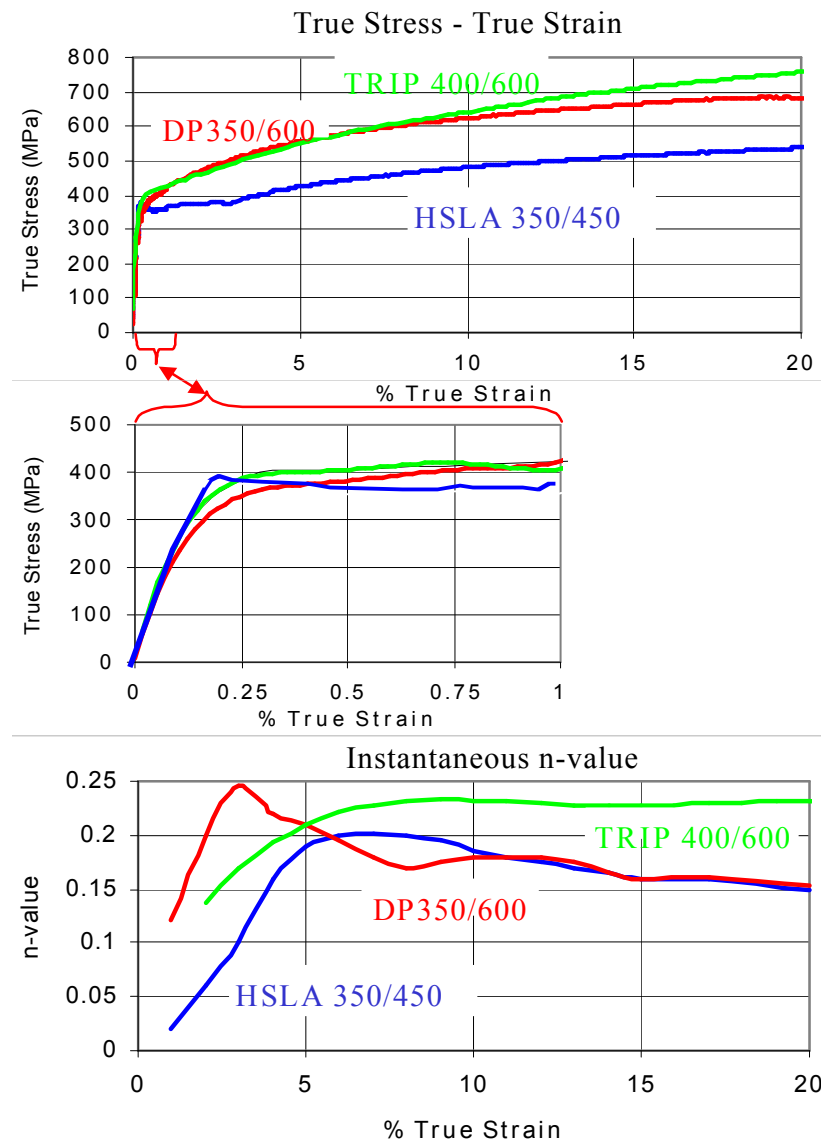


Figure 2.4.3.3.2-1 True stress-strain and instantaneous n-value for HSLA 350/450, DP350/600, and TRIP 400/600

2.4.3.3.3 Formability Dual Phase

At a strain range of 5 to 15%, HSLA 340 and DP350/600 have similar n-values. Also, DP has an r-value of 1.0. These facts may seem to imply that there is no advantage in formability for either steel grade. But, dual phase steels exhibit rapid stain hardening prior to 5% strain. This characteristic allows strain to be distributed across greater volumes of material and delays the onset of local necking. As a result, the formability of DP is better than that of a conventional high strength steel of similar yield strength, as illustrated in [Figure 2.4.3.3.3-1](#).

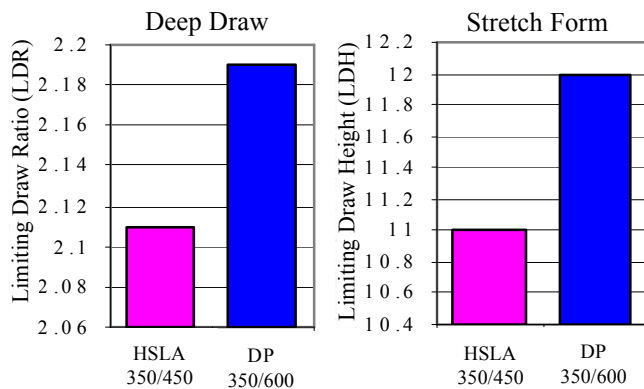


Figure 2.4.3.3.3-1 Comparison of DP350/600 and HSLA350/400 for LDR and LDH6

TRIP

As discussed in [Section 2.4.3.2](#), TRIP steels can sustain their n-value much longer than other grades. Even though the initial n-value is lower than that of dual phase steels, it increases and maintains itself into high strain ranges, which gives TRIP an advantage in severe stretch applications.¹

TRIP steels have a relatively low r-value, approximately 1.0. Despite this fact, TRIP has excellent deep drawability. The mechanics of this contradictory phenomenon are complicated, but in simple terms the microstructure of TRIP steel inhibits local thinning between a flange and wall section, thus improving formability.¹

2.4.3.3.4 Structural Steel Performance of AHSS

The superior formability of advanced high strength steels, compared with conventional high strength steels of similar initial yield strengths, give the automotive designer more flexibility to optimize part geometry. This section discusses other component performance criteria that also affect vehicle performance such as stiffness, strength, durability, and crash energy management.

Stiffness

The stiffness of a component is controlled by material modulus of elasticity (E) and component geometry (including gauge). Since the modulus of elasticity is constant for steel, changing the grade will not influence vehicle stiffness; the designer must modify component geometry. The enhanced formability of AHSS offers greater design flexibility, which will allow a designer to improve component stiffness without increasing mass or sacrificing strength. Reductions in gauge can be offset by changes in geometry or the use of continuous joining techniques such as laser welding or adhesive bonding.

Strength

Component strength is a function of its geometry and yield and/or tensile strength. As noted previously, advanced high strength steels offer improvements in design flexibility due increased formability and enhanced work hardening capability. Additionally, these grades of steels also have excellent bake hardening ability. The combination of superior work hardening and excellent bake hardening enhances the final as-manufactured strength of AHSS components. Component material strengths for a typical HSLA grade and a similar Dual Phase grade are compared in [Figure 2.4.3.3.4-1](#).⁶ In order to optimize the mass of a vehicle, it is important to design to the

final as-manufactured strength to avoid the over design that occurs when the part is based on as-rolled material properties.

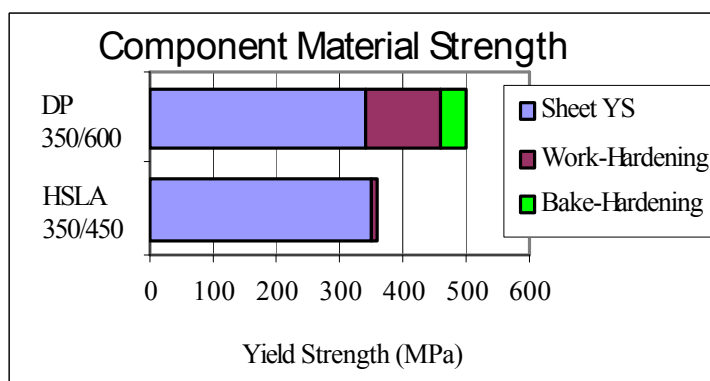


Figure 2.4.3.3.4-1 Comparison between DP350/600 and HSLA350/450 subjected to a 2% strain and bake hardened

Fatigue

Fatigue in a structural component involves complicated relationships among several factors that include geometry, thickness, applied loads and material endurance limit¹. It has been shown that the endurance limit of a material increases with tensile strength.⁷⁻⁸ Superior work and bake hardening significantly increase the as-manufactured strength of AHSS components, which will result in a better fatigue performance.⁹

Crashworthiness

Crashworthiness requirements are becoming increasingly stringent. As a result, materials must be able to absorb more energy in a crash scenario. Steel exhibits sensitivity to strain rate under a dynamic load such as a crash. This condition is shown in [Figure 2.4.3.3.4-2](#). The automotive designer/analyst should incorporate this effect into computer simulations to accurately predict crash performance because it has been shown that properly considering strain rate effects will improve model accuracy.^{10,11,12}

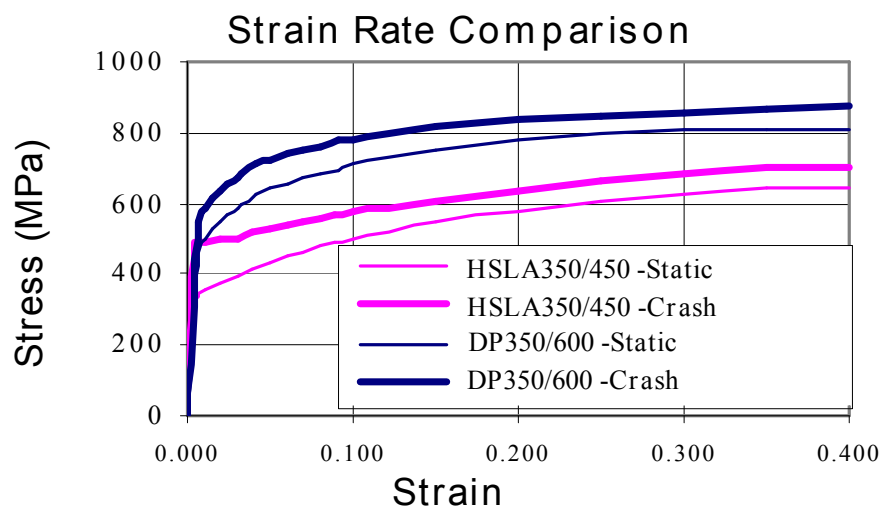


Figure 2.4.3.3.4-2 Static and dynamic stress strain curves for a conventional HSS, HSLA350/450, and an AHSS, DP350/600³

Dual phase steel is predicted to have a significant advantage in energy absorption based on a comparison of the area under curves found in [Figure 2.4.3.3.4-2¹](#). The higher energy absorption is attributed to the high work hardening rate and a high flow stress that distribute the strain more evenly and consequently engages greater volumes of material in the crash event. Work hardening and bake hardening improve the energy absorption because the formed and baked component will have a higher flow stress than the as-rolled material from which the component was manufactured.[12, 13, 14](#)

2.4.4 AVAILABILITY AND TYPICAL MATERIAL PROPERTIES

Availability of hot and cold rolled sheet steels materials in regards to width and thickness, coupled with typical mechanical properties measured over thousands of tests made by steel producers and the Materials Uniformity Task Force of the Auto/Steel Partnership, is summarized in [Table 2.4.4-1](#). Obviously, all materials are not available in every width and/or thickness and some widths and/or thicknesses may only be available from a limited number of producers. Consequently, producers must be consulted to determine availability of particular materials.

**Table 2.4.4-1 Compilation of AISI and A/SP materials property data
typical property values**

Mat'l	SAE Class.	Grade		Strength		Total Elng.	n	r	Hard.	Width Range		Thickness	
				Yield	Tensile					Rb	(mm)	(in)	
		SAE	AISI	MPa/ksi	MPa/ksi	%					(mm)	(in)	(mm)
HR	SAE J2329	1	CQ	269/39	386/56	35	0.19	N/A	60	610 - 1829	24 - 62	1.00 - 9.53	0.070 - 0.500
HR	SAE J2329	2	DQ	248/36	338/49	37	0.19	1.1	54	610 - 1829	24 - 72	1.00 - 9.53	0.055 - 0.375
HR	SAE J2329	3	DDQ	234/34	331/48	41	0.20	1.1	55	610 - 1829	24 - 72	1.00 - 9.53	0.055 - 0.375
CR	SAE J2329	1	CQ	296/43	331/48	35	0.20	1.1	50	610 - 1829	24 - 62	0.38 - 3.30	0.020 - 0.120
CR	SAE J2329	2	DQ	186/27	317/46	38	0.22	1.5	42	610 - 1829	24 - 72	0.38 - 3.30	0.015 - 0.130
CR	SAE J2329	3	DQ	186/27	317/46	42	0.22	1.5	42	610 - 1829	24 - 72	0.38 - 3.30	0.015 - 0.130
CR	SAE J2329	4	DDQ	172/25	310/45	44	0.23	1.7	38	610 - 1829	24 - 72	0.38 - 3.30	0.015 - 0.130
CR	SAE J2329	5	EDDQ	159/23	303/44	46	0.23	2.0	32	610 - 1829	24 - 72	0.38 - 3.30	0.015 - 0.130
CR	SAE J2340	180A	Dent Resist	200/29	350/50	40	0.22	1.7	63	610 - 1829	24 - 72	0.64 - 2.79	0.025 - 0.110
CR	SAE J2340	210A	Dent Resist	210/30	375/54	39	0.21	1.6	65	610 - 1829	24 - 72	0.64 - 2.79	0.025 - 0.110
CR	SAE J2340	250A	Dent Resist	270/39	400/58	36	0.20	1.5	68	610 - 1829	24 - 72	0.64 - 2.79	0.025 - 0.110
CR	SAE J2340	280A	Dent Resist	300/43	430/62	36	0.18	1.4	70	610 - 1829	24 - 72	0.64 - 2.79	0.025 - 0.110
CR	SAE J2340	180B	Bake Hard	200/29	320/46	39	0.20	1.7	52	610 - 1829	24 - 72	0.64 - 2.79	0.025 - 0.110
CR	SAE J2340	210B	Bake Hard	221/32	352/51	41	0.19	1.6	54	610 - 1829	24 - 72	0.64 - 2.79	0.025 - 0.110
CR	SAE J2340	250B	Bake Hard	255/37	379/55	39	0.18	1.4	58	610 - 1829	24 - 72	0.64 - 2.79	0.025 - 0.110
CR	SAE J2340	280B	Bake Hard	324/47	421/61	37	0.17	1.1	67	610 - 1829	24 - 72	0.64 - 2.79	0.025 - 0.110
HR	SAE J2340	300S	HSS	340/49	450/65	30	0.17	N/A	72	610 - 1829	24 - 72	1.00 - 9.53	0.055 - 0.375
CR	SAE J2340	300S	HSS	340/49	379/55	28	0.17	1.0	70	610 - 1829	24 - 72	0.64 - 2.79	0.025 - 0.110
HR	SAE J2340	340S	HSS	407/59	483/70	28	0.16	N/A	75	610 - 1829	24 - 72	0.64 - 2.79	0.025 - 0.110
CR	SAE J2340	340S	HSS	379/55	455/66	26	0.17	1.3	72	610 - 1575	24 - 62	0.64 - 2.03	0.025 - 0.080
HR	SAE J2340	300X	HSLA	350/51	407/59	32	0.17	N/A	72	610 - 1829	24 - 72	1.00 - 9.53	0.055 - 0.375
CR	SAE J2340	300X	HSLA	352/51	469/68	28	0.16	1.1	70	610 - 1829	24 - 72	0.38 - 3.30	0.015 - 0.130
CR	SAE J2340	300Y	HSLA	350/51	407/59	25	0.17	N/A	72	610 - 1829	24 - 72	0.38 - 3.30	0.015 - 0.130
HR	SAE J2340	340X	HSLA	407/59	483/70	30	0.17	N/A	75	610 - 1829	24 - 72	1.00 - 9.53	0.055 - 0.375
CR	SAE J2340	340X	HSLA	365/53	476/69	27	0.15	1.1	76	610 - 1524	24 - 60	0.76 - 3.18	0.030 - 0.125
CR	SAE J2340	340Y	HSLA	365/53	476/69	26	0.15	1.1	76	610 - 1524	24 - 60	0.76 - 3.18	0.030 - 0.125
CR	SAE J2340	380X	HSLA	462/67	524/76	26	0.14	1.0	80	610 - 1524	24 - 60	0.76 - 3.18	0.030 - 0.125
CR	SAE J2340	380Y	HSLA	462/67	524/76	24	0.14	1.0	80	610 - 1524	24 - 60	0.76 - 3.18	0.030 - 0.125
HR	SAE J2340	420X	HSLA	476/69	531/77	27	0.15	N/A	87	610 - 1829	24 - 72	1.00 - 9.53	0.055 - 0.375
CR	SAE J2340	420X	HSLA	462/67	524/76	25	0.15	1.0	87	610 - 1524	24 - 60	0.76 - 3.18	0.030 - 0.125
CR	SAE J2340	420Y	HSLA	462/67	524/76	22	0.15	1.0	87	610 - 1524	24 - 60	0.76 - 3.18	0.030 - 0.125
HR	SAE J2340	490X	HSLA	531/77	600/87	24	0.13	N/A	90	610 - 1829	24 - 72	1.00 - 9.53	0.055 - 0.375
CR	SAE J2340	490X	HSLA	531/77	600/87	19	0.13	N/A	90	610 - 1524	24 - 60	0.76 - 3.18	0.030 - 0.125
CR	SAE J2340	490Y	HSLA	531/77	600/87	17	0.13	N/A	90	610 - 1524	24 - 60	0.76 - 3.18	0.030 - 0.125
HR	SAE J2340	550X	HSLA	586/85	676/98	17	0.12	N/A	96	610 - 1829	24 - 72	1.00 - 9.53	0.055 - 0.375
CR	SAE J2340	550X	HSLA	586/85	676/98	17	0.12	N/A	96	610 - 1524	24 - 60	0.76 - 3.18	0.050 - 0.125
HR/CR	SAE J2340	550Y	HSLA	586/85	676/98	17	0.12	N/A	96	610 - 1524	24 - 60	0.76 - 3.18	0.050 - 0.125
CR	SAE J2340	490R	Rec Anneal	540/78	600/87	15	N/A	N/A	90	610 - 1524	24 - 60	0.76 - 3.18	0.050 - 0.125
CR	SAE J2340	550R	Rec Anneal	600/87	700/101	12	0.12	N/A	96	610 - 1524	24 - 60	0.76 - 3.18	0.050 - 0.125
CR	SAE J2340	700R	Rec Anneal	750/108	800/116	11	N/A	N/A	610 - 1524	24 - 60	0.76 - 3.18	0.050 - 0.125	
CR	SAE J2340	830R	Rec Anneal	900/130	1000/145	4	N/A	N/A	610 - 1524	24 - 60	0.76 - 3.18	0.050 - 0.125	
HR/CR	SAE J2340	500DH	Dual Phase	340/49	550/80	25		N/A	90	610 - 1524	24 - 60	0.48 - 2.16	0.050 - 0.125
HR/CR	SAE J2340	600DH	Dual Phase	550/80	710/103	17		N/A	96	610 - 1524	24 - 60	0.48 - 2.16	0.050 - 0.125
HR/CR	SAE J2340	600DL1	Dual Phase	550/80	710/103	18		N/A	96	610 - 1524	24 - 60	0.48 - 2.16	0.050 - 0.125
HR/CR	SAE J2340	600DL2	Dual Phase	550/80	710/103	23		N/A	96	610 - 1524	24 - 60	0.48 - 2.16	0.050 - 0.125
HR/CR	SAE J2340	700DH	Dual Phase	600/87	760/110	15		N/A	97	610 - 1524	24 - 60	0.48 - 2.16	0.050 - 0.125
HR/CR	SAE J2340	800DL	Dual Phase	580/84	860/125	10		N/A	104	610 - 1524	24 - 60	0.48 - 2.16	0.050 - 0.125
HR/CR	SAE J2340	950DL	Dual Phase	680/98	1050/152	10		N/A	106	610 - 1524	24 - 60	0.48 - 2.16	0.050 - 0.125
HR/CR	SAE J2340	1000DL	Dual Phase	810/117	1070/155	7		N/A	106	610 - 1524	24 - 60	0.48 - 2.16	0.050 - 0.125
HR/CR	SAE J2340	800M	Martensite	800/116	900/131	N/A		N/A	610 - 1295	24 - 51	0.48 - 1.50	0.020 - 0.060	
HR/CR	SAE J2340	900M	Martensite	900/130	1025/149	5		N/A	610 - 1295	24 - 51	0.48 - 1.50	0.020 - 0.060	
HR/CR	SAE J2340	1000M	Martensite	960/139	1090/158	N/A		N/A	610 - 1295	24 - 51	0.48 - 1.50	0.020 - 0.060	
HR/CR	SAE J2340	1100M	Martensite	1030/149	1180/171	5		N/A	610 - 1295	24 - 51	0.48 - 1.50	0.020 - 0.060	
HR/CR	SAE J2340	1200M	Martensite	1140/165	1340/194	5		N/A	610 - 1295	24 - 51	0.48 - 1.50	0.020 - 0.060	
HR/CR	SAE J2340	1300M	Martensite	1200/174	1400/203	5		N/A	610 - 1295	24 - 51	0.48 - 1.50	0.020 - 0.060	
HR/CR	SAE J2340	1400M	Martensite	1260/183	1480/214	5		N/A	610 - 1295	24 - 51	0.48 - 1.50	0.020 - 0.060	
HR/CR	SAE J2340	1500M	Martensite	1350/196	1580/229	5		N/A	610 - 1295	24 - 51	0.48 - 1.50	0.020 - 0.060	

REFERENCES FOR SECTION 2.4

1. J.R. Shaw, B. K. Zuidema, "New High Strength Steels Help Automakers Reach Future Goals for Safety, Affordability, Fuel Efficiency, and Environmental Responsibility" SAE Paper 2001-01-3041.
2. SAE Specification J2340, Categorization and Properties of Dent Resistant, High Strength, and Ultra High Strength Automotive Sheet Steels, Oct 1999, Society of Automotive Engineers, 400 Commonwealth Drive, Warrendale, PA, 15096-0001.
3. ULSAB-AVC Consortium, Technical Transfer Dispatch #6, "ULSAB-AVC Body Structure Materials," May, 2001.
4. Konieczny A. A. , United States Steel Internal Report
5. J. R. Fekete, A.M. Stibich, M. F. Shi, "A Comparison of Energy Absorption of HSLA vs. Dual Phase Sheet Steel in Dynamic Crush", SAE Paper 2001-01-3101.
6. J. R. Shaw, K. Watanabe, M. Chen, "Metal Forming Characterization and Simulation of Advanced High Strength Steels" SAE Paper 2001-01-1139, 2001.
7. K. Eberle, Ph. Harlet, P. Cantineaus, and M. Vande Populiere, "New thermomechanical strategies for the realization of multiphase steels showing a transformation induced plasticity (TRIP) effect," 40th MWSP Conference, Vol. XXXVI, Iron and Steel Society, Warrendale, PA, (1998), 83-92.
8. J-O. Sperle, "Fatigue Strength of High Strength Dual-Phase Steel Sheet," Int. Journal of Fatigue 7 no 2 (1985) pp. 79-86.
9. K. Mahadevan, P. Liang, J. R. Fekete, "Effect of Strain Rate in Full Vehicle Frontal Crash Analysis," SAE Technical Paper no. 2000-01-0625, Society of Automotive Engineers, Warrendale, PA, USA.
10. Simunovic, S., Shaw, J., Aramayo, G., "Material modeling effects on impact deformation of ultralight steel auto body", SAE Paper 2000-01-2715, 2000.
11. S. Simunovic, J. Shaw, "Effect Material Processing in Full Vehicle Crash Analysis," SAE Technical Paper No. 2000-01-1056, Society of Automotive Engineers, Warrendale, PA, USA.
12. T. Dutton, S. Iregbu, R. Sturt, A. Kellicut, B. Cowell, K. Kavikondala," The Effect of Forming on the Crashworthiness of Vehicles with Hydroformed Frame Siderails", SAE Paper 1999-01-3208, 1999
13. X. M. Chen, M. F. Shi and P. M. McKune, S.M. Chen," Applications of High Strength Steels in Hydroforming Dual Phase Vs. HSLA", SAE Paper 2001-01-1133, 2001.

14. B. K. Zuidema, S. G. Denner, B. Engl, J. O. Sperle, "New High Strength Steels Applied to the Body Structure of ULSAB-AVC" SAE Paper 2001-01-3042, 2001

BIBLIOGRAPHY FOR SECTION 2.4

Refer to [Section 2.15](#) for a comprehensive bibliography for [Section 2.1](#) to [2.14](#).

2.5 STEEL COMPANY PROVIDED STRESS STRAIN CURVES

The relationship between the stress and strain that a material displays is known as a stress-strain curve. Stress-strain curves might be needed in the inelastic finite element analysis. It is unique for each kind of steel and is found by recording the amount of deformation (strain) at distinct intervals of tensile or compressive loading as explained in [Section 23.12](#). The best source of the stress-strain curves are from the steel manufacturers.

[Figure 2.5-1](#) shows the sample stress strain curves for a HR 80 ksi, DP 590 HR, and a HR 50 ksi. [Figure 2.5-2](#) shows the sample stress strain curves for a BH210 and a BH180EG. [Figure 2.5-3](#) shows the sample stress strain curves for a DP600/590 HDGA and a Galvanized 50 ksi. [Figure 2.5-4](#) shows the sample stress strain curve for a DDS-CR.

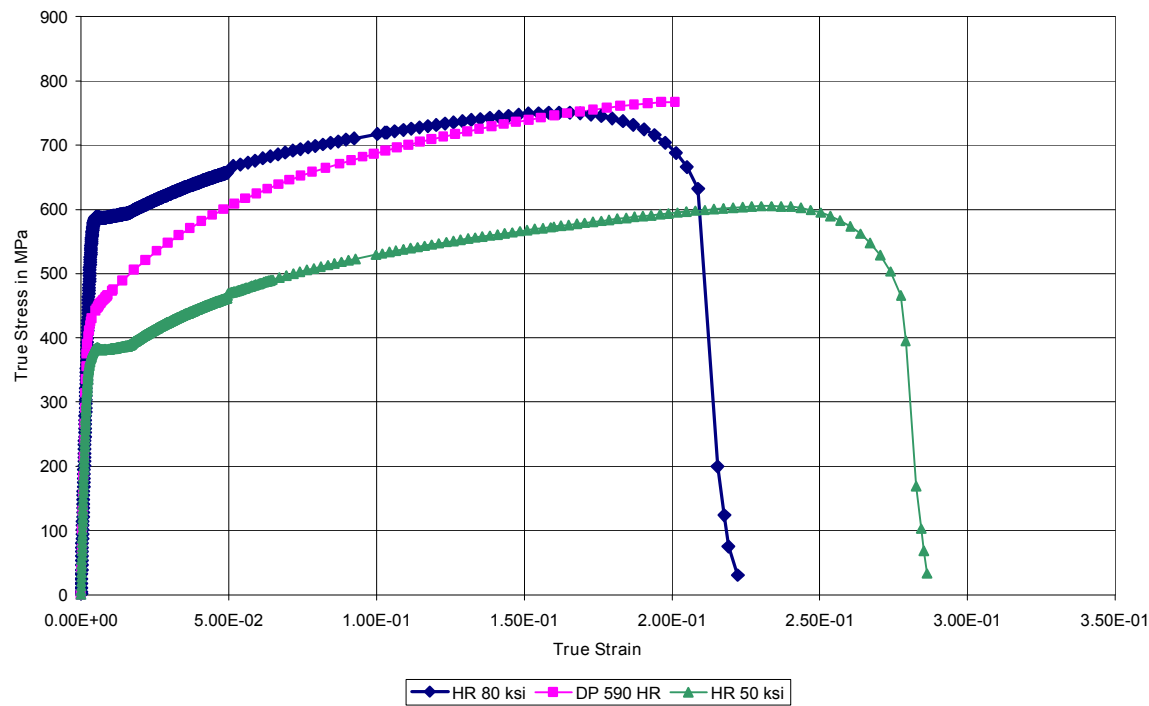


Figure 2.5-1 Sample stress-strain curves for a HR 80ksi, DP 590 HR, and a HR 50ksi

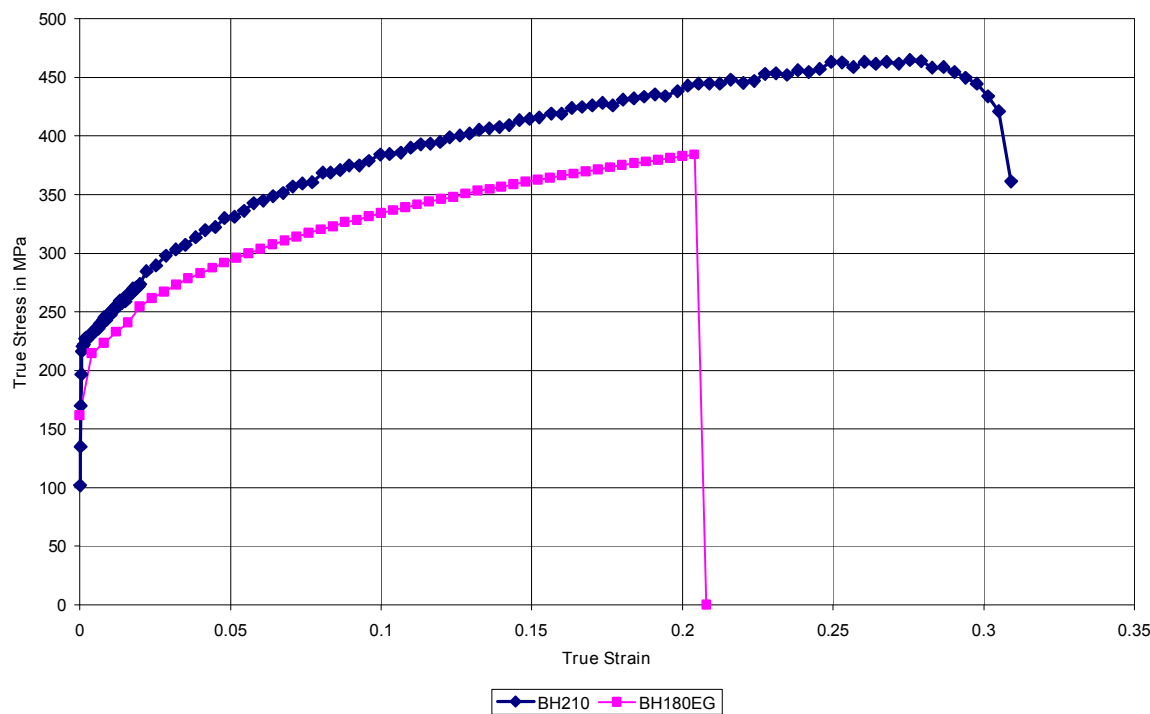


Figure 2.5-2 Sample stress-strain curves for a BH210 and a BH180EG

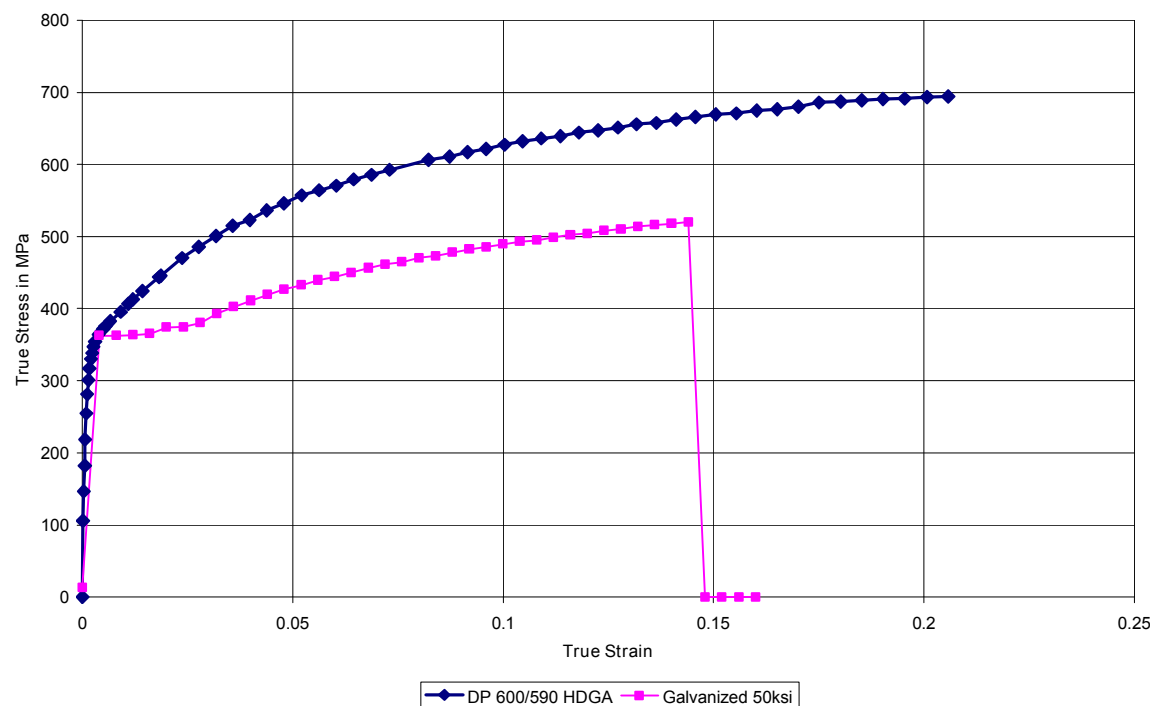


Figure 2.5-3 Sample stress-strain curves for a DP600/590 HDGA and a Galvanized 50 ksi

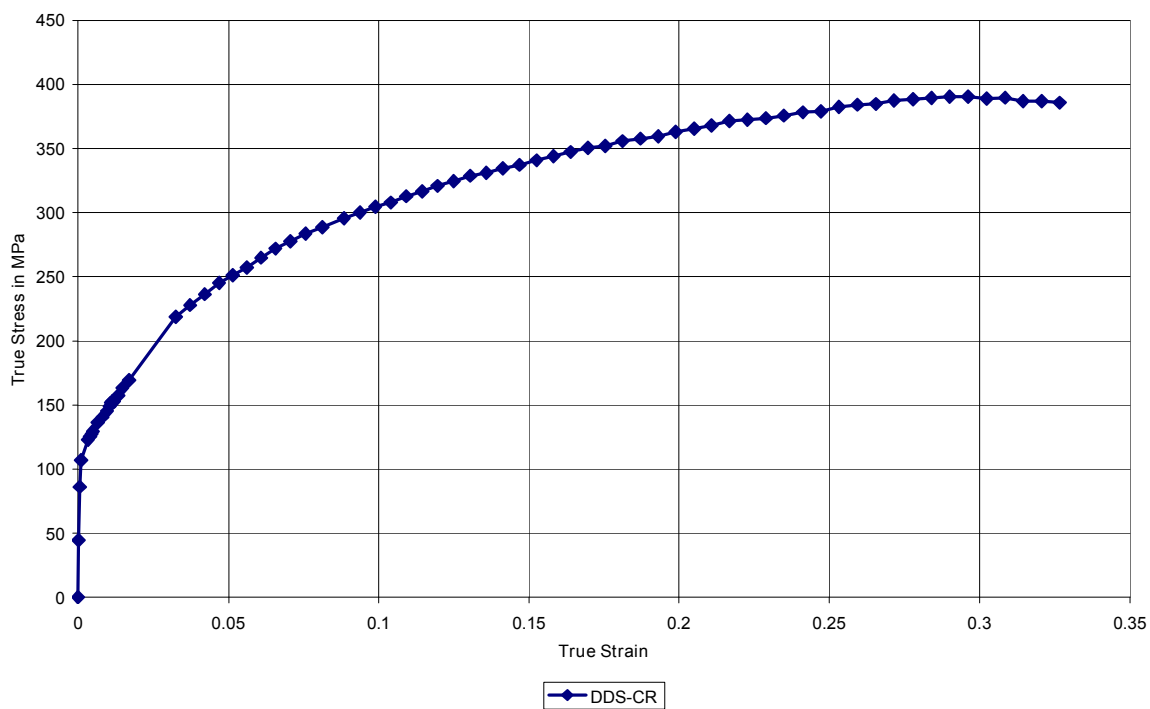


Figure 2.5-4 Sample stress-strain curves for a DDS-CR

2.6 WELDABILITY OF HIGH STRENGTH STEELS

When high strength steel is used in welded applications, welding procedures must be suitable for the steel chemistry and intended service. Unspecified chemical elements, when present, are subject to the limits stated in [Table 2.6-1](#). The sum Cu, Ni, Cr, and Mo must not exceed 0.50% on heat analysis. When one or more of these elements is specified, the sum does not apply; only the individual limits on the remaining unspecified elements will apply as described in J2340.

Table 2.6-1 Chemical limits on unspecified elements

Element	Type A,B, &R %	Type S %	Type X & Y %	Type D & M %
Phosphorus	0.100	0.100	0.060	0.020
Sulfur	0.015	0.020	0.015	0.015
Copper	0.200	0.200	0.200	0.200
Nickel	0.200	0.200	0.200	0.200
Chromium	0.150	0.150	0.150	0.150
Molybdenum	0.060	0.060	0.060	0.060

Note: Maximum phosphorus must be less than 0.050 % on Grades 180A & 180B

Used by permission from SAE

In welding high strength steels it is important to consider several factors usually not considered in welding lower strength steels: for example, welding process, welding parameters and material combinations. Integration of these types of considerations can result in a successful system of welding for HSS. Various welding methods (arc welding, resistance welding, laser welding and high frequency welding) all have unique advantages in welding specific sheet steel combinations. Considerations for production rate, heat input, weld metal dilution, weld location access, etc., may make one system more weldable than another system. For instance, a HSS that is problematic for spot welding may not exhibit the same difficulty in arc or high frequency welding. In fact, a low heat input resistance seam welding method has been successfully employed for commercial production of bumper beams with a 1300M grade. In general, caution should be exercised in spot welding an HSS to itself because of possible weld metal interfacial fracture tendencies, but even a problematic HSS can be spot welded to a low carbon mild steel.

The resistance spot weldability requirements for low strength steels evaluate the operational robustness of the candidate steel. This often embodies measurements of current range and electrode wear (for galvanized coatings). The resistance spot weldability requirements for HSS may be similar to those of low strength steels. End use requirements will determine required spot weld performance. These requirements may limit the current range and/or electrode life based on individual application weld quality specifications. For instance, fast quenching of the weld may damage the weld metal integrity causing interfacial fracture, or excessive weld heat input may cause metallurgical changes that soften the heat affected zone. Both of these conditions could result in a loss of joint strength. Incorporation of appropriate weld and temper cycles or modification of weld chemistry through selective dilution of the joint can lead to acceptable weld strength and thus ensure the retention of advantages to using HSS for weight reduction in automotive components.

The resistance spot weld behavior for uncoated and coated sheet steels having a minimum yield strength up to 420 MPa, as defined by this Recommended Practice, shall be determined by the

test procedure defined in Weld Quality Test Method Manual, published by the Resistance Welding Task Force, Auto/Steel Partnership ; and the American Welding Society, Recommended Practices for Test Methods for Evaluating the Resistance Spot Welding Behavior of Automotive Sheet Steel Materials, (AWS/ANSI/SAE Standard D8.9-97). Acceptance criteria must be agreed upon between customer and supplier. Note these standard test methods are intended for strength levels up to 420 MPa (60 ksi), and modifications may be required for higher strength levels. Due to unique properties of HSS, selection of the weld process parameters should be determined in consultation with the steel supplier.

BIBLIOGRAPHY FOR SECTION 2.6

Refer to [Section 2.14](#) for a comprehensive bibliography for [Section 2.1](#) to [2.13](#).

2.7 TOLERANCES FOR HOT AND COLD ROLLED SHEET STEELS

The current standard for sheet steel thickness and tolerances are detailed in SAE J1058.

2.8 COATED STEEL SHEETS

The need in the automotive industry to improve corrosion resistance has brought about an increased use of metallic coated steel sheets in place of the cold rolled (uncoated) sheets formerly used. Metallic coated includes hot dipped galvanized and electrolytically coated sheets. Preprimed and prepainted sheets are also available, and can be obtained either with or without the metallic coating on the underlying steel substrate. Block diagrams for typical finishing and coating flowlines are shown in [Figure 2.8-1](#).

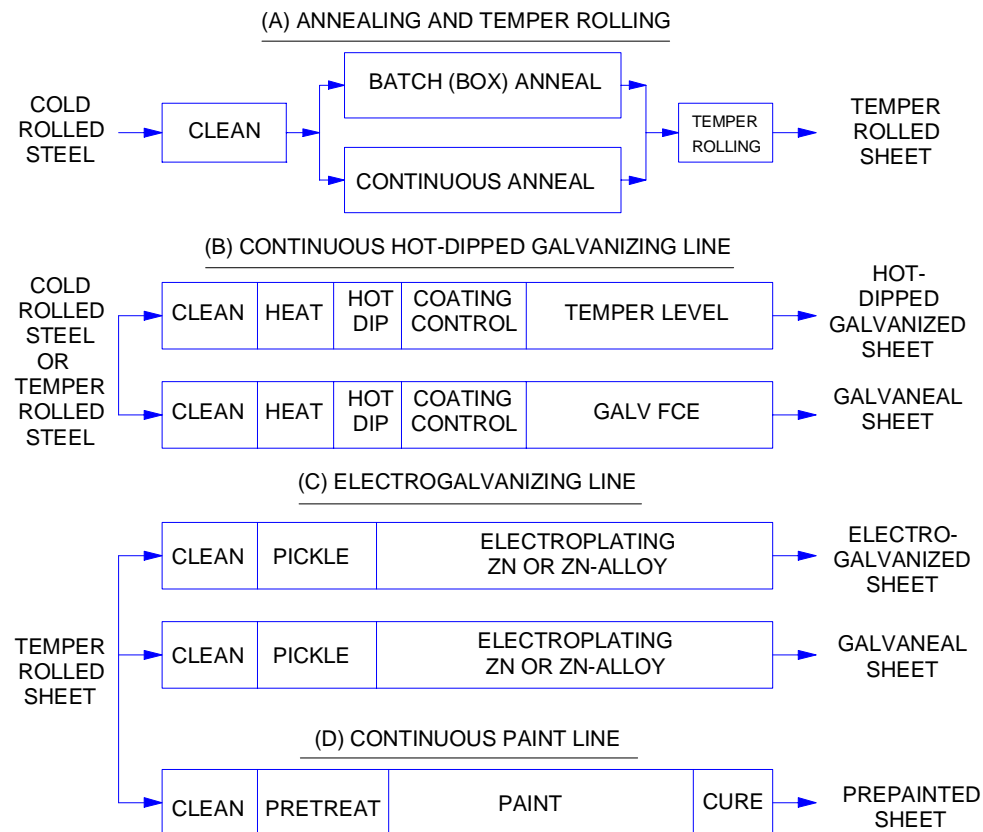


Figure 2.8-1 Typical finishing and coating flowlines

2.8.1 HOT DIPPED METALLIC COATED SHEETS

Hot dipped coating lines are used to produce galvanized coatings, galvannealed coatings, aluminum coatings, aluminum-zinc alloy coatings, and terne (alloys of 12% to 25% tin, balance lead) coatings. Terne alloys are environmentally unacceptable to the automotive industry. The galvanized products are in greatest demand for automotive applications. Variations include two side coated, differentially coated, and one side coated products in a variety of coating masses (thicknesses), finishes, and zinc-iron alloy combinations. Process temperatures differ significantly for the various coatings, and the higher temperatures encountered in some operations can significantly alter the mechanical properties for these materials compared with cold rolled or electrogalvanized sheet. Advanced steel making and processing techniques have been developed to minimize these differences in mechanical properties.

2.8.2 ELECTROLYTIC METALLIC COATED SHEETS

Electrolytic coated sheets are mainly used for body panels, trim, and hardware applications. The electrolytic coating process does not significantly alter the mechanical properties of the cold rolled sheet; it has the least effect of any of the normally used coating processes on the mechanical properties of the steel sheet.

2.8.3 PREPRIMED STEELS

Improved methods of handling and processing sheet steel have generated interest in the use of preprimed and prepainted steels. The use of two-sided preprimed steel has been investigated for the purpose of eliminating in-plant priming operations. A trial run of front fenders was performed to determine the feasibility of fabrication, and a body assembly plant was studied to determine the effects on manufacturing operations. The potential advantages include reductions in:

1. Floor space
2. Capital equipment
3. Preparation for paint
4. Labor cost

The potential disadvantages include problems with:

1. Stamping scrap mix
2. Contamination of scrap
3. Corrosion resistance at cut edges
4. Spot welding

In the trial stamping run, the coating withstood the bending and stretching associated with the forming operations with no loss of integrity. It was therefore concluded that body panels can be formed from preprimed sheet in existing metal forming presses using existing dies. Some material handling equipment will require modification to prevent damage to the coating. Shipping costs will be increased somewhat because it will be necessary to separate the stampings to prevent damage to the coating, and the number of stampings per truck load will be reduced. The cost increase will depend to a great extent on the shipping distance.

The body assembly plant study indicated that the preprimed panels can be processed through the assembly plant with only minor alterations in some material handling operations. Some assembly operations must also be revised. Preprimed steel is not compatible with welding, but appears to be fully compatible with fastening operations utilizing mechanical fasteners, deformation of the parent metal, and adhesive bonding.

2.8.4 PREPAINTED STEELS

A similar trial run of hood outer panels was performed using fully topcoated prepainted steel. Various topcoat colors matching those of the assembly plant paint shop and specially formulated to withstand the metal forming operations were applied to the steel surface via the conventional paint lines. Potential advantages and disadvantages were categorically the same as for preprimed steel, but greater in magnitude.

The coatings withstood the forming operations with no loss of integrity. It was therefore concluded that body panels of similar configuration can be formed from fully topcoated prepainted sheet in existing metal forming presses using existing dies. Other conclusions, regarding processing, shipping, and assembly operations, were essentially the same as for preprimed steel. Paint suppliers have expressed confidence that they can supply paint formulations to meet in-plant color requirements when market demand justifies the effort.

2.8.5 EFFECTS ON FORMABILITY

Two related material factors influence the formability of coated sheets: the substrate and the coating. The characteristics of the coating, although less important to the forming process than those of the substrate, can have significant effects on the forming process because they can affect metal flow over tool and die surfaces.

The following guidelines can be helpful in designing parts using coated steel sheet.

1. The formability of most hot dipped galvanized and galvanneal sheet grades is slightly lower than the same steel produced in the uncoated condition.
2. Relative to other hot dipped galvanized sheets, ultra low carbon stabilized steel sheets exhibit very good substrate properties after hot dipped galvanizing.
3. The electrogalvanizing process does not significantly affect the mechanical properties of the substrate.
4. Direct contact with steel suppliers in the application of galvanized steels to forming is recommended because of the diversity of galvanized steels and the knowledge each supplier has about his own products.
5. Difficulty with forming coated sheets can be minimized by designing parts with lower forming severity.
6. Where possible, larger die radii are preferred for the forming of galvanized sheet.
7. Where possible, stretch forming is preferred to draw forming for galvanized sheet.
8. Simple substitution of electrogalvanized sheet for uncoated sheet may require changes in binder pressure.
9. Careful selection of lubricants is particularly important for galvanized steel sheets, and previous experience with uncoated sheet may not be applicable.

BIBLIOGRAPHY FOR SECTION 2.8

Refer to [Section 2.14](#) for a comprehensive bibliography for [Section 2.1](#) to [2.13](#).

2.9 LAMINATED VIBRATION DAMPING STEELS (LVDS)

2.9.1 INTRODUCTION

The term “laminated steel” generally applies to products consisting of two layers of steel bonded to a plastic core. In this discussion, the term “laminated vibration damping steels” (LVDS) refers to a product consisting of steel outer skins bonded together by a 0.025 mm (0.001”) thick viscoelastic material. The total thickness of available product currently ranges from 0.8 to 3.0 mm (0.032 to 0.120”). Caution should be exercised in the designing with laminated steels, because laminated steel panels of same thickness possess lower section modulus than those with solid steel panels.

When a component made from LVDS is subjected to structure-borne excitation, the amplitudes of resonant vibrations are much lower than for a similar component made from conventional sheet steel. The amplitude reduction normally leads to less radiation of airborne noise. Extensive laboratory and vehicle tests have quantified the performance characteristics of LVDS for vehicle noise, vibration and harshness (NVH). Studies have shown that LVDS can benefit vehicle level performance not only for structure-borne noise, but also for the higher frequency ranges that cause speech interference inside the passenger compartment.

The viscoelastic materials used in LVDS are currently formulated to optimize damping performance at 27C (80F), 54C (130F), 77C (170F) and 99C (210F). This latitude has been helpful in optimizing structural damping in various stamped sheet steel body and chassis components including oil pans, valve covers, engine accessory drive covers, transmission pans, heat shields and sheet steel body members.

2.9.2 MECHANICAL PROPERTIES

The mechanical properties of LVDS (yield strength, ultimate strength, % elongation, strain hardening, etc.) are totally determined by the properties of the steel. These and the forming characteristics of LVDS allow vehicle programs the flexibility of either adding it into the vehicle to improve NVH performance, or designing it into the vehicle to optimize the NVH system performance.

2.9.3 FORMING CHARACTERISTICS

Formability of LVDS is totally determined by the draw quality of the steel. They can therefore be processed using tools designed for standard metal fabricating operations such as slitting, roll forming, brake forming, stamping, drawing and punching. It is suggested that hold down or clamp pressures be increased, tighter die clearances be utilized and radii kept as generous as possible. In some instances the use of a pre-applied dry lube can greatly enhance formability. When holes other than pilot are to be punched, expanding the die progression to reduce individual drawing stages, making the center of the material first during drawing stages, and punching holes last helps to prevent misalignment of hole centers on the skins.

2.9.4 POST-FORMING PROCESSING AND TREATING

LVDS can survive paint bake ovens, E-Coat cycles, vapor degreasing, standard cleaning and treating operations, etc. The following treatments typically have no effect on the physical properties:

- Heat treatment at 232C (450F) for 40 minutes
- Oil soak at 150C (300F) for 1 hour
- Environmental cycling from -31C (-25F) to 107C (225F) for 5 cycles
- ASTM-D-117-64 salt spray for 250 hours
- ASTM-D-2247-68 humidity cabinet for 250 hours
- Exposure to forming lubricants
- Heat-stability testing from 38C (100F) to 205C (400F) in 14C (25F) increments.

2.9.5 FASTENING SYSTEMS

The LVDS viscoelastic core is thin and weldable. Therefore the product can be spot welded, projection welded, MIG welded and seam welded without shunting. Welding parameters are similar to those for solid metal substrates.

Adhesive bonding and lock seaming have also been performed successfully. LVDS can be used in multiple configurations with other sealers and adhesives.

Bolted joints that sandwich the material between the bolt head and nut may encounter torque retention problems because of the potential for relaxation in the 0.04 mm (0.001") thick viscoelastic layer. Steps to reduce the torque loss are as follows:

- During stamping, coin the area to be torqued.
- Automatic torque equipment should allow for torque/re-torque.
- After final assembly, re-torque.

2.10 STAINLESS STEELS

Stainless steels combine good formability with excellent resistance to corrosion and elevated temperatures. Alone or in combination with other materials, low maintenance stainless steels enhance beauty, assure long life, save mass, and provide optimum performance in safety-related components.

The alloy characteristics and typical mechanical properties for a number of different stainless steel grades currently in use are shown in [Table 2.10-1](#) and [Table 2.10-2](#).

Table 2.10-1 Stainless steel alloy characteristics

	Ferritic 51400	Martensitic 51400	Austenitic 30300	Precipitation Hardening (PH)
Heat Treatable	No	Yes	No	Yes
Magnetic	Yes	Yes	No	Yes
Characteristic Microstructure	Ferrite	Martensite	Austenite	Martensite (as hardened)
Formability	B	D	A	C
Strength	D	A	C	B
Corrosion Resistance	C	D	A	B
Oxidation Resistance	A	D	B	D
Weldability	B	D	A	D

A = Highest, D = Lowest

Table 2.10-2 Nominal mechanical properties of stainless steels

SAE Grade	UNS Grade	Condition**	Yield Strength MPa (ksi)	Tensile Strength MPa (ksi)	Percent Elongation in 50mm (2 in.)	Hardness RB
30201	S20100	A	260 (38)	655 (95)	40	90
30301	S30100*	A	205 (30)	515 (75)	40	92
		1/4 H	515 (75)	860 (125)	---	---
		1/2 H	760 (110)	1035 (150)	---	---
		3/4 H	930 (135)	1205 (175)	---	---
		FH	965 (140)	1275 (185)	9	41C
30304	S30400	A	205 (30)	515 (75)	40	92
30304L	S30403	A	170 (25)	485 (70)	40	88
30316	S31600	A	205 (30)	515 (75)	40	95
41409	S40900	A	205 (30)	380 (55)	22	80
51410	S41000	A	275 (40)	485 (70)	20	80
51420	S42000	A	370 (54)	605 (88)	28	88
51440B	S44003	FH	425 (62)	740 (107)	18	96
51430	S43000	A	205 (30)	450 (65)	22	88
51439	S43900	A	205 (30)	450 (65)	22	88
	18 Cr-Cb	A	310 (45)	470 (68)	34	80
	17-4 PH	A	100 (145)	1100 (160)	15	28C

* Austenitic stainless steels, 200 and 300 series, can be cold worked to high tensile and yield strengths and yet retain good ductility and toughness. Data for various tempers of Type 30100 are given to illustrate this characteristic. Data on other grades are available from the steel supplier.

** A = Annealed, 1/4 H = 1/4 Hard, 1/2 H = 1/2 Hard, 3/4 H = 3/4 Hard, FH = Full Hard

2.11 COMPARATIVE COST AND MASS

The cost and mass comparison for various types of steel must ultimately be made by evaluating alternative designs for a specific component. However, some general guidelines can be applied to determine the potential advantages of high strength steel. For example, in those cases where the yield strength can be fully utilized, the required thickness can be reduced by using appropriate formulas for tensile, flexural, torsional, or combined stress.

In many cases it is not possible to take full advantage of the high yield strength materials. The geometry of the component and the type of applied load may dictate a failure mode that is governed to some degree by stiffness. In some cases the forming and fabricating constraints must be evaluated against the material properties to determine whether the desired design can be produced, or how closely it can be approximated.

Where stiffness governs the design, there is a tendency to conclude that high strength steels will offer no advantage because all steels have the same modulus of elasticity. It may, however, be advantageous to modify the geometry of the component somewhat to increase the stiffness. For example, deep thin walled sections may tend to fail by buckling, either locally (such as in the web or flange of a section) or across the entire section (such as a long column in compression). In the latter case, a deeper section may be beneficial. Local buckling can be avoided or delayed by designing one or more stiffeners into critical areas to raise the stress level before buckling occurs and allow the design to take advantage of a higher yield strength material. Section 3.1 includes quantified design data for carbon steel that will assist the designer in identifying areas of a thin walled member that are subject to local buckling, and where increasing the local stiffness is beneficial.

Designs using stainless steels are currently governed by the ASCE specifications¹ and are too extensive to be covered in this manual. However, previous comments concerning designs with higher strength steels are also appropriate for stainless steels, except that consideration should be given to the anisotropy and low proportional limit.

Many factors affect overall component cost such as corrosion resistance, component life, and subsequent processing operations. Material costs, which can vary widely, are only one factor in the overall cost. A more expensive material that meets performance requirements and requires less processing may generate lower overall cost than a less expensive material. General cost guidelines can be offered to assist the designer in these tradeoffs that typify the initial stages of design.

[Table 2.11-1](#) gives approximate comparative cost data for twelve types of steel that can be used to advantage by the automotive designer.

Table 2.11-1 Approximate relative costs of various sheet steels
(Based on popular widths and thicknesses)

Type	Approximate Relative Cost
Hot Rolled Carbon	0.80
Cold Rolled Carbon	1.00
Bake Hardenable	1.10
Hot Dipped Galvanized	1.12
Aluminized	1.21
Electrogalvanized	1.35
HSLA	1.15
Dual Phase	1.40
Martensitic	1.50
Aluminum Sheet Type 5052	4.8
Austenitic Stainless Type 304	5.7*
Ferritic Stainless Type 409	2.6*
Martensitic Stainless Type 410	2.8*
PH Stainless 17-4	9.0*

* Stainless steel costs are strongly influenced by cost of expensive alloys such as chromium and nickel, which can cause more price variability than with carbon steels.

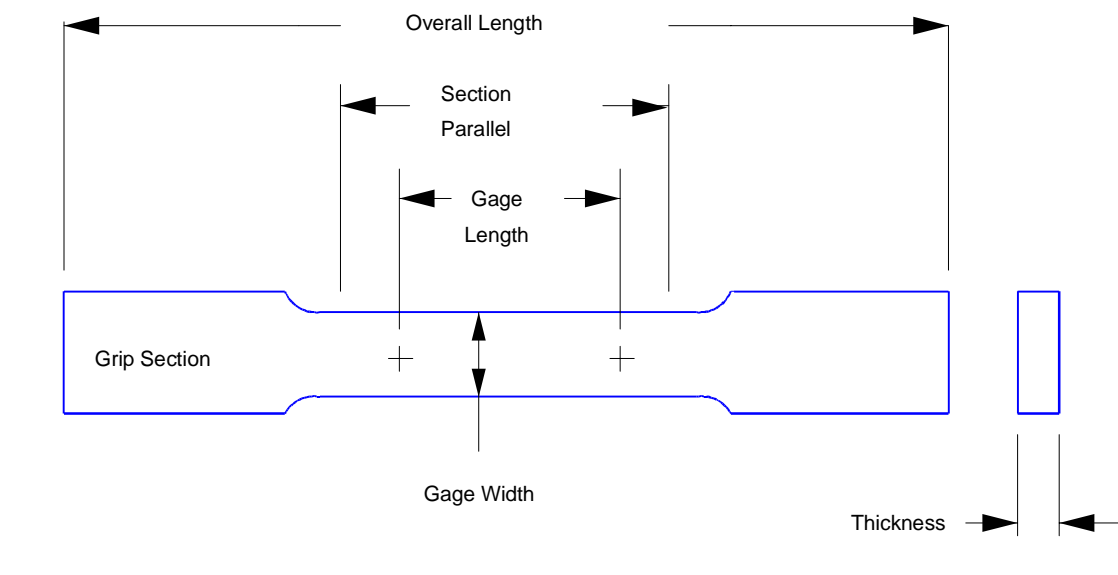
Although sheet steel products are sold on the basis of mass, there are specific points at which there are step increases in the cost per unit of mass. These points relate to thickness, width of original blank, degree of formability required, strength level required for structural function, and the type and amount of corrosion protection required. The step points vary among steel suppliers and cannot be easily identified. However, they are generally based on productivity. For example:

1. More production time per pound is required to produce thinner gauges.
2. When widths are narrow, less steel is processed through a production line during a given time.
3. Greater degrees of formability or higher strength levels require more expensive grades of steel.
4. Any increase in alloy content results in a higher cost product.
5. Greater degrees of corrosion protection also increase the cost of steel.

2.12 MECHANICAL TESTING

2.12.1 INTRODUCTION

Mechanical properties are specified for certain automotive applications. The more common properties are those obtained in a tension test or hardness test made on a representative sample of the sheet steel. The standard sheet specimen used in the tension test is shown in [Figure 2.12-1](#).



Rectangular Tension Test Specimen for Sheet (1/2 Inch Wide Test)

Dimension	inch	mm
Overall Length	8	200
Gage Length	2.000 ± 0.005	50 ± 0.10
Gage Width	0.500 ± 0.010	12.5 ± 0.25
Thickness	Thickness of Material	

Figure 2.12-1 Standard sheet tension test specimen

ASTM A370 describes the standard tension test. In this test, an increasing axial load is continuously applied by a tension testing machine to the specimen until the specimen fractures. During the test the elongation of the gage length on the specimen is continually measured. The relationship between the applied load and corresponding elongation is plotted as a load versus elongation diagram. The applied load divided by the original cross sectional area of the specimen is the engineering stress. The change in length of the gage length divided by the original gage length, expressed as a percent, is the engineering strain or percent elongation.

Stress strain curves generated from the standard tension test are illustrated in [Figure 2.12-2](#) below. Yield strength may be depicted and described in two ways, depending on the stress-strain characteristics of the steel as it begins to yield:

- The minimum stress in the yield point elongation region (YPE) for materials exhibiting discontinuous yielding.
- The stress at 0.2 percent strain offset, for materials exhibiting a continuous yielding stress strain curve.

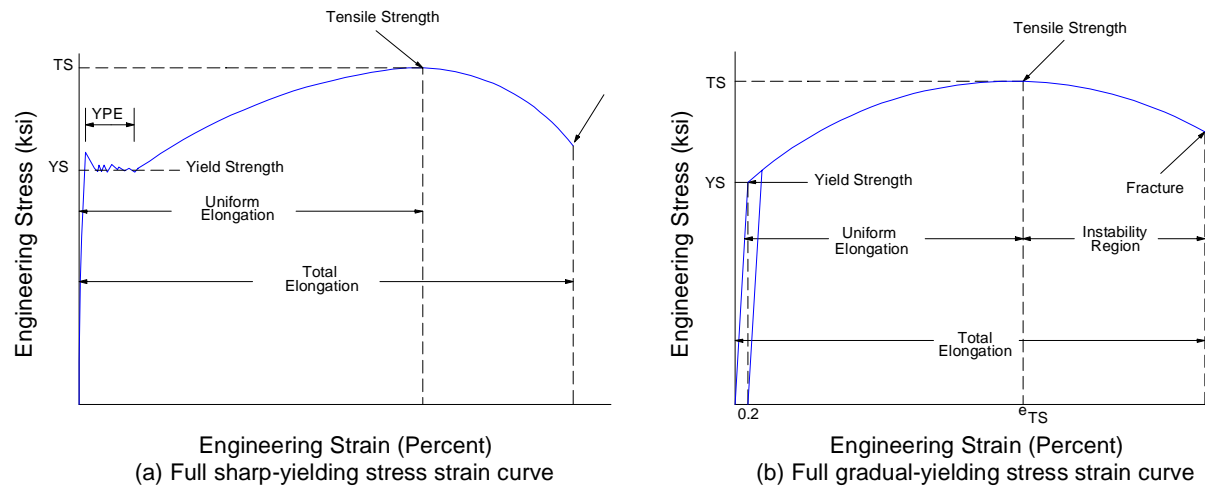


Figure 2.12-2 Complete stress-strain curves showing continuous and discontinuous yielding.

2.12.2 METALLURGICAL TERMS

Modulus Of Elasticity

The modulus of elasticity is the slope of the stress versus strain diagram in the initial linear elastic portion of the diagram . It is a measure of the stiffness of the metal. The value for steel is approximately 200,000 MPa (29,500 ksi). The value does not change appreciably with changes in composition, steel manufacturing processes, or fabrication operations.

Yield Strength

The stress at which the metal yields or becomes permanently deformed is an important design parameter. This stress is the elastic limit below which no permanent shape changes will occur. The elastic limit is approximated by the yield strength of the material, and the strain that occurs before the elastic limit is reached is called the elastic strain. The yield strength is defined in three ways, depending on the stress-strain characteristics of the steel as it begins to yield. The procedures in SAE J416, ASTM E8, and ASTM A370 describe the testing for tensile properties. Stress-strain curves showing continuous and discontinuous yielding are shown in [Figure 2.12-2](#).

Tensile Strength

Tensile strength is the maximum load sustained by the specimen in the tension test, divided by the original cross sectional area. The tension test described in ASTM A370 is explained in an earlier portion of this report. Also see [Figure 2.12-2](#).

Uniform Elongation

The strain to maximum load in the tension test is called the uniform elongation. It is the limit of plastic strain that is uniformly distributed over the strained area. Following the uniform elongation, deformation is concentrated in one region of the specimen, creating a localized reduction in cross section referred to as necking.

Hardness

Hardness is the resistance of metal to indentation. There is no absolute scale for hardness. Each of the different hardness tests has its own scale of arbitrarily defined hardness. The most common test used to measure the hardness of steel sheet is the Rockwell hardness test. The Rockwell hardness number is derived from the net increase in depth of impression as the load on an indenter is increased from a fixed initial load and then returned to the initial load.

Elongation

The Elongation is a direct measure of ductility and represents an important consideration in evaluating formability. Elongation is usually reported as a percent increase in length within the 50 mm gage length of the tension test specimen.

Work Hardening Exponent, n value

The work hardening exponent, n , is related to the steepness of the stress-strain curve in the plastic deformation region; it also correlates with the uniform elongation of the steel and the ratio of the tensile strength to yield strength. Determination of the n value from load elongation curves is described in ASTM E 646. Most important, the strain hardening exponent correlates to the ability of the metal to be stretch formed. A higher n value indicates a capability for the metal to strain harden in areas that have been cold worked by deformation processes. This capacity to transfer strain contributes to a better response to biaxial stretch deformation modes.

Plastic Strain Ratio, r Value

The plastic strain ratio r is a measure of the resistance to thinning as metal is drawn, controlled by the crystallographic orientation of its structure, which is dependent on the chemical composition and processing of the material. The procedure for measuring r value can be found in ASTM E517. For anisotropic materials, the r value changes with test direction, and for convenience is measured in directions longitudinal (0 deg.), diagonal (45 deg.), and transverse (90 deg). Higher r values indicate a greater resistance to thinning, and are directly related to an increased ability of the sheet to be formed by deep drawing.

2.13 INFLUENCE OF STRAIN RATE ON YIELD STRENGTH

It is well known that the mechanical properties of sheet steels are affected by strain rate. The dynamic yield strength is used in [Section 3.3.4](#) for predicting dent resistance, and is also necessary for crash energy management calculations.

Five selected sheet steels (25AK, 35XF, 50SK, 50XF and 100XF) were tested under tension and compression at various strain rates from 0.0001 to 1.0 per second in a research program conducted at the University of Missouri-Rolla sponsored by the American Iron and Steel Institute ([References 1,2,3,4,5](#)). Complete engineering stress-strain curves are shown in [Figure 2.13-1](#) for a gradual yielding steel with a nominal yield strength of 35 ksi tested in longitudinal tension at strain rates of 0.0001, 0.01 and 1.0 in./in./sec.

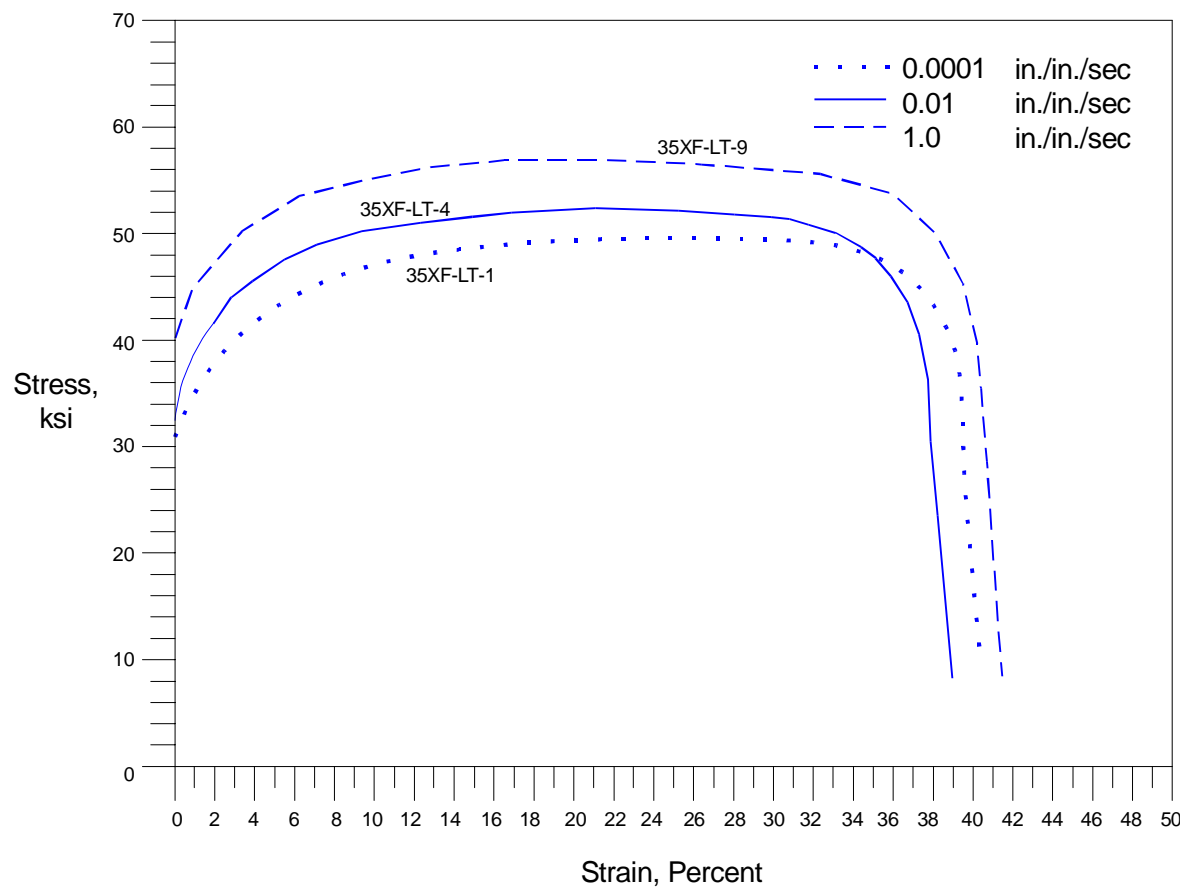


Figure 2.13-1 Tensile stress-strain curves for 35XF-LT steel under different strain rates, virgin materials

[Figure 2.13-2](#) shows tensile stress-strain curves for a steel with a yield plateau and nominal yield strength of 50 ksi. Many other stress-strain curves are given in the reports cited. Based on 250 coupon tests and some extrapolation, the following generalized equations were developed to predict the tensile and compressive yield strengths for strain rates ranging from 0.0001 to 100 per second.

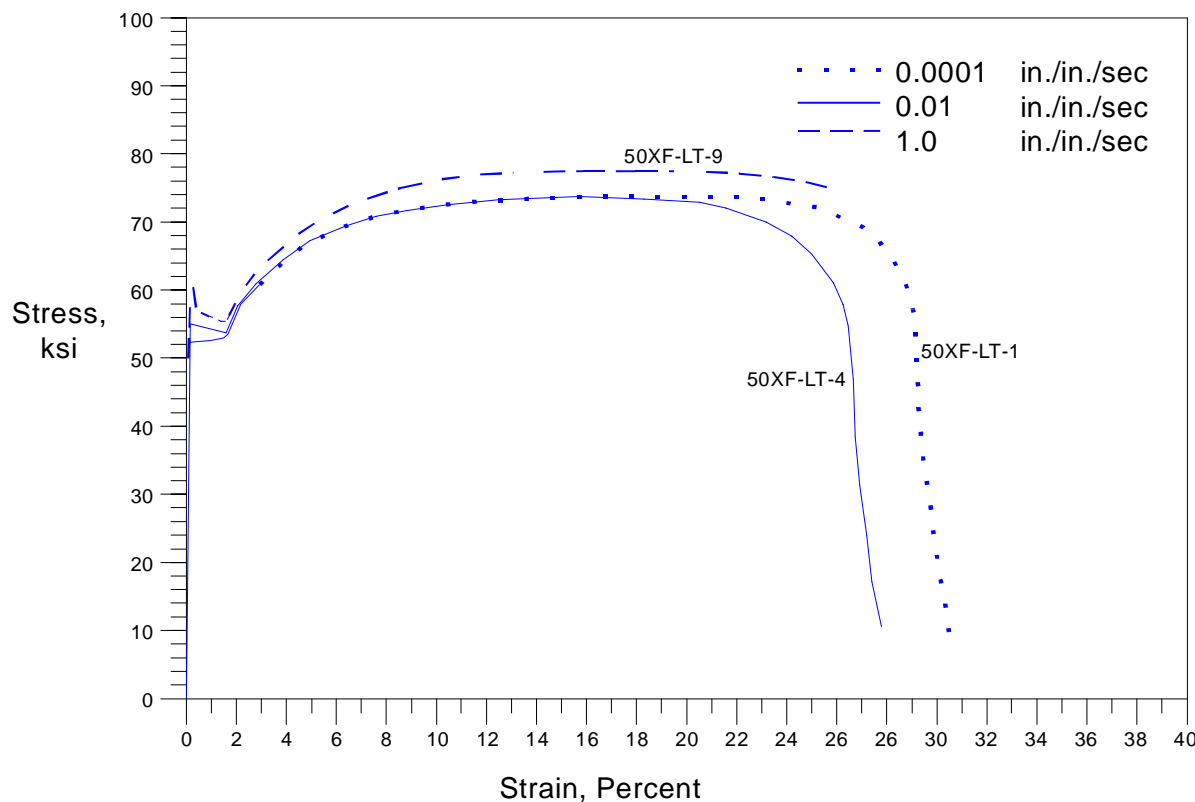


Figure 2.13-2 Tensile stress-strain curves for 50XF-LT steel under different strain rates, virgin materials

$$(F_y)_{\text{pred}} = \left(A e^{(B/F_y)} + 1 \right) (F_y)_s$$

Equation 2.13-1



where

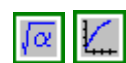
$$A = a_1 + b_1 \log(\dot{\epsilon}) + c_1 \log(\dot{\epsilon})^2$$

Equation 2.13-2



$$B = a_2 + b_2 \log(\dot{\epsilon}) + c_2 \log(\dot{\epsilon})^2$$

Equation 2.13-3



for tensile yield stress:

$$\begin{array}{ll} a_{1t} = 0.023 & a_{2t} = 77.7 \\ b_{1t} = 0.009 & b_{2t} = 0.069 \\ c_{1t} = 0.001 & c_{2t} = -0.595 \end{array}$$

for compressive yield stress:

$$\begin{array}{ll} a_{1c} = 0.033 & a_{2c} = 64.9 \\ b_{1c} = 0.004 & b_{2c} = 11.1 \\ c_{1c} = 0.000 & c_{2c} = -1.87 \end{array}$$

where $(F_y)_{\text{pred}}$ = predicted dynamic yield strength

$(F_y)_s$ = static yield strength

$\dot{\epsilon}$ = strain rate

[Figure 2.13-3](#) and [Figure 2.13-4](#) are graphic representations of the previous equations.

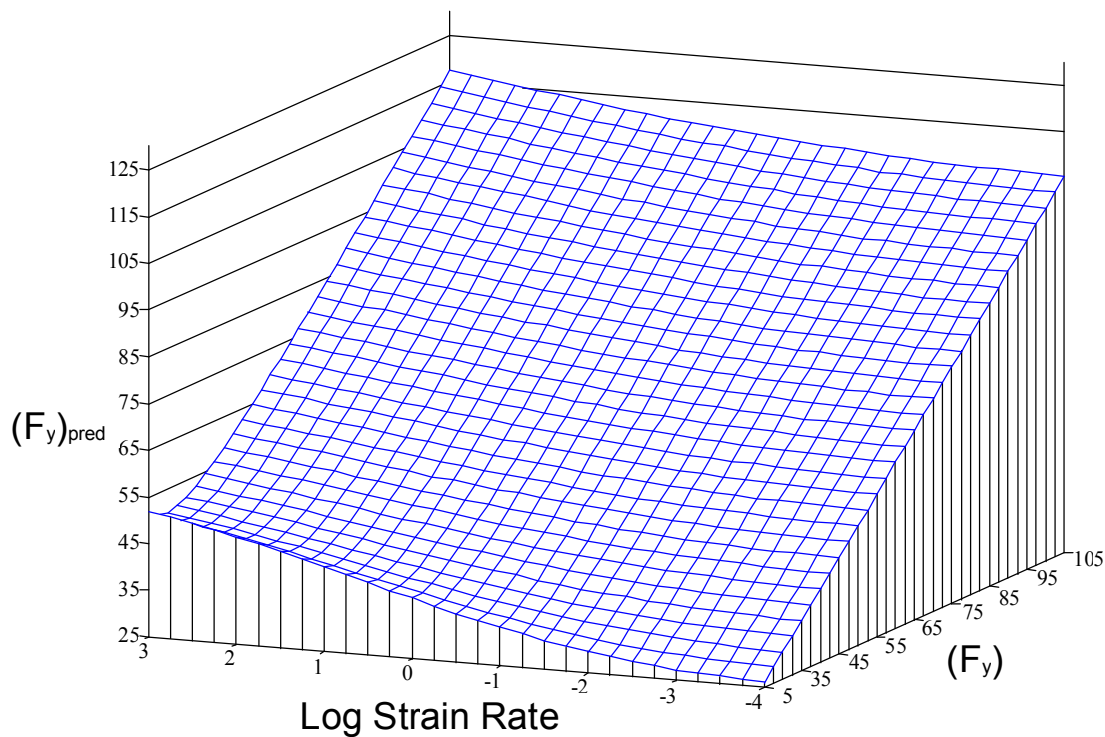


Figure 2.13-3 Generalized prediction of dynamic tensile yield stress

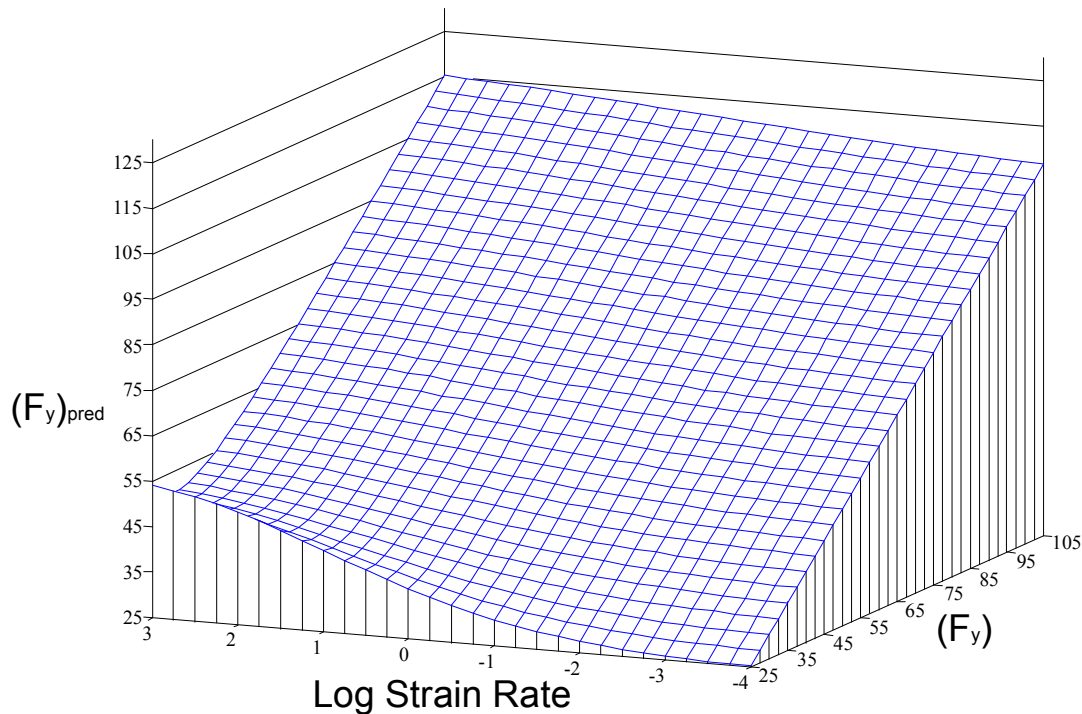


Figure 2.13-4 Generalized prediction of dynamic compressive yield stress

More recently, the Auto/Steel Partnership sponsored a strain rate characterization project at Los Alamos National Laboratory using strain rates up to 65000/second and obtaining the true stress-strain curves. Example of such curves for a DQSK and an HSLA material are shown [Figure 2.13-5](#). Many other curves are given in Reference [6](#).

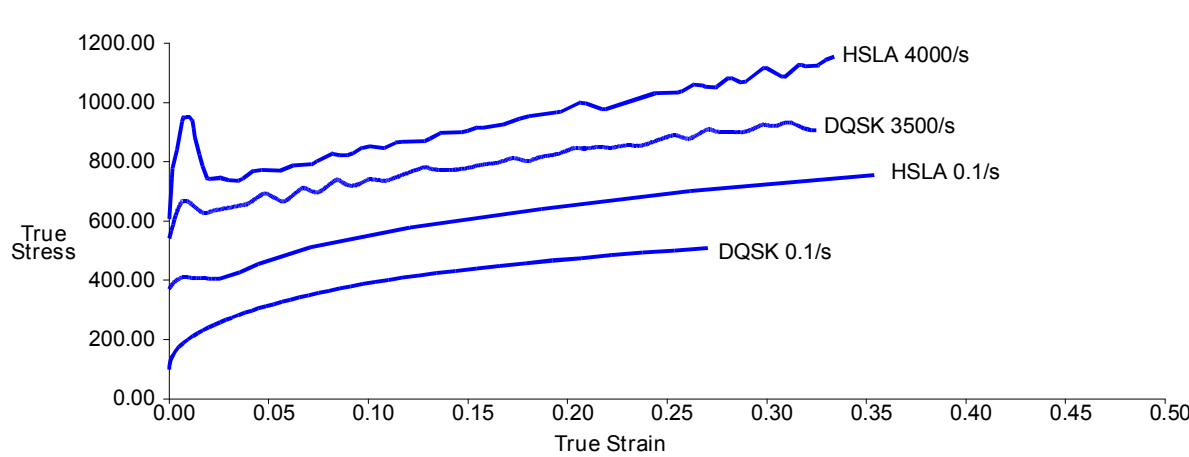


Figure 2.13-5 True Stress/Strain Curves for 0.05%C Mild Steel and 50 ksi HSLA Steel at 25°C

REFERENCES FOR SECTION 2.13

1. Kassar, M. and Yu, W.W., Design of Automotive Structural Components Using High Strength Sheet Steels: Effect of Strain Rate on Material Properties of Sheet Steels and Structural Strengths of Cold-Formed Steel Members, Fourteenth Progress Report, Civil Engineering Study 90-2, University of Missouri-Rolla, May 1990.
2. Kassar, M. and Yu, W.W., Effect of Strain Rate on Material Properties of Sheet Steels, ASCE, Journal of Structural Engineering, Vol. 118, No. 11, November, 1992.
3. Pan, C.L., and Yu, W.W. Design of Automotive structural Components Using High Strength Sheet Steels: Influence of Strain Rate on the Mechanical Properties of sheet Steels and Structural Performance of Cold-Formed Steel Members, Eighteenth Progress Report, Civil Engineering Study 92-3, University of Missouri-Rolla, December, 1992.
4. Pan, C.L., and Yu, W.W., Influence of Strain Rate on the Structural Strength of Cold-Formed Steel Automotive Components, Proceedings of Automotive Body Materials, International Body Engineering Conference, (M. Nassim Uddin, Ed.), September, 1993.
5. Pan, C.L., Yu, W.W., Schell, B. and Sheh, M., Effects of Strain Rate on the Structural Strength and Crushing Behavior of Hybrid Stub Columns, Proceedings of Automotive Body Design & Engineering, International Body Engineering Conference, (M. Nassim Uddin, Ed.), September, 1994.
6. Cady, C.M., Chen, S. R., Gray III, G.T., Lopez, M.F., Carpenter II, R.W., and Korzekwa, D., Dynamic Material Testing and Constitutive Modeling of Structural Sheet Steel for Automotive Applications, Final Progress Report, Los Alamos National Laboratory, August 1996.

2.14 STRENGTH INCREASE FROM COLD WORK OF FORMING

When flat steel is cold formed into any shape its mechanical properties are modified and its base thickness may be changed. The effect of cold forming on the mechanical properties of a particular steel section is shown in [Figure 2.14-1](#).

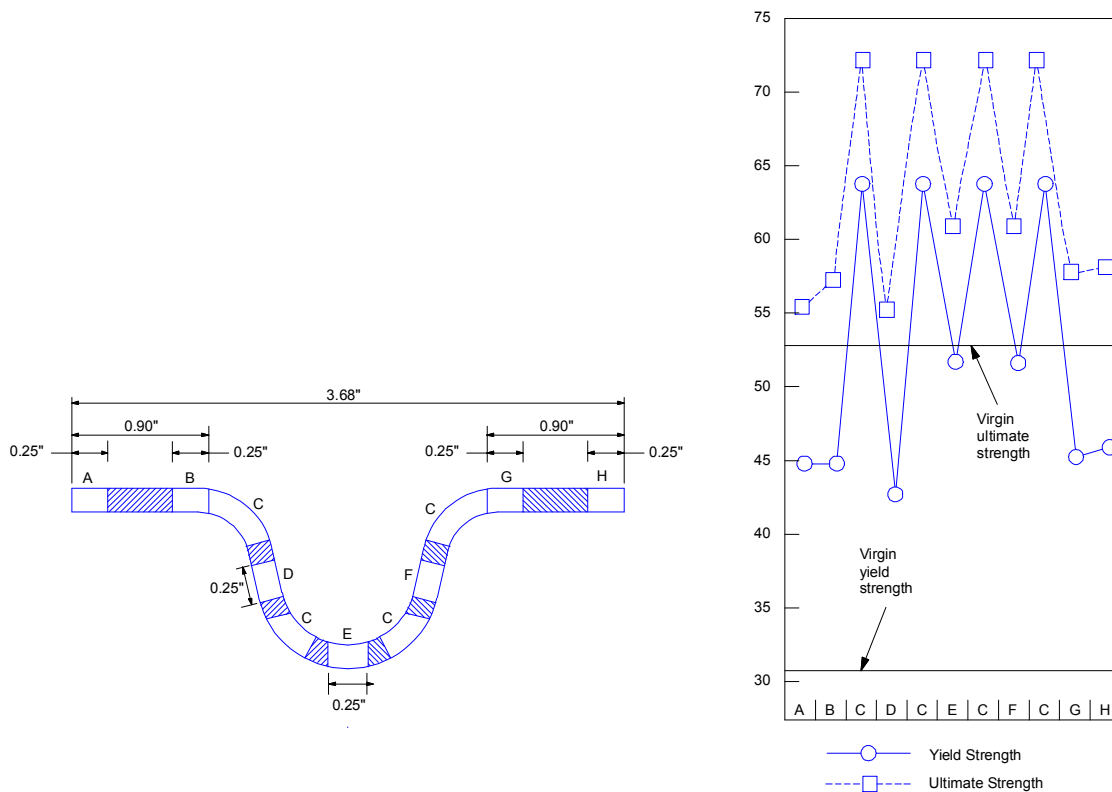


Figure 2.14-1 Effect of cold work on mechanical properties in a cold-formed steel section¹

Sufficient research has been conducted by AISI² to permit a good estimate of the increased yield strength due to simple bending of a flat sheet. Corner bends have a higher yield strength and lower ductility than the flat portion of a cross section, and a slightly reduced thickness. The additional yield strength is primarily a function of the corner inside-bend-radius-to-thickness ratio, R/t , of the bend and F_u/F_y , the ratio of tensile-to-yield strength of the as-received material.

If the extra capacity resulting from the increased yield strength is ignored during preliminary design phases, the analysis will underestimate the component strength, and in that sense be conservative. However, in seeking minimum weight designs it may be appropriate to take advantage of the increased strength due to cold forming. Also, it may be advisable to avoid underestimating the strength of a component in crash energy management situations where progressive failure may be a design objective.

The AISI Specification has a procedure that can be used to evaluate numerically the increased yield strength due to cold work of forming, using the variables R/t and F_u/F_y . Based on this approach, the increased yield strength from cold bending can be determined by substituting F_{ya} for F_y , where F_{ya} is the average yield strength. The increased strength is limited to certain situations; the limitations and methods for determining F_{ya} are outlined below.

(a) For axially loaded compression members and flexural members whose proportions are such that the flat width of each of the component elements of the section remains fully effective, the design yield strength, F_{ya} , of the steel shall be determined on the basis of one of the following methods:

- (1) full section tensile tests,
- (2) stub column tests, or
- (3) computed as follows:

$$F_{ya} = CF_{yc} + (1-C)F_{yf}$$

Equation 2.14-1



where:

F_{ya} = average yield strength of the steel in the full section of compression members, or full flange sections of flexural members.

C = for compression members, ratio of the total corner cross-sectional area to the total cross-sectional area of the full section.

= for flexural members, ratio of the total corner cross-sectional area of the controlling flange to the full cross-sectional area of the controlling flange.

F_{yf} = weighted average tensile yield strength of the flat portions established by tests or virgin yield strength if tests are not made.

$F_{yc} = B_c F_{yv}/(R/t)^m$, tensile yield strength of corners. This equation is applicable only when $F_{uv}/F_{yv} \geq 1.2$, $R/t \leq 7$, and the included angle $\leq 120^\circ$.

$$B_c = 3.69 (F_{uv}/F_{yv}) - 0.819 (F_{uv}/F_{yv})^2 - 1.79$$

$$m = 0.192 (F_{uv}/F_{yv}) - 0.068$$

R = inside bend radius

t = base metal thickness, before bending

F_{yv} = tensile yield strength of virgin steel

F_{uv} = ultimate tensile strength of virgin steel

(b) For axially loaded tension members, the yield strength shall be determined by either method (1) or method (3) prescribed in paragraph (a) above.

(c) The effect of any welding on mechanical properties of a member shall be determined on the basis of tests of full section specimens containing within the gage length such welding as is intended for use.

The increased yield strength due to cold forming should not be used when determining the inelastic reserve strength of a member.

A similar approach could be used for other types of cold forming if the distribution and magnitude of yield strengths were known.

REFERENCES FOR SECTION 2.14

1. Karren, K. W. and G. Winter: "Effects of Cold-Straining on Structural Sheet Steels", Journal of the Structural Division, ASCE Proceedings, vol. 93, Feb. 1967
2. American Iron and Steel Institute, Specification for the Design of Cold formed Steel Structural Members, 1996 Edition, Washington, D. C.

2.15 BIBLIOGRAPHY FOR SECTIONS 2.1 TO 2.14

<u>Section</u>	<u>Document</u>
2.5	Uniformity of Automotive Sheet Steel Vol. 1, Vol.2, Material Uniformity Task Force, Auto/Steel Partnership, 2000 Town Center, Southfield, MI, 48075 Uniformity of High Strength Steels Vol. 1, Vol. 2, Material Uniformity Task Force, Auto/Steel Partnership, 2000 Town Center, Southfield, MI, 48075 SAE Specification J2329, Categorization and Properties of Low Carbon Automotive Sheet Steels, Oct 1999, Society of Automotive Engineers, 400 Commonwealth Drive, Warrendale, PA, 15096-0001. SAE Specification J2340, Categorization and Properties of Dent Resistant, High Strength, and Ultra High Strength Automotive Sheet Steels, Oct 1999, Society of Automotive Engineers, 400 Commonwealth Drive, Warrendale, PA, 15096-0001. SAE Specification J1058, Standard Sheet Steel Thickness and Tolerances, Jan 1998, Society of Automotive Engineers, 400 Commonwealth Drive, Warrendale, PA, 15096-0001. Uniformity of Properties on High Strength Automotive Sheet Steels, Vol.1 , Vol.2, Oct 1998, Material Uniformity Task Force, Auto/Steel Partnership, 2000 Town Center, Southfield, MI, 48075.
2.6	Mechanisms of Electrode Wear on Welding Hot Dipped Galvanized Steel, June 1994, Resistance Welding Task Force, Auto/Steel Partnership, 2000 Town Center, Suite 320, Southfield, MI, 48075 Finite Element Modeling of Electrode Wear Mechanisms, May 1995, Resistance Welding Task Force, Auto/Steel Partnership, 2000 Town Center, Ste 320, Southfield, MI, 48075 Weld Quality Test Method Manual, Oct. 1997, Resistance Welding Task Force, Auto/Steel Partnership, 2000 Town Center, Ste 320, Southfield, MI, 48075 Resistance Spot Welding Electrode Wear on Galvannealed Steels, Sept 1997, Resistance Welding Task Force, Auto/Steel Partnership, 2000 Town Center, Ste 320, Southfield, MI, 48075
2.8	Uniformity of Coating Weights and Properties on Automotive Sheet Steels, Vol. 1, Vol. 2, Aug. 1995, Material Uniformity Task Force, Auto/Steel Partnership, 2000 Town Center, Southfield, MI., 48075

3. DESIGN

Section 3 is specific to the design of thin-wall sheet steel members. Sections 3.1 to 3.12 provide information that will guide the body designer to the "best first guess", help interpret the results generated by the computer, and suggest appropriate design modifications to be plugged into the next iteration.

Symbols used in Section 3 are tabulated in Appendix A.

Introduction To Sections 3.1-3.4

Sections 3.1 to 3.4 present information regarding the design of automotive components using sheet steels to meet strength as well as stiffness criteria. Although many of the expressions presented are very detailed, the intent of these sections is to present preliminary design information. The information will help the designer make the correct decisions early in the design process, before incurring the cost of more sophisticated procedures such as finite element analysis.

All numerical expressions are given in nondimensional format or are presented with SI metric as the primary system of units. All strength expressions are presented in terms of their critical or ultimate value with no factor of safety in the expressions.

Only a portion of the information presented is derived from expressions in the current AISI design specifications¹ used by the construction industry. The rest is current and recent research or general reference information that is applicable to the design of sheet steel automotive components. The information is presented with some background relative to its application, but the amount of background is limited to keep the document a manual rather than a textbook.

More detailed information is available on straight members with simple configuration than on curved members and members of complex shapes. However, the information on straight members can provide the necessary background for evaluating more complex configurations.

REFERENCES FOR SECTION 3

1. American Iron and Steel Institute, Specification for the Design of Cold -Formed Steel Structural Members, 1986 Edition with 1989 Addendum, Washington, D.C.

3.1 STRAIGHT LINEAR MEMBERS

This section presents detailed information related to the strength and stiffness of straight members under tensile, compressive, flexural and torsional loads plus various combinations of these loads.

3.1.1 TENSION IN MEMBERS

Cold formed members in tension can be used in many applications up to the point that yielding is reached. At this point only a small fraction of the member's elongation potential has been employed. In addition to the percent elongation, the minimum tensile-to-yield ratio should be known. Most steels designed per the AISI specifications have a tensile-to-yield ratio that meets or exceeds 1.17. The higher strength steels in which this ratio is less than 1.17, and which may have a limited minimum elongation, should be used with caution when subjected to yield stresses. A minimum tensile-to-yield ratio of 1.08 and minimum total elongation of ten percent on two inch gage length (or seven percent on eight inch gage length) is specified¹ for steels used for construction to insure proper structural behavior.

Of special concern for tension design are the tensile limitations that may be imposed by fatigue considerations, as discussed in [Section 3.5](#), and the ductility requirements needed for energy management, as discussed in [Section 3.6](#).

If tensile stress is localized, such as in flexure of members, it is possible to strain members beyond the yield strain and to take advantage of this inelastic straining. Localized yielding can be tolerated at points of stress concentration provided the strain history of the location is known.

Although the virgin yield strength is typically used to evaluate the tensile (or compressive) load capacity of a member, advantage can be taken of the increased yield strength obtained by cold forming. [See Section 2.14](#).

3.1.2 COMPRESSION IN MEMBERS

Cold formed members in compression must be examined for their capacity as influenced by overall instability as is done for other members. The effective slenderness ratio, which is the product of the effective length factor (K) and the member length (L) divided by the radius of gyration, represents the primary variable influencing overall instability.

In addition, local instability must be examined for the flat or mildly curved portions of a member cross section due to the slenderness of these portions or components. In this case the ratio of width to thickness (w/t) is the primary variable. The presence of the corners in a section permits the section to continue to carry load after buckling of the flat elements has occurred.

The basic approach used¹ is first to determine the limiting stress level based on overall instability. Then the effect of local instability is evaluated at this level of stress. This effect is introduced by evaluation of the effective area of the cross section at this stress. If strength is not of prime consideration, the effective areas and other properties such as moment of inertia can be evaluated at the stress level that is deemed most appropriate for the situation.

3.1.2.1 Local Instability of Flat Elements

There are two basic types of flat elements that must be considered: the stiffened or partially stiffened compression element (sce) and the unstiffened compression element (uce). This is illustrated for the lipped channel shown in [Figure 3.1.2.1-1](#).

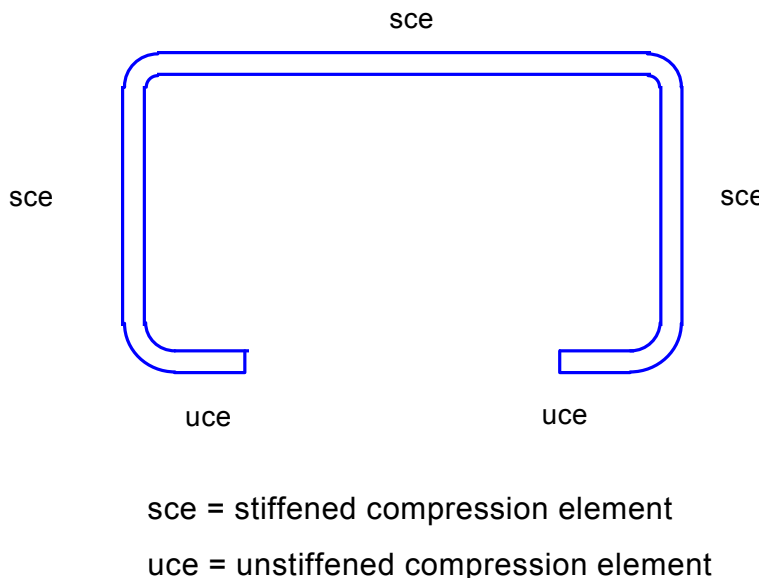


[Figure 3.1.2.1-1](#) Stiffened and unstiffened elements of a compression member

The behavior of these two types of flat elements is similar. However, it has been customary to treat the local instability differently for stiffened and unstiffened compression elements. For stiffened compression elements a portion of the element is ignored to account for post-buckling behavior. For unstiffened elements, the stress limit has been reduced in the past to account for loss of full section capacity². With the 1986 AISI Specification¹, both types of elements are being treated using the effective width approach.

3.1.2.1.1 Fully Stiffened Compression Elements Without Intermediate Stiffeners



A stiffened compression element without intermediate stiffening is a completely flat compression element, of which both edges parallel to the direction of stress are stiffened by a web, flange, or stiffening lip. The stiffening elements must meet certain criteria which will be discussed later. The local buckling behavior is illustrated in [Figure 3.1.2.1-1\(b\)](#).

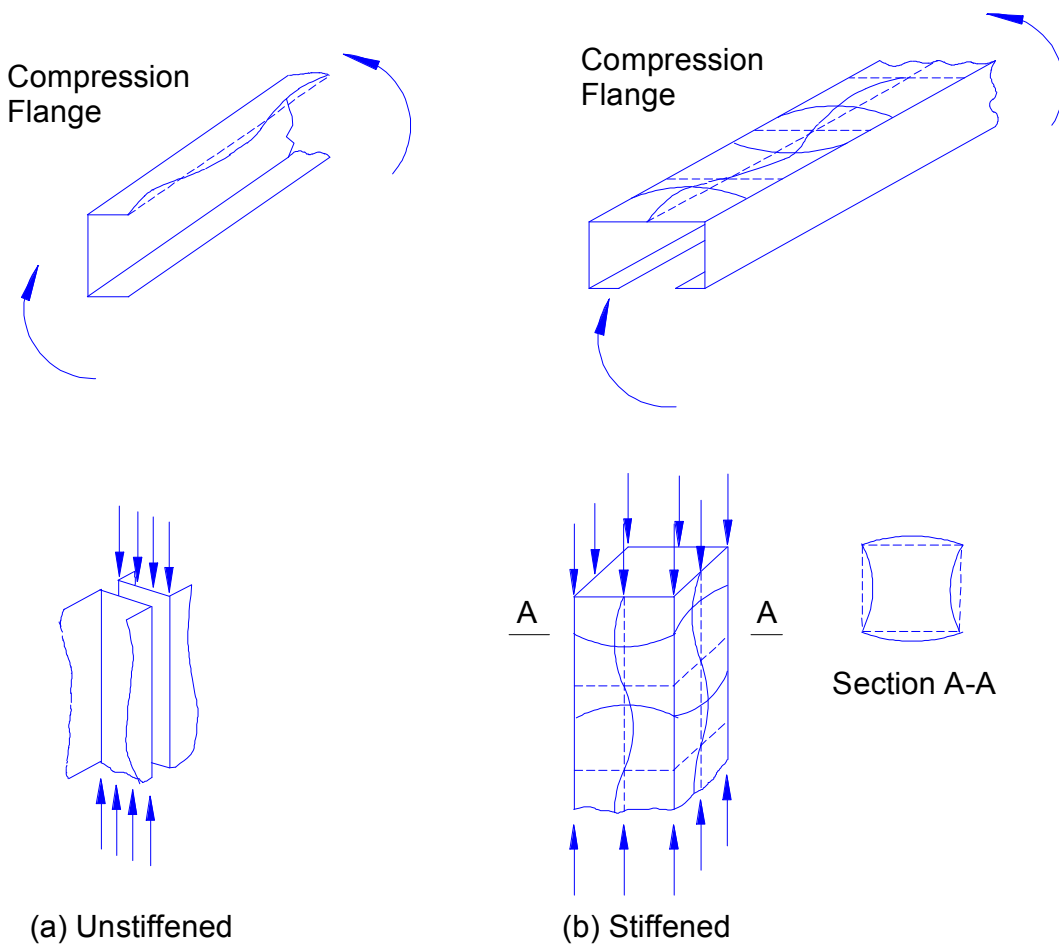


Figure 3.1.2.1.1-1 Local buckling of compression elements

The buckling illustrated occurs only upon achieving a certain stress level in the flat element. The effective width should be determined when the slenderness factor l exceeds a value of 0.673.

The slenderness factor

$$\lambda = 1.052 \left(\frac{w}{t} \right) \frac{\sqrt{f}}{\sqrt{k}}$$

Equation 3.1.2.1.1-1

A row of two icons. The first icon is a square root symbol ($\sqrt{\alpha}$). The second icon is a graph of a parabola opening upwards, representing a square function.

where f = stress in the element

E = modulus of elasticity of the element.

For steel, $E = 200,000 \text{ MPa} (29,500 \text{ ksi})$

k = buckling coefficient for the flat plate

w, t are defined in Figure 3.1.2.1.1-2.

Equation 3.1.2.1.1-1 with $f = F_y$ is valid for materials with yield strengths up to $F_y = 552 \text{ MPa}$ (80 ksi). For stiffened compression elements with a higher yield strength, recent research³ suggests that a reduced yield strength be substituted for the limiting value of f in Equation 3.1.2.1.1-1 and used in all subsequent calculations to determine section ultimate capacity. The reduced yield strength for a stiffened compression element, F_{yrs} , is obtained as follows:

$$F_{yrs} = \left(1.0 - 0.2 \sqrt{\frac{w}{t}} \sqrt{\frac{F_y}{E}} \right) F_y$$

Equation 3.1.2.1.1-2



This expression was obtained from tests with w/t ratios ranging from 18 to 137, F_y values ranging from 580 to 1055 MPa (84 to 153 ksi), and $\sqrt{\frac{w}{t}} \sqrt{\frac{F_y}{E}}$ values from 0.27 to 0.84.

At $l = 0.673$ the limit width-thickness ratio (at which full capacity is achievable) can be evaluated as

$$\text{limit } \frac{w}{t} = 0.64 \sqrt{\frac{kE}{f}}$$

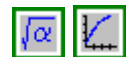
Equation 3.1.2.1.1-3



For fully stiffened compression elements under uniform stress, $k = 4$, which gives a w/t value (identified as $(w/t)_{lim}$ in Reference 2) at which buckling begins of

$$\left(\frac{w}{t} \right)_{lim} = S = 1.28 \sqrt{\frac{E}{f}}$$

Equation 3.1.2.1.1-4

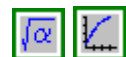


In metric and U.S. customary units

$$S = \frac{572}{\sqrt{f}} \quad f \text{ in MPa}$$

$$S = \frac{220}{\sqrt{f}} \quad f \text{ in ksi}$$

Equation 3.1.2.1.1-5



Fully stiffened refers to elements stiffened by other stiffened elements, such as the walls of the box section and the web of the lipped channels in Figure 3.1.2.1.1-2 and Figure 3.1.2.1.1-3. The value S will also represent a benchmark w/t limit when considering other types of flat elements, as will be seen later.

For w/t beyond the value S , the effective width, b , is less than the actual width w . For purposes of section analysis, the effective width is divided in two, and each half is positioned adjacent to each stiffening element, as illustrated in Figure 3.1.2.1.1-2 and Figure 3.1.2.1.1-3. Thus the width ($w - b$) is completely removed at the center of the flat width when evaluating the section properties.

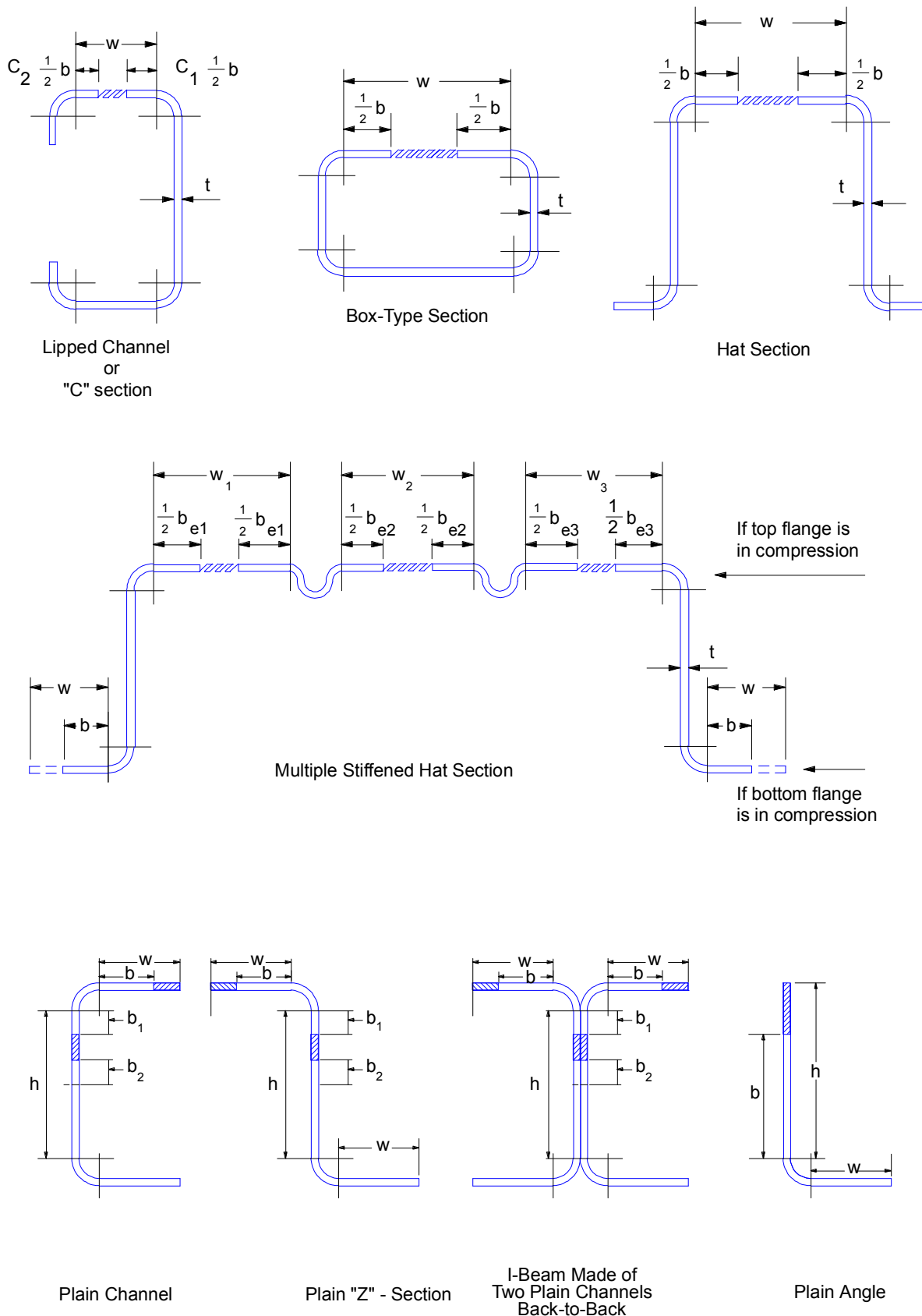


Figure 3.1.2.1.1-2 Effective width concept-flexural members

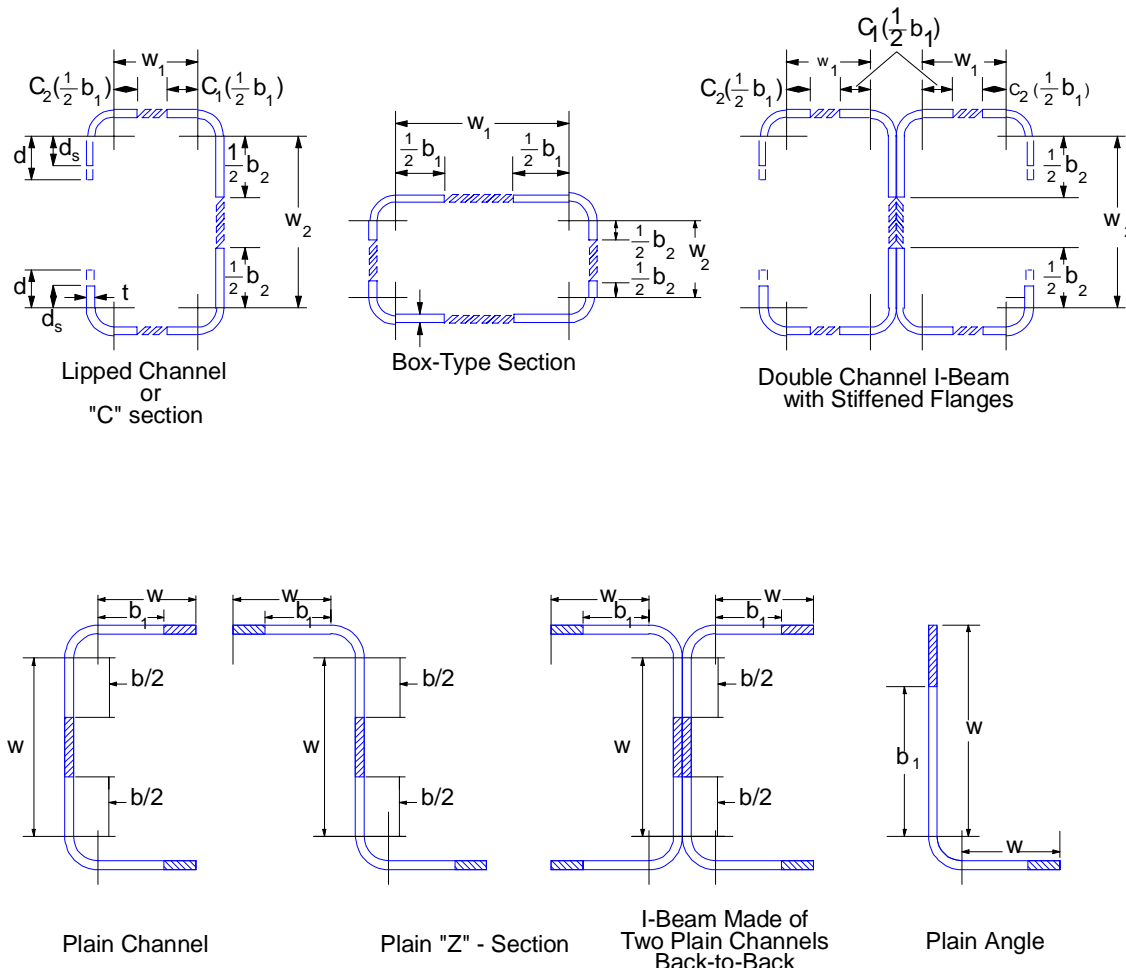
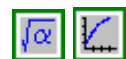


Figure 3.1.2.1.1-3 Effective width concept-compression members

The value of \mathbf{b} is calculated from the general 1986 AISI Specification¹ expression

$$b = w \left(1 - \frac{0.22}{\lambda} \right)$$

Equation 3.1.2.1.1-6



where λ is given in [Equation 3.1.2.1.1-1](#).

For a fully stiffened compression element (with $k = 4$ and $S = 1.28 \sqrt{\frac{E}{F_y}}$), [Equation 3.1.2.1.1-6](#) is

$$b = tS \left(1.486 - \frac{0.486S}{w/t} \right)$$

Equation 3.1.2.1.1-7



It should be noted in [Equation 3.1.2.1.1-7](#) that the effective b/t increases only a limited amount beyond the value of S . This increase with w/t can be considered a second order effect in preliminary design work by considering a flat width to either be fully effective or limited to a

single value of b which is independent of w/t . This is the procedure used in the Japanese specifications⁴.

By arbitrarily substituting $w/t = 2.5S$ into the [Equation 3.1.2.1.1-7](#) this expression for b/t becomes $1.29S$. Thus a good approximation to the AISI expression for stiffened compression members, which is very close to the Japanese expression, is as follows:

$$\begin{aligned} b = w & \quad \text{for } \frac{w}{t} \leq 1.29S \\ b = (1.29S)t & \quad \text{for } \frac{w}{t} > 1.29S \end{aligned}$$

Equation 3.1.2.1.1-8



For the case where $f = 345 \text{ MPa (50 ksi)}$, $b = w$, for w up to $40t$; for w greater than $40t$, $b = 40t$. [Figure 3.1.2.1.1-4](#) can be used in the evaluation of the more exact effective width b using [Equation 3.1.2.1.1-6](#) for any flat compression element.

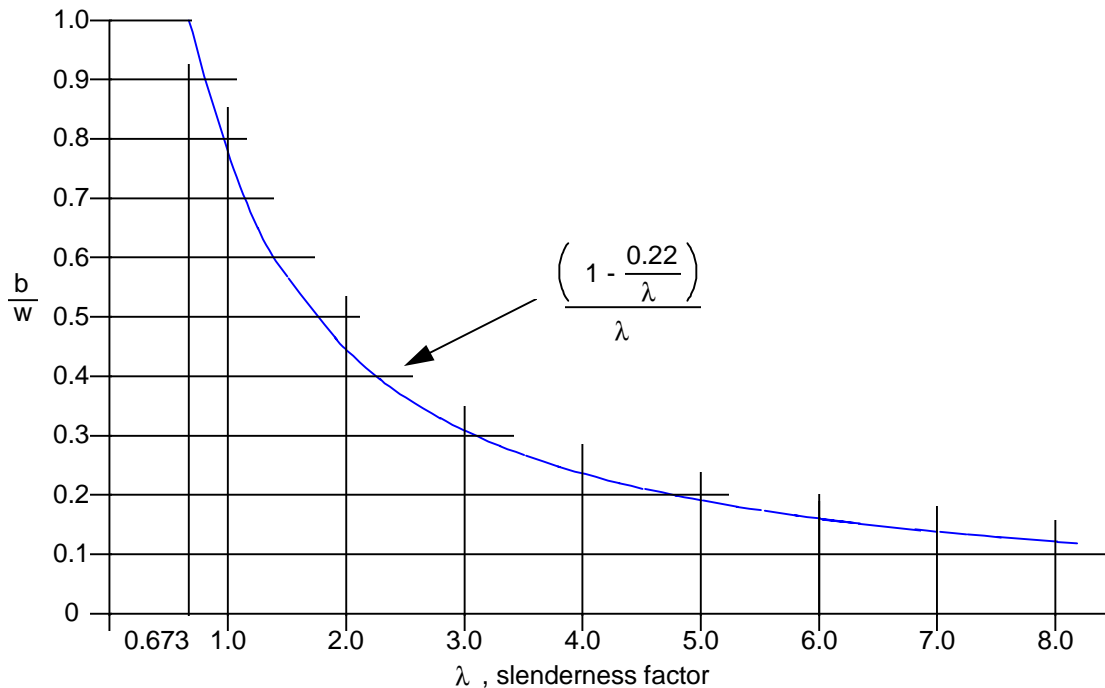


Figure 3.1.2.1.1-4 Effective width evaluation



[Figure 3.1.2.1.1-5](#) can be used in the evaluation of the slenderness factor λ which is needed in [Figure 3.1.2.1.1-4](#).

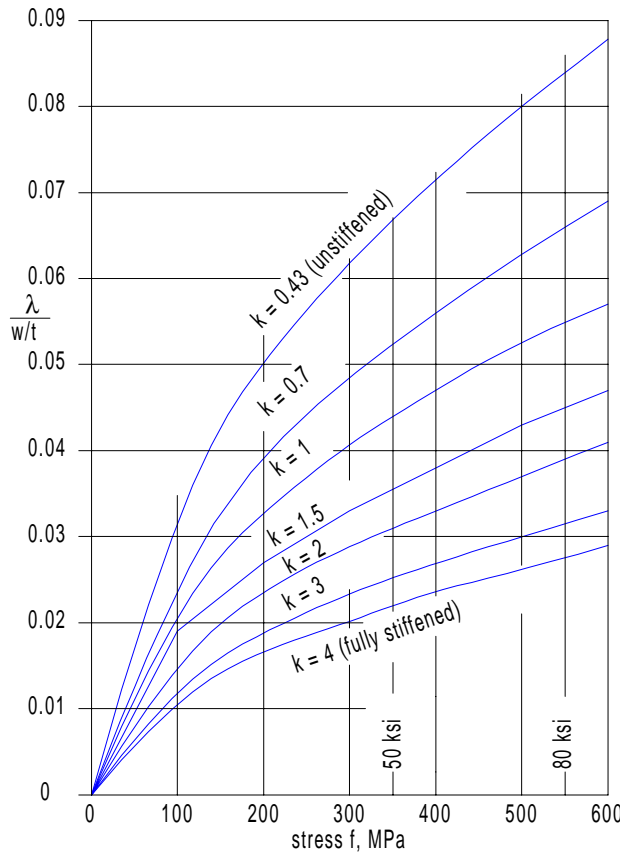


Figure 3.1.2.1.1-5 Slenderness factor evaluation $\sqrt{\alpha}$

If a circular hole of diameter ϕ exists in the stiffened element, the value of b is limited to $w-\phi$. The effective width may be reduced further due to slenderness effects. In this case a lesser effective width can be evaluated as

$$b = w \left(1 - \frac{0.22 - \frac{0.8\phi}{w}}{\lambda} \right)$$

Equation 3.1.2.1.1-9 $\sqrt{\alpha}$ \checkmark

where $\frac{\phi}{w} \leq 0.50$

$$\frac{w}{t} \leq 70$$

and the hole spacing is greater than $0.5w$ and 3ϕ .

The value of compressive stress f should be the value at failure of the section for strength evaluation. For evaluation of deflection or for performance at operating conditions the stress f should be the value of stress occurring at the level of loading being considered.

The value of the buckling coefficient k is 4 if the flat element is stiffened by web members which are stiffened elements. A web member is a shear carrying element of a section whereas edge stiffeners as shown in [Figure 3.1.2.1.1-2](#) are not web members. A w/t limit of 500 applies if the flat element is supported by two web members. Other types of stiffened elements may have k less than 4. These will be discussed after unstiffened elements are examined.



3.1.2.1.2 Unstiffened Compression Elements.....

The unstiffened compression element is illustrated in [Figure 3.1.2.1-1](#). At small **w/t** ratios, the yield stress of the element can be achieved. At large **w/t** ratios, the elastic buckling stress and post buckling characteristics control the element capacity.

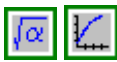
The 1986 AISI Specification¹ treats unstiffened elements in the same manner as stiffened elements by using the effective width concept. This approach is still conservative, but less so than the allowable stress method used in earlier AISI specifications.

The maximum **w/t** recommended by AISI for unstiffened elements is 60. Noticeable flange tip deformations (see [Figure 3.1.2.1-1\(a\)](#)) are likely for **w/t** ratios greater than 30.

The effective width approach can be employed for unstiffened compression elements by using the slenderness factor λ in [Equation 3.1.2.1.1-1](#) with a **k** value of 0.43. This value of **k** at a $\lambda = 0.673$ from [Equation 3.1.2.1.1-3](#) produces the limiting **w/t** for full capacity.

$$\text{limit } \frac{w}{t} = 0.42 \sqrt{\frac{E}{f}}$$

Equation 3.1.2.1.2-1



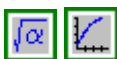
The value in [Equation 3.1.2.1.2-1](#) is equal to 0.33 **S** where **S** is the limiting value for a fully stiffened compression element.

The effective width **b** can be evaluated using [Figure 3.1.2.1.1-4](#) and [Figure 3.1.2.1.1-5](#) with **k** = 0.43. The effective width is placed adjacent to the bend radius as shown in [Figure 3.1.2.1.1-2](#) for multiple stiffened hat section.

It is possible to simplify the effective width expression above as was done for stiffened elements. The simple limit is 0.33 of that in [Equation 3.1.2.1.1-8](#).

$$\begin{aligned} b &= w && \text{for } \frac{w}{t} \leq 0.426S \\ b &= 0.426St && \text{for } \frac{w}{t} > 0.426S \end{aligned}$$

Equation 3.1.2.1.2-2



For **f** = 345 MPa (50 ksi) the 0.426 **S** parameter has a value of 13.

For unstiffened compression elements with a yield strength greater than 550 MPa (80 ksi), recent research⁴ suggests that a reduced yield strength should be substituted for the limiting value of **f** in all calculations to determine section ultimate capacity. The reduced yield strength for an unstiffened compression element, **F_{yru}**, is obtained as follows:

$$F_{yru} = \left(1.079 - 0.6 \sqrt{\frac{w}{t}} \sqrt{\frac{F_y}{E}} \right) F_y \leq F_y$$

Equation 3.1.2.1.2-3

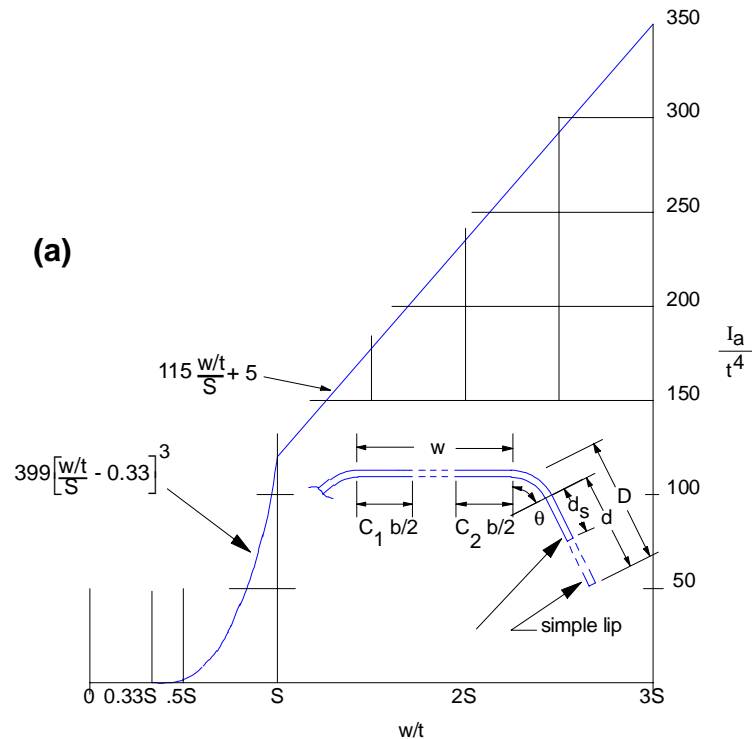


This expression was obtained from tests with **w/t** ratios from 5.6 to 53, **F_y** values ranging from 580 to 1055 MPa (84 to 153 ksi), and $\sqrt{\frac{w}{t}} \sqrt{\frac{F_y}{E}}$ values from 0.13 to 0.53.

3.1.2.1.3 Stiffened Elements With Edge Stiffener



Illustrations of stiffened elements with edge stiffener appear in [Figure 3.1.2.1.1-2](#), [Figure 3.1.2.1.1-3](#) and [Figure 3.1.2.1.3-1\(a\)](#).



I_s = Stiffener moment of inertia

I_a = Minimum or adequate value of the stiffener for a fully stiffened compression element.

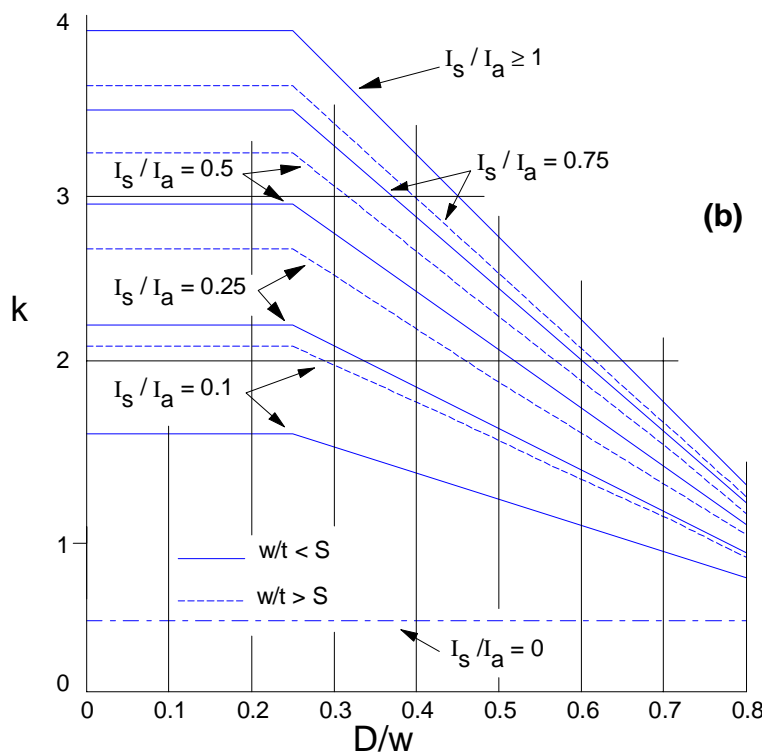


Figure 3.1.2.1.3-1 Edge stiffening evaluation, k



If $w/t \leq 0.33 S$, which is a value of 10.3 for a 345 MPa (50 ksi) yield stress, no edge stiffener is required. This, in effect, means that the compression element is fully effective as an unstiffened compression element for $w/t \leq 10.3$.

For w/t between 0.33 S and $2S$, a simple lip bent at angle θ to the stiffened compression member can be used as a stiffening element as long as D/w is less than 0.8. The definitions of w , D and θ are illustrated in [Figure 3.1.2.1.3-1\(a\)](#). Edge stiffeners other than a simple lip (see [Figure 3.1.2.1.3-2](#)) can be employed to a w/t of $3S$.

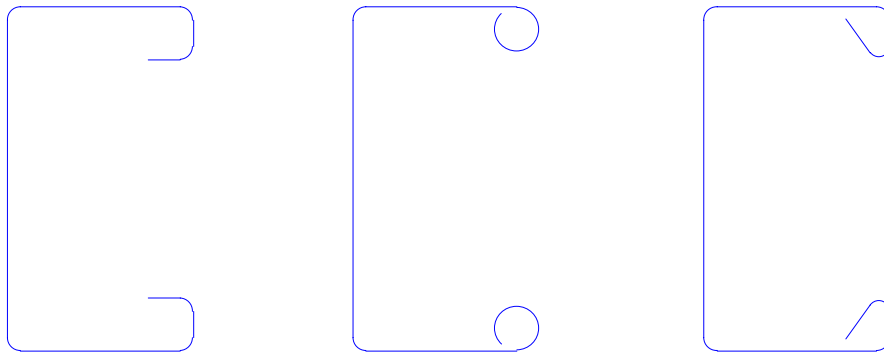


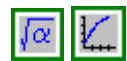
Figure 3.1.2.1.3-2 Edge stiffeners other than simple lip

The evaluation of the edge stiffener requirements in the 1986 AISI Specification¹ covers many situations. The provisions cover simple lips where the bend is other than 90 degrees. They cover situations where the lip is less than the minimum stiffness required to fully stiffen the element. The provisions also consider the influence of loss of effectiveness of the lip if the lip is too long relative to the length of the element being stiffened.

With the use of [Figure 3.1.2.1.3-1](#), evaluation of the effective properties of the stiffened element and the lip can be performed with relative ease. The previous specifications considered only the case where $k = 4$ and the stiffener moment of inertia, I_s , exceeded the minimum or adequate value I_a .

$$I_s = t^4 \left(\frac{d}{t} \right)^3 \frac{\sin^2 \theta}{12}$$

Equation 3.1.2.1.3-1

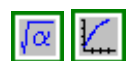


$$I_a = 0$$

$$\text{for } \frac{w}{t} \leq 0.33S$$

$$I_a = 399t^4 \left(\frac{w}{t} - 0.33 \right)^3 \text{ for } 0.33S \leq \frac{w}{t} < S$$

Equation 3.1.2.1.3-2



$$I_a = t^4 \left(115 \frac{w}{t} + 5 \right) \text{ for } \frac{w}{t} > S$$

However, if the depth of the lip **D** is large relative to the flat width it is stiffening, the onset of buckling for flat width **w** occurs at a lower **w/t** ratio as evidenced by the reduction in **k** for larger **D/w**.

If the **I_s** < **I_a**, a further reduction in the buckling coefficient **k** occurs.

$$k = 3.57 \left(\frac{I_s}{I_a} \right)^n + 0.43 \quad \text{for } \frac{D}{w} < 0.25$$

where **k** ≤ 4.0

$$\begin{aligned} n &= \frac{1}{2} && \text{for } \frac{w}{t} < S \\ n &= \frac{1}{3} && \text{for } \frac{w}{t} \geq S \end{aligned}$$

Equation 3.1.2.1.3-3



$$k = \left(4.82 - 5 \frac{D}{w} \right) \left(\frac{I_s}{I_a} \right)^n + 0.43 \quad \text{for } 0.25 < \frac{D}{w} \leq 0.8$$

$$\text{where } k \leq 5.25 - 5 \frac{D}{w}$$

This reduces the effective width of both the stiffened element and the stiffening lip. The reduced width of the lip is

$$d_s = d'_s \left(\frac{I_s}{I_a} \right) \leq d'_s$$

Equation 3.1.2.1.3-4



where **d'_s** = effective width of the unstiffened lip per [Section 3.1.2.1.2](#)

The reduced area of the lip is

$$A_s = A'_s \left(\frac{I_s}{I_a} \right) \leq A'_s$$

Equation 3.1.2.1.3-5



where **A'_s** = actual area of lip for a non-simple lip.

The coefficients **C₁** and **C₂** in [Figure 3.1.2.1.1-2](#) and [Figure 3.1.2.1.1-3](#) are calculated as follows:

$$C_1 = 2 - \frac{I_s}{I_a}$$

$$C_2 = \frac{I_s}{I_a}$$

Equation 3.1.2.1.3-6



Equation 3.1.2.1.3-7



where **C₁** is ≥ 1
C₂ is ≤ 1

Previously, no information was available to ascertain the influence of a stiffener which had less than the adequate moment of inertia. Thus, the element previously had to be considered unstiffened in this case.

[Example 3.1-1](#) in [Section 6.2.1.1](#) illustrates the use of the procedure.

3.1.2.1.4 Multiple Stiffened Flat Elements



To improve the effectiveness of flat compression elements, intermediate stiffeners can be added. [Figure 3.1.2.1.4-1](#) illustrates two types of multiple stiffened elements.

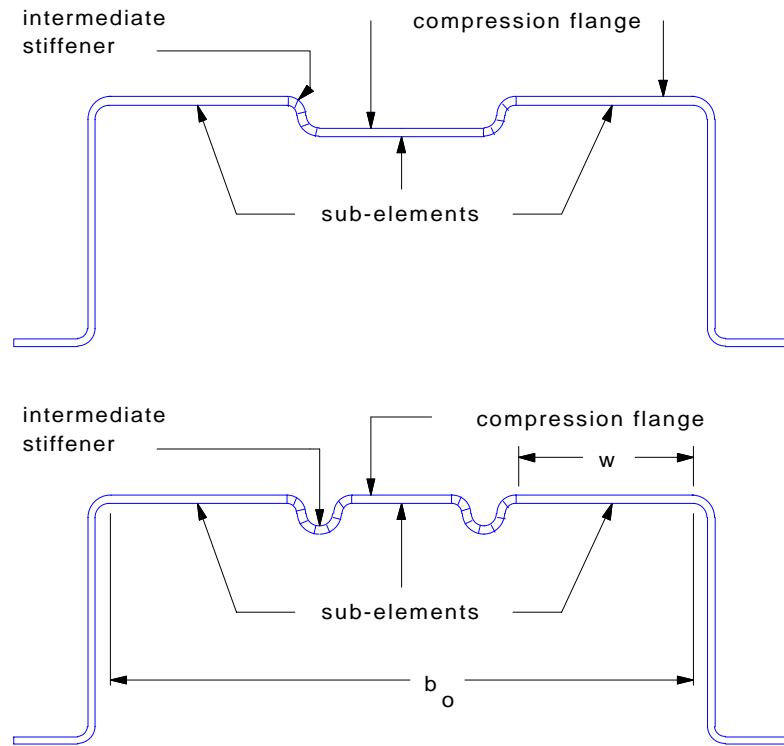


Figure 3.1.2.1.4-1 Multiple-stiffened compression elements

[Figure 3.1.2.1.4-2](#) illustrates a stiffened flat element with a single intermediate stiffener. A single intermediate stiffener must have a moment of inertia $I_s \geq I_a$ in order for the subelement w to be fully stiffened and $k = 4$. I_a can be determined from [Figure 3.1.2.1.4-2\(a\)](#) or as follows:

$$I_a = t^4 \left(50 \frac{b_o}{S} - 50 \right) \quad \text{for } \frac{b_o}{t} < 3S$$

$$I_a = t^4 \left(128 \frac{b_o}{S} - 285 \right) \quad \text{for } \frac{b_o}{t} > 3S$$

Equation 3.1.2.1.4-1



When $I_s < I_a$ the value of k is reduced, as indicated in [Figure 3.1.2.1.4-2](#),

$$k = 3\sqrt{I_s/I_a} + 1 \quad \text{for } \frac{b_o}{t} < 3S$$

$$k = 3\sqrt[3]{I_s/I_a} + 1 \quad \text{for } \frac{b_o}{t} > 3S$$

Equation 3.1.2.1.4-2

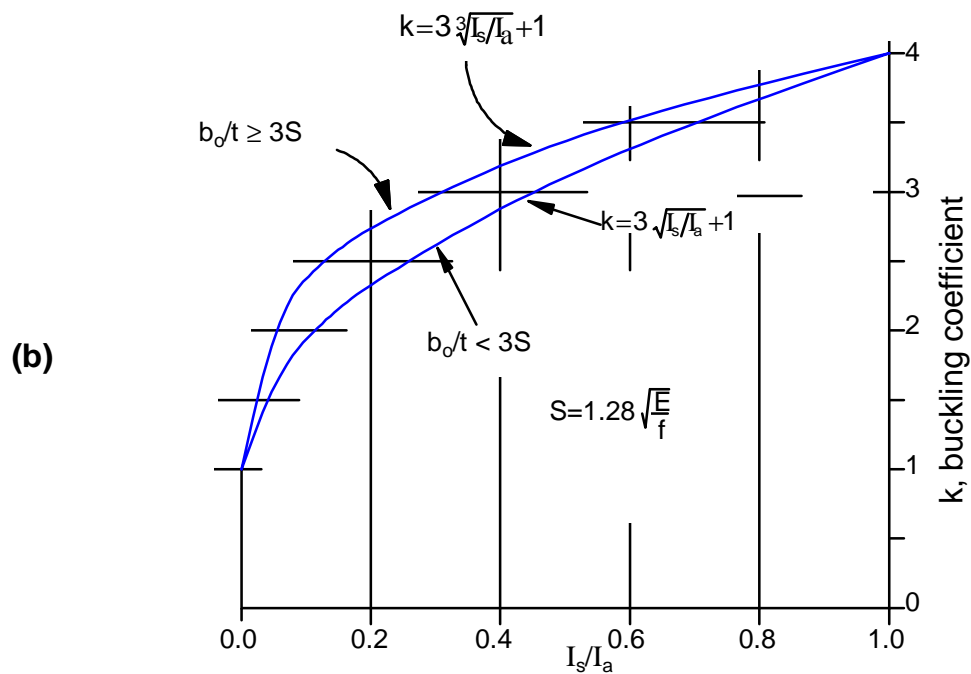
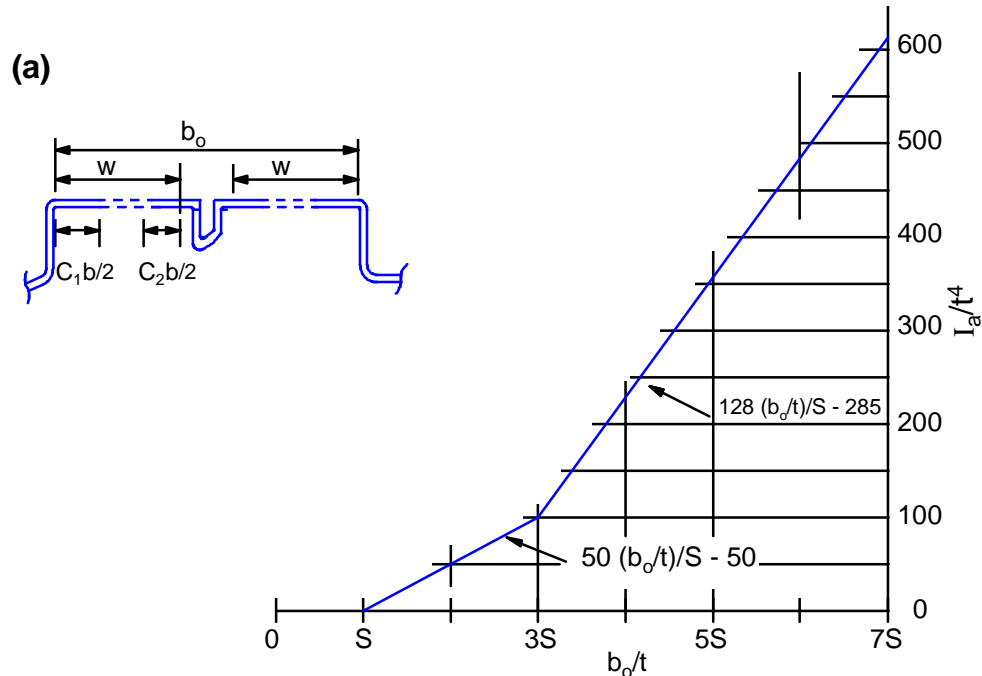


[Figure 3.1.2.1.4-2](#) Evaluation of effectiveness of uniformly compressed element with single intermediate stiffener



If $I_s = 0$, the result degenerates to that of a fully stiffened element without intermediate stiffeners. The reduced area of the stiffeners is

$$A_s = A'_s \frac{I_s}{I_a} \leq A'_s$$

Equation 3.1.2.1.4-3



where A'_s = area of intermediate stiffener

The coefficients C_1 and C_2 are calculated in [Equation 3.1.2.1.3-6](#) and [Equation 3.1.2.1.3-7](#), respectively.

For a multiple stiffened element, if adequate stiffeners are spaced so closely that w/t of all subelements is less than S (defined in [Equation 3.1.2.1.1-4](#)) then the entire intermediately stiffened element is fully effective. In this case an equivalent thickness, t_s , can be computed

$$t_s = \sqrt[3]{\frac{12I_{sf}}{b_o}}$$

Equation 3.1.2.1.4-4



where I_{sf} is the moment of inertia of the entire multiple stiffened element (flats and stiffeners).

b_o is the entire width between webs (shear carrying elements) (See [Figure 3.1.2.1.4-1](#)).

This t_s can be used to evaluate a flat-width ratio b_o/t_s for determining the effective width of the element, since the buckling behavior of the orthotropic plate of width b_o is the same as that for a flat plate of thickness t_s .

If the w/t ratio of the subelements is larger than S , the AISI Specifications¹⁻³ indicate that only the two intermediate stiffeners, the one adjacent to each web, shall be considered effective. Furthermore, the I_s of each stiffener must be at least the value of I_a as defined below in order for the stiffener to be considered and w be the subelement width rather than b_o .

$$\frac{I_s}{t^4} \geq \frac{I_a}{t^4}$$

$$\text{where } \frac{I_a}{t^4} = 3.66 \sqrt{\left[\frac{w}{t}\right]^2 - 0.136 \frac{E}{F_y}} \geq 18.4$$

Equation 3.1.2.1.4-5



If the $w/t \leq 60$, the effective width b of each subelement is the same as calculated for fully stiffened elements. If w/t is greater than 60, the effective width b must be further reduced due to 'shear lag', which produces lower stresses away from the webs as the flange tends to deflect in toward the neutral axis. This reduced effective width can be expressed as

$$b_e = b - 0.10t \left(\frac{w}{t} - 60 \right) \text{ for } \frac{w}{t} \geq 60$$

Equation 3.1.2.1.4-6



In addition, an effective stiffener area less than the actual area must be used due to the lower stress from shear lag. See [Figure 3.1.2.1.4-3](#), which shows the lower stress at the stiffener.

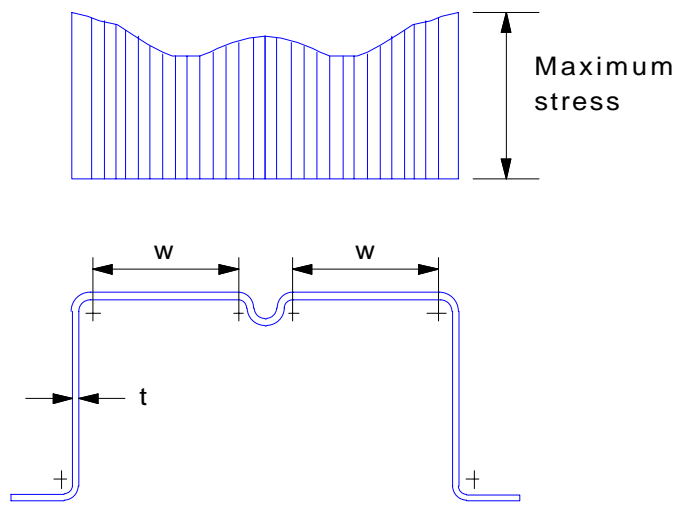


Figure 3.1.2.1.4-3 Stress distribution in compression flange with intermediate stiffener.

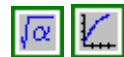
[Table 3.1.2.1.4-1](#) or [Equation 3.1.2.1.4-7](#) can be used to obtain the value of the area reduction factor, α .

Table 3.1.2.1.4-1 Reduction factor, α , for computing effective area of stiffener ($A_s = \alpha A'_s$) for multiple-stiffened elements and wide stiffened elements with edge stiffeners

w/t	Flat Width Ratio, b/t												
	20	25	30	35	40	45	50	55	60	70	80	90	100
60	1.00	1.00	1.00	1.00	1.00	1.00	1.00	1.00	1.00				
62	0.95	0.96	0.97	0.97	0.98	0.98	0.99	0.99	1.00				
64	0.91	0.92	0.93	0.94	0.95	0.96	0.97	0.98	0.99				
66	0.86	0.87	0.89	0.90	0.92	0.93	0.95	0.96	0.98				
68	0.81	0.83	0.85	0.87	0.89	0.91	0.93	0.95	0.97				
70	0.76	0.78	0.80	0.83	0.85	0.88	0.90	0.92	0.95	1.00			
72	0.70	0.73	0.76	0.79	0.82	0.84	0.87	0.90	0.93	0.98			
74	0.65	0.68	0.71	0.75	0.78	0.81	0.84	0.87	0.90	0.97			
76	0.60	0.63	0.67	0.70	0.74	0.77	0.81	0.84	0.88	0.95			
78	0.54	0.58	0.62	0.66	0.69	0.73	0.77	0.81	0.85	0.92	1.00		
80	0.48	0.52	0.57	0.61	0.65	0.69	0.73	0.77	0.82	0.90	0.98		
82	0.43	0.47	0.52	0.56	0.60	0.65	0.69	0.74	0.78	0.87	0.96		
84	0.37	0.42	0.46	0.51	0.56	0.61	0.65	0.70	0.75	0.84	0.94		
86	0.31	0.36	0.41	0.46	0.51	0.56	0.61	0.66	0.71	0.81	0.91	1.00	
88	0.25	0.30	0.36	0.41	0.46	0.51	0.57	0.62	0.67	0.78	0.89	0.99	
90	0.19	0.24	0.30	0.36	0.41	0.47	0.52	0.58	0.63	0.74	0.86	0.97	1.00
100	0.16	0.21	0.26	0.31	0.36	0.41	0.46	0.51	0.56	0.66	0.76	0.86	0.96
110	0.14	0.18	0.23	0.27	0.32	0.36	0.41	0.45	0.50	0.59	0.68	0.77	0.86
120	0.12	0.16	0.20	0.24	0.28	0.33	0.37	0.41	0.45	0.53	0.62	0.70	0.78
130	0.10	0.14	0.18	0.22	0.25	0.29	0.33	0.37	0.41	0.48	0.56	0.64	0.72
140	0.09	0.12	0.16	0.19	0.23	0.26	0.30	0.34	0.37	0.44	0.51	0.59	0.66
150	0.07	0.11	0.14	0.17	0.21	0.24	0.27	0.31	0.34	0.41	0.47	0.54	0.61

$$\alpha = \left(3 - \frac{2b_e}{w} \right) - \frac{1}{30} \left(1 - \frac{b_e}{w} \right) \left(\frac{w}{t} \right) \text{ for } 60 < \frac{w}{t} < 90$$

Equation 3.1.2.1.4-7



$$\alpha = \frac{b_e}{w} \quad \text{for } \frac{w}{t} > 90$$

where b_e is from [Equation 3.1.2.1.4-6](#)

[Example 3.1-1](#) in [Section 6.2.1.1](#) illustrates how to evaluate the effective area for a channel section, and the advantage of intermediate stiffeners, using the procedures of this section.

3.1.2.2 Local Instability of Cylindrical Tubular Members



Local buckling can occur in tubular members of short or moderate length. Relative length can be evaluated by the parameter $\frac{L^2}{Rt}$ where:

$$\frac{L^2}{Rt} < 3 \quad \text{for short tubes}$$

$$3 < \frac{L^2}{Rt} < 52 \quad \text{for moderate - length tubes}$$

$$\frac{L^2}{Rt} > 52 \quad \text{for long tubes}$$

For extremely long tubes, column buckling may occur. Using the area and moment of inertia of a tubular section, the elastic critical stress can be expressed as

$$f_{cr} = \frac{\pi^2 E}{2} \left(\frac{R}{L} \right)^2$$

Equation 3.1.2.2-1



For steel, this expression becomes

$$f_{cr} = 986,960 \left(\frac{R}{L} \right)^2 \text{ MPa}$$

Equation 3.1.2.2-2



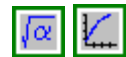
$$f_{cr} = 145,000 \left(\frac{R}{L} \right)^2 \text{ ksi}$$

$\frac{L^2}{Rt}$ must be considerably greater than 52 for the Euler buckling to occur.

For very short tubes, where the radius is extremely large as compared to its length, the critical buckling stress approaches that for a wide-flat plate, which is

$$f_{cr} = \frac{\pi^2 Et^2}{12(1-\mu^2)L^2}$$

Equation 3.1.2.2-3



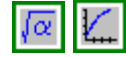
where μ = Poisson's ratio = 0.3 for steel

For steel, this expression becomes

$$f_{cr} = 180,760 \left(\frac{t}{L} \right)^2 \text{ MPa}$$

$$f_{cr} = 26,660 \left(\frac{t}{L} \right)^2 \text{ ksi}$$

Equation 3.1.2.2-4



The moderate length tubes may buckle locally into a diamond pattern. The critical buckling stress for this case is

$$f_{cr} = CE \frac{t}{R}$$

Equation 3.1.2.2-5



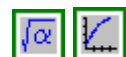
Theoretically, C is 0.605 for steel.

The inward buckling causes transverse compressive membrane stresses. Since nothing is able to resist these compressive stresses, this buckling is accompanied by a sudden drop off in load. Due to this snap through buckling, a value of C one-third or less of the theoretical value is usually recommended for design purposes.

A value of $C = 0.165$ was recommended by Plantema⁴. This leads to an elastic critical stress for steel of

$$f_{cr} = 0.165E \frac{t}{R} = \frac{0.33E}{\frac{D}{t}}$$

Equation 3.1.2.2-6



This elastic value is valid for $D/t \geq 0.448 E/F_y$ which for $F_y = 345 \text{ MPa}$ (50 ksi) is $D/t \geq 260$. At the D/t limit of $0.448E/F_y$, f_{cr} is at 75 percent of the yield stress of the tube.

According to the 1980 provisions of AISI, full yield stress is not achieved until $D/t \leq 0.114 E/F_y$, which is 66 for $F_y = 345 \text{ MPa}$ (50 ksi). Between the D/t ratios of $0.114 E/F_y$ and $0.448 E/F_y$, a transition expression is used to describe the inelastic buckling. This stress reduction did not interact with overall instability considerations in the 1980 AISI Specifications².

The approach presented here follows that used in the 1986 AISI Specification¹. Instead of considering the total area with a stress limit based on local instability, a reduced area is used with a stress of F_y to reflect the effect of local buckling. This can be accomplished by using the transition expression and [Equation 3.1.2.2-6](#) as the means of calculating an equivalent area for a cylindrical tubular member.

This equivalent area, A_o , is expressed as follows:

$$A_o = A \quad \text{for} \quad \frac{D}{t} \leq 0.114 \frac{E}{F_y}$$

$$A_o = \left(\frac{2}{3} + \frac{0.038 \frac{E}{F_y}}{\frac{D}{t}} \right) A \quad \text{for} \quad 0.114 \frac{E}{F_y} < \frac{D}{t} \leq 0.448 \frac{E}{F_y}$$

$$A_o = \left(\frac{0.336 \frac{E}{F_y}}{\frac{D}{t}} \right) A \quad \text{for} \quad \frac{D}{t} \geq 0.448 \frac{E}{F_y}$$

Equation 3.1.2.2-7



where A = total area of cylindrical tubular section
 F_y = yield stress in tubular member.

[Figure 3.1.2.2-1](#) shows the A_o/A ratio for $D/t \leq 300$.

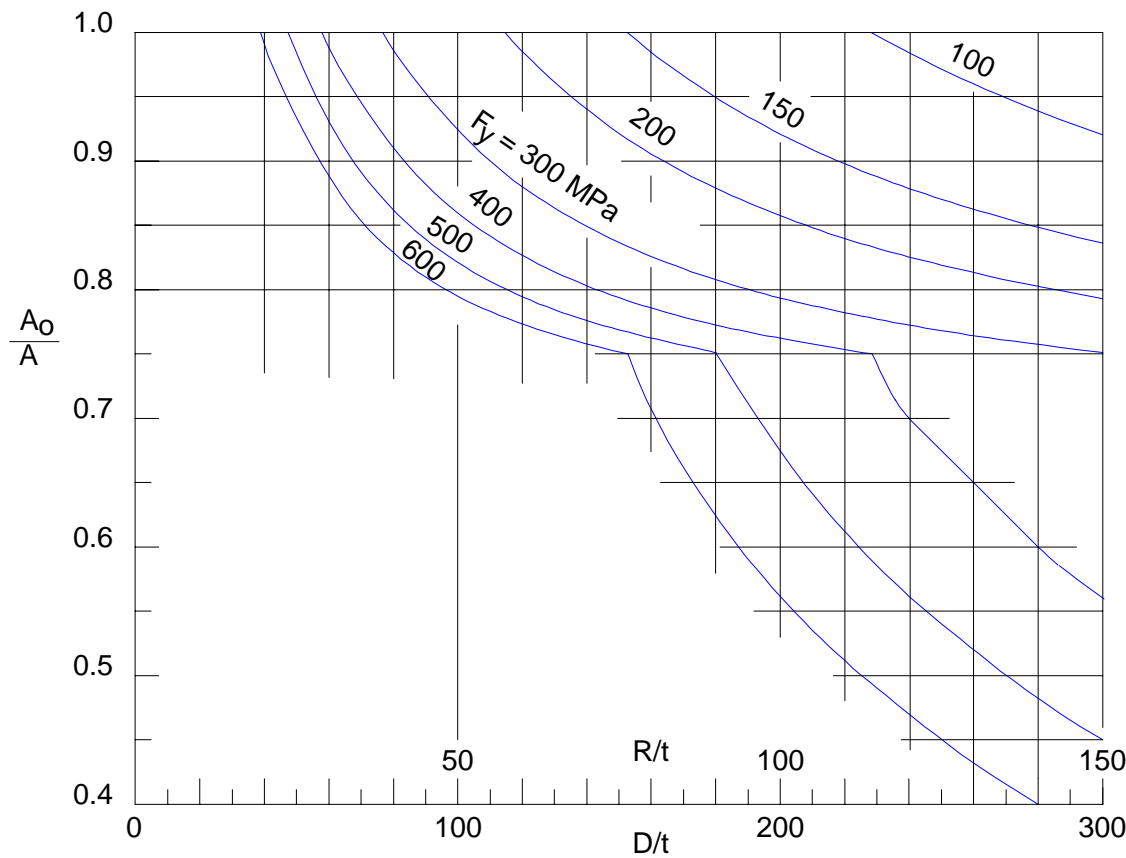


[Figure 3.1.2.2-1](#) Equivalent area for cylindrical tubular compression members 

When inelastic column (overall) buckling occurs in a tubular member subject to local buckling, a further reduction in the load capacity occurs. An effective area, A_e , used to reflect the resultant load capacity, is defined in [Section 3.1.2.5](#).

For tubular members, it is not economical to design using $D/t > 0.448 E/F_y$ since the critical stress drops off rapidly in the elastic range. It is extremely rare to use a tubular section with D/t beyond 200. In fact, the third expression in [Equation 3.1.2.2-7](#) is not in the 1986 AISI Specifications¹. Using the smallest thickness available for A570 steel, 0.6477 mm (0.0255 in.), a D/t of 200 is reached for a tube diameter of 129.5 mm (5.1 in.).

A tubular member at $D/t = 100$, e.g. $D = 64.77$ mm (2.55 in.) and $t = 0.6477$ mm (0.0255 in.), may not be uncommon. With these dimensions the effective length would have to be in excess of about one meter before column buckling would become a significant factor in the design. At $L = 1000$ mm the parameter L^2/Rt is 47,674.

3.1.2.3 Local Instability of Curved Plate Elements



Local instability of curved plate elements of constant radius, braced along one or both sides by a corner bend, is an extension of the evaluation of flat plate elements in [Section 3.1.2.1](#) of this chapter. Simple examples of stiffened and unstiffened elements are illustrated in [Figure 3.1.2.3-1](#).

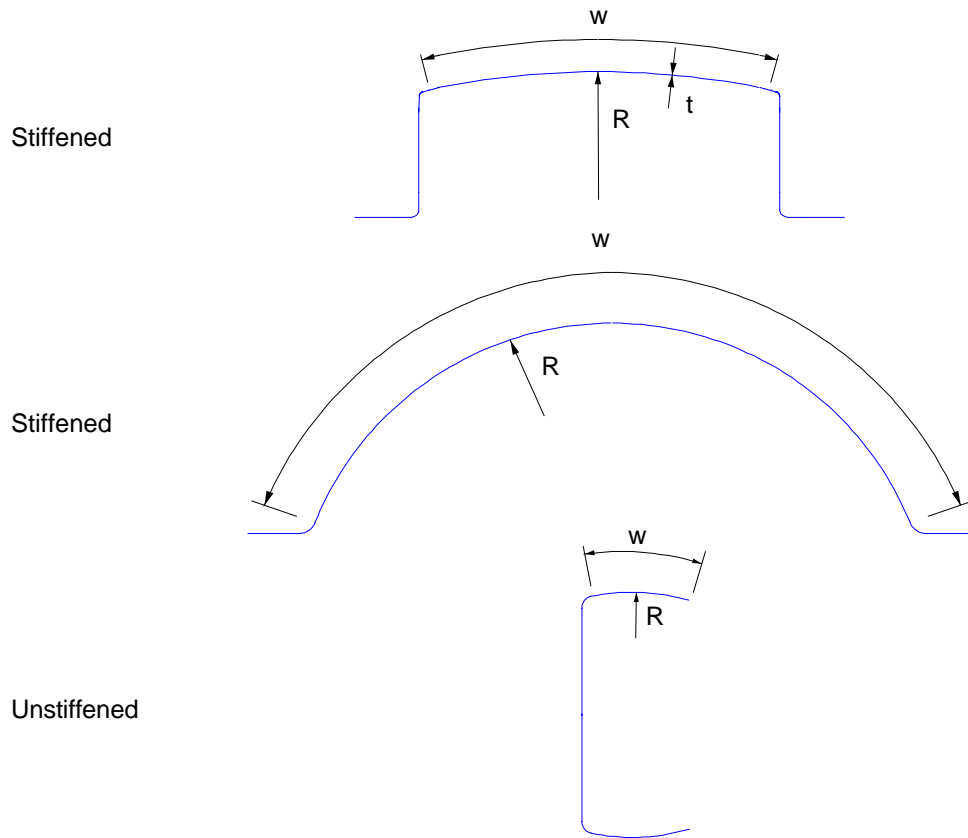


Figure 3.1.2.3-1 Examples of stiffened and unstiffened curved elements

For most linear members, the length of curved elements is beyond the length where flat plate buckling per [Equation 3.1.2.2-4](#) will occur. Local buckling will be similar to that for a cylinder which is represented by [Equation 3.1.2.2-5](#), as long as a sufficient arc length is present to develop the buckling mode.

Elastic buckling of curved plate elements lies somewhere between those of flat plates and complete cylinders. An expression to predict this elastic buckling was developed based on energy methods and can be expressed as a combination of the buckling stress of a complete cylinder and that of a flat plate^{5, 6}.

$$f_{crp} = \sqrt{\left(f_{crc}\right)^2 + \left(\frac{f_{crf}}{2}\right)^2 + \frac{f_{crf}}{2}}$$

Equation 3.1.2.3-1



where f_{crp} = buckling stress of curved panel with radius R

$f_{crc} = 0.3E \frac{t}{R}$ = buckling stress of full cylinder with radius R

f_{crf} = buckling stress of flat plate ([Equation 3.3.1.3-1](#)) with w equal to the length of the arc.

Inelastic buckling values can be obtained from the above expression by using tangent or secant modulus of elasticity in place of E, the elastic modulus of elasticity (see [Figure 3.3.3-2](#)). [Equation 3.1.2.3-1](#) only predicts the critical stress, but does not consider any post buckling behavior as is used for flat plates.

Recent tests of stub columns at the University of Missouri-Rolla⁶ were used as the basis for the following empirical expression for buckling of an unstiffened curved plate element.

$$\frac{f_{crp}}{E} = 0.0407 \left(\frac{t}{R} \right) + 0.452 \left(\frac{t}{w} \right)^2$$

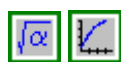
Equation 3.1.2.3-2



Tests were conducted using sheet steels with yield strengths varying from 26.5 ksi (183 MPa) to 88.3 ksi (609 MPa). A tangent modulus expression was formulated which gives good estimates for the buckling load when f_{crp} is larger than the proportional limit. It was found to be satisfactory to consider the proportional limit at 0.7 F_y in which case,

$$E_t = E \frac{f_{crp}}{F_y} \frac{\left(1 - \frac{f_{crp}}{F_y}\right)}{0.21}$$

Equation 3.1.2.3-3



The tangent modulus of elasticity E_t would be substituted for E in [Equation 3.1.2.3-2](#) if f_{crp} , using E, exceeds 0.7 F_y .

The curved elements shown in [Figure 3.1.2.3-1](#) have the benefit of being stiffened on either one or both sides by a stiffened element or edge stiffener when a sharp bend of close to 45° is created.

In these cases there is post buckling capability, just as for flat compression elements. The effective width concept for the ultimate strength of curved panels has been researched^{7, 8} and found to be a satisfactory approach.

In this approach the effective width b is exactly as defined for flat elements. However, unlike a flat element, the ineffective portion of a curved element is assumed to carry the critical buckling

stress of a circular cylinder with the same radius and thickness as the panel. This is illustrated in [Figure 3.1.2.3-2](#).

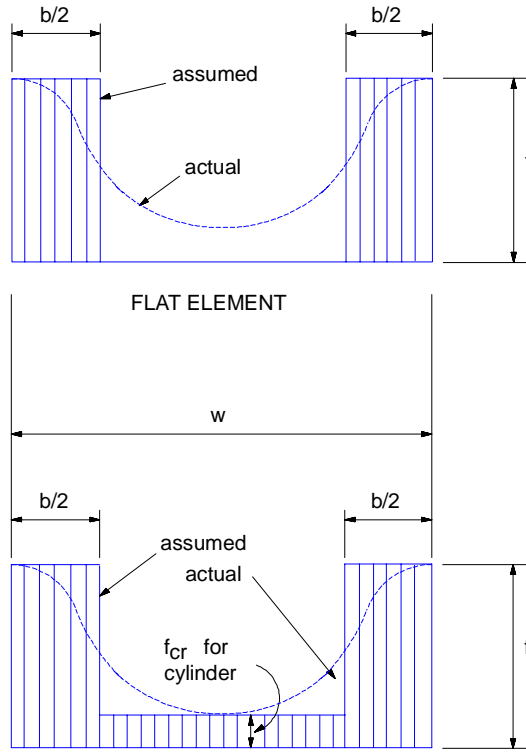


Figure 3.1.2.3-2 Effective width concept for flat and curved elements

Instead of completely neglecting the center portion as done for flat elements, use of an effective thickness

$$t_e = \left(\frac{A_o}{A} \right) \left(\frac{F_y}{f} \right) t$$

Equation 3.1.2.3-4

is appropriate where A_o/A is from [Figure 3.1.2.2-1](#). This procedure is demonstrated in [Example 3.1-2](#) in [Section 6.2.1.2](#).

3.1.2.4 Local Instability of Sections with Curved and Straight Elements

When the curved segment is tangent with a straight segment, the evaluation of each is not as straightforward as when the two segments are separated by a sharp bend. A curved segment with $R/t \leq 7$ is normally used to stiffen the edge of a flat element. In this case the flat element width is measured from the point of tangency.

For a curved element with

$$\frac{R}{t} \leq \frac{0.057 E}{F_y} \left(\frac{R}{t} \leq 33 \text{ for } F_y = 345 \text{ MPa (50 ksi)} \right)$$

yield strength of the element can be achieved. However, measuring w from the point of tangency may not be conservative. It may not be reasonable to consider that the curved element can

provide a stiffened edge. Thus, at some point the flat element should be taken as half of a stiffened element or even as an unstiffened element. This is illustrated in [Figure 3.1.2.4-1](#).

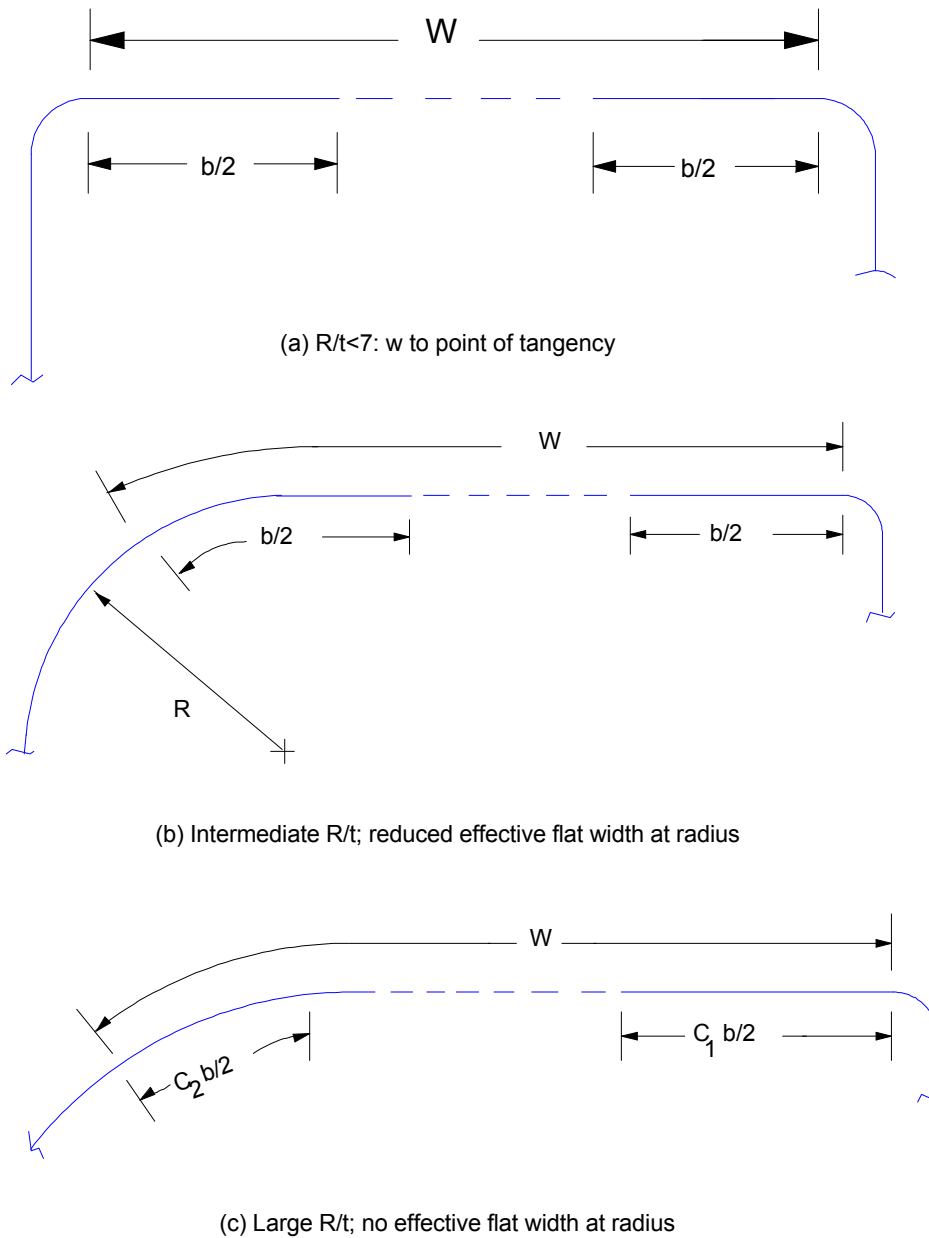


Figure 3.1.2.4-1 Effective flat width with varying corner radii

No quantitative information is available on these matters; however, conservative assumptions can be made that should be satisfactory for preliminary analysis, as outlined in [Example 3.1-3](#) in [Section 6.2.1.3](#).

For a section composed of a number of flat and curved elements, evaluation of a critical stress for the section can be a problem. Two methods are explained in [Reference 5](#) for evaluating a critical stress for such a section. Each bases the overall critical stress on the areas and critical stresses of the various components. One method uses the buckling capacity of the curved element as an upper limit value while the other does not.

The approach used must consider all of the components in the section and their relationship to one another. If the section has sharp radius corners with

$$\frac{R}{t} < 0.057 \frac{E}{F_y}$$

then post buckling capacity can be achieved; if not, then the radius portion or flat portion tangent to the radius will limit the capacity. If the sharp radius corners are not distributed around the cross section, the post buckling strength may not be of any value, as the effective section properties at post buckling stresses may produce a load which is less than the elastic buckling load.

Tests were conducted at the University of Missouri-Rolla^{6, 9, 10, 11} on the sections shown in [Figure 3.1.2.4-2](#)

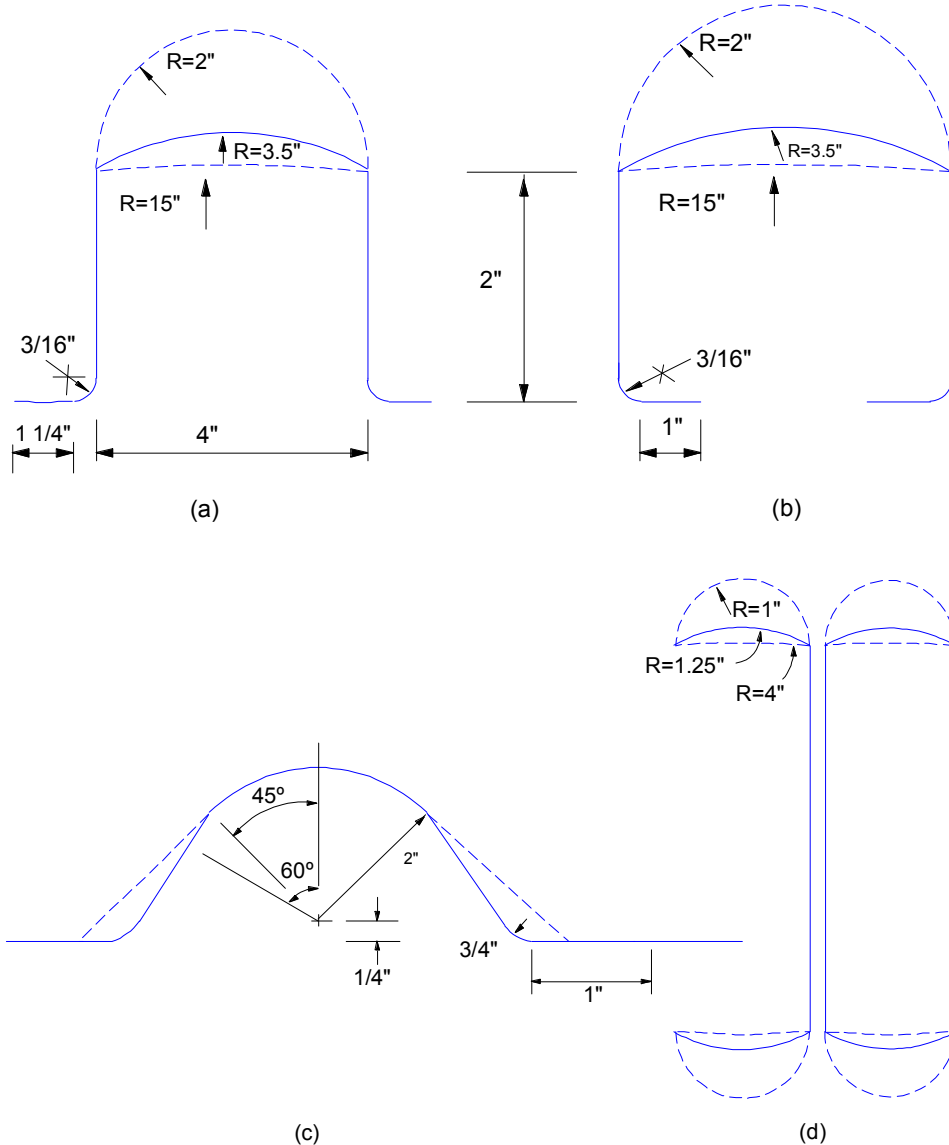


Figure 3.1.2.4-2 University of Missouri-Rolla test specimens

Stub column tests were done on these specimens with lipped channel or hat sections being connected in pairs for the test. In some of the tests, the flat widths were stiffened so that the buckling stress of the curved elements could be achieved prior to flat plate buckling. Post buckling capability existed only for the sections with large radius ($R = 100$ mm [4 in.] and 380 mm [15 in.]) where sharp bends existed at the ends of the curved segment.

The recommended procedure for evaluating the axial load capacity of a section with curved elements based on these tests is as follows:

1. Use [Equation 3.1.2.3-2](#) for f_{crp} for unstiffened curved elements and [Equation 3.1.2.3-1](#) for stiffened curved elements with E_t from [Equation 3.1.2.3-3](#) used for E when $f_{crp} > 0.7 F_y$.
2. Use f_{crp} as the stress at which the effective width is determined for all flat elements.
3. Determine the axial capacity as the stress f_{crp} times the net area of the cross section found by removing all ineffective flat portions from the total area.

The axial capacity of the section at any stress less than f_{crp} can be obtained by using that stress instead of f_{crp} in steps 2 and 3.

3.1.2.5 Overall Stability of Members



The axial stress capacity has been calculated in the 1980 and earlier AISI specifications using the total area, A , of the cross section. A factor Q , which represents the ratio of the effective to total area at stress F_y was used to reduce the limiting stress.

The effect of the Q factor was imposed only to the inelastic portion of the column equations. The elastic portion of the column equation (the Euler load) was unaffected by the effective area. The reasoning was that at the lower stress (less than half of QF_y) the section would typically have a Q of one.

This approach was changed in the 1986 AISI Specification¹. The axial stress is now based on the effective area instead of the total area. This effective area is calculated at the ultimate stress determined by the member's lateral buckling integrity, i.e., its slenderness ratio and its yield stress. The limiting stress equations are basically the same as used previously, but are presented in a much simpler form.

The provisions are as follows:

$$F_{cu} = F_e \quad \text{for } F_e \leq \frac{F_y}{2}$$

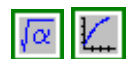
$$F_{cu} = F_y \left(1 - \frac{F_y}{4F_e}\right) \quad \text{for } F_e > \frac{F_y}{2}$$

Equation 3.1.2.5-1



where $F_e = \frac{\pi^2 E}{\left(\frac{KL}{r}\right)^2}$ for flexural buckling

Equation 3.1.2.5-2



The previous relations are applicable for doubly symmetric sections, closed cross sections, or any other sections not subject to torsional-flexural buckling. For sections subject to torsional-flexural buckling, an appropriate F_e can be computed using procedures in the 1986 AISI Specification¹. The axial capacity is then determined by

$$P_u = A_e F_{cu}$$

Equation 3.1.2.5-3



In the previous equations,

- P_u = axial load capacity
- A_e = the effective area at the stress F_{cu}
- F_{cu} = ultimate compression stress under concentric loading
- $\pi^2 E$ = 1,974,000 MPa (291,000 ksi)
- K = effective length factor
- L = unbraced length of member
- r = radius of gyration of full, unreduced cross section
- F_y = yield strength of steel

The format is so simple that design aids are not very useful. Knowing F_y and having calculated KL/r , determine F_e , F_y/F_e and then F_{cu} . Determine A_e for the section at the stress F_{cu} and then calculate P_u .

This procedure is applicable to cylinder tubular members as discussed in [Section 3.1.2.2](#). Capacity reduction in the inelastic range is considered by an effective area

$$A_e = \left[1 - \left(1 - \frac{F_y}{2F_e} \right) \left(1 - \frac{A_o}{A} \right) \right] A$$

Equation 3.1.2.5-4



where A_o is defined by the second expression in [Equation 3.1.2.2-7](#).

In order to extend the application of this concept to include the third expression in [Equation 3.1.2.2-7](#), the following procedure is recommended:

- 1) Compute A_o/A using [Equation 3.1.2.2-7](#) or [Figure 3.1.2.2-1](#).
- 2) If F_e is greater than $F_y/2$, determine A_e from [Equation 3.1.2.5-4](#) and then compute $P_u = A_e F_{cu}$, which is [Equation 3.1.2.5-3](#). If F_e is less than $F_y/2$ then compute $P_u = AF_e$.
- 3) If A_o/A is less than 0.75, compute $A_o F_y$ and let P_u be the lesser of $A_o F_y$ and P_u , calculated above in 2.

When considering sections of various shapes that have curved elements, the effective area of the curved elements can be taken as A_o .

The only problem with the new approach ([Equation 3.1.2.5-1](#), [Equation 3.1.2.5-2](#), and [Equation 3.1.2.5-3](#)) is the need to calculate A_e for each level of stress F_{cu} encountered for a given section. This is a place where the simplified effective width approach given in [Equation 3.1.2.1.1-8](#) and [Equation 3.1.2.1.2-2](#) might be useful.

For sections composed of flat elements, another idea is to use the old approach where A_e had to be calculated only at yield stress (A_{ey}). This can be done very easily using the above equations simply by redefining the radius of gyration r . If $r = \sqrt{\frac{I}{A_{ey}}}$ rather than $\sqrt{\frac{I}{A}}$, then [Equation 3.1.2.5-1](#), [Equation 3.1.2.5-2](#) and [Equation 3.1.2.5-3](#) give identical answers for P_u , as does the 1980 AISI Specification³. In this case, I is based on the full unreduced cross section and A_{ey} , the effective area at F_y , is used in calculating P_u .

For channel, Z-shape and single angle sections with unstiffened flanges, the axial capacity may be limited by torsional buckling instead of flexural (or torsional-flexural) buckling. In this case, the axial capacity P_u for torsional buckling should be calculated as follows¹:

$$P_u = \frac{A\pi^2 E}{25.69 \left(\frac{w}{t} \right)^2}$$

Equation 3.1.2.5-5



where A = area of the full, unreduced cross section

w = flat width of the unstiffened element

t = thickness of the unstiffened element

The smaller of the ultimate loads from [Equation 3.1.2.5-3](#) and [Equation 3.1.2.5-5](#) should be used.

[Example 3.1-4](#) in [Section 6.2.1.4](#) illustrates the use of column [Equation 3.1.2.5-1](#).

3.1.3 FLEXURE OF MEMBERS

Flexure capacity can be limited by the yield stress, the yield strain (in compression), local instability or overall lateral instability. The flexural stress acting in conjunction with shear and/or compression load can further reduce the flexural capacity. However, inelastic straining can increase the flexural capacity beyond that at first yield, provided sources of instability are eliminated. The flexural capacity of sections composed of flat elements and of cylindrical sections will be examined.

3.1.3.1 Flexural Capacity of Members with Flat Elements.....



Flexural members may have flat elements, either stiffened or unstiffened, which are subjected to either uniform compression, uniform tension, or a varying stress condition.

If the element has uniform compressive stress, the element can be treated as in [Section 3.1.2.1](#). The effective width concept would be used. Since the load enters the flanges of flexural members from the webs and is developed gradually with bending moment, factors other than compression stress and element slenderness can determine the effective width of the flanges.

3.1.3.1.1 Effective Width - Short Spans

For short span beams, shear lag causes a flange effective width which is less than the actual width between webs. The type of load and the ratio of span L to width w_f are the principal variables. The width w_f is the flange projection for an I or C section or half the distance between webs for multiple web sections as shown in [Figure 3.1.3.1.1-1\(a\)](#). Curves for determining the effective width from L/w_f ratio are shown in [Figure 3.1.3.1.1-1\(b\)](#).

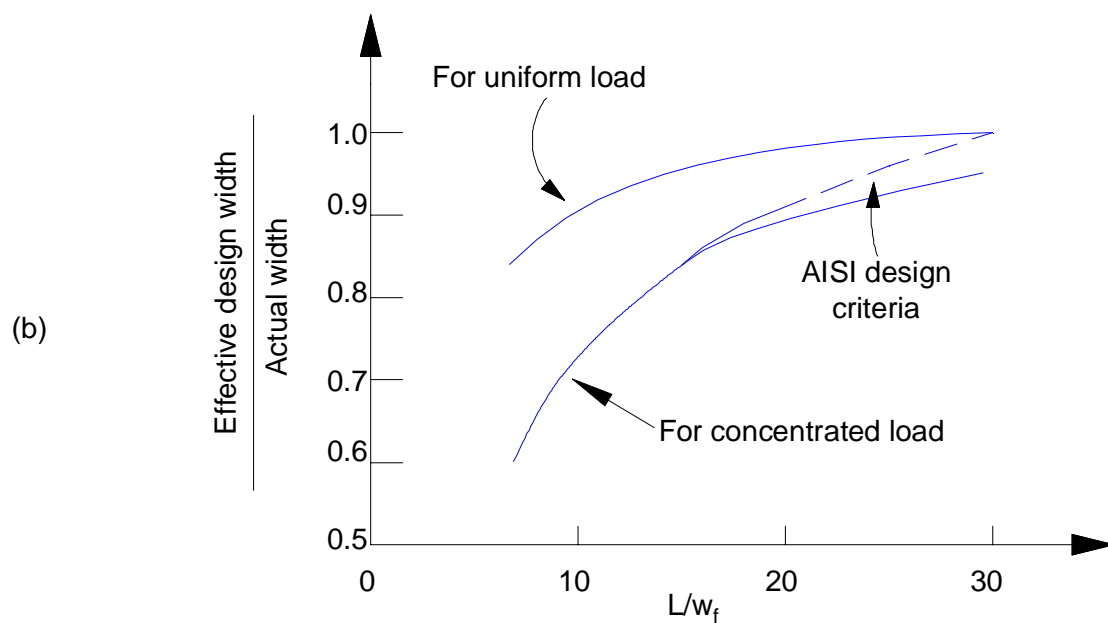
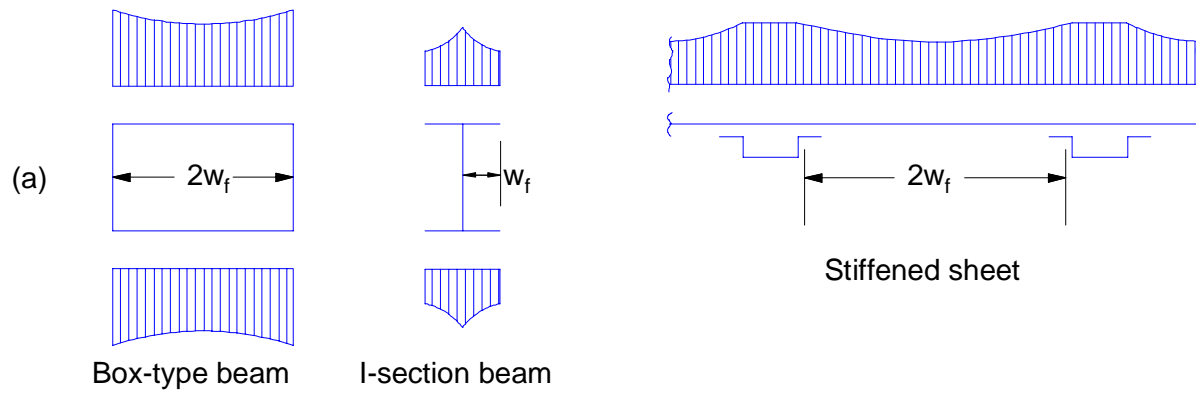


Figure 3.1.3.1.1-1 Definition of w_f : effective width of beam flanges with small 

For compression use the lesser of the effective width determined from [Section 3.1.2.1](#) and that determined using [Figure 3.1.3.1.1-1\(b\)](#). For tension on flange element use only [Figure 3.1.3.1.1-1\(b\)](#) to evaluate effective width.

If the w/t ratio of a stiffened compression element is less than $0.86 S_y$ where $S_y = 1.28 \sqrt{\frac{E}{F_y}}$, it may be possible to permit inelastic stress redistribution in the web and improve the ultimate moment capacity of the section beyond that of the yield moment.

3.1.3.1.2 Effect of Stress Variation

A linear stress variation exists across the flat elements that are the webs of the flexural members. The variation may be as in [Figure 3.1.3.1.2-1\(a\)](#), where maximum tension and compression

stresses are the same, or as in [Figure 3.1.3.1.2-1\(b\)](#), where either the tension or compression stress of an element is larger than that on the other edge.

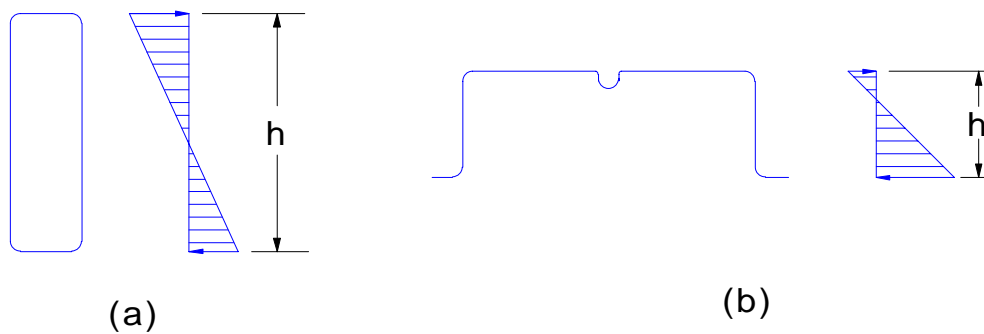


Figure 3.1.3.1.2-1 Flexural stress variation

The web height is limited in the AISI specifications to $h/t = 200$ (where h is the depth of the flat portion of web) when this web is not stiffened transversely or longitudinally. The h/t ratio may be increased to 260 when intermediate stiffeners are used and to 300 when intermediate plus bearing stiffeners are used. The h/t limitation is more severe than the w/t limit for fully stiffened uniformly compressed elements because these elements must also transfer shear.

If the larger of the two stresses is tension, then the likelihood of having the compression stress control is quite small if $h/t < 200$. For the case where the compression stress is larger, the limiting stress can be evaluated from one of the two expressions below. If the stiffener at the compression side of the web is a stiffened element, it imparts more rotational restraint leading to a higher buckling load than can be achieved by an unstiffened element (See [Figure 3.1.3.1.2-2](#)).

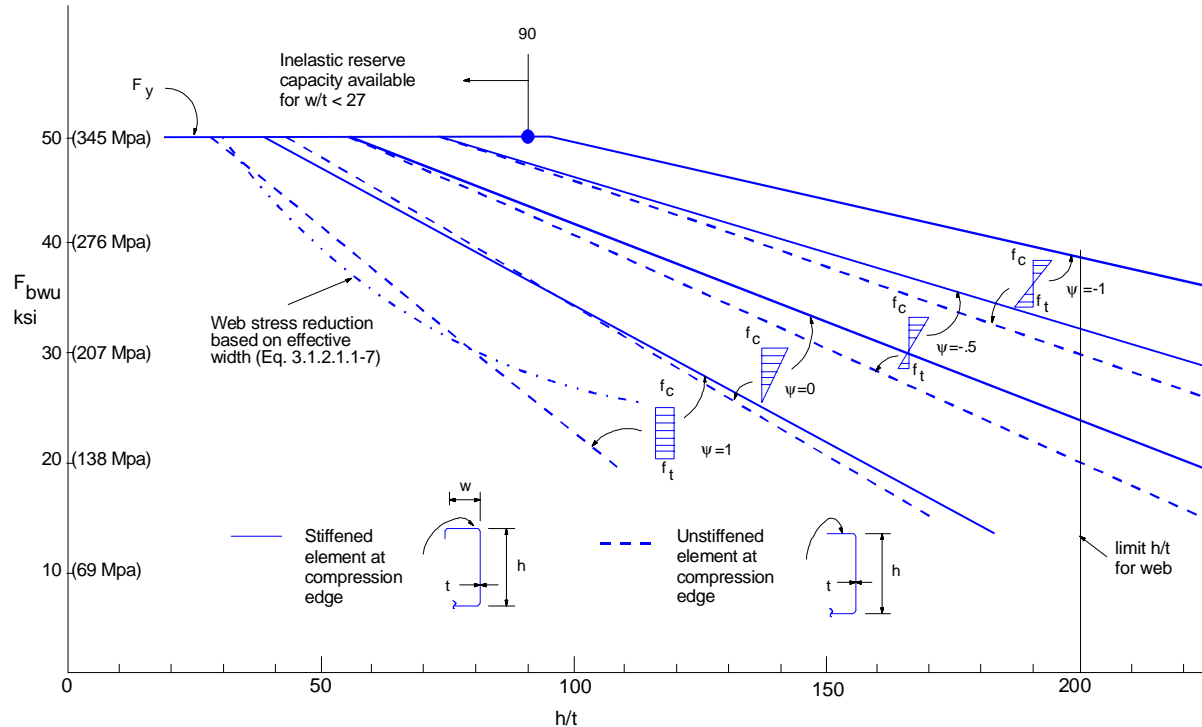


Figure 3.1.3.1.2-2 Stress reduction in web per [Equation 3.1.3.1.2-1](#) and [Figure 3.1.3.1.2-2](#)



The following expressions are a generalization of the expression¹² for webs in the 1980 AISI Specification².

Stiffened element

$$F_{bwu} = \left(1.197 - 0.247 \frac{h}{t} \sqrt{\frac{F_y}{kE}} \right) F_y$$

Equation 3.1.3.1.2-1



Unstiffened element

$$F_{bwu} = \left(1.229 - 0.374 \frac{h}{t} \sqrt{\frac{F_y}{kE}} \right) F_y$$

Equation 3.1.3.1.2-2



$$\text{where } k = 4 + 2(1 - \psi)^3 + 2(1 - \psi)$$

Equation 3.1.3.1.2-3



$$\psi = \frac{f_t}{f_c} = \frac{f_2}{f_1}$$

Equation 3.1.3.1.2-4



(See [Figure 3.1.3.1.2-2](#) and [Figure 3.1.3.1.2-3](#))

The parameter k represents the buckling factor for a plate as a function of the variation of tensile to compressive stress ratio. A plot of these expressions is shown in [Figure 3.1.3.1.2-2](#) for $F_y = 345 \text{ MPa}$ (50 ksi).

Note that when $y = 1$ (uniform stress) an h/t between 30 and 39 is where buckling begins to reduce the stress limit. Note that if the equation for uniform compression on a stiffened element is plotted in [Figure 3.1.3.1.2-2](#), it compares favorably with the lower bound value if w/t is considered equivalent to h/t .

As the amount of compression force over the element decreases and pure flexure is approached, the element can achieve the stress levels indicated for $y = -1$, which form the basis for the 1980 AISI provisions.

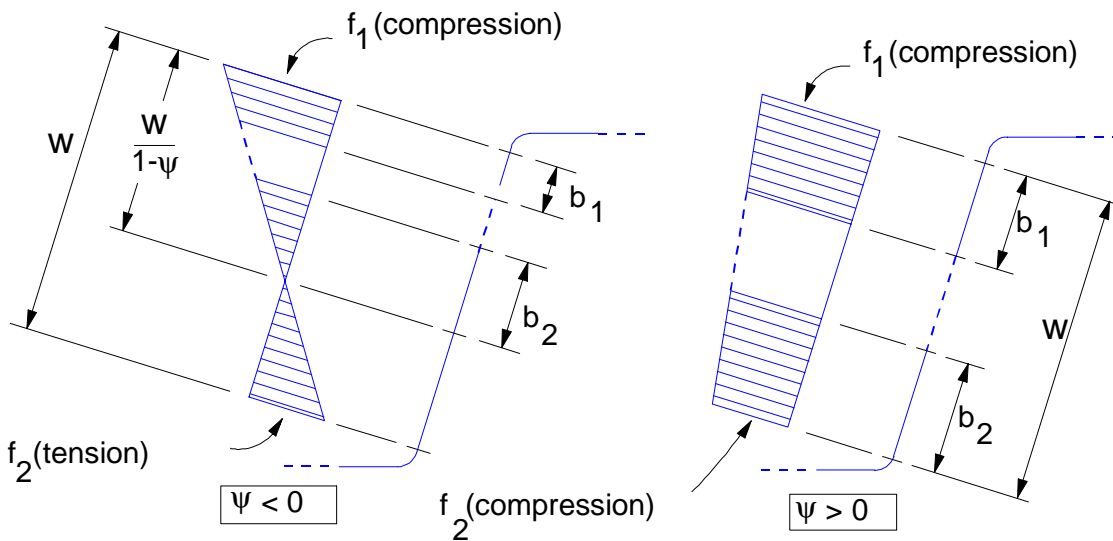
The 1986 AISI Specification¹ eliminates [Equation 3.1.2.1.2-1](#) and [Equation 3.1.2.1.2-2](#) replaces them with an effective width concept consistent with that used for elements under uniform compression. These relationships, in fact, are a generalization of those developed for a uniformly compressed stiffened element in [Section 3.1.2.1.1](#).

The effective width of the compression portion of the flat element is shown as b_1 and b_2 in [Figure 3.1.3.1.2-3](#) with

$$b_1 = \frac{b_e}{3 - \psi}$$

Equation 3.1.3.1.2-5





Effective Elements and Stresses on Effective Elements

Figure 3.1.3.1.2-3 Stiffened elements with stress gradient and webs

For principally flexural stress variation the width b_2 should be defined as

$$b_2 = \frac{b_e}{2} \quad \text{for } \psi \leq -0.236$$

$$b_2 = b_e - b_1 \quad \text{for } \psi > -0.236$$

Equation 3.1.3.1.2-6

where b_e = effective width \mathbf{b} as determined from [Equation 3.1.2.1.1-6](#) with λ determined using \mathbf{k} from [Equation 3.1.3.1.2-3](#).

$b_1 + b_2 \leq \frac{W}{1+\psi}$, the compression portion of the web calculated on the basis of effective section.

The widths \mathbf{b}_1 and \mathbf{b}_2 are plotted in [Figure 3.1.3.1.2-4\(a\)](#) over the entire practical range of ψ . The w/t ratio at which the flat width becomes fully effective is presented in [Figure 3.1.3.1.2-4\(b\)](#) in terms of parameter \mathbf{S} .

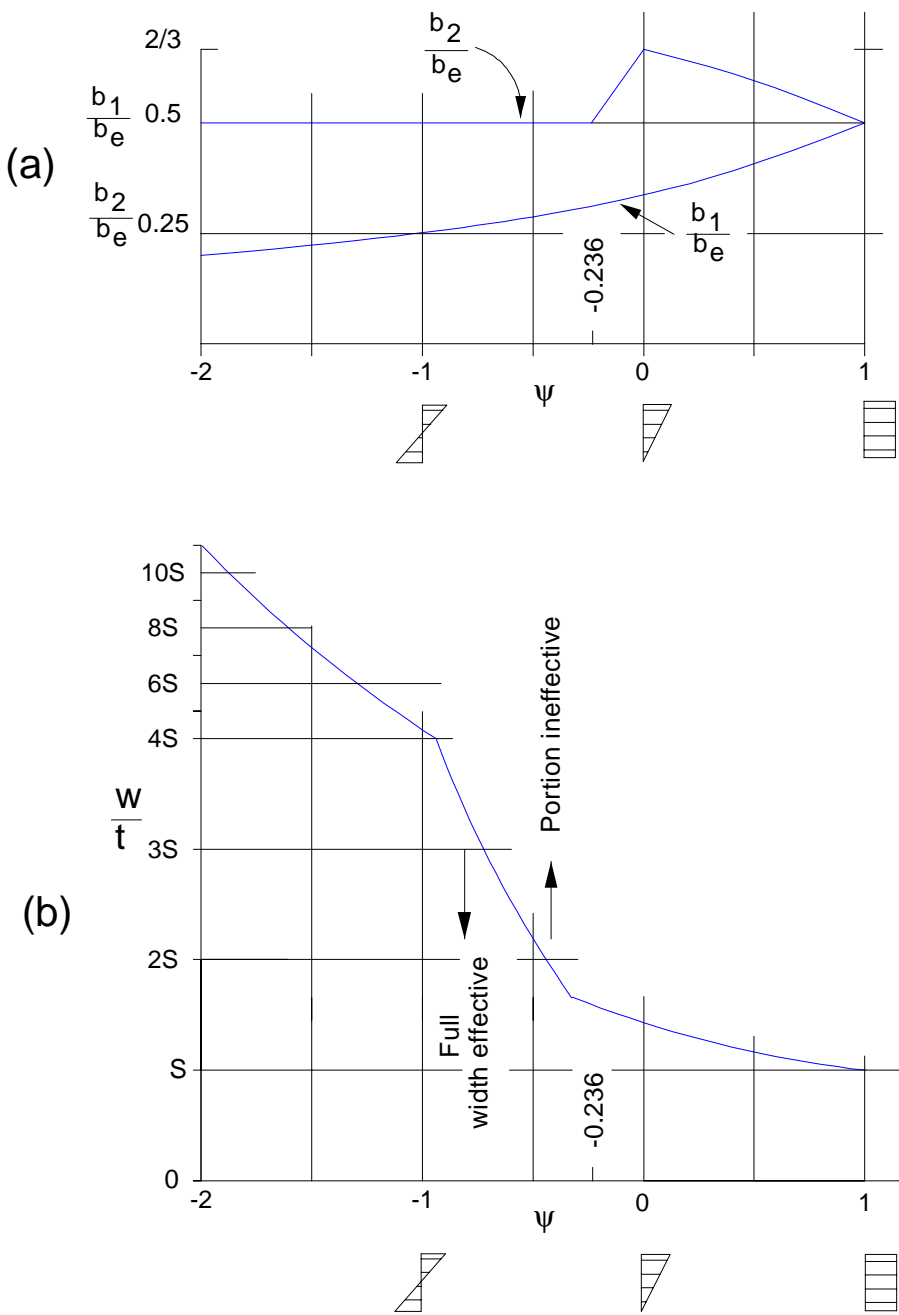


Figure 3.1.3.1.2-4 Effective width for nonuniform compression



The b_1 and b_2 value need not be calculated if w/t is less than the limit. If this is done b_1 plus b_2 will exceed the compression portion of the web when ψ is less than -0.236.

A comparison of the effective width procedure with the stress limit procedure ([Equation 3.1.3.1.2-1](#) and [Equation 3.1.3.1.2-2](#)) indicates that the stress limit procedure is more conservative as the stress variation across the element becomes more flexural (ψ approaches -1).

[Example 3.1-5](#) in [Section 6.2.1.5](#) illustrates how to evaluate the effective web area.

3.1.3.1.3 Inelastic Stress Redistribution

Inelastic stress redistribution allows the section to strain beyond yield under some circumstances. If the w/t ratio of the stiffened element (flange) under compression and the depth/thickness ratio of the compression portion of the web are both less than

$$\frac{1.11}{\sqrt{\frac{F_y}{E}}} \quad (27 \text{ for } F_y = 345 \text{ MPa or } 50 \text{ ksi})$$

the section can be permitted to strain beyond yield provided that the section is not subject to any overall instability, the shear stress is less than $0.577 F_y$, and the web inclination is less than 30° . The effect of cold forming is not included in determining F_y .

Per the AISI specification, the maximum compression strain limit is defined as $C_y e_y$. The strain in compression is limited to 3 times the yield strain $e_y = F_y/E$; there is no limit on tensile strain. The uniformly stiffened compression element (flange) cannot be a multiple stiffened element or stiffened by an edge stiffener; it must be stiffened by two stiffened elements (webs). Thus, only tubular shapes or hat sections can achieve this additional capacity with post yield compression straining.

For fully stiffened compression elements without intermediate stiffeners ([Section 3.1.2.1.1](#)),

$$\begin{aligned} C_y &= 1 & \text{for } \frac{w}{t} \leq \lambda_1 \\ C_y &= 3 - 2\left(\frac{w/t - \lambda_1}{\lambda_2 - \lambda_1}\right) \text{ for } \lambda_1 < \frac{w}{t} < \lambda_2 \\ C_y &= 3 & \text{for } \frac{w}{t} \geq \lambda_2 \end{aligned} \quad \text{Equation 3.1.3.1.3-1}$$



where

$$\lambda_1 = \frac{1.11}{\sqrt{F_y/E}} \quad \text{Equation 3.1.3.1.3-2}$$



$$\lambda_2 = \frac{1.28}{\sqrt{F_y/E}} \quad \text{Equation 3.1.3.1.3-3}$$



For other types of elements, $C_y = 1$.

The computation process to include the inelastic stress might be tedious for hand calculation. Thus, for preliminary design purposes, it is conservative to simply limit compression strain to e_y for

$$\frac{w}{t} > \frac{1.11}{\sqrt{\frac{F_y}{E}}}$$

The strain of $3F_y/E$ at $F_y = 345$ MPa (50 ksi) is essentially 0.005 mm/mm. This illustrates that the inelastic straining permitted is actually quite small relative to the total elongation available in most sheet steel.

[Figure 3.1.3.1.3-1](#) illustrates the stress distribution that can occur in flexure.

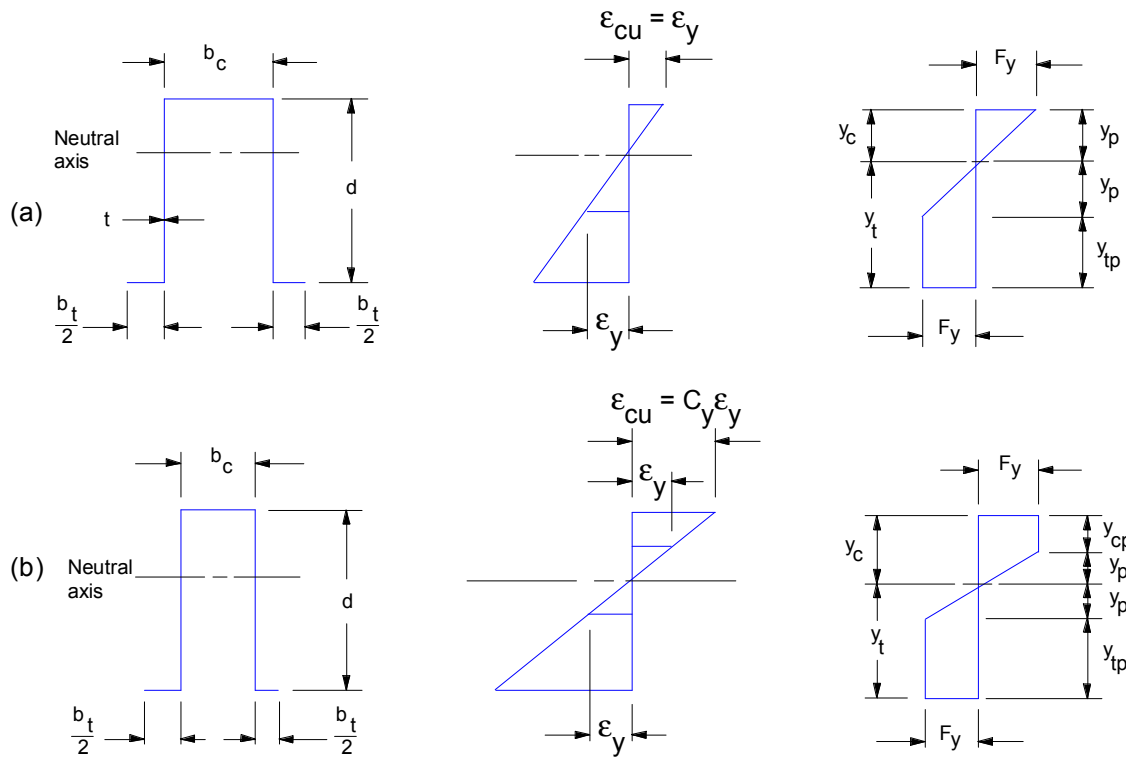


Figure 3.1.3.1.3-1 Stress distribution and ultimate moment in sections with yielded

Case (a) illustrates yielding in tension where no inelastic compression strain is employed which can be used for

$$\frac{w}{t} > \frac{1.11}{\sqrt{\frac{F_y}{E}}}$$

Case (b) illustrates the case where the compression strain is taken to $C_y \epsilon_y$ where the maximum $C_y = 3$. The case where $C_y = 3$ and no tension yield occurs is a highly unlikely situation and is not covered. Both (a) and (b) are governed by the following equations:

$$y_c = \frac{b_t - b_c + 2d}{4}$$

Equation 3.1.3.1.3-4

$$y_t = d - y_c$$

Equation 3.1.3.1.3-5

$$y_p = \frac{y_c}{\epsilon_{cu} / \epsilon_y}$$

Equation 3.1.3.1.3-6

$$y_p = \frac{y_c}{3} \text{ when } C_y = 3$$

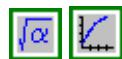
Equation 3.1.3.1.3-7

$$y_{cp} = y_c - y_p$$

Equation 3.1.3.1.3-8

$$y_{tp} = y_t - y_p$$

Equation 3.1.3.1.3-9



$$M_u = F_y t \left[b_c y_c + 2y_{cp} \left(y_p + \frac{y_{cp}}{2} \right) + \frac{4}{3} (y_p)^2 + 2y_{tp} \left(y_p + \frac{y_{tp}}{2} \right) + b_t y_t \right] \quad \text{Equation 3.1.3.1.3-10}$$

$$M_u = F_y t \left[b_c y_c + \frac{52}{27} y_c^2 + d(d - 2y_c) + b_t(d - y_c) \right]; \quad C_y = 3 \quad \text{Equation 3.1.3.1.3-11}$$

$$M_u = F_y t \left[b_c y_c + \frac{4}{3} y_c^2 + d(d - 2y_c) + b_t(d - y_c) \right]; \quad C_y = 1 \quad \text{Equation 3.1.3.1.3-12}$$



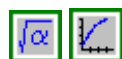
3.1.3.2 Flexural Capacity of Cylindrical Members



Cylindrical members in flexure, such as tubular door intrusion beams, can achieve a plastic moment, which is at least 1.29 times the moment at first yield. The plastic moment can conservatively be calculated as:

$$M_p = 4R^2 t F_y$$

Equation 3.1.3.2-1

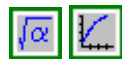


M_p is limited to 1.25 M_y in the 1986 AISI Specification¹. The ultimate moment will be less than M_p for the larger D/t values. Provisions for M_u based on 1986 AISI Specification¹ expressions and related source material are:

$$M_u = M_p \quad \text{for } \frac{D}{t} \leq \frac{0.071E}{F_y}$$

$$M_u = \left(0.775 + \frac{0.016 \frac{E}{F_y}}{\frac{D}{t}} \right) M_p \quad \text{for } \frac{0.071E}{F_y} < \frac{D}{t} \leq \frac{0.320E}{F_y}$$

Equation 3.1.3.2-2



$$M_u = \left(\frac{0.264 \frac{E}{F_y}}{\frac{D}{t}} \right) M_p \quad \text{for } \frac{0.320E}{F_y} < \frac{D}{t} < \frac{0.72E}{F_y}$$

The ultimate moment M_u is equal to the yield moment at $D/t = 0.336 E/F_y$ which is $D/t = 195$ for a 345 MPa (50 ksi) yield stress. The limit for use of the third expression of [Equation 3.1.3.2-2](#) is based on the limit of test data¹³ and extends beyond the limit imposed in the 1986 AISI Specification¹.

3.1.3.3 Shear Stresses for Web Members



In the webs of flanged members it is customary to compute the shear stress as a uniform value of

$$\tau_v = \frac{V}{ht}$$

Equation 3.1.3.3-1



The actual maximum shear stress at the neutral axis of the flexural member may be 25 percent larger than the average value. Limit criteria are based on the average value.

The theoretical maximum possible shear stress is the shear yield stress, which is the tensile yield value divided by 3%. Due to the minor consequences of such yielding, the AISI factor of safety on shear yield is only 1.44. Consistent with the elastic approach, it is thus valid to use $2/3 F_y$ as the shear yield for design purposes. The capacity is reduced by web slenderness using parameter h/t . The ultimate shear force

$$V_u = \frac{2}{3}htF_y \quad \text{for } \frac{h}{t} \leq 2.236\sqrt{\frac{E}{F_y}}$$

$$V_u = 1.49t^2\sqrt{F_y E} \quad \text{for } 2.236\sqrt{\frac{E}{F_y}} < \frac{h}{t} < 3.285\sqrt{\frac{E}{F_y}}$$

$$V_u = 4.895 \frac{t^3}{h} E \quad \text{for } \frac{h}{t} \geq 3.285\sqrt{\frac{E}{F_y}}$$

Equation 3.1.3.3-2  

The above expressions are for webs that are unreinforced (no stiffeners). With web stiffeners that subdivide the web into rectangular panels, an increase in the shear capacity is realized. A shear buckling coefficient greater than the 5.34 used in the above equations will produce the appropriate equations (see AISI Specification¹).

If the web member is curved over its depth, its elastic shear capacity is larger than that given by the third expression in [Equation 3.1.3.3-2](#) due to its curvature. With an arc length of h , the web shear capacity V_u can be expressed per [Reference 7](#).

$$V_u = 4.895 E \frac{t^3}{h} + 0.10 E \frac{t^2 h}{R}$$

Equation 3.1.3.3-3  

[Design Procedure 3.1-12](#), located in [Section 5.2](#), incorporates the procedure described in this section. This procedure and others shown in [Section 5](#) are implemented in AISI/CARS.

3.1.3.4 Combined Flexural and Shear Stresses.....

For webs subjected to both bending and shear where local instability is present, neither of the individual capacities is reached. Instead, the moment and shear force should be limited by the following expression.

$$\left(\frac{M}{M_u}\right)^2 + \left(\frac{V}{V_u}\right)^2 \leq 1$$

Equation 3.1.3.4-1  

This expression is applicable for unreinforced webs. For reinforced webs, a somewhat more liberal interaction expression can be used (see AISI Specification¹).

For sections where yielding is reached and where inelastic straining is possible, there is minimal interaction between shear and flexural capacities. No shear-flexure interaction expression need be used in this case.

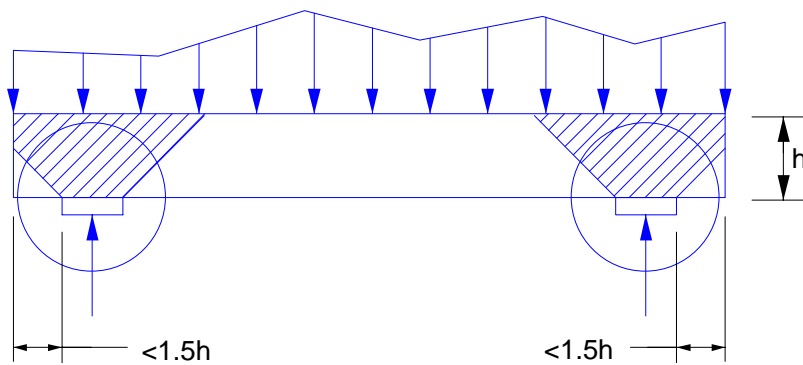
[Design Procedure 3.1-13](#), located in [Section 5.2](#), incorporates the procedure described in this section. This procedure and others shown in [Section 5](#) are implemented in AISI/CARS.

3.1.3.5 Transverse Concentrated Loads and Reactions

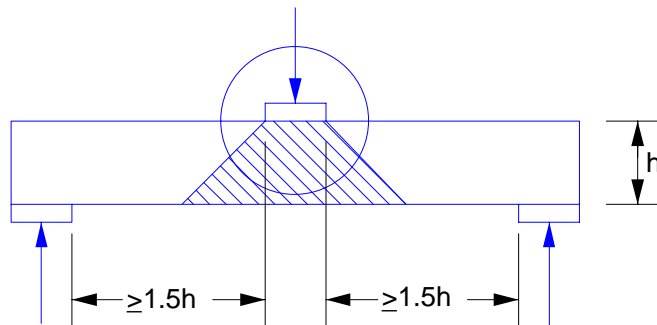
Transverse loads applied to the webs can cripple the webs. A large number of variables affect the crippling capacity of a web that is not reinforced at or near the load locations. The list of variables is as follows:

1. Single web having rotational flexibility or double web having a high degree of restraint against rotation
2. Exterior or interior location of the load or reaction
3. Proximity of another load or reaction on the opposite edge of the web
4. The length of the load or reaction, N
5. The web thickness, t
6. The height of the web, h
7. The corner bend radius, R
8. The angle between the plane of the web and the plane of the bearing surface
9. The yield stress of the material

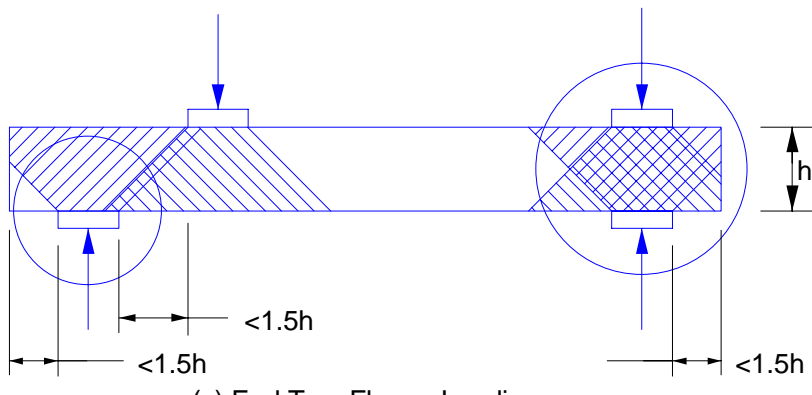
The expressions in the 1980 AISI Specification² and 1981 Design Guide¹⁴ are based on tests where $R/t \leq 6$, $N/t \leq 210$, $N/h \leq 3.5$, and $F_y \leq 386$ MPa (56 ksi) and thus apply for this range. Later testing with higher strength steels has led to changes in web crippling equations. All equations presented here do not consider another load or reaction in close proximity on the opposite edge of the web, or two flange loading. They represent either end or interior one flange loading only. See [Figure 3.1.3.5-1](#).



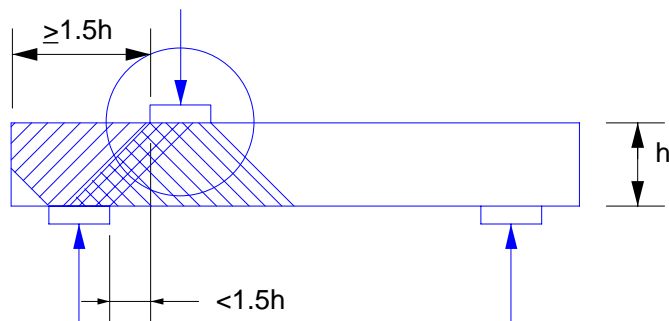
(a) End One-Flange Loading



(b) Interior One-Flange Loading



(c) End Two-Flange Loading



(d) Interior Two-Flange Loading

Figure 3.1.3.5-1 Types of loading and assumed distribution of reaction or load



3.1.3.5.1 Beams with Single Webs.....

The analysis of beams with single webs is divided into two categories that are defined by applied loads and reactions. The two categories are:

- (1) reactions at interior supports and concentrated loads located in the span and
- (2) end reactions or concentrated loads on the outer end of cantilevers.

- (1) For reactions at interior supports and for concentrated loads located in the span

$$P_{cu} = C_t C_h C_R C_N C_F C_\theta$$

Equation 3.1.3.5.1-1



where:

$$\begin{aligned} C_t &= 17.13 t^2 \\ &= 2.485 t^2 \end{aligned}$$

for P_{cu} in N with t in millimeters

Equation 3.1.3.5.1-2



$$\begin{aligned} C_h &= 291 - 0.40 \frac{h}{t} \\ &= 291 \end{aligned}$$

for $F_y < 1165 \text{ MPa (169 ksi)}$

Equation 3.1.3.5.1-3



$$\begin{aligned} C_R &= 1.06 - 0.06 \frac{R}{t} \\ &= 0.7 \end{aligned}$$

for $1 \leq \frac{R}{t} < 6$

Equation 3.1.3.5.1-4



$$\begin{aligned} C_N &= 1 + 0.007 \frac{N}{t} \\ &= 0.75 + 0.011 \frac{N}{t} \end{aligned}$$

for $\frac{N}{t} \leq 60$

Equation 3.1.3.5.1-5



$$\begin{aligned} C_F &= \left(1.375 - 0.375 \frac{F_y}{F_o} \right) \frac{F_y}{F_o} \\ &= 1.26 \end{aligned}$$

for $F_y < 631 \text{ MPa (91.5 ksi)}$

Equation 3.1.3.5.1-6



$$F_o = 345 \text{ MPa (50 ksi)}$$

$$C_\theta = 0.7 + 0.3 \left(\frac{\theta}{90} \right)^2$$

θ defined in Appendix A

Equation 3.1.3.5.1-7



The above relationships incorporate results from recent data^{15, 16, 17} which were evaluated in a University of Missouri-Rolla report¹⁸. They include specimens having yield stresses to 745 MPa (108 ksi) and ultra high strength yields from 1165 to 1300 MPa (169 to 189 ksi).

The presence of a high concentrated load at a point of high bending moment will reduce the capacity of the concentrated load as well as the bending moment capacity. The ultimate strength version of the 1980 AISI Specification⁴ expression is

$$1.07 \frac{P}{P_{cu}} + \frac{M}{M_u} \leq 1.42$$

Equation 3.1.3.5.1-8



which should be checked in addition to checking

$$\frac{P}{P_{cu}} \leq 1$$

Equation 3.1.3.5.1-9

$$\frac{M}{M_u} \leq 1$$

Equation 3.1.3.5.1-10

Additional testing ([References 19, 20, 21, 22](#)) has led to the development of completely new equations for interior single webs. Two modes of web crippling failure are considered to exist: an overstressing or localized bearing failure and a web buckling failure. These equations have been developed for a limited range of parameter variation. These expressions will undoubtedly be refined and altered based on future testing.

Based on overstress,

$$P_{cy} = Ct^2 F_y \left(1 + 0.217 \sqrt{\frac{N}{t}} \right) \left(1 - 0.0814 \frac{R}{t} \right)$$

Equation 3.1.3.5.1-11



where $C = 7.80$ for N, mm, MPa units
 $= 7.80$ for kip, inch, ksi units

In evaluation of P_{cy} in the previous equation, the following limiting values apply:

$$\begin{aligned} \left(1 + 0.217 \sqrt{\frac{N}{t}} \right) &\leq 3.17 \\ (1 - 0.0814 R/t) &\geq 0.43 \end{aligned}$$

The presence of high bending moment may reduce the concentrated load to an amount P_{cm} which can be obtained from the following interaction equation.

$$1.1 \frac{P_{cm}}{P_{cy}} + \frac{M}{M_u} \leq 1.42$$

Equation 3.1.3.5.1-12



Web buckling may control the concentrated load capacity based on the following expression.

$$P_{cb} = Ct^2 \left(1 + 2.4 \frac{N}{h} \right) \left(1 - 0.0017 \frac{h}{t} \right) \left(1 - 0.12 \frac{e}{h} \right)$$

Equation 3.1.3.5.1-13



where $C = 5650$ for N, mm units
 $= 820$ for kip, inch units

In the previous equation,

$$\begin{aligned} \left(1 + 2.4 \frac{N}{h}\right) &\leq 1.96 \\ \left(1 - 0.0017 \frac{h}{t}\right) &\leq 0.81 \\ \left(1 - 0.12 \frac{e}{h}\right) &\geq 0.40 \end{aligned}$$

Other variables are defined in [Appendix A](#).

Should the value of the expression in parentheses be beyond the limiting values, use the limiting values for the expression in [Equation 3.1.3.5.1-13](#). P_{cu} is the lesser of the values obtained for P_{cm} and P_{cb} .

(2) For end reactions or for concentrated loads on outer ends of cantilevers

From the AISI Guide for Preliminary Design¹⁴, in slightly altered form, the ultimate load is

$$P_{cu} = Ct^2 \left(1.15 - 0.15 \frac{R}{t}\right) \left(98 + 4.2 \frac{N}{t} - 0.022 \frac{N h}{t^2}\right) C'_f \quad \text{Equation 3.1.3.5.1-14} \quad \boxed{\sqrt{\alpha}} \quad \boxed{L}$$

where $C = 16.06$ for N, mm, MPa units
 $= 2.33$ for kip, inch, ksi units

$$\begin{aligned} C'_f &= \left(1.60 - 0.6 \frac{F_y}{F_o}\right) \frac{F_y}{F_o} && \text{for } F_y < 458 \text{ MPa (66.5 ksi)} \\ &= 1.07 && \text{for } F_y \geq 458 \text{ MPa (66.5 ksi)} \end{aligned} \quad \text{Equation 3.1.3.5.1-15} \quad \boxed{\sqrt{\alpha}} \quad \boxed{L}$$

where $F_o = 345 \text{ MPa (50 ksi)}$

[Equation 3.1.3.5.1-14](#) is limited to use with materials having yield strengths less than or equal to 552 MPa (80 ksi) per [Reference 20](#).

A new alternative approach similar to that for interior loads has been suggested^{19, 20}. This approach is based on tests of materials with yield strengths as high as 1140 MPa (165 ksi).

Based on overstress,

$$P_{cy} = Ct^2 F_y \left(1 + 0.0122 \frac{N}{t}\right) \left(1 - 0.247 \frac{R}{t}\right) \quad \text{Equation 3.1.3.5.1-16} \quad \boxed{\sqrt{\alpha}} \quad \boxed{L}$$

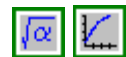
where $C = 9.9$ for N, mm MPa units
 $= 9.9$ for k, in, ksi units

In the above equation, the term $(1 - 0.247 R/t)$ should be as calculated, but not less than 0.32, which occurs for $R/t > 2.75$. The term $(1 + 0.0122 N/t)$ should not exceed 2.22 in evaluating P_{cy} .

Since no moment exists to reduce P_{cy} , it should be compared directly with the failure caused by web buckling

$$P_{cb} = Ct^2 \left(1 - 0.00348 \frac{h}{t}\right) \left(1 - 0.298 \frac{e}{h}\right)$$

Equation 3.1.3.5.1-17



where $C = 9550$ for N, mm, MPa units
 $= 1385$ for kip, inch, ksi units

$$\left(1 - 0.00348 \frac{h}{t}\right) \geq 0.32$$

$$\left(1 - 0.298 \frac{e}{h}\right) \geq 0.52$$

e = clear distance between the closest opposite bearing location measured along the beam

Should the value of the expressions in parentheses be beyond the limiting values, use the limiting values in [Equation 3.1.3.5.1-17](#). P_{cu} would be the smaller of P_{cb} and P_{cy} .

3.1.3.5.2 Sections With High Degree of Restraint Against Web Rotation



Types of web construction with a high degree of rotational restraint are illustrated in [Figure 3.1.3.5.2-1](#).

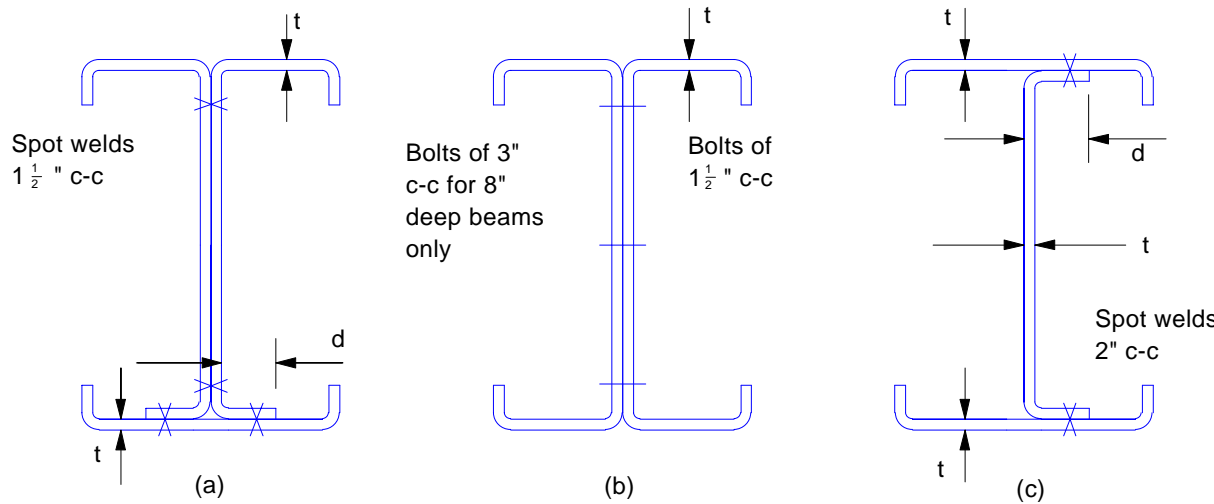


Figure 3.1.3.5.2-1 Typical cross sections used in investigation of web crippling.
High degree of restraint against web rotation.

Webs in hat, channel, zee or tubular sections fall into the first category, which was covered in [Section 3.1.3.5.1](#).

A slightly simplified adaptation of the AISI specification values (using a factor of safety of 2.0) for the capacity of each web thickness, which are in the AISI Preliminary Design Guide¹⁵, is given here.

- (1) For end reactions or for concentrated loads located on the outer end of cantilevers

$$P_{cu} = Ct^2 F_y \left(10 + 1.25 \sqrt{\frac{N}{t}} \right) \quad \text{for } F_y \leq 410 \text{ MPa (60 ksi)}$$
Equation 3.1.3.5.2-1  

where $C = 1$ in N, mm, MPa units
 $= 1$ in kip, inch, ksi units

- (2) For reactions at interior supports or for concentrated load located on the span where the edge of bearing is more than $1.5 h$ from the ends

$$P_{cu} = Ct^2 F_y \left(15 + 3.25 \sqrt{\frac{N}{t}} \right) C'_F$$
Equation 3.1.3.5.2-2  

where C is defined above
 C'_F is defined in [Equation 3.1.3.5.2-3](#)

Recent tests at the University of Missouri-Rolla¹⁹ using steels with yield values from 410 to 786 MPa (60 to 114 ksi) indicated that "end one flange load" can produce a premature failure as shown in [Figure 3.1.3.5.2-2](#), which can substantially reduce load capacity.

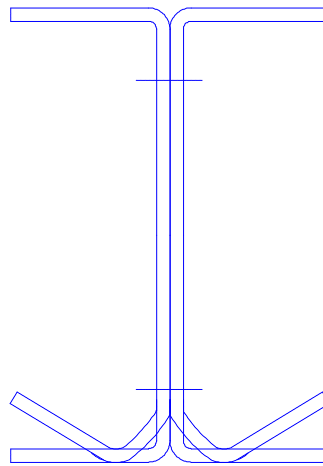


Figure 3.1.3.5.2-2 Sketch showing premature failure at web-flange junction

This failure at the web-flange junction is technically not web crippling and can be avoided by any detail that would tend to prevent the individual flange from rotation about its connection to the other, such as a tie between flanges. Based on this and the fact that the AISI expression is based on tests with $F_y \leq 386$ MPa (56 ksi), it is recommended that [Equation 3.1.3.5.2-1](#) be limited in use to $F_y \leq 410$ MPa (60 ksi).

In 1988, the problem of premature failure of I-beams at the web-flange junction was studied further at the University of Missouri-Rolla. Based on a limited amount of test data and the finite element method, a design equation was developed for cold-formed steel I-beams using high strength sheet steels when they are subjected to end one-flange loading with flanges not connected to bearing plates. For details, see [Reference 23](#).

Similar tests²⁰ for the interior condition indicated that [Equation 3.1.3.5.2-2](#) can be used for higher strength steels. Based on a review of the test data it appears appropriate to apply a C'_F factor for higher strength steels and limit its application due to lack of data for very high strength steels. Define C'_F as follows:

$$\begin{aligned} C'_F &= 1 && \text{for } F_y < 410 \text{ MPa (60 ksi)} \\ C'_F &= 1.15 - \frac{F_y}{2733} && \text{for } 410 \leq F_y \leq 820 \text{ MPa} \\ &= 1.15 - \frac{F_y}{400} && \text{for } 60 \leq F_y \leq 120 \text{ ksi} \\ C'_F &= 0.85 && \text{for } F_y > 820 \text{ MPa (120 ksi)} \end{aligned}$$

Equation 3.1.3.5.2-3



[Example 3.1-6](#) in [Section 6.2.1.6](#) illustrates the application of web crippling analysis.

3.1.3.6 Overall Lateral Instability



Overall or member instability can only occur if the compression side of a flexural member is laterally unbraced and the moment of inertia about the bending moments axis is larger than that about the perpendicular axis. The flexural member would like to buckle so that it can bend about the axis with the least moment of inertia - the minor principal axis.

When a flexural member buckles, it attempts to both translate laterally and twist ([Figure 3.1.3.6-1](#)).

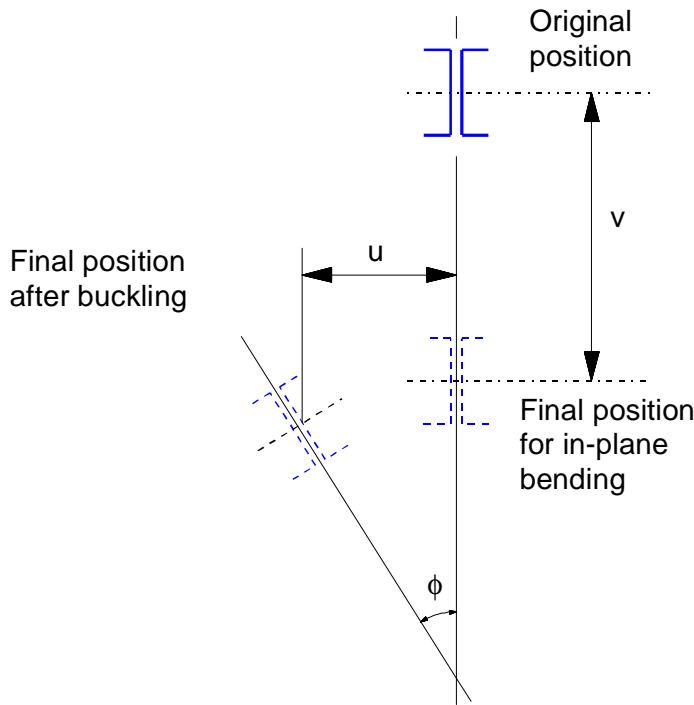


Figure 3.1.3.6-1 Position of I-beam after lateral buckling

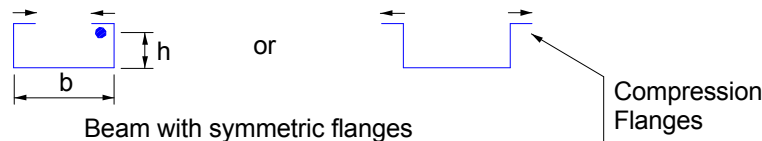
The member twists because the compression flange wants to buckle while the tension flange wishes to remain straight and restrains the translation on the tension side.

Tubular sections, which have a very large torsional stiffness relative to I and channel shaped sections, usually have no lateral buckling problem. For example, rectangular tubular shapes have no strength reduction even at a depth to width ratio of 10 with unbraced length to width ratio of 0.086 E/F_y (Per [Reference 1](#) and AISC Commentary). Even hat sections with two webs have a large torsional stiffness as compared to single web members and are thus economical to use if lateral buckling is a problem. The lack of twist flexibility inhibits the lateral buckling.

Lateral translational restraint of the tension flange and rotational restraint of the web in channel or I-sections also improves the lateral buckling strength of these sections. Treatment of these effects is beyond the scope of this document. Laterally unbraced compression flanges, i.e., flanges that totally rely on the restraint (rotational and translational) that is provided by the tensile flange ([Figure 3.1.3.6-2](#)), are addressed in the AISI Cold Formed Steel Design Manual.

Notes:

1. Arrows indicate probable direction of collapse due to shear.



2. b is portion of tension flange supporting web.



3. h is distance from tension flange to centroid of equivalent column.

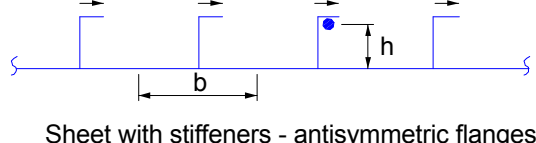


Figure 3.1.3.6-2 Compression flanges relying on tension flange restraint

Flanged open sections receive torsional stiffness from two sources. One is the St. Venant torsional stiffness (usually denoted as J), which produces torsional shear stresses. The other is the warping stiffness which produces weak axis flexural and shear stresses in the flanges.

Since the thickness of cold formed members is small, the St. Venant torsional stiffness, which is a function of t^3 , is ignored. The warping stiffness in combination with the weak axis translational stiffness is used to evaluate the lateral integrity of I or channel shaped members using the elastic critical moment.

$$M_e = \pi^2 E C_b d \frac{I_{yc}}{L^2}$$

Equation 3.1.3.6-1



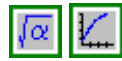
where L = effective unbraced length of the compression flange

d = the depth of the section along web

I_{yc} = moment of inertia of the compression portion of a section about the centroidal axis of the entire section parallel to the web, using the full unreduced section.

$$C_b = 1.75 + 1.05 \frac{M_1}{M_2} + 0.3 \left(\frac{M_1}{M_2} \right)^2 \leq 2.3$$

Equation 3.1.3.6-2



C_b is the bending coefficient which reflects the severity of buckling over the unbraced length based on the moment gradient. M_1 and M_2 are the moments at the ends of the unbraced length. M_1 and M_2 are equal and opposite in sign for uniform bending moment leading to $C_b = 1$. $C_b = 1.75$ when $M_1 = 0$. C_b should be taken as unity when the moment at any point in the unbraced length is larger than the end moments M_1 and M_2 .

The critical moment, M_c , is the lateral buckling moment as affected by inelastic material properties. The lateral buckling moment curves are given in [Figure 3.1.3.6-3](#) as a function of $\frac{M_e}{S_f}$ where M_e is from [Equation 3.1.3.6-1](#) and M_y is as follows:

$$M_y = S_f F_y$$

Equation 3.1.3.6-3



where S_f = elastic section modulus of the full unreduced section for the extreme compression fiber

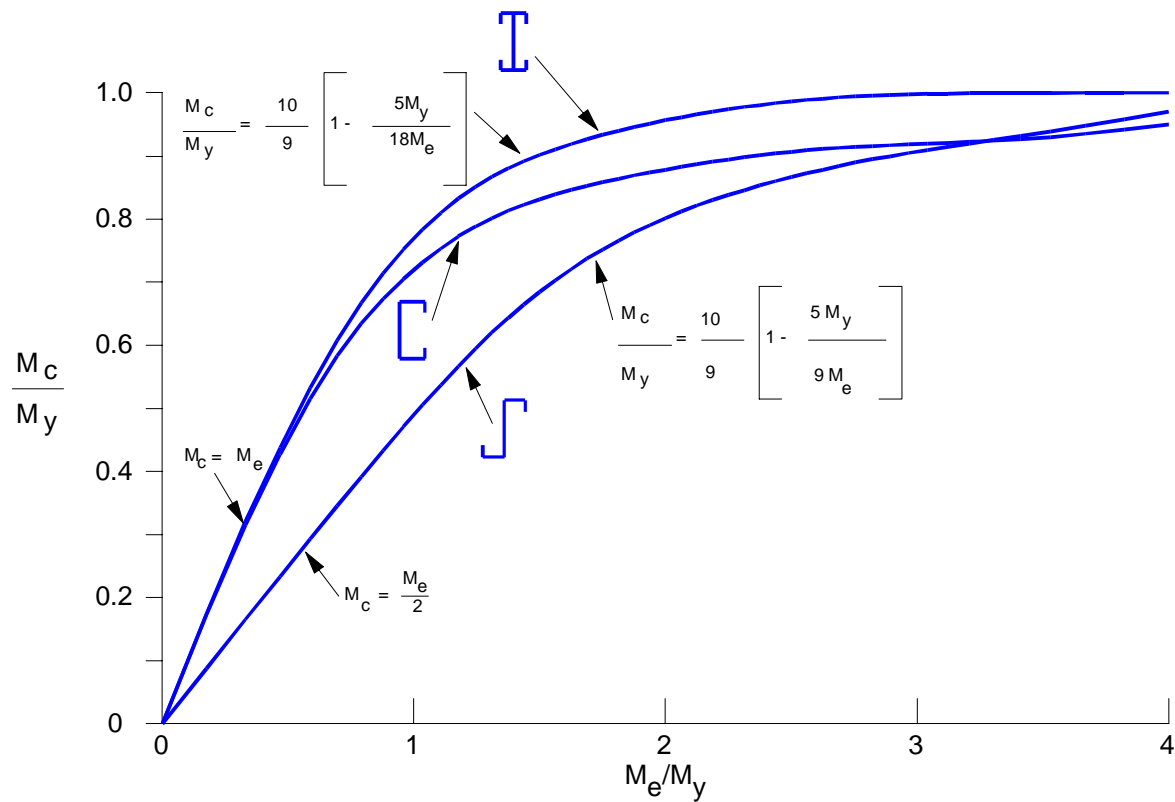


Figure 3.1.3.6-3 Lateral buckling curves for I, C, and Z sections.....



There is an elastic portion, a transition region where inelastic behavior affects the lateral buckling capacity, and a region where the capacity is simply limited by the yield stress of the material.

This chart has a curve for Z shaped sections as well. Z shaped sections will buckle at a moment half of M_e from [Equation 3.1.3.6-1](#). This is the basis for the Z curve. The I and Z shapes follow the same criteria used previously, whereas the equation for the C shapes is different. The value

of M_u in this approach requires the calculation of an effective section modulus S_c , which is to be determined at stress M_c/S_f

$$M_u = \left(\frac{M_c}{S_f} \right) S_c = \text{lateral buckling ultimate moment}$$

Equation 3.1.3.6-4



where S_f = elastic section modulus of the full unreduced section for the extreme compression fiber

S_c = elastic section modulus of the effective section calculated at a stress

$$\frac{M_c}{S_f} \text{ in the extreme compression fiber}$$

Evaluation of lateral buckling capacity is illustrated in [Example 3.1-7](#) in [Section 6.2.1.7](#).

3.1.3.7 Combined Axial and Flexural Overall Stability



The capacity of a member under combined axial and flexural loads is customarily evaluated by means of an interaction equation which reflects the individual flexural and axial capacities. The interaction expression is based on the stress expression $f_a + f_b \leq F$ where F is the stress limit which can be written

$$\frac{f_a}{F} + \frac{f_b}{F} \leq 1.0$$

Equation 3.1.3.7-1



If different stress limits exist for flexure and axial effects, then [Equation 3.1.3.7-1](#) may be rewritten as:

$$\frac{f_a}{F_a} + \frac{f_b}{F_b} \leq 1.0$$

Equation 3.1.3.7-2



This expression can be written in terms of force and moment by multiplying terms by area and section modulus, respectively. The expression can then be generalized to consider biaxial bending as follows:

$$\frac{P}{P_u} + \frac{M_x}{M_{ux}} + \frac{M_y}{M_{uy}} \leq 1.0$$

Equation 3.1.3.7-3



where P = applied axial load

P_u = axial load capacity

M_x, M_y = applied bending moments about each principal axis

M_{ux}, M_{uy} = ultimate bending moment calculated for each principal axis separately with no axial load

[Equation 3.1.3.7-3](#) can be used directly for three situations:

1) Tension

For tension, $P_u = P_y = AF_y$.

2) Compression at points of axial load bracing

In this case, $P_u = A_e F_y$. [Equation 3.1.3.7-3](#) with this maximum P_u should also be checked between points of axial load bracing if C_m (defined later) less than 1 is used.

3) Compression in regions between axial load bracing where the ratio $P/P_u \leq 0.15$

In this case P_u is based on axial capacity considering slenderness effects per [Equation 3.1.2.5-1](#). M_{ux} and M_{uy} should include local buckling effects and also lateral buckling effects (per [Equation 3.1.3.6-3](#)) if the section is laterally unbraced in bending at the location being examined.

If the axial stress in compression is less than 15 percent of the axial stress capacity, the axial load is considered to have a negligible second order effect on the bending moments. If the axial stress ratio is more than 15 percent, the moments are considered to be magnified by a factor

$$\frac{C_m}{\left(1 - \frac{P}{P_e}\right)}$$

Equation 3.1.3.7-4

where P = axial load

P_e = Euler buckling load

$C_m = 0.85$

Equation 3.1.3.7-5

The value 0.85 is typical. An exception is when the compression member is laterally braced against joint translation and is rotationally restrained at the ends and subjected only to end moments, in which case

$$C_m = 0.6 - 0.4 \left(\frac{M_1}{M_2} \right) \geq 0.4$$

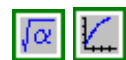
Equation 3.1.3.7-6

where $\frac{M_1}{M_2}$ is the ratio of the smaller to larger end moments

This ratio is -1 for uniform moment and can vary to a ratio of +1 under complete reverse curvature. Thus C_m is to be used with M_2 ; $C_m M_2$ represents an equivalent midspan moment.

When $P/P_u > 0.15$, the interaction expression

$$\frac{P}{P_u} + \frac{C_{mx} M_x}{\left(1 - \frac{P}{P_{ex}}\right) M_{ux}} + \frac{C_{my} M_y}{\left(1 - \frac{P}{P_{ey}}\right) M_{uy}} \leq 1.0$$

Equation 3.1.3.7-7

where all terms are as defined in [Equation 3.1.3.7-3](#), is to be used to check a compression member in its unbraced region. The variable P_{ex} , for bending about the x-axis or in the y-plane, is

$$P_{ex} = \frac{\pi^2 E I_x}{(K_x L_x)^2}$$

Equation 3.1.3.7-8

where L_x = the actual axial unbraced length in the y-plane of bending

K_x = corresponding effective length factor

I_x = moment of inertia of the full unreduced section about the x-axis of bending

A corresponding set of definitions exists for P_{ey} . When [Equation 3.1.3.7-7](#) is employed, [Equation 3.1.3.7-3](#) (situation 2) should also be checked since the C_m factors may cause [Equation 3.1.3.7-3](#) (situation 2) to be more critical. This is especially true if C_m is calculated from end moments.

If the section being examined is a cylindrical tube subjected to biaxial bending, the vector sum of the moments should be obtained. The section should then be treated as an uniaxial bending problem in the interaction [Equation 3.1.3.7-3](#) and [Equation 3.1.3.7-7](#). The biaxial interaction expression is accurate for rectangular sections, but becomes increasingly conservative as the section loses its corners and becomes more rounded.

3.1.4 TORSION OF MEMBERS



Linear members may be subjected to torsional loads or may twist during application of other types of loading. Torsional stresses introduced by the twisting are often much less important than the torsional deformation that occurs. The twist strength and stiffness of various section shapes will be examined as well as buckling that involves torsion.

3.1.4.1 Strength and Stiffness

Members that have a mass of concentrated cross-sectional area, such as a square or circular solid, have good torsional properties. However, these shapes are not economical based on the amount of material. Torsional integrity in the economic thin wall stamping depends on whether the section is an open or closed section.

3.1.4.1.1 Closed Shapes

Closed shapes are tubular sections. Tubes can be circular, elliptic, square, rectangular, or some unusual shape. When these shapes are twisted, they undergo little distortion or visible displacement because they are very stiff.

The shear stress in these sections can be evaluated from the following expression.

$$\tau_t = \frac{T}{2at}$$

Equation 3.1.4.1.1-1



where T = the applied torque

t = tube wall thickness

a = area enclosed by the mean perimeter of the tube wall

In a circular tube $a = \pi R^2$. This stress exists at all locations along the perimeter as long as the wall thickness remains constant.

The torsion stiffness is evaluated by means of determining the angle of twist per unit length which can be expressed as

$$\phi = \frac{T}{JG}$$

Equation 3.1.4.1.1-2



where $G = \frac{E}{2(1+\mu)}$ = the shear modulus of elasticity

Equation 3.1.4.1.1-3



$$J = \frac{4a^2}{\sum \left(\frac{l}{t} \right)}$$

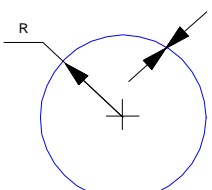
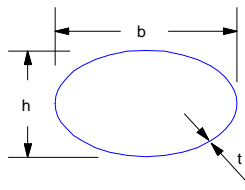
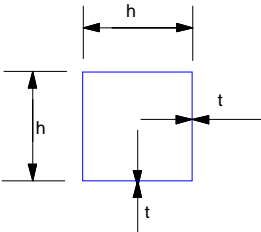
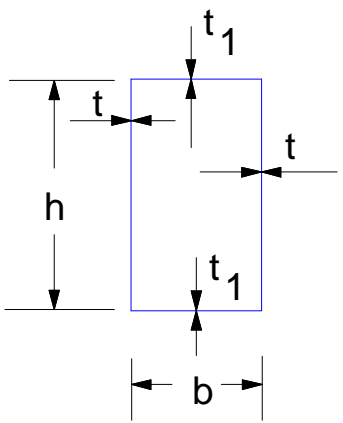
Equation 3.1.4.1.1-4



l/t is the ratio of length of each part on the perimeter divided by its respective thickness.

This constant J is equal to the polar moment of inertia for a circular tube. The torsion properties for several basic shapes are given in [Table 3.1.4.1.1-1](#).

Table 3.1.4.1.1-1 Torsional shear stress and stiffness formulas for closed sections

$v_t = \frac{T}{2\pi R^2 t}$ $J = 2\pi R^3 t$		Equation 3.1.4.1.1-5 Equation 3.1.4.1.1-6	
$v_t = \frac{T}{\frac{\pi}{2} b h t}$ $J = \frac{\pi b^2 h^2 t}{2 \sqrt{2(b^2 + h^2)}}$		Equation 3.1.4.1.1-7 Equation 3.1.4.1.1-8	
$v_t = \frac{T}{2h^2 t}$ $J = h^3 t$		Equation 3.1.4.1.1-9 Equation 3.1.4.1.1-10	
$v_t = \frac{T}{2bht}$ $v_{t1} = \frac{T}{2bht_1}$ $J = \frac{2tt_1 b^2 h^2}{bt + ht_1}$ $J = \frac{2b^2 h^2 t}{b + h}$ for $t_1 = t$		Equation 3.1.4.1.1-11 Equation 3.1.4.1.1-12 Equation 3.1.4.1.1-13 Equation 3.1.4.1.1-14	

3.1.4.1.2 Open Shapes

When a section is made up of thin straight or curved segments, which are not closed to form tubular shapes but left "open" to form sections such as a channel, hat, Z or I, the torsional behavior is substantially different. These sections usually have two components contributing to torsional stiffness - St. Venant's torsion and torsion resistance due to restraint from warping. There are some sections such as angles, tee and cruciform shapes that have only St. Venant torsional stiffness.

St. Venant torsional stiffness for open shapes is given by a modified polar moment of inertia \mathbf{J} , which is

$$\mathbf{J} = \frac{1}{3} \sum I t^3$$

Equation 3.1.4.1.2-1



where I = the length of an element of the cross section
 t = the corresponding thickness of the element

The equation is applicable to sections with large I/t ratios. The length I can be curved as well as straight.

The shear stress for thin wall open shapes can be evaluated from the following expression:

$$\mathbf{v}_t = \frac{Tt}{\mathbf{J}}$$

Equation 3.1.4.1.2-2



This is a maximum shear stress occurring at the faces of the through thickness, t . The largest shear occurs in the element with the largest thickness. In cold formed sections made from a single flat piece of material with radius corners, the shear stress v_t is essentially the same along the entire length. The variable I can be taken as the length of the entire section for this case.

The angle of twist per unit length can be evaluated from [Equation 3.1.4.1.1-2](#) where \mathbf{J} is the value computed using [Equation 3.1.4.1.2-1](#). Under St. Venant torsional deformation, the flat or curved elements of a member remain straight along its length. The elements only warp from the shear into a parallelogram shape, but do not bend or curve along their length.

If a section has flange and/or webs some distance apart, twisting usually forces these elements to bend in addition to warping. The flexural stiffness depends on the end restraint conditions and the span length.

The torsion analysis of beams including the effect of flexural and shear stresses from warping restraint is beyond the scope of this document. Refer to Yu¹³ for a treatment of this topic. [Example 3.1-8](#) in [Section 6.2.1.8](#) illustrates the difference in relative torsional stiffness of open and closed sections.

3.1.4.2 Torsional, Torsional- Flexural Buckling

Often, when the unbraced length of members becomes relatively short, it is assumed that buckling will not occur. However, this is when torsional buckling is likely to occur for an open section.

Pure torsional buckling can occur under axial load for doubly symmetric sections or point symmetric sections such as a Z-section. If such a member has a relatively small slenderness ratio, is of small thickness (small J) and has limited warping stiffness, it is more likely to buckle torsionally. Yu^{12} indicates that since the torsional buckling stress is similar to the local buckling stress, this type of member will not fail by torsional buckling if correctly designed for local buckling.

For singly symmetric shapes such as illustrated in [Figure 3.1.4.2-1](#), buckling can occur about the y-axis.

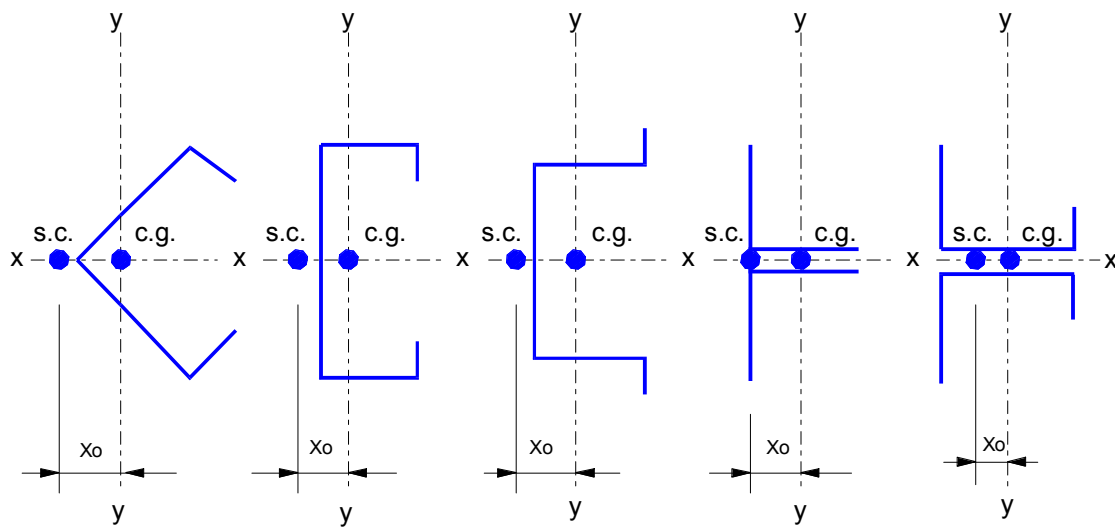


Figure 3.1.4.2-1 Singly symmetric open sections

This is the likely failure mode when the axial load is centered at or to the left of the shear center (away from the centroid). Inelastic behavior is to be expected at failure due to the low slenderness ratio causing $F_u > F_y/2$.

When the eccentricity places the load to the right of the c.g. the member may begin to buckle about the y-axis, but failure can also occur in a torsional - flexural mode (the y-axis flexural and torsional modes coupled) at a lower load. An I section of relatively thin material with an I_x value close to or larger than the I_y value is a likely candidate for torsional - flexural buckling.

Should such conditions exist, either the section should be changed to a closed section or the procedures in Sections C4.2 and C3.1.2 of the 1986 AISI Specification¹ should be employed to obtain F_e and M_e respectively.

REFERENCES FOR SECTION 3.1

1. American Iron and Steel Institute, Specification for the Design of Cold-Formed Steel Structural Members, 1986 Edition with December 11, 1989 Addendum, Washington, D.C.
2. American Iron & Steel Institute, Specification for the Design of Cold-Formed Steel Structural Members, September, 1980.

3. Pan, Lan-Cheng, "Effective widths of High Strength Cold-Formed Steel Members", PhD Thesis, University of Missouri-Rolla, 1987.
4. Plantema, F.J., "Collapsing Stresses of Circular Cylinders and Round Tubes," report S. 280, Nat. Luchtvaarlaratorium, Amsterdam, Netherlands, 1946.
5. Parks, B., and Yu, W.W., "Design of Automotive Structural Components Using High Strength Sheet Steels: Preliminary Study of Members Consisting of Flat and Curved Elements", Fourth Progress Report, Civil Engineering Study 83-5, University of Missouri-Rolla, August, 1983.
6. Parks, B., and Yu, W.W., "Design of Automotive Structural Components Using High Strength Sheet Steel: Structural Behavior of Members Consisting of Flat and Curved Elements", Ninth Progress report, Civil Engineering Study 87-2, University of Missouri-Rolla, June, 1987.
7. Sechler, E.E. and Dunn, L.G., Airplane Structural Analysis and Design, New York, NY, John Wiley and Sons, Inc., 1942.
8. Barton, M.V., Fundamentals of Aircraft Structures, New York, NY, Prentice-Hall, Inc., 1948.
9. Parks, M. B., Santaputra, C. and Yu, W.W., "Structural Behavior of Members Consisting of Curved Elements", Proceedings of the Sixth International Conference on Vehicle Structural Mechanics, April, 1986.
10. Parks, M. B. and Yu, W.W., "Structural Behavior of Members Consisting of Flat and Curved Elements", Proceedings of the SAE International Congress and Exposition. February, 1987.
11. Parks, M. B. and Yu, W.W., "Local Buckling Behavior of Stiffened Curved Elements", International Journal on Thin-Walled Structures, Vol. 7, No. 1, Elsevier Applied Science, London, U.K., 1989
12. Yu, Wei-Wen, Cold Formed Steel Design, Second Edition, 1991, John Wiley & Sons, Inc., New York, N. Y.
13. Structural Stability Research Council, T.V. Galambos, editor, Guide to Stability Design Criteria for Metal Structures, Fourth Edition, John Wiley & Sons, New York, N.Y. 1988.
14. American Iron and Steel Institute, Guide for Preliminary Design of Sheet Steel Automotive Structural Components, 1981 Edition.
15. Errera, S.J., "Automotive Structural Design Using the AISI Guide," SAE Technical Paper Series 820021, February 22-26, 1982.
16. Levy, B.S., "Advances in Designing Ultra High Strength Steel Bumper Reinforcement Beams," SAE Technical Paper Series 830399.

17. Vecchio, M.T., "Design Analysis and Behavior of a Variety of As Formed Mild and High Strength Sheet Materials in Large Deflection Bending", SAE Technical Paper Series 830398.
18. Santaputra, C., and Yu, W.W., "Design of Automotive Structural Components Using High Strength Sheet Steels: Strength of Beam Webs", Third Progress Report, Civil Engineering Study 83-4, University of Missouri-Rolla, August, 1983.
19. Santaputra, C., and Yu, W.W., "Design of Automotive Structural Components Using High Strength Sheet Steels: Structural Behavior of Beam Webs Subjected to Web Crippling and a Combination of Web Crippling and Bending," Fifth Progress Report, Civil Engineering Study 84-1, University of Missouri-Rolla, October, 1984.
20. Santaputra, C., and Yu, W.W., "Design of Automotive Structural Components Using High Strength Sheet Steels: Web Crippling of Cold Formed Steel Beams", Eighth Progress Report, Civil Engineering Study 86-1, University of Missouri-Rolla, August, 1986.
21. Santaputra, C., Parks, M. B., and Yu, W.W., "Web Crippling of Cold-Formed Steel Beams Using High Strength Sheet Steels", Proceedings of the Sixth International Conference on Vehicle Structural Mechanics, April, 1986.
22. Santaputra, C., Parks, M. B., and Yu, W.W., "Web Crippling Strength of Cold-Formed Steel Beams", Journal of Structural Engineering, ASCE, Vol. 115, No. 10, October, 1989.
23. Lin, S.H., Hsiao, L.E. , Pan, C.L. and Yu, W.W., "Design of Automotive Structural Components Using High Strength Sheet Steels: Structural Strength of Cold-Formed Steel I-Beams and Hat Sections Subjected to Web Crippling", Tenth Progress Report, Civil Engineering Study 88-5, University of Missouri-Rolla, June, 1988.

3.2 CURVED MEMBERS

When linear members are curved, the analysis of the member is no longer as simple as it is for a straight member. The stability considerations change from those in a straight member. The stresses at a location diverge from that obtained from normal flexural theory. Furthermore, additional stresses occur that can be more of a problem than the flexural stresses. The flexibility of curved members also tends to increase with increase in curvature.

The first section will cover the member in a moderately curved situation where overall member behavior is the major concern. The second section will cover the member cross section and how it behaves when curved, especially when highly curved.

3.2.1 EFFECT ON FLEXURAL AND COMPRESSION BEHAVIOR

A curved member, if restrained from relative lateral translation of the ends, can exhibit completely different in-plane behavior than a straight member or a curved member with end movement. Under compression induced by lateral loads, such a member will buckle as shown in [Figure 3.2.1-1](#).

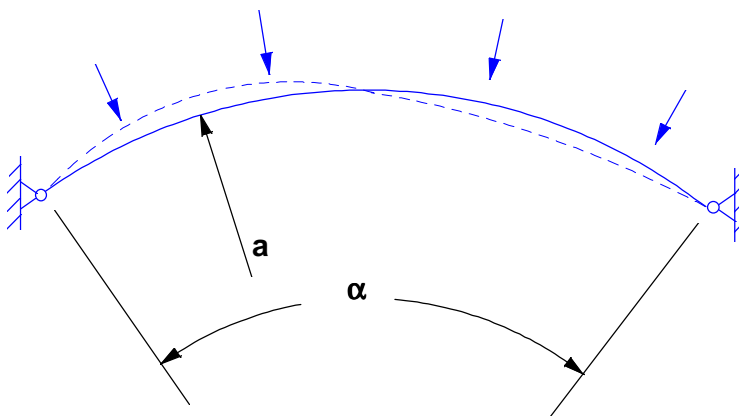
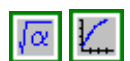


Figure 3.2.1-1 Buckling of curved compression members

The effective length is approximately half of the arc length. The effective length can be calculated as:

$$\frac{L_{\text{eff}}}{L} = \frac{\pi}{\sqrt{4\pi^2 - \alpha^2}}; \alpha \leq \pi$$

Equation 3.2.1-1



where α = included angle in radians

If the ends are rotationally restrained, the effective length will be even lower. [Equation 3.2.1-1](#) can still be used if the inflection point location near the ends can be determined or estimated. Measure to the inflection point in this case.

Often a tie member is employed to keep the ends from translating. This is especially important when the curved member becomes very shallow and requires large thrust with little end displacement to carry the load.

When the rise-to-span ratio (see [Figure 3.2.1-2](#)) is less than about 0.07, the member should be analyzed together with its tie system to evaluate the end displacement or the member should be considered only as a flexural member under lateral loads.

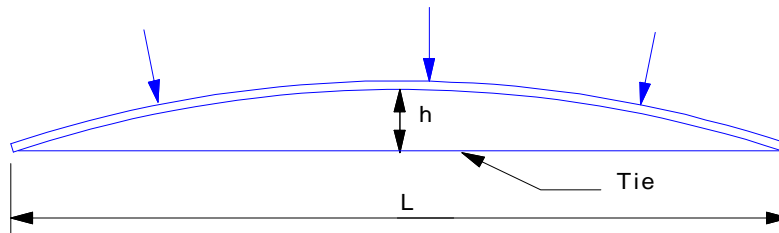


Figure 3.2.1-2 Curved compression member with tie

If a curved member is subjected to end loads as shown in [Figure 3.2.1-3](#) and the ends can deflect, the situation is that of a column with initial eccentricity.

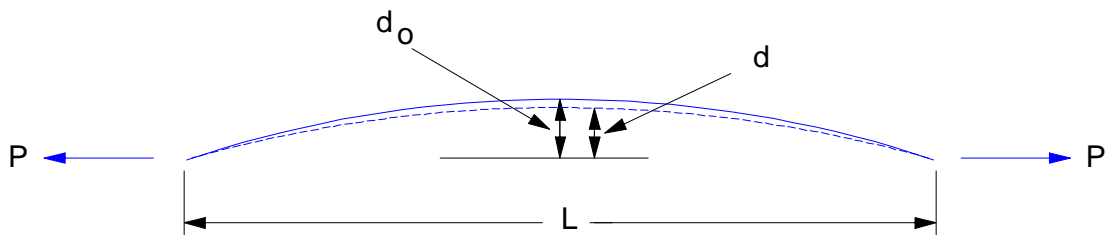


Figure 3.2.1-3 Curved member with end loading

If the value of d_o is small relative to its length, the final lateral position d and the corresponding maximum stress f_{max} can be evaluated as follows:

$$d = \frac{d_o}{\left(1 + \frac{P}{P_e}\right)}$$

Equation 3.2.1-2



$$f_{max} = \frac{P}{A} \left(1 + \frac{d_o c}{r} \frac{P_e}{P + P_e}\right)$$

Equation 3.2.1-3



where A = cross sectional area

r = radius of gyration

c = distance to extreme fiber

P_e = Euler load from [Equation 3.2.1-4](#)

P = applied load; tension positive, compression negative

$$P_e = \frac{\pi^2 E A}{\left(\frac{L_{eff}}{r}\right)^2}$$

Equation 3.2.1-4



The stress f_{max} can be compared with the axial stress limit or the axial and flexural stress can be computed separately and used in the interaction equations in [Section 3.1.3.7](#).

Considering the curved member in [Figure 3.2.1-3](#) as a single straight member for purposes of computer modeling is acceptable for $d_o / L < .07$. When this is done the axial stiffness is reduced. An effective area can be estimated for modeling purposes as:

$$A_{\text{eff}} = \frac{A}{1 + 0.52 \left(\frac{d_o}{r} \right)^2}$$

Equation 3.2.1-5



where r is the radius of gyration of the section.

For larger curvatures the curved member would best be considered as a series of straight line or shallow curved segments.

If a curved member is subjected to uniform moment, its lateral stability can be larger or smaller than for a straight member of the same length in which bending occurs about the strong axis. Timoshenko¹ illustrates this for sections with St. Venant torsional stiffness, but with no warping stiffness. Flexure producing compression on the outside of the bend produces a buckling moment less than that of a straight bar while compression on the inside of the bend leads to a higher buckling moment than in a straight bar.

For curved members subject to lateral buckling (especially if the outside is in compression) it is very important to restrain the ends of the curved member against weak axis rotation in order to achieve significant lateral stability. Significant improvement of lateral stability can be achieved by intermediate lateral bracing. Examination of the member should also include a careful evaluation of the integrity of the cross section under flexure, as covered in the next section.

3.2.2 BEHAVIOR OF SECTIONS AT LOCATIONS OF HIGH CURVATURE

Behavior of sections that are not straight or mildly curved diverge from normal flexural theory in several aspects.

3.2.2.1 Sections with Webs in Plane of Curvature



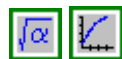
The inner fibers of a curved section have flexural stresses higher than obtained from normal flexural theory. Radial stresses are developed in the webs from the bending moments. The portions of flanges away from the webs lose their effectiveness and transverse bending occurs.

When a/c , the ratio of radius of the curved beam to the distance from inner fiber to centroidal axis (see [Figure 3.2.2.1-1](#)) is less than 10, the stress increase at the inner fiber should be considered. A corresponding decrease from normal flexural theory occurs at the outer fiber of the section. At a/c of 10 the stress increase is about 7 percent.

The stress in a curved member can be calculated using the Winkler-Bach formula:

$$f_b = \frac{M}{Aa} \left[1 + \frac{y}{Z(a+y)} \right]$$

Equation 3.2.2.1-1



where A = cross sectional area of the section

y = distance from the centroidal axis (+ y away from center of curvature)

Z = section property defined in [Equation 3.2.2.1-2](#) to [Equation 3.2.2.1-4](#)

The neutral axis moves toward the center of curvature as shown in [Figure 3.2.2.1-1](#). Its location can be determined directly from [Equation 3.2.2.1-1](#).

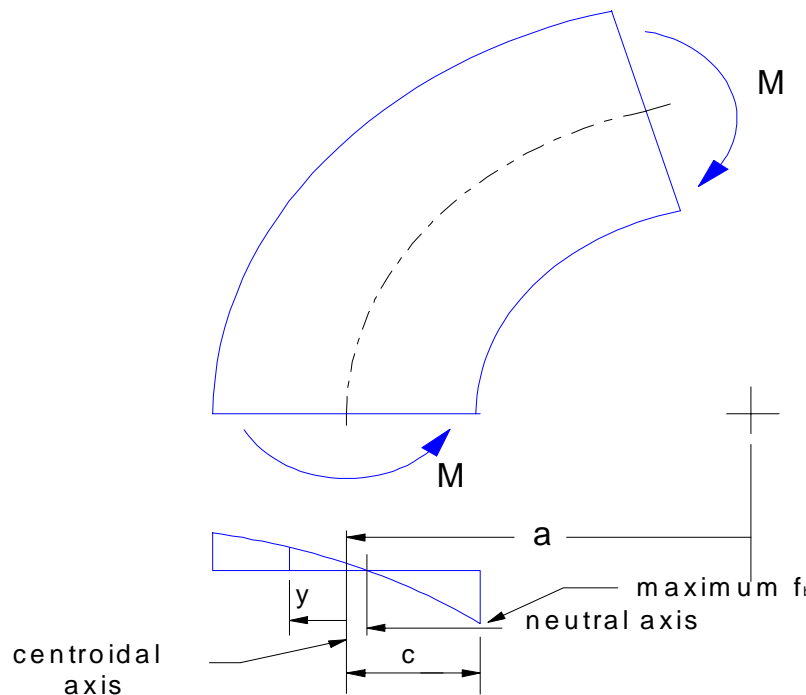


Figure 3.2.2.1-1 Flexural stress in a curved member

$$Z = -1 + \frac{a}{h} \ln \frac{a+c}{a-c}$$

Equation 3.2.2.1-2



where a , c , and h are defined in [Figure 3.2.2.1-2\(a\)](#)

$$Z = -1 + \frac{a}{A} \left[b \ln \frac{a_o}{a_i} - (b - t_w) \ln \frac{a_o - t}{a_i + t} \right]$$

Equation 3.2.2.1-3



where a , a_i , a_o , b , t , and t_w are defined in [Figure 3.2.2.1-2\(b\)](#)

$$Z = -1 + \frac{a}{A} \left[(b'_o + t_w) \ln a_o - (b'_i + t_w) \ln a_i - b'_o \ln (a_o - t) + b'_i \ln (a_i + t) \right]$$

Equation 3.2.2.1-4



where a , a_i , a_o , b'_o , c , t , and t_w are defined in [Figure 3.2.2.1-2\(c\)](#)

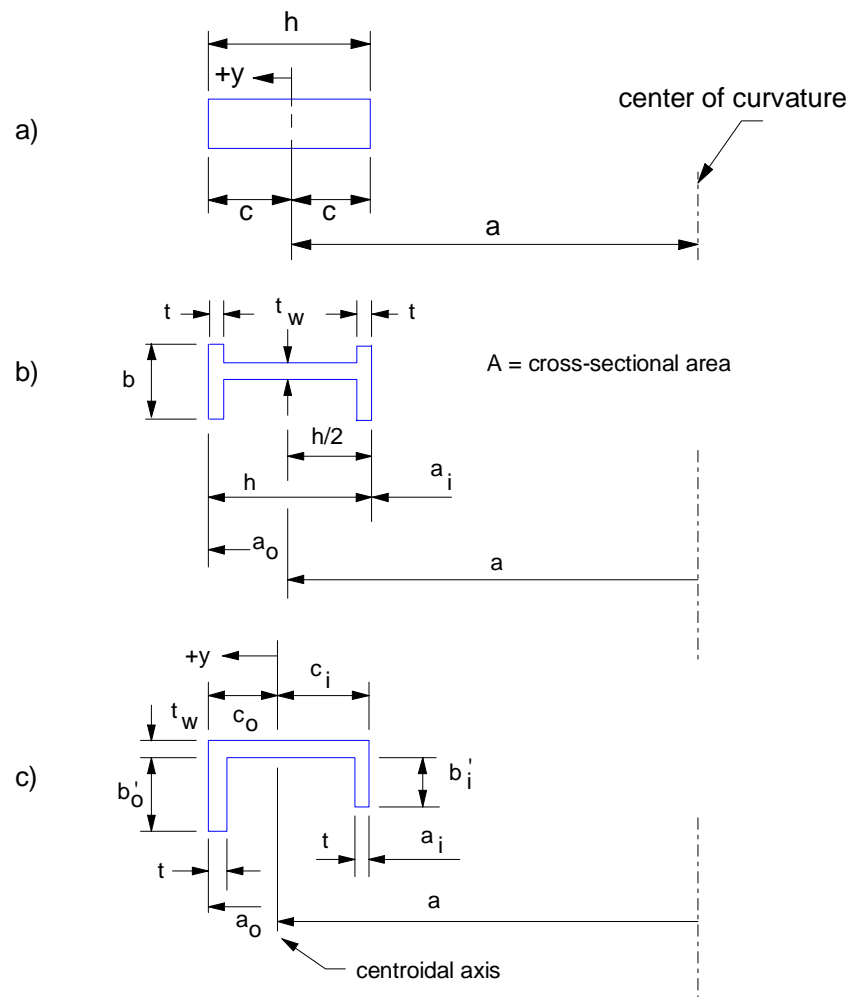


Figure 3.2.2.1-2 Section property Z for curved members

When the section has a flange, the flexural stress in the curved flange distorts the flange. Tension pulls the flange inward and compression pushes the flange outward away from the webs as illustrated in [Figure 3.2.2.1-3](#) for I and rectangular tube sections.

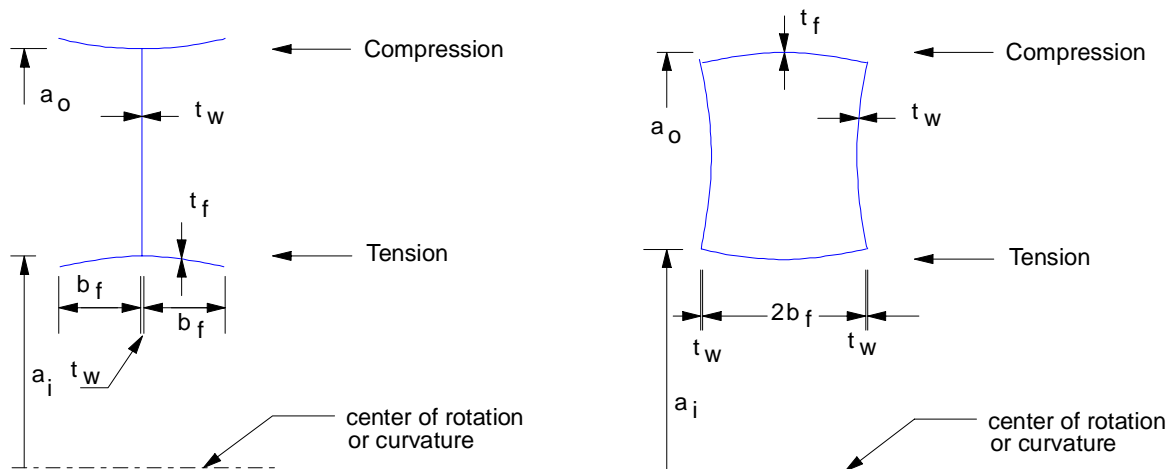


Figure 3.2.2.1-3 Flange distortion in curved members

As a result, the tips of the flanges or the region of the flange away from the webs relieves itself of stress.

This has led to the use of an effective width concept² much like that used for the stiffened compression flange. However, in this case, the effective width is independent of stress level and the concept works well for relatively thin flanges as well as for thick flanges. This effective width can be approximated simply by the following relationship:

$$b' = 0.7\sqrt{a_f t_f} \leq b_f$$

Equation 3.2.2.1-5



where b' = effective flange width adjacent to web

a_f = radius of curvature at flange

t_f = flange thickness

b_f = flange width beyond web as shown in [Figure 3.2.2.1-3](#)

The lesser of the effective width for compression flanges per [Section 3.1.2.1](#) and b' should be used. The b' value is likely to control for thin wall sections. The centroidal axis and area should be evaluated using the effective section with Z being computed using [Equation 3.2.2.1-4](#) since the flange widths are likely to be unequal.

It is recommended to minimize the bend radius at the corners for maximum stiffness. For purposes of analysis, ignore the bend radii and measure b' from the face of the web. The standard moment of inertia of the section considering the b' effective widths as shown in [Figure 3.2.2.1-2](#) is quite satisfactory for stiffness computations. The correct I is never more than 8 percent larger than the standard I .

Transverse bending stress in the flanges is likely to be larger than the circumferential stress evaluated by [Equation 3.2.2.1-1](#). This bending stress induced from the flange distortion illustrated in [Figure 3.2.2.1-3](#) can be calculated approximately from the following expression:

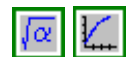
$$f_{btr} = B f_b$$

Equation 3.2.2.1-6



$$\text{where } B = 1.7 \frac{b_f}{\sqrt{a_f t_f}} \leq 1.7$$

Equation 3.2.2.1-7



The f_b used should be the stress at the center of the flange ($t_f/2$ from face), but the outer fiber stress is acceptable for thin-flanged sections.

The radial stress in the web can also be significant. It is critical in the web at the junction with the flange. This stress as illustrated in [Figure 3.2.2.1-4](#) can be approximated from hoop tension relationships to be:

$$f_r = \frac{F_f}{a_f t_w}$$

Equation 3.2.2.1-8



The numerator, F_f , is the flange force so the stress at the center of the flange is the proper value to use. This force, if compressive, in conjunction with compressive circumferential stresses in the web can lead to web crippling.

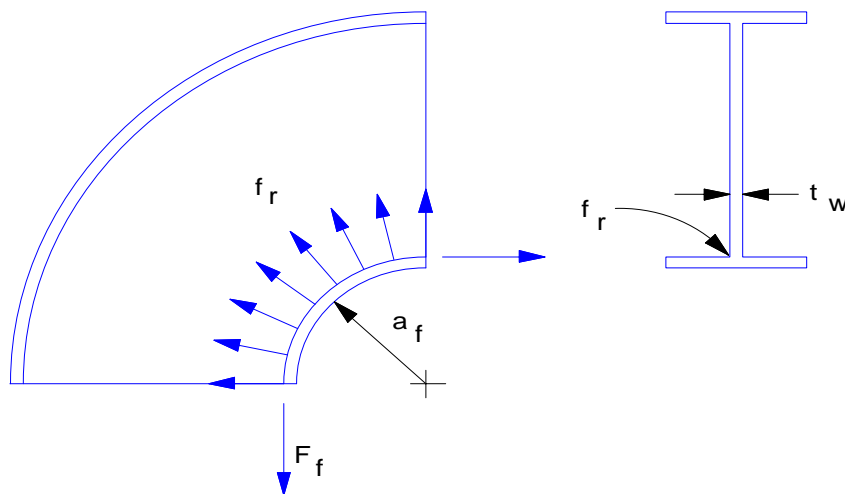


Figure 3.2.2.1-4 Radial web stress in curved members

[Example 3.2-1](#) in [Section 6.2.2.1](#) illustrates the evaluation of section properties and stresses in a curved member with web(s) in the plane of curvature.

3.2.2.2 Curved Circular Tubular Members

When a circular member which is curved is subject to flexure, it distorts in a manner illustrated in [Figure 3.2.2.2-1](#).

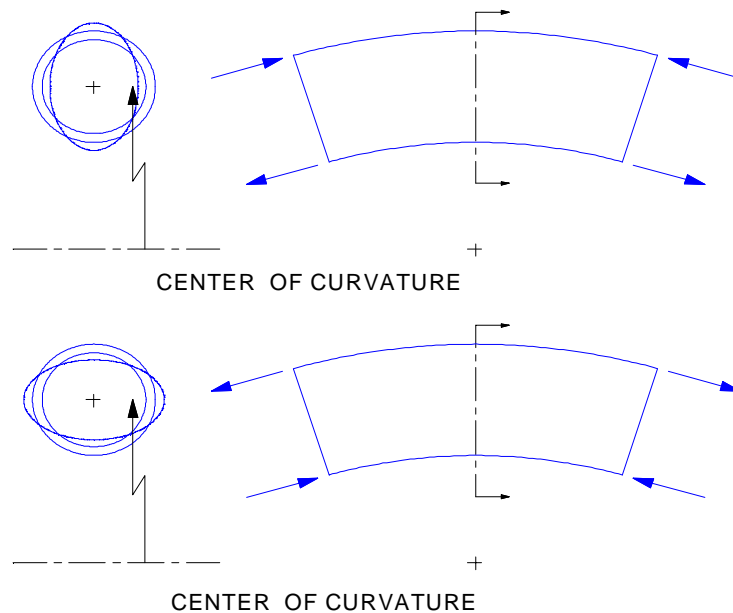


Figure 3.2.2.2-1 Distortion in curved circular members

When the inner portion is in tension and the outer portion in compression, the section will ovalize and elongate in the plane of bending. When the stresses are reversed, the section will flatten.

This behavior increases the flexibility and the stresses beyond that calculated from normal flexural theory. The parameter that defines the situation is:

$$at/R^2$$

where a = radius of curvature to centroidal axis
 t = wall thickness
 R = pipe radius

This parameter is called the flexibility characteristic, g , in piping design.

With the flexibility characteristic, the following expressions from von Karman^{3.4.5} can be used to modify the tube moment of inertia in order to obtain a proper flexibility.

$$\text{effective } I = jI$$

Equation 3.2.2.2-1



$$\text{where } j = 1 - \frac{9}{10 + 12g^2}; g \geq 0.335$$

Equation 3.2.2.2-2



To obtain a value for the maximum stress from flexure, a stress intensification factor, i , can be used to modify the standard stress calculated.

$$f_{b\max} = \frac{iMR}{I}$$

Equation 3.2.2.2-3



$$\text{if } g < 1.472; i = \frac{2}{3j\sqrt{3q}} \geq 1$$

Equation 3.2.2.2-4



$$\text{if } g \geq 1.472; i = \frac{1-q}{j}$$

$$\text{where } q = \frac{6}{5 + 6g^2}$$

Equation 3.2.2.2-5



A somewhat simpler set of expressions for i and j are used in pipe stress analysis work.

$$j = \frac{g}{1.65} \leq 1$$

Equation 3.2.2.2-6

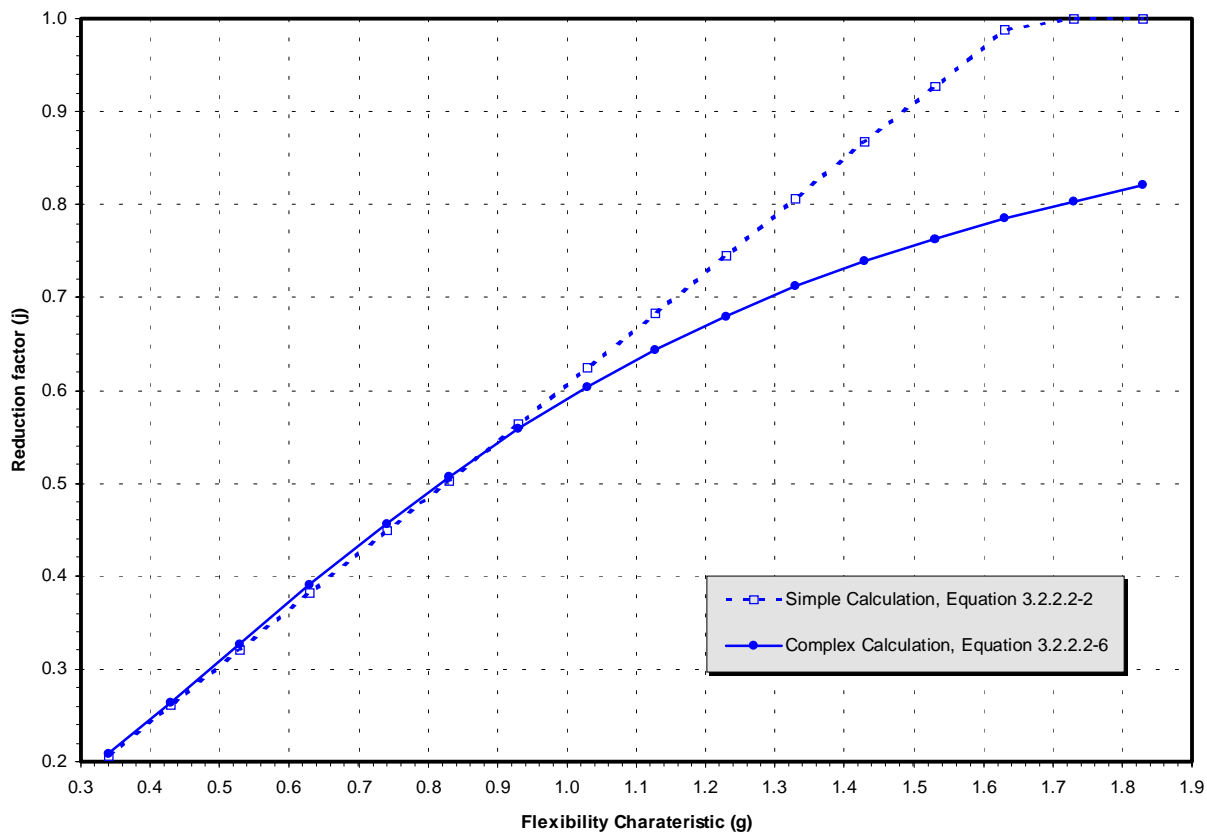
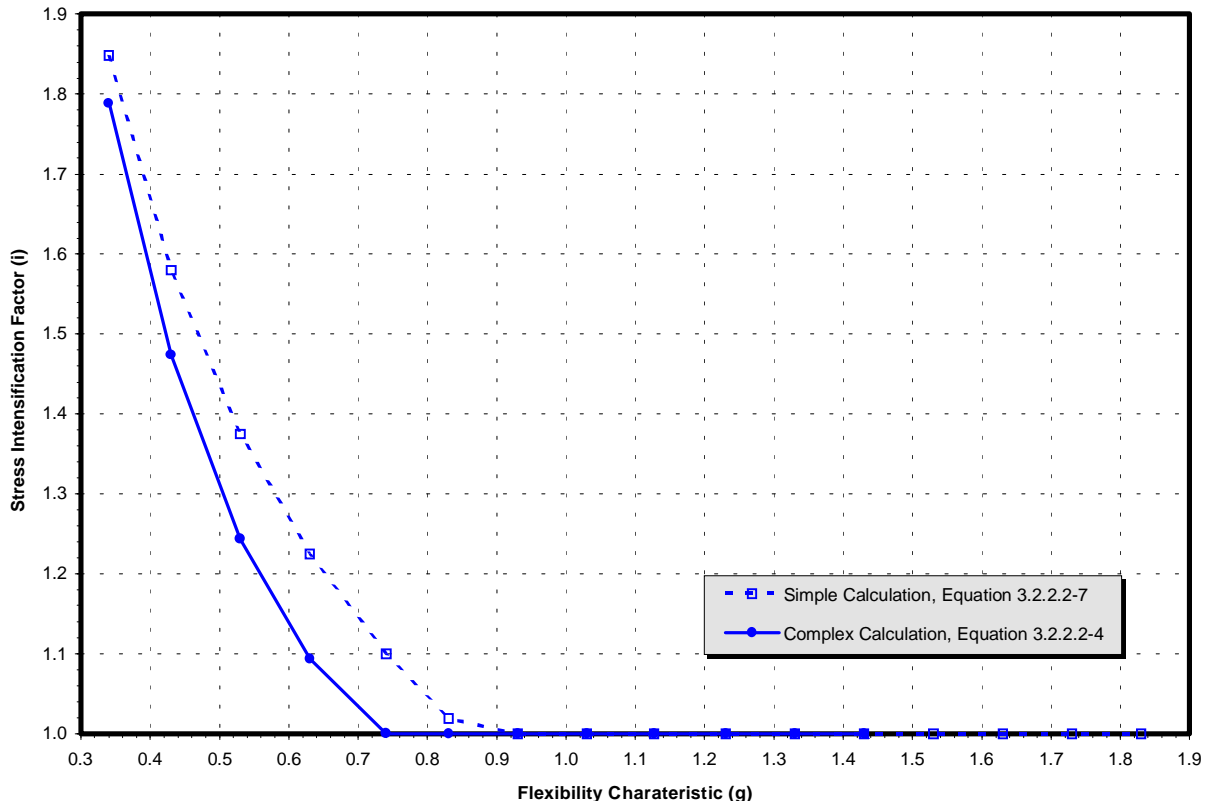


$$i = \frac{0.9}{g^{2/3}} \geq 1$$

Equation 3.2.2.2-7



The use of both these sets of expressions should be limited to cases in which a/R is greater than or equal to 2. The agreement between the two approaches is reasonably good for low levels of g used in [Example 3.2-2](#) in [Section 6.2.2.2](#). The values of j are reasonably close until $g > 1.2$ (see [Figure 3.2.2.2-2](#)). The value of i drops below 1 for $g > 0.73$ using [Equation 3.2.2.2-4](#) while i reaches 1 at $g = 0.854$ in [Equation 3.2.2.2-7](#) (see [Figure 3.2.2.2-3](#)).

**Figure 3.2.2.2-2** Inertia reduction factor (j)**Figure 3.2.2.2-3** Stress intensification factor (i)

REFERENCES FOR SECTION 3.2

1. Timoshenko, S.P. and Gere, J.M., *Theory of Elastic Stability*, McGraw-Hill Book Company, Inc., New York, NY 1961.
2. Seely, F.B. and Smith, J.O., *Advanced Mechanics of Materials*, John Wiley & Sons, Inc., New York, NY, 2nd Ed., 1952.
3. Von Karman, Th., "Uber die Formanderung dunnwandiger Rohre, insbesondere federnder Ausgleichrohre," Z. Vereines Dtsch. Ing., vol. 55, p 1889, 1911.
4. Roark, R.J. and Young, W.C., *Formulas for Stress and Strain*, fifth edition, McGraw-Hill Book Company, Inc., New York, NY 1975.
5. Avallone, E.A. and Baumeister, T., *Mark's Standard Handbook for Mechanical Engineers*, 9th Ed., pp 5-61 - 5-63, McGraw-Hill Book Company, Inc., New York, New York, 1987.

3.3 SURFACE ELEMENTS

This section presents an overview of the behavior of three dimensional sheet components that cover a surface or area. They may be flat, curved about a single axis, or doubly curved. These surface elements may be subjected to lateral or in-plane loadings. The load can be carried by these elements by shear or by flexural or axial action.

This section gives a basic understanding of the expected structural behavior and presents the variables that govern that behavior. References furnish the more specific data that may be required.

Flat surfaces are discussed first. This is followed by singly curved surfaces and then doubly curved surfaces. This leads to a discussion of dent resistance.

3.3.1 FLAT SURFACES



Flat plates or panels subjected to loads normal to their surface have flexural deformation and flexural stresses just as linear members subjected to distributed lateral loads. However, flexural stresses exist in both directions at all points on a plate. Deflections and the stresses are functions of plate dimensions and edge conditions.

3.3.1.1 Flexure

The expression for maximum deflection of a rectangular plate subjected to a uniformly distributed load per unit area, q , can be written in the following form:

$$\frac{w_m}{t} = \frac{C_w q \left(\frac{L_1}{t}\right)^4}{E \left[\left(\frac{L_1}{L_2} \right)^2 + 1 \right]^2}$$

Equation 3.3.1.1-1



where w_m = maximum plate deflection

t = plate thickness

L_1 = shorter of the rectangular plate dimensions

L_2 = larger of the rectangular plate dimensions

E = modulus of elasticity

C_w = deflection coefficient that varies with edge restraint and with $\frac{L_1}{L_2}$ ratio

Without considering a change in C_w , it can be observed that there is a significant difference between a square panel in which $L_1/L_2 = 1$ and a very long narrow panel where $L_1/L_2 = 0$. The exact ratio of the center deflections of a square plate to that of a long narrow plate of the same L_1 is 0.32.

This difference reflects the fact that in a square plate, the load spans both ways and the torsional plate stiffness (and resulting twisting moments developed) enhances the plate's load carrying capacity. The aspect ratio L_1/L_2 has an effect on the maximum stress in the plate, f_{bm} similar to the effect it has on deflection. This stress is:

$$f_{bm} = \frac{C_f q \left(\frac{L_1}{t} \right)^2}{\left(\frac{L_1}{L_2} \right)^2 + 1}$$

Equation 3.3.1.1-2



where C_f is a coefficient that is a function of edge restraint and aspect ratio L_1/L_2 .

With simply supported edges, the stress f_{bm} in a square plate is 0.38 of the f_{bm} value in a long narrow plate. In a long narrow plate, the load spans across the short dimension L_1 creating a one way bending situation except near the side supports. Values of C_f and C_w can be obtained for numerous variations of plate shape and edge condition from data provided in [Reference 1](#).

The flexural stiffness of the plate can be improved very economically by simply corrugating the sheet. See [Figure 3.3.1.1-1\(a\)](#).



(a) Corrugated sheet



(b) Sheet with multiple stiffeners

Figure 3.3.1.1-1 Ribbed and corrugated sheet

This produces a substantial stiffness and load capacity improvement in the direction of the ribs. Even stiffeners such as shown in [Figure 3.3.1.1-1\(b\)](#) can produce a significant improvement in flexural properties. The ribbed or corrugated plate basically exhibits one way flexural behavior, since the perpendicular direction retains the properties of a flat plate.

3.3.1.2 Membrane Behavior

The presence of the side support has a pronounced effect on plate behavior. The plate begins to develop significant in-plane stresses after deflecting an amount $w_m > t$. If the span-to-thickness ratio is large, a plate will rely on in-plane or membrane stresses for most of its load carrying capacity.

The center deflection under combined bending and membrane stress, w_o , can be expressed in the form

$$w_o = \frac{w_m}{1 + C_o \left(\frac{w_o}{t} \right)^2}$$

Equation 3.3.1.2-1



where w_m = bending deflection from [Equation 3.3.1.1-1](#) or [Equation 3.3.1.2-2](#)

C_o = coefficient which is a function of rotational and in-plane edge restraint

The problem is now nonlinear in that the plate stiffness increases with increasing deflection. C_o is smallest if the edge of the plate is free to move radially. Values for circular plates of radius a_p are provided in [Table 3.3.1.2-1](#).

Table 3.3.1.2-1 Deflection coefficients for circular plates

Rotational Edge Restraint	C_o		C'_w
	Free	Immovable	
Clamped	0.146	0.471	0.171
Simply Supported	0.262	1.852	0.696

C'_w in the [Table 3.3.1.2-1](#) is the deflection coefficient for a circular plate. The center deflection of a circular plate with radius a_p under uniform pressure q can be expressed as:

$$\frac{w_m}{t} = \frac{C'_w q}{E} \left(\frac{a_p}{t} \right)^4$$

Equation 3.3.1.2-2



The tensile membrane force developed is restrained by an infinitely stiff compression ring in the case of the immovable edge. A compression ring is developed in the outer portion of the plate if the plate has a free edge. This is illustrated in [Figure 3.3.1.2-1](#). It is possible to buckle the plate from the ring compression developed. In practice the edge usually has a stiffener (e.g. bent lip) which provides additional area for the ring and moment of inertia to resist ring buckling. Thus, the coefficient C_o usually ranges between the free and immovable values.

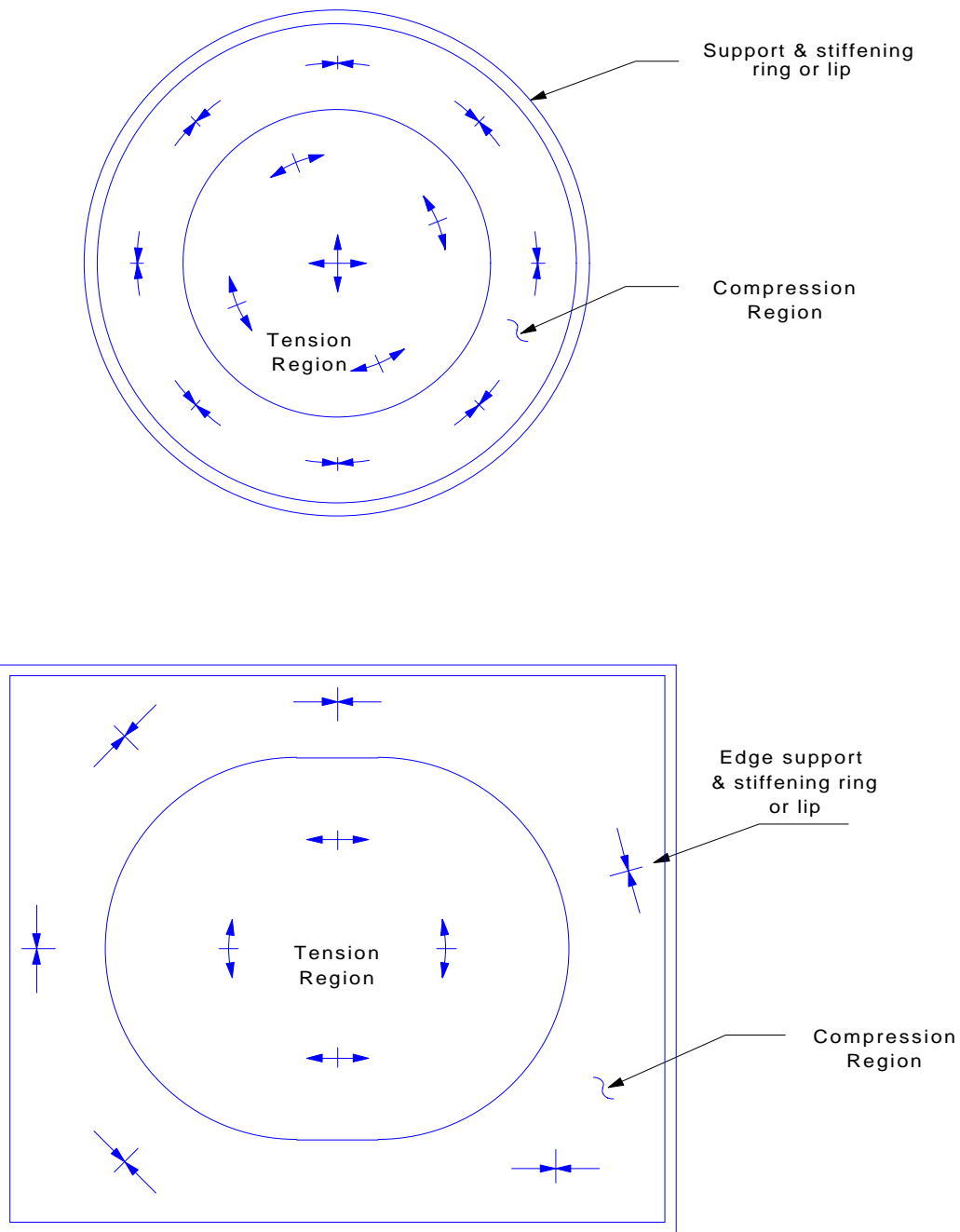


Figure 3.3.1.2-1 Membrane action in flat plate

The membrane and bending stresses developed are a function of the parameters shown in [Table 3.3.1.2-2](#). Stress coefficients for circular plates are given in [Reference 1](#).

Table 3.3.1.2-2 Membrane and bending stress parameters

Membrane	$E \left(\frac{w_o}{a_p} \right)^2$
Bending	$E \left(\frac{w_o t}{a_p^2} \right)$

The coefficients for circular plates can be used to approximate the situation for square plates or plates close to square by inscribing a circular plate over the actual plate. To be somewhat more conservative, the radius of the plate used in calculation should be taken as a bit larger than that of the inscribed circle. Tabulated information on membrane stresses and deflection of rectangular plates is given in [Reference 2](#).

If the flat plate is very thin the flexural integrity of the plate can be completely ignored. For the case of a circular membrane clamped along the circumference under uniform pressure q , the center deflection can be evaluated as:

$$w_o = 0.662 a_p \sqrt[3]{\frac{qa_p}{Et}}$$
Equation 3.3.1.2-3 

The corresponding tensile membrane stresses at the center and perimeter of the membrane are as follows:

$$(f_r)_{r=0} = 0.423 \sqrt[3]{E \left(\frac{qa_p}{t} \right)^2}$$
Equation 3.3.1.2-4 

$$(f_r)_{r=a} = 0.328 \sqrt[3]{E \left(\frac{qa_p}{t} \right)^2}$$
Equation 3.3.1.2-5 

Note that deflection is proportional to the cube root of the load intensity, but stress is proportional to the 2/3 power of the load intensity.

Stiffening beads are added to floor pans, dash panels and cargo box floors. In addition to increasing the flexural stiffness normal to the sheet, the beads are oriented to increase the load capacity for axial loadings imposed in crashes. (Beads oriented perpendicular to the direction of impact decrease the crush loads while beads oriented parallel increase crush loads.) The beads also suppress vibrations.

[Design Procedure 3.3-2](#), located in [Section 5.4](#), incorporates the procedure described in this section. This procedure and others shown in [Section 5](#) are implemented in AISI/CARS.

3.3.1.3 Compressive Integrity

The integrity of the flat plate loaded in compression in one direction forms the basis of the effective width concept used for flat elements of cold formed members, as described earlier in this Chapter. The basic equation for the critical stress representing the buckling of the rectangular plate is:

$$f_{cr} = \frac{k\pi^2 E}{12(1-\mu^2)\left(\frac{w}{t}\right)^2}$$

Equation 3.3.1.3-1



where **w** and **k** are as shown in [Figure 3.3.1.3-1](#) for the simply supported flat plate.

In the figure, **m** is the number of half sine waves in the buckled configuration.

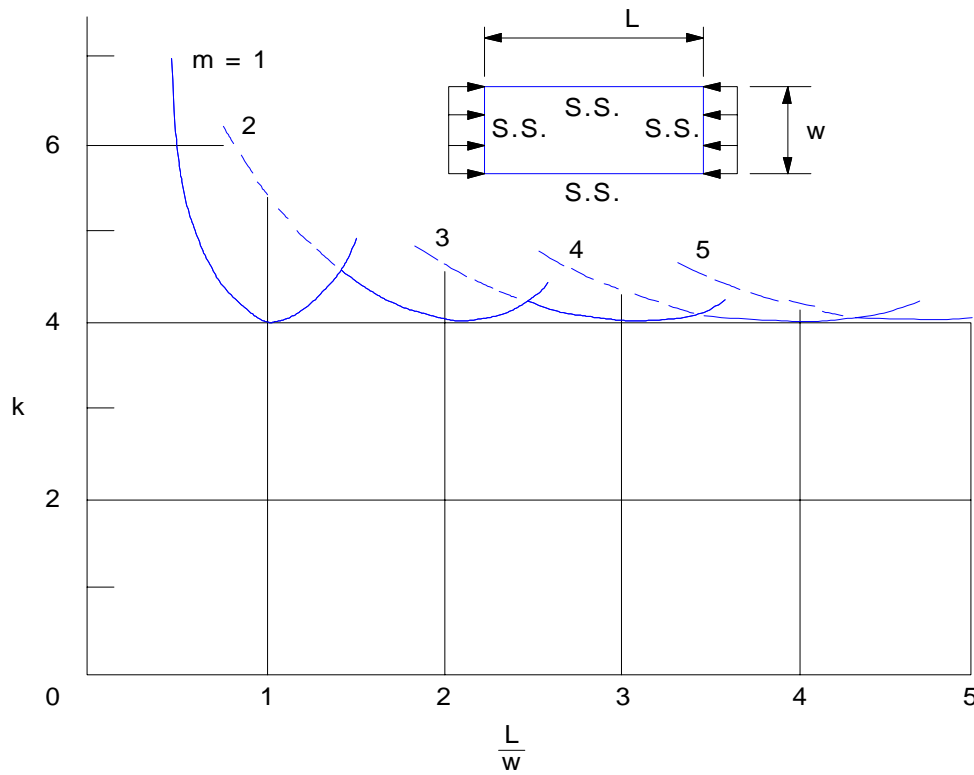


Figure 3.3.1.3-1 Buckling coefficient for simply supported flat plate

The expression in [Equation 3.3.1.3-1](#) is applicable when **L** is equal to or greater than **w**. For **L** small relative to **w**, the buckling load will approach the Euler load for the plate. At **L = w**, the plate buckling load (four sides simply supported) is four times that of the plate with two sides free. Thus, the edge support is very beneficial.

Values of **k** for other edge conditions and other loads on a rectangular plate are given in [Reference 3](#). Other plate buckling information for flat plates is tabulated in [Reference 2](#).

Stiffening of a flat plate by attaching angles or other shapes to the flat plate can significantly improve the axial load capacity. The stiffening can also be achieved by corrugating or adding ribs to the plate as per [Figure 3.3.1.1-1](#).

3.3.2 SINGLY CURVED SURFACES



The addition of a single parabolic or cylindrical curvature to a flat plate can produce a sizable increase in lateral load carrying capacity. This type of surface is the same as that shown in [Figure 3.2.1-1](#). The lateral load is carried to the support primarily by means of in-plane compressive load. The plate bending is small relative to that of a flat plate on the same span.

The effective length for use in compression load design can be determined from [Equation 3.2.1-1](#). Thus, in the elastic range, the critical buckling stress is

$$f_{cr} = \left[\left(\frac{2\pi}{\alpha} \right)^2 - 1 \right] \left[\frac{E}{12(1-\mu^2) \left(\frac{a}{t} \right)^2} \right]$$

Equation 3.3.2-1



The ends of the curved plate must be restrained from translation in order for this buckling load to be achieved.

The bending induced depends on the type of loading. A uniform normal pressure produces no bending for a circular arch shape. A uniform pressure over a horizontal surface produces no bending on a parabolic arch shape. Any concentrated or non-uniform distributed load produces flexural stresses which must be evaluated in conjunction with the axial loads using [Equation 3.1.3.7-7](#).

The addition of stiffening along the edges of a thin singly curved plate can provide a substantial improvement in the stiffness and strength of the plate. The edge support is estimated to provide about four times the critical stress obtained from [Equation 3.3.2-1](#) provided that the stress remains in the elastic range. The addition of corrugations or ribs along the curved surface can further improve the integrity of the surface.

If the rise-to-span ratio is small, buckling can be in a symmetrical mode rather than the unsymmetrical mode shown in [Figure 3.2.1-1](#).

3.3.3 DOUBLY CURVED SURFACES



The spherical shape is the most common doubly curved surface in that it has only one degree of curvature. A uniform pressure of q produces a membrane stress

$$f_m = \frac{qa}{2t}$$

Equation 3.3.3-1



where a is the spherical radius and t is the thickness of the spherical surface (See [Figure 3.3.3-1\(a\)](#)).

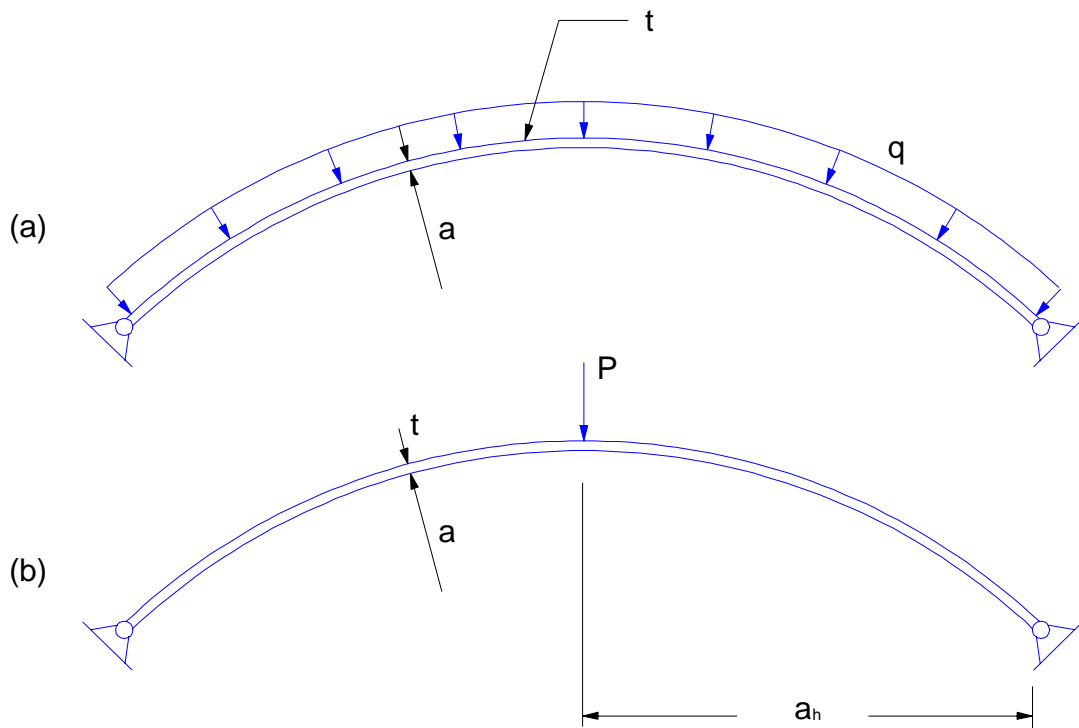
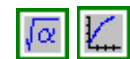


Figure 3.3.3-1 Spherical surfaces subjected to lateral load

An external pressure q of sufficient magnitude will lead to a buckling load which can be represented by the following equation.

$$q_{cr} = CE \left(\frac{t}{a} \right)^2$$

Equation 3.3.3-2



The theoretical value of C is approximately 1.2. However, the spherical shape is extremely sensitive to imperfections. So the achievable value of C is typically no more than 0.3 to 0.4. The amount of imperfection and edge effects (usually edge deflections) can reduce the value of C even further.

If the surface is not of a single thickness t , but stiffened by ribs in some manner, [Equation 3.3.3-2](#) can be extended to the form

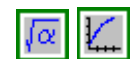
$$q_{cr} = CE \left(\frac{t_m}{a} \right)^2 \left(\frac{t_B}{t_m} \right)^{3/2}$$

Equation 3.3.3-3



where $t_m = \frac{A_s}{S_s}$, equivalent membrane thickness evaluated

Equation 3.3.3-4



as the stiffener area divided by the stiffener spacing

where $t_b = \sqrt[3]{\frac{12I_s}{S_s}}$, equivalent bending thickness evaluated

Equation 3.3.3-5



from the stiffener moment of inertia

If the in-plane buckling stress exceeds the proportional limit of the material, the above buckling expression should have E replaced by $\sqrt{E_s E_t}$ where E_s and E_t are the secant and tangent moduli of elasticity, respectively. See [Figure 3.3.3-2](#) for the definition of E_s and E_t . This can significantly reduce the buckling load. Use of a high yield strength material can produce a marked improvement in buckling resistance and allow more post buckling deformation prior to the onset of permanent deformations. Sharp yielding steels can have a proportional limit almost equal to the yield strength, while gradually yielding steels can have a proportional limit of only 70 percent of yield, or less. The cold working of the steel that occurs in achieving the spherical shape may increase the proportional limit.

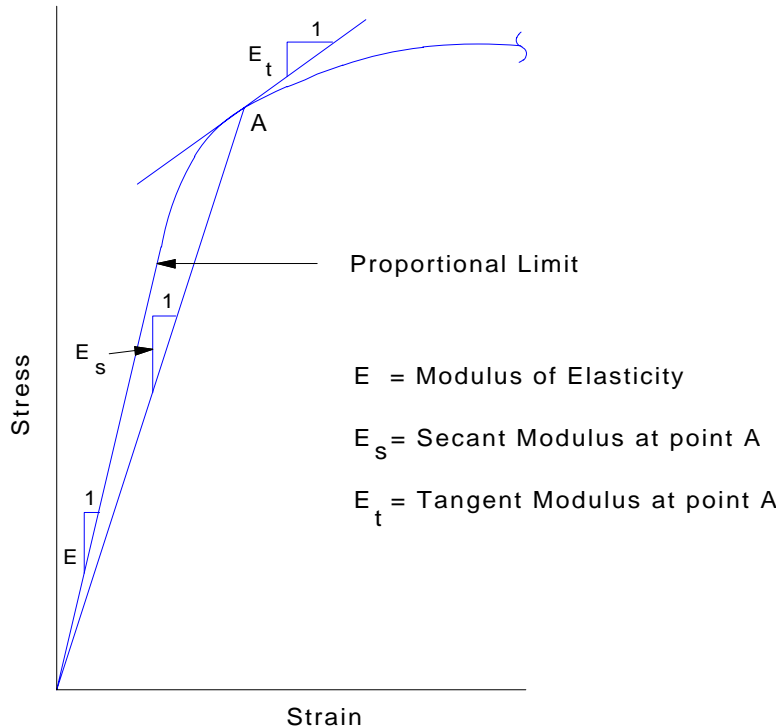


Figure 3.3.3-2 Compression stress strain curve illustrating various moduli

Additional information on shell stability can be found in [References 4 and 5](#). One example of note in [Reference 4](#) is that of a concentrated load on a spherical shell as shown in [Figure 3.3.3-1\(b\)](#). The load P will produce an inward dimple at the load as buckling occurs. The following expression approximates the theoretical buckling load for this case.

$$P_{cr} = \left[\frac{Et^3}{a} \right] \left[\sqrt{0.152(\gamma + 74.9)} - 2.88 \right] \quad \text{for } 20 < \gamma < 100$$

Equation 3.3.3-6



$$P_{cr} = \left[\frac{Et^3}{a} \right] \left[\sqrt{0.093(\gamma + 11.5)} - 0.94 \right] \quad \text{for } 100 < \gamma < 500$$

$$\text{where } \gamma = \frac{(a_h)^4}{(a^2 t^2)}$$

Equation 3.3.3-7



a_h = horizontal radius of spherical shell ([Figure 3.3.3-1\(b\)](#))

Bending stresses and membrane stresses produced by a concentrated load or a load over a small circular area are given in [Reference 2](#). Also given are expressions for evaluating the stresses induced in a spherical shell from edge displacements and edge loads.

[Design Procedure 3.3-3](#), located in [Section 5.4](#), incorporates the procedure described in this section. This procedure and others shown in [Section 5](#) are implemented in AISI/CARS.

3.3.4 DENT RESISTANCE



Body panels are typically formed into doubly curved shapes for styling and to achieve the most economical panel. The surface stiffness, the critical oil canning load as well as the denting energy are all considered in the design.

The expressions in this section for stiffness, dent resistance and oil canning load are based on technical papers published in the 1970's and early 1980's, which address empirical or theoretical approaches to a very complex issue. Stiffness, dent resistance and oil canning of body panels are known to be very sensitive to many variables, such as material properties, panel dimensions, panel curvature, edge conditions, sample fixturing and speed of loading. The following discussion is based on point loads, which is representative of small projectiles such as hail damage. However, it is not representative of palm denting. The designer is cautioned that testing is recommended to establish the actual performance of any body panel.⁶

The theoretical stiffness of a spherical shape under a concentrated load is of the form

$$K = \frac{P}{\delta} = \frac{C'E t^2}{a\sqrt{1-\mu^2}}$$

Equation 3.3.4-1



where a = spherical radius
 C' = a constant

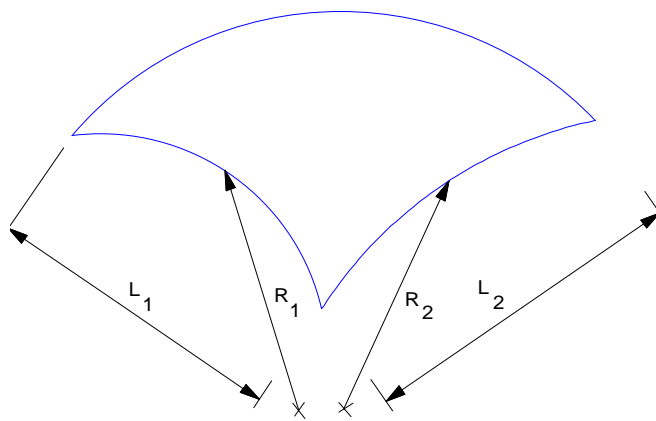
Since the curvature will seldom be the same in the two orthogonal directions, the expression above is generalized by replacing the curvature ($1/a$) with

$$\frac{1}{a} = \frac{\left(\frac{L_1^2}{R_1}\right) + \left(\frac{L_2^2}{R_2}\right)}{2 L_1 L_2}$$

Equation 3.3.4-2



where L_1, L_2 = the rectangular panel dimensions as shown in [Figure 3.3.4-1](#) with $L_1 \leq L_2$
 R_1, R_2 = the panel radii of curvature in the two orthogonal directions

**Figure 3.3.4-1** Doubly curved surface

The theoretical shell stiffness expression can be written in the following form^{7,8}

$$K = \frac{9.237 Et^2 H_c \pi^2}{k L_1 L_2 \sqrt{1-\mu^2}}$$

Equation 3.3.4-3

$$\text{where } H_c = \text{crown height} = \frac{L_1^2}{8R_1} + \frac{L_2^2}{8R_2}$$

Equation 3.3.4-4

$$k = \text{spherical shell factor} = A\alpha^2$$

Equation 3.3.4-5

$$\alpha = 2.571 \sqrt{\frac{H_c}{t}} \text{ for Poisson's ratio} = 0.3$$

Equation 3.3.4-6

A is obtained from [Table 3.3.4-1](#).

$\frac{H_c}{t}$ has an upper limit of 60.

Table 3.3.4-1 Alpha vs. A

Alpha (α)	A	Alpha (α)	A
0	1.000	10	0.069
1	0.996	11	0.053
2	0.935	12	0.044
3	0.754	13	0.037
4	0.506	14	0.032
5	0.321	15	0.028
6	0.210	16	0.025
7	0.148	17	0.022
8	0.111	18	0.019
9	0.085	19	0.017
		20	0.016

A simplified expression for spherical shell factor **k** in steel is:

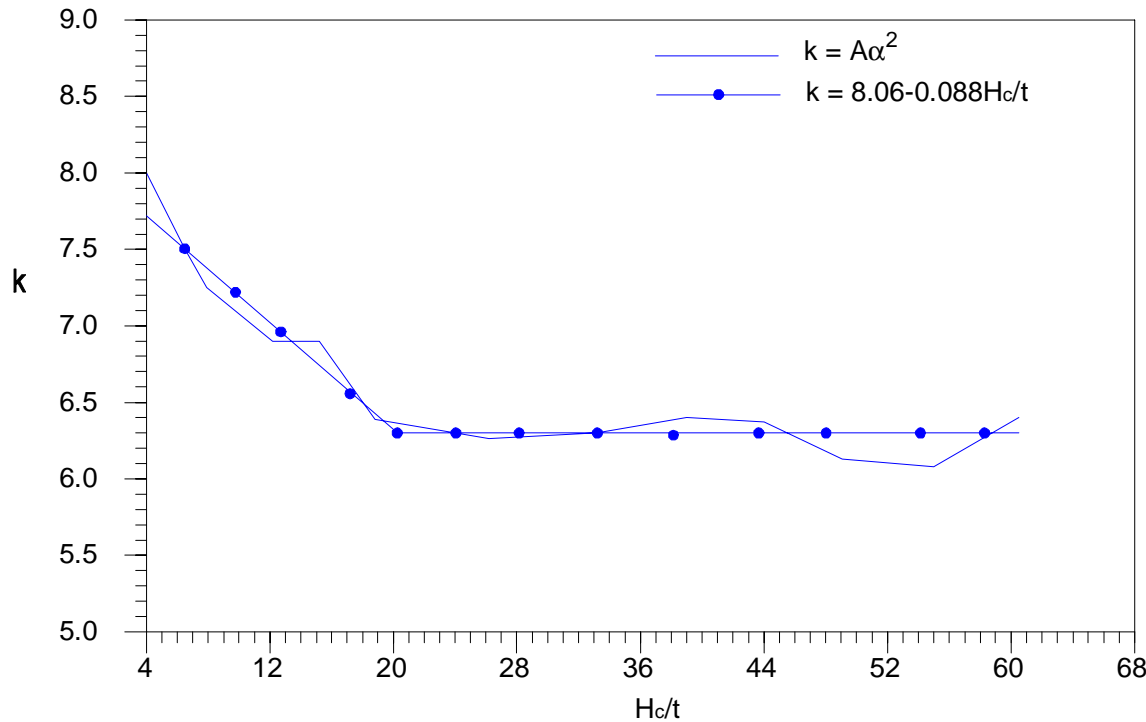
$$k = 8.06 - 0.088 \frac{H_c}{t} \quad \text{for } 4 \leq \frac{H_c}{t} < 20$$

$$= 6.3 \quad \text{for } 20 \leq \frac{H_c}{t} \leq 60$$

Equation 3.3.4-7



Both methods of determining the spherical shell factor, **k**, are plotted as a function of the crown height ratio, H_c/t , in [Figure 3.3.4-2](#).

Figure 3.3.4-2 k vs. H_c/t

Alternatively, an empirical expression for curved panel stiffness is

$$K = C_2 t$$

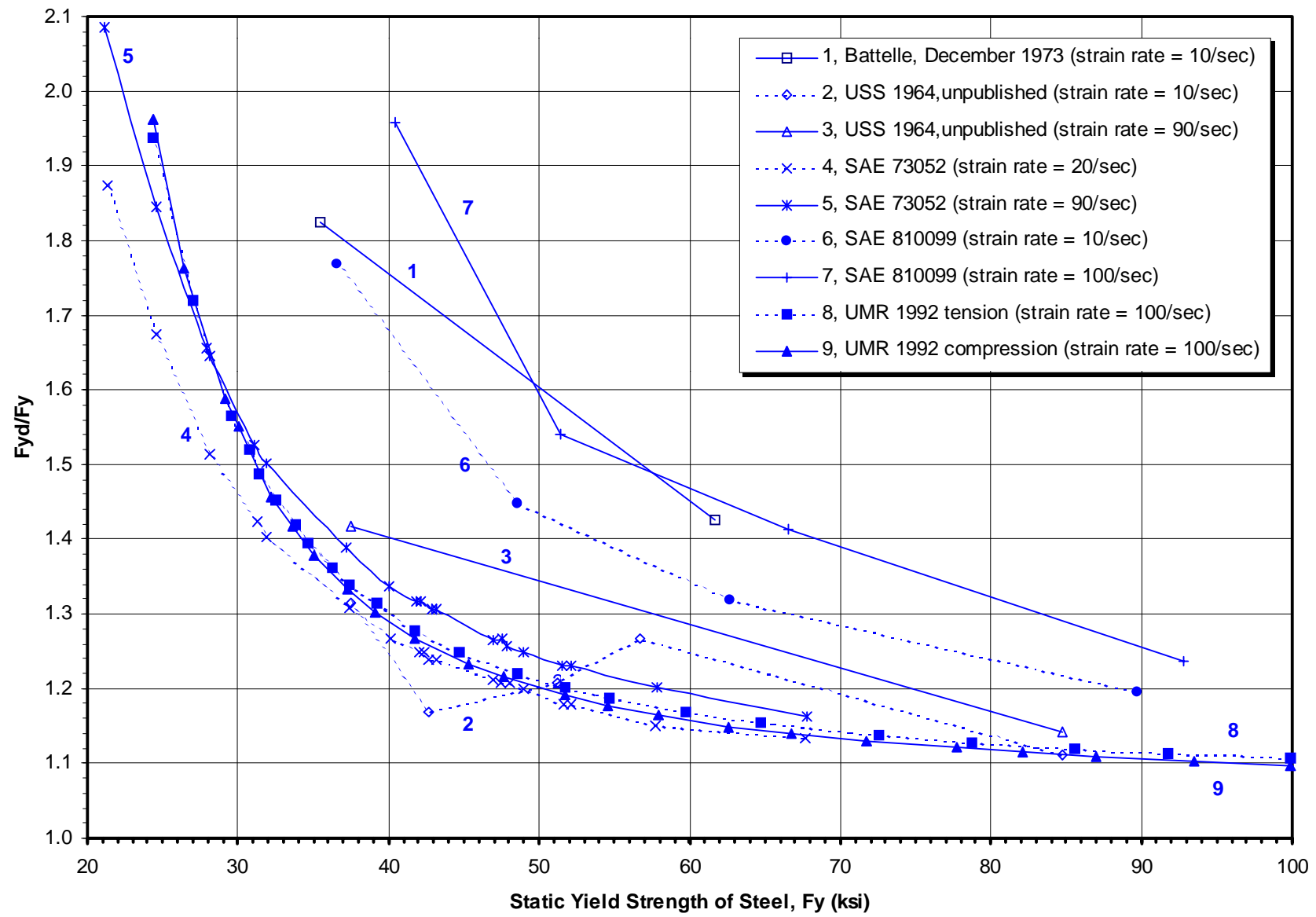
Equation 3.3.4-8



where **C₂** is a function of panel geometry which was derived using steel panels ([Reference 7](#)). The designer should determine the minimum stiffness required.⁹

The denting resistance is evaluated in terms of minimum denting energy. The designer should also determine the minimum denting resistance required. It has been shown ([Reference 10](#)) that the dent resistance is proportional to $F_{yd}t^2$ if F_{yd} is evaluated at the appropriate dynamic strain rate rather than being taken as the typical "static" value obtained from a test machine.

The dynamic strain rate corresponding to denting (10 to 100 per second) is many orders of magnitude higher than the typical static tensile test strain rate (0.001 per second). The ratio of dynamic to static yield strength of steels at strain rates of up to 100/sec are shown in [Figure 3.3.4-3](#), based on the data given in [Reference 11](#). It is up to the designer to select an appropriate factor from [Figure 3.3.4-3](#) to evaluate F_{yd} or to use an appropriate value of F_{yd} obtained from another source. The influence of strain rate on yield strength is also discussed in [Section 2.13](#).

Figure 3.3.4-3 F_{yd}/F_y versus F_y for steel

Grade 35XF, 50XF and 100XF materials were tested at strain rates of 0.0001, 0.01 and 1.0 per second in a research program performed at the University of Missouri-Rolla.^{11, 12, 13} Both tension and compression tests were performed. A method was developed to predict the yield and ultimate strengths of these steels for strain rates up to 1000 per second.

The denting energy based on an empirical curve fit ([References 7](#) and [8](#)) can be expressed as

$$W = 56.8 \frac{(F_{yd}t^2)^2}{K}$$

Equation 3.3.4-9



where K = panel stiffness per [Equation 3.3.4-3](#)

t = panel thickness

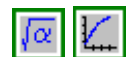
F_{yd} = yield strength of the panel at high strain rate

This formula defines a dent as 0.001 inch (0.025 mm) permanent deformation in the panel. The stiffness often tends to control over the dent resistance except when the panel size is small.

Oil canning load often controls panel designs over both stiffness and dent resistance. Of concern are the degree of oil canning, which determines the likelihood of a panel buckling measured by the parameter λ , and the critical buckling load P_{cr} at which the panel would collapse and reverse its curvature. The critical oil canning load ([References 9](#) and [14](#)) is given as

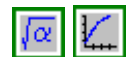
$$P_{cr} = \frac{CR_{cr}\pi^2 Et^4}{L_1 L_2 (1 - \mu^2)}$$

Equation 3.3.4-10



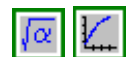
where $C = 0.645 - 7.75 \times 10^{-7} L_1 L_2$ in millimeter units
 $= 0.645 - 0.0005 L_1 L_2$ in inch units

Equation 3.3.4-11



$$R_{cr} = 45.929 - 34.183\lambda + 6.397\lambda^2$$

Equation 3.3.4-12



$$\text{with } \lambda = 0.5 \sqrt{\frac{L_1 L_2}{t}} \sqrt{\frac{12(1 - \mu^2)}{R_1 R_2}}$$

Equation 3.3.4-13



This expression is valid for

$$\frac{R_1}{L_1} \text{ and } \frac{R_2}{L_2} > 2$$

$$\frac{1}{3} < \frac{L_1}{L_2} < 3$$

$$L_1 L_2 < 1200 \text{ in}^2 (0.774 \text{ m}^2)$$

The designer should determine the minimum critical oil canning load required. Since oil canning is controlled by geometry and modulus of elasticity, it appears that there is no advantage in using high strength steels. However, high strength is necessary to maintain the elastic behavior under large deformations so that an elastic recovery is more likely to occur.

Example 3.3-1 shown in Section 6.2.3.1 illustrates the use of the equations for stiffness, denting, and oil canning in the design of a body panel.

REFERENCES FOR SECTION 3.3

1. Timoshenko, S.P. and Woinowsky-Krieger, S., *Theory of Plates and Shells*, McGraw-Hill Book Co., Inc., New York, N.Y., 1959.
2. Roark, R. J. and Young, W.C., *Formulas for Stress and Strain*, McGraw-Hill Book Co., Inc., New York, NY, Fifth Edition, 1975.
3. Yu, Wei-Wen, *Cold-Formed Steel Design*, 1991, John Wiley & Sons, Inc.
4. Timoshenko, S.P. and Gere, J.M., *Theory of Elastic Stability*, McGraw-Hill Book Company, Inc., New York, NY, 1961.
5. Structural Stability Research Council, Theodore V. Galambos, editor, *Guide to Stability Design Criteria for Metal Structures*, 4th Edition, John Wiley & Sons, New York, NY, 1988.
6. Auto/Steel Partnership Dent Resistance Task Force, Report on Steel Body Panel Performance Characteristics, Volume 1 and 2, July 1991.
7. Vadhavkar, A.V., Fecek, M.G., Shah, V.C., and Swenson, W.E., "Panel Optimization Program (POP)", SAE Technical Paper No. 810230 (February, 1981).
8. Mahmood, H.F., "Dent Resistance of Surface Panel and Slam Area", SAE Technical Paper No. 810099 (February 1981).
9. Swenson, W.E., Jr. and Traficante, R.J., "The Influence of Aluminum Properties on the Design, Manufacturability and Economics of an Automotive Body Panel", SAE Technical Paper No. 820385 (February, 1982).
10. Johnson, T.E., Jr., and Schaffnit, W.O., "Dent Resistance of Cold-Rolled Low-Carbon Steel Sheet", SAE Technical Paper No. (May, 1973).
11. Pan, Chi-Ling and Yu, Wei Wen, "Design of Automotive Structural Components Using High Strength Sheet Steels: Influence of Strain Rate on the Mechanical Properties of Sheet Steels and Structural Performance of Cold-Formed Steel Members", Eighteenth Progress Report, Civil Engineering Study 92-3, University of Missouri-Rolla, December, 1992.
12. Kassar, Maher and Yu, Wei-Wen, "Design of Automotive Structural Components Using High Strength Sheet Steels: The Effect of Strain Rate on Mechanical Properties of Sheet Steels", Eleventh Progress Report, Civil Engineering Study 89-2, University of Missouri-Rolla, January, 1989.
13. Kassar, Maher and Yu, Wei-Wen, "Design of Automotive Structural Components Using High Strength Sheet Steels: The Effect of Strain Rate on Mechanical Properties of Sheet

Steels", Twelfth Progress Report, Civil Engineering Study 89-4, University of Missouri-Rolla, August, 1989.

14. Lohwasser, A.K. and Mahmood, H.F., "Surface Panel Oil Canning Analysis - Theoretical Development", Technical Memorandum, No. 9-611, Chrysler Corp., April 1979.

3.4 CONNECTIONS

There are four basic systems that are commonly used to join sheet steel body members with other members: welding, mechanical fasteners, mechanical fastening by deformation of the parent metal and adhesive bonding. Each system offers advantages and disadvantages, which are discussed in [Sections 3.4.1](#) through [Section 3.4.6](#). In some cases, the systems are combined to optimize the performance of the joint, such as weldbonding, which is discussed in [Section 3.4.7](#).

The following checklist will assist in identifying the factors to be weighed in selecting the optimum system.

1. Assess the Application and Operating Environment.
 - 1.1 Determine the type and intensity of applied load.

Type of load is essential; typical types are long-term or continuous, occasional, fatigue, and impact (high strain rate).

Sources may be anticipated or accidental. Anticipated loads, which are usually quantified, include those computed from suspension G loads; low-speed bumper impacts; rough road tests; and door, hood and deck lid slam.

Accidental loads, which are not readily quantified, include high speed collision, rollover, and low speed (parking lot) collisions.
 - 1.2 Assess potential problem areas

Potential problem areas may include long term structural degradation, potential for rattles, galvanic and atmospheric corrosion, differential rates of thermal expansion, and repairability.
 - 1.3 Design the joint

Select the system or combination that will meet the design requirements.

Evaluate the shape and size of the contact areas of the members to be joined and the relationship between the type and direction of load and the joint configuration.
 - 1.4 Determine the side benefits

Examine the side benefits that may be derived, such as galvanic separation, moisture barrier, and effects of load distribution that may eliminate or require local reinforcements and stiffeners on all affected members.
 - 1.5 Review the cosmetic requirements

Witness marks are generally prohibitive on appearance surfaces, but may be tolerable on other surfaces.

1.6 Review the effect on materials

Check the compatibility of joining method on materials, such as possible degradation of properties developed by heat treatment, capability for joining dissimilar materials, and toleration of pre-coated stock.

2. Determine which system(s), alone or in combination, is acceptable.

The joint must be accessible to equipment such as weld guns, adhesive application systems and screw drivers.

3. Confer with manufacturing engineers (and suppliers of adhesives or fasteners where they are alternatives).

3.1 Determine the cost of modifying plant operations to accommodate the fastening system.

3.2 Assess the effects on the components to be joined in terms of mass, material cost and process cost. Material cost includes the cost differential for the material required to fabricate the components and the cost of any fasteners or adhesives that are employed.

3.3 Estimate operating costs for each process, such as the cost of energy, maintenance, floor space required and amortization.

4. Determine all of the implications for each option on the entire vehicle and select the optimum system for the joint.

3.4.1 WELDED CONNECTIONS

The great majority of welded connections in automotive structures are spot welds. This section will therefore be confined to a discussion of the strength of spot welded joints. Weldability, a description of the spot welding process, and quality control of spot welding are described in [Section 4.3-1](#) and in [Reference 1](#). The spacing of spot welds to achieve structural criteria is presented in [Section 3.4.4](#).

The strength that a spot weld, or a pattern of welds, will exhibit in a particular application can be predicted to some extent from tabulated data compiled from test specimens. Welded joints in real world applications will rarely behave like the test specimens. Therefore, proper application of the data requires a basic understanding of spot weld testing methods.

Spot welds are tested in a variety of ways in order to evaluate their mechanical properties in various modes of loading. These tests include the peel, chisel and a variety of tension, torsion and fatigue tests.

3.4.1.1 Peel Test

The peel test is the most commonly used mechanical test for spot welds. It is widely accepted because of the following factors:

1. Ease of performance
2. Low cost
3. The ability to use it on the shop floor for quality control

This test is performed by making two welds on a sample. The first weld serves as a shunt weld to carry part of the current, so the second weld is a more realistic example of what is found in the manufactured automobile. For the purposes of the test, the second spot weld is peeled to destruction.

Research in evaluating the factors that affect the peel test ([Figure 3.4.1.1-1](#)) has demonstrated that the smaller the distance between the spot weld and the pulling tab, the greater the maximum load.

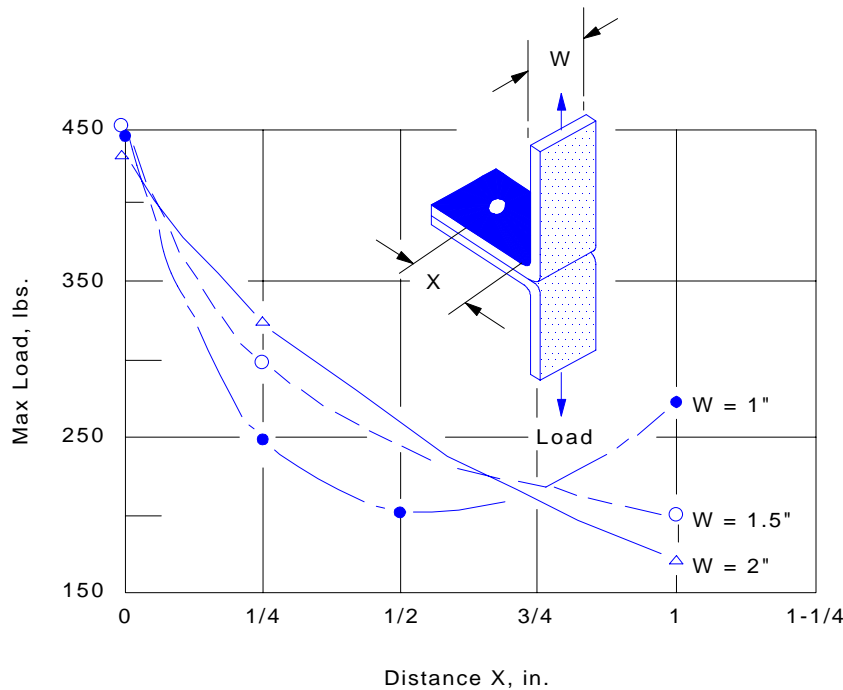


Figure 3.4.1.1-1 Effect of geometry on quantified peel test

Thus, the results generated may be somewhat operator dependent. It has also been observed on marginally acceptable HSLA materials, that conducting the peel test while the specimen is still warm from welding promotes nugget pullout. In contrast, testing identical specimens after cooling results in a partial fracture of the weld metal. Even with these findings, little work has been done to characterize and qualify the peel test data.

3.4.1.2 Chisel Test

Chisel testing is similar to the peel test. The difference is that forcing a chisel, or wedge, between the sheets near the spot weld location may more easily produce an interfacial failure. The stress distribution at the weld for chisel or peel loading is illustrated in [Figure 3.4.1.3-2\(a\)](#).

3.4.1.3 Tensile Tests

Recently, tensile tests have become more popular in the automotive industry. Numerous tensile test specimen geometries ([Figure 3.4.1.3-1](#)) have been utilized to determine tensile properties of spot welds.

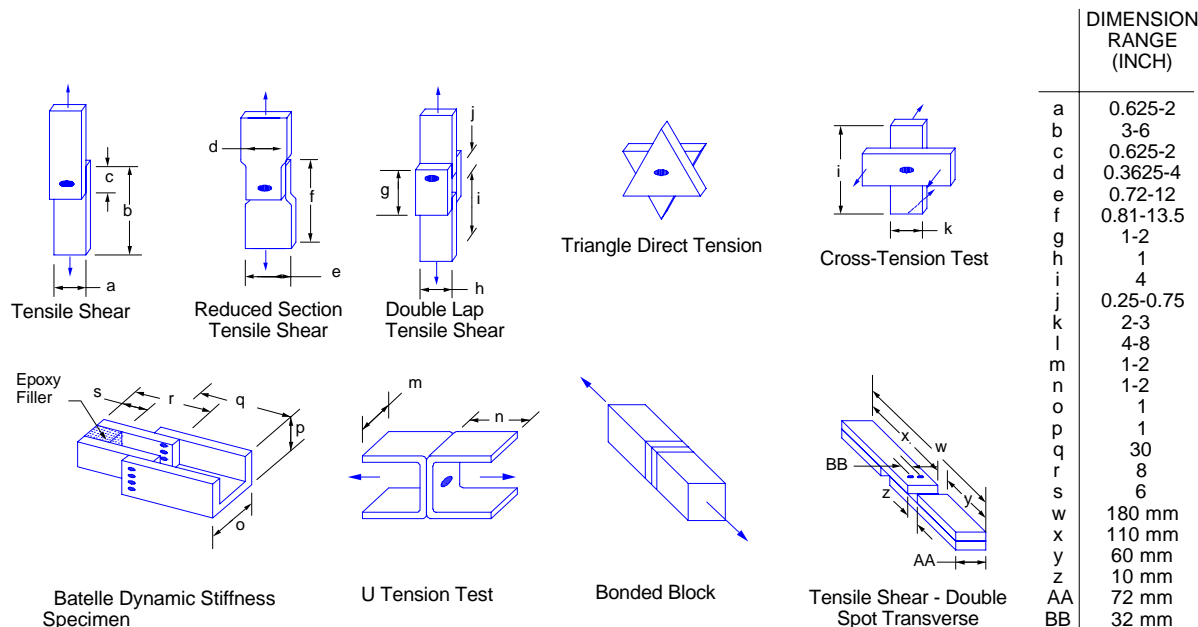


Figure 3.4.1.3-1 Various tensile test specimens

Stress distribution in spot welds of various test geometries is illustrated in [Figure 3.4.1.3-2](#).

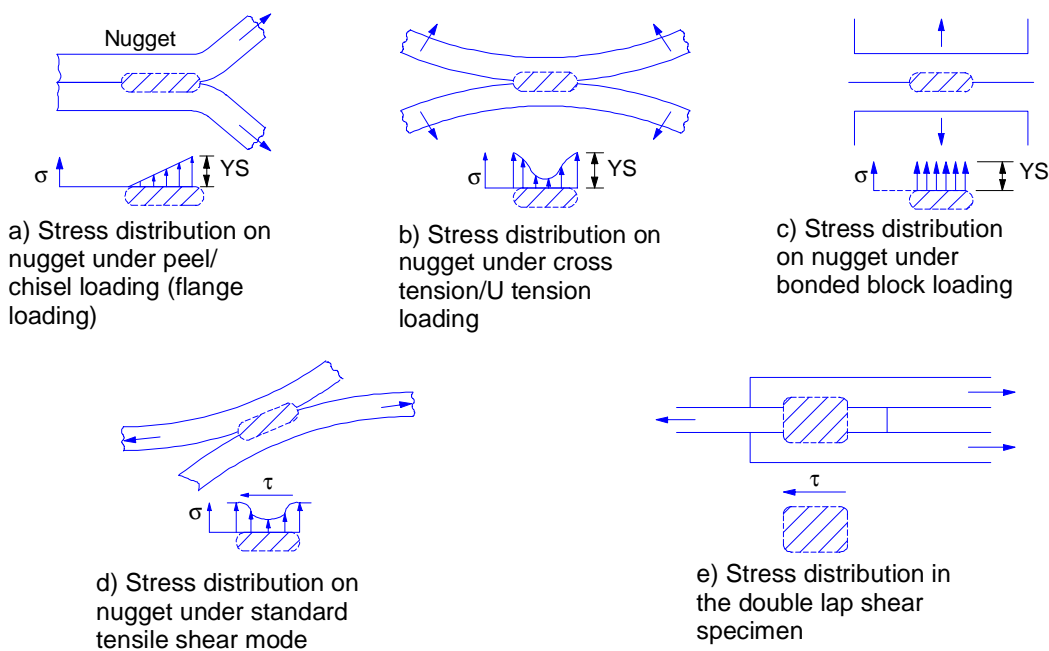


Figure 3.4.1.3-2 Stress distribution around spot welds of various test geometries

Specimens consist either of those designed to measure normal stress or those that measure shear stress. The lap shear or tensile shear specimen is made bylapping one piece of material over another piece, making a spot weld, then pulling the pieces in opposite directions until failure. Other types of specimen designs include a normal bonded block type specimen, although this is not used very often. Normal tensile tests include the cross weld test and the U-tensile test.

The important finding of test data is that welds made in different geometries have different strengths. For example, the lap shear geometry carries the highest load. Besides specimen geometry, other factors that affect spot weld strength include sheet size, nugget size, weld time, hold time, spot array, coatings, and testing procedures.

3.4.1.4 Torsion Testing

The torsion test ([Figure 3.4.1.4-1](#)) is also used to evaluate spot weld properties.

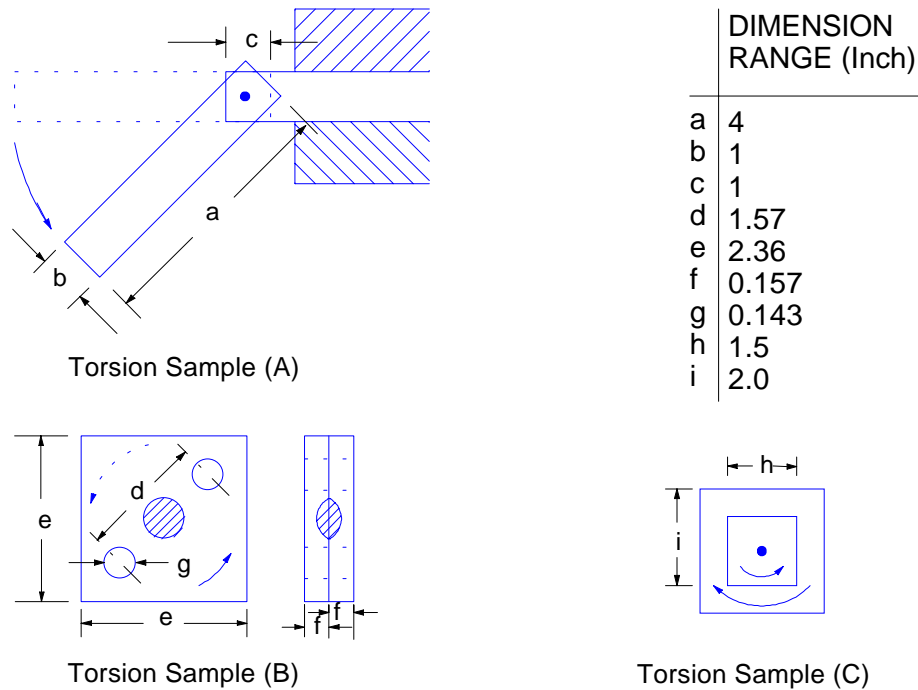


Figure 3.4.1.4-1 Torsion test specimens

The angle of twist before nugget failure has been used as a measure of spot weld ductility, while the maximum torque has been used to evaluate spot weld strength. Generally, most torsion tests are similar. Although popular in the past, these tests are used less today. They are, however, useful in characterizing various types of steels. Usually, good forming steels that have high ductility have low torques, with large twist angles. In contrast, high strength steels tend to have higher torques with lower twist angles. When a weld is made with some expulsion, it tends to reduce both the torque and the twist angle. All the factors that affect tensile tests also have been observed to affect torsion testing.

3.4.1.5 Fatigue Testing

Fatigue testing of spot welds has gained considerable interest in recent years. However, there are unanswered questions about the factors that affect fatigue testing of spot welds such as the effect of specimen geometry, sheet size, nugget size, weld time, hold time, spot array and composition.

One major point concerning fatigue testing is illustrated in [Figure 3.4.1.5-1](#).

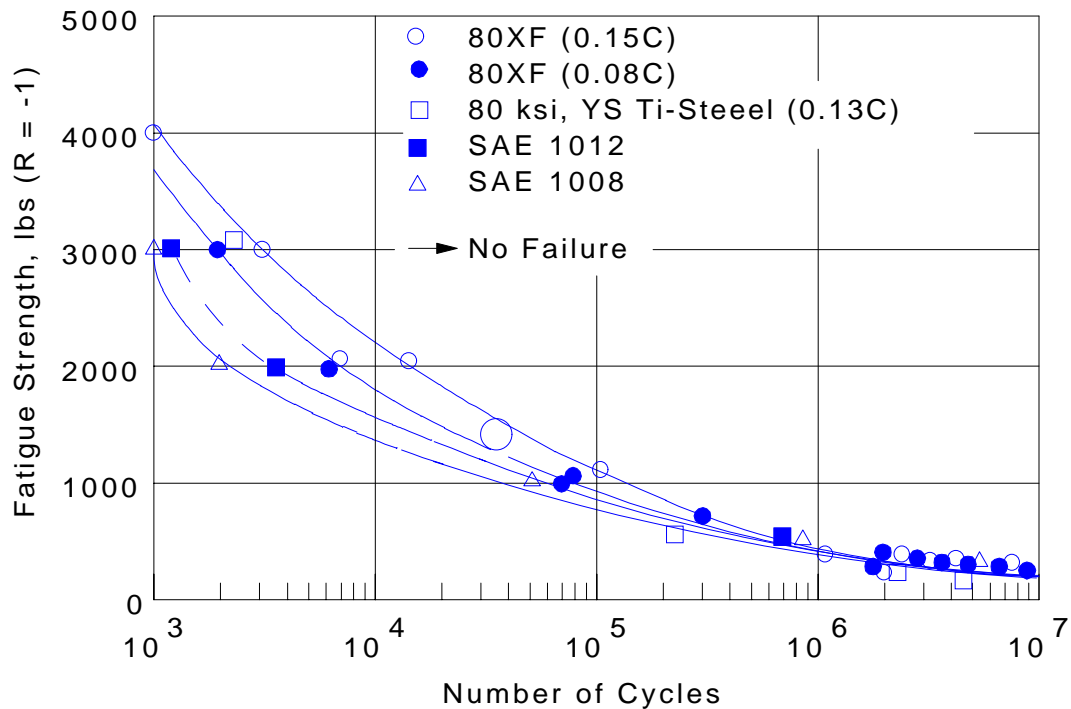


Figure 3.4.1.5-1 Fatigue endurance curves; high strength and low-carbon steels

The line with triangles indicates SAE 1008 standard carbon steel in comparison with high strength low alloy. At a low number of fatigue cycles, the high strength low alloy material has a definite advantage in fatigue strength. At high cycles (between 10^6 and 10^7), this advantage appears to be reduced. Thus, a concern in the auto industry is the small difference in the fatigue strength at high cycles between high strength steels and plain carbon type steels.

Another observation concerns the critical diameter of a spot weld. Once a critical diameter is reached, the failures behave in a normal crack mode, with the crack growing through the sheet; that is, the nugget is pulled out. If the diameter of the nugget is smaller than this critical size, rather than pulling out a nugget during fatigue testing, the result is an interfacial failure.

3.4.1.6 Shear Strength Values

Conservative shear strength values have been used to provide allowable shear values in the 1980 AISI specification² for spot welds on various sheet thicknesses. The allowable values employ a factor of safety of 2.5. Somewhat less conservative shear strength values, which are shown in [Table 3.4.1.6-1](#), form the basis of the allowable shear values in the 1986 AISI specification³.

Table 3.4.1.6-1 Resistance weld capacity.
Ultimate shear strength per spot V_{su}

Thickness of thinnest outside sheet (inches)	V_{su} (kips)	Thickness of thinnest outside sheet (mm)	V_{su} (kN)
0.010	0.130*	0.25	0.58
0.020	0.437	0.51	1.94
0.030	1.000	0.76	4.45
0.040	1.423	1.02	6.33
0.050	1.654	1.27	7.36
0.060	2.282	1.52	10.15
0.070	2.827	1.78	12.57
0.080	3.333	2.03	14.82
0.094	4.313	2.39	19.18
0.109	5.987	2.77	26.63
0.125	7.200	3.18	32.03
0.188	10.000*	4.77	44.48
0.250	15.000*	6.35	66.72

* From AWS C1.1-66 Tables 3.1-1 and 3.1-3. Remainder of values either taken from or interpolated from AWS C1.3-70 Table 2.1.

These values are applicable to all structural grades of low carbon steel, but also give conservative values for medium carbon and low alloy steels as well. These values do not consider capacity reductions due to fatigue loading.

3.4.1.7 Tensile Strength of Arc Spot Welds

The tensile strength of arc spot welds was recently studied at the University of Missouri-Rolla^{4, 5}. Results of more than 260 welded connection tests indicate that the primary parameters that influence the tensile strength of an arc welded connection are the thickness of the sheet, the diameter of the weld, and the tensile strengths of the sheet and weld. Design recommendations were developed for predicting the tensile strength of arc spot welds.

3.4.2 MECHANICAL FASTENERS

Where access to both sides of a joint is available, resistance spot welding is the primary method of joining sheet steel. However, mechanical fasteners have been successfully used when:

- Anti-corrosion coatings or adhesives are incompatible with spot welding
- The steel is too thin to be reliably spot welded
- A neat, flash free appearance is desired
- Spot welds are too close together, causing shunting

Where after-paint repairs of spot welds are required, or where only single side access is available, blind or pop rivets or self-piercing and threading screws are used.

Mechanical fasteners are conveniently divided into two sided and one sided. Two sided fasteners, typically a bolt and nut, require two parts at each location. One sided fasteners, such as self tapping screws, require one part per location.

Fasteners are available in a wide variety of grades, head styles, threads, lengths, locking devices, and other design variations. The number of different fasteners, which tends to proliferate within a company, can become enormous. Many companies are recognizing the cost incurred for each fastener type (and part number) that is on their books, and are taking significant steps toward reducing the number of different fasteners within their system. Designers are being encouraged to consult company standards and specify fasteners within those standards whenever possible.

3.4.2.1 Two sided Fasteners

Two sided fasteners, typically bolts, are commonly employed to connect thicker sheet gauges. The nuts may be transported in bulk to the point of assembly or attached to one of the members by means such as projection welding. In some cases bolts are threaded into tapping plates, which are thick plates with tapped threads welded to one of the members. Although the SAE standard for hex bolts⁶ includes coarse, fine and 8-thread series, the automotive industry now uses coarse threads almost exclusively.

The strength classification system used by SAE for bolts and machine screws utilizes grade numbers, with the higher numbers indicating higher strengths⁷. In the systems used for some machine screws⁸ and for metric⁹, the numbers have quantitative relationships to the strength of the fastener. The system used for nuts, in sizes 1/4 to 1-1/2 in. inclusive, is similar to that used for bolts, but the system includes only three grades¹⁰.

The tensile strengths and proof loads for bolts,^{7,9} machine screws⁸ and nuts¹⁰, as a function of their size, grade, and thread, have been standardized and published for use in design. Where shear strength is the governing factor, it may be taken at 60 percent of tensile strength.

3.4.2.1.1 Clamping Load and Nut Torque

Some attachments that utilize a nut on a bolt (or stud) require that a specified clamping load be developed and sustained. In those cases, criteria governing clamping loads must be met in addition to the design considerations for mechanical fasteners, which are discussed in [Section 3.4.2.3](#).

The clamping force developed when a nut is torqued on a bolt is determined by the applied torque and the surface condition of the threads and bearing areas. The maximum clamping load that can be developed is a function of the strength of the bolt. Normally the proof load (the maximum load that the bolt can sustain without permanent deformation) is specified. When selecting a nut and bolt to develop a specified clamping load, the nut should be of the same or higher grade than the bolt. For example, either a grade 5 or a grade 8 nut can be used with a grade 5 bolt, but a grade 2 nut should not be used.

The clamping load is related to the tightening torque by the formula

$$T = kPd$$

Equation 3.4.2.1.1-1



where T = torque applied to the nut

k = a constant that depends on the surface coating and type of lubrication (if any) on the threads and bearing areas. Typical values are listed in [Table 3.4.2.1.1-1](#).

P = axial load on the bolt or stud

d = nominal bolt or stud diameter

The value of **kPd** must be divided by 12 when **T** is in lb ft; it must be divided by 1000 when **T** is in **Nm** and **d** is in mm.

Table 3.4.2.1.1-1 Typical k values for nut torquing

Type of Surface		Dry or Lubricated	k value
Nut	Bolt and Bearing		
zinc	steel	dry	0.22
steel	steel	dry	0.20
cadmium	cadmium	dry	0.17
zinc	steel	machine oil	0.16
cadmium	steel	wax or oil	0.15
---	---	phosphate and oil	0.12
---	---	moly disulphide	0.09

Some manufacturing facilities employ torque-to-yield power wrenches, which detect the point at which the bolt begins to yield and automatically stop. Where this type of wrench is available, a torque-to-yield specification may be used instead of specifying a torque value.

When bolts or machine screws are inserted into tapping plates, the plate can be made thick enough so that the length of thread engagement is sufficient to permit development of the full strength of the bolt. Nuts generally provide sufficient threads to permit development of the full strength of the bolt, provided that the nut is of equal or higher grade than the bolt, as recommended above.

3.4.2.2 One Sided Fasteners

One sided fasteners are widely used because they offer a quick, economical means of fastening that does not require backup operations, access to the opposite side of the joint, or opposite side components, such as loose nuts, weld nuts or tapping plates. The types of one sided fasteners most commonly used in automotive bodies are self tapping screws, self-drilling tapping screws, and thread rolling screws. (This discussion will follow SAE J478a and consider the fasteners commonly called sheet metal screws as type A self tapping screws.) One sided fasteners are hardened to levels that enable them to deform or cut the sheets into which they are installed. The required hardness determines the strength of the fastener. For example, thread rolling screws typically exhibit approximately twice the strength of machine screws, and typically 25 percent higher strength than self tapping screws.

3.4.2.2.1 Self Tapping and Self-Drilling Tapping Screws

Self tapping screws are installed through holes in the top sheet into holes in the bottom sheet. The holes are of such sizes that the screw thread draws the sheets tight while cutting a thread or forming threads in the bottom sheet. With a self-drilling tapping screw, the hole is cut into the bottom sheet or both sheets by the screw, which then cuts a thread in the sheet or sheets. The clamping force developed by these types of screws is limited by the thickness and mechanical properties of the sheet. The threads form an interference fit in the bottom sheet, which makes them resistant to loosening, depending on the length of thread engagement.

The penetrating capability of a self-drilling tapping screw may limit its usage, particularly in smaller screw sizes. For example, a #6 screw, which is 3.51 mm (0.138 in.) diameter, can drill through sheet up to 2.3 mm (0.09 in.). This penetration amounts to approximately 0.65 times the diameter, or three threads. A #12 screw, which is 5.49 mm (0.216 in.) diameter, can drill through steel up to 13 mm (0.5 in.). This penetration is 2.3 D or 6.5 threads.

3.4.2.2.2 Thread Rolling Screws

Thread rolling screws are becoming more useful as sheet metal gauges become thinner to meet the demand for lighter mass vehicles. Thread rolling screws pass through a clearance hole in the upper sheet into an extruded hole in the bottom sheet ([Figure 3.4.2.2-1](#)).

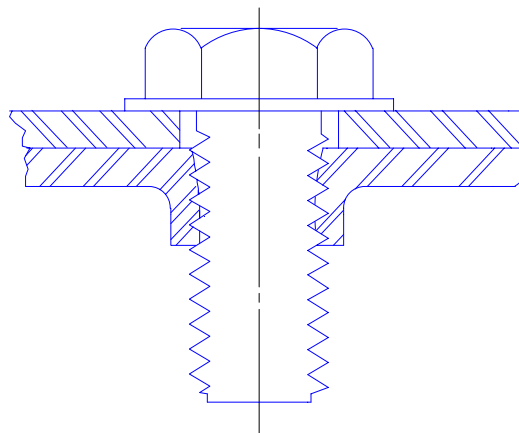
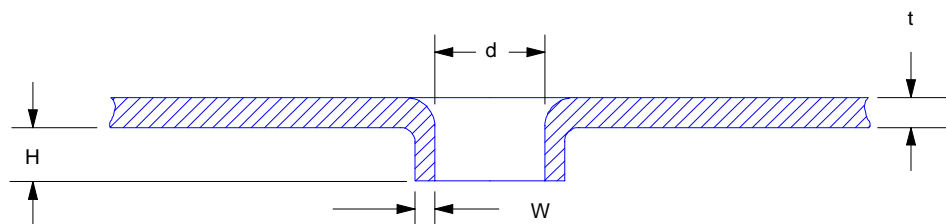


Figure 3.4.2.2-1 Typical thread rolling screw installation

The profile and design dimensions of the thread, combined with the dimensions of the extruded hole, enable the screw to roll a thread into the hole as it is driven. The sheet steels for which thread rolling screws are being specified generally have adequate forming properties to allow the extruded hole to be formed to the required dimensions within required tolerances.

Typical dimensions for extruded holes are shown in [Figure 3.4.2.2-2](#), and typical locating dimensions are shown in [Figure 3.4.2.2-3](#).



d per manufacturers specifications, typically 0.85 to 0.90 D_n
 where D_n = Nominal thread size (maximum thread diameter)
 $0.20 D_n \leq t \leq 0.75 D_n$
 $0.5t \leq W \leq 0.6t$
 H minimum $\approx 0.25 D_n$ (for $W = 0.6 t$)
 maximum $\approx 0.30 D_n$ (for $W = 0.5 t$)
 Length of thread engagement $\approx 0.95 (t + H)$

Figure 3.4.2.2-2 Recommended dimensions for extruded holes

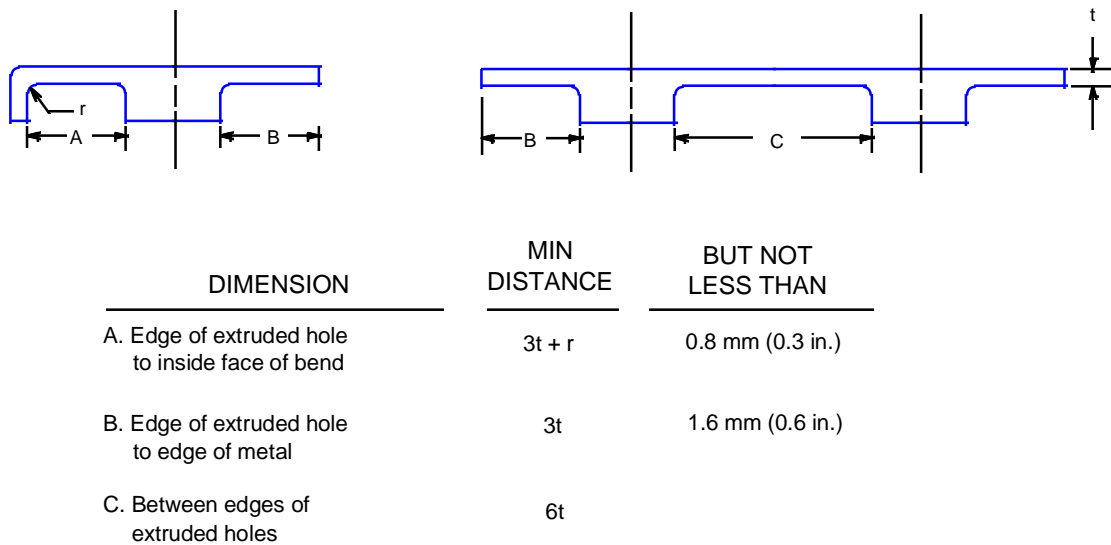


Figure 3.4.2.2.3 Recommended dimensions for spacing extruded based holes, on manufacturing criteria

The dimensions shown are fairly conservative, and they reflect the restrictions imposed by material properties and manufacturing processes. Variations can sometimes be made in consultation with the appropriate manufacturing and materials personnel. It should be noted that the dimensions for hole location are also subject to the discussion on spacing and edge distance in [Section 3.4.2.3](#), relative to the strength of the joint. Those relationships do not, however, reflect the benefit of the additional material at the extruded hole.

Thread rolling screws also form an interference fit in the bottom sheet, which makes them highly resistant to loosening under vibration. In addition, there is some latitude to increase the torque required to drive the screw by reducing the diameter of the extruded hole, consequently increasing the interference between the hole and screw. This latitude may be advantageous in the assembly plant, where a single driving tool is employed to install several different fasteners that require drive torques which vary somewhat. Suppliers of thread rolling screws frequently have their own patented thread profile, so that the drive torque data may vary from one manufacturer to another.

It is sometimes possible to provide sufficient length of thread engagement and wall thickness in the extruded hole to develop the full tensile strength of the thread rolling screw. In those cases, the minimum tensile strength of the screw governs the design, and published data on tensile strength are available¹¹. If the extruded hole does not develop the full strength of the screw, the threads in the extruded hole are more likely to strip than the threads on the screw.

The strength of the threads in the extruded hole may, therefore, govern the strength of the joint. However, several factors make accurate prediction difficult. The extruding and thread rolling operations cold work the metal and increase the thread strength. Conversely, part or all of the extrusion may have a relatively thin wall, particularly with thin gauge sheet steel, which tends to diminish thread strength. If the strength of the joint is critical, tests should be run to determine the best available thread profile and optimize the dimensions of the extruded hole.

3.4.2.2.3 Clamp-Up Fasteners

Clamp-up fasteners ([Figure 3.4.2.2.3-1](#)) are also installed from one side.

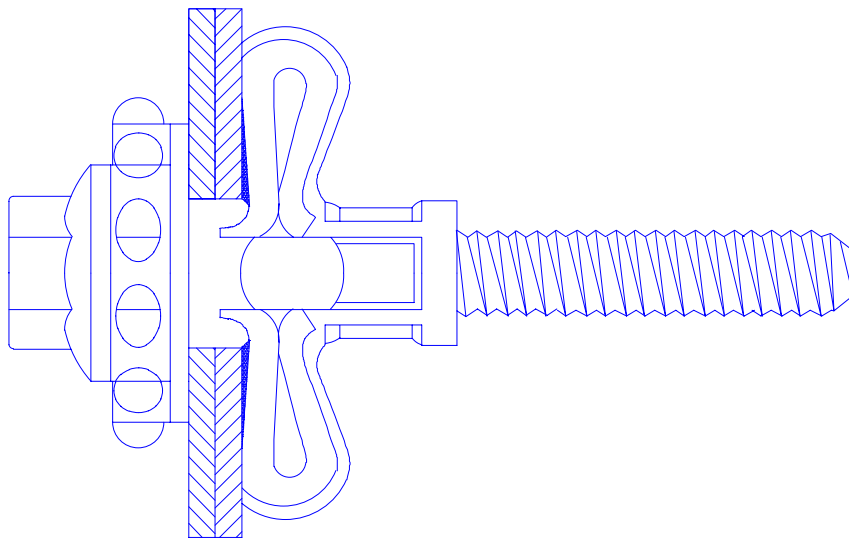


Figure 3.4.2.2.3-1 Clamp-up type fastener

They are detailed so that, in effect, they have two washers and are thus more resistant to pullover. (See discussion of pullover in [Section 3.4.2.3](#)). They also tend to hold better under vibrating loads than the self tapping screw, when joining thin sheets.

3.4.2.2.4 Pop Rivets

Pop rivets are another type of one sided fastener that can be used to connect sheet steel. During installation, the fastener pin is drawn through the rivet (which acts as a sleeve) causing it to expand and fill the hole. The tensile capacity of this connection is often less than the shear capacity; however, the shear capacity is good for its size.

3.4.2.2.5 One-Side Fasteners Requiring Two-Side Access

Self-piercing, hardened steel fasteners are forced through the sheet metal from one side of the joint. However, access is required for a backup die on the opposite side. Depending on the process, either the die side or both sides are swaged or cold-formed over to lock the sheets together. This type of fastener is not as repeatable as conventional "aircraft" structural rivets, and joint strengths are not as high. However they develop higher static strengths than do mechanically fastened joints.

Self-piercing fasteners offer two principal design advantages:

1. Joints may exceed the normal 2.5-3:1 maximum metal thickness ratio for welding¹².
2. The tolerance stackups resulting from pre-punched holes, and the need to drill at assembly are eliminated.

Two design/processing factors affect the joint strength.

1. The joints are generally stronger when the fastener is inserted through the thinner sheet first with the clinch in the heavier piece of metal.
2. Lubricants should be removed from the joint because they may reduce the long term joint strength.

The phases of joint formation for one style of fastener are shown in [Figure 3.4.2.2.5-1](#). A cross section of the joint is shown in [Figure 3.4.2.2.5-2](#). The head of the fastener may be convex, as illustrated in [Figure 3.4.2.2.5-1](#) or flush as illustrated in [Figure 3.4.2.2.5-2](#).

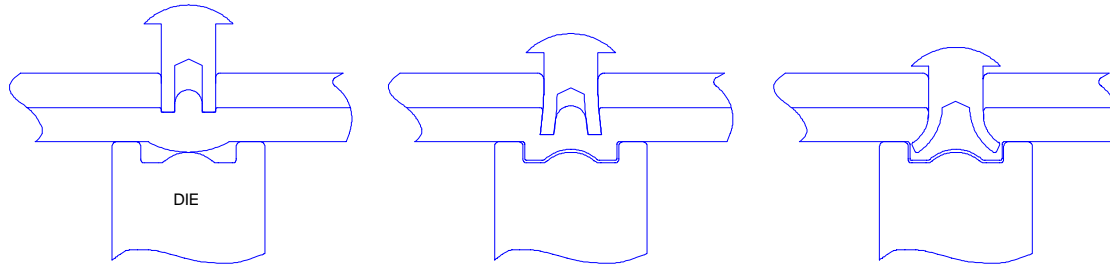


Figure 3.4.2.2.5-1 Phases of joint formation with a self-piercing fastener

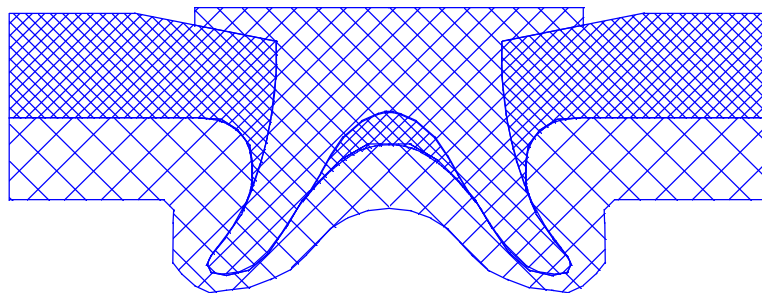


Figure 3.4.2.2.5-2 Cross section of a joint formed with a self-piercing fastener

Automotive applications of this type of fastener include:

- Two piece control arm stampings, which are being partially fastened at key locations.
- Zinc coated steel seat structure panels 0.7 mm (0.028 in.) thick, which are being fastened to pre-painted steel seat brackets 3.0 mm (0.125 in.) thick

3.4.2.3 Design Considerations for Mechanical Fasteners



3.4.2.3.1 Pullover

Sheet connections in single shear with thickness of 5 mm (3/16 in.) and smaller (i.e. with limited flexural stiffness) will tend to pull over the fastener. The fastener connecting two sheets in single shear will rotate to accommodate the pullover. Manufacturers' test results for #12 self tapping screws are indicated as pullover values instead of shear values in sheets of 1.27 mm (0.05 in.) thickness or less. This implies that considerations other than fastener shear integrity can control the shear capacity of a connection as illustrated in [Figure 3.4.2.3.1-1](#).

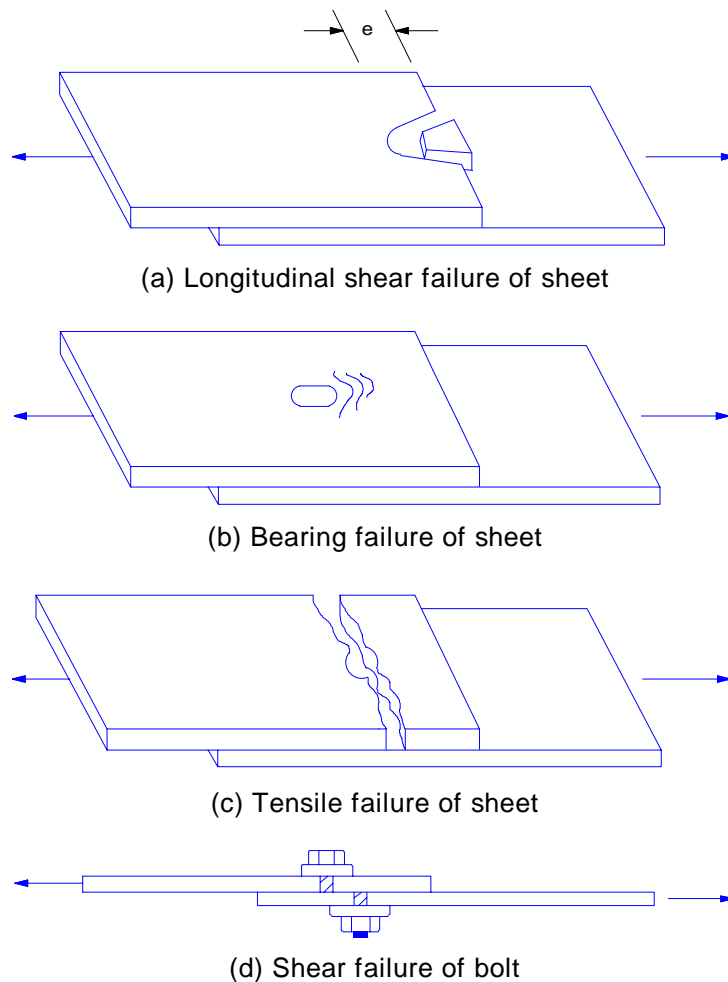


Figure 3.4.2.3.1-1 Types of failure of bolted connections

3.4.2.3.2 Spacing and Edge Distance for Bolts

The spacing and edge distance for bolts must be controlled in order to achieve the desired strength. The minimum bolt spacing should be **3d** (where **d** is the bolt diameter) between center of bolt holes. The distance from the center of any standard hole to the end or edge of member or plate should be at least **1.5d**. In addition, the distance e_{min} from the center of a standard hole to the end of the part or to the nearest edge of an adjacent hole in the direction of the line of force should be limited, to prevent the type of failure shown in [Figure 3.4.2.3.1-1\(a\)](#), to

$$e_{min} = \frac{V_u}{F_u t}$$

Equation 3.4.2.3.2-1



where V_u = ultimate shear force to be transmitted
 t = thickness of thinnest part
 F_u = tensile strength of thinnest part.

Simply use consistent units for stress and dimension in the evaluation of e_{min} .

3.4.2.3.3 Bearing Stress Limits

The ultimate bearing stress, F_{bu} , of the fastener against the sheet can also limit the shear capacity. The bearing stress is calculated as V_u/dt , where d is the nominal (gross) diameter of the fastener and V_u and t are as defined in [Equation 3.4.2.3.2-1](#). Bearing failure is illustrated in [Figure 3.4.2.3.1-1\(b\)](#).

Although the bearing limit is better for steels with larger F_u/F_y ratios, the primary variable is the restraint provided to the sheet adjacent to the bolt. If washers are used under both nut and bolt head or the plate is confined by other plates on each side, the ultimate bearing stress is as follows when the deformation around the bolt holes is not a design consideration.

$$F_{bu} = 3.0F_u$$

Equation 3.4.2.3.3-1



If an outside sheet is attached with bolts having no washers, then the ultimate bearing stress on that outside sheet should be limited to

$$F_{bu} = 2.2F_u$$

Equation 3.4.2.3.3-2



To achieve these bearing limits, the end distance e_{min} would have to be greater than **1.5d** and based on evaluation of [Equation 3.4.2.3.2-1](#).

3.4.2.3.4 Sheet Tensile Capacity

The tensile capacity of the sheet is the last thing to check ([Figure 3.4.2.3.1-1\(c\)](#)). For sheet with thickness $t < 5$ mm (3/16 in.), the capacity is a function of the presence of washers and conditions of single or double shear. The conservative expression that is applicable to cases with no washer under the bolt head or nut is

$$F_t = \left(1.0 - r + \frac{2.5rd}{s}\right)F_u \leq F_u$$

Equation 3.4.2.3.4-1



where r = the force transmitted by the bolt or bolts at the section considered, divided by the tension force in the member at that section. If r is less than 0.2, it may be taken equal to zero.

d = nominal (gross) diameter of the fastener.

s = spacing of bolts perpendicular to line of stress. In the case of a single bolt, s is the width of sheet.

F_t = ultimate tensile stress on net section

Use of this expression can be facilitated by the chart in [Figure 3.4.2.3.4-1](#).

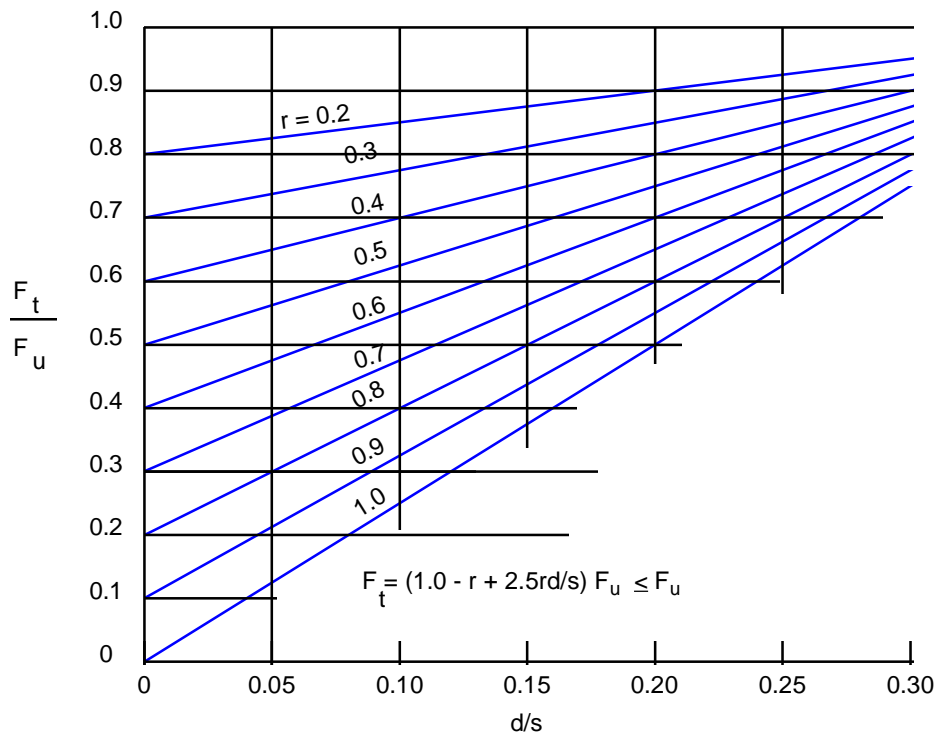


Figure 3.4.2.3.4-1 Ultimate tension stress on net section for bolted connections

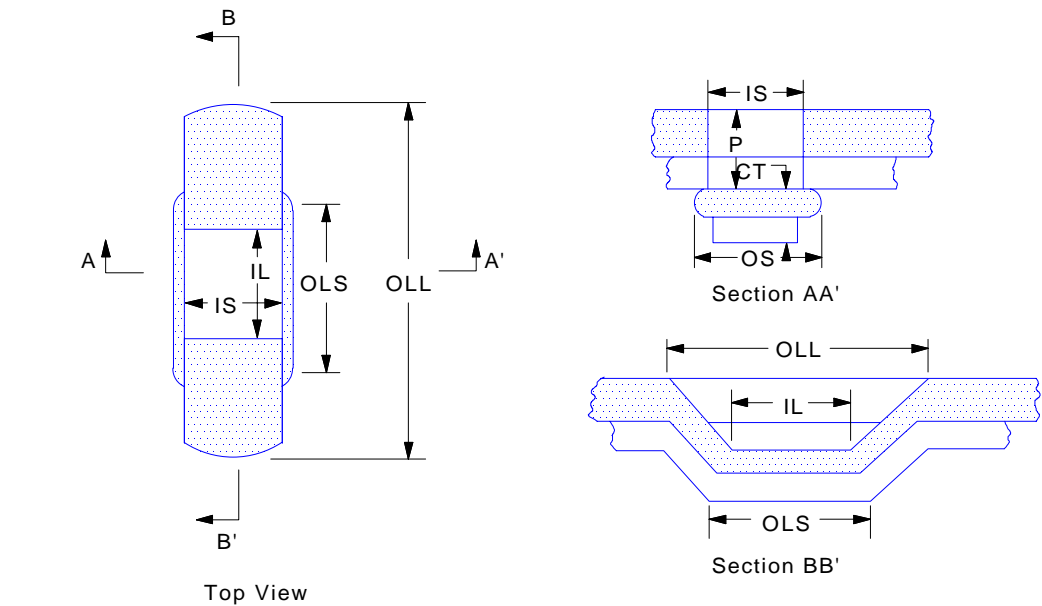
For information on the exact criteria for connections with washers, see the 1986 AISI Specification³.

3.4.3 MECHANICAL JOINING

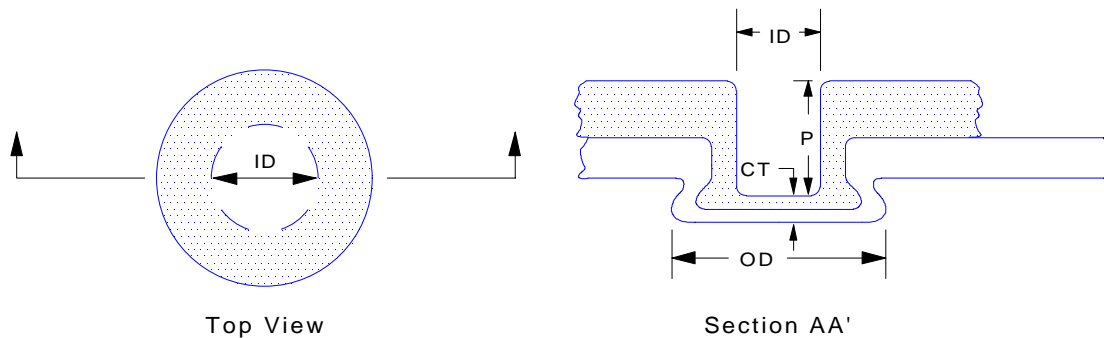
Where an alternative to spot or arc welding is required, and access for a backup die is available, mechanical clinch fastening may be used. The process is accomplished by mechanically joining two sheets directly, rather than using bolts or screws. It requires established minimum elongations of the clinched materials. Two mechanical joining methods are shown in [Figure 3.4.3-1](#). The general guideline for clinching is to place the most formable or thickest piece on the punch side so that it can support the loads imposed by the tools.

The conventional mechanical joint is formed by first piercing or slitting the sheets; then the tabs are pressed to lock the two sheets together. The technique shown in [Figure 3.4.3-1\(a\)](#) is one employed to join two lapped sheets. The strength under static and fatigue loading is not as good as that of a spot weld^{13, 14, 15}.

The button type mechanical joint has better behavior than the conventional mechanical joint¹³. It exhibits better static strength, better energy absorption on peeling and since it has no cracks, it has better fatigue properties. The button type mechanical joint has high cycle fatigue properties comparable to those of a spot weld even though its static properties are lower.



(a) Schematic of conventional mechanical joint



(b) Schematic of button-type (crack free) mechanical joint

Figure 3.4.3-1 Mechanical joint types

Examples of automotive applications of mechanical joining include:

- Assembly of very thin gauge, aluminized mild steel or ferritic steel heat shield assemblies.
- Assembly of adhesively bonded deck lid or hood inner and outer panels to fixture them before ELPO heat or to improve shear and peel strength. Also avoids "crows feet" caused by welding heat.
- Assembly of steel brackets sandwiched to plastic fender panels.
- Assembly of steel fan blades
- Assembly of steel chassis stampings prior to welding to minimize distortion.

3.4.4 SPACING OF MECHANICAL CONNECTIONS



The spacing of mechanical connections between components, to develop a composite section, is typically based on several strength considerations. Little is presently known regarding the composite stiffness that is achieved. Flexural and axial stiffnesses are usually close to that

expected. However, when open sections are attached intermittently to produce a closed section, the expected torsional stiffness is not achieved. Apparently, such sections behave as open sections between connection points. Connection integrity must be more than that required by strength in order to approach the stiffness obtained from continuous connection between components.

An example of a strength consideration is the connection between a pair of channel shapes to form either an **I** or tubular section in compression. AISI requires a connection spacing that limits the slenderness ratio of the channel between connectors to half the critical slenderness ratio of the composite section.

Where a flat sheet in compression is attached to another element, AISI recommends a spacing that prevents Euler buckling at the stress level desired. The effective length factor is considered at 0.6 and the radius of gyration is $t/\sqrt{12}$ for the cover sheet of thickness t . This leads to an expression in the AISI Specification with parameters t/\sqrt{f} where f is actual stress in the plate. This expression does not have a constant factor of safety since it is based on elastic buckling only. It will tend to be unconservative as the stress f approaches the yield stress.

An alternate to the above can be employed for compression members. The alternate procedure is to employ the relative slenderness approach used for connecting channels.

Letting $K = 0.6$ for the plate of thickness t

$$\left(\frac{0.6s}{t}\right) \leq C\left(\frac{KL}{r}\right) \text{ from which } s \leq 0.48 Ct\left(\frac{KL}{r}\right)$$

Equation 3.4.4-1



where KL/r is the critical slenderness ratio of column.

With factor $C = 1$, the slenderness of the plate just matches that of the section; with $C = 0.5$, the slenderness ratio of the plate is half that of the section. [Equation 3.4.4-1](#) considers inelastic buckling since the limiting stress is governed by [Equation 3.1.2.5-1](#) using the KL/r of the section.

If the flat sheet or cover plate is used in a flexural member where KL/r is not calculated, establish a pseudo KL/r from the maximum stress required in bending. Determine KL/r from [Equation 3.1.2.5-1](#) by letting F_u equal the maximum bending stress in compression. This procedure is illustrated in [Example 3.4-1](#) shown in [Section 6.2.4.1](#).

Another design consideration for connection spacing of a flat plate (or any plate that laps with another leaving an unstiffened edge) is to prevent premature buckling of the unstiffened edge. This can be achieved if the spacing is kept to three times the projecting flat width w , (see [Figure 3.4.4-1](#)). This $3w$ value need not be less than $500t/\sqrt{F_y}$ (millimeters) since the unstiffened element can yield at this spacing. The $500t/\sqrt{F_y}$ is again likely to govern in most cases.

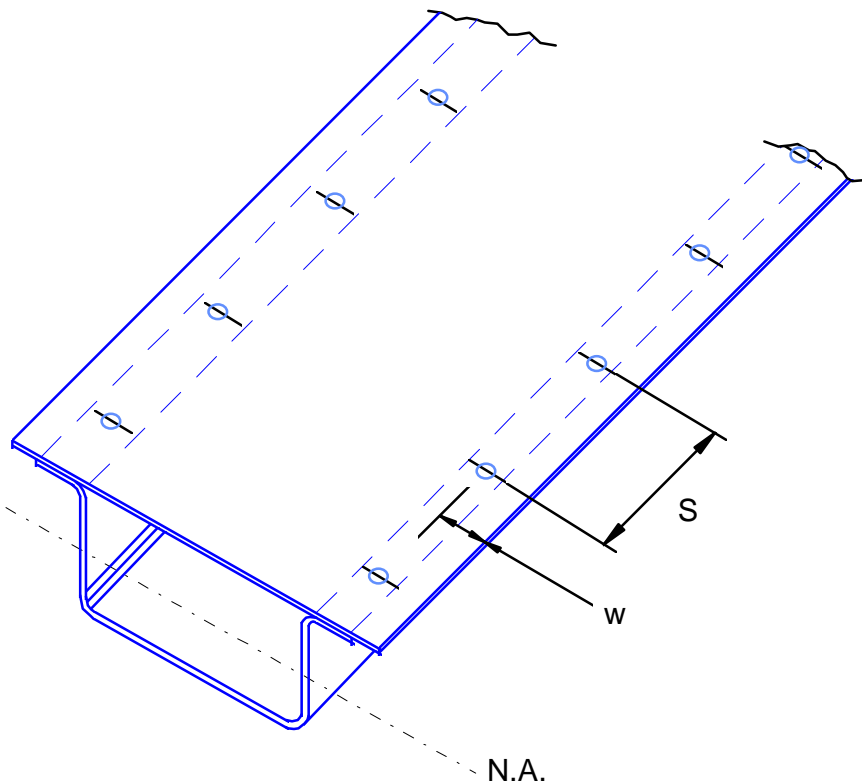


Figure 3.4.4-1 Spaced connection of flat element

The strength of the connection must also be checked, of course. For a flexural member, a longitudinal shear stress calculation is required. If the flat plate acts like a flange, the shear force per attachment point, V_s , is calculated as

$$V_s = \left(\frac{s}{n} \right) V_m \frac{Q}{I}$$

Equation 3.4.4-2

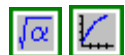


where V_m = maximum shear force in the beam
 Q = moment of the plate area about the section neutral axis
 I = section moment of inertia
 n = number of attachment points per location along section
 s = spacing of attachment points

Under axial load, there is no equation that dictates the shear requirement. Yu¹⁶ recommends using 2 percent of the axial load as a shear force that can be employed in [Equation 3.4.4-2](#) to compute the required V_s . Another approach would be to check the ability to transfer the axial load on the cover plate from the rest of the section into the plate over a certain length of the compression member.

$$V_s = \frac{\left(\frac{s}{n} \right) P_p}{L'}$$

Equation 3.4.4-3



where P_p = axial force in cover plate
 L' = length over which it is desired to transfer load

The value of L' could be as much as a quarter of the unbraced length of the member or may be only twice the depth of the section.

[Example 3.4-1](#) illustrates the evaluation of the spacing criteria for connection of a flat plate.

3.4.5 ADHESIVES

This section gives an overview of the types of adhesives available to the body designer and their characteristics, especially as they relate to the performance of the adhesive bonded joint. A glossary of terms relevant to adhesives is included in [Section 3.4.8](#).

Adhesive materials are basically plastics. Their characteristics and their performance in a given application will therefore be distinctly different from that of the steel members that they join. For example, the modulus of elasticity and design strength of steel are unaffected by temperature changes that vehicle bodies experience. However, for some adhesives they vary considerably over the same temperature range. The performance of the joint will also be distinctly different from joints made by welding or mechanical fastening.

Adhesives, like all plastics, are classified as either thermoplastic or thermosetting. Thermoplastics can be repeatedly heated to the point where they become liquid, and resolidified by cooling. Thermosets solidify by a chemical reaction called crosslinking, in which the molecules form bonds with adjacent molecules to form a solid state. The thermoset reaction does not result from the addition or removal of heat (although in many cases it is accelerated at elevated temperatures) and it is not reversible.

Structural and nonstructural are the two major categories for the adhesives that are used to bond sheet steel. In some literature, the distinction is made on the basis of application; that is, adhesives are called structural when used in applications where joints are integral parts of load bearing structures, such as B pillar to roof rail attachment. Adhesives are called nonstructural when used in applications where loads are negligible, such as the attachments of trim. In other literature the distinction is based on capability; that is, adhesives are called structural if they can be used in structural applications such as the one described above, and they are called nonstructural if they are not suitable for such applications. In this manual the latter distinction, capability, is applied.

The properties of all adhesives allow them to serve additional functions as sealants, insulators, and corrosion barriers. [Table 3.4.5-1](#) summarizes the properties and characteristics of five types of structural adhesive.

Table 3.4.5-1 Summary of properties and characteristics of structural adhesives¹⁷

	Epoxy	Polyurethane	Modified Acrylic (Reactive)	Cyanoacrylate	Anaerobic
Typical Cure Time: hr @ °F	2-24 @ 70 0.1-4 @ 300	0.2-0.5 @ 70	0.05-1 @ 70 for handling	0.5-5 @ 70	1-12 @ 70 0.05-2 @ 250
Number of Components	One or Two	One or Two	One or Two	One	One
Mixing	Some	Some	Some	No	No
Materials Bonded	Most	Most smooth, non porous	Most smooth, non porous	Most non porous	Metals, Glass thermosets
Gap Filling Characteristics	Tends to become brittle when thick	Excellent	Excellent	Poor	Poor
Substrate Preparation Required	Can bond oily Surfaces	Surface treatment and cleaning important	Some can bond oily surfaces	Yes	Yes
Service Temperature Range °F	-67 to 250	-250 to 175	-100 to 250	-67 to 175	-67 to 300
Impact Resistance	Good	Excellent	Good	Poor	Fair
Maximum Lap Shear Strength: psi @ 70° F	2200	2200	3700	2700	2500
Typical T-Peel Strength: lb/in.	< 3 - 20	80	30	< 3	10
Remarks	Good for dissimilar materials. Low Shrinkage. Variable pot life.	Excellent for low temperatures and dissimilar materials.	Good for bonding dissimilar materials.	Brittle, low shrinkage. Thin films are best.	May cause crazing of some thermoplastics. Thin films best.

3.4.5.1 Structural Adhesives

Structural adhesives are classified as either one or two part. This classification is important because the systems have different processing characteristics. One part adhesives are easy to dispense, but cure slowly, often requiring heat. Two part adhesives cure rapidly, but usually require mixing and dispensing equipment.

3.4.5.1.1 Epoxies

Epoxies are available as one or two part adhesives. One part epoxies require heat to cure; two part may utilize mild heating to speed curing. Epoxies have exceptional shear strength and can be chemically modified to increase peel strength or durability. One part epoxies generally have superior environmental durability and oil resistance compared with two part. This makes one part epoxies useful for bonding coated steel after stamping.

3.4.5.1.2 Urethanes

Urethanes are also available as one or two part adhesives. They require less heating to develop handling strength than epoxies. Cure can sometime be accelerated by adding water. Urethanes have shear strength that is equal to epoxies, and better peel strength. However, they may require a clean or primed surface for bonding. Urethanes are used for bonding glass to painted metal.

3.4.5.1.3 Acrylics

Acrylics are also available as one or two part adhesives and they cure rapidly without the need for fixturing. They are well suited to bonding metal because of their oil resistance, but the best acrylics currently have an objectionable odor. Since zinc is a catalyst for curing acrylics, galvanized steel could be potentially used as the catalyst. The actual surface area of zinc that is available to the acrylic is important. For example, electrogalvanized is rougher than hot dip galvanized, and would therefore have a higher potential for success. Special formulations are required to bond both sides of one side galvanized steel.

3.4.5.1.4 Cyanoacrylates

Cyanoacrylates cure rapidly and react with the moisture on the surface of the steel to induce cure. However, they cure too quickly to bond large areas. They require well mated surfaces because they cannot be used to fill gaps, and they will not tolerate oil on the adherends.

3.4.5.1.5 Anaerobic Adhesives

Anaerobic adhesives cure when oxygen is removed from the joint; this is especially useful when the joint is in a confined space. They are best suited for thread locking applications.

3.4.5.2 Nonstructural Thermoplastic Adhesives

Two categories of nonstructural thermoplastic adhesives are currently used in automotive body applications: vinyl plastisols and hot melt adhesives.

3.4.5.2.1 Vinyl Plastisols

Vinyl plastisols heat cure and require fixturing. They are oil resistant and, although they are not structural adhesives, have high peel strength. Vinyl plastisols are used to assemble the hood inner and outer panels.

3.4.5.2.2 Hot Melt Adhesives

Hot melts are thermoplastic adhesives that bond very quickly. They are applied as a hot liquid that wets the surface and gains adhesive strength as the liquid solidifies. Hot melts have difficulty in bonding to nonpainted metals because metals, depending on the surface area, may dissipate the heat before the adhesive wets the surface.

3.4.5.3 Physical Properties of Adhesives in Vehicle Design

The physical properties of an adhesive determine where it can be effectively used in automotive applications. For example, impact resistance is important in the front or "crush zones"; joints in the passenger compartment are designed for stiffness and strength. An understanding of the properties of adhesives is therefore important for selection of the optimum adhesive.

There are two principal modes of failure in a bonded joint: adhesive and cohesive. Adhesive failure occurs at the interface of the adhesive and adherend, whereas cohesive failure occurs within the adhesive. The two modes are shown schematically in [Figure 3.4.5.3-1](#).

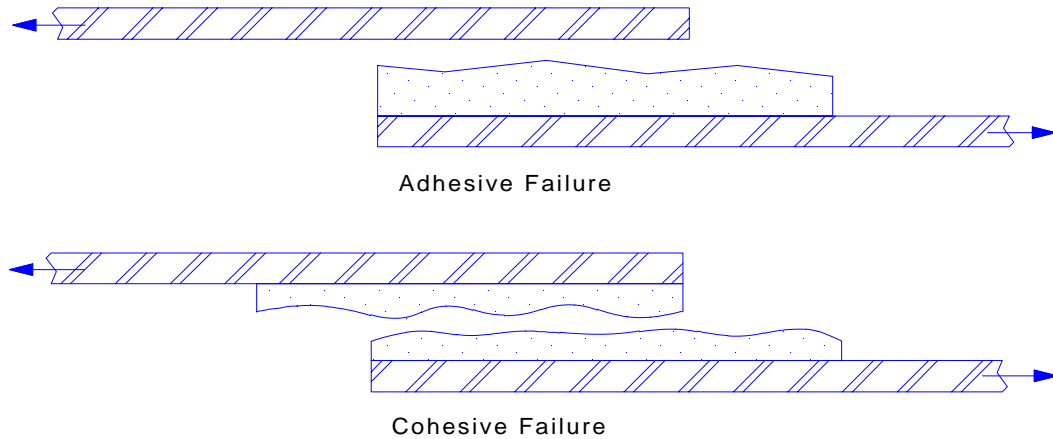


Figure 3.4.5.3-1 Adhesive and cohesive failures

Cohesive failure is the preferred mode because the life of the bonded joint can be predicted to some degree of accuracy, provided that applied loads and environmental conditions are as anticipated.

3.4.5.3.1 Impact Strength

Impact strength is essential for bonding components that are prone to large deflections, and subject to impact loading, as in a collision. In order for the adhesive to absorb impact energy without disbonding, it must exhibit high elongation and high peel strength. These properties allow the adhesive to stretch and flex before failure. Therefore, an elastic adhesive is generally selected when impact strength is the major consideration. Urethanes and toughened epoxies (modified to increase elongation and peel) are good choices for impact absorbing applications since they have more peel strength than rigid epoxies. [Figure 3.4.5.3.1-1](#) shows the relationship between load and deflection for rigid (brittle) and flexible (elastic) adhesives.

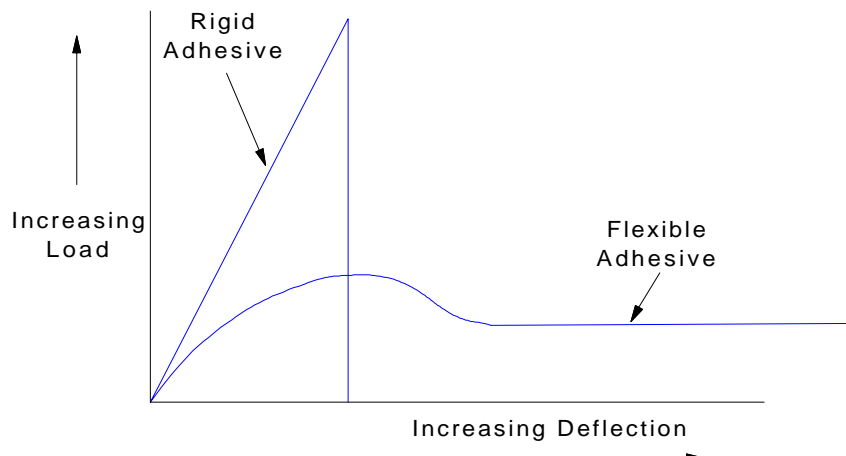


Figure 3.4.5.3.1-1 Adhesive load deflection properties.
Typical characteristics for static loading¹⁸

[Figure 3.4.5.3.1-2](#) shows the peel stress distribution for rigid and flexible adhesives.

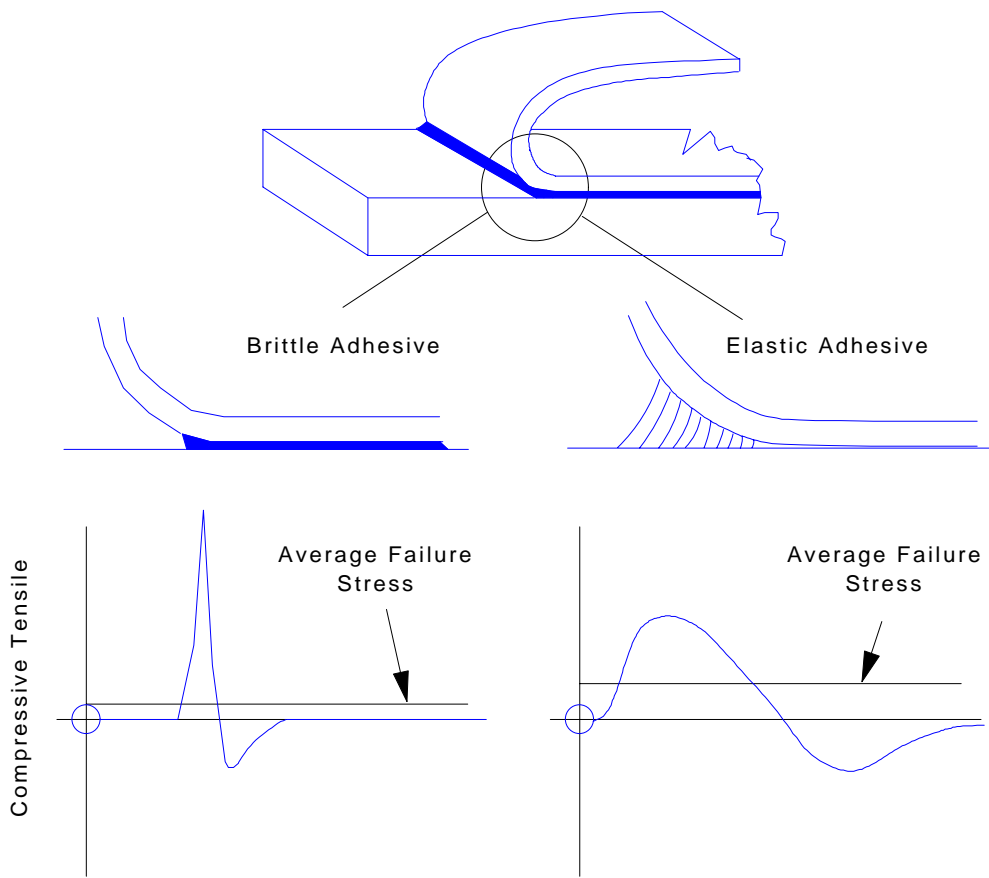


Figure 3.4.5.3.1-2 Peel stress distribution¹⁹

Adhesives become more rigid when suddenly loaded, as in the sudden impact of a collision. Thus, an elastic adhesive has more impact strength than static load tests indicate. Although the properties of adhesives may be reasonably well characterized, testing is always needed to determine if the adhesive retains both the minimum load bearing and impact characteristics necessary for a given application.

3.4.5.3.2 Peel Versus Shear Strength

Peel and shear are two of the four types of loading discussed in [Section 3.4.6.1](#). Since bonded joints often experience load combination, adhesive selection often involves a trade-off. Applications demanding high shear strength require a rigid adhesive; applications demanding high peel strength require a flexible adhesive.

Most rigid adhesives are too brittle for joints with simple geometries, such as lap joints, that require high shear strength. A rigid adhesive can be blended with a more flexible component, a process called toughening the adhesive. The addition of the flexible component allows the adhesive more elongation before bond failure, which increases peel strength and reduces shear strength. The trade-off is illustrated in [Figure 3.4.5.3.2-1](#).

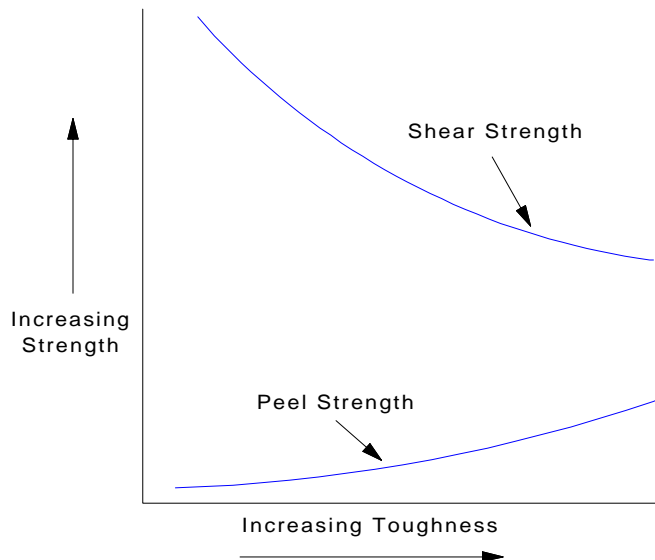


Figure 3.4.5.3.2-1 Strength-toughness trade-off in an adhesive¹⁸

Epoxies are usually toughened (modified to increase elasticity and peel strength) for automotive applications. Urethane adhesives have high peel strength and are usually stiffened (modified to reduce elasticity) to obtain high shear strength. In vehicle design, the high peel strength of urethanes makes them an excellent choice for bonding painted metal to glass. However, unlike epoxies, urethanes have poor oil resistance, and so toughened epoxies are used for bonding of oily steels in high strength applications.

3.4.5.3.3 Bond Life Versus Load

The load that a bonded joint can withstand, under conditions of long term continuous loading, is a function of the expected life. Typical of plastics, the design strength must be reduced when long term continuous loading is anticipated. For a life of five to ten years, design strength should be 10 to 20% of the ultimate strength of the joint. When the anticipated life is very short, in the order of one month or less, the design strength may be as high as 50 to 75% of ultimate. The relationship is shown schematically in [Figure 3.4.5.3.3-1](#).

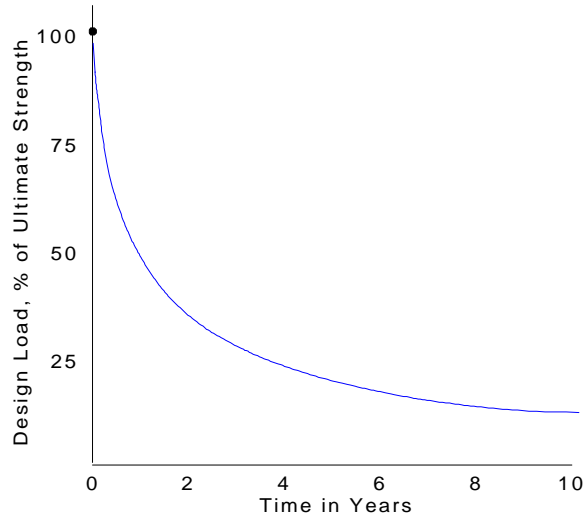


Figure 3.4.5.3.3-1 Schematic design load vs. time relationship for adhesive bonded joints

Actual values for design strength at expected life depend on the adhesive formulation and the anticipated loading.

3.4.5.4 Other Factors Affecting Performance Operating Temperature

Adhesives exhibit thermal properties that must be considered when selecting an adhesive. Some adhesives lose their elasticity at lower temperatures. Maximum shear strength generally occurs at a temperature within the useful range, and decreases at lower and higher temperatures. [Figure 3.4.5.4-1](#) shows typical relationships between shear strength and temperature for several structural adhesives.

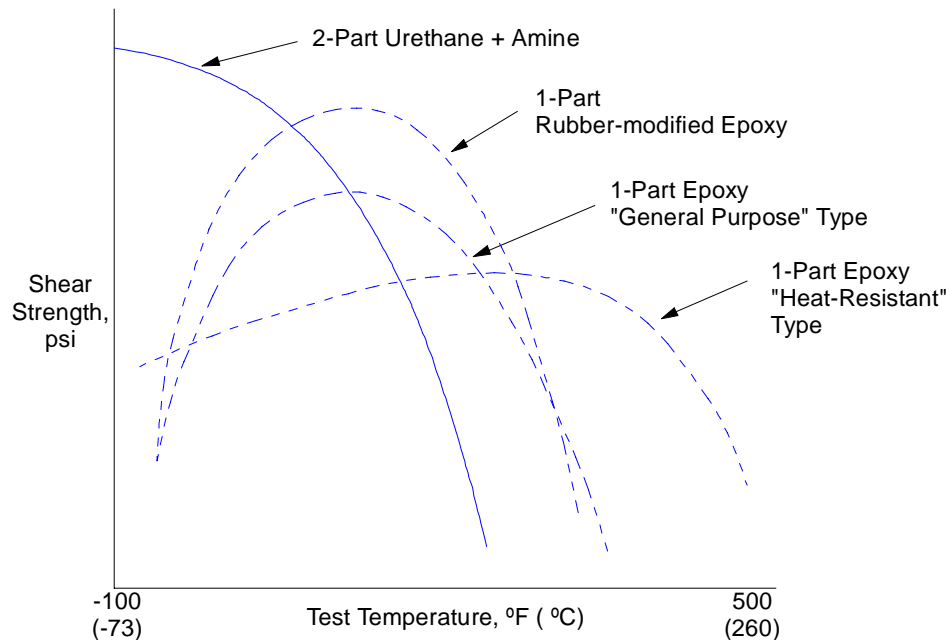


Figure 3.4.5.4-1 Effect of temperature on shear strength¹⁹

Therefore, for automotive applications the elongation and peel strengths of an adhesive must be tested over the entire anticipated temperature range. Although the properties of rigid adhesives are less temperature dependent than flexible adhesives, their peel strength is too low for normal conditions.

High temperature resistance must be considered for adhesive joints near the engine or exhaust system of the car. As temperature increases, rigid adhesives soften and become more flexible. Although the rigid adhesive loses its shear strength upon softening, its peel and impact strength increase.

3.4.5.4.1 Bondline Thickness

Peel and shear strength are both affected by bondline thickness. [Figure 3.4.5.4.1-1](#) shows that bondline thickness should be kept to a minimum to fully exploit the shear and peel strengths of the adhesive.

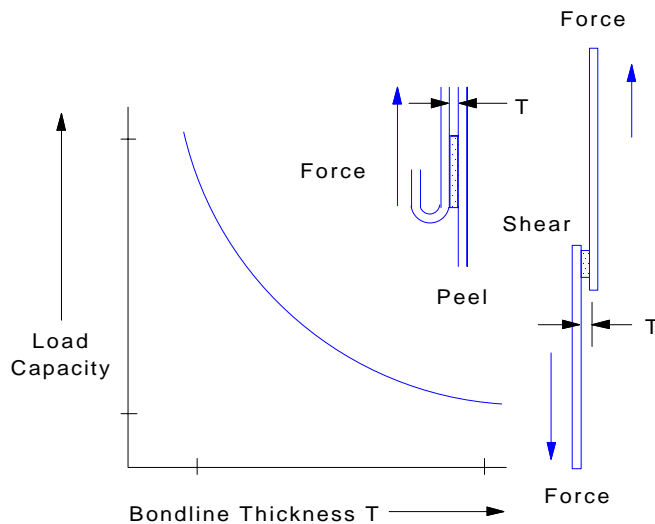


Figure 3.4.5.4.1-1 Load capacity vs. bondline thickness

3.4.5.4.2 Curing

Many adhesives require a curing cycle, in which the temperature of the adhesive is elevated, causing it to develop its full strength. It is current practice to tailor the adhesive so that it will cure in the paint ovens. The economic advantages are obvious; however two areas require special precautions:

1. Anticipated changes in paint oven temperatures must be known in advance so that adhesives can be modified and tested to meet production schedules. Adhesives suppliers usually assume this responsibility.
2. Adhesives that will operate at high temperatures (above 230°F or 110°C) require higher curing temperatures. The designer must ensure that paint oven temperatures will be high enough, or that a special cure cycle will be employed.

3.4.6 DESIGN FOR ADHESIVE BONDING

Adhesive bonding can be an economical and effective means for joining sheet steels. Bonding may, however, be overlooked if the designer is not familiar with the process. Structural bonding using adhesives has been employed in the aircraft industry since World War II, and it is finding numerous applications in automotive sheet steel body components. Design guidelines for bonding sheet steels have been developed and published¹⁹. This section focuses on automotive body applications.

Adhesive bonding offers a number of advantages over welding and mechanical fastening:

1. Sheet steel can be joined to materials that are dissimilar, including those with widely varying thicknesses and thermal properties.
2. Adhesive bonding produces a relatively uniform distribution of loads, and it does not impose discontinuities (such as holes) in the sheet steel. These characteristics lead to relatively good fatigue resistance.
3. Mechanical properties of the steel, such as those developed by heat treatment, can be preserved.

4. With proper design, the process does not leave a witness mark to mar cosmetic surfaces, such as the indentation that is left by spot welding.
5. A bonded joint develops a continuous contact area between surfaces that is attractive. It also provides a tight seal, which can act as a nonconductive layer (insulator) across the joint and as a barrier to corrosive environments.
6. Adhesives can be used in combination with spot welding or mechanical fastening to improve the performance of the joint.

The use of adhesive bonding imposes special conditions and requires the input of materials and manufacturing as well as design personnel. Among the problems that the team must address are:

1. build variations
2. surface conditions of the parts to be bonded
3. processing steps
4. substrates (coated or uncoated steel)
5. substrate lubricants
6. preparation and storage of adhesive
7. health of workers (toxicology)

3.4.6.1 Types of Static Load

There are four types of static load to which bonded joints may be subjected: tension, cleavage, shear and peel. These are illustrated in [Figure 3.4.6.1-1](#).

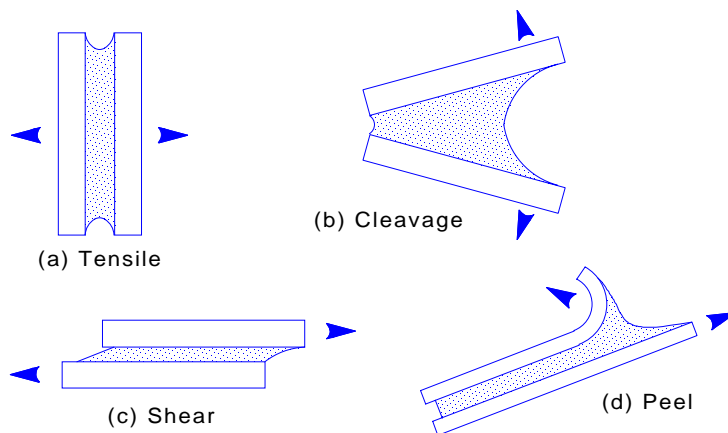


Figure 3.4.6.1-1 Types of static load

The designer should bear in mind that bonded joints usually experience a combination of these loads. Load types are discussed individually in this section to identify the characteristics of each and clarify their behavior.

In pure tensile loading, [Figure 3.4.6.1-1\(a\)](#), the forces are applied perpendicular to the plane of the joint, and the stress is distributed uniformly over the bond. This type of loading occurs when the applied loads are uniformly distributed, or when the members are rigid enough to effect uniform distribution of concentrated loads. Pure tensile loading is rare and impractical for joining sheet materials, as [Figure 3.4.6.1-2](#) would suggest.

Cleavage occurs when tensile forces are applied nonuniformly over the bond as shown in [Figure 3.4.6.1-1\(b\)](#). Adhesives will fail at lower cleavage loads than tensile loads, because localized stresses are higher than the stress associated with uniform distribution. Pure cleavage occurs only when the members are sufficiently rigid to avoid deflections that induce peel loading.

Shear, shown in [Figure 3.4.6.1-1\(c\)](#), occurs when the applied loads are parallel to the plane of the joint, and distributed uniformly. Pure shear is desirable, but it rarely occurs in bonded sheet metal structures because the members must be sufficiently rigid to remain parallel to the applied load, and thus avoid deflection that induces cleavage loading ([Figure 3.4.6.1-2](#)).

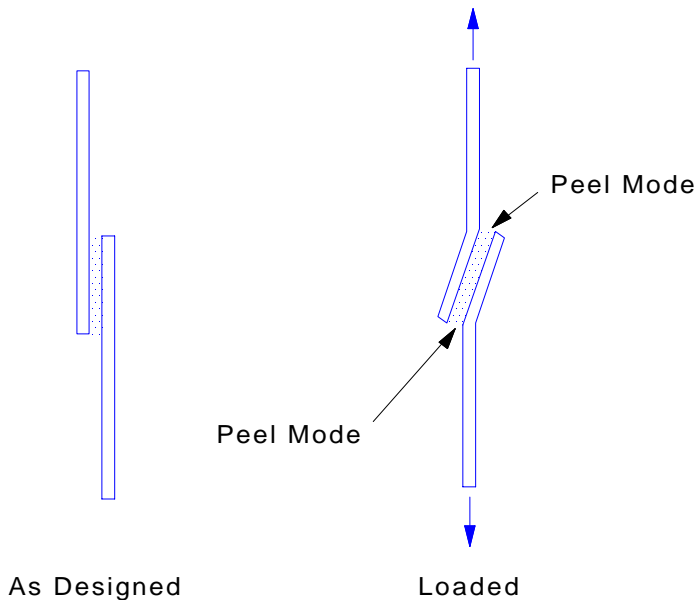


Figure 3.4.6.1-2 Peel forces may be generated at the bond ends when lap joints are subjected to a tensile load

Peel, illustrated in [Figure 3.4.6.1-1\(d\)](#), is undesirable because the stresses in the adhesives are concentrated on a very thin line at the edge of the bond. Since most automotive body components are made from relatively thin gage steel, most of the joints designed for automotive bodies will experience some degree of peel.

3.4.6.2 Adhesive Design Data

The designer must rely on test data to design bonded joints. While the performance of the joint will ultimately be verified by testing, the initial design will rely on test data. The data must adequately indicate whether bonding is feasible, and support a reasonably accurate first design approximation. ASTM test methods for developing tensile, lap shear, and peel data are illustrated in [Figure 3.4.6.2-1](#) and [Figure 3.4.6.2-2](#).

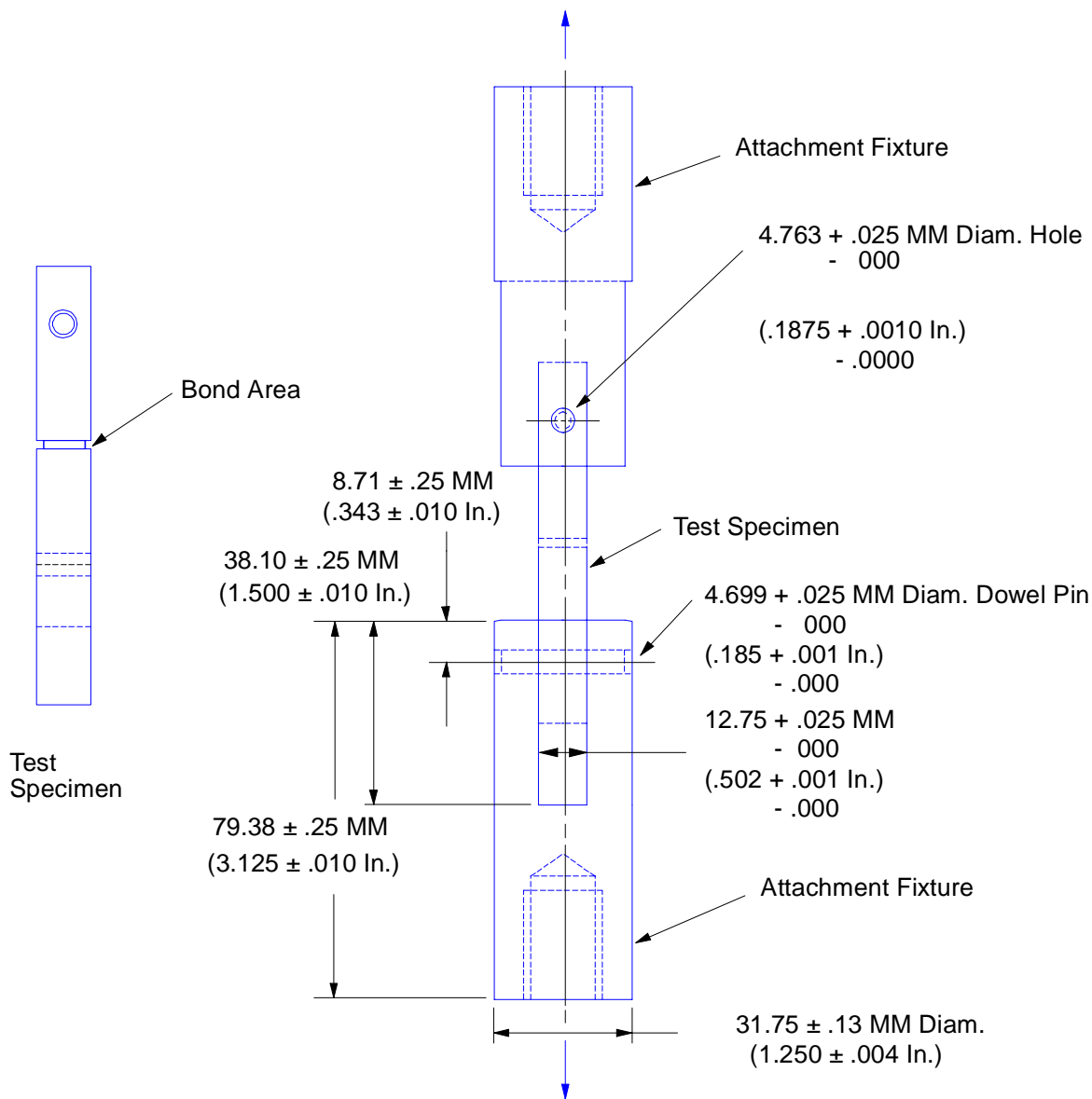
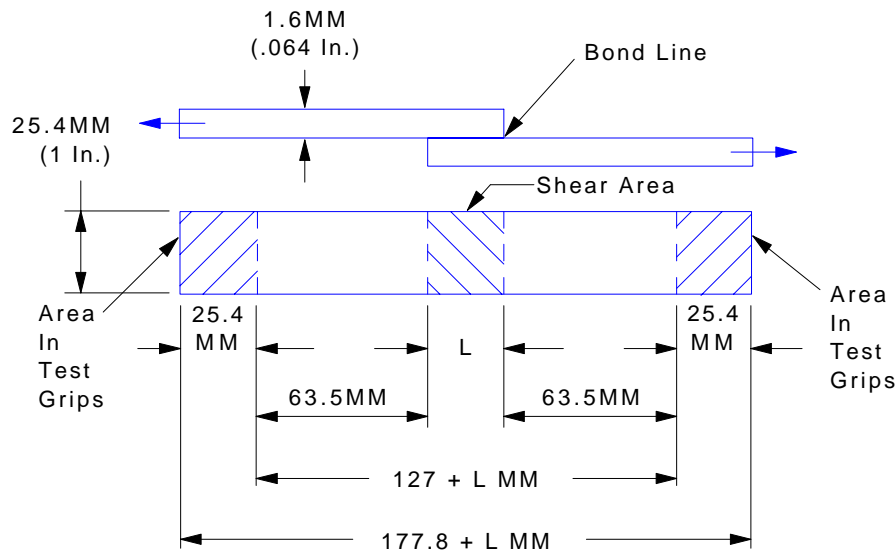
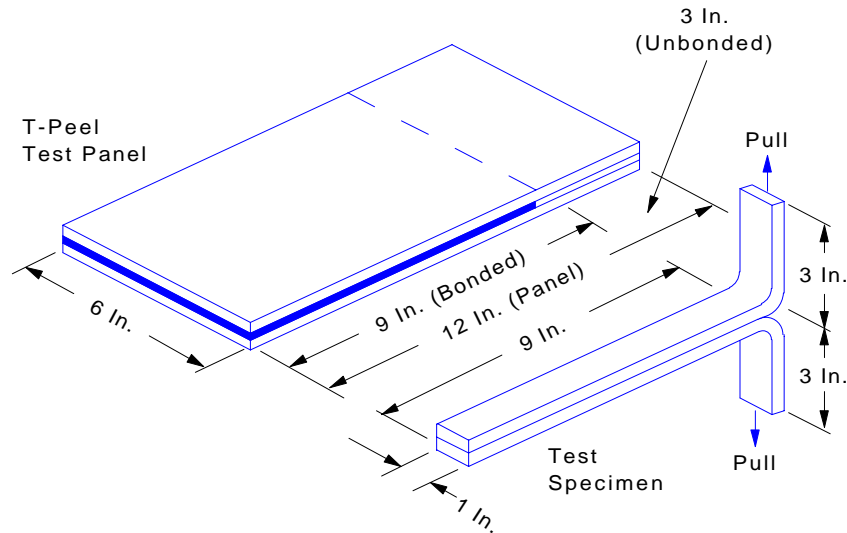


Figure 3.4.6.2-1 Test specimen and attachment fixtures for tensile test
(from ASTM D2095-62T)

The dynamic performance of a bonded joint is also of interest, particularly on joints that are subject to loads imposed by vehicle crash conditions. Efforts are now being made to establish test procedures that can be used to quantify the dynamic performance of bonded joints in sheet steel structures.



(a) Lap Shear Specimen (From ASTM D1006-62)



(b) Test Panel and T-Peel Specimen (From ASTM D1876-61T)

Figure 3.4.6.2-2 Lap shear and T-peel test specimens

Predicting the performance of an adhesive bonded assembly based on data derived from tests on standard test specimens presents certain difficulties. They can be handled if the designer understands the relationship between laboratory results and real world performance. There are four factors that must be considered when correlating test data with the design at hand.

1. ASTM test methods are designed to compare adhesives and minimize substrate effects. The values derived are good for rigid members, but overestimate the strength of joints using drawing quality sheet steels.
2. Test specimens used on tests other than ASTM may not be subjected to a single pure load condition. The specimens, like the bonded joint, may deflect somewhat so that the adhesive is loaded in several directions.

3. The joint will be subjected to load combinations that are less predictable and less controllable than for the test specimen. For example, [Figure 3.4.6.1-2](#) shows a combination of shear and peel in a joint with a simple geometric configuration. The peel is induced when the offset load causes the steel sheet to bend. The mode of loading becomes less predictable as the geometry of the joint becomes more complex.
4. Test data on standard specimens are based on the bonding technique as well as the adhesive. Factors such as substrate surface preparation, adhesive application, and curing, which are integral parts of published test data, may not be achieved or well controlled in practice.

Difficulties in correlating test data with real world performance can be minimized by utilizing good design practice. Ultimately the joint must be tested and the results evaluated against the design performance requirements.

3.4.6.3 Design Considerations

The design requirements of a bonded joint may be met by following four principles that are essential to good design practice:

1. Adhesives are strongest when loaded in shear. Design to maximize shear and minimize peel, cleavage and tension forces.
2. Use the maximum feasible bond area.
3. Avoid stress concentrations.
4. Consult with appropriate manufacturing and adhesives personnel to ensure that the adhesive and assembly techniques are optimized.

It is especially important to minimize peel, which is a concern whenever thin gage steel is joined. For example, [Figure 3.4.6.3-1\(a\)](#) shows a joint that may be appropriate for spot or resistance seam welding when the joint is accessible from only one side. However, this configuration is inappropriate for adhesive bonding, because the mode of loading would be mostly peel. Two design alternatives for a bonded joint, which introduce shear as the principal loading mode, are shown in [Figure 3.4.6.3-1\(b\)](#).

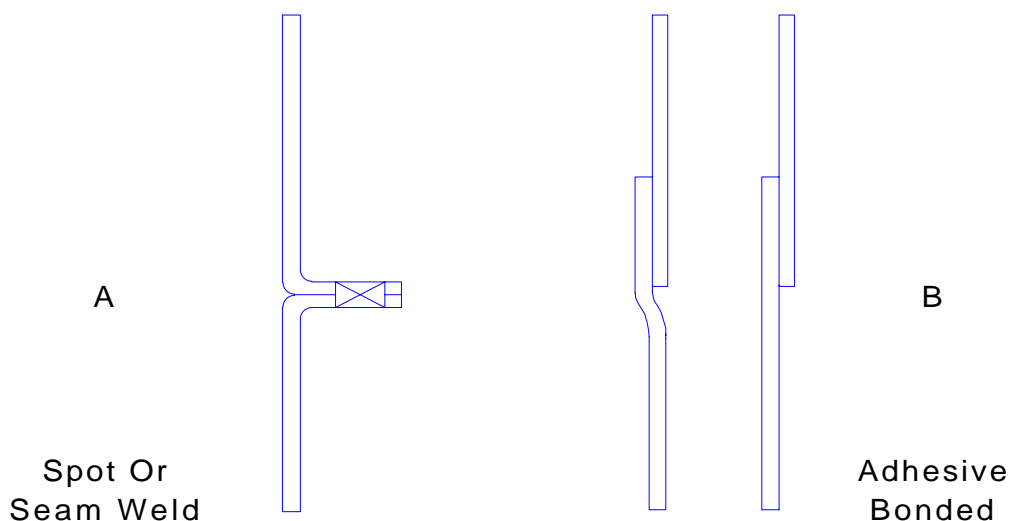


Figure 3.4.6.3-1 Alternative joint designs

When only one side of a joint is accessible, a spot or seam weld flange may be acceptable. If the members are bonded, a lap joint is preferred.

It is not always possible to redesign a joint to minimize peel. In those cases another type of fastening with adequate resistance to peel, such as spot welding or mechanical fastening, may be combined with bonding to develop the desired joint properties. Spot welding or mechanical fastening may also be required to fixture the joint while the adhesive develops handling strength (see [Section 4.4.2](#)). All such factors should be identified early in the design so that supplementary fastening can be designed to meet both requirements.

The adhesive application process must be factored into the design of the joint if the adhesive is to be constrained from wiping onto visible metal surfaces. When the adhesive is spread over 80 percent of the flange width or less ([Figure 3.4.6.3-2](#)), the application process can usually be controlled to confine the adhesive within the flange. The design strength of the joint will be based on a bond width that is less than the flange width.

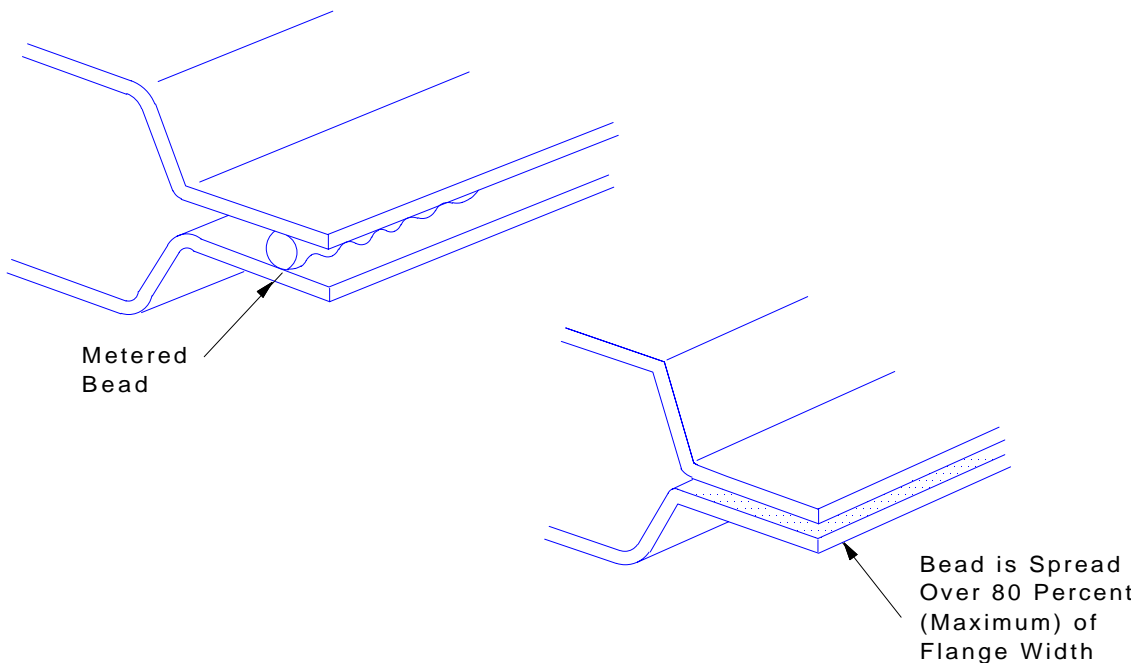


Figure 3.4.6.3-2 Squeeze out control by providing adequate flange width

Alternatively, [Figure 3.4.6.3-3](#) and [Figure 3.4.6.3-4](#) show joints that have been designed so that the full width of a designed area is bonded, and any excess adhesive is squeezed into nonvisible areas.

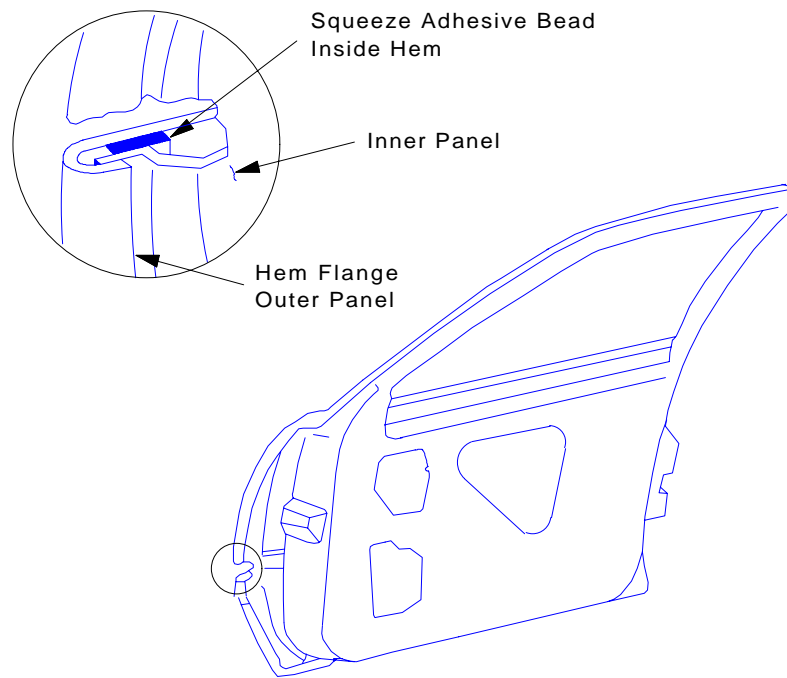


Figure 3.4.6.3-3 Squeeze out control of a bonded joint for a door hem in a visible area¹⁸

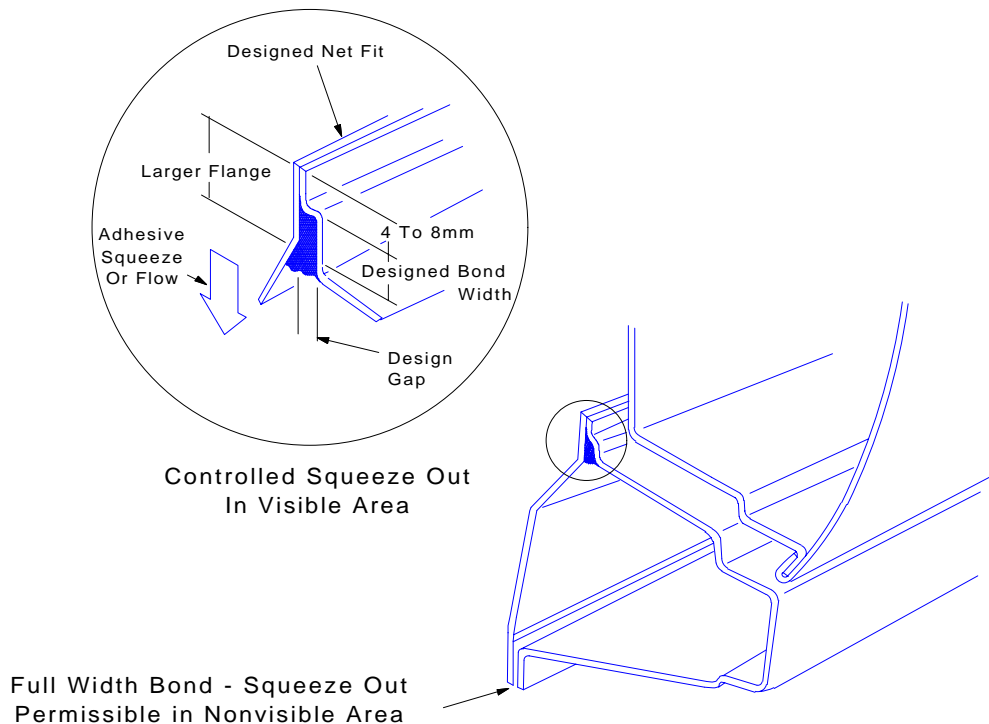


Figure 3.4.6.3-4 Squeeze out control of bonded joints for visible and nonvisible areas of a sill¹⁸

Figure 3.4.6.3-5 shows a joint that was designed so that the assembly operation would force any excess adhesive into nonvisible areas. These alternatives allow the joint design to utilize the full flange width.

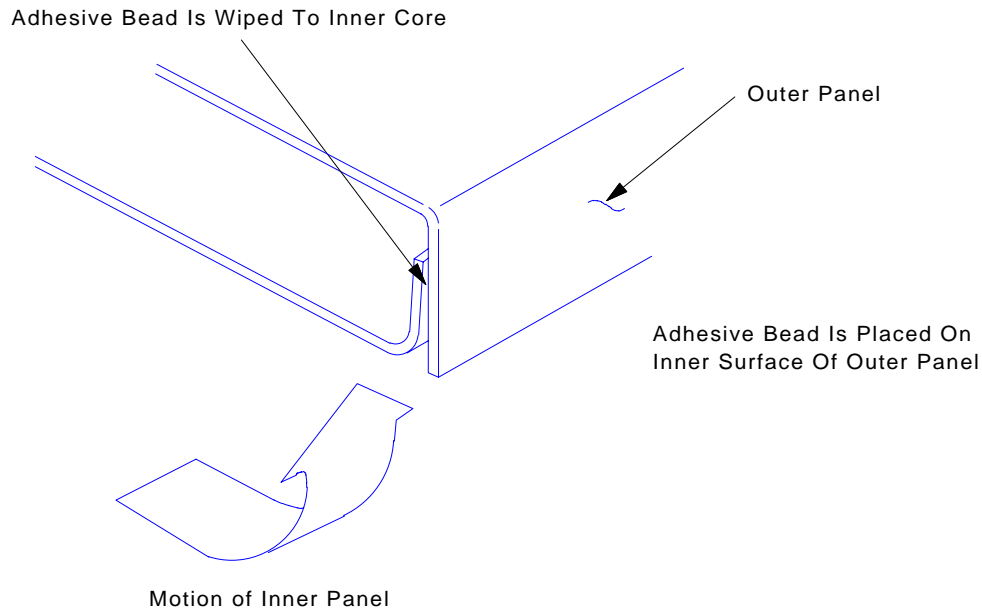


Figure 3.4.6.3-5 Adhesive squeeze out controlled by assembly operation¹⁸

The bonded joint may include features such as standoff pads or dimples along the bond surface that provide a gap to control the bondline thickness for consistent bond strength (recall [Figure 3.4.5.4.1-1](#)). Standoff pads can additionally provide locations for spot welds or mechanical fastening that will improve the performance of the joint or retain the members while the adhesive cures ([Figure 3.4.6.3-6](#)).

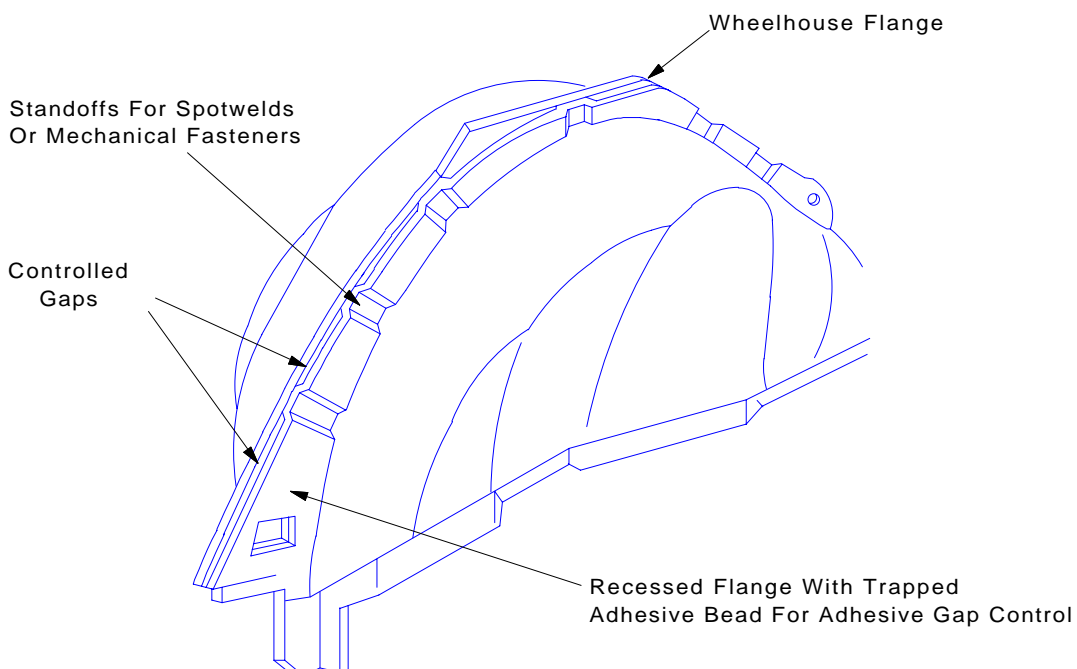


Figure 3.4.6.3-6 Standoffs utilized to form controlled gaps for adhesive and provide surfaces for spotwelds or mechanical fasteners¹⁸

3.4.6.4 Distribution of Shear Stresses in a Lap Joint

The distribution of shear stresses in the adhesive governs the strength of the joint to a great extent. Shear stresses are distributed uniformly across the width of a lap shear joint (direction perpendicular to the applied load). They are not uniformly distributed along the length (direction parallel to the applied load) because the steel and adhesive layers make up an elastic system in which strain, and consequently stress, is nonuniform. The strength of a lap joint is therefore proportional to its width, but is not proportional to its overlap length ([Figure 3.4.6.4-1](#)).

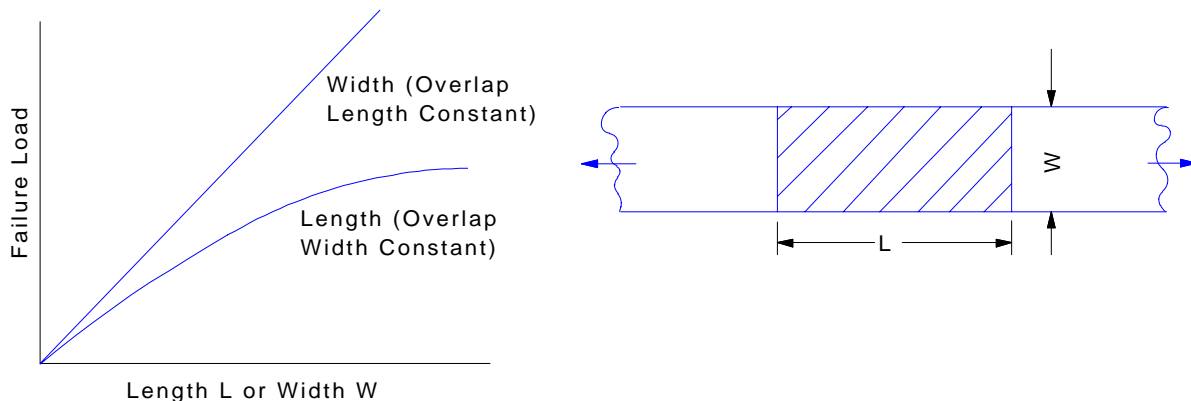


Figure 3.4.6.4-1 Effect of overlap and width on a typical lap-shear joint

[Figure 3.4.6.4-2](#) shows the typical stress distribution in a simple lap-shear joint.

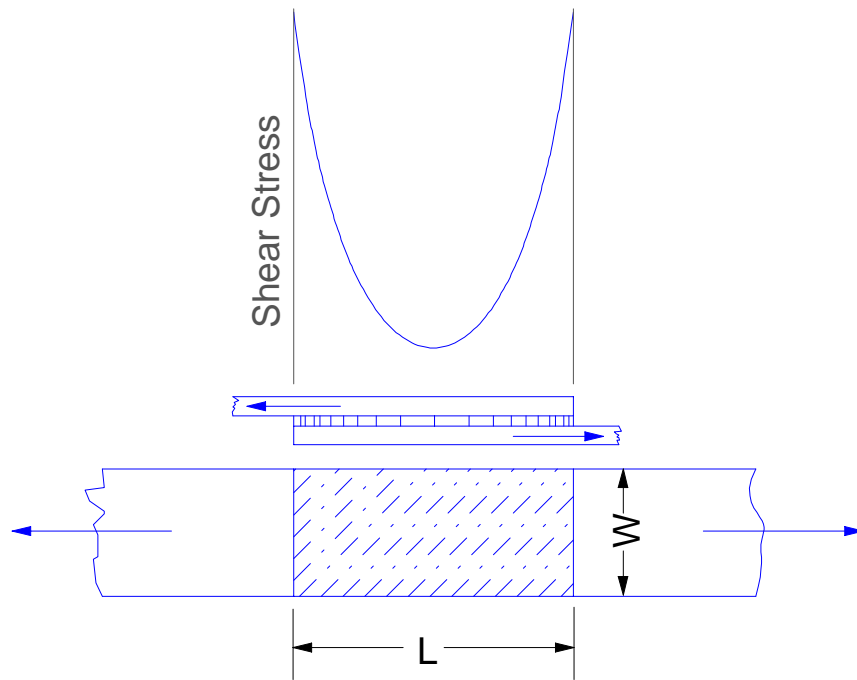


Figure 3.4.6.4-2 Typical stress distribution in a lap-shear joint parallel to the applied load

The figure indicates that the stress distribution in the direction parallel to the applied load is nonlinear as well as nonuniform. Therefore the strength of the joint cannot be predicted by simple calculations.

The relationship between the mean failure stress of an adhesive, the thickness of the steel, and overlap length has been demonstrated by De Bruyne²⁰.

Figure 3.4.6.4-3 shows the mean failure stress versus "joint factor", which is the ratio of the square root of metal thickness to overlap length.

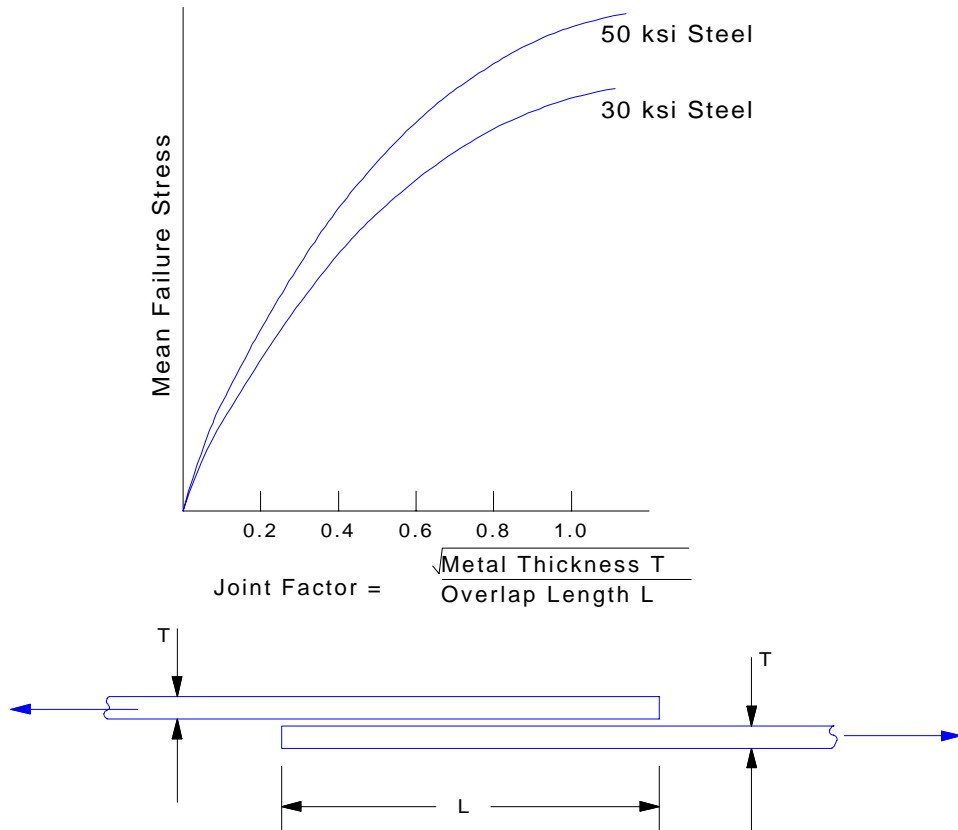


Figure 3.4.6.4-3 Typical mean failure stress vs. joint factor¹⁹ for a lap-shear joint¹⁹

At low values of joint factor, the failure stress is proportional to the square root of metal thickness, and essentially independent of the steel yield strength. The figure implies that the designer can vary factors such as metal thickness and length of overlap, within limits, to obtain the desired strength. The joint factor must be determined for each adhesive and for the strength of the steel.

3.4.6.5 Selection and Specification of Adhesives

Selecting an adhesive is a very complex process. The designer wants a strong adhesive that will never fail. Management wants the lowest overall cost; that is, material cost, equipment cost, maintenance cost and labor cost must all be minimized. Manufacturing engineering wants an adhesive that is safe and easy to use. The manufacturing manager wants an adhesive that is compatible with existing assembly practices. An applications engineer must select an adhesive that comes close to satisfying the needs of each group.

Fortunately, considerable amounts of information and assistance are available. Adhesive manufacturers and users are developing much needed technical information. The amount of practical experience grows every day as adhesives are used in new applications.

3.4.7 WELDBONDING

The term "weldbonding" describes the process of joining steel with a combination of spot welds and a structural adhesive. The process can lead to improved joint stiffness, strength and fatigue life, depending on the adhesive chosen and the spot weld spacing.

Weldbonding processes take advantage of the resistance to peel loading offered by spot welds and the resistance to shear loading offered by the adhesive. In a weld bonded joint, the adhesive distributes the load over a greater area of sheet metal surfaces, which results in a wider stress distribution across the members being joined, and reduced stress levels.

- Under static loading, reduced stresses in some cases increases the spring rate of the joint.
- Under cyclic loading, the more uniform distribution of stresses around the spot welds substantially increases fatigue life.
- Under dynamic loading, the wider uniform stress distribution will enable the joint to absorb more impact energy. Spot welds maintain the integrity of the joint after the adhesive has failed during large plastic deformations. [Figure 3.4.7-1](#) compares the impact energy absorption by spot welded, adhesive bonded and weldbonded joints.

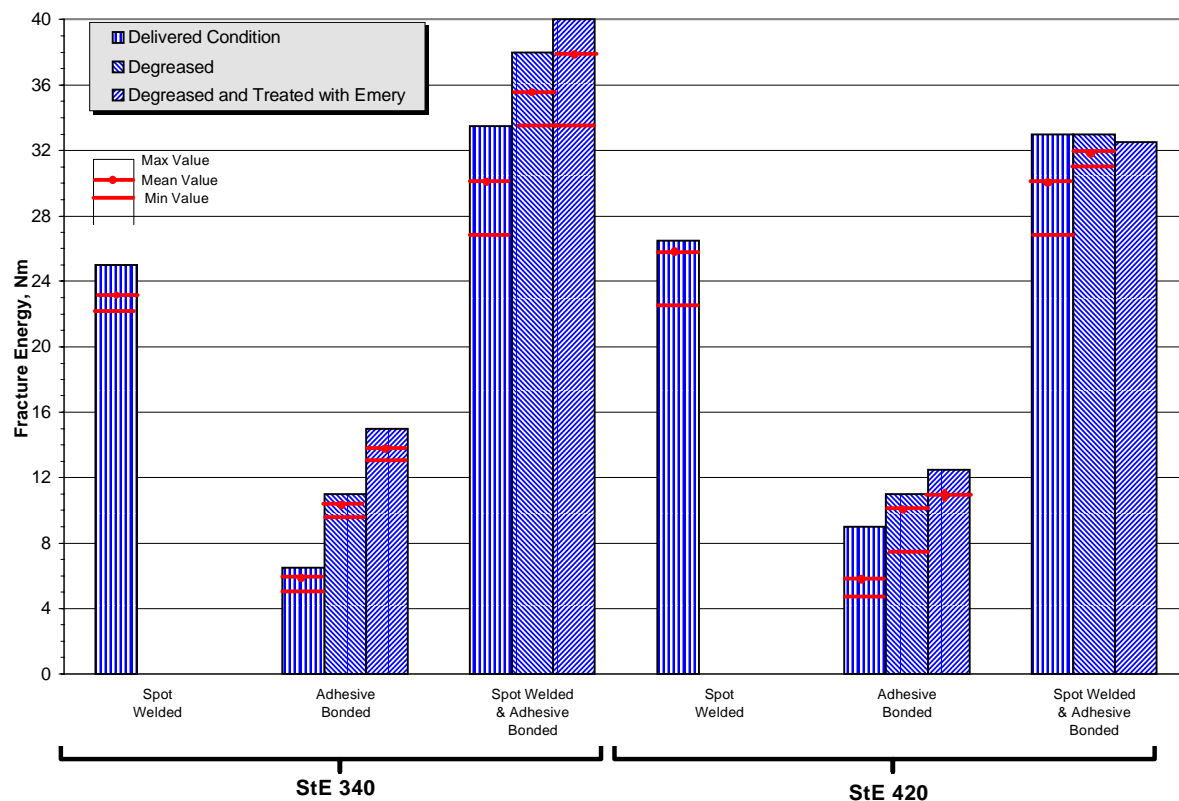


Figure 3.4.7-1 Impact energy absorption for various joints

Four design parameters affect the performance of weldbonded joints: weld spacing, adhesive type, width of weld flange and the type of loading for which the joint is designed.

Weld spacing will have the greatest effect when an adhesive with a low modulus of elasticity is used. The flexible adhesive allows the spot welds to be loaded, and they contribute more to the overall joint characteristics (refer to [Section 3.4.1](#) Welded Connections, and [Section 3.4.4](#) Spacing of Mechanical Connections for more information on spot welds and their spacing).

Adhesive type will influence weldbonded joint stiffness, strength, and fatigue life since different adhesives have varying moduli and tensile strengths (refer to [Section 3.4.5](#) Adhesives for more information).

Weld flange width contributes directly to the area bonded, and thus the area over which the load is applied. A larger bonded area will decrease the stress level in that location, increasing the fatigue life and increasing the amount of energy that can be absorbed from impact loading.

The type of applied load will affect how a weldbonded joint can perform. A joint designed so that the load will be in shear will best take advantage of the stiffness and strength of adhesives in shear. The spot welds in a joint designed so that the load will be tension or peel will contribute more to the stiffness and strength of the joint than will the adhesive because of the relatively low mechanical properties of adhesives in these types of loading.

Any location on the body-in-white may be a candidate for weld bonding. Some of the most common locations are:

- Areas with difficult weld gun access. Weld flanges that are difficult to reach with spot welding equipment and maintain the desired weld pitch are natural candidates.
- Fatigue life applications. Any joint that is sensitive to fatigue could have structural adhesive added to improve its fatigue life. Weldbonded joints can improve fatigue life while containing the cost and mass incurred by alternatives such as increased metal thickness or added reinforcements. Components loaded by the suspension, or by trailer towing, and latch strikers are examples of fatigue sensitive areas.
- Energy absorption applications. Weldbonded joints have proven to absorb more energy than spot welded joints. Downgaging of front and rear rail sections may be possible if crash energy absorption can be maintained. Structural adhesive can be applied along the entire length of the rails or in strategic locations to control the crash energy absorbed and possibly the crush mode. Potential applications include:
 - Front body hinge pillars, center pillar, and rocker section to increase the energy absorbed during a side impact.
 - Roof rails to absorb more energy during a vehicle rollover.

3.4.8 GLOSSARY OF ADHESIVE TERMS

The glossary in [Table 3.4.8-1](#) is applicable to adhesives that are used in automotive body applications. Some of the terms are not used in the text of this manual; they are included for the convenience of the reader who is utilizing other sources.

Table 3.4.8-1 Glossary of adhesive terms

Adhesive Term	Definition
Adherend	A material joined by an adhesive
Bondline Thickness	The gap between the adherends that is filled by adhesive
Cure, Curing	Cause and adhesive to develop its final chemical and mechanical properties; more appropriate with thermosetting adhesives (see set)
Curing Agent	A chemical component that accomplishes curing
Engineering adhesive	A structural adhesive meeting specific performance criteria; e.g., a minimum shear of 500 psi
Fixturing	Any technique that supports the joint until the adhesive develops handling strength
Gel	(See definition of set)
Handling Strength	Strength developed in and adhesive during curing that is less than full cure but sufficient to allow the bonded components to be moved or otherwise handled
Hot Melt	An adhesive that bonds upon cooling
Induction Curing	A heat curing process where heating is produced by an electromagnetic field
Net Fit	Metal-to-metal or adhered-to-adherend contact
Non Structural Adhesive	Monomer based composition that may or may not polymerize to form a permanent bonded barrier between two adherends forming a non load bearing joint
One Part Adhesive	An adhesive that requires no mixing
Open Time	The maximum allowable time period (for a two part adhesive) between mixing the adhesive and joining the adherends
Peel	A type of loading that imposes a very high edge stress to the boundary of bonded area (Figure 3.4-18)
Peel Strength	Resistance of an adhesively bonded joint to fail in a prying or peel mode; measured in force per unit area
Set (Gel)	Convert the adhesive from its dispensed state to a nonflowing state exhibiting some adhesion; more appropriate with thermoplastic adhesive (see cure)
Shear	A type of loading that imposes stress that is distributed across the bonded area in the plane of the joint
Shear Strength	Resistance to an applied load of an adhesively bonded joint in the plane of the bondline; measured in force per unit area
Structural Adhesive	Monomer based composition that polymerizes to form a high modulus, high strength, permanent adhesive to bond two relatively rigid adherends, forming a load bearing joint
Thermoplastic	A polymer that repeatedly softens when heated
Thermoset	A polymer that cures by crosslinking and does not soften upon reheating
Toughening	Decreasing the brittle characteristics of an adhesive by adding appropriate constituents to the formulation
Two-Part Adhesive	An adhesive consisting of a resin and a curing agent, which begins curing when the components are mixed
Viscosity	The resistance to flow of a liquid
Weldbonding	Joining process using adhesive bonding supported by resistance spot welding

REFERENCES FOR SECTION 3.4

1. American Iron and Steel Institute, Committee of Sheet Steel Producers, *Spot Welding Sheet Steel*, Washington, D.C.
2. American Iron and Steel Institute, *Specification for the Design of Cold-Formed Steel Structural Members*, September, 1980, Washington, D.C.
3. American Iron and Steel Institute, *Specification for the Design of Cold Formed Steel Structural Members--1986 Edition*, Washington, D.C.
4. LaBoube, R.A. and Yu, W.W. "Tensile Strength of Arc Spot Weld Connections", Proceedings of the International Conference on Steel and Aluminum Structures, Singapore, May, 1991.
5. LaBoube, R.A. and Yu, W.W. "Behavior of Arc Spot Welds in Tension", Journal of Structural Engineering, ASCE, Vol. 199, No. 7, July 1993.
6. SAE Standard J105, *Hex Bolts*, Society of Automotive Engineers, Inc., 400 Commonwealth Drive, Warrendale, Pa.
7. SAE Standard J429 Aug 83, *Mechanical and Material Requirements for Externally Threaded Fasteners*, Society of Automotive Engineers, Inc. 400 Commonwealth Drive, Warrendale, Pa.
8. SAE Standard J82 Jun 79, *Mechanical and Quality Requirements for Machine Screws*, Society of Automotive Engineers, Inc. 400 Commonwealth Drive, Warrendale, Pa.
9. SAE Standard J1199 Sep 83, *Mechanical and Material Requirements for Metric Externally Threaded Steel Fasteners*, Society of Automotive Engineers, Inc. 400 Commonwealth Drive, Warrendale, Pa.
10. SAE Standard J995 Jun79, *Mechanical and Material Requirements for Steel Nuts*, Society of Automotive Engineers, Inc. 400 Commonwealth Drive, Warrendale, Pa.
11. SAE Standard J81 Jun79, *Thread Rolling Screws*, Society of Automotive Engineers, Inc. 400 Commonwealth Drive, Warrendale, Pa.
12. Hill, Howard, *Introduction To The Self-Piercing Riveting Process and Equipment*, Advanced Technologies and Process Sessions, IBEC '94, Detroit, Michigan, September, 1994.
13. Sawhill, J.M., Jr., and Sawdon, S.E., *A New Mechanical Joining Technique for Steel Compared with Spot Welding*, SAE Technical Paper No. 830128 (March, 1983).
14. Larson, Johnny K., *Clinch Joining - A Cost Effective Joining Technique for Body-In-White Assembly*, Advanced Technologies and Process Sessions, IBEC '94, Detroit, Michigan, September 1994.

15. Strandberg, Osten and Lennblad, Johan, *FE Modeling Of The Clinch Joining Process*, Advanced Technologies and Process Sessions, IBEC '94, Detroit, Michigan, September 1994.
16. Yu, Wei-Wen, *Cold Formed Steel Design*, 1985, John Wiley & Sons, Inc.
17. Adapted from "Bonding Advice: How to Select the Right Adhesive", *Modern Metals*, May 1987.
18. Adapted from American Iron and Steel Institute, *Adhesive Bonding of Sheet Steels*, Washington D.C., 1987.
19. American Iron and Steel Institute, Committee of Sheet Steel Producers, *Production Design Guide for Adhesive Bonding of Sheet Steel*, Washington, D.C., 1976 (Out of print).
20. Adapted from De Bruyne, N.A. and Houwink, H., *Adhesion and Adhesives*, p 98, London, Elsevier Publishing Co., 1951 (Cited by Irving Skeist in *Handbook of Adhesives*, Second edition, p 109).

3.5 DESIGNING AGAINST FATIGUE FAILURES

3.5.1 INTRODUCTION

Great strides have been made in the last four decades in understanding and in designing to prevent fatigue failures in vehicle components. Safety and reliability have become bywords to the vehicle industry at a time when fuel economy has dictated the use of the most sophisticated design procedures to optimize the use of materials without increasing the probability of component failure. The concerns of the design engineer focus on the overall structure as well as its components when exposed to service conditions that result in numerous fluctuating loads and attendant stress and strain histories which may result in fatigue failure. With the need to provide an economical design through mass reduction, many of the older design procedures have been set aside in lieu of the more recent and comprehensive design procedures. Previously, large factors of safety were designed into components because of lack of knowledge and understanding of interactive effects. These safety factors are no longer needed since the development of extensive computer software packages. These software packages not only calculate the flow of loads through components and the stresses at stress concentrations, but also are able to encompass large volumes and many channels of real time loading histories, and combine the two for fatigue life evaluations of complete vehicle body and chassis systems.

3.5.1.1 Objective

The primary purpose of this section is to present an overview of the various fatigue design procedures and to indicate when each is most applicable. Generally sufficient information is presented to make the calculations, given the appropriate material properties and loading histories anticipated. Fatigue properties of many common grades of sheet steels are included but the reader is encouraged to search the technical literature, check company files, or conduct tests on materials being considered for use. Comments are made concerning material variability and effects of manufacturing on fatigue properties of steels. Environmental effects on fatigue, such as corrosion and temperature, are beyond the scope of this section. Although fatigue life prediction procedures are reviewed, the designer must establish the anticipated loading history for the component being designed. Comments are made regarding the means of obtaining these loading histories. Finally, and most importantly, the reader is encouraged to use the references to obtain more detailed information on analytical procedures and material properties appropriate for a particular component. This is particularly important in cases where the reader is working with a fatigue critical or sensitive component. This summary is intended as a primer and not a final authority on fatigue design of vehicle components.

3.5.1.2 Steps in Fatigue Design

The current fatigue design procedures used to design structures and components have evolved primarily from experience based on a gradual application of the new methods and followed by good correlating test results. An overview of various features of the process is shown in [Figure 3.5.1.2-1](#), but the underlying principles for all the elements can be summarized by three necessary ingredients for problem solution:

1. Structure or Component Load Histories: The external loads on a component or structure flow through the material and cause the cyclic stressing of fatigue critical locations. One needs the number of cycles, directions and magnitudes of all significant external loads.

Deciding which loads or magnitudes are significant for analysis may be an iterative process.

2. Geometry: An analysis must be made of how the measured loads translate into local "hot-spot" stress or strain. The transform can be computed from tabulations of stress concentration factors, photoelastic experiments, or from finite element analysis (FEA) results.
3. Material: Cyclic deformation and fatigue properties must be available for the component materials of the structure. The cyclic deformation information is used by material models, including the newer multiaxial models to follow the stress-strain behavior at the critical location. The fatigue properties are used to predict the failure (cracking) of the critical location.

Figure 3.5.1.2-1 shows that a number of factors influence the basic three elements of design listed above. Past service or performance experience may, for example, influence the material used, or suggest adjustment of the design load levels. The material deformation and fatigue properties may also be altered by processing, such as cold work, welding, or shot peening, or by non-standard environments like corrosion, wear, or high temperature usage. Their effects can be expressed in changes to the room temperature stress/strain-life curves, as in high temperature fatigue where a lowering of the strain-life curve occurs, or by an alteration in the applied stress levels; e.g. a shot peened surface can be simulated by superimposing a compressive stress over the load induced stresses.

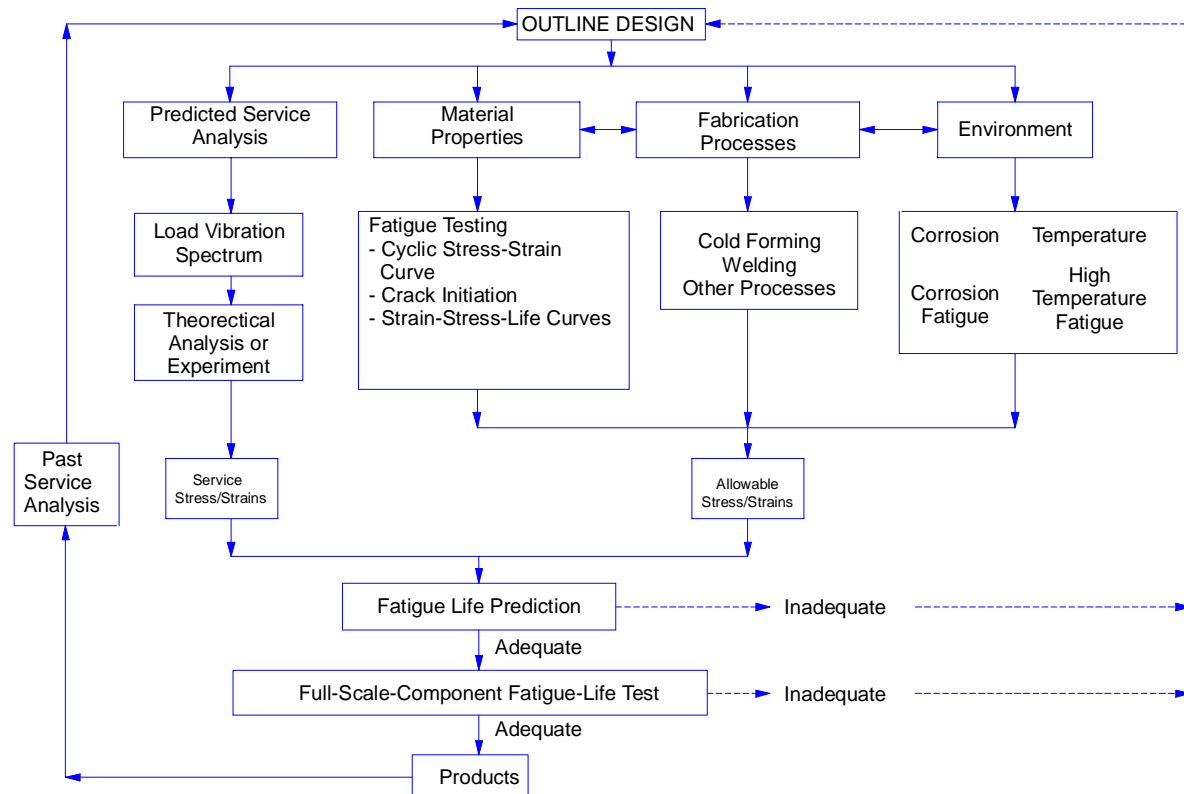


Figure 3.5.1.2-1 Fatigue design flow chart

3.5.1.3 Fatigue Mechanisms

Fatigue is failure under repeated loading. There are three stages in a fatigue failure:

- Crack initiation
- Crack propagation
- Final fracture

In the short life fatigue region of axially loaded specimens ($N_f < 100,000$ cycles approximately), the initiation phase completes within a very short portion of the life¹ and most of the life is spent propagating a small crack. In "long-life" fatigue near the fatigue limit, a majority of life is spent in developing and coalescing microstructural cracks, while the propagation phase from grain size level crack to final fracture tends to comprise a small fraction of life. The first two stages are often not easily separated quantitatively. However, in vehicle design, failure is considered to have occurred as soon as a fatigue crack is initiated or becomes visible. In most cases, the crack propagation life is ignored and provides a safety factor against catastrophic failure. In cases where loads cannot be transferred to other members during crack propagation, however, localized regions subjected to plastic strain reversals may show virtually no visible sign of damage before final catastrophic crack growth through the member. Thus, detection of a crack cannot be used as a method of failure prevention in vehicle design. However, in other industries, where components are very high cost (e.g.: stamping press) and no critical safety issues arise, it is expedient to estimate the remaining life before replacement, using the crack propagation techniques.

Figure 3.5.1.3-1 shows the most widely used technique in the ground vehicle industry. The local stress-strain method starts at the top and then branches to the middle left. The crack propagation version thereof, which represents the future evolution of the methodology, branches to the right. Both methods assume that the designer-analyst can measure or simulate the local stress-strain behavior at the critical fatigue location. After individual hysteresis loops have been extracted or "counted", damage is presently usually assessed by applying the Smith/Watson/Topper parameter, which is the maximum stress multiplied by strain amplitude (left branch). In the crack propagation method, damage could be computed from the amount of crack propagation each loop would create, da/dn , vs. ΔK curve in the right branch of the figures, where K is the stress intensity factor at the crack tip. Both methods lead to a fatigue life prediction. For the immediate future it is expected that the methods depicted in the left branch will dominate the ground vehicle durability analysis applications, but it is also highly probable that the philosophy of the right branch, or a variant of it, will continue to gain in acceptance and usage

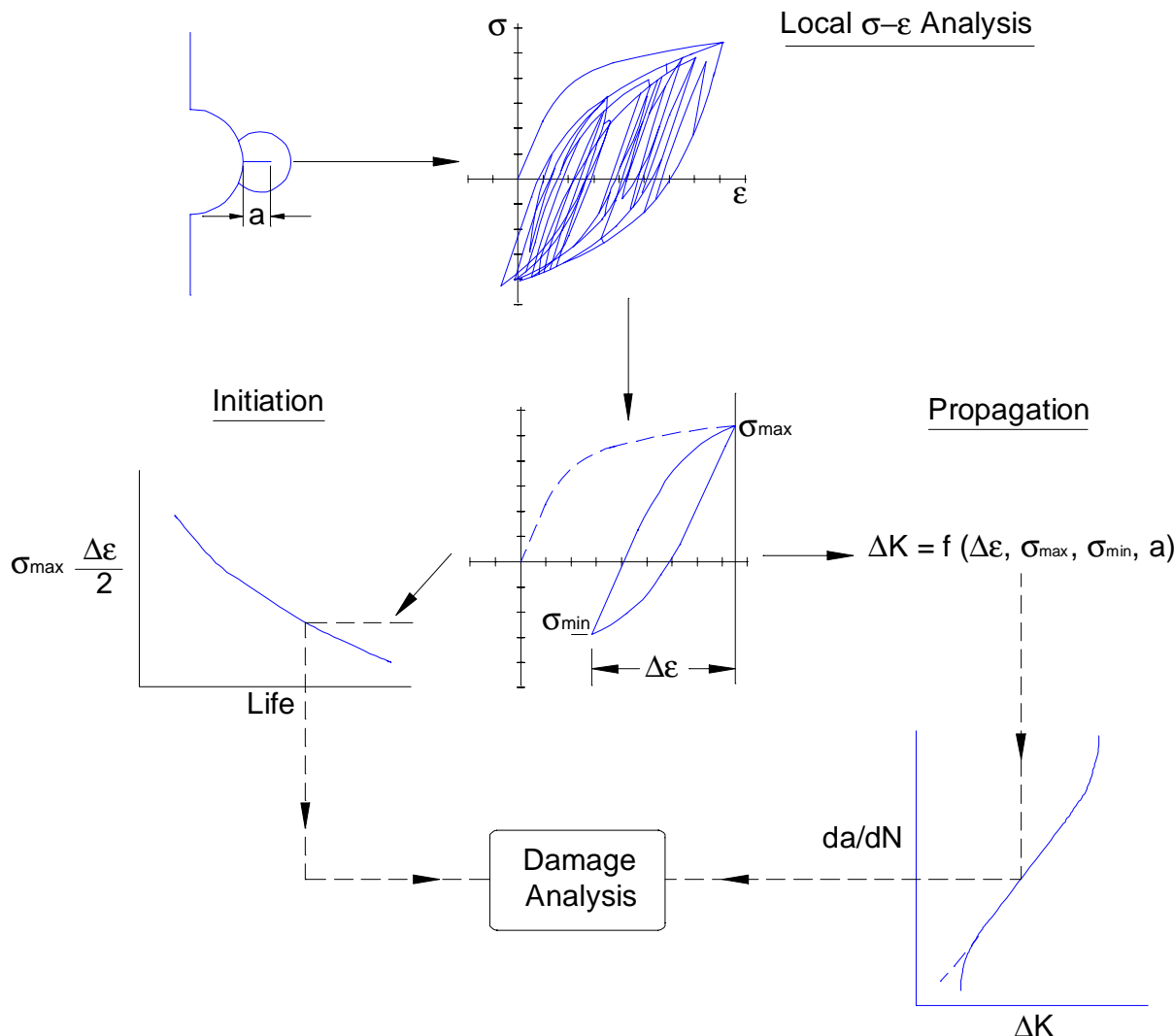


Figure 3.5.1.3-1 Using estimates of local stress-strain behavior to compute fatigue damage with either a mean stress parameter ($\sigma_{max} - \frac{\Delta\epsilon}{2}$) or by computing crack propagation.

3.5.1.4 Basic Fatigue Design

Three methods are generally used to perform initial design or analyze existing components.

- **Stress-Based Design:** uses the "S-N" (stress vs. cycles to failure) curve of specimens tested in constant amplitude stress control to characterize the material, and the computed value of the stress near the failure location to evaluate fatigue projected fatigue life. The load history, for cycle and damage counting, must be assessed in terms of the same notch stress. The method cannot handle load events that cause local plasticity and is therefore limited to designs in the long life region of the material fatigue curve. Components that are not expected to have significant plasticity, as in the case of some engine components, can be designed using this method. In most ground vehicle components the method has been superceded by the local stress-strain approach described below.

- **Crack Propagation Methods:** are used extensively in the aircraft industry to assess the residual strength and remaining life of components with unexpected fatigue cracks. Usually the initial design is based on some form of stress-based or local stress-strain fatigue assessment, and then subsequently checked for crack propagation resistance in the event that some fatigue cracking is missed by the mandatory periodic inspections of aircraft. Such an inspection technique would be very difficult to apply to the ground vehicle products, however, and a more conservative design is applied, in terms of proving ground severity or length, to prevent all critical fatigue cracks, and consequently crack propagation assessments are not commonly used for design.
- **Local Stress-Strain Methods:** are sometimes referred to as "Strain Based" techniques, but in actuality their use requires the computation of both local stress and local strain at the critical location or fatigue "hot spot". The method is now the predominant technique for fatigue assessment of ground vehicle structures and components, and due to its importance will be the subject of the remainder of this section.

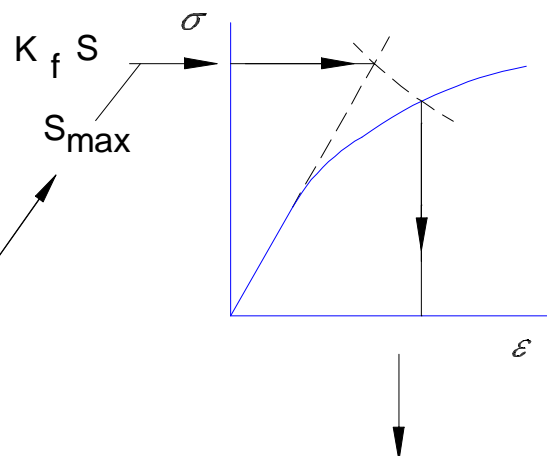
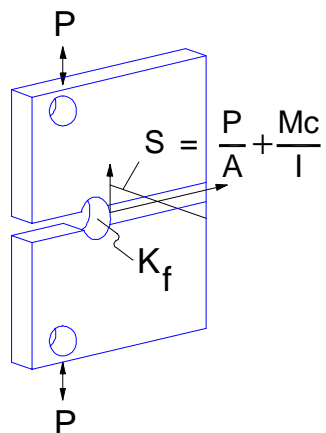
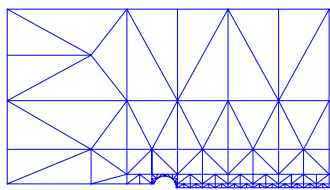
The principal element of the modern fatigue properties database is strain-controlled fatigue data for materials typically utilized in the construction of earth moving, automotive, truck vehicles, and presumably any other industries that design fatigue stressed structures and components. Strain-controlled fatigue data allows the life of a component to be estimated from what is called a "local stress-strain approach" [e.g.: Smith/Topper² or Topper/Wetzel/Morrow³].

The method assumes that, while a component may be subject to nominal elastic stresses in most of its structure, local plastic deformation will occur at unavoidable points of stress concentration, and at these locations cracks will eventually initiate, and may propagate to component failure. Although it is possible to design components to maintain even such local stresses beneath the cyclic yield and prevent initiation, weight constraints often mandate finite structural life, which in turn necessitates a reliable fatigue life prediction methodology.

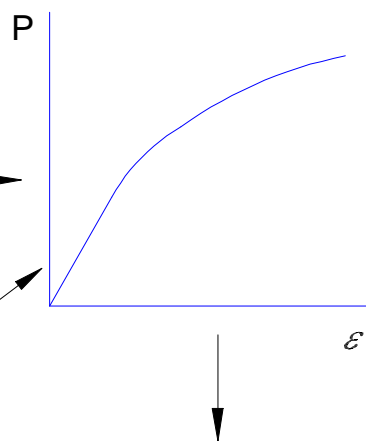
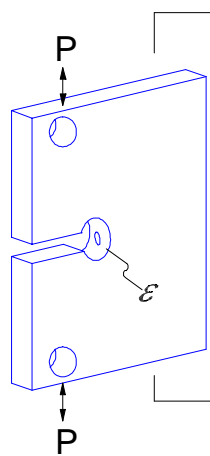
The methodology ([Figure 3.5.1.4-1](#)) requires the definition of two properties or relationships: A stress-strain equation, and a strain-life equation. Other terms are often introduced to aid in the understanding of material deformation and fatigue behavior, elastic strain, plastic strain, reversals to failure, but the fundamental variables that are observed in the material tests are Stress, Strain, and Cycles; all other terms are derived from these three measurements. Since there are only three variables, then only two relationships need to be defined, it does not really matter which. It could for instance be stress-life and strain-life, but typically stress-strain and strain-life are commonly defined. In present day usage, however, some of the derived variables are often used to express other concepts, and redundant sets of equations fitted in different ways can cause life prediction difficulties, but a reference back to the fundamental variables will clear up most fitting problems.

Analytical

Strength of Materials

Finite Elements

Plastic

Experimental

Component Calibration

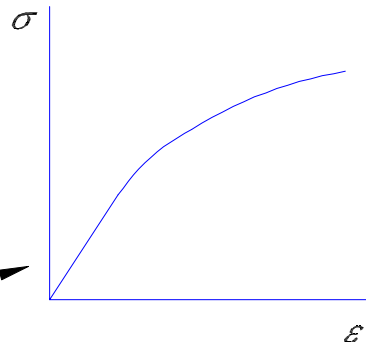
Local ε - History

Figure 3.5.1.4-1 Techniques for assessing the local stress and strain magnitudes at critical locations

3.5.1.5 Component Life Estimation

There are a number of methods available for life prediction, which use the basic strain life data to estimate component life. Briefly, in increasing degree of complexity, these consist of:

1. Component Load life testing: When estimation of a realistic local stress at the fatigue critical location is very difficult (e.g.: complex welded or brazed structures) it may be expedient, if the structure itself is inexpensive to test a number of samples of the structure with constant amplitude loading. The loads are usually selected to replicate the expected service loads. The method becomes difficult when realistic boundary conditions are problematic, and is very difficult to use when the samples are expensive. The advantage is that the geometry or notch analysis and the material properties are inherent in the specimen, which can save considerable analysis time. Given that a constant amplitude load vs. life curve has been generated the fatigue damage of various service or test load histories can be assessed using the Palmgren-Miner rule.^{4, 5}
2. Component with Simple Geometry: In a notched plate specimen subjected to a specified loading history, the location of principal interest is the notch root where failure will take place. The stress history or strain history at the notch root developed by the loading history of the component is determined by finite element analysis or experimentally with a strain gage. The damage caused by the various cycles is then summed for each event and a fatigue history determined. Computer models of the local plastic stress-strain behavior are available to delineate the individual hysteresis loops, while other code segments compute their damage.
3. Complex Structures: Complex structures such as vehicle bodies have many load input locations, and many potential fatigue critical sites. In the last decade the methods used on simpler components, described briefly above, have been extended to handle multichannel loads and applied to all parts of the vehicle structure. The key has been the combination of finite element modeling, using unit load analysis for each force vector, followed by time-based superposition of load effects to compute the stress histories of each element of the structure. Given an element stress history one can simply repetitively compute the expected fatigue damage for each element in the structure⁶
4. Multiaxial Deformation Cases: Although significant advances have been made in the estimation of fatigue under multiaxial loading, it is still very problematic to compute a variable, complex stress-strain path reliably. Selecting a fatigue "event" such as a closed hysteresis loop is another problem, with a final difficulty of assessing the damage of stress-strain events that have multiaxial stress and strain components. Although some solutions are available, their implementation should be used with great caution and large factors of safety. Basic theories and analysis procedures for multiaxial loading conditions are reviewed in [Section 3.5.8](#).

Fatigue life predictions involve use of the linear damage law (Palmgren-Miner Rule), a method of cycle counting from the known service history, and a cumulative damage determination involving the fatigue properties of the material to be used. In [Section 3.5.6](#), the variability of fatigue properties and the effect of cold work (forming) on these properties are reviewed.

In the past, most of the interest of vehicle designers has been on fatigue of non-welded parts. However, in recent years, with the mass reductions required by improved fuel economy, attention has been focused on fatigue behavior of fabricated joints, such as spot welded and arc welded joints. All welds contain imperfections or weld contours, which are crack like. Thus, the analyses

must focus primarily on crack propagation or stress threshold levels below which cracks will not propagate. Fracture mechanics procedures are most amendable to this type of behavior and are described in [Section 3.5.7](#).

3.5.1.6 Design Verification Testing

Two types of testing are common to the ground vehicle industry; test track evaluations and bogie testing. In test track evaluations the component in question is used in a vehicle that is driven on a test track having a surface simulating the worst anticipated loadings the vehicle is expected to see during its service life. In a bogie test, the component is subjected to a predetermined number of cycles of some extreme loading in a laboratory test that has been correlated to service life conditions. Each vehicle company has its own procedures and testing requirements that remain as confidential information within the company. If appropriate, the reader should seek this information from company sources.

Fatigue failure is highly statistical due to variabilities in loads, geometry and material properties. In [Section 3.5.9](#), a summary of the useful formulas to characterize uncertainties in fatigue properties based on testing results is given.

3.5.2 MONOTONIC PROPERTIES

It is important to be familiar with the definitions of terms relating to monotonic loading of materials. Monotonic stress-strain properties are determined from tension tests of smooth polished specimens of circular or rectangular cross sections as described in SAE J416⁷ and ASTM E8⁸ procedures. Full sheet thickness specimens are generally tested from sheet steels. The load applied to the specimen and elongation in the uniform gage length are measured to determine the stress-strain behavior of the steel being evaluated. Monotonic properties are defined from either engineering stress-strain curve, based on the original cross sectional area and gage length, or true stress and true strain curve, based on the instantaneous cross sectional area and gage length dimensions ([Figure 3.5.2-1](#)).

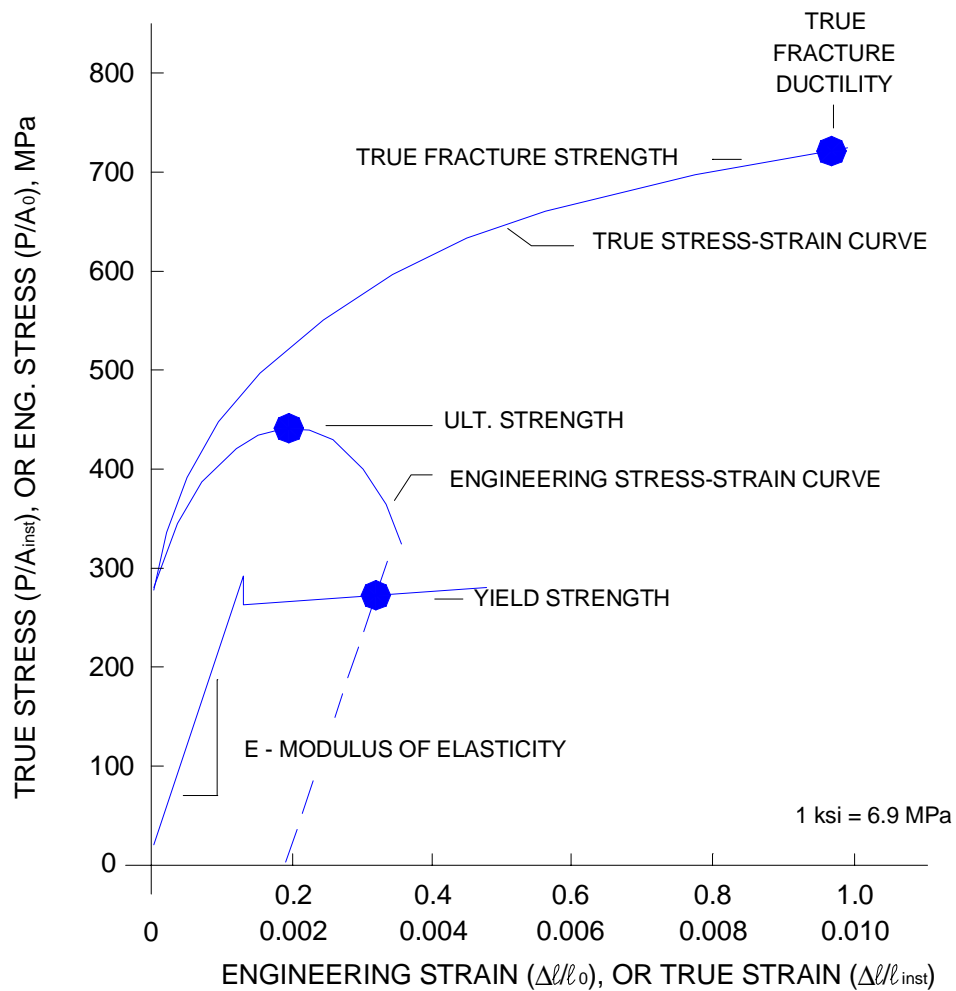


Figure 3.5.2-1 Monotonic engineering^g and true stress-strain curves and properties for 1020 H.R. steel^g

Engineering and true stresses and strains are defined by:

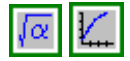
$$\text{Engineering stress} = S = \frac{P}{A_0}$$

Equation 3.5.2-1



$$\text{Engineering strain} = e = \frac{\Delta\ell}{\ell_0}$$

Equation 3.5.2-2



$$\text{True stress} = \sigma = \frac{P}{A_{inst}}$$

Equation 3.5.2-3



$$\text{True strain} = \varepsilon = \frac{\Delta\ell}{\ell_{inst}}$$

Equation 3.5.2-4



where Subscript "o" refers to the original dimension.

Subscript "inst" refers to the dimension of the specimen at the instant the load or elongation is measured.

P = applied load.

ℓ = gage length in the uniform cross section corresponding to some applied load.

A = minimum cross sectional area of the specimen in the uniform gage length.

The following relationships between engineering and true stresses and between engineering and true strains are valid up to necking in a tension test:

$$\sigma = S(1+e)$$

Equation 3.5.2-5



$$\epsilon = \ln(1+e)$$

Equation 3.5.2-6



Other monotonic material properties of interest are:

$$\text{Modulus of Elasticity} = E = \frac{\text{stress}}{\text{strain}} = \frac{\Delta S}{\Delta e}$$

Equation 3.5.2-7



where E is also known as the elastic or Young's Modulus representing the slope of the linear elastic region of the stress-strain curve.

Yield Strength S_y or σ_y is the stress corresponding to a 0.2 percent offset strain and can be determined by constructing a line parallel to the elastic modulus and passing through 0.2 percent strain at zero stress ([Figure 3.5.2-1](#)).

$$\text{Ultimate Tensile Strength} = S_u = \frac{P_{\max}}{A_o}$$

Equation 3.5.2-8



where S_u is the engineering stress at maximum load when tensile instability, i.e., necking, occurs in a tensile specimen

$$\text{Percent Reduction in Area} = \% RA = \frac{A_o - A_f}{A_o} \times 100$$

Equation 3.5.2-9

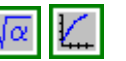


where A_f is area of the minimum cross section at fracture.

If the true stress, σ , and true plastic strain, ϵ_p , values for a steel are plotted on a log-log scale, the data can generally be fitted with a straight line ([Figure 3.5.2-2](#)) according to the equation:

$$\sigma = K \epsilon_p^n$$

Equation 3.5.2-10



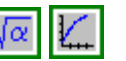
where K is the Monotonic Strength Coefficient

n is the Monotonic Strain Hardening Exponent.

K is the true stress corresponding to a true plastic strain of one and n is the slope of the true stress and true plastic strain log-log plot. ASTM Standard E646¹⁰ describes the process for obtaining K and n values. The total true strain is then given by adding its elastic and plastic parts:

$$\epsilon = \epsilon_e + \epsilon_p = \frac{\sigma}{E} + \left(\frac{\sigma}{K} \right)^{\frac{1}{n}}$$

Equation 3.5.2-11



A significant increase of the strain rate in a tensile test generally increases strength but reduces ductility of the material. For high strength steels, however, this effect is usually small at room temperature.

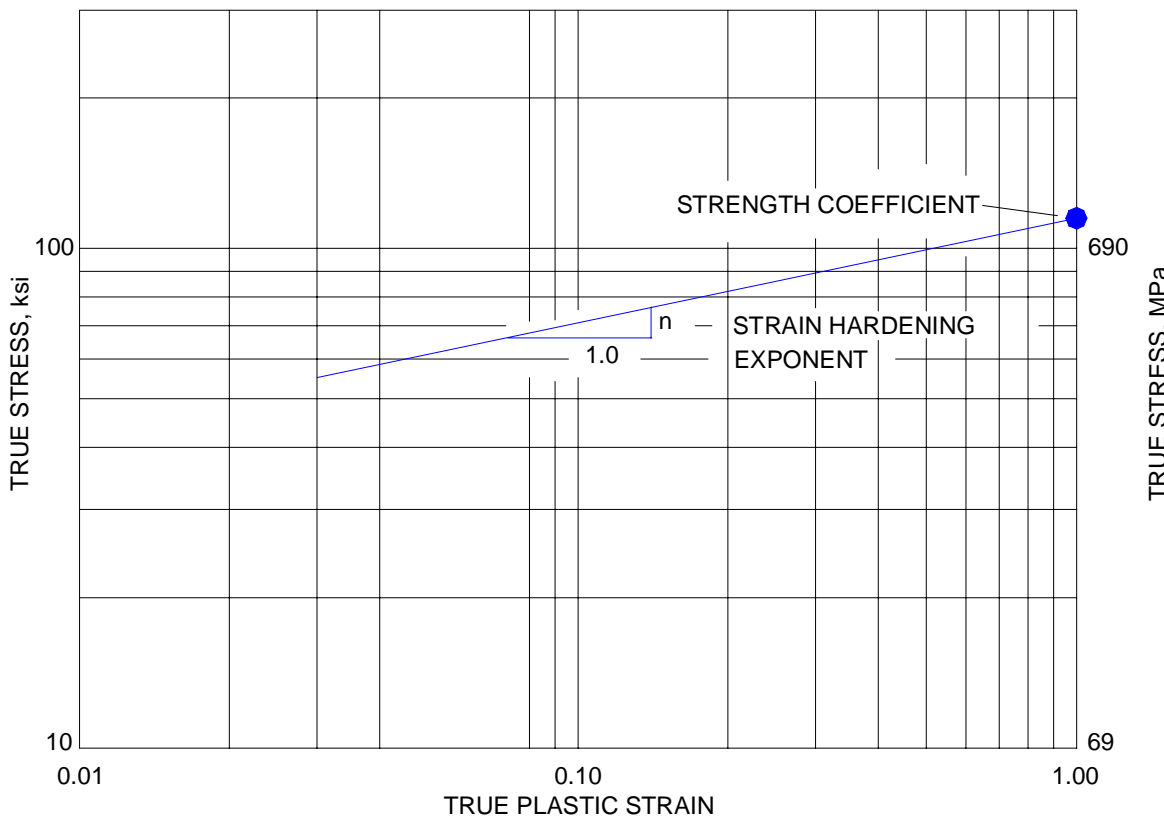


Figure 3.5.2-2 Monotonic true stress vs. true plastic strain curve for 1020 H.R. steel⁹

Other terms of interest are:

$$\text{True Fracture Strength} = \sigma_f = \frac{P_f}{A_f}$$

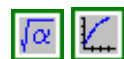
Equation 3.5.2-12



Bridgeman correction factors^{9, 11} should be used to adjust σ_f for triaxial stresses in the necked region of the specimen.

$$\text{True Fracture Ductility} = \varepsilon_f = \ln\left(\frac{A_o}{A_f}\right) = \ln\left[\frac{100}{(100 - \% RA)}\right]$$

Equation 3.5.2-13



$$\text{Percent Elongation} = \% \text{elong.} = \left(\frac{l_f - l_o}{l_o} \right) \times 100$$

Equation 3.5.2-14



It should be cautioned that special procedures⁹ are necessary to properly account for rectangular cross sectional areas when measuring fracture areas.

Measures of energy absorption capacity of the material are resilience and tensile toughness. Resilience is the elastic energy absorbed by the specimen and is equal to the area under the elastic portion of the stress-strain curve. Tensile toughness is the total energy absorbed during deformation (up to fracture) and is equal to the total area under the engineering stress-strain curve. A high tensile toughness is an indicator of a material with both high strength and ductility.

In a monotonic compression test, the initial part of the stress-strain curves is similar to that in monotonic tension test. Therefore, material properties such as modulus of elasticity E and yield strength S_y may be defined from the initial part of the stress-strain curve in a similar manner to that in monotonic tension test. However, necking does not occur in compression and as a result, the engineering ultimate strength is the same as engineering fracture strength in a compression test. For a ductile steel, the specimen does not usually fracture in compression, but it deforms into an increasingly larger diameter pancake shape.

3.5.3 LOAD-CONTROLLED CYCLIC PROPERTIES

Stress-life fatigue design procedures have been widely used in the past and are still used today. The most common applications of this methodology are for long or infinite life design of smooth or mildly notched components, where strains are predominantly elastic.

3.5.3.1 Terminology

The stress-life fatigue design methodology is based on nominal stress fluctuations in the component. Laboratory data are generated using smooth specimens of round or rectangular cross sections. Four testing modes have been used for loading: axial, rotating bending, flexural bending, and torsion, with axial loading currently being the most popular. The nomenclature used in describing cyclic loading is shown in [Figure 3.5.3.1-1](#).

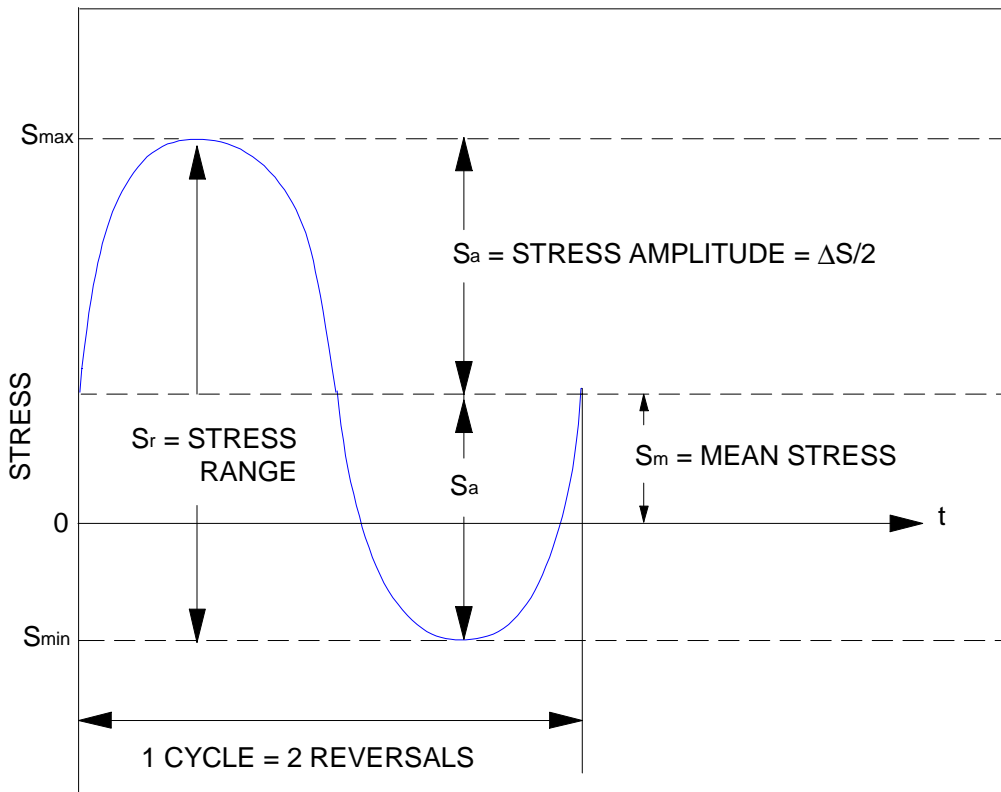


Figure 3.5.3.1-1 Cyclic Stress nomenclature

The fatigue life N_f is the number of cycles of stress or strain that a given specimen sustains before failure of a specified nature occurs.

The nominal stress S is the stress at a point calculated for the net cross section by simple elastic theory, without taking into account the effect of the stress provided by a geometric discontinuity.

The maximum stress S_{max} is the stress having the highest algebraic value in the stress cycle, tensile stress being considered positive and compressive stress negative.

The minimum stress S_{min} is the nominal stress having the lowest algebraic value in the cycle, tensile stress being considered positive and compressive stress negative.

The mean stress S_m is the algebraic average of the maximum and minimum stresses in one cycle; that is,

$$S_m = \frac{S_{max} + S_{min}}{2}$$

Equation 3.5.3.1-1



The stress range S_r , is the algebraic difference between the maximum and minimum stresses in one cycle; that is,

$$S_r = S_{max} - S_{min}$$

Equation 3.5.3.1-2



The stress amplitude S_a is one half of the stress range; that is,

$$S_a = \frac{S_r}{2} = \frac{S_{max} - S_{min}}{2}$$

Equation 3.5.3.1-3



The stress ratio R is the algebraic ratio of the minimum to the maximum stress; that is,

$$R = \frac{S_{min}}{S_{max}}$$

Equation 3.5.3.1-4



An S-N diagram is a plot of the number of cycles to failure of a specimen versus the applied stress. The plotted stress can be S_{max} , S_{min} , S_r , or S_a ; the stress ratio as well as the loading mode should be specified. The data are plotted either as semi-log ([Figure 3.5.3.1-2](#)) or log-log curves ([Figure 3.5.3.2-1](#)).

The fatigue strength at N_f cycles S_n is the hypothetical value of stress for failure at exactly N_f cycles as determined from an S-N diagram. The value of S_n is generally taken as the value (can be S_{max} , S_{min} , or S_a) for which 50 percent of the samples survived N_f cycles. The term mean-fatigue strength at N_f cycles is also used.

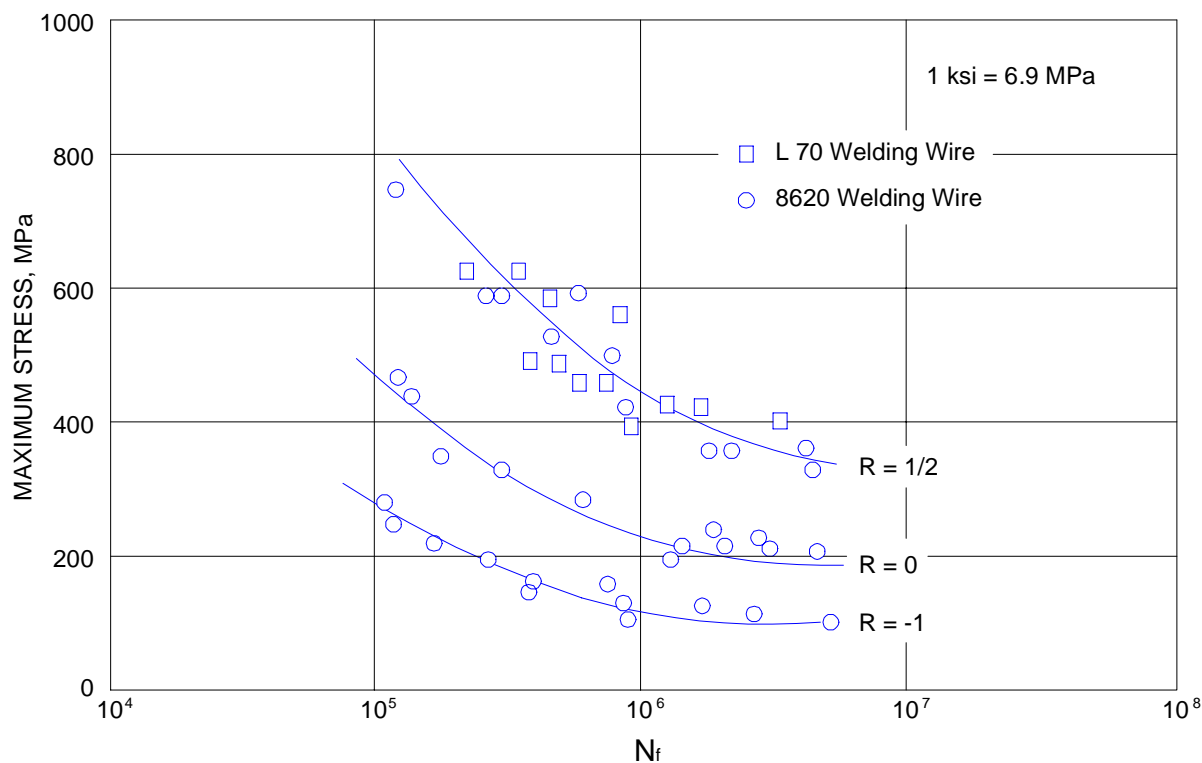


Figure 3.5.3.1-2 Semi-log S-N curve¹²

3.5.3.2 S-N Curves for Smooth Specimens Under Load Control

To determine the fatigue resistance of a material, as measured by an **S-N** curve, specimens of the material are subjected to different constant amplitude, fully reversed loading amplitudes until the specimen fractures. The resulting life for each specimen is plotted (log scale) against the corresponding applied stress amplitude (or σ_{\max} or σ_{\min}). For most steels, a stress value is encountered below which the specimen will not fail. This value is commonly referred to as the fatigue limit or the endurance limit. Thus the fatigue behavior is described by a curve of some changing slope for finite life, and a curve of zero slope for infinite life. The intersection of these curves is referred to as the knee of the curve and generally occurs at fatigue lives of 10^5 to 5×10^6 cycles. In corrosive or other aggressive environments, however, the knee of the curve can disappear and an endurance limit corresponding to infinite life does not usually exist. Also, some metals, such as aluminum, do not exhibit an endurance limit.

For any material, the **S-N** curves are usually displaced from one another for different testing modes. The differences between these curves are generally attributed to differences in stress gradient, the equations used to calculate the stresses, and the volume of material subjected to the imposed stresses. [Figure 3.5.3.2-1](#) shows test results from axial (push-pull) and rotating bending specimens, indicating considerably shorter fatigue lives in axial loading, compared to rotating bending. In axial loading, the entire gage section volume is subjected to the maximum stress, whereas in rotating bending only the perimeter of the minimum cross section is subjected to the maximum stress. In addition, specimen misalignment in axial loading can induce an additional bending stress on the specimen. These effects cause shorter fatigue lives in axial or push-pull loading.

Figure 3.5.3.2-2 shows a schematic diagram of the number of cycles necessary to initiate a crack and to fracture in a fatigue specimen. For long lives, almost the entire life is spent in initiating a crack. Initiation is defined here as a crack on the order of 1 mm in length. Different testing modes can result in different cyclic lives for initiation and for propagation at the same applied nominal stress. Thus the resulting total life curves will be different for different testing modes. If crack growth represents a significant portion of the total fatigue life, fracture mechanics may be a better approach to quantify the fatigue life.

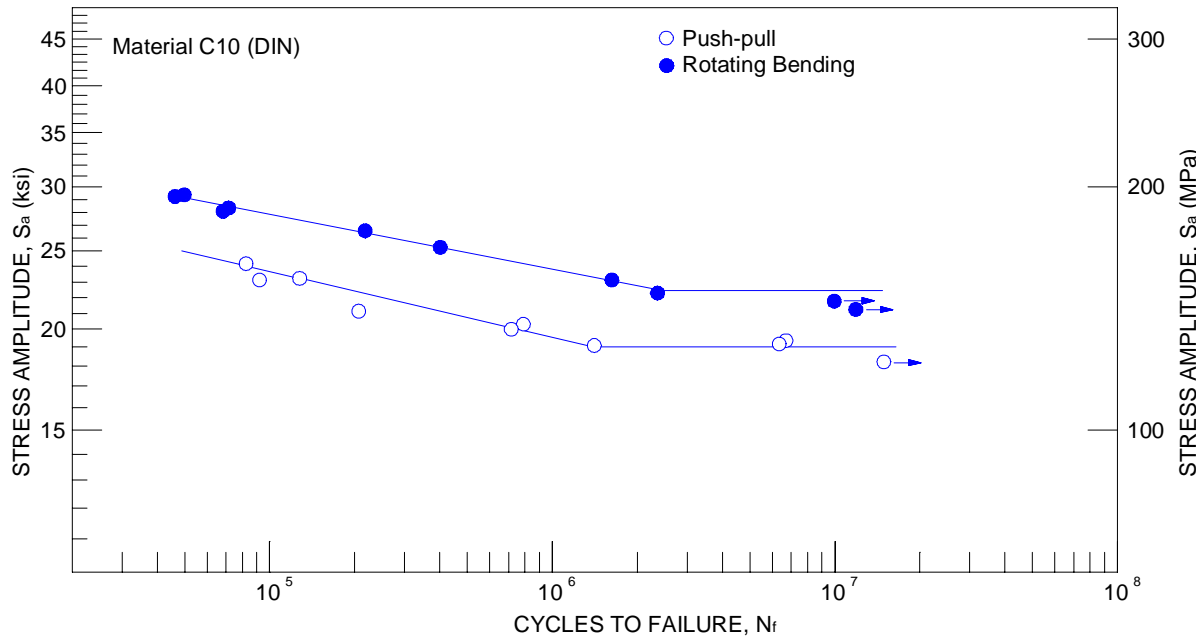


Figure 3.5.3.2-1 Experimental results for axial (push-pull) and rotating bending fatigue tests⁹

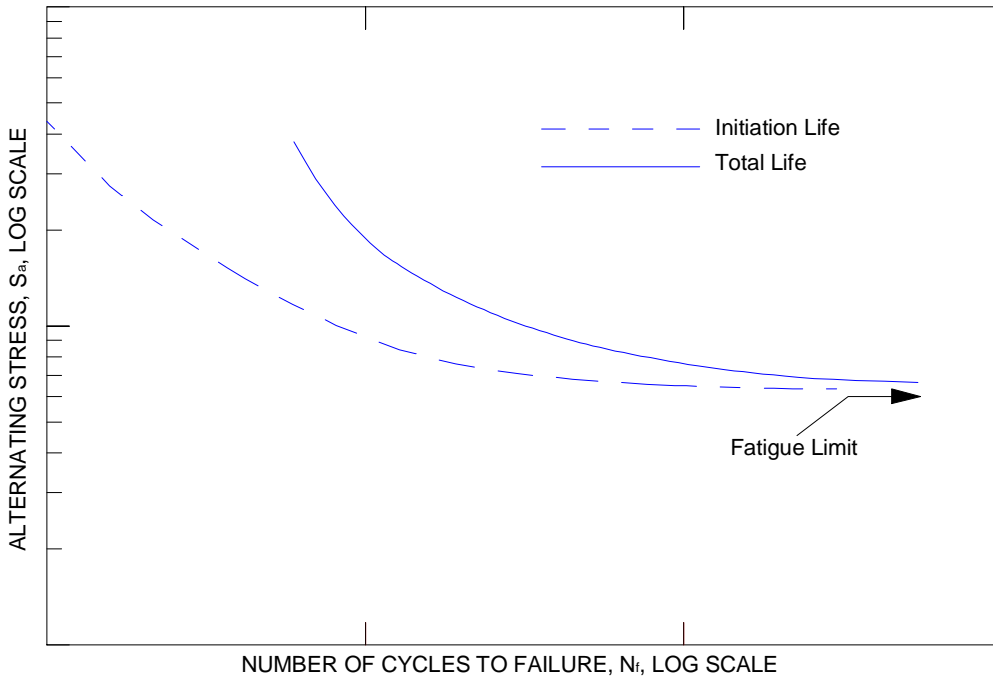


Figure 3.5.3.2-2 Initiation and total life for a schematic S-N curve¹²

The fatigue limit or endurance limit for steels has been correlated with the tensile strength of the steel being tested. For wrought carbon and alloy steels, the stress amplitude for the fatigue limit for fully reversed loading of $R = -1$ is generally about one half of the value of the tensile strength¹³ (Figure 3.5.3.2-3). However, cast alloys generally exhibit fatigue limits less than one half the tensile strength (Figure 3.5.3.2-4)¹³.

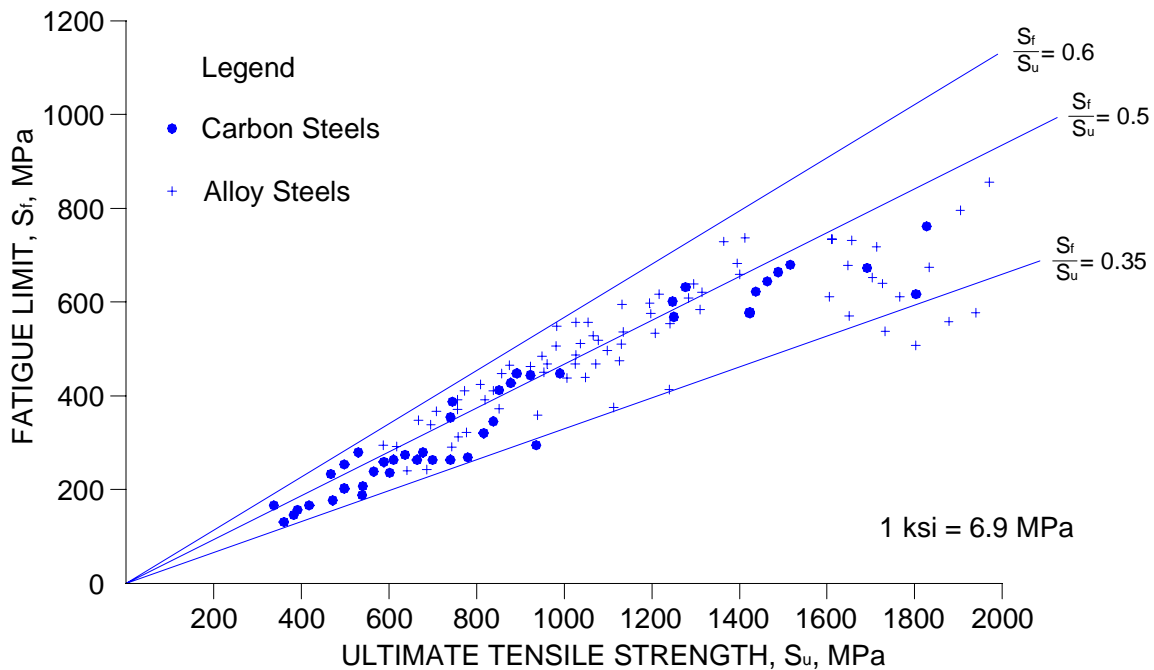


Figure 3.5.3.2-3 Relation between rotating bending fatigue limit ($R = -1$) and ultimate tensile strength of wrought steels¹³

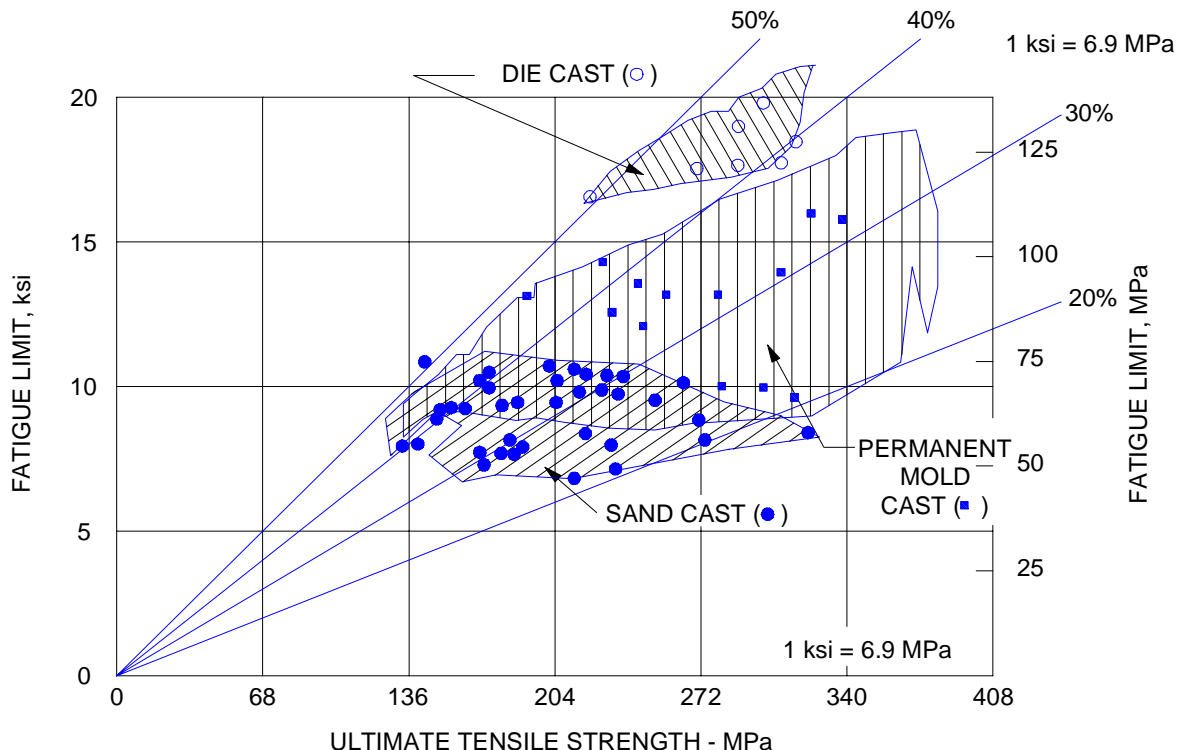


Figure 3.5.3.2-4 Fatigue limit to ultimate tensile strength ratios for casting alloys (separately cast specimens)¹³

To use terminology consistent with low cycle fatigue and strain life procedures, the **S-N** curve can be plotted on a log-log scale using true stress, σ_a , values for the engineering stress, S , and reversals to failure ($2N_f$) (Figure 3.5.3.2-5). The straight line relationship on this log-log plot is given by:

$$\sigma_a = \sigma'_f (2N_f)^b$$

Equation 3.5.3.2-1



where b = slope of the curve (fatigue strength exponent)

σ'_f = value of σ_a at one reversal (fatigue strength coefficient)

This equation, however, is only valid for finite fatigue lives because it does not reflect a fatigue limit. Hence, the curve should be limited to stress amplitudes greater than S_f shown in Figure 3.5.3.2-5. On the other hand, when making life predictions for automotive components, periodic overloads can eliminate the fatigue limit and Equation 3.5.3.2-1 can be used for fatigue lives greater than 10^6 reversals¹⁴.

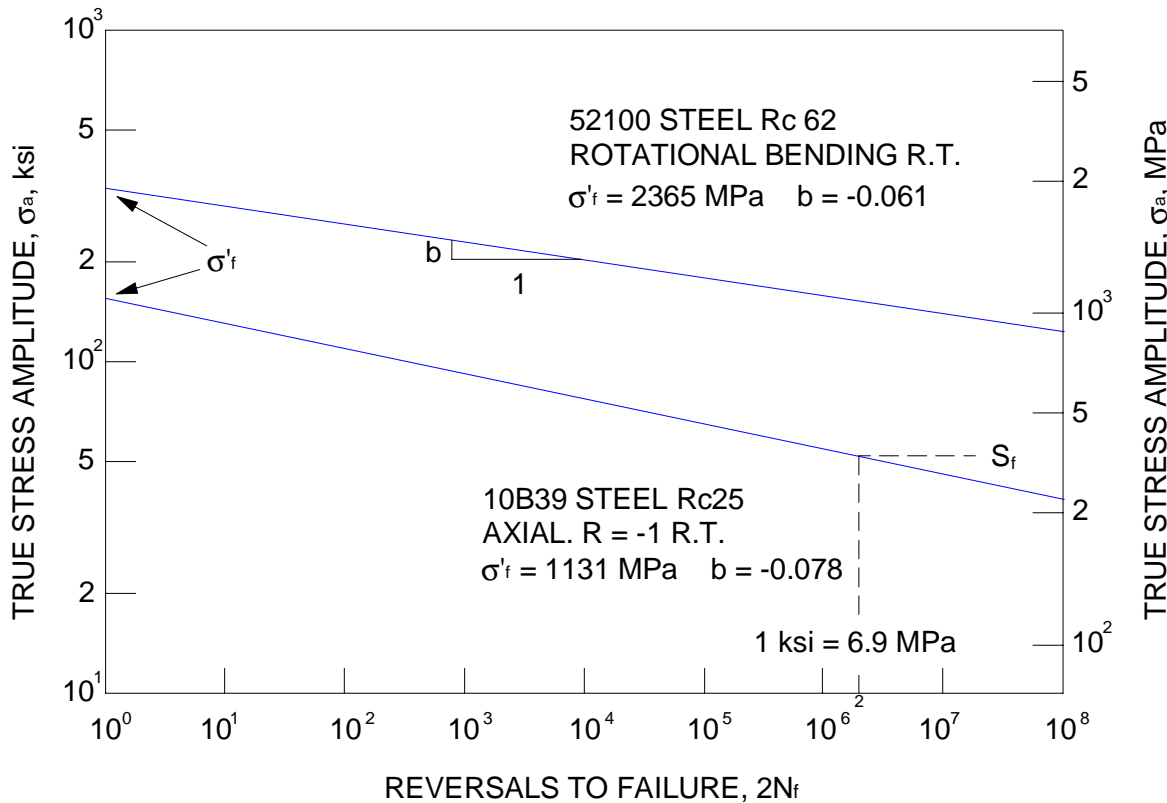


Figure 3.5.3.2-5 Illustration of log-log linear true stress vs. reversals to failure curves for high and mild strength steels⁹

3.5.3.3 Specimens with Notches Under Load Control

A local stress concentration, such as a notch or change in section size, will be the most likely location for a fatigue crack to initiate. The most common means of characterizing the severity of a notch is from a theoretical stress concentration factor, K_t . The theoretical stress concentration factor K_t is the ratio of the greatest stress in the region of a stress concentration, as determined

by the theory of elasticity, to the corresponding nominal stress. Values for K_t can either be found in compendiums¹⁵, or determined from finite element analysis, or determined experimentally. An example of K_t values for a stepped bar in bending is shown in [Figure 3.5.3.3-1](#). However, all of these stress concentration factors are based upon elastic analyses and are generally not correlated to fatigue testing.

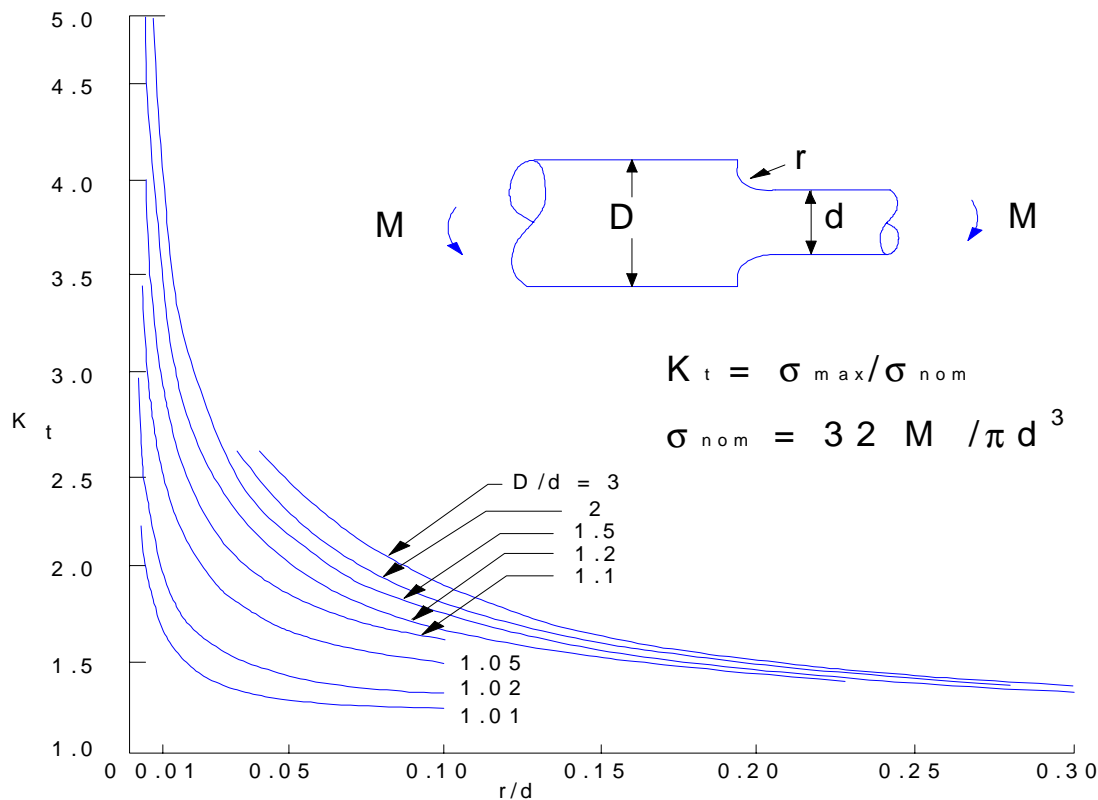


Figure 3.5.3.3-1 Stress concentration factor, K_t , for bending of a stepped round bar with a shoulder fillet (based on photoelastic tests of Leven & Hartman, Wilson & White) ([Reference 15](#))

The fatigue notch factor K_f is the ratio of the fatigue strength of a specimen with no stress concentration to the fatigue strength at the same number of cycles with the stress concentration for the same conditions. The fatigue notch factor, K_f , is less than the theoretical value, K_t , thus reflecting the ability of steels to strain plastically and partially reduce the theoretical stress concentration. In addition, differences in the volume of material being plastically strained for different specimen sizes and geometries add to the discrepancies between K_t and K_f values. When specifying K_f , it is necessary to specify the geometry and the values of S_{\max} , S_{\min} , and N_f for which it has been determined.

The fatigue notch sensitivity q is the measure of the degree of agreement between K_f and K_t for a particular specimen of a particular size and material, loaded in a certain manner, containing a stress concentration of a specific size and shape. The most common definition is:

$$q = \frac{K_f - 1}{K_t - 1}$$

Equation 3.5.3.3-1



Although K_f values are best determined experimentally, the following relationship has been proposed for notched parts¹³:

$$K_f = 1 + \frac{K_t - 1}{1 + \frac{a}{r}}$$

Equation 3.5.3.3-2



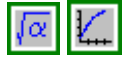
where r = notch root radius

a = material constant depending upon material strength.

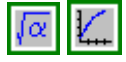
Relationships for "a" have been postulated for heat treated and hot rolled steels and as a function of tensile strength. Such a relationship for relatively high strength steels subjected to axial or bending fatigue is given by Peterson¹⁵:

$$a = 0.0254 \left(\frac{2070}{S_u} \right)^{1.8} \text{ mm for } S_u \geq 550 \text{ MPa}$$

Equation 3.5.3.3-3



$$a = 0.001 \left(\frac{300}{S_u} \right)^{1.8} \text{ in for } S_u \geq 80 \text{ ksi}$$



3.5.3.4 Mean Stress Effects in Load-Controlled Tests

Most laboratory fatigue testing data are obtained for constant amplitude loading. As shown in [Figure 3.5.3.1-2](#), the mean stress has a significant effect upon the fatigue life. For example, in [Figure 3.5.3.1-2](#), for a constant life of 10^6 cycles an increasing R ratio corresponds to a higher tensile mean stress and a lower stress amplitude. A compressive mean stress, on the other hand, increases the fatigue life. Thus, the mean stress must be accounted for in life predictions. It should also be noted that the effect of residual stress on fatigue life is the same as the effect of a mean stress, unless the residual stress relaxes, usually due to plastic deformation at high load levels.

A common method of estimating mean stress effects is with the use of a modified Goodman diagram. This diagram is a plot of the stress amplitude versus the mean stress for a constant life ([Figure 3.5.3.4-1](#)). Goodman proposed a linear relationship as an approximation for a constant life line diagram. The ultimate tensile strength of the steel is plotted as the mean stress for a stress amplitude of zero. The other end of the line is fixed by the stress amplitude for fully reversed loading ($R = -1$) corresponding to the fatigue life being plotted. Thus, different constant life lines would be represented by a family of straight lines, all emanating from the ordinate axis (x-axis) at the ultimate tensile strength.

Each line is represented by the equation:

$$S_a = S_{cr} \left(1 - \frac{S_m}{S_u} \right)$$

Equation 3.5.3.4-1



where S_a = stress amplitude for the same life as S_{cr}

S_{cr} = stress amplitude for the constant life line at an $R = -1$

S_m = mean stress

S_u = ultimate tensile strength

Because of the conservative nature of the linear Goodman constant life line, Gerber suggested a parabolic relationship of the form

$$S_a = S_{cr} \left(1 - \frac{S_m^2}{S_u^2} \right)$$

Equation 3.5.3.4-2



This equation provides a reasonable approximation to data for ductile steels.

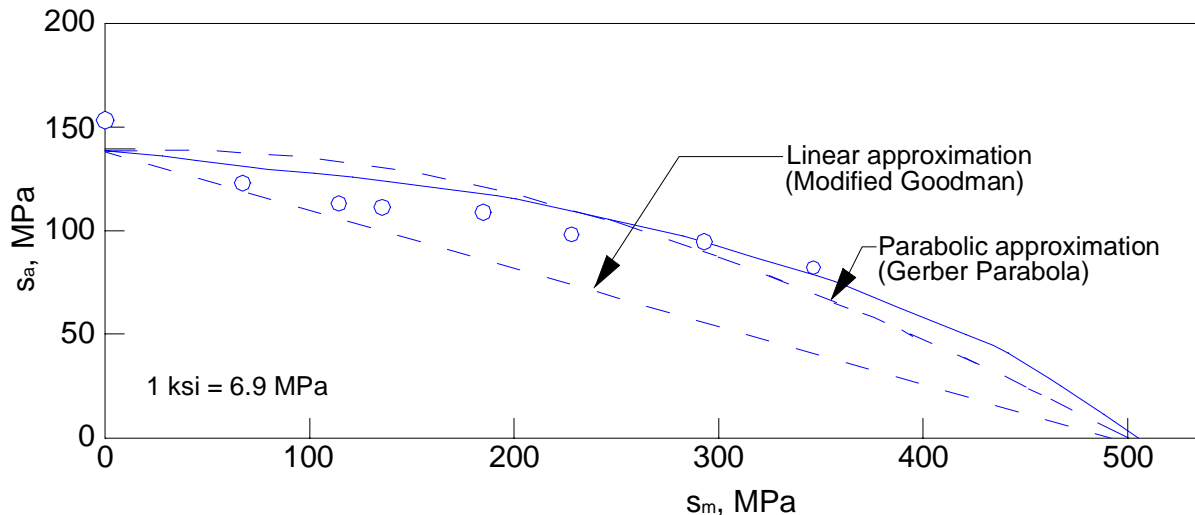
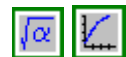


Figure 3.5.3.4-1 A constant life line diagram for modified Goodman and Gerber approximations⁹

Using true stress and true strain notations, [Equation 3.5.3.2-1](#) can be modified¹³ for mean stress σ_m , as

$$\sigma_a = (\sigma_f' - \sigma_m)(2N_f)^b$$

Equation 3.5.3.4-3



In fatigue life analysis and applications, however, the difference between true and engineering stresses are often negligible such that $\sigma_a = S_a$ and $\sigma_m = S_m$. Data for 1045 steel in [Figure 3.5.3.4-2](#) shows how the fatigue life curve is translated downward for an increase in tensile mean stress of 690 MPa (100 ksi). It should be recognized, however, that if the mean stress is a residual stress, then at shorter lives the residual stress relaxes due to plastic deformation, and as a result the two lines shown in [Figure 3.5.3.4-2](#) will merge at short lives.

Use of [Equation 3.5.3.4-3](#) for a constant life line diagram is identical to the Goodman approach ([Equation 3.5.3.4-1](#)) except that the intercept on the mean stress axis is the fatigue strength coefficient instead of the ultimate tensile strength. [Figure 3.5.3.4-3](#) shows the family of constant life lines for 4340 steel. This methodology of accounting for mean stress is particularly useful because [Equation 3.5.3.4-3](#) can be arranged as;

$$2N_f = \left(\frac{\sigma_a}{\sigma_f' - \sigma_m} \right)^{1/b}$$

Equation 3.5.3.4-4



and fatigue life can be directly calculated from the fatigue properties of σ_f' and b for a given steel.

For materials behaving in a brittle manner, another equation can be used¹.

$$\sigma_a(\sigma_a + \sigma_m) = (\sigma'_f)^2 (2N_f)^{2b}$$

Equation 3.5.3.4-5

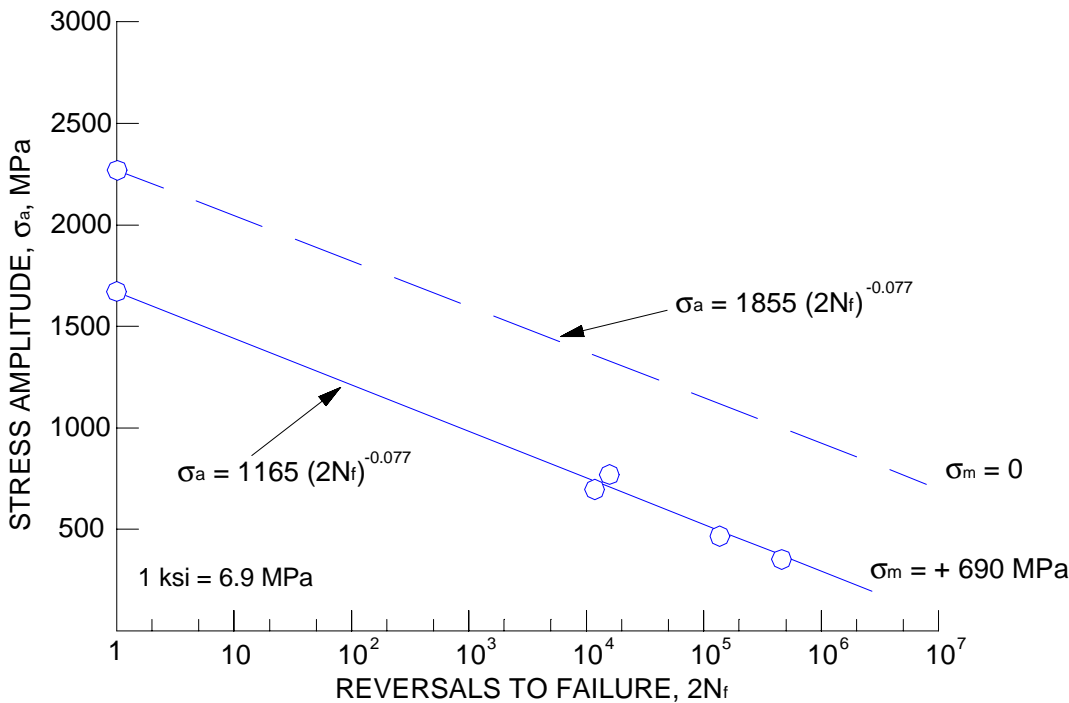


Figure 3.5.3.4-2 Fatigue strength vs. life relations for 1045 steel (386 BHN) as influenced by mean stress⁹

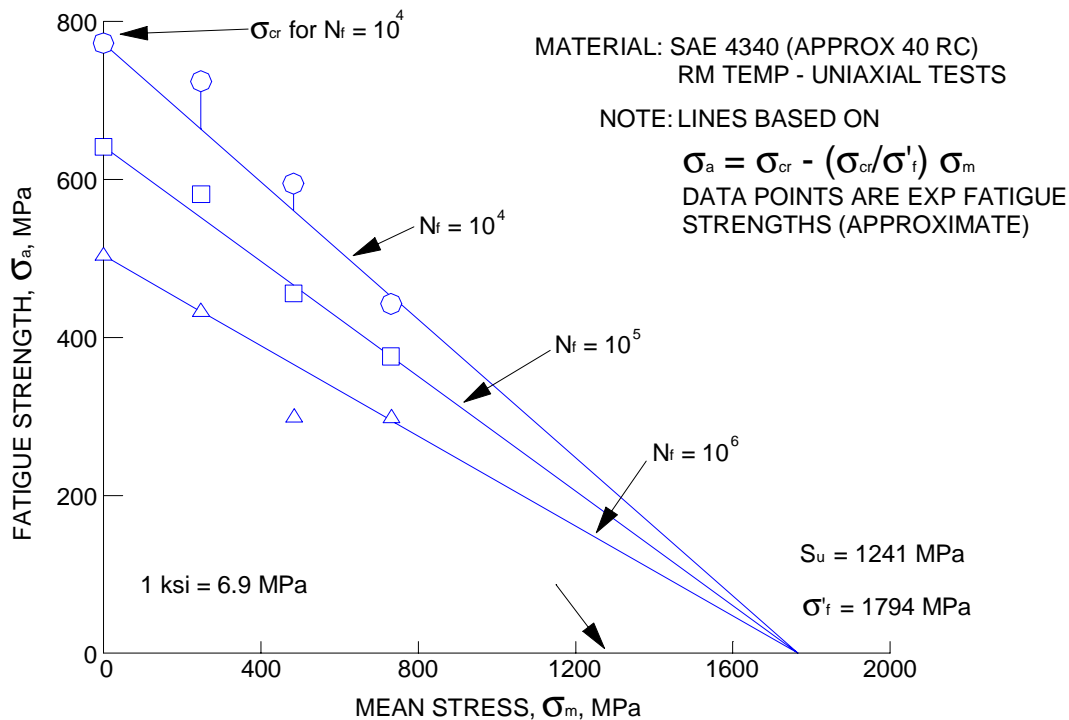


Figure 3.5.3.4-3 Constant life-line diagram for 4340 steel using the fatigue strength coefficient approach¹³

3.5.4 STRAIN CONTROLLED CYCLIC PROPERTIES

Consider a structure containing a notch or stress concentration factor subjected to some constant load or elastic stress fluctuation. The cyclic response of the material at the root of the notch will be much different from that of the surrounding body because of inelastic deformations at the notch root. If a strain gage is placed on the notch face, the fatigue behavior of the localized plastic zone can be simulated by testing smooth specimens under strain controlled conditions equal to those measured by the strain gage ([Figure 3.5.4-1](#)).

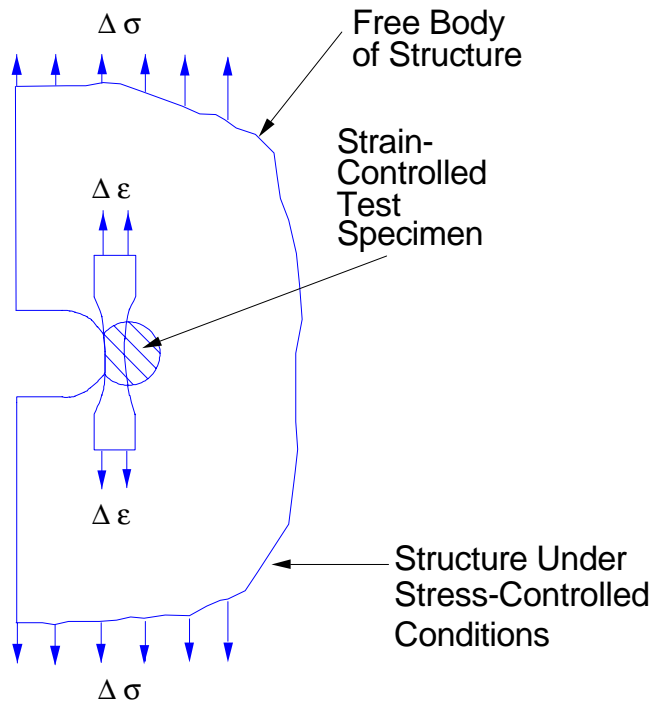


Figure 3.5.4-1 Strain controlled test specimen simulation for stress concentrations in structures^{[12](#)}

The cyclic stress-strain resulting from strain controlled cycling of smooth specimens will be significantly different from that obtained for load controlled cycling. For example, in constant load (stress) cycling of SAE 960 steel, the steel cyclically softens resulting in an expanding stress-strain hysteresis loop with increasing numbers of cycles ([Figure 3.5.4-2](#)).

With increasing numbers of constant stress ($S_a = 414$ MPa or 60 ksi) cycling, cyclic creep occurs in the tensile direction until very large cyclic strains and fracture occurs. When the same material was cyclically loaded at constant strain cycles corresponding to the same stress amplitude of 414 MPa, the material cyclically softened but did not exhibit cyclic creep. The hysteresis loops measured at different cycles in the life of the specimen for this strain controlled testing are shown in [Figure 3.5.4-3](#).

Thus, strain controlled fatigue behavior has received a great deal of attention in the past two decades. This methodology is particularly suited to finite life and low cycle fatigue behavior where significant plastic straining occurs at notches.

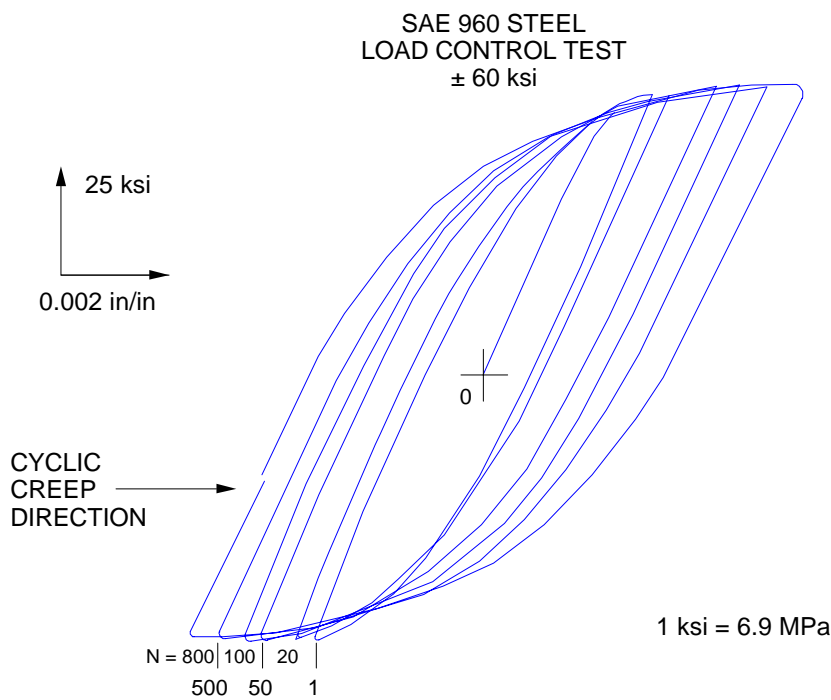


Figure 3.5.4-2 Cyclic softening and the early stages of cyclic creep in 960 steel during stress-mode cycling⁹

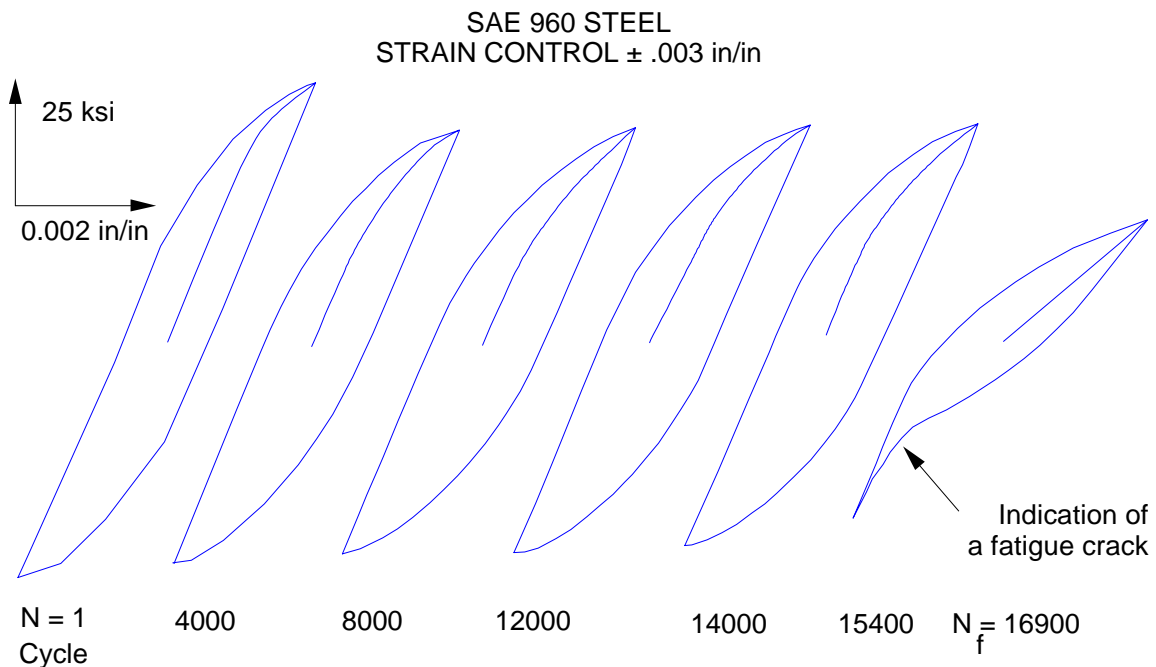


Figure 3.5.4-3 Cyclic softening in 960 steel but without cyclic creep during strain mode cycling⁹

3.5.4.1 Smooth Specimen Data Under Strain Control

Cyclic properties are determined by cyclic strain control test of axially loaded smooth polished specimens. Generally a gage length to thickness ratio of less than 3 is necessary to prevent buckling during fully reversed straining. In a strain controlled test, the stress and strain are periodically recorded with an x-y plotter to develop a hysteresis loop ([Figure 3.5.4.1-1](#)). Although cyclic softening or hardening may occur during the initial cycles of straining, a stable hysteresis loop generally occurs after about 20 to 50 percent of the fatigue life of the specimen.

The total strain range, $\Delta\epsilon$, for a hysteresis loop is equal to twice the strain amplitude, ϵ_a (i.e., $\Delta\epsilon=2\epsilon_a$), and the total stress range, $\Delta\sigma$, is equal to twice the stress amplitude σ_a (i.e., $\Delta\sigma=2\sigma_a$). Moreover, the total strain amplitude can be represented as the sum of its elastic and plastic components ([Figure 3.5.4.1-1](#)) such that

$$\epsilon_a = \frac{\Delta\epsilon}{2} = \frac{\Delta\epsilon_e}{2} + \frac{\Delta\epsilon_p}{2} = \frac{\Delta\sigma}{2E} + \frac{\Delta\sigma_p}{2}$$

Equation 3.5.4.1-1



because $\Delta\epsilon_e = \frac{\Delta\sigma}{E}$, where E is Young's modulus.

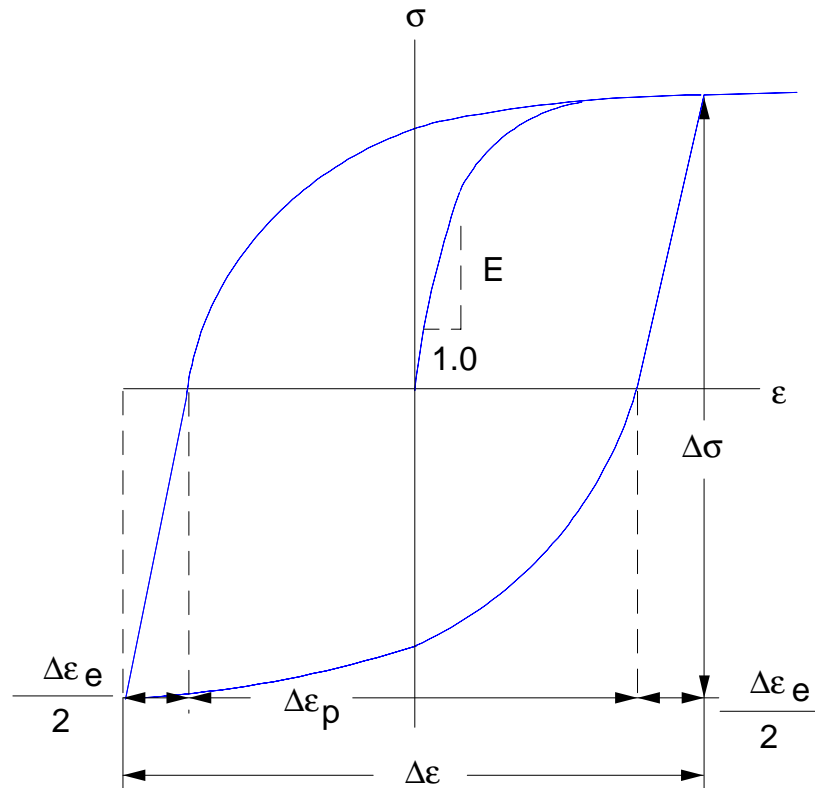


Figure 3.5.4.1-1 Schematic of a stress-strain hysteresis loop¹²

A log-log plot of the stable plastic strain amplitude, $\Delta\epsilon_p/2$ versus the number of reversals to failure, $2N_f$, generally results in a straight line relationship ([Figure 3.5.4.1-2](#)) given by the equation

$$\frac{\Delta\epsilon_p}{2} = \epsilon'_f (2N_f)^c$$

Equation 3.5.4.1-2



where ϵ'_f = fatigue ductility coefficient

c = fatigue ductility exponent

N_f = number of cycles to failure; therefore $2N_f$, is equal to the number of reversals to failure.

The fatigue ductility coefficient, ϵ'_f , and fatigue ductility exponent, c , are the intercept and slope of the regression analysis between true plastic strain amplitude, $\Delta\epsilon_p/2$, versus reversals to failure, $2N_f$, data in a log-log plot.

Similarly, a log-log plot of the stable stress amplitude, $\Delta\sigma/2$, versus the number of reversals to failure, $2N_f$, results in a straight line relationship given by the equation:

$$\frac{\Delta\sigma}{2} = \sigma_a = \sigma'_f (2N_f)^b$$

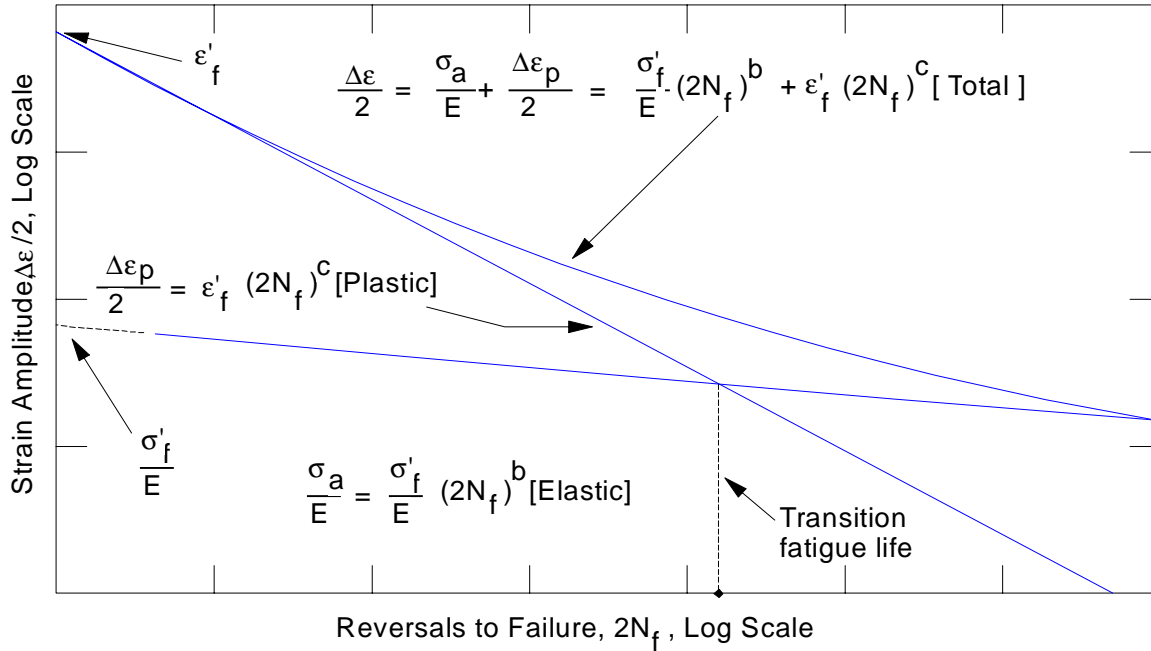
Equation 3.5.4.1-3



where σ_a = true stress amplitude

σ'_f = fatigue strength coefficient

b = fatigue strength exponent

Figure 3.5.4.1-2 Strain life plot ¹²

The fatigue strength coefficient, σ'_f , and fatigue strength exponent, b , are the intercept and slope of the regression analysis between true elastic strain amplitude, $\Delta\epsilon_e/2$, versus reversals to failure, $2N_f$, data in a log-log plot.

Dividing [Equation 3.5.4.1-3](#) by the modulus of elasticity, E , gives the elastic strain amplitude in terms of the fatigue strength coefficient, the fatigue strength exponent and the fatigue life:

$$\frac{\Delta \varepsilon_e}{2} = \frac{\sigma_a}{E} = \frac{\sigma_f'(2N_f)^b}{E}$$

Equation 3.5.4.1-4

Combining [Equation 3.5.4.1-1](#), [Equation 3.5.4.1-2](#) and [Equation 3.5.4.1-4](#) results in the strain-life relationship:

$$\frac{\Delta \varepsilon}{2} = \frac{\sigma_f'(2N_f)^b}{E} + \varepsilon_f'(2N_f)^c$$

Equation 3.5.4.1-5

which is represented as a heavy curve in [Figure 3.5.4.1-2](#)

Thus, [Equation 3.5.4.1-5](#) is a mathematical expression composed of an elastic and a plastic component for the strain controlled fatigue behavior of a steel.

The transition fatigue life, N_t , obtained when the elastic and plastic components of the strain are equal (i.e., $\Delta \varepsilon_p / \Delta \varepsilon_e = 1$) is given by the relation:

$$2N_t = \left(\frac{E\varepsilon_f'}{\sigma_f'} \right)^{\frac{1}{b-c}}$$

Equation 3.5.4.1-6

[Equation 3.5.4.1-5](#) and [Equation 3.5.4.1-6](#) and [Figure 3.5.4.1-2](#) show that total fatigue lives less than N_t are governed primarily by the plastic strain amplitude (ductility), whereas the total fatigue lives greater than N_t are governed primarily by the elastic strain amplitude (elastic stress). Thus, transition life can be considered as the point of separation between low cycle and high cycle fatigue.

Moreover, it is claimed that the fatigue ductility coefficient ε'_f , and the fatigue strength coefficient, σ_f' determined from regression analysis of fatigue data, can be approximated by the logarithmic ductility of material D and true fracture strength, σ_f , respectively, obtained from a monotonic tension test¹³. Logarithmic ductility of material is given by the equation below.

$$D = \ln(1 - \text{reduction in area})^{-1}$$

Equation 3.5.4.1-7

3.5.4.1.1 Transient Cyclic Stress-Strain Behavior

The stress-strain behavior for metals depends on the initial condition (heat treated, cold worked, etc.) of the metal and on the test conditions used. When exposed to fully reversed cyclic plastic strain amplitudes of constant magnitude, the metal may exhibit

1. Cyclically neutral behavior
2. Cyclically hardening behavior
3. Cyclically softening behavior, or
4. Complex cyclic behavior.

These behaviors can be illustrated by observing the variation in stress as a smooth specimen is subjected to completely reversed, constant amplitude strain fluctuations with a zero mean value, as shown in [Figure 3.5.4.1.1-1](#). If the stress magnitude required to apply the constant strain cycles remains constant ([Figure 3.5.4.1.1-1\(a\)](#)) the metal is cyclically neutral, which implies that the metal's cyclic stress-strain properties are identical to its monotonic stress-strain properties (engineering stress and strain properties obtained from a tension test). If the stress to apply a constant strain increases ([Figure 3.5.4.1.1-1\(b\)](#)) the metal cyclically hardens; if the stress to apply a constant strain decreases ([Figure 3.5.4.1.1-1\(c\)](#)) the metal cyclically softens. A metal exhibits complex cyclic behavior when cyclic softening, or hardening, behavior occur for different strain ranges.

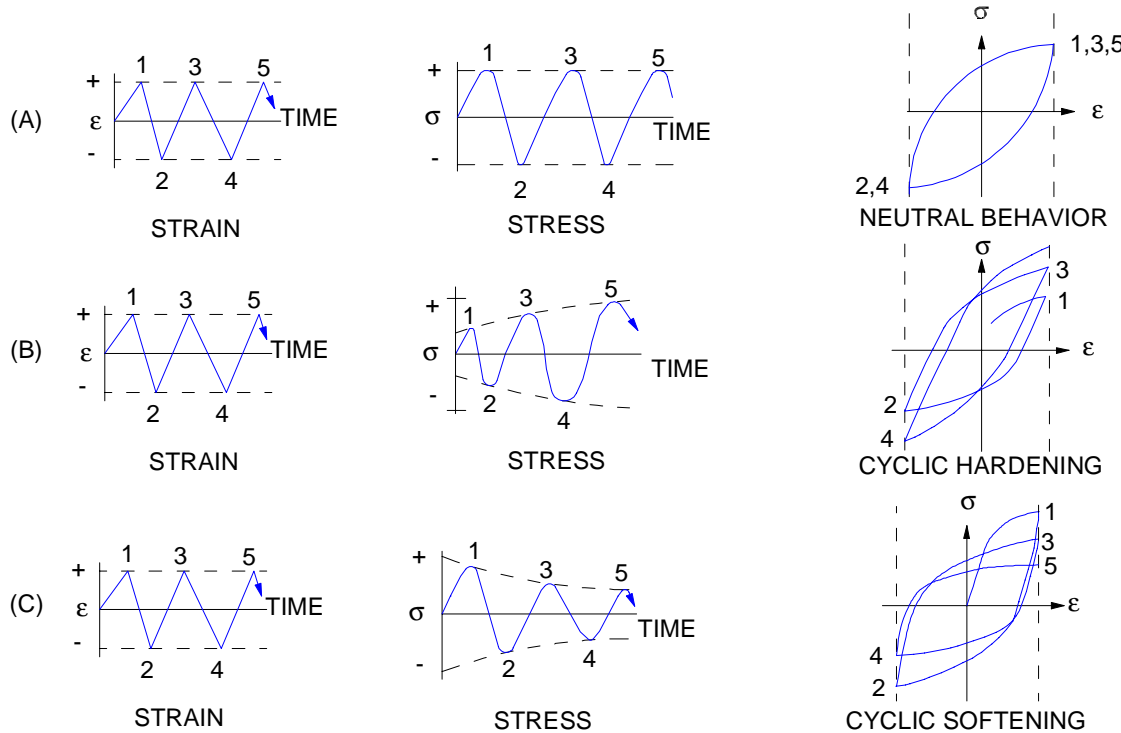


Figure 3.5.4.1.1-1 Schematic representation of cyclic hardening and cyclic softening¹⁶

3.5.4.1.2 Cyclically Neutral Stress-Strain Behavior

Many steels subjected to constant cyclic strain amplitude usually exhibit an initial transient behavior, but reach an essentially cyclically stable stress-strain behavior that corresponds to a constant hysteresis loop. This stable behavior is usually reached after about 20 to 50 percent of the total fatigue life of the specimen. The stabilized stress values are plotted at the corresponding strain values to construct a cyclic stress-strain curve similar to a monotonic stress-strain curve. This procedure is shown schematically in [Figure 3.5.4.1.2-1\(a\)](#). Superposition of the cyclic and monotonic stress-strain curves ([Figure 3.5.4.1.2-1\(b\)](#)) shows how different steels may exhibit significantly different stress-strain behavior when cyclically loaded than when tested monotonically.

Another means of producing the cyclic stress-strain curve consists of subjecting a specimen to blocks of gradually decreasing and then increasing strain amplitudes, as shown in [Figure 3.5.4.1.2-2](#). A maximum strain amplitude of ± 1.5 to 2.0 percent is usually sufficient to

cyclically stabilize the metal quickly without the danger of causing the specimen to neck, fail, or buckle before a stable state is achieved. The cyclic stress-strain curve is then determined by the locus of superimposed hysteresis loop tips.

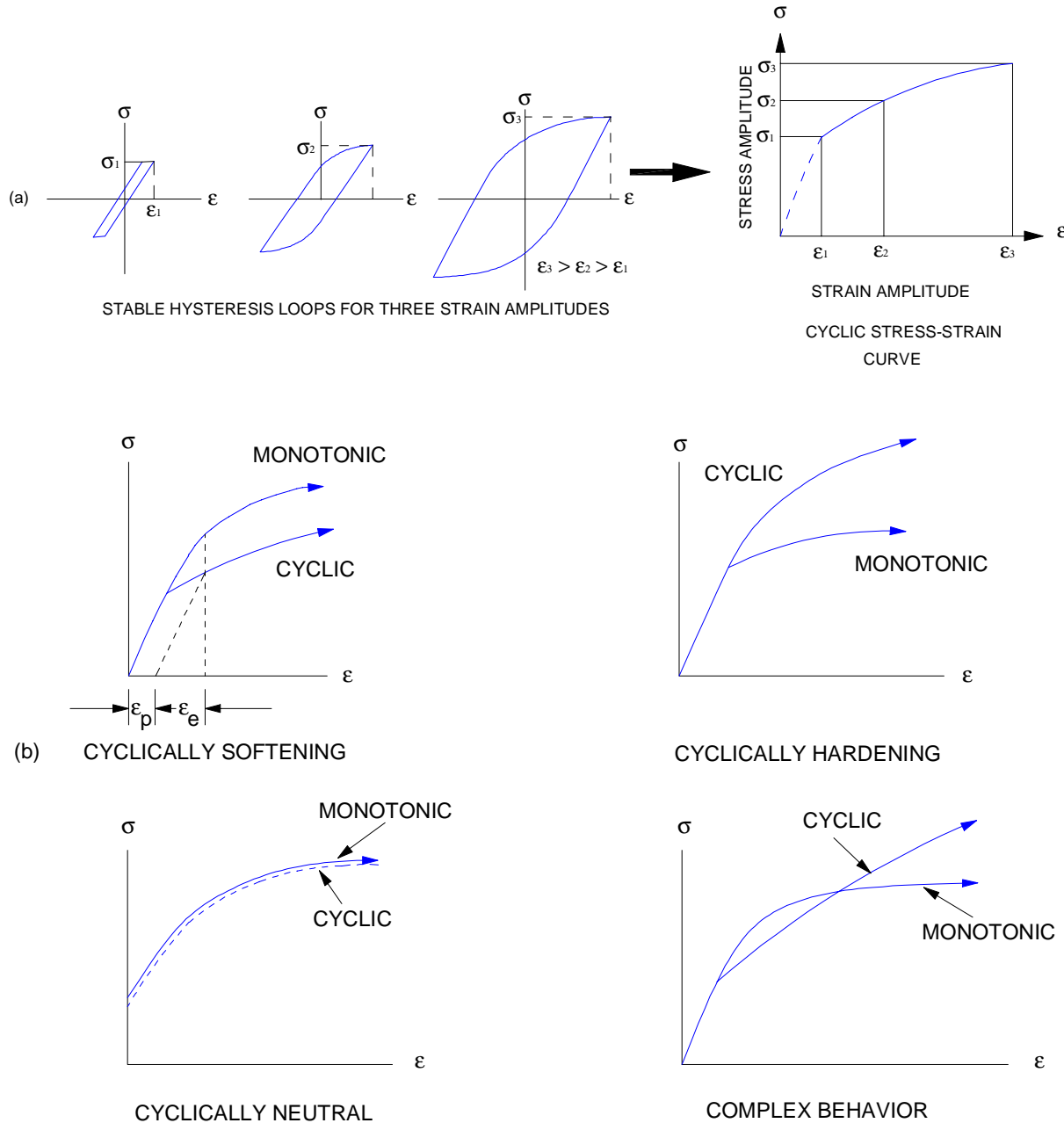


Figure 3.5.4.1.2-1 Cyclic stress strain curves for various behaviors¹⁶

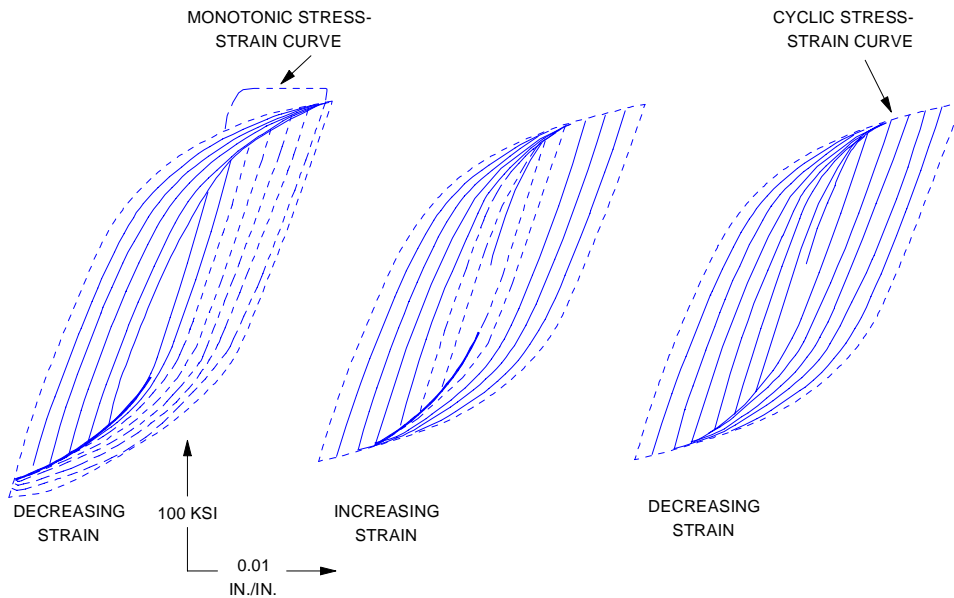


Figure 3.5.4.1.2-2 Stress strain record of incremental step test on quenched and tempered SAE 4142, 380 BHN ¹⁶

3.5.4.2 Specimens with Notches Under Strain Control

As described in [Section 3.5.3.3](#), for Specimens With Notches Under Load Control, the theoretical stress concentration factor, K_t is determined from the elastic global and local stresses and strains of a notch. The theoretical stress concentration factor however, is related to the fatigue notch concentration factor, K_f , through the fatigue notch sensitivity index, q , according to [Equation 3.5.3.3-2](#).

Another, more straightforward, means of determining the fatigue notch concentration factor is to machine a notch into a specimen of the material to be characterized and to test the specimen in completely reversed axial load control until fracture. The results from the notched specimen are compared to the smooth specimen results and the K_f is determined.

Perhaps the most common means of determining the K_t is the Neuber¹⁷ approach in which K_t is determined by the geometric mean value of the elastic stress and strain concentration factors K_σ and K_ϵ respectively. Thus,

$$K_t = \sqrt{K_\sigma K_\epsilon}$$

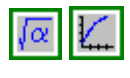
Equation 3.5.4.2-1



Because in real materials the stress and strains at the root of notches are plastic and not elastic and because real materials have varying responses to cyclic loads in the presence of a high stress concentration, a stress concentration factor ([Reference 2](#)), K_t , is derived from the Neuber relationship as:

$$K_t = \sqrt{\frac{\Delta\sigma \Delta\epsilon}{\Delta S \Delta e^2}}$$

Equation 3.5.4.2-2



where $\Delta\sigma$ and $\Delta\epsilon$ are the local true stress and strain ranges at the notch root and ΔS and Δe are nominal or global stress and strain ranges remote from the notch.

In fatigue, since small notches have less effect than expected based on K_t , several researchers proposed replacing K_t in Neuber's approach by fatigue notch concentration factor, K_f .

It is convenient to incorporate the modulus of elasticity, E , and Hooke's relationship between ΔS and Δe and rewrite [Equation 3.5.4.2-2](#) in the form:

$$K_f = \sqrt{\frac{\Delta\sigma \Delta\varepsilon E}{\Delta S^2}}$$

Equation 3.5.4.2-3



Thus, the fatigue notch factor is affected by the product of the local stress and strain range, the modulus of elasticity and the global stress range. Note that [Equation 3.5.4.2-2](#) is valid for nominally elastic behavior.

Values of K_f are experimentally determined for various materials by testing small notched specimens in the laboratory for all stress ranges ΔS , in the stress range histogram. By rewriting [Equation 3.5.4.2-3](#) as,

$$K_f \Delta S = \sqrt{\Delta\sigma \Delta\varepsilon E}$$

Equation 3.5.4.2-4



[Equation 3.5.3.2-1](#) and [Equation 3.5.4.1-5](#) can be substituted into the right side to obtain,

$$K_f \Delta S = \left[4E \sigma_f' \varepsilon_f' (2N_f)^{b+c} + 4\sigma_f'^2 (2N_f)^{2b} \right]^{1/2}$$

Equation 3.5.4.2-5

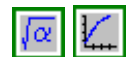


[Figure 3.5.4.2-1](#) shows the curve calculated from the right side of [Equation 3.5.4.2-5](#) for 1020 steel.⁹

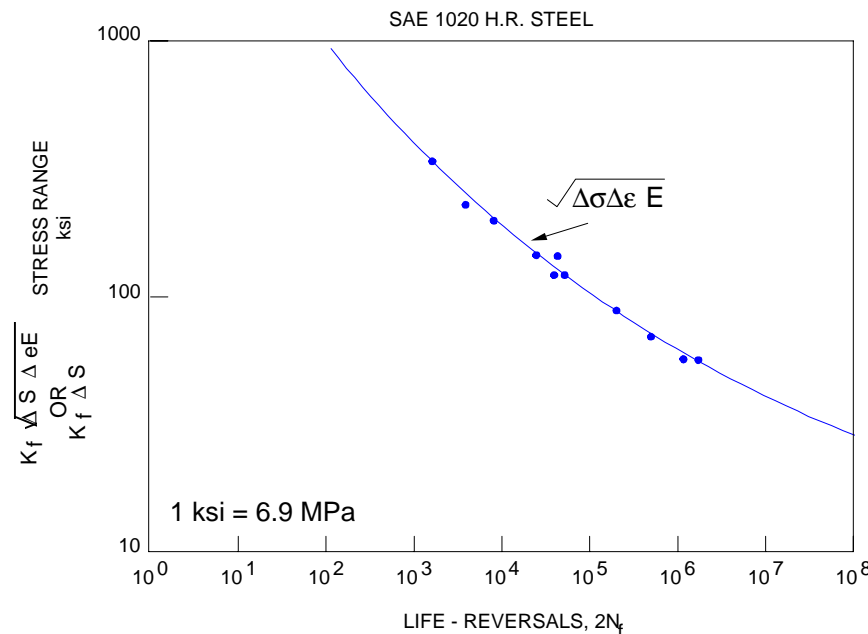


Figure 3.5.4.2-1 Neuber curve for 1020 H.R. steel⁹

K_f is determined for a notched specimen by taking the value of the curve at the reversals to failure, $2N_f$, and dividing it by the nominal elastic stress range, ΔS . Neuber plots for three sheet steels (with different tensile strength) cyclically loaded in the presence of a drilled hole ($K_t = 2.5$) are shown in [Figure 3.5.4.2-2](#). As can be seen from [Figure 3.5.4.2-2](#), as the tensile strength increases the material becomes more notch sensitive.

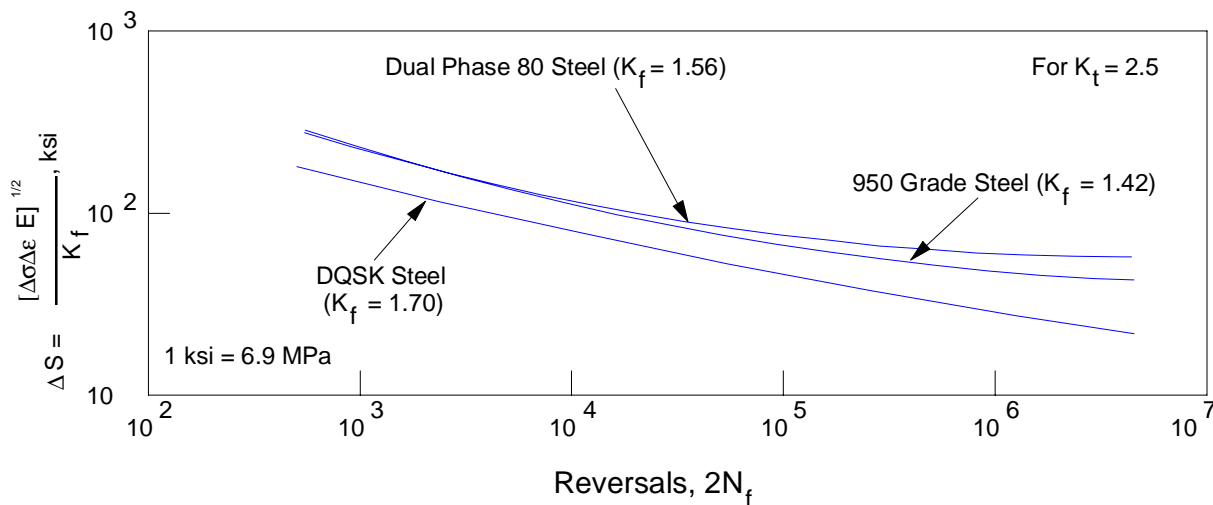


Figure 3.5.4.2-2 Neuber plots of notched fatigue - test data for DQSK, 950 grade and dual phase 80 steels¹⁶

An example calculation is given in [Section 6.2.5](#) for the strain-life estimates of steels of different tensile strengths. The difference in fatigue strength for the two steels is discussed for initiating a crack after 500,000 cycles of a double notched tensile sheet.

3.5.5 FATIGUE LIFE PREDICTIONS

Fatigue lives are predicted by a variety of methods, including load-life, stress-life (S-N), local strain (strain-life), and linear elastic fracture mechanics (LEFM). The load-life, S-N and strain-life approaches are based on crack initiation while the LEFM approach is based on crack propagation. In some cases both the load-life and S-N approaches can be used to predict the total life which includes crack initiation plus crack propagation.

All the crack initiation methods are based on a cumulative damage approach. The linear cumulative damage approach proposed by Palmgren ([Reference 4](#)) and Miner ([Reference 5](#)) is widely used as the best available method.

In order to predict fatigue lives based on a cumulative damage approach, a cycle counting method is required. The cycle counting method breaks the time history into small events in which the fatigue calculation for the entire history can be performed by summing the damage caused by each event. Four methods of cycle counting will be explained here, namely; range counting, level crossing counting, rainflow counting, and time-at-level counting.

After the cycle counting a detailed analysis using material properties is required to determine the damage caused for different ranges of load, stress or strain.

The particular methodology appropriate for an individual designer will depend primarily upon the service (time) history, geometry and material property information available. These analyses are very complex and time consuming, generally requiring computer algorithms. The reader is advised to review the references cited for more detailed information and procedures. Only a brief overview of the methodologies are included below and no working knowledge can be assumed with such a cursory review.

3.5.5.1 Linear Damage Law

The linear damage law proposed by Palmgren⁴ and Miner⁵ (P-M) assumes that the percentage of life used is proportional to the summation of the cyclic ratios for each loading condition. Thus, it is necessary to first determine the number of cycles for various loading ranges from the loading history of the component and the corresponding cyclic life of the material for each range are then summed to determine the damage:

$$D = \frac{n_1}{N_1} + \frac{n_2}{N_2} + \frac{n_3}{N_3} + \dots + \frac{n_n}{N_n} \quad \text{Equation 3.5.5.1-1}$$

where D = damage,

$n_1, n_2, n_3, \dots, n_n$ = cycles occurring in service at loading levels of 1, 2, 3, ..., n

$N_1, N_2, N_3, \dots, N_n$ = cycles to failure for the material in question at the loading levels of 1, 2, 3, ..., n.

When the sum of the ratios becomes equal to one, failure is predicted.

If a sequence of histories is repeated a number of times, then the P-M equation can be written as:

$$B \sum \frac{n_i}{N_i} = 1 \quad \text{Equation 3.5.5.1-2}$$

where B is the number of repeats (blocks) to failure

3.5.5.2 Cycle Counting

Four of the most common methods of cycle counting are range counting, level-crossing counting, rain-flow counting, and time-at-level counting. Currently, most researchers consider rain-flow counting to give the best representations of the service cycles in variable amplitude fatigue analysis.

3.5.5.2.1 Range Counting

Range counting separates the variable amplitude service history into individual ranges. A range is the difference between the value of the peak and the valley of a signal. As shown in [Figure 3.5.5.2.1-1](#), range counting develops a matrix of ranges and number of occurrences.

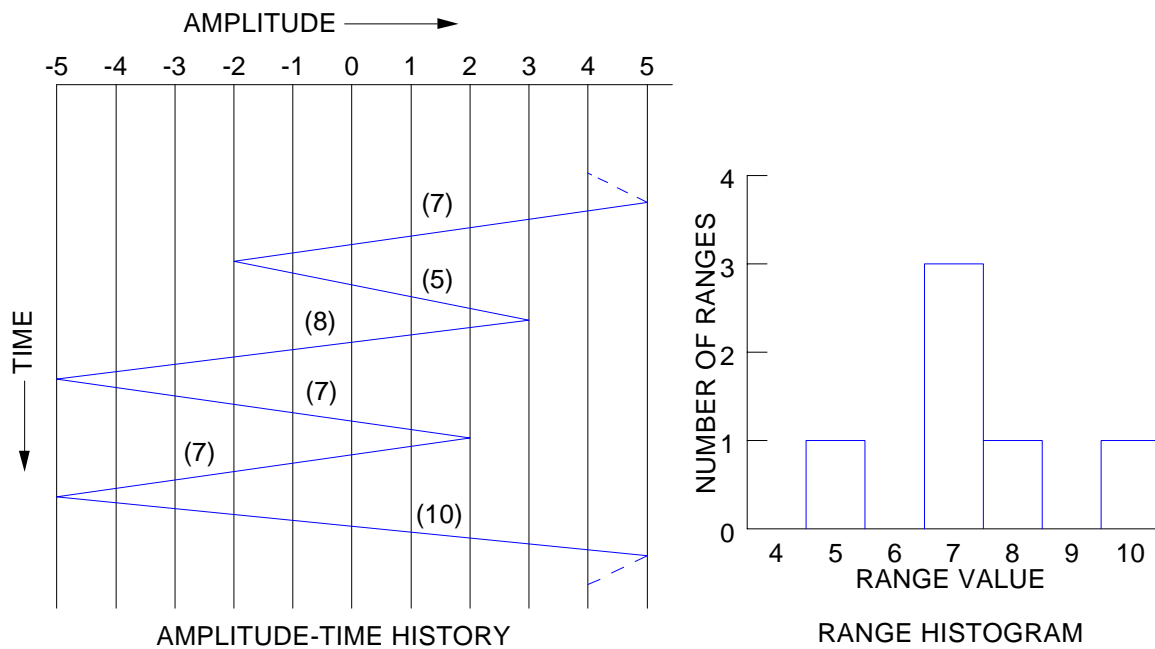


Figure 3.5.5.2.1-1 Range counting example¹⁸

3.5.5.2.2 Level-Crossing Counting

In level-crossing counting, the number of times (occurrences) the signal crosses each level is determined. Positive and negative values are defined according to that level for which a positively sloped or negatively sloped signal crosses the level ([Figure 3.5.5.2.2-1](#)).

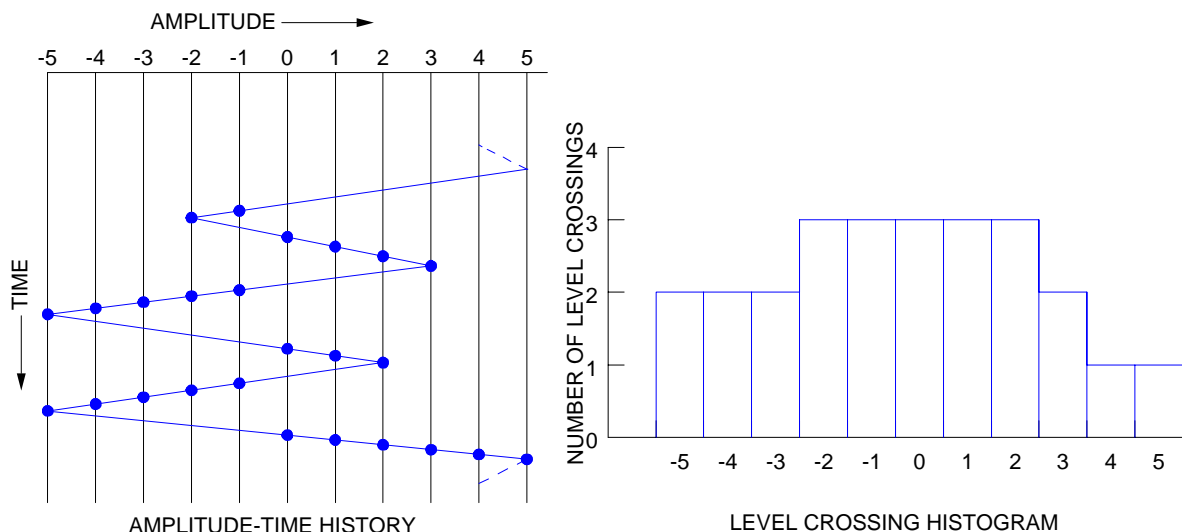


Figure 3.5.5.2.2-1 Level crossing counting example¹⁸

From the level-crossing histogram, a cumulative frequency of crossing occurrences is determined ([Figure 3.5.5.2.2-2](#)).

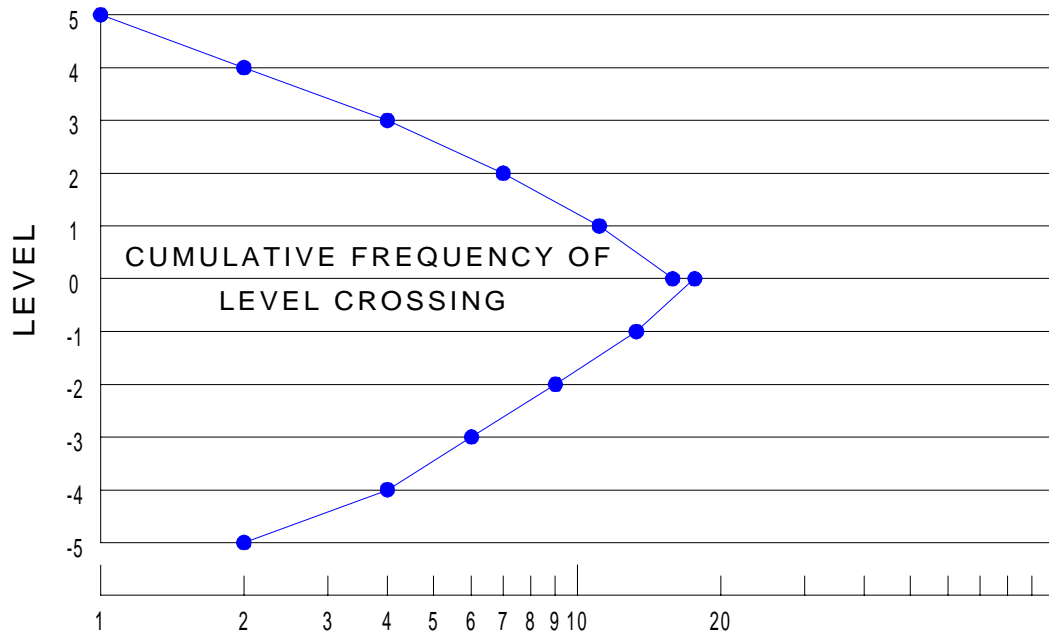


Figure 3.5.5.2.2-2 Cumulative distribution plot ¹⁸

The positive and negative levels are then paired to define cycles as shown in [Figure 3.5.5.2.2-3](#) for the history shown in [Figure 3.5.5.2.2-1](#).

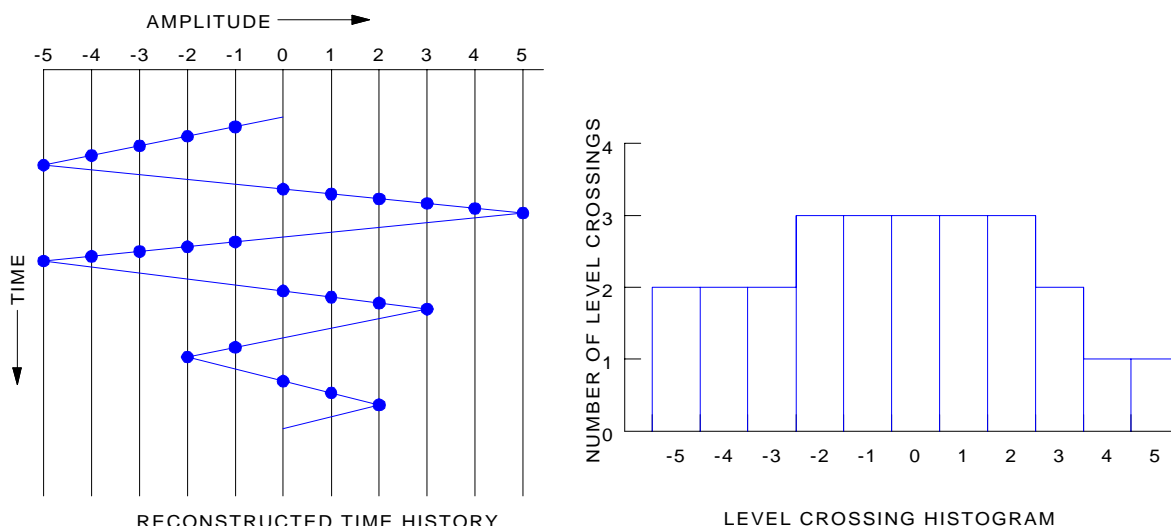


Figure 3.5.5.2.2-3 Reconstructed time history ¹⁸

3.5.5.2.3 Rain-Flow Counting

Although rain-flow counting may appear similar to range counting, it is different in that rain-flow does not necessarily pair adjacent peaks and valleys to define a cycle. Instead it pairs those that define a closed hysteresis loop in the stress-strain response of a material subjected to variable amplitude loading. Rainflow cycle counting is important since it predicts the closed hysteresis loops with which the fatigue damage is associated.

The name, rain-flow, comes from the concept of rain flowing down a series of pagoda roofs when the time axis is orientated vertically. The beginning of a half cycle or range is defined by the location of the start of the rain flow. The end of the cycle or step of the rain-flow occurs if:

1. Starting at a peak, it comes opposite a more positive peak than where it started; or starting at a valley it comes opposite a more negative valley than where it started, or
2. It runs into a rain-flow from the roof above, or
3. It reaches the end of the signal.

[Figure 3.5.5.2.3-1](#) shows a rainflow cycle count. For simplicity only rainflow ranges and number of cycles are shown.

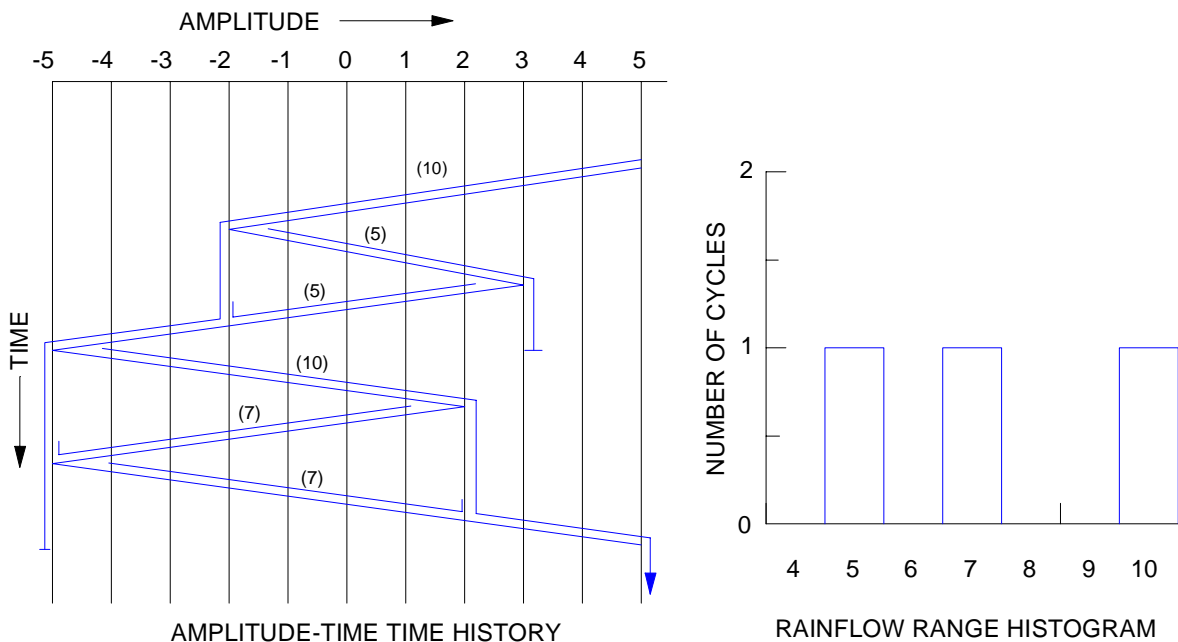


[Figure 3.5.5.2.3-1](#) Rainflow counting example¹⁸

[Figure 3.5.5.2.3-2](#) shows a more detailed 3-D histogram of the same history as in [Figure 3.5.5.2.3-1](#) with range, mean and number of rainflow cycles.

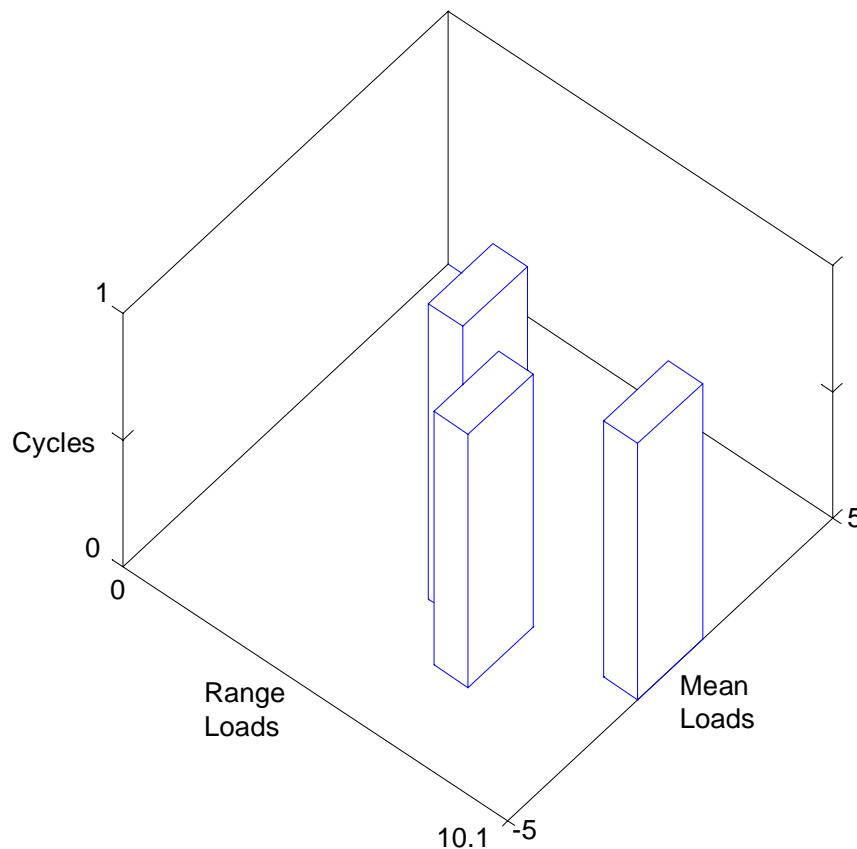


Figure 3.5.5.2.3-2 3-D rainfall counting example of the history in [Figure 3.5.5.2.3-1](#)

In a new recent definition of rainflow, the greatest peak or valley in the time history is chosen as the starting point and the time history is arranged to start and end with this maximum peak or valley. This results in all half cycles being paired to form full cycles. Rainflow cycles are then counted depending on the comparison of two adjacent ranges. If the first range is less than or equal to the second range, a rainflow cycle is counted. The range and mean values of the rainflow cycle are recorded, and its peak and valley are discarded for purposes of further cycle counting. If no cycle is counted, then one moves ahead and defines new ranges. This continues until a count can be made and all peaks and valleys in the time history are covered.

Note that because most cumulative damage histories are represented by repeated blocks of variable amplitude cycles, the maximum absolute value of the history is chosen as the starting point. The history in [Figure 3.5.5.2.3-3](#) is represented by a set of contained stress-strain hysteresis loops and as mentioned before, each of these closed loops represent a rainflow cycle.

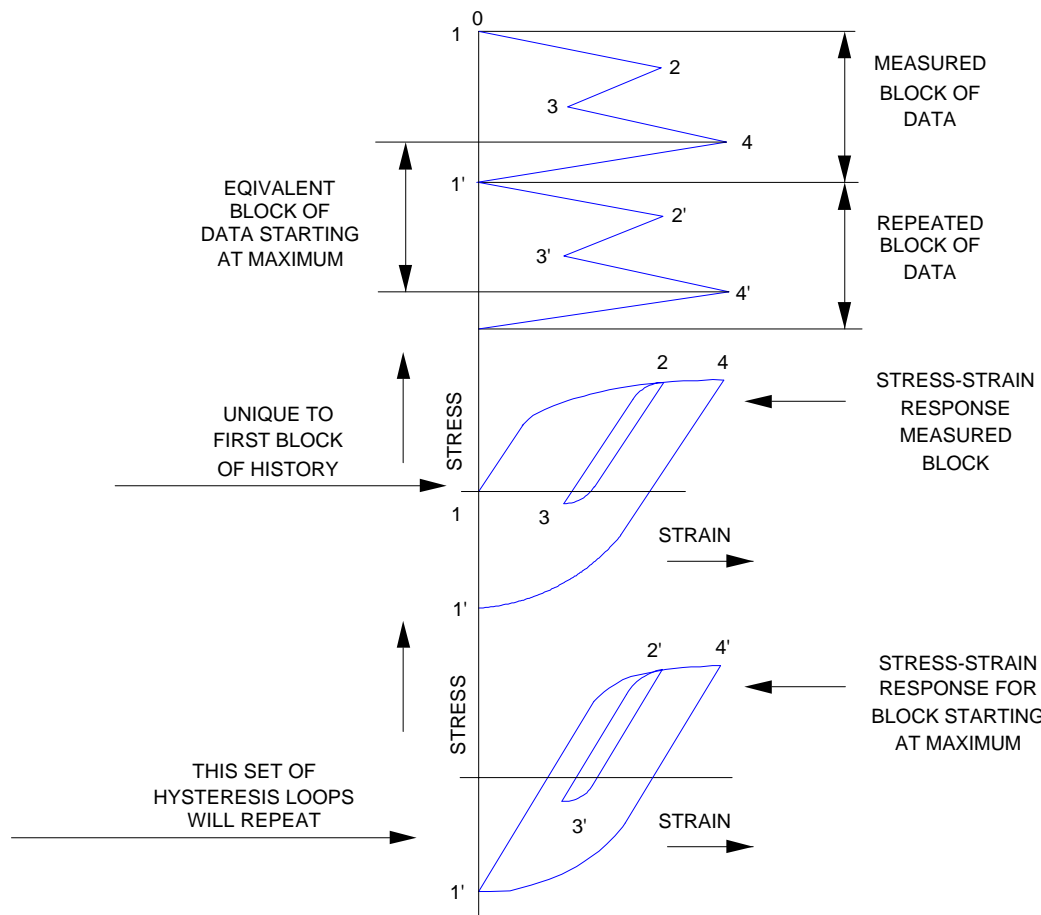


Figure 3.5.5.2.3-3 Logic for starting counting at largest absolute value¹⁸

3.5.5.2.4 Time-at-Level Counting

The time-at-level counting procedure develops a histogram of levels and the amount of time the signal is at each particular level ([Figure 3.5.5.2.4-1](#)).

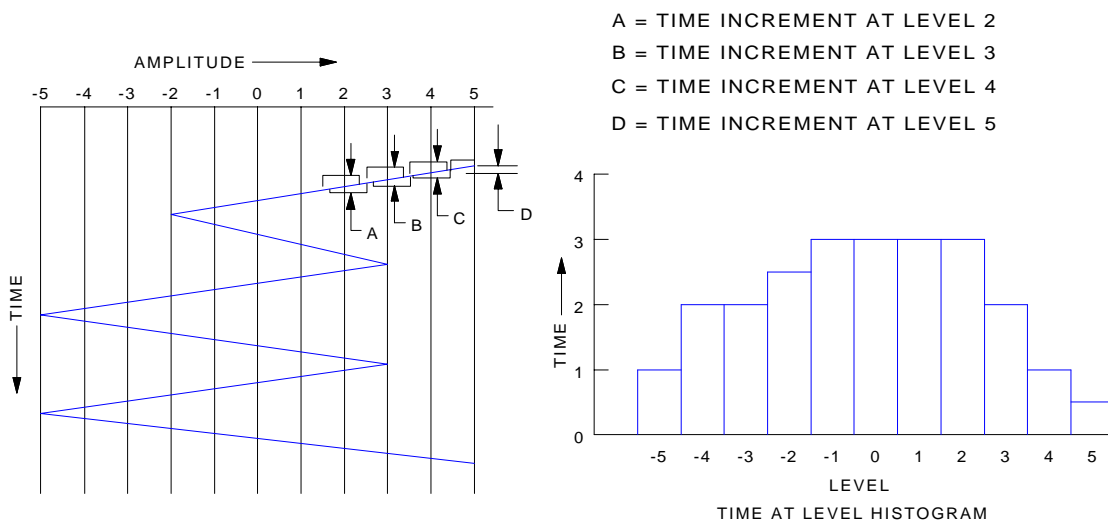


Figure 3.5.5.2.4-1 Time at level example¹⁸

3.5.5.3 Cumulative Damage Determination

As mentioned before, fatigue lives are predicted by a variety of methods, including load-life, S-N, strain-life, and LEFM. All of these methodologies require good service history data, material property data, geometry information and appropriate equations and procedures to establish the fatigue damage.

One of the most difficult tasks of the engineer is to determine the level of analytical sophistication appropriate for the component being considered. In making this decision, the accuracy of each of the three components of the design must be considered; the accuracy of the service history input, the accuracy of the cumulative damage methodology, and the accuracy of the material property data. For example, decisions such as the appropriate model for incorporation of mean stress effects on life predictions must be evaluated. As a second example, it has been shown that the loading sequence can significantly alter the fatigue life of a component. Tests of notched and smooth specimens subjected to an initial overload cycle in tension were compared to those for which the initial overload was in compression ([Figure 3.5.5.3-1](#)).

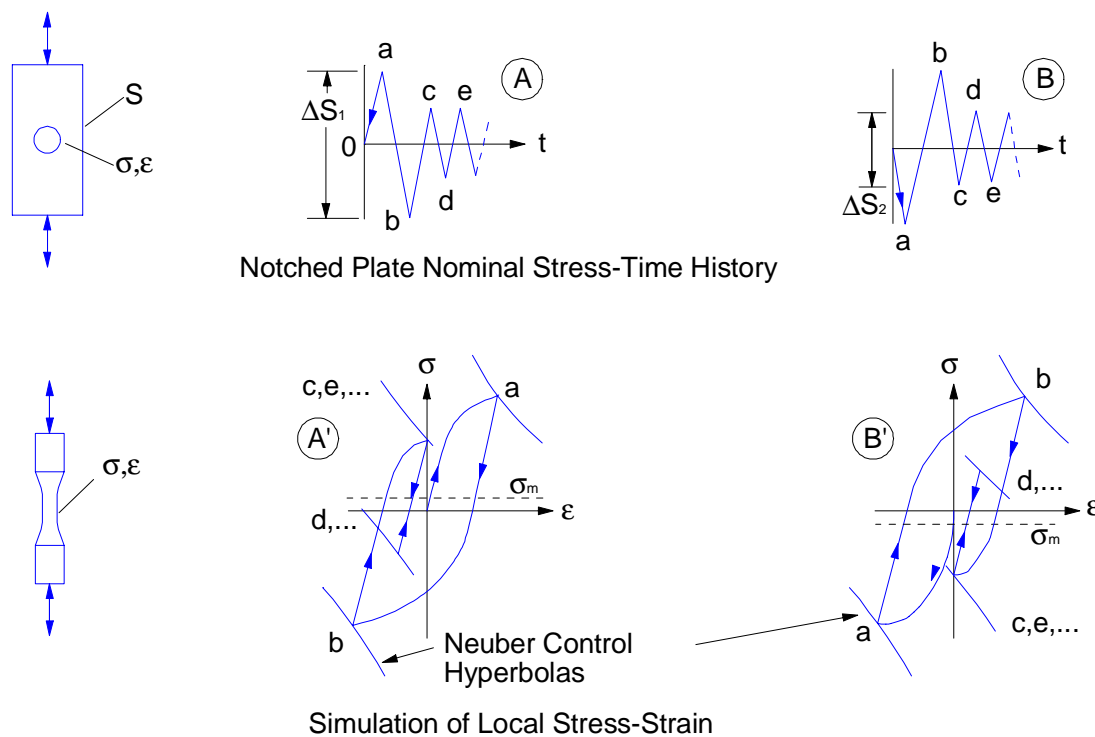


Figure 3.5.5.3-1 Sequence effects example (from Stadnick and Morrow)¹⁹

[Figure 3.5.5.3-1](#) shows that for low applied stress ranges, an initial high-low overload produces tensile local mean stress while an initial low-high overload produces compressive local mean stress.

The load-life analysis is the most straight forward procedure because it is a test of the actual component manufactured from the material being considered, incorporating all of the stress concentrations of concern. No additional stress analysis is needed. However, prototypes must be built and tested and any new material being considered must be used to build another prototype.

The stress-life (S-N) analyses has the advantage of evaluating different materials for a particular component design. Procedures outlined in [Section 3.5.3.2](#), [Section 3.5.3.3](#) and [Section 3.5.3.4](#) are necessary for evaluating mean stress effects and assessing stress concentration values. As previously discussed, stress-life calculations are most appropriate for long life considerations. Significant notch root plasticity and large mean stress effects are not reflected in these results. Also, empirical K_f values give much greater accuracy than estimations of stress concentrations based on K_t and q values. The notch root strain-life (local strain-life) analysis is suited for long, intermediate and short life calculations. However, it is best suited for intermediate and short life calculations where significant notch root plasticity occurs. The procedures outlined in [Section 3.5.4.1](#) and [Section 3.5.4.2](#) are used for incorporating mean stress effects.

The two general models for considering the mean stress effects are Morrow and Smith-Watson-Topper (SWT). Morrow modified the elastic term of the strain-life equation ([Equation 3.5.4.1-5](#)) for introducing the local mean stress into the strain-life equation. The SWT model assumes that by fatigue life for any condition of local mean stress depends on the product of $(\sigma_{mean} + \sigma_a)\epsilon_a$. [Equation 3.5.5.3-1](#) and [Equation 3.5.5.3-2](#) show the modified strain life equations to include the mean stress effects based on Morrow and SWT respectively. Both the Morrow and SWT approaches are in current use by the fatigue community, and no consensus exists as which one is superior to the other. Overall, the belief of the fatigue community is that the SWT approach provides good results and is a good choice for general use. However, a review of current literature suggests that the Morrow approach provides better results for compressive mean stresses while SWT gives non-conservative results.

$$\frac{\Delta\epsilon}{2} = \left(\frac{\sigma'_f - \sigma_m}{E} \right) (2N_f)^b + \epsilon'_f (2N_f)^c$$

Equation 3.5.5.3-1

$$(\sigma_a + \sigma_m) \frac{\Delta\epsilon}{2} = (\sigma'_f)^2 (2N_f)^{2b} + \sigma'_f \epsilon'_f (2N_f)^{b+c}$$

Equation 3.5.5.3-2

Sequential effects, using rain-flow counting, can also be incorporated if appropriate. Also as mentioned in [Section 3.5.3.3](#), empirical K_f values should be used rather than theoretical K_t values.

A sixth cumulative damage methodology, fracture mechanics, is best suited for calculating the fatigue life in growing a small preexisting crack to final failure. In this approach, a factor called the stress intensity factor, K , is used to characterize the severity of the crack situation and depends on loading, geometry and crack size. Some researchers have extended this methodology to include initiation of cracks from notches. These procedures incorporate empirical factors to compensate for the many inaccuracies, such as the unavailability of accurate stress intensity factors for very shallow cracks, particularly when emanating from a sharp notch or stress concentration. In the following sections, procedures are presented that utilize fracture mechanics for understanding the behavior of fabricated design details that contain crack-like imperfections. The design stress values from these data are based on large numbers of actual tests and incorporate significant factors of safety.

3.5.6 VARIABILITY OF FATIGUE PROPERTIES

3.5.6.1 Fatigue Data Generation

Fatigue data are generated following the ASTM-E 466 standard practice for load controlled fatigue testing and ASTM-E606 for strain controlled fatigue testing. For sheet steels, a supplemental procedure was developed by the Auto/Steel Partnership (A/SP) Sheet Steel Fatigue Program in 1996²⁰. Fatigue data are normally reported by using the data sheet developed by the SAE FD&E committee shown in [Figure 3.5.6.1-1](#). In addition to fatigue data, steel microstructure and monotonic properties of the steel are also provided.

MONOTONIC PROPERTIES:		Correlation Coeff., r	Material _____
Mod. of Elast. E	GPa($\times 10^3$ ksi)		Condition _____
Yield Strength, 0.2% S_y	MPa(ksi)		Hardness _____ HB
Ultimate Strength, S_u	MPa(ksi)		Material Source _____
Strength Coeff., K	MPa(ksi)		Specimen Orientation _____
Strain Hard. Exp., n			Other Specs. _____
Red. in Area, %RA			Composition _____
True Frac. Strength, σ_f	MPa(ksi)		
CYCLIC PROPERTIES:			
Yield Strength, 0.2% S'_y	MPa(ksi)	Reference _____	
Strength Coeff., K'	MPa(ksi)	Date _____	
Strain Hard. Exp., n'			
Fatigue Strength Coeff., σ'_f			
Fatigue Strength Exp., b			
Fatigue Ductility Coeff., ϵ'_f			
Fatigue Ductility Exp., c			
MICROSTRUCTURE:			
Grain Size _____			
Comments: _____			

Sheet of _____

Figure 3.5.6.1-1 Material characterization data sheet of SAE

[Table 3.5.6.1-1](#) and [Table 3.5.6.1-2](#) are compilations of fatigue properties for various steel products taken from SAE publication J1099²¹. [Table 3.5.6.1-1](#) is for the sheet steels and [Table 3.5.6.1-2](#) is for the bar steel products. In the past three years, the A/SP Sheet Steel Fatigue Program has generated fatigue data for several steel grades currently used for automotive body panels and structures, including IF steels, rephosphorized steels and HSLA steels. In addition, there is large amount of fatigue data available in published technical papers. Among those, the handbooks by C. Boller and T. Seeger²² and by The Society of Materials Science, Japan²³ are the ones with the biggest compilations.

Table 3.5.6.1-1 Monotonic and Cyclic Properties for Some Sheet Steels (Reference 21)

Steel Grade	Material Condition	Yield Strength (MPa)	Ultimate Tensile Strength (MPa)	σ_f' (MPa)	b	ε_f'	c	K' (MPa)	n'
1004	Hot rolled	287	378	1159	-0.142	1.300	-0.649	781	0.180
1004	Hot rolled	472	490	1019	-0.124	1.450	-0.701	561	0.180
1005	Hot rolled	226	321	888	-0.137	0.280	-0.505	1208	0.260
1005	Hot rolled	234	356	878	-0.129	0.460	-0.536	834	0.200
1005	Hot rolled	245	323	1024	-0.151	0.290	-0.509	1254	0.270
1005	Hot rolled	267	359	776	-0.126	0.240	-0.466	626	0.170
1008	Hot rolled	252	363	1225	-0.143	0.350	-0.522	1706	0.240
1008	Hot rolled	273	399	1016	-0.136	0.210	-0.473	958	0.220
1008	Hot rolled	234	331	1124	-0.172	0.460	-0.543	1443-c	0.318-c
1008	Hot rolled	255	365	1007	-0.159	0.500	-0.054	1234-c	0.290-c
1010	Hot rolled	200	331	499	-0.100	0.104	-0.408	867-c	0.244-c
1015	Hot rolled	228	414	884	-0.124	0.729	-0.581	945-c	0.213-c
1020	Hot rolled	262	441	1384	-0.156	0.337	-0.485	1962-c	0.321-c
1020	Cold rolled	255	393	697	-0.116	0.136	-0.405	1233-c	0.286-c
1025	Hot rolled	306	547	934	-0.107	0.590	-0.520	1042-c	0.207-c
HF50	Hot rolled	342	416	1111	-0.117	0.940	-0.676	694	0.132
HF50	Hot rolled	359	442	686	-0.074	0.337	-0.540	761	0.129
HF50	Hot rolled	361	441	732	-0.090	1.384	-0.703	684	0.124
HF50	Hot rolled	375	461	889	-0.055	0.345	-0.563	632	0.092
HF50	Hot rolled	383	448	959	-0.102	3.189	-0.794	745	0.116
HF50	Hot rolled	385	448	1088	-0.116	2.828	-0.790	785	0.127
HF50	Hot rolled	403	479	1000	-0.102	0.563	-0.622	1014	0.151
HF50	Hot rolled	417	492	1218	-0.118	1.932	-0.771	1056	0.147
HF50	Hot rolled	428	474	1378	-0.143	3.091	-0.807	694	0.110
HF60	Hot rolled	416	481	895	-0.191	0.967	-0.750	587	0.094
HF60	Hot rolled	431	479	1113	-0.109	0.754	-0.670	1029	0.143
HF60	Hot rolled	434	525	1074	-0.105	0.429	-0.598	1152	0.163
HF60	Hot rolled	456	534	913	-0.091	0.226	-0.552	1134	0.161
HF60	Hot rolled	459	533	744	-0.063	0.451	-0.598	792	0.103
HF60	Hot rolled	466	558	976	-0.880	1.007	-0.705	876	0.106
HF70	Hot rolled	505	570	1461	-0.123	6.052	-0.904	934	0.101
HF70	Hot rolled	521	628	1230	-0.104	4.202	-0.843	1251	0.173
HF80	Hot rolled	557	617	1239	-0.108	1.053	-0.771	1125	0.122
HF80	Hot rolled	569	697	1428	-0.105	1.816	-0.861	1287	0.118
HF80	Hot rolled	579	756	2126	-0.152	3.217	-0.934	1389	0.133
HF80	Hot rolled	580	654	1145	-0.091	1.104	-0.717	1091	0.124
HF80	Hot rolled	581	645	1451	-0.113	5.289	-0.958	1122	0.170
HF80	Hot rolled	585	635	1379	-0.112	1.979	-0.820	984	0.100
HF80	Hot rolled	596	657	1512	-0.119	2.214	-0.826	981	0.096
HF80	Hot rolled	605	681	1818	-0.134	1.641	-0.830	1387	0.139
HF80	Hot rolled	642	719	2008	-0.131	7.185	0.985	1285	0.115
DDQ+	Cold rolled	152	306	607	-0.116	0.125	-0.437	832	0.234
DDQ+	Galvannealed	140	292	430	-0.083	0.066	-0.430	641	0.201
DDQ+	Hot dip galvanized	179	303	564	-0.103	0.122	-0.428	635	0.178
DDQ	Hot dip galvanized	150	279	545	-0.102	0.082	-0.388	1143	0.289
DQSK	Cold rolled	171	307	591	-0.105	0.155	-0.450	694	0.196
DQSK	Hot dip galvanized	185	321	875	-0.134	0.142	-0.418	824	0.214
CQ	Hot dip galvanized	314	352	561	-0.089	15.240	-0.956	419	0.088
HF40	Cold rolled	279	370	753	-0.103	0.222	-0.477	596	0.134
HF50	Cold rolled	357	490	536	-0.047	4.117	-0.883	481	0.049
HF50	Cold rolled	439	496	571	-0.057	2.046	-0.787	516	0.640
HF60	Cold rolled	424	501	572	-0.053	20.116	-0.810	531	0.068
50Y60T	Cold rolled	417	554	912	-0.095	0.127	-0.366	935	0.174
80Y90T	Cold rolled	603	747	2744	-0.173	0.448	-0.548	2221	0.267

(Reprinted with permission from SAE J1099 JUN98©1998 Society of Automotive Engineers, Inc.)

Where:
 σ_f' = Fatigue strength coefficient
b = Fatigue strength exponent
 ε_f' = Fatigue ductility coefficient
c = Fatigue ductility exponent
K' = Cyclic strength coefficient
n' = Cyclic strain hardening exponent

Note: The suffix "-c" indicates K' and n' values are calculated by $K' = \sigma_f' / (\varepsilon_f')^{n_c}$ and $n' = b/c$, respectively.
 Those values without the suffix "-c" are from experimental results.

Table 3.5.6.1-2 Monotonic and Cyclic Properties for Some Bar Steels (Reference 21)

Steel Grade	Material Condition	Hardness BHN	Yield Strength (MPa)	Ultimate Tensile Strength (MPa)	RA %	σ_f' (MPa)	b	ϵ_f'	c	K' (MPa)	n'
1035	Hot rolled		443	641		2034	-0.172	3.670	-0.860	865	0.140
1035	Hot rolled		448	623		1491	-0.152	1.560	-0.729	838	0.090
1040	Cold drawn		637	759		1311	-0.103	0.848	-0.612	915	0.131
10V40	Hot rolled		572	802		1287	-0.092	0.315	-0.577	1371	0.150
1045	Cold drawn, annealed	225	517	752	44	916	-0.079	0.486	-0.520	1022-c	0.152-c
1045	Quench & tempered	500	1689	1827	51	2661	-0.093	0.196	-0.643	3371-c	0.145-c
1045	Quench & tempered	595	1862	2241	41	3294	-0.104	0.220	-0.868	3947-c	0.120-c
1045	Normalized	192	423	718	48	1439	-0.127	0.525	-0.522	1401-c	0.212-c
1045	Heat treated	277	620	942	39	2906	-0.161	0.786	-0.579	1770-c	0.191-c
1045	Heat treated	336	787	1322	21	3403	-0.151	0.458	-0.560	2066-c	0.165-c
1045	Heat treated	410	865	1516	6	4385	-0.167	0.491	-0.491	3048-c	0.208-c
1045	Heat treated	563	1636	2297	18	5813	-0.154	1.379	-1.082	3083-c	0.075-c
1045	Heat treated	500	1729	1956	38.3	2636	-0.086	0.210	-0.551	3366-c	0.157-c
1045	Heat treated	390	1275	1344	59	1785	-0.086	1.207	-0.825	1751-c	0.104-c
10B21	Heat treated	318	999	1048	67.6	1204	-0.063	3.709	-0.832	1089-c	0.076-c
10B21	Heat treated	255	806	834		922	-0.063	2.377	-0.753	858-c	0.083-c
10B22	Heat treated	255	806	834		841	-0.043	1.928	-0.738	809-c	0.058-c
15B27	Heat treated	250	772	847	69	938	-0.057	1.689	-0.784	903-c	0.072-c
15B27	Heat treated	264	854	916	66.5	1062	-0.059	1.575	-0.782	1026-c	0.075-c
4130	Heat treated	366	1358	1427	54.7	1655	-0.076	0.803	-0.672	1696-c	0.114-c
4130	Heat treated	259	778	896	67.3	1261	-0.077	0.985	-0.648	1264-c	0.119-c
4140	Heat treated	293	848	938		1163	-0.062	2.360	-0.765	1084-c	0.082-c
4140	Heat treated	475	1895	2033	20.0	1832	-0.070	0.400	-0.867	1974-c	0.081-c
4142	Heat treated	400	1447	1551	47.0	1787	-0.084	1.195	-0.859	1756-c	0.098-c
4142	Heat treated	450	1860	1929	37.0	2079	-0.086	2.620	-0.972	1910-c	0.088-c
4142	Heat treated	380	1378	1413	48.0	2143	-0.094	0.637	-0.761	2266-c	0.124-c
4142	Heat treated	670	1619	2446	6.0	2549	-0.078	0.003	-0.436	7119-c	0.179-c
4142	Heat treated	450	1584	1757	42.0	1937	-0.076	0.706	-0.869	1997-c	0.088-c
4142	Heat treated	475	1722	1929	35.0	2161	-0.081	0.331	-0.854	2399-c	0.094-c
4340	Heat treated	409	1371	1468	38.1	1879	-0.859	0.640	-0.636	1996-c	0.135-c
4340	Heat treated	275	834	1048		1276	-0.075	1.224	-0.714	1249-c	0.105-c
4340	Heat treated	243	634	827	43.4	1198	-0.095	0.522	-0.563	1337-c	0.168-c
4340	Heat treated		1102	1171	56.0	1165	-0.058	5.492	-0.850	1037-c	0.069-c
5160	Heat treated	430	1488	1584	39.7	2054	-0.081	1.571	-0.821	1964-c	0.099-c
5160mod	Heat treated		1565	1755		3553	-0.125	11.532	-1.095	2065	0.089
51V45	Quench & tempered		1871	2108		4585	-0.150	35.560	-1.442	2799	0.090
52100	Heat treated	519	1922	2912	11.1	2709	-0.096	0.243	-0.642	3348-c	0.150-c
	Cast Steel										
0030	Cast	137	303	496	46	655	-0.083	0.280	-0.552	738-c	0.136-c
0050A	Cast	192	415	787	19	1338	-0.127	0.300	-0.569	1165-c	0.171-c
	Cast	174	402	583	26	869	-0.101	0.150	-0.514	896-c	0.141-c
	Cast	206	542	702		1117	-0.101	0.780	-0.729	786-c	0.960-c
8630	Cast	305	985	1144	29	1936	-0.121	0.420	-0.693	1502-c	0.122-c

(Reprinted with permission from SAE J1099 JUN98©1998 Society of Automotive Engineers, Inc.)

Where: σ_f' = Fatigue strength coefficient

b = Fatigue strength exponent

 ϵ_f' = Fatigue ductility coefficient

c = Fatigue ductility exponent

K' = Cyclic strength coefficient

n' = Cyclic strain hardening exponent

Note: The suffix "-c" indicates K' and n' values are calculated by $K' = \sigma_f' / (\epsilon_f')^{n'}$ and $n' = b/c$, respectively.
Those values without the suffix "-c" are from experimental results.

3.5.6.2 Effect of Tensile Properties on Fatigue Performance

Fatigue performance is dependent upon the tensile strength of the steels. It has been shown that for high cycle fatigue the endurance limit is proportional to the tensile strength of the steel. A rule of thumb that has been used for a long time, is that the endurance limit is 50% of the ultimate tensile strength²⁴. However, experimental results have shown that the endurance limit is microstructure sensitive. The fatigue ratio, i.e. the ratio of endurance limit and tensile strength, is often less than 0.5. For example, the endurance ratio was found to be as low as 0.35 for some dual phase steels. It is thus recommended to use a ratio value of 0.4 when no fatigue data is available. For low cycle fatigue, steels of higher tensile strength normally exhibit higher fatigue strength at high life levels. However, their fatigue strength at low life region may be lower due to poor ductility.

3.5.6.3 Variability of Fatigue Properties Within a Steel Grade

Numerous investigations have been conducted that show no statistically significant difference in strain life fatigue properties of sheets taken from different parts of a coil, different coils of the same heat, and different heats of the same steel grade^{25, 26}. A more systematic study has been conducted by A/SP Sheet Steel Fatigue Program recently to investigate the variability of fatigue properties for a steel grade from heat to heat and among different steel producers. Three coils from different heats were tested for three different steel producers. The strain life curves for an IF steel grade are given in [Figure 3.5.6.3-1](#) and [Figure 3.5.6.3-2](#). [Figure 3.5.6.1-1](#) is for the three coils from a single producer. The variability is rather small. From coil to coil the fatigue life can vary by a factor of 1.4 to 2.0 for the same strain level applied. This small variability is the result of the tight control of tensile properties by today's steel producers. The variability among three steel producers are shown in [Figure 3.5.6.3-2](#) where strain-life curves of all nine coils were plotted. The variability of fatigue life increases when more steel producers are included. The fatigue life can vary by a factor of 1.6 to 3.7.

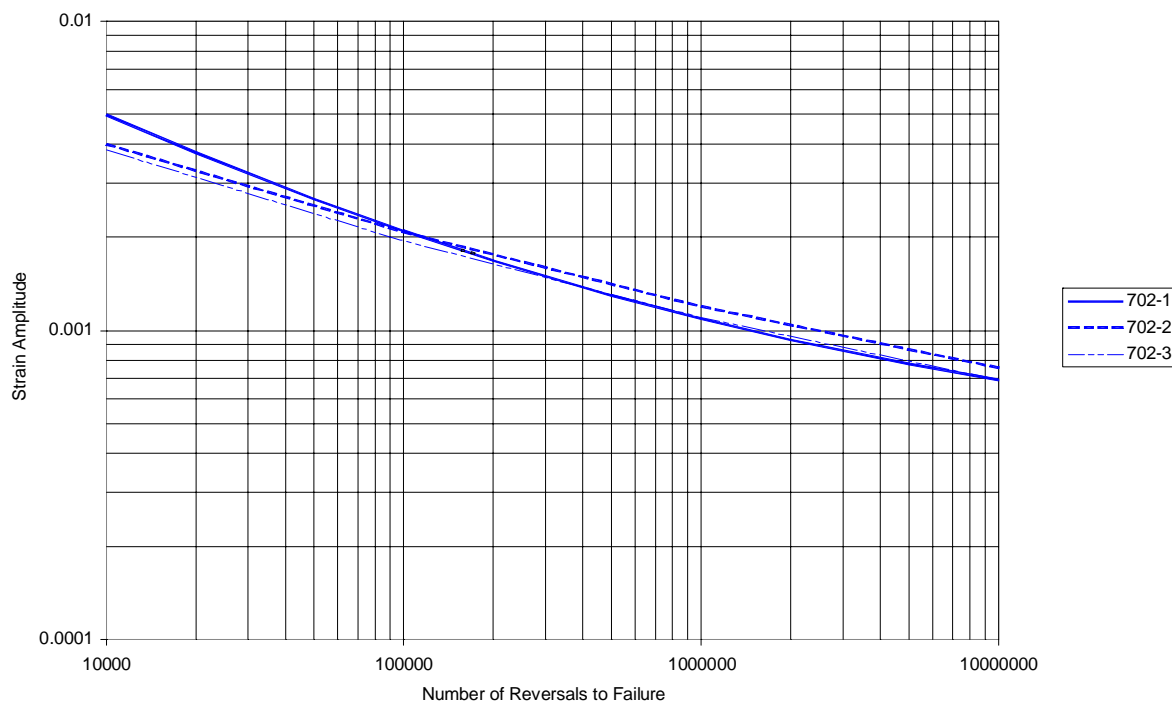


Figure 3.5.6.3-1 Strain life curves for steels from three different coils of the same steel grade. The steels were provided by a single producer.

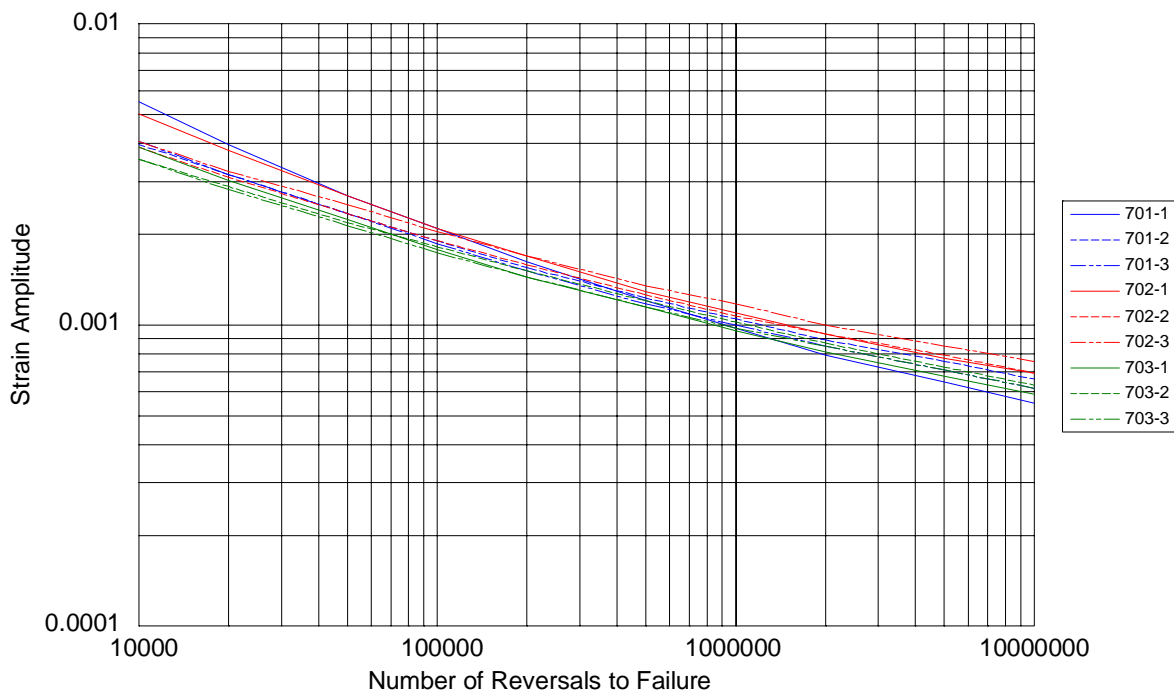


Figure 3.5.6.3-2 Strain life curves for steels from nine coils produced by three different producers #701, #702, and #703

3.5.6.4 Effects of Cold Work on Fatigue Properties

A majority of fatigue data published in the open technical literature was determined by testing as-produced sheet steels, which are normally in the fully annealed or temper rolled condition. However, automotive body panels or structures are often subjected to cold working during stamping. Often, the amount of cold work is much higher than that applied during temper rolling. Therefore, the effect of cold working on fatigue properties has been an important subject for durability analysis. However, research work on the subject is very limited so far and the results are often contradictory.

The only systematic work published so far was sponsored by AISI in 1983²⁷. An 80DF (045 DF), 50XF (050 XF), and a 1006 steel were deformed to various strain levels under uniaxial tension, plane strain (cold rolling) deformation, and in-plane balanced biaxial stretching. Results from monotonic and cyclic tests showed that, at long lives, the fatigue life was increased by prior deformation (effect of work hardening on fatigue endurance strength) whereas, at short lives the fatigue life either remained the same or was reduced. The phenomena at short lives, or high strain fatigue condition, were attributed to the cyclic softening or the formation of microcracks during severe cold working. Cyclic softening is a process where rearrangement of the microstructure takes place so that the work hardening result may be completely or partially eliminated. The cyclic yield strength increased with the amount of prior deformation but less rapidly than the monotonic yield strength, reflecting the cyclic softening effect. This work also concluded that small and moderate amounts of cold working have little effect on the strain controlled fatigue properties of steels.

It should be pointed out that cold working provides higher yield strengths and is one of the important strengthening mechanism. In component design it is often used as an extra safety

factor. However, design engineers should be aware that when the component is subjected to cyclic loading, this beneficial factor might not be effective.

3.5.7 FATIGUE BEHAVIOR AND MODELS OF SHARPLY NOTCHED AND WELDED COMPONENTS

As mentioned earlier, some fabricated parts, such as those that have been spot welded or arc welded, contain imperfections that have stress concentrations much higher than those considered when making stress-life and strain-life calculations using stress concentration factors. These crack-like imperfections are best analyzed using fracture mechanics crack growth procedures since the stress concentration factors are so high that very few (if any) cycles are necessary to initiate a crack. Although some investigators have used strain controlled cyclic analyses to analyze these problems, the following discussions will focus on crack growth procedures.

3.5.7.1 Arc Welded Components

Because of the presence of crack-like imperfections in arc welds, most of the fatigue life of arc welded components is believed to be spent in propagating a crack, even at long lives. In the past few decades significant strides have been made in understanding and quantifying crack growth behavior in steels through the use of fracture mechanics. Many generalities have been identified regarding crack growth behavior in steels²⁸. For all intents and purposes, the crack growth rate (in air) for all steels is the same, independent of strength, toughness, or chemistry. As expected, only the component of the cyclic loading that causes the crack to open contributes to the growth of the crack. Hence, mean stress effects for crack growth are much different than those that occur during the initiation of a crack (stress-life and strain-life analyses). In fact, only the stress range causing crack opening is significant²⁹ and mean stress effects are generally ignored as long as the mean stress does not lead to crack closure. Finally, for a particular crack length and component geometry, there is a threshold stress range below which the crack will not propagate in steels. This threshold stress range is also independent of the grade and properties of the steel but is affected by mean stress.

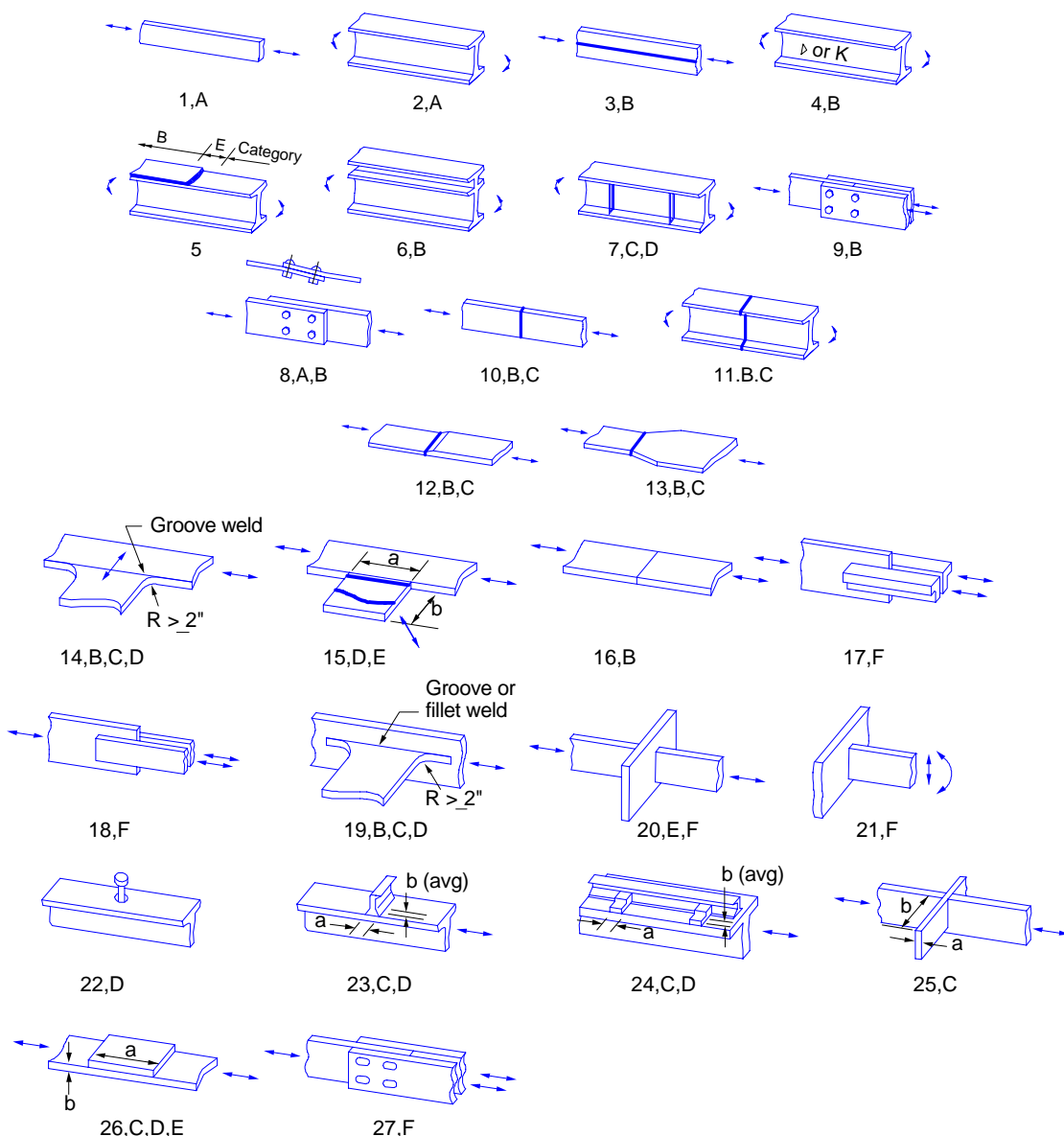
Understanding of these generalities is important because they help the designer to understand what variables and limitations are important when designing fabricated automotive components. Although the automotive industries clearly design components against the initiation of cracks in fatigue loading, welded components will contain such crack-like imperfections and the design must comprehend the component life as limited by crack growth considerations.

A vast amount of research has been conducted in recent years to formulate fatigue design procedures of bridge structures³⁰. In essence, these procedures categorize different design details according to the severity of local stresses (stress concentration) caused by the design details. These concepts have recently been extended to steel sheet fabricated details^{31,32}. In this work, over 100 fatigue tests have been conducted on a wide variety of sheet steel grades and thicknesses used to fabricate many different design details tested over numerous stress ranges and stress ratios. Although some additional work is needed to further classify mean stress effects and variable amplitude loading, these procedures are quite reliable, particularly for long life estimates. The stress range fatigue life design of fabricated components is based upon six stress range categories. These six allowable applied stress ranges are shown in [Table 3.5.7.1-1](#) for various cyclic lives.

Table 3.5.7.1-1 Allowable Range of Stress (F_{sr} , MPa (ksi))(From Reference 30)

CATEGORY	Cycles		
	20,000 to 100,000	2,000,000	More Than 2,000,000
A	414 (60)	166 (24)	166 (24)
B	310 (45)	124 (18)	110 (16)
C	221 (32)	90 (13)	69 (10)
D	186 (27)	69 (10)	48 (7)
E	145 (21)	55 (8)	35 (5)
F	103 (15)	62 (9)	55 (8)

The six categories, A through F, represent various levels of notch severity and residual stress intensity as defined by the American Association of State Highway and Transportation Officials (AASHTO) (Figure 3.5.7.1-1).



NOTE: LETTERS DESIGNATE FATIGUE-DESIGN CATEGORIES ACCORDING TO AASHTO SPECIFICATION

Figure 3.5.7.1-1 Illustrative examples³⁰

Because the fatigue crack growth rate in steels is not dependent upon material properties, the fatigue design categories and allowable stress ranges are independent of steel grade. A plot of these values is shown in [Figure 3.5.7.1-2](#).

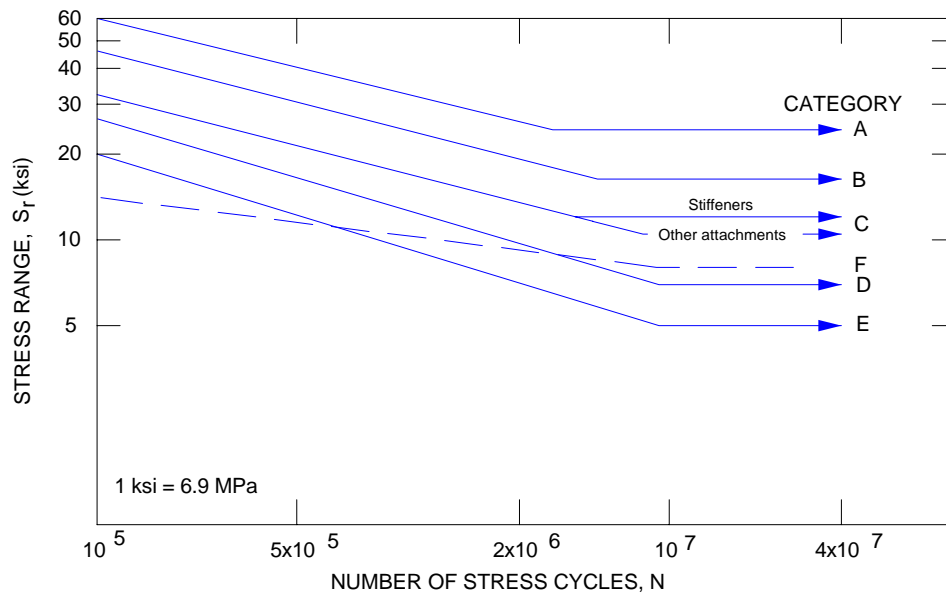


Figure 3.5.7.1-2 S_r - N fatigue design curves for bridges and buildings³⁰

Test results from various steel sheet fabricated details are compared to these corresponding categories in [Figure 3.5.7.1-3](#) through [Figure 3.5.7.1-6](#). Examples of some of these categories found in a suspension system are shown in [Figure 3.5.7.1-7](#).

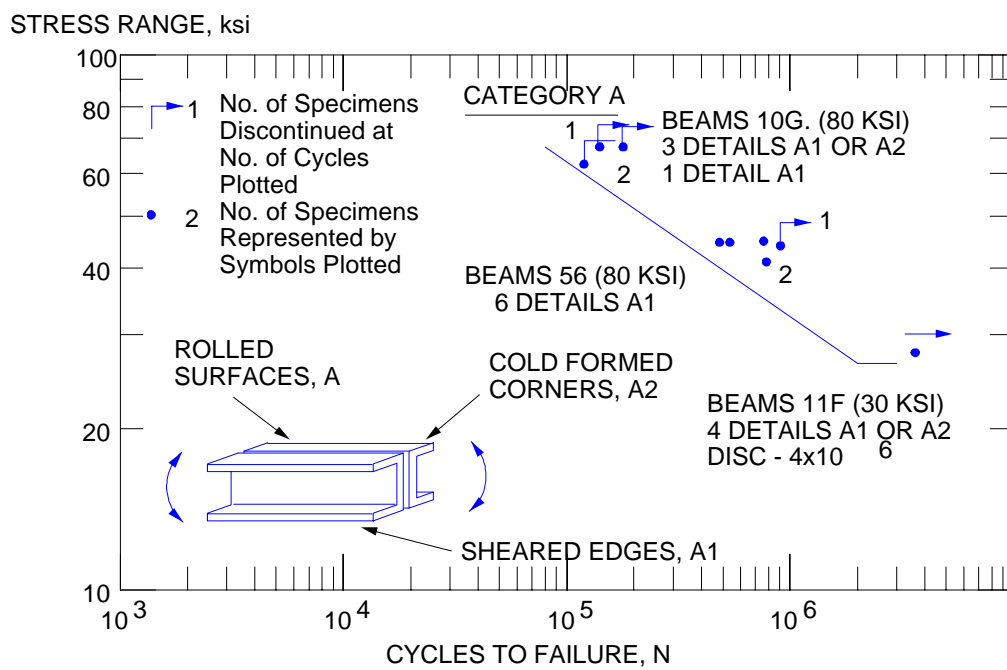


Figure 3.5.7.1-3 Fatigue tests on 4 inch deep beams (category A)³¹

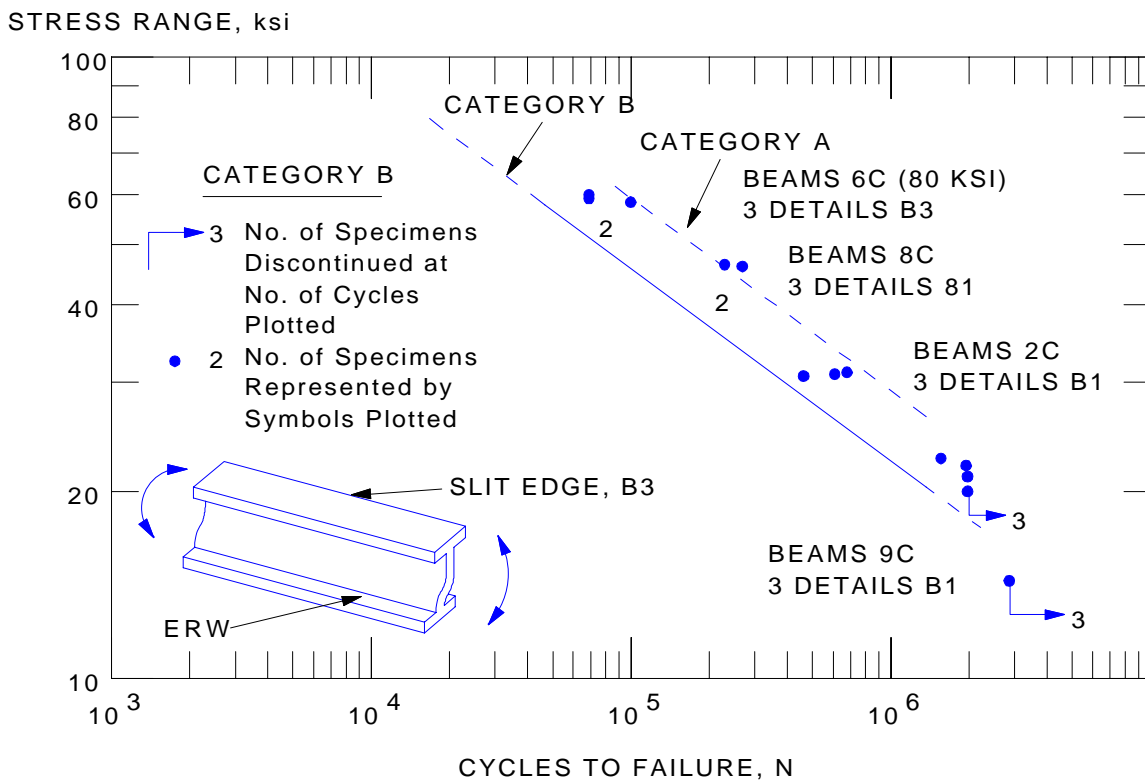


Figure 3.5.7.1-4 Fatigue tests on 4 inch deep beams (category B)³¹

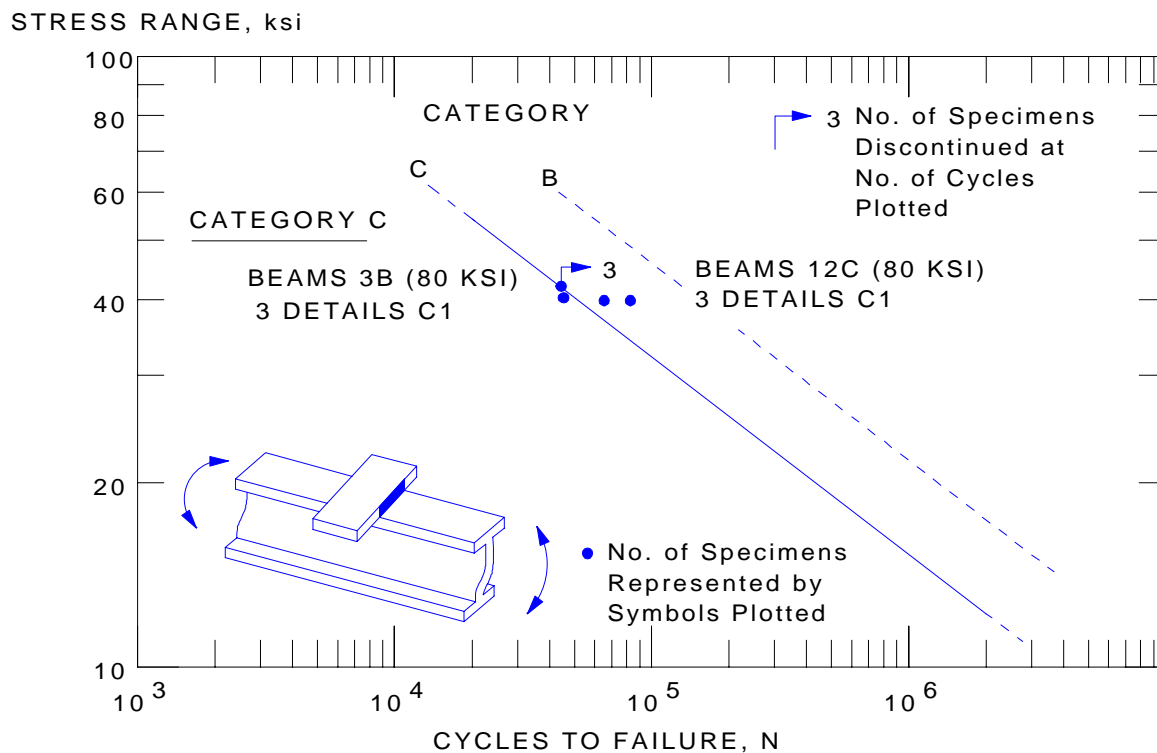


Figure 3.5.7.1-5 Fatigue tests on 4 inch deep beams (category C)³¹

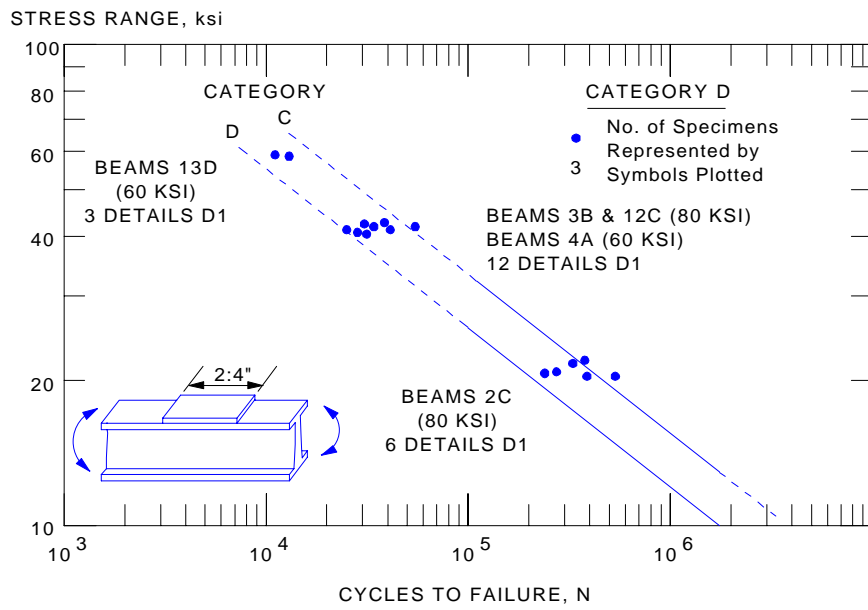


Figure 3.5.7.1-6 Fatigue tests on 4 inch deep beams (category D)³¹

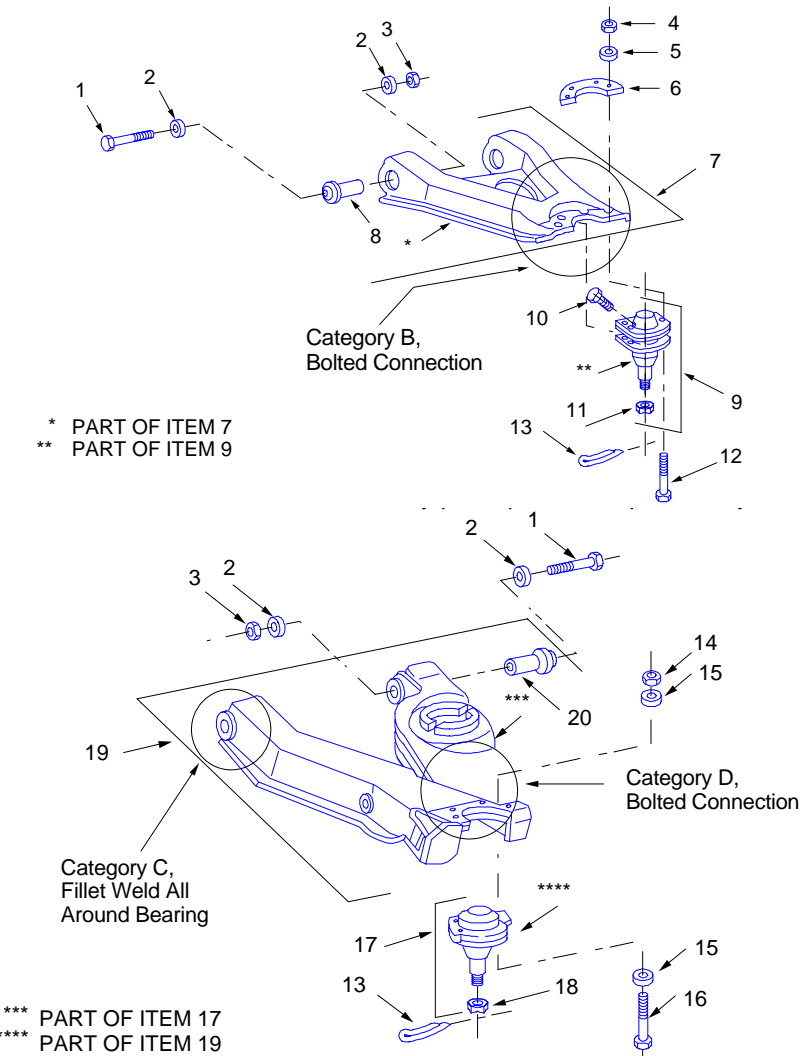


Figure 3.5.7.1-7 Examples of category B, C and D of heavy pick-up truck suspension system

3.5.7.2 Spot Welded Components

With the recent mass reductions of automobiles for improved fuel economy, more attention has been given to fatigue life of spot welded joints. Previously, spot welded components were not considered fatigue critical because large factors of safety were incorporated through the use of heavy gage steel material. However, much interest has now arisen in designing against fatigue failures of spot welded components.

Early fatigue tests showed the importance of spot welded stiffeners in the fatigue process³³. The stiffness of the joint in turn affects the rotation of the weld nugget during loading. This rotation causes a crack-like opening between the two sheets ([Figure 3.5.7.2-1](#)) and a resultant opening mode of cracking and a shearing mode of cracking³⁴.

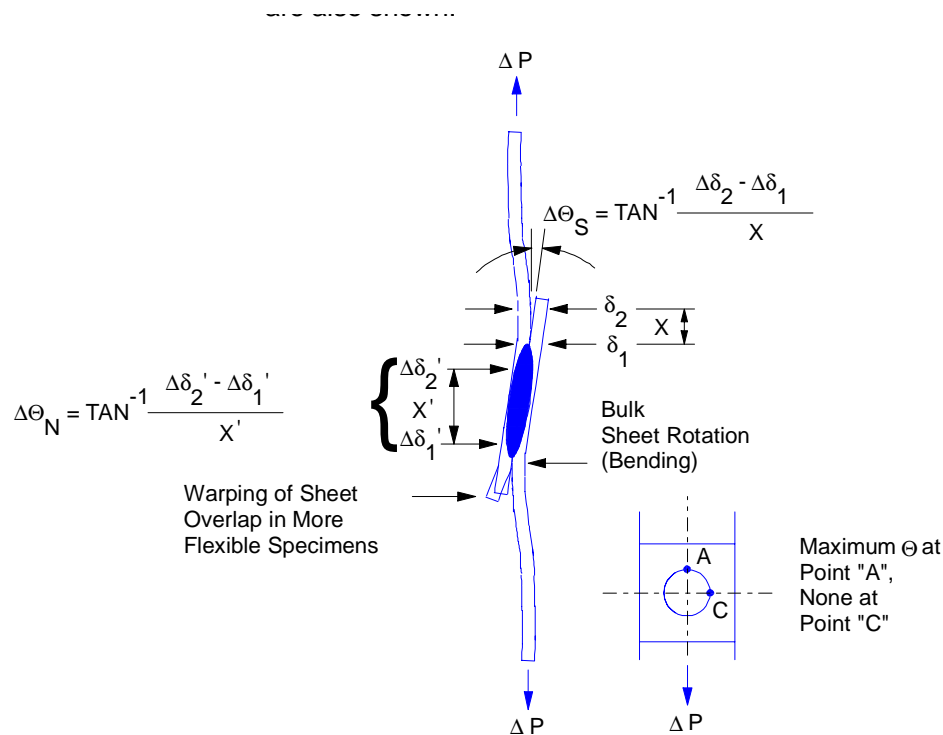


Figure 3.5.7.2-1 The reaction of a spot welded sheet to tensile-shear loading. Methods of measuring the resultant sheet and nugget rotation are also shown³⁴.

The opening mode, which is the most common mode of failure, causes sheet cracking at the toe of the weld through the thickness of the sheet in the heat affected zone of the weld ([Figure 3.5.7.2-2](#))

This opening mode of crack extension is referred to as K_I in fracture mechanics terminology³⁵. The shear mode of cracking during cycle loading occurs through the weld nugget as a mode K_{III} . Although both of these cracking modes are always active, most of the failures occur due to the sheet (K_I) tensile stress mode of cracking. Because of the crack-like opening between the sheets as the nugget rotates under the applied load, the fatigue life of a spot weld is spent primarily in crack propagation. Increases in base metal strength have no significant effect upon long life ([Figure 3.5.7.2-3](#)) but show some improvement in short life behavior³⁵.

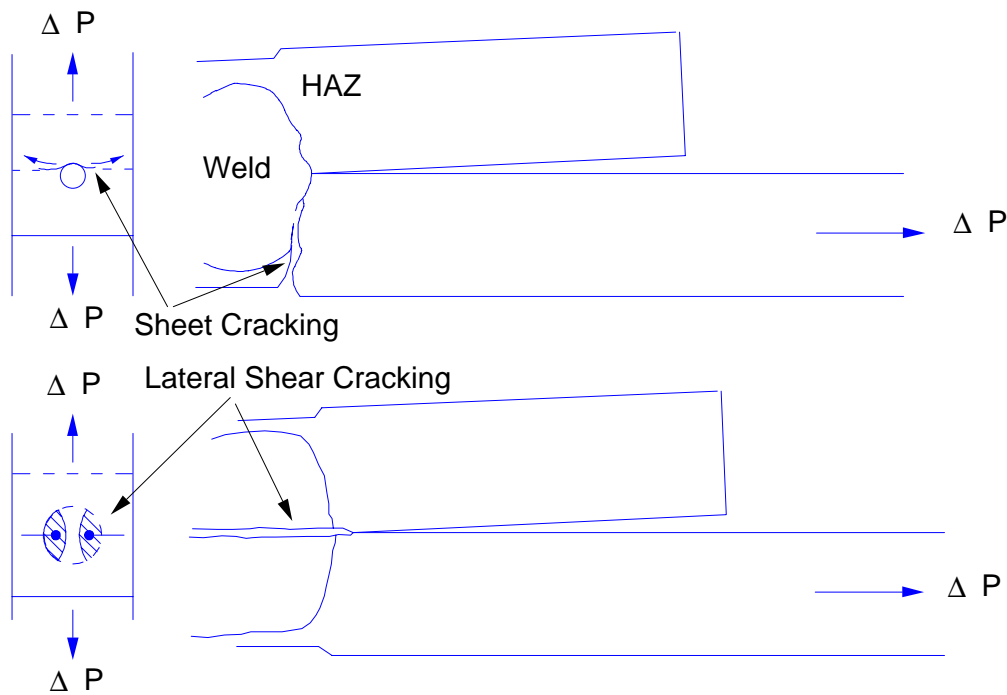


Figure 3.5.7.2-2 Illustration of the two types of fatigue cracking (sheet and shear) which can occur concurrently from tensile shear loading³⁴

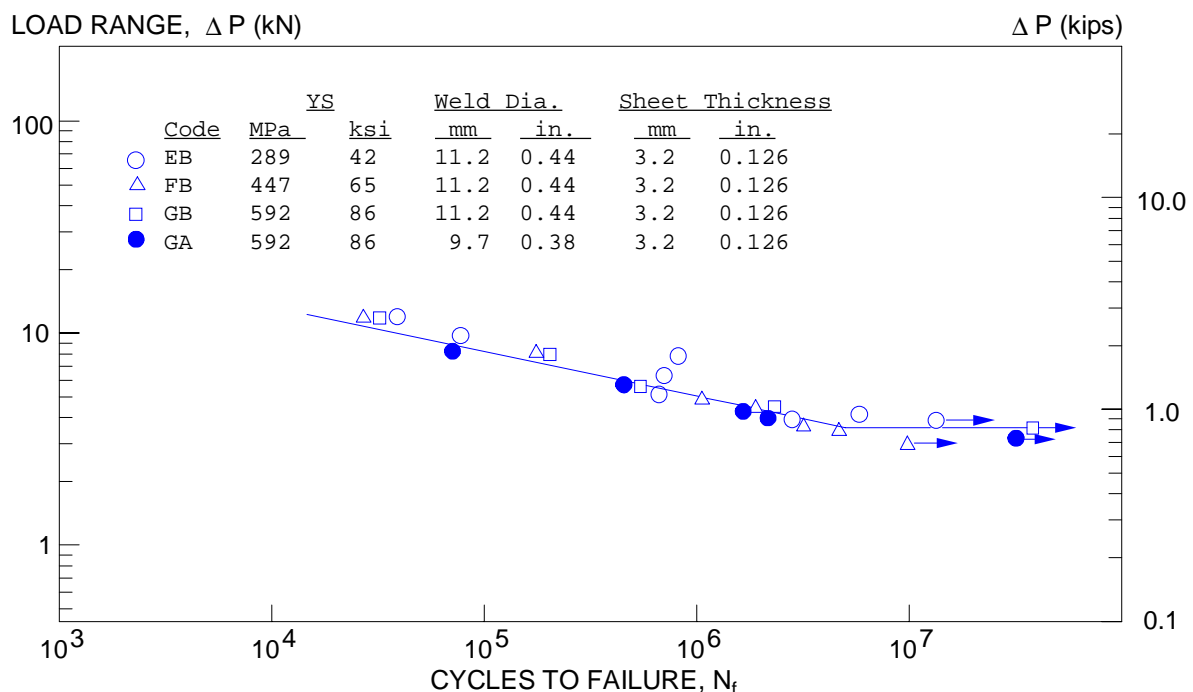


Figure 3.5.7.2-3 Tensile-shear spot-weld fatigue - test data for the 3.2 mm (0.126 inch) thick sheet with two weld diameters

Increasing stiffness decreases the nugget rotation and crack opening resulting in increased fatigue life ([Figure 3.5.7.2-4](#) and [Figure 3.5.7.2-5](#)). R ratio effects and residual stress effects follow trends typical of fatigue crack growth rate behavior^{[36](#)}.

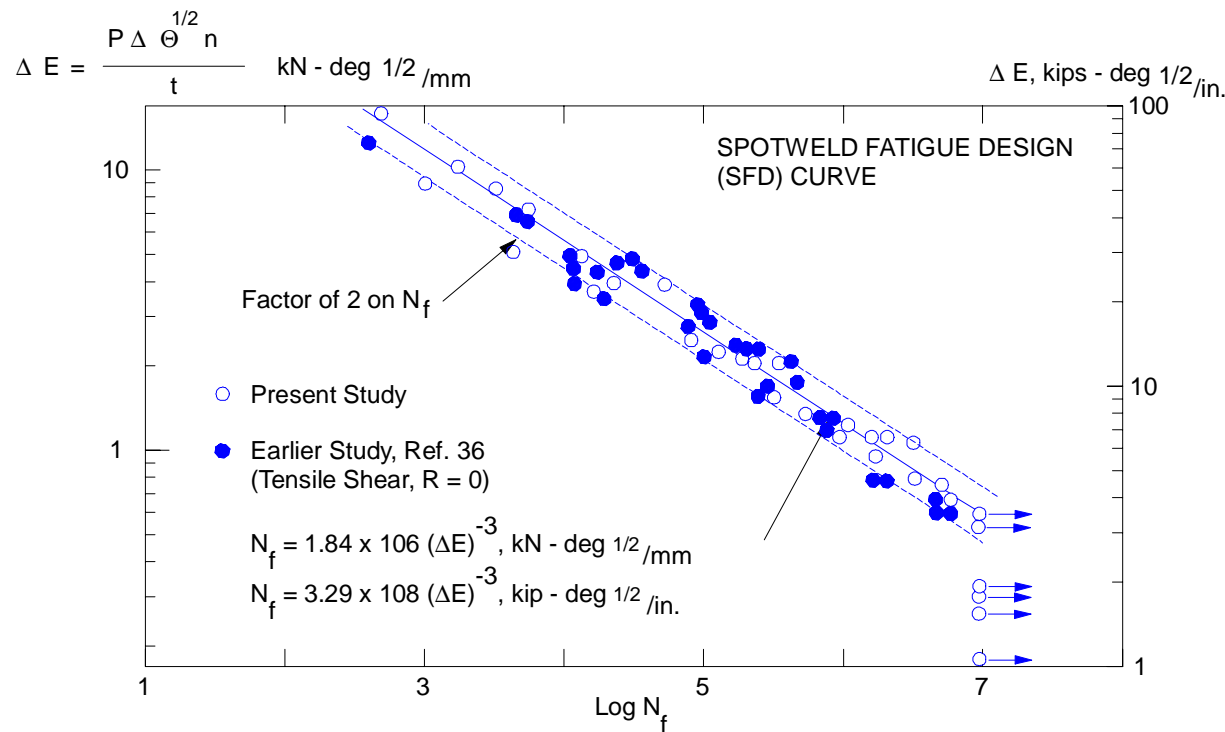


Figure 3.5.7.2-4 Spot-weld fatigue design (SFD) curve showing the relationship between tensile-shear fatigue life and the correlation parameter, A.E.^{[35](#)}

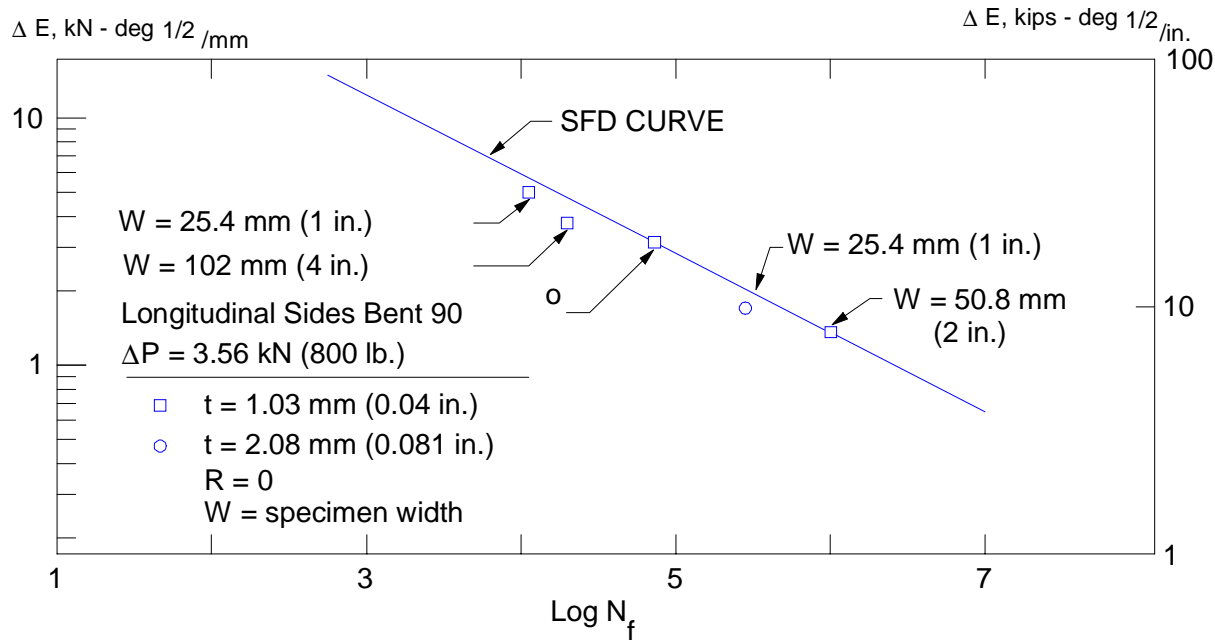


Figure 3.5.7.2-5 Examples of how variations in joint stiffness influence the spot weld fatigue life^{[35](#)}

A recently completed report sponsored by AISI³⁷ showed improvements in spot welded fatigue performance due to tensile preloading, which is believed to result in large compressive residual stresses at the notch root. Coining (Figure 3.5.7.2-6) and a forging pulse (Figure 3.5.7.2-7) of the electrode after the welding current is stopped result in improved spot weld fatigue performance. However, these improvements were only observed to be stable at long lives of HSLA steels and not for low carbon steel weldments.

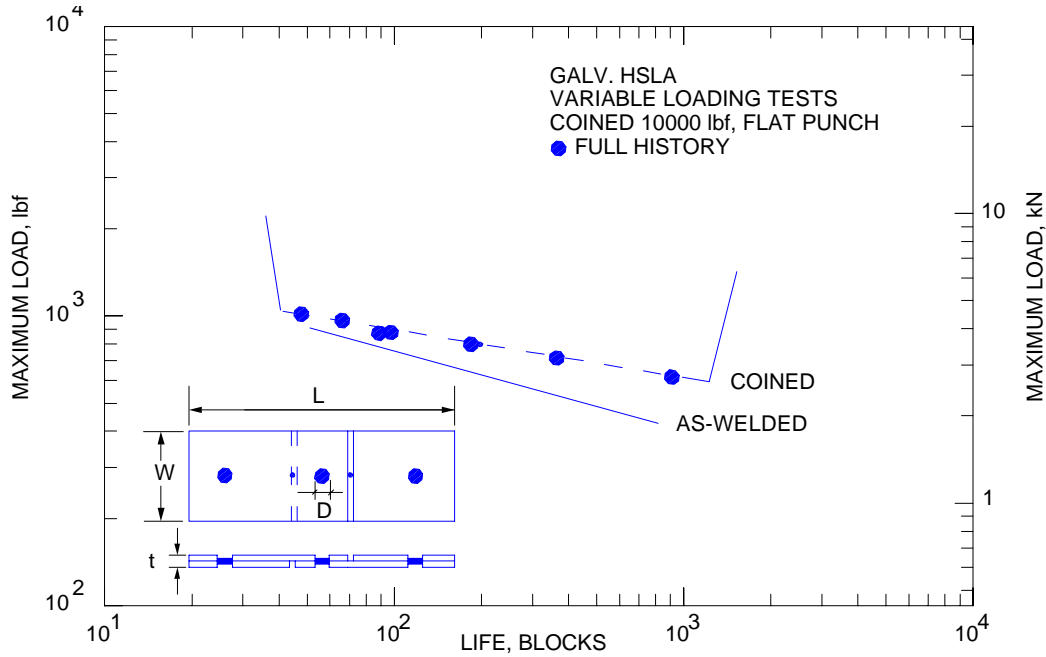


Figure 3.5.7.2-6 Fatigue test results for 10,000 lbf. Coined (flat punch) galvanized AISI 050XF tensile-shear spot weldments subjected to full Ford weld history. (task 24)³⁷

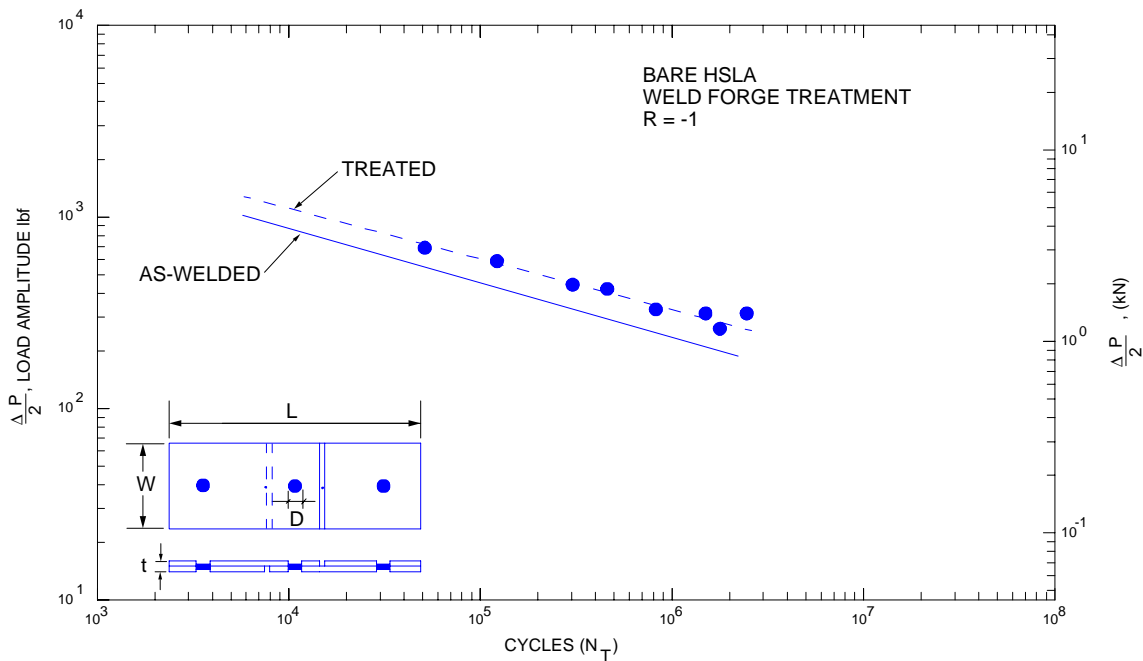


Figure 3.5.7.2-7 Fatigue test results for weld-forge treated bare AISI 050XF tensile shear spot weldments ($R=-1$). (task 25)³⁷

3.5.7.3 Recent Advances in Life Predictions of Resistance Spot Welds

The ability to predict accurately the fatigue life of spot welded structures is always a formidable challenge throughout the automotive industry. Significant improvements in understanding of fatigue behavior and in the ability to deal with it in engineering practice have been made in the last decade. Some impressive new technologies and theories are becoming available to assist engineers in more reliably assessing the fatigue performance of spot welded structures. The following three sections provide valuable overviews of current efforts to general analysis approaches to fatigue life predictions. These methods incorporate the latest understanding of crack initiation and propagation phenomena in explaining a variety of mean stress (or R-ratio) and mixed loading mode effects.

3.5.7.3.1 Stress Index K_i

Per Swellam³⁸, a general parameter (K_i) is an empirically derived quantity to represent the magnitude of the stress field at the periphery of the spot weld, based on the concepts of mixed mode fracture mechanics and experimental data. The method involves the following assumptions:

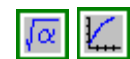
- A) Linear elastic fracture mechanics (LEFM).
- B) The spot welded joint is considered to be two half-spaces jointed by a circular area.
- C) A modified equivalent stress factor can be related to fatigue lives.

The K_i is used to correlate the fatigue behavior of all spot weld sizes and can be expressed in terms of the normal (N), shear (V), and bending (M) forces applied to the weld nugget as shown in [Figure 3.5.7.3.1-1](#). When spot welds are modeled by beam elements, the interface forces and moments are simply obtained from the output of the beam elements. It is noted that the forces and moments are referred to the interface and not to the mid-plane of the plane elements simulating the spot-welded sheets.

The K_i is defined as follows:

$$K_i = (1-R)^{0.85} \sqrt{\frac{K_{I,max}^2 + \beta K_{II,max}^2}{\frac{8t^2w}{D^3} \left(\frac{36t^2}{D^2} + 1 \right)}}$$

Equation 3.5.7.3.1-1



where R = stress ratio,

β = 2 or 3 for low-carbon or HSLA steel

t = metal sheet thickness

w = metal sheet width

D = weld nugget diameter, and with

$$K_I = K_{axial} + K_{moment} = \frac{N}{D\sqrt{\frac{\pi D}{2}}} + \frac{6M}{D^2\sqrt{\frac{\pi D}{2}}}$$

Equation 3.5.7.3.1-2



$$K_{II} = K_{shear} = \frac{V}{D\sqrt{\frac{\pi D}{2}}}$$

Equation 3.5.7.3.1-3



Some expressions for K_i of common spot-weld geometries under cyclic loading with $R = 0$ are given³⁹ as follows:

A) Tensile-shear (TS) specimen

$$K_i = \frac{F}{2t\sqrt{\pi w(36t^2 + D^2)}} \sqrt{36t^2 + \beta D^2}$$

Equation 3.5.7.3.1-4



A) Cross-Tension (CT) specimen

$$K_i = \frac{F}{2t\sqrt{\pi w(36t^2 + D^2)}} (D + 3e)$$

Equation 3.5.7.3.1-5



A) Coach-peel (CP) specimen

$$K_i = \frac{F}{2t\sqrt{\pi w(36t^2 + D^2)}} (D + 6e)$$

Equation 3.5.7.3.1-6



A) Double-shear (DS) specimen

$$K_i = \frac{F}{2t\sqrt{\pi w(36t^2 + D^2)}} D \sqrt{\beta}$$

Equation 3.5.7.3.1-7



where e = moment arm (e.g., offset of the applied force F in [Figure 3.5.7.3.1-1](#))

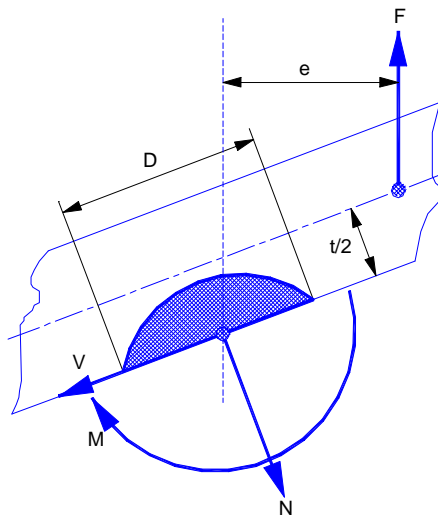


Figure 3.5.7.3.1-1 Resolved components N , V , and M at the nugget for a general applied force F

As illustrated in [Figure 3.5.7.3.1-2](#) adopted from [Reference 39](#), stress index (K_i in MPa $\sqrt{\text{mm}}$) versus total fatigue life (N_f in cycles) for tensile-shear, cross-tension, double-shear, coach-peel, tensile-shear sheet-to-tube, and cross-tension plate-to-plate spot welded specimens made of low carbon and HSLA steels (total of 622 data) is expressed as follows:

A) 50% reliability line:

$$K_i = 1223N_f^{(-0.187)}$$

[Equation 3.5.7.3.1-8](#)



A) Three-standard-deviation design curve (99.7% reliability):

$$K_i = 433N_f^{(-0.187)}$$

[Equation 3.5.7.3.1-9](#)

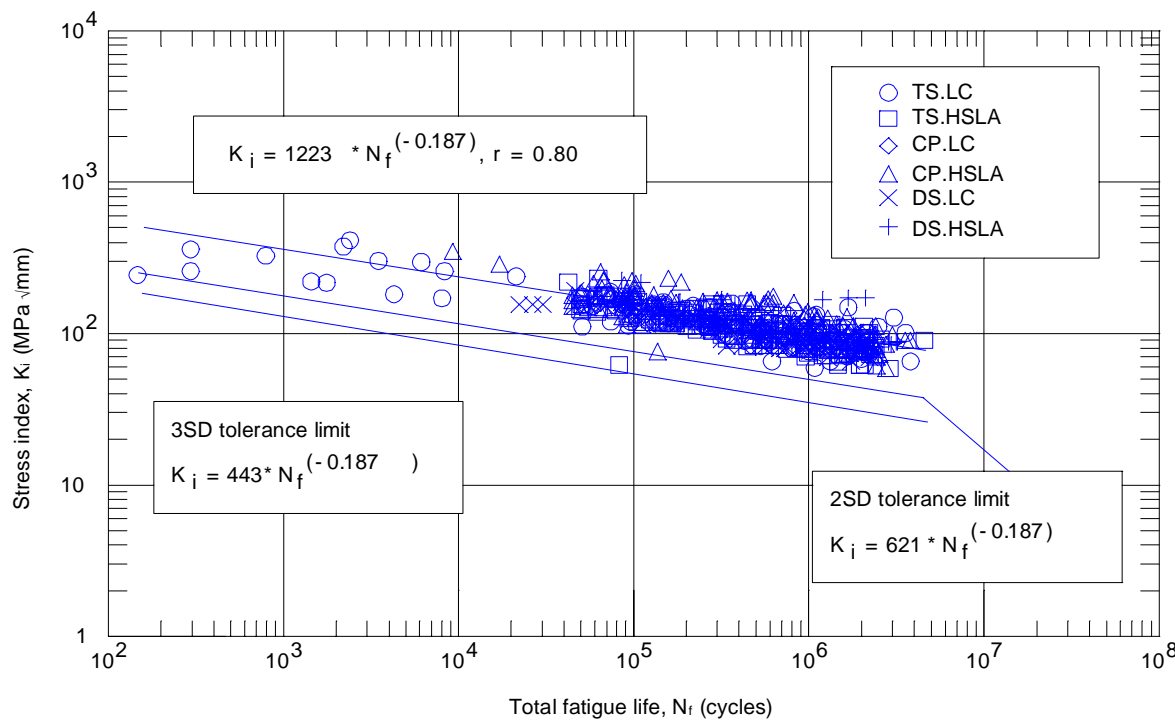


[Figure 3.5.7.3.1-2](#) K_i versus cycle to failure (adopted from [Reference 37](#))

An example calculation is given in [Section 6.2.5.1](#) for the fatigue life of a tensile-shear spot welded specimen subjected to a cyclic force.

3.5.7.3.2 Local Stress Parameters

Zhang⁴⁰ assumes that the notch stress is the summation of the singular stress derived from the stress intensity factors and the non-singular stress approximated by nominal stresses. The singular stress derived in [Reference 40](#) is asymptotic and valid only for small notch root radius ($\rho \rightarrow 0$), while the non-singular stress approximated by nominal stresses becomes valid for larger ρ .

Two stress parameters (local notch stress range, $\Delta\sigma_t$, and equivalent stress intensity factor range (SIF), ΔK_{eq}) near the crack tip are proposed and have shown acceptable correlation of test data across specimens and weld sizes. In general, the life prediction models can be expressed:

$$\Delta\sigma_{t,max} = A(N_f)^B$$

Equation 3.5.7.3.2-1



And

$$\Delta K_{eq} = C(N_f)^D$$

Equation 3.5.7.3.2-2



where A, B, C, and D are the fatigue properties of the spot welded specimens.

As shown in [Figure 3.5.7.3.2-1](#), the maximum "tangential stress" along the interior surface of a blunt crack tip, $\sigma_{t,max}$, are derived ([Reference 40](#)) in terms of forces and moments on the spot weld nugget as follows:

$$\sigma_{t,max} = \frac{4\sqrt{S_x^2 + S_y^2}}{\pi Dt} \left(1 + \frac{\sqrt{3} + \sqrt{19}}{8\sqrt{\pi}} \sqrt{\frac{t}{\rho}} \right) + \frac{6\sqrt{M_x^2 + M_y^2}}{\pi Dt^2} \left(1 + \frac{2}{\sqrt{3}\pi} \sqrt{\frac{t}{\rho}} \right) + \frac{4N_z}{\pi D^2} \left(1 + \frac{5D}{3t\sqrt{2\pi}} \sqrt{\frac{t}{\rho}} \right)$$

Equation 3.5.7.3.2-3



where D = diameter of the spot weld nugget

t = thickness of the metal sheet

ρ = curvature radius of the spot welded notch

S_x and S_y = in-plane shear forces on the nugget

N_z = out-of-plane normal force on the nugget

M_x , M_y , and M_z = moments acting on the nugget.

It is assumed that the notch root radius $\rho = 0$ mm is used for all specimens.

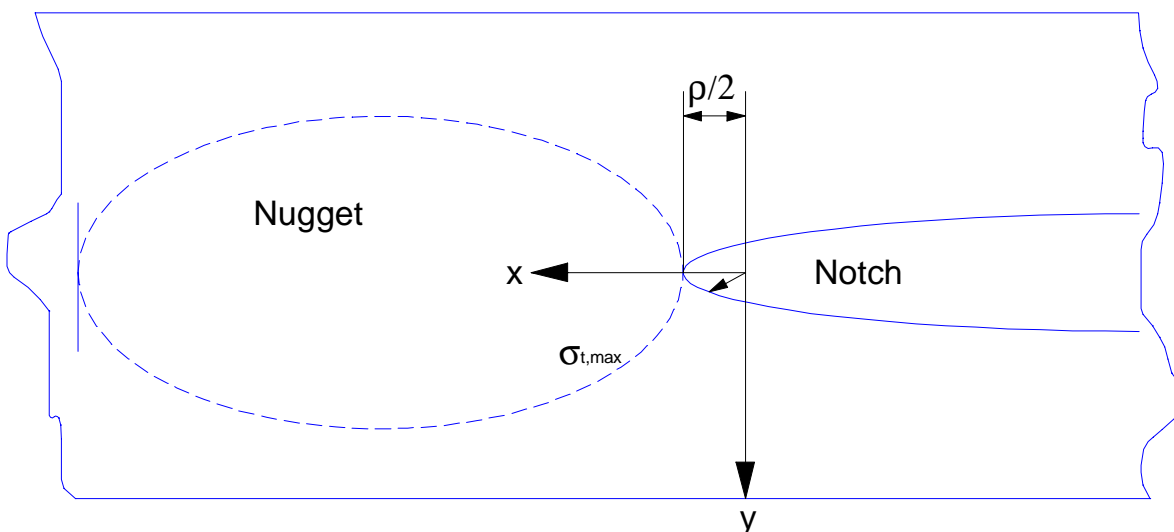
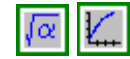


Figure 3.5.7.3.2-1 Maximum tangential stress at spot welds with a curvature radius ρ

Due to the mixed loading condition at spot welds, an equivalent stress intensity factor is proposed ([Reference 40](#)) for fatigue life predictions as follows:

$$K_{eq} = \begin{cases} +\sqrt{K_I^2 + K_{II}^2 + K_{III}^2} & \text{for } K_I \geq 0 \\ -\sqrt{K_I^2 + K_{II}^2 + K_{III}^2} & \text{for } K_I < 0 \end{cases}$$

Equation 3.5.7.3.2-4



where

$$K_I = \frac{\sqrt{3}\sqrt{S_x^2 + S_y^2}}{2\pi D\sqrt{t}} + \frac{2\sqrt{3}\sqrt{M_x^2 + M_y^2}}{\pi D t \sqrt{t}} + \frac{5\sqrt{2}N_z}{3\pi D\sqrt{t}}$$

Equation 3.5.7.3.2-5



$$K_{II} = \frac{2\sqrt{S_x^2 + S_y^2}}{\pi D\sqrt{t}}$$

Equation 3.5.7.3.2-6



$$K_{III} = \frac{\sqrt{2}\sqrt{S_x^2 + S_y^2}}{\pi D\sqrt{t}} + \frac{2\sqrt{2}M_z}{\pi D^2\sqrt{t}}$$

Equation 3.5.7.3.2-7



It is noted that the stress intensity factors from above include the effects of nugget diameter and sheet thickness, which is fundamentally different from those given by Swellam ([Reference 38](#)) where effects of the sheet thickness and width are considered in a geometric modification factor.

Some approximate expressions for stress intensity factors and notch stress of common spot-weld specimens are given ([Reference 40](#)) as follows:

A) Tensile-shear (TS) specimen

$$K_I = \frac{\sqrt{3}F}{2\pi D\sqrt{t}}$$

Equation 3.5.7.3.2-8



$$K_{II} = \frac{2F}{\pi D\sqrt{t}}$$

Equation 3.5.7.3.2-9



$$K_{III} = \frac{\sqrt{2}F}{\pi D\sqrt{t}}$$

Equation 3.5.7.3.2-10



$$\sigma_{t,max} = \frac{4F}{\pi Dt} \left(1 + \frac{\sqrt{3} + \sqrt{19}}{8\sqrt{\pi}} \sqrt{\frac{t}{\rho}} \right)$$

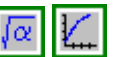
Equation 3.5.7.3.2-11



A) Cross-Tension (CT) specimen

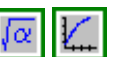
$$K_I = \frac{3\sqrt{3}Fe}{16\pi Dt\sqrt{t}}$$

Equation 3.5.7.3.2-12



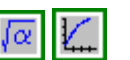
$$K_{II} = \frac{3Fe}{32\pi Dt\sqrt{t}}$$

Equation 3.5.7.3.2-13



$$\sigma_{t,max} = \frac{3Fe}{4\pi Dt^2} \left(1 + \frac{2\sqrt{3} + \sqrt{13}}{8\sqrt{\pi}} \sqrt{\frac{t}{\rho}} \right)$$

Equation 3.5.7.3.2-14



A) Coach-peel (CP) specimen

$$K_I = \frac{2\sqrt{3}Fe}{\pi Dt\sqrt{t}}$$

Equation 3.5.7.3.2-15



$$\sigma_{t,max} = \frac{6Fe}{\pi Dt^2} \left(1 + \frac{2}{\sqrt{3\pi}} \sqrt{\frac{t}{\rho}} \right)$$

Equation 3.5.7.3.2-16



After correlating fatigue test data from different weld sizes and different specimen configurations, as shown in [Figure 3.5.7.3.2-2](#) and [Figure 3.5.7.3.2-3](#), Zhang⁴¹ concluded that the fatigue life or the fatigue strength of spot welds could be better predicted in terms of the local notch stress range. This may explain why the spot welded joint behaves more like a blunt crack where the notch stress is of relevance than like a sharp crack where the stress intensity factors are of relevance.

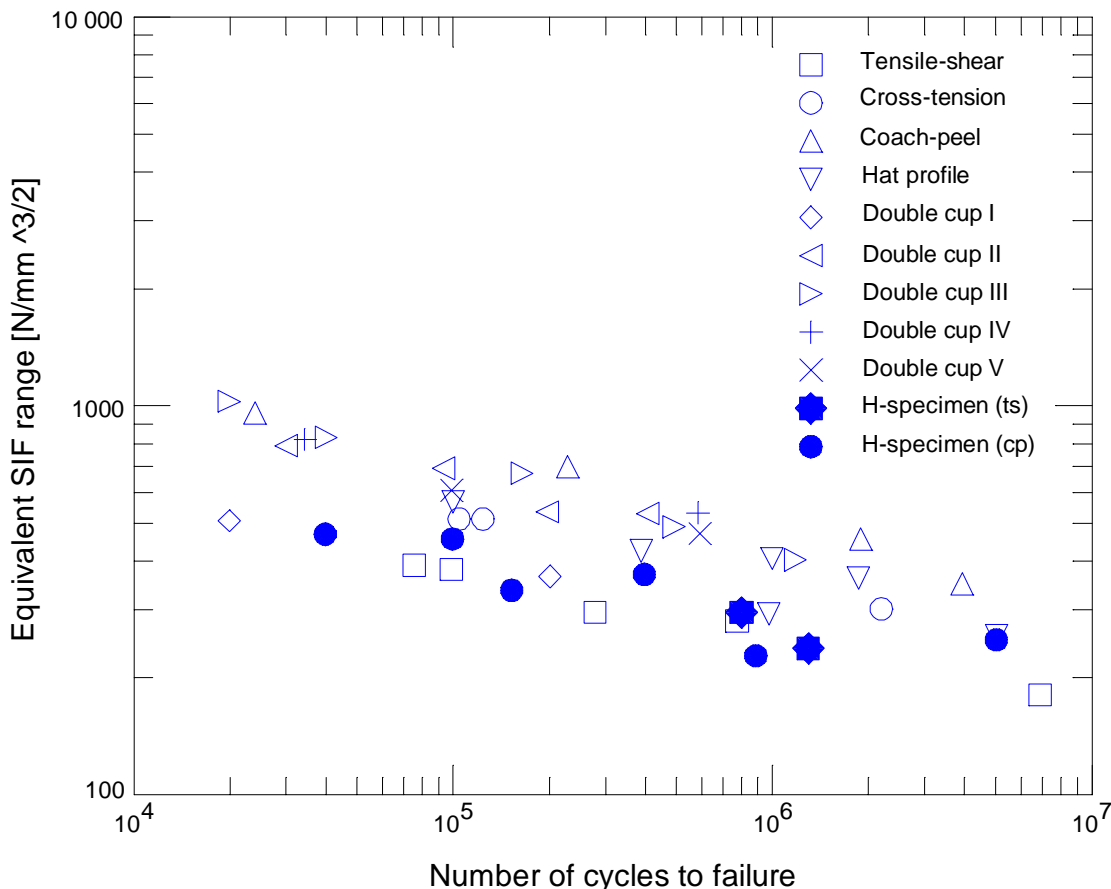


Figure 3.5.7.3.2-2 Equivalent stress intensity factor (SIF) versus life
(adopted from [Reference 41](#))

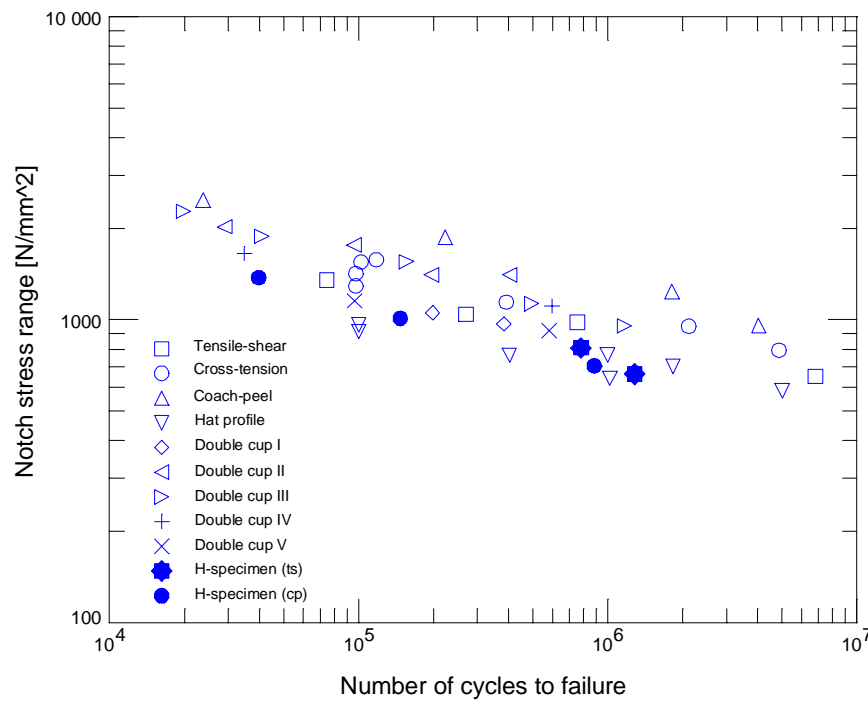


Figure 3.5.7.3.2-3 Local notch stress range versus cycle to failure (adopted from [Reference 41](#))

3.5.7.3.3 Structural Stress

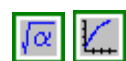
The maximum structural stress or hot-spot stress at spot welds is related analytically to the interface forces and moments that the spot welds transfer from one metal sheet to another. In Rupp's model⁴², two types of failure mechanisms (cracking in the sheet metals and cracking through the weld nugget) were considered on the spot welded joints. Thus, Rupp's model can differentiate nugget fracture from sheet fracture while Sheppard's model⁴³ focuses mainly on the sheet fracture. Both methods are supported by experiments in such a sense that the fatigue test data gathered from different weld and specimens can be well correlated by the maximum structural stress. Rupp's model has been programmed into commercial fatigue softwares such as MSC-FATIGUE and LMS-FALANCS, and widely used by the automotive industry.

3.5.7.3.3.1 Cracking in sheet metal

In case of cracking in the sheet metal, the theoretical radial stresses of a circular plate with central loading (normal force, bending moment, and lateral force) were modified to calculate the local nominal stresses of a spot weld joint. In [Figure 3.5.7.3.3.1-1](#), the radial stress, due to a normal force \mathbf{N} applied to a small rigid circular plate with a diameter D_p centered in a larger flexible circular plate with a diameter D_p , a thickness t , and clamped boundary conditions are given⁴⁴ as follows:

$$\sigma_r = \frac{3N}{\pi t^2} \left(\frac{\ln \frac{D_p}{D}}{1 - \left(\frac{D}{D_p} \right)^2} - \frac{1}{2} \right)$$

Equation 3.5.7.3.3.1-1



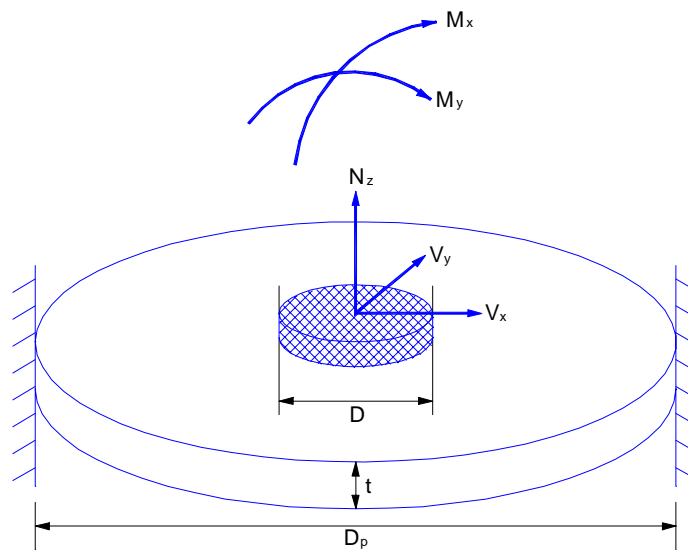


Figure 3.5.7.3.3.1-1 Circular plate model for sheet metals

The radial stress resulting from a bending moment **M** is

$$\sigma_r = \frac{2\beta M}{D_p t^2}$$

Equation 3.5.7.3.3.1-2



And, the radial stress due to a lateral force **V** is

$$\sigma_r = \frac{V}{\pi D t}$$

Equation 3.5.7.3.3.1-3



Assuming **Dp** = 10 **D** and $\beta = 9.36$, the above equations due to **N** and **M** can be rewritten as follows:

$$\sigma_r = \frac{1.744N}{t^2}$$

Equation 3.5.7.3.3.1-4



and

$$\sigma_r = \frac{1.872M}{Dt^2}$$

Equation 3.5.7.3.3.1-5



For different geometry of spot welded specimens, the radial stresses due to **N** and **M** was modified as follows:

$$\sigma_r = G \frac{1.744N}{t^2}$$

Equation 3.5.7.3.3.1-6



and

$$\sigma_r = G \frac{1.872M}{Dt^2}$$

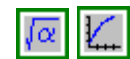
Equation 3.5.7.3.3.1-7



where \mathbf{G} is the geometric correction factor defined in the following

$$\mathbf{G} = 0.6\sqrt{t}$$

Equation 3.5.7.3.3.1-8



\mathbf{G} was the empirical constant for steel spot welds, used to collapse all the fatigue data with different sheet thickness into one small scattering band.

The schematic of a typical spot weld can be shown in [Figure 3.5.7.3.3.1-2](#). Cracking in the sheet metal may appear in either the upper or the lower sheets, and is modeled by local forces and moments at Points 1 and 2.

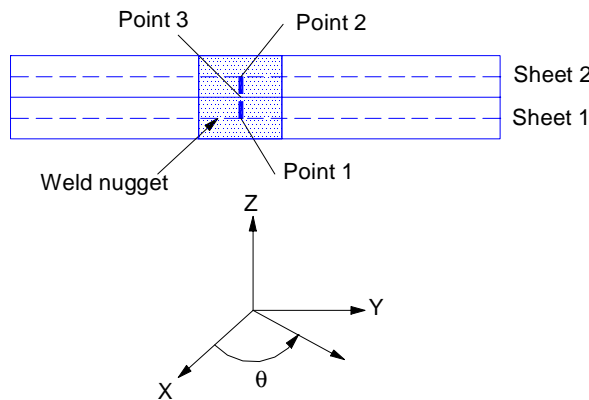


Figure 3.5.7.3.3.1-2 Schematic of a typical spot weld

The stresses at Points 1 and 2 can be expressed in terms of angle θ around the circumference of a spot weld:

$$\sigma_{r1} = -\sigma(r, V_{x1}) \cos \theta - \sigma(r, V_{y1}) \sin \theta + \sigma(r, N_{z1}) + \sigma(r, M_{x1}) \sin \theta - \sigma(r, M_{y1}) \cos \theta$$

Equation 3.5.7.3.3.1-9



$$\sigma_{r2} = -\sigma(r, V_{x2}) \cos \theta - \sigma(r, V_{y2}) \sin \theta - \sigma(r, N_{z2}) - \sigma(r, M_{x2}) \sin \theta + \sigma(r, M_{y2}) \cos \theta$$

Equation 3.5.7.3.3.1-10



where

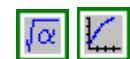
$$\sigma(r, V_{xi}) = \frac{V_{xi}}{\pi D t_i}$$

Equation 3.5.7.3.3.1-11



$$\sigma(r, V_{yi}) = \frac{V_{yi}}{\pi D t_i}$$

Equation 3.5.7.3.3.1-12



$$\sigma(r, N_{zi}) = G_i \frac{1.744 N_{zi}}{t_i^2}$$

Equation 3.5.7.3.3.1-13



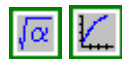
$$\sigma(r, M_{xi}) = G_i \frac{1.872 M_{xi}}{D t_i^2}$$

Equation 3.5.7.3.3.1-14



$$\sigma_{(r,M_{yi})} = G_i \frac{1.872 M_{yi}}{D t_i^2}$$

Equation 3.5.7.3.3.1-15



in which $i=1$ or 2 .

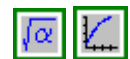
Note that since G_i are derived empirical factors, the diameter of the weld nugget and the thickness of the sheet metal should have dimensions in mm. Forces are in Newtons and moments in Newton-mm. The radial stresses are calculated at intervals around the circumference of the weld nugget, say at 10-degree intervals, and the maximum radial stress amplitude is used as the fatigue damage parameter.

3.5.7.3.3.2 Cracking in nugget

Per Heyes and Fermer⁴⁵, the maximum in-plane principal stress, expressed as a function of angle θ along the circumference of the spot weld, is used as the damage parameter at Point 3 (center of a nugget shown in [Figure 3.5.7.3.3.1-2](#)), which is calculated as follows:

$$\sigma_{1,3} = \frac{\sigma}{2} \pm \sqrt{\left(\frac{\sigma}{2}\right)^2 + \tau^2}$$

Equation 3.5.7.3.3.2-1



where

$$\sigma = \sigma_{N_{z3}} + \sigma_{M_{x3}} \sin \theta - \sigma_{M_{y3}} \cos \theta$$

Equation 3.5.7.3.3.2-2



$$\tau = \tau_{V_{x3}} \sin^2 \theta + \tau_{V_{y3}} \cos^2 \theta$$

Equation 3.5.7.3.3.2-3

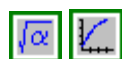


where the stresses are derived on the formulas of a beam subjected to tension, shear, and bending.

The normal stress, bending stress, and the maximum shear stress are determined as below:

$$\tau_{V_{x3}} = \frac{16 V_{x3}}{3\pi D^2}$$

Equation 3.5.7.3.3.2-4



$$\tau_{V_{y3}} = \frac{16 V_{y3}}{3\pi D^2}$$

Equation 3.5.7.3.3.2-5



$$\sigma_{N_{z3}} = \frac{4 N_{z3}}{\pi D^2} \quad N_{z3} > 0$$

Equation 3.5.7.3.3.2-6



$$\sigma_{M_{x3}} = \frac{32 M_{x3}}{\pi D^3}$$

Equation 3.5.7.3.3.2-7



$$\sigma_{M_{y3}} = \frac{32 M_{y3}}{\pi D^3}$$

Equation 3.5.7.3.3.2-8



3.5.7.3.3.3 Fatigue life predictions

It is required a S-N curve obtained from a fit of experimental data for a relation of equivalent stress amplitude and total fatigue life. The S-N curve is generalized as follows:

$$\sigma_{a,R=0} = \sigma'_{f,R=0} (2N_f)^b$$

Equation 3.5.7.3.3-1



where $\sigma_{a,R=0}$ is the stress amplitude at $R=0$

$\sigma'_{f,R=0}$ is the interception at one reversals and b is the slope of the S-N curve.

It is noted that the stress amplitude in this equation can be referred either to the maximum radial stress amplitude for cracking in sheet metal in [Equation 3.5.7.3.3.1-9](#) and [Equation 3.5.7.3.3.1-10](#) or to the maximum in-plane principal stress amplitude for cracking in nugget as illustrated in [Equation 3.5.7.3.3.3-1](#).

In some situations where the baseline fatigue properties are determined at cyclic loading at $R=0$, the mean stress sensitivity factor M is introduced to relate the baseline data to other loading with different mean offsets at the high cycle fatigue region (e.g., 2×10^6 cycles for steels). It is useful for applications on welds, where the Goodman approach will tend to overestimate the effect of mean stresses. M is defined as

$$M = \frac{S_a - S_{a,R=0}}{S_{m,R=0} - S_m}$$

Equation 3.5.7.3.3-2



where S_a and S_m are the stress amplitude and the mean stress at 2×10^6 cycles

$S_{a,R=0}$ and $S_{m,R=0}$ are the stress amplitude and the mean stress at $R = 0$ and 2×10^6 cycles.

The mean stress sensitivity factor $M=0.1$ is assumed for steels in [Reference 41](#).

Based on given M , σ_a and σ_m to a specific fatigue life in cycles, the equivalent stress amplitude $\sigma_{a,R=0}$ can be derived as follows:

$$\sigma_{a,R=0} = \frac{\sigma_a + M\sigma_m}{M+1}$$

Equation 3.5.7.3.3-3



3.5.8 MULTIAXIAL FATIGUE

Many engineering components are subjected to multiaxial loadings more complicated than simple uniaxial, bending or torsional loads. The most common fatigue analysis of multiaxial loadings is a straightforward extension of the uniaxial method⁴⁶, as summarized below. Since multiaxial fatigue is still an actively researched area, the readers are encouraged to keep up with the latest publications⁴⁷.

3.5.8.1 The Critical Plane Approach

Cyclic multiaxial problems usually involve fluctuations of principal stress directions. For example, two histories of a transmission shaft are shown in [Figure 3.5.8.1-1](#), where the bending stress, σ_{xx} , is plotted against the torsional stress, σ_{xy} , for every point in history. On the left is a approximately pure bending history and on the right is a biaxial history. By neglecting the relatively small circumferential stress, σ_{yy} , the principal stress direction can be estimated by the angle ϕ as indicated in the figure for each point in history. Its variation throughout history therefore becomes more complicated as the biaxiality of stress history increases. As a result, the failure plane and hence fatigue life is difficult to estimate without a detailed analysis, unlike for uniaxial loadings. To cope with this, the critical plane approach is generally adopted which assumes that fatigue failure will initiate on a plane where the largest amount of fatigue damage is accumulated. This means that fatigue analysis has to be performed for all potential failure planes before the most critical plane as well as fatigue life can be determined.

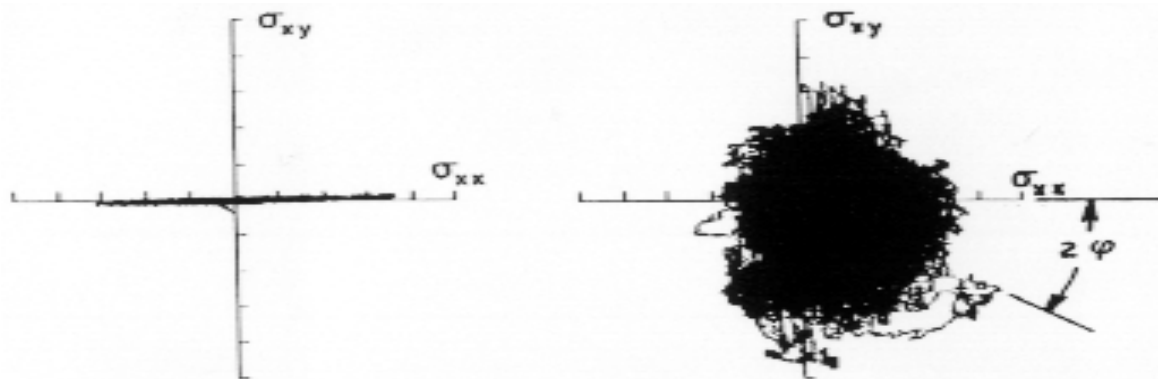


Figure 3.5.8.1-1 Stress distribution for a pure bending history and a biaxial history

3.5.8.2 Multiaxial Damage Parameter

There has been sufficient experimental evidence suggesting that uniaxial parameters such as the normal strain amplitude is not adequate in predicting fatigue failure for complex multiaxial problems. Over the years many multiaxial damage parameters have been proposed⁴⁸. Three simple parameters are mentioned here as examples:

$$\text{Von Mises' equivalent stress, } \sigma_{\text{eq}} = \sqrt{\frac{(\sigma_1 - \sigma_2)^2 + (\sigma_2 - \sigma_3)^2 + (\sigma_3 - \sigma_1)^2}{2}} \quad \text{Equation 3.5.8.2-1} \quad \boxed{\sqrt{\alpha}} \quad \boxed{\checkmark}$$

where σ_1 , σ_2 , and σ_3 are the three principal stresses in decreasing order.

The Von Mises stress is a measure commonly used to equate a multiaxial stress state with a uniaxial one. Since it is a scalar and is always positive, its lack of direction and sign makes it suitable only for proportional or near-proportional multiaxial loadings. The same scalar nature, however, makes the parameter a better choice when searching for 'hot spots' in complicated structures before a detailed and more time-consuming fatigue analysis is performed on critically loaded areas.

Brown and Miller's parameter = $\gamma_a + K\epsilon_a$

Equation 3.5.8.2-2



where γ_a , and ϵ_a are the shear strain amplitude and normal strain amplitude, respectively; K is a material constant.

This parameter⁴⁹ tries to improve fatigue life predicting capability of the uniaxial parameter γ_a after experimental data show that cyclic shear with simultaneous normal deformation is more damaging than simple shear cycling.

Modified Smith – Watson – Topper parameter = $\sigma_{max}\epsilon_a + \tau_{max}\gamma_a$

Equation 3.5.8.2-3



This parameter⁵⁰ tries to improve fatigue life predicting capability of the uniaxial Smith-Watson-Topper parameter $\sigma_{max} \epsilon_a$, by including contributions from the shear component.

To determine the adequacy of a multiaxial damage parameter requires a sufficient number of constant amplitude tests preferably of various proportionalities. By plotting the parameter against the observed fatigue life from each test , a narrow band with minimal scatter should form if the damage parameter is a proper one. A parameter-life curve can then be established and serve as the material's fatigue curve to be used in fatigue analysis of complex histories.

3.5.8.3 General Iterative Procedures

The most general multiaxial fatigue analysis therefore involves repetitions of the following steps (a-d), similar to uniaxial problems, for all material planes before the most critical plane and its associated fatigue life can be determined.

- a) Select a material plane, usually defined by the rotational angle between the plane's normal and a reference axis in a given coordinate system;
- b) Obtain both the normal and shear stress/strain histories on the plane by performing stress/strain transformations;
- c) Rainflow count ([Section 3.5.5.2.3](#)) a stress (or strain) component to determine fatigue events. Since in general multiaxial loadings the normal and shear component are not necessarily in phase, the component being rainflowed depends on the fatigue mechanism. For example, the Brown and Miller criterion was initially proposed based on fatigue cracks occurring on shear dominant planes, and thus the shear component should be rainflowed. Similarly, the Smith-Watson-Topper criterion was based on fatigue cracks appearing on normal stress dominant planes, the normal component should be rainflowed.
- d) Calculate the value of the selected damage parameter for each fatigue event; determine the corresponding damage from the parameter-life equation; and sum up the damage.

3.5.8.4 Consistent Application of Multiaxial Method

The multiaxial method outlined above is now applied to simple torsional tests to illustrate how the method should be applied consistently both to baseline tests (for establishing material's fatigue property purposes) and to general complex histories for fatigue design purposes.

Let us use the Brown and Miller parameter as an example. If a fully reversed simple torsional test of strain amplitude (ϵ_{xy})_a is observed to last (N_f) cycles, to use the critical plane approach, it is first determined that the normal and shear strain amplitude on a material plane θ degrees from the loading axis (Figure 3.5.8.4-1) is $\epsilon_a = (\epsilon_{xy})_a \sin 2\theta$ and $\gamma_a = (\epsilon_{xy})_a \cos 2\theta$, respectively. The value of Brown and Miller parameter on the θ plane is then $(\epsilon_{xy})_a [\cos 2\theta + K \sin 2\theta]$. This parameter reaches its maximum value $\sqrt{(1+K^2)} (\epsilon_{xy})_a$ when $\tan(2\theta)=K$.

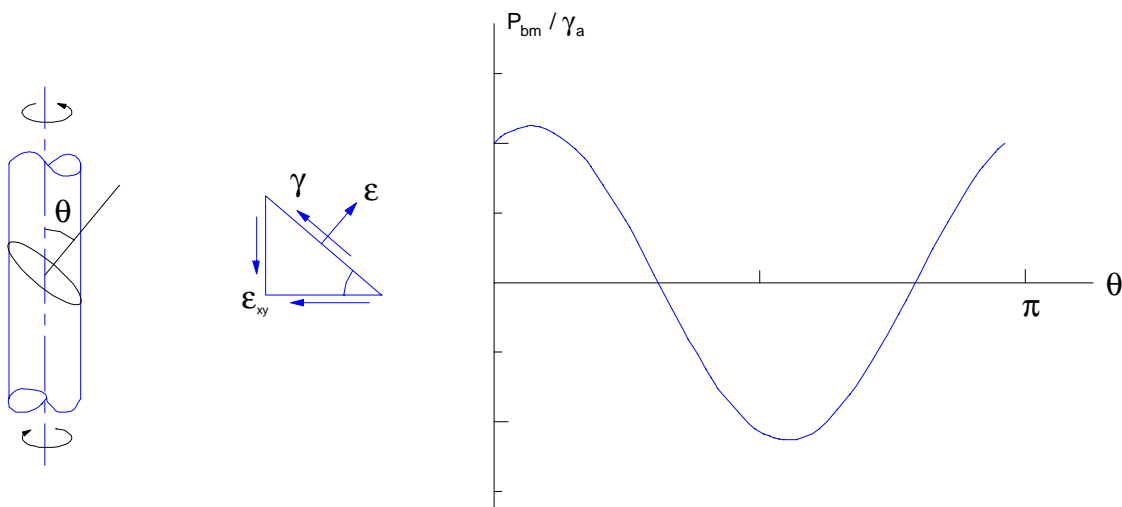


Figure 3.5.8.4-1 Damage parameter variation on different material planes

Therefore, on the parameter versus life plot, a point $[\sqrt{(1+K^2)}(\epsilon_{xy})_a, N_f]$ should be entered. If such data points from various tests do form a narrow band, then the resulting curve can be established as the material's fatigue property, a Brown and Miller parameter versus fatigue damage relationship, which is to be used for fatigue analysis of complicated histories. This parameter-life relationship can be continuously improved as more constant amplitude test data, even from modes different from torsional, become available, and the critical plane approach as described above be employed.

3.5.8.5 Further Research Issues

Multiaxial fatigue is a very complex subject and remains an actively researched field. Only the least controversial approach is summarized above. Many interesting areas such as multiaxial notch stress correction, multiaxial rainflow method, multiaxial cyclic relaxation/ratcheting, and effects of multiaxial overload are still evolving. The readers should therefore be aware of the limitations of the current method and try to remain informed of the newest development, particularly if the current method is suspected to underpredict fatigue damage.

3.5.9 STATISTICAL FATIGUE PROPERTIES

The reliability of fatigue life predictions for components under variable amplitude loads is affected by variability in loads, material properties, modeling errors, and cumulative damage value. It is well known that test data in fatigue life and the fatigue strength of materials exhibit

scattered results, even though the specimens come from the same batch. The uncertainty in material properties can be a result of the materials product form, for example, forging, extrusion or plate material. This can lead to changes in material strength depending on where the test specimens are extracted from in the material. Past experience in the automotive industry has shown that variations of drivers, road surfaces and weather conditions are the major contributors to loading variability. Modeling errors (errors between measured and predicted data) are a consequence of a model's inability to duplicate the actual physical mechanism operating in an experimental test. The combination of uncertainty in life prediction techniques, material properties, and type of loading histories also affect the randomness of the cumulative damage value.

The intent of this section is to characterize uncertainties in fatigue properties. Although numerous methods^{51, 52, 53} to determine the statistical fatigue properties have been published, a summary of the useful formulas is described in the following sections. Step-by-step calculations are illustrated with the assumptions and limitations addressed. The reader is referred to [Reference 54](#) for details of determining and investigating the uncertainties in loading histories, material properties, and the parameters used in the fatigue reliability models.

3.5.9.1 Load-Life (P-N) Method

Typical P-N data (P_i , N_i) is defined by the expression

$$P_a = P_f' (N_f)^m$$

Equation 3.5.9.1-1



where P_a = load amplitude

P_f' = fatigue strength coefficient

m = fatigue strength exponent

N_f = cycles to failure.

Taking logarithms (base e) of both sides yields

$$\ln(N_f) = -\frac{1}{m} \ln(P_f') + \frac{1}{m} \ln(P_a)$$

Equation 3.5.9.1-2



Hence

$$Y = A + BX$$

where $Y = \ln(N_f)$;

$X = \ln(P_a)$;

$A = (-1/m) \ln(P_f')$,

$B = 1/m$

It is assumed that the slope of the P-N curve (m) and the variance of Y estimates on X (s^2) are constant. At a specific load level P_a and constant slope m , it can be shown

$$\sigma_{\ln N_f}^2 = \sigma_A^2 = \sigma^2$$

Also the relationship of $A = -1/m \ln(P_f')$ leads to the following

$$\sigma_A^2 = \frac{1}{m^2} \sigma_{\ln(P_f')}^2$$

Equation 3.5.9.1-3



Assuming that P_f' is log-normally distributed, $C_{P_f'}$ can be obtained as follows:

$$\sigma_A^2 = \frac{1}{m^2} \sigma_{\ln(P_f')}^2$$

Equation 3.5.9.1-4



$$\sigma_A^2 = \frac{1}{m^2} \ln(1 + C_{P_f'}^2)$$

or

$$C_{P_f'} = \sqrt{\exp(m^2 \sigma_A^2) - 1}$$

Equation 3.5.9.1-5



Therefore, the estimated COV of P_f' is

$$\hat{C}_{P_f'} = \sqrt{\exp(m^2 s^2) - 1}$$

Equation 3.5.9.1-6



The mean of P_f' is given as follows:

$$\mu_{P_f'} = \exp\left(-\frac{\hat{A}}{\hat{B}}\right)$$

Equation 3.5.9.1-7



Assuming that N_f is base e log-normally distributed, C_{N_f} can be determined as follows:

$$\sigma_{\ln(N_f)}^2 = \ln(1 + C_{N_f}^2)$$

Equation 3.5.9.1-8



$$\ln(1 + C_{N_f}^2) = \sigma_A^2 = \sigma^2$$

which leads to the following

$$C_{N_f} = \sqrt{\exp(\sigma_A^2) - 1}$$

Equation 3.5.9.1-9



Hence, the estimated COV of N_f is

$$\hat{C}_{N_f} = \sqrt{\exp(s^2) - 1}$$

Equation 3.5.9.1-10



An example calculation is given in [Section 6.2.5.3](#) for the fatigue properties using the Load-Life Method.

3.5.9.2 Stress-Life Method

Typical S-N data (σ_a , $2N_f$) is defined by the expression proposed by Basquin⁵⁵ in 1910:

$$\sigma_a = \sigma_f' (2N_f)^b$$

Equation 3.5.9.2-1



where σ_a = true stress amplitude
 σ_f' = fatigue strength coefficient
 b = fatigue strength exponent
 $2N_f$ = reversals to failure

Taking logarithms (base e) of both sides yields

$$\ln(2N_f) = -\frac{1}{b} \ln(\sigma_f') + \frac{1}{b} \ln(\sigma_a)$$

Equation 3.5.9.2-2



Hence

$$Y = A + BX$$

where $Y = \ln(2N_f)$;
 $X = \ln(\sigma_a)$;
 $A = (-1/b) \ln(\sigma_f')$,
 $B = 1/b$

With the identical assumptions in [Section 3.5.9.1](#), the estimated **COV** of $2N_f$, **COV** of σ_f' , and the mean of σ_f' are given as follows:

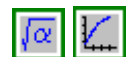
$$\hat{C}_{2N_f} = \sqrt{\exp(s^2) - 1}$$

Equation 3.5.9.2-3



$$\hat{C}_{\sigma_f'} = \sqrt{\exp(b^2 s^2) - 1}$$

Equation 3.5.9.2-4



$$\hat{\mu}_{\sigma_f'} = \exp\left(-\frac{\hat{A}}{\hat{B}}\right)$$

Equation 3.5.9.2-5



An example calculation is given in [Section 6.2.5.4](#) for the fatigue properties using the Stress-Life Method.

3.5.9.3 Plastic Strain-Life Method

Typical ϵ_p - $2N_f$ data (ϵ_a^p , $2N_f$) is often defined by the following expression, as independently proposed by Coffin⁵⁶ and Manson⁵⁷ in the 1950s:

$$\epsilon_a^p = \epsilon_{f'} (2N_f)^c$$

Equation 3.5.9.3-1



where ϵ_a^p = plastic strain amplitude

$\epsilon_{f'}$ = fatigue ductility coefficient

c = fatigue ductility exponent

$2N_f$ = reversals to failure

Taking logarithms (base e) of both sides yields

$$\ln(2N_f) = -\frac{1}{c} \ln(\epsilon_{f'}) + \frac{1}{c} \ln(\epsilon_a^p)$$

Equation 3.5.9.3-2



Hence

$$Y = A + BX$$

where $Y = \ln(2N_f)$;

$$X = \ln(\epsilon_a^p);$$

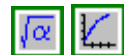
$$A = (-1/c) \ln(\epsilon_{f'});$$

$$B = 1/c$$

With the identical assumptions in [Section 3.5.9.1](#), the estimated COV of $2N_f$, COV of σ_f' , and the mean of σ_f' are given as follows:

$$\hat{C}_{2N_f} = \sqrt{\exp(s^2) - 1}$$

Equation 3.5.9.3-3



$$\hat{C}_{\sigma_{f'}} = \sqrt{\exp(c^2 s^2) - 1}$$

Equation 3.5.9.3-4



$$\hat{\mu}_{\sigma_{f'}} = \exp\left(-\frac{\hat{A}}{\hat{B}}\right)$$

Equation 3.5.9.3-5



An example calculation is given in [Section 6.2.5.5](#) for the fatigue properties using the Plastic Strain-Life Method.

3.5.9.4 Total Strain-Life Method

It is assumed that the total strain amplitude can be decomposed into elastic and plastic components:

$$\varepsilon_a = \varepsilon_a^e + \varepsilon_a^p$$

Equation 3.5.9.4-1



where the elastic strain amplitude can be related to the stress amplitude by $\varepsilon_a^e = \sigma_a / E$.

Based on [Equation 3.5.9.2-1](#) and [Equation 3.5.9.3-1](#), [Equation 3.5.9.4-1](#) can be rewritten as follows:

$$\varepsilon_a = \frac{\sigma_{f'}^e}{E} (2N_f)^b + \varepsilon_{f'} (2N_f)^c$$

Equation 3.5.9.4-2



Thus, the quantities $\sigma_{f'}^e$, b , $\varepsilon_{f'}$, and c are the fatigue properties for the total strain-life approach and the statistical properties of these quantities were determined and illustrated in the previous sections.

3.5.9.5 Cyclic Stress-Strain Curve

The following relationships exist between cyclic stress-strain and strain-life properties

$$K' = \frac{\sigma_{f'}^e}{(\varepsilon_{f'})^{n'}}$$

Equation 3.5.9.5-1



$$n' = \frac{b}{c}$$

Equation 3.5.9.5-2



where K' is the cyclic strength coefficient
 n' is the cyclic strain hardening exponent.

An example calculation is given in [Section 6.2.5.6](#) for the Statistical Cyclic Stress-Strain properties.

REFERENCES FOR SECTION 3.5

1. N. W. Dowling, "Mechanical Behavior of Materials: Engineering Methods for Deformation, Fracture, and Fatigue", 2nd Edition, Prentice Hall, 1998.
2. Smith, K.N. and Topper, T.H., "Basis of Structural Fatigue," SAE Paper No. 700777, Warrendale, PA.
3. Topper, T.H., Wetzel, R.M., and Morrow, J.D., "Neuber's Rule Applied to Fatigue of Notched Specimens," Journal of Materials, JMSLA, Vol. 4, No. 1, March 1969.
4. Palmgren, A., "Die Lebensdauer Von Kugellagern," ZVDI, Vol. 68, No. 14, 1924.
5. Miner, M.A., "Cumulative Damage in Fatigue," *Journal of Applied Mechanics*, Vol. 12, 1945.
6. Conle, F. A., and Mousseau, C. W., "Using Vehicle Dynamic Simulations and Finite Element Results to Generate Fatigue life for Contours for Chassis Components", Int. J. Fatigue, Vol. 13, No. 3, 1991, pages 159 - 205.
7. "Tensile Test Specimens", SAE J416, 1999.
8. ASTM Standard E8, "Tension Testing of Metallic Materials," American Society for Testing and Materials, 1999.
9. LaPointe, N.R., "Monotonic and Fatigue Characterizations of Metals," *ibid*, Paper No. 80679.
10. ASTM Standard E646, "Tensile Strain-Hardening Exponents (n-Values) of Metallic Sheet Materials," American Society for Testing and Materials, 1999.
11. American Society for Testing and Materials, "A Guide for Fatigue Testing and the Statistical Analysis of Fatigue Data," ASTM STP No. 91A, 1963.
12. American Iron and Steel Institute, "Sheet Steel Properties and Fatigue Design for Ground Transportation Engineers", Committee of Sheet Steel Producers, Document SG 836 281 RI, Washington, D.C.
13. Fatigue Design Handbook, Advances in Engineering, Volume 4, Society of Automotive Engineers, Edited by J.A. Graham, J.F. Millan, and F.J. Appl, 1968.
14. Grover, H.J., "Fatigue of Aircraft Structures," Naval Air Systems Command, Department of the Navy, NAVAIR 01-1A-13, 1966.
15. Peterson, R.E., Stress Concentration Factors, John Wiley and Sons, 1974.

16. Barsom, J.M., Klippstein, K.H., and Shoemaker, A.K., "State of the Art Report on Fatigue Behavior of Sheet Steels for Automotive Applications," Report to the American Iron and Steel Institute, AISI Project 1201-409D, United States Steel Corporation, February 1980.
17. Neuber, H., "Theory of Stress Concentration for Shear Strained Prismatical Bodies with Arbitrary Nonlinear Stress Strain Law," Transactions of the American Society of Mechanical Engineers, Journal of Applied Mechanics, December 1961.
18. Tucker, L.E., "Cumulative Damage Analysis," *Proceedings of the SAE Fatigue Conference, P-109*, Paper No. 820686, SAE, April 1982.
19. Socie, D., "Variable Amplitude Fatigue Life Estimation Methods," *ibid*, Paper No. 820689.
20. "Testing Procedures for Strain Controlled Fatigue Test (Supplement Instructions for A/SP Fatigue Program)", Auto/Steel Partnership Sheet Steel Fatigue Program, 1997.
21. "Technical Report on Low Cycle Fatigue Properties, Ferrous and Non-Ferrous Materials", SAE J1099, 1998.
22. "Materials Data for Cyclic Loading", C. Boller and T. Seeger, Elsevier, 1987.
23. "Databook of Fatigue Strength of Metallic Materials", The Society of Materials Science Japan, Elsevier, 1996.
24. "Metal Fatigue", N. E. Frost, K. J. Marsh, and L. P. Pook, Clarendon Press, London, 1974, p. 46.
25. Holt, J.M, and Stewart, B.K., "Strain Controlled Fatigue Properties of USS EX-TEN F50 Steel," SAE Paper No. 790460, Warrendale, PA.
26. Archbhaumik, D., "Steel Variability Effects on Low Cycle Fatigue Behavior of a Single Grade of High Strength Low Alloy Steel," *Metallurgical Transactions A*, Volume 10A, March 1979.
27. Holt J.M. and Charpentier, P.L., "Effect of Cold Forming on the Strain Controlled Fatigue Properties of HSLA Steel Sheets, "Metals/Materials Technology Series, 1983 Metals Engineers, American Society for Metals, Paper No. 8306-071, Philadelphia, PA.
28. Rolfe, S.T. and Barsom, J.M., *Fracture and Fatigue Control in Structures*, Prentice-Hall, 1977.
29. Ewing K.W., Wilson, M.L., Heimbuch, R.A. Woney, D.K., and Hinchens, A.F., "Fatigue of Welded High Strength Low Alloy Steels," SAE Paper No. 800374, Warrendale, PA.
30. Fisher, J.W., *Bridge Fatigue Guide-Design and Details*, American Institute of Steel Construction, New York, New York, 1977.
31. Klippstein, K.H., "Fatigue Behavior of Steel Sheet Fabrication Details," SAE Paper No. 810436, Warrendale, PA.

32. Klippstein, K.H., "Fatigue of Fabricated Steel Sheet Details-Phase II," SAE Paper No. 850366, Warrendale, PA.
33. Orts, D.H., "Fatigue Strength of Spot Welded Joints in a HSLA Steel," SAE Paper No. 810355, Warrendale, PA.
34. Davidson, J.A., "Design Related Methodology to Determine the Fatigue Life and Related Failure Mode of Spot-Welded Sheet Steels," *Metals/Materials Technology Series*, 1983 International Conference on Technology and Applications of High-Strength Low-Alloy (HSLA) Steels, American Society for Metals, Paper No. 8306-022, Metals Park, OH.
35. Davidson, J.A. and Imhof, E.J., Jr., "The Effect of Tensile Strength on the Fatigue Life of Spot-Welded Sheet Steels," SAE Paper No. 840110, Warrendale, PA.
36. Davidson, J.A., "A Review of Fatigue Properties of Spot-Welded Sheet Steels," SAE Paper No. 830033, Warrendale, PA.
37. Lawrence, F.V. Jr., Cutter, H.T., and McMahon, J.C., "Improvement of Steel Spot-Weld Fatigue Resistance," Final Report to AISI, College of Engineering, University of Illinois, Urbana, Illinois, April 1985.
38. Swellam, M. H. M., *A Fatigue Design Parameter for Spot Welds*, Ph.D. Thesis, Department of Civil Engineering, University of Illinois at Urbana-Champaign, 1991.
39. Lawrence, F. V., Jr., A Professional Development Course of Fatigue of Weldments, April 18 & 19, 1996.
40. Zhang, S., "Stress Intensities at Spot Welds," International Journal of Fracture, 88, pp. 167-185, 1997.
41. Zhang, S., "Approximate Stress Intensity Factors and Notch Stresses for Common Spot-Welded Specimens," Welding Journal Research Supplement, May 1999, pp. 173-179.
42. Rupp, A., Störzel, K., and Grubisic, V., "Computer Aided Dimensioning of Spot-Welded Automotive Structures," SAE Technical Paper 950711, 1995.
43. Sheppard, S. D. and Strange, M., "Fatigue Life Estimation in Resistance Spot Welds: Initiation and Early Growth Phase," *Fatigue and Fracture of Engineering Materials and Structures*, Vol. 15, No. 6, 1992, pp. 531-549.
44. Cook, R. D., Roark's Formulas for Stress and Strain, Sixth Edition, McGraw-Hill Book Company, New York, 1989.
45. Heyes, P. and Fermer, M., "A Program for the Fatigue Analysis of Automotive Spot-Welds Based on Finite Element Calculations," SIAT '96/SAE Technical Paper 962507, Symposium on International Automotive Technology (SIAT'96), Pune, India, December 5-7, 1996.
46. Multiaxial Fatigue, American society for Testing and Materials, STP 853, Miller, K.J. and Brown, N.W., eds., Philadelphia, PA, 1985.

47. Socie, D. F., and Marquis, G. B., "Multiaxial Fatigue", Society of Automotive Engineers, Inc., 2000.
48. C.-C. Chu, "Critical Plane Fatigue Analysis of Various Constant Amplitude Tests for SAE1045 Steels," SAE Paper 940246, 1994.
49. Brown, M.W. And Miller, K.J., "A Theory for Fatigue under Multiaxial Stress-Strain Conditions," Proceedings The Institution of Mechanical Engineers, Vol. 187, No. 65, 1973.
50. K.N. Smith, P. Watson, and T.H. Topper, "A Stress Strain Function for the Fatigue of Metals, Journal of Materials, JMSLA, 5(4), pp.767-778, 1970.
51. Wirshing, P. H. and Wu, Y. T., Probabilistic and Statistical Methods of Fatigue Analysis and Design," Pressure Vessel & Piping Technology 1985 A Decade of Progress, 1985, pp. 793-819.
52. Shen, C. C., The Statistical Analysis of Fatigue Data, Ph.D. Thesis, Department of Aerospace and Mechanical Engineering, University of Arizona, 1994.
53. Socie, D. F. and Park, K., "Analytical Descriptions of Service Loading Suitable for Fatigue Analysis," Proceedings of the 10th International Conference on Vehicle Structural Mechanics and CAE, SAE P308, 1997, pp. 203-206.
54. Lee, Y., Lu, M., Segar, R. C., Welch, C. D., and Rudy, R. J., "Reliability-based Cumulative Fatigue Damage Assessment in Crack Initiation, International Journal of Materials and Product Technology, Vol. 4, No. 1, 1999, pp. 1-16.
55. Basquin, O. H., "The Exponential Law of Endurance Tests," Am. Soc. Test Mater. Proc., Vol. 10, 1910, pp. 625-630.
56. Coffin, L. F. Jr., "A Study of the Effects of Cyclic Thermal Stresses on a Ductile Metal," Trans. ASME, Vol. 76, 1954, pp. 931-950.
57. Mason, S. S., "Behavior of Materials under Conditions of Thermal Stress," Heat Transfer Symposium, University of Michigan Engineering Research Institute, 1953, PP. 9-75.

BIBLIOGRAPHY FOR SECTION 3.5

Landgraf, R.W., "Fundamentals of Fatigue Analysis," Proceedings of the SAE Fatigue Conference, P 109, Paper No. 820677, SAE, April 1982.

Reemsnyder H.S., "Stress Analysis," ibid, Paper No. 820683.

Nelson D.V. and Socie D.F., "Crack Initiation and Propagation Approaches to Fatigue Analysis," Design of Fatigue and Fracture Resistant Structures, STP 761, American Society for Testing and Materials, 1982.

Brichmeier, J.E. and Smith, K.V., "Optimization of a Light Truck Rough Road Durability Procedure Using Fatigue Analysis Methodology," *ibid*, Paper No. 820693.

Bickerstaff, D.J., Birchmeier J.E., and Tighe, W.R., "Overview of Design Approaches for Optimizing Fatigue Performance of Suspension Systems," *ibid*, Paper No. 820676.

3.6 CRASH ENERGY MANAGEMENT

Automotive vehicle structural crashworthiness is defined as the capability of an automotive structure to provide adequate protection for the vehicle and its passengers in the event of a crash. The vehicle structure and the occupant restraint system interact to protect vehicle occupants ¹. The structure needs to maintain enough space inside the vehicle so that the occupant restraints can operate effectively. It must also provide some degree of ridedown to assist the restraint system in controlling occupant acceleration, thereby limiting injury potential during a crash. Reduction of intrusion must be balanced against more aggressive deceleration curves.

Currently, three Federal Motor Vehicle Safety Standards (FMVSS) must be met by vehicles sold in the U.S.:

- 208 Frontal impact at $\pm 30^\circ$ and Flat Frontal Impact
- 214 Dynamic impacts
- 301 Frontals, lateral and rear

Possible future U.S. standards and European standards apply to frontal impacts (partial overlaps).

Most of the components of the vehicle system, such as interior arrangement, restraint systems, engine and power train packaging, steering systems, and suspensions, influence the vehicle crash performance.

Sheet steel products constitute the principal material used in automotive vehicle structures. The material properties of sheet steel have a major influence on the vehicle structural crashworthiness performance and its energy absorption capability. This section will focus on providing some design guidance in the crash energy management aspects related to body and chassis structures manufactured from sheet steel.

3.6.1 FACTORS AFFECTING CRASH ENERGY MANAGEMENT

Crashworthiness and crash energy management are dependent on vehicle size, mass and even styling. With smaller vehicles becoming more common, exacerbated by the proliferation of multipurpose vehicles (MPV) and small trucks, there is cause for concern for occupant safety in large-to-small vehicle collisions. When the smaller vehicles are designed for the expected service loads and minimum mass, it can be difficult to meet all of the design parameters, and often the "best compromise" is the result.

The main energy management components, such as longitudinal rails that provide the major portion of the energy absorption, undergo large plastic deformations. The work hardening effect and strain rate sensitivity of the material, as well as dynamic instability of the rails must be considered in their design.

Perhaps the greatest challenge is the front structure design. There are stringent requirements for geometric packaging in order to fit in the components, while attempting to maintain crush space for managing crash energy. Frequently this results in a complex structure, and adequate strength and structural stability becomes very difficult to achieve. To overcome these obstacles, designers need to pursue novel concepts and solutions, both in structural design and packaging of

vehicle components. In order to maintain minimum vehicle mass, the structure cannot be overdesigned. The best design and analytical tools available must be applied early in the design sequence, when modifications are possible, to resolve these packaging-mass-structure issues satisfactorily.

The general development of a vehicle structural design for crash energy management involves 3 major areas:

- Front structure
- Body and side structure
- Rear structure

These three areas are convenient for analysis, and are used as a means of dividing the vehicle for design purposes.

3.6.2 DYNAMIC CRASH SEQUENCE

The desirable dynamic crash sequence is progressive in nature. The initial contactor (bumper or side) deforms first, then the next structural component, and the following component until the energy is absorbed. Each section involved in the crash must exhibit enough resistance to the load transmitted from the previous section so that plastic deformation of the previous section can dissipate energy. The body compartment must be designed to withstand the anticipated crush loads for the various defined impact speeds from defined impact directions with adequate body integrity to allow for proper function of the restraint system.

In designing the structural components for progressive crush, the effect of crush velocity and section stability on the anticipated crush force must be considered. The equations for section stability and suggested solutions for this parameter are detailed in [Section 3.1.2](#) of this design manual, which provides an excellent resource for compressive load stability analysis.

3.6.3 RAIL CRUSH MODES

The longitudinal rails in the vehicle structure form the major force path in the energy management of a vehicle during a crash. These components are also the most difficult to modify after the vehicle packaging and architecture concepts are completed. These considerations imply that the crash energy absorbing capability of the major structural rails should be included as part of the vehicle design specifications. Moreover, the accuracy of an initial estimate of the force and crush space is important to attaining the vehicle goals, including crash and functional requirements within the vehicle mass targets.

Since energy is the product of force times crush distance, the "ideal" rail compression mode would be a continuous axial compression with no bending. In this case the material folds in an accordion-like fashion until a near solid condition is reached. The length in the solid condition is approximately 40% - 50% of the initial length and provides optimum energy absorption per material mass. The initial force to induce the first plastic deformation is extremely high, and may put undue force capacity requirements on the supporting structure. This condition has only been achieved in the laboratory ([Figure 3.6.3-1](#)) with seamless square tubing (short column loading) under carefully controlled conditions, and is not considered a practical design solution.

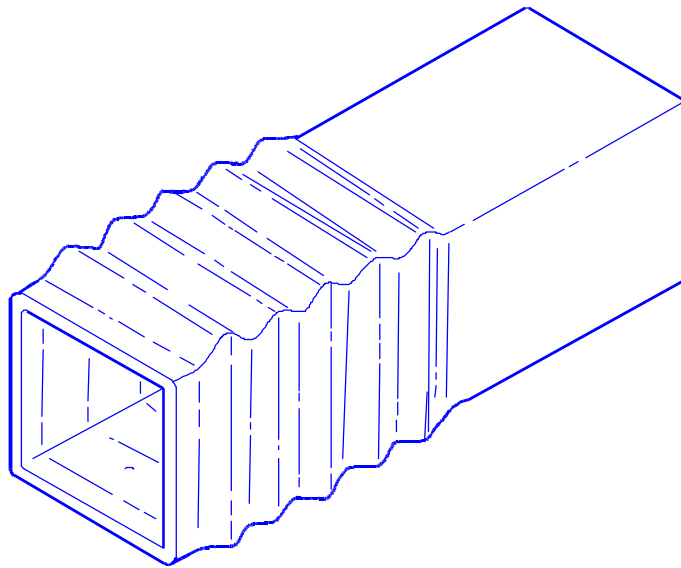


Figure 3.6.3-1 Ideal collapse of a square seamless steel tube

Pre-convoluting the rails, with the convolutions progressively becoming deeper toward the point of load application, reduces the peak loading and provides for axial compression with high energy absorbing efficiency. An example of a front rail with this configuration is shown in [Figure 3.6.3-2](#). [Figure 3.6.3-3](#) shows a schematic representation of the load versus crush relationship for axial crush with and without initiators and for bending. While there has been some success with this design approach, the front drive small vehicles, with conflicting space and component mounting requirements, will limit the application of this approach. Instead, other crush initiators, such as judiciously placed holes or corner "crippling" indentations, may help to approach this condition.

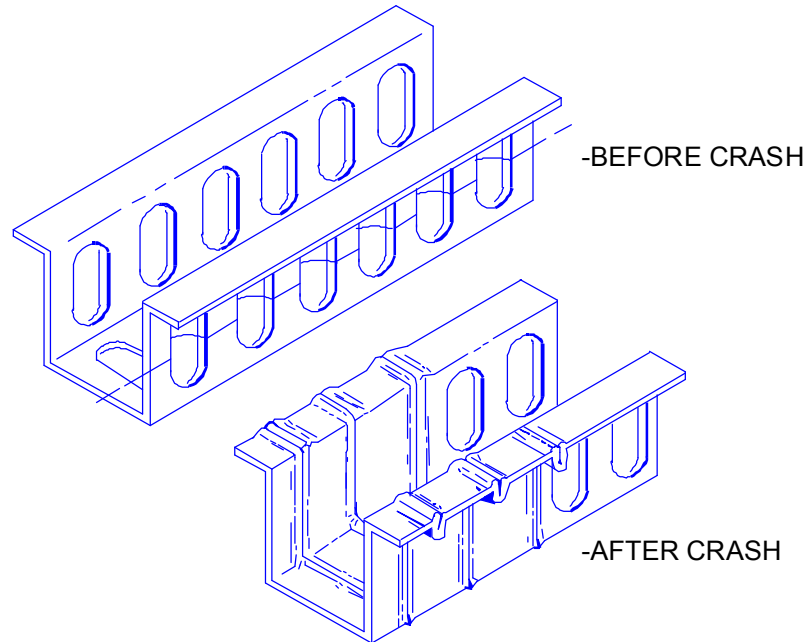


Figure 3.6.3-2 Front rail - pre-convoluted

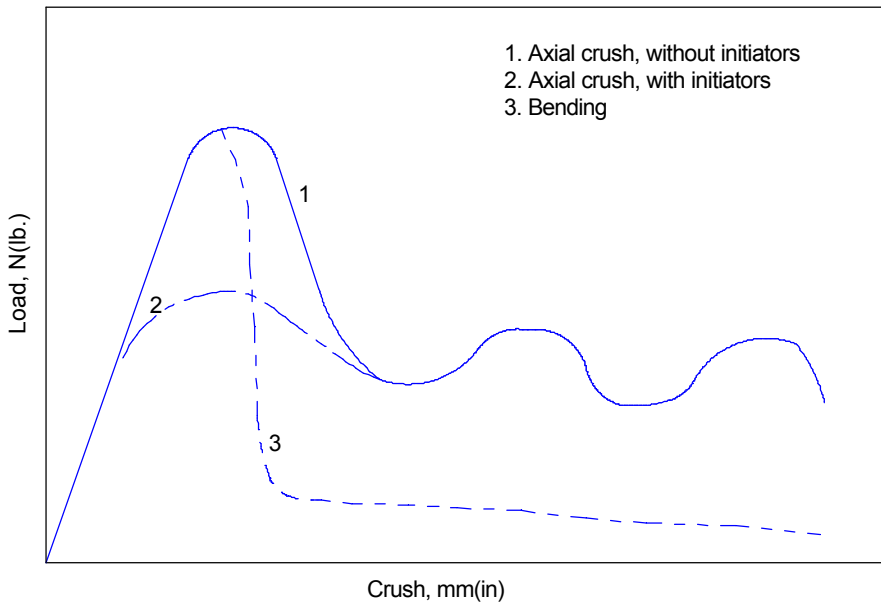


Figure 3.6.3-3 The use of initiators reduces the high initial crush load without diminishing the remaining crush characteristic. Bending results in a very high initial load followed by significantly less energy absorption.

In all cases, there will be a propensity for the structure to fail in a bending mode in a crash. In this case, energy is absorbed in the formation and rotation of discrete plastic hinges, which are formed at locations of maximum bending moment or diminished bending strength. Typical locations include built-in ends, bends, natural stress risers and structural imperfections. This condition is illustrated in [Figure 3.6.3-4](#). The hinges strain a much lower percentage of the metal than does an axial collapse, so that the average crush load, and consequently the total energy absorbed, is significantly lower. A premature loss of energy absorption capacity will alter the crash behavior of the vehicle, many times in an unpredictable manner. In combination with crush initiators, some internal reinforcement or spacers may be added to the interior of the rail to keep the walls apart, thus delaying the hinge effect by increasing the bending moment capability of the rail section. This will impose some mass and cost penalty, but additional reinforcement is usually necessary to meet performance requirements.

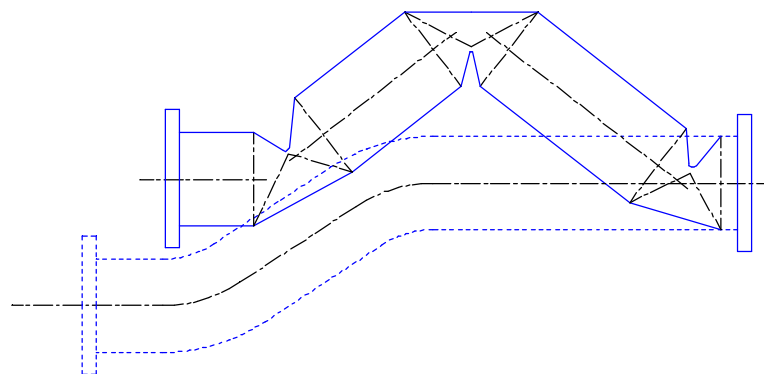


Figure 3.6.3-4 Schematic illustration of bending in a frame rail

3.6.4 PARAMETERS AFFECTING AVERAGE CRUSH FORCE OF RAIL SECTIONS

The parameters affecting the average crush force of rail sections can be generally categorized as:

1. Overall section geometry
2. Material tensile strength
3. Wall thickness
4. Weld flange configuration

Figure 3.6.4-1 through **Figure 3.6.4-4** quantify these variables based on actual static crush tests. The test samples are 305 mm (12.0 in.) long (short column) and were statically crushed. The samples were fabricated from 1.40 mm (0.055 in.) thick cold rolled steel, having an average strength of 247 MPa (35.8 ksi). The results are plotted for average static crush force. The average static force of the base sample is assigned a value of 100%. It should be cautioned that these data are for comparative purposes. In a typical vehicle structure, the collapsed portion of the column is unstable in bending and will buckle in a global mode as the column compresses in a crash, resulting in lower than expected loads.

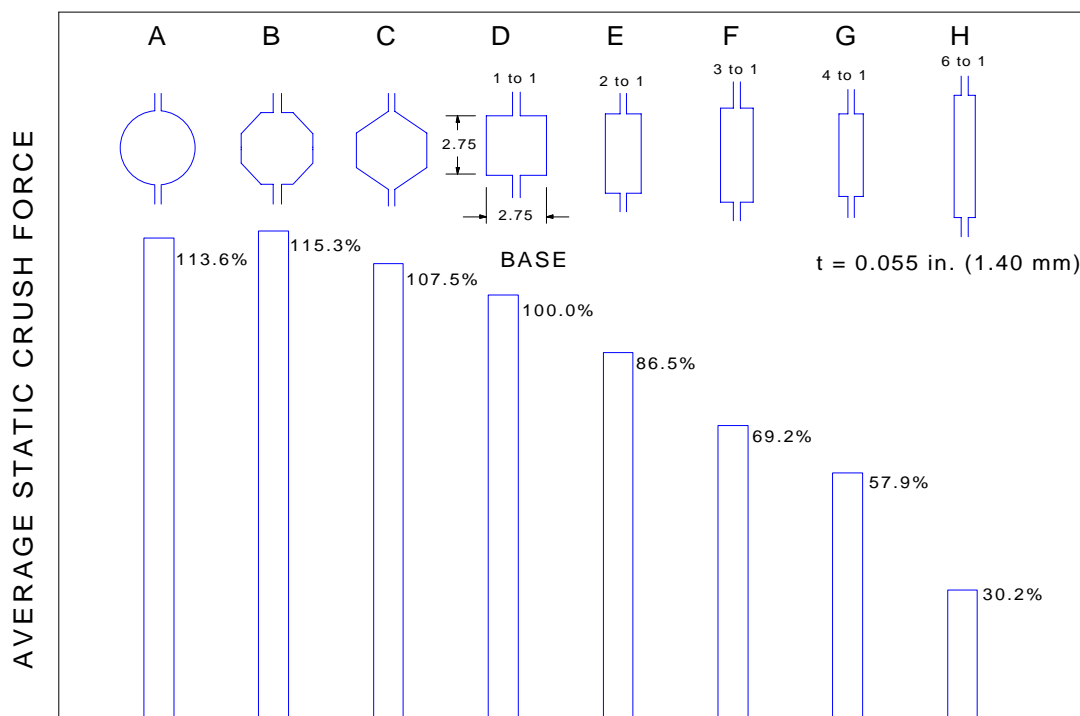


Figure 3.6.4-1 Average static crush force vs. section shape
(All samples were the same mass and length)

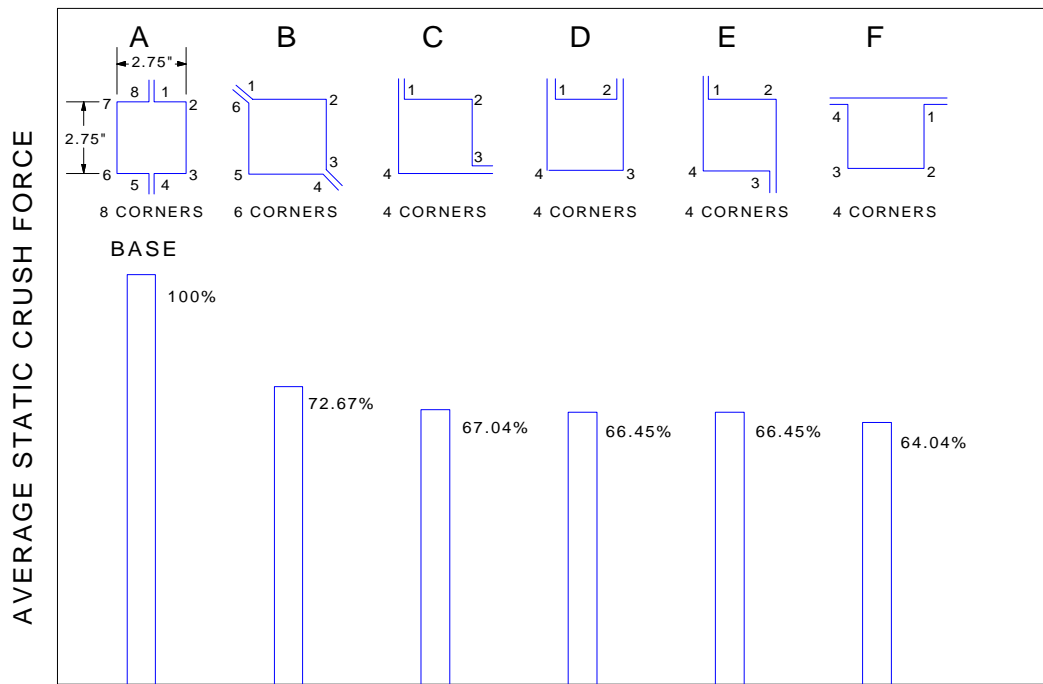


Figure 3.6.4-2 Average static crush force vs. weld flange configuration
(All samples were the same mass and length)

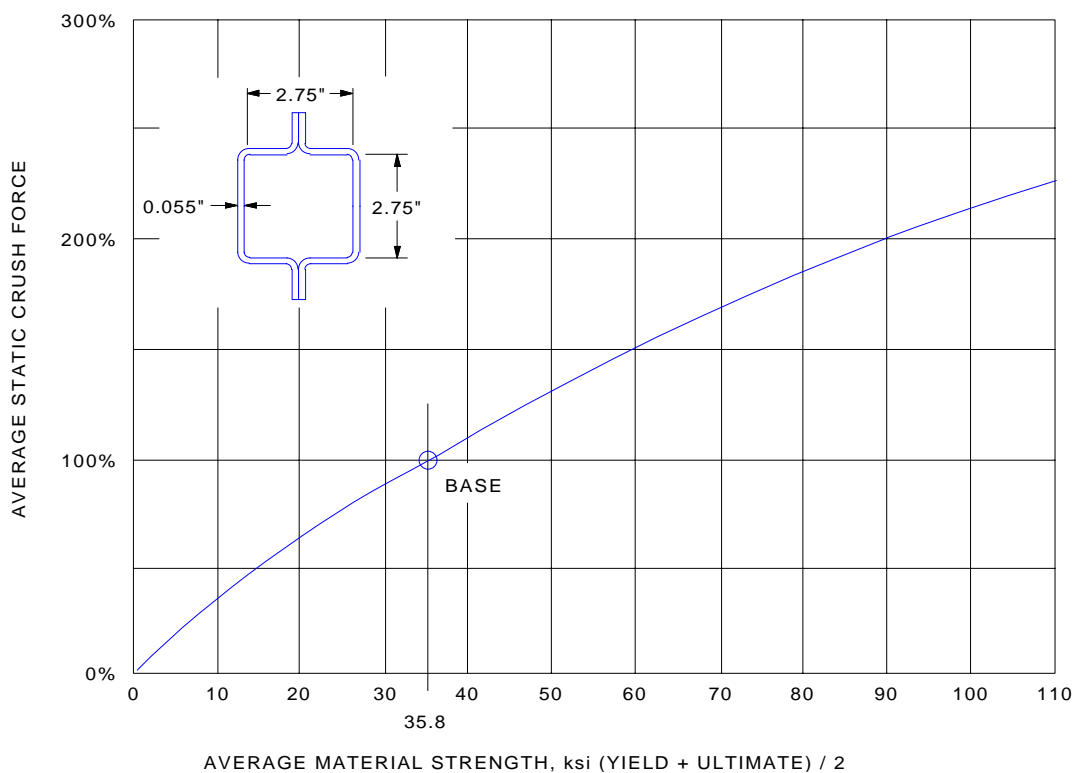


Figure 3.6.4-3 Average static crush force vs. average material strength
(for 0.055" metal thickness)

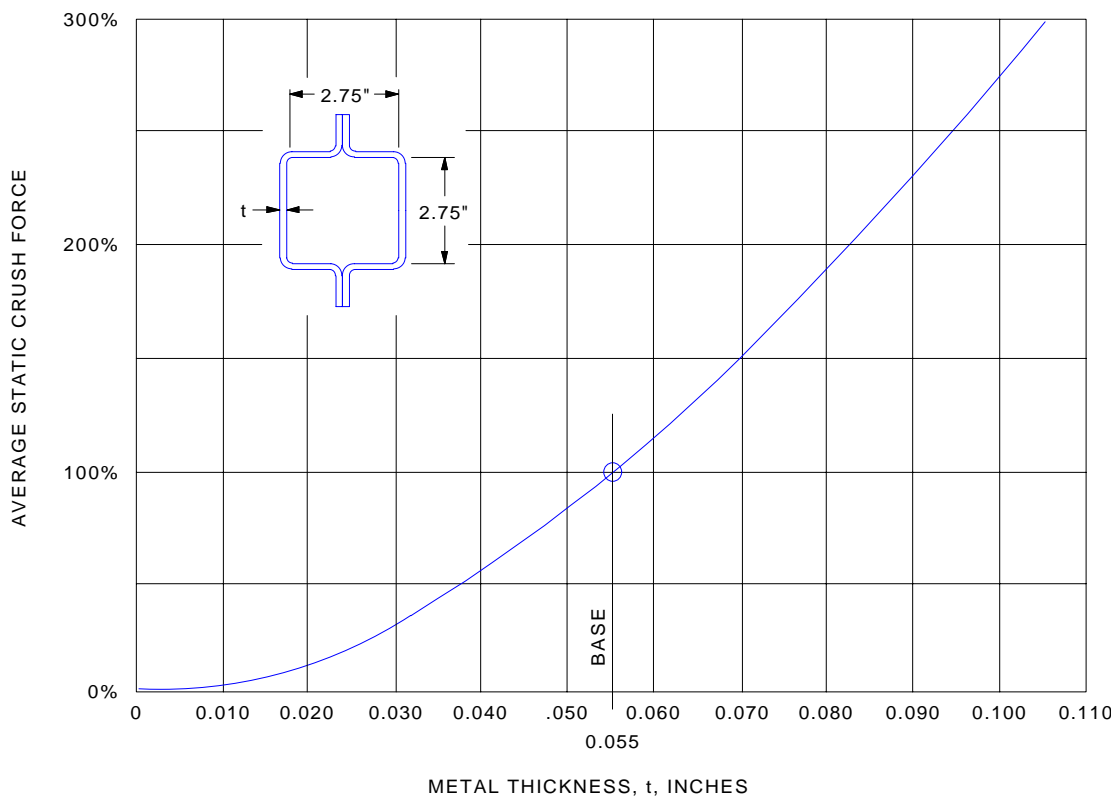


Figure 3.6.4-4 Average static crush force vs. metal thickness
(for 35.8 ksi average of yield and ultimate strength)

3.6.5 STATIC/DYNAMIC CRUSH FORCE DESIGN CONSIDERATIONS

Accurately predicting the crash performance of a vehicle structure and the energy managed by each of the major structural components requires an in-depth understanding of crash mechanics, and reliable material data. In full vehicle studies, the variables include global structure, section shapes, yield and ultimate strengths, strain hardening and strain rate.

Some of the material properties required to predict the crush characteristics are:

1. Stress-strain properties representative of the material for large plastic deformation
2. Change in properties under dynamic loading conditions
3. Strain hardening
4. Ductility properties
5. The variability that can be expected for production steels

Other factors, such as Poisson's ratio, are also pertinent to compressive loading conditions². In addition to the material properties, the section geometry and crush mode (e.g. bending, compressive buckling, or a combination) also affect the dynamic crush force properties.

The effect of the sum of the material property variables can be loosely categorized as the "dynamic factor" needed to predict the dynamic crush load capability from quasi static tests or computed static force capability.

Accurate crush load prediction, therefore, can only be expected if the assumption of crush modes and dynamic factors are identical to the actual assembled vehicle performance. This means that the constraints applied to structural members for test or computational analysis must force the crush mode to be a paradigm of the future vehicle.

Examples of the average dynamic crush force compared to static force are shown in [Figure 3.6.5-1](#) and [Figure 3.6.5-2](#). These data were generated from drop tower tests at 30 MPH. The drop head mass was adjusted to prevent bottoming out of the samples. This adjustment resulted in a crush of approximately 50% of the initial length. These tests are for some of the same short column sections that were used for static tests ([Sec 3.6.4](#)).

To arrive at a "dynamic factor", the static values of average force were calculated for the same crush distance as produced by the dynamic test of the same sample. The dynamic factor was defined as the ratio of dynamic to static crush force.

[Figure 3.6.5-1](#) compares 5 different section shapes. Section "E" had a failure mode different from the static test, resulting in a misleading dynamic factor of 3.15. The rest of the data follow the static tests quite well.

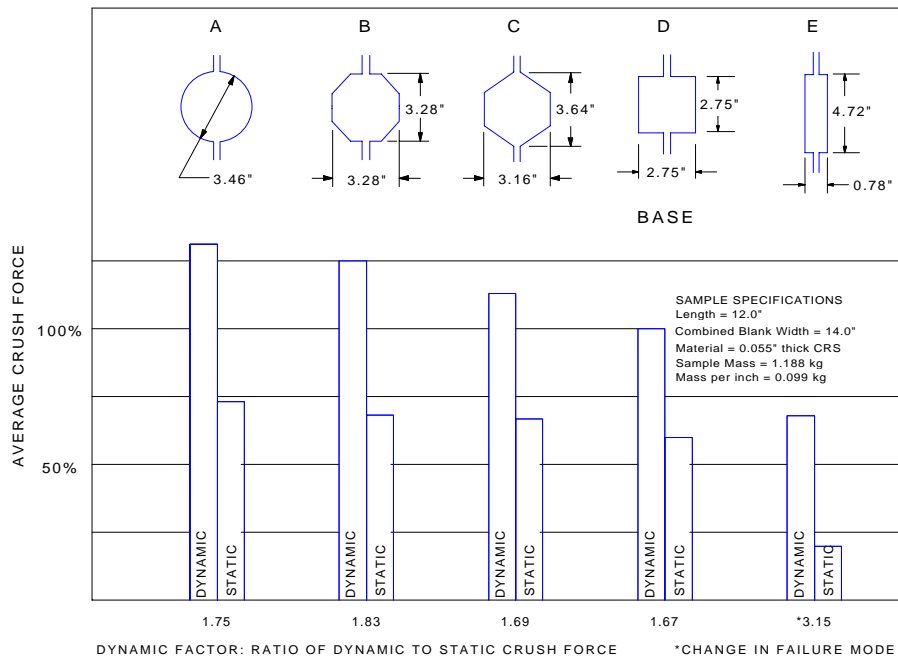


Figure 3.6.5-1 Average crush force, static and dynamic, at 50% crush vs. shape section (all samples were the same mass and length)

[Figure 3.6.5-2](#) and [Figure 3.6.5-3](#) show that dynamic effects of weld flange configuration and metal thickness (in the range of automotive structures) also indicate a nearly linear relationship to static tests.

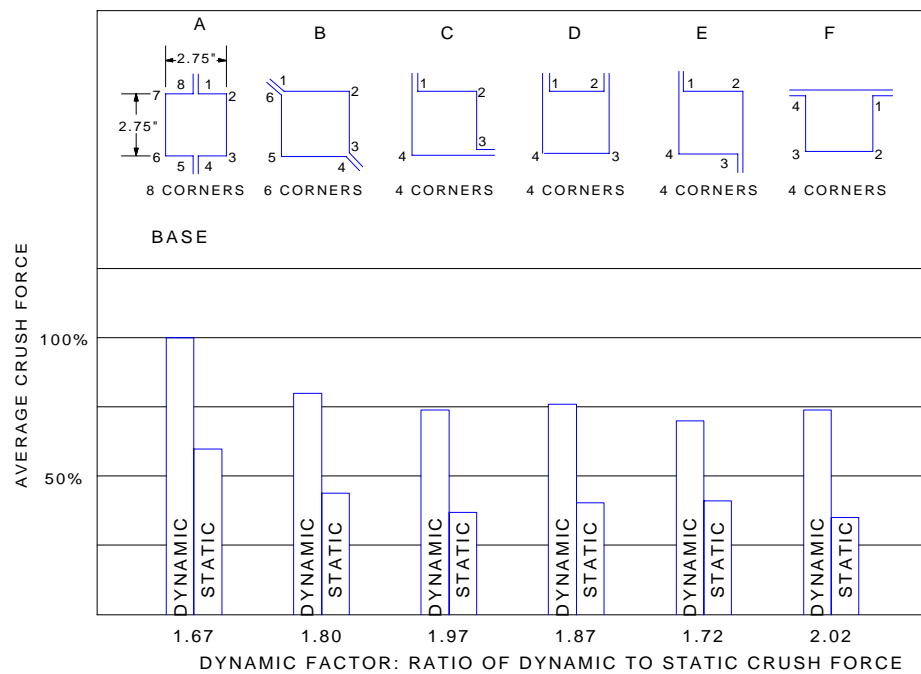


Figure 3.6.5-2 Average crush force, static and dynamic, at 50% crush vs. weld flange configuration (all samples were the same mass and length)

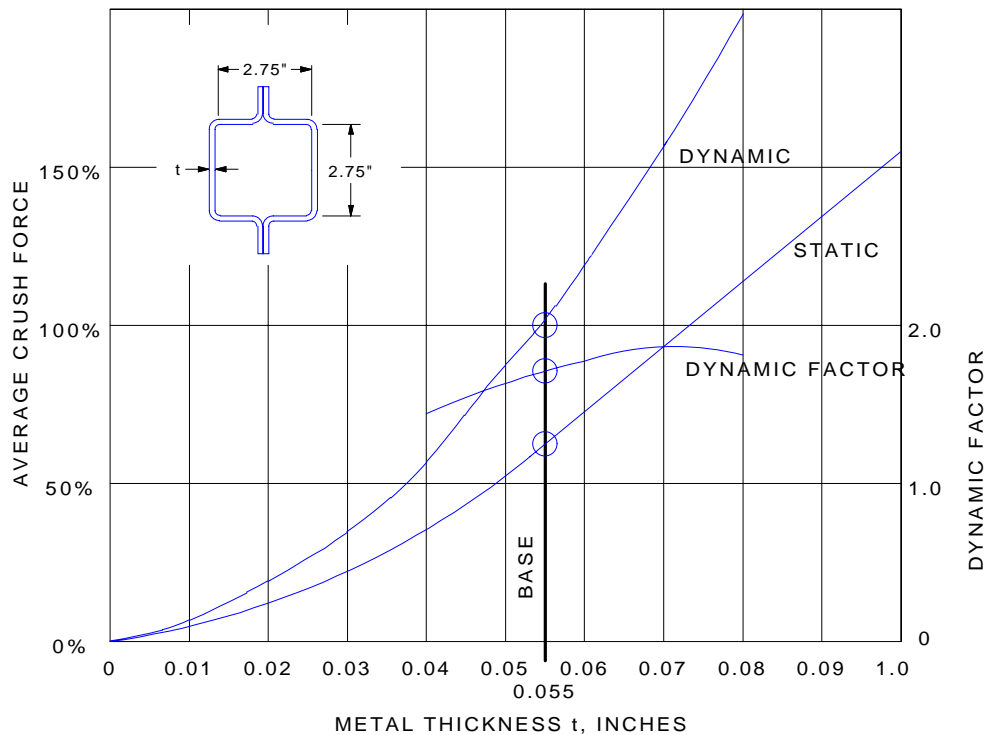


Figure 3.6.5-3 Average crush force, static and dynamic, at 50% crush vs. metal thickness (for 35.8 ksi average of yield and tensile strength)

[Figure 3.6.5-4](#) shows a decrease in dynamic effect as the average of the yield and tensile strength of the material increases.

As with the static crush force data, the dynamic data, generated under ideal conditions, should be treated as qualitative in application to vehicle design. The compressive crush mode of the structure will control the force capability to a large extent.

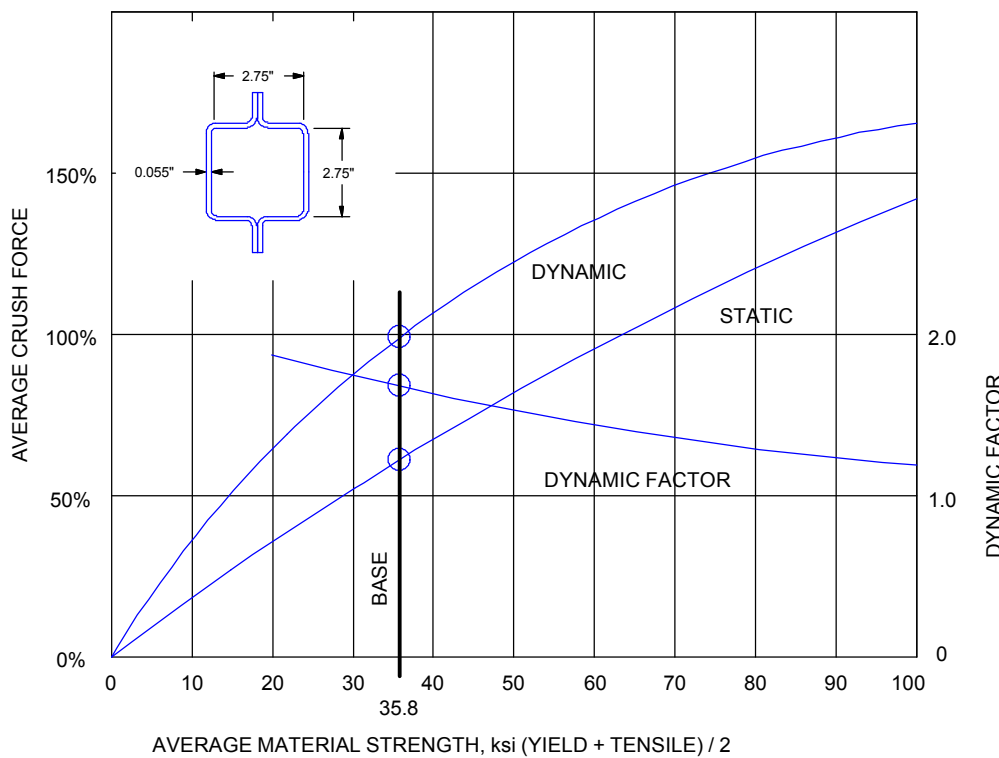


Figure 3.6.5-4 Average crush force, static and dynamic, at 50% crush vs. average material strength

3.6.6 ANALYTICAL TOOLS USED FOR CRASHWORTHINESS DESIGN

Analytical tools have been developed over the years, and are still a developing technology. Current computer tools are dependent on research into large deformation non linear computer finite element solutions, as well as the computer resources needed to support this technology.

There are several analytical methods that have been developed over the years to help the crashworthiness engineer predict the performance of vehicles in a crash. These include Lumped Parameter Modeling (LPM), Finite Element (FE) modeling, and combinations of these techniques.

One of the early approaches developed, LPM, uses the solution to a set of differential equations to represent a vehicle structure as nonlinear springs and lumped masses to compute vehicle crash performance. An LPM model is shown in [Figure 3.6.6-1](#).

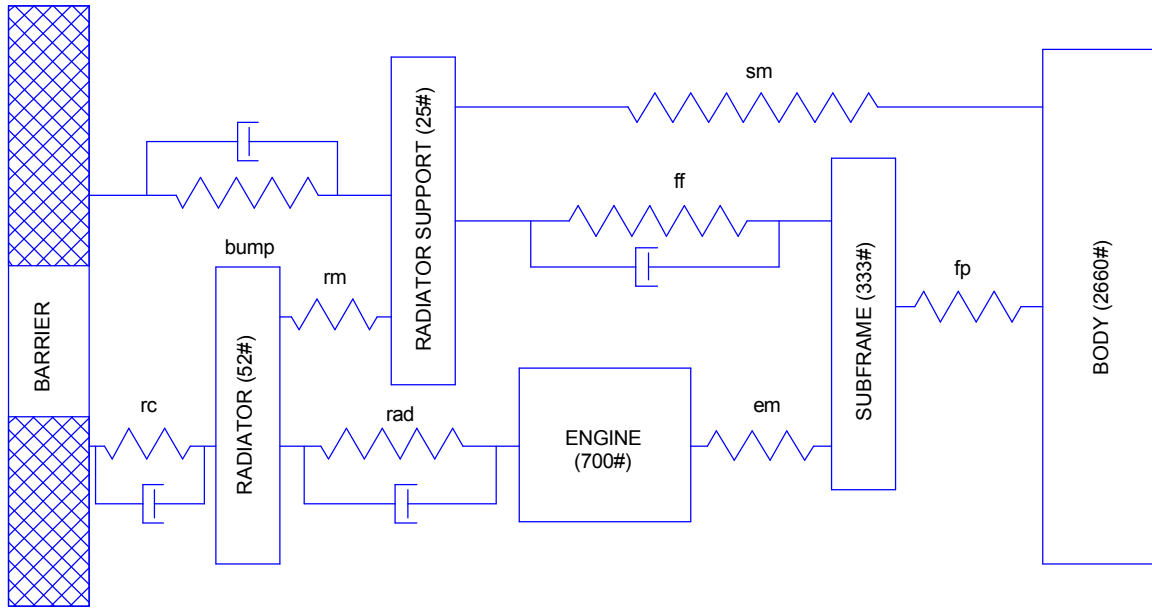


Figure 3.6.6-1 One-dimensional LMS frontal barrier impact simulation model ³.

LPM has been used successfully to predict vehicle crash performance ⁴, but is dependent on the skill and experience of the engineer, and knowledge of crash mechanics, for success. Crush data for the LPM approach is obtained from "hand calculations" for the main structural members, static and dynamic (drop tower or partial structure barrier) crush testing, or finite element analysis, to represent the structural parts.

The LPM approach is relatively simple and effective, but has some deficiencies. The structural data used to model the nonlinear springs are difficult to obtain, both because of the knowledge required in setting up test constraints and in timely buildup of test parts. Obtaining test parts of sufficient fidelity for test can cause delay in evaluating the ongoing design. This is especially a problem in the current emphasis on "fast to market" vehicle design programs.

The next logical step, which depends on research and computer capability, is the use of large deformation, nonlinear, finite element models to predict the crash performance of vehicles. Currently the main codes in use have the capability to completely model the vehicle structure and occupant system. The structural simulations have been generally successful; however the skill and knowledge on the part of the analyst are still of paramount importance. While the construction of a finite element model is a time consuming task, its accuracy justifies the use. Developments in FE modeling techniques, such as auto meshing and parameter based input, will make the modeling process faster in the future.

3.6.7 ANALYTICAL TOOL APPLICATION EXAMPLE

With the modeling tools that are available, the crashworthiness engineer can choose the best approach for the analysis at hand. The most difficult analysis is for a car that is new from the "ground up". However, a complete new design is almost unknown; there is always some

1. Obtain components and subassemblies that are similar to the new vehicle from existing FE models.
2. Assemble the available components into a partial "new" vehicle structure.
3. From the soft line design, add the missing structure as LP spring mass models.
4. Estimate the force deflection properties (the nonlinear springs) using the techniques in [Section 3.1](#) of this manual or, alternatively, some drop tower tests of pretest sections.
5. As the design progresses, periodically update the model.
6. Convert the model to FE when enough detail is available.

The first model can be relatively crude, with estimated parameters, such as crush space and configuration, based on soft line design proposals. The preliminary model will suffice to provide reasonable early estimates of crash performance in the hands of an experienced analyst, and will provide an "early warning" of any areas that may need special attention in the final design.

This technique, coarse to fine analysis, provides an analytical approach that parallels the design throughout the process, and tends to minimize changes for energy management considerations after the design is completed. Full scale crash tests are not completely eliminated, but will be used more for validation of the analysis than for design purposes.

3.6.8 CRUSH BEHAVIOR OF HYBRID STUB COLUMNS

In Chapter 3 of the forthcoming AISI Safety Book, Mahmood and Fileta describe a method proposed by Wierzbicki and Abromowicz for determining P_m , the mean crush load of thin-wall plate-type columns. For a thin-wall rectangular section of uniform material thickness and strength, the predicted mean crush load can be expressed as :

$$P_m = 9.56\sigma_0 t^{5/3} C^{1/3}$$

Equation 3.6.8-1



where $C = \frac{1}{2}(b+d)$
 $\sigma_0 = (0.9 \text{ to } 0.95) \sigma_u$
 $\sigma_u = \text{the ultimate strength of the material,}$
 $b \text{ and } d = \text{the lengths of the sides of the rectangular box column, and}$
 $t = \text{the uniform wall thickness.}$

The crush behavior of hybrid stub columns (fabricated from components with different properties) and columns made from components with similar materials of different thicknesses, has recently been studied and reported [5 6 7](#). The specimens used for the experimental work included box shaped and hat shaped stub columns, which were fabricated from two components of either the same material or from two different materials.

[Figure 3.6.8-1](#) shows the typical cross sections of these stub columns. Two sheet steels, 25AK and 50SK, were selected for this study. The nominal yield strengths were 172 MPa (25 ksi) and 345 MPa (50 ksi) respectively, and the thicknesses were 1.98 mm (0.78 in.) and 1.88 mm (0.074 in.) respectively.

Following material testing under strain rates from 0.0001 to 1.0 per second, a total of 144 stub columns were tested at the University of Missouri-Rolla using strain rates from 0.0001 to 1.0 per second ([Reference 6](#)). In addition, 52 drop silo tests of hybrid stub columns were conducted at General Motors Corporation ([Reference 7](#)). The impact velocities used for the tests were 28.5 and 43.2 km/hr (17.7 and 28.5 mph).

The results of the tests indicated that the static and dynamic crush performance of hybrid stub columns is affected by loading rate, sectional geometry, and the stress-strain relationship of the material. As shown in [Figure 3.6.8-2](#), the average mean crush loads dramatically increased when loading rates increased from quasi-static to 43.2 km/hr (26.8 mph), due to the strain rate effect ([Reference 7](#)).

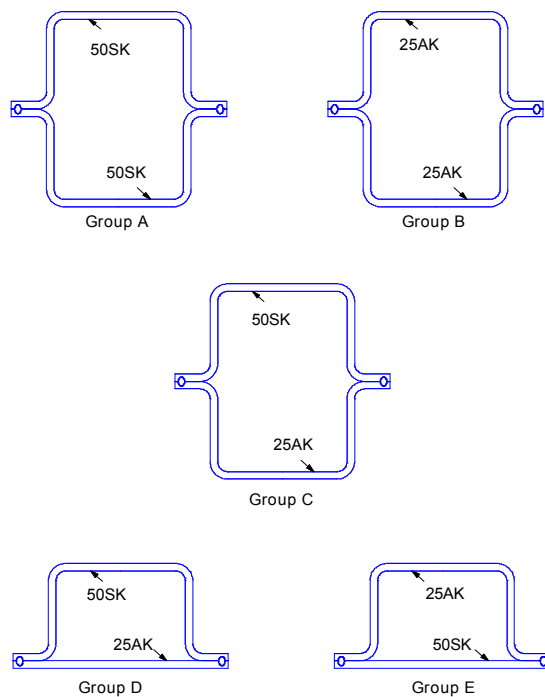


Figure 3.6.8-1 Cross sections of stub columns

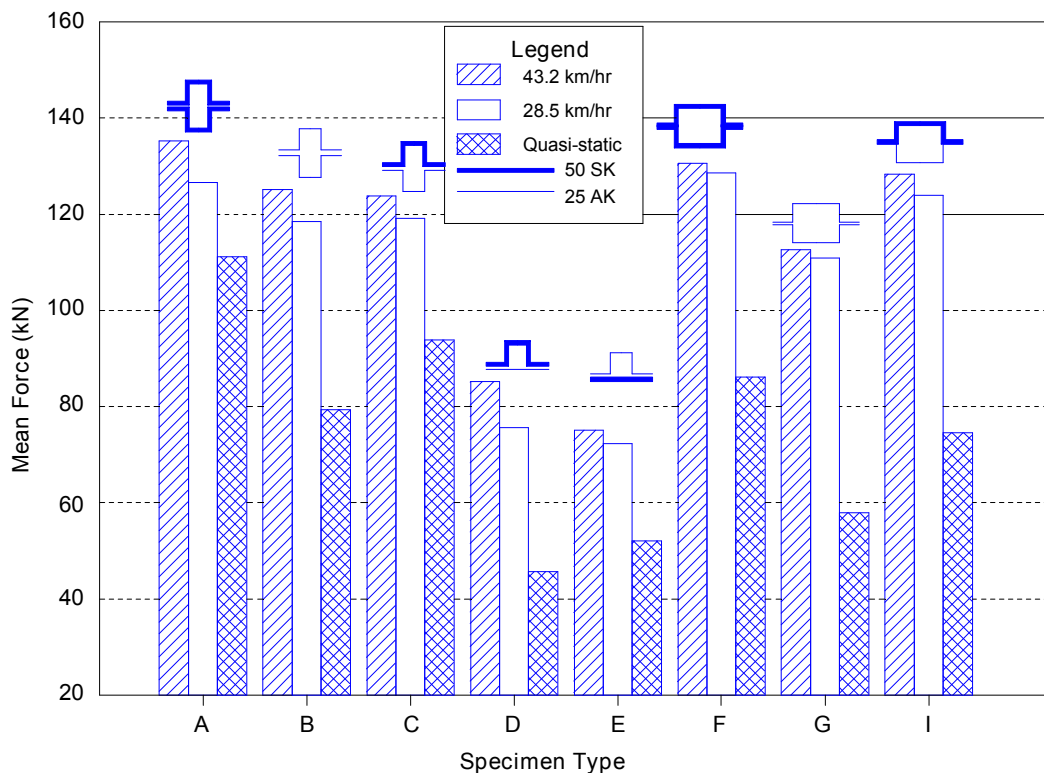


Figure 3.6.8-2 Average mean crush load comparison for stub columns

For the purpose of preliminary design, the mean crushing load of the hybrid stub columns consisting of two different materials may be estimated by using the following equations ([Reference 6](#)).

$$P_{\text{mean}} = [0.141(\alpha - 1.144) + 0.361] P_u$$

Equation 3.6.8-2



- where α = aspect ratio, $d'/b' \leq 1.14$
 b' = overall width of the stiffened flange of box-shaped and hat-shaped stub columns ([Figure 3.6.8-1](#))
 d' = overall depth of the cross section ([Figure 3.6.8-1](#))
 P_u = computed ultimate load based on the dynamic tensile stress determined by [Equation 2.13-1](#)

According to [Reference 6](#), the ultimate strength of a stub column fabricated from two different materials may be calculated by using [Equation 3.6.8-3](#):

$$P_u = (A_e)_1 (F_y)_1 + (A_e)_2 (F_y)_2$$

Equation 3.6.8-3



In the above equation, the subscripts 1 and 2 represent components in the stub column fabricated from two different materials.

The effective design widths to be used for determining the effective cross sectional areas, $(A_e)_1$ and $(A_e)_2$ are computed on the basis of the dynamic tensile stresses, $(F_y)_1$ and $(F_y)_2$, respectively. It should be noted that the yield strengths and the cross sectional areas of the two components are different.

[Equation 3.6.8-3](#), to compute the ultimate load, is based on tests of columns whose lengths were short enough to avoid overall column buckling, and both ends of the column were flat and parallel.

For more information please refer to the AISI Technical Report "State of the Art Review of Automobile Structural Crashworthiness" AU 2301 and its references.

The Auto/Steel Partnership acknowledges the contribution of Ford Motor Corporation Body and Chassis Engineering Office for the illustrations in [Figure 3.6.3-1 & Figure 3.6.3-2](#), [Figure 3.6.4-1](#) through [Figure 3.6.4-4](#), and [Figure 3.6.5-1](#) through [Figure 3.6.5-4](#).

REFERENCES FOR SECTION 3.6

1. Paluszny, A. "State-of-the-art Review of Automobile Structural Crashworthiness", American Iron and Steel Institute, June 1992.
2. Fischer, R., "Occupant Protection In Car To Car Impacts", SAE Technical Paper No. 740316 (1974).
3. Magee, C.L. Keynote Address "Design for Crash Energy Management - Present and Future Developments", The Seventh International Conference on Vehicle Structural Mechanics, April, 1988.

4. Fischer, R. and Haertle, J. "Use of Computer Modeling in New Vehicle Design", SAE Technical Paper No. 840863 (1984).
5. Schell, B.C., Sheh, M.Y., Tran, P.H., Pan, C.L. and Yu, W.W., "Impact and Static Crush Performance of Hybrid Hat Section Stub Columns", Proceedings of Automotive Body Design & Engineering, international Body Engineering Conference (M. Nasim Uddin, Ed.), September 1993.
6. Pan, C.L., Yu, W.W., Schell, B.C. and Sheh, M.Y., "Effect of Strain Rate on the Structural Strength and Crushing Behavior of Hybrid Stub Columns", Proceedings of Automotive Body Design & Engineering, international Body Engineering Conference (M. Nasim Uddin, Ed.), September 1994.
7. Fleming, T.J. and Schell, B.C., "Non-Linear Explicit Finite Element Simulation of the Dynamic Axial Crush of Double-Hat Section Columns", Proceedings of Automotive Body Design & Engineering, international Body Engineering Conference (M. Nasim Uddin, Ed.), September 1994.

3.7 DESIGNING AGAINST CORROSION

3.7.1 INTRODUCTION

In recent decades, attention has focused on body corrosion in automobiles, and significant advances have been made in the number and sophistication of corrosion-protection systems and techniques. This section examines some of the major environmental causes and categorizes the various types of corrosion that result. It highlights the broad range of countermeasures now available and briefly explores future needs.

3.7.1.1 Background

The automotive and steel industries have a long history of cooperative efforts, which have steadily improved the North American passenger vehicle. Some 50 years ago, car makers sought greater strength and durability in their vehicles and the steel producers responded by cold rolling very wide sheets of low-carbon steel, which opened the way to the greater safety of all-steel bodies. Later, better drawing steels were developed to accommodate designs with more complex body panel and fender shapes. More recently, steel producers expanded their offerings of higher-strength steels to shed pounds cost-effectively from components and assemblies for improved vehicle fuel economy.

Currently, the adoption by the major producers of high-technology methods of steel making, rolling, and annealing have resulted in the production of sheet steels with much more consistent properties.

Other cooperative efforts also have been undertaken. As road salt usage climbed in the United States and Canada, vehicle damage from corrosion increased. The auto industry and its suppliers responded with design changes and improvements in the materials used. These efforts began with galvanized steel rocker panels in the late 1950's, expanded to a broad range of coatings for other vulnerable components, and achieved an important turning point in vehicle corrosion protection. The cooperative efforts will continue as gains already achieved ([Figure 3.7.1.1-1](#)) form the basis ^{1,2} for further improvements and for "fine tuning" of protective systems and techniques through more selective - and more effective - use of each.

1995 SAE Parking Lot Survey Results

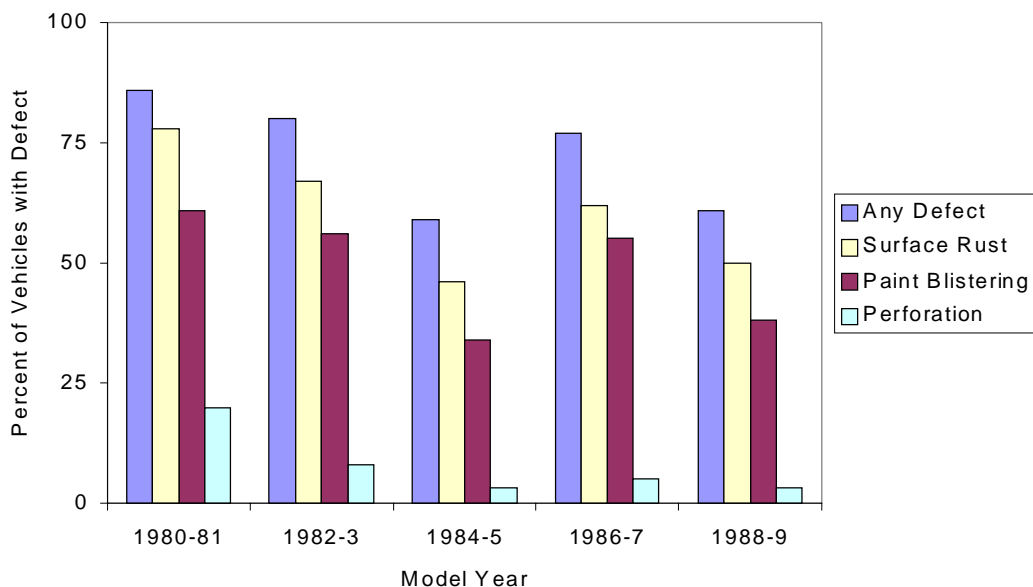


Figure 3.7.1.1-1 Corrosion of automobiles as determined by SAE parking lot surveys, showing the decrease in corrosion of cars accompanying the increasing use of coated sheet. (Plotted from data given in Reference 1)

3.7.1.2 Defining the Problem

Corrosion menaces most vehicles in the US and Canada to varying degrees. The worst car body and chassis damage occurs in the "salt belt" (Figure 3.7.1.2-1)³, an area that surrounds the Great Lakes and loops eastward through the northeastern states and the Canadian provinces of Ontario, Quebec, and the Maritimes.

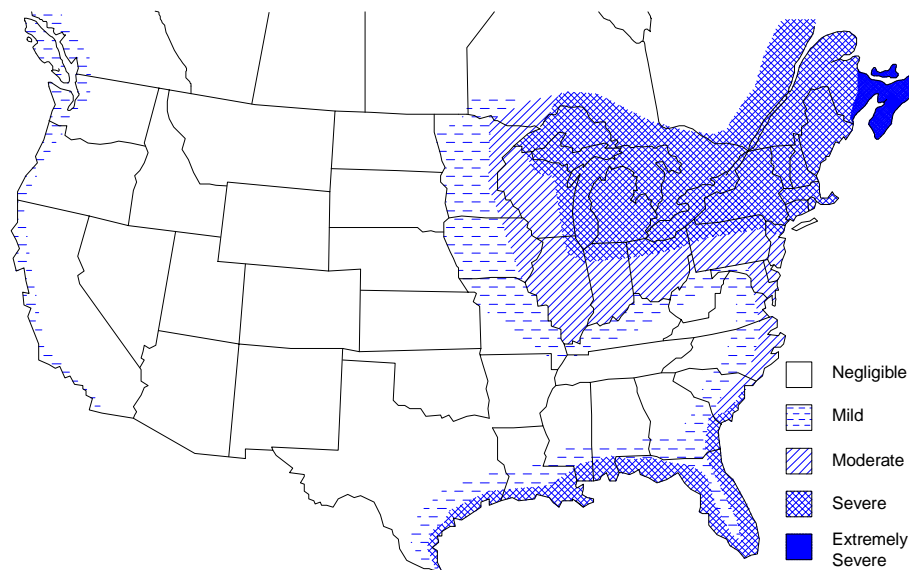


Figure 3.7.1.2-1 Vehicle corrosion environment in Canada and the United States

In this international zone, roughly 10 to 20 million tons of salt are applied to roads and streets each winter to depress the melting point of ice and snow and keep these thoroughfares open for traffic⁴. More judicious spread rates per mile have been offset by additional roads being de-iced. Today, motorists expect bare pavement all year round.

Vehicle corrosion results when lower body panels and under-vehicle components are exposed to road slush containing the de-icing chemicals⁵. The causes of corrosion, however, are not limited to wintertime activity, nor are they confined to vehicles driven in the "salt belt". Long after the snows have gone, dormant deposits of road salts on these vehicles can renew their corrosive action when rewetted by spring rains and road splash. While corrosion also occurs in vehicles in other northern states, damage usually is less severe where winter temperatures normally are too low for effective use of de-icing chemicals.

Alternative chemicals to sodium chloride are being evaluated to reduce the corrosion caused by highway de-icing salts, but they are more costly⁶.

Other environmental causes of corrosion across the country cannot be ignored. For example, air pollution in industrial centers poses a threat, particularly where levels of sulfur dioxide⁴ and chloride are high. Dust control procedures⁷ on rural roads also add to the threat in summer. And in coastal regions, year-round exposure to salt-laden spray, mist, and other airborne chemicals in combination with high humidity also can produce corrosion damage.

3.7.2 TYPES AND FORMS OF CORROSION

Vehicle corrosion assumes several different forms or types, causing damage that ranges from minor to severe. An important first step in defining and dealing with the overall problem is to classify the several forms of corrosion attack and to qualify their effects.

3.7.2.1 Uniform Corrosion

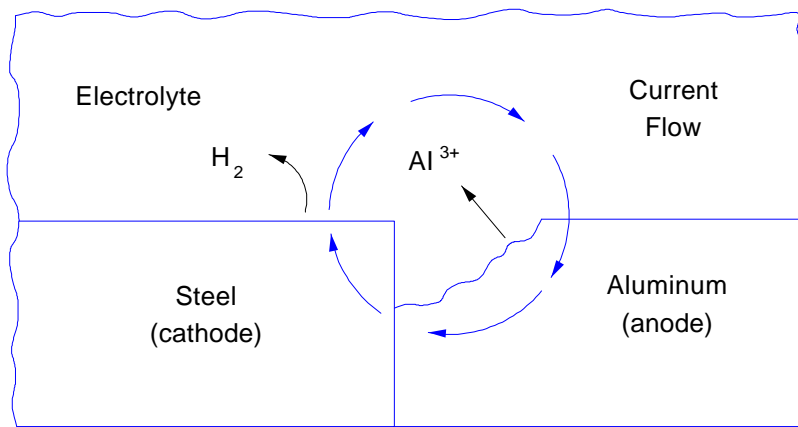
Uniform corrosion proceeds evenly over the entire exposed surface of an uncoated part and eventually causes a general thinning of the metal. It is the best known type of corrosion, but also is the least damaging. In automotive applications, uniform corrosion usually is not related to perforation or structural damage.

3.7.2.2 Galvanic Corrosion

Galvanic corrosion, sometimes referred to as two-metal or bimetallic attack, occurs when dissimilar metals are in contact in the presence of an electrolyte. The more active, or anodic, metal corrodes rapidly while the more noble, or cathodic, metal is not damaged. On the galvanic scale, aluminum and zinc are more active than low-carbon steel and, in the presence of a chloride-containing electrolyte, will corrode preferentially when in contact with steel ([Figure 3.7.2.2-1](#))^{8,9}.

This form of corrosion has had a strong influence on limiting the use of aluminum in automotive applications that would be in direct contact with steel. To prevent an aluminum-to-steel contact, isolating techniques, such as nonconductive or barrier type spacers or sealers, are required.

The galvanic corrosion mechanism also can be turned into a benefit and it is widely employed as the primary protection system for steel. A thin zinc or zinc-alloy coating on steel will corrode preferentially and this sacrificial action provides long term protection for the substrate.

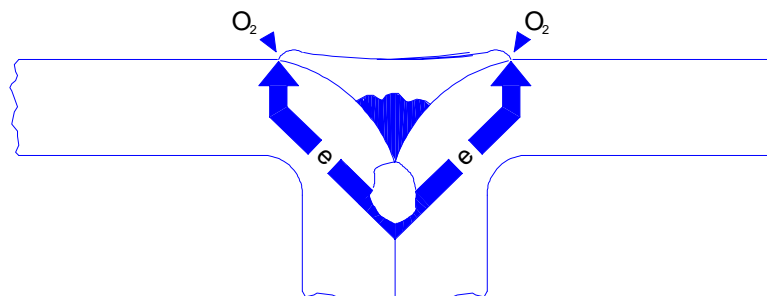


Galvanic corrosion occurs when two metals of dissimilar activity are placed in contact with one another in the presence of an electrolyte. The more active metal will react anodically and corrode in preference to the less active metal which, as the cathode, is protected.

Figure 3.7.2.2-1 Galvanic or bimetallic corrosion

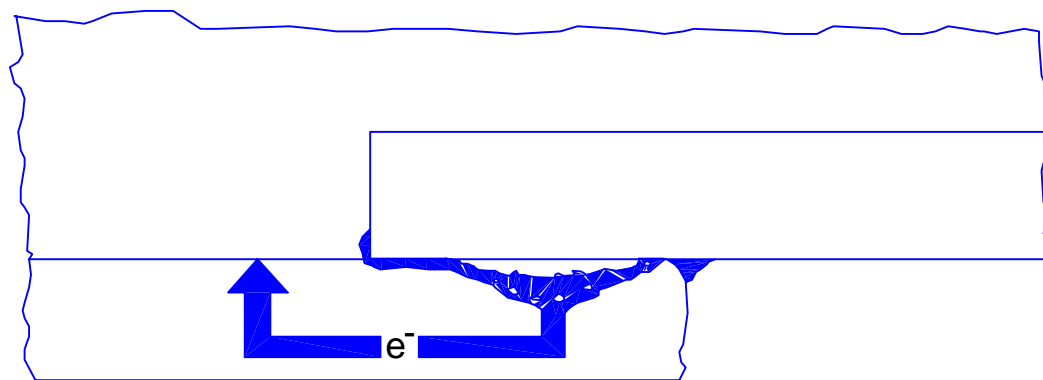
3.7.2.3 Crevice Corrosion

Crevice corrosion is the most damaging type encountered in the automobile because it's sharply focused on localized areas and usually is invisible in its early stages. The attack is swift, often resulting in unexpected or premature failure. Crevice corrosion attack is usually associated with small volumes of stagnant solution or electrolyte trapped in holes, on gasket surfaces, at joints (Figure 3.7.2.3-1 and Figure 3.7.2.3-2)⁸ under fasteners, and in surface deposits or poultices (Figure 3.7.2.3-3).⁸



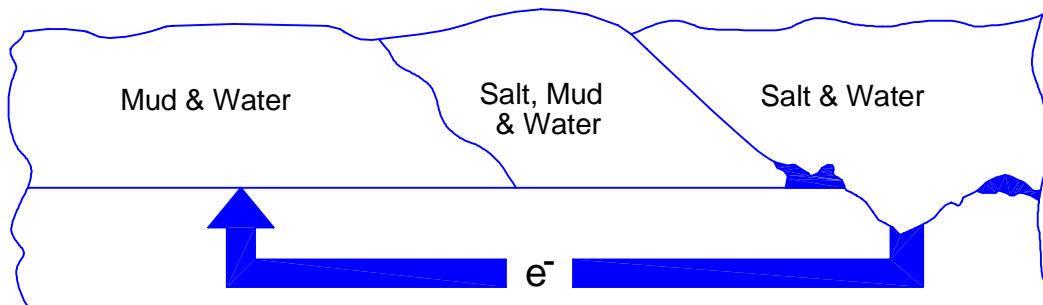
Crevice corrosion is caused by a gradient between the oxygen at the surface of the electrolyte and oxygen-starved electrolyte at the bottom of the crevice. Typical of weldments, sheet-metal joints, and rough surfaces where water may be trapped, the oxygen gradient also causes a rough microfinished surface to corrode faster than a smooth surface.

Figure 3.7.2.3-1 Crevice corrosion at weld joint



Crevice corrosion also can occur between tightly sealed joints where the concealed metal surface is oxygen starved and electrolyte may seep between irregularities in the mating surfaces. This condition also occurs where moisture-bearing materials (such as felt) are in contact with the steel.

Figure 3.7.2.3-2 Crevice corrosion at lap joint

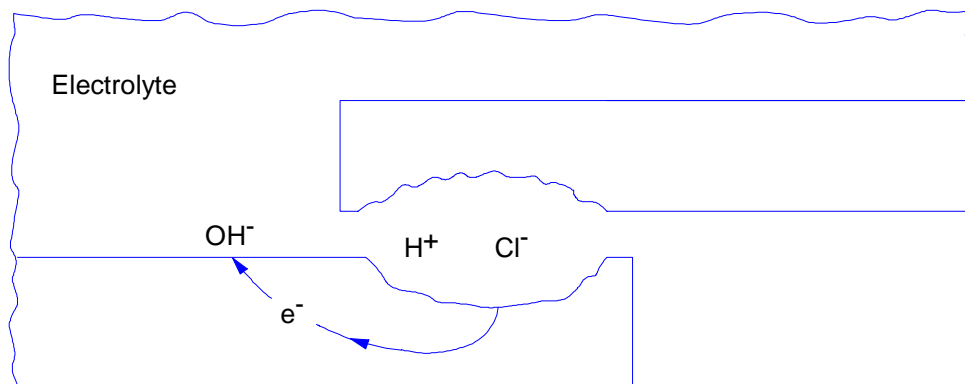


Electrolyte composition gradients are probably the most common cause of corrosion. Clumps of mud frequently collect under car fenders. The varying concentrations of salt and water encourage corrosion.

Figure 3.7.2.3-3 Poultice corrosion

The mechanism of crevice corrosion will depend upon the type of metal and the conditions of exposure. Sometimes crevice corrosion can be explained on the basis of differences in metal ion concentration between the crevice and surrounding surfaces. Often, it is described as oxygen concentration cell corrosion, caused by oxygen availability at the surface of the electrolyte and oxygen starvation at the surface of the metal.

Other studies^{10, 11} have shown that although metal ion and oxygen concentration differences exist, the corrosion mechanism is more complex and can be explained by acid formation within the crevice. Although oxygen is depleted in the crevice, metal dissolution continues because the excess of positively charged metal ions is balanced by the migration of anions (especially chloride ions) from the bulk solution into the crevice ([Figure 3.7.2.3-4](#)).⁸ The metal chloride concentration in the crevice increases. Hydrolysis of the metal chloride follows and the pH falls to approximately 3 within the crevice¹². This sets up an autocatalytic anodic process in shielded areas.



Crevice corrosion showing acid formation and increased chloride ion concentration within the crevice.

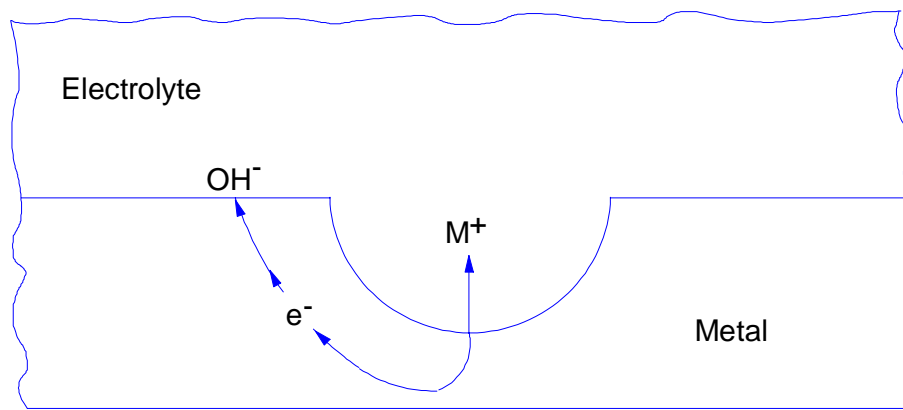
Figure 3.7.2.3-4 Crevice corrosion at lap joint

Crevice corrosion remains a major problem because of current unitary manufacturing techniques where the body is a mass of box sections and joints¹³. It is almost impossible to eliminate the minute cracks between joined surfaces that are prime sites for crevice attack. The severity of crevice corrosion is evidenced by widespread inner-vehicle and under-vehicle corrosion and its resulting perforation of body panels and chassis components. This is caused by mud packs or poultices in a predominantly chloride medium.

Metals or alloys that rely on passive layers or oxide films for corrosion protection, for example aluminum alloys and stainless steels, are particularly susceptible to crevice attack in chloride media. The high concentration of chloride or hydrogen ions destroys the films, resulting in increased metal dissolution rates. These materials can be alloyed to improve their crevice corrosion resistance. In addition, designing to minimize crevices and maintenance to keep surfaces clean are used to combat the problem.

3.7.2.4 Pitting Corrosion

Pitting corrosion is a localized attack, usually caused by chlorides. The mechanism governing pit growth is similar to that of crevice corrosion. In fact, pits are "mini" crevices which usually have diameters equal to their depth. They can occur so closely spaced that they give the appearance of a roughened surface. This is a self-initiating form of crevice corrosion, in that the corrosion process creates the pit (or crevice) which propagates, at an accelerated rate, and eventually perforates the metal. Initiation of pits usually results from metal inhomogeneities, breaks in protective films, surface deposits, defects, or imperfections. (Figure 3.7.2.4-1).⁸



Similar to crevice corrosion, pitting corrosion occurs at localized areas where oxygen has been depleted, pH has become lowered and chloride has become enriched.

Figure 3.7.2.4-1 Pitting corrosion

In summary, all four main types of corrosion occurring on an automobile involve destruction of the metal through reaction with the environment, and all are electrochemical in nature and require the presence of water. The presence of chlorides, as in de-icing salts, simply accelerate the attack.

3.7.3 CORROSION OF PAINTED STEEL

Corrosion of auto body components is usually classified according to initial location and direction of attack. When attack initiates at an interior surface or within a closed or semiclosed part, it is termed "perforation", or "inside-out" corrosion. Corrosion that initiates on visible exterior surfaces, usually at nicks or scratches in the paint, is called "cosmetic", or "outside-in" corrosion.

3.7.3.1 Perforation Corrosion

Perforation corrosion can lead to serious structural damage that may go undetected until it becomes visible on the external surface after penetrating the metal from within. Repair can be difficult and costly, often involving replacement of entire panels and sometimes requiring fabrication of new attachments or other custom work.

Much of the problem is caused by road debris collecting in packs or poultices, which are trapped in pockets and corners and on ledges and vertical surfaces ([Figure 3.7.3.1-1](#)).⁸

The poultices hold the salty electrolyte in intimate contact with the metal. This, and the lack of rapid runoff and thorough air-drying of the metal, accounts for corrosion occurring on vertical and upper interior surfaces. Plugging of drain holes is another cause of perforation corrosion. This leads to an accumulation of a damp, salty poultice in the lower interior of doors, rocker panels, and tailgates that produces corrosion and eventual penetration of the sheet.

A major factor contributing to perforation corrosion is the inherent difficulty in adequately cleaning, phosphating, and applying primer to interior surfaces of body assemblies. By insuring

that all internal surfaces are completely protected, the use of precoated sheet has proven to be particularly effective in preventing perforation corrosion.

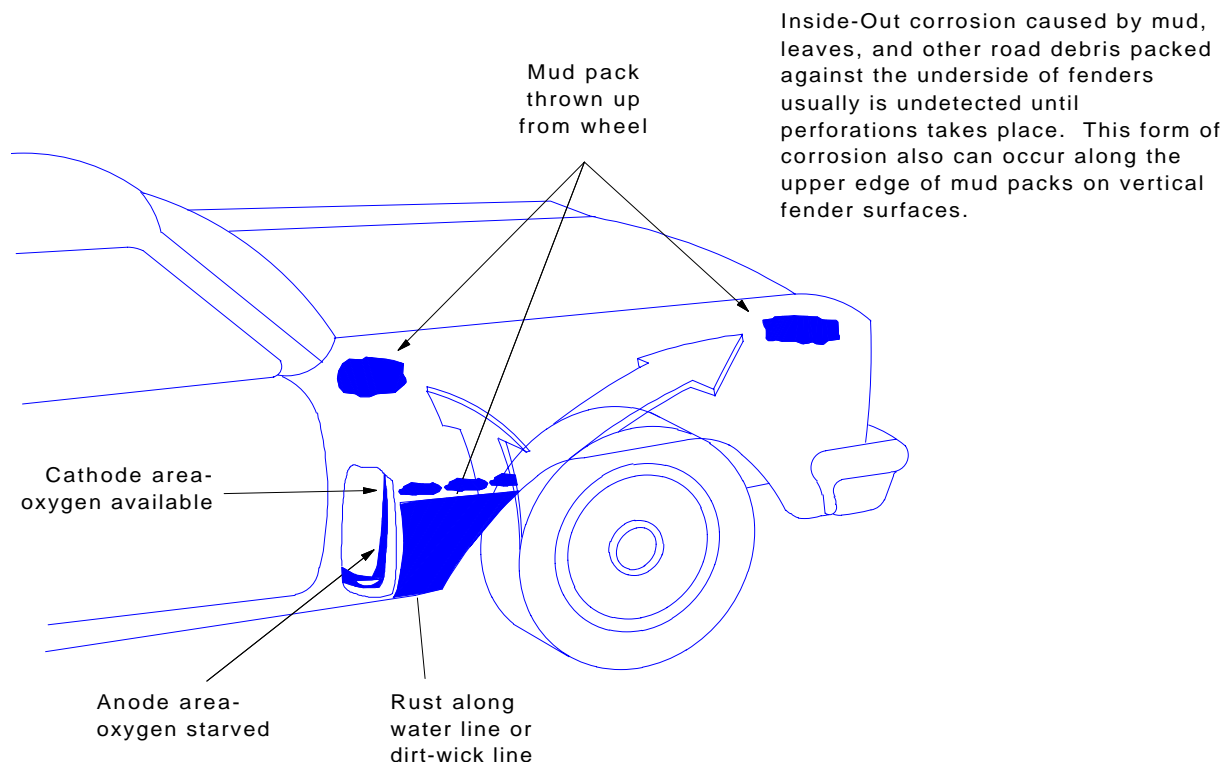


Figure 3.7.3.1-1 Inside out Corrosion

3.7.3.2 Cosmetic Corrosion

Cosmetic corrosion begins at points of exterior damage to the paint system that locally expose the steel substrate. When bare metal is exposed to the environment, the main concern is poor appearance due to corrosion products, particularly red rust and stain, and the lateral spread of paint damage resulting from undercutting and blistering.

Scab Corrosion

Scab corrosion is a term applied to cosmetic corrosion when it occurs at exterior joints and crevices that trap moisture, dirt, and salts. Typical locations for this kind of corrosion are at the contact area between window moldings and cowl or tulip panels. Scab corrosion is not necessarily a galvanic reaction (caused by dissimilar metals), as it occurs frequently at joints of similar metals. Scab corrosion is minimized by use of a steel sheet with a zinc or zinc alloy coating on the exterior surfaces.

Filiform Corrosion

Filiform corrosion is a type of cosmetic corrosion that occurs under paint films on metallic surfaces. Although not immediately apparent, the attack appears as a network of threadlike filaments under the coating. It does not damage or destroy components, but it does have an adverse effect on appearance. Filiform generally occurs only within a range of relative humidity of about 55-85%.¹⁴

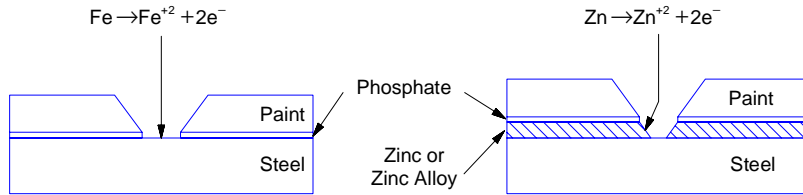
3.7.3.3 Mechanisms of Paint Undercutting

Mechanisms of paint undercutting have been the subject of considerable current research.^{15, 16}

Figure 3.7.3.3-1 shows some of the factors involved during the undercutting corrosion of painted, cold-rolled, zinc, and zinc-alloy coated steel sheet at areas of localized paint damage.

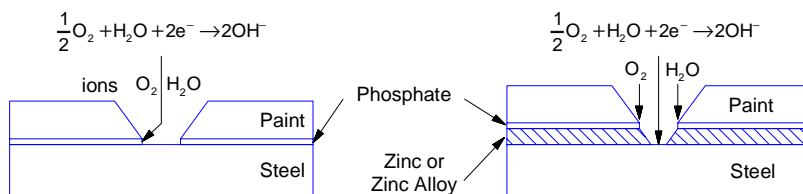
Anodic Reaction

Corrosion begins at exposed metal in the presence of electrolyte. Iron (in uncoated steel) or Zn (in precoated steel) gives up electrons to the base metal and ions are freed to the electrolyte. In zinc and zinc-alloy coated material, the exposed steel is protected galvanically.



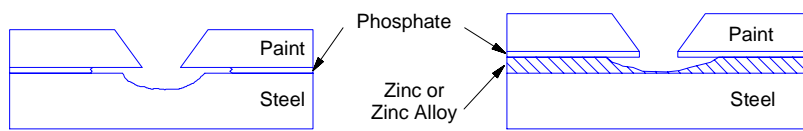
Cathodic Reaction

Hydroxyl ions are generated as a result of the cathodic reaction for both materials. With uncoated steel, OH⁻ is produced on the steel surface.



Mode of Attack

With uncoated steel, the exposed steel substrate is attacked, while the phosphate film beneath the paint layer is dissolved by the high pH solution formed by the OH⁻ ions. For zinc-coated steel, the coating dissolves the paint film and galvanically protects the exposed steel. Under very wet conditions, cathodic delamination may occur on coated surfaces.



Corrosion Products

In steel, iron oxide precipitates as a result of a series of chemical reactions and forms an unsightly red rust deposit. Zinc forms ZnO or Zn(OH)₂ or zinc hydroxy chloride depending on the type of corrosive environment. The white zinc corrosion product is less objectionable in appearance than red rust and also acts to protect the underlying steel.

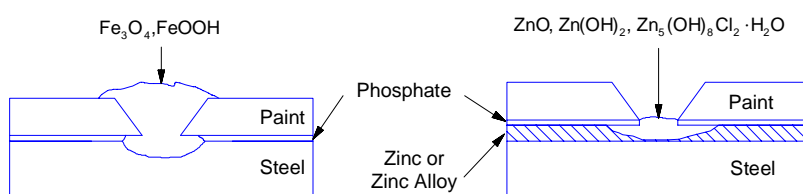


Figure 3.7.3.3-1 Corrosion processes at damaged paint site

In the case of cold-rolled sheet, exposure to wet conditions leads to anodic dissolution of the steel at the exposed area with the formation of unsightly red rust. The migration of water, oxygen, and ions through and under the paint film causes a cathodic reaction to take place beneath the paint adjacent to the damaged region. Electrons flow through the steel to balance the separated anodic and cathodic reactions. The high pH solution that is developed at the steel/paint interface causes a loss of paint adhesion, which is termed cathodic disbonding. Depending on the types of

paint system, pretreatment, and substrate, cathodic disbonding can proceed by one or more of several possible mechanisms, including:

1. Saponification of the paint resin, a degradation of the polymer by hydroxyl ions,
2. Dissolution of the phosphate layer, or
3. Reduction of an oxide layer on the metal surface.

During subsequent exposure to drying conditions, oxygen becomes available for increased cathodic activity at the area of initial damage, allowing anodic dissolution to spread into the delaminated region, thus leading to further attack by anodic undermining. Formation of voluminous rust beneath the film may lead to further damage caused by mechanical wedging.

Repeated exposure to wetting and drying cycles leads to a continuing attack of the steel substrate, formation of red corrosion products, and loss of paint adhesion.

With zinc and zinc-alloy coated steel, exposure to wet conditions does not result in rusting at the damaged site because of the sacrificial galvanic action of the zinc coating. In this case, as shown in [Figure 3.7.3.3-1](#), the zinc coating corrodes preferentially, acting as the anode in a galvanic couple, with the exposed steel acting as the cathode. While the steel is thus protected, there is some loss of paint adhesion due to anodic undermining as the zinc coating is consumed. There may be further loss of adhesion in advance of the dissolution front owing to cathodic disbonding.

Zinc ions that are produced by dissolution of the coating migrate to the exposed steel surface where they combine with hydroxyl ions from the cathodic reaction, thus forming a white precipitate. The white precipitate is generally less objectionable in appearance than red rust. It also serves to inhibit the cathodic reaction in this region and slows the rate of zinc dissolution. Red rust will eventually develop on the exposed steel once the available zinc in the coating is consumed.

During intervals of dryness, both anodic and cathodic reactions are halted and the spread of paint damage is stopped. This serves to explain why the degree of paint delamination for zinc and zinc-alloy coated steels exposed to actual service conditions is less than that of cold-rolled steel, even though the results are opposite when these materials are tested under conditions of continual wetness, such as in a salt-spray test.

3.7.4 PRECOATINGS

Application of a metal coating to both sides of the sheet steel for automobile body or chassis parts is one of the most effective methods of combating corrosion².

Since the 1980's, there has been a major increase in the use of pre-coated steels in the North American automobile. The pre-coated sheet steels currently available are listed in [Table 3.7.4-1](#) with descriptions of the pre-coatings and typical automotive applications.

Table 3.7.4-1 Precoated Steel Sheet for Automobiles

Coating	Description	Typical Applications
Hot-Dip Zinc	Galvanized sheet, produced by the hot-dip process. Available with regular spangle, minimized spangle and extra smooth surfaces. Wide range of coating masses available. Typical coating mass are 60-100 g/m ² .	Inner and outer body panels, structural components.
Hot-Dip Zinc-Iron	Galvannealed sheet. Produced by heat treating hot-dip galvanized steel to form a zinc-iron alloy coating containing about 10% iron. Typical coating masses are 40-60 g/m ² .	Inner and outer body panels, structural components.
Hot-Dip Aluminum-Silicon Alloy	Type 1 aluminum-coated. Coating is an aluminum-silicon alloy containing 8 to 12% silicon. Coating masses are class 25 (38 g/m ²) and class 40 (60 g/m ²).	Exhaust systems, catalytic converters, chassis components.
Hot-Dip Aluminum-Zinc Alloy	Galvalume sheet. Coating is an alloy of 55% aluminum, 1.5% silicon, balance zinc. Typical coating mass is 75g/m ² .	Exhaust systems, air cleaner covers, core plugs, brake shields, floor pan covers.
Hot-Dip Lead-Tin Alloy	Terne is a lead-tin alloy containing 3 to 15% tin with a wide range of available coating masses. Hot dipping after flash electrodeposition of 1 to 1.5% nickel produces nickel terne.	Fuel tanks, fuel lines, brake lines, radiator and heater components, air cleaners.
Electroplated Zinc	Pure zinc coatings produced by electrodeposition. Range of coating masses available. Current use includes 30 to 100 g/m ² . Typical costing masses are 60 and 70 g/m ² . Available in one or two-side and differentially coated.	Inner and outer body panels.
Electroplated Zinc-Iron Alloy	Electrodeposited zinc-iron alloy coating containing 10 to 20% iron. Typical coating masses are 30-50 g/m ² .	Inner and outer body panels.
Electroplated Zinc-Nickel	Electrodeposited zinc-nickel alloy coating containing 10 to 14% nickel. Typical coating masses are 20 to 40 g/m ² .	Inner and outer body panels.
Electroplated Tin	Tinplate. Cold rolled sheet with a thin electrodeposited tin layer.	Oil filter and heater components.
Organic-Metallic Composite	Proprietary weldable organic coating and pretreatment applied by roll coating, usually to one side, over metallic-coated (usually electrodeposited) sheet. Typical combinations are 1 to 2 µm organic over zinc-nickel alloy, and a 5 - 10µm zinc-rich organic over zinc. Metallic coating can be one or two-side, but is usually one-side to provide barrier protection to the interior surfaces of outer body panels.	Inner and outer body panels, fuel tanks.

The principal precoated steels used in automotive applications today are metallic coated sheets, typically of either pure zinc or zinc alloy compositions. From 1981 to 1996, the shipments of coated sheet steel for North American consumption have shown a dramatic increase.¹⁷ See Figure 3.7.4.4-1

Precoated steels are generally characterized by a coating mass designation. In general, corrosion resistance increases with coating mass¹⁸.

3.7.4.1 Hot Dipped Coated Steel

Hot-dip coatings are produced by a continuous process of immersing steel strip into a molten bath of the desired coating metal. The hot-dip process is currently the most cost-effective way to deposit heavy, corrosion-resistant coatings on a steel substrate. Recent advances in the production of uniform, lighter hot-dip coatings have made this process more attractive for exposed quality auto body panels. During the 1990's, steel companies throughout the world greatly increased their capacity to produce high quality coated sheet by installing modern, high-speed hot-dip coating lines.

The types of hot-dip coated sheet steels for applications in the automotive industry for body panels include pure zinc coatings and zinc-iron (Galvanneal) diffusion coatings.

Pure Zinc Coatings

Pure zinc coatings are available for automotive use with coatings ranging from approximately 20 to 160 g/m² per side. Heavier pure zinc coatings give the best galvanic or sacrificial corrosion resistance to cold-rolled steel substrates. Two-side hot-dip zinc-coated steels impart sacrificial protection from red rust to the exposed surface (cosmetic corrosion resistance) in applications such as rocker panels; and because hot-dip products are available in heavier coating masses, they are particularly suited to the inner surface of exterior body panels to prevent perforation corrosion.

Zinc-Iron (Galvanneal) Diffusion Coatings

Heating the strip immediately following its withdrawal from the zinc-coating bath produces zinc-iron coatings. This annealing process causes iron from the steel substrate to diffuse into the zinc coating. This results in an alloyed coating composed of approximately 10% iron (balance zinc). These coatings usually range in coating mass from 30-60 g/m².

Zinc-iron coatings provide less sacrificial protection of exposed steel than pure zinc coatings; however, alloying zinc with iron lowers the corrosion rate of the coating. Zinc-iron alloy coatings are also more weldable. They are suited for exterior skin panels, inner panels, and structural components. Hot-dipped coated steels for use in automobile components other than body panels include aluminum-coated steels (type 1), aluminum (55%)/zinc, zinc/aluminum (5%), long terne, and nickel terne.

Aluminum-coated steels (Type I)

Aluminum-coated steels (Type I) contain 8-12% silicon in the coating. They have enhanced high-temperature corrosion performance and are primarily used for making parts of the automotive exhaust system, including intermediate pipes, muffler parts, and tail pipes. Aluminum-coated steels are also used for some structural components.

Aluminum (55%)/Zinc

Aluminum (55%)/Zinc-coated steels have similar applications involving high-temperature corrosion resistance. Typical applications include heat shields, mufflers, and underhood parts.

Zinc/Aluminum (5%)

Zinc/Aluminum-coated steels are claimed to offer some ductility and corrosion resistance advantages over pure zinc coatings.

Long Terne

Long Terne-coated steel has a coating of lead alloy containing nominally 8% tin. It protects against corrosion in gas tanks, fuel lines, and brake lines and does not contaminate gasoline or brake fluid. Less active than the steel substrate, it does not provide galvanic protection if the coating is penetrated. Nickel terne-coated steel includes an electrolytic flash coating of nickel (1 to 1.5 g/m²) underneath a conventional lead/tin coating for enhanced corrosion resistance. The use of terne is decreasing because of concerns about the effects of lead on the environment.

A variation of long terne-coated steel employs a subsequent prepainted organic coating on each surface for some fuel tanks. The outer surface has a zinc-rich organic coating to provide added exterior corrosion protection, while the inner surface has an aluminum-rich organic coating to augment the lead/tin coatings resistance to gasoline, and low concentrations of methanol and ethanol containing fuels.

3.7.4.2 Electroplated Steel

Steel sheet with an electroplated metallic coating is widely used for outer skin auto body panels because of enhanced coating thickness control, appearance, formability, and weldability. For production of automotive sheet steel, electroplating consists of a continuous, relatively low-temperature process in which a negatively charged steel strip is passed between positively charged anodes. Metallic ions of the desired coating elements, in an electrolyte solution, are reduced at the steel strip thereby plating the surface.

Pure Zinc Coatings

Electroplated zinc coatings range from approximately 20 to 100 g/m² per side for automotive body panel use. For outer body panels, 60 g/m² is the most popular.

Zinc Alloy Coatings

The most commonly produced zinc alloy coatings are zinc-iron (10 to 20% Fe) and zinc-nickel (10 to 14% Ni). These coatings are typically supplied for automotive applications in coating masses ranging from 20 to 50 g/m². The advantages claimed for the zinc-alloy coating systems include better weldability and paint adhesion.

Several other binary and tertiary zinc-based alloy coatings for automotive use have been reported in the literature; however, none is being used extensively on commercial vehicles.

Duplex Coatings

Duplex coatings are designed to provide two-layer interaction. A thick bottom layer provides the bulk of the corrosion protection to the substrate, while the top layer, generally a flash coating (0.5 to 5 g/m²), enhances other desirable properties for automotive body sheet applications, such as weldability, paintability (cratering resistance), formability, and surface appearance. Examples of duplex coatings for automotive applications include 80 to 90% iron zinc over zinc-iron, and chrome-chrome oxide layers over pure zinc.

3.7.4.3 Organic Precoated Steel

For many years, Zincrometal (a registered trademark of Metal Coatings International), a weldable two-layer, one-side primer consisting of a zinc-containing chromium-oxide base layer with zinc-rich organic top layer on cold-rolled steel, was used extensively for making outer skin panels for automobiles. It provides enhanced passivation and corrosion protection from perforation corrosion and limited sacrificial protection to the substrate through the use of metal

powders in the organic layer. However, the need for better corrosion resistance and stamping performance led to the decline of Zincrometal in favor of two-side metallic coated steel sheet.

More recently, a variety of thin-film organic treatments, including zinc-rich primers, organic composites, and organic silicate composites, have emerged for use over zinc and zinc-alloyed coated sheet. These usually involve a treatment with a chromate corrosion-inhibiting layer and either a thin (5-10 μm) zinc-rich organic or a very thin (1-2 μm) clear organic layer.^{19,20} The organic metallic-coated sheet steels were developed primarily for use in unexposed automotive applications. In these applications, additional corrosion protection is desired because full electrocoat primer coverage is often difficult to achieve due to inherent difficulties of cleaning and phosphating of interior surfaces and limited access of the electrocoat primer. Additionally, it is believed that the use of an organic layer will permit a decrease in metallic coating thickness while still providing equivalent corrosion protection.

3.7.4.4 Precoated Steel Usage

Existing and projected precoated steel usage varies in the three main automobile producing areas in the world²¹.

Japan

The choice of corrosion protection used in Japan differs with the individual manufacturer. The most common automotive materials include:

1. Hot-dip zinc-iron alloy (galvanneal)
2. Electroplated zinc-nickel
3. Organic composite coatings over zinc-nickel
4. Electroplated zinc
5. Electroplated zinc-iron duplex (high iron flash topcoat on one side only, mainly for exposed parts)

Coating masses generally range from 15 to 45 g/m².

Incentives for the Japanese auto makers to use zinc-alloy coatings of relatively low coating mass included welding equipment limitations and the high cost of electricity in Japan which made heavy coatings expensive. However, recent trends indicate that the coating masses for automotive steel in Japan are gradually increasing due to the need to provide added corrosion protection for the highly corrosive environments encountered in many North American markets. More future materials emphasis is being placed on exposed quality hot-dipped coated sheet, such as galvannealed coatings, to afford greater corrosion protection.

Europe

European car makers use a wide variety of methods to minimize corrosion damage and there is no consistent pattern of precoated steel usage. A few manufacturers have gone to an "all galvanized concept", while others use very little precoated steel, relying on corrosion resistance from organic coatings and waxes. Nevertheless, manufacturers have generally increased their consumption of coated sheet steel in recent years to where coated sheet accounted for about 43% of the mass of European auto bodies in 1987. This trend is expected to continue. The types of coated sheet products in use include:

1. Hot-dip zinc for unexposed parts

2. Electroplated zinc for exposed parts
3. Electroplated zinc-nickel
4. One-side zinc-rich prepainted electroplated zinc

The use of Zincrometal has declined and there are no major use of galvannealed sheet.

North America

The corrosion protection trend among domestic North American auto makers is widespread application of two-side precoated steel (90 percent of the body-in-white). The corrosion protection requirements are fairly well established by each manufacturer for the near future. Thus coated sheet product selection has emphasized manufacturability; i.e., forming, joining, and painting criteria. The coated sheet products used by the domestic North American manufacturers include both hot-dip and electroplated pure zinc and zinc-iron coatings in masses of 40 to 100 g/m² per side. The product mixes of the "transplant auto makers" are generally influenced by their parent company.

Future trends include reducing some coating masses, using organic films to enhance corrosion protection of metallic coated sheet products, and increasing applications of galvannealed sheet.

The current and future higher usage of precoated steel by the North American manufacturers is a reflection of the philosophy that use of such materials is good technically, and a cost-effective way of providing durability in a highly corrosive environment ([Figure 3.7.4.4-1](#), [Figure 3.7.4.4-2](#), and [Figure 3.7.4.4-3](#)).

Coated sheet products used by the North American auto makers are generally:

1. 60 g/m² electroplated zinc for exposed panels
2. 60-70 g/m² hot dip zinc for unexposed panels
3. 40-50 g/m² hot-dip zinc-iron alloy (galvanneal) for both exposed and unexposed panels

US SHIPMENTS OF COATED SHEET

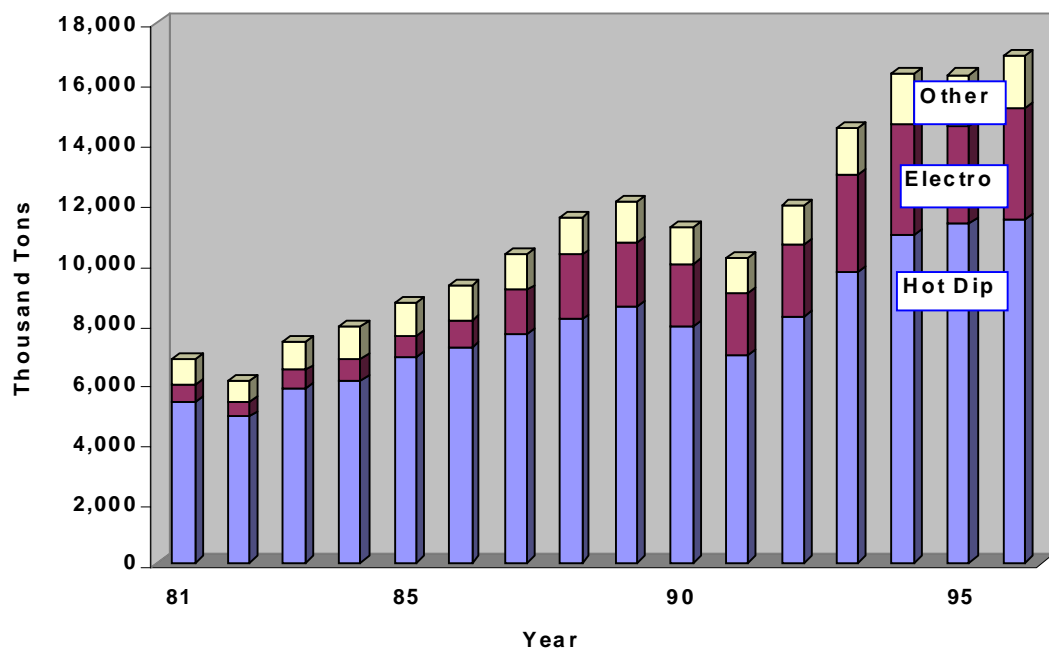


Figure 3.7.4.4-1 U.S. shipments of coated steel sheet products, showing the increase in use of coated sheet steel products resulting by the automotive industry switch from bare cold rolled to coated sheet. (Plotted from data given in [Reference 22](#))

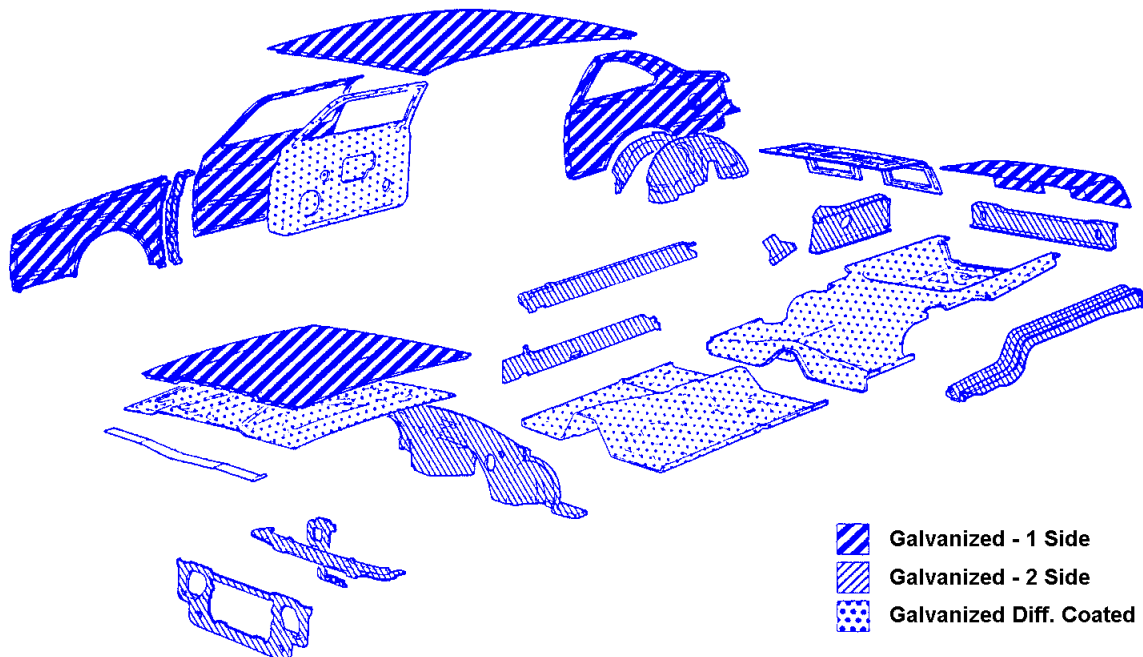


Figure 3.7.4.4-2 1989 T-Bird/Cougar body corrosion protection precoated and non-ferrous

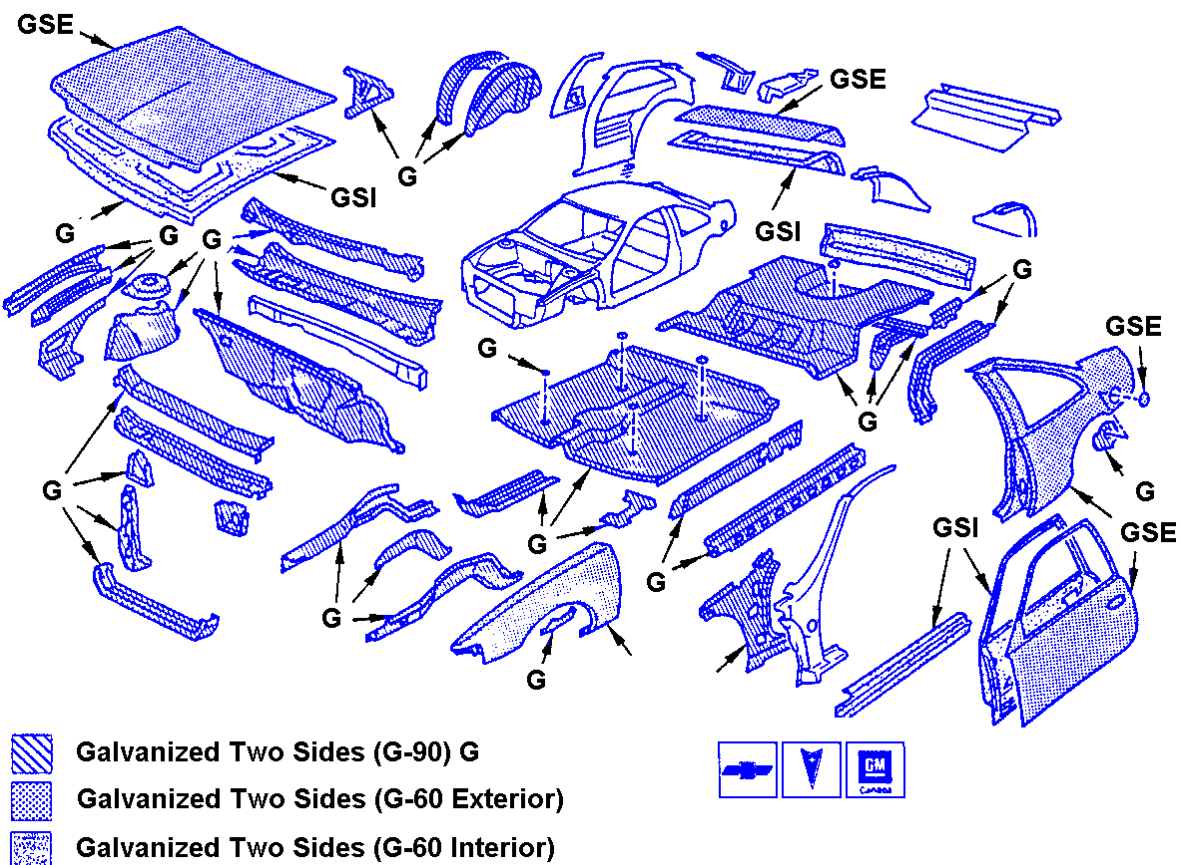


Figure 3.7.4.4-3 1990 GM-10 Coupe precoated metals

3.7.5 ASSEMBLY COATINGS FOR CORROSION PROTECTION

Several different types of coatings, such as zinc rich primers, waxes, and seam sealers, have historically been applied, after fabrication and during assembly, to provide supplemental corrosion protection of automobiles. Most of these coatings functioned by excluding the corrosive environment from the substrate; thus the protection provided was strictly barrier. The purpose of these coatings was to provide additional rather than sole protection against corrosion. The extensive usage of sacrificial galvanized steel has greatly diminished the need for many of these coatings.

Several different types of post coatings have been used successfully, but now have limited usage due to the increased use of galvanized steels.

Zinc-Rich Spray Primer

Zinc-rich spray primer is generally classified as a paint; however, it contains approximately 90% zinc by mass and should not be confused with the usual primers, surfacers, and topcoats used in painting an automobile. This material was applied to joints and interior surfaces after fabrication and prior to assembly. The industry had used this material as a spray-on 40 micron-thick protective coating for local protection during the last 25 years.

Weld-Through Coatings

Weld-through coatings were developed as an alternative material to the zinc-rich spray paint. They are gummy and weldable, and provide excellent protection even when applied to oily steel substrates. Welding fumes and handling of coated parts are disadvantages of this material.

Corrosion-Preventive Wax

Corrosion-preventive wax is a spray-on coating, applied by wands or automation, usually after painting. It is a solvent-based, perhaps aluminum-filled (for visibility) wax-containing corrosion inhibitor. Applied to a minimum dry film thickness of 50 microns, it develops a tack-free film after air curing that provides additional barrier corrosion protection in body cavities, seams, and hem areas. Typical applications have been the inside of the lower front fender, inside of doors, rear wheelhouse joints, and lower-quarter panel joints.

Two other types of assembly coatings that are still being used in numerous applications are chip resistant coatings and sound deadeners.

Chip-Resistant Coatings

Chip-resistant coatings are applied under the topcoat to the areas of the vehicle subject to stone chipping and road blast. They can be vinyl, urethane, or powder-spray coatings. The vinyl materials are applied to inner wheelhouse panels and lower exterior body side, and are used at about 400 microns thickness. The urethane and powder materials are spray applied and are used on the more visible portion of the vehicle, as well as on the leading edge of hood panels. Typical thicknesses used are 100 microns for the liquid urethane coatings and up to 250 microns for powder coatings.

Sound Deadeners

Sound deadeners are used primarily for sound deadening and not corrosion protection. Typically they are spray applied after paint, at about 800 microns thickness, on the inside of door panels, quarterpanels, wheel wells, and the tunnel area surrounding the driveshaft. Historically, these materials have deteriorated with age, hardened, cracked, or had poor adhesion, thus providing numerous corrosion sites. Newer versions of these materials, which include water-borne products, have improved adhesion, as well as greater resistance to cracking and flaking, than previously used materials. An example of current assembly coating on a vehicle is shown in [Figure 3.7.5-1](#).

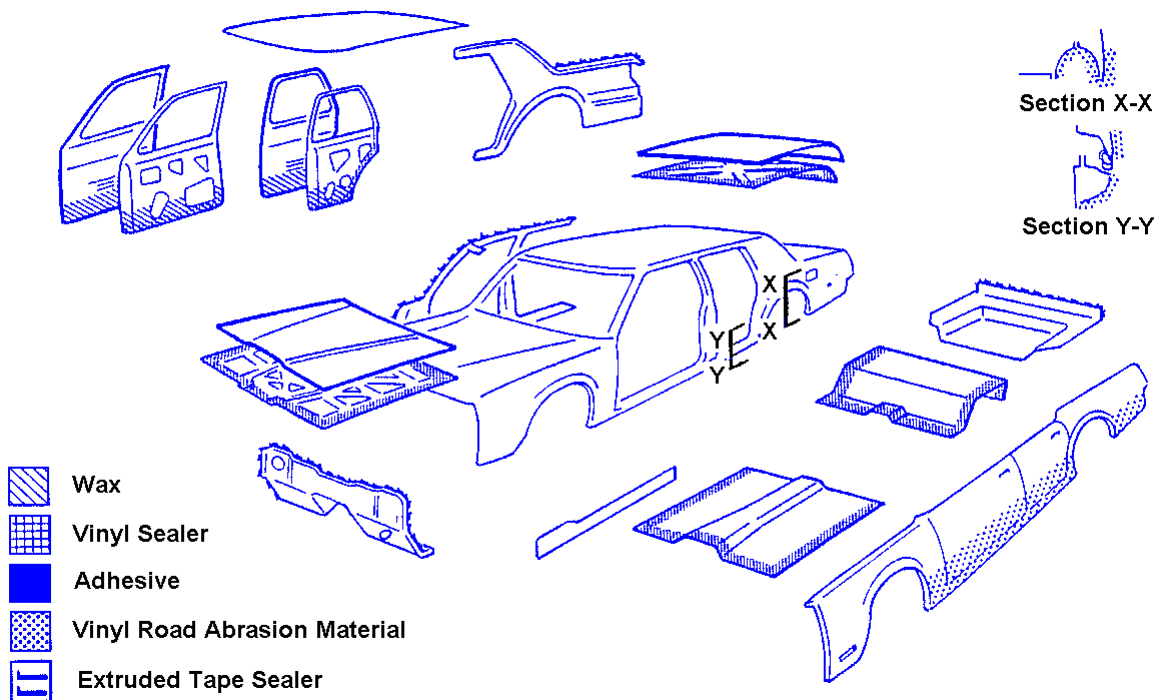


Figure 3.7.5-1 Assembly coatings

3.7.6 PHOSPHATE PRETREATMENT

The zinc phosphate pretreatment process reacts with the metal surface to form a nonmetallic crystalline coating^{23, 24, 25}. The coating is resistant to alkaline corrosion by-products and inhibits underfilm corrosion²⁶. It also serves as a nonconductive insulating layer to isolate corrosion sites and, by its structure, provides physical anchoring sites for the primer applied over it. Zinc phosphate coatings have been used successfully for years by the automotive industry to enhance the adhesion of organic finishes to the metal and to achieve superior corrosion resistance with these finishes. Phosphate coatings representing the latest technology will contain zinc, nickel, iron, and manganese as part of the chemical composition²⁷. Phosphate baths have also been formulated to apply coatings equally well to all the different metallic surfaces represented in the car body today.

3.7.6.1 Zinc Phosphate Coatings

The zinc phosphate coating can be applied to the car body at the assembly plant in either a spray or an immersion processing stage ([Figure 3.7.6.1-1](#)).

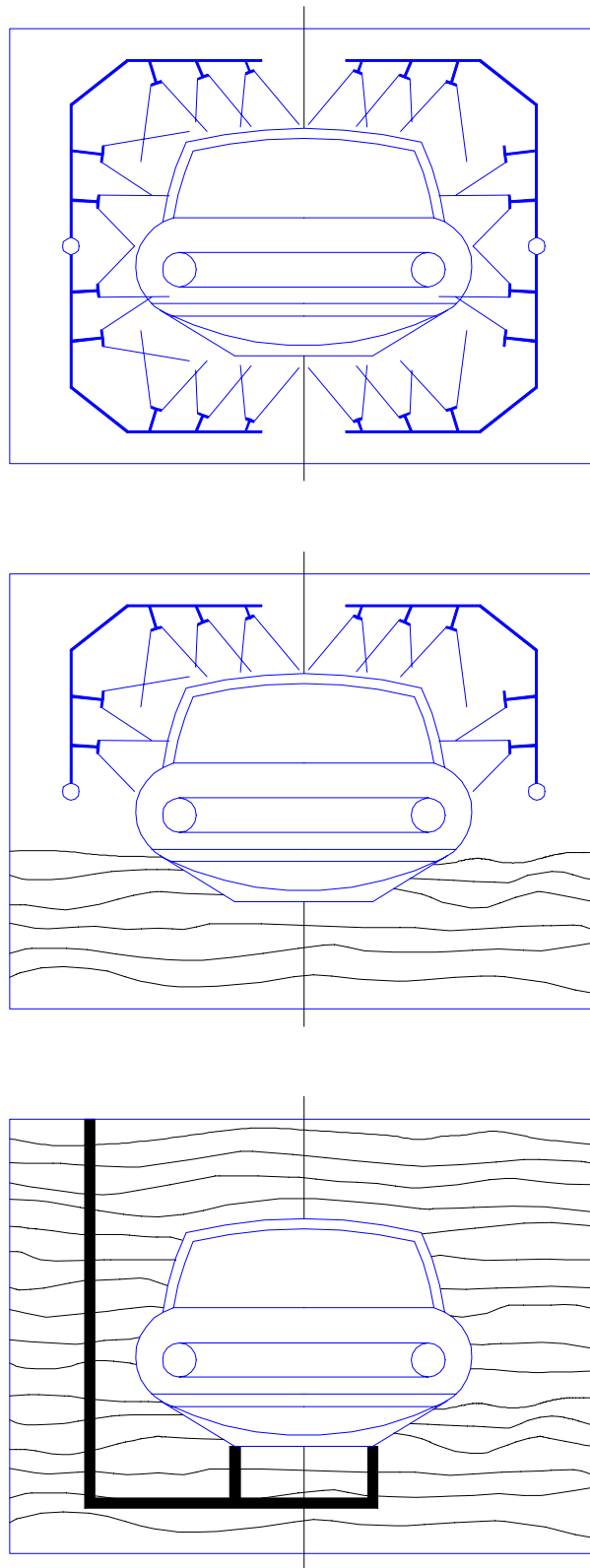


Figure 3.7.6.1-1 In North America, phosphate coatings are applied by spraying, partial-immersion and full dip immersion systems

The method chosen for phosphate application usually determines the method used in the other stages. Although effective on exterior surfaces, spray application has difficulty reaching

enclosed and internal surfaces. Immersion application, on the other hand, can coat all surfaces of the car body, and thus this method also enhances inside out corrosion resistance. For this reason, immersion application is designed into new plants and into lines upgraded because of age or manufacturing changes. The typical processing sequence includes the following treatments:²⁸

1. Body Shop Cleaning/Precleaning
2. Cleaning (2 Stages)
3. Rinsing
4. Rinse Conditioning
5. Phosphating
6. Rinsing
7. Post-treating
8. Deionized Water Rinsing

Cleaning

At some assembly plants, additional cleaning is provided in the body shop to remove excessive dirt, grinding dust, and heavy oils. A precleaning step is used to remove sealer, chalk, and ink marks. Manual wiping or automatic spray application may be used. Alkaline cleaners containing builders and surfactants are used to remove processing and stamping oils and soils from the metal surface. Modern cleaners are formulated with inhibitors to reduce etching of the surfaces of reactive metals found in today's vehicles.

Recent developments in cleaner technology have led to lower operating temperatures. Where the usual cleaner temperature was about 140° F, the newer cleaners operate satisfactorily at 120° F. In addition to energy savings, the use of such cleaners also results in less sealer removal and redeposition in the cleaner sections. With increased interaction between oil suppliers and pretreatment companies, this scenario would help facilitate easily removable lubricants. This would result in cost savings as more lower temperature applications, aqueous cleaner recovery and recycling of the lubricant from the cleaning process.

Rinsing

Rinsing removes the residual processing chemicals from the previous stages that would interfere with subsequent operations or compromise the performance of the coating system. The final deionized water rinse is especially critical to remove any salts that may contaminate the electrodeposition primer bath.

Conditioning

Conditioning agents are colloidal suspensions of titanium phosphates (Jernstedt salts)²⁹ applied prior to phosphate deposition in a rinse step or separately in a spray riser. They nucleate crystallization of the phosphate coating, which results in a dense phosphate coating of small crystal size.

Recent developments include the use of liquid rinse conditioners for easier product delivery. Also, dust contamination from the usage of powders is eliminated.

Phosphating

In the phosphating step, the metal surfaces react with an acidic solution containing zinc, nickel, and/or manganese as their acidic phosphate salts. The change in the pH at the

solution/metal interface causes solubility changes and the growth of phosphate crystals that are integral to the surface. Additives such as oxidizing agents serve to accelerate the deposition of a crystalline coating. Other additives may be needed to improve the treatment of zinc and aluminum surfaces. Because of automotive weight restrictions, aluminum is becoming an important component in the mix for pretreatment. Phosphating of aluminum requires use of new bath compositions. The baths are controlled by maintaining the required level of acidity, accelerator level, and metal concentrations. The use of coated steels has led to the development of products that replace part of the zinc in the zinc phosphate coating with nickel and/or manganese. Some European manufacturers have had success using electrodeposited zinc coated steels that were prephosphated at the production line. This approach reduces rusting in transit, lowers the use of lubricating liquids in the stamping plant, improves housekeeping in the stamping plant, and reduces chemical consumption at the assembly plant. Treatment of enclosed surfaces and hem flanges does not depend on the application method, and it is claimed that the treatment and performance of bimetallic couples is improved. When prephosphated sheet is processed in the assembly plant phosphate washer, cleaner strength must be controlled, and the two phosphate systems involved must be closely matched to avoid appearance and performance problems.

Post-Treating

Although the most commonly used post-treatments contain chromium ions, new types have been developed that are based on organic monomers or polymers and/or inorganic salts. These newer types are of interest because of their environmental acceptability.

The need for the application of a post-treatment depends on total system requirements. Although this step is generally employed in the United States and Europe, Japanese car manufacturers do not use a post-treatment step³⁰, except for manufacturing facilities located in the United States.

Future trends are to eliminate post-treatments and utilize DI water only.

3.7.6.2 Characterization of Phosphates

Phosphate coatings are characterized by composition, uniformity, coating mass per unit area, crystal size, and morphology. The coating mass is typically greater than 1.5 g/m² but less than 4 g/m². Present-day phosphate systems aim for a crystal size of about 15 microns or less if applied by spray and 10 microns or less if applied by immersion. Crystal morphology is a function of conditioning, the application method, and phosphate bath composition. Immersion processing generally results in nodular crystals while spray processing gives plate-like crystals. Phosphate coatings containing a higher concentration of Fe (phosphophyllite)³¹, Ni, or Mn have been shown to outperform coatings containing only Zn (hopeite).³²

The right combination of characteristics will yield the optimum paintable surface and form the foundation for the total corrosion resistant system applied to the metal surface.

3.7.6.3 Future Developments

Improvements in metal treatment technology are continuing. Among these are better performance, process simplification, automatic bath control, and on-line monitoring of coating characteristics. Increasingly restrictive environmental legislation will require waste minimization through the use of alternative compositions or ancillary processes. Analogous to these compositions are current research studies on nickel free baths which results in minimization of heavy metal additions to bath and sludge.

3.7.7 PAINTS AND PAINTING SYSTEMS

The North American automobile industry employs an electrocoat primer, in some instances a surfacer or guide coat, and a color topcoat system on car bodies. Major developments, particularly in the primers, offer significant improvements in corrosion protection.

In North America, the conversion from spray priming to cathodic electrodeposition of primer is complete. This rapid change occurred between 1976 and 1983, indicating the wide acceptance of cathodic electrodeposition epoxy primer for greatly improved corrosion resistance.

In electrophoretic deposition systems - variously called electrodeposition, electrocoating, E-Coat, and ELPO - the metal substrate is immersed in an aqueous bath and coated with a charged organic primer under the influence of an electrical field.

The advantages of electrodeposition include uniform coverage without pinholes, edge protection, penetration into enclosed areas, elimination of fire hazards and air pollution, and reduction of water pollution problems. In addition to adaptability to full automation, it offers more efficient utilization of the paint. Originally, cathodic electrocoated primers had poor stability and developed less "throwing power" than the anodic types, but both problems now have been solved. The major benefit of cathodic electrodeposition is the substantial improvement in corrosion resistance of the primed steel, particularly on marginal quality phosphated surfaces.

In the cathodic electrodeposition primer systems, the vehicle body is the cathode, and the dissolved metal ions tend to migrate in the same direction as the cationic resin, which coats the cathodic part. In addition to avoiding the possibility of anodic attack on the conversion coating or substrate, the electrodeposited cationic resins are alkaline in nature and tend to be inherently good corrosion inhibitors.

Electrodeposition of primer is at least a partial solution to the problems of tougher upcoming ambient air standards and energy conservation needs. It is much less polluting and, in many cases, also eliminates the need for the large dryoff oven after phosphating. The use of lead free electrodepositon primers contributes to the use of environmentally friendly coatings.

3.7.7.1 Changes in Cathodic Electrodeposition Epoxy Primers

By 1985, most paint lines in North American automobile assembly plants converted to high build (30-35 μm coating thickness) cathodic electrodeposition primers. In many plants this change resulted in the elimination of the primer surfacer or guide coat.

However, in the late 1980's, a trend developed away from the high-build electrocoats toward intermediate coating thickness of about 22 μm . The use of a primer surfacer or guide coat has regained favor to optimize the appearance of the topcoat and to improve chip resistance. Further improvements in the cathodic electrocoat are designed for better stone chip resistance and lower bake temperatures.

3.7.7.2 Improving Chip Resistance and Use of Color-Keyed Spray Primers

The continuing effort to improve field performance of paint systems has resulted in the addition of chip-resistant primers to the paint process. These may include either high-build products

sprayed on the cured electrocoat, or powder primers or slurries applied on the electrocoat prior to cure. Thin film primers are often painted on the front of hoods to provide additional stone protection.

To allow use of brighter topcoat colors or replace the use of expensive base coat material on less critical surfaces, some U.S. manufacturers are spray-applying color-keyed primers. These materials may be similar in color to topcoat color families, but are lower in cost and can produce significant paint cost savings. As a result of this process change, some automotive manufacturers are evaluating the use of medium build electrocoats ($20\text{-}25 \mu\text{m}$) in combination with color keyed primers to produce the $30\text{-}35 \mu\text{m}$ primer film currently applied with high film build electrocoats.

3.7.7.3 Trends in Topcoats

Environmental regulations limiting the release of organic solvents have forced many changes in topcoat technology. Non-aqueous acrylic dispersion lacquers and thermoplastic acrylic lacquers have been eliminated due to their high solvent content. Currently, various topcoat systems are used for North American automobiles. They include:

1. Non-aqueous dispersion enamels
2. High solids solution enamels
3. High solids base coat/clear coat enamels
4. High solids base coat/two-component clear coats
5. Water borne base coats/enamel clear coats
6. Various combinations of the last three base coat/clear coat systems.

The non-aqueous dispersion enamels have almost been completely replaced by high solids solution enamels. Many plants have proceeded directly to base coat/clear coat technology for both metallic and non-metallic colors. These paints, in many cases, are applied directly over electrocoat primers. Base coat/clear coat systems provide attractive finishes with a deep luster that are more resistant to chalking, fading, and chemical spotting than are conventional enamels.

All base coat/clear coat systems, with the exception of waterborne base coats, are essentially applied wet-on-wet. Waterborne base coats are of interest because of their lower solvent content, and better orientation of the aluminum flakes. Two factors that are driving further changes in topcoats are stricter solvent emission regulations and chemical spotting problems due to atmospheric fallout. Lower emissions requirements have resulted in an emphasis not only on water borne base coats, but also on powder clear coats. These types of systems are currently being field tested on vehicles. To reduce problems of chemical spotting, many auto manufacturers have begun to use two-component clear coats as part of their paint system. These clear coats may be either urethane or non-urethane type materials. They require more sophisticated application techniques and equipment. Improvements in chemical resistance may also be obtained with certain powder clear coats.

The complete paint system film build with and without primer surfacers is shown in [Table 3.7.7.3-1](#). The total system film thickness may range from $85\text{-}110 \mu\text{m}$.

Table 3.7.7.3-1 Typical Paint System Film Build

Topcoat	With Primer Surfacer	Without Primer Surfacer
Electrocoat and Primer	20-25 μm	30-35 μm
Primer Surfacer	15-25 μm	
Base coat	5-25 μm	15-20 μm
Clear coat	40 μm	40 μm

3.7.7.4 Autodeposition Coatings ³³

The automotive industry is showing increased interest in the use of autodeposition coatings for protecting steel and iron components. In the autodeposition coating process, a resinous coating is applied to a metal article as the result of chemical reaction of the metal surface with the coating solution. Since any surface that is wetted by the solution is coated, the system has unlimited "throwing power" into recessed or enclosed structures. Current commercial coatings are based on polyvinylidene chloride or acrylic resins. The PVDC coating process emits no volatile organic compounds (VOC), has no heavy metal effluent, and cures at 80° to 100°C. The acrylic coating process has low VOC emissions, requires a chromium rinse, and cures at 130° to 180°C. Current applications include various underhood and underbody components as well as housings, springs, and shafts.

Although current applications of autodeposition coatings are single-coat functional coatings for steel and iron components, developments for coating galvanized steel and primers for conventional and powder topcoats are being realized.

3.7.8 IMPROVING THE PROTECTION

3.7.8.1 Design Considerations

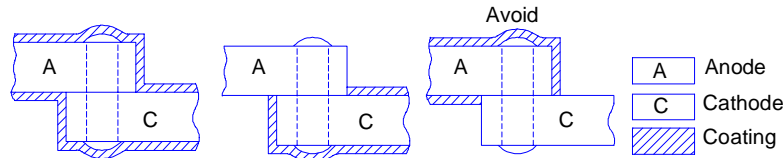
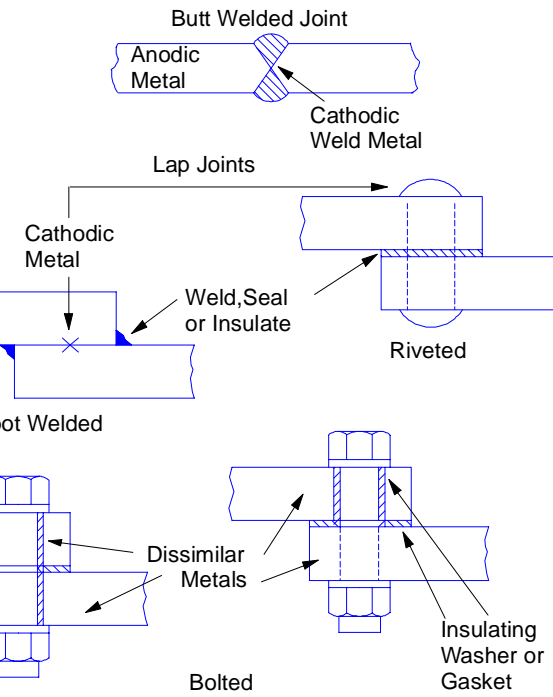
Design will continue to play an important role in controlling corrosion. As is widely recognized, the configuration of a part or assembly has an influence on - and often is the determining factor in - the type and severity of corrosion that occurs in service. It also determines the ease with which protective measures can be applied after assembly. Attention to design considerations becomes even more important wherever significant thickness reductions are involved.

For many years, preferred component configurations and assembly practices to minimize corrosion have been outlined and discussed in a growing body of design concept literature.³⁴ The importance of these factors - joints, closed sections and entrapment areas, and others - was again reviewed by Rowe in 1977³⁵ and the concepts detailed in [Figure 3.7.8.1-1](#) through [Figure 3.7.8.1-5](#) are based on his paper.

To minimize corrosion attack in butt welded and lap joints, the weld material (or rivet or bolt) should be less active than the larger area metals being joined.

In lap joints, use of fillet welds, insulating material, or a seam sealer is recommended.

In bolting dissimilar materials, use of insulating washers or gaskets and bushings is required in a corrosive environment.



Coatings should be applied to both anode and cathode or to cathode only; never to the anode only. Damage to coating on anode would result in serious corrosion due to small anode-large cathode combination.

Joints exposed to direct splash should be protected by flanges. These may have to be angled to protect without creating entrapment sites.

Entrapment sites in offset lap welds and standing seams should be eliminated with a sealer or a bead weld.

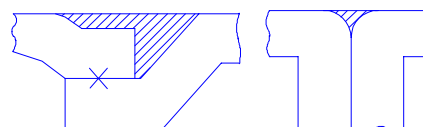
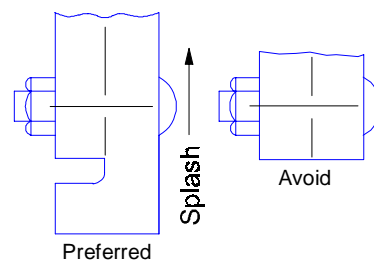
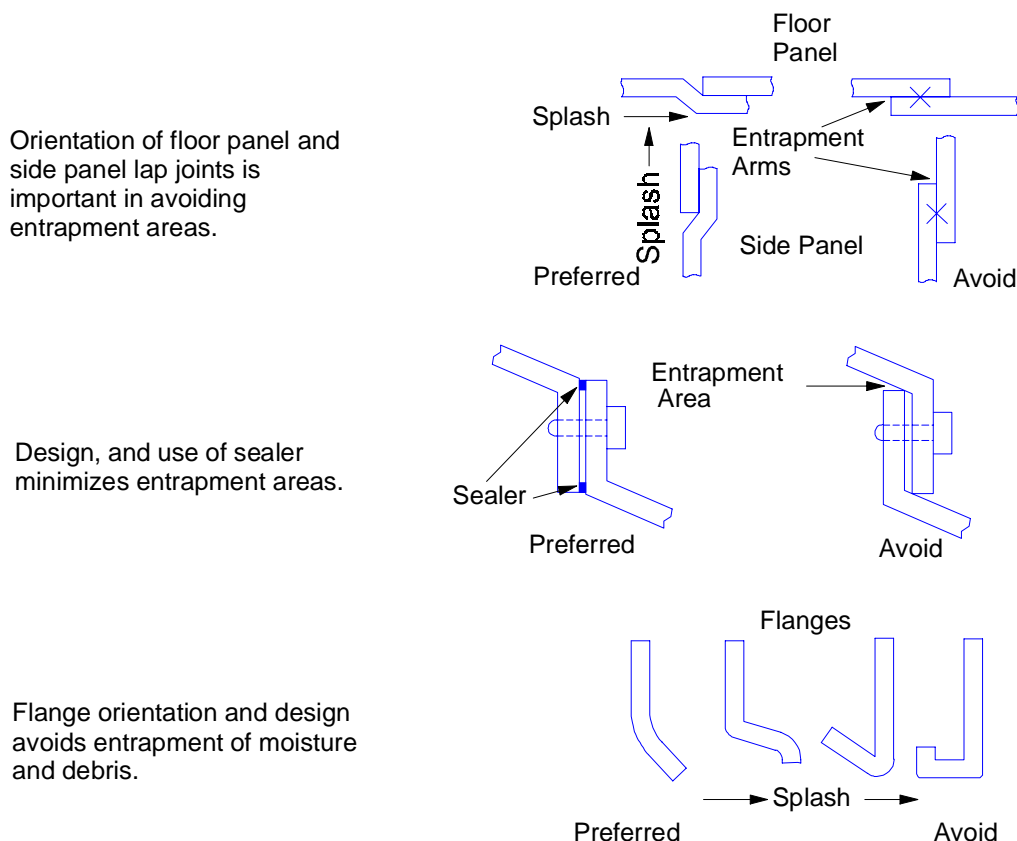
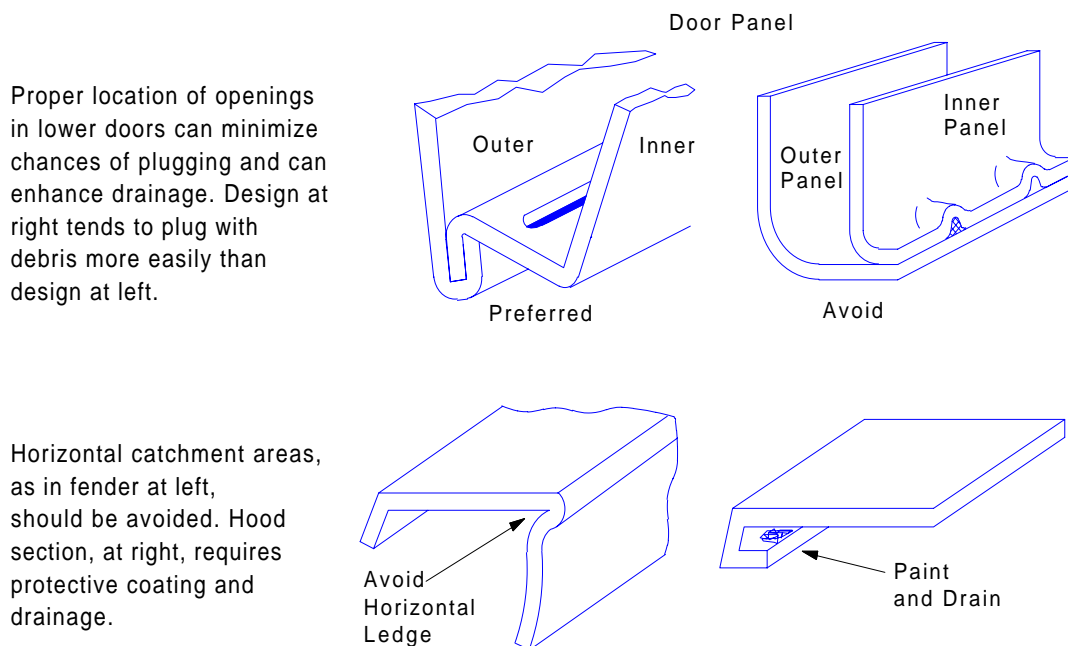
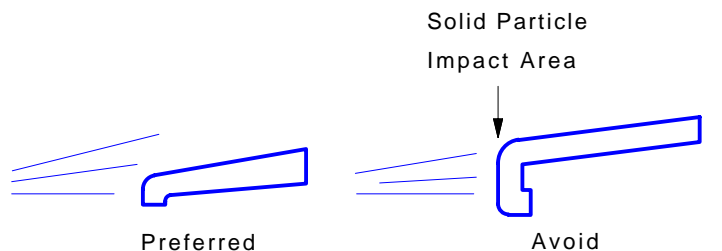


Figure 3.7.8.1-1 Preferred design textures for joints and faying surfaces

**Figure 3.7.8.1-2** Avoiding entrapment areas**Figure 3.7.8.1-3** Controlling entrapment areas

The vertical rise of components in the path of airborne solids should be minimized.



Sharp contours and certain directional design features should be minimized. (Arrows indicate areas of concern).

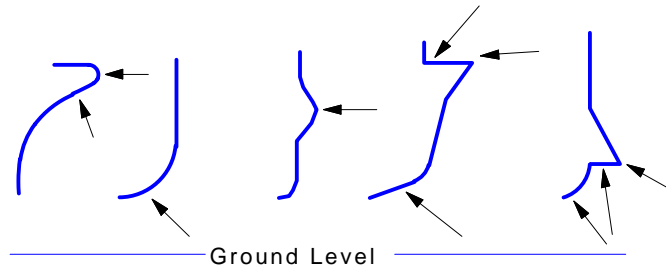
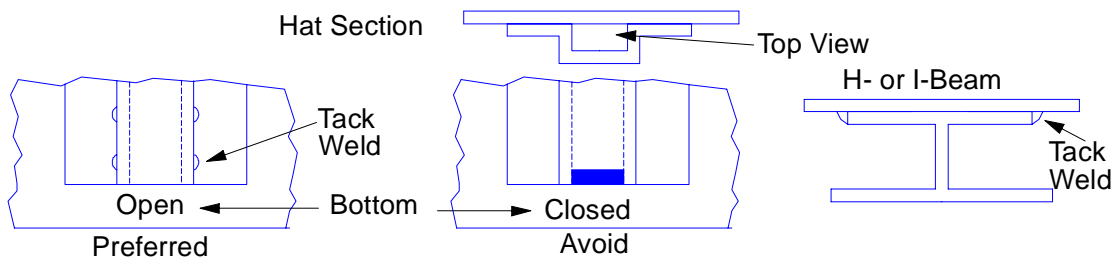
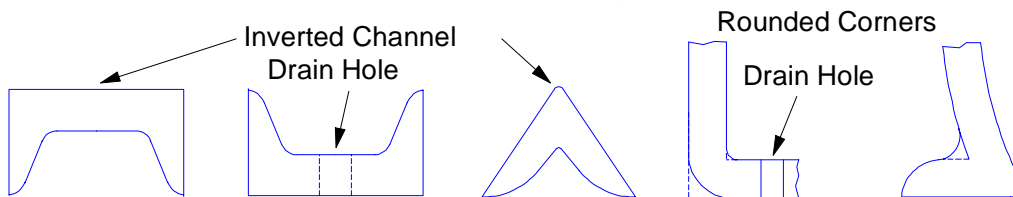


Figure 3.7.8.1-4 Other design features



Hat section and H- or I-beam reinforcements are good designs but hat section should be open at bottom for easy drainage.



If not inverted, channels require drain holes to avoid entrapment areas; angle sections should have rounded corners, smooth tapers, and drain holes as indicated.

Figure 3.7.8.1-5 Design and orientation of structural members and reinforcements

3.7.8.2 Aftermarket Rustproofing

The interest in aftermarket rustproofing to provide additional corrosion protection to North American-built vehicles has greatly diminished. The use of precoated steels, electrodeposition primer, and comprehensive post assembly coatings of waxes, sealers, urethane and vinyl have made aftermarket rustproofing unnecessary, according to most North American auto makers. Manufacturers of rust-inhibiting compounds are now supplying directly to the assembly lines.

The corrosion resistance is already built into today's vehicles.

3.7.8.3 Cathodic Protection

Cathodic protection of automobiles, in the form of sacrificial protection, is achieved using zinc coated steels to minimize body and chassis perforation corrosion, and stainless steel clad aluminum trim to control corrosion of steel body panels at trim areas.

Cathodic protection, in the form of impressed current protection, has been reported as not successful in controlling automobile body corrosion.³⁶ Field tests have demonstrated that the problems associated with automobile cathodic protection using anodes include the high resistivity of the non immersion environment.

3.7.9 CORROSION TEST METHODS

One of the most important and challenging tasks facing the corrosion and coatings engineers in automotive companies, steel companies, and other suppliers is that of evaluating coated steels and ranking candidate materials. Corrosion occurring over long service in the North American deicing salt/snow belt is difficult to simulate in a short time. Available methods include field surveys, on-vehicle testing, proving ground testing, atmospheric corrosion testing and laboratory testing. The ability of many of the currently methods to duplicate on-vehicle test results has been studied and ranked by the A/SP corrosion Task Force³⁷.

3.7.9.1 Field Surveys

Field surveys involve inspection, often destructive, of the sheet steel components of actual vehicles with a well-defined history in a corrosive environment.

Obviously, if properly conducted with appropriate controls, this is the best and most direct way of comparing the performance of automotive materials. The environment is real, and component design and vehicle dynamics are taken into account.

However, it is time-consuming, tedious, expensive, and virtually confined to the automotive companies themselves. Faster, cheaper, yet dependable methods of evaluating materials are usually required.

3.7.9.2 On-Vehicle Testing

On-vehicle testing involves installing special racks with coupons on vehicles and subjecting the coupons to yearly inspections. An SAE Recommended Practice (J1293) was developed for under-vehicle corrosion testing in 1980, and updated in 1990 ([Figure 3.7.9.2-1](#)) following the work of an SAE Task Force of the Iron and Steel Technical Committee, Division 32.

It is now customary to carry out under-vehicle testing of the as-received metal precoated steels (compared with uncoated mild steel) as well as phosphated and cathodic primed metallic coated steels.

Measurements taken are usually percent surface area of base metal attack and density and depth of pitting. Although the measurements are relatively easy, the work is time consuming and tedious, and overall interpretation requires experience and good technical judgment.

On-vehicle testing of fully painted coupons of candidate materials on racks is also performed, with racks located on bumpers³⁸, truck boxes¹⁸, and trailers.

Mobile testing is a good, relatively inexpensive method of testing that probably provides the closest simulation of actual service. As with field surveys, the test is lengthy, with at least two winters in a corrosive environment required for the under-vehicle testing, and considerably longer for the on-vehicle testing of the full paint system. In designing on-vehicle test programs, sufficient material should be provided to allow for possible attrition due to accidents, vandalism and changes in ownership.

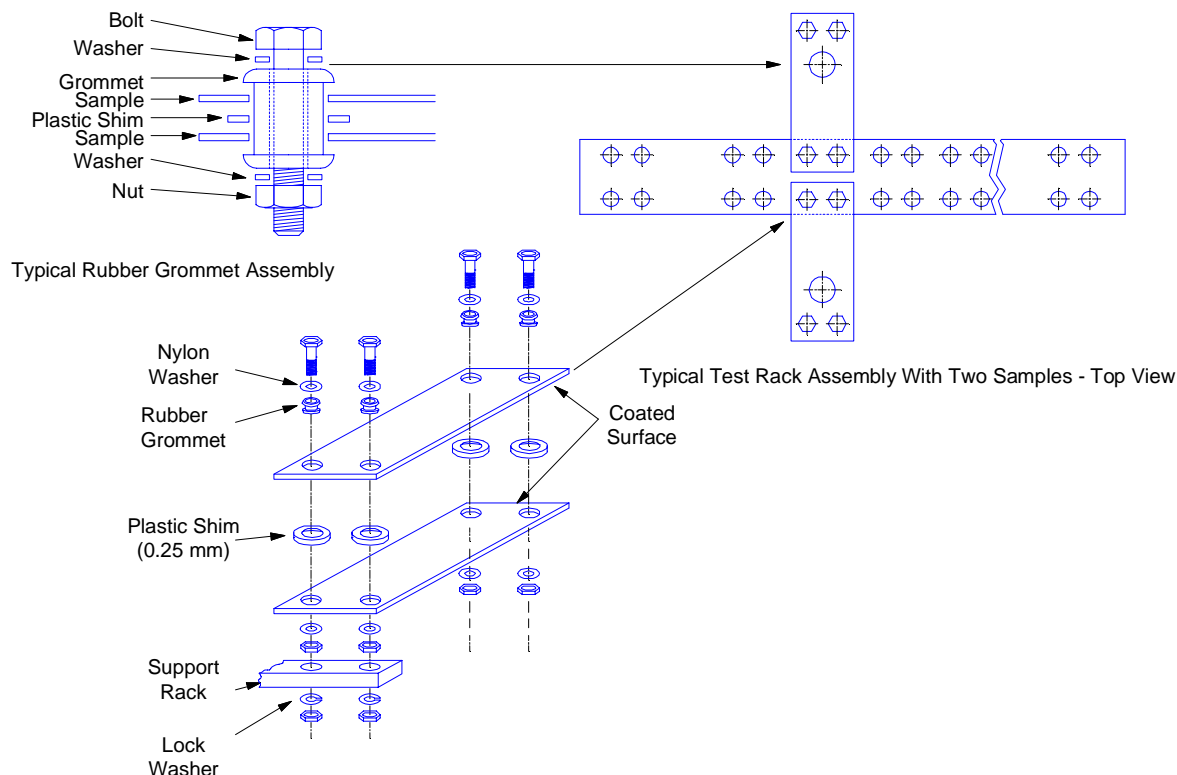


Figure 3.7.9.2-1 Under vehicle corrosion test assembly (SAE J1293)

3.7.9.3 Proving Ground Testing

Proving ground testing involves testing of prototype and production vehicles on the automotive company's proving grounds. Each automotive company has developed cycles to produce accelerated corrosion of vehicles. Test times can range from ten weeks to ten months, depending on the goal of the test proving ground. Corrosion/durability tests can simulate field experience in general metallic corrosion, cosmetic corrosion, and functional corrosion of various components and systems.³⁹ However, perforation corrosion is more difficult to accelerate.

In addition to testing of full vehicles in a realistic corrosive environment, the proving ground also tests components, assemblies, and painted test panels. These are either attached to test vehicles or towed on trailers.

For testing of perforation corrosion, a useful and practical method involves "mini-door" assemblies towed on trailers.⁴⁰ This allows simultaneous testing of a large array of simulated door enclosures, all subjected to the same environment at the proving ground. The mini-doors are subsequently taken apart, and both the amount and location of corrosion are determined. This has been used to quantitatively evaluate many different types and combinations of pre-coated steel in a way that would not be practical on full vehicles.⁴¹

3.7.9.4 Atmospheric Corrosion Testing

Atmospheric corrosion testing of the type used to rank coated steels for use in construction applications is used on a limited basis to rank automotive materials.

The outdoor scab test, also referred to as the modified Volvo test⁴², is often used for evaluating cosmetic corrosion resistance. In this test, test panels are placed outdoors on racks and sprayed with salt water twice weekly. Typical test times are one or more years.

3.7.9.5 Laboratory Testing

Laboratory testing includes salt spray (fog) testing per ASTM B117, laboratory cyclic testing and electrochemical testing.

Salt Spray (Fog) Test ASTM B117

Historically, the salt spray test has been one of the most widely used laboratory tests in automotive materials evaluation and development. However, it does not simulate the vehicle corrosion environment, either in the deicing salt/snow belt areas or coastal areas of North America, and accordingly often ranks materials differently than actual service exposure.

It is sometimes used for detecting marginal systems or highlighting poor quality samples of a system that is already known. While it may be relatively inexpensive and easy to carry out, agreement among different salt spray cabinets is often poor. Under no circumstance should it be used for research or materials development.

Laboratory Cyclic Testing

Cyclic laboratory corrosion tests involve repeated intervals of salt spray or salt water immersion, exposure to controlled humidity and temperature, and drying. Such tests provide a more realistic simulation of the environment experienced by road-driven vehicles, and they are being used increasingly in the evaluation of coated sheet products, phosphate pretreatments, and paint systems. As described in [Section 3.7.3.3](#), the mechanisms of corrosion and the relative behavior of materials under alternating wet-and-dry conditions are significantly different from what occurs under constantly wet conditions¹⁶.

In the past, each automotive company, and many of their suppliers, has developed its own cyclic corrosion test involving the use of different chemical conditions, temperatures, humidities, time periods, specimen size, configurations, and evaluation method. It has been reported that ranking of materials in the different tests does not correlate very well and little has been published on correlation between cyclic test results and actual service results.⁴³ Also the multiplicity of tests leads to confusion and problems.

A task force of the Auto/Steel Partnership, consisting of technical representatives of the major North American automakers, chemical suppliers, and steel sheet producers, has undertaken an effort to improve and standardize laboratory cyclic corrosion test. The SAE J2334 Cosmetic Corrosion Lab Test, developed by the Partnership and issued by SAE International in November 1998, shows excellent correlation to field corrosion in the North America snow belt³⁸. The test includes two test cycles to accommodate both manual operation and automatic corrosion chamber testing. Development of a perforation corrosion test procedure by the Partnership is on going⁴⁴.

Electrochemical Testing

Because corrosion is generally an electrochemical process, electrochemical measurements can provide a great deal of information on rates and mechanisms of corrosion. Techniques such as linear polarization, potentiodynamic polarization, and electrochemical impedance spectroscopy are being used increasingly, spurred by the ongoing development of electronic instruments, computers and software. While these methods are particularly well-suited to fundamental studies, their application to materials evaluation has been limited by high equipment costs, need for skilled operators, and lack of standard practices.

Moreover, most electrochemical methods do little more than monitor the progress of corrosion. For purposes of materials testing, simpler means such as visual evaluation can often be conducted more quickly, at lower cost, and with greater certainty.

REFERENCES FOR SECTION 3.7

1. T. C. Simpson, A. W. Bryant, G. Hook, R. A. Daley, R. J. Swinko, and R. W. Miller, "U. S. Automotive Corrosion Trends Over the Past Decade, Paper No. 394", in Corrosion and Corrosion Control of Aluminum and Steel in Lightweight Automotive Applications, NACE International, Houston, TX (1995).
2. Townsend, H. E., Coated Steel Sheets for Corrosion-Resistant Automobiles, Materials Performance, 30 (10), 60-65 (1991).
3. General Motors Milford Proving Grounds, "*Vehicle Corrosion Environment Canada and the United States*", Internal Document, October 1990.
4. Baboian, R., "Environmental Aspects of Automotive Corrosion Control", in Corrosion and Corrosion Control of Aluminum and Steel in Lightweight Automotive Applications, NACE International, Houston, TX (1995).
5. American Public Works Association, "*Vehicle Corrosion Caused by De-icing Salts*", Special Report #34, September 1970.
6. McCrum, R. L., "*Calcium Magnesium Acetate and Sodium Chloride as Highway Deicing Salts - A Comparative Study*", Materials Performance, Volume 28, Number 12, December 1989, pages 24-28.
7. "*Dust Control, Road Maintenance Costs, Cut with Calcium Chloride*" Public Works Vol. 121, No. 6, May 1990, pp. 83-84.

8. Townsend, H. E., Behavior of Painted Steel and Aluminum Sheet in Laboratory Automotive Corrosion Tests, Corrosion, 52 (1), 66-71 (1996).
9. Bittence, J. C., "Waging War on Rust, Part I: Understanding Rust", Machine Design, October 7, 1976, pages 108-113; Part II: "Resisting Rust," Machine Design, November 11, 1976, pages 146-152.
10. Rosenfeld, L. and Marshakov, J. K., "Mechanism of Crevice Corrosion", Corrosion Vol. 20, 1964, p. 115t.
11. France, Jr., W.D., "Crevice Corrosion in Metals", Localized Corrosion - Cause of Metal Failure, ASTM STP 516, American Society Testing & Materials, 1972, p. 164.
12. Hospadaruk, V., "Corrosion Fundamental and Their Application to Automobiles", Automotive Corrosion by Deicing Salts, R. Baboian, NACE, Houston 1981.
13. Fenton, J., "Long Term Corrosion Prevention", Automotive Engineer Vol. 9, No. 1, February/March 1984, p. 39.
14. Uhlig, H., "Filiform Corrosion, " Corrosion and Corrosion Control, Wiley, New York, 1971, p. 252.
15. Van Ooij, W. J., and Sabata, A., Corrosion 46 (2) p. 162-171 (1990).
16. Shastry, C. R., and Townsend, H. E., Corrosion 45 (2), p. 103-119 (1989).
17. Carson, C. G., and Peterson, P. T., "Challenges and Opportunities for Coated Steel Products", Proceedings of the USI 23rd Annual Meeting and Conference, Berlin, Federal Republic of Germany, October 1989.
18. Ostermiller, M. R., and Townsend, H. E., On-Vehicle Cosmetic Corrosion Evaluation of Coated and Cold-Rolled Steel Sheet, Proceedings of the Sixth Automotive Corrosion and Prevention Conference, P-268, Society of Automotive Engineers, Warrendale, PA (1993), pp. 65-83
19. Dorsett, T. E., Development of a Composite Coating for Pre-Coated Automotive Sheet Metal, SAE Paper 862027, December 1986.
20. Watanabe, T., et al., Development of Organic Composite Coated Steel Sheets with Bake Hardenability and High Corrosion Resistance, Proceedings of International Conference on Zinc and Zinc Alloy Coated Steel Sheet, GALVATECH '89, September 1989.
21. Ostermiller, M. R., Phiepho, L. L., Singer, L. and Raymond, L., "Advances in Automotive Corrosion Resistance," Proceedings of the Fourth International Conference on Zinc and Zinc-Alloy Coated Sheet, The Iron and Steel Society of Japan, Tokyo, pp. 678-685 (1998)
22. U.S. Shipments of Steel Mill Products", in Metal Statistics 1997, Ferrous Edition, American Metal Market, New York (1997).

23. Rausch, W., Die Phosphatierung von Metallen, (Eugene G. Lenz Verlag, 1974).
24. Lorin, G., Phosphating of Metals, (Finishing Publications, 1974).
25. Freeman, D. B., Phosphating and metal pre-treatment, (Woodhead-Faulkner, Cambridge, England, 1986).
26. Knaster, M. B. and Parks, J. M., Mechanism of Corrosion and Delamination of Painted, Phosphated Steel During Accelerated Corrosion Testing, Paper No. 860110, National SAE Meeting, 1986.
27. Mischke, P., Manganmodifizierung Stetzt Sich Durch, Industrie Anzeiger, 78/1987, p. 26.
28. Preparing Steel for Organic Coatings, Products Finishing Directory, 1989, p. 6.
29. Jernstedt, G. W., US Patent 2,310,239 Jernstedt, G. W., Trans. Electrochemical Society, 83, (1943), 361.
30. Simpson, M. W. and Zurilla, R. W., Phosphate Final Rinse Options, Pretreat 90, November 1990.
31. Richardson, M. D. W. and Freeman, D. B., Pretreatment and Cathodic Paint Performance - Use of the "*P/P&H Ratio*", Trans. IMF, 1986.
32. Kent, G. D. and Petschel, M., Polycrystalline Conversion Coatings, Products Finishing, September 1988.
33. Jones, T. C., and Fristad, W. E., Applications and Advances in Autodeposition Coatings," in Corrosion Prevention, SP-1265, Society of Automotive Engineers, Warrendale, PA, pp.1-10 (1997).
34. "*Prevention of Corrosion of Metals*", Handbook Supplement HSJ 447, Society of Automotive Engineers, Warrendale, PA 1981.
35. Rowe, L. C., "*The Application of Corrosion Principles to Design*", Paper No. 770292, presented at SAE Automotive Engineering Congress, Detroit, Michigan, February 1977.
36. Baboian, R., "*Cathodic Protection of Automobiles - Does It Work?*" Materials Performance, Vol. 26, No. 7, July 87, p. 82-88.
37. H. E. Townsend, D. D. Davidson, and M. R. Ostermiller, "Development of Laboratory Corrosion Tests by the Automotive and Steel Industries of North America", in Proceedings of the Fourth International Conference on Zinc and Zinc-Alloy Coated Sheet Steels", The Iron and Steel Institute of Japan, Toyko (1998), pp. 659-666.
38. M. W. Simpson, W. B. van der Linde, D. C. McCune, and H. E. Townsend, License-Plate Cosmetic Corrosion Tests of Automotive Coated Steel Sheet, NACE International Paper No. 98553 (1998).

39. Schumacher, W. A., "Proving Ground Vehicle Corrosion Testing", Automotive Corrosion & Prevention Conference, Dearborn Michigan, December 5-7, 1983.
40. Ostermiller, M. R., Piepho, L. L., Singer, L., Oldenburg, W. C., and Dorsett, T. E., "Simulation of Perforation Corrosion Mechanism Using 'Mini-Door' Test Panels", ASM World Conference, September 24-30, 1988, Published in Corrosion Resistant Automotive Sheet Steels, L. Allegra Ed., ASM International, Metals Park, Ohio.
41. Oldenburg, W., Dorsett, T., and Masterson, T., "Perforation Corrosion Performance of Various Materials Using Mini-Door Test Specimens Correlated with Vehicle Road and Laboratory Test Results", S.A.E. Automotive Corrosion and Prevention Conference, December 4-5, 1989, Paper No. 892579. Published in S.A.E. Publication, p. 228.
42. Stephens, M. L., Davidson, D.O., Soreide, L. E., and Shiffer, R. J. Paper No. 862013, Society of Automotive Engineers, Warrendale, Pennsylvania (1986).
43. Kent, Gary D., Hacias, Kenneth J., and Fotinos, Nicephoros A., "Laboratory Evaluation of Automotive Conversion Coatings", Paper No. 831812, SAE Automotive Corrosion and Prevention Conference, Dearborn, Michigan, December 5-7, 1983.
44. "SAE J2334, Cosmetic Corrosion Lab Test", SAE International, Warrendale, PA (1998).

3.8 DESIGN FOR ROLL FORMING

Roll forming offers an alternative to stamping for some body components. The process entails very low costs for tools and equipment and it offers very high production rates. [Section 4.2](#) contains a discussion of the roll forming process, which is helpful in understanding design for roll forming. This section outlines techniques for utilizing the economic advantages of the roll forming process.

The design principles for components made by stamping and roll forming are distinctly different due to the differences in the mechanics of manufacturing operations. The optimum design practice and the tolerances that can be maintained with either process must ultimately be verified by consulting with manufacturing personnel. The following discussion will acquaint the designer with the fundamental principles of designing for roll forming and will facilitate interaction with the roll former's manufacturing personnel.

3.8.1 DIMENSIONING PRINCIPLES

3.8.1.1 Design to Inside Surfaces

During roll forming, the sheet steel is usually wrapped around the male die. It is therefore generally preferable to dimension cross sections to inside surfaces as illustrated [Figure 3.8.1.1-1](#). Exceptions sometimes occur due to the method of forming, industrial standards or application. For example tubular products, which are not completely formed around a male die, are frequently defined by the outside diameter.

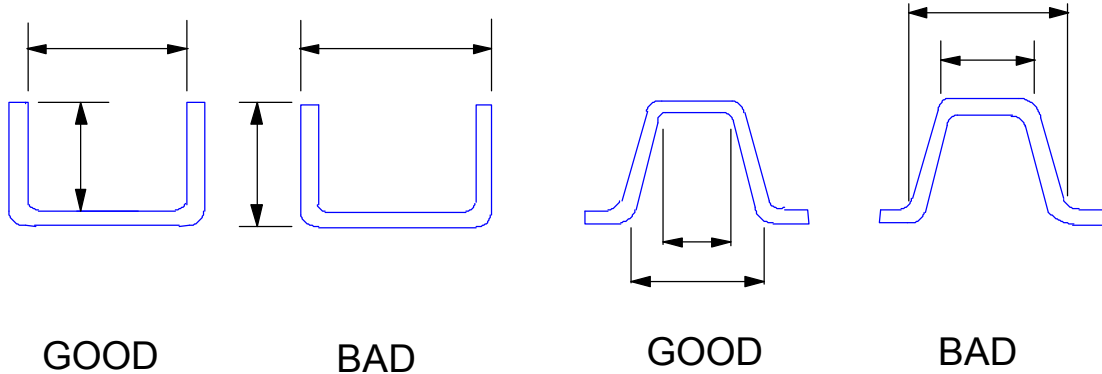


Figure 3.8.1.1-1 Dimension to inside surfaces

3.8.1.2 Establish Dimensions from the Same Surface

It is preferable to establish both reference points of a dimension from the same surface as illustrated in [Figure 3.8.1.2-1](#). Otherwise the specified tolerance must include variations in the thickness of the sheet steel as well as the variations produced by the roll forming operation.

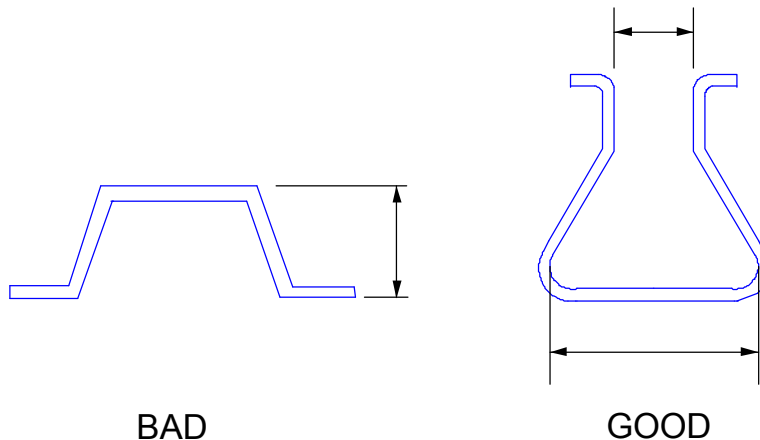


Figure 3.8.1.2-1 Establish both reference points of a dimension from the same surface

3.8.1.3 Dimension to Critical Features

Tool makers generally prefer that the section be dimensioned to the construction points formed at the intersections of the elements rather than to the centers of radii and tangent points, as shown in [Figure 3.8.1.3-1\(a\)](#). This system best reflects the progression of roll forming operations. However, the stackup caused by this system may generate unacceptable tolerances on critical dimensions, such as the opening. Base line dimensioning shown in [Figure 3.8.1.3-1\(b\)](#), which is commonly used in the automotive industry, will give closer control by relating dimensions and tolerances to component functions. The difference in preferred systems of dimensioning are best resolved by direct discussions between design and tooling engineers early in the design process.

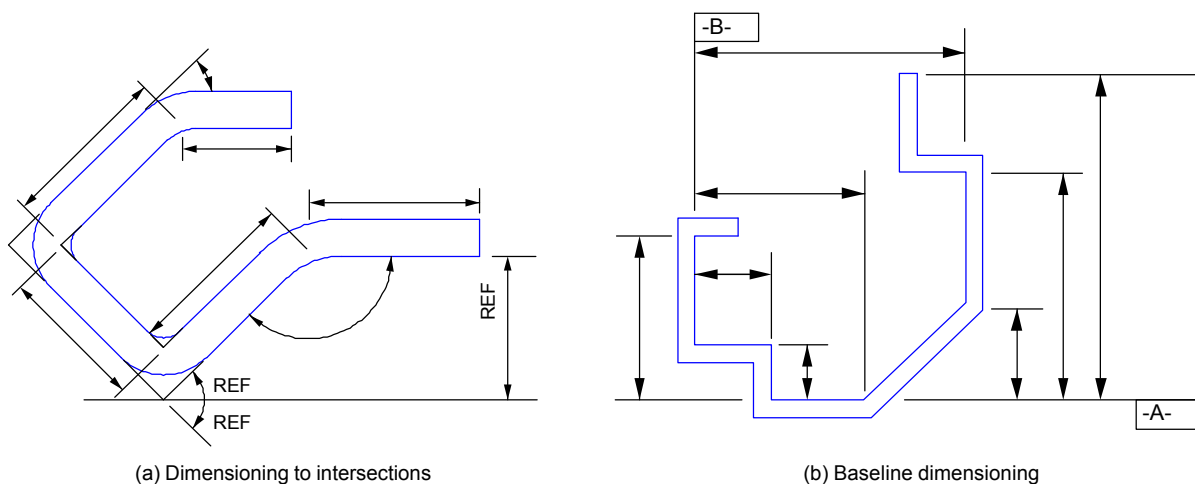


Figure 3.8.1.3-1 Dimensioning systems

3.8.2 TOLERANCES

Five types of tolerances are applicable to roll formed components:

1. Length and related factors
2. Section dimensions, linear and angular
3. Straightness and flatness deviations
4. Features such as holes, notches and dimples
5. Others such as burr and appearance

3.8.2.1 Length, Width and Related Tolerances

The length of a roll formed component is generated in the cut-off operation, which produces three types of variation: length, squareness and burr. Length tolerance is affected by variations in cut-off operations, which are largely influenced by the type and condition of the machines, controls and tools. Squareness is not generally specified because roll forming mills can usually hold the deviation from perpendicular closer than required. This is especially true for the relatively narrow strips used for automotive body components. Where off-square ends are required, the angle and tolerance should be specified. Burrs may also be generated in cut-off operations; they are addressed later in this section.

Variations in the width of the strip affect certain dimensions of the section. For example, the opening shown in [Figure 3.8.2.1-1](#) (dimension "g") is formed by return lips whose length is directly affected by strip width. The figure shows two design alternatives, both of which concentrate strip width variations on elements that do not affect the opening dimension.

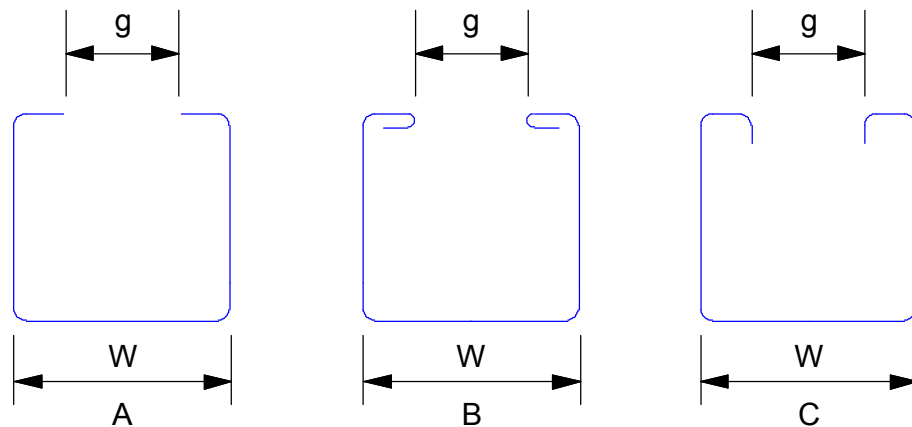


Figure 3.8.2.1-1 The gap width g is affected by variations in strip width in A. Methods for eliminating the effects are illustrated in B and C.

3.8.2.2 Section Tolerances

Guidelines for tolerancing roll formed components are found in documents such as ANSI Y14.5M, the Canadian CSA B78.2 and Delta Standard of Tolerancing Roll Formed Products.

[Figure 3.8.2.2-1](#) illustrates the interpretation of tolerances on several common roll formed sections.

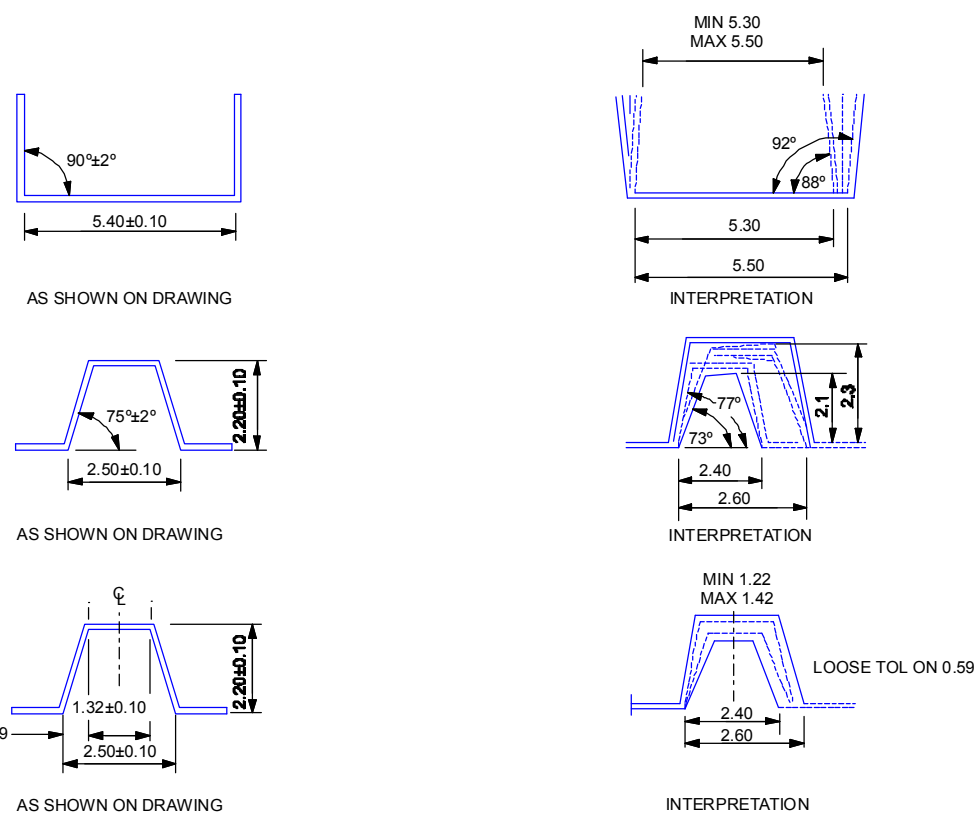


Figure 3.8.2.2-1 Interpretation of tolerances on roll formed sections

3.8.2.3 Straightness Deviations

Straightness deviations of roll formed components are best understood from the mechanics of the roll forming operation (See [Section 4.2](#)). As the strip progresses from flat to final form, residual stresses are induced. These stresses, combined with variations in material properties and dimensions, cause distortions in the finished component. The distortions may be aggravated by manufacturing variables such as improper tool design, incorrect roll alignment and insufficient maintenance of equipment.

Residual stresses and material variations may cause variations due to springback; they can also cause bow, camber, twist, flare, wavy edges, wavy center and herringbone effect. Preperforated features, such as holes, notches and embossments usually increase these deviations. The conditions are defined in [Figure 3.8.2.3.2-1](#) to [Figure 3.8.2.3.6-1](#).

3.8.2.3.1 Springback

Springback in roll formed products is similar to that in stampings. It is caused by the elastic component of deformation in the metal, which deflects the section when the tool forces are released. The amount of springback is primarily a function of metal thickness, material strength, forming radius and gap between the rolls.

3.8.2.3.2 Bow and Camber

Bow is the deviation in the longitudinal direction perpendicular to the plane of the roll forming shafts, which are normally horizontal ([Figure 3.8.2.3.2-1](#)). It is usually specified as a function of length, such as X in. bow per Y in. length (or mm per mm). For short lengths, the maximum

bow is usually specified. Camber or sweep is deviation in the plane parallel to the roll forming shafts, and is normally specified in the same terms as bow ([Figure 3.8.2.3.2-1](#)). The final decision about component orientation is determined by manufacturing personnel and may not be as anticipated by the designer. It is therefore advisable to specify the direction of bow and camber tolerances on the drawing.

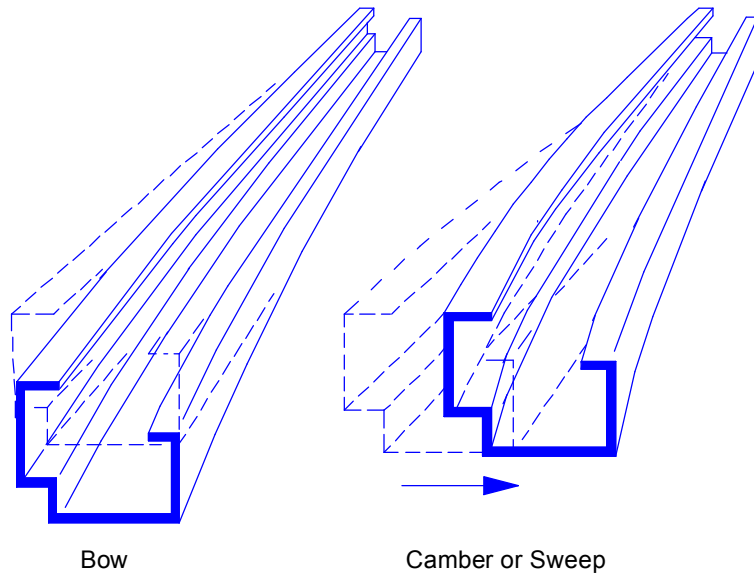


[Figure 3.8.2.3.2-1 Bow and camber straightness deviation](#)

3.8.2.3.3 Twist

Twist is the angular variation of a flat surface over the length of a component ([Figure 3.8.2.3.3-1](#)). It is measured by clamping one end of the component on a flat surface and measuring the deviation at the other. Twist is frequently specified as a function of component length, such as X° per Y mm (in.).

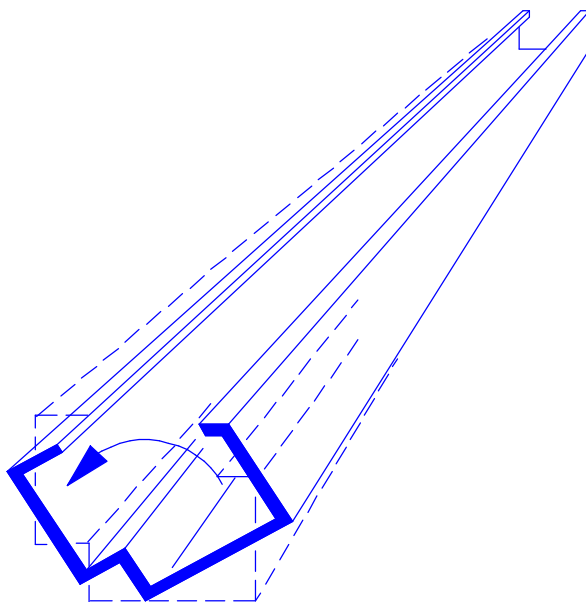


[Figure 3.8.2.3.3-1 Twist straightness deviation](#)

3.8.2.3.4 Flare

Flare, which is typical of roll forming, is a measure of the amount that the edges of the strip turn inward or outward adjacent to the cut end ([Figure 3.8.2.3.4-1](#)). Tolerances specified for flare override, and do not add to, dimensional and angular tolerances.

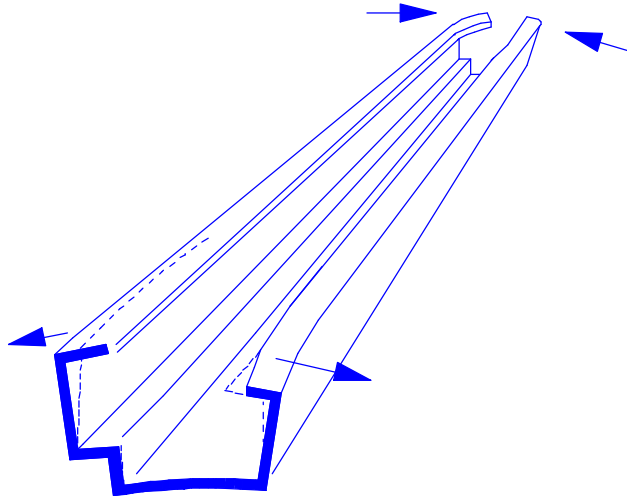


[Figure 3.8.2.3.4-1 Flare straightness deviation](#)

The direction of flare is usually inward at the front end (first through the rolls) and outward at the tail. With high strength material or deep sections, both ends may flare outward. The length to which the flare tolerance is applied is sometimes specified, typically 50 to 150 mm (2 to 6 in.). Components formed from pre-cut blanks usually exhibit more flare than those made from continuous strip. The amount of flare in components made from continuous strip is not influenced by the method of cutting.

3.8.2.3.5 Cross Bow

Cross bow is the deviation of a surface from flat, measured from the starting and ending points of the flat surface or full section, parallel with the roll forming shafts ([Figure 3.8.2.3.5-1](#)).

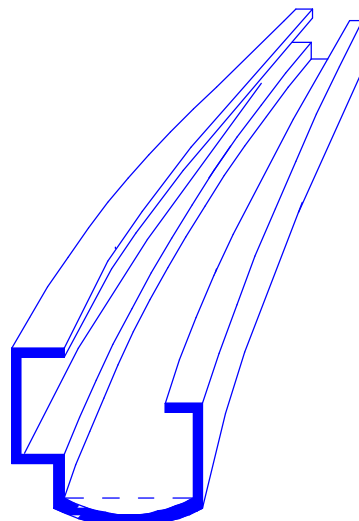


[Figure 3.8.2.3.5-1 Cross bow straightness deviation](#)

3.8.2.3.6 Waviness and Herringbone

Wavy edges, wavy center (oil canning), and herringbone effects are typical of wide flat sections formed from thin material. These deviations are seldom measured and can not be well defined ([Figure 3.8.2.3.6-1](#)). Acceptance limits are sometimes established by visual inspection, usually employing light reflected at a shallow angle.

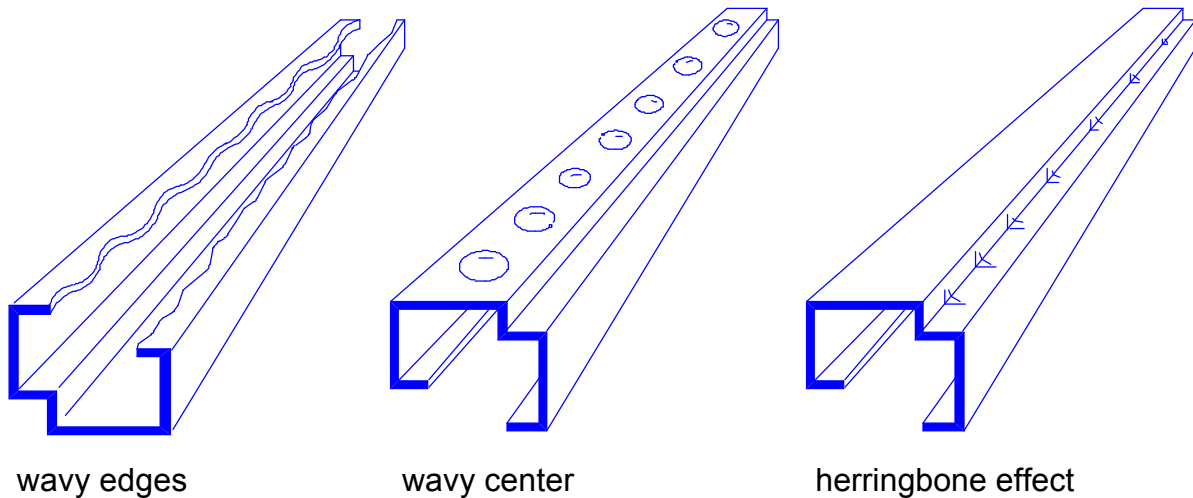


[Figure 3.8.2.3.6-1](#) Defects that are not readily measured

3.8.2.4 Holes, Notches and Dimples

Dimensioning and tolerancing other features such as holes, notches and dimples should follow ANSI Standard 514.5. The implications of the various manners of applying the dimensions and tolerances are demonstrated in the U-channel shown in [Figure 3.8.2.4-1](#). The channel can be formed from pre-cut blanks or formed from continuous strip and cut after forming. The holes can be pierced individually, by twos, by threes, or by sixes. The piercing operations can occur before, during or after forming. These variables generate sixteen different ways to produce the simple component by roll forming. (Theoretically there are twenty-four combinations; in this case, eight are not practical.) Each way uniquely affects tolerances. Where these types of variations exist, tolerances should be determined in consultation with manufacturing engineers to achieve the required tolerances at maximum economy.



[Figure 3.8.2.4-1](#) There are 16 different ways of manufacturing this simple U-channel by roll forming. Each of the ways has a unique effect on tolerances.

3.8.2.5 Burrs and Appearance Factors

Burrs are formed by cutting and piercing operations such as cut-off and notching dies. The burr height can be appreciable if the die is dull, damaged or incorrectly set up. It can also be diminished by subsequent operations that "iron off" the burr. Tolerances for burrs and acceptance standards for appearance factors are usually covered by separate specifications. In critical cases, such as where a burr may cause assembly problems, the drawing should indicate the permitted direction of the burr or clarify that the plus tolerance includes burr.

3.8.3 MATERIAL FACTORS

3.8.3.1 Mechanical Properties

The mechanical properties of sheet steel in strengths up to 275 MPa (40 ksi) yield and with normal ductility have little effect on dimensional tolerances. As strength increases further and ductility decreases, larger bending radii are required and springback increases. Ultra-high strength steels may require 15° to 20° overbend to achieve a 90° bend. The increased springback makes it necessary to increase overbend, and it aggravates the dimensional variations caused by variations in material thickness and yield strength.

Springback variations are worse with ultra high strength steel because specifications usually define the minimum strength in the direction of rolling, but do not limit maximum strength. Neither strength nor elongation is specified across the direction of rolling, and they may fluctuate within one coil. Since the main bending stresses created during forming are oriented across the direction of rolling, allowable yield strength variations can contribute to substantial springback variations.

3.8.3.2 Coatings

Sheet steel that is coated with aluminum, zinc or paint, and plastic laminated sheet steels can be roll formed. The coatings do not affect tolerances but may impose limits on forming operations. For example, roll pressures that are needed in some cases to form the section can cause shiny streaks on the surface. Proper design of the rolls and use of the correct lubricants are necessary to prevent the rolls from picking up pieces of the coatings. Polishing and other surface treatments on the rolls also help to minimize the amount of coating pickup.

3.8.4 CURVED COMPONENTS

Roll forming offers the latitude to sweep or curve the component in the longitudinal direction. This capability allows for curved components to be economically fabricated by roll forming. Components can be curved after they are cut to length, but it is usually more economical to curve continuously, then cut to length. Curving is a well developed science, but it has not yet been documented. Therefore, in most cases the development of tools and techniques are based on the experience of the tool designer and on trial and error.

3.8.4.1 Effects of Curving

Curving produces different effects on the component cross section than do normal service loads. Normal service loads induce stresses only within the elastic range of the material, whereas curving operations force the material well into the plastic deformation range. The bending loads

applied in curving operations induce plastic tensile strain on the outside of the section and compressive on the inside. Since the material volume does not change, the outer surfaces become thinner and the inner surfaces thicker as shown exaggerated in [Figure 3.8.4.1-1](#).

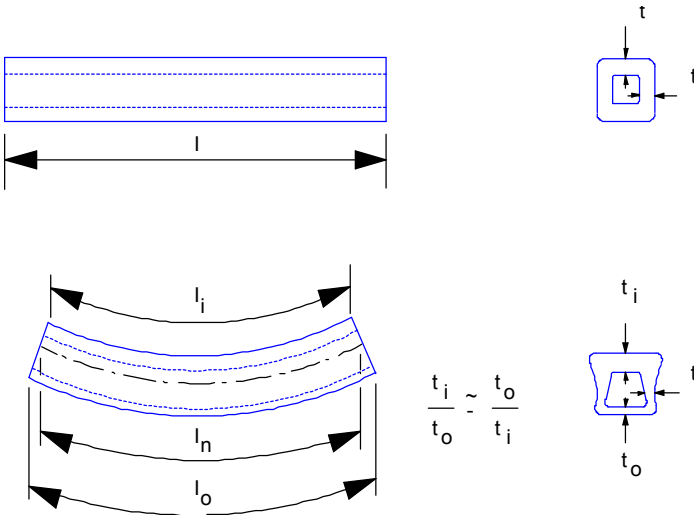


[Figure 3.8.4.1-1](#) Curving induces plastic strain that changes section properties

The redistribution of material shifts the neutral axis toward the inside surface. Other factors associated with manufacturing processes and material characteristics also contribute to the shift of the neutral axis. Curving produces effects that may cause changes in the shape of the cross section. This behavior is discussed for curved members in [Section 3.2.2](#). Elements that are subject to tensile strain tend to move toward the center of curvature, and elements subject to compressive deformation tend to move away. These tendencies produce the effects shown in [Figure 3.8.4.1-2](#). Note that the asymmetrical angle section tends to twist.

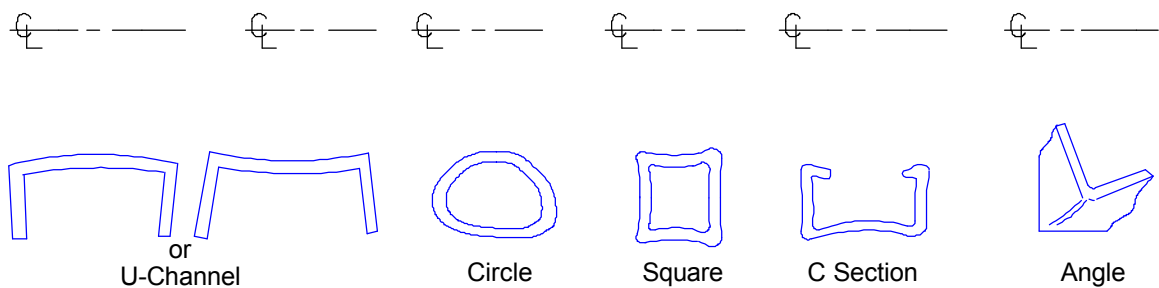


[Figure 3.8.4.1-2](#) Distortions in common sections caused by the tendency for material in tension to move toward the center of curvature

The tensile side of the section usually experiences less trouble than the compressive side in continuous curving because the material is pushed through the curving rolls. The compressive forces subtract from the tensile stresses on the outside, and stresses rarely exceed ultimate tensile. However, the compressive forces add to the compressive stresses on the inside, increasing the possibility of buckling in wide, thin elements of the section.

Another effect of curving is web crippling; several types are shown in [Figure 3.8.4.1-3](#). Crippling is aggravated by cutouts in the web such as holes, slots and notches. The section distortions illustrated in [Figure 3.8.4.1-2](#) and [Figure 3.8.4.1-3](#) can be minimized or eliminated by using tools that support the section during curving, such as forming shoes. Distortions can also

be minimized through good component design practice, such as the use of stiffeners. (See [Section 3.1.2.1](#).)

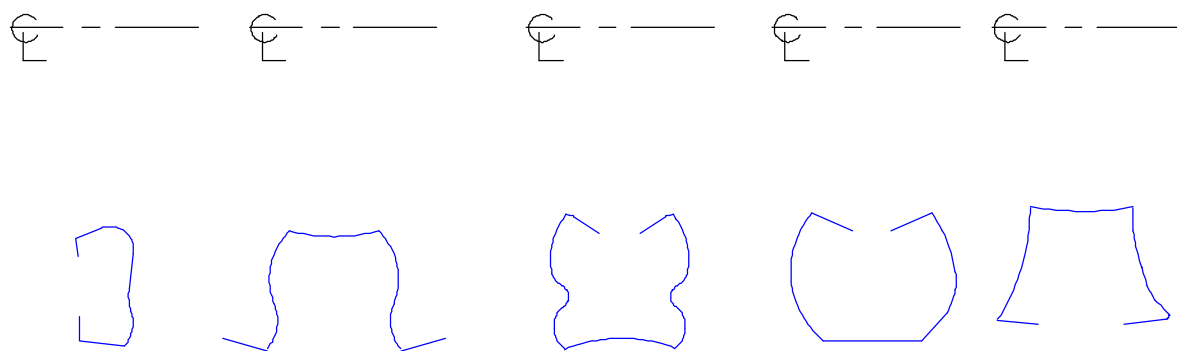


Figure 3.8.4.1-3 Distortions in common sections caused by web crippling

3.8.4.2 Design of Curved Components

Several design factors influence the minimum radius of curvature for a section. Recognizing these factors will help the designer anticipate the amount of curvature that can be attained and recognize the tradeoffs that can be made.

3.8.4.2.1 Material Thickness

The thinner the material, the larger the minimum curving radius because thinner material has more tendency to buckle and is thus more difficult to compress.

3.8.4.2.2 Section Height

The higher the section (in the direction of curving), the larger the minimum curving radius because the amount of strain is proportional to the distance from the neutral axis of the section. The mutual effects of section height, curving radius and material thickness are shown schematically in [Figure 3.8.4.2.2-1](#).

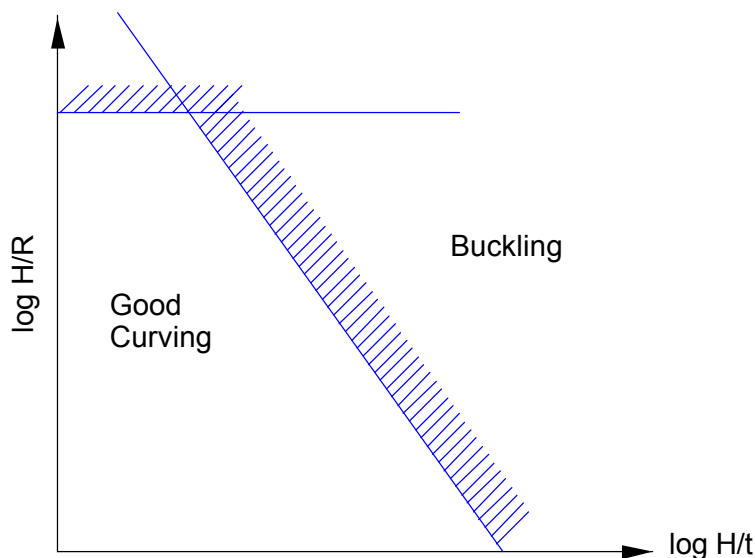


Figure 3.8.4.2.2-1 Mutual effects of section height (H), curving radius (R) and material thickness (t)

3.8.4.2.3 Section Shape

Wider flat compressed elements in a section are more prone to buckling than narrower flat or curved elements. [Figure 3.8.4.2.3-1](#) shows methods for reducing the length of flat elements or replacing them with curved elements. The figure also indicates that it is more helpful to modify elements on the compression side than on the tension side because the compression side experiences more difficulties as noted above.

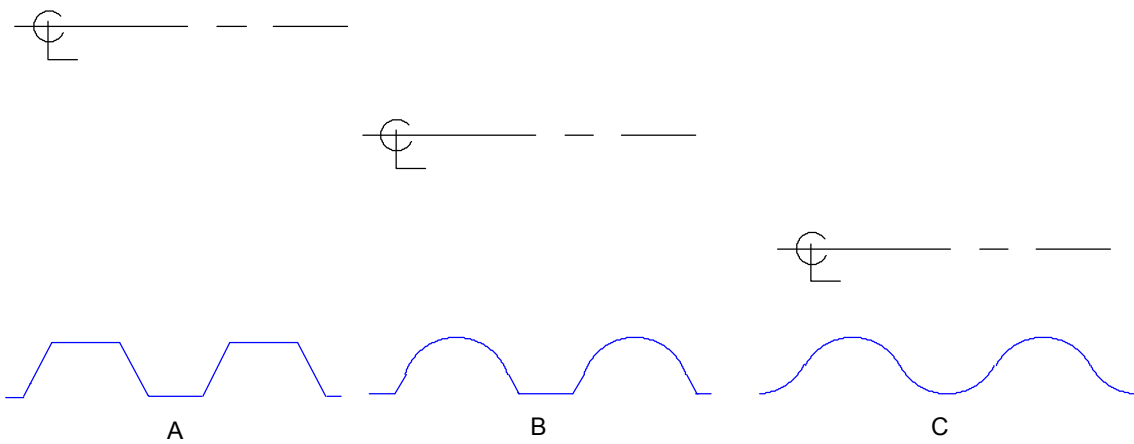


Figure 3.8.4.2.3-1 The relatively large minimum curving radius for Section A can be reduced by substituting curved elements for flat on the compression side. Substituting curved for flat on the tension side also gives a further reduction.

3.8.4.2.4 Use of Stiffeners

Stiffeners can be added to some sections subject to crippling to increase stiffness of critical elements. The use of these stiffeners is similar to those used for load carrying members subjected to stresses within the elastic range discussed in [Section 3.1](#). The principles developed in that section can be applied qualitatively to curving operations, but not quantitatively because the formulae assume that the stresses are within the elastic limit. [Figure 3.8.4.2.4-1](#) illustrates stiffeners applied to the legs of the U channel to reduce the crippling tendency.

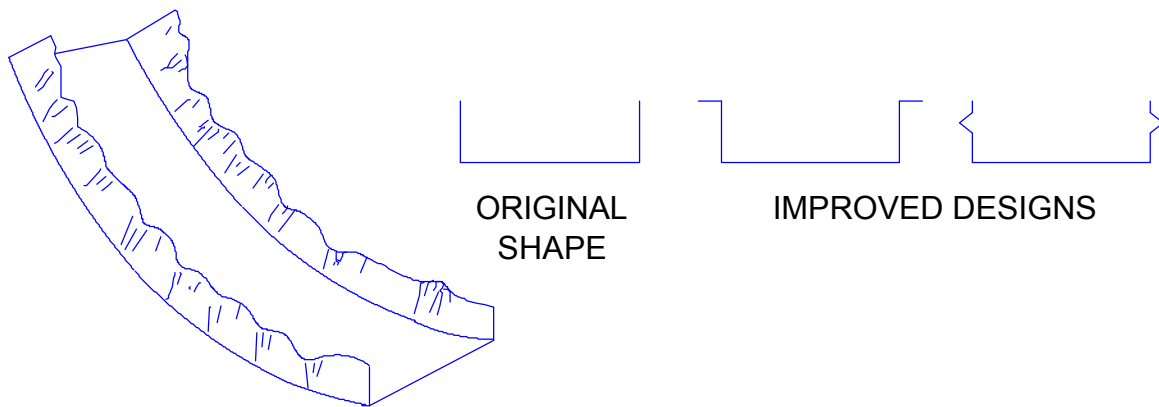


Figure 3.8.4.2.4-1 Stiffeners on the legs of the channel reduce the tendency of the legs to cripple in curving operations

3.8.4.2.5 Hidden Bend Lines

Bends made in the section enhance its strength and rigidity, but they make the component more difficult to curve, particularly when they prohibit roll contact on areas of the section that are critical to the bending operation. It is easier to curve components with rolls if all of the bend lines are accessible to the rolls. For example, the C section and the hat section [Figure 3.8.4.2.5-1](#) have the same blank size, thickness, width, height and section modulus about a horizontal axis.

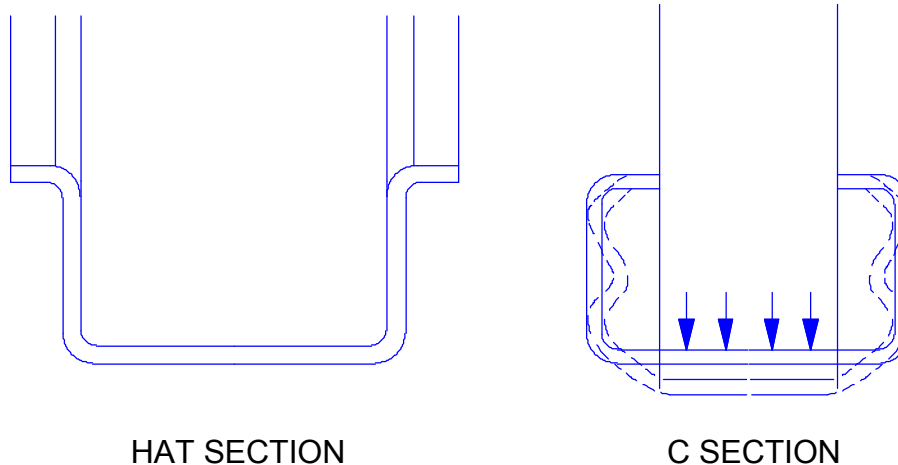


Figure 3.8.4.2.5-1 The curving rolls can reach the bend lines of the hat section but not the C section. Distortion of the C section can occur as illustrated.

All of the bend lines in the hat section are accessible to the rolls. However, the rolls are obstructed from the bend lines at the junction of the web and legs of the C section, so it can distort during curving. Therefore, the hat section can be curved to a smaller radius than the C section. This principle does not apply if the sections are curved with shoes (curved bronze members that are fitted to both surfaces of the metal and do not rotate).

3.8.4.2.6 Cut-Outs and Dimples

The economy of roll forming makes it desirable to form cut-outs of various types and formations such as dimples as a part of the roll forming operation. However, these features complicate curving. The undesirable effects of these features can be minimized by observing the following precautions.

1. Dimples, lances and embossed holes require grooves in the curving tools to prevent the tools from flattening them. These protrusions should therefore be located far enough from the bend lines to allow maximum surface contact between the curving tool and material.
2. Hole-to-hole distances in surfaces subject to tensile strain will increase and the holes will elongate. The opposite will be true of holes in surfaces subjected to compressive strain. These effects should be accounted for in design if they adversely affect product function.

3. Holes too close to the edge of a leg or web in areas subject to compressive strain can cause buckling, as illustrated in [Figure 3.8.4.2.6-1](#).

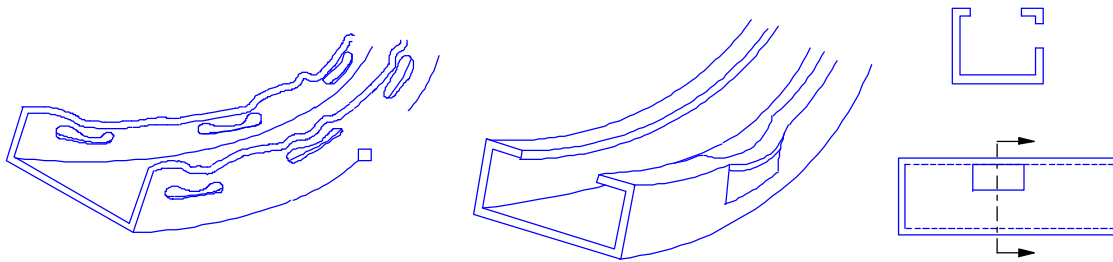


Figure 3.8.4.2.6-1 Holes located too close to the edge of compression element can cause buckling

4. Flare, as noted above, occurs at the beginning and end of sections. Deep cut-outs, such as those shown in [Figure 3.8.4.2.6-2](#), simulate cut-offs and induce flare. Curving with rolls can accentuate flare at cut-outs; the use of curving shoes can minimize or eliminate it.

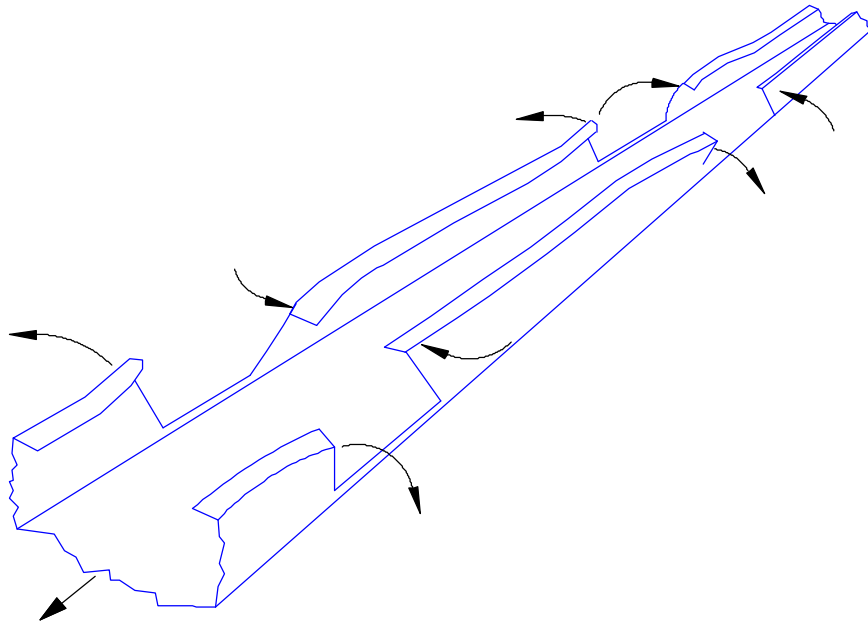


Figure 3.8.4.2.6-2 Deep cut-outs can cause flare

5. Deep cut-outs can also weaken a section and induce buckling during curving as shown in [Figure 3.8.4.2.6-3](#). If the cut-out is on only one side, the component can be expected to twist. These problems can also be minimized or eliminated by using curving shoes.

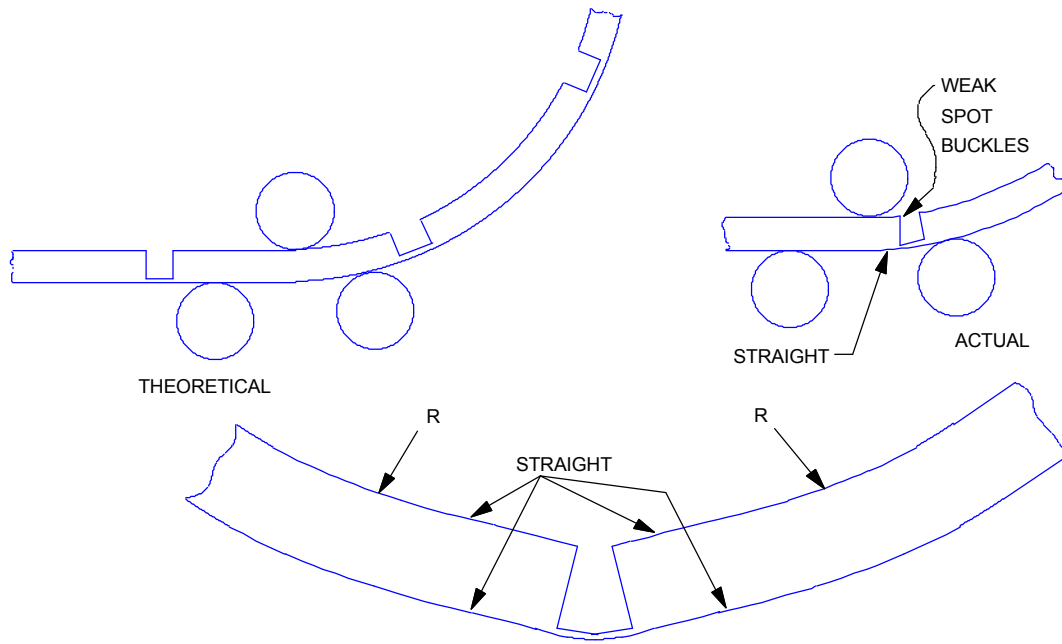


Figure 3.8.4.2.6-3 Deep cut-outs can induce buckling during curving

3.9 SPECIAL DESIGN CONSIDERATIONS

Advances in materials and manufacturing technology are creating new opportunities for design alternatives that improve performance and reduce cost and mass. This section addresses areas of body design where advances in design, materials and manufacturing technology can be utilized to increase performance and improve cost effectiveness.

3.9.1 TAILOR WELDED BLANKS

Tailor welded blanks are used for two purposes:

- Combine several steel options into a welded blank prior to stamping. By combining varying thicknesses, coatings and material grades, the product and manufacturing engineers can tailor the blank to take advantage of the different properties of the steels within the part.
- Integrate and eliminate parts, resulting in savings for tooling, operational costs, and lead time.

Tailor welded blanks are currently used for:

- Door inner panels
- Body side frames
- Underbody frame rails
- Engine compartment rails
- Center pillar inner panels

They may be considered for any application to realize one or more of the following benefits:

- Fewer parts
- Fewer dies
- Fewer spot welds
- Reduced design and development time
- Lower manufacturing costs
- Less purchased material due to better utilization
- Mass reduction
- Improved dimensional accuracy
- Improved structural integrity
- Improved safety

3.9.1.1 Types of Welds

Four types of welds are used or have been considered for tailor welded blanks:

- Laser beam, with and without filler wire
- Resistance mesh seam
- High frequency induction
- Electron beam (non-vacuum)

Currently, laser beam and resistance mesh seam welds are employed in vehicles built in North America. These processes are illustrated in [Figure 3.9.1.1-1](#) and [Figure 3.9.1.1-2](#).

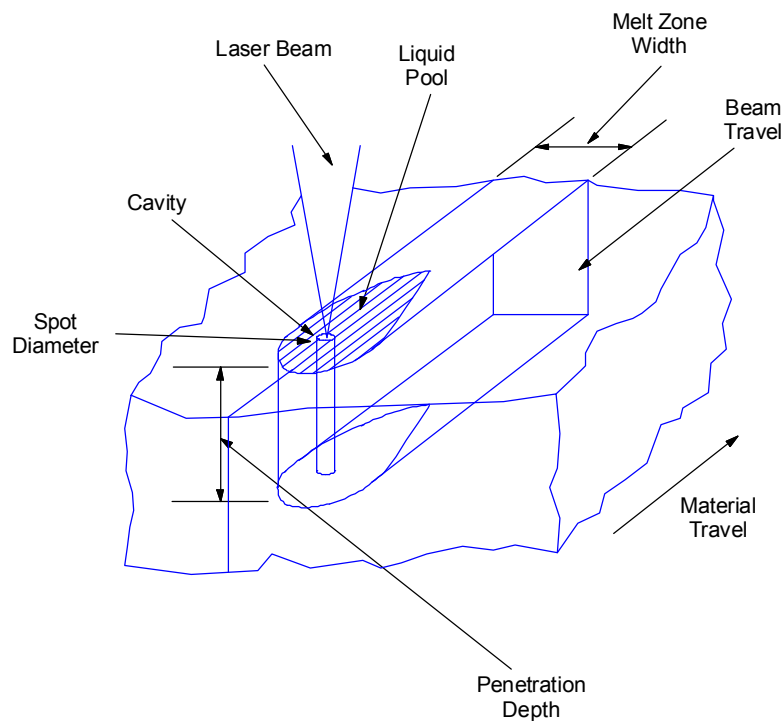


Figure 3.9.1.1-1 The laser beam butt seam welding process

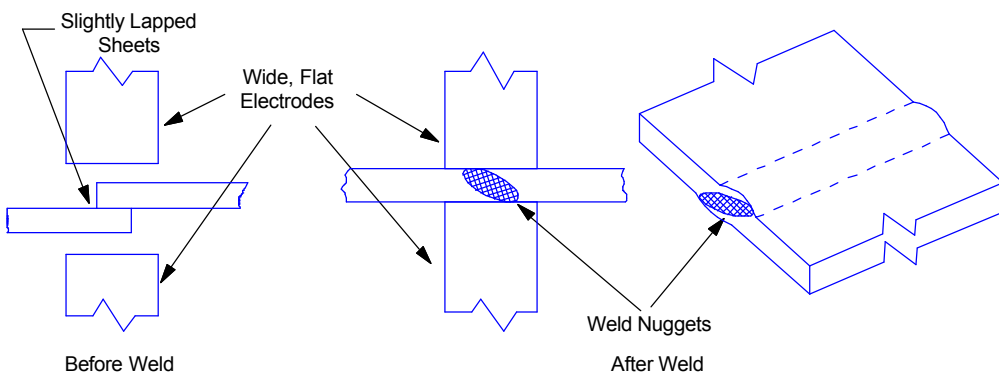


Figure 3.9.1.1-2 The resistance roller mesh lap seam welding process

3.9.1.2 Welding Process Selection Criteria

The welding process selection is driven by factors such as:

- Cost
- Structural requirements
- Stamping process requirements
- Blank welding capability
- Availability of material
- Aesthetic requirements

Resistance mash seam welding requires an overlap and produces a seam that is 10% to 50% thicker than the thicker of the materials. The latitude to reduce the thickness is limited by process requirements. Thicknesses toward the low (10%) limit are usually achieved by a post-weld planishing operation, which compresses the weld joint between steel rollers. The heat affected zone is approximately twice the width of the weld. Currently available tailor welded blank mash seam welding processes are able to produce welds in lengths from 50 mm (2.0 in.) to 2500 mm (100 in.) in a straight line only. Edge preparation is unnecessary unless welding multiple piece blanks, such as for a bodyside ring. Gauge limitations are:

- Minimum thickness 0.7 mm (0.030 in.)
- Maximum thickness 3.0 mm (0.120 in.)
- Total thickness 5.0 mm (0.200 in.)
- Maximum material thickness ratio 3:1

Laser beam tailor welding produce a narrower heat affected zone than mash seam, but requires precision shearing of the blank edges to assure a good fit up prior to welding. The joint is concave when no filler wire is used, as shown in [Figure 3.9.1.2-1](#).

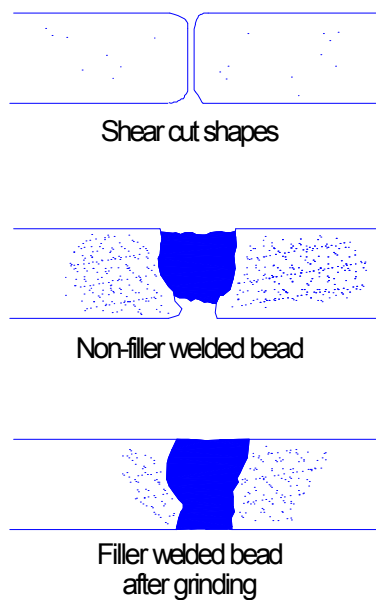


Figure 3.9.1.2-1 The effect of filler wire use and grinding on a laser beam butt seam weld

The use of a filler and post-weld grinding produces a weld that is flush with the parent metal when the two pieces of stock being joined are of equal thickness. Maximum weld length is currently about 3800 mm (150 in.), and the process can weld non-parallel lines. However, maintaining edge alignment becomes more difficult with welds over 500 mm (20 in.) in length, and edge preparation becomes more critical. Gauge limitations are:

- Minimum thickness 0.7 mm (0.030 in.)
- Maximum thickness 3.0 mm (0.120 in.)
- Maximum material thickness ratio 3:1

Neither process is currently being used for a "Class A" exposed surface on an outer panel. However laser welded blanks are being used on secondary exposed surfaces, such as the bodyside frame and door inner panels. Other advantages of laser welding include:

- Where appearance is important and where weather seal surface or wind noise is important, the laser weld process may have advantages over resistance mash seam due to surface geometry.
- Hem flange requirements may favor laser beam welding.
- Laser welding has a narrower heat affected zone. For example, the heat affected zone of a mash seam weld joining two pieces of 1.0 mm (0.040 in.) stock is typically 4 to 8 mm (0.16 to 0.32 in.), while the width for a laser weld is 2 to 3 mm (0.080 to 0.12 in.).
- Laser welding is more suitable for joining coated steel because it is a non-contact process, and its narrower heat affected zone burns off less of the coating.

Where either process is acceptable, resistance mash seam welds generally cost less to produce.

3.9.1.3 Potential Applications for Tailor Welded Blanks

Potential product applications are best identified by recognizing the advantages, particularly in terms of economics, of tailor welded blanks, which include:

1. Part integration and tooling cost reduction
2. Improved material yield
3. Mass reduction and structural integrity
4. Reduced dimensional variation

Other product considerations are discussed in [Section 3.9.1.4](#).

In assessing the economic effects of part integration, product engineers and designers should assess the following factors:

- Total reduction in parts count, including engineering, design and assembly costs.
- Total reduction in the number of tools, including the costs of designing, building and operating them.
- Cost reduction derived from the selective use of coated steels and different strengths and thicknesses of steel.

Material yield is affected by three factors:

- Part design
- Draw die development
- Blank nesting

Parts made in draw dies typically have material utilization ranging from 30% to 80%. In other terms, a material utilization rate of 80% means that 1.25 kg (lb) of material must be purchased to produce one kg (lb) of product; a utilization rate of 30% requires the purchase of 3.3 kg (lb) to produce one kg (lb) of product. Parts that are nearly rectangular in outline, made from blanks that nest efficiently, tend toward the upper end of the range. Those that are very irregular and cannot be nested efficiently tend toward the lower end.

In some cases it is possible to split the blank into pieces that can be nested efficiently, then weld them to produce the desired shaped blank. [Figure 3.9.1.3-1](#) illustrates one way in which material that would otherwise have been engineered scrap is utilized to improve nesting and increase material utilization. [Table 3.9.1.3-1](#) summarizes material utilization in typical body applications.

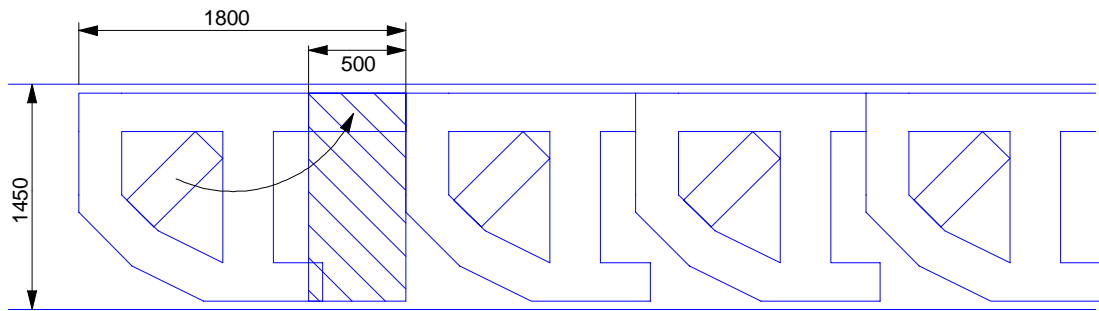


Figure 3.9.1.3-1 By utilizing stock that would otherwise be engineered scrap and making tailor welded blanks, blank nesting is improved and purchased stock reduced by 28%.

Table 3.9.1.3-1 Effect of Part Shape on Material Consumed

Part Shape	Typical Parts	Blank Mass (kg)	Panel Mass (kg)	Eng. Scrap	Stock Mass/Panel Mass
Rectangular or Trapezoidal	Roof Outer	11.35	9.03	20%	1.25
	Hood Outer	12.45	9.98	20%	1.25
	Rocker Outer	2.70	2.15	20%	1.25
	Deck Lid Outer	9.60	6.01	37%	1.60
Irregular	Front Fender	5.94	3.04	49%	1.95
	Quarter Outer (coupe)	16.53	7.52	54%	2.20
	Quarter Inner (coupe)	9.92	5.85	41%	1.70
	Quarter Outer (sedan)	14.76	4.76	68%	3.10
	Quarter Inner (sedan)	4.32	1.19	72%	3.63
	Front Body Hinge Pillar	6.39	1.86	71%	3.44

The manufacturing engineers generally determine the economic feasibility of using tailor welded blanks, and the product engineers evaluate the effects of the composite structure on the product.

The factors that drive the potential for mass reduction from the use of tailor welded blanks also drive the potential for improved structure. The following illustrations may allow a reduction in mass, improvement in structure or a combination of both. Structure includes both NVH (noise, vibration and harshness) and crashworthiness considerations.

- Joining sheet stock of varying thicknesses allows material thickness to conform more nearly to structural requirements, and eliminates the tendency for one critical feature to drive the thickness of the entire part.
- The weld joints require little or no overlapping of metal, as is required with spot welded or bonded joints.
- The continuous welds generate a monolithic structure, which is inherently stronger and stiffer than spot welded or adhesive bonded reinforcements.

Dimensional variations can be reduced significantly by the use of tailor welded blanks. Variations are reduced by:

- Eliminating stack-up tolerances.
- Eliminating distortions, such as those caused by welding guns when parts do not meet exactly.

Reduction in dimensional variations have been reported by both domestic and foreign manufacturers. For example, door opening variations have been reduced by as much as 50%.

3.9.1.4 Other Product Considerations

In addition to the applications noted above, production experience with tailor welded blanks indicates satisfactory performance, and in some cases improved product performance, in the following areas.

3.9.1.4.1 Crashworthiness

The following have been concluded from tests of axial and bending modes on components made from tailor welded blanks.

- Rectangular thin wall section beams formed by laser and mash seam tailor welded blanks performed satisfactorily in crush tests at speeds up to 42 km/hr (26 mph) and 25 km/hr (15.5 mph).
- There was minimal difference between laser and mash seam welded blanks in terms of maximum energy absorption, peak load and maximum crush distance.
- The energy absorption of rails formed by tailor welded blanks increases significantly with steel sheet thickness and slightly with material yield strength.
- Galvanized sheet surfaces showed minimal effects on crashworthiness performance.
- High strength steels enhanced the local stability in the axial mode of collapse.

3.9.1.4.2 Sealing Compounds

Since the welds used in tailor welded blanks are continuous, compared with intermittent spot welds, no sealing compounds are required at the weld joints. Savings are realized from the elimination of investment, material and application costs. Environmental benefits and minor mass savings may also accrue.

3.9.1.4.3 Corrosion Resistance and Coating Adhesion of the Weld Seam

Corrosion resistance of coated stock is affected by the width of the heat affected zone, because the heat of welding destroys the coating. In general, the narrower the zone, the better the corrosion resistance. Paint adhesion is highly dependent on the formation of a good phosphate coating prior to painting. The formation of the phosphate coat is adversely affected in the heat affected zone. Where high levels of corrosion resistance are required, special attention to corrosion resistance of the seam will be required.

The information in this section was extracted from Tailor Welded Blank Design and Manufacturing Manual, Auto/Steel Partnership, 50 30-01 895 MPG, July 1995. Please consult this source for additional information and references.

3.9.2 VALUE ENGINEERING/VALUE ANALYSIS

3.9.2.1 Introduction

Value engineering/value analysis,¹ (VE/VA) was originally developed to identify and eliminate unnecessary manufacturing costs without reducing product functionality, reliability, durability or appearance. It has been successfully applied to a variety of steel products and processes simultaneously improving functionality and reducing cost.

VE/VA is a disciplined, clean sheet approach to problem solving. It focuses on specific product design and manufacturing process characteristics. VE/VA comprises two related disciplines: value engineering (VE) and value analysis (VA). VE is employed up front, is design focused, and is done before production tooling is established. VA is employed to improve value after the start of production.

3.9.2.2 Advantages of VE/VA

Traditional approaches to cost reduction focus on eliminating obvious unnecessary cost. Today's competitive global marketplace demands a more comprehensive approach. The VE/VA provides that. It:

1. Asks "How can we maintain or improve reliable performance of this part for the least cost?"
2. Is function oriented.
3. Addresses unnecessary cost, both obvious and not obvious.
4. Maintains or improves performance for the customer.

VE/VA helps engineers get new ideas in steel materials and processes to market faster, at a price the customer is willing to pay. The power of the VE/VA technique is derived from five key ingredients:

1. The synergistic power of a multi-disciplinary team.
2. Positive atmosphere.
3. An easy to follow, disciplined approach to gathering the required information.
4. Active participation in the decision making process by those people who will implement the proposals that are generated.
5. Systematic, logical series of separate problem solving steps involving separate types of mental activity, including:
 - Exhaustive accumulation of facts and data.
 - Identification and improvement of assumptions.
 - Penetrating functional analysis.
 - Creative brainstorming.
 - Critical judgment and evaluation.
 - Systematic searching of the creative thoughts to maximize advantages and minimize disadvantages.

3.9.2.3 How the VE/VA Process Works

The VE/VA process is performed in six distinct steps:

1. Gather information

Define the scope of the project and gather the most accurate, up-to-date information from appropriate sources.

2. Define functions

During this stage, the questions "What does the product or process do?" and "How much does it cost to do that?" are answered in very specific terms. This process identifies functions with high value-improvement potential.

3. Generate creative alternatives

Creative forces and abilities are called upon in a brainstorming session to generate a great number of alternate methods of providing the selected functions.

4. Evaluate and develop proposals

The ideas generated in the creative stage are combined and developed into proposals for implementation.

5. Recommend proposals

The most promising proposals are critically reviewed with the appropriate audience for "buy-in".

6. Implement proposals

Effective follow-up ensures that the appropriate activity such as testing and validation of the proposal are carried out. Related cost savings and performance improvement are documented.

Timely execution of these six steps will avoid most product development problems in the design phase. It also helps to achieve a fundamental objective of most projects: to meet or exceed customer requirements at reduced cost.

3.9.2.4 Value Defined

Value is a relationship between product function and cost, and may be defined by the equation:

$$\text{Value} = \frac{\text{Function}}{\text{Cost}}$$

Equation 3.9.2.4-1



where function = those things that the product, process or procedure must do to satisfy the customer

cost = expenditures of resource including time, money, people, energy and material

The equation indicates that the greatest value improvement occurs when function is increased while simultaneously reducing cost.

Ultimately, value depends on the effectiveness with which every usable concept, material, process and approach to the problem has been identified, analyzed and implemented. Maximizing value is the goal of every VE/VA effort. VE/VA brings better combinations into focus with less expenditure of resources.

3.9.2.5 Details of a VE/VA Program

Detailed information on how to conduct a VE/VA program for steel automotive body components has been developed for AISI and is available on request¹.

3.9.3 DESIGN GUIDELINES FOR ULTRA-HIGH STRENGTH STEELS

High strength and ultra-high strength steels (UHSS) with moderate ductility have become increasingly important in automotive structural design. In particular, they enable body engineers to meet various safety requirements at minimum mass and cost. UHSS are produced by a continuous heat treatment, which includes a controlled high temperature heating followed by a water quench and a mild reheat cycle. UHSS are relatively isotropic in mechanical properties, have maximum through-coil uniformity, and are available in thicknesses from 0.5 to 2.0 mm (0.020 to 0.080 in.).

There are some design limitations due to manufacturing considerations. Ductility generally decreases as yield strength increases. Lower ductility of UHSS limits bendability, defined as the ratio of bending radius to stock thickness (r/t), to a minimum of about 4. In addition, springback, which increases with the yield strength of the material, is higher in UHSS than in mainstream sheet steels. Most UHSS can be formed in stamping dies, as long as provision is made for lower ductility and limitations in bending radii. Bend stretching, drawing and flanging are all possible.

Most of the UHSS can be formed by roll forming. Pre-piercing and post-roll forming operations, such as sweeping and limited stamping, are routinely practiced. Hence, components with essentially constant cross section are excellent candidates for UHSS. Because of the relatively low tooling costs and high production rates of roll forming, this technology is used extensively to exploit the mass reduction potential of the UHSS. Most of the applications for door intrusion beams, bumper reinforcing beams and structural tubing are roll formed.

As sweep curvature is increased, roll forming operations become more challenging because increasing curvature increases both tensile and compressive stresses. Two options are available to ensure ease of production:

1. Maintain maximum allowable beam depth (for minimum mass) and reduce yield strength to increase ductility. For example, several high sweep bumpers are produced in 965 MPa (140 ksi) yield strength steel rather than 1300 MPa (190 ksi).
2. Reduce depth and increase thickness, reducing the strains from sweeping, and permitting the use of 1300 MPa (190 ksi) steel, again to minimize mass.

Design guidelines for UHSS are discussed in several publications [2,3,4](#).

Deflection of UHSS components can involve large elastic deflections as well as localized plastic deformation, such as crippling. Successful application of FEA requires that both the overall load-deflection curve and the local deformation be accurately predicted. When full curve tensile properties are required, refer to individual steel suppliers.

REFERENCES FOR SECTION 3.9

1. Freeze, D.E., A Report on Value Engineering /Value Analysis, American Iron and Steel Institute, AU-2004, 1992.
2. Borchelt, J.E. and Subbaraman, B., Design of Ultra-High Strength Sheet Steel Beams , SAE Paper 900428, March, 1990, Warrendale, Pa.
3. Shapiro, J.M., Cline, R.S. and Subbaraman, B., Application of Ultra-High Strength Sheet Steels for Mass and Cost Savings , IBEC, 1993.
4. Borchelt, J.E., Shapiro, J.M. and Subbaraman, B., Application of Empirical Relationship Developed for Ultra-High Strength Steels in Bumper Design , SAE Paper 900737, March, 1990, Warrendale, Pa.

3.10 DESIGN GUIDELINES FOR SHEET STEEL

The impact of design on manufacturing is not always obvious. Therefore, the efficient use of steel in the design of body components requires cooperative effort between design and manufacturing engineers, and that the designer have a basic knowledge of the influence of sheet metal designs on manufacturing. This section provides guidance on how various sheet metal designs impact manufacturing, and thus the cost of tooling, and component quality and cost.

In order to remain competitive in the worldwide automotive marketplace, manufacturers must produce high-quality, minimum-cost steel bodies consistent with requirements for timely introduction of new models and freshened redesigns. Tooling costs, which are driven by the number and complexity of the dies required to make a component, play a major role in these design decisions. Improvement can be made only by careful attention to the impact of design features on manufacturing, on a part by part basis.

For this reason, each automobile company has developed manuals that attempt to convey to the body designer those aspects of a design that cause difficulty in manufacture, and the acceptable parameters that should be incorporated in the design to guarantee manufacturability. The parameters are frequently organized by panel, and focus on specific characteristics of specific panels. If, however, the reasons for the difficulty in manufacture are not clearly stated and generalized, the manual runs the risk of becoming a sterile collection of rules which differ from panel to panel.

The information in this section identifies some general characteristics or manufacturing issues that add cost to the product or pose difficulties in quality assurance and briefly discusses their important elements. The section contains seven subsections, each of which can be read independently. None is comprehensive. The topics covered are all relevant to the design of low cost sheet metal components and are included based on inputs of lists of characteristics surveyed during the first assessment of the manufacturability of a design.

No attempt is made to develop rules, since there are few designs that cannot be manufactured with the expenditure of enough time and money and the application of enough forming operations, dies, and presses. However, the manufacturing issues associated with many designs create major difficulties. This section provides the designer with information that will better enable him to identify critical design features early in the design process and provides data to make a more informed tradeoff between manufacturing difficulty and functionality before the design is released.

The impact of material selection on manufacturability is discussed in [Sections 2.3, 2.5](#), and [2.8.5](#). These sections should be reviewed to gain the background for the following discussion.

3.10.1 DESIGN FOR COMPONENT CONSOLIDATION

Component consolidation depends on shape and process considerations, and opportunities for consolidation exist in both large and small assemblies. For example, body side apertures and floor pans can be redesigned to combine components. Smaller assemblies can be redesigned to save mass and increase performance by tabbing individual parts for assembly or by specifying a particular geometry where components join with other parts. Minor components, such as brackets that are used for assembling the body-in-white, and then become redundant, can often be eliminated when other joining techniques are designed into the body.

Since styling delivers product forms that engineering cannot easily change, for reasons of appearance, major outer body panels are not generally candidates for redesign. Opportunities for consolidating parts are primarily confined to non-visible areas such as underbodies.

3.10.1.1 Influences of Steel Suppliers' Equipment

The width and thickness of steel sheets are limited by the steel suppliers' equipment. Designs can be maximized within width constraints, while reducing both scrap and mass, by employing known technology. For example, designers typically combine two or more drawn shapes into a floor pan because steel sheets are not available to the required width for one-piece design in the desired gauge. Recently, very wide one-piece drawn floor pans have been produced from laser welded blanks ([Figure 3.10.1.1-1](#)).

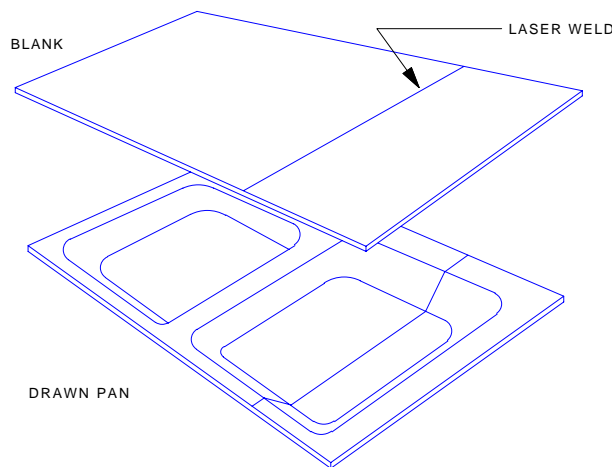


Figure 3.10.1.1-1 One-piece floor pan made from a laser welded blank

Door surrounds are traditionally made from pillars, headers and sills. They can now be combined into one large stamping, or aperture panel ([Figure 3.10.1.1-2](#)), but this tends to create large areas of engineered scrap (see [Section 3.10.3](#)). However, smaller stampings can be formed from the material in the openings either simultaneously or later in another press. Quarter panels can also be integrated into the aperture for further consolidation. (See the case study in [Section 6.1.1](#).)

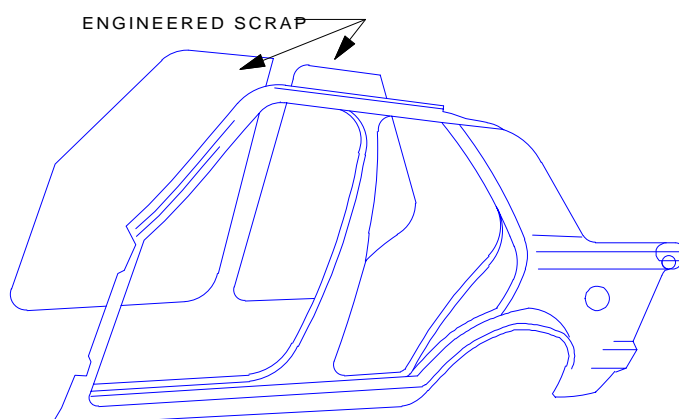


Figure 3.10.1.1-2 One-piece body side aperture panel

When possible, the designer can create common parts that can be used for both sides of the vehicle. This saves a line of dies, increases the volume of production from the line of dies, increases manufacturing efficiency, and decreases cost. Further savings can be realized if designers design components that are common to several platforms.

3.10.1.2 Manufacturing Processes

The designer can utilize new processes or revisit old ones in consolidating components. One new technique is laser welding steel pieces into blanks and finished stampings. Either laser welding or mash-seam welding provides the opportunity to vary thickness and strength within the same blank to enhance product performance. Laser welds are preferred for appearance and integrity, but are currently more costly. For example, blanks are made by welding steel of varying thicknesses and stamping them into door inner panels to increase strength at the hinge face of the door ([Figure 3.10.1.2-1](#)) while eliminating smaller reinforcements. For additional information, see [Section 3.9.1 Tailor Welded Blanks](#).

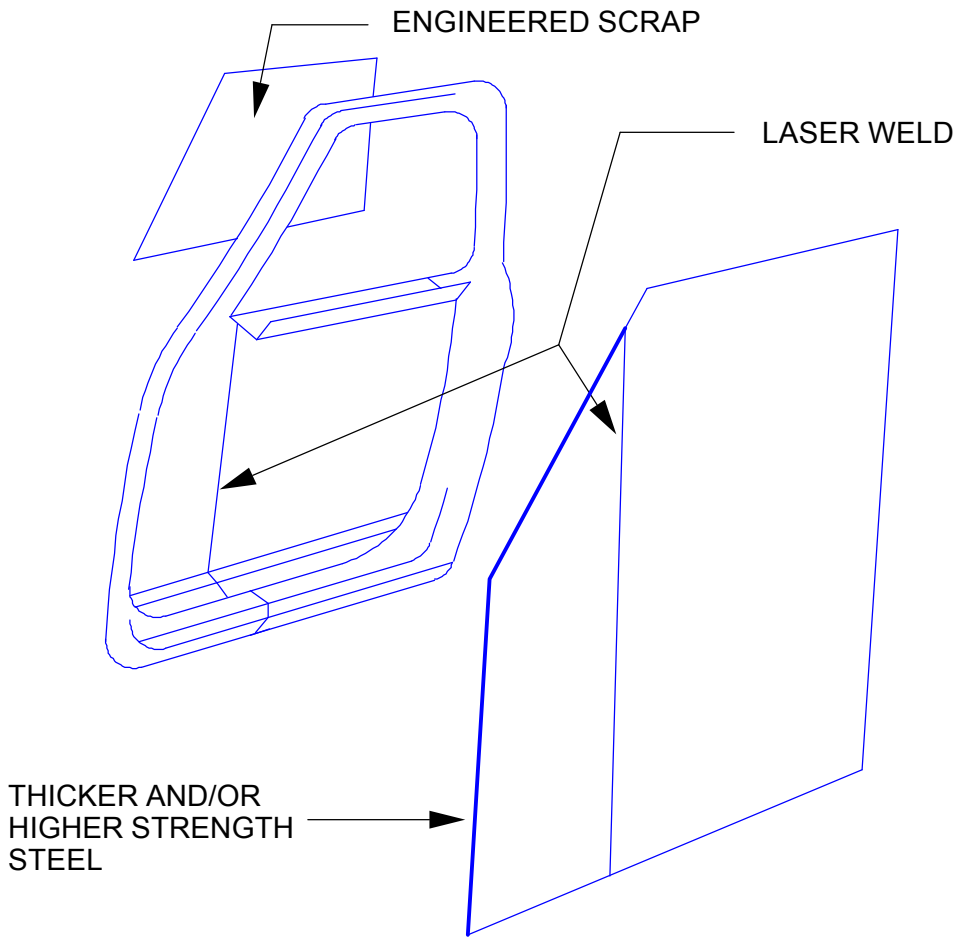


Figure 3.10.1.2-1 Laser welded door inner panel

Blanks for B-pillars are laser welded from two pieces with the lower portion thicker, for improved crash resistance ([Figure 3.10.1.2-2](#)). Laser welded tailored blanks are now available to further increase function and significantly reduce engineered scrap ([Figure 3.10.1.2-3](#)).

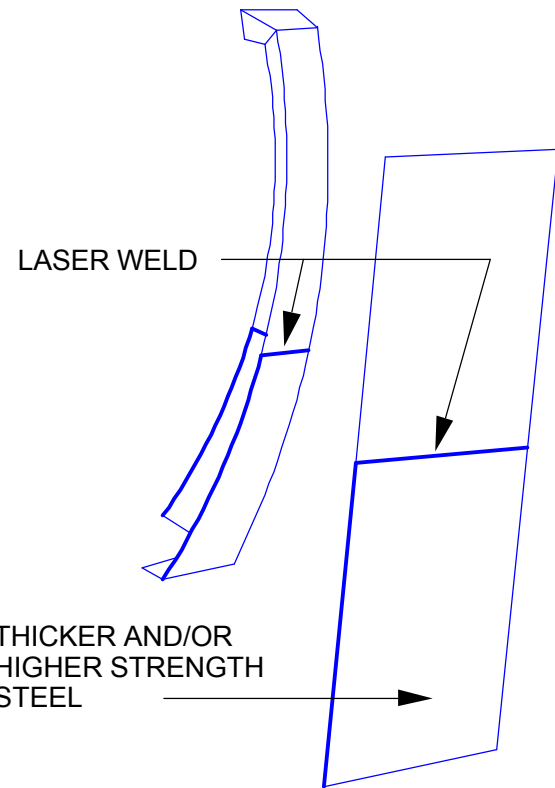


Figure 3.10.1.2-2 Laser welded "B" pillar

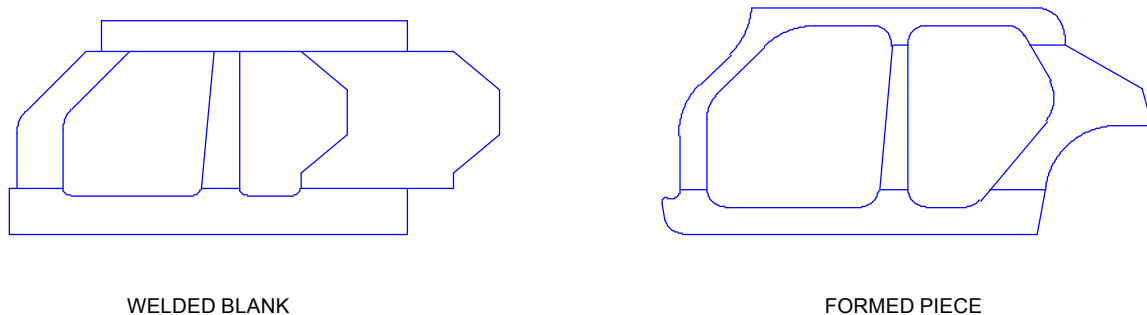


Figure 3.10.1.2-3 Laser welded tailored blanks

Some one-piece intrusion beams for doors are now made by hot forming very high-strength sheet steel. Most beams are typically made of three or more stampings to satisfy the product demands. The one-piece beams are made from net shape blanks that are formed at 1800°F (980°C), then held in the die for typically 20 seconds and rapidly cooled to room temperature. The beams are dimensionally accurate, and tensile strength can exceed 200 ksi (1380 MPa).

3.10.2 TOLERANCING AND PROCESS CAPABILITY

Tolerancing is used to convey the critical design specifications of a product. The specifications are sometimes applied to dimensional characteristics in order to meet fit-and-finish requirements for features such as mating surfaces, trim edges, holes and pins. They are also applied to requirements for various manufacturing operations and to requirements for tooling, gaging, and assembly.

In general, tolerances are restrictive specifications and should be made only as close as necessary to ensure that the component functions satisfactorily. For example, some features, such as principal locating points, exterior surfaces, and mating surfaces, require close tolerances. Others, such as stiffening beads, drain holes, and lightening holes can function with loose tolerances. Unnecessarily close tolerances increase tooling and production costs, lower die life, and may require 100% inspection. Looser tolerances mean simpler manufacturing processes. Any potential conflict over preferred tolerances is best resolved by direct discussions between design and tooling engineers early in the design process.

Some of the various types of tolerances applicable to stamping processes are:

1. Surface controls, such as exterior and mating surfaces
2. Angular controls, such as channel sections
3. Features, such as holes and notches
4. Others, such as burr and appearance

3.10.2.1 Surface Controls

Surface controls can be divided into four categories: exterior or visible panels, interior or non-visible panels, mating surfaces, and trim edges.

Exterior or visible panels, such as hoods, decklids and doors, have surfaces that are visible on a parked vehicle. The surface profiles for these visible panels require close tolerances ([Figure 3.10.2.1-1](#)).

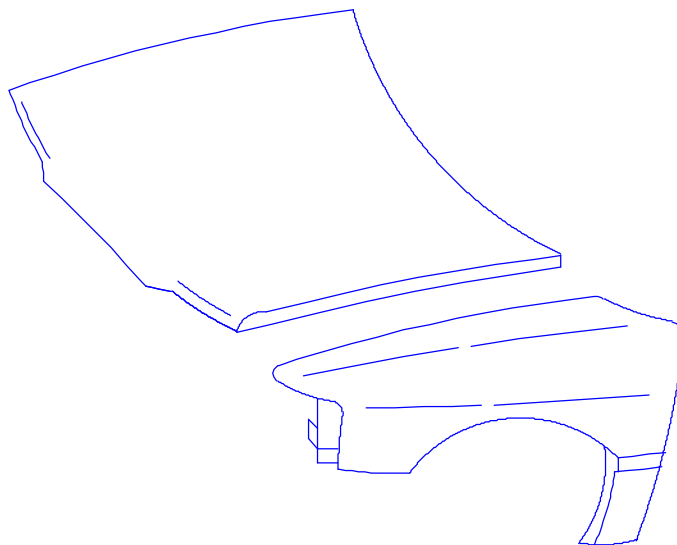


Figure 3.10.2.1-1 Hood outer panel & fender - visible surface

Interior or non-visible panels, such as wheelhouses, inner hoods, inner decklids and underbodies, are not visible on a parked vehicle. Since styling does not have input to these panels, the tolerances are determined on functional requirements only. The tolerances on these panels should be as loose as possible, consistent with functional requirements. Floor pan non-visible surfaces are illustrated in [Figure 3.10.2.1-2](#).

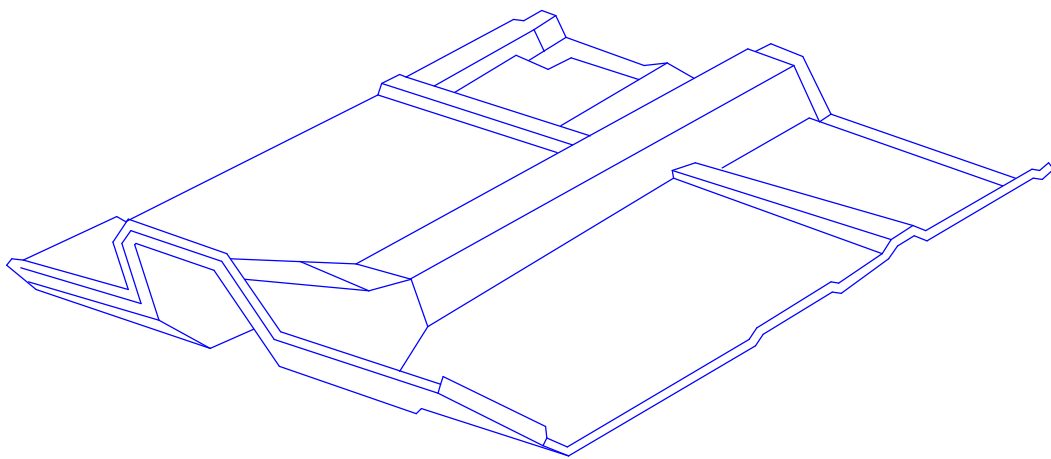


Figure 3.10.2.1-2 Floor pan - non-visible surface

Mating surfaces are required to facilitate some stamping and assembly processes, such as attaching tapping plates, welding at flanges, and attaching seals. Where spot welding is performed, it is necessary to have good contact between mating surfaces so that the welding current can pass through both pieces. Flatness of the mating surfaces should therefore be specified. If tolerances closer than normal are specified, corrective operations such as coining, grinding, or straightening may be required, and cost is increased. Mating surfaces at a roof to aperture joint are shown in [Figure 3.10.2.1-3](#).

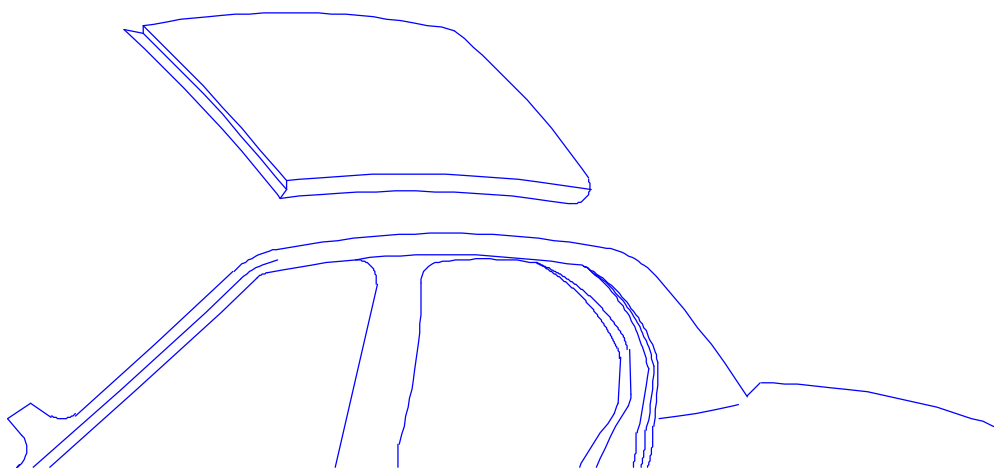


Figure 3.10.2.1-3 Roof to aperture joint - mating surface

Flanges adjacent to trim edges are often hemmed or welded to other flanges. In these cases it is necessary to specify tolerances on the trim edges to maintain the minimum flange width. [Figure 3.10.2.1-4](#) illustrates an assembly of hood inner and outer, which requires minimum flange widths.

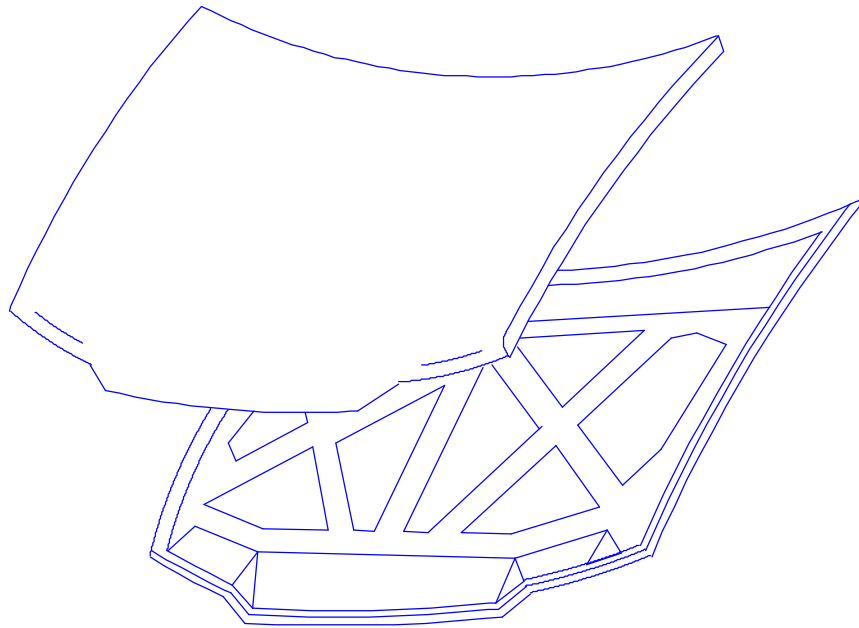


Figure 3.10.2.1-4 Assembly of hood inner and outer requires minimum flange length

3.10.2.2 Angular Control

During forming of channel sections, the vertical walls spring back when the tool forces are released. The amount of springback varies with material thickness, mechanical properties, and forming radii (see [Section 3.10.5.1](#)). To maintain closer tolerance on vertical angles, such as the rail section shown in [Figure 3.10.2.2-1](#), it is necessary to control tolerances on material thickness and properties; this may in turn increase the cost of the material.

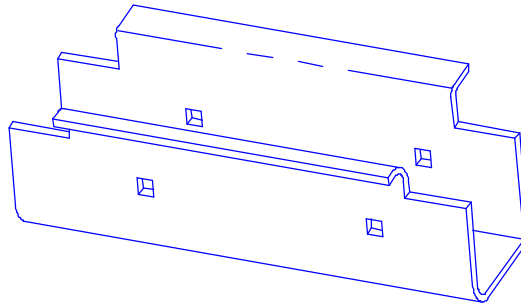


Figure 3.10.2.2-1 Close angular tolerances on the vertical walls of a channel section are difficult to hold due to springback

3.10.2.3 Features Such as Holes and Notches

The tolerances on features such as radii on non-visible surfaces, lightening holes, drainage holes, and stiffening beads should be as loose as possible to avoid costly tooling and processing.

Standard size punches with standard tolerances should be considered for the holes. If tolerances closer than standard are required, the holes must be punched after forming. This procedure reduces production rates and increases tooling cost, increasing piece cost. [Figure 3.10.2.3-1](#) illustrates lightening holes in a decklid inner panel.

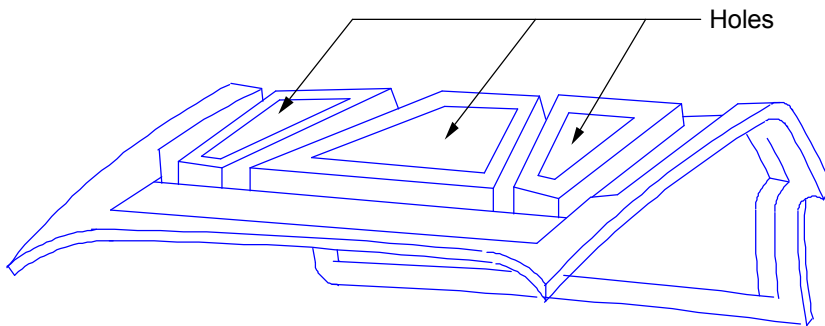


Figure 3.10.2.3-1 Features such as lightening holes in a decklid should be specified to loose tolerances

3.10.2.4 Burr and Appearance

Tolerance for appearance and burr height limits should be avoided unless they affect the function of the component. Removal of burrs or sharp edges incurs additional expense.

3.10.3 BLANKING AND REDUCTION OF ENGINEERED SCRAP

More steel is purchased to manufacture a sheet metal component than is incorporated in the finished form or in the finished body-in-white. The unused or scrap material originates as either manufactured scrap or engineered scrap, which is sometimes termed offal. Manufactured scrap occurs when components, either finished or unfinished, are damaged beyond repair during manufacture. It may, in principle, be eliminated with appropriate care during manufacture.

Engineered scrap is defined and discussed in [Section 4.1.8](#). It is inherent in design of the component and the manufacturing process, and cannot be reduced or eliminated during manufacture irrespective of the care and attention devoted to the manufacturing operation. Engineered scrap can be minimized in design. However, all aspects of the design must be considered to make a balanced judgment. For example, it would be impractical to retain all of the metal in the lightening holes of a hood inner panel to reduce engineered scrap. Similar judgment should be applied to all designs.

3.10.3.1 Reuse of Engineered Scrap

A portion of engineered scrap has the potential to be reused. This usually consists of major areas of flat or nearly flat, essentially undeformed regions, which can be easily recycled through additional blanking and forming operations. Typical examples might be cutout sections in a windshield ring, side ring, hood inner or sun roof.

Although reuse is an obvious and very attractive way to minimize engineered scrap, there are numerous issues. First, the material must be collected. However, transfer press lines are usually set up to move stampings through the line and drop engineered scrap down chutes to underground conveyor belts. Ejecting cutouts to the side of the press line for recovery is frequently impractical and sometimes impossible. Conventional press lines present fewer difficulties, but scrap collection typically reduces productivity due to the additional material handling required.

In principal, the cutouts could be retrieved from the existing scrap processing facilities. It is difficult, however, to obtain large pieces because engineered scrap is frequently trimmed into smaller, less usable segments to make them less prone to jam the scrap chutes. Further, even if large pieces of scrap are segregated, they may be bent or damaged during handling, causing difficulties in feeding them into the downstream die. However, scrap is much more readily collected from a blanking die.

Reuse of scrap introduces additional complexities beyond the collection difficulties, including:

1. The gage, coating and grade of the scrap must match those required for the second stamping.
2. The number of stampings to be made from the scrap should be consistent with the number available from the stamping from which it is obtained. Thus utilization of scrap across car lines with differing sales volumes creates additional difficulties.
3. To minimize handling and shipping, the scrap should be used in the plant in which it is generated. Thus, small stampings that would be natural candidates for scrap utilization can not be outsourced.

[Section 6.1.4](#) is a case study illustrating the use of engineered scrap to fabricate door anti-flutter bars.

A related approach is to use the scrap in the die by integrating a second die to form a smaller stamping simultaneously with the large one. If the small and large stampings have a strong functional relationship, it may be possible to defer separating them until subsequent processing, such as at the assembly plant, to simplify handling.

Although important, scrap utilization programs rarely make a major impact on engineered scrap generation when initiated after vehicle production is started. A reduction in engineered scrap values of 3 percentage points, for example from 44% to 41%, is optimistic without a major concerted effort early in a vehicle program. A reduction of 1.5% is more typical. Thus the most effective approach to reducing engineered scrap is through component and process design early in the program.

3.10.3.2 Blank Nesting

Blank nesting, or the locations of the blanks on the incoming steel strip, is probably the most significant single factor influencing engineered scrap. Blanks with simple shapes offer the best opportunity to minimize engineered scrap as shown in A of [Figure 3.10.3.2-1](#).

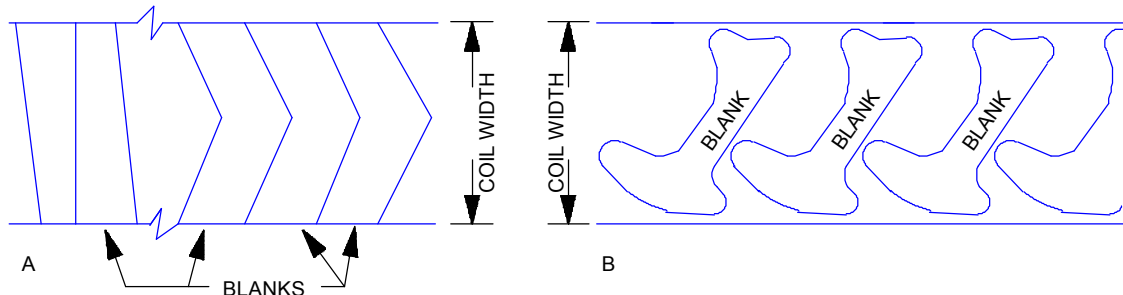


Figure 3.10.3.2-1 The blanks at A nest and permit essentially 100% utilization of incoming steel. The blanks at B do not.

On the other hand, stampings that use an irregularly shaped or developed blank, as shown at B, necessitate careful blank nesting to minimize scrap.

The product design can markedly influence the efficiency of nesting, and thus the amount of engineered scrap, by the extent to which it incorporates features that force a deviation from the simple shapes in [Figure 3.10.3.2-1](#) example A. For example, design B in [Figure 3.10.3.2-2](#) will lead to more engineered scrap than design A, because of the "ears" on one end of B corresponding to the attached "C" pillar.

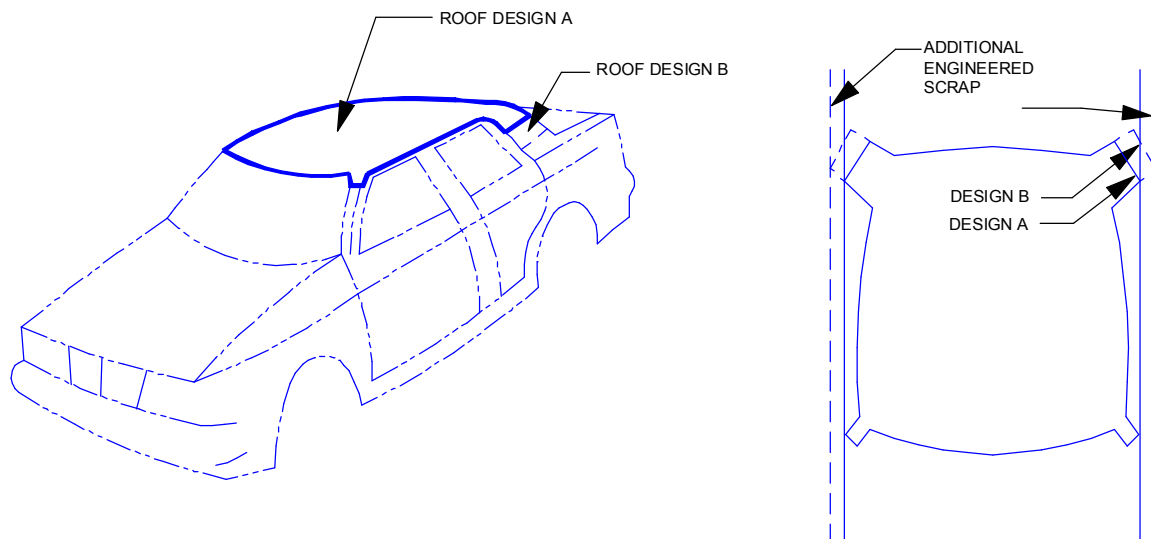


Figure 3.10.3.2-2 The design of the roof panel influences the stock width and consequently the amount of engineered scrap

A second example is shown in [Figure 3.10.3.2-3](#) for a "B" pillar. The difference in length of the section at the bottom, and hence the difference in engineered scrap, is directly related to the bottom flair. Furthermore, the unavailability or limited availability of wide coil widths may force a less than optimum nesting, particularly for large stampings.

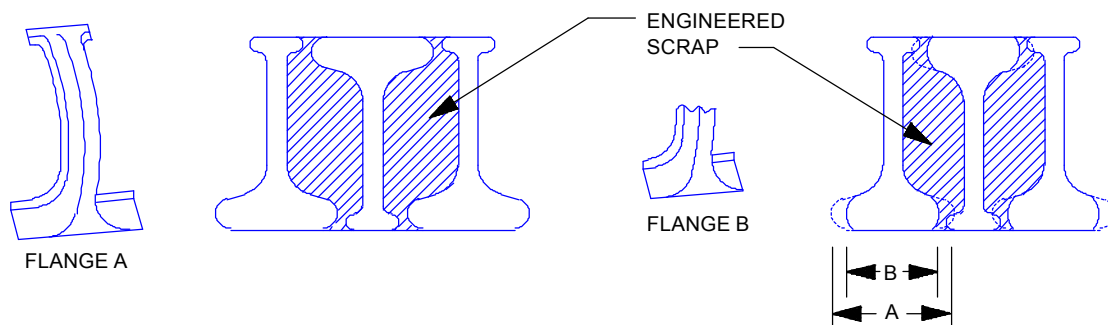


Figure 3.10.3.2-3 The length of the flange at the bottom of the B pillar affects the amount of engineered scrap

3.10.3.3 Reducing Binder Scrap

Another major opportunity to reduce engineered scrap lies in reducing binder scrap. The most effective way to reduce binder scrap is to use a form or "crash" die, eliminating the binder completely and using a developed blank. However, as mentioned above, this may lead to an increase in engineered scrap during blanking by reducing the efficiency of nesting.

Less dramatic, but no less significant savings can be achieved by:

1. Minimizing the depth of draw to reduce the height of the draw wall and hence the overall blank size.
2. Double attaching components to "share" the binder loss between two or more components.

In general, consolidation also leads to engineered scrap reduction by eliminating some of the binder regions and attaching surfaces from individual components. If, however, many of the individual stampings are manufactured on a form die, and the consolidated component requires a draw die, the anticipated reduction may not be realized.

3.10.3.4 Alternate Manufacturing Processes

For open or closed channel sections, roll forming offers the opportunity to reduce engineered scrap significantly. Since a limited amount of sweep can be developed in the section, roll forming need not be restricted to straight forms. See [Sections 3.8 and 4.2](#) for more detailed discussions of design for roll forming and the roll forming process. An extension of this, which offers the opportunity to also vary section geometry, is hydroforming of tubes.

Another approach is to make use of recently developed technology for laser welding and mash seam welding. These processes enable blanks of irregular shape to be fabricated as an assembly of simpler shapes that can be individually blanked with much less engineered scrap. An example might be a body side panel, [Figure 3.10.3.4-1](#), where engineered scrap can be minimized and material effectiveness optimized by fabricating the blank from a series of more regular shapes. Also, the ability to fabricate a blank for a large panel from small segments offers an opportunity to use smaller pieces of scrap generated in other operations.

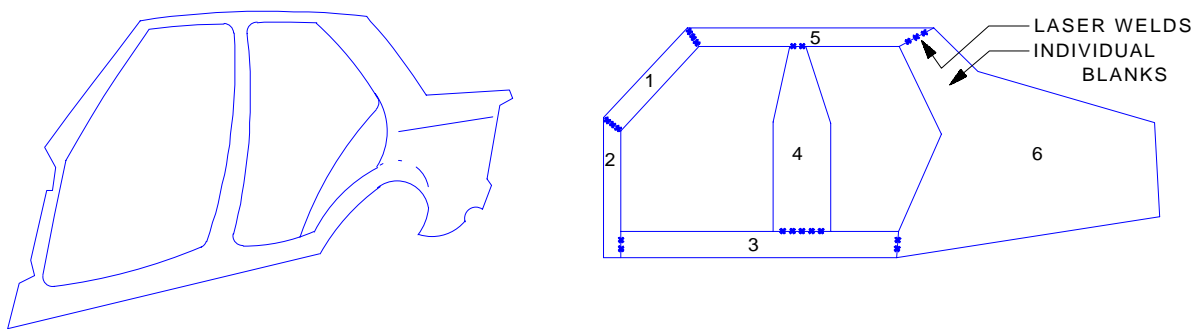


Figure 3.10.3.4-1 Schematic of side ring comprising six individual blanks laser welded to form one composite blank

See [Section 4.3.3](#), and the case studies in [Sections 6.1.3 and 6.1.4](#) for a more detailed discussion and examples of laser welding.

3.10.4 DRAWING AND TRIMMING OPERATIONS

3.10.4.1 Drawing Operations

Stamping of sheet metal to form automotive body components to the desired shape stretches the metal in at least one direction and often compresses it in the other. It is done in a draw die assembly consisting of a die cavity, a punch, and usually a blank holder or pressure pad. Ideally, the stamping is drawn to the finished shape in one operation. For a more detailed discussion of drawing operations, see [Section 4.1](#).

The following guidelines should be followed to achieve the most efficient and least costly drawing operations.

3.10.4.1.1 Minimize the Depth of Draw

The depth of draw affects the complexity and cost of the die and press. A shallow draw, as shown in [Figure 3.10.4.1.1-1](#), may permit the use of a single action die and press rather than a more costly and slower double action die and press. Minimal draw depth may also allow less costly grades of sheet steel and potentially reduce engineered and manufactured scrap. Conversely, deeper draws may require more than one operation, causing additional die and production costs.

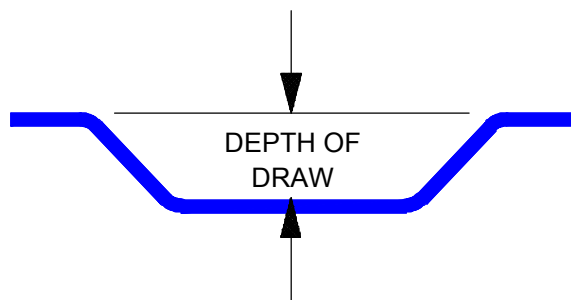


Figure 3.10.4.1.1-1 Minimize depth of draw where practical

3.10.4.1.2 Avoid Backdraft

The backdraft illustrated in [Figure 3.10.4.1.2-1](#) makes the component impossible to form in a simple die and press. The angled portion would have to be drawn in an open position, then the shape completed in a subsequent operation. This significantly increases tool cost.

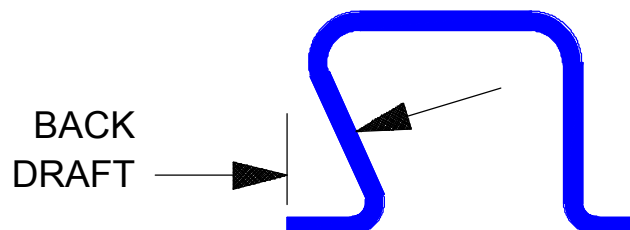


Figure 3.10.4.1.2-1 Back drafts require extra operations that increase tool cost

3.10.4.1.3 Design for Open End Draw

If the component can be designed for open end draw, as shown in [Figure 3.10.4.1.3-1](#), it could be formed in a simple form die, whereas the closed end draw in the figure requires a complex draw die. The open-end draw die also reduces engineered scrap because no binder stock is required in the open end.

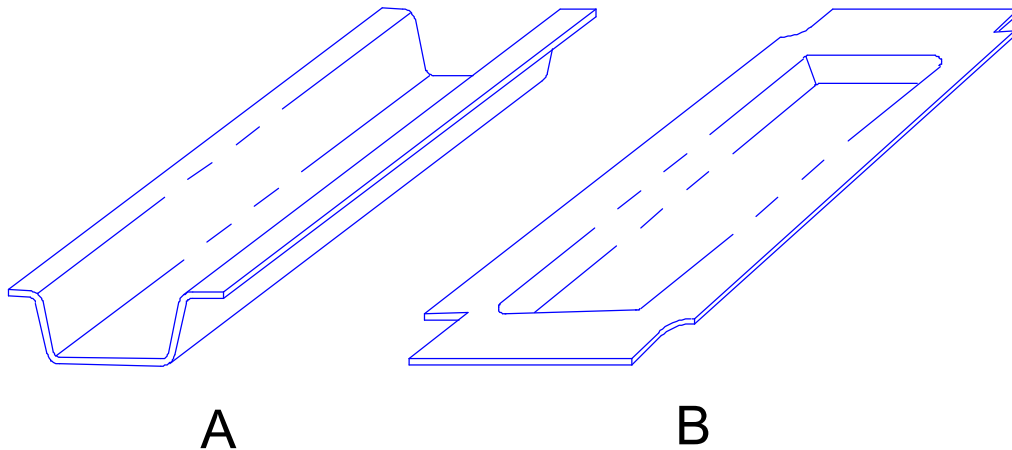


Figure 3.10.4.1.3-1 The open end form at A requires lower tooling cost and generates less scrap than the closed end draw at B

3.10.4.1.4 Soften Locally Severe Shape Changes

The large radii and open angle walls shown in [Figure 3.10.4.1.4-1 B](#) facilitate the use of simpler and less costly die processing. Both material cost and manufactured scrap are reduced.

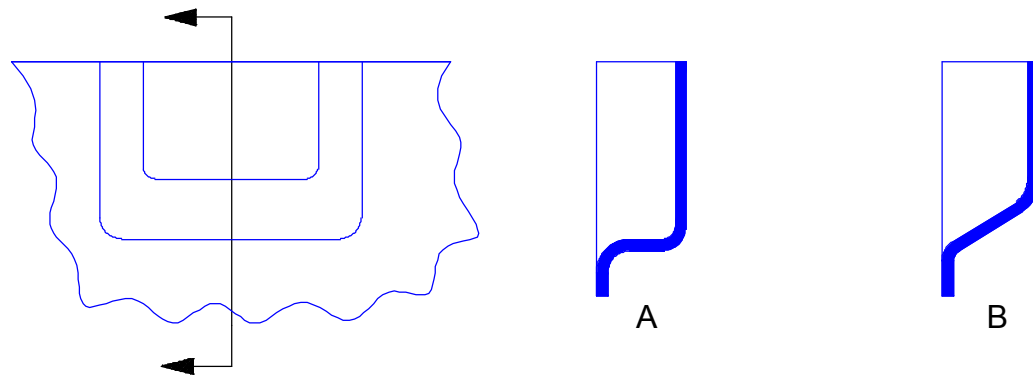
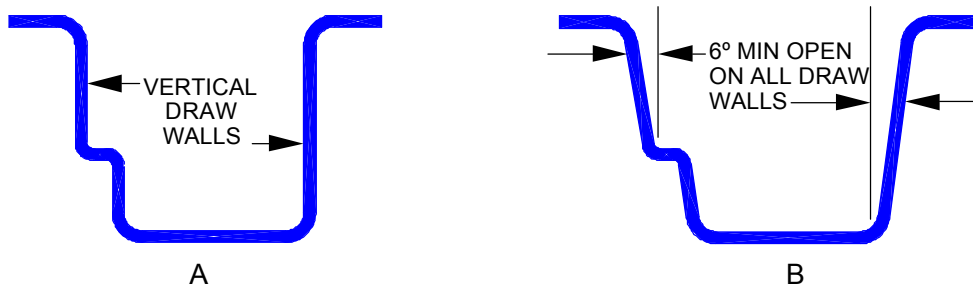


Figure 3.10.4.1.4-1 The large radius and open angle wall in Section B are preferable to the small radius and horizontal wall at A

3.10.4.1.5 Keep Draw Walls Open in the Die Position

Vertical draw walls, shown in [Figure 3.10.4.1.5-1](#), usually add forming operations and increase the manufactured scrap, while reducing the production rate, because of springback. (See the discussion on springback in [Section 3.10.5.1](#))



[Figure 3.10.4.1.5-1](#) The vertical walls at A require additional forming.
The open walls at B do not.

3.10.4.1.6 Keep Draw Walls the Same Depth

Draw walls of unequal depth can cause the stamping to twist, often requiring subsequent straightening operations. The preferred design, shown in [Figure 3.10.4.1.6-1B](#), virtually eliminates the tendency to twist, thereby reducing the number of die operations. Blanking cost and manufactured scrap may also be reduced. Where it is not possible to keep the opposing flanges at the same height, it may be possible to form two pieces simultaneously in a symmetrical configuration by double attaching, as shown in [Figure 3.10.4.1.6-1C](#), then separating them.



[Figure 3.10.4.1.6-1](#) It is preferable to keep opposing flanges at the same height as at B.
Where this is not possible, two pieces may be formed
simultaneously by double attaching as shown at C.

3.10.4.1.7 Observe Forming Limits

The amount of stretch imparted to the metal must be within the safe region of the forming limit diagram for the material. (See the discussion of forming limit diagrams in [Section 4.1.5.4](#).) This guideline is best observed through close cooperation between component designers and die construction sources who have the capability to make reasonable estimates of actual strains. Keeping all stretched areas comfortably within the safe region virtually eliminates costly splits due to minor process variations during manufacturing.

3.10.4.2 Trimming Operations

Automotive sheet metal stampings are trimmed during fabrication to remove excess metal that is required for processing. Trimming is generally accomplished in a die that has an upper punch and a lower die block of the same shape except for a trim clearance between them. The clearance depends on the type and thickness of the sheet metal. The punch first stretches, then shears the metal when the punch and die block meet.

The following guidelines should be followed to achieve the most efficient and least costly trimming operations.

3.10.4.2.1 Design to Permit Trimming in One Direction

The component should be designed so that all trim angles are in the same plane as closely as possible. (See [Figure 3.10.4.2.1-1](#).) This will permit trimming in one direction and eliminate the need for added trim dies or for adding cams to trimming operations. Trim edges will remain in better condition, reducing manufactured scrap.

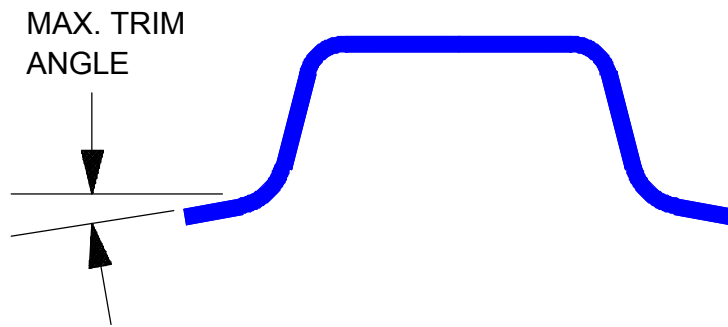


[Figure 3.10.4.2.1-1](#) Keeping all trim angles within an established minimum will simplify trimming operations

3.10.4.2.2 Keep Trim Walls Open

Open trim walls permit trim shearing in a single operation for lower tool cost and less manufactured scrap. A minimum of 10° is recommended, as shown in [Figure 3.10.4.2.2-1](#).

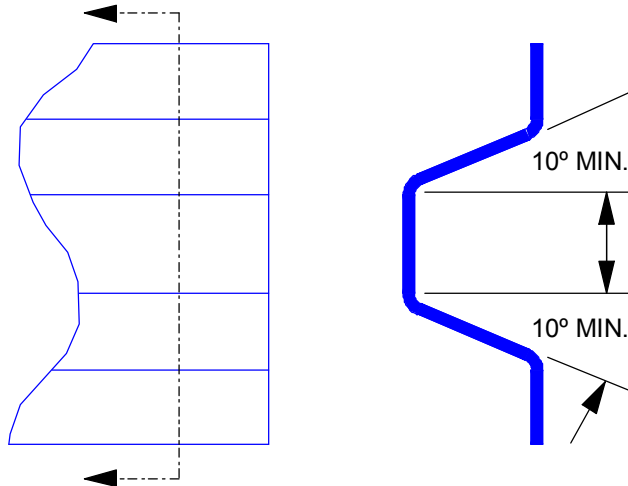


[Figure 3.10.4.2.2-1](#) A minimum 10° open flange walls facilitates trim shearing

3.10.4.2.3 Avoid Sharp Trim Corners

Sharp trim angles require a more complex trim steel arrangement, increasing die construction and maintenance costs. A minimum corner angle of 60° is recommended, as shown in [Figure 3.10.4.2.3-1](#).

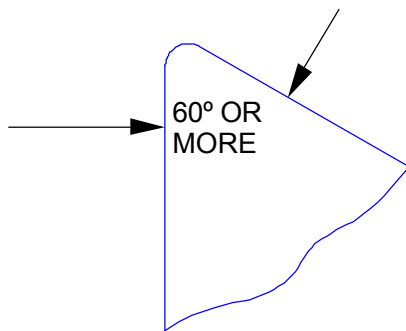


Figure 3.10.4.2.3-1 Avoid trim corners less than 60°

3.10.4.2.4 Provide Relief At Flanges

The plastic flow of sheet metal during a flanging operation requires relief. A relief dimension of at least two metal thicknesses is required as shown in [Figure 3.10.4.2.4-1](#). The preferred design is shown at C. Where this is not possible, notches should be provided as shown at B. The condition at A should be avoided.

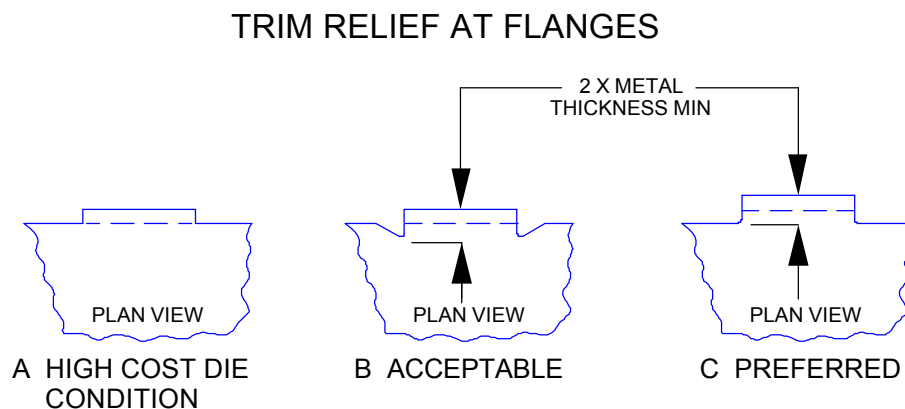


Figure 3.10.4.2.4-1 Provide a relief notch of at least two metal thicknesses to facilitate flanging

3.10.4.2.5 Keep Trim Notches Wide and Open

Narrow trim notches with parallel side walls create difficult and costly die conditions. Notch width should be a minimum of four times metal thickness, and sides should be a minimum of 5° open as illustrated in [Figure 3.10.4.2.5-1](#).

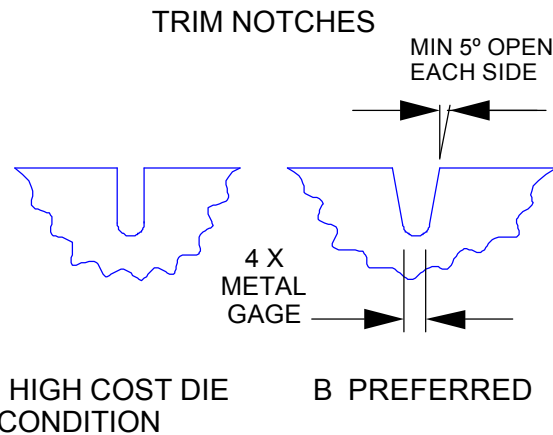


Figure 3.10.4.2.5-1 Notches should be wide and open to facilitate flanging

3.10.5 FLANGING AND PIERCING GUIDELINES

The following guidelines will help the stamping designer to incorporate some of the most commonly required flanged and pierced features with major reductions in tooling requirements and costs. Direct interaction between the component designer and the manufacturing engineer is required in most cases to achieve the most efficient design.

3.10.5.1 Flanging

Flanges are common features generally added to facilitate welding and bonding or to provide stiffness. The die members generally required to form a flange ([Figure 3.10.5.1-1](#)), consist of:

1. A post or punch conforming to the component form.
2. A holding pad with springs, nitrogen cylinders, or air cylinders to clamp the stamping against the post or punch as the press ram descends.
3. A flange steel mounted solidly to the upper or lower die.

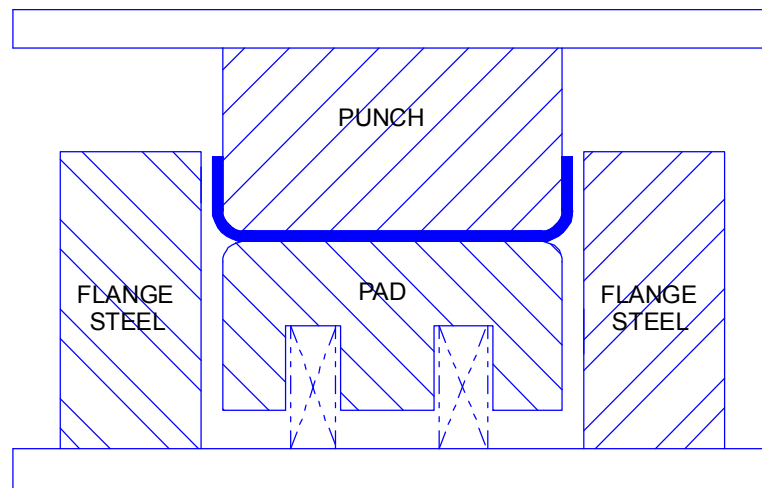


Figure 3.10.5.1-1 Flanging die members

The direct flange die is the most economical die to form a flange. The flanges can be on one or more sides of a stamping, but must be oriented in the same direction, ([Figure 3.10.5.1-2](#)). They will not be parallel due to springback.



Figure 3.10.5.1-2 Flanges made by a direct flange die must be oriented in the same direction and will not be parallel due to springback

3.10.5.1.1 Springback

Springback is caused by the elastic characteristic of steel. It generally ranges from 3° in mild steel to 6° in higher-strength steels. Two flanges oriented in the same direction that are formed with parallel die tooling will therefore not be parallel when the stamping is removed from the die ([Figure 3.10.5.1.1-1](#)).

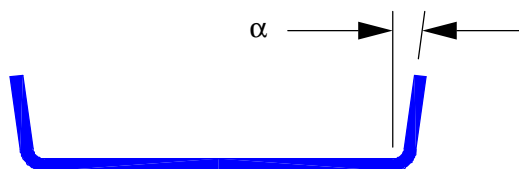


Figure 3.10.5.1.1-1 The elasticity of steel causes springback in the flange

The condition should therefore be avoided in the design to avoid costly added operations. If mandatory, multiple die operations are required, and the dimensional variation will be increased due to the location error from one die to another ([Figure 3.10.5.1.1-2](#)).

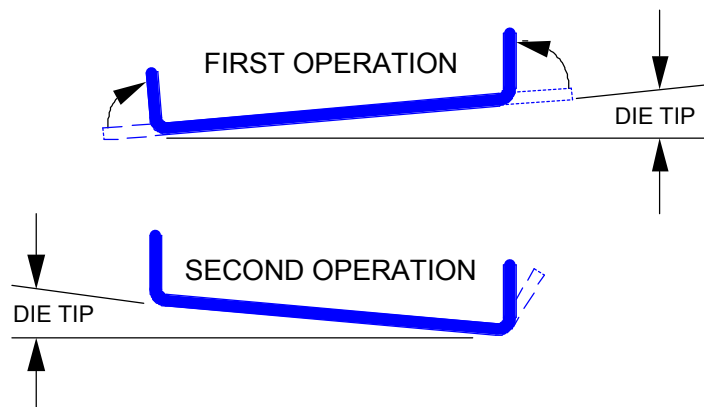
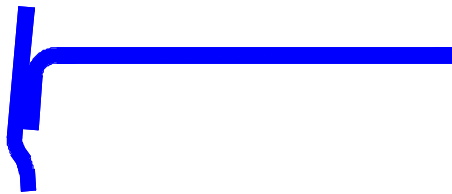


Figure 3.10.5.1.1-2 Multiple die operations are required when flanges oriented in the same direction are parallel

Cost is minimized when springback is recognized and the mating component designed to match the springback condition as shown in [Figure 3.10.5.1.1-3](#). (See also [Figure 3.10.7-3](#).)



[Figure 3.10.5.1.1-3](#) Mating components should be designed to match the springback condition

3.10.5.1.2 Flanging in Opposite Directions

When the design requires flanges oriented in opposite directions, a double pad flange die is required ([Figure 3.10.5.1.2-1](#)). This type of die is more expensive to construct and maintain than a single pad die, which is used when flanges are oriented in one direction.

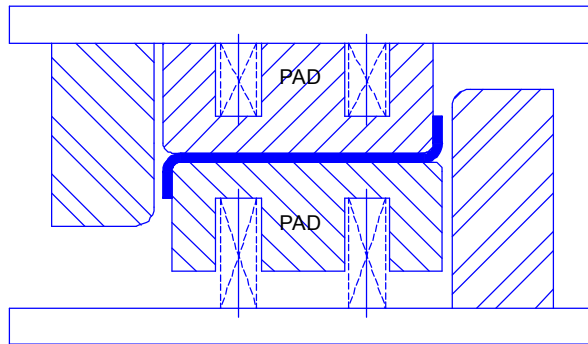


[Figure 3.10.5.1.2-1](#) Die forming flanges in opposite directions

A major advantage of this type of die is the ability to create parallel flanges in opposite directions. The stamping can be tipped in the double pad die to compensate for springback on both flanges as shown in [Figure 3.10.5.1.2-2](#). Two parallel flanges are formed in a single die operation at less cost and with better quality than with the multiple die operations required when the two parallel flanges are oriented in the same direction.

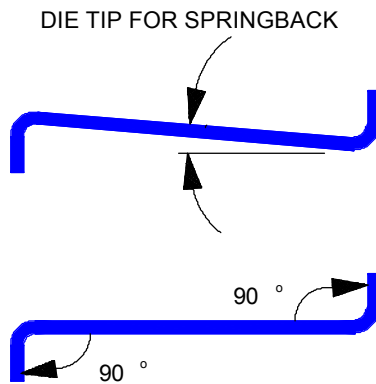


[Figure 3.10.5.1.2-2](#) Parallel flanges oriented in opposite directions can be formed by tipping the piece in the die

3.10.5.1.3 Flange Holding Surface

The design must provide sufficient surface area adjacent to the flange to permit the die to clamp or hold the workpiece as the flange is formed, as shown in [Figure 3.10.5.1.3-1](#). A dimension A at least two times B is preferred because it produces the lowest tooling cost. A equal to B is possible with increased tool cost. A less than B is normally not practical.

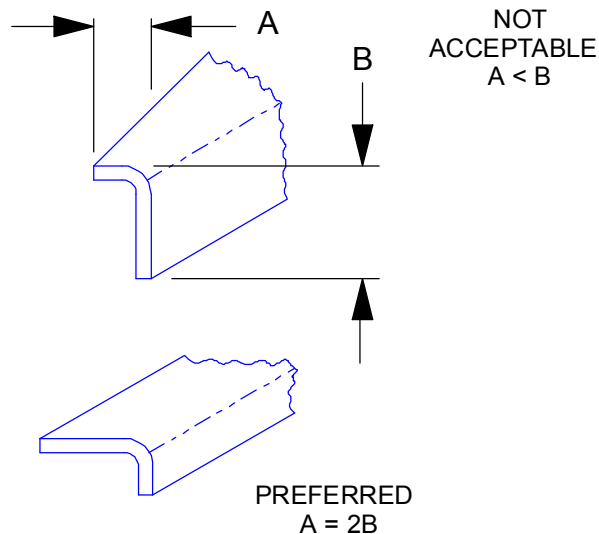


[Figure 3.10.5.1.3-1](#) Provide adequate hold down area for flanging operation

3.10.5.1.4 Return Flanges

Return flanges ([Figure 3.10.5.1.4-1](#)) create the need for added dies, which increase both fixed and variable costs.



[Figure 3.10.5.1.4-1](#) A return flange directed toward the workpiece requires added dies

A return flange directed away from the workpiece ([Figure 3.10.5.1.4-2](#)) can be incorporated into the tooling at nominal cost.

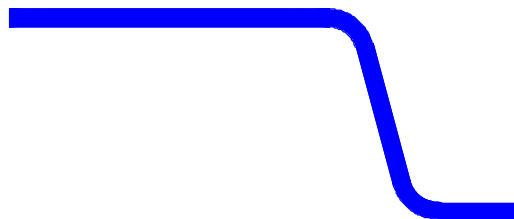


[Figure 3.10.5.1.4-2](#) A return flange directed away from the workpiece can be incorporated into the die

3.10.5.1.5 Corners on Flanges

Flanges with closed corners should be avoided to maximize quality and minimize tooling cost. The closed corner, shown at A in [Figure 3.10.5.1.5-1](#), requires compressing the metal, which causes wrinkles under optimum conditions and overlapped metal in the more extreme conditions. Relief notches, shown at B and C, should be added in all corners to improve quality and reduce tooling cost.

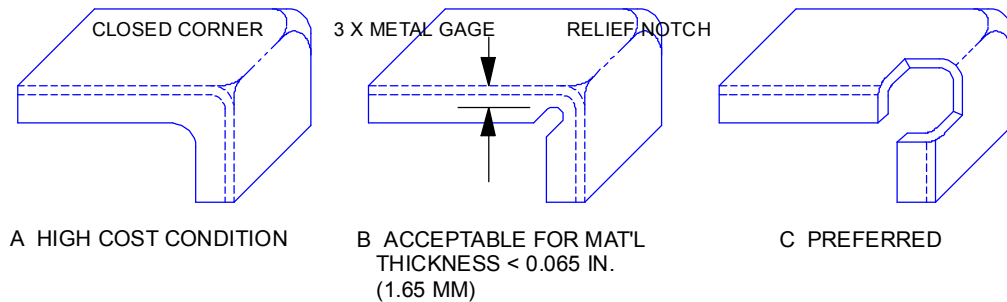


Figure 3.10.5.1.5-1 Avoid flanges with closed corners

3.10.5.1.6 Flanged Holes

The two designs shown in [Figure 3.10.5.1.6-1](#) are generally used to strengthen a hole. The traditional flanged hole at A requires two operations: piercing and flanging. In the preferred design at B, the depressed area or racetrack for the hole is formed when the shape is established, and only a single operation is required to pierce the hole.



Figure 3.10.5.1.6-1 The traditional flanged hole at A requires one more operation than the racetrack design at B

3.10.5.1.7 Die Lock

Some flange designs can cause die lock or back draft conditions ([Figure 3.10.5.1.7-1](#)). These conditions increase tooling cost because expensive fill slides are required to fill the back draft area during forming. The fill slide then moves away to allow the stamping to be removed from the die.

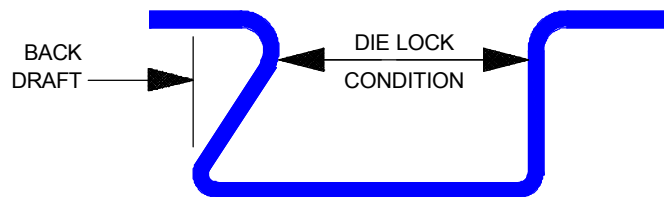


Figure 3.10.5.1.7-1 The backdraft causes a potential die lock and increases tooling cost

Some die lock conditions are not possible for mass production, such as the one shown in [Figure 3.10.5.1.7-2](#).

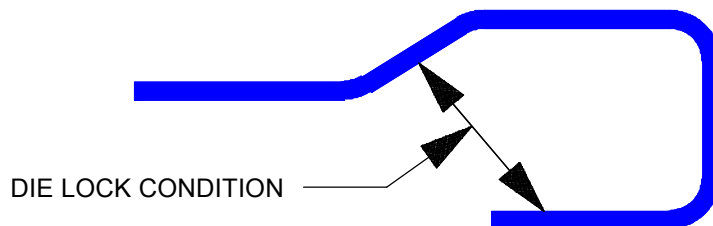


Figure 3.10.5.1.7-2 This die lock condition is not possible for mass production

3.10.5.2 Piercing Hole Size Variety

The first guideline for piercing is to design to standard hole sizes. Tooling components used for piercing are consumable and have a relatively short life compared with other die components, and replacements are kept on hand in the stamping facility. Standardizing hole sizes and shapes will reduce tool replacement inventory in the stamping plant.

There are two other major cost issues in addition to the obvious inventory costs associated with the variety of piercing tools: downtime cost and quality cost. Downtime cost is incurred when the inventory system fails to have a tool available for replacement during a production run. Quality cost is incurred when an incorrect tool is installed and poor quality components are produced. In some cases the sizes vary by as little as 0.004 in.(0.1 mm).

3.10.5.2.1 Combining Piercing and Trimming Operations

Piercing operations are combined with trimming operations in most die processes to minimize the number of dies required to complete the stamping. The pierced holes must be within approximately 15° of the trimming direction to maximize this opportunity. Holes that are not within this guideline must be pierced in other dies within the process. In some cases, the angle of trim may be obvious to the designer, but usually the manufacturing engineer must determine it. [Figure 3.10.5.2.1-1](#) illustrates holes that can be combined with the trim operation and the limit of 15° .

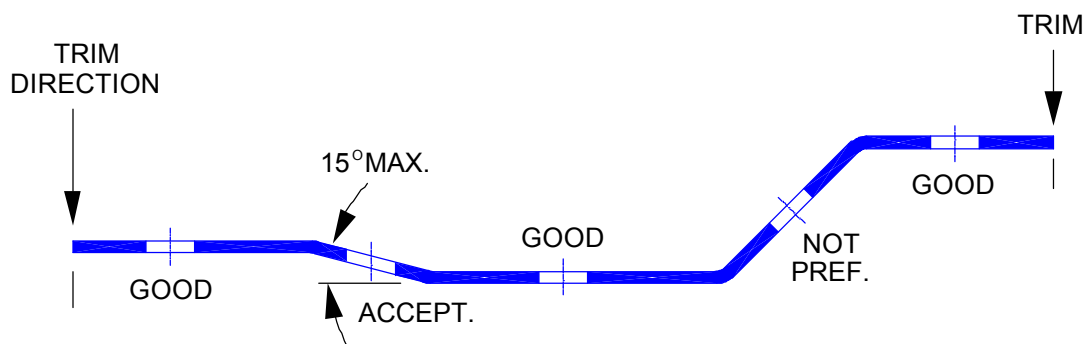
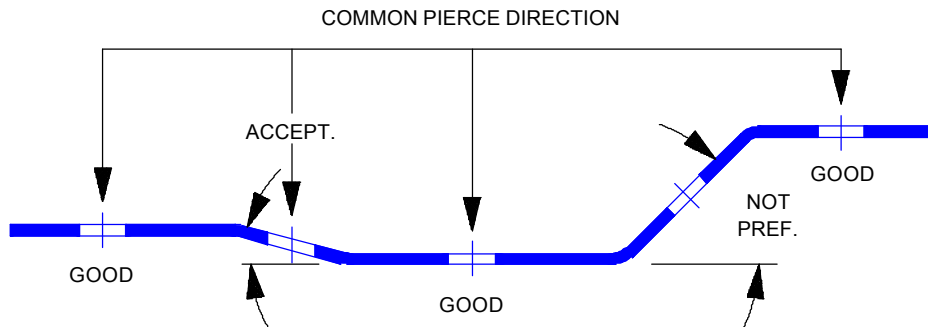


Figure 3.10.5.2.1-1 Holes oriented within 15° of the trimming direction can be pierced in the trimming operation

3.10.5.2.2 Common Direction of Piercing

When the piercing and trimming operations cannot be combined, the lowest tooling cost is achieved when all holes are in a common pierce direction and the surfaces being pierced are oriented to each other within 15° , as shown in [Figure 3.10.5.2.2-1](#).



[Figure 3.10.5.2.2-1](#) Holes oriented within 15° of each other can be pierced in one operation

Wherever possible, holes in side walls or flanges should be avoided to eliminate piercing operations that require expensive cams (see [Section 3.10.6](#)) or adding dies to the process ([Figure 3.10.5.2.2-2](#)).



[Figure 3.10.5.2.2-2](#) Avoid holes in side walls

3.10.5.2.3 Limitations on Pierced Hole Locations

The locations of holes to be pierced must be considered to ensure that the construction of all die features is strong and rigid enough for mass production. Holes located too close to a trim line or too close to a wall weaken die features, so that high die maintenance is required to avoid component distortion. Maintaining at least the required minimum distance between holes also allows standard die components to be used, reducing die construction cost.

The general guidelines for hole locations are illustrated in [Figure 3.10.5.2.3-1](#).

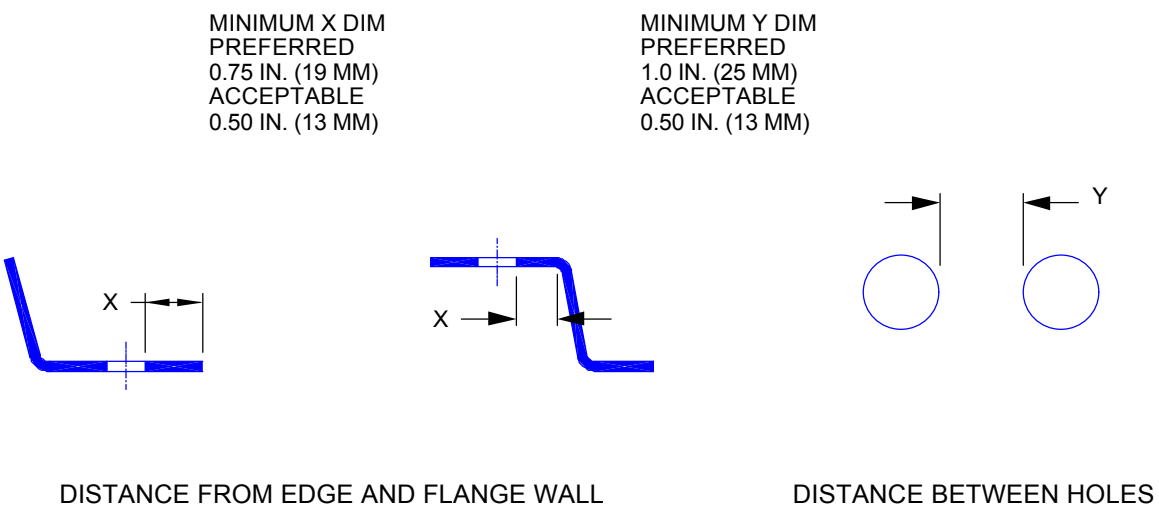


Figure 3.10.5.2.3-1 Limitations on the locations of pierced holes

3.10.6 CAMS

As product and manufacturing engineers work more closely to reduce costs and lead times, they are also making significant progress in containing the number of operations required to produce a quality sheet metal stamping. One technique is the use of more cams to trim, pierce, flange and form the stamping.

A cam is used to actuate a die member at an angle to the vertical press stroke. The type of cam employed to form a feature, and consequently the additional manufacturing cost, depends primarily on the direction of cam movement relative to the press stroke.

Although cams are a viable means of reducing the number of tools, their use entails higher initial costs and higher maintenance costs. Their use, while not ideal, provides the ability to manufacture a panel with fewer, but more costly dies, and allows the designer more flexibility to refine vehicle design.

When designers want to make use of cams, the following guidelines will minimize die complexity and cost:

1. Holes that must be cam pierced should be kept in the same orientation to minimize the complexity of cam construction and reduce the required number of cam operations ([Figure 3.10.6-1](#)). Holes on two separate surfaces that are oriented within 15° of each other will allow one cam to pierce both surfaces, eliminating a second cam and cam operation.
2. On narrow U-shaped forms, wherever possible, holes should be located opposite each other to balance thrust. ([Figure 3.10.6-2](#)).
3. On panels with a return flange, such as hoods, the face should be 15° or more from vertical ([Figure 3.10.6-3](#)). This will allow the main die pad to hold the panel, eliminating the cam mounted pad, thus simplifying the die design and reducing cost.

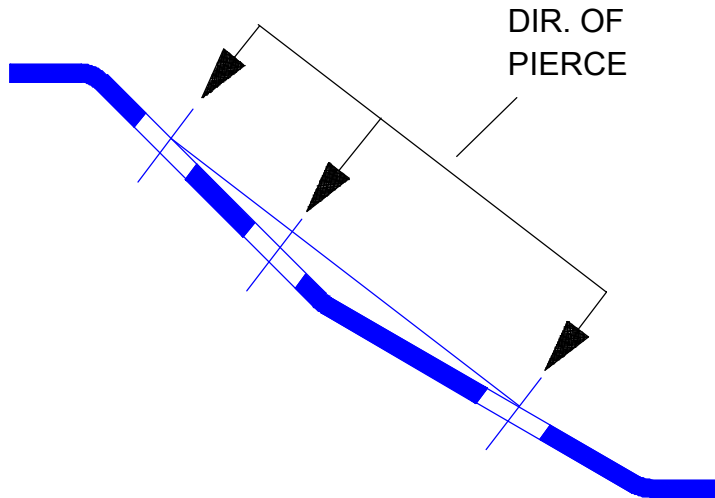


Figure 3.10.6-1 Cam pierced holes should be kept in the same orientation



Figure 3.10.6-2 Holes located opposite each other balance thrust loads

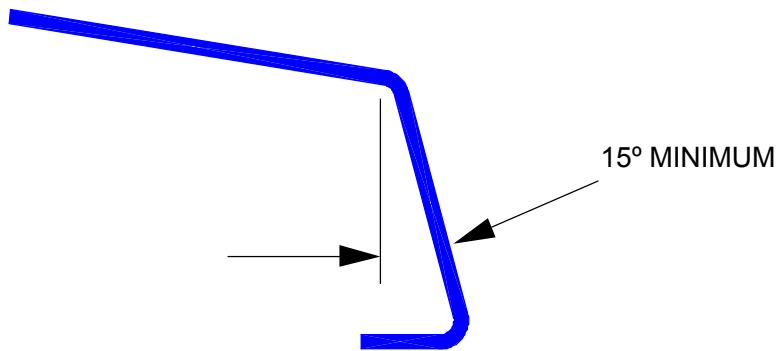


Figure 3.10.6-3 Return flange faces 15° or more from vertical simplify the die

3.10.7 ASSEMBLY CONSIDERATIONS

Many studies have been directed toward simplification or elimination of assembly operations. In addition to cost, factors such as quality, feasibility, and scrap projections must be considered. For example, operations can be eliminated by part consolidation, but the cost and feasibility must be compared with the cost of several simpler components plus assembly. Both manufacturing and design personnel can make significant contributions to cost-effective designs by giving detailed consideration to the assembly process in the early stages of design.

One important aspect of designing for assembly is the special considerations that must be given to variances in the components making up the assemblies. Mass-produced stampings inherently require a liberal tolerance, which is generally defined with a note on the drawings based on normal stamping capability. When the general tolerance is not tight enough, tighter limits are set. When it is possible to achieve and maintain the tighter tolerances, cost is usually increased. Therefore, in the interest of lower piece cost, components and assemblies should be designed within the general tolerance wherever possible. To do this, the designer must be aware of the impact that variances have on assembly operations.

A number of things can be done in the design phase to facilitate assembly by accommodating the variations inherent in steel stampings. Several examples have been drawn from a typical unitized underbody rail section.

1. Minimize coordination points by providing clearance except where welds are to be made. The two stampings in [Figure 3.10.7-1](#) are to be spot welded in three locations. The clearance provided in the step ensures contact on the vertical flange. In general, clearance should be provided in all areas except where welds are to be placed.
2. Design a gap between bend radii of nesting stampings by making the radius of the inner member larger than that of the outer member as shown in [Figure 3.10.7-2](#). This will ensure proper nesting when the radius of the outer member grows due to die wear.
3. Springback (see [Section 3.10.5.1](#)) affects the alignment of stampings for welding. Channels should be designed open, as shown in [Figure 3.10.7-3](#), or with formations in the side walls to avoid the need to restrike. Direct the clamp location and weld sequence to minimize distortion.
4. Both the maximum and minimum tolerance stack must be considered when designing joints. Trim and assembly tolerance must provide a minimum weld flat and must not interfere at the offset. (See [Figure 3.10.7-4](#).)
5. Dimensional variations affect critical coordination. It is therefore important to minimize component movement when fixture forces are removed by attaching in the region that must be coordinated. The stamping shown in [Figure 3.10.7-5](#) is positioned with a tab and pin. (Note the clearance between the stamping and pin.) The weld on the side wall will minimize component movement when the pin is removed.

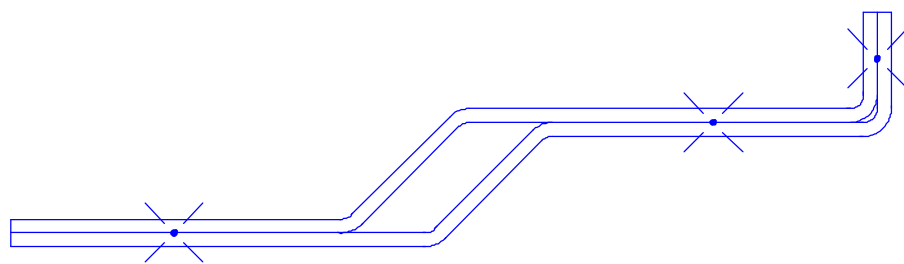


Figure 3.10.7-1 Provide clearance between surfaces that are not welded or bonded

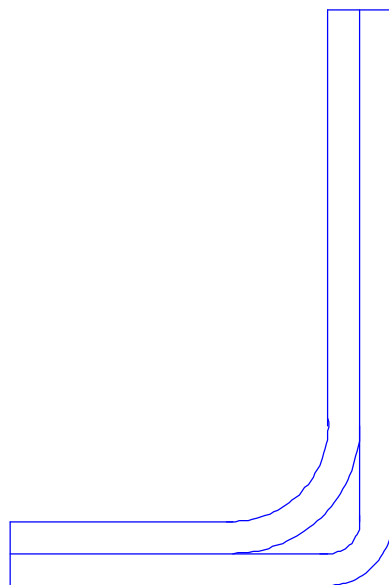


Figure 3.10.7-2 Maintain a gap between nesting radii

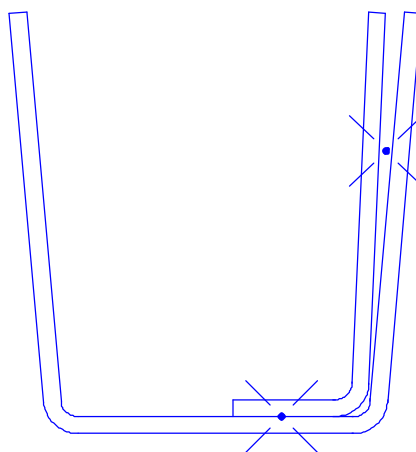


Figure 3.10.7-3 Channels should be designed open to aid in alignment for welding

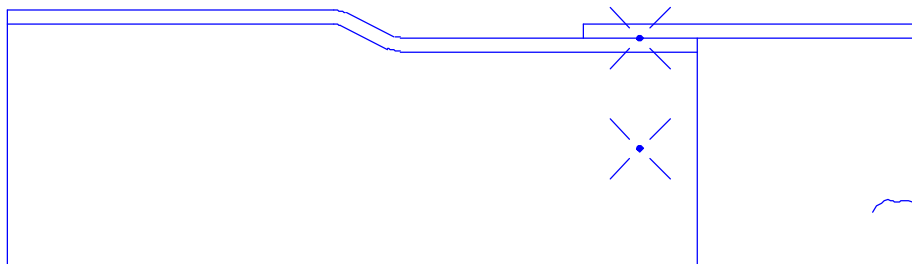


Figure 3.10.7-4 Joint design should consider both maximum and minimum tolerance stack

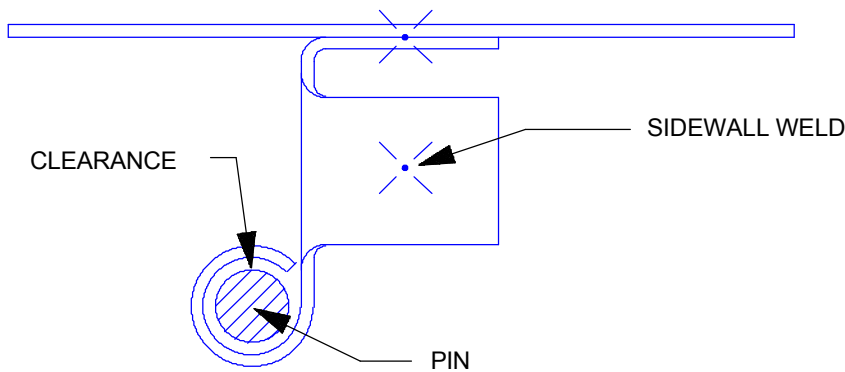


Figure 3.10.7-5 Minimize the dimensional variations due to fixturing

The above examples focus on one aspect of the many problems that must be anticipated during design. It is important for the designer to build a good working knowledge of the techniques used to solve similar problems. Early involvement of manufacturing personnel can reduce the number of late, costly, and often compromising revisions necessary to facilitate assembly of a mass produced, quality body.

3.11 AISI/CARS GEOMETRIC ANALYSIS OF SECTIONS (GAS)

THEORY.....



This section presents an overview of the theory and solution algorithms used in the Geometric Analysis of Sections (GAS) module of AISI/CARS. The complete presentation of all the pertinent theories is beyond the scope of this section. Additional information can be obtained from the bibliography at the end of this section.

[Section 3.11.1](#) provides an introduction to the solutions provided by GAS. [Section 3.11.2](#) identifies the analysis methods and approximations used in GAS. [Section 3.11.3](#) provides the equations used in GAS to calculate nominal properties of a homogeneous or hybrid cross section. [Section 3.11.4](#) provides the equations used in GAS to calculate nominal properties of a composite cross section. [Section 3.11.5](#) provides the equations used in GAS to calculate effective properties of a cross section. [Sections 3.11.6](#) and [3.11.7](#) provide the equations used in GAS to calculate axial capacity, flexural capacity of a member respectively. [Section 3.11.8](#) provides the equations used in GAS to evaluate the combined axial and flexural overall stability of a member. [Section 3.11.9](#) provides the equations for the calculations of axial force deflection properties of stub columns.

3.11.1 INTRODUCTION

GAS can be used to calculate cross section properties and member capacities. The cross section properties computed by GAS, either the nominal or the effective properties, are the properties of a cross section at any point along the member length. GAS can be used to calculate the nominal and effective properties of a cross section at any point along the member length. The nominal properties are calculated without considering the stress condition on the cross section. All components of the cross section are considered to be fully effective. The effective cross section properties are calculated by determining the effective portion of each component or segment of the section according to its stress state and boundary conditions. The effective cross section properties are based on the combined effectiveness of each segment of the cross section.

Member capacities, as calculated by AISI/CARS, are based on the assumption that the member is prismatic (i.e., a constant cross section along the entire member length). Therefore, engineering judgment should be used when determining member capacities for a selected cross section of a non-prismatic member. GAS can calculate the axial capacity and flexural capacity of a member. The capacity of a member under combined axial and flexural loads can be evaluated using the GAS analysis option - Combined Axial And Flexural Overall Stability

3.11.2 ANALYSIS METHODS AND APPROXIMATIONS

In general, GAS utilizes the "linear" or "midline" method for section modeling and analysis. In this method the material of the section is considered to be concentrated along the centerline or midline of straight or curved line elements. The accuracy of the linear method for computing the properties of a given section depends on the thickness of the segments and the configuration of the section.

Yu¹ has discussed the accuracy of this method and concluded that: "For the thickness of steel sheets generally used in cold-formed steel construction the error in the moment of inertia determined by the linear method is usually negligible".

GAS also utilizes thin-walled theory for the calculation of the following torsional properties - Torsional constant, Warping constant, and Shear center location. The formulae for torsional properties are only applied to cross sections with continuous segments since a discontinuity would prevent shear flow across the section.

A cross section is considered thin-walled if its thickness is an order of magnitude smaller than its other dimensions so that the shear stress may be assumed to be uniform through the thickness. It is customary to use 10 as the lower bound limit for the cross section height to thickness ratio or the cross section width to thickness ratio for sections with uniform thickness. For cross sections with non-uniform thickness, it is left to the judgment of the user to determine the applicability of the GAS solutions.

The formulae for torsional properties apply only to straight line segments. GAS converts an arc segment into a number of smaller line segments at 15 degree intervals. For example, a 90° arc will be represented as six straight line segments.

3.11.3 NOMINAL PROPERTIES FOR HOMOGENEOUS OR HYBRID CROSS SECTIONS

A homogeneous cross section is defined as a section consisting of one material or more than one material with the same modulus of elasticity and yield strength. A hybrid cross section is a section consisting of more than one materials with the same modulus of elasticity but different yield strength. GAS calculates nominal properties for a homogeneous or hybrid cross section as shown in [Table 3.11.3-1](#).

Table 3.11.3-1 Nominal Properties for Homogeneous or Hybrid Cross Sections

Property	Description
Area	Area of the section
c_x	X coordinate of the centroid
c_y	Y coordinate of the centroid
I_{xx}	Moment of inertia about the x axis
I_{yy}	Moment of inertia about the y axis
I_{xy}	Product of inertia
θ	Reference angle
I_{uu}	Moment of inertia about the major principal axis, u
I_{vv}	Moment of inertia about the minor principal axis, v
S_{x+}	Section modulus about the x axis in the positive y direction
S_{y+}	Section modulus about the y axis in the positive x direction
S_{x-}	Section modulus about the x axis in the negative y direction
S_{y-}	Section modulus about the y axis in the negative x direction
S_{u+}	Section modulus about the u axis in the positive v direction
S_{v+}	Section modulus about the v axis in the positive u direction
S_{u-}	Section modulus about the u axis in the negative v direction
S_{v-}	Section modulus about the v axis in the negative u direction
r_x	Radius of gyration about the x axis
r_y	Radius of gyration about the y axis
J	Torsional Constant
C_w	Warping Constant
e_x	X coordinate of the shear center
e_y	Y coordinate of the shear center
C_{uu}	Shear coefficient about the u axis
C_{vv}	Shear coefficient about the v axis
J_{open}	Torsional constant of the open portion
J_c	Torsional constant of the closed portion
$t_o\max$	Maximum thickness in the open portion
$t_c\min$	Minimum thickness in the closed portion
A_o	Enclosed area
I_{yc}	Moment of inertia of the compression portion about the neutral axis using the full unreduced section.
j	Section property for torsional-flexural buckling
w	Flat strip width

3.11.3.1 Area

The total area, A, of the section is computed using the following equation:

$$A = \sum l t$$

Equation 3.11.3.1-1

where l = segment length
 t = segment thickness

3.11.3.2 Centroid

The centroid is the location where the area of a section can be considered to be concentrated for computations of first moments.

The centroid of a section is defined as (c_x, c_y) in the global coordinate system. The centroid is computed using the following equations:

$$c_x = \frac{\sum x_i A_i}{A} \quad \text{Equation 3.11.3.2-1}$$

$$c_y = \frac{\sum y_i A_i}{A} \quad \text{Equation 3.11.3.2-2}$$

where x_i, y_i = coordinates of the center of segment i

A_i = area of segment i

3.11.3.3 Moments of Inertia

The moment of inertia is the second moment of the area about a reference axis. The moment of inertia of a cross section is the summation of contributions from all the line and arc segments that define the section:

$$I_{xx} = I_{xxl} + I_{xcc} \quad \text{Equation 3.11.3.3-1}$$

$$I_{yy} = I_{yyl} + I_{yyC} \quad \text{Equation 3.11.3.3-2}$$

$$I_{xy} = I_{xyl} + I_{xyC} \quad \text{Equation 3.11.3.3-3}$$

where I_{xxl} , = moments of inertia contribution from straight line segments

I_{yyl} ,

I_{xyl}

I_{xcc} , = moments of inertia contribution from curved segments (arcs)

I_{yyC} ,

I_{xyC}

The line method is used for calculating the moment of inertia of straight segments. Each straight segment in the section is idealized as a line of finite length, l, and thickness, t. It is assumed that each segment forms an angle, α , with the positive x axis of the global coordinate system, and the centroid of each segment is a distance, c , from the centroid of the entire section. See [Reference 2](#) for additional details. The moments of inertia of straight segments are computed using the following equations:

$$I_{xxl} = \Sigma \left(\left(\frac{lt^3}{12} \right) \cos^2 \alpha + \left(\frac{tl^3}{12} \right) \sin^2 \alpha + tlc_{xx}^2 \right) \quad \text{Equation 3.11.3.3-4}$$

$$I_{yyl} = \Sigma \left(\left(\frac{lt^3}{12} \right) \sin^2 \alpha + \left(\frac{tl^3}{12} \right) \cos^2 \alpha + tlc_{yy}^2 \right) \quad \text{Equation 3.11.3.3-5}$$

$$I_{xyl} = \Sigma \left(\left(\frac{tl^3 - lt^3}{24} \right) \sin(2\alpha) + tl c_{xx} c_{yy} \right) \quad \text{Equation 3.11.3.3-6}$$

where l = segment length

t = segment thickness

α = angle between segment and positive x axis

c_{xx} = perpendicular distance from the x axis to the segment center

c_{yy} = perpendicular distance from the y axis to the segment center

The area method is used for the calculation of moments of inertia contribution by the curved segments. The moments of inertia contributed by curved segments are found with the following equations:

$$I_{xxc} = \Sigma \left(\left(\frac{r_2^4 - r_1^4}{16} \right) (2\alpha_2 - \sin 2\alpha_2 - 2\alpha_1 + \sin 2\alpha_1) + A_i (c_{xx} - c_{cx})^2 \right) \quad \text{Equation 3.11.3.3-7}$$

$$I_{yyc} = \Sigma \left(\left(\frac{r_2^4 - r_1^4}{16} \right) (2\alpha_2 - \sin 2\alpha_2 - 2\alpha_1 - \sin 2\alpha_1) + A_i (c_{yy} - c_{cy})^2 \right) \quad \text{Equation 3.11.3.3-8}$$

$$I_{xyc} = \Sigma \left(\left(\frac{r_2^4 - r_1^4}{8} \right) (\sin^2 \alpha_2 - \sin^2 \alpha_1) + A_i (c_{xx} - c_{cx})(c_{yy} - c_{cy}) \right) \quad \text{Equation 3.11.3.3-9}$$

where r_1 = inner radius of the segment

r_2 = outer radius of the segment

α_1, α_2 = angles between segment ends and the positive x axis

c_{xx} = perpendicular distance from the x axis to the segment centroid

c_{yy} = perpendicular distance from the y axis to the segment centroid

c_{cx}, c_{cy} = distance between center of curvature and the segment centroid

A_i = area of the segment

3.11.3.4 Reference Angle

The reference angle, q , is defined as the angle between the principal axes and the centroidal axes. Principal axes are defined as those axes for which the product of inertia, I_{xy} , vanishes. To calculate q , the following equation (page 495 of [Reference 3](#)) is used:

$$\theta = 0.5 \arctan \left(\frac{2I_{xy}}{I_{yy} - I_{xx}} \right) \quad \text{Equation 3.11.3.4-1}$$

3.11.3.5 Principal Moments of Inertia

Principal moments of inertia, I_{uu} and I_{vv} , are the moments of inertia about the principal axes of the section. They are obtained using:

$$I_{uu} = \frac{(I_{xx} + I_{yy}) + (I_{xx} - I_{yy})\cos 2\theta - 2I_{xy}\sin 2\theta}{2} \quad \text{Equation 3.11.3.5-1}$$

$$I_{vv} = I_{xx} + I_{yy} - I_{uu} \quad \text{Equation 3.11.3.5-2}$$

where I_{xx} , I_{yy} , I_{xy} and θ are defined in [Sections 3.11.3.3](#) and [3.11.3.4](#)

3.11.3.6 Section Modulus

GAS calculates section moduli, S_x and S_y , using the following equations:

$$S_x = \frac{I_{xx}}{c_{xxmax}} \quad \text{Equation 3.11.3.6-1}$$

$$S_y = \frac{I_{yy}}{c_{yymin}} \quad \text{Equation 3.11.3.6-2}$$

where c_{xxmax} = the distance from the x axis to the extreme fiber

c_{yymin} = the distance from the y axis to the extreme fiber

GAS calculates section moduli, S_u and S_v , based on principal moments of inertia, I_{uu} and I_{vv} using the following equations:

$$S_u = \frac{I_{uu}}{c_{uumax}} \quad \text{Equation 3.11.3.6-3}$$

$$S_v = \frac{I_{vv}}{c_{vemax}} \quad \text{Equation 3.11.3.6-4}$$

where c_{uumax} = the distance from the principal axis u to the extreme fiber

c_{vemax} = the distance from the principal axis v to the extreme fiber

3.11.3.7 Radius of Gyration

The radii of gyration, r_x and r_y are computed by using the following equations:

$$r_x = \left(\frac{I_{xx}}{A} \right)^{1/2} \quad \text{Equation 3.11.3.7-1}$$

$$r_y = \left(\frac{I_{yy}}{A} \right)^{1/2} \quad \text{Equation 3.11.3.7-2}$$

where I_{xx} , I_{yy} , and A are defined in previous sections

3.11.3.8 Torsional Constant

Three different approaches (from [References 2 and 4](#)) are used to compute the torsional constant (J) for different types of sections.

1. For open-cell sections⁴

$$J = \sum ab^3 \left[\frac{16}{3} - 3.36 \frac{b}{a} \left(1 - \frac{b^4}{12a^4} \right) \right]$$

Equation 3.11.3.8-1

where the summation is carried out over all elements

a is half of the element length

b is half of the element thickness

2. For single celled sections, the following equation is used to compute the torsional constant of the elements around the cell.

$$J_c = \frac{4A_o^2}{\Sigma(l/t)}$$

Equation 3.11.3.8-2

where $S(l/t)$ is the sum of the length/thickness ratios of the elements around the cell

A_o is the area enclosed by the mean perimeter of the cross section.

If there are any elements that are not part of the cell, their contribution is accounted for by using the formula for open-cell sections and adding it to the J computed from the above formula.

3. For multi-cell sections, a set of simultaneous equations (one for each cell) is solved. The system of equations defines the rotation of each cell due to an applied torque ($1/G$). Continuity requires that each cell in a multi-cell section rotate through the same angle. There is an additional equilibrium equation of the form,

$$T = 2\sum(qA_{oi})$$

Equation 3.11.3.8-3

where q is the shear flow in each cell

the summation is over all the cells in the section.

The system of equations are then solved for the angle of twist of the section. J_c is found by taking the reciprocal of the angle of twist. The torsional constant of the section, J , is the sum of J_{open} and J_c .

$$J = J_{open} + J_c$$

Equation 3.11.3.8-4

3.11.3.9 Warping Constant

GAS calculates the warping constant for open-cell sections. The warping constant is assumed to be negligible for closed sections.

The warping constant, C_w , is defined as⁵:

$$C_w = \int_0^E w_n^2 t ds$$

Equation 3.11.3.9-1

where t = segment thickness
 w_n = normalized unit warping

Normalized unit warping is defined as:

$$w_n = \frac{1}{A} \int_0^E w_o t \, ds - w_o \quad \text{Equation 3.11.3.9-2}$$

where w_o = unit warping with respect to the shear center

w_o can be obtained by:

$$w_o = \int_0^s p_o \, ds \quad \text{Equation 3.11.3.9-3}$$

where p_o = distance between the tangent line at the point and the shear center

For thin-walled open cross sections with discrete segments, the integration in the formula can be simplified using a summation as follows:

$$w_{oj} = \sum_{i=0}^j p_{oij} l_{ij} \quad \text{Equation 3.11.3.9-4}$$

$$w_{nj} = \frac{1}{A} \left(\frac{1}{2} \sum_{i=0}^n (w_{oi} + w_{oj}) t_{ij} l_{ij} \right) - w_{oj} \quad \text{Equation 3.11.3.9-5}$$

$$C_w = \frac{1}{3} \sum_{i=0}^n (w_{ni}^2 + w_{ni} w_{nj} + w_{nj}^2) \quad \text{Equation 3.11.3.9-6}$$

where p_{oij} = distance between segment ij to the shear center
 t_{ij} = segment thickness between points i and j
 l_{ij} = segment length between points i and j

3.11.3.10 Shear Center

The shear center is the location in a cross section where no torsion occurs when flexural shears act in planes passing through that location. The shear flow in any element can be calculated using:

$$q = \frac{VQ}{I} \quad \text{Equation 3.11.3.10-1}$$

where V = shear force
 Q = sum of the first moment of all elements between the point of interest and a free edge
 I = moment of inertia of the entire section

By definition, the sum of the moments caused by the shear flow about the shear center must equal zero. The sum of the moments about the centroid of the section is used to compute the offset from the centroid to the shear center in each coordinate direction e_x and e_y .

The above method can be applied in a straightforward manner to open-cell sections, whereas, the location of the shear center of a closed multicell section is considerably more difficult. First an artificial cut must be made in each cell in order to obtain an open section so that the shear flow can be calculated. Then, the cells of the section are closed and a set of simultaneous equations (one for each cell) is solved in order to calculate redundant shear flows around each cell. The moments caused by these shear flows about the centroid are then added to the moments caused by the open cell shear flows, and the resulting offsets from the centroids to the shear center are determined. The shear center is located by adding the offsets to the coordinates of the centroid. See [Reference 6](#) for additional details on locating the shear center.

3.11.3.11 Shear Coefficient

Shear coefficients are defined as the ratio of the shear stress at the neutral axis to the average shear stress on the cross section.[3, 7](#) The shear coefficient is calculated using the following equation:

$$\text{Shear coefficient} = \frac{ayA}{It} \quad \text{Equation 3.11.3.11-1}$$

where
 a = area beyond the neutral axis
 y = distance between the centroid of the area beyond the neutral axis and the neutral axis
 A = total area of the section
 I = moment of inertia of the section
 t = total thickness of segments on the neutral axis

3.11.3.12 Section property for torsional-flexural buckling - j

Section property for torsional-flexural buckling, j , is defined as follows:

$$j = \frac{1}{2I_y} \left(\int_A x^3 dA + \int_A xy^2 dA \right) - x_0 \quad \text{Equation 3.11.3.12-1}$$

where x_0 = the distance from the shear center to the centroid along the principal x-axis, taken as negative. For singly-symmetric sections, x-axis is the axis of symmetry oriented such that the shear center has a negative x-coordinate.

3.11.3.13 Flat Strip Width - w

Flat strip width is the width of the strip required to produce the given shape of the cross section.

Flat strip width, w , is defined as follows:

$$w = \sum w_i \quad \text{Equation 3.11.3.13-1}$$

where w_i = Flat strip width of segment i

For straight segments, w_i equates the segment length.

For curved segments with radius up to two times the thickness, w_i is defined as follows⁸:

$$w_i = 0.01745\alpha(r + \frac{t}{3}) \quad \text{Equation 3.11.3.13-2}$$

where α = angle of the curved segment
 r = inside radius
 t = thickness

For curved segments with radius larger than two times the thickness, w_i is defined as follows⁸:

$$w_i = 0.01745\alpha(r + \frac{t}{2}) \quad \text{Equation 3.11.3.13-3}$$

where α = angle of the curved segment
 r = inside radius
 t = thickness

3.11.4 NOMINAL PROPERTIES FOR COMPOSITE SECTIONS

A composite section is defined as a section which is composed of materials with different moduli of elasticity. GAS calculates nominal properties for a composite cross section as shown in [Table 3.11.4-1](#).

Table 3.11.4-1 Nominal Properties For Composite Sections

Property	Description
Area	Area of the section
c_x	X coordinate of the centroid
c_y	Y coordinate of the centroid
I_{xxt}	Moment of inertia about the x axis
I_{yyt}	Moment of inertia about the y axis
I_{xyt}	Product of inertia
θ_t	Reference angle
I_{uut}	Moment of inertia about the major principal axis, u
I_{vvt}	Moment of inertia about the minor principal axis, v
S_{xt+}	Section modulus about the x axis in the positive y direction
S_{yt+}	Section modulus about the y axis in the positive x direction
S_{xt-}	Section modulus about the x axis in the negative y direction
S_{yt-}	Section modulus about the y axis in the negative x direction
S_{ut+}	Section modulus about the u axis in the positive v direction
S_{vt+}	Section modulus about the v axis in the positive u direction
S_{ut-}	Section modulus about the u axis in the negative v direction
S_{vt-}	Section modulus about the v axis in the negative u direction
r_{xt}	Radius of gyration about the x axis
r_{yt}	Radius of gyration about the y axis

3.11.4.1 Area

The same method used in [Section 3.11.3.1](#) is used for composite section calculations. The computed cross section area is the physical cross section area rather than the transformed cross section area.

3.11.4.2 Centroid

The centroid of a section is defined as (c_x, c_y) in the global coordinate system. c_x and c_y are computed from the following equations:

$$c_x = \frac{\sum x_i t_{ei} l_i}{A} \quad \text{Equation 3.11.4.2-1}$$

$$c_y = \frac{\sum y_i t_{ei} l_i}{A} \quad \text{Equation 3.11.4.2-2}$$

where x_i, y_i = coordinate of the center of segment i

t_{ei} = equivalent thickness of segment i

l_i = length of segment i

A = area

3.11.4.3 Moments of Inertia

The transformed section method is used in GAS to calculate the moments of inertia of a composite section. The procedure is to transform the section, consisting of more than one material, into an equivalent cross section composed of only one material.

First the equivalent thickness of each segment, is computed by:

$$t_{ei} = t_i \frac{E_i}{E_1} \quad \text{Equation 3.11.4.3-1}$$

where t_{ei} = equivalent thickness of segment i

t_i = thickness of segment i

E_1 = Young's modulus of the transformed section

E_i = Young's modulus of segment i

The moments of inertia of the transformed section for line segments is obtained by:

$$I_{xxt} = \sum \left[\left(\frac{l t_e^3}{12} \right) \cos^2 \alpha + \left(\frac{t_e l^3}{12} \right) \sin^2 \alpha + t_e l c_{xx}^2 \right] \quad \text{Equation 3.11.4.3-2}$$

$$I_{yyt} = \sum \left[\left(\frac{l t_e^3}{12} \right) \sin^2 \alpha + \left(\frac{t_e l^3}{12} \right) \cos^2 \alpha + t_e l c_{yy}^2 \right] \quad \text{Equation 3.11.4.3-3}$$

$$I_{xyt} = \sum \left[\left(\frac{t_e l^3 - l t_e^3}{24} \right) \sin(2\alpha) + t_e l c_{xx} c_{yy} \right] \quad \text{Equation 3.11.4.3-4}$$

where l = segment length

t_e = equivalent segment thickness

α = angle between the segment and the positive x axis

c_{xx} = perpendicular distance from the x axis to the segment center

c_{yy} = perpendicular distance from the y axis to the segment center

The moment of inertia of the transformed section of curved segments is obtained by using the same formula for homogeneous cross section calculation except that the equivalent thickness is used to compute the inner and outer radii of the segment.

3.11.4.4 Reference Angle

The reference angle θ_t for a composite section is obtained using:

$$\theta_t = 0.5 \arctan \left(\frac{2I_{xyt}}{I_{yyt} - I_{xxt}} \right) \quad \text{Equation 3.11.4.4-1}$$

where I_{xyt} , I_{xxt} and I_{yyt} are defined in [Section 3.11.4.3](#)

3.11.4.5 Principal Moments of Inertia

Principal moments of inertia of a composite section are obtained using:

$$I_{uut} = \frac{(I_{xxt} + I_{yyt}) + (I_{xxt} - I_{yyt}) \cos(2\theta_t) - 2I_{xyt} \sin(2\theta_t)}{2} \quad \text{Equation 3.11.4.5-1}$$

$$I_{vvt} = I_{xxt} + I_{yyt} - I_{uut} \quad \text{Equation 3.11.4.5-2}$$

where I_{xxt} , I_{yyt} , I_{xyt} and θ_t are defined in [Section 3.11.4.3](#) and [Section 3.11.4.4](#).

3.11.4.6 Section Modulus

GAS calculates section moduli, S_{xt} and S_{yt} , using the following equations:

$$S_{xt} = \frac{I_{xxt}}{n_x c_{xxmax}} \quad \text{Equation 3.11.4.6-1}$$

$$S_{yt} = \frac{I_{yyt}}{n_y c_{yyymax}} \quad \text{Equation 3.11.4.6-2}$$

where c_{xxmax} = the distance from the x axis to the extreme fiber

c_{yyymax} = the distance from the y axis to the extreme fiber

n_x = modular ratio at the extreme fiber for c_{xxmax}

n_y = modular ratio at the extreme fiber for c_{yyymax}

Modular ratio n_i is defined as:

$$n_i = \frac{E_i}{E_1} \quad \text{Equation 3.11.4.6-3}$$

where E_1 = Young's modulus of the transformed section

E_i = Young's modulus of segment i

GAS calculates section moduli, S_{ut} and S_{vt} , based on principal moments of inertia, I_{uut} and I_{vvt} , using the following equations:

$$S_{ut} = \frac{I_{uut}}{n_u c_{uumax}} \quad \text{Equation 3.11.4.6-4}$$

$$S_{vt} = \frac{I_{vvt}}{n_v c_{vvmax}} \quad \text{Equation 3.11.4.6-5}$$

where c_{uumax} = the distance from the u axis to the extreme fiber

c_{vvmax} = the distance from the v axis to the extreme fiber

n_u = modular ratio at the extreme fiber for c_{uumax}

n_v = modular ratio at the extreme fiber for c_{vvmax}

3.11.4.7 Radius of Gyration

The radii of gyration of a composite section are computed using the following equations:

$$r_{xt} = \left(\frac{I_{xxt}}{A} \right)^{1/2} \quad \text{Equation 3.11.4.7-1}$$

$$r_{yt} = \left(\frac{I_{yyt}}{A} \right)^{1/2} \quad \text{Equation 3.11.4.7-2}$$

where A = area computed in [Section 3.11.4.1](#)

I_{xxt}, I_{yyt} = moments of inertia of the transformed section as computed in [Section 3.11.4.3](#)

3.11.5 EFFECTIVE CROSS SECTION PROPERTIES

The effective-width concept, which accounts for the post-buckling strength of a thin-walled cross section, has been developed in [Section 3.1](#). The effective width concept applies only to elements in compression; elements in tension are fully effective. The post-buckling strength is the additional load carried by elements of the cross section, after they have buckled locally, by means of a redistribution of stress.

Under the effective-width concept, only certain portions of the plate width are considered to be effective in carrying loads after exceeding the local-buckling stress.

The effective cross section consists of the effective portions of all segments. [Section 3.11.5.1](#) presents the procedures for the effective cross section determination of a homogeneous section. [Section 3.11.5.2](#) presents the procedures for the effective cross section determination of a hybrid section. GAS computes the section properties for an effective cross section as shown in [Table 3.11.5-1](#). The same procedures for calculating area, centroid, moments of inertia, reference angle, and section modulus for nominal cross section properties are used for effective section properties calculation. The equations are shown in [Section 3.11.1](#) to [Section 3.11.4](#). The algorithm for Reference Load calculation is presented in [Section 3.11.5.7](#).

Table 3.11.5-1 Effective Cross Section Properties

Property	Description
Area	Area of the section
c_x	X coordinate of the centroid
c_y	Y coordinate of the centroid
I_{xx}	Moment of inertia about the x axis
I_{yy}	Moment of inertia about the y axis
I_{xy}	Product of inertia
θ	Reference angle
I_{uu}	Moment of inertia about the major principal axis, u
I_{vv}	Moment of inertia about the minor principal axis, v
S_{x+}	Section modulus about the x axis in the positive y direction
S_{y+}	Section modulus about the y axis in the positive x direction
S_{x-}	Section modulus about the x axis in the negative y direction
S_{y-}	Section modulus about the y axis in the negative x direction
S_{u+}	Section modulus about the u axis in the positive v direction
S_{v+}	Section modulus about the v axis in the positive u direction
S_{u-}	Section modulus about the u axis in the negative v direction
S_{v-}	Section modulus about the v axis in the negative u direction
r_x	Radius of gyration about the x axis
r_y	Radius of gyration about the y axis
I_{yc}	Moment of inertia of the compression portion about the neutral axis using the full unreduced section.
P	Reference axial load
M_{x+}	Reference positive moment about the x axis
M_{x-}	Reference negative moment about the x axis
M_{y+}	Reference positive moment about the y axis
M_{y-}	Reference negative moment about the y axis

3.11.5.1 Effective Cross Section Determination of A Homogeneous Section

The procedures used in GAS to determinate the effective cross section of a homogeneous section under specified stress level are described as follows:

1. Compute the normal stress distribution based on a given stress level (per [Section 3.11.5.4](#)) assuming all the segments are fully effective.
2. Determine the segment type (per [Section 3.11.5.5](#)) of each segment.
3. Based on the computed stress distribution and the segment type, calculate the effective width of each segment (per [Section 3.1.2](#) and [Section 3.1.3](#)).
4. Calculate the cross section properties of the section (per [Section 3.11.1](#) and [Section 3.11.4](#)) based on the effective portion of each segment.
5. Compute the stress distribution using the calculated effective section.
6. Calculate the effective width of each segment based on the revised stress distribution.
7. Calculate the cross section properties of the section based on the effective portion of each segment.
8. Repeat Steps 5 to 7 until the area and moments of inertia of the effective section converge.

3.11.5.2 Effective Cross Section Determination of A Hybrid Section

Effective cross section determination of a hybrid section is based on the research results done by University of Missouri-Rolla^{9,10}. Since the research results are for ultimate axial load of stub columns and yield moments of hybrid beams, only the analysis option of "Yield Stress" Stress Level is available in GAS for hybrid sections.

For a hybrid section under ultimate axial load, the following procedures are used in GAS to determine the effective cross section:

1. Set the stress of each segment to be the yield strength of its material.
2. Determine the segment type (per [Section 3.11.5.5](#)) of each segment.
3. Based on the stress distribution and the segment type, calculate the effective width of each segment (per [Section 3.1.2](#) and [Section 3.1.3](#)).

For a hybrid section under yield moment, the following procedures are used in GAS to determine the effective cross section:

1. A position of the neutral axis is assumed.
2. Determine the location of the controlling yield strain - extreme fiber at compression side or extreme fiber at tension side.
3. From strain distribution and the assumed linear elastic-plastic stress-strain relationship, the stress in each element is computed.
4. Determine the segment type (per [Section 3.11.5.5](#)) of each segment.
5. Based on the computed stress distribution and the segment type, calculate the effective width of each segment (per [Section 3.1.2](#) and [Section 3.1.3](#)).
6. Repeat Step 1 to 4 until $\Sigma A_e \sigma = 0$ where A_e is the effective area of each element and σ is the stress in the element.

Please note that GAS assumes the stress-strain relationship to be linear elastic-plastic, a sharp-yielding type of stress-strain curve. For sections with materials of gradual-yielding stress-strain curve, use GAS results with caution. Another assumption made by GAS is that the neutral axes are parallel to the local coordinate axes. If the principal axes of the cross section are not parallel to the local coordinate axes, error message will be issued.

3.11.5.3 Normal Stress Calculation

The stress calculation in GAS is mainly for calculating effective cross section properties. Since only normal stress is needed for effective cross section properties, GAS computes the normal stress distribution in the cross section under specified axial loads and moments.

3.11.5.3.1 Normal Stress in a Homogeneous Section Induced by Axial Load

The normal stress induced by axial load, σ_a , in a homogeneous section can be obtained by the following equation:

$$\sigma_a = \frac{P}{A} \quad \text{Equation 3.11.5.3.1-1}$$

where P = applied axial compression load
 A = total area of the section

3.11.5.3.2 Normal Stress in a Composite Section Induced by Axial Load

It is assumed that there are "n" kinds of materials in the section. Segments of the same material are put into one group. Therefore, we have "n" groups of segments for a section.

The first step is to determine how the axial load is apportioned among the "n" groups. This is easily done by the method of consistent deformations. Assume the segments undergo the same total shortening in the axial direction. Each group of segments will carry a portion of the load proportional to its axial stiffness, i.e., proportional to AE . Therefore, the loads on each group of segments, P_j , $j=1$ to n are given by:

$$P_j = P \frac{A_j E_j}{\sum_{i=1}^n A_i E_i} \quad \text{Equation 3.11.5.3.2-1}$$

where A_i = area of group i
 E_i = Young's modulus of group i

The normal stress in the segment is given by:

$$\sigma_a = \frac{P_j}{A_j} \quad \text{Equation 3.11.5.3.2-2}$$

3.11.5.3.3 Normal Stress in a Homogeneous Section Induced by Moments

The normal stress induced by moments, σ_m , in a homogeneous section is computed by:

$$\sigma_m = \frac{(M_y I_{xx} + M_x I_{xy})X - (M_x I_{yy} + M_y I_{xy})Y}{I_{xx} I_{yy} - I_{xy} I_{xy}} \quad \text{Equation 3.11.5.3.3-1}$$

where M_x, M_y = defined moments
 X, Y = distance from the centroid to the point where stress is calculated

3.11.5.3.4 Normal Stress in a Composite Section Induced by Moments

The normal stress induced by moments, σ_m , in a composite section may be computed by:

$$\sigma_m = n \frac{(M_y I_{xxt} + M_x I_{xyt})X - (M_x I_{yyt} + M_y I_{xyt})Y}{I_{xxt} I_{yyt} - I_{xyt} I_{xyt}} \quad \text{Equation 3.11.5.3.4-1}$$

where n = modular ratio

M_x, M_y = defined moments

X, Y = distance from the centroid to the point where stress is calculated

3.11.5.3.5 Total Normal Stress

The total normal stress is the sum of σ_a and σ_m

$$\sigma_T = \sigma_a + \sigma_m \quad \text{Equation 3.11.5.3.5-1}$$

3.11.5.4 Stress Distribution in a Homogenous Section Under Different Stress Levels

GAS offers four different stress levels for effective cross section properties calculation:

1. Yield Stress
2. Specified Stress
3. Stress from Loads
4. At First Onset Of Local Buckling

For "Yield Stress" and "Specified Stress" levels, the loading direction must be specified. The loading direction can be:

1. Compressive Axial Load
2. Positive M_x
3. Negative M_x
4. Positive M_y
5. Negative M_y

The stress level "Yield Stress", means the maximum stress in the cross section reaches the yield stress under the specified direction of loading. The stress level "Specified Stress", means the maximum stress in the cross section reaches the user specified value under the specified direction of loading. The procedures to calculate the stress distribution under "Yield Stress" and "Specified Stress" are very similar and they are described as follows:

1. Apply a unit load in the user specified loading direction and compute the stress distribution using the equations in [Section 3.11.5.3](#).
2. Find the maximum stress in the cross section under the unit load.

3. Compute the scaling factor. For "Yield Stress", the scaling factor is equal to the material yield stress divided by the maximum stress under the unit load. For "Specified Stress", the scaling factor is equal to the user specified stress value divided by the maximum stress under the unit load.
4. Multiply the scaling factor to all the stresses under the unit load and obtain the stress distribution in the cross section.

For "Stress from Loads", the user inputs the loads and GAS computes the stress distribution using the equations in [Section 3.11.5.3](#).

For "At First Onset Of Local Buckling", GAS uses the following procedures to find the stress distribution when the first onset of local buckling occurs.

1. Use the procedures for the Stress Level "Yield Stress" and compute the effective area. If the effective area is equal to the total area, the stress distribution is obtained. If not, continue.
2. Use the procedures for the Stress Level "Specified Stress" and set the stress to be $F_y - F_y/500$.
3. Compute the effective area.
4. Repeat Steps 2 to 3 and reduce the specified stress by $F_y/500$ until the effective area is equal to the total area.

3.11.5.5 Segment Type Determination

Based on the geometry and stress condition in a segment, GAS determines the type of each segment of a section. There are seven segment types for the purpose of effective width calculations:

1. Uniformly compressed stiffened elements
2. Stiffened elements with a stress gradient
3. Unstiffened elements in compression
4. Uniformly compressed elements with an edge stiffener
5. Uniformly compressed elements with a single intermediate stiffener
6. Edge stiffened elements with intermediate stiffeners or stiffened elements with more than one intermediate stiffener
7. Tension elements

For every line in the cross section, GAS requires the line type to be specified as one of the following:

1. Segment
2. Edge Stiffener
3. Intermediate Stiffener
4. Unstiffened

An Edge Stiffener is used to provide a continuous support along a longitudinal edge of the compression flange to improve the buckling stress. In other words, an Edge Stiffener is used to stiffen the compression flange. An Intermediate Stiffener Line is a line associated with an intermediate stiffener in the compression flange. An unstiffened compression element is a flat

compression element that is stiffened at only one edge parallel to the direction of stress. The unstiffened compression element is illustrated in [Figure 3.1.2.1-1](#).

For every arc in the cross section, GAS requires the arc type to be specified as one of the following:

1. Segment
2. Intermediate Stiffener
3. Fully Effective
4. Unstiffened

The Fully Effective arc is assumed to be fully effective in the calculation and no effective width calculation will be done for that arc. Therefore, the Fully Effective arc should only be used for an arc which the user believes to be fully effective such as a fillet. An Intermediate Stiffener arc is an arc associated with an Intermediate Stiffener. An unstiffened compression curved element is a curved element that is stiffened at only one edge parallel to the direction of stress. The unstiffened curved element is illustrated in [Figure 3.1.2.3-1](#).

If a line or an arc is a "Segment", GAS will determine the segment type according to the following criteria^{[11](#)}:

1. Stiffened if connected on both ends.
2. Edge stiffener if one end free and connected to only one element on the other end when both the edge stiffener and the stiffened element is under uniform compression or a compressive stress gradient (but not a stress reversal).
3. Unstiffened for all other elements not satisfying items (a) or (b).
4. If the cross section consists of two elements, both of them are unstiffened elements.
5. If the cross section consists of three elements, the two elements with free end are unstiffened elements.

3.11.5.6 Effective Width Calculations

GAS uses the procedures and equations presented in [Section 3.1](#) of this manual to calculate the effective width of various element types under specific loading conditions. This section summarizes the procedures utilized by GAS and includes some of the equations from [Section 3.1](#) for easy reference. Refer to [Section 3.1](#) for additional information.

3.11.5.6.1 Effective Width of Uniformly Compressed Stiffened Elements

The effective width, b , of uniformly compressed stiffened elements is determined using [Figure 3.1.2.1.1-4](#) or as follows:

$$b = w \quad \text{when } \lambda \leq 0.673 \quad \text{Equation 3.11.5.6.1-1}$$

$$b = \rho w \quad \text{when } \lambda > 0.673 \quad \text{Equation 3.11.5.6.1-2}$$

where w = width of the element

ρ is determined by:

$$\rho = \frac{1 - \frac{0.22}{\lambda}}{\lambda} \quad \text{Equation 3.11.5.6.1-3}$$

Where λ is a slenderness factor determined by

$$\lambda = 1.052 \left(\frac{w}{t} \right) \sqrt{\frac{f}{E}} \quad \text{As per Equation 3.1.2.1.1-1} \quad \boxed{\sqrt{\alpha}} \quad \boxed{L_{\text{eff}}}$$

where f = stress in the element
 E = Young's modulus of the element
 k = plate buckling coefficient
 w = width of the element
 t = thickness of the element

3.11.5.6.2 Effective Width of Stiffened Elements with a Stress Gradient

The effective widths, b_1 and b_2 , as shown in [Figure 3.1.3.1.2-3](#), are determined as follows:

$$b_1 = \frac{b_e}{3 - \psi} \quad \text{As per Equation 3.1.3.1.2-5} \quad \boxed{\sqrt{\alpha}} \quad \boxed{L_{\text{eff}}}$$

$$b_2 = \begin{cases} \frac{b_e}{2} & \text{for } \psi \leq -0.236 \\ b_e - b_1 & \text{for } \psi > -0.236 \end{cases} \quad \text{As per Equation 3.1.3.1.2-6} \quad \boxed{\sqrt{\alpha}} \quad \boxed{L_{\text{eff}}}$$

where b_e = effective width determined for a uniformly compressed stiffened element with f_1 substituted for f and k determined as follows:

$$\text{where } k = 4 + 2(1 - \psi)^3 + 2(1 - \psi) \quad \text{As per Equation 3.1.3.1.2-3} \quad \boxed{\sqrt{\alpha}} \quad \boxed{L_{\text{eff}}}$$

$$\psi = \frac{f_t}{f_c} = \frac{f_2}{f_1} \quad (\text{See Figure 3.1.3.1.2-3 for } f_1 \text{ and } f_2.) \quad \text{As per Equation 3.1.3.1.2-4} \quad \boxed{\sqrt{\alpha}} \quad \boxed{L_{\text{eff}}}$$

3.11.5.6.3 Effective Width of Unstiffened Elements in Compression

The effective width of an unstiffened compression element with uniform compression is determined by:

$$\begin{aligned} b &= w && \text{for } \frac{w}{t} \leq 0.426S \\ b &= 0.426St && \text{for } \frac{w}{t} > 0.426S \end{aligned} \quad \text{As per Equation 3.1.2.1.2-2} \quad \boxed{\sqrt{\alpha}} \quad \boxed{L_{\text{eff}}}$$

$$\left(\frac{w}{t}\right)_{\lim} = S = 1.28 \sqrt{\frac{E}{f}}$$

As per [Equation 3.1.2.1.1-4](#)

The effective width of an unstiffened compression element and an edge stiffener with a stress gradient is determined for a uniform compressed stiffened element with $f = f_3$ as shown in [Figure 3.1.3.1.2-3](#) and $k = 0.43$.

3.11.5.6.4 Effective Width of Uniformly Compressed Elements with an Edge Stiffener

Based on the value of the width/thickness ratio, w/t , of the element, the effective width calculation of a uniformly compressed element with an edge stiffener can be evaluated using [Figure 3.1.2.1.3-1](#) or as follows:

1. For $\frac{w}{t} \leq \frac{S}{3}$

$$b_e = w$$

Equation 3.11.5.6.4-1

2. For $\frac{S}{3} < \frac{w}{t} \leq S$

b_e is calculated according to the stiffened element procedure

$$\text{For } 0.8 \geq \frac{D}{w} > 0.25$$

$$k = \left(4.82 - 5 \left(\frac{D}{w} \right) \right) \left(\frac{I_s}{I_a} \right)^{1/2} + 0.43 \leq 5.25 - 5 \left(\frac{D}{w} \right) \quad \text{Equation 3.11.5.6.4-2}$$

$$\text{For } \frac{D}{w} \leq 0.25$$

$$k = 3.57 \left(\frac{I_s}{I_a} \right)^{1/2} + 0.43 \leq 4.0 \quad \text{Equation 3.11.5.6.4-3}$$

where D = Depth of a simple lip

I_s = Moment of inertia of the stiffener

I_a = Adequate moment of inertia of the stiffener, as defined by the relationship:

$$I_a = 399 \left(\frac{\frac{w}{t}}{S} - 0.33 \right)^3 t^4 \quad \text{Equation 3.11.5.6.4-4}$$

3. For $\frac{w}{t} \geq S$, b_e is calculated according to the stiffened element procedure

$$\text{For } 0.8 \geq \frac{D}{w} > 0.25$$

$$k = \left(4.82 - 5\left(\frac{D}{w}\right) \right) \left(\frac{I_s}{I_a} \right)^{1/3} + 0.43 \leq 5.25 - 5\left(\frac{D}{w}\right) \quad \text{Equation 3.11.5.6.4-5}$$

$$\text{For } \frac{D}{w} \leq 0.25$$

$$k = 3.57 \left(\frac{I_s}{I_a} \right)^{1/3} + 0.43 \leq 4.0 \quad \text{Equation 3.11.5.6.4-6}$$

$$\text{where } I_a = \left(\frac{115 \frac{w}{t}}{S} + 5 \right) t^4 \quad \text{Equation 3.11.5.6.4-7}$$

3.11.5.6.5 Effective Width of Uniformly Compressed Elements with Single Intermediate Stiffener

Based on the value of the width/thickness ratio, b_o/t , of the element, the effective width calculation of a uniformly compressed element with an intermediate stiffener can be evaluated using [Figure 3.1.2.1.4-2](#) or as follows:

1. For $\frac{b_o}{t} \leq S$

$$b = w \quad \text{Equation 3.11.5.6.5-1}$$

2. For $S < \frac{b_o}{t} < 3S$

b is calculated according to the stiffened element procedure

$$k = 3 \left(\frac{I_s}{I_a} \right)^{1/2} + 1 \leq 4 \quad \text{Equation 3.11.5.6.5-2}$$

$$\text{where } I_a = \left(50 \frac{\frac{b_o}{t}}{S} - 50 \right) t^4 \quad \text{Equation 3.11.5.6.5-3}$$

$$3. \text{ For } \frac{b_o}{t} \geq 3S$$

b is calculated according to the stiffened element procedure

$$k = 3 \left(\frac{I_s}{I_a} \right)^{1/3} + 1 \leq 4 \quad \text{Equation 3.11.5.6.5-4}$$

$$\text{where } I_a = \left(128 \frac{\frac{b_o}{t}}{S} - 285 \right) t^4 \quad \text{Equation 3.11.5.6.5-5}$$

3.11.5.6.6 Effective Width of Edge Stiffened Elements - Other Cases

For the determination of the effective width, the intermediate stiffener of an edge stiffened element or multiple stiffeners of a stiffened element shall be disregarded unless each intermediate stiffener has adequate moment of inertia as follows:

$$I_a = 3.66t^4 \left[\left(\frac{w}{t} \right)^2 - \left(\frac{0.136E}{F_y} \right) \right]^{1/2} \quad \text{Equation 3.11.5.6.6-1}$$

If the spacing of intermediate stiffeners between two webs is such that the subelement, b, between stiffeners is less than w, as determined for a fully stiffened element, then only two intermediate stiffeners (those nearest each web) shall be considered effective.

If the spacing of intermediate stiffeners between a web and an edge stiffener is such that the subelement between stiffeners b is less than w, as determined for a fully stiffened element, then only one intermediate stiffener, that nearest the web, shall be considered effective.

If $w/t > 60$, the effective width, b_e , of the subelement or element shall be determined as follows:

$$b_e = b - 0.10t \left(\frac{w}{t} - 60 \right) \quad \text{for } \frac{w}{t} \geq 60 \quad \text{As per Equation 3.1.2.1.4-6}$$

where w/t = flat-width ratio of subelement or element

b = effective width determined from fully stiffened element procedure

If intermediate stiffeners are spaced so closely that for the elements between stiffeners, $b = w$ as determined in fully stiffened elements, then all the stiffeners may be considered effective. In computing the flat-width to thickness ratio for the entire multiple-stiffened element, such elements shall be considered as replaced by an "equivalent element" without intermediate stiffeners whose width, b_o , is the full width between webs or from the web to the edge stiffener, and whose equivalent thickness, t_s , is determined as follows:

$$t_s = \sqrt[3]{\frac{12I_{sf}}{b_o}} \quad \text{As per Equation 3.1.2.1.4-4}$$

where I_{sf} = moment of inertia of the full area of the multiple-stiffened element, including the intermediate stiffeners

3.11.5.6.7 Effective Width of Curved Elements

The effective width calculation for curved elements stiffened by bends larger than 45° is as defined for flat elements. However, unlike a flat element, the ineffective portion of a curved element is assumed to carry the critical buckling stress of a circular cylinder with the same radius and thickness as the element. Instead of completely neglecting the center portion as is done for stiffened flat elements, use an effective thickness:

$$t_e = \left(\frac{A_o}{A} \right) \left(\frac{F_y}{f} \right) t$$

As per [Equation 3.1.2.3-4](#)



where A_o/A is from [Figure 3.1.2.2-1 \(Section 3.1\)](#)

F_y = Material yield stress

f = Stress in the element

t = Segment thickness

3.11.5.7 Reference Load

Reference load is the load corresponding to the computed stress distribution for the effective cross section properties calculation. No reference load is computed for the Stress Level of "Stress from Load" since the load is specified by the user.

For a homogenous section under axial load, the reference load, P , is computed by:

$$P = A_e F$$

[Equation 3.11.5.7-1](#)

where A_e = Effective area

F = F_y for Stress Level of Yield Stress or user-specified stress of Stress Level of Specified Stress

For a homogenous section under moment, the reference load, M , is computed by:

$$M = S_e F$$

[Equation 3.11.5.7-2](#)

where S_e = Effective section modulus

F = F_y for Stress Level of Yield Stress or user-specified stress of Stress Level of Specified Stress

For a hybrid section, the ultimate axial load is computed by:

$$P = \sum A_e F_y$$

[Equation 3.11.5.7-3](#)

where A_e = Effective area of each segment

F_y = material yield strength of each segment

For a hybrid section, the yield moment is calculated by the following integral over the effective section:

$$M = \int \sigma y dA$$

[Equation 3.11.5.7-4](#)

where σ = normal stress

y = distance to the neutral axis.

3.11.6 AXIAL CAPACITY

The axial capacity is determined by

$$P_u = A_e F_{cu}$$

As per [Equation 3.1.2.5-3](#)



where P_u = axial load capacity

A_e = the effective area at the stress F_{cu}

$\pi^2 E$ = 1,974,000 MPa (291,000 ksi)

K = effective length factor

L = unbraced length of member

r = radius of gyration of full, unreduced cross section

F_y = yield strength of steel

F_{cu} = ultimate compression stress under concentric loading determined as follows:

$$F_{cu} = F_e \quad \text{for } F_e \leq \frac{F_y}{2}$$

As per [Equation 3.1.2.5-1](#)



$$F_{cu} = F_y \left(1 - \frac{F_y}{4F_e} \right) \quad \text{for } F_e > \frac{F_y}{2}$$

For doubly-symmetric sections, closed sections and any other sections which can be shown not to be subject to torsional or torsional-flexural buckling, the elastic flexural buckling stress, F_e , shall be determined as follows:

$$F_e = \frac{\pi^2 E}{\left(\frac{KL}{r} \right)^2}$$

As per [Equation 3.1.2.5-2](#)



For singly-symmetric sections subject to torsional-flexural buckling, F_e shall be taken as the smaller of F_e calculated according to [Equation 3.1.2.5-2](#) and F_e calculated as follows:

$$F_e = \frac{1}{2\beta} [(\sigma_{ex} + \sigma_t) - \sqrt{(\sigma_{ex} + \sigma_t)^2 - 4\beta\sigma_{ex}\sigma_t}]$$

Equation 3.11.6-1

where

$$\beta = 1 - \left(\frac{x_o}{r_o} \right)^2$$

Equation 3.11.6-2

$$\sigma_{ex} = \frac{\pi^2 E}{(K_x L_x / r_x)^2}$$

Equation 3.11.6-3

$$\sigma_t = \frac{1}{Ar_0^2} [GJ + \frac{\pi^2 EC_w}{(K_t L_t)^2}] \quad \text{Equation 3.11.6-4}$$

where x_0 = Distance from the shear center to the centroid along the principal x-axis
 r_x, r_y = Radii of gyration of the full cross section about the centroidal principal axes.
 r_0 = polar radius of gyration of the full cross section about the shear center

$$r_0 = \sqrt{r_x^2 + r_y^2 + x_0^2} \quad \text{Equation 3.11.6-5}$$

where K_x, K_t = Effective length factor for bending about the x-axis and for twisting
 L_x, L_t = Unbraced length for bending about the x axis and for twisting

3.11.7 FLEXURAL CAPACITY

The flexural capacity of a member shall be calculated either on the basis of initiation of yielding in the effective section or on the basis of the inelastic reserve capacity

3.11.7.1 Based on Initiation of Yielding

The flexural capacity shall be determined as follows:

$$M_u = S_c F_{cu} \quad \text{Equation 3.11.7.1-1}$$

where F_{cu} = ultimate stress
 S_c = Elastic section modulus of the effective section calculated with the extreme compression or tension fiber at F_{cu}

If the member is not subject to torsional flexural buckling,

$$F_{cu} = F_y \quad \text{Equation 3.11.7.1-2}$$

If the member is subject to flexural torsional buckling

$$F_{cu} = \frac{M_c}{S_f} \quad \text{Equation 3.11.7.1-3}$$

where S_f = Elastic section modulus for the extreme compression fiber
 M_c = Critical moment calculated as follows:

$$\begin{aligned} M_c &= M_y \text{ for } M_e \geq 2.78M_y && \text{Equation 3.11.7.1-4} \\ M_c &= \frac{10}{9}M_y \left(1 - \frac{5M_y}{18M_e}\right) \text{ for } 2.78M_y > M_e > 0.56M_y \\ M_c &= M_e \text{ for } M_e \leq 0.56M_y \end{aligned}$$

where M_y = Moment causing initial yield at the extreme compression fiber of the full section
 $= S_f F_y$
 M_e = Elastic critical moment

For bending about the symmetry axis of singly, doubly and point symmetric sections, M_e is computed as:

$$M_e = C_b r_0 \sqrt{\sigma_{ey} \sigma_t} \quad \text{Equation 3.11.7.1-5}$$

where

$$C_b = \frac{12.5 M_{max}}{2.5 M_{max} + 3 M_A + 4 M_B + 3 M_C} \quad \text{Equation 3.11.7.1-6}$$

where: M_{max} = absolute value of maximum moment in the unbraced segment
 M_A = absolute value of moment at quarter point of unbraced segment
 M_B = absolute value of moment at centerline of unbraced segment
 M_C = absolute value of moment at three-quarter point of unbraced segment
 r_0 = polar radius of gyration of the full cross section about the shear center

$$\sigma_{ey} = \frac{\pi^2 E}{(K_y L_y / r_y)^2} \quad \text{Equation 3.11.7.1-7}$$

$$\sigma_t = \frac{1}{A r_0^2} [GJ + \frac{\pi^2 E C_w}{(K_t L_t)^2}] \quad \text{Equation 3.11.7.1-8}$$

where A = Full cross section area
 C_w = Warping constant
 J = St. Venant torsion constant
 K_y, K_t = Effective length factor for bending about the y-axis and for twisting
 L_y, L_t = Unbraced length of bending about the y axis and for twisting

For point-symmetric sections, use half of the value calculated by [Equation 3.11.7.1-5](#) for M_e .

For bending about the centroidal axis perpendicular to the symmetry axis for singly-symmetric section,

$$M_e = C_s A \sigma_{ex} [j + C_s \sqrt{j^2 + r_0^2 (\sigma_t / \sigma_{ex})}] / C_{TF} \quad \text{Equation 3.11.7.1-9}$$

where

$$C_{TF} = 0.6 - 0.4 \left(\frac{M_1}{M_2} \right) \quad \text{Equation 3.11.7.1-10}$$

where M_1 is the smaller and M_2 the larger bending moment at the ends of the unbraced length in the plane of bending. When the bending moment at any point within an unbraced length is larger than that at both ends of

this length, and for members subject to combined compressive axial load and bending moment, $C_{TF} = 1$.

$C_s = 1$ for moment causing compression on the shear center side of the centroid

$C_s = -1$ for moment causing tension on the shear center side of the centroid.

j = torsional-flexural buckling property defined in [Equation 3.11.3.12-1](#).

$$\sigma_{ex} = \frac{\pi^2 E}{(K_x L_x / r_x)^2}$$
Equation 3.11.7.1-11

3.11.7.2 Based on Inelastic Reserve Capacity

Inelastic stress redistribution allows the section to strain beyond yield under some circumstances. The flexural capacity based on inelastic reserve capacity is determined using the maximum compression strain of $C_y e_y$, no limit is placed on the maximum tensile strain. The e_y is the yield strain which equals to F_y/E and C_y is the compression strain factor determined as follows:

For stiffened compression elements intermediate stiffeners,

$$\begin{aligned} C_y &= 1 && \text{for } \frac{w}{t} \leq \lambda_1 \\ C_y &= 3 - 2\left(\frac{w/t - \lambda_1}{\lambda_2 - \lambda_1}\right) && \text{for } \lambda_1 < \frac{w}{t} < \lambda_2 \\ C_y &= 3 && \text{for } \frac{w}{t} \geq \lambda_2 \end{aligned}$$
Equation 3.11.7.2-1

where

$$\lambda_1 = \frac{1.11}{\sqrt{F_y/E}}$$
Equation 3.11.7.2-2

$$\lambda_2 = \frac{1.28}{\sqrt{F_y/E}}$$
Equation 3.11.7.2-3

For other types of elements, $C_y = 1$.

3.11.8 COMBINED AXIAL AND FLEXURAL OVERALL STABILITY

The capacity of a member under combined axial and flexural loads is customarily evaluated by means the interaction ratio of an interaction equation.

For $P/P_u \leq 0.15$,

$$\frac{P}{P_u} + \frac{M_x}{M_{ux}} + \frac{M_y}{M_{uy}} \leq 1.0$$
As per [Equation 3.1.3.7-3](#)



where P = applied axial load

- P_u = axial load capacity
 M_x, M_y = applied bending moments about each principal axis
 M_{ux}, M_{uy} = ultimate bending moment calculated for each principal axis separately with no axial load

When $P/P_u > 0.15$, the interaction expression

$$\frac{P}{P_u} + \frac{C_{mx}M_x}{\left(1 - \frac{P}{P_{ex}}\right)M_{ux}} + \frac{C_{my}M_y}{\left(1 - \frac{P}{P_{ey}}\right)M_{uy}} \leq 1.0 \quad \text{Equation 3.11.8-1}$$

where all terms are as defined in [Equation 3.1.3.7-3](#), is to be used to check a compression member in its unbraced region. The variable P_{ex} , for bending about the x-axis, is

$$P_{ex} = \frac{\pi^2 EI_x}{(K_x L_x)^2} \quad \text{Equation 3.11.8-2}$$

where L_x = the actual axial unbraced length in the y-plane of bending

K_x = corresponding effective length factor

I_x = moment of inertia of the full unreduced section about the x-axis of bending

The value of C_m is 0.85 typical. An exception is when the compression member is laterally braced against joint translation and is rotationally restrained at the ends and subjected only to end moments, in which case

$$C_m = 0.6 - 0.4 \left(\frac{M_1}{M_2} \right) \geq 0.4 \quad \text{As per } \text{Equation 3.1.3.7-6} \quad \boxed{\alpha} \quad \boxed{L}$$

where $\frac{M_1}{M_2}$ is the ratio of the smaller to larger end moments

3.11.9 AXIAL FORCE DEFLECTION PROPERTIES OF STUB COLUMNS

As shown in [Figure 3.11.9-1](#), the force deflection curve of a short compressive column experiencing local buckling can be divided into two regions – before the first onset of local buckling and after the first onset of local buckling¹².

Before the first onset of local buckling (P_o), the member exhibits linear-elastic behavior and the slope of the line can be computed as:

$$K = \frac{AE}{L} \quad \text{Equation 3.11.9-1}$$

where A is the cross section area
L is the member length.

After the first onset of local buckling (from P_o to P_u), the slope changes according to the loading. The tangent line slope of the curve at P_i can be computed as:

$$K_{ti} = \frac{A_{ei}E}{L}$$

Equation 3.11.9-2

where A_{ei} is the effective area of the member when subject to load P_i .

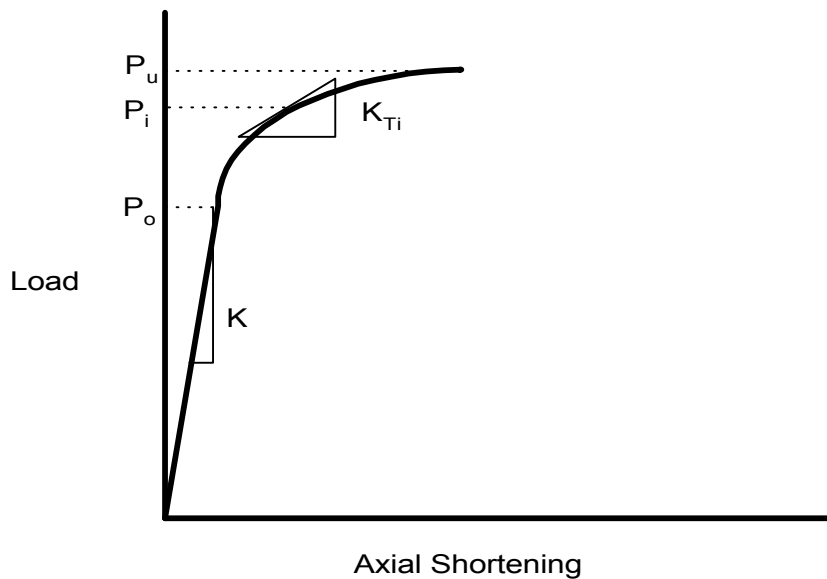


Figure 3.11.9-1 Axial Force Deflection Properties of Stub Column

REFERENCES FOR SECTION 3.11

1. Yu, Wei-Wen Cold-Formed Steel Design, Second Edition, John Wiley & Sons. Inc., 1991.
2. General Motors Corporation, COMSEC Thin Walled Section Analysis, GM Engineering Report CPE-049, June 1987.
3. Timoshenko, S. P. and Gere, James M., Mechanics of Materials, Van Nostrand Reinhold Company, 1972.
4. Warren C. Young, Roark's Formulas for Stress and Strain, Sixth Edition, McGraw-Hill, New York 1989.
5. Galambos, Theodore V, Structural Members and Frames, McGraw-Hill, Inc., 1978.
6. Paz, Mario, Strehl, C. Patrick and Schrader, Preston Computer Determination of the Shear Center of Open and Closed Sections, Computers and Structures, v. 6, June 1975, pp 117-125.
7. The James F. Lincoln Arc Welding Foundation, Design of Welded Structures, 1966.
8. American Society for Metals, Metal Forming Handbook, Volume 4, 1998.
9. Pan, C.L. and Yu, W.W., Design of Automotive Structural Components using high strength Sheet Steels: Effect of Strain Rate on the Structural Strength and Crusing Behavior of Cold-Formed Steel Stub Columns, Nineteenth Progress Report, Civil Engineering Study 93-1, University of Missouri-Rolla, July 1993.
10. Pan, C.L. and Yu, W.W., Design of Automotive Structural Components using high strength Sheet Steels: Effect of Strain Rate on the Structural Strength of Cold-Formed Steel Hybrid Beams, Twentieth Progress Report, Civil Engineering Study 93-1, University of Missouri-Rolla, June 1995.
11. Shiunn-Jang Wang, Computer Determination of the Effective Properties of Sections with Arbitrary Shape , ASCE First Congress on Computing in Civil Engineering, 1994.
12. Shiunn-Jang Wang, Sam Errera, Douglas G. Prince, Determine Member Strength of Automotive Steel Components Considering Local Buckling Effects, SAE 2000 International Body Engineering Conference, October 2000.

BIBLIOGRAPHY FOR SECTION 3.11

1. American Iron and Steel Institute, Cold-Formed Steel Design Manual, August 1986 Edition with December 11, 1989 Addendum, Washington D.C.
2. Desktop Engineering Int'l Inc., DE/CAASE User's Manual, August, 1994.

3. Chrysler Corporation, SECRIP User Manual, February 1977.
4. Ford Motor Company, BEAMSTRESS User's Training Notes, June 1989.
5. Inland Steel Company, BEAM1 User's Manual"
6. ARMCO Steel Company, SDSECT User's Manual"
7. Boresi, Arthur P., Sidebottom, Omar M., Seely, Fred B. and Smith, James O. Advanced Mechanics of Materials, McGraw-Hill, Inc., 1980.
8. Roark, R. J. and Young, W. C., Formulas for Stress and Strain, Sixth Edition, McGraw-Hill, New York.
9. Park, R. and Paulay, T., Reinforced Concrete Structures, John Wiley & Sons, Inc., 1975.
10. Johnston, Bruce G., Guide to Stability Design Criteria for Metal Structures, 3rd Edition, Structural Stability Research Council, 1975
11. American Iron and Steel Institute, Guide for Preliminary Design of Sheet Steel Automotive Structural Components, 1981.
12. American Iron and Steel Institute and Desktop Engineering Int'l, Inc., AISI/CARS 2000, May 2000.

3.12 DESIGNING FOR STAMPING OPERATIONS

For additional information see [Section 3.10 Design Guidelines for Sheet Steel](#) and [4.1 Stamping Operations](#).

3.12.1 INTRODUCTION

The objective of this section is to lead technical personnel through the complete product/manufacturing development cycle, with special emphasis toward how team involvement can impact the stamping plant and its out-the-door product. The major focus for discussion in this section will be light gage, body-in-white components and outer skin (show surface) panels. Information on the work of manufacturing engineers, which is not normally performed by the design engineer, is presented to enhance the design engineers' understanding of those functions.

The Product/Manufacturing Development Team should represent the following disciplines: Stylist, Product Designers, Sheet Metal Metallurgical Engineers, Manufacturing (stamping and assembly plant) Engineers and Technicians, and Welding Personnel. Establishment of guidelines, targets, and procedures should be their first order of business. Participation and compromise will determine how effectively the development team will enable their company to improve its competitive position with world class quality products, produced at a world market competitive price.

3.12.2 STYLING

Prior to concept approval, styling personnel, body design engineers, and manufacturing engineers with expertise in major body sheet metal stampings (white metal parts), should meet to study and evaluate the styling of outer skins for manufacturability and estimated piece cost. It is imperative that the concerns of all participating disciplines be thoroughly discussed and evaluated, and compromises be reached. Manufacturing must be willing to accept reasonable styling challenges in order to create a marketable vehicle. Conversely, styling must not pursue a design that is not manufacturing friendly.

3.12.2.1 Review Guidelines

The following features impact material utilization (cost) or quality. A thorough analysis must be conducted until a complete understanding of all potential problem areas is achieved by all participating parties.

- General shape and contour for formability should be soft and flowing ([Figure 3.12.2.1-1](#)).
- Draw depth of panel should not exceed 4". This may allow for total lockout of sheet metal ([Figure 3.12.2.1-1](#)). Advantages of stretch forming will be discussed later in this section.
- Panel sweep should never go below acceptable minimum standards ([Figure 3.12.2.1-2](#)).
- Severe transitions in shape must be held to a minimum. Sudden length of line changes cause poor draw conditions. Reverse areas should be held to minimum depth ([Figure 3.12.2.1-3](#)). Irregular styling features such as grooves and ditches male/female styling character lines/shapes) can cause poor panel conditions at the beginning of the draw

punch contact (trapped metal, skid lines and impact lines). Female feature lines avoid panel skid lines ([Figure 3.12.2.1-3](#)).

- Sharp corners in the product design will cause poor die conditions and usually result in generating manufacturing scrap ([Section 3.12.12.1](#)).

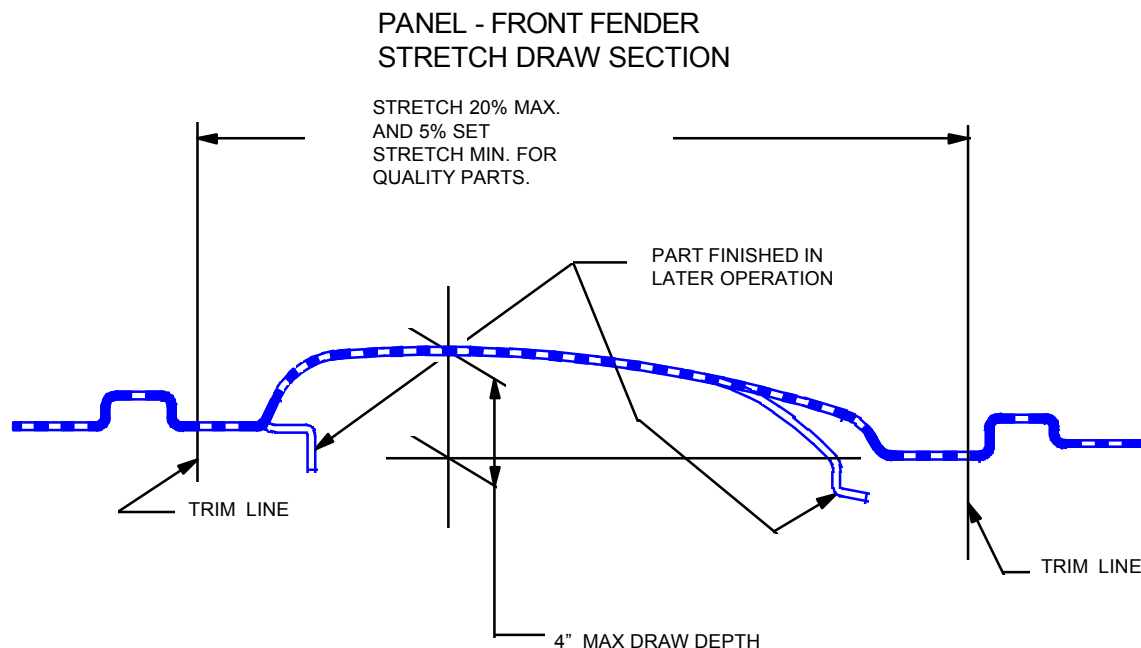


Figure 3.12.2.1-1 Preferred quality panel

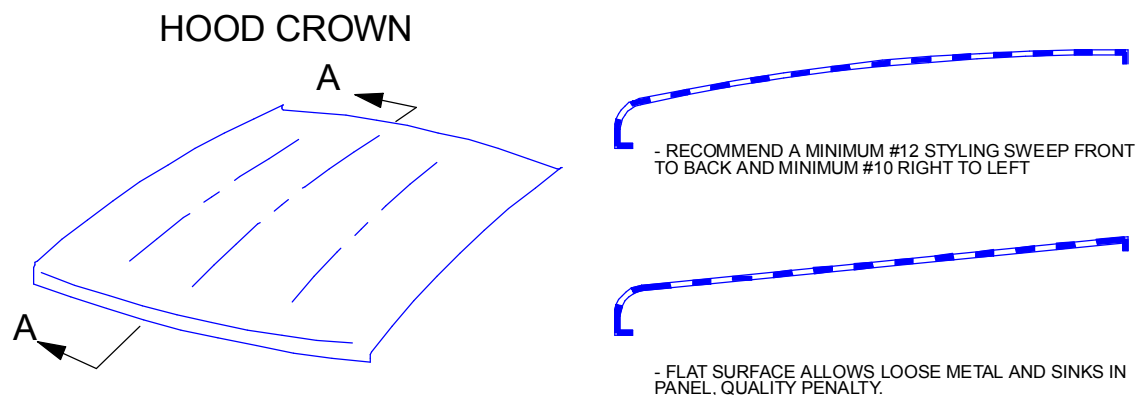


Figure 3.12.2.1-2 Panel sweep minimum standards

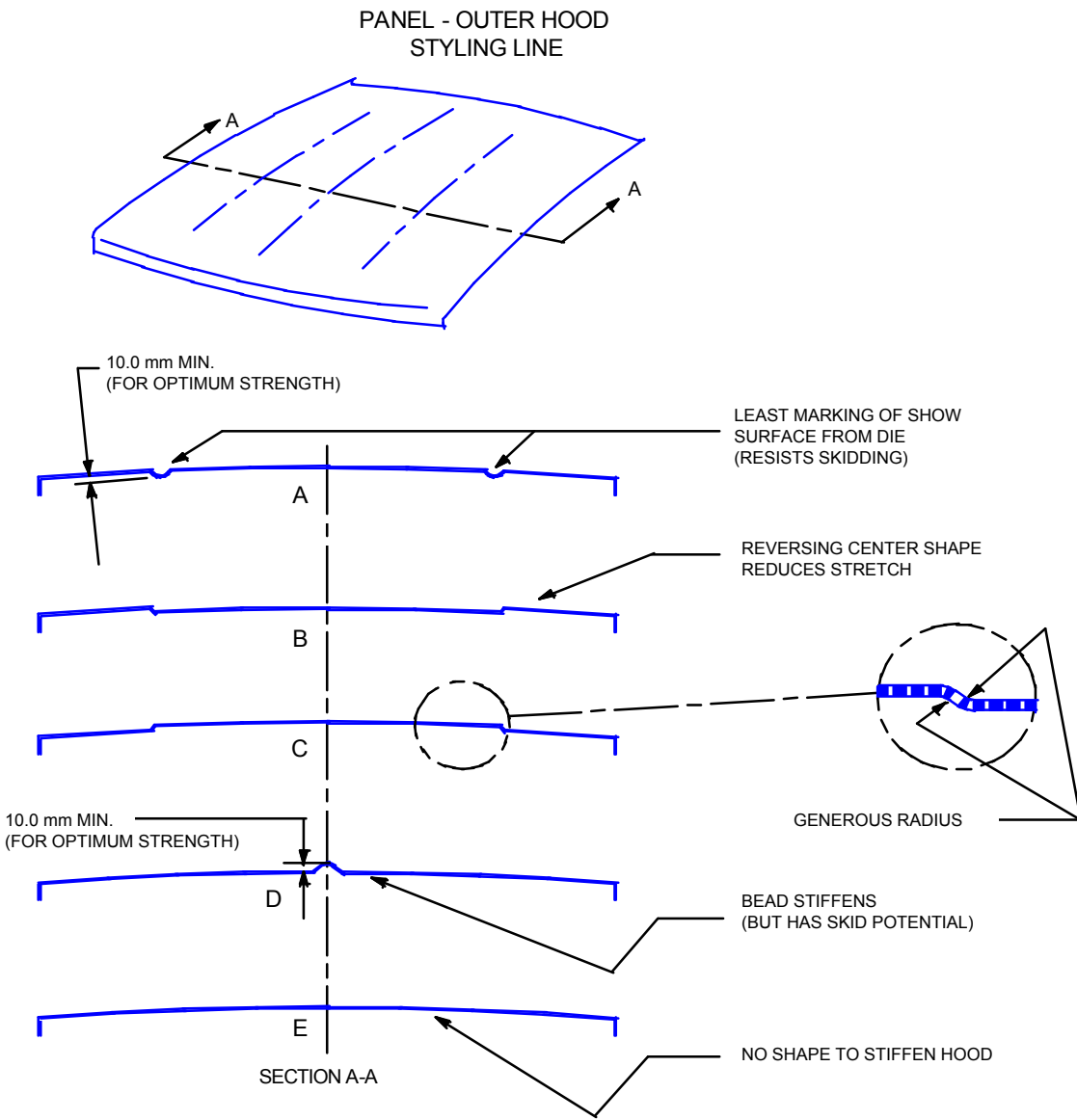


Figure 3.12.2.1-3 Transitions and irregular styling

- Panel cut lines and joint lines must be reviewed for feasibility and manufacturability, as well as achieving good material utilization and also to avoid increasing die cost and lead time ([Figure 3.12.2.1-4](#)).
- Multipiece panels, as compared to one or two piece panels, can only be evaluated by performing a preliminary cost quality study. [Figure 3.12.2.1-5](#) illustrates a one, two, and three piece quarter panel.

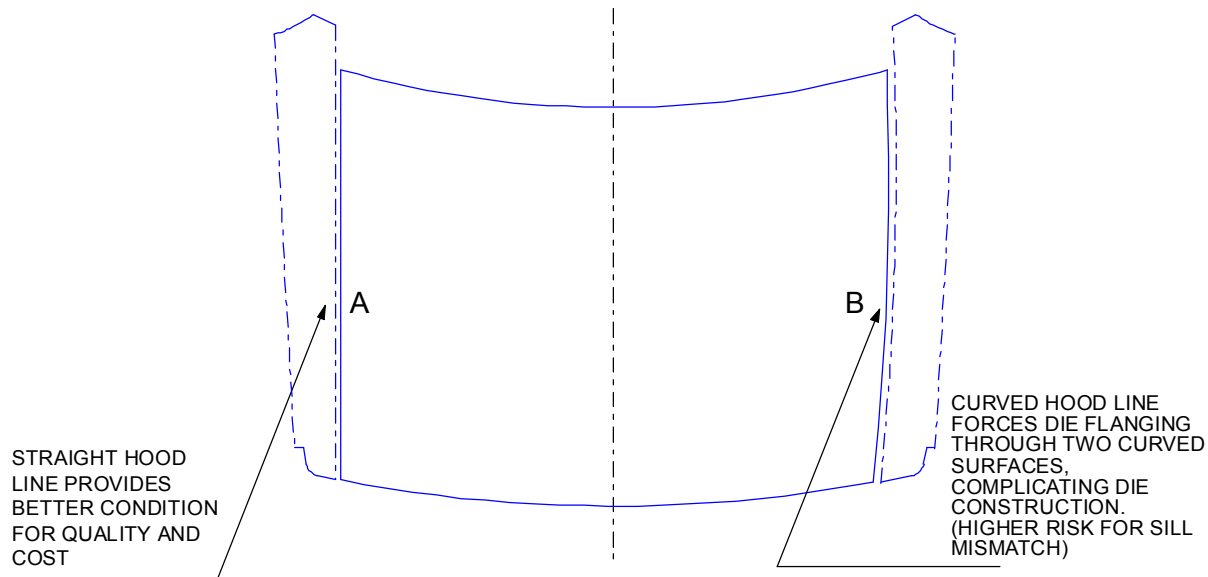


Figure 3.12.2.1-4 Panel cut lines and joint lines

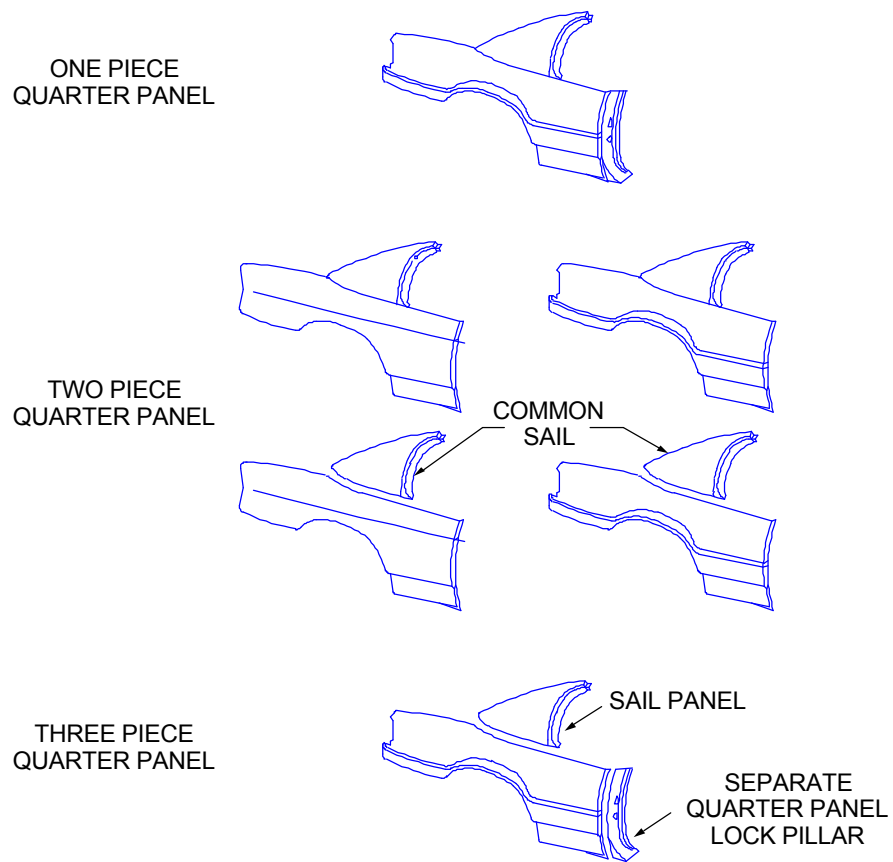


Figure 3.12.2.1-5 One, two and three piece quarter panels

Breaking Up Panels

Breaking up panels may have other advantages. For example, removing the sail or lock pillar from the quarter panels could reduce manufacturing operations and tooling cost, and allow for less expensive future face lifts. A preliminary cost study may be necessary.

Advantages

- One Piece - Requires fewer dies. No sub-assembly. Deproliferation of parts.
- Two Piece - Cheaper to make styling changes and maintain one common part.
- Three Piece - Eliminates the need for deep draw operation by eliminating the attached lock pillar. Quarter panel can be stretch formed. Provides for improved material usage. Accommodates styling changes more easily and cheaply.

Disadvantages

- One Piece - Requires larger dies and more time required for construction. Frequently leads to poor material utilization.
- Two Piece - Requires more dies. Requires welding operation and may require metal finish.
- Three Piece - Requires more dies and additional welding and metal finishing.

Manufacturing Concern

If manufacturing accepts a challenge involving a draw or form panel, pick surface data from the clay model and make a proof die to obtain drawability verification. Preliminary funding must be available to accomplish this, so that no time is lost.

Blank and Material Considerations

Product and manufacturing engineers should review the profile of large panels for an early estimate of the shape and size of the blank that will be needed, and evaluate the impact on engineered scrap.

3.12.3 PRODUCT DESIGN CRITIQUE

When product definition has been sufficiently established for the initial product planning to begin, product/manufacturing personnel must concentrate on panel break lines, reverse areas on surface panels, and evaluation of male and female character lines.

Prior to product engineering cross section review meetings, it is imperative that the manufacturing and assembly plant engineers have already accumulated sufficient knowledge regarding previous similar parts. Having this previous panel historical data available enables the engineers to move forward to attain the goal of Continuous Improvement.

The vehicle development group provides preliminary panel cross sections as the vehicle packaging function evolves. This is usually the first opportunity for the manufacturing engineers to see inner panels, structural reinforcements, and bracket configurations, in addition to outer panel flanging ([Figure 3.12.3-1](#)). Each cross section must be evaluated as to formability, material, and the number of operations required to produce a specific panel. Minimizing engineering and manufactured scrap must be a primary function in the manufacturing comprehensive panel analysis. This may mean redesigning problem areas of the part.

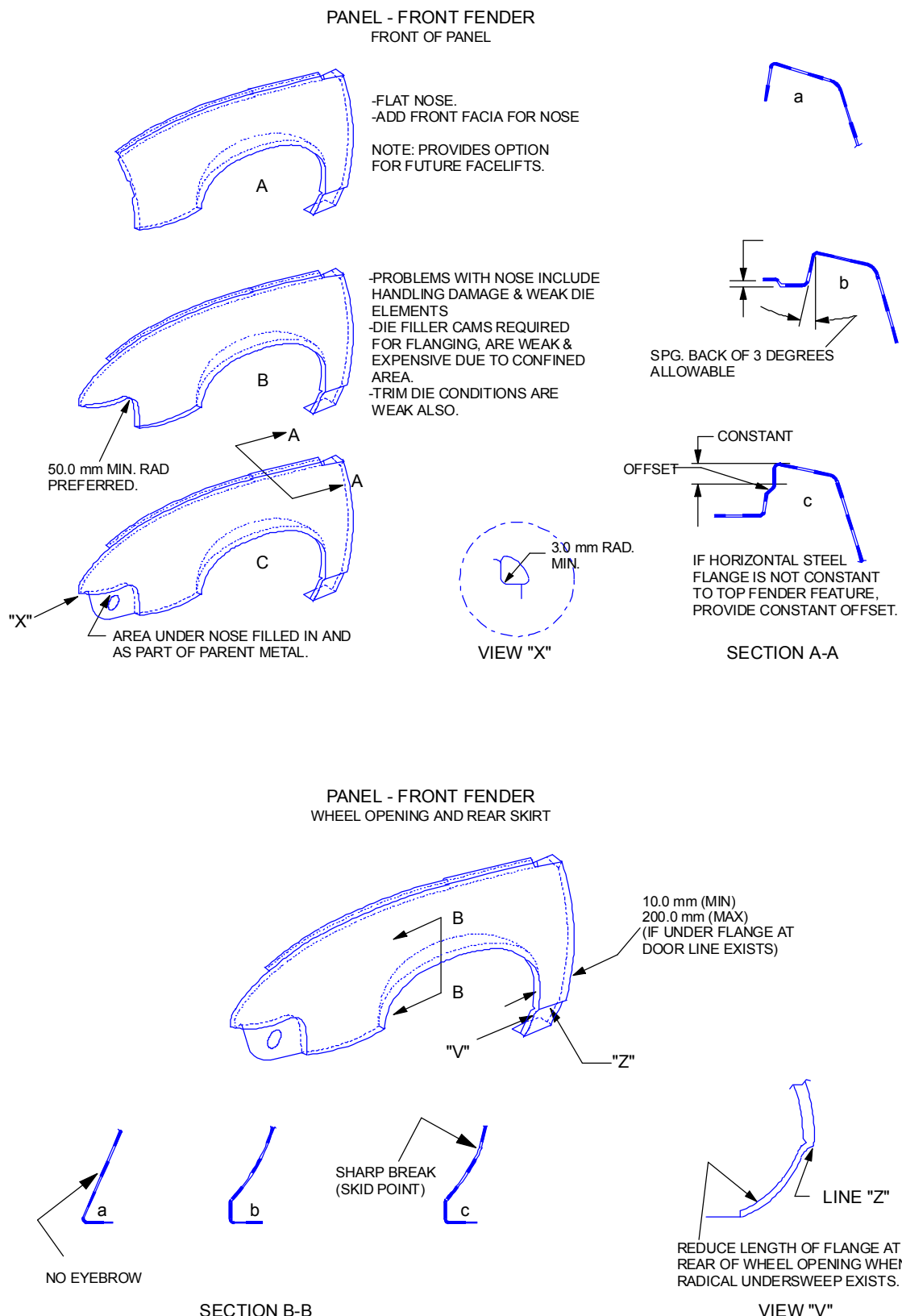


Figure 3.12.3-1 Preliminary panel cross sections

The optimum manufacturing process will provide for the absolute minimum blank size without jeopardizing the panel quality. Engineers must continue to:

- Review the panel design with the product engineer
- Pursue changes that will improve quality and reduce costs
- Estimate the blank size and shape and determine the potential blank nest
- Analyze critical blank nest points with the product engineer.

Knowing part relationship to adjacent components can have a positive influence toward improving material utilization by removing material at critical nest points and adding it to an adjacent part.

A part that will generate excessive engineered scrap (above acceptable level) should be analyzed for manufacturing from a tailored blank.

3.12.3.1 Material

Material thickness is usually based on established norms, classified by family of parts. However, with new materials coupled with new manufacturing and sub-assembly processes, thicknesses are being reduced. Historically, significant thickness variations for common parts have been evident between product groups. Acceptable minimum guidelines for each family of parts may be similar to those listed in [Table 3.12.3.1-1](#).

Table 3.12.3.1-1 Minimum Thickness Guidelines

Family of Parts	Acceptable Minimum Thickness
Outer skins	0.70 - 0.78 mm
Inner panels	0.60 - 1.00 mm
Under body	1.20 - 2.20 mm
Frame and engine cradle	1.80 - 2.20 mm
Brackets	1.80 - 4.00 mm

Variations due to part size, shape and structural analysis may be necessary. As a general rule, the thinnest acceptable gage of material should be used. Note, however, that the use of thinner material can adversely affect formability and may increase tooling cost. Minimum material gage will reduce cost and mass, but will not offset the ratio of engineered scrap.

The type of material selected will be determined by the function of the part. Listed below are several different types of sheet metal that are being utilized today.

- Commercial quality
- High strength
- Work hardenable
- Bake hardenable
- Exposed surface
- Dent resistant
- Killed quality
- Drawing quality
- Dead soft
- Lock forming quality

Processed sheet steel is obtainable as:

- Hot rolled sheet steel
- Cold rolled sheet steel
- Hot-dipped galvanized (two sides) steel
- Electrolytic zinc, zinc-iron alloy and zinc-nickel alloy coated steel

3.12.3.1.1 Tailor Welded Blanks

Tailor welded blanks may be beneficial in terms of material utilization and possibly eliminate reinforcements by using a heavier gage material where required ([Figure 3.12.3.1.1-1](#)).

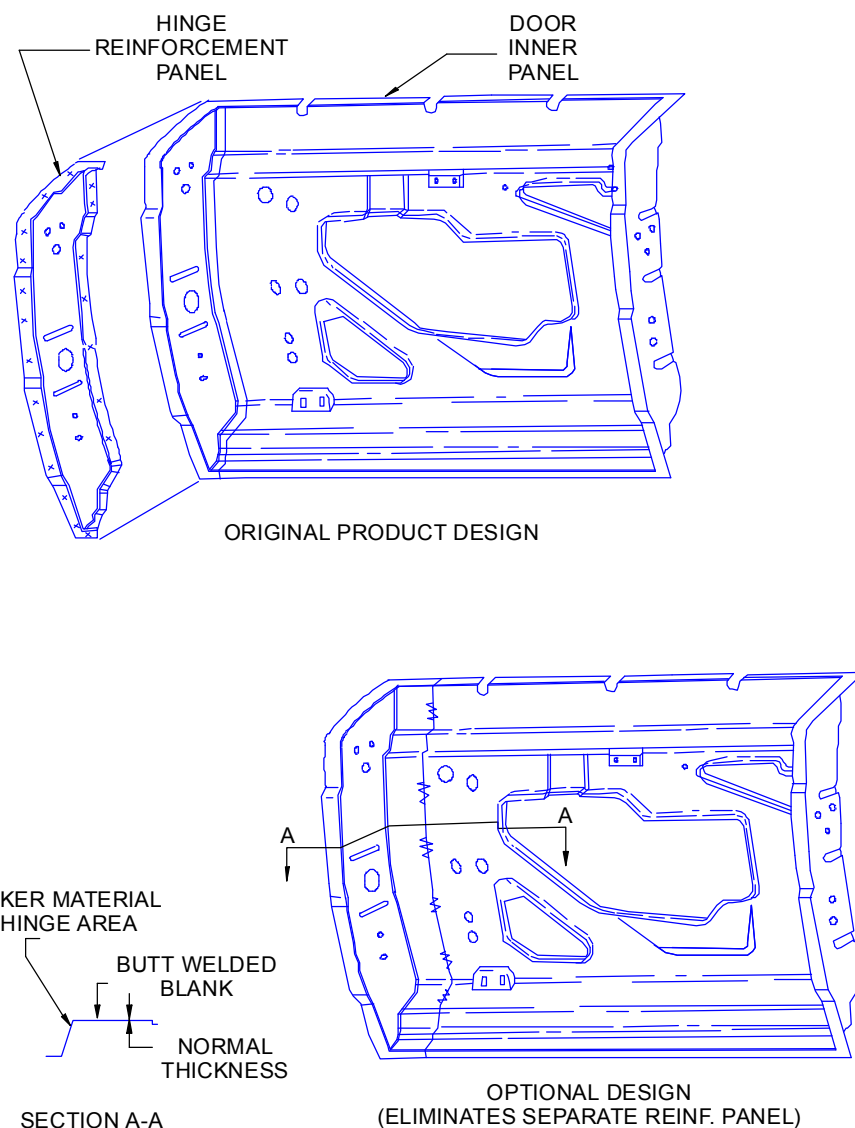


Figure 3.12.3.1.1-1 Example of a welded blank for a door inner panel. (Two different material thicknesses were used to avoid the door hinge reinforcement.)

Welded blanks should be considered when there are advantages over one piece blanks, as in the following situations:

- The welded blank may cost less than an equivalent one piece blank, because the configuration of the blank may not lend itself to efficient blank nesting and thereby generate excessive engineered scrap.
- Stock for a welded blank may be more readily available than stock for an equivalent one piece blank if the coil size exceeds 72". This may result in a premium cost to the customer.
- The blank may have a shape that would waste more material if it were made in one piece instead of being welded. Sometimes material can be saved by welding projecting portions, such as tabs and ears.
- The welded blank may reduce the cost of stamping and assembly tooling. Flat or simple shapes are welded in a layout designed to avoid the presence of seams in certain areas of the blank (may allow the use of automatic welding equipment). Placement of weld joints may be critical to formability, die function and die maintenance.

For a fuller discussion of tailor welded blanks, refer to [Section 3.9.1](#).

3.12.4 MANUFACTURING ENGINEERING PRE-PROCESSING

Simultaneously with the panel familiarization period, additional support data must be gathered that will assist in early pre-process planning. When the panel is believed to be manufacturable, pre-processing can begin. The sheet metal manufacturing engineer has the responsibility of specifying the necessary equipment, such as dies, welders, presses and automation, to perform an operation or series of operations to produce a part. However, the equipment available should never determine the selected process. The best process should be determined by cost and quality. Then the production plant can be selected that has the equipment available to utilize this state-of-the-art process.

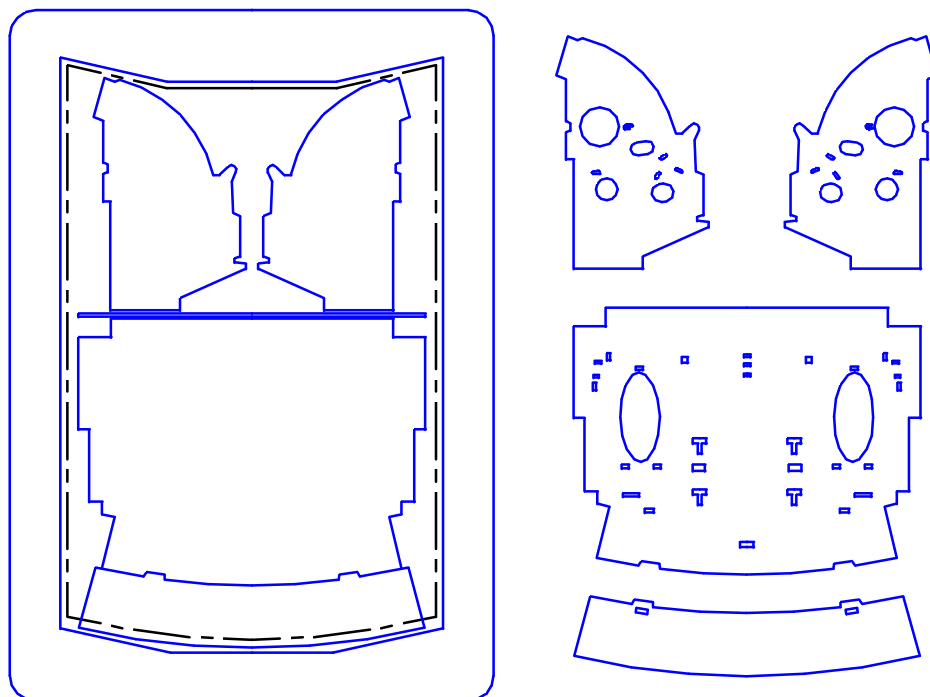
In general, when establishing pre-processing tooling requirements, some factors should be studied individually and relative to other factors. For example, the number of operations in a progressive die, press line, or transfer press operation should never be decreased because of equipment availability or a management mandate specifying a stated not-to-exceed number of operations. Reducing the number of operations (hits), after the product design has been established and the optimum process determined, has proven to be false economy in the long term. Design for manufacturing will assist this process.

3.12.4.1 Pre-Process Criteria

Some criteria for determining the pre-process selection:

- Does panel/process create usable engineered scrap?
- Can the part be produced from available engineered scrap?
- Can the part be produced from engineered scrap simultaneously during another primary part operation?
- Can the part be made from a developed blank? This type of a blank is the most cost effective for material utilization. (It requires no trim operation and generates the least amount of engineered scrap.)

- Is a draw operation required?
- Can material be totally locked out?
- Can the part be manufactured simultaneously with a dissimilar part or parts? ([Figure 3.12.4.1-1 A,B](#))
- Does panel require proof tooling?
- Is full or partial trim required?
- Can critical nest points be revised to improve the blank nesting? ([Figure 3.12.4.1-2](#))
- Can the part be made double (two parts tied together or one right and one left hand part joined together)? ([Figure 3.12.4.1-3](#))
- Should the panel be designed as one piece or multi-piece structure? ([Figure 3.12.4.1-4 A,B](#))
- Was a tailor welded blank considered?
- Can holes be pierced in blank or trim die?
- Is redraw or restrike operation required?
- Have break lines, character lines, key, door handle and fuel opening depressions been analyzed?
- Have all sharp corners been eliminated?



(A) Draw die cavity shows 4 parts tied together and drawn simultaneously

(B) Drawing shows 4 parts completely finished & separated

Figure 3.12.4.1-1 Parts manufactured simultaneously

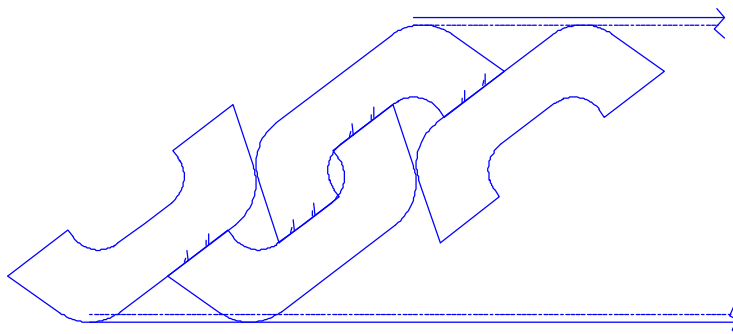


Figure 3.12.4.1-2 Example of nipping off corners of blank/part to reduce coil size

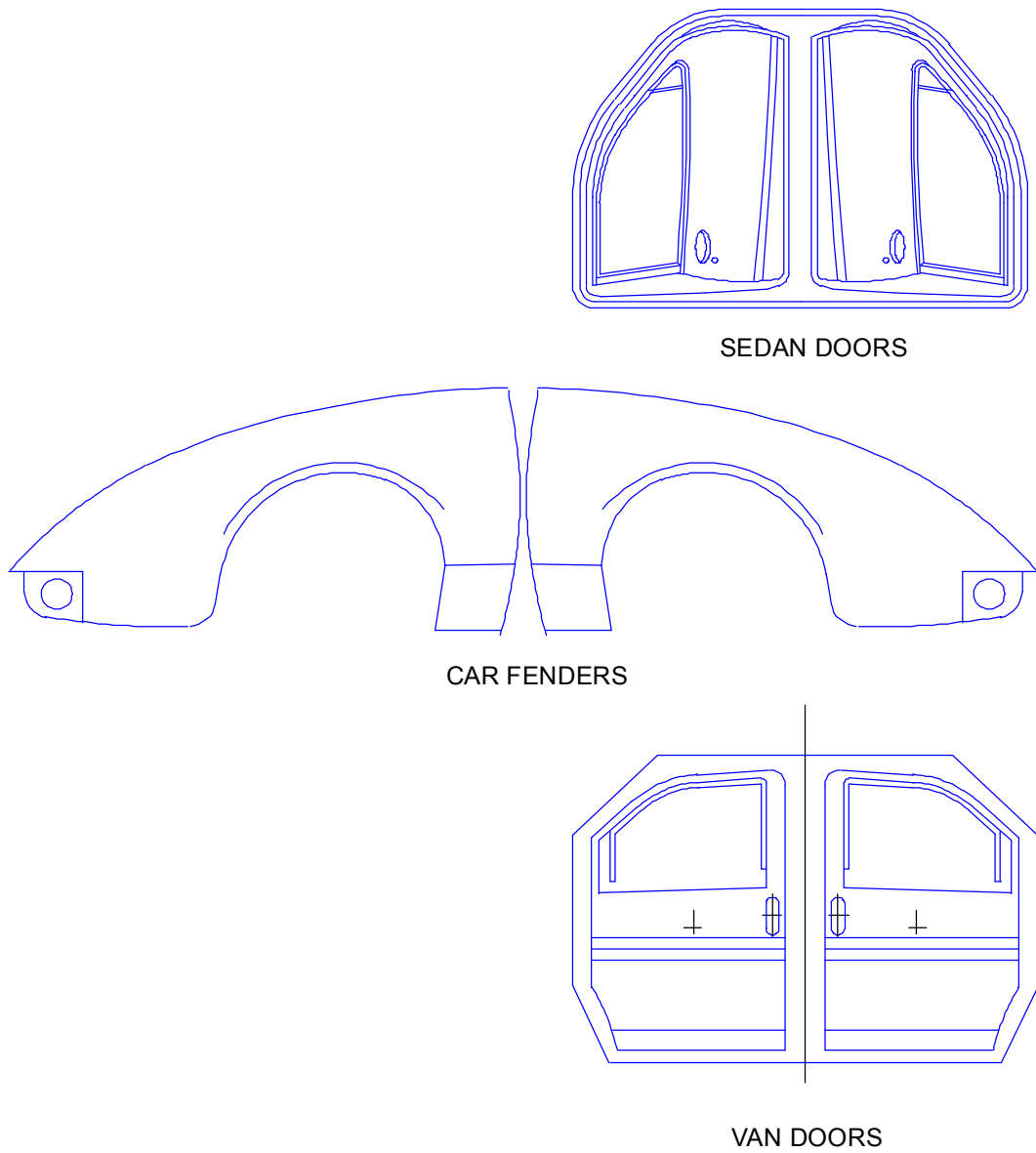
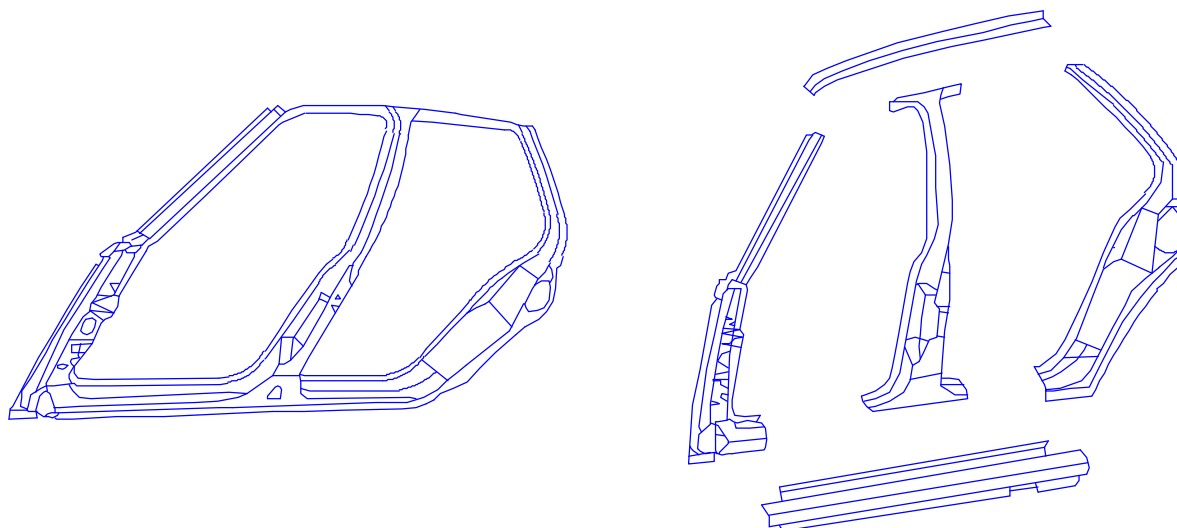


Figure 3.12.4.1-3 Double attached parts



ADVANTAGES

- Combines several stampings into one
- Reduces die requirements
- Eliminates weld-fab operations
- Simplifies assembly operations
- Improves dimensional quality
- Potential tooling cost reduction
- Reduces floor space required
- Reduction in wind noise and water leak potential
- Part deproliferation

ADVANTAGES

- Individual stampings are easier to form
- Reduces tooling lead time required for restyling
- Detail stamping dimensional quality easier to control
- Material savings potential
- Engineering changes are easier to implement
- Sheet metal press flexibility
 - Smaller press/less tonnage required
 - Smaller/lighter part handling equipment required
 - Transfer and progressive presses compatible
- More flexible for different model uses

DISADVANTAGES

- Requires longer lead time for tooling (extensive die tryout)
- Reduces the flexibility of press assignment. Requires larger presses, more tonnage and part handling problems
- Engineering changes for dies are more difficult and time consuming
- Product & process engineering must be accurate and complete at early stages
- Restricts material selection for design
- Increases engineering scrap

DISADVANTAGES

- Requires more component part handling
- Requires more difficult and costly assembly & fabrication operations (labor cost)
- Wind noise and water leak potential
- Possible material scheduling problems
- Dimensional stack up problems
- More checking fixtures are required

Figure 3.12.4.1-4 Single vs. multipiece

3.12.4.2 Influencing Factors

Functions that influence the pre-processing tooling requirements are:

- Type of dies
- Number of operations
- Size of part
- Production rate
- Part handling (automation)
- Disposal of scrap/slugs
- Draw die bead selection
- Engineered scrap handling
- Press requirements
- Development tooling
- Design life of part
- Annual volume
- Type of draw die
- Material utilization

3.12.4.3 Types of Dies

Determining the proper die selection is extremely important before establishing preprocessing requirements. Some die options are listed below.

- Blank Die (1 per strike/2 per strike)
- Compound blank and pierce die
- Progressive notch, pierce, and cutoff blank die
- Progressive die to make part complete (utilized to manufacture brackets and reinforcements)
- Line dies with pick and place automation
- Line dies with manual or semi-automatic operation
- Transfer die with die mounted transfer
- Transfer die with press mounted transfer
- Transfer press with lead off toggle operation
- Transfer press with coil feed equipment or automatic blank feed automation
- Draw die (toggle, stretch form, lock stretch self contained)
- Form die (with or without developed blank)
- Trim die (or trim and pierce die)
- Flange die (or return flange die)
- Pierce die
- Cam die
- Redraw die
- Coin die
- Restrike die
- Pre-form die

- Pre-draw die
- Multi-slide tooling

3.12.4.4 Pre-Process Proof Die Planning

Although computerized methods are being developed, proof tooling coupled with the third party specialist review process, is still critical to achieve the maximum material utilization with the optimum manufacturing process.

For example, investigating the possibility of making a panel double (two parts tied together) ([Figure 3.12.4.4-1](#)), the proof die provides an excellent opportunity to try out two different ideas. One proposed development can be engineered on one side of the kirksite die, while another idea can be developed on the opposite side of the lead die. When complete, all features can be examined and the best solution selected.

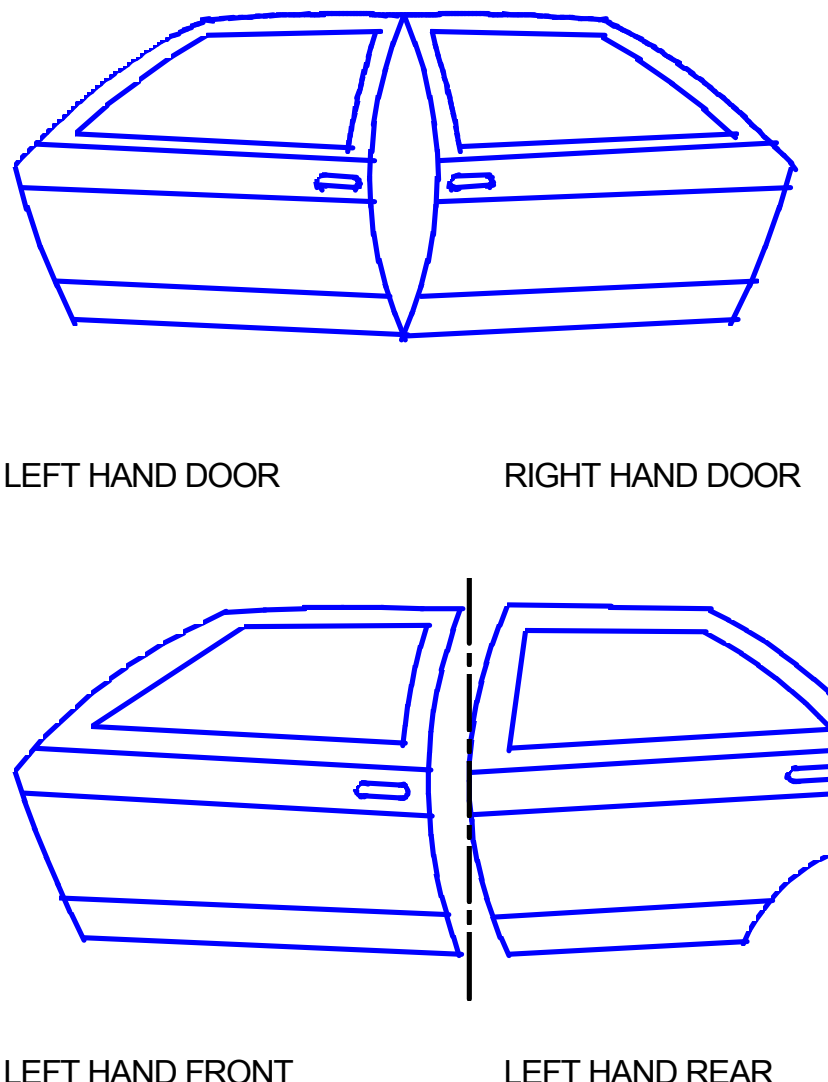


Figure 3.12.4.4-1 Investigating a panel double in a proof die

3.12.4.5 Proof and Prototype Defined

Proof tooling and prototype tooling are two distinctly different sets of tools, scheduled at different times for different intended purposes. Proof tooling is used for verification of panel manufacturability. It is essential that it be representative of the production tooling, including panel setup, die action, binder ring shape, and punch opening. It is often used to produce prototype parts, but this is not the primary function. The prototype die often uses a flat die ring and produces only the basic panel shape. The panel may be finished by hand to obtain the desired part. Hence, prototype dies may give no assurance that the conditions evaluated are suitable for manufacturing. Therefore the prototype part may not be truly representative of the manufacturing process.

3.12.5 PROOF DIE DEVELOPMENT VERIFICATION

Kirksite proof draw die tooling offers the advantage of knowing that the production process will be successful and that a panel redesign will not be required after the production tooling has been completed. It is a powerful tool in the quest for improved panel quality and should be used to the maximum extent possible. Accurate early blank configuration can be determined with engineered kirksite draw die gaging. Thus, blank configuration can be accurately determined, permitting engineered blank nest analysis (examination of critical nest points) very early in the program. It also permits a very systematic approach to developing the proper bead selection for the draw die, possibly utilizing total sheet metal lockout, which provides optimum panel quality with a minimum size blank.

When should the engineer decide to utilize a proof die? Opponents say it should only be done on a selective basis, such as:

- When the new panel is considerably different from any previous panel.
- The severity of the panel shape is a concern.
- If there are changes in dimensional requirements.
- A different material is being contemplated.

Proponents say it should be used for all major stampings that require a draw die application and all other parts where manufacturability is a concern. Product engineering always requests that early prototype parts be made, so why not use the manufacturing process, with relatively inexpensive soft tooling, to furnish the product personnel with parts that are representative of the product design intent.

3.12.5.1 Advantages and Disadvantages of Proof Dies

A summary of the advantages and disadvantages of utilizing the proof tooling approach to determine early processing requirements are:

Advantages

- A proof die provides an early evaluation of the formability of the panel and, with proper program timing, allows modifications to be made to both the product design and manufacturing process, prior to production die design.
- It is the most cost effective and timely means of proving panel formability and process capabilities, as opposed to making revisions to the hard (production) dies. During

primary tryout of the production dies, timing constraints usually do not provide for time consuming modifications to be made to either the panel or the dies.

- The manufacturing engineer is provided with early determination of die pressure requirements (usually nitrogen).
- Blank configuration and blank nesting can more accurately be determined.
- Accurate and engineered draw die gaging can be developed to minimize the blank size.
- The best selection and location of the die beads can be determined, for attaining optimum panel quality with minimum steel requirement.
- Material selection can also be evaluated early in the program. Part structural or quality improvement modifications can be made to the material, the product design or the manufacturing process.
- Prototype parts for the product engineer can be obtained from the proof tooling source. These costs can be shared by both the product and manufacturing groups. These parts will accurately depict the product design intent. There will be no welding, heating or hammer forming of the product panel, because these metal forming methods are not representative of the design intent. Prototype parts are always required, so why not always build a proof die.
- A proof die allows for early circle grid analysis of the drawn stamping. Incremental draw depth panels (breakdown panels) are available to resolve formability problems. Binder shapes can be modified quickly and inexpensively to the soft kirksite die.
- It provides reference panels, to be utilized when analyzing possible hard die problems.
- The production press equipment selection is verified. It is an absolute must that the kirksite die be tried out in a press that very closely simulates the actual production press for ram speed and press tonnage.
- Soft die tooling can be provided for questionable secondary operations. (Example: Hood and fender curved splitline.)
- Critical last minute tooling or product changes are avoided, thereby enabling the tight timing schedules to be maintained.
- Different draw concepts can be tried on panels that are tied together and made double.

Disadvantages

- It causes additional tooling cost (shared with prototype part cost).
- Additional time and manpower are required to participate in the program. (Rebuttal: it is better to spend the time at the beginning of the project than at the ever-critical program conclusion.)
- Storage of reference panels can create space problems.
- The fact that the proof die must be tried out in a mechanical press, simulating the actions of the production plant press. This can present a problem to most proof die construction sources. It may necessitate the transfer of the proof die to another source for tryout, perhaps the actual production plant. Failure to try out this die in the proper press can lead to erroneous conclusions about the ability of the die shape and material to produce a quality stamping.

3.12.6 DRAW DIES

During the pre-process phase of the program, the selection of the proper draw die (beginning with the proof die program) is extremely critical to minimize the material requirements to develop and manufacture a quality panel. Also, paralleling the selection of the proper draw die is the importance of determining the correct draw die bead and accurate (engineered) draw die gaging of the blank. This enables establishment of accurate material cost by developing a very accurate blank, examining the critical nest points (for possible revisions) and determining the optimum blank nest. It absolutely ensures the manufacturability of the panel.

3.12.6.1 Types of Draw Dies

During the analysis of the draw die selection process, the manufacturing engineer should be aware of the great advantage of the four piece draw die. It allows for easy adjustment in the draw depth of the panel, which could result in a smaller blank, if the depth of draw can be reduced.

1. The lock stretch form die ([Figure 3.12.6.1-1](#)) is a three piece die that utilizes a toggle press, without nitrogen, and provides for total material lockout. This die is restricted to panels with soft profiles and shallow draw depth (maximum 4").

Typical Applications

- Fenders
- Door Outer
- Quarter Panels with separate door lock pillar
- Hood Outer
- Truck Cab Backs
- Deck Lids
- Roofs

Positives

- Low engineered scrap
- Best overall surface stretch and panel rigidity
- Clean-up of blank surface distortion (wrap buckles)
- Clean draw operation - no metal movement through beads or off binder
- Most computer-development friendly
- Minimum construction cost and lead time
- Lowest die maintenance
- Low noise level and press shock

Negatives

- Punch galling: requires heat treatment or chrome plating
- Difficult control of male character line skid
- Limited reverse draw ability
- Panel will require turnover automation
- Punch cannot assist in wrapping (unless specially designed)
- Restricted as to press type and location
- Slower press cycle time (toggle press)

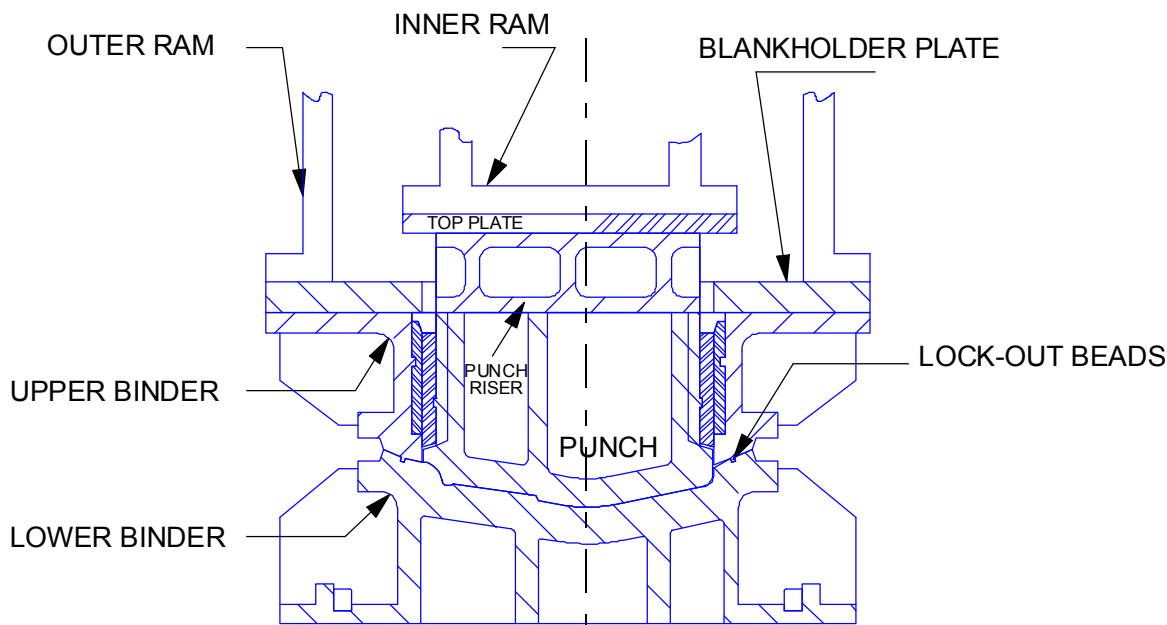


Figure 3.12.6.1-1 Lock stretch form die (toggle type) total material lockout

2. The lock stretch form die ([Figure 3.12.6.1-2](#)) is a four piece die that utilizes self-contained nitrogen floating lower binder and provides for total material lockout.

Typical Applications

Same as lock stretch form die, toggle, (1)

Positives

Same as lock stretch form die (1), plus

- No panel turnover required
- Punch can assist wrapping
- Faster press cycle time (no toggle press)
- Easy to revise draw depth

Negatives

Same as lock stretch form die, toggle (1), plus

- Increased construction cost and lead time
- High press tonnage required early in press stroke
- High noise level and greater shock on press and die
- Nitrogen system requires additional maintenance

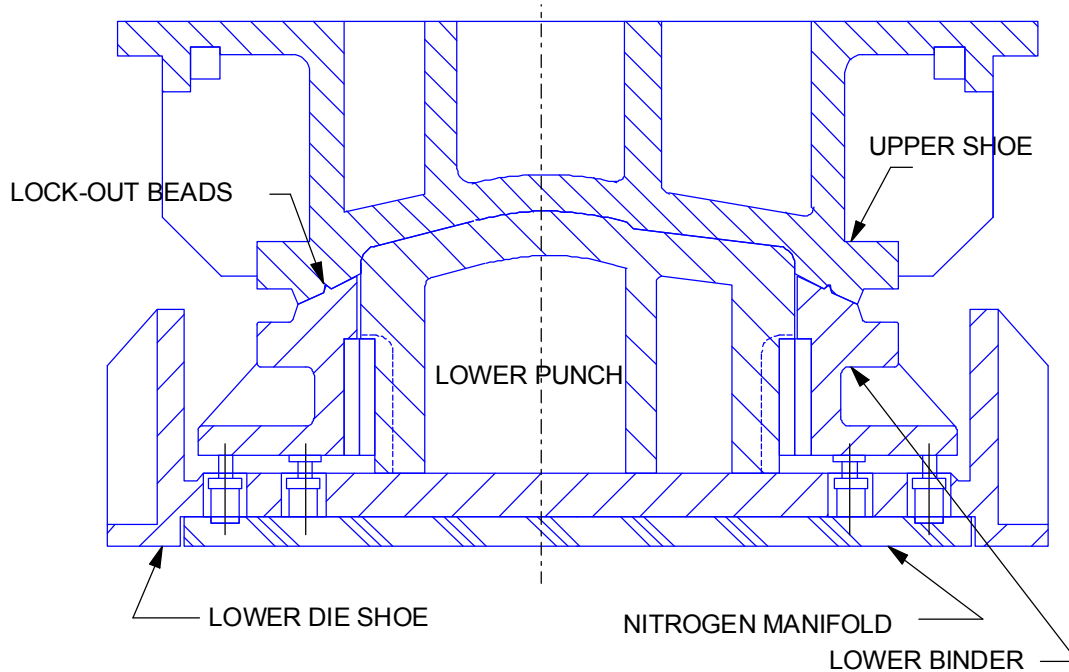


Figure 3.12.6.1-2 Lock stretch form die (nitrogen self-contained) total material lockout

3. Draw die, a four piece die that utilizes self contained nitrogen floating lower binder and provides for controlled material flow.

Typical Applications

Most large panels that require a draw binder, controlled material flow and assigned to transfer or pick and place automated press line.

Positives

Same as lock stretch form die, nitrogen (2), plus best press location and type of press flexibility

Negatives

Identical to lock stretch form die, nitrogen (2)

4. Draw die, a three-piece die that utilizes a toggle press, without nitrogen, and provides for controlled material flow.

Typical Applications

All large panels that require a draw binder, controlled material flow and assigned to a transfer or pick and place press line with a lead off toggle press.

Positives

- Low noise level and press shock
- Reduced construction and lead time
- Greater flexibility for depth of draw

Negatives

- Restricted press location and press type
- Requires panel turnover automation
- Punch cannot assist in wrapping the panel unless specially designed
- Limited reverse draw ability
- Slower press cycle time (toggle press)

5. Stretch draw die, a four piece die that utilizes a toggle press with a self-contained nitrogen floating lower binder and provides two-stage controlled material flow.

Typical Application

Most large panels that require a draw binder, controlled material flow, reverse draw requirements, and assigned to transfer or pick and place press line with a lead-off toggle press.

Positives

- Greater flexibility for reverse draw
- Low amount of engineered scrap
- Panel turnover not required
- Greater overall surface stretch and panel rigidity
- Punch can assist in wrapping panel

Negatives

- Slower press cycle time (toggle press)
- High tonnage required early in press stroke
- Noise level and press shock are high
- Increased die maintenance
- Highest construction cost and lead time requirement
- Limited depth of draw
- Restricted press location and press type

Refer to [Table 3.12.6.1-1](#) for a comparison of form/draw operations.

Table 3.12.6.1-1 Rating Matrix for Form/Draw Operations

ATTRIBUTES	TYPE OF FORM/DRAW OPERATION				
	LOCK STRETCH FORM DIE (Self Contained Type)	LOCK STRETCH FORM DIE (Toggle Type)	DRAW DIE (Self Contained Type)	DRAW DIE (Toggle Type)	STRETCH DRAW DIE (4) PIECE (Toggle & Self Contained Type)
BEST MATERIAL UTILIZATION	1	2	4	5	3
MOST PRODUCT FRIENDLY	1	3	2	4	5
HIGHEST OVERALL QUALITY	1	2	3	4	5
MOST UNIVERSAL APPLICATION	5	4	3	1	2
LOWEST TOOLING COST	3	1	4	2	5
LOWEST DIE MAINT.	2	1	3	4	5

NOTE: Comparing Rating Matrix: 1=Best, 5= Worst

3.12.6.2 Die Beads and Material Flow-Lockout

This section is devoted to the application of die beads and metal restrictors in a draw or form die. Die beads should be utilized to capture maximum material savings, while maintaining control of material flow to attain optimum panel quality. Two basic bead applications will be discussed. They are:

- Total material lockout and gripper bead styles, which are normally applied when panel draw depths are moderate to shallow and possess few if any male styling features. Total sheet metal lockout is the most economical way to produce panels, by minimizing sheet metal material requirements. By design, stretch formed or drawn panels are of the highest quality while minimizing die maintenance due to restricted metal flow. There are one or two other types of lockout beads available.
- Material flow bead styles, which are applied where draw depths are severe enough to indicate that sheet metal flow off the binder is inevitable. This type bead is often accompanied by one or two additional secondary beads.

There are approximately six variations of bead styles and combinations that will be discussed briefly ([Figure 3.12.6.2-1](#)).

1. Single male bead (squared style) uses the least material in performing its single bead function and is recommended as the best primary bead to use.

2. One male bead and one male or female secondary bead. The secondary bead is applied only when absolutely necessary.
3. One male bead and two male or female secondary beads.
4. One small male or female bead set outboard of the punch opening.
5. Two male or female beads set outboard of the punch opening.
6. Single male bead, radius style. Due to the large radius this bead uses more material.

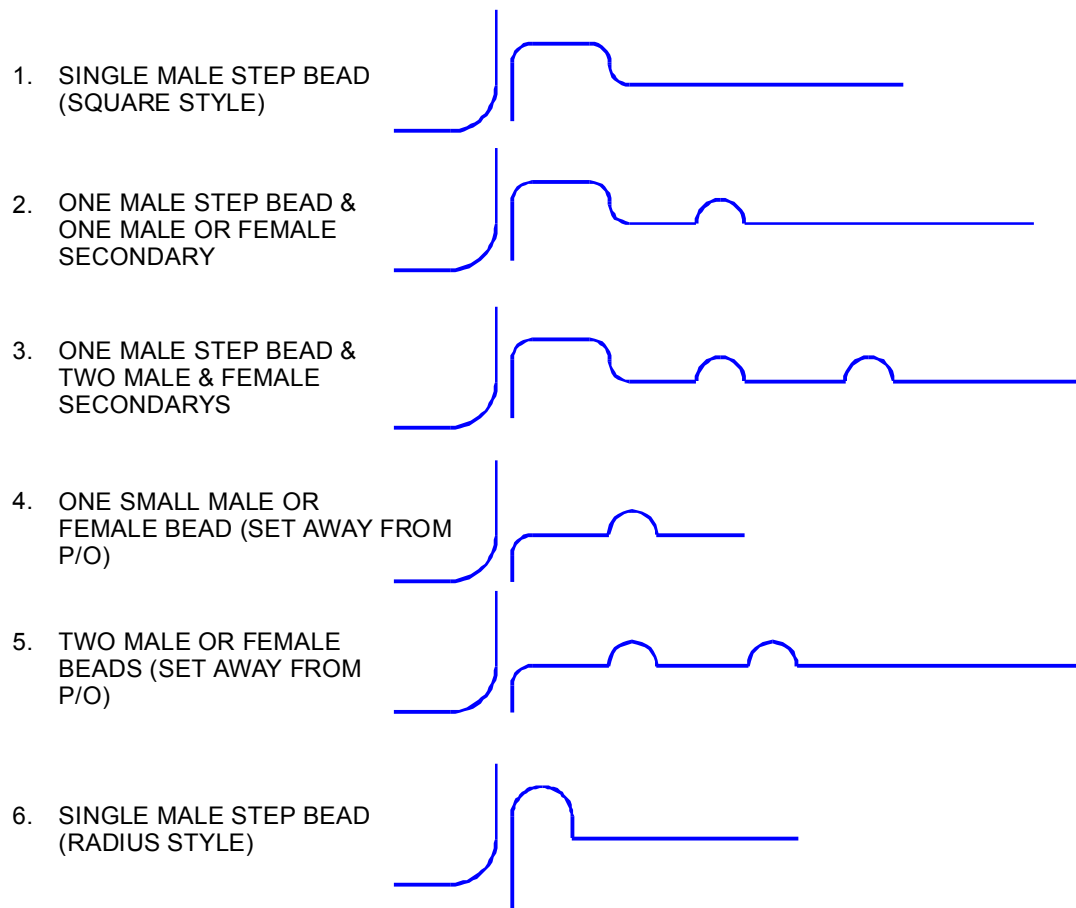


Figure 3.12.6.2-1 Metal flow bead styles

3.12.7 CIRCLE GRID ANALYSIS

Circle grid analysis is a technique used during the proof die tryout. Review of the grids can determine potential problem areas where strain exceeds an acceptable limit. A typical grid pattern shown in [Figure 4.1.5.3-1](#) is etched on to the flat blank surface. After the proof die is cycled in a mechanical press with this blank, the drawn panel can be analyzed for the amount of stretch at each individual circle. Breakdown panels can also be checked by varying the different depths of draw in perhaps one inch increments, until the draw punch is on the bottom of the die cavity. The amount of strain at each circle is determined by comparing the major and minor diameters of the ellipses with the original circle diameter ([Figure 4.1.5.3-2](#)). The major diameter of the ellipse is always larger than the initial circle diameter, so that major stretch is always positive. The minor diameter may be greater or less; minor stretch may thus be either positive or negative.

Also, the assigned steel source will usually provide a service that utilizes ultrasound equipment that will detect material strain.

For additional information on Circle Grid Analysis see [Section 4.1.5.3](#).

3.12.8 FORMING LIMIT DIAGRAM

The forming limit diagram is derived from the circle grid analysis to provide useful information to die designers, part designers, and steel suppliers. The percent of major and minor strain is plotted on a forming limit diagram shown in [Figure 4.1.5.4-1](#). That particular illustration applies only to low carbon steel (1.0 mm thick). Positive minor strain allows for some increase in strain, whereas negative minor strain will permit a substantial increase in strain.

When areas of failure or potential failure are observed, adjustments can be made to binder pressure, increase radii, die beads, lubrication, or increase in sheet metal thickness. It is mandatory to ensure that all points fall safely below the marginal zone, so that process changes such as die wear, material lubrication, and changes in sheet metal chemistry will not shift any points into the marginal zone.

For additional information on the forming limit diagram see [Section 4.1.5.4](#).

3.12.9 OPTIMIZING BLANKING EFFICIENCY

The most efficient, cost effective blank is the developed blank that produces a finished part with no trimming operation required. This type of blank is possible when the part shape is simple, with little compound curvature, and possesses simple flange break lines. Developed blanks are primarily used to manufacture black metal parts such as heavy metal frame or engine cradle parts. The part raw edges must have increased tolerances for flange length to avoid a finish trim die operation.

Some lighter gage sheet metal parts are candidates for developed blank consideration such as windshield pillars, and roof bows. Simple brackets and reinforcements should be evaluated, especially if tolerances can be increased in non-critical areas. However, most body sheet metal panels (body in white) require binder control due to their severe shape and must be drawn to achieve an acceptable panel. In those cases the draw development (proof die) offers the first indication of blank configuration so that preliminary blanking plans can be formulated. Remember that coil widths exceeding 72" may result in a premium cost (penalty). Once the rough blank outline is known, an engineering blank nesting review process must be performed.

3.12.9.1 BLANK CONFIGURATION AND NESTING

The decision as to which type of blanking system to implement sometimes proves difficult. Several options are usually available; each may be attractive, yet a clear cut direction is not obvious. Each option must be reviewed, and the most cost effective system must be established. The manufacturing engineer may have to solicit assistance from other groups to establish a reliable cost analysis.

Examples of the various blank producing options and general blank considerations are provided on the pages that follow.

1. Square sheared blank ([Figure 3.12.9.1-1](#)) requires the most basic blank production equipment, normally a general purpose cutoff die.

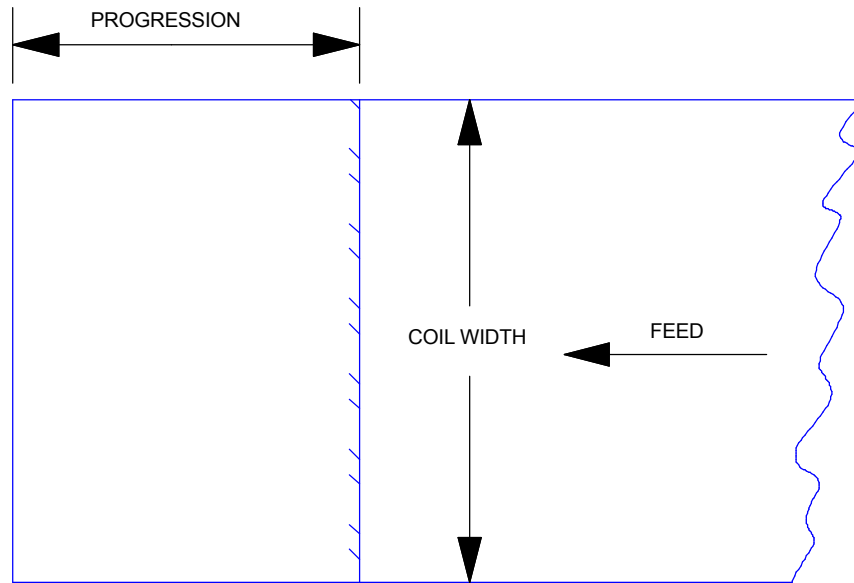


Figure 3.12.9.1-1 Square blank (one per stroke)

2. Trapezoidal blank - two per stroke ([Figure 3.12.9.1-2](#)). This blank requires a specific blank die dedicated to the blank shape.

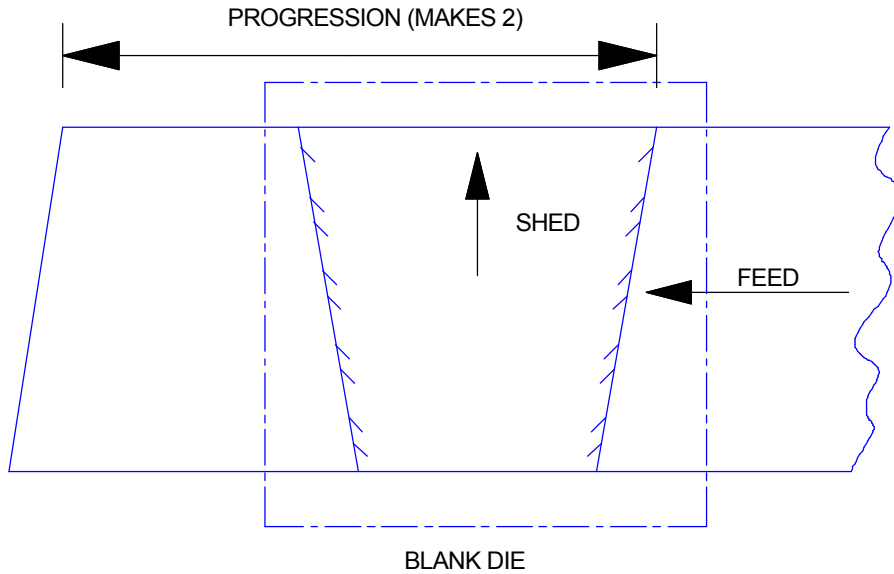


Figure 3.12.9.1-2 Trapezoidal blank (two per stroke)

3. Chevron style blank ([Figure 3.12.9.1-3](#)) is generally used for hood inner and outer panels, and requires a specific dedicated die. To achieve this common cutline, the nose and cowl of the panel must be somewhat compatible.

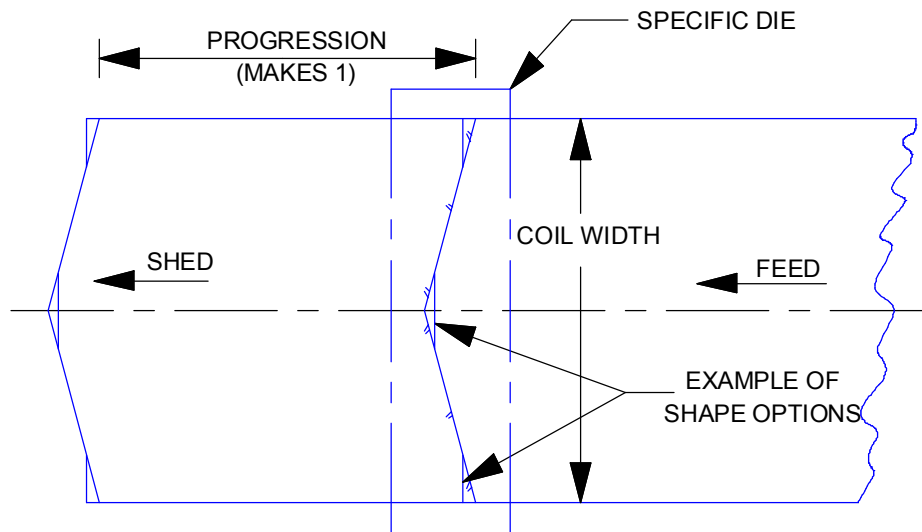
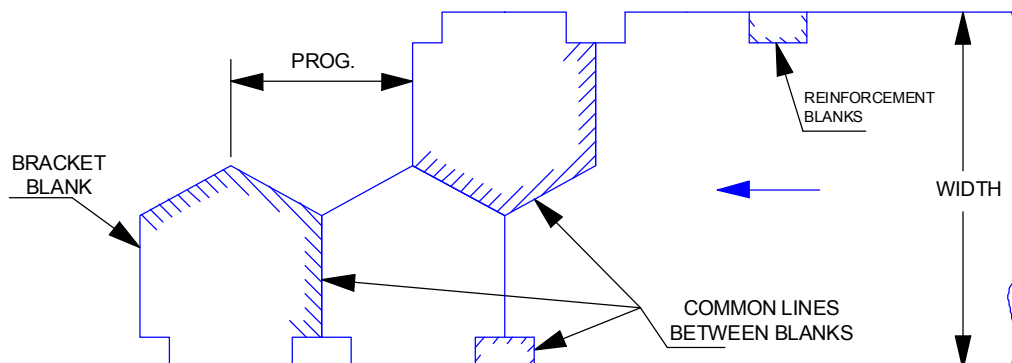


Figure 3.12.9.1-3 Chevron shape cut (one per stroke)

4. Nested blanks - two per stroke ([Figure 3.12.9.1-4](#)). Illustrations indicate no pre-cutting or notching exists. All blanks that indicate a close nest potential should be analyzed for every nesting possibility. The engineer should explore all rotational combinations, with the obvious goal to achieve the least number of square inches used. Strive for common cutlines to eliminate the material web.



100% TOTAL MATERIAL UTILIZATION:
COMMON LINE NESTING: THE WEB SHOULD BE ELIMINATED
WHEREVER POSSIBLE TO REDUCE STOCK USAGE. COMMON LINE
NESTING, SHOWN IN THE ADJOINING ILLUSTRATION, SHOULD
BE APPLIED WHEREVER POSSIBLE.

Figure 3.12.9.1-4 Nested blanks (two per stroke)

5. Nested blanks with progressive precutting ([Figure 3.12.9.1-5](#))

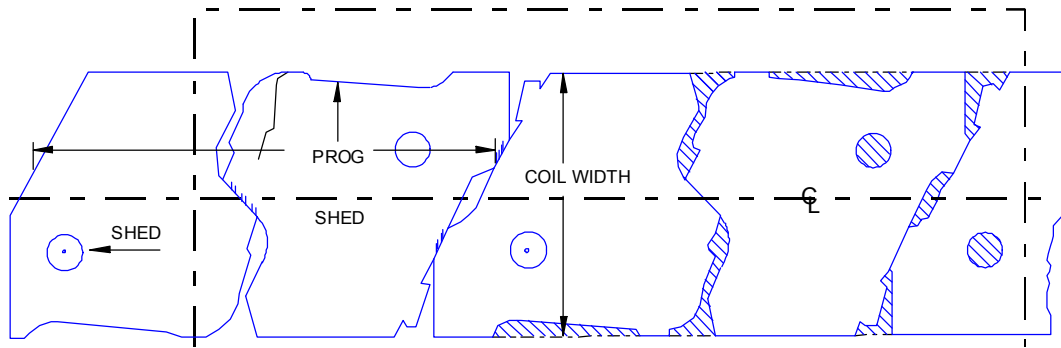


Figure 3.12.9.1-5 Multiple part blanking (progressive cuts)

6. Multiple part blanking ([Figure 3.12.9.1-6](#)). Each part that is being blanked must have a sub-die. This makes it possible to remove a sub-die and blank one specific blank from virgin steel, should a shortage of a specific blank occur. This type of blanking operation is desirable for reducing labor costs per piece and increases material utilization. In addition, it minimizes handling and die sets.

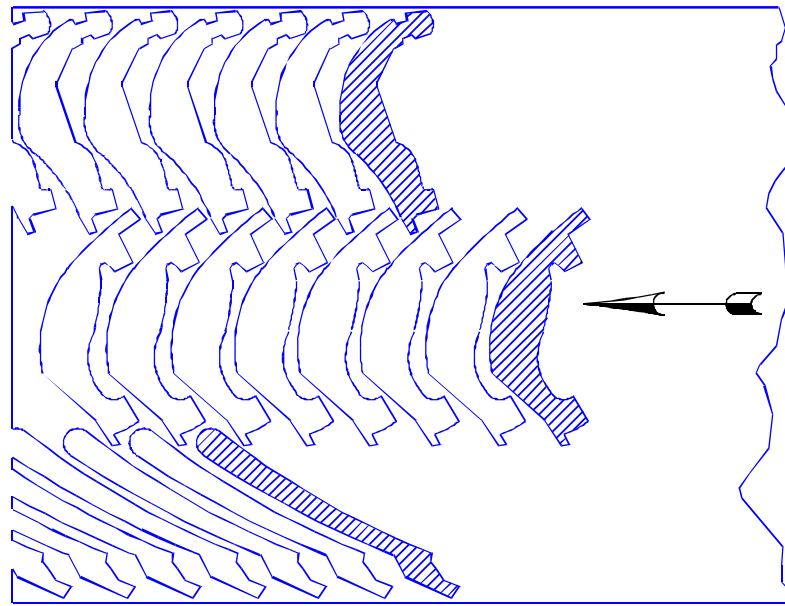


Figure 3.12.9.1-6 Multiple part blanking (three separate nests combined)

7. Compound blank and pierce die. ([Figure 3.12.9.1-7 \(A\)](#)) This type of die is used when the outside perimeter and the relationship of interior holes or other configurations must be guaranteed repeatable. All cuts are made simultaneously. This type of die more accurately maintains this relationship than does the progressive notch, pierce and cutoff die. ([Figure 3.12.9.1-7 \(B\)](#) illustrates typical compound blank and pierce part.)

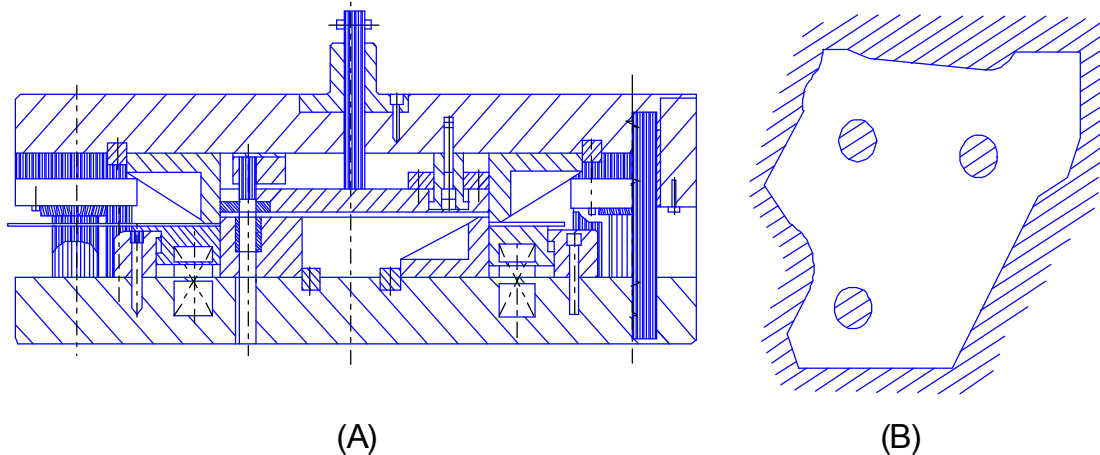
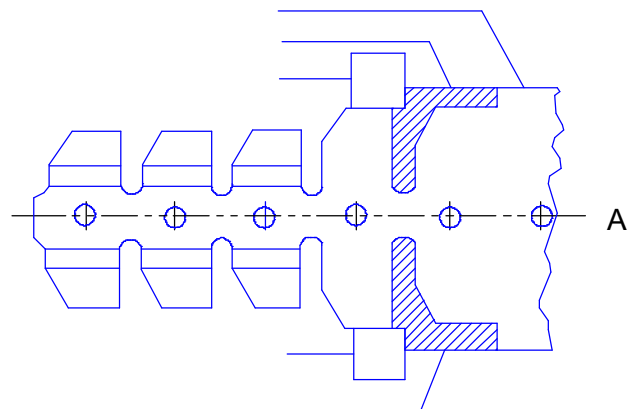


Figure 3.12.9.1-7 Compound blank & pierce part

8. Progressive die nesting ([Figure 3.12.9.1-8 A](#)) The beginning of a progressive die sequence is a cutting operation to isolate the part configuration. This will allow forming operations to progressively take place. With the coil edge blank die a significant reduction in coil width is achieved, thereby reducing piece cost. When the coil edge becomes the edge of the part, tolerances must increase to accept the variation in coil width ([Figure 3.12.9.1-8 B](#)).

A NOTCHED EDGE ON ONE OR BOTH SIDES OF THE COIL CAN BE USED IF A QUALIFIED EDGE IS NECESSARY. THIS TECHNIQUE MAY BE MORE ECONOMICAL THAN PAYING THE EXTRA CHARGE FOR A CUT OR SLIT EDGE.



STRIP EDGE USAGE: THE COIL OR STRIP WIDTH CAN BE REDUCED BY USING THE MATERIAL EDGE TO ESTABLISH THE BLANK AND PART EDGE. HOWEVER, THE ADVANTAGE SHOULD BE CAREFULLY COMPARED WITH THE POSSIBLE INCREASED MATERIAL COST FOR A CUT EDGE.

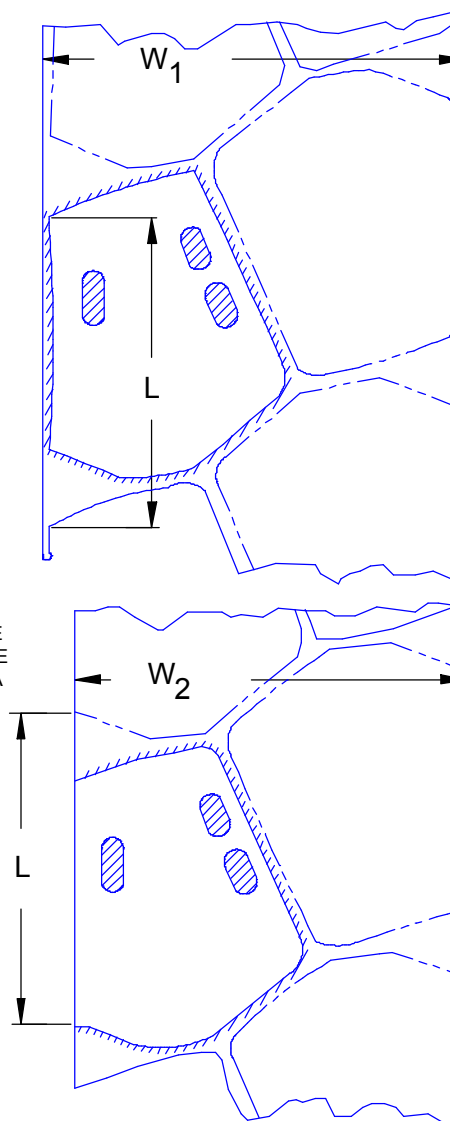
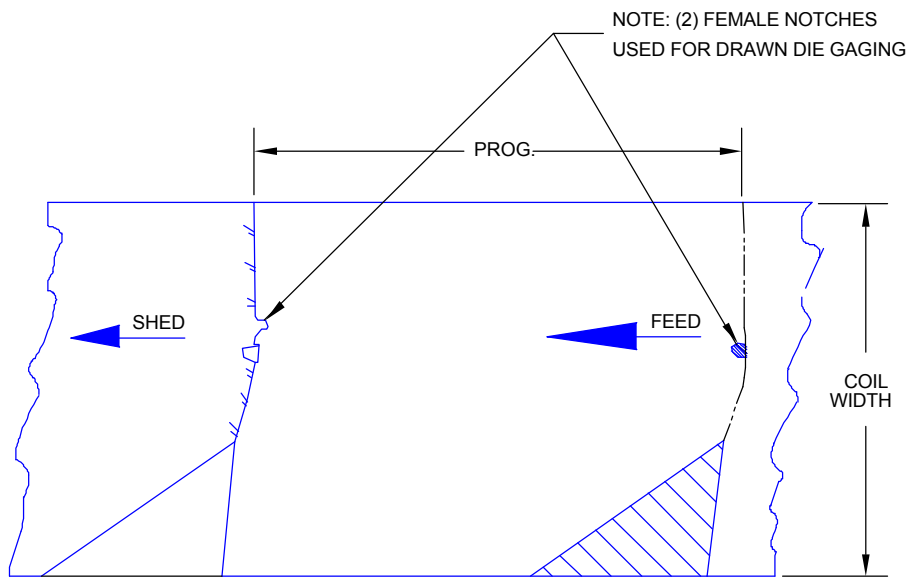


Figure 3.12.9.1-8 Notched edge & strip edge usage

9. Coil edge blank utilizing positive blank gaging holes or notches ([Figure 3.12.9.1-9](#)). When utilizing the coil edge of the blank it is mandatory that gaging holes or notches be provided so the blank can accurately (with repeatability) be located in the draw or form die. Coil edge variations are normally too great, causing very loose draw die gaging. When die gaging variation is adjustable and opened up to accept a maximum coil edge blank, proceeded by a blank from minimum width coil (coil camber also impacts this gaging), the blank is allowed to shift around in the draw or form die. As irregular blank shifts occur, this tendency will create manufactured scrap or costly nonproductive repairs.



[Figure 3.12.9.1-9](#) Sample blank nest (Gage notches cut at same stroke)

In conclusion, do not use alternate, less cost effective configurations such as cut off or trapezoidal blanks just to save on blank die construction or because it is the only blanking equipment available at the assigned production plant. Avoiding the construction of a blank die will generate only a short-term cost savings and will be exceeded by the additional cost of purchasing a larger coil width for the design life of the part. The engineers must determine and analyze the critical nest points and develop the most cost effective blank possible.

3.12.10 ENGINEERED SCRAP

Many blanking operations, in order to obtain the necessary blank configuration, will generate a certain amount of engineered scrap, which is sometimes referred to as offal. The manufacturing engineer must effectively examine the pieces of engineered scrap to determine if certain pieces can be used to economically produce other stampings ([Figure 3.12.10-1](#)). Ideally, the engineer will select another part, with identical production volume requirements, from the same new model vehicle. Potential useful engineered scrap must be categorized and documented ([Figure 3.12.10-2 A,B](#)).

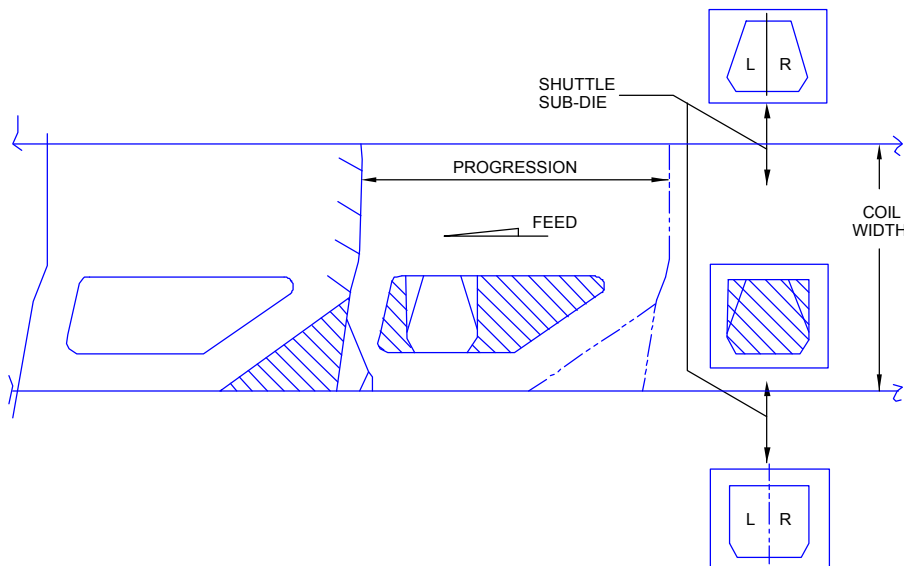


Figure 3.12.10-1 Use of sub dies blank offal or blank part from offal during primary blanking operations

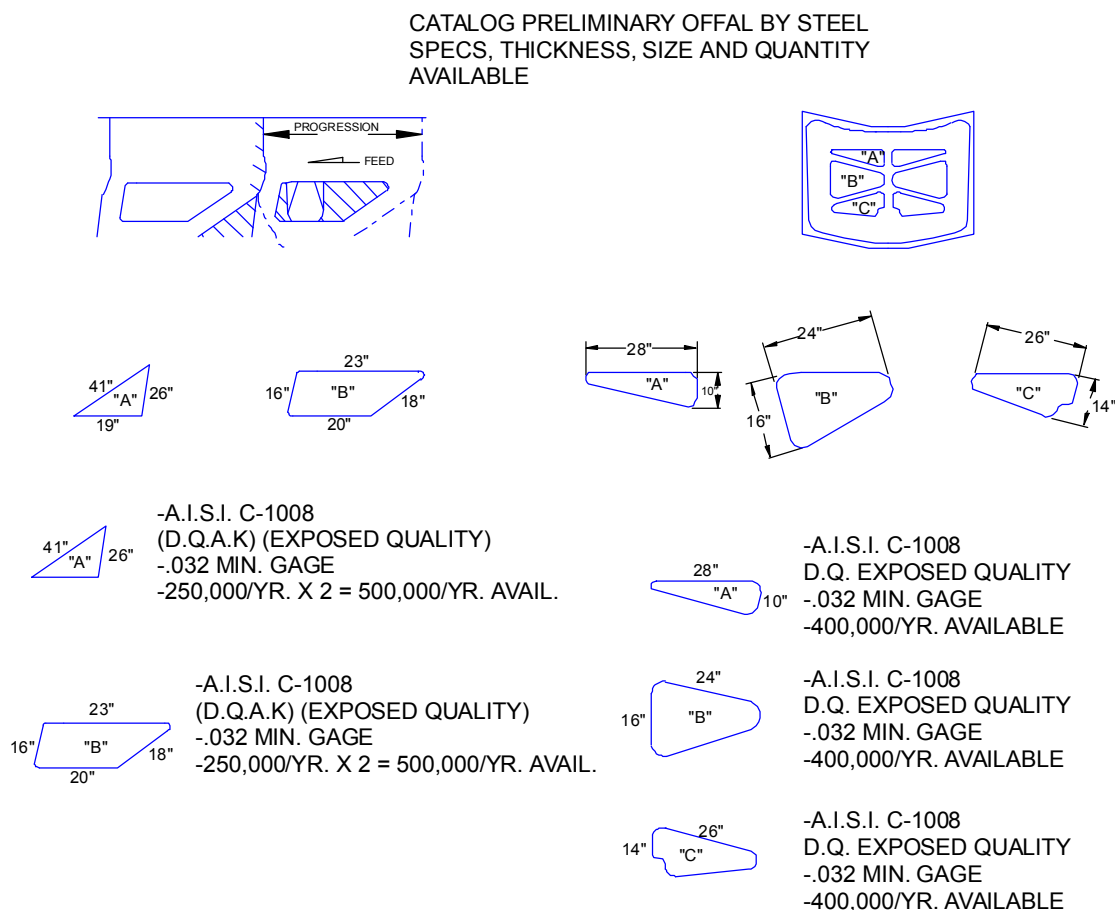
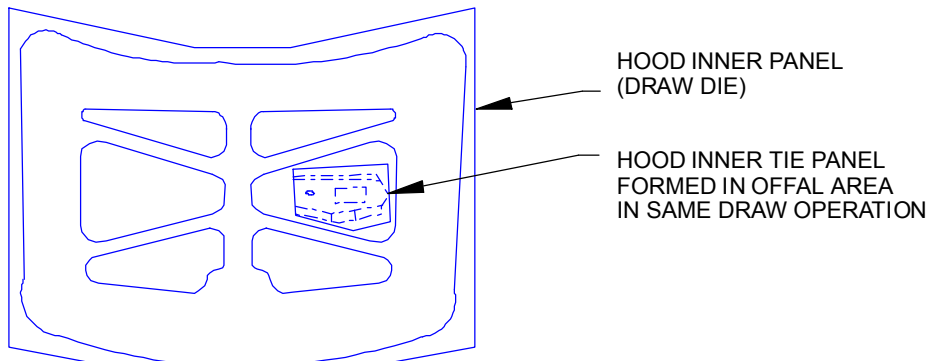


Figure 3.12.10-2 Document preliminary engineered scrap

A review of the following factors must be analyzed to determine if cost factors indicate the effective use of engineered scrap to manufacture another part. A definition of primary and secondary part operations may be helpful.

- Primary utilizes virgin coil steel to produce a part and is also the operation that generates the useful engineered scrap. ([Figure 3.12.10-3](#))
- Secondary is the operation that manufactures the part made from engineered scrap. ([Figure 3.12.10-3](#))



EXAMPLE:
HOOD INNER PANEL
HOOD INNER TIE PANEL

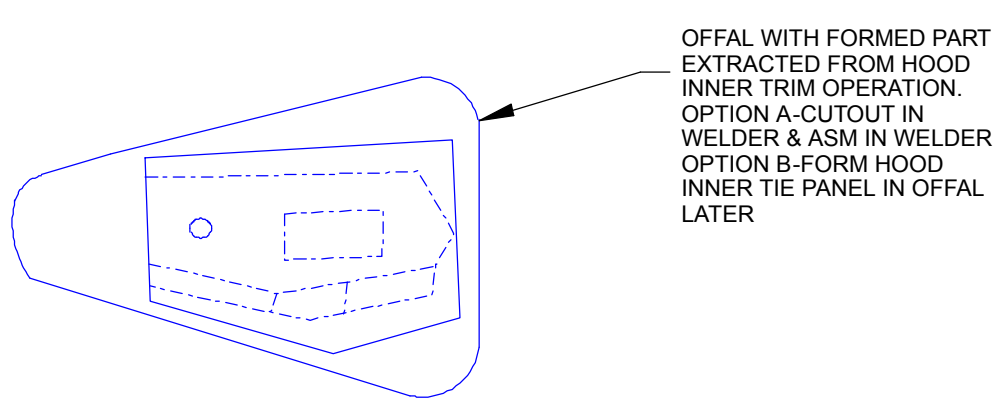
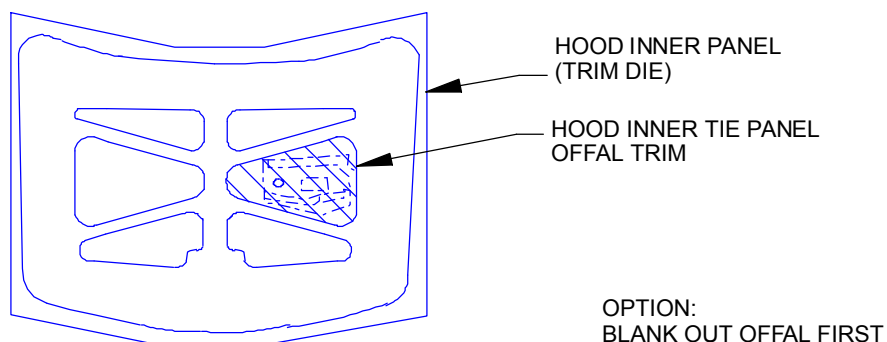


Figure 3.12.10-3 Investigate possibility of making multiple parts

Factors for consideration in determining the cost effectiveness of using engineered scrap:

- Recovery method of the engineered scrap
- Whether a re-blanking operation is required
- Manually stacking and pre-positioning the engineered scrap (Handling ergonomics are now more stringent.)
- Banding of engineered scrap required for transportation to a secondary press operation
- Cost impact on primary blank die design
- Whether the steel specifications of the primary part will meet all the requirements for the secondary part
- Schedule coordination (utilize sub-dies)
- Service consideration (utilize sub-dies)
- What will be done if primary part is canceled (utilize sub-dies)
- What is scrap value of engineered scrap
- What will be done if primary/secondary part changes (sub-dies)
- Overhead burden of personnel and facilities that are dedicated to material utilization (Factor in these costs.)
- Credit for material avoidance (Engineered scrap eliminates the virgin steel cost for secondary part.)
- Whether production requirements are compatible. (Rule of thumb: available engineered scrap must equal 100% of production requirements of secondary part, plus a safety factor of approximately 25%. This is overcome when sub-die construction is utilized to manufacture the secondary part in the primary die.)

3.12.10.1 SUB DIES

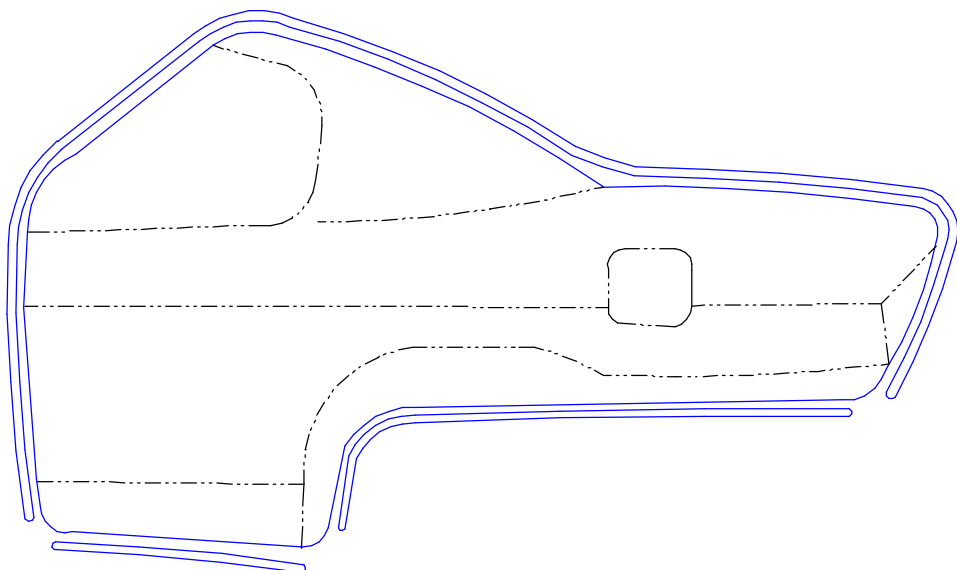
When utilizing engineered scrap to make a secondary part blank or a partial or fully completed part, the use of sub-dies ([Figure 3.12.10-1](#)) integrated into the primary part tooling is mandatory. Sub-dies can be removed from the primary die and set up for the independent manufacture of the secondary blank or part, by using virgin coil steel for any additional blank requirements. Therefore, it is no longer mandatory that the primary and secondary parts have identical volumes. Sub-dies are also effective if only one of the parts (either primary or secondary) remains active for future production requirements and the other part would only be needed to fill service part requests.

3.12.11 FACTORS INFLUENCING MATERIAL UTILIZATION

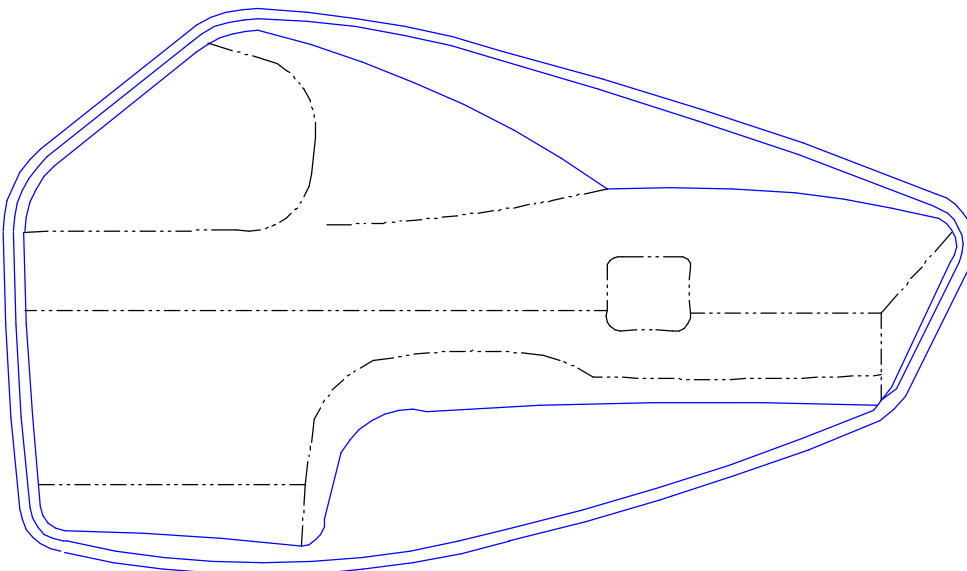
Material utilization assessment must be performed early in the program. During the proof die development program, it is imperative that minimizing the blank size be as important a goal as learning about the panel formability. Significant reductions in vehicle cost can be generated with a strong and effective material utilization program, early in the project. Attention also must be given toward engineering draw/form die blank gaging. Temporary gaging, haphazardly utilized, will not permit an accurate blank development.

Key factors for review to optimize material utilization:

- Strive to use a nested development blank as this is the absolute minimum amount of material usage. Use of a cutoff blank should be the last alternative, because it generally requires more material. This decision is usually made with the rationale being a cost avoidance in blank die construction. A cost study would be required to determine blank die cost avoidance, as compared with the additional material required, from cutoff die, the annual volume and anticipated design life of the panel.
- Test form or drawability without draw beads. Beads usually require a larger blank. Add beads only when and where necessary. Locate beads at closest proximity to the punch opening. Beads were discussed more in [Section 3.12.6.2](#).
- Material utilization penalties are usually incurred when parts are tied together and the parts are not symmetrically opposite.
- During blank development, keep reducing the blank size until the panel quality is affected. Then, gradually increase the blank configuration until acceptable quality requirements are obtained. This assures optimum blank size.
- Minimize addendum length (extra material, outside part trim, used to manufacture the panel).
- Keep binder opening close to part (punch) outline. This improves material flow and panel quality, and can enhance blank nesting ([Figure 3.12.11-1](#)).
- Challenge material specifications by attempting to downgrade projected requirements (both gage and chemistry).

**TOP EXAMPLE**

KEEP BINDER OPENING CLOSE TO CONFIGURATION OF PART.
MINIMIZE MATERIAL BY PROVIDING FOR POSSIBLE BLANK
NESTING. CONTROLS MATERIAL FLOW BY KEEPING STOCK ON
BINDER.

**BOTTOM EXAMPLE**

REQUIRES LARGE BLANK AND REDUCES BLANK NESTING
POSSIBILITIES. IF MATERIAL IS ALLOWED TO PULL OFF BINDER,
THE ABILITY TO CONTROL THE MATERIAL FLOW IS LOST. THIS
USUALLY RESULTS IN A POOR QUALITY DRAW PANEL.

Figure 3.12.11-1 Binder opening close to part outline

3.12.11.1 MINIMIZE DRAW PUNCH OPENING AND DRAW DEPTH

Historically it was routine to always maintain the product trim line on created trimmable addendums on the draw punch whenever possible. It was rare to lay a trim line on the binder due to the potential of trim line length variations. However, due to current pressures to become world class in material utilization, the above can no longer be maintained as a “standard” method of creating developments.

All flanges must now be scrutinized for the potential of laying out on the binder, as this may allow a shallower draw depth and result in less material usage ([Figure 3.12.11.1-1 a,b](#)). It is understood that all flanges can not and should not lie on the binder, due to draw mark run-in, on all outer skin panel surface.

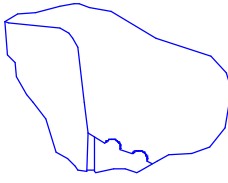
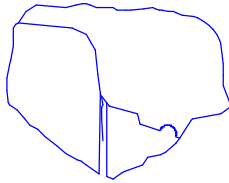
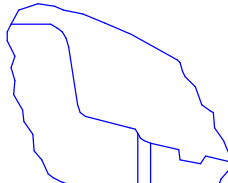
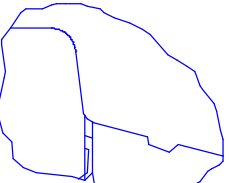
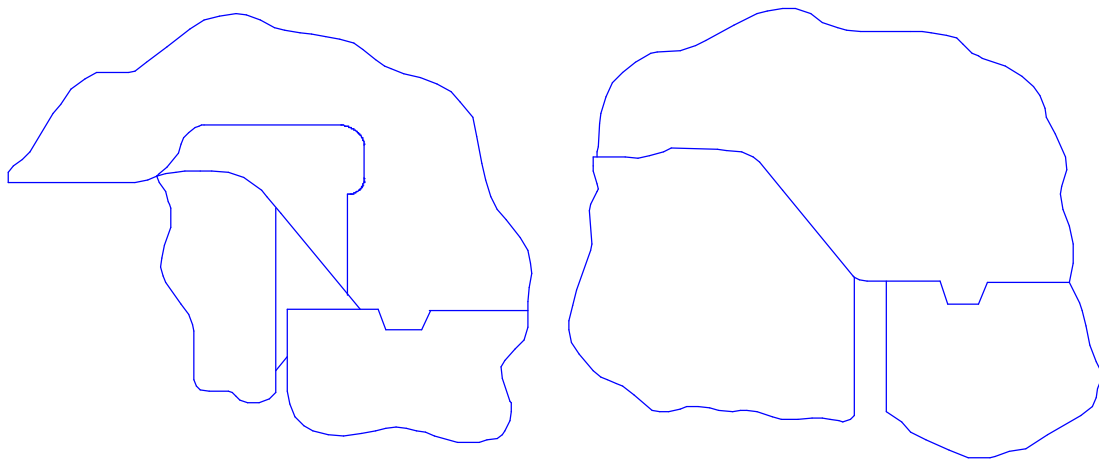
			
HISTORIC DESIGN	PREFERRED NEW DESIGN	HISTORIC DESIGN	PREFERRED NEW DESIGN
ADVANTAGES	ADVANTAGES	ADVANTAGES	ADVANTAGES
<ul style="list-style-type: none"> • PANEL IS HOME- NO NEED TO FLANGE 		<ul style="list-style-type: none"> • LEAST MATERIAL USAGE • RAM TRIM - NO SLIDE • SCRAP SHEDDING - NO PROBLEM 	
DISADVANTAGES	DISADVANTAGES	DISADVANTAGES	DISADVANTAGES
<ul style="list-style-type: none"> • REQUIRES EXPENSIVE CAM TRIM SLIDE • SCRAP MUST BE SHED UNDER SLIDE • EXCESSIVE MATERIAL USAGE 		<ul style="list-style-type: none"> • REQUIRES RAM FLANGING • SPRINGBACK FROM DRAW RADIUS 	
(a) MINIMIZE DRAW DEPTH MOVE TRIM LINE FROM PUNCH TO BINDER		(b) MINIMIZE PUNCH OPENING PROFILE AND MOVE TRIM LINE FROM PUNCH TO BINDER	

Figure 3.12.11.1-1 Scrutinize laying out on the binder

When reviewing punch opening ([Figure 3.12.11.1-2](#)) profile decisions on a proof die development, it is absolutely mandatory that the manufacturing engineer have a basic knowledge of the critical nest points. These points are the area that demands a concentrated effort toward reducing draw depths and moving punch opening and die beads closer to the punch.



PREFERRED NEW DESIGN

HISTORIC DESIGN

ADVANTAGES

1. MORE BINDER STRENGTH INSIDE BEAD.
2. BEAD CAN NOW BE IN CLOSER TO DRAW WALL - MATERIAL SAVINGS
3. ELIMINATES USELESS SPOTTING

Figure 3.12.11.1-2 Minimize punch opening profile section examples

3.12.12 FINALIZE MANUFACTURING PROCESSES

Prior to finalizing the process and commencing the die design, the manufacturing engineer must have gathered all pertinent program data and implemented it into the development tooling (proof die).

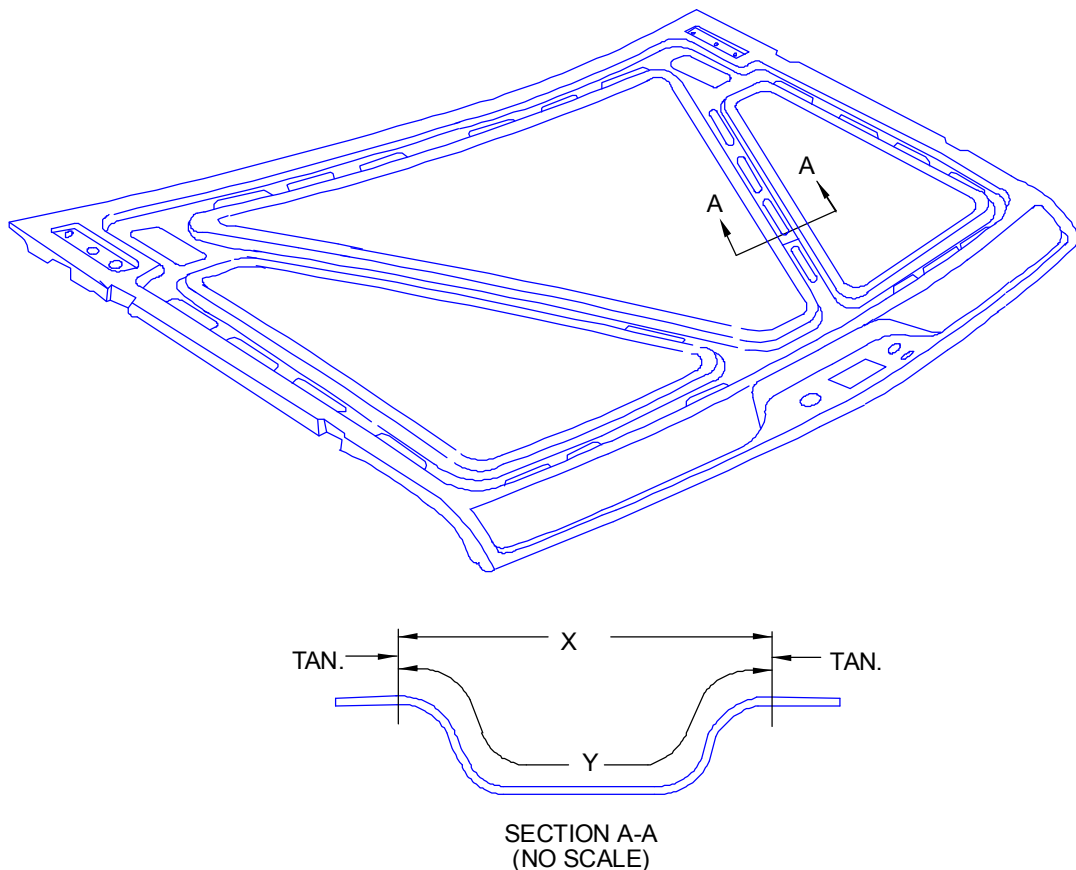
Part concessions should all have attained final approval from the product engineer. Material gage and chemistry was finalized, with assistance from the metallurgical engineer (if required). Input from third-party reviews has all been agreed upon and implemented into the final process. Critical nest points and preliminary blank nesting has been approved. (This will be finalized with the production dies.) All press data has been determined and fed into the process. Approved strain documentation is available. Thus far, the Product/Manufacturing Development Team should have attained all their goals and objectives.

3.12.12.1 Manufacturing Scrap Avoidance

Manufacturing scrap is defined as defective production parts that are produced during the stamping plant operations, or during transportation of panels to the assembly plant. The Product/Manufacturing Development team members must direct more of their attention toward the factors that can cause manufactured scrap. Emphasis toward reducing or eliminating these non-productive costs during manufacture or transportation of panels is the responsibility of the production plant and all associated engineering personnel. Purchasing additional raw material is necessary to replace the defective parts. This material also results in additional productive and

non-productive labor costs to replace the panels lost from initial part inventories. The production plant must also focus on reducing or eliminating part repairs. Repairs only result in increased panel costs. Some of the causes of manufacturing scrap or repairs are discussed.

- Utilizing coil edge blanks without positive blank gaging holes or notches. ([Figure 3.12.9.1-9](#).) This subject was discussed more extensively in [Section 3.12.9.1](#) (scrap).
- Draw/form die gaging must be engineered for accuracy and repeatability (scrap).
- Flange die steels improperly hardened. When inserts are too soft, galling will occur on panel flanges causing ripping or tearing of the flange (possible repair or scrap).
- Raw material - not to specifications (scrap).
- Trim die steel improperly hardened. When inserts are too soft or have improper die steel clearance, this will result in excessive panel burrs. Shavings or slivers are also generated. This causes dirt/foreign material contamination to outer skin panels (repairs - metal finish).
- Broken die punches - holes missing (repair).
- Excessive material strain ([Figure 3.12.12.1-1](#)) (scrap).
- Failure to utilize pilots or positive stop gaging for progressive die operations (scrap).
- Excessive part carrier ribbon flex, on progressive dies (scrap).
- Avoid blank turnover operation (added cost and possible mutilation).
- Failure to monitor operation (spot check) (scrap/repair).
- Failure to establish control limits and monitor operation (scrap).
- Excessive tensile and yield strength ranges, especially for high strength steel parts (scrap).
- Relieve die post and pad areas on surface panels to alleviate surface contamination (repair).
- Poor packaging (scrap or repairs).
- Automation malfunctions (scrap).



REDUCING MANUFACTURING SCRAP CAN BE ACCOMPLISHED WITH THE PRODUCT AND MANUFACTURING ENGINEER JOINTLY DESIGNING PANELS THAT ARE MORE FRIENDLY TO THE MANUFACTURING PROCESS.

NOTE: CHANNEL SECTIONS THAT ARE NOT CLOSE TO OUTSIDE EDGE OF PANEL, AND THEREFORE VOID OF METAL FLOW SHOULD BE RESTRICTED TO NO MORE THAN 25% STRETCH. (COMPARING LINE "Y" TO LINE "X" IN SECTION A-A.)

Figure 3.12.12.1-1 Excessive material strain (example of a hood inner panel)

3.12.13 BEGIN DIE DESIGN

It is sometimes necessary to begin limited die design earlier than originally anticipated due to the long lead time requirements of some major panels. However, if the design start can occur after all the pre-described information is gathered, normally expectations of a high quality more efficient design can be achieved. This is possible because more thought will be devoted to optimizing the die design, rather than the designer being involved in the fix up - catch up mode. Also, the blank die design can begin with a high degree of certainty that only minor modifications would be anticipated during production die primary and secondary tryout. An additional benefit is that the blank die can be built simultaneously with the other dies, thereby providing actual production die cut blanks for the production draw and line die tryout. Also, if additional pilot parts are required, costly hand cut blanks would not have to be fabricated.

Assuming that the die development program (proof die/dies) and prototype parts program ran concurrently, a comfort level should exist regarding the structural finite element analysis, which was conducted by product engineering, in attaining design intent. It is imperative that all die designs and press line automation comprehend and engineer Quick Die Change requirements into all tooling. All production plants must meet stringent die change (world class) objectives to achieve just in time inventories.

3.12.14 DIE CONSTRUCTION (GENERAL CONTRACTOR)

The optimum procedure is to have the construction source as the general contractor, with total responsibility for panel development (proof dies), design of both the dies and automation required, and tryout of the total system including the welding of sub-assemblies.

The general contractor should not be responsible for just front fenders. As an example, the contract should include the total front end assembly, hood assembly, fender assembly and all motor compartment, structural sheet metal. This responsibility would include furnishing all prototype and pilot parts. The general contractor then sells the total front end assembly to the customer. Sub-contracting of components (parts, automation, welding) is allowed, but still falls under the umbrella of the responsibilities of the general contractor. (Optimum program would be to assign entire body in white to a single source.)

The construction source must have all program data available to assume total project responsibility. This data must all be on site of the general contractor. Typical data would include:

- All pertinent proof die panel development data. This information describes all steps taken to achieve the final successful draw stampings. Included in this process would be all attempts that failed to produce a stamping of high quality with minimum size blank.
- A complete set of one inch incremental break-down draw panels
- Analysis of blank nesting proposals and critical nesting points
- Metallurgical reports on material
- Production press line information (including automation)
- Draw die pressure requirements and accurate panel gaging
- Die face data and digitized proof die data
- Production plant layout for welded assemblies

An extensive discussion of construction and tryout of welding equipment is beyond the scope of this section.

3.12.15 PRIMARY TRYOUT

Primary tryout of the production dies is performed at the general contractor's construction facility. When the die construction and die spotting has been completed, set all the dies in presses that closely simulate the action of the production plant equipment, then proceed to make a draw panel and drill coordinating holes in panel. Using locator pins in each die lower post,

nest each panel onto these pins and then cycle the press. Not distorting the coordinating holes indicates the panel has been completely stabilized. Then proceed to analyze:

- Blank size and configuration
- Addendum
- Circle grid draw stamping
- Critical nest points of blank
- Die beads (fully seated and are the correct size)
- Further reduction of blank size, if possible
- Scrap and slug shedding properly
- Trim and flange steel hardened
- Pressure requirements established and identified with a die tag
- Die gaging, accurate and repeatable
- Establish dimensional control limits
- Verify that material selection is correct
- Flame hardening of draw punch and all reverse areas
- All dies shipped to the production facility with approved blank and a panel off each die operation
- Any blank changes from proof die to production die identified and documented.

3.12.16 SECONDARY TRYOUT

This phase of the program takes place in the complete production plant environment that includes presses, dies, welders, automation, and packaging containers. It is essential during this phase of the program that a more disciplined attitude be developed and adhered to for approval of any engineering changes, so as not to jeopardize the final program objectives of cost, quality and timing. To accomplish this the product design world must establish a start and stop date for events that take place at the proving grounds. If additional vehicle testing is required, the start of production date will have to be modified. It can no longer be an acceptable practice that start and stop dates are not established and adhered to. The consequence of this means altering the new model introduction date. Crunching and compressing program tooling due to delay in other phases has proven quality and production start-up problem. Each timing phase is critical.

Both primary and secondary tryout periods of the program help to provide the manufacturing engineer and plant personnel with a final attempt to reduce the blank size (raw material reduction results in substantial cost reductions for the projected design life of the specific model program. Also, they must focus on potential areas that could produce non-productive manufacturing scrap or repairs.

The following functions must be performed during secondary tryout and verified:

- Press/die locators are in line with automation to avoid panels being mislocated.
- Die gaging is accurate with automation and it is positive and repeatable.

- Produce panels for statistical process control analysis.
- Harden or possibly chrome plate draw die binders.
- Try out secondary part from engineered scrap (if applicable).
- Attempt to use discarded outer panel blanks to make inner panels. Example: hood outer blanks to make hood inner panel.
- Identify and document the blank size changes from primary to secondary tryout.

In conclusion, review, record and publish pertinent data to avoid repeating problems for future new model programs.

3.12.17 REVIEW FOR TECHNICAL LIBRARY

A comprehensive review must be made, by the entire Product/Manufacturing Development Team, of all factors that either directly or indirectly influenced the optimum use of material, or impacted panel cost, quality or timing. This data must be documented and recorded. This will promote continued improvement for all future model change programs. To ignore establishing this historical panel information library will jeopardize progress toward improving a competitive manufacturing position. Failure to determine the root cause of problems and faults can no longer be tolerated. Additionally, development of check sheets for each phase of the program is necessary to prevent items from slipping through the cracks.

Each benchmark of the program is critical to reach a successful program conclusion. Items or delays at the beginning of the program must be recognized as to their impact farther along in the program. Attempting to catch up at a later stage in the project has proven to cause both cost and quality problems at the conclusion.

Each separate project discipline must take responsibility for its own start and stop dates. Delaying changes seldom produces good results; generally it only maintains the status quo.

4.1 STAMPING OPERATIONS

4.1.1 INTRODUCTION

Historically, the progression of an automotive sheet metal body stamping from conception to production has been a segmented series of events. Styling, part design, material selection, die design, die build, die tryout, and part production have been performed in a sequential manner. Interaction between adjacent stages has been minimal at best. For example, die designers have had little input into the design of the part, and rarely did they interact with the press room tryout staff. The activities of each segment in the sequence have been conducted within its own sphere of work by its own group members. Interaction among the different groups has been very limited.

Today, simultaneous engineering requires that representatives from all units involved in the conception to production sequence become involved together at the earliest possible point in the design. Ideally, the simultaneous engineering concept even brings specialists from material, lubricant, and other outside suppliers into the initial design phase, where major design changes can be made most easily in a cost and time effective manner.

Interaction of various functions requires a number of common crossover points for all participants: identical language, understanding of basic sheet metal formability, formability limits, press shop terminology, and a framework for analysis. Only then can diverse participants communicate and understand each other to accomplish the best, low cost design that will have optimum manufacturing feasibility.

This section describes the methods available to form sheet metal stampings, the equipment used to accomplish the forming, and some of the tradeoffs necessary to maintain manufacturing feasibility.

4.1.2 BREAKDOWN OF A COMPLEX STAMPING

Stamping operations convert coils of steel received from the steel mill into parts. The parts are rarely used in their as formed condition; they are usually assembled with other stampings or parts by welding, bonding, or mechanical fastening. Subsequent operations are important in that they place constraints on the part design and forming operations. For example, welding may require a weld flange of minimum width that must be buckle free.

4.1.2.1 Geometrical Configuration Versus Forming Mode

Two methods are used to divide a complex part into its component sections. The first method, by the geometry of the part, is generally used by the stylist and part designer. It describes the final geometry and dimensions of the functional part independent of how the geometry was obtained. The second method, by forming operations or forming mode, is used by the die designer to generate the required geometry. It consists of a initial stamping which then usually undergoes a number of additional operations, such as restrike, trim, flange, and punch, before it becomes a finished part. The initial stamping may or may not resemble the final part.

A distinction is made here between a stamping and a part. A stamping is the deformed sheet anywhere in the production cycle; it represents some stage along the production cycle. The initial stamping usually needs to undergo several forming and processing sequences before it

becomes a part and leaves the stamping operation. When a stamping becomes a part, it may not yet be suitable to put on the automobile. For example a door panel needs an inner door part, outer door part, door intrusion beam, locks, hinges, etc. The finished part is the final goal of the stylist and the part designer; intermediate stamping operations are the concern of the die designer.

[Figure 4.1.2.1-1](#) shows a complex part that represents geometries commonly found in typical automotive body panels. The geometry of the part can be prescribed by specifying the dimensions of the top surface, the side walls, the corners, and the flanges. Added to this overall stamping geometry are sub areas such as embossments, holes, slots, and other functional zones. The part designer thinks in terms of the required geometry to accomplish the required function or the geometry needed to fulfill the styling shape, usually without concern about how the part is to be made. The geometry usually is not hard to define. For example, the part print [Figure 4.1.2.1-1\(a\)](#) could require the lower left corner radius to be 1 x metal thickness (1t) or 15 x metal thickness (15t). The 1t radius may actually be required for clearance or other purposes or it may be simply an arbitrary number put on the part print because it "looks crisp". A 1t radius, however, restricts the depth of the initial stamping and probably will require two or three stamping operations to generate the specified part surface. A 1t radius corner may be impossible to produce or cost prohibitive in some part configurations.

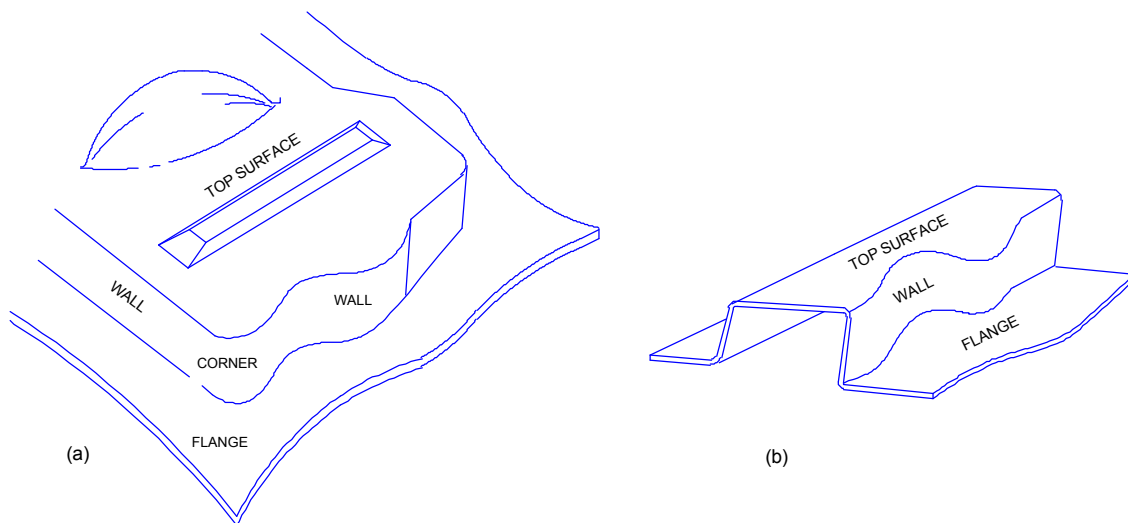


Figure 4.1.2.1-1 Schematic of a part with a combination of geometries

The second method of breaking down a complex part is by its forming operations or forming modes. Typical forming operations are listed in [Table 4.1.2.1-1](#), defined in [Section 4.1.2.2 Description of Forming Modes](#), and detailed in [Section 4.1.6](#). Note that specific geometric shapes can be created by more than one forming operation or mode, as illustrated [Figure 4.1.2.1-1\(b\)](#). The geometric characteristics are similar to [Figure 4.1.2.1-1\(a\)](#), but the forming operations are different.

Table 4.1.2.1-1 Relationship between part geometry and forming mode

GEOMETRY	FIRST OPERATION	SUBSEQUENT OPERATION
Top Surface	None Stretch Emboss	Restrike Emboss
Corner	Cup Draw	Redraw Ironing
Wall	Bending Bend-and-Straighten Shrink Flange Stretch Flange	Post Stretch
Flange	Draw Bead Contours	Trim and Reflange
Other	Blank	Trim Pierce Punch Extrude

4.1.2.2 Description of Forming Modes

4.1.2.2.1 Stretching

In the most common stretching mode, the blank is completely clamped at the die ring or binder by hold down pressure or lock beads ([Figure 4.1.2.2.1-1\(a\)](#)). A contoured punch is then pushed through the die opening into the clamped blank. All deformation Stretching occurs in the metal that is originally within the die opening. The deformation state is biaxial tension, which results in a thinning of the metal over the entire dome. In the laboratory, stretchability is commonly evaluated by a hemispherical punch.

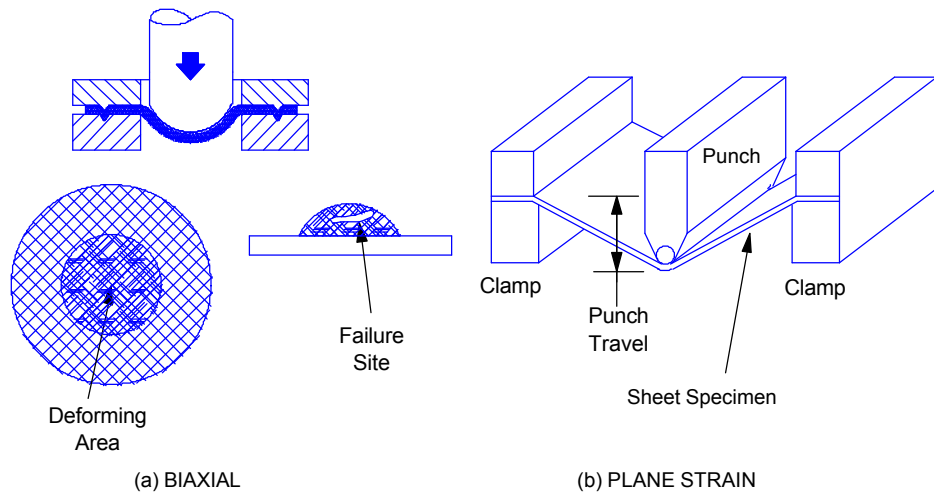


Figure 4.1.2.2.1-1 Stretch forming in which no deformation is allowed in the flange area and all deformation occurs in the die opening over the punch

Plane strain stretching is a special case of stretching ([Figure 4.1.2.2.1-1\(b\)](#)), where the punch is very long compared to its width. Again the blank is securely clamped at the ends. Deformation now occurs only across the punch face; no deformation occurs along the punch length. This deformation mode is commonly found in character lines and the edge of stampings.

4.1.2.2.2 Deep (Cup) Drawing

In the deep (cup) drawing mode of forming, a circular blank is drawn into a circular die by a flat bottom punch ([Figure 4.1.2.2.2-1](#)). This mode is also called radial drawing because the flange is pulled radially toward the die opening. The resulting decrease in blank circumference causes a circumferential compression of the metal. Buckles are controlled by the blank holder pressure. No deformation takes place under the head of the flat punch.

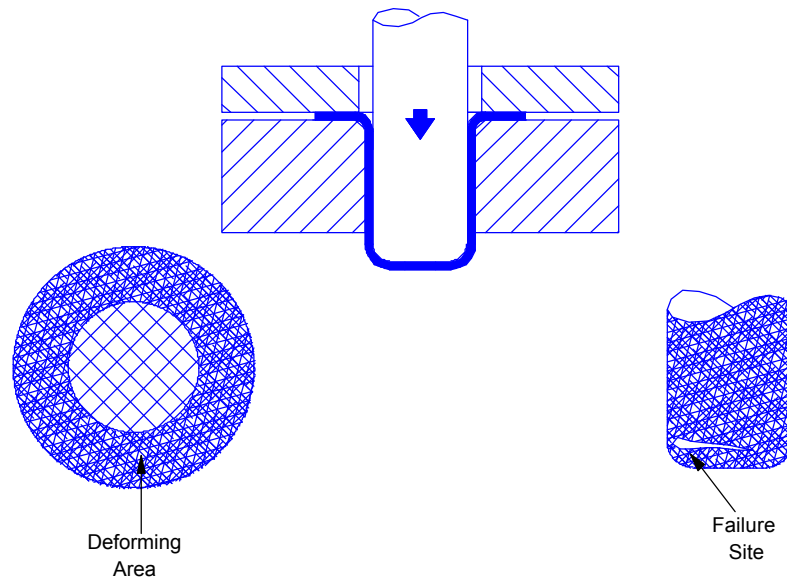


Figure 4.1.2.2.2-1 Deep (cup) drawing

4.1.2.2.3 Bending

Bending is one of the most common methods used to change the shape of sheet metal. V -bend and U-bend are shown in [Figure 4.1.2.2.3-1\(a\)](#). In each case a punch forces the metal into a long channel die as both free edges swing upward. The wiping bend or flanging operation, shown in [Figure 4.1.2.2.3-1\(b\)](#), varies in that one edge is held securely while the punch wipes or swings the free edge down.

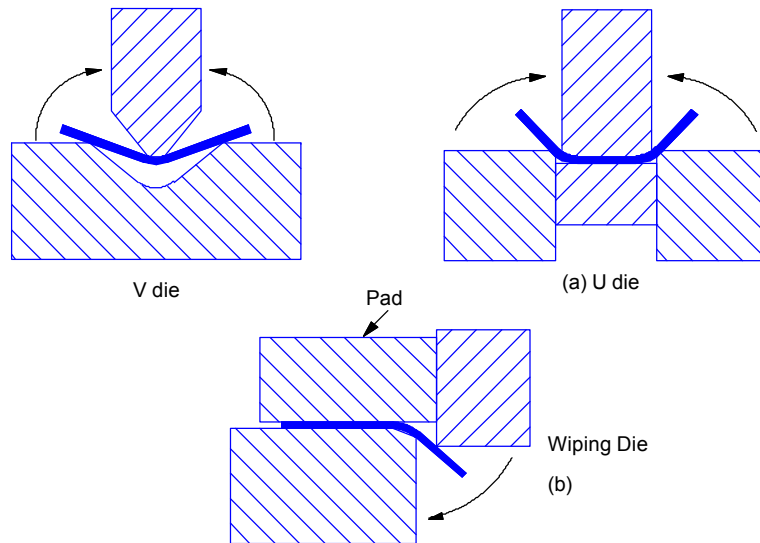


Figure 4.1.2.2.3-1 Types of bending along a straight bend line

All bending operations have several characteristics in common. First, one or more metal edges swing through space. This swing must be calculated to allow for sufficient room in the tooling. Second, the metal bends along a narrow line that acts much like a plastic hinge. Third, metal outside the plastic hinge is unstrained and remains in the as received condition.

4.1.2.2.4 Flanging

Flanging along a straight line is identical to the bending described above. When the line of bending is changed from straight to curved, another degree of complexity is added to the operation. The metal outside the plastic hinge no longer remains in the as received condition; it experiences either tensile (positive) or compressive (negative) deformation.

Shrink flanging is one form of flanging ([Figure 4.1.2.2.4-1\(a\)](#)). As the name implies, the flange length shrinks during forming. Each radial zone (shaded region) is folded 90° along a radial line to form the flange or wall. Since the arc length of the final flange or wall is smaller than the arc length of the element from which it was formed, compression must take place in the circumferential direction. The greater the flange depth, the greater the amount of compression. In addition, the compression is the largest at the top of the flange and is zero at the flange radius. Stretch flanging is the opposite to shrink flanging ([Figure 4.1.2.2.4-1\(b\)](#)). Here a tensile stretch is required to generate the increase in line length. Hole expansion is a common example of stretch flanging.

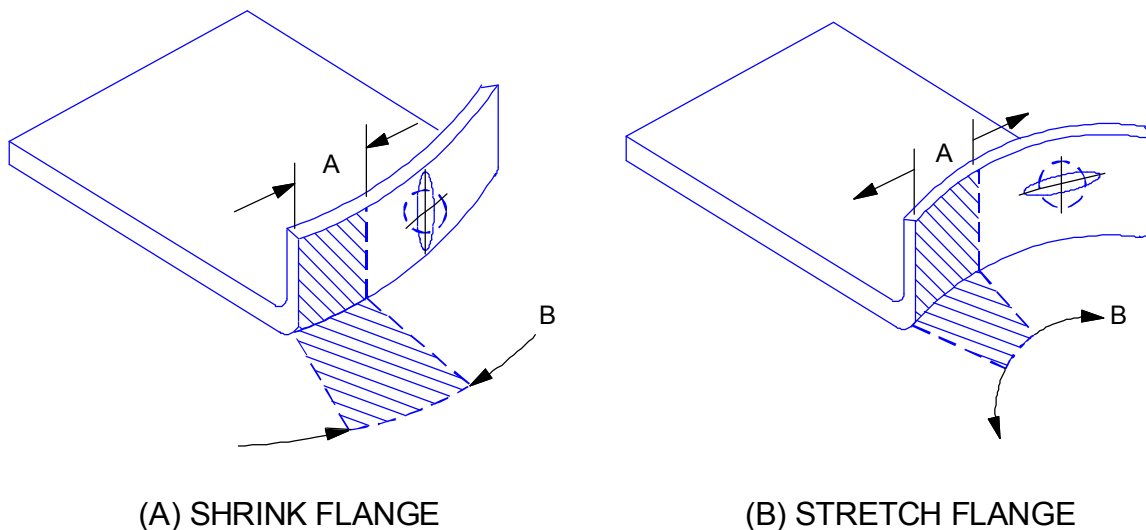


[Figure 4.1.2.2.4-1](#) Bending along a curved bend axis

4.1.2.2.5 Bend-and-Straighten

A bend-and-straighten operation generates a final shape that is identical with that generated by a bending operation ([Figure 4.1.2.2.5-1](#)). However, the intermediate steps are very different and generate different characteristics in the final product. In the bend-and-straighten operation, the swing of the metal is prevented by the blank holder. The bottom radius is formed around the punch by a bend operation while a simultaneous bend is formed around the die radius.

Thereafter, each additional element in the final wall begins in the flange and is pulled towards the radius zone. Because the die radius line is straight, no compression is created along the radius line. Upon entering the die radius zone, the element is bent to conform to the radius contour. When leaving the radius zone, the element must be unbent or straightened to conform again to the straight wall. Thus, this operation is descriptively called bend -and-straighten.

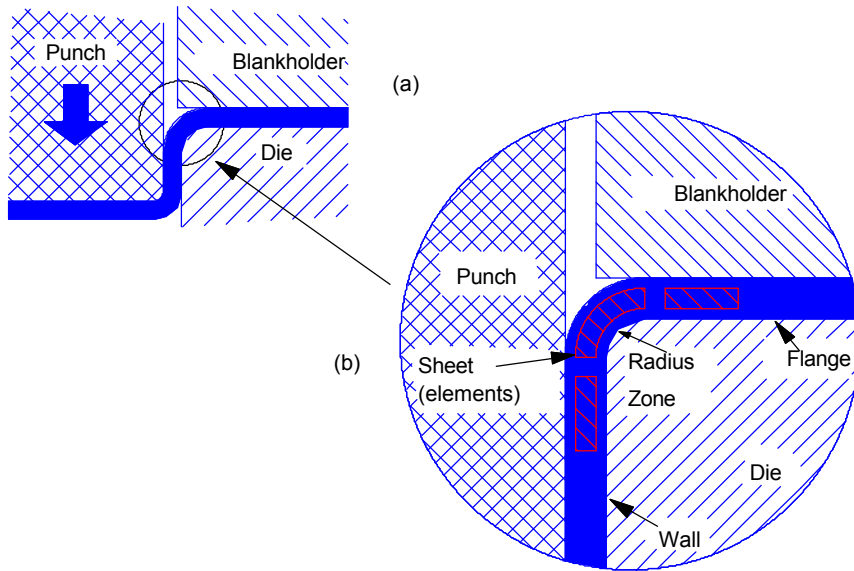


Figure 4.1.2.2.5-1 Bend and straighten

The primary difference between bending and bend -and-straighten is the condition of the final wall. In the bend operation, the final wall is swung into position and remains in the unworked state. During the bend -and-straighten operation, the metal is worked first in one direction (tension or compression depending on the convex or concave side of the bend) and then worked in the reverse direction. This bending and unbending hardens the metal and reduces the residual formability of the material for subsequent stamping operations. Substantial portions of the major panels are formed by the bend -and- straighten mode of deformation.

4.1.2.3 Interaction of Forming Modes

Forming modes usually interact because most stampings are composed of several distinct areas, each of which is formed by one of the primary forming modes. The two shapes shown [Figure 4.1.2.1-1](#) are reproduced in [Figure 4.1.2.3-1](#) with the geometrical designations replaced by the respective forming modes used to generate the geometrical shapes.

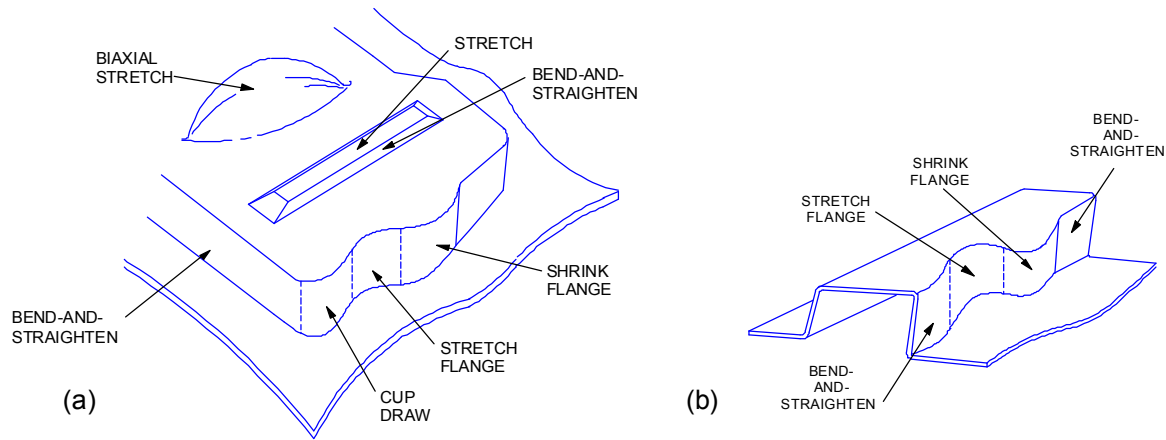


Figure 4.1.2.3-1 Schematic of a part with composite forming operations

When the forming modes have been identified, the analysis of the stamping can begin. One method of analysis is the length of line technique. Here the required length of line is analyzed for each of the directions and zones in the stamping. An example is shown in [Figure 4.1.2.3-2](#).

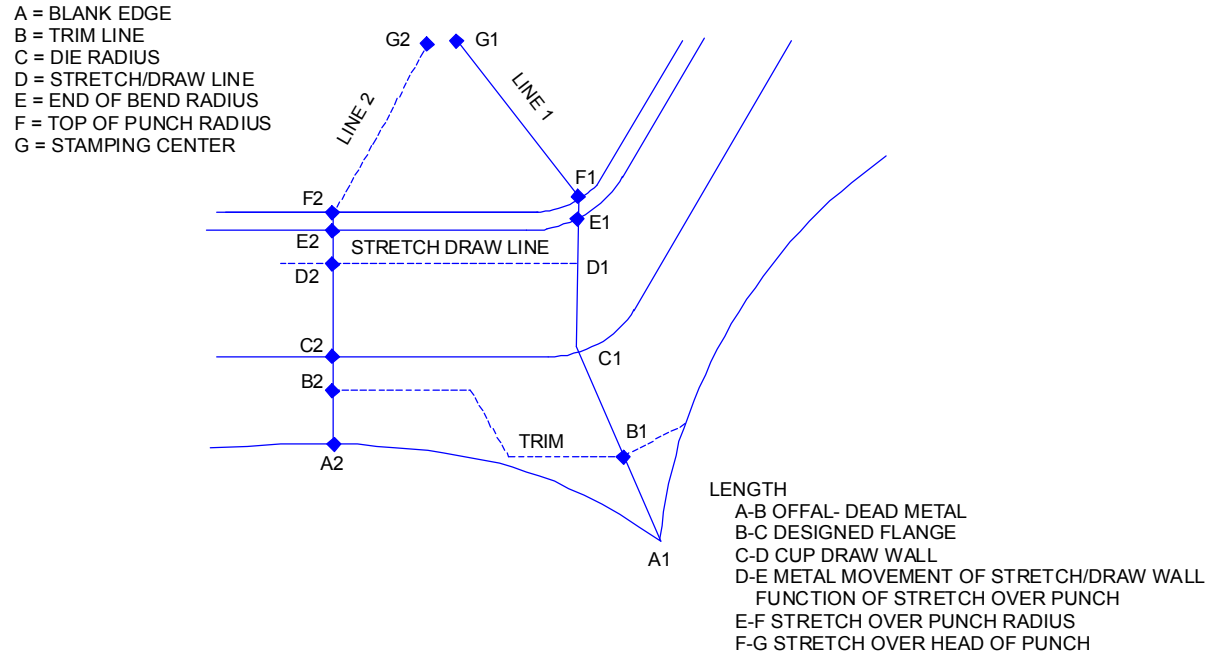


Figure 4.1.2.3-2 Line analysis of a complex stamping

In this complex stamping, note that the wall geometry of line 1 is generated by a radial or cup drawing mode. This is determined by examining the plan view of the stamping ([Figure 4.1.2.3-3](#)). Note that the four corners can be combined to form a complete cup, which is created by radial or cup drawing. By contrast, the wall geometry of line 2 is generated by a bend -and- straighten operation. It is therefore important to identify the known forming modes within a stamping.

Each of the forming modes requires different material properties for optimum formability. Both the design parameters and material properties will vary greatly - often in the opposite direction - depending on the forming mode.

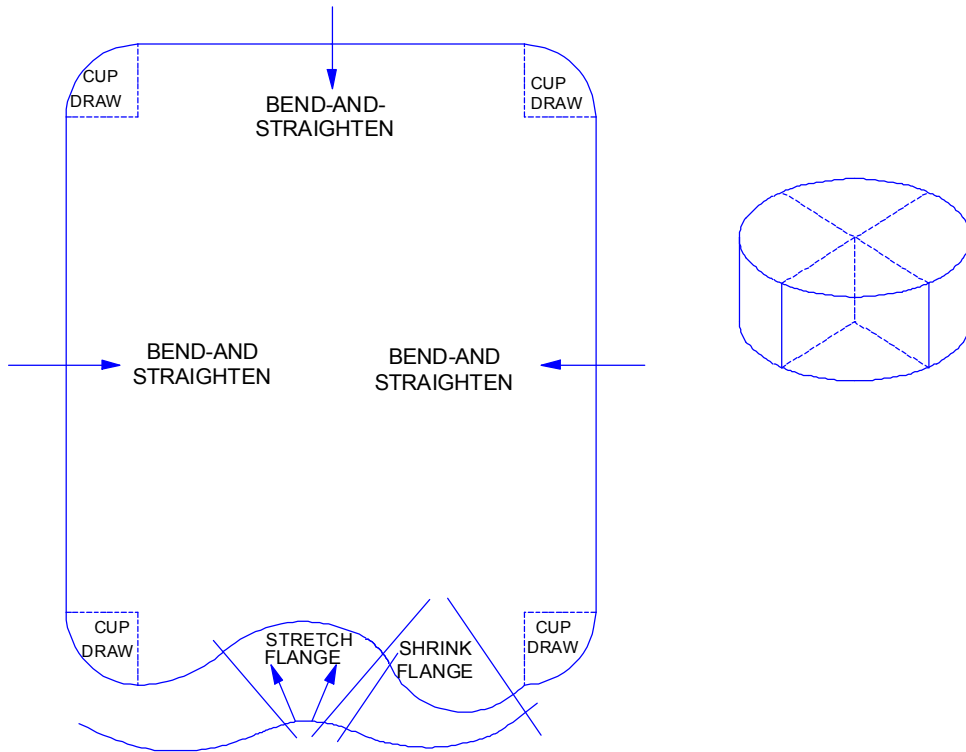


Figure 4.1.2.3-3 Plan view showing cup draw segments in corners

After the first stamping is formed, a wide option of secondary forming operations is available to change the shape created by each of the initial forming modes. For example, trimming and reverse flanging of the initial flange may present problems. The bend-and-straighten section remained at the initial blank thickness, but the metal in the corner cup draw has increased in thickness, up to 40 percent.

These forming modes are interactive and are constantly changing in response to a large number of variables. For example, the blank width may be increased to provide an additional flange, after trimming, to meet subsequent welding requirements. The additional flange will restrict metal flow from the binder (hold down) area and thereby increase the depth of the stamping required by stretching over the punch. This may drive the deformation over the punch into a failure condition. This trend can be reversed by increasing the die radius to allow easier flow of the extended blank into the die cavity. However, if the die radius is now too large for the final part, a restrike operation will be required to sharpen the radius to the required (not desired) dimension. These are the interactions that must be considered by the simultaneous engineering team.

Unfortunately, an increase or decrease in interface lubricity, with respect to the surface characteristics of the incoming steel, can inadvertently cause the same reaction in the die and cause variations from part to part. Thus, the first task at hand is to understand the forming modes and how they interact to provide the desired part shape, and therefore the required stamping.

4.1.3 SEQUENCE OF OPERATIONS

The production sequence becomes important after the part has been designed and the forming modes selected. This sequence may place additional limits on the forming modes and even on the initial part design. In any case, knowledge of terminology is important to simultaneous engineering.

4.1.3.1 Initial Blank

The stamping operation begins with a blank, which is created either by shearing or blanking ([Figure 4.1.3.1-1\(a\)](#)). Shearing is a straight cut across the coil width to form a square or rectangular blank. Blanking creates a blank bounded by a contoured line composed of straight and curved segments. While shearing is easier to perform, it may waste metal.

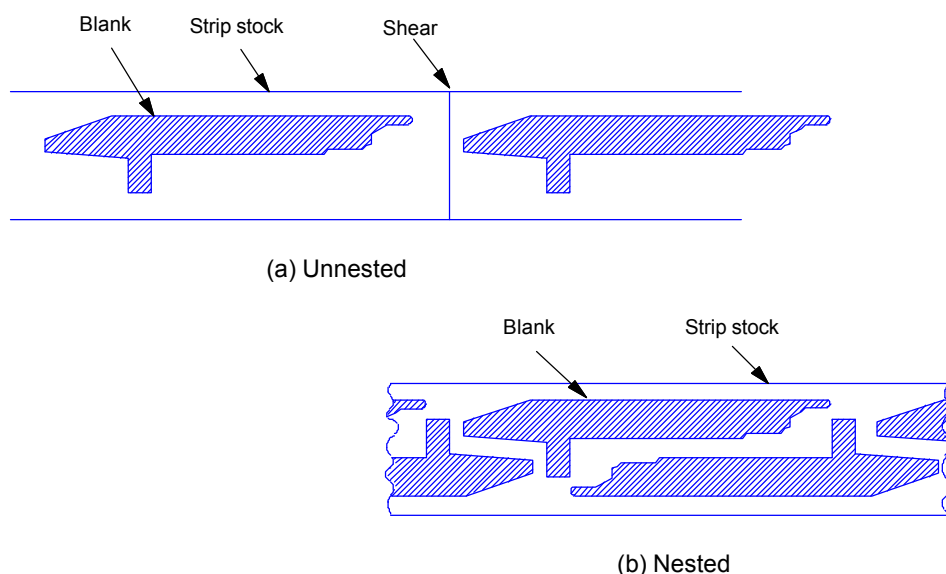


Figure 4.1.3.1-1 Nesting irregular blanks in layout to save material

Contoured blanks can be nested ([Figure 4.1.3.1-1\(b\)](#)) to reduce the metal that must be removed as trim (offal or engineered scrap). This trim metal is intentionally and unavoidably wasted from the initial blank on every stamping. Sometimes large segments of offal can be reapplied on smaller parts, but careful study of the economics must be made. The costs of steel collection, storage, reapplication, accounting, scheduling, etc. may outweigh the savings generated by the amount of the scrap metal actually used.

Another reason for contouring the blanks by a blanking operation is to match the blank perimeter to the perimeter of the die opening. Matching encourages more uniform metal flow into the die cavity, prevents excessive buckling in the flange, and reduces the drag of extra flange metal behind critical zones. A third reason for contouring the blanks is to create the final flange/part contour in the blank in order to eliminate a trimming operation after forming.

Shearing or blanking operations can be performed in several ways. They may be performed in material receiving, where coils of steel are blanked and the stacks of blanks shipped to the press line. Blanks may be made at the head of the press line as the coil is unwound into a washer, blanker, oiler combination. Blanks may also be created in the die at the start of the forming stroke.

4.1.3.2 First Forming

The first forming operation may be the operation where the majority of the stamping shape is formed, or it may be a preform. A preform is a stage that typically gathers metal into a zone for later use. For example, a dome of metal is created in the center of the blank while the metal on the edges is unrestrained and free to move [Figure 4.1.3.2-1](#). This preform operation allows the necessary length of line to be generated without excessive tension, localized metal thinning over tight radii, and possible breakage. The main forming sequence then follows to generate the major panel shape.

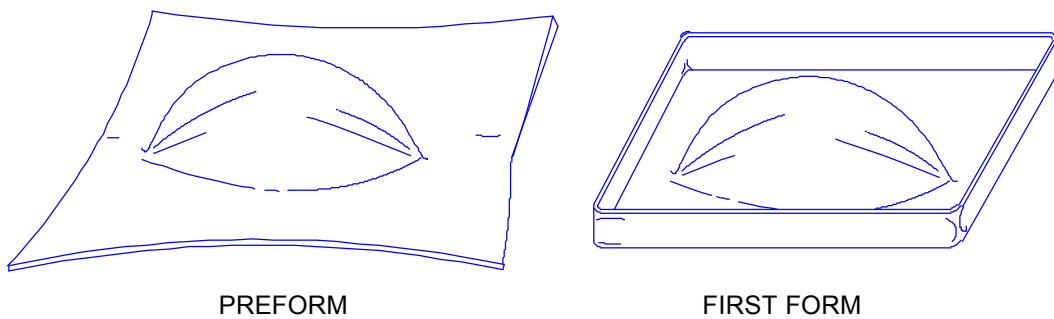


[Figure 4.1.3.2-1](#) Preforming allows metal to flow into critical areas before the surrounding metal is locked.

If the sequence were reversed, the edges of the stamping would be restrained or even locked. Instead of metal flowing from the binder, the entire length of line would be generated by stretching the limited length of metal. Any number of preform stages may precede the major forming operations; the number is a function of the part requirements and each requires a separate die.

A typical first forming operation would be:

1. Blank insertion

The blank may be inserted by hand, automatic feed equipment, gravity slide, or many other methods.

2. Blank positioning

This is accomplished by hand, stops, guide pins, index fingers, or other methods.

3. Closing the hold down (binder) ring (if equipped)

This action places restraint on the blank to control metal flow into the die cavity and reduce buckling within the flange material. The binder ring may be in a single plane or may be developed in the third dimension ([Figure 4.1.3.2-2](#)). The developed binder preforms the blank closer to the contours of the punch. This helps to eliminate metal being trapped under the punch, avoids pulling metal into the die on sharp radii, encourages uniform metal flow, and balances forces on the punch to avoid skidding of the character line.

4. Punch Action

The punch now moves towards the blank, contacts the blank, and moves the specified distance into the die cavity. The main portion of the forming is accomplished during this segment.

5. Retraction

The punch and blank holder ring retract to create a die opening. The height of the die opening depends on the stroke of the press and the dimensions of the die set; it must be greater than the height of the stamping being withdrawn.

6. Ejection

Various lever, air, spring, arm, and other systems are used to remove the stamping from the die.

7. Transfer

Manual, semi-automatic, or automatic systems are used to transfer the stamping from one die to the next. The next die may be in the same press in the case of progressive die sets or transfer presses. It may be in the next press in a press line, elsewhere in the plant, or in another plant somewhere across the country.

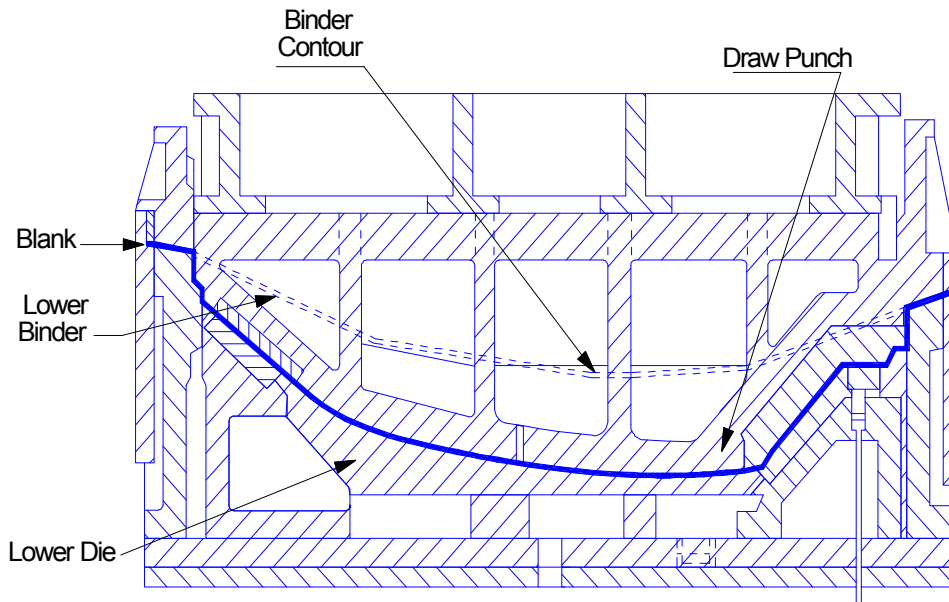


Figure 4.1.3.2-2 A contoured (developed) binder

4.1.3.3 Subsequent Operations

A wide variety of stamping operations may be subsequently performed, such as redraw, restrike, rim, flange, reverse flange, punch, pierce or extrude. Descriptions of these operations are best found in handbooks and will not be detailed here.

Any one of the subsequent operations may be the finish or final operation, depending on the die designer. The only requirement of the finish operation is that the part be finished as it leaves this operation in compliance with the part print. During the production day, numerous stampings are removed from the finish operation, taken to checking fixtures to determine accuracy to part print, to "green rooms" for visual evaluation of surface quality, and to other part quality audits.

4.1.4 PRESS AND TOOLING DESCRIPTIONS

4.1.4.1 Presses

Presses are identified by different methods. Some of the more common methods are:

1. Tonnage

Typical identifications are 300 ton, 600 ton, 200 ton outer slide/400 ton main ram.

2. Source of Power

Occasionally the source of power is manual, either hand or foot powered. Mechanical powered presses, sometimes called toggle presses, store energy in a flywheel, and transfer it to the workpiece by gears, cranks, eccentrics, or levers. Hydraulic cylinders apply the load in hydraulic presses.

3. Number of slides

Presses may be classified as single action, double action or triple action.

4. Type of frame

Mechanical presses are classified as straight side or gap frame.

5. Forming function

Presses are classified as blanking presses, press brakes, draw presses, trim presses, four slide presses, etc.

6. Size of the press opening and press bed

The content of the press line, in terms of total number of presses and the capabilities of each, is essential to the design and manufacturing of a part. Large stamping plants have a fixed number of presses of fixed size and types in each line. The number of dies can be less than the number of presses. However, when the number of dies exceeds the number of presses available, a major problem occurs and off-line operations are required. Thus, the complexity of a given part may be governed by the number and type of dies and the number of operations that can be performed in each die. Simultaneous engineering is advantageous because the characteristics are known for the press line to be used in forming each stamping. The alternative is to design to a uniform set of specifications for all die sets and presses.

4.1.4.2 Dies

One or more dies is placed within the press opening. Die is a generic term used to denote the entire press tooling used to cut or form sheet metal. The term is also used to denote just the female half of the press tool ([Figure 4.1.4.2-1](#)). The major components of the die are the guidance system, punch, blank holder and female die. There are many variations. For example, the punch may be attached to the lower bed of the press and the female die cavity moved up and down on the main ram. Details of die design and die construction can be found in a number of good textbooks and reference manuals and will not be included here.

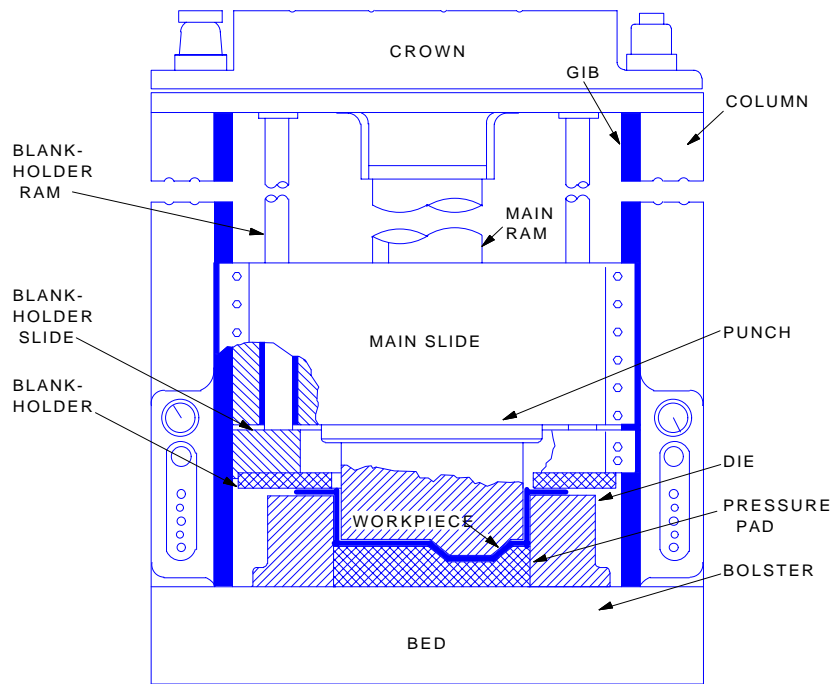


Figure 4.1.4.2-1 Major components of a hydraulic press and die

4.1.5 GENERAL METAL DEFORMATION

4.1.5.1 Stress and Strain

Simple sheet metal forming is based on the concept of applying a sufficient force on a sheet of metal to create a permanent deformation. Deformation processes rely on the capacity of a material to respond in a predictable manner when subjected to applied stresses. There are four principal types of response: elastic, uniform, necking, and fracture. Please refer to [Section 2.12](#) for a discussion of these responses in terms of material properties.

When the level of stress exceeds the yield strength of the material, the deformation is composed of both elastic and plastic deformation. When the sheet of metal is unloaded from the plastic deformation region, the plastic component of deformation is retained and the shape generated by plastic deformation remains.

The elastic component attempts to neutralize itself; this reverse of deformation is called springback. The elastic stresses that can not be neutralized remain as a complex set of residual stresses, which may or may not affect the stamping. They may be relieved in subsequent forming operations, upon heating the stamping (paint bake oven), or in service. The residual stresses may react with a mechanical magnification that can cause major distortion in the form of reduced part depth, twist, flare, camber, curl, and many other undesirable forms. Elimination, or at least minimization, of springback is another specialized art in sheet metal forming.

Plastic deformation continues with increasing stress until the forming limit of the material is exceeded. An obvious goal for the simultaneous engineering team is to develop an acceptable part geometry by careful selection of the material, forming modes, dies, and presses such that the stamping remains in the uniform deformation region and the resultant springback does not violate the required dimensional accuracy of the final part.

4.1.5.2 Material Formability Parameters

A number of parameters or sheet metal characteristics can be measured and correlated to the capability of the sheet metal to be formed by different forming modes. Unfortunately, different forming modes correlate with different parameters. Therefore, when sheet steel is made, the critical forming mode must be known so that the value of the appropriate forming parameter can be maximized. The parameters of interest to the simultaneous engineering team are work hardening exponent (n), plastic strain ratio (r), strain rate hardening exponent (m), total elongation, yield strength, and forming limit. These parameters are discussed in [Section 2.12.2](#) except forming limit, which is discussed in [Section 4.1.5.4](#).

4.1.5.3 Circle Grid Analysis

Circle Grid strain analysis (CGA) is a technique employed during die tryout, and sometimes during production, to analyze and quantify plastic deformation in sheet metal. Analysis of the grids can suggest methods for reducing forming severity¹, making die tryout more of a science and less an art.

A sheet of steel is prepared for CGA by etching a circle grid onto the surface. Many different grid patterns exist. A typical grid, shown in [Figure 4.1.5.3-1](#), consists of 0.1 in. diameter circles arranged in rows and columns on 0.125 in. centers, and a 0.25 in. square grid pattern. The etched pattern remains intact while the steel is processed through the forming operations. Plastic deformation in the steel causes the circles to deform into ellipses. The amount of plastic strain at each circle can be observed and quantified by measuring the major and minor diameters of the ellipses. The relatively small size of the circles, and fairly precise measuring procedures give a detailed, quantified pattern of plastic strain in the stamping.

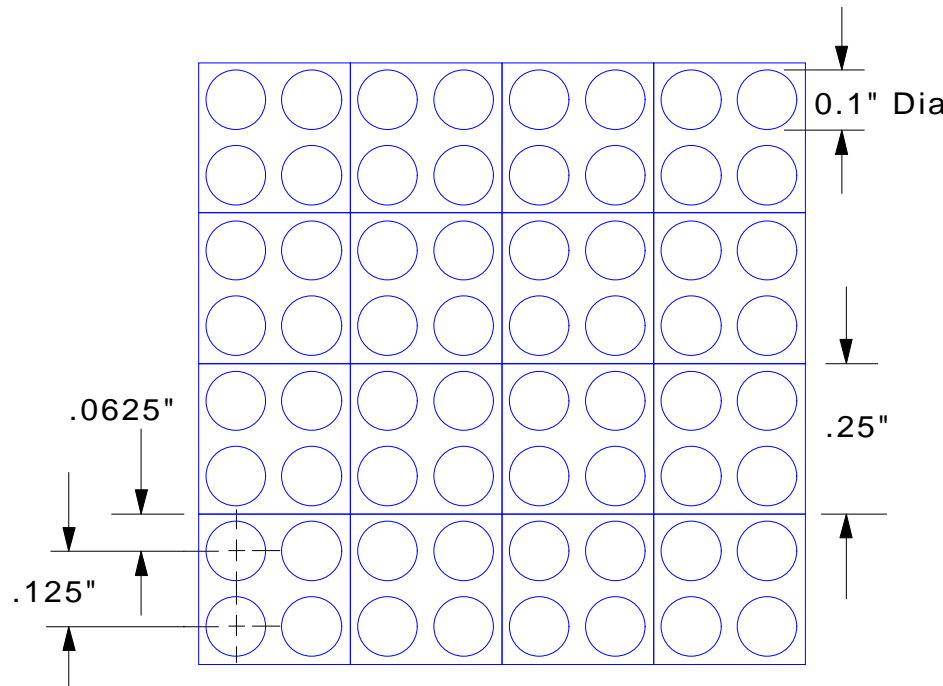


Figure 4.1.5.3-1 Typical circle grid pattern

A series of CGA runs is often made through various stages of metal forming. When deep draws are required, the press may be stopped at several increments of punch travel (such as 25%) and the samples compared to track the plastic strain at each location on the part. When stampings are made on progressive dies, samples are made for each stage. This procedure indicates at what stage forming problems occur as well as where the critical locations are on the part.

The orientation of the major axis indicates the direction of major strain. Strain is quantified by comparing the major and minor axes with the original diameter of the circles according to the formula:

$$\% \text{ Strain} = \frac{l_2 - l_1}{l_1} \times 100$$

Equation 4.1.5.3-1



where l_1 = initial circle diameter

l_2 = final major or minor ellipse diameter

The major diameter of the ellipse is always larger than the initial circle diameter, so that major stretch is always positive. The minor diameter may be greater or less; minor stretch may thus be either positive or negative (see [Figure 4.1.5.3-2](#)).

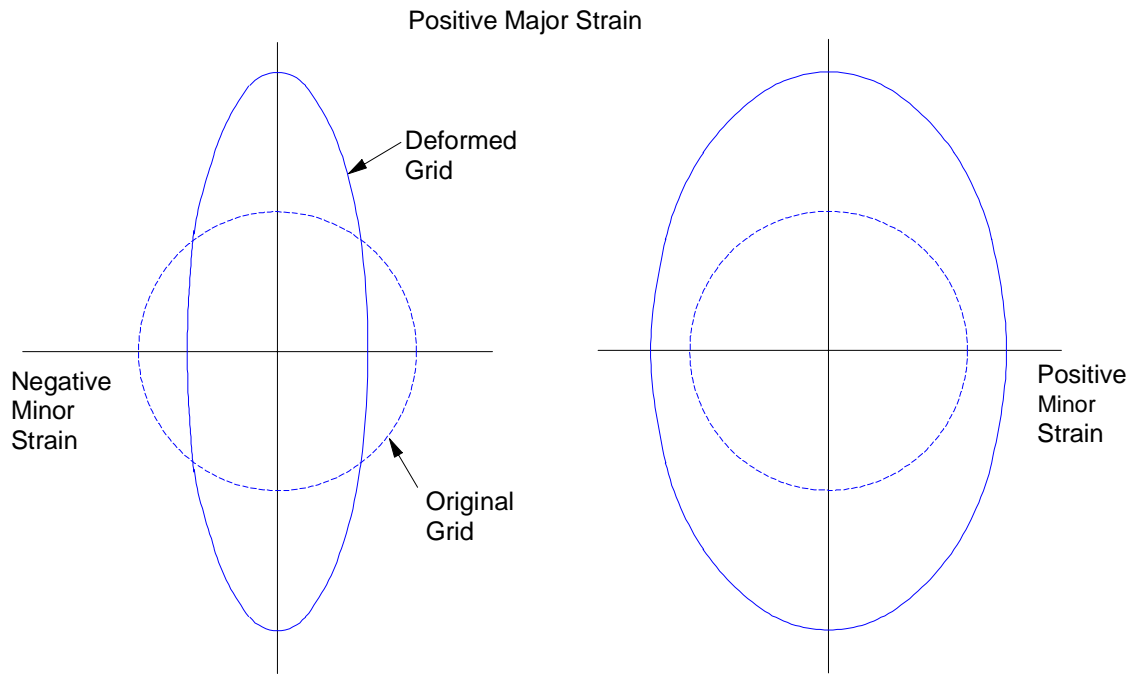


Figure 4.1.5.3-2 Representation of strains by etched circles

4.1.5.4 Forming Limit Diagram

The forming limit diagram (FLD) is derived from the circle grid analysis to provide information useful to die designers, part designers, and steel suppliers. The percent of major and minor strain, which are computed in the CGA, are plotted on a forming limit diagram such as the one shown in [Figure 4.1.5.4-1](#), which applies to a low carbon, low strength steel 1 mm (0.04 in.) thick.

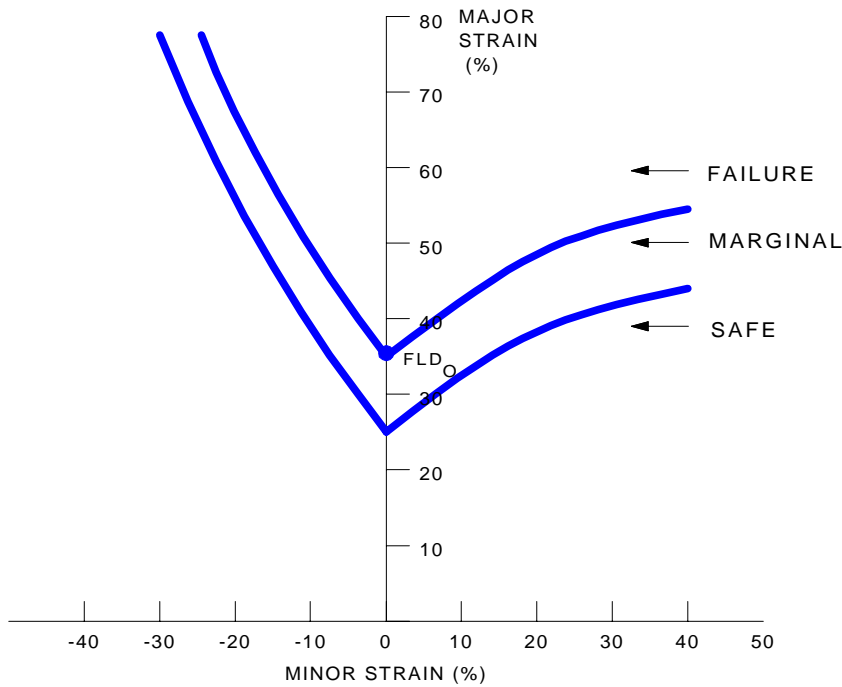


Figure 4.1.5.4-1 Typical forming limit diagram

The diagram has a vertical axis for positive major strain and a horizontal axis for positive and negative minor strain. Two parallel curves separated by 10% strain on the vertical scale divide the diagram into three zones. Points on the stamping with large amounts of strain are plotted in relation to the axes. Locations that plot in the upper, or failure zone, will regularly fail by severe necking or tearing. Those in the intermediate, or marginal zone, will experience some failures depending on material and process variables. Those that fall into the lower, or safe zone, should not experience failures. The FLD indicates that the maximum allowable strain, and consequently the maximum length of line that can be generated in any direction, is influenced by the minor strain associated with it. The lowest value of major strain occurs when the minor strain is zero (plane strain). Positive minor strain allows some increase in major strain; negative minor strain allows substantial increase.

When areas of failure or potential failure are indicated, variables are adjusted such as binder pressure, die clearance, lubrication, steel grade or thickness. Best procedure ensures that all points fall safely below the marginal zone so that process changes, such as die wear and variations in die lubricant and sheet stock, will not shift any points into the marginal zone.

All forming limit curves for the grades of steel used in automotive bodies have essentially the same shape. The difference is their vertical position on the diagram, which is determined by the work hardening exponent, n , (Section 2.12.2) and thickness of the steel. [Figure 4.1.5.4-2](#) shows the relationship of n value and thickness to the plane strain intercept (FLD_0) for low carbon steel. The FLD_0 locates the curve on the grid. These characteristics allow the analyst to use one curve for all steel grades just by positioning it correctly on the vertical axis.

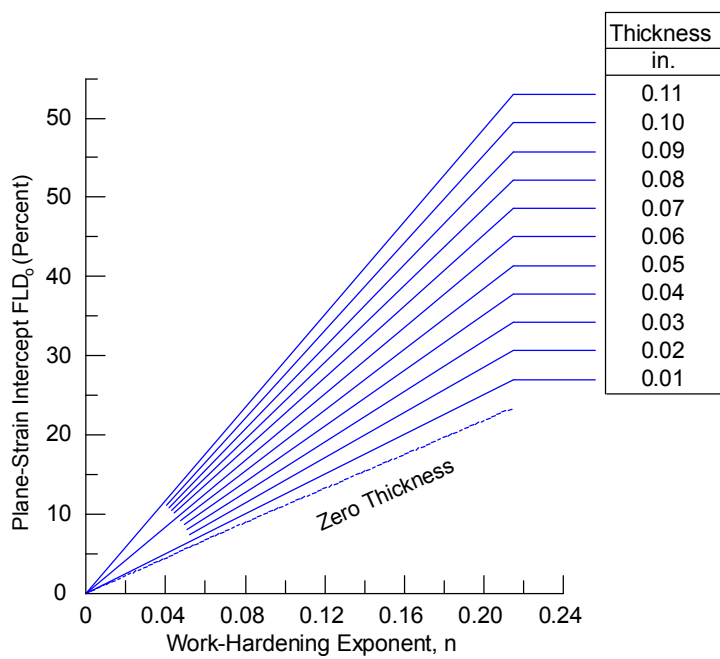


Figure 4.1.5.4-2 Effects of n value and metal thickness on formability of low carbon steel

In the absence of data for the work hardening exponent, yield strength can be used in combination with material thickness as a first approximation for locating the curve on the major strain axis. [Figure 4.1.5.4-3](#) shows the relationship of yield strength and thickness to FLD_0 . The figure indicates that FLD_0 increases with increasing metal thickness, and increases with decreasing yield strength down to approximately 47.5 ksi. These factors indicate potential problems from decreased formability when metal thicknesses are decreased and yield strength increased. Both reduce FLD_0 , decreasing the formability as illustrated in [Figure 4.1.5.4-3](#). In some cases, down gauging will require redesign of some features to reduce maximum strain, such as increased radii, reduced depth of draw, and sloped side walls.

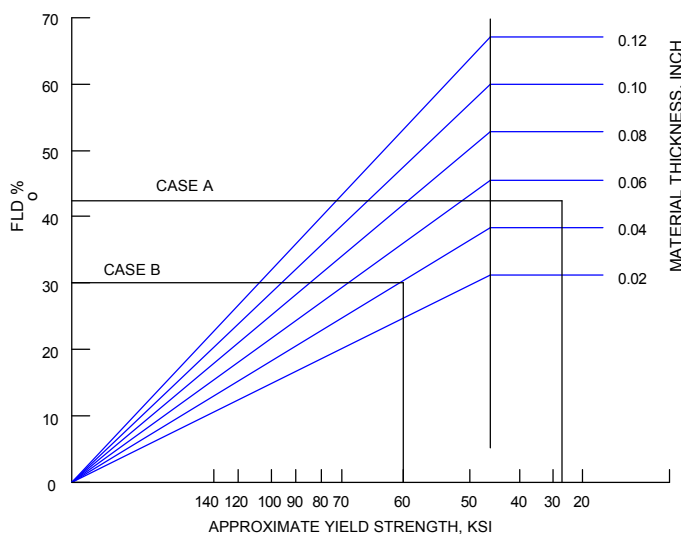


Figure 4.1.5.4-3 Effects of yield strength and metal thickness on formability. The increase in yield strength from 27 ksi to 60 ksi and the accompanying reduction in metal thickness from 0.052 in. to 0.040 in. reduces FLD_0 from 42% to 30%.

4.1.6 SHEET METAL FORMING OPERATIONS

4.1.6.1 Cutting

Cutting operations in one plane are classified by the terms shearing, blanking, slitting, piercing, and lancing. Cutting operations in more than one plane are classified by the terms trimming and parting.

4.1.6.1.1 Shearing

Shearing is done by a blade along a straight line. The work metal is placed between a stationary lower blade and a movable upper blade and is severed by bringing the blades together. Nondeveloped blanks are generated by shearing.

4.1.6.1.2 Blanking

Blanking involves a cutting action about a closed shape, which is the piece retained for further processing. The closed shape may be composed of any number of straight and curved line segments. Developed or contoured blanks are generated by blanking.

4.1.6.1.3 Slitting

Slitting is cutting lengths (usually coils) of sheet metal into narrower lengths by means of one or more pairs of circular knives. This operation often precedes shearing or blanking and is used to produce exact blank or nesting widths.

4.1.6.1.4 Piercing

Piercing is forming a hole in sheet metal with a pointed punch with no metal fallout.

4.1.6.1.5 Lancing

Lancing makes an opening without completely separating the cut piece from the body of the metal sheet, such as for louvers.

4.1.6.1.6 Trimming

Trimming removes unwanted metal from the finished part that was required for some previous stamping operation, such as binder areas, or was generated by a previous stamping operation, such as the earing zone on the top of a deep drawn cup.

4.1.6.1.7 Parting

Parting operations are used to separate two identical or mirror image parts that were formed together (typically for the expediency of making two parts at one time or to balance the draw operation of a nonsymmetrical part). Parting is also an operation that involves two cutoff operations to produce contoured blanks from strip. Scrap is produced in this parting process.

4.1.6.1.8 Sheet Metal Cutting Theory

The same basic theory of sheet metal cutting applies to all of the operations detailed above. The cutting occurs by a combination of metal penetration and actual fracture of the metal. The clearance of the cutting knives is a critical factor in both the visual appearance and the residual ductility of the cut edge. For low strength, low carbon steel an aim of ten percent clearance is used for automotive body panel stock.

The most important stamping consideration for cutting is the residual ductility in the cut edge. [Figure 4.1.6.1.8-1](#) shows the residual stretchability as a function of burr height. Here the burr height is the measure of damage inflicted during the cutting operation. [Figure 4.1.6.1.8-2](#) gives more specific information. Here the hole expansion values are provided for different strength steels as a function of the quality of the blanked hole.

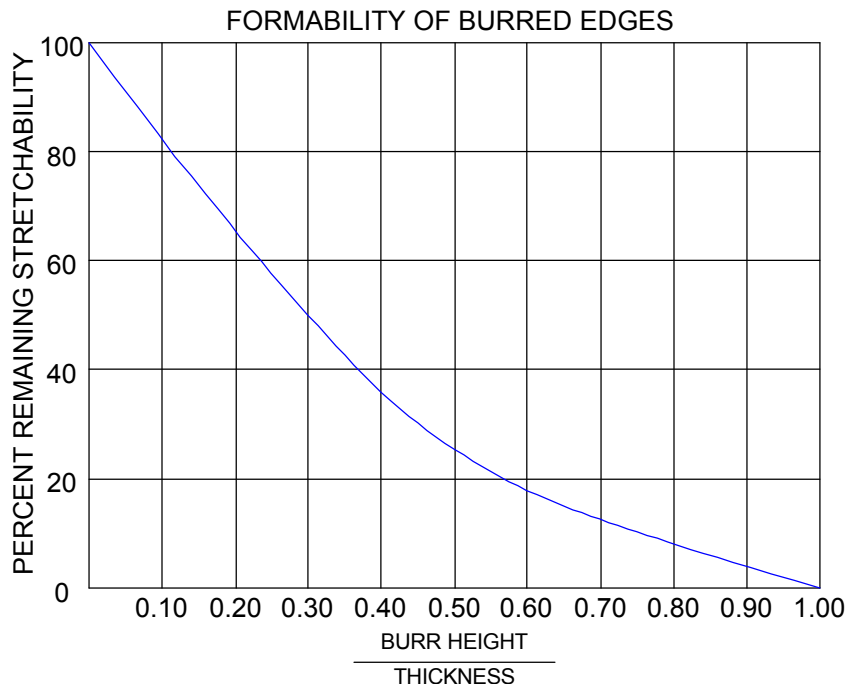


Figure 4.1.6.1.8-1 Reduction in blank edge stretchability due to blanking damage

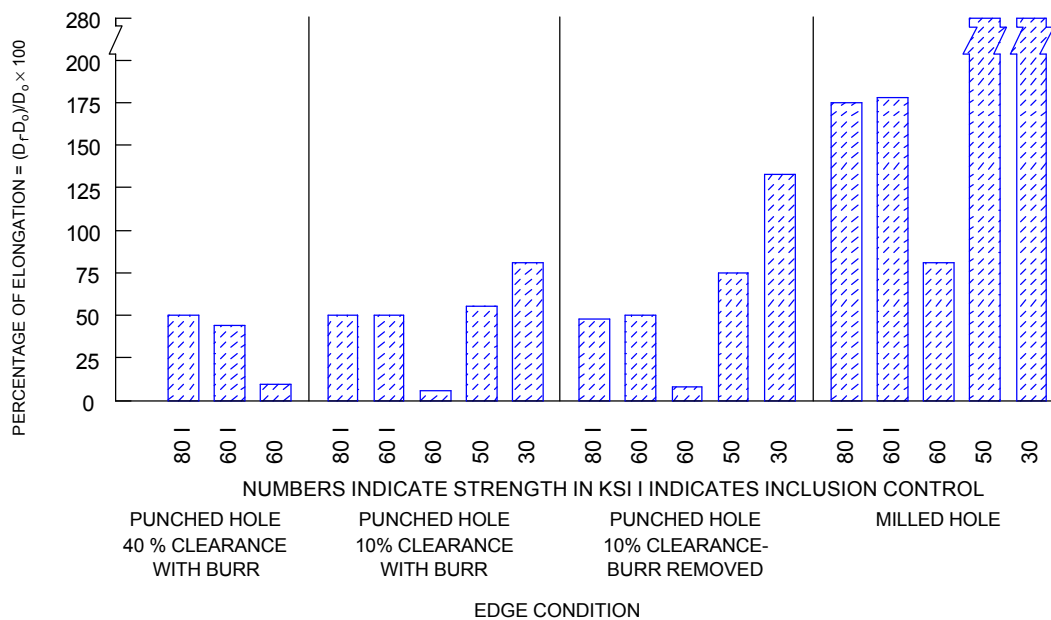


Figure 4.1.6.1.8-2 Measured percent hole elongations as a function of hole quality and steel grade

If the stretching required to make the part exceeds the residual stretchability after cutting, several avenues are available for restoring the edge stretchability. One is improving the quality of the original cutting operation. A second is an additional cut of higher quality. A third is shaving or milling the cut edge before subsequent tensile straining. A fourth is heating the cut edge to reduce the effects of the cutting operation, or "thermal deburring". If these steps are not feasible, the stamping or the part will have to be redesigned to reduce the required stretching on the blanked edge.

Metallic coatings and painted coatings can flake off the cut edge as small slivers. They may adhere to the cutter and then fall onto subsequent pieces, causing imprint damage during forming operations.

4.1.6.2 Bending

Bending is one of the most common methods used to change the shape of sheet metal. Almost all sheet metal forming operations involve bending. Bending is different from other forming modes in that a severe strain gradient is developed from one surface to the other. During bending, the maximum tensile strain occurs on the convex surface of the stamping, while the maximum compressive strain occurs on the concave surface. Somewhere within the sheet metal is a neutral axis, which does not change length. A common design assumption is that the surface area of the bend, and the thickness at the bend, do not change.

The convex tensile and concave compressive stresses tend to magnify the elastic recovery or springback reaction when the forming loads are removed. Harder or higher yield strength materials, thinner sheets, and larger bend radii increase the tendency for springback. Methods for controlling springback include overbending and stretch bending. Overbending does not reduce springback but simply adds an increment to the original bend such that the original bend angle minus the springback will equal the design angle. Stretch bending actually reduces the amount of springback by adding a through thickness tensile component, which eliminates the tensile/compressive stress gradient.

The radius of a bend in sheet metal forming is generally specified in terms of thickness of metal being bent. A sheet with a thickness of 0.75 mm (0.03 in.) bent over a radius of 3 mm (0.12 in.) would have a 4t bend. Bends therefore can vary from zero thickness to infinity (no bend) at one location and the bending can change from one location to another, even reversing the direction of the bend.

In designing bends, the best approach is to use a finite element program. Lacking that, there are many standards for bend requirements of materials in general and for specific kinds of materials under special conditions. These should be referenced when selecting a material and its bending radii.

For automotive stampings the metal thickness of cold rolled steel is generally in the range of 0.5 mm (0.02 in.) to 1.8 mm (0.07 in.). The outer body panels will cover a smaller range from 0.6 mm (0.025 in.) to 0.9 mm (0.035 in.). The bend radii for most of these stampings should be between 3t and 9t. Larger radii, up to 25t, are used if the design requires a rounded look. Too sharp a bend will cause excessive tearing, especially if there are tensile forces associated with the bend. Sharper bends usually require a restrike operation. Too large a bend radius introduces the possibility of excessive springback and the necessary larger spacing needed between the bend dies can cause loss of control of the metal being bent.

Bends are most frequently made to angles up to 90° by the vertical movement of a punch into a die opening. A hinge die can be used to overbend beyond 90°. Further bending and flattening to form a hem can be accomplished by a subsequent punch action against a backing plate.

4.1.6.3 Bend-and-Straighten

In the bend-and-straighten mode, metal flows in a straight path from the binder zone into the die radius, over the die radius in the bending operation, and out of the die radius in the straightening operation. Tensile strain is generated on the convex surface during bending and on the concave side during straightening. Because the tension on the concave side follows compression (which work hardens the metal and depletes usable formability), the concave side is more severely affected. Severity of this operation depends on the ratio of the bend radius to the sheet metal thickness. When the die radius is less than $4t$, the operation is too severe. However, when the die radius exceeds $10t$, an unsupported band is created between the die radius and the punch radius. The ideal die radius is $6t$ to $8t$.

Any tension created in the binder area can add a stretch component to the pure bend-and-straighten operation. This restraint can be created by additional binder or hold down pressure or by the insertion of "draw beads" into the binder surface. The beads are placed in the bend-and-straighten areas to restrict metal flow into the die cavity, creating an added stretch component. (Strictly speaking, draw beads resist drawing and induce stretching; they would be more accurately identified as stretch beads.)

4.1.6.4 Flanging

Flanges are short vertical bends at the edges of a panel or surrounding a hole. When bending a flanged inside corner, the corner radius should be at least $14t$ and the length of the flange should be at least $4t$. If an outside corner is to be formed with a flange, the minimum radius of the corner should be $5t$ and the angle of the corner no sharper than 60°.

In hemmed corners where the metal of the flange is folded back against the sheet, the minimum allowed corner radii are increased to $24t$ for an inside and $7t$ for an outside corner, again no sharper than 60°.

Flanges and hems are used to straighten the edges of sheet metal parts, give a smooth rounded edge to a part, or to provide hidden joints. They can be either concave or convex but in either case problems of too little metal for an inside flange, or too much metal for an outside flange, must be handled during the bending process. This is accomplished by limiting the width of the flange, cutting notches in the corner flange metal to reduce the amount of metal to be bent and stretched or shrunk, or designing offsets to take up excess metal. Offsets are displacements of a few metal thicknesses, similar to those used to form license plate numbers. For corner flanges, the offsets can be considered designed wrinkles. Edges that must be strengthened further than is possible by hemming are curled.

Shrink flanging tends to generate buckles and loose metal. Careful control of punch/die clearances is required to produce a "clean" flange. In contrast, stretch flanges suffer from edge cracking and tearing if the stretching limits are exceeded. The simplest analysis is to calculate the increase in length of line assuming that the stretch flange is made up of segment(s) of a circle.

The elongations for steel are compared to the experimental hole expansion limits shown in [Figure 4.1.6.1.8-2](#). These limits are conservative for stretch flanges. Unlike the true hole expansion test where the entire hole perimeter is subjected to the same elongation, the adjacent metal in a stretch flange may be undeformed or may even be in the shrink flanging mode. Thus

adjacent areas to the stretch flange may be able to feed metal into the stretch zone and reduce the required elongation.

4.1.6.5 Hole Expansion

Typical limits for hole expansion for steel are given in [Figure 4.1.6.1.8-2](#). The maximum amount of elongation depends on the quality of the edge of the expanding hole and the stretchability of the steel. The hole expansion capacity of the steel increases with increasing n value, m value, total elongation, and r_m value (See [Section 2.12.2](#)).

4.1.6.6 Biaxial Stretch

Limits for biaxial stretch are defined by forming limit diagrams, which are briefly described above. Unfortunately, the distribution of stretch over a punch is very nonuniform and varies from point to point, both in major strain and minor strain. This variation is due to punch geometry, lubrication, and many other factors. The most accurate analysis is accomplished during soft tooling tryout. Some predictive capabilities are available with mathematical modeling programs. As a very rough calculation, the maximum depth of a hemispherical segment is equal to 80 percent of the sum of the punch radius and the die radius. A complete hemispherical shape is not achieved for steel except for unusual lubrication conditions.

4.1.6.7 Deep (Cup) Drawing

The cup drawing operation is rather well defined compared to the stretch forming operation. The design limits are defined by the Limiting Drawing Ratio (LDR).

$$LDR = \frac{D}{d}$$

Equation 4.1.6.7-1



where D = the diameter of the largest blank that can be successfully drawn into a cup with a diameter d .

The Limiting Drawing Ratio is a function of the r value of steel ([Figure 4.1.6.7-1](#)), the thickness of the steel ([Figure 4.1.6.7-2](#)), and the radii of the punch and die ([Figure 4.1.6.7-3](#)). These Limiting Drawing Ratio values can be obtained only for optimum draw radii as outlined [Figure 4.1.6.7-4](#).

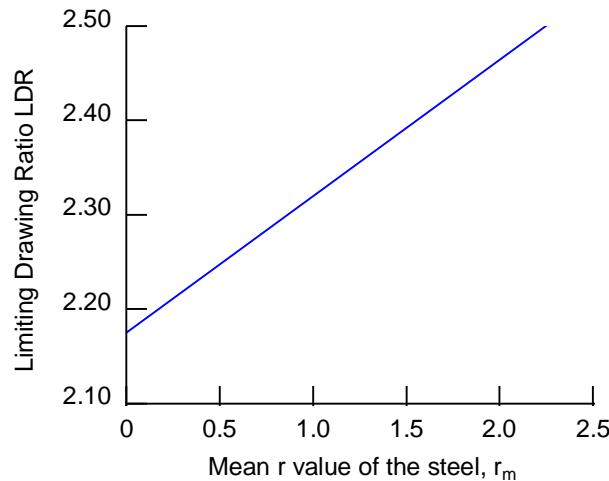


Figure 4.1.6.7-1 The limiting drawing ratio, LDR, as a function of r_m

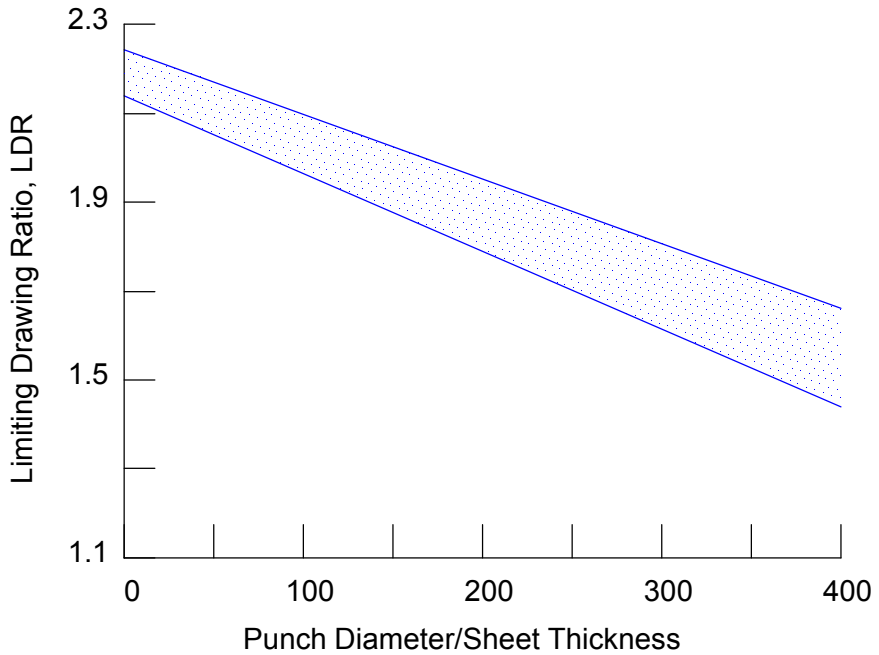


Figure 4.1.6.7-2 The limiting drawing ratio, LDR, decreases as sheet thickness decreases for a given punch diameter

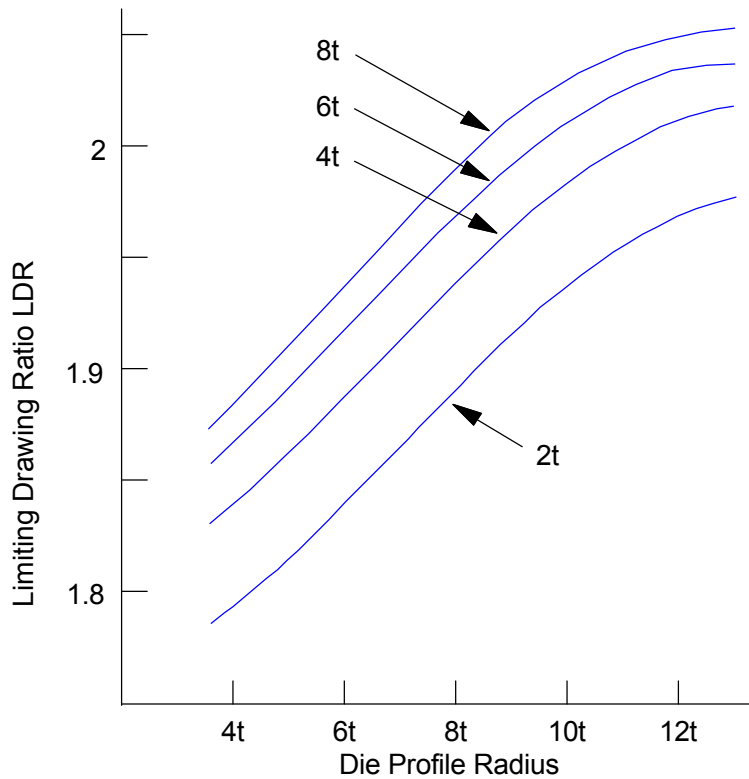


Figure 4.1.6.7-3 The limiting drawing ratio is a function of both the die profile radius and the punch profile radius (t = sheet thickness)

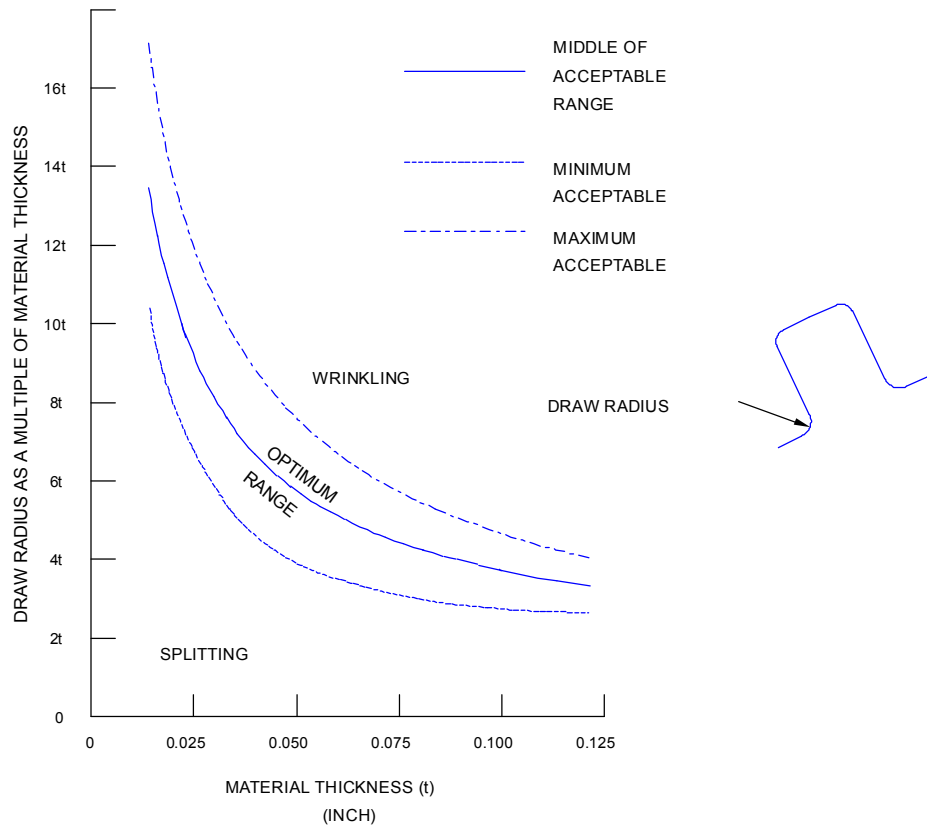


Figure 4.1.6.7-4 The optimum draw radius depends on the material thickness

If a deeper cup is required relative to the diameter of the cup, then one or more redraw operations is necessary ([Figure 4.1.6.7-5](#)).

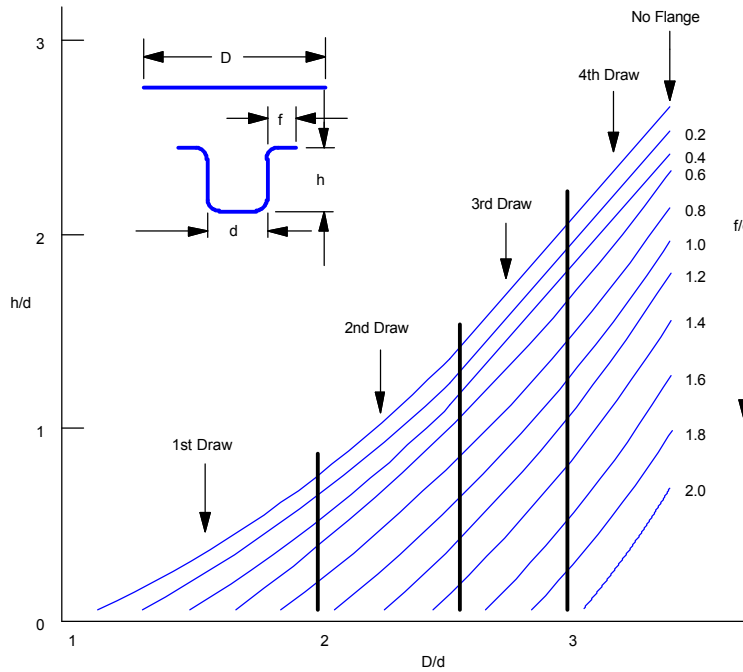


Figure 4.1.6.7-5 Calculation of a number of redraws

The stretch forming and cup drawing operations are usually in tandem along any analysis line. However, the variables for each of these forming operations are often in direct opposition to each other, as indicated in [Table 4.1.6.7-1](#).

Table 4.1.6.7-1 Comparison of stretch versus draw modes of forming

VARIABLE	STRETCH	DRAW
Critical radius	Punch	Die
Metal movement over die	None	All
Lubricant with slip	Over punch nose	Binder area
No lubricant	Binder area	Punch nose
Lubricant cooling	Not needed	Die radius corner
Anti-galling lubricant	None	Straightening zone
Sheet thickening	No	Yes
Clearance	1t	1.25t
Location of thinning	Away from pole (top)	Punch radius (bottom)
Fracture	End of stroke	Early to 1/3 stroke
Location of fracture	Changes with lubricant	Independent of lubricant
Location of wrinkles	Over punch nose	Flange of cup
Trim allowance	Large (binder area)	Small (earing only)
Important property	n	r
Press speeds effect	Limited by n reduction	r independent of speed
Maximum press speeds	<100 strokes/minute	>250 strokes/minute
Maximum punch force	End of stroke	Early to 1/3 stroke
Maximum force to mechanical press capacity	Matched	Mismatched
Binder force	10 or more times punch force	5-40 percent of punch force
Reason for binder force	Stop metal movement in flange	Prevent wrinkles in flange
Subsequent hits	To sharpen radii	To increase cup depth
Blank size/shape	Trial-and-error die tryout	Calculated
Sticking	No problem-lifters used	Problem-knockouts used
Punch venting	Prevent bursting on down stroke	Prevent vacuum on retract
Loose metal	Oil can on large punch radii	Cup edge wrinkles, die R>10t
Lüder's lines	A common problem	Seldom a problem
Critical surface smoothness	Punch and die opening sheet	Binder and flange sheet
Blank area to roughen	Binder	Punch
Major appearance problems	Pimples and dimples	Scratches, galling, impact line
Fiber direction	Critical	Non critical
Blank preformed	Usually	Rarely

4.1.7 ANALYSIS TECHNIQUES

4.1.7.1 Shape Analysis

Shape analysis is a method for determining the forming severity of stamped parts. Forming severity indicates, through a numerical value, how near a part is to failure or fracture. Shape analysis is based on stretching and deep drawing actions in sheet metal forming. These actions occur when a blank is stretched over a punch nose and drawn into a die cavity. They influence each other and react with the tooling to affect the onset and character of failure. They are very sensitive to the "tip" of the part relative to the axis of the punch and die cavity.

The shape analysis concept is extendible to any sheet metal undergoing similar modes of strain. Determining the forming severity permits reduction in strain and improvement in material economy and process efficiency by changes in the material, forming process, or part shape. The method can also be applied to parts of various designs, parts made of different materials and with different tooling, and parts on which different forming lubricants are used.

In shape analysis, the critical forming area of a part is selected for analysis. A line representing the profile of one-quarter of a cup shape is marked on the part through the critical area ([Figure 4.1.7.1-1](#)). The cup center, the outer edge of the cup, and the boundary between stretch and draw types of strain are marked. Measurements are made of the amount that the lines lengthen due to the forming actions. Proportions of stretch and draw cup are calculated. Laboratory cups and domes made from the same material give forming parameters that are compared to the measurements, and the forming severity is calculated. From the forming severity and other parameters, the need for changes in shape, process, or material can be determined. Analysis can be made of other areas of the stamping and compared for severity.

Additional information and illustrations of the shape analysis technique can be found in a handbook on tooling and manufacturing [2](#).

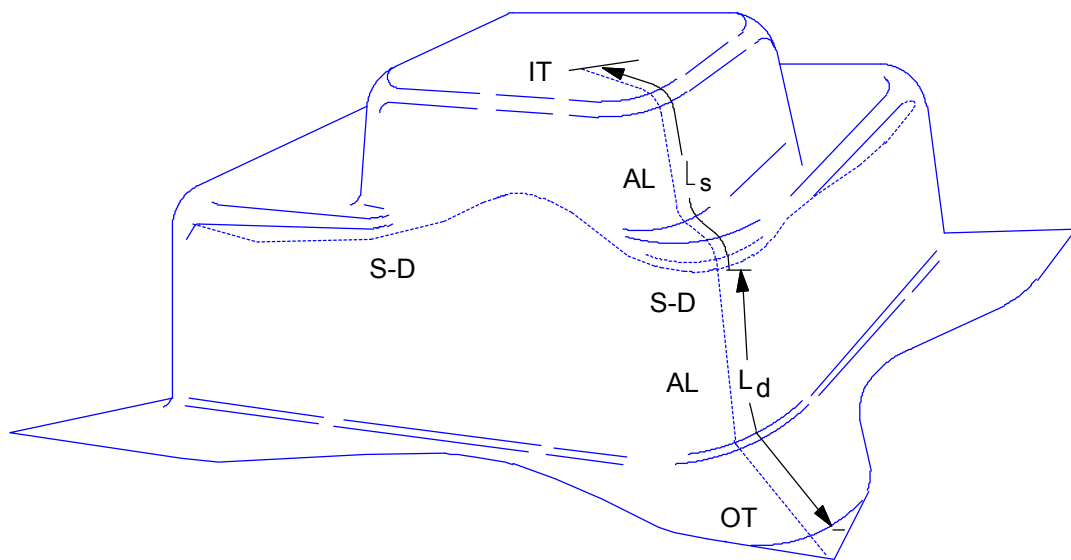


Figure 4.1.7.1-1 Deep drawn pan illustrating analysis line locations for measurements using shape analysis techniques

4.1.7.2 Mathematical Modeling

Different types, levels, and complexities of mathematical modeling are emerging as design and analysis tools for sheet steel formability. They describe the deformation behavior of sheet metal by mathematical equations. The deformation of the sheet metal is calculated based on finite element analyses and the stresses and resulting strains developed in the forming cycle.

A discussion of the various mathematical modeling techniques is beyond the scope and intent of this section.

4.1.7.3 Circle Grid Analysis

Circle grid analysis (CGA) techniques can be used when a first hit of the stamping has been made on prototype or hard tools to determine sheet metal flow patterns, the respective forming modes, and the resulting severity. CGA and the related forming limit diagrams are discussed in [Section 4.1.5.3](#) and [Section 4.1.5.4](#).

4.1.8 ENGINEERED SCRAP

Engineered scrap, sometimes termed "offal", is the excess raw material that is inherent in the design and production of steel stampings. In some organizations, offal identifies the material that can be utilized for another part. Engineered scrap is an important part of the material cost because it is only partially recoverable. It is unavoidable because a steel body stamping utilizes less, often substantially less, than 100% of the material in the blank or coil. Perimeter material that is required to clamp the blank during forming operations is discarded. Interior openings, such as the window openings in a door, are also frequently discarded although in some cases the material is used to make another part ([Figure 4.1.8-1](#)). Engineered scrap is recycled, but it brings a markedly reduced price compared with the price of sheet stock.

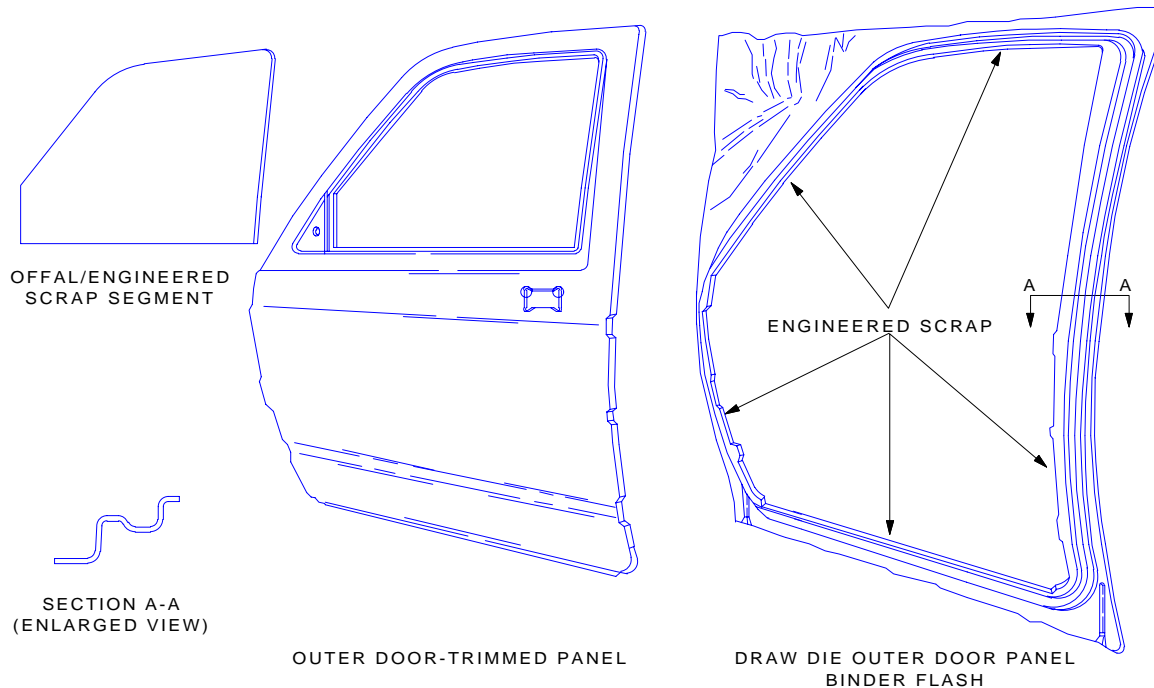


Figure 4.1.8-1 Engineered scrap from an outer door panel

Individual profit centers may develop special formulas for computing engineered scrap. The simplest concept is expressed by the formula:

$$\text{Engineered Scrap} = \frac{\text{Mass of metal consumed} - \text{mass of parts produced}}{\text{Mass of metal consumed}}$$

Equation 4.1.8-1



The high percentage of material that becomes engineered scrap (more than 30% is common) and its low value combine to make engineered scrap reduction a prime potential area for body-in-white cost reduction. It can potentially be minimized by joint efforts between design and manufacturing engineers in the following areas:

1. Assessment of part design and its impact on material requirements to reduce the blank size or length of coil required.
2. Assessment of draw die or form die development to minimize the amount of perimeter material required to process the part.
3. Nesting of blanks, where possible, to reduce the sheet size or length of coil required.
4. Assignment of cut out material, where possible, to recover material that would otherwise be scrapped.
5. After several manufacturing runs have been made, quality has been established and manufacturing parameters have been fine tuned, conduct a review to determine if further blank size reductions are possible.

REFERENCES FOR SECTION 4.1

1. American Iron and Steel Institute, Sheet Steel Formability , August 1984, Washington D.C.
2. The Tool and Manufacturing Engineers Handbook - Volume 2 - Forming, Society of Manufacturing Engineers , Dearborn, Michigan, 1984 pp 1-24 to 1-33.

BIBLIOGRAPHY FOR SECTION 4.1

1. Dinda, S., James, K.F., Keeler, S.P. and Stine, P.A. How to Use Circle Grid Analysis for Die Tryout, Metals Park, Ohio, American Society for Metals, 1981
2. Keeler, S.P. A Short Course in Circle Grid Analysis , Livonia, Michigan, National Steel Corporation, 1986

4.2 ROLL FORMING

4.2.1 INTRODUCTION

Roll forming is a high speed forming process that can be used to form a variety of automotive body components. The starting material, usually a flat strip in coil form or occasionally in precut strip configuration, is formed and at the same time longitudinally moved by pairs of rotating tools, until the finished shape exits at the end of the mill.

Most roll forming lines process 0.15 to 10 mm (0.006 to 0.390 in.) thick material at a speed of 20-70 m/min (65-270 ft/min). A mill running only 50 percent of the time at approximately 60 m/min (200 ft/min) forming speed produces almost 15,000 m (50,000 ft) of product in a single 8 hour shift. Practically any material that can be formed by other processes can also be roll formed.

4.2.2 GENERAL DESCRIPTION

Products are usually roll formed at room temperature (hence the name cold roll forming) producing straight, longitudinal bend lines without changing the thickness of the material. Roll forming, however, has the capability to shape parts at high temperature, produce curved parts, bend perpendicular to the direction of rolling and change the thickness of the material [1, 2, 3](#).

Roll forming, like any other manufacturing process, has its limitations but its advantages far outweigh its disadvantages. Because of its high productivity the trend is to incorporate as many other operations into the roll forming lines as is economically feasible. This arrangement permits the production of the finished or semi-finished components from strip within seconds, without material handling and storage between operations. Since roll forming lines can be made flexible and programmable and produce parts with practically no scrap, the roll forming process can easily fit into the concepts of Just in Time Production, Flexible Manufacturing System, or Net Shape Process.

Roll forming is used to manufacture a large variety of products. Typical roll formed automotive components are: frame and panel members, seat adjusting parts, crash barriers, trims, window components, bumpers [4](#), channels, van components, sun visor supports, radiator parts, and tubular components. [Figure 4.2.2-1](#) and [Figure 4.2.2-2](#) show examples of the roll formed components. Products can be made out of mild or high strength steels, uncoated, galvanized or prepainted, as well as stainless steels or bimetals.

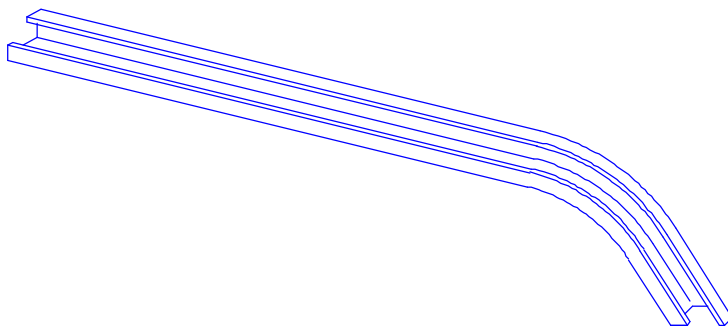


Figure 4.2.2-1 Minivan sliding door track 2 side galvanized 0.075", Chrysler Corp

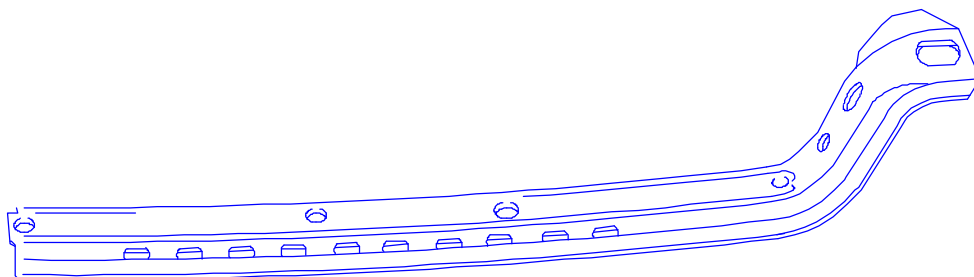


Figure 4.2.2-2 Adjustable curved seat track, A.G. Simpson

Different metallic and nonmetallic materials can be combined into one product in the roll forming process. The different materials can be held together by mechanical joining, welding, adhesive bonding or plastic can be extruded on the metal. Roll forming can produce parts with insulating material attached to it or make laminated sandwich composites.

4.2.3 ROLL FORMING LINE

The basic roll forming line consists of an uncoiler, a roll form mill and a cutoff press. A simple line, however, may consist of a single roll forming mill fed with precut strips. At the other end of the scale are more complex lines that may have two uncoilers; several prenotching presses, cutoff, and/or piercing and forming presses; and two or three roll forming mills. They may contain other production equipment such as resistance, high frequency or other welders; adhesive applicators; rotary piercing or embossing units; automated part feeders and assembly units; curving rolls or blocks; painting and packaging equipment; or robots. Computers or programmable controllers are frequently utilized to manufacture products with variable hole patterns, lengths, widths or weld spacings in one setup.

A small percentage of roll forming lines are fed with precut blanks. Precutting can be done on separate machinery or a cut to length line can be installed ahead of the roll former. If the blanks are precut on separate machinery, they can then be fed into the line manually or by an automatic sheet feeder. The advantage of a precut line is that a cut off die change is not required for each different profile.

The disadvantages of rolling pre-cut blanks are:

1. The length of finished products usually cannot be less than approximately two times the horizontal center distance between roll forming stands.
2. Productivity is lower.
3. It is more difficult to keep tight tolerances.
4. End flare is more pronounced than in sections made from a continuous strip.
5. More forming passes are required to compensate for flare or tolerance problems.

Therefore, most products are made from coils (reels) and are cut to length after forming in the line. Material for so called "continuous" roll forming is supplied in coil form. The coils are placed on an uncoiler (frequently called decoiler or reel) positioned ahead of the roll former. Most uncoilers are equipped with adjustable brakes to prevent unreeling when the line is suddenly stopped and some have an optional drive to ease the feeding of thicker materials or heavier coils. Uncoiler drives are also used when a loop is required between the uncoiler and the

next intermittently operated or stationary equipment. They may also be equipped with a peeler table (or feeder) leading the end of the coil directly to the next equipment.

To minimize the unproductive coil change time, double arm uncoilers can be used. While one mandrel (arm) supplies the material to the roll former, the other one can be loaded. For automotive applications double uncoilers are recommended. Occasionally the tail end of the last coil and the leading end of the new coil are welded together in a coil end joiner. If it is advisable to run the roll former without any interruption, such as in the case of welded tube manufacturing or painting, a strip accumulator can be installed between the roll former and the end joiner. The accumulator has enough material stored to supply the mill while the new coil is fed into the line and welded to the tail end of the last coil.

Strip flatteners/straighteners are usually not required for products that are just roll formed. They may be used, however, if products are prepierced before roll forming.

Roll forming mills are available in many variations ⁵. They can be divided into two major types: outboard and inboard mills. In outboard mills the rolls are mounted on cantilevered (overhanging) shafts. This type of mill is used to form lighter metal strips or the edges of wider sheets. Two outboard mills facing each other on a common base with adjustable distance between them are called duplex mills. For automotive purposes usually the inboard (standard or conventional) type of mill is used. In this type of mill the shafts (sometimes called spindles or arbors) are supported at both ends. The vertical distance between the shafts is variable and either both top and bottom or at least the bottom shafts are driven. To roll form the products within the specified tolerances, the mill must have enough stands (passes) with adequate diameter shafts. The shaft shoulders, against which the rolls are set, should be aligned within 0.075 mm (0.003 in.) in the vertical and 0.25 mm (0.010 in.) in the horizontal direction.

To minimize tool changeover time and eliminate set up time it is recommended that a rafted type of roll forming mill be used. In the case of rafted mills the stands, shafts and rolls are fastened to removable steel plates. To change the mill from one profile to another only one or a few rafts have to be replaced.

Roll forming mills, in addition to the usual housings, shafts and rolls, have other units to help or complete forming. Among them are the entry rolls, entry guides, side stands, strip supports between stands, rotary piercers, straighteners and curving stands. All these units can play an important role during manufacture of the product.

In most roll forming lines a cutoff press is used to cut the formed product to specified lengths. The cutoff press can be used for piercing, notching, bending, embossing, swageing or for other operations in addition to cutting the product to length. It is common to apply prepiercing presses to pierce holes or to make notches, dimples, embossments, etc. in the flat strip or partially formed section. Most lines contain one prepiercing press, but occasionally three to four presses and two to three mills are combined in a single line to manufacture more complex parts. The maximum speed of the line is frequently restricted by the maximum number of press hits per minute. Therefore high capacity, relatively fast presses should be used for prepiercing and for cutting the pieces to length.

To avoid product buckling and/or distortion of the product during cutting, the cut-off die must be accelerated to the speed of the roll formed section while the material is cut through. Different methods are used to sense the length to be cut and accelerate the die. The combination of the length sensing system, die accelerator and other components will influence the length tolerance ⁶.

Prepiercing and other operations in the starting strip can be accomplished also with "flying" tools in the so called tight strip arrangement or with stationary dies having a loop ahead and after the press.

4.2.4 COMBINING OTHER OPERATIONS WITH ROLL FORMING

The productivity of roll forming is so high that it is desirable to incorporate as many other operations in the line as is economically and technically feasible. In most cases the combined operations can be executed without additional operators. Therefore, this eliminates the labor cost of the added operations (with the exception of setup cost) as well as material handling and inventory between operations. Some of the operations that can be included in roll forming lines are illustrated in [Figure 4.2.4-1](#).

Piercing holes		Curving or sweeping	
Notching corners		Marking (stamped, embossed, inked)	
Lancing tabs		Coining, locally or in a continuous line	
Stitching materials together		Arc or laser welding	
Louvering for ventilation		Resistance, high frequency or induction welding	
Mitering corners		Adhesive bonding, caulking	
Slitting edges or center		Painting	
Cutting to length		Extruding plastic on rolled product	
Embossing		Packaging	
Bending across rolling		Others	

Figure 4.2.4-1 Operations that can be completed in roll forming line

Any of the additional operations can be carried out before, between, or after roll forming. The relative location of the operations are frequently dictated by the product design or availability of equipment. Careful consideration should be given however to the dimensioning and tolerancing of the drawing because it can have a significant influence on the cost of equipment, tooling and manufacturing. (Please refer to [Section 3.8](#) for information on dimensioning and tolerancing.) Close cooperation between the part designer, tool designer and manufacturing personnel can reduce costs and improve quality.

4.2.5 FLOW OF MATERIAL AND TOOLING

During roll forming the flat strip entering the mill is gradually formed, step by step, until it reaches its final shape. [Figure 4.2.5-1](#) shows in a simplified way how a flat strip is formed into a U channel. While the corner line AB travels in a straight line, the edge DF travels a longer, helical way and must be elongated by EF to have continuity. Once it is fully formed, the edge FG is compressed back to the same length as the corner BC. Naturally, the longer the leg (FB distance) and the shorter the distance between the first and last pass in the roll forming line (AB distance), the greater is the strain created. Further strain is created by the brake applied to the uncoiler, by the surface speed differential between rolls, by the complexity of shape and by the lateral movement of the flat surfaces, as shown in [Figure 4.2.5-2](#).

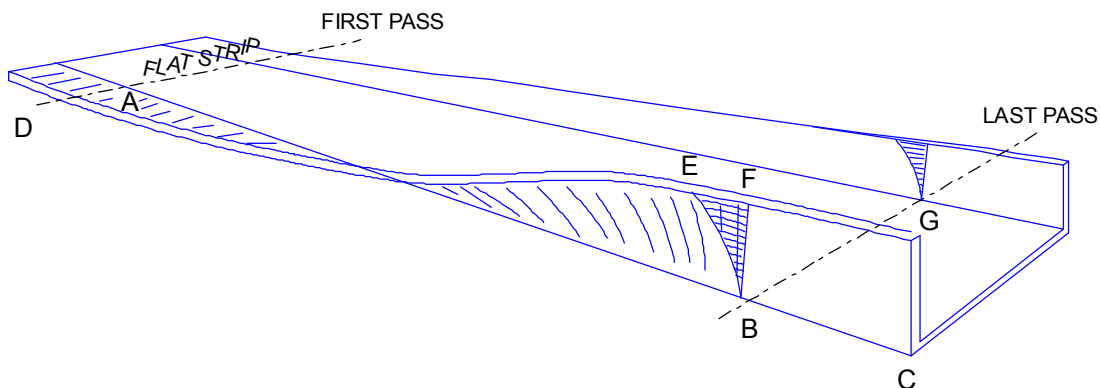


Figure 4.2.5-1 Theoretical flow of material during forming of a "U" channel. (Total elongation EF developed in DF distance is "compressed" back at F).

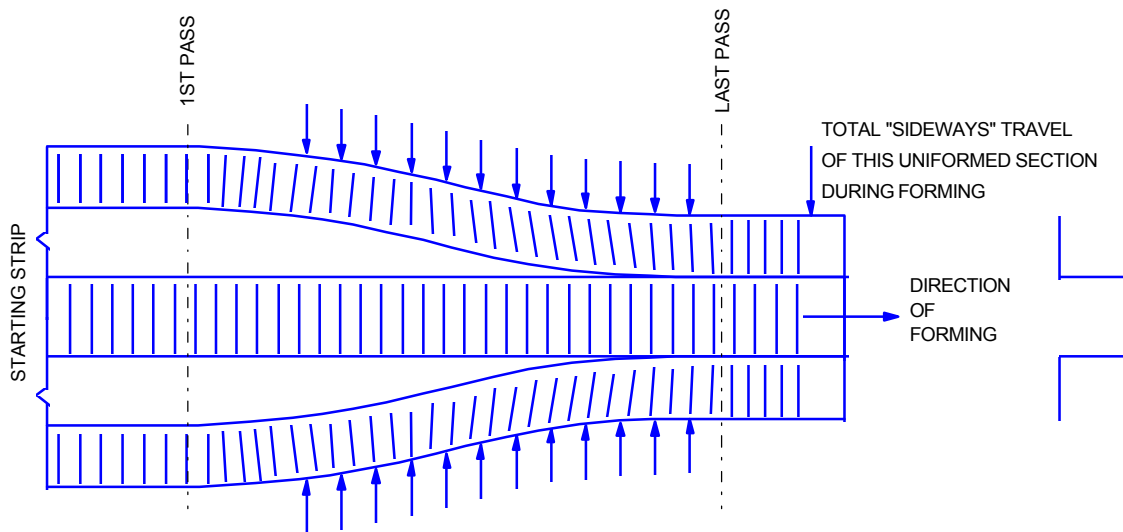


Figure 4.2.5-2 Flow of material with legs and bottom remaining in horizontal position

The actual strain will be even larger than the anticipated one caused by the idealized smooth flow shown on the previous two figures because frequently the deformation is concentrated in a short distance² where the material enters the rolls.

Further stresses and strains will be created by the imperfections of the incoming strip such as camber, twist, uneven thickness, wavy edge or wavy center. Roll forming mill and tool discrepancies, such as misaligned uncoiler or entry guides, bent shafts, misaligned tools, and worn or incorrectly designed tools can also contribute to the stresses developed in the part during forming.

The residual stresses in the different segments of the finished shape can deform the final product. In addition to springback, a variety of deviations from the straight line may occur as shown in [Figure 4.2.5-3](#). Springback, affecting both the formed angle and formed radius, is affected by the modulus of elasticity. It will be amplified by increased work hardening properties, as well as by increased forming radius, increased gap between rolls and by reduced material thickness.

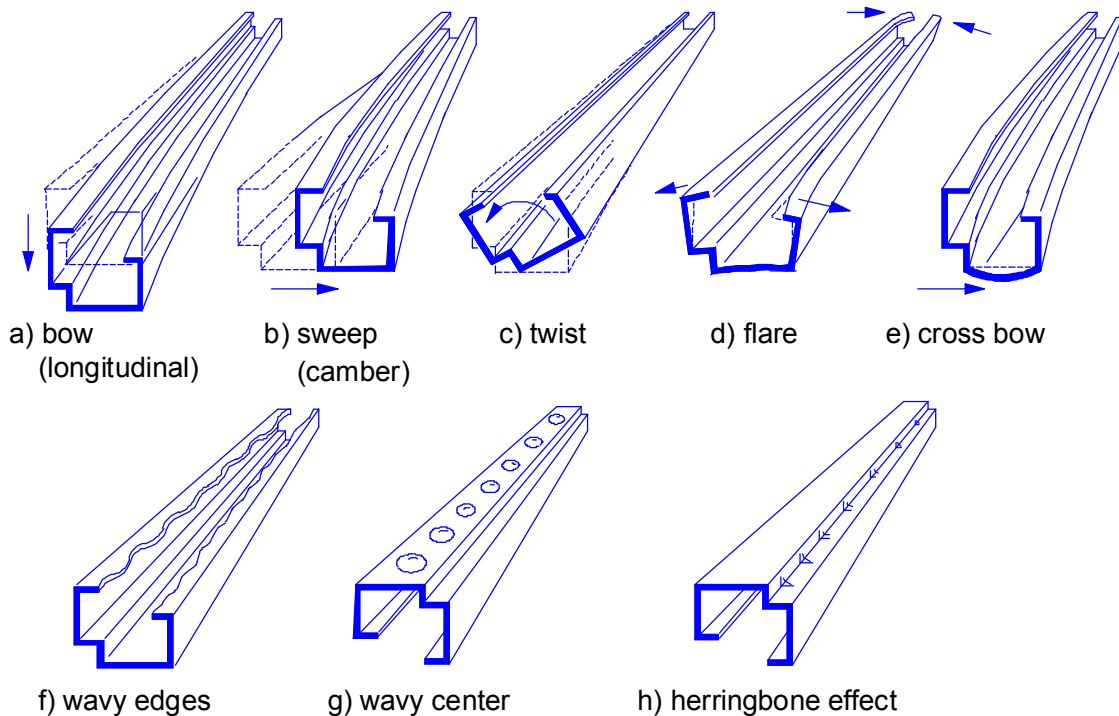


Figure 4.2.5-3 Residual stresses in material may create undesirable effects

The designer of the rolls establishes the number of passes required to produce the shape within specified tolerances. In addition to anticipating the flow of material through the mill, the tool designer must also consider the following:

1. Finished section: length of legs, open or "blind" corners, width of nonstiffened segments, etc.
2. Orientation: how the section will exit from the mill (any critical surface should be on the top side for visual inspection), direction of burrs, position of tools for any subsequent operations in the line (punching, welding, cleaning, painting, etc.)
3. Material: maximum and minimum thicknesses (including tolerances), deviation in mechanical properties, scratch sensitivity of surfaces, etc.
4. Other operations: before, between, or after roll forming.
5. Equipment: roll forming mill shaft diameters, number of passes, horizontal and vertical shaft distances, side roll stands, availability of lubrication, press capacity, etc.

The roll material or roll surface treatment specified by the tool designer will depend on the anticipated quantities to be manufactured, the type of material to be formed and the consistency of the shape required. For automotive purposes rolls are usually made out of D2 (high chrome, high carbon) tool steel, heat treated to 59-62 HRC and polished. Chrome plating is occasionally specified but it is not required for hot rolled, pickled and oiled or cold rolled material. Other surface treatments such as titanium nitride will considerably increase the tooling cost, but they provide excellent wear resistance and longer tool life.

Tool costs may appear to be high at first glance, but considering that millions of parts may be produced before replacement is required, the cost per piece of a well designed tool is relatively low. The tool designer must rely on information provided by others. Therefore, the product drawings and other documents should give all the necessary information needed for good tool design.

4.2.6 MATERIAL TO BE FORMED

Practically any steel specified for formed products in an automobile can be roll formed. Frequently, the material specification for roll formed products are less critical than they are for other operations; for example, killed or semikilled steels are usually not required for roll forming. Minimum bending radii for different steels specified in suppliers recommendations and in standards can be followed. In certain cases even smaller bending radii can be used than shown on the tables. Cold rolled, hot rolled, pickled and oiled, galvanized or prepainted steel can be processed through roll forming lines.

Metallic coated steel, however, requires good lubrication to avoid coating pickup by the rolls. Roll forming lines can handle steels with a wide variety of mechanical properties, including high strength steels⁸. Due to different springback properties, ranging from 0° to 30° per 90° bend, the rolls to form products to tight tolerances must be designed for a specific material and for a specific thickness. Material with more uniform mechanical properties and uniform thickness will produce more uniform products.

High strength steels, especially in the 690 to 1,380 MPa (100 to 200 ksi) yield strength range, having low elongation and high springback properties, will have higher residual stresses after roll forming. These stresses may cause extensive end flares or objectionable deformations around prepierced holes and will make secondary operations such as curving difficult. Careful roll design can reduce these undesirable effects although a large fluctuation in mechanical properties across the width of strip makes it more difficult to form to tight tolerances.

Strip dimensions seldom represent restrictions; equipment to roll form 0.15 to 10 mm (0.006 to 0.390 in.) thick and 3 to 1520 mm (0.125 to 60 in.) wide steel strips are commonly available.

4.2.7 DESIGN CONSIDERATIONS

The design of automotive components is covered by other sections of this manual. This section will give additional guidelines about the influence of roll forming on product design. It also highlights some of the advantages provided and restrictions created by roll forming.

4.2.7.1 Bending Radii

The minimum bending radii for different material thicknesses and qualities are available in supplier's data sheets and standards. The inner radii of the forming rolls are usually made to

match the specified minimum radii, based on the maximum material thickness (including thickness tolerance) to be formed.

It is possible to form sharp inner corners in profiles made out of steel by grooving the flat strip as shown in [Figure 4.2.7.1-1](#). The reduced strength of corners due to reduced material thickness and notch effect should be taken into consideration.

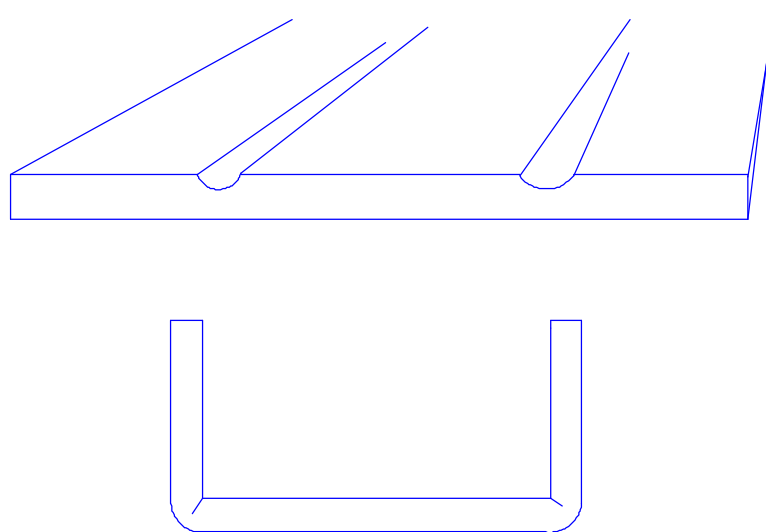


Figure 4.2.7.1-1 Grooving strip to form sharp corners

High strength steels require larger bending radii (typically two to five times material thickness) and considerable overbend to compensate for springback. The designer should provide sufficient space for overbending ([Figure 4.2.7.1-2](#)).

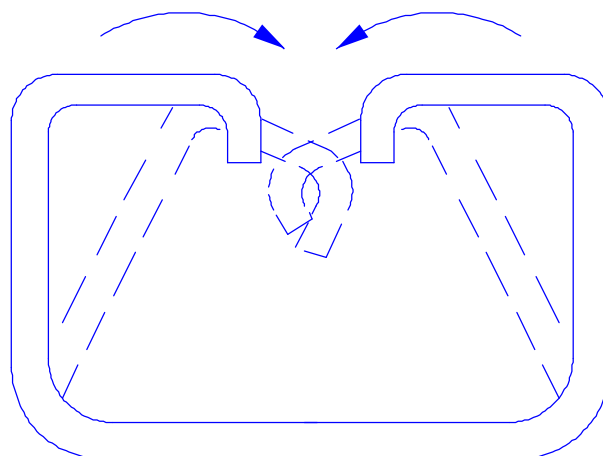


Figure 4.2.7.1-2 Space for overbending must be provided when springback is significant

Forming angles under 90° is usually simple. Bending over 90° requires more passes. When part of the section is bent over 90° , or another part of the formed section is covering the corner to be bent, a blind corner is created. The male die can not reach into the blind corner and the pressure applied on the segments to be formed may bend other segments as shown in [Figure 4.2.7.1-3](#). Some of these difficulties can be overcome by creating a false break to provide access to the corner as shown in [Figure 4.2.7.1-4](#), then eliminating the false break.

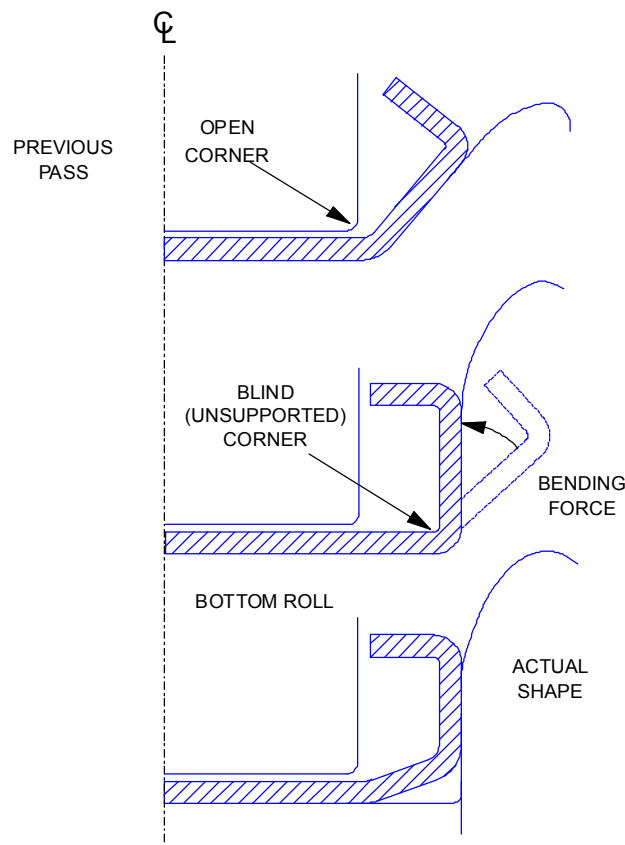


Figure 4.2.7.1-3 Possible additional bendline at unsupported section

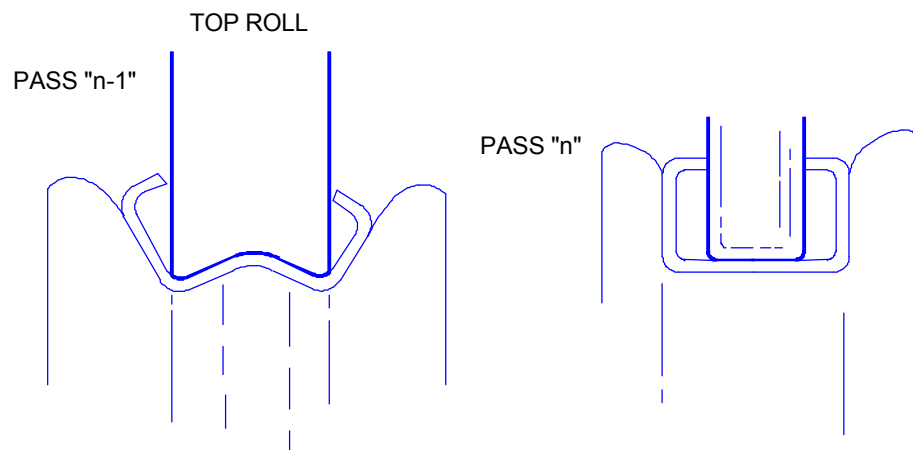
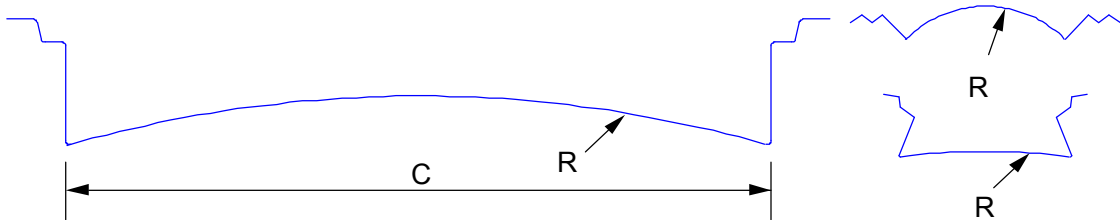


Figure 4.2.7.1-4 "Straightening back" false break

Roll designers prefer to work with reasonably tight radii which helps to set the profile. Forming very large radii as shown in [Figure 4.2.7.1-5](#) requires only one or two passes. The strain in the material, however, barely exceeds the elastic limit. As a result of the limited permanent deformation the tolerance may be large on the radius and chord.



[Figure 4.2.7.1-5](#) Tight tolerance is difficult to maintain on a large radius

4.2.7.2 Width of Nonformed Sections

An unformed segment that is too wide or too narrow, located between the edge of the strip and the first bend line or between two bend lines, can create problems. [Figure 4.2.5-1](#) shows how the edges are stretched during forming. The longer the leg, the greater will be the strain. If the strain at the edge is beyond the elastic limit, it is difficult to compress the thin metal back at the straight section and the result will be a wavy edge ([Figure 4.2.7.2-1](#)). Waviness may be eliminated by applying an additional stiffening bend closer to the edge as shown on the right hand side of [Figure 4.2.7.2-1](#). Starting with a strip that has a wavy edge or excessive camber can contribute to the waviness of the finished product.

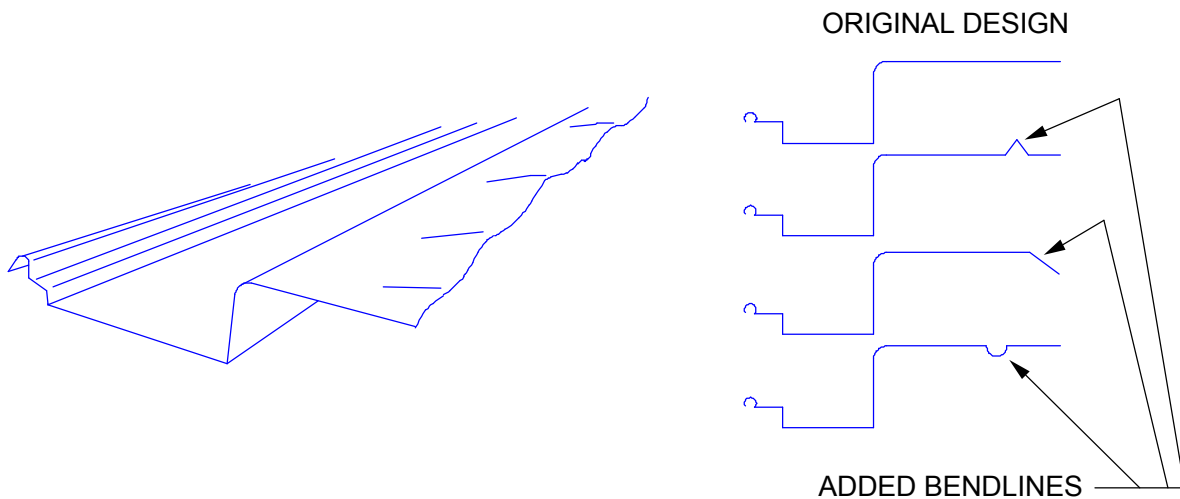


[Figure 4.2.7.2-1](#) Edges of wide unstiffened sections have a tendency to wave.
Added bendline(s) shown on right hand side can eliminate waviness.

Too short a leg may create forming problems ([Figure 4.2.7.2-2](#)). For easier forming and for better tolerances it is preferred to keep the length of the leg at least four times the material thickness.

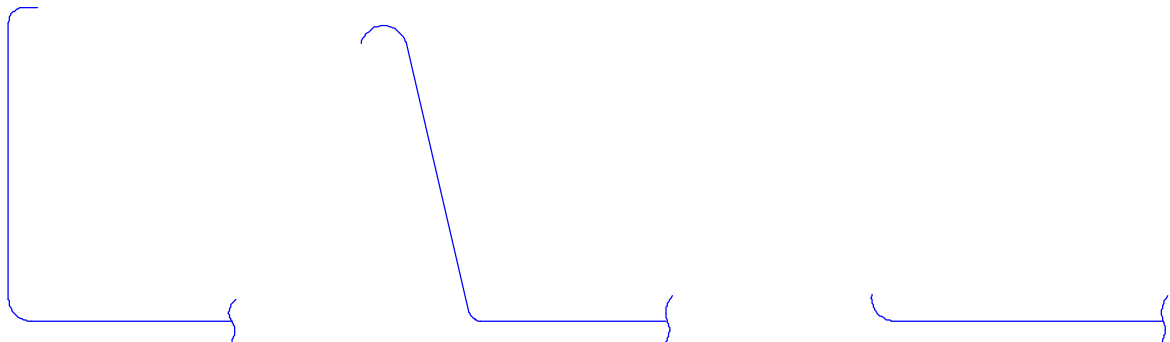


Figure 4.2.7.2-2 A short leg is difficult to form

When stiffeners or other ribs are designed, the slenderness of the mill dies should be considered. Thin rolls ([Figure 4.2.7.2-3](#)) can easily chip or break, stopping production for one to three days. Extreme side pressure can easily be exerted on the rolls if the gap between the rolls at one side becomes smaller than the material thickness.

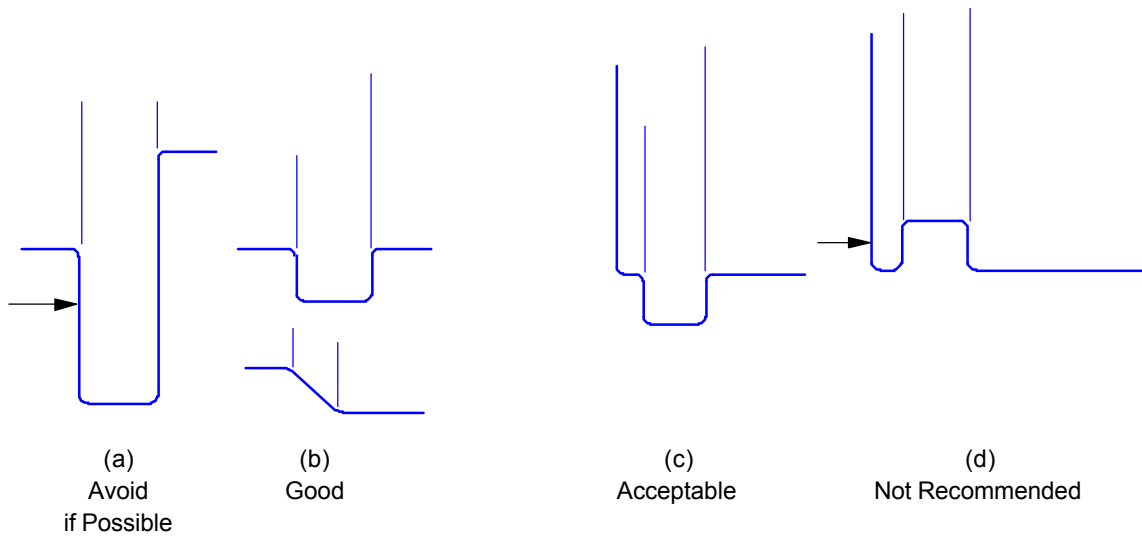


Figure 4.2.7.2-3 Stiffener rib designs

4.2.7.3 Bend Line Discontinuity

The designer usually recognizes that bend lines increase the strength of the section, but the weakness introduced by any discontinuity of the bend line may be overlooked.

[Figure 4.2.7.3-1](#) illustrates a few examples where, by design or by incorrect forming, the straight bend line is discontinuous or damaged. Even corner embossing, which greatly increases the strength in one direction, will reduce the strength of the section in the other direction.

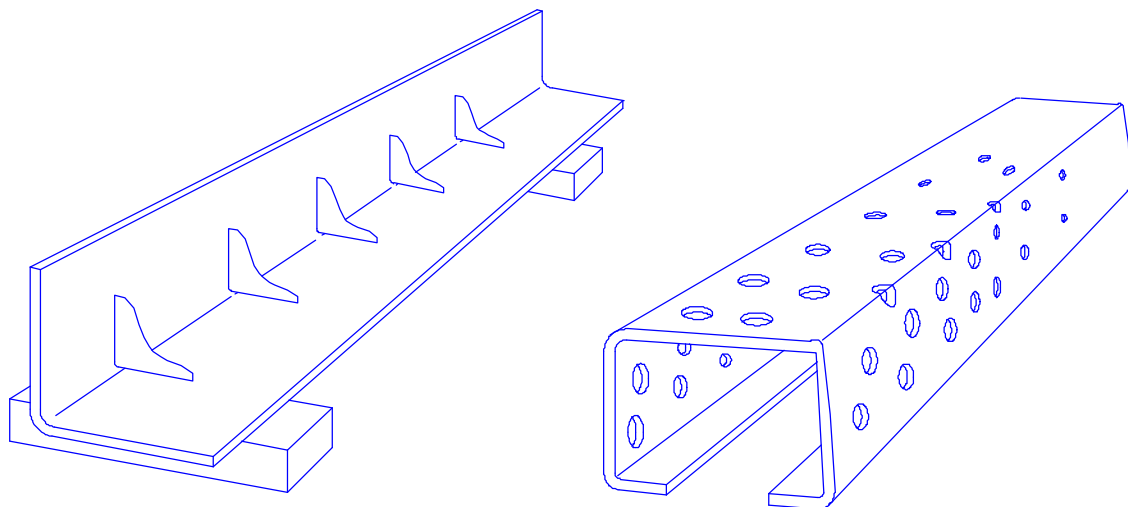


Figure 4.2.7.3-1 Discontinued bendlines have reduced strength

Cutouts at the bend line may represent another problem. If the cutout is too close to the bend line, the leg may be too short to be bent, and remain in its original plane after forming ([Figure 4.2.7.3-2](#)). Holes too close to the edge of the strip may leave too little material outside the hole, which stretches to such a degree during forming that it will buckle inward or outward in the final shape ([Figure 4.2.7.3-3](#)). Holes pierced in the flanges of curved panels may show even more severe deformation in the compressed elements ([Figure 4.2.7.3-4](#)).

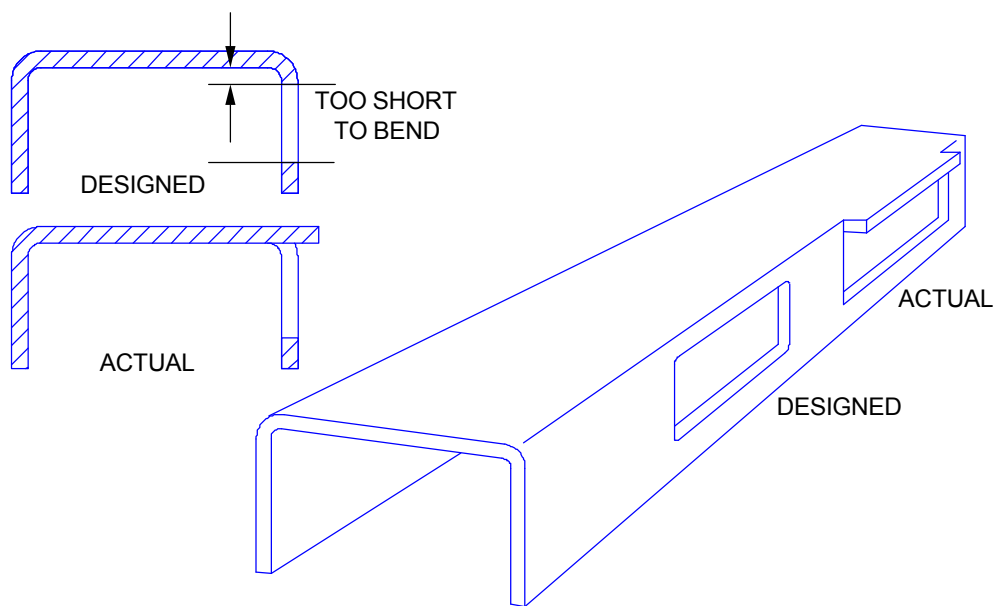


Figure 4.2.7.3-2 Effect of cutout too close to bendline

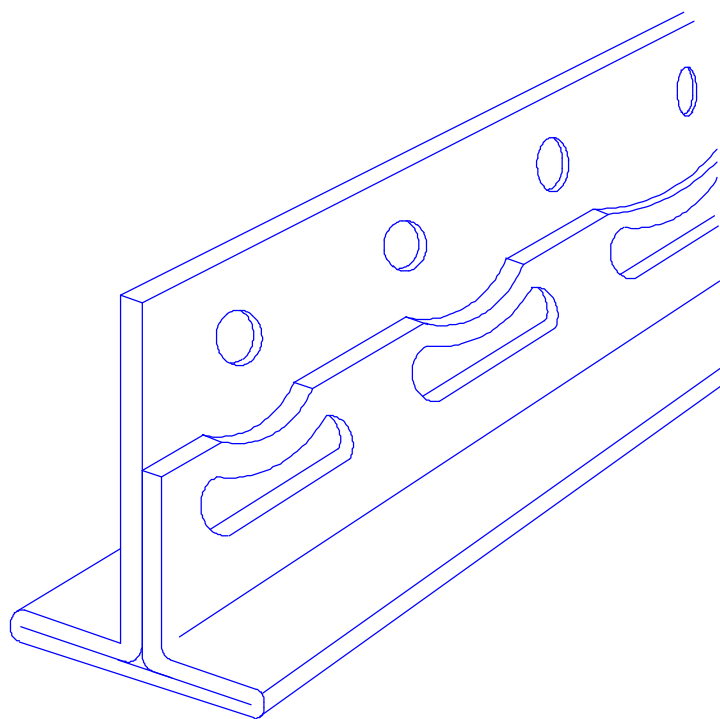


Figure 4.2.7.3-3 Effect of overstretched edge when holes are close to edge (effect was eliminated by modifying rolls)

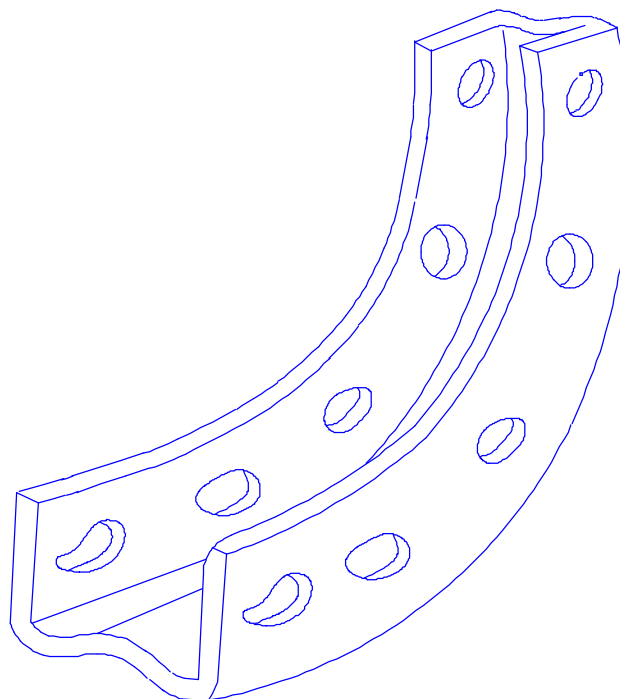


Figure 4.2.7.3-4 Tension and compression caused by curving can significantly distort pre-pierced holes

4.2.8 SPECIAL CONSIDERATIONS AND SPECIAL APPLICATIONS

The primary considerations of a part designer are the function, appearance and cost of the product. The method of manufacturing, however, should not be overlooked because it will influence all three basic considerations. Therefore, it is highly recommended that the tool designer and manufacturing personnel experienced in roll forming be involved in the conceptual stage of product design. At this stage, certain minor details, which can greatly influence the cost and quality of the finished part, can still be changed or modified. In most cases newly designed parts are roll formed with existing equipment. Therefore, the capacities of the equipment must also be taken into consideration.

There are some special cases where new equipment can be built to produce new parts. In these cases, only the available funds and time restrictions will restrict the introduction of new or unusual manufacturing methods. Some examples related to roll forming are:

1. Interrupted roll forming: It is possible to lift the upper forming rolls by hydraulic cylinders, servo motors, or cams, to create noncontinuous forming operations. For example, grooves in a product may be stopped at a certain distance before the end ⁹.
2. Variable hole, welding or other patterns: Specific punches or other equipment can be activated or deactivated in the line by the command of a computer, N/C or programmable controller.
3. Variable width product: Nonparallel edges of pie shaped sections can be roll formed with special equipment or special arrangement.
4. Variable radii curving: With appropriate control, products can be curved to two or more radii.
5. Very short pieces: Simple methods are available to roll form very short, (3 mm or 1/8 in.), pieces.
6. Forming at elevated temperature: Roll forming of preheated material in conventional mills is possible, but special mills can be built to roll form at high (hot forming) temperatures.
7. Ring forming: Rings can be produced in two different ways. One method is to roll form the section, curve it and cut it to length in the line. The cut ends are then welded together as in the case of bicycle rims. The other method starts with a flat, welded, continuous ring formed in several steps to its final shape as in the case of manufacturing automotive wheel rims.
8. Forming "dogleg" shapes in the longitudinal directions: Variable radii curving method mentioned previously can be applied or longitudinal sections may be bent by equipment similar to the automatic tube benders in the line.

The above list shows only a few possibilities to utilize roll forming lines for unusual applications. Although the major portion of the roll formed product will be formed on conventional roll formers, the high volume automotive components can provide opportunities to employ some existing, unusual methods or to develop new technology for profitable production.

REFERENCES FOR SECTION 4.2

1. High Production Roll Forming, Source Book; SME, January 1983.
2. Metals Handbook, "Forming", Volume 4, ASM, (1973).
3. Tool & Manufacturing Engineers Handbook, "Forming", Volume 2, SME, (1984).
4. Ferry, J.W. Techniques and Limitations for Cold Roll Forming High Strength Steel Bumper Components, "High Procuction Roll Forming", Source Book: SME, January, 1983.
5. Halmos G.T., Guidelines for Purchasing Roll Forming Lines, "Technology of Roll Forming Conference", Toronto, September, 1984, SME.
6. Halmos G.T., "Length Tolerances for Roll Formed Parts", Precision Metal; December 1981, Vol. 39, No. 12, p. 33-36.
7. Bhattacharyya D., Development of a Logical Flow Chart for Selection of Roll Schedules, Symposium on Sheet Metal Forming, Theory and Practice", McMaster University, Hamilton, Ontario, May, 1986.
8. Halmos, G.T., "Roll Forming HSLA Steels", International Conference on Technology and Application of HSLA Steels, Philadelphia, Pennsylvania, October, 1983, ASM: also The Fabricator, July/August, 1984, Vol. 14, No. 5, p. 12.
9. Pugh, G.H., "Interrupted Roll Forming; Sheet Metal Industries", April 1970, Vol. 47, No. 4.

4.3 WELDING PROCESSES

The design engineer is often asked to design automotive components that require welded assemblies. The choice of welding joint design, welding process, and the selection of welding procedures can substantially affect the cost and performance of the welded assembly.

This section covers several welding processes that are used for auto body and component manufacturing. A general process comparison chart is presented in [Table 4.3-1](#).

Table 4.3-1 Process Comparison Chart

Welding Process	RSW ^(a)	RSEW ^(b)	Projection Welding	Resistance Butt/Flash	LBW ^(c)	GMAW ^(d)	FCAW ^(e)
Joint design	Overlap flange	Overlap flange	Lap, attachments	Butt	Butt, flange, overlap	Butt, plug, overlap, groove	Butt, fillet, overlap, groove
Part fit-up	Some tolerance	Some tolerance	Some tolerance	Wide tolerance	Critical	Wide tolerance	Wide tolerance
Filler possible	No	No	No	No	Yes	Yes	Required
Material	All steels with and without coatings	All steels with and without coatings	Most steels	Most steels	Most steels	All steels and alloys	Low carbon, alloy, some stainless
Thickness (mm)	Min = 0.25 Max ≈ 8.0	Min = 0.25 Max ≈ 8.0	Wide range	Min = 0.75	All common body gauges	Min = 0.25	Min = 0.25
Cost of equipment	High	Low to moderate	Low to moderate	Moderate	High	Low	Low
Cost per weld	Low	Low	Low	Low	Moderate	Low	Low
Quality of weld	Good	Good	Good	Good	Very good	Good	Good
Distortion	Some	Moderate	Low	Generally NA	Low	Moderate	Moderate
Skill factor	Low	Low	Low	Low	Generally automatic	High	High

- Legend:
- (a) Resistance spot welding
 - (b) Resistance seam welding
 - (c) Laser beam welding
 - (d) Gas metal arc welding
 - (e) Flux-cored arc welding

4.3.1 RESISTANCE WELDING (RW)

4.3.1.1 Process Description

RW processes use the inherent resistance of the components to be attached, combined with very high current flows, to generate heat required for welding. The RW processes encompass a very

wide range of technologies, the best known of which include RSW, RSEW, resistance projection welding, etc. All RW systems contain three essential components. These are:

- An electrical system for supplying the currents required for welding
- A force application system to bring the components together under the required pressures for welding
- A cooling system to localize heat within the workpiece and protect the electrode from thermally induced changes.

How the required currents, forces, and cooling are supplied largely defines the differences between these processes.

RW technologies are widely used in sheet metal fabrication industries, especially in the automotive industry. The primary reason is the relatively low cost of joining in high-volume applications. Though the capital costs of RW are high, processing speeds are typically very fast, there are no consumables, no shielding is required, and the processes tend to be extremely robust to the manufacturing environment. Therefore, in view of manufacturing costs, the RW technologies are generally quite advantageous.

4.3.1.1.1 Resistance Spot Welding (RSW)

RSW is the most widely used RW process. The basic configuration for RSW is given in [Figure 4.3.1.1.1-1](#). Typically, the parts to be joined are assembled in a lap-type configuration. Water-cooled electrodes are then brought into contact with the workpieces under high forces. These electrodes serve three functions. First, the electrodes conduct the current into the weld area, facilitating heating. Second, the electrodes apply high force to the welding area, both to stabilize contact resistance (allowing stable current flow and facilitating stable heat generation), and to constrain the growing weld nugget. Although it is not recommended, welding forces have the additional advantage of mitigating the effects of poor fit-up (realistic in auto body welding). Finally, the electrodes provide cooling to the growing weld. This feature thermally drives the growing weld to the center of the stackup, and facilitates proper attachment of the component sheets.

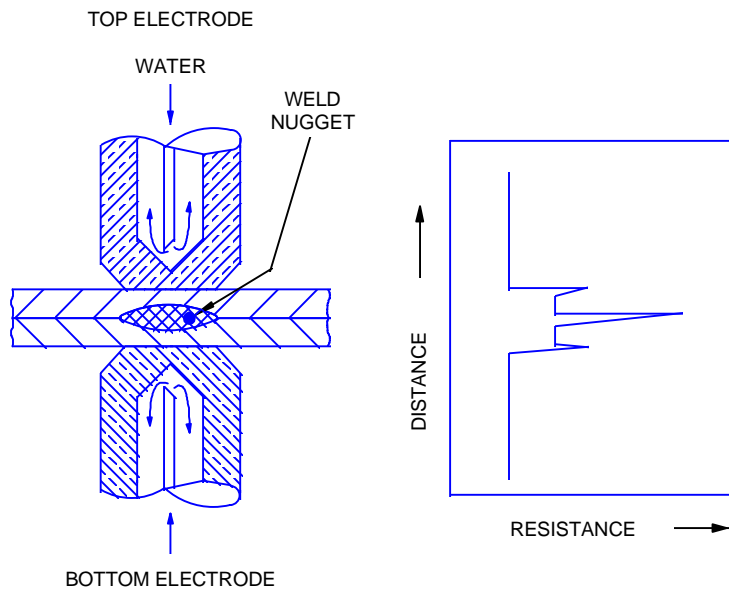


Figure 4.3.1.1.1-1 Schematic RSW process

The distribution of heat during the spot welding process depends on the resistance elements [electrode/sheet contact resistance, bulk resistances, and sheet/sheet contact resistance(s)] in the stackup. A typical variation in resistances for a stackup of uncoated steels (before the initiation of welding current) is presented in [Figure 4.3.1.1.1-1](#). Typically, the pre-current flow stackup shows high contact resistances at the sheet-sheet and electrode-sheet contact surfaces, with substantially lower resistances in the bulk. As the weld cycle begins, current flow through the contact resistances generates heat, causing contact asperities to collapse and contact resistance to drop. At the same time, bulk resistance increases and continues heating the components until a molten zone (nugget) is formed at the sheet-sheet interface. The temperature at the electrode-sheet interface is controlled by the cooling action of the water-cooled electrodes, effectively concentrating the heating at the sheet-sheet interface, where the nugget ultimately forms.

Numerous organizations and companies have published recommended practices or specifications for RW steels.^(1, 2, 3, 4, 5, 6, 7, 8, 9, 10, 11, 12, 13, 14, 15, 16, 17, 18, 19) These specifications detail most of the critical requirements for RW, including the process conditions (forces, currents, weld times), electrode geometries, required flange widths, etc. In addition, these documents also detail some basic weld performance information, including weld sizes and mechanical strengths.

Most sheet steels can be welded using relatively simple welding conditions. A typical welding profile includes four time segments: squeeze, weld, hold, and off. The squeeze time is required to allow the mechanical system to supply the required force and come to mechanical equilibrium prior to initiating weld current. The weld time is simply the duration of current flow. The hold time is an allotted period to allow the weld nugget to re-solidify after welding. The off time allows the electrodes to return to home position, and allow any automation to index. Depending on the stackup configuration and equipment employed, RW can be done at rates ranging from 10-60 welds/min. Because optimum welding parameters are different for different substrates, sheet thicknesses, coatings and stackup combinations, they must be varied to suit the material(s) being welded. General guidelines are available through AWS, RWMA, other standards issuing bodies, and the automotive specifications.

When welding high-strength steel, higher heat is needed, dictating larger electrodes. Therefore the weld flanges must be wider than those with mild steels.

Applications for RW cover the myriad of sheet metal fabrication. In automotive applications, body fabrication and assembly accounts for as many as 6000 spot welds per vehicle. Frame and sub-component assemblies also extensively use RSW.

4.3.1.1.2 Resistance Seam (RSEW) and Mash Seam Welding (MSEW)

RSEW is a variant of RSW in which copper wheels, rather than single-point copper electrodes are used. RSEW is typically done with similar press-type equipment as used for RSW. The same types of electrical, mechanical, and force and cooling systems are required to accomplish RSEW. Components for joining are oriented in a similar lap configuration. The major difference between seam and spot welding is that current is fired continuously or pulsed through rolling wheels, rather than single-point electrodes.

RSEW is typically done by firing multiple pulses of current as the electrodes roll along the surface of the workpieces. Generally, the duration of the current pulse (typically less than 0.1 sec) is extremely fast relative to the motion of the electrode wheels, so an effective spot is made. The process proceeds, then, as a series of overlapping spots as the wheels move along the

surface. Depending on the speed of the wheels and the rate of current pulsing, a number of joint types can be made, as shown schematically in [Figure 4.3.1.1.2-1](#). If the delay between current pulses is relatively long compared with the speed of the welding wheels, the process will produce a series of discrete spots, virtually indistinguishable from a row of spots made with conventional spot welding. This is an extremely high-speed way of creating such rows of spots, and is used extensively where leak-tight joints are not required. An example of this is attachment of roofs onto automobile bodies. If the pulsation frequency is increased relative to the wheel speed, the individual spots will overlap. The use of such overlapping spots is a common way to achieve leak-tight RSEW. Typical applications for this variant of the RSEW process include automobile gasoline tanks and catalytic converters.

A major advantage when using pulsation RSEW for fabricating leak-type joints is that it is quite robust to a range of manufacturing variations. Most notably, minor changes in speed as well as changes in direction can be made while maintaining leak-tight integrity. General guidelines for RSEW are available in a number of the standard references.^(4, 5, 8, 19, 20)

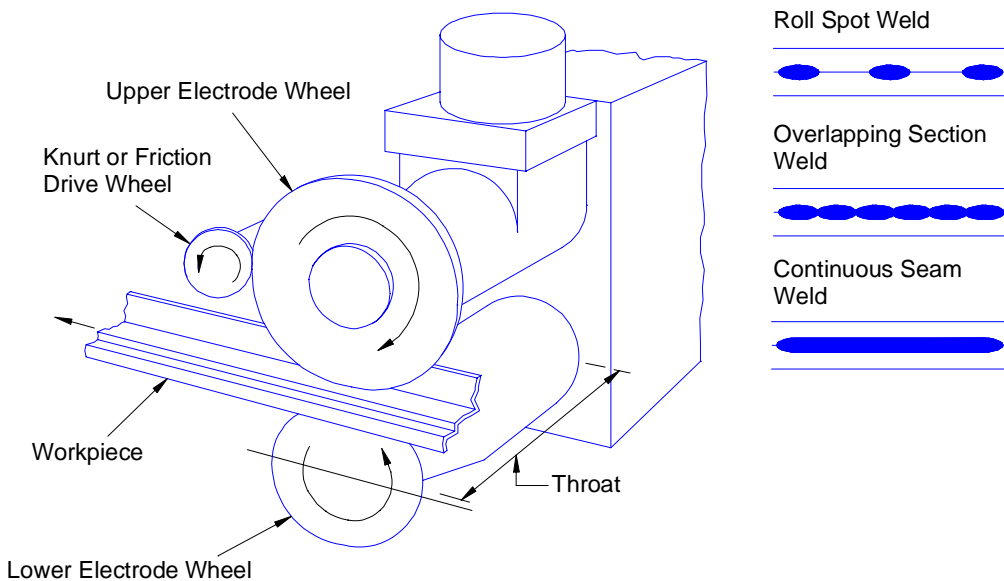


Figure 4.3.1.1.2-1 Description of RSEW Process

Generally, RSEW operations are conducted with flood cooling, which allows heat to be maintained in a manner similar to RSW. Where water cannot be tolerated, internal cooling of the electrode wheels is also used. In no case, however, should RSEW be done without some cooling.

The mesh seam electric welding (MSEW) Process is related to RSEW, and is used to make lap joints that are only slightly thicker than the unwelded sheet. The basic process is illustrated in [Figure 4.3.1.1.2-2](#). Essentially, the parts are overlapped by 0.5 to 1.5 times material thickness. Seam welding wheels are then passed along the joint. The resulting heat allows the joint to collapse under the influence of the welding wheels, consolidating the joint. The resulting joints, if fabricated properly, are solid state in character, with minimal retained buildup in the joint area. Post planishing is sometimes used to make the resulting mashed joint of equal thickness with the base material. The process has been demonstrated to be effective for joining both similar and dissimilar thickness materials.

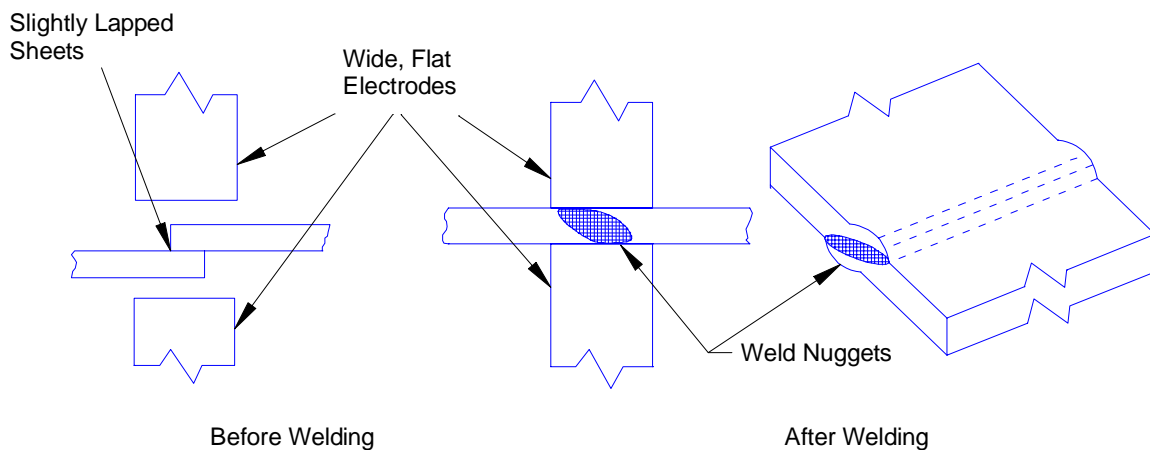


Figure 4.3.1.1.2-2 Resistance MSEL Process

MSEL is used in a variety of sheet metal fabricating industries. Applications range from materials as thin as 0.1 mm (can applications) to as thick as 3 mm (steel drum and water heater applications). In automotive applications, MSEL is used for tailor-welded blanks. In addition to welding materials of different thicknesses, MSEL is used to weld materials of different strength levels and with different coating types into a single component, where it is very cost competitive. Unlike conventional seam welding, standard practices are not available.

A variant of RSEW, the “electrode wire seam welding” process (sometimes called Soudronic welding), employs an intermediate copper wire electrode between each wheel electrode and the workpiece (see [Figure 4.3.1.1.2-3](#)). Using a complex mechanical arrangement, the wire is continuously fed from a spool to a groove in the periphery of each welding wheel to provide a continually renewed electrode surface. This approach prevents the buildup of coating/paint residue from a coated or pre-painted sheet steel, and therefore is well suited to the welding of automotive fuel tanks²⁰.

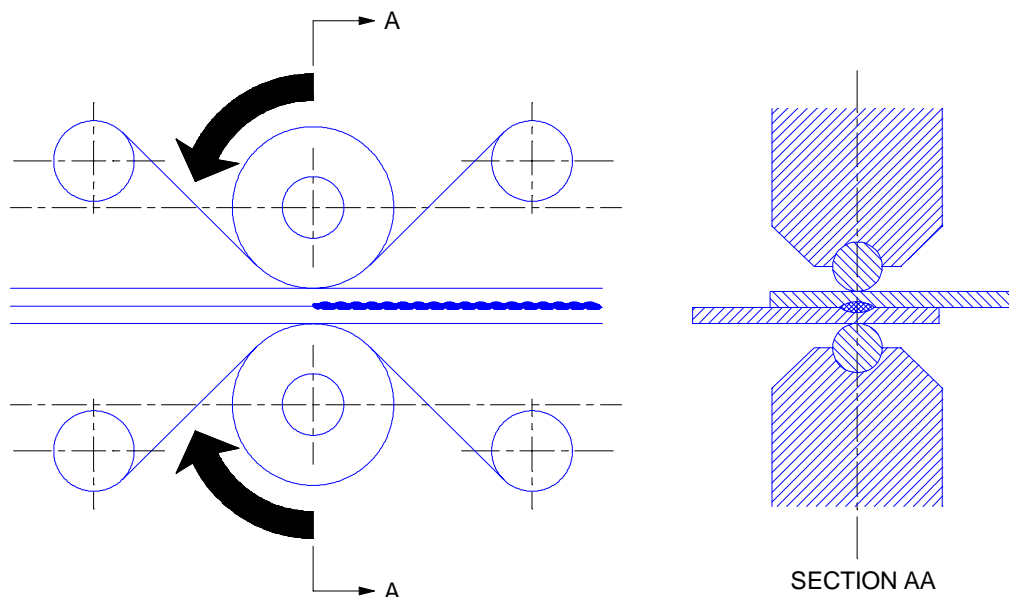


Figure 4.3.1.1.2-3 Electrode Wire Seam Welding Process

4.3.1.1.3 Resistance Projection Welding

Resistance projection welding is another variant of RSW. It is typically used as an alternate process to attach sheet components in a lap configuration, irregular components to sheet, or irregular components to one another. The basic resistance projection welding process is illustrated in [Figure 4.3.1.1.3-1](#). The figure illustrates the sheet-to-sheet or “embossed” projection welding process. A projection is first stamped onto one of the two sheets to be joined. The sheets are then positioned in a lap configuration for joining with standard RW equipment. Welding cycles are similar to those used for RSW. During welding, the projection serves as a point contact between the two sheets to be joined. This point contact acts to focus welding current, and therefore heating, at that location.

The weld development proceeds in two stages. Over the first few cycles, the projection collapses and some solid-state bonding results. With additional weld time, this hot region at the residual projection tip continues to heat, and a nugget similar to a resistance spot weld develops. Embossed projection welding is well described in the recommended practice documents. Recommended practices include projection designs, designs for the stamping tools, welding schedule information, minimum weld size and mechanical properties information.^(4, 5, 8, 21, 22)

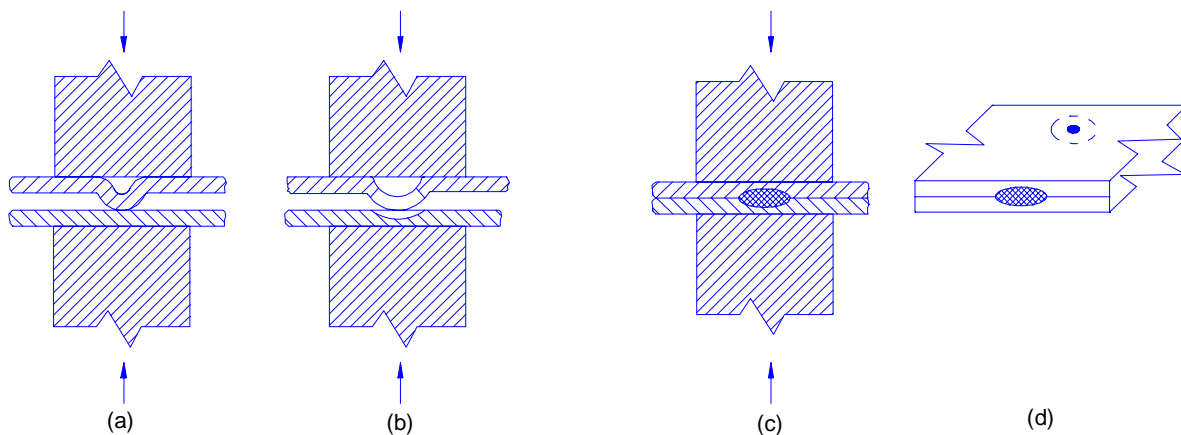


Figure 4.3.1.1.3-1 Resistance Projection Welding Process

Solid projection welding is related to embossed projection welding. Solid projection welding is used in joining components to sheet metal. Applications range from annular projection welding to nut welding. In these applications, either a machined projection or a physical discontinuity acts as the projection for welding. Solid projection welding differs from embossed projection welding in that there is no surrounding sheet to constrain a growing weld nugget. As a result, the welds by necessity take advantage of only the solid-state part of the process. Surprisingly, there are also few guidelines for either projection designs or weld processing for solid projection-type welds. Most such information is derived empirically, on an application-to-application basis.

The ability of the projection(s) to locate current flow (and subsequent heating) provides projection welding with a number of advantages over conventional RSW. For the embossed variant of the process, these advantages include closer spot spacings, narrower flange widths, and the ability to accommodate a wide variety of stackup configurations. Of particular note is

new technology using embossed projection welding which offers the potential of “mark-free” welding on one side. This technology takes advantage of current localization associated with the projection and very short weld times. The major advantage of solid projection welding is the ability to join a variety of shapes and configurations in a cost-effective way.

The major drawback of projection welding is in the manufacture of the projections themselves. Embossed projections often can be formed as part of ancillary stamping operations simply by modifying the die. Where this is not possible, or the component does not experience other forming operations, the projections must be stamped in a secondary operation, adding cost. Forming solid projections is typically much more difficult. For weld nuts and some embossments, forming the projections must be consistent with other cold heading operations. This restriction often limits obtainable projection geometries, and subsequent weld quality. Projections with more precision, particularly annular projections, are often machined at additional cost.

4.3.1.1.4 Resistance Upset (Butt) Welding

Resistance butt welding utilizes RW-type hardware (transformers, forcing systems, controls) to create solid-state joints. Resistance upset welding is used in a number of automotive applications, ranging from wheel rims to steering wheels. The basic configuration for welding is shown in [Figure 4.3.1.1.4-1](#). Essentially, parts to be welded are loaded in a butt configuration under very high compressive stress, typically 75-150 MPa. On initiation of the welding current, material between the jaws softens and the parts are forged together under the applied stress. The resulting joints are solid state in character, with bonding completely across the joint interface. Joining is typically very rapid, usually less than 1-2 seconds, so production rates can be very high.

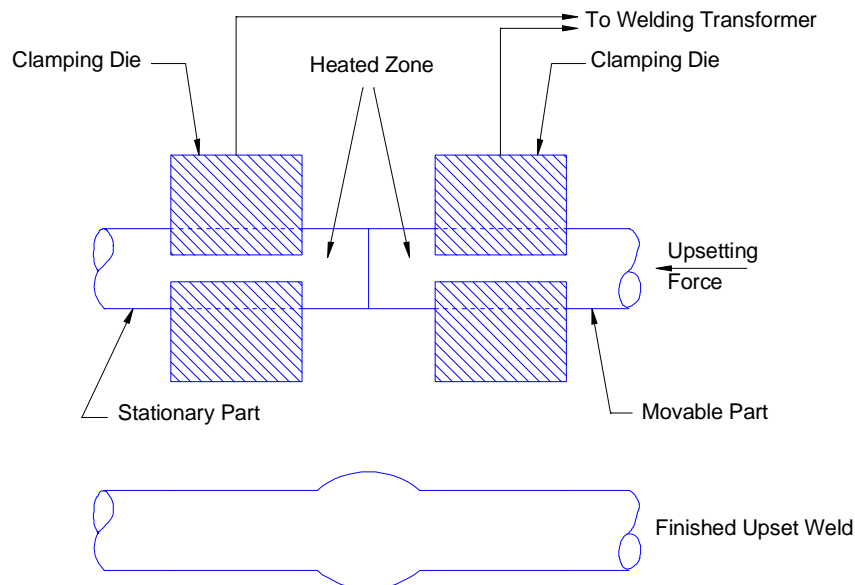


Figure 4.3.1.1.4-1 Schematic of Resistance Upset (Butt) Welding

While resistance butt welding can be quite attractive for some applications, there are a number of restrictions that limit its use. Most notably, resistance butt welding is generally restricted to applications of relatively simple geometry. In order to accomplish balanced heating and forging, the workpieces must be of similar, uniform cross section and geometry. This generally restricts the process to bar and flat strip. In addition, given current distribution problems during welding,

strip widths are generally restricted to about 500 mm. The applications of resistance butt welding are also limited by the current delivery capabilities of the equipment. Most resistance butt welding applications require about 80-120 A/mm² (50-75 kA/in.²). The largest power supplies today are limited to about 200 kA, limiting welding cross sections to about 2500 mm² (4 in.²). Finally, all resistance butt welds have some degree of extruded flash from the joint area, which must either be removed in an additional processing step or tolerated in the final product.

4.3.1.1.5 High-Frequency (HF) Welding

HF welding composes a group of welding technologies that utilize HF currents, typically greater than 10 kHz. The most common of these is HF tube welding, shown schematically in [Figure 4.3.1.1.5-1](#). This variant of the process typically uses 100 kHz to 450 kHz current and a coil to induce current flow in flat stock that is being formed into a tube. Closure of the tube is accomplished by a set of pinch rolls at a location termed the “vee” of the configuration. Current flow in the tube occurs around the body of the tube, along the edges of the vee, and finally across the apex of the vee itself. The vee effectively acts as a current concentrator, localizing heating. Heating and forging conditions occur at the vee similar to those seen for resistance butt welding. The major advantage of HF welding is the relatively high welding speeds. In some applications, line speeds greater than 100 m/min can be obtained. Applications for HF welding have included exhaust pipe tubing, as well as tubing for sub- and full-frame structures.

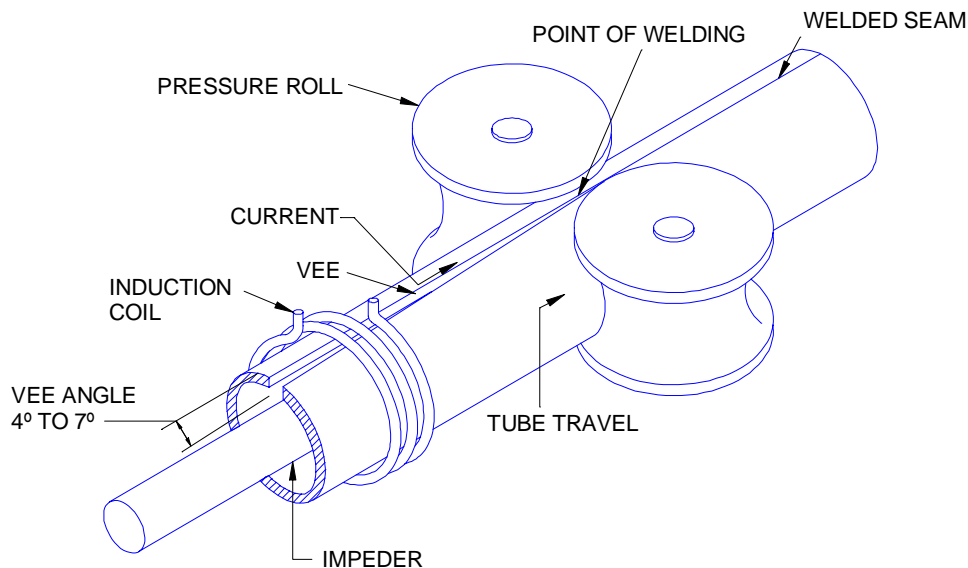


Figure 4.3.1.1.5-1 Tube Seam Welding by HF Induction Welding

The major drawbacks to HF welding include limited weldable geometries, generally restricted to longitudinal seams, and quality control. In general, only the longitudinal seams on tubes are HF welded. A variant of HF welding is used in production, however, for manufacturing tailor-welded blanks. For tube fabrication, lack of quality control combined with high line speeds can be a problem. The concern here is that if weld quality lags, given the processing line speeds, considerable scrap will be generated in a short period of time.

4.3.1.2 Design Considerations

Successful weldment design requires understanding of both the weldability of the material and the weld joint placement. The process descriptions and cited references will provide the basis for design using a resistance welding process. However, consultation with each automotive company's welding design specifications is recommended.^(21, 23, 24)

In all cases, resistance spot welding produces some local surface indentation or marking (if a solid backup is used on one side) in the area of the weld. This condition will be influenced by part fit-up, weld time and electrode force. For this reason, spot welds are not generally used in surface critical conditions.

4.3.1.3 Material Considerations

Many of the welding technologies described above are relatively mature, with most problems related to how these technologies apply to newer materials. With regard to sheet steels, the range of such products is extensive. These include bare steels, high-strength steels (HSS), and a range of coated steels. Nuances of resistance welding the various steel types are covered in the following sections. It is of note that most of the information provided here is for RSW. Much of this information is transferable to the other processes, keeping in mind the differences in the processes themselves.

4.3.1.3.1 Uncoated/Mild Sheet Steel

Uncoated/mild sheet steels have been resistance welded in production for many decades. These steels typically have relatively high contact resistances, which break down readily as the weld current is applied. These materials can therefore be welded at relatively moderate currents. Materials typically exhibit very wide current ranges (>2000 A), and demonstrate electrode lives of many tens of thousands of welds. Sheet thicknesses ranging from less than 0.25 mm to greater than 10 mm have been readily resistance welded in production applications. These steels are equally amenable to all types of RW processes.

4.3.1.3.2 Zinc-Coated Sheet Steels

A variety of coated sheet steels are now used in vehicle construction. The most common of these are the zinc-coated steels. Zinc-coated steels commonly fall under three classifications: hot-dipped galvanized (HDG) steels, electrogalvanized (EG) steels, and galvannealed steels. All are readily weldable by RW.

The resistance welding of these steels differs dramatically from their uncoated counterparts. The primary reason is the effect of the coatings on the various contact resistances. The zinc on the surface, in any of its forms, represents a relatively soft layer at the interfaces. Under the applied welding load, these surfaces preferentially deform, resulting in lower sheet-to-sheet and electrode-to-sheet contact resistances. Representative contact resistances for a variety of zinc-coated sheet steels, as well as uncoated sheet steel, are presented in [Table 4.3.1.3.2-1](#). Clearly, the coated steels show order of magnitude reductions in contact resistance compared with bare steel. The lower contact resistances result in large increases in the required welding currents. Some comparable currents for welding different coated steels are presented in the table. The free zinc (HDG and EG) coated steels require roughly 50-100% more current than their bare counterparts. The coatings and higher welding current produce several effects. First, initiation of the weld nugget is delayed in the weld cycle because the initial heating melts the coating and

causes much of the current to be shunted through the molten coating annulus formed at the faying surface. Second, the alloying of the electrode faces with the coating increases their resistance and causes a shift in the heat balance. These first two factors combine to result in much narrower current ranges with coated sheet steels. Finally, the surfaces of the electrodes experience much more heating, increasing alloying of the coating with the electrode and reducing electrode life.

Table 4.3.1.3.2-1 Typical Weldability Data for 0.88-mm-Thick Mild Steel
(2.2-kN Electrode Force and 6-mm Electrode Face Diameter)

Coating Type	Contact Resistance ($\mu\Omega$)	Typical Welding Current (kA)	Typical Electrode Life (No. of Welds)
Uncoated	1500-3000	7-9	20,000
HDG	50-150	11-13	1,000-3,000
EG	10-50	11-13	2,000-5,000
Galvannealed	300-500	8-10	3,000-8,000

The greater electrode heating is the primary source of the fundamental concern for RSW-coated sheet steels: accelerated electrode wear. Electrode wear has been a concern for galvanized steels for decades. Compared with uncoated steels, electrode lives for coated steel are appreciably shorter. Representative electrode lives for typical coated steel products are presented in the table. Recent work has shown that this reduction in electrode life is directly related to overheating of the electrodes. Essentially, overheating allows a substantial depth of copper to soften in the electrode face, allowing the copper to distort, resulting in mushrooming.^(25, 26) The higher temperatures also result in accelerated alloying between coating and electrode, producing brittle layers of higher resistance on the surface. The alloying leads to wear by pitting of the electrode surfaces.

It is of note that generally electrogalvanized steels demonstrate substantially longer electrode lives than HDG steels. Recent work has demonstrated that the aluminum content of the coating plays a major role in electrode wear. Higher aluminum content in both HDG and galvannealed steels reduces electrode life.

4.3.1.3.3 Aluminum-Coated Steels

Aluminum-coated steels are used for a range of high-temperature applications, particularly exhaust systems, including exhaust pipes, brackets, heat shields, etc. Aluminum-coated steels are readily resistance weldable but, as with zinc-coated steels, the process is affected by electrode wear. Aluminum readily alloys with the copper electrodes, causing considerable wear. The problem is exacerbated by the relatively high contact resistance associated with aluminum oxide on the coating surface. The effect is to preferentially heat the surfaces, accelerating electrode wear. Typical electrode lives with Al-coated steels are less than 1000 welds.

4.3.1.3.4 Preprinted Steels

Weldable organic (or pre-painted) steels come in two configurations: single-side painted, and with conducting paints. Single-side painted steels can be welded to unpainted steel sheets using a series-type process. Series welding places the welding and shunt electrodes on the same side of

the stackup. Joints can be made without damaging the paint on the back side when very short times are used. Also, the application of a projection onto the unpainted component also allows concentration of current, and welding with minimal damage to the paint. However, the possibility of dimpling, which is associated with the projection, may be a consideration. Steels with conducting paints, or “weldable primers” typically are coated with paints containing conducting pigments.⁽¹¹⁾ These pigments range from zinc particles to Fe₂P. During application of the welding force, the conducting pigment particles are compressed together, creating conducting paths. These paths allow current flow and local heating and subsequent softening of the paint. The softened paint is then extruded, allowing full conduction, and subsequent welding.

4.3.1.3.5 High-Strength Steel (HSS)

HSS offers a number challenges for RW.^(7, 8, 9, 10, 27, 28) Most of these challenges have been grouped under the term “hold-time sensitivity”, which is defined by peel test behavior. A material that is considered hold-time sensitive will exhibit button-type failures of spot welds when short (0-5 cycles) hold times are used, but interfacial (or partial) failure when longer hold times (30-60 cycles) are used. Two classes of hold-time sensitivity have been defined, each corresponding to a different classification of HSS. Rephosphorized grades of steel demonstrate hold-time sensitivity due to solidification cracking related to phosphorus additions. Extensive empirical work has shown, however, that hold-time sensitivity in these grades of steels can be avoided if the phosphorus content is maintained below 0.06%. Dual-phase grades of steels, with higher carbon and manganese additions, exhibit hold-time sensitivity through the formation of relatively hard martensites. Similar empirical work has shown that hardness hold-time sensitivity can be avoided by maintaining carbon levels below 0.1%. Hold-time sensitivity is also a problem in plain carbon steel when carbon content is greater than approximately 0.08 to 0.09%.

Hold-time sensitivity is essentially a cooling rate-related phenomenon. As a result, factors that increase the cooling rate in the weld also increase hold-time sensitivity behavior. These include thinner sheet and smaller weld sizes. Using thicker sheets (and subsequently larger weld sizes) will mitigate some of the compositional effects described above.

It is of note that many of the dual-phase HSS (high carbon, manganese) will use compositions inherently hold-time sensitive. For these applications, more advanced weld schedules are required. The application of post-weld tempering has been found to be very effective in reducing weld hardnesses, and minimizing (or eliminating) hold-time sensitivity effects. These methods offer great potential as more hardenable grades of steels are applied in auto body construction.

4.3.2 ARC WELDING PROCESSES

Arc welding processes use electrical energy to melt or fuse metals to produce a joint between two or more parts. All processes are characterized by an electrical arc between an electrode and the workpieces. The processes of current use or interest are GMAW, FCAW, and plasma arc welding (PAW). AWS (American Welding Society) or company standards may be used to define required weld quality in automotive applications.^(27, 29) These processes, their advantages and disadvantages, and their applications for autobody manufacturing are described in the following sections.

4.3.2.1 Gas Metal Arc Welding (GMAW) – Process Description

The GMAW process (also known as Metal Inert Gas, MIG, or MAG welding) is characterized by an arc that is formed between the end of a continuously fed electrode wire and the workpiece (see [Figure 4.3.2.1-1](#)). The solid wire is continuously fed through a contact tip in the torch, and melts to form the weld bead joining the base metals. The wire feed rate is balanced to the burnoff rate to maintain a stable arc. The wire type is selected to give the weld metal a matching (but typically overmatching) strength compared with the base metal. The weld area around the arc is protected by a shielding gas supplied from the torch.

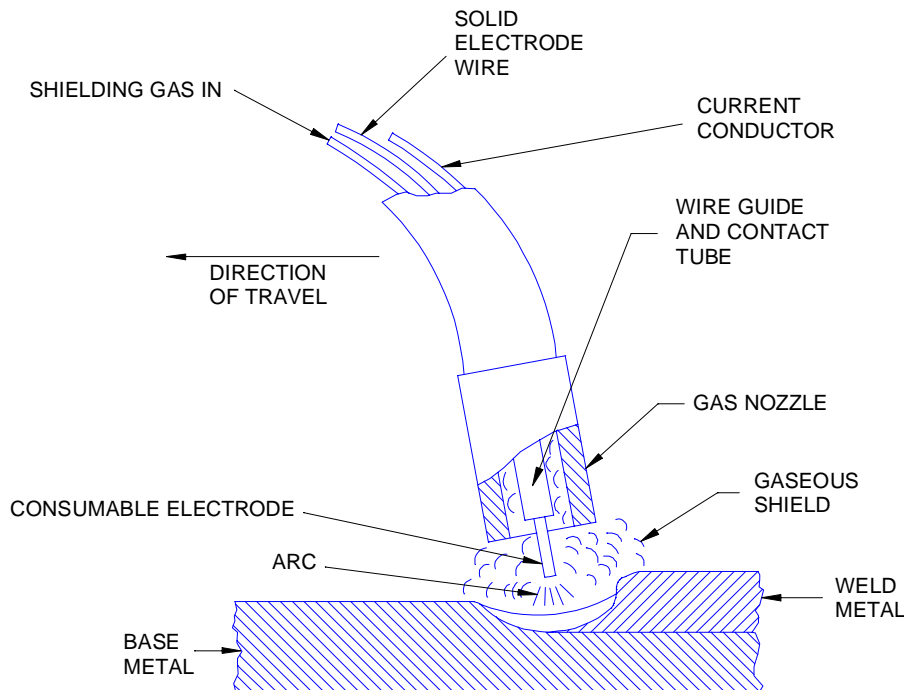


Figure 4.3.2.1-1 GMAW Process

GMAW weldments can be made in all positions, especially using “short-circuit” transfer, or pulsed current, P-GMAW; thus the process is ideally suited to automation, especially through arc welding robots. Gap tolerance for GMAW is good, with joint gaps up to one sheet thickness (1T) being tolerable.

The welding parameters that must be controlled to produce acceptable welds include welding current, arc voltage, wire feed speed, torch travel speed, torch travel and work angles, and shielding gas flow rate. The joint gap should be minimized to achieve the best joint quality and productivity.

4.3.2.1.1 GMAW – Advantages and Disadvantages

The major advantages of the GMAW process are its high productivity and reliability coupled with low cost. The process is suited for automation, and very little cleanup is required after welding. The equipment can be deployed on welding robots with relative ease, and single-side access only is required. In addition, the process is suitable for many different alloys including, among others, carbon and low-alloy steels, stainless steels and aluminum alloys.

The disadvantages of GMAW are the plant ventilation that is required to remove welding fumes, and the protection that is needed from strong drafts to avoid loss of shielding gas efficiency, which can lead to porosity. Welding of coated steels can cause porosity by volatilization of zinc-rich coatings. This can be mitigated by correct development and implementation of welding procedures.

4.3.2.1.2 GMAW – Applications

The GMAW process is suitable for a variety of alloys as noted above in butt, fillet, and lap joints. Joint fit-up is less critical than for Gas Tungsten Arc Welding (GTAW) and laser beam welding (LBW).

Typical applications on sheet metal body in white (BIW) are short welds of an inch or less, either in a lap-fillet configuration, or by spot or plug welding. Many attachment welds are made using GMAW, such as door hinges to door pillars. The process is suitable for welding vehicle frames, including tubular spaceframes. A sub-set of GMAW operations is GMA brazing, which uses silicon bronze filler wire to braze steel components such as roof-to-quarter panel components.

4.3.2.1.3 Variant GMAW Processes

Pulsed GMAW (P-GMAW) offers increased control of metal transfer compared with conventional constant-voltage GMAW. This gives the P-GMAW weld improved cosmetic appearance and reduction in spatter and cleanup considerations compared with constant-voltage GMAW.

Variable polarity (VP or AC) GMAW is a new variant of GMAW in which the balance of electrode polarity is adjustable to change the degree of penetration achieved during the weld. This variant of GMAW is designed to be even more tolerant to joint gaps (even up to $2\times$ metal thickness) and to minimize distortion associated with the heat input of the process when welding sheet thicknesses. These two features make the process potentially attractive for sheet metal BIW fabrication. Commercial equipment is currently available from a limited number of sources for welding steel and aluminum alloys.

Twin-wire GMAW exploits the benefits of two torches and two arcs in a single weld pool to achieve productivity gains in excess of three times that of single-wire GMAW. The most suitable systems for robotic operation incorporate two wires in a single torch using two contact tips and sequencing the current pulsing to minimize arc interference. Several commercial systems are available and applications range from 1.6-mm sheet to thicker materials. Applications include frame manufacturing, such as in light trucks and SUVs, and a wide array of suspension and axle components.

4.3.2.2 Flux-Cored Arc Welding (FCAW)

The operation of the FCAW process is essentially similar to that of the GMAW process. The main difference is that FCAW uses a flux- or metal-cored consumable that consists of a tubular metal sheath wire, which contains either a flux or a powdered metal core. Some FCAW consumables operate without a supply of shielding gas, but most of those suitable for welding components relevant to the automotive industry employ a shielding gas, usually a mixture of argon and carbon dioxide.

4.3.2.2.1 FCAW – Advantages and Disadvantages

Most of the advantages and disadvantages of FCAW are similar to those for GMAW. An additional consideration for FCAW is that the weld metal is partially protected by a slag coating which has to be removed after welding. This additional operation is a considerable disadvantage in a high-productivity welding environment. The wire must be handled with caution to minimize moisture pickup, which will affect hydrogen content and may cause subsequent cracking in low-alloy and higher strength steels.

Since metal-cored wire consumables do not contain fluxing agents, they do not produce a slag covering. The advantage of metal-cored wires is that they have higher melting efficiency than do solid wires, and thus present the opportunity for gains in productivity through increased welding speed or deposition rate.

4.3.2.2.2 FCAW – Applications

The FCAW process, which utilizes flux- or metal-cored wires, is typically used for carbon, low alloy, and stainless steels. The metal-cored wire consumables have been used to considerable advantage on fabrication of exhaust components such as Type 409 stainless steels. Metal-cored wires are also available for carbon and low-alloy steels, and provide productivity advantages through increased melting efficiency compared with solid steel wires.

Both flux- and metal-cored wire consumables can be used to weld butt, fillet, and lap joints. The applications can be similar to GMAW with brackets, body panels, spaceframe welding, and component parts being suitable.

4.3.2.3 Plasma Arc Welding (PAW)

The PAW process is like GTAW (Gas Tungsten Arc Welding) except that a copper nozzle protects the tungsten electrode. The nozzle has an orifice that focuses the arc to produce an increased power density compared with the conical arc of GTAW. PAW should be considered and used as an arc welding process most similar to Laser Beam Welding (LBW). PAW can be used in the melt mode (conduction mode) or keyhole mode. The melt mode is similar to GTAW, but with increased tolerance to variation in torch-to-workpiece distance (because of the columnar arc shape) higher power density, and increased tolerance to electrode contamination which is important when welding coated steels. Melt mode PAW can be used with or without cold wire addition.

4.3.2.3.1 PAW – Advantages and Disadvantages

The advantage of PAW is that it can be used with or without filler wire addition, and provides good control of heat input relative to wire addition. This can be used to advantage for a variety of joints where low distortion and good cosmetic appearance is important. The high penetration capability in the keyhole mode, allowing sheet stackups up to 8-mm thick to be welded without pilot holes, is a considerable advantage.

The main disadvantage to PAW for conventional joints is that good fit-up is required as the process is not very tolerant to joint gaps in the spot welding context, or in a lap-fillet joint configuration. For joints such as butt and lap-fillet joints this can be improved by adding filler wire. The equipment is also more expensive than that for GMAW.

4.3.2.3.2 PAW – Applications

Applications of PAW are currently limited to some brazing operations for roof-to-quarter panel joints, and to hemming of door outers to inners. The potential applications are larger than those currently being exploited.

4.3.2.3.3 PAW – Variant Processes

Plasma brazing is analogous to GMA brazing, but uses independent control of wire and heat through a separate heat source and external cold wire feed. This can be used to advantage to minimize spatter associated with arc starting in GMA brazing. The independent control of heat and wire enables better control of distortion, and also minimizes porosity compared with GMA brazing.

Plasma spot welding can be accomplished using the PAW process in the melt mode to produce a spot weld in multiple stackups, without addition of filler wire or the use of pilot holes. The ability to weld several sheet metal thicknesses, up to 8 mm in total thickness without pilot holes (such as are used in plug and slot welds for GMAW/FCAW) offers a considerable advantage. The equipment can be readily automated, or attached to a robot, and has good tolerance to variations in torch-to-workpiece distance because of the columnar nature of the arc.

4.3.3 LASER BEAM WELDING (LBW)

Laser processing is accomplished by a transfer of energy from a coherent beam of light to the material it is impacting. The power density and the interaction time of the light determine how the material is affected. Typical laser processes that can be achieved include heat treating, cladding, welding, cutting, and drilling. In all laser processing the energy is converted from light into thermal heating of the target material to achieve the desired result.

4.3.3.1 LBW -- Process Description

LBW requires a concentrated beam on a surface at a high enough level to melt the material (see [Figure 4.3.3.1-1](#)).⁽³⁰⁾ The critical concentration of energy is approximately 10^4 W/cm^2 for most ferrous alloys. At this power density, the energy transfer from the laser beam into the part occurs in two dimensions, and the depth of the weld is determined by the flow of material in the molten pool. This type of weld is very similar in appearance to a GTAW weld with a low depth-to-width ratio and is called “conduction mode welding”. At higher power densities, $>10^6 \text{ W/cm}^2$, the transfer of energy occurs in three dimensions. The three-dimensional heating is made possible by the high power density, which heats the molten material enough that it vaporizes. The pressure from the expansion of the substrate material causes the formation of a “keyhole”. Keyhole mode welding has the characteristic of a very high depth-to-width ratio.

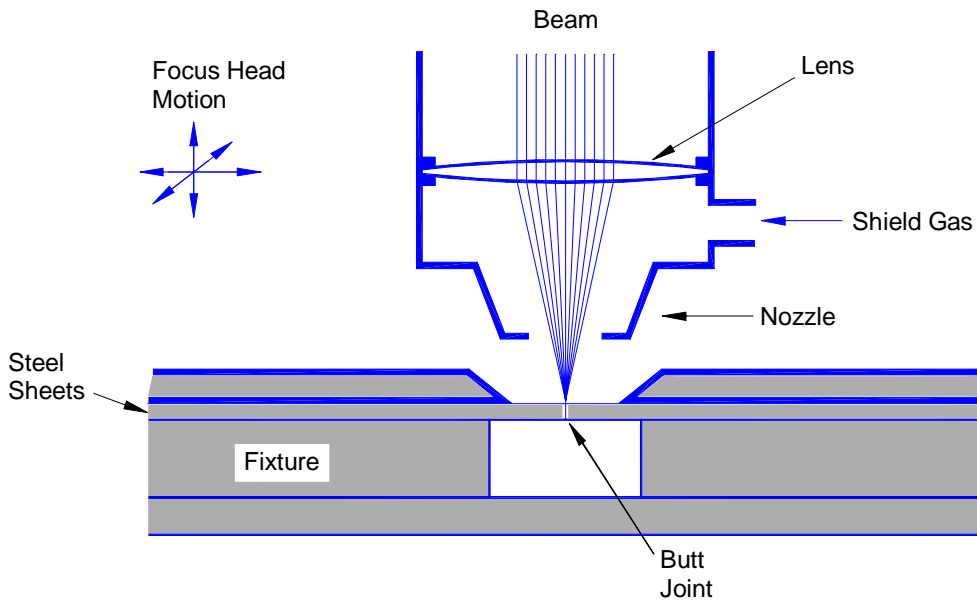


Figure 4.3.3.1-1 Example of Laser Welding Arrangement that may be Used for Tailor Blank Welding (The laser beam can be either CO₂ or Nd:YAG.)

In addition to the power density, there are other factors that determine whether a weld will be conduction or keyhole mode.⁽³⁰⁾ The melting point of the material, the reflectivity of the material, the relative speed between the material and the beam, the wavelength of the laser, and the power density profile of the laser beam are all factors that determine the configuration of the weld.

While there are major differences in the conduction and keyhole-mode laser welding, there are some similarities. Both processes can be accomplished in air, unlike electron beam (another high power density process), which requires a vacuum. Both processes can be accomplished without filler material being added (autogenous). Filler material can be added as shim, wire, or powder to address fit-up problems, meet positive re-enforcement requirements, or to alter the chemistry of the weld metal. Gases are often used to increase the transfer of energy in the keyhole welding process and shielding gases are also used to decrease the oxidation of the molten material, insure weld integrity, and improve the visual appearance of the weld.

4.3.3.2 Types of Lasers (CO₂ vs. Nd:YAG)

There are two primary laser types used for automotive welding of steel alloys: CO₂, a gas laser, and the Nd:YAG laser, a solid-state laser. The CO₂ laser operates at 10.6-μm wavelength while the Nd:YAG operates at 1.06-μm wavelength. While both lasers can use mirrors and lenses to direct and focus the beam, the shorter wavelength of the Nd:YAG permits it to be delivered by glass fibers (200- to 1000-μm diameter). Fiber delivery enables the use of Nd:YAG lasers in standard robotic systems for delivery, while CO₂ lasers are restricted to specially designed workcells, gantries, or complex manipulators. These factors can impact the capital investment and operation costs.

Also related to the wavelength are the safety issues associated with the different lasers. Because the processing is performed in an automated fashion, most laser processing is accomplished in

enclosures or at safe distance from workers. The only protection that is normally required in the area is for the eyes. For the CO₂ lasers, plastic safety glasses are sufficient, while the shorter wavelength of the Nd:YAG requires special glasses for eye protection.

Although there are system and safety issues, both types of laser are used in industrial facilities. The only concerns may be controlling the temperature of certain components and vapors or moisture in any beam-delivery system.

4.3.3.3 Typical Applications

The use of lasers in the fabrication of automotive components is growing rapidly.⁽³⁰⁾ Laser welding has permitted a number of major innovations such as tailor-welded blanks and three-dimensional cutting and welding of hydroformed parts.

The two major classes of laser welding applications are thin gauge and thick gauge. Thin gauges, typically less than 3 mm, can either be conduction or keyhole-mode welded. The mode will depend on the joint configuration (lap or butt joint) and the properties desired from the welded joint. To maximize production, higher processing speeds can be achieved with keyhole-mode welding, but welds are narrower. Narrower welds may potentially impact joint fit-up requirements. Poor fit-up can result in undercut which reduces the strength of lap joints. Conduction mode welding is slower but can reduce fit-up requirements and produces larger interfaces in lap joint welds.

Thick gauges, typically 3 mm and greater, normally require keyhole welding. The high depth-to-width ratio of the keyhole mode welding permits very deep welds to be made with minimal heat input. With these parameters there is less heat, and therefore little or no distortion, potentially minimizing post-weld processing or the impact on surrounding material.

4.3.3.3.1 Body Applications (Tailor Blanking)

One of the largest current applications of lasers in the automotive industry is in fabricating tailored blanks, where sheets of steel in various thicknesses, grades and coatings are welded prior to stamping to maximize performance and reduce waste. Examples include door rings, inner door panels, floor panels, and shock towers. For a fuller discussion, please refer to [Section 3.9.1, Tailor Welded Blanks](#).

4.3.3.3.2 Other Components

Lasers are also used to weld a number of other automotive components, such as:

1. Engine, transmissions, and suspension components
2. Exhaust manifolds, catalytic converters, mufflers
3. Temperature and pressure sensors, ABS sensors, electronic packages
4. Air bag igniters and inflators

4.3.3.4 Advantages/Disadvantages

The advantages and disadvantages of laser welding determine the best application of the process. Often the advantages and disadvantages occur in manufacturing steps before or after the laser welding process.

Laser welding has many advantages over other welding techniques. It is a very low heat input process less than 10% of the heat of arc processes. This means that there is little distortion of the workpiece or modification to the properties of the material in the vicinity of the weld. This may reduce or eliminate secondary processes or allow for welding to occur very late in the assembly process. Also, because high depth-to-width ratios are possible, lap joints can be accomplished in very thick materials. Other advantages of the process include:

1. Improved visual appearance
2. Little or no distortion or waviness
3. Capability to weld through multiple layers
4. Single-sided access

Laser welding may additionally offer mass reduction by decreasing or eliminating flanges normally required for spot welding. The use of continuous weld beads may also increase the stiffness of the structure compared with a spot-welded structure.

While laser welding has a number of advantages it also has disadvantages. One disadvantage is that laser welding is a “line-of-sight” process meaning that the weld joint must be visible for the weld to be made. Laser welding is a “thermal process” which means that there will be some distortion due to differential heating of the part during welding.

Some of the general disadvantages are:

1. Sensitivity to part fit-up
2. Sensitivity to the surface condition
3. Potentially poor weld quality when lap welding coated sheet steels due to trapped gases in the metal
4. High cost of equipment, which can be offset by productivity

4.3.3.5 Materials

Laser welding can be performed on a wide range of ferrous and non-ferrous alloys. Most steel alloys are very weldable either in the conduction or keyhole modes. The alloy composition and post-weld processing must be considered when selecting the welding parameters due to the high cooling rates associated with laser welding. High cooling rates can induce high hardness, high yield strength, low ductility, or low toughness in the weld metal or in the heat-affected zone (HAZ) of the weld. Despite this fact, laser welded tailored blanks have readily formable joints. The degradation of properties is of special concern for high-alloyed steels where martensite may form in the weld metal or HAZ.^(30,31)

Any coating on the steel may be a concern. The relatively low boiling point of zinc can make the laser weld unstable causing “blow holes” and porosity in the weld. This is a major problem for lap joints and less of a problem for butt welds. To prevent this problem in lap joints a gap may be established between the plates to allow for the zinc vapors to escape.

4.3.3.6 Design Considerations

If laser welding is considered in the design of a component, some major advantages can be utilized. The ability to adjust the stiffness of a joint by variations in the weld length or configuration allows for “fine tuning” of the structural performance of a joint.

The ability to make continuous welds with very low distortion has a number of advantages. The elimination of post-process grinding or straightening decreases production costs or can eliminate the need for sealers or other measures to take up irregularities in the joint.

4.3.4 OTHER WELDING PROCESSES

In the last few decades, a number of new, so-called single-shot solid-state processes have come into limited use in the automotive industry. The most common of these is friction welding, which uses relative motion of the workpieces to generate heat for bonding. Metallurgically, this process is quite similar to resistance butt welding described above with the exception that friction heating, rather than resistance heating, is used to achieve temperatures for forging.

Two variants of friction welding are used in automotive manufacture today: direct-drive friction welding and inertia welding. The primary differences between these two processes are the energy sources for friction heating. Direct-drive friction welding uses a continuously driving motor to achieve rotational velocities for friction heating. Friction heating is then done at a constant speed for a fixed time prior to forging. Inertia welding first stores energy in a rotating flywheel prior to welding. On contact of the workpieces, the energy of the flywheel is dissipated as friction heat (in the workpieces). Both variants of the process yield exceptional quality welds. Typical applications for friction welding in the automotive industry include engine valves and axle spindles. Friction welding has an implied advantage over resistance butt welding in that the amount of heat generated is based only on the motor or flywheel size. Therefore, sections of several tens of thousands of square millimeters can be welded.

Friction welding, however, suffers many of the drawbacks of resistance butt welding, including high equipment costs, the need for flash removal and part geometry restrictions. Since parts must be round, friction welding is limited to a relatively few automotive applications, and currently no body applications.

Magnetically impelled arc butt welding (MIAB) has also seen limited use in the automotive industry. MIAB welding allows joining of relatively thin-walled tube sections in relatively short times. The parts are positioned in a butt configuration similar to resistance butt or friction welding. The welding equipment uses relatively high-voltage DC power applied across the parts, a forging system for upsetting the parts, and magnetic coils around the parts. On welding, the parts are gapped, and an arc is established locally across the gap. Under the influence of the magnetic coils, the arc is driven around the periphery of the parts, generating uniform heat along the bond line. After sufficient heat is generated, the parts are upset together. The process is capable of short cycle times, similar to that for resistance butt and friction welding. In addition, non-round sections and very thin-wall tubing can be welded. The process has seen extensive use for applications such as prop shafts and spindles in Europe; however, the technology has not been used in North America.

The process has similar drawbacks to resistance butt and friction welding in that equipment costs are high, and flash removal may be a concern. An additional concern with MIAB welding is that joinable wall thicknesses are relatively limited. Generally, the process is not recommended for parts with wall thicknesses greater than 3 mm.

REFERENCES FOR SECTION 4.3

1. American Motors Corporation, Criteria for Evaluation of Resistance Spot Welds (Mild and HSLA Steels), Manufacturing Engineering Standard 76-8.
2. American Welding Society D8.7-78, Specification for Automotive Weld Quality – Resistance Spot Welding (1978).
3. American Welding Society D8.6-77, Standard for Automotive Resistance Spot Welding Electrodes (1977).
4. American Welding Society C1.3-70, Recommended Practice for Resistance Welding Coated Low Carbon Steels (1970).
5. American Welding Society C1.1-66, Recommended Practice for Resistance Welding (1966).
6. Auto/Steel Partnership Report AZ-017-02 997 1.0C EG, “Weld Quality Test Method Manual” (Oct. 31, 1997).
7. Chrysler Corporation, Resistance Spot Welding – High Strength Steel Structural Components, Process Standard PS-6328 (Aug. 31, 1978).
8. DelVecchio, E. J., Resistance Welding Manual, 4th Edition, Resistance Welder Manufacturers’ Association, Philadelphia, PA (1989).
9. Dickinson, D. W., Welding in the Automotive Industry, Report SG 81-5, American Iron and Steel Institute (Aug. 1981).
10. Ford Motor Company Specification BA 13-4, Resistance Spot Weldability Test for High Strength Low Alloy (HSLA) Steel (Sept. 26, 1980).
11. Ford Motor Company Specification BA13-3, Welding Acceptance Test for ZINCROMETAL (Nov. 25, 1972).
12. Ford Motor Company Specification BA13-1, Welding Acceptance Test for Galvanized Steel (June 8, 1971).
13. Ford Motor Company, Resistance Welding Cap Electrodes, Manufacturing Standard WC-1 (July 1971).
14. General Motors Corporation, CPC Group, Specifications and Procedure for Determining the Weldability of Zinc Preprimed Sheet Steel, Specification MDS-246 (revision of July 16, 1985).
15. General Motors Corporation, Automotive Weld Quality – Resistance Spot Welding Low Carbon Steel, Engineering Standard GM 4488P (Apr. 1985).
16. General Motors Corporation, CPC Group, Specification MDS-247, Specifications and Procedure for Determining the Weldability of Body Steel Materials (revision of July 18, 1984).

17. Howe, P., "Spot Weld Spacing Effects on Weld Button Size," Paper C3, Proceedings of AWS Sheet Metal Conference VI (Oct. 1994).
18. IIW, Recommended Practice for Spotwelding Zinc-Coated Sheets, Document III/399/71 (May 1971).
19. Welding Resistance: Spot and Seam, Military Specification MIL-W-6858D (Oct. 20, 1964).
20. Vol. 2, Welding Handbook, 8th Ed, American Welding Society, Miami, FL, 1991, p.555
21. "Welding and Brazing," Metals Handbook, Vol. 6, ASM, pp. 401-484 (1971).
22. Welding, Resistance, Spot and Projection for Fabricating Assemblies of Carbon Steel Sheet, Military Specification MIL-W-46154(MR) (Oct. 20, 1970).
23. American Iron and Steel Institute Report SG 85-2, "Solutions to Manufacturing Problems Using Galvanized Steel," W. J. Riffe ed. (second printing June 1986).
24. American Welding Society D8.4-61, Recommended Practice for Automotive Welding Design (1961).
25. Auto/Steel Partnership Report ZSP7060 0997 1C EWI, "Resistance Spot Welding Electrode Wear on Galvannealed Steels" (Sept. 1997).
26. Auto/Steel Partnership Report AZ019 01 694 2.5C EWI, "Mechanisms of Electrode Wear During Resistance Spot Welding Hot-Dipped Galvanized Steel" (June 1994).
27. Chrysler Corporation, Resistance Weldability Test for Uncoated High Strength Steels, Laboratory Procedure LP461K-167 (revision of Sept. 4, 1981).
28. Chrysler Corporation, Resistance Weldability Test for Galvanized High Strength Steels, Laboratory Procedure LP461K-167 (revision of Nov. 25, 1981).
29. American Welding Society D19.0-72, Welding Zinc-Coated Steel (1972).
30. Steen, W. M., Laser Material Processing, Springer-Verlag, 1991.
31. Belforte, D. and Levitt, M., The Industrial Laser Annual Handbook, 1990 Edition, Pennwell Books (1990).

BIBLIOGRAPHY FOR SECTION 4.3

1. American Iron and Steel Institute Report SG-936 282-10M-RI, "Spot Welding Sheet Steel."
2. American Welding Society Specification D8-8, Specification for Automotive and Light Truck Components Weld Quality – Arc Welding (1997).
3. American Welding Society D8.5-66, Recommended Practice for Automotive Portable Gun Resistance – Spot Welding (1966).

4. Chrysler Corporation, Resistance Weldability Test for Galvanized and Galvannealed Low Carbon Hot and Cold Rolled Steel Sheet, Process Procedure LP461K-170 (revision of Jan. 26, 1984).
5. Chrysler Corporation, Resistance Spot and Arc Welding Automotive Components, Process Standard PS-1682 (Aug. 30, 1983).
6. Resistance Welding Equipment Standards, Resistance Welder Manufacturers' Association, Bulletin 16.

4.4 ADHESIVE BONDING

Adhesives must be adaptable to the manufacturing environment. The sequence of operations associated with bonding is as distinct from welding or mechanical fastening as the equipment employed. This section gives an overview of the adhesive bonding process, including the dispensing (and mixing) of the adhesive, handling the assembly while the adhesive sets, the compatibility of the adhesive with the adherends, and compatibility with downstream processing.

4.4.1 DISPENSING ADHESIVES

The manufacturing problems associated with dispensing adhesives depend to a great extent on whether a one or two-part adhesive is being dispensed.

4.4.1.1 One-part Adhesives

One-part adhesives are relatively easy to dispense. The amount of adhesive dispensed and the location of the adhesive on the adherends must be controlled in order to bond effectively. One-part adhesives have high viscosities, hence after-flow (stringers) can be a problem. Viscosity problems are avoided by keeping the pot at a constant temperature. In general, the dispensing of these adhesives is trouble free.

4.4.1.2 Two-part Adhesives

Two-part adhesives begin curing as soon as they are mixed; therefore the timing associated with mixing and dispensing is critical for achieving well bonded joints. A fairly sophisticated delivery system, such as the one illustrated in [Figure 4.4.1.2-1](#), is needed to mix the adhesive properly and deliver it to the joint at the proper time.

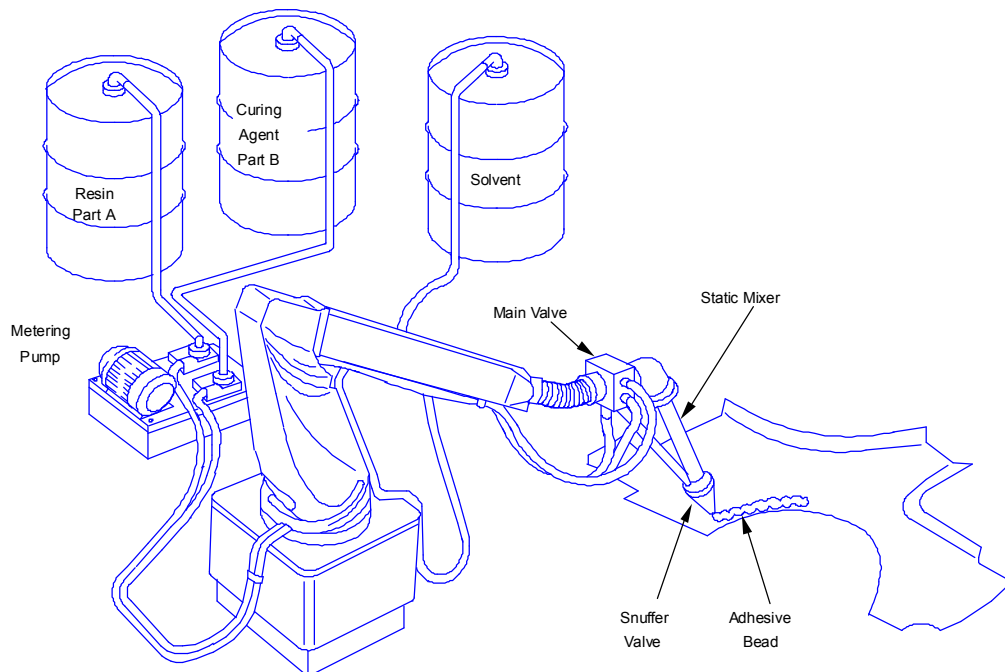


[Figure 4.4.1.2-1](#) Typical two-part adhesive robot dispensing system [1](#)

Resin viscosity, mix ratios, mix chemistry, and mix times must all be controlled. Downtime is routinely needed to purge and clean the dispensing equipment. Backup equipment and labor must be available to prevent work stoppages. Disposable mixers can be used to reduce downtime, but they entail additional costs. Nevertheless, two-part adhesives develop handling strength rapidly, and require less fixturing than one-part adhesives. These characteristics make them a reasonable choice for many joining applications.

The latitude to vary the mix ratio of a two-part adhesive is convenient; then open time and viscosity can be varied, within limits, to adjust the bonding process to production parameters. Changes should be made with caution, because they will tend to affect the physical properties of the adhesive, depending on the sensitivity of the adhesive to mix ratio. An adhesive that is not overly sensitive to mix ratio is advantageous since it will offer more latitude for variation, and consequently more latitude to accommodate manufacturing variables. In any case, maintenance schedules and dispensing parameters must be revised as the mix ratio is changed.

A major disadvantage in the use of two-part adhesives is the possibility of the adhesive curing in the dispenser. This problem may be avoided either by frequent maintenance of the dispensers or by the use of disposable static mixers. The static mixer should be placed at the dispensing tip; otherwise the tubing and conduit that are placed after the static mixer must be discarded with the mixer.

The key advantage of two-part adhesives over one-part adhesives is the ability to achieve handling strength rapidly. They also respond very quickly to mild heating, so that localized heat sources can be used to accelerate the chemical reaction after dispensing ([Figure 4.4.1.2-2](#)).

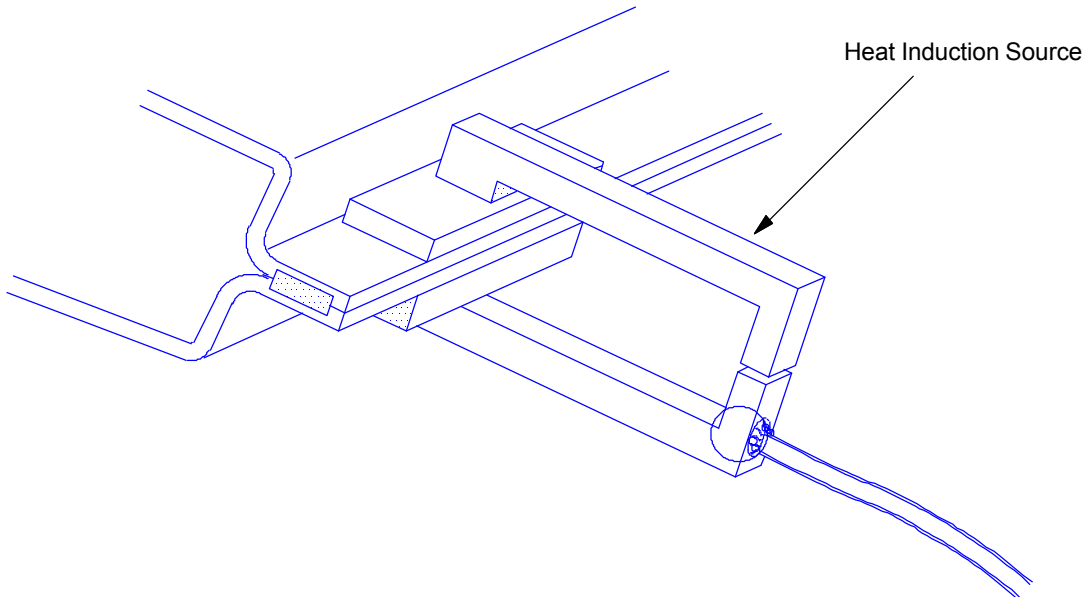


Figure 4.4.1.2-2 Localized heating can be applied to accelerate the chemical reaction and develop handling strength [1](#)

Productivity is improved because of the shorter cycle time. In each application, the balance between the amount of fixturing required, allowable variations in the physical properties of the adhesive, and the cycle time must be determined. Input from the entire design, manufacturing, and materials team is essential to reach an appropriate balance.

4.4.2 HANDLING STRENGTH AND FIXTURING

Handling strength must be developed rapidly in a bonded joint so that the assembly can quickly move to the next processing step. This is a key concern when using any adhesive. One method, mentioned above, is to apply localized heat sources to accelerate the chemical reaction.

Fixturing is often used to maintain the integrity of the assembled joint until the adhesive develops handling strength. Many fixturing methods are available for use with one-part and slow curing two-part adhesives. Three are commonly employed for sheet steel:

1. Mechanical fixturing methods, such as rivets, Tog-L-Loc™, or widely spaced spot welds, are illustrated in [Figure 4.4.2-1](#) and [Figure 4.4.2-2](#). These fasteners may be used to enhance the structural performance of the joint, as described in [Section 3.4](#), or they may be used only to support the parts during handling, with the cured adhesive providing the strength needed in service.

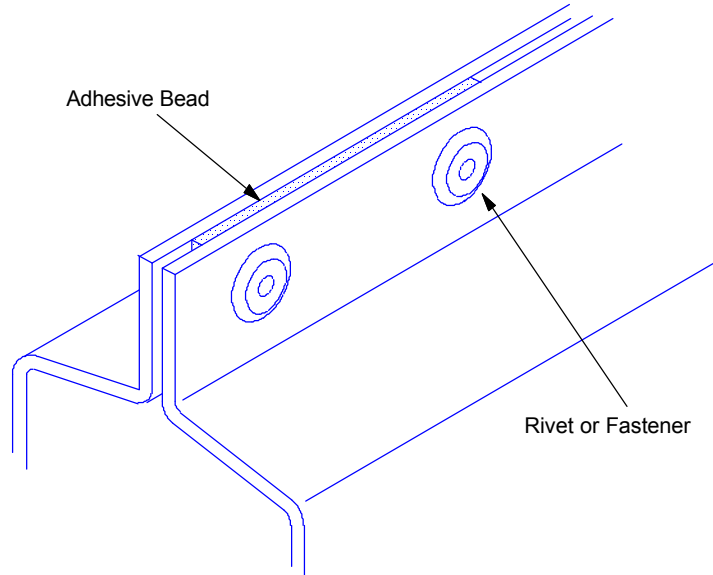


[Figure 4.4.2-1](#) Mechanical fasteners, such as rivets, can be employed to develop handling strength ¹

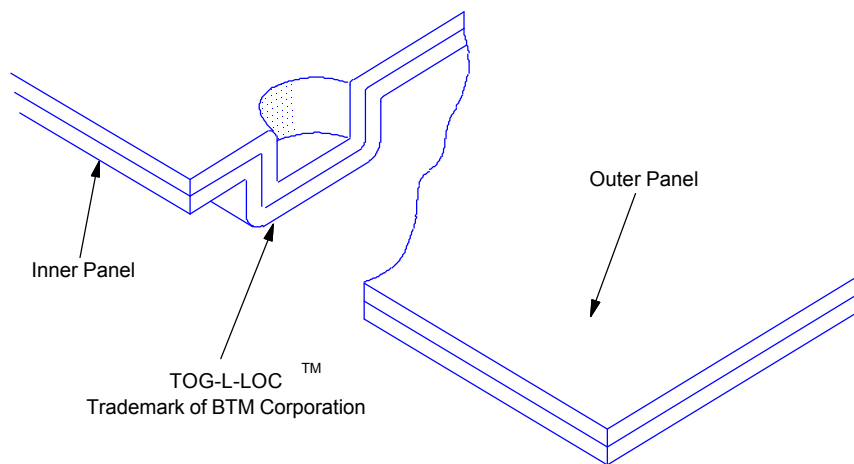


[Figure 4.4.2-2](#) Mechanical fastening can be employed to develop handling strength ¹

2. The sheet can be bent in a variety of ways to secure the joint. [Figure 4.4.2-3](#) and [Figure 4.4.2-4](#) show examples of this type of fixturing.

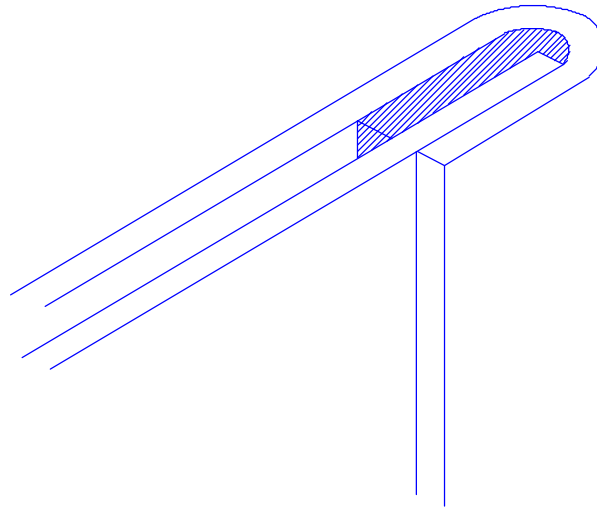


Figure 4.4.2-3 A hem flange can be used to fixture components while the adhesive develops handling strength. The adhesive has been confined by the flange, eliminating squeeze-out or run-out ¹

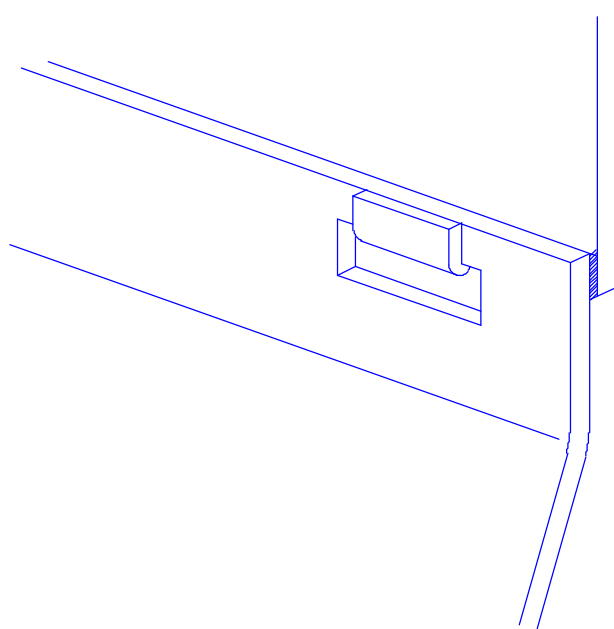


Figure 4.4.2-4 “Toy tabs” are a convenient means of fixturing ¹

3. A small amount of a faster curing adhesive, such as a hot melt, can be used for fixturing. Care must be taken so that the hot melt does not flow out of the joint in the paint ovens.

4.4.2.1 Trip Curing

Trip curing mechanisms are a convenient alternative to fixturing and a means to achieve handling strength quickly. These techniques initiate the cure of the adhesive shortly after dispensing. One such mechanism is induction heating, which can be used with some one-part epoxies ([Figure 4.4.1.2-2](#)). The cure of one-part urethane adhesives can be accelerated by injecting water into the adhesive stream. Other trip curing mechanisms involve pretreating the sheet with a catalyst ([Figure 4.4.2.1-1](#)) or adding a pressure activated catalyst within the adhesive ([Figure 4.4.2.1-2](#)). The last two methods are, strictly speaking, two-part adhesives. However, since the catalyst's function is only to partially cure the adhesive, and since no mixing occurs while dispensing the adhesive, they may be considered one-part adhesives with trip curing. There are efforts currently underway to use metal coatings or lubricants to trip cure adhesives.

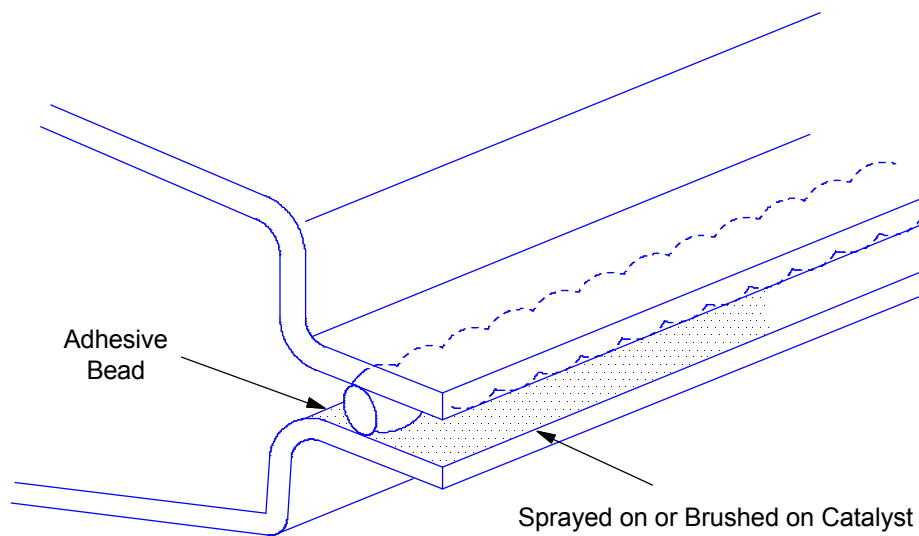


Figure 4.4.2.1-1 A catalyst may be applied to one of the steel surfaces to act as a trip-curing mechanism

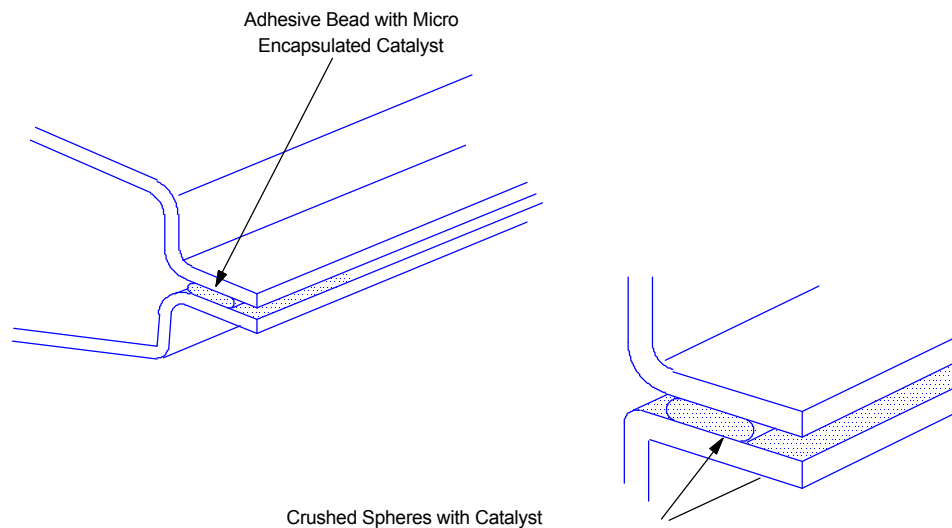


Figure 4.4.2.1-2 The catalyst may be encapsulated in micro glassbeads that crush and release the catalyst as the adhesive bead is compressed

4.4.3 SUBSTRATE CONSIDERATIONS

The compatibility of the substrate with the adhesive is very important. The steel surface, its coating, and any working fluids such as drawing compounds, lubricants, and mill oils must be evaluated for adhesive compatibility.

The performance of one-part epoxies is not generally affected by mill oils. The high viscosity epoxies displace most of the oil and they absorb the remainder. The longer the adhesive sits on the steel before curing, the more oil it can absorb. This absorption capability makes one-part epoxies more reliable and less sensitive to surface contaminants.

One-part acrylics and two-part epoxies can be applied to mill-oiled surfaces if there is no substantial puddling of oil. However, two-part urethane adhesives require a prepared surface, such as a solvent wipe or priming, for bonding.

Drawing compounds pose a special problem since they are diluted with water. If moisture is trapped at the adhesive/steel interface, it can cause a one-part adhesive to expand uncontrollably when heated, disrupting the bond. The presence of trapped moisture will also reduce the long term properties of most adhesives. Therefore it is important that drawing compounds or other sources of water be removed from the adherends before applying the adhesive.

When steel is joined to plastic, special care must be taken because mold release agents on the plastic often interfere with adhesive bonding. Materials such as sheet molding compounds (SMC) require special attention since the mold release agent is an integral part of the material. SMC parts require wiping or abrading the substrate prior to bonding. Primerless adhesive systems aimed specifically at SMC applications are being developed.

Adhesives are sensitive to surface conditions; thus substrate compatibility is essential. An effective way to avoid compatibility problems would be to standardize all surface treatments, including those used by steel suppliers, those used within the stamping plants and those used within the assembly plants.

4.4.4 COMPATIBILITY WITH DOWNSTREAM PROCESSING

The adhesive should not affect any processing done after bonding, nor should the bond be affected by subsequent processing. The adhesive must be inert. This is especially important when bonding automotive assemblies, since an assembly will go through cleaning, pretreating, rinsing and painting before heat curing, and it is undesirable to have any of these processes contaminated with adhesive. It is best to use an adhesive that cures before the assembly arrives at the next processing step. If the adhesive cannot be completely cured, any degree of cure will improve its inertness; therefore, trip curing may be helpful. Contamination problems can be avoided by using a high-viscosity adhesive that will not wash out of the assembly and by using an adhesive resistant to subsequent chemical processing.

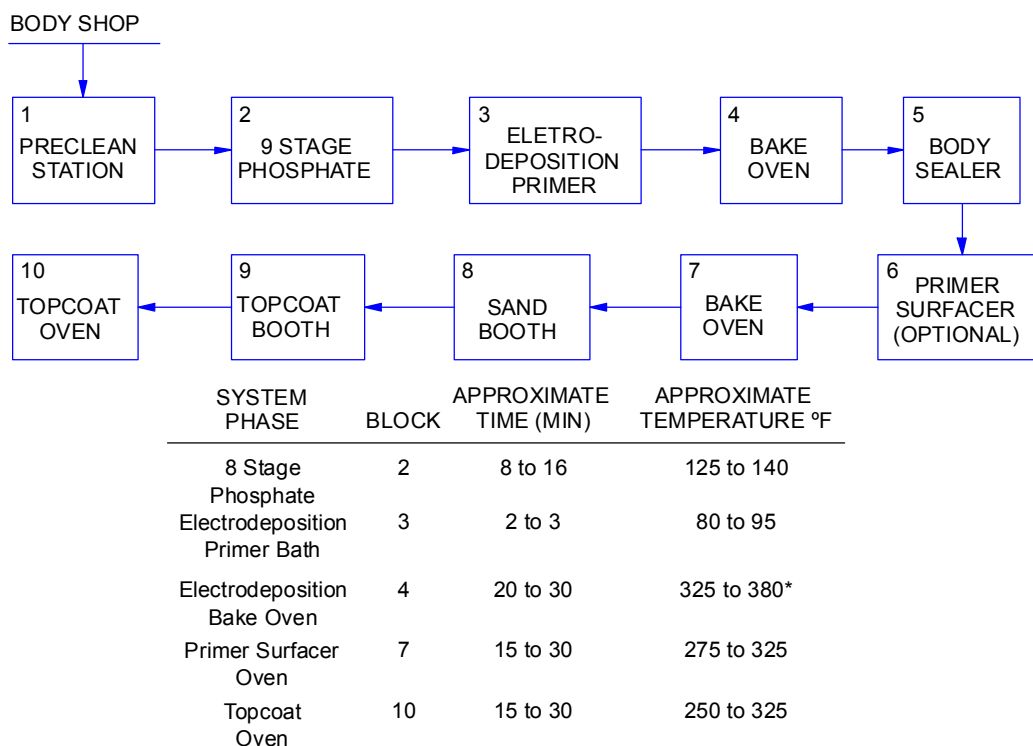
Adhesive read-through is an occasional downstream problem. Read-through is observed on an exterior panel when an adhesive on its inside surface shrinks excessively in a paint oven. It is most visible when an inner panel is bonded to an outer panel such as a deck lid or hood. As expected, thin panels are more prone to read-through than thick panels. Low shrinkage adhesives and proper production control can minimize or eliminate this problem.

REFERENCES FOR SECTION 4.4

1. Adapted from "Adhesive Bonding of Sheet Steels", 1987, American Iron and Steel Institute, Washington, D.C.

4.5 FINISHING SYSTEMS

The finishing process in a modern assembly plant includes a wide range of operations such as cleaning, pretreating, painting and application of supplemental coatings. These operations are intended to produce a vehicle finish with a high level of customer appeal as well as durability and corrosion resistance. [Figure 4.5-1](#) is a block flow diagram of a typical automotive finishing system. Currently various corrosion resistant coatings are available, such as Zn (zinc) and ZnFe (zinc-iron) which are applied by both the EG (electrogalvanize) and HDG (hot dip galvanize) processes. There may be significant differences in the ways that products respond to finishing processes, depending on the coatings. The designer should be aware of these effects before specifying a material and coating process.



*Certain oven zones may have ambient temperatures of 410 °F; during a line stop, the surface temperature can approach 410 °F.

Figure 4.5-1 Typical automotive finishing system

4.5.1 PRETREATMENT

Prior to the pretreatment phase, cleaning is done in the body shop to remove sheet metal fines and to prepare the unit for highlighting and inspection. Mill oils, draw compounds, and shop soils such as metal filings are removed in one or more stages of the spray washers. Bodies may be cleaned before or after the installation of doors, deck lids and front end sheet metal. The proprietary cleaners used in the washers are formulated to remove light soils and provide temporary corrosion protection. They must not inhibit or interfere with the subsequent phosphate process. It is therefore important that mill oils and drawing compounds be evaluated for removability as well as lubricating characteristics. Any contaminants remaining on the surface of the unit prior to painting may cause a defect that requires a paint repair.

4.5.1.1 Preclean

A preclean operation is performed, prior to entering the phosphate unit, in which a water based cleaner is applied to the body, either by hand wiping or misting nozzles ([Figure 4.5-1](#) block 1). This phase is intended to soften soils and promote more effective removal during the cleaning stages. Following this step the body enters the first stage of the phosphate unit (block 2).

4.5.1.2 Zinc Phosphate Coating

A high quality zinc phosphate coating is the basis for good paint system performance. Its purpose is to provide a base for paint adhesion and minimize under-film corrosion if the paint film is broken. Each stage may be total spray, total immersion or partial immersion; each is usually one to two minutes in length. A phosphate unit may consist of eight or more stages, which may be all spray, all immersion or a combination. Blocks 1 through 8 in [Figure 4.5.1.2-1](#) show the individual stages in a typical eight-stage zinc phosphate system.

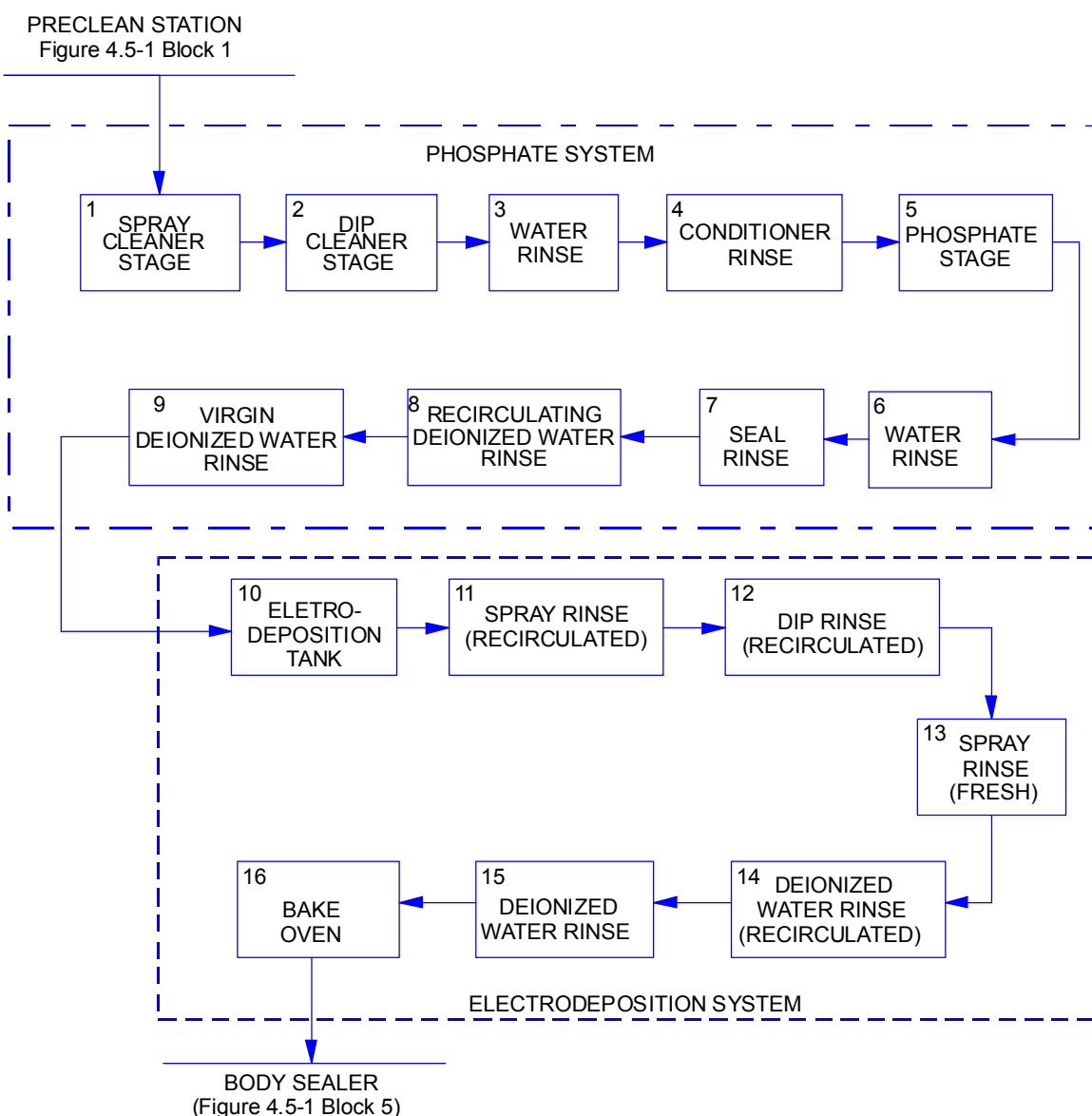


Figure 4.5.1.2-1 Phosphate/electrodeposition system

Spray systems use nozzles to direct the process solutions onto the body. Side, floor and overhead nozzles insure complete coverage of the exterior surfaces of the body. Generally, interior surfaces and box sections are only partially covered by spray or flood nozzles directed through openings in the body. The spray system offers effective cleaning of the exterior surfaces by impingement of the solutions. It offers the advantages of relatively short length of equipment and lower chemical concentrations. The major disadvantages are higher maintenance costs and poor interior coverage. The use of coated steels on interior surfaces can reduce the occurrence of inside-out corrosion, which may result from poor cleaning of interiors.

Immersion systems dip the body into the process solutions. As the body moves through the bath, pumps and piping circulate the solutions, improving coverage on interior sections. In order to obtain maximum effectiveness, interior sections must be designed to allow for the flow of solutions within them. An immersion system offers optimum crystal size, easier chemical control, improved coverage on interior sections and easier maintenance. Disadvantages are greater length of equipment and higher initial cost.

Partial immersion is a combination of spray on the upper portion of the body and immersion on the lower. The compromise between total spray and total immersion is determined by equipment cost, length of equipment, maintenance and effectiveness of the operation.

In a modern nine-stage unit, cleaning and rinsing are accomplished in the first four stages. Two widely used configurations are clean-rinse-clean-rinse ([Figure 4.5.1.2-1](#) blocks 1 through 4) and clean-clean-rinse-rinse. Cleaners used in the phosphate unit must not only clean the metal but also be compatible with the phosphate bath chemistry so as not to inhibit formation of the phosphate coating. For this reason the phosphate system is considered a process and all chemicals are purchased from the same supplier who formulates the bath chemistry to accommodate the processing of various metals.

Immediately before entering the phosphate stage the metal is treated with a proprietary compound to promote a uniform, fine grained phosphate coating (conditioner rinse, block 4). In the phosphate stage (block 5), the coating is formed by spraying or dipping the body in an acidic solution of zinc phosphate, together with other compounds. The crystals are formed on the metal surface through subsequent precipitation of the zinc phosphate. The small grained, tightly compacted uniform coating formed in the process enhances paint adhesion and corrosion resistance. Following the phosphate stage the body is rinsed with water to remove any residual chemicals (block 6).

In the next stage (block 7), the body is rinsed with a material containing chromium compounds to improve the corrosion performance.

The final stage of the phosphate process is a virgin deionized water rinse (block 9) that dilutes any process solutions remaining on the body which, if left on the surface, would reduce durability and cause paint contamination.

4.5.2 ASSEMBLY PLANT PAINT PROCESS

The first step of the paint process in a modern assembly plant is the application of a corrosion resistant primer over the zinc phosphate coating ([Figure 4.5-1](#) block 3). Although some plants still use spray or dip application, most of the automobiles produced worldwide utilize an electrodeposition process. A typical electrodeposition process and subsequent bake operation are

amplified in blocks 9 through 15 in [Figure 4.5.1.2-1](#). After application of the primer the coating is cured by a 325-380°F bake, depending on the material, for approximately 20 to 30 minutes ([Figure 4.5-1](#) block 4).

After the application of corrosion resistant primer, the seams, hem flanges and drain holes are sealed with any one of a variety of materials (block 5). Flowable sealers, thumb grade sealers and hot melt patches are usually applied manually, although robot application for flowable sealers is increasing. A short oven bake of 10-15 minutes may be used to set up or gel the sealers. More commonly, the sealers are co-baked with the paint system.

The next step in many processes is the application of a primer-surfacer (block 6), which is formulated to fill minor surface imperfections and supply a base for the color coats. Lately, these primers have been formulated to provide a chip resistant layer to protect the metal from stone damage and corrosion. These can be solvent borne liquid or solvent free powder coatings. The liquid primers can be applied by air or rotary atomized equipment (with or without electrostatics) while the powder coatings require electrostatic rotary atomized equipment. After a bake in the range of 135 to 175°C (275 to 350°F), depending on the material, (block 7) and cool down, the body can be sanded (block 8).

The oven bake cycle is important when bake hardenable steels are used. For a discussion of bake hardenable steels, see [Section 2.5.3](#).

Several methods of sanding may be employed including wet, moist and dry. The total body is usually sanded by the wet process, which utilizes air driven sanders and large quantities of water. Moist sanding involves localized sanding to remove dirt or surface imperfections. Dry sanding may be applied to specific locations or to the total body. As the name implies, it is performed without water. Residual dust must be removed after completion of the sanding operation by water washing, vacuum, air blow off or tack cloth.

The final phase of the painting operation is the application of the color coat (block 9). The majority of the automobiles built worldwide are top coated with enamels. A few lacquer plants remain in operation while awaiting conversion to enamel. High solids enamels and base coat/clear coat are widely used in the United States. However, these are now being replaced by a combination of high solids water borne color base coats and high solids solvent borne clearcoats to meet U.S. Clean Air regulations. A combination of air and rotary atomized equipment is generally used. The topcoat is cured by a 250 to 325°F bake for 15 to 30 minutes, depending on the material (block 10).

4.5.3 PAINT APPLICATION METHODS

A wide variety of paint application methods has been historically used in the automotive industry. The basic categories are dip, flow coat, electrodeposition, air atomized spray and centrifugal atomized spray. Most modern automotive paint lines use a combination of different types of application equipment to obtain the lowest emissions and paint usage with the best finish appearance.

Dip painting is accomplished by immersing the part to be coated in the paint. This method has used both solvent base and water base paints. There are several disadvantages with the process. Paint film thickness is less at the top of the part than the bottom, and the reduced film thickness may cause durability problems. Drips may occur on bottom edges causing both cosmetic and durability problems. Edge coverage is also a problem. Interior areas coated with a dip primer

may experience a problem known as solvent wash where trapped solvent vapors wash away the uncured paint.

Flow coat painting utilizes a series of small diameter pipes to flow the paint onto the parts. Interior coverage is usually less than with a dip material. The other disadvantages of the process are the same as with the dip process.

Electrodeposition painting is accomplished by immersing the part to be coated in the paint and applying a charge to the part, which attracts the paint particles. The part may be either positively or negatively charged; most automotive lines today are negatively charged. Process equipment is complex consisting of power supply, pumps, filters, heater, cooler, storage tanks and rinsing equipment.

Major advantages of the electrodeposition process are high transfer efficiency (paint applied versus paint consumed), improved interior section coverage, lower solvent emissions, uniform film thickness and reduced labor. Disadvantages are in the complex and expensive equipment that is required. The process also renders interior coverage highly design dependent. Although the part is completely immersed in the paint, only the areas of the interior sections that receive a current density high enough to cause deposition of the paint are coated. There is a tradeoff between enough holes in an interior section for paint coverage and the adverse effect of the holes on structural and acoustical properties. This, together with the problem of trapped air, presents major design and processing concerns.

The air atomized spray gun is a widely used method for applying primer-surfacers and color coats. This type of gun uses compressed air to break up the liquid paint into finely divided particles, which allows rapid solvent evaporation as the paint is applied to the part. A major disadvantage of this type of process is low transfer efficiency and, in the case of solvent based paints, high solvent emission from the paint booth stacks. Air atomized electrostatic guns use a combination of compressed air at lower pressures and gun tip design to break up the liquid paint before an electrical charge is applied. This method produces more efficient paint usage (greater transfer efficiency). Today's higher solids paints, combined with electrostatic charging of the paint, have improved transfer efficiency and reduced solvent emissions.

The latest development in paint application is the disc or bell. With this method the liquid paint is atomized as it comes off a rapidly rotating (20,000 to 60,000 rpm) disc or bell shaped rotor. An electric charge, typically 80,000 volts, together with low pressure shaping air, directs the paint onto the object to be coated. Transfer efficiency is greater, and solvent emissions are therefore less with this system compared to air atomized application.

4.6 THIN-WALLED WELDED STEEL TUBE FORMING

Seam welded cold-rolled steel tubing can be an alternative to assemblies of two stamped shells welded into tubular structures. The tubing can be mandrel/die bent and may be additionally formed to the desired shape hydraulically. Typical pre-formed cross sections used in structural automotive parts are circular and rectangular.

Several processes are employed for forming tubing. The selection depends on the complexity of the end product.

- When only reorientation of a constant section is required, the tubing is bent.
- When more than reorientation of a constant section is needed, the bent section can be locally compressed in an open cavity.
- When more complex reshaping is needed, the bent tube can be placed in a closed die set where a pressurized fluid is introduced into the ends of the tube, reshaping it to the confines of the cavity, in a process known as hydroforming.
- If more shape changes are needed, hydroforming can be performed at higher pressures or be combined with compression bulge forming.

Following is a description of these processes, starting with tubing fabrication and progressing from the simplest to the most complex reshaping processes.

4.6.1 FABRICATING THIN WALLED STEEL TUBING

Thin walled steel tubing for automotive applications is fabricated in a high speed, continuous process. The type of steel selected depends on the requirements of the application and the forming process. Tubing for hydroforming is typically made from 1008-1010 aluminum killed steel or medium strength HSLA steel, either in ASTM half-thickness tolerance hot rolled or ASTM regular-thickness tolerance cold rolled coils. The sheet is slit to a strip of width required for the perimeter of the tubular section. The strip then passes through rolls where it is formed into a closed circle, and the edges are welded either by a high frequency butt or TIG weld as shown in [Figure 4.6.1-1](#).

The rough weld joint may then be cleaned up. Normally only the outside is cleaned up unless subsequent processing utilizes mandrels that require a smooth inner surface. The tubing may also be annealed, depending on the material. The tubing is then longitudinally stretched or circumferentially compressed to precisely set the outer perimeter. If another shape, such as a rectangle is required, the round tube is rolled to the new shape. If the steel is bare, the tubing is pickled and oiled. Finally, the continuous tube is cut into straight, finite lengths for further processing, and washed clean of cutting fluids and chips.

The steel coil is processed into tubing at either a steel processing plant or a tube fabricating facility. The added processing cost, which depends on the number of finishing operations, typically ranges from \$0.11-0.22 per kg (\$100-200 per ton or \$0.05-0.10 per pound).

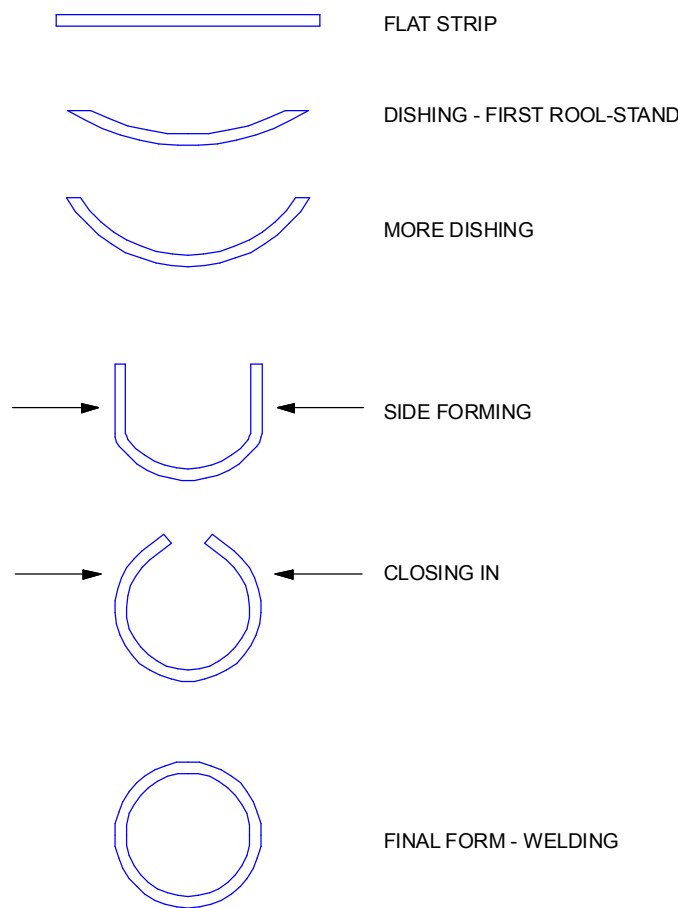


Figure 4.6.1-1 Tube forming process

4.6.2 MANDREL OR DIE RESHAPING OF TUBULAR SECTIONS

If a tube with a constant cross section of various orientations is sufficient, a bent or twisted tube is the most economical solution, sometimes with the addition of local smashing, as shown in [Figure 4.6.2-1](#). Processing is performed in high speed tube benders. Instrument panel support bars and utility vehicle frame rails are examples of these applications.

Tube bending limits are driven by necking or thinning constraints on the outer wall; the forming limit of the material must not be exceeded. Therefore, a forming limit diagram for a particular steel may be required. To estimate bending radius limits:

- Assume a neutral axis located one third the section height from the inside diameter.
- Calculate the elongation of the outer fibers after bending.

Wrinkling may also occur on the inside of the bend if the inside bending radius is too small. This may also be a forming limit or product stability limitation for sections with a low ratio of thickness-to-diameter¹. NC feedback controlled bending of tubes tends to produce better dimensional repeatability than stamping and post-welding. In some cases, NC bent-and-drilled structure sub-parts have been so repeatable that clamping and control points have been minimized on the final assembly fixtures.

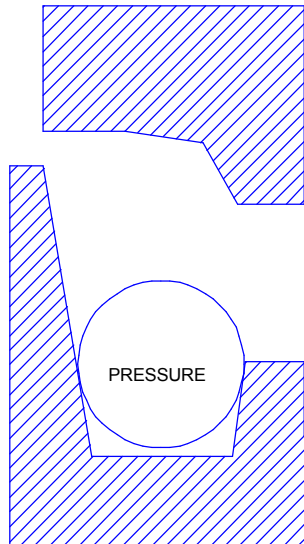


Figure 4.6.2-1 Local tube compression

4.6.3 DIE BENDING

If a straight tube can be dropped into a tubular width cavity, the part can be reshaped in a single plane die-and-punch operation. The process allows limited reshaping of the perimeter, punching of holes and local compression. It does not require special tube bending equipment.

4.6.4 HYDROFORMING

Processing techniques for hydroforming were originally patented in Japan in 1962. The process was initially restricted to a few part suppliers. After the patents expired, the process reappeared and matured in the pipe fitting industries. It is relatively new to the automotive body, exhaust and chassis structure industries. The process is divided into two principal types: low pressure and high pressure. A typical setup for hydroforming is shown in [Figure 4.6.4-1](#).

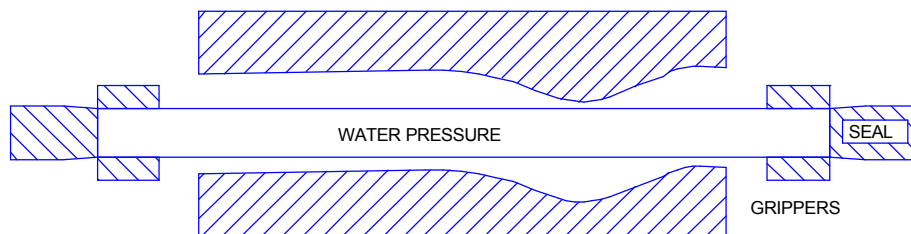


Figure 4.6.4-1 Typical hydroforming setup

4.6.4.1 Low Pressure Hydroforming

If a constant perimeter length (less than 5 percent expansion) with reshaping will satisfy the product needs, or if greater dimensional control is needed than for die struck parts, low pressure hydroforming of die bent or mandrel bent tubes is a low investment process. Cycle times are slightly longer than for a bent or mechanically formed tube, and shorter than for a high pressure process.

Low pressure hydroforming is arbitrarily defined by the Tube and Pipe Fabricators Association as a process using fluid at pressures less than 83 MPa (12,000 psi). The fluid is typically water with a rust inhibitor. A complete cycle consisting of preform loading, forming, depressurizing and unloading ranges from 15 seconds to more than a minute.

A companion process, called pressure sequencing, is used at the same pressure range. It consists of applying a pre-pressure, and varying the applied pressure as the dies are closed.

The preform consists of a straight, bent, twisted or locally deformed tube. Die splits must be designed to allow the preform to drop into the cavity and the finished part to be extracted from the cavity. The preform must have sufficient dimensional repeatability to drop readily into the hydroforming cavity; conversely, the dies must be able to tolerate the expected variations in the preforms. The design limits of the cavity split lines for insertion of the preform into the hydroform cavity may limit the final complexity of the finished parts.

Forming pressures less than 28 MPa (4000 psi) generally produce one percent perimeter expansion or less, and sections with nearly equal wall thickness. Perimeter expansion is governed by yield strength, work hardening and initial wall thickness as well as pressure. Forming pressures above 28 MPa (4000 psi) are used for parts that require more consistent forming beyond the yield strength, and perimeter stretching up to five percent. Normally, the higher the applied pressure, the higher the initial investment for tooling, hydraulic interfaces to the tubing, and pressurizing equipment. Both pressure levels seem to equalize the strain over the entire part and improve part repeatability beyond that of NC controlled bent parts.

A hydroforming die set generally requires only one pair of dies. The amount of die wear, and consequently the required die maintenance, depends on the extent to which the metal being formed slides over the die surfaces. Press platens are used to bring the dies together; in some cases the dies form the tube to some extent as they close, as implied in [Figure 4.6.4-1](#).

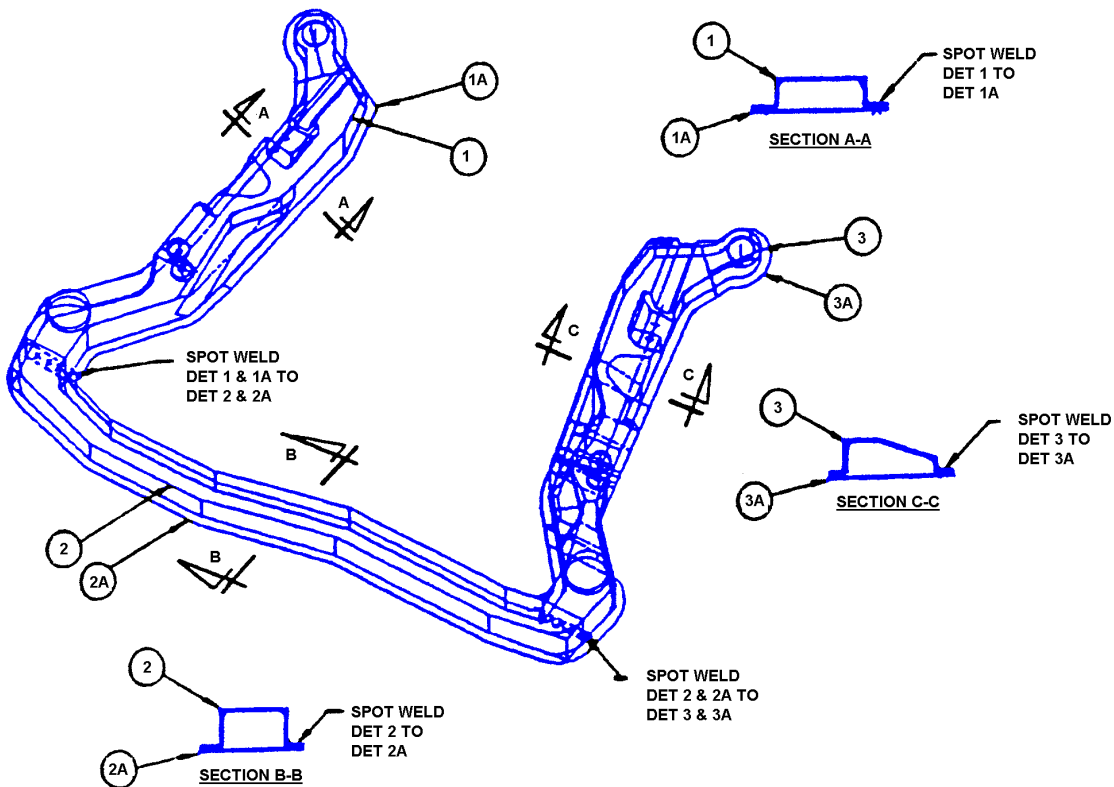
End-of-tube hydraulic fittings are typically unique to the processor or are proprietary. As the forming pressure increases, the sizing and condition of the ends of the tubing become more critical.

After the part is formed and any post end-of-tube treatment is completed, a portion of tube ends may be removed. These operations normally generate less engineered scrap than does conventional stamping processes.

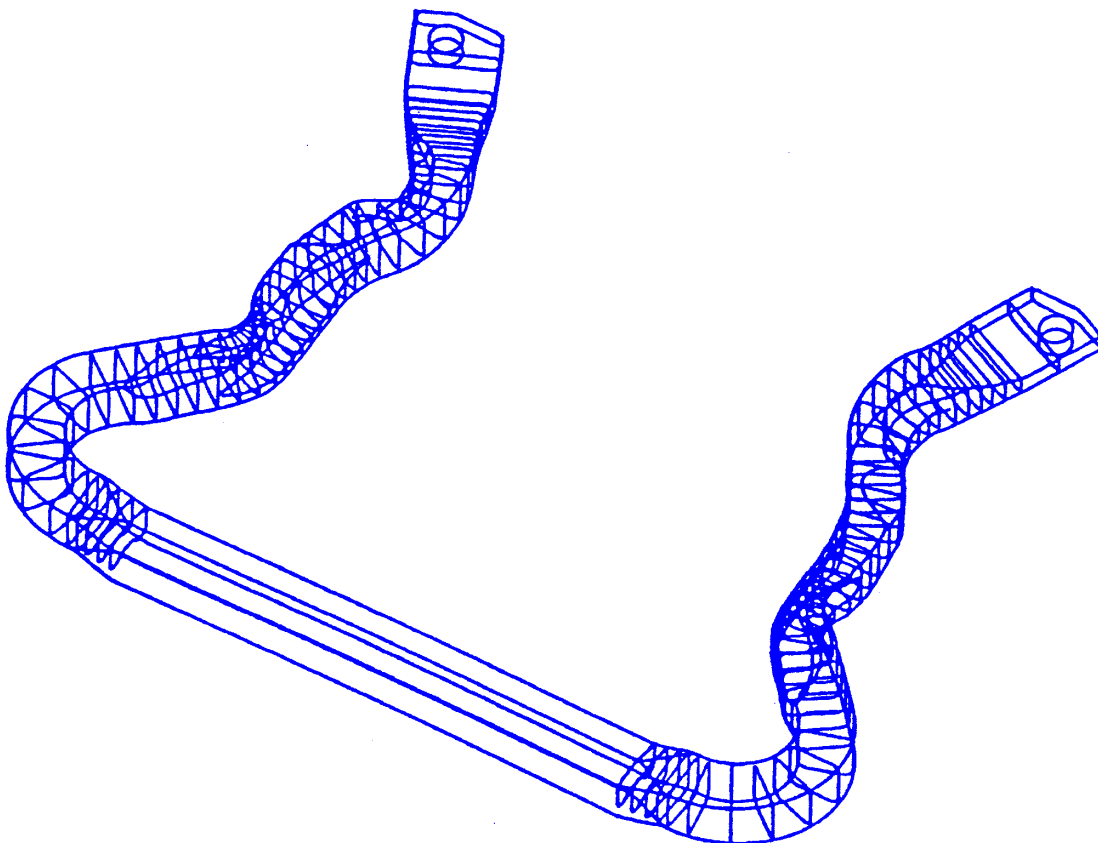
Examples of production low pressure hydroformed structures are:

1. Instrument panel support beams, 600,000-700,000 units per year for a single plant line.
2. Front suspension cradles, 350,000-450,000 units per year.
3. Radiator surround sub-assemblies, 300,000-400,000 units per year.

Part count has typically been cut in half for these structures. The radiator surround is less than 1.5 mm (0.060 in.) thick, is made out of cold rolled Galvanneal steel and is processed through the body ELPO tank. Suspension cradles are being made out of both mild steels and HSLA steels with yield strengths up to 310 MPa (45 ksi) minimum (See [Figure 4.6.4-1](#)).



(a) Suspension cradle as a six piece stamping assembly



(b) Suspension cradle as a single piece hydroformed tube

Figure 4.6.4.1-1 Suspension cradles

4.6.4.2 High Pressure Hydroforming

High pressure hydroforming may be required when either of the following is required:

- Additional expansion of the perimeter, up to 25 percent, with limited thickness reduction
- Wrinkle removal

If greater perimeter expansion or less thickness reduction is required, high pressure hydroforming combined with compression bulge forming, as illustrated in [Figure 4.6.4.2-1](#), may be required.

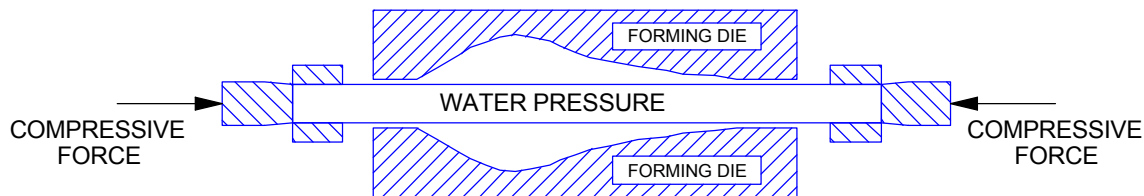


[Figure 4.6.4.2-1](#) Typical compression bulge forming setup

High pressure hydroforming is arbitrarily defined as an expansion process using fluid pressure greater than 83 MPa (12,000 psi). Typical high forming pressures are in the range of 103 to 276 MPa (15,000 to 40,000 psi), with some options as high as 827 MPa (120,000 psi). High pressure hydroforming cycle times are longer than low pressure because;

- Presses are larger
- Tooling is more complex
- Inter-stage annealing has been used, but should be avoided in low carbon steels.

Bulge forming near the end of a tube, over a fairly straight section, can expand an AKDQ steel tube by more than fifty percent. In general, bulge formed cross sections seem to require larger minimum radii than do pure hydroformed sections.

Examples of production or prototyped high pressure hydroformed tubular structures are:

1. Frame front rails.
2. Rear suspension sub-frame members.
3. Steering column energy absorption bellows.
4. D-pillar for a low volume station wagon.

4.6.5 SIMULTANEOUS PROCESSING

In addition to reshaping the section of the tubular structure, holes can be punched using the fluid as a backup anvil, as illustrated in [Figure 4.6.5-1](#). A variety of shapes, including round, square, oval and D-shaped, can be punched. The process presents two potential problems.

1. If slugs are removed from the holes, they must be removed in a way that does not allow them to fall back into the die. In some cases they can be retained in the tube and not interfere with part function or subsequent processing.
2. The holes tend to elongate in the direction of greatest strain, which may present a problem when cage nuts are employed.

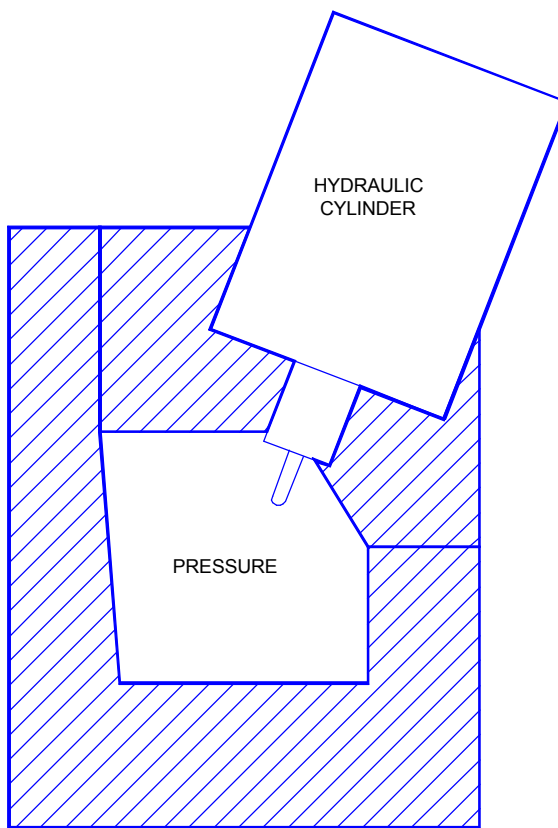


[Figure 4.6.5-1](#) Piercing operation using fluid pressure for a back-up anvil

The hole size and location tolerances are comparable with those achieved by traditional machining and piercing operations.

Holes are typically pierced inward into the tube. If no extrusion is necessary, holes can be clean pierced. There will typically be a depression around the hole, but it does not generally cause problems for inserts. Extruded holes are also pierced to receive thread-forming fasteners. For example, pierced and extruded holes are being used to secure components such as fender assemblies, intercooler mounting brackets, transmission coolers, air intake filters and some structural components to radiator closures.

Holes in rolled corners can be pierced in the hydroforming die, and they remain nearly circular. The holes can be used to receive self tapping or thread forming screws to attach cosmetic panels or brackets. A plan for in-plant or field service repairs of these threaded holes will be required.

4.6.6 POST-HYDROFORMING PROCESSING

Pierced holes may be spin or flow drilled to open up the holes or to provide increased surface area for threads of structural fasteners. The process employs a high speed spinning tool to push the steel, rather than remove it. Drilling is typically used to improve the roundness of holes or to provide more accurate gaging locators.

Depending on the required complexity, tube ends can be removed by processes such as shearing, sawing and plasma cutting. Mandrels can be inserted a limited distance into the tube ends to permit resizing or reshaping. ELPO treatment of zinc alloy pre-coated steel, within limits, has been successful.

4.6.7 SUMMARY OF ADVANTAGES AND DISADVANTAGES

Hydroforming tubing provides the potential for the following advantages compared with alternative stamped and welded structures:

- Reduced tooling costs
- Part integration
- Integration of piercing and punching operations
- Elimination of pinch weld flanges
- Less or negligible die wear
- Potential improvements in dimensional repeatability

The dimensional repeatability of hydroforming versus alternate processes is shown in [Table 4.6.7-1](#). The numbers are unitless based on hydroforming at 1.0.

Table 4.6.7-1 Dimensional repeatability of hydroforming versus alternate processes

Process	Stamped and Welded	Swept or Bent with Partial Yielding	Swept or Bent with Full Yielding	Swept or Bent plus Hydroformed
Relative Dimensional Variation	2.0.-3.0	2.0-2.5	1.5	1.0

Hydroforming may incur disadvantages or limitations compared with stamping and welding, such as:

- Difficulty of incorporating internal brackets
- Limits on perimeter length variation
- Relatively long cycle times
- Post processing operations for end treatments
- May require single sided spot welding, laser welding or MIG welding to attach bracketry
- May require special presses
- Incomplete ELPO treatment

The process appears to be neutral relative to mass reduction. However, in locations where high mass percentages of weld flanges might occur, and the flanges are not needed to mount other parts, some mass savings may be realized.

REFERENCES FOR SECTION 4.6

1. Gillanders, John, *Pipe and Tube Bending Manual*, Fabrication and Manufacturing Association International, Rockford, Illinois, 1994.

BIBLIOGRAPHY FOR SECTION 4.6

1. Automotive Industries Staff, *Hybrid Hydroformed Frame*, Automotive Industries, April 1995.
2. Brooke, Lindsay; Kobe, Gerry; and Sawyer, Christopher A.; *Manufacturing On Fire!*, Automotive Industries, November 1993.
3. Bruggemann, Charles and Shah, Sanjay, *Hydroform Structures*, IBEC-2 Conference, Detroit, Michigan, 1994.
4. Christensen, William L., *Hydroforming of Tubular Sections*, FabSpec, Inc., World Tube Conference, Tube and Pipe Fabrication Association, Schaumburg, Illinois, October 1994.
5. Irving, Robert, *Automotive Engineers Plunge into Tomorrow's Joining Problems*, Welding Journal, American Welding Society, December 1994.
6. Mason, Murray, *Hydroformed Tubes for Automotive Body Structure Applications*, TI Vari-form, SAE paper 930575, March 1993.
7. McElroy, John, *1995 Oldsmobile Aurora*, Automotive Industries, September 1993.
8. Sawyer, Christopher A., *Hydro-forming is Hot*, Automotive Industries, June 1991.
9. Author unknown, *Hydroforming process blow moulds steel*, Metallurgia, April 1992.

4.7 HYDROFORMING SHEET STEEL

The practice of hydroforming sheet metal products has existed for many years. Hydroforming processes have exhibited several distinct advantages, which include:

- Intricate or very deep shape making capabilities due to a more uniform strain distribution of the sheet metal material
- Excellent surface finish
- The capacity to produce rigid panels due to strain hardening
- Ability to handle modest directional die-lock conditions
- Shorter tooling development times
- Reduced tooling and parts costs at low production volumes

However, the processes have been historically identified with three disadvantages:

- Slow process, sometimes requiring several minutes per cycle (although several parts can often be made per cycle)
- Expensive capital costs requiring dedicated, specialized presses
- Minimal automation requiring hand feeding of blanks and part removal

Recently, hydroforming processes have been developed that offer, in specific applications:

- Reduced mass parts
- Improved quality parts
- The use of existing presses and skilled labor

The processes are designed to replace existing draw die operations and produce hydroformed sheet metal parts. The press action is utilized to apply a force that effects a seal to prevent the leakage of fluid, which is usually water with a rust inhibitor added. Part shape, quality and strength are improved by developing uniform strain distributions. There are two basic systems for controlling the interaction of the fluid and the tool:

1. Sheet steel is forced into a female cavity by water under pressure, supplied either by a pump or by press action, as shown in [Figure 4.7-1](#)
2. Sheet steel is deformed by a male punch, which acts against fluid under pressure, as shown in [Figure 4.7-2](#)

The potential for cost savings is enhanced through a low cost tooling strategy that utilizes a master shoe and die inserts. The master shoe is defined as the equipment that can be used for any part that is made in the press. Die inserts contain the specific part shapes. Unlike standard dies, which may require matched male and female inserts, hydroform dies require only one insert, which results in significant tooling cost savings.

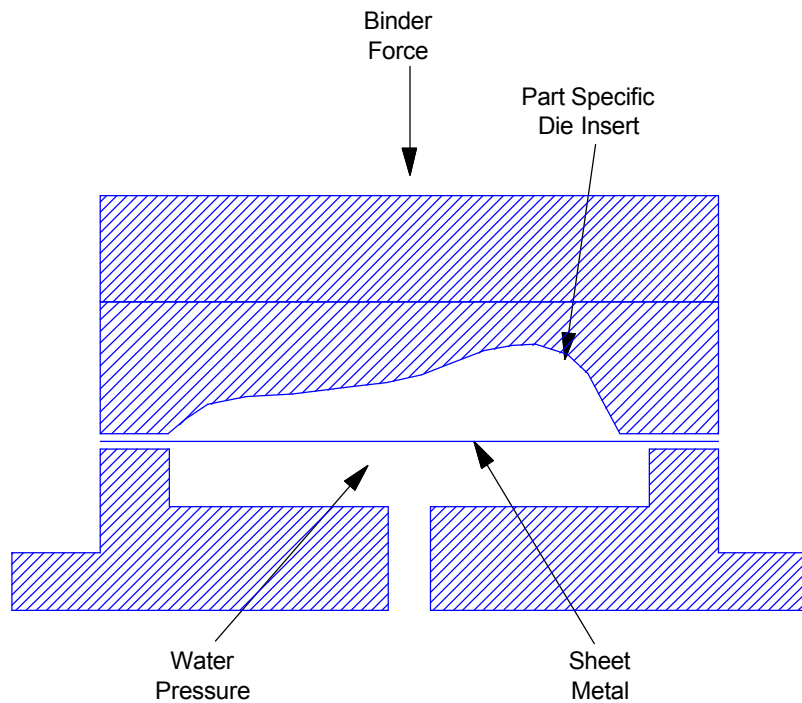


Figure 4.7-1 Hydroforming using fluid under pressure to form the shape in a female cavity

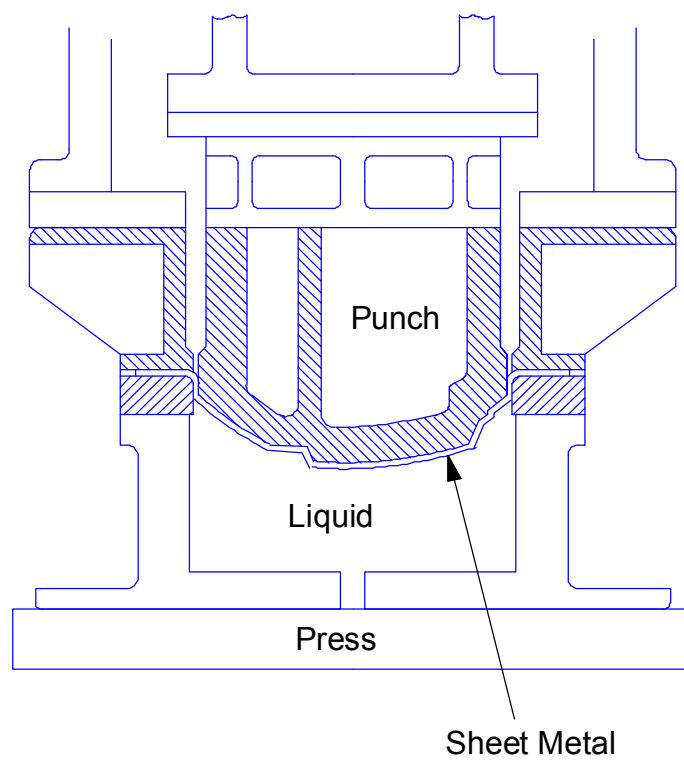


Figure 4.7-2 Hydroforming using a male punch to form the shape against fluid under pressure

Examples of parts made by hydroforming include very deep drawn quarter panels, rear compartment panels and fenders on low volume production vehicles and oil pans for mass production truck diesel engines.

Table 4.7-1 gives illustrative quantitative information on the current features of hydroforming technology. Values are based on typical applications, and will vary according to the application and type of hydroforming process employed.

Table 4.7-1 Features of Current Hydroforming Technology

Feature	Current Hydroforming Technology
Tooling Requirement	Only one part specific die is required.
Tooling Cost, Draw Stage Only	Typical cost \$350,000 for the first part, \$50-100,000 for additional parts that use the same master shoe.
Production speeds	2 to 12 parts per minute, depending on depth and size.
Sheet Metal Blank Requirements	Sheet metal blank requirements: HS: Lockout enables smallest blank size.
Surface Quality	Excellent surface quality on fluid side. Typical quality on die side.
Prototype tool to production time	6 to 12 months, because prototype developments can be used in production.
Ease of making engineering changes	Simple design minimizes change time. Low cost die materials could further reduce timing.
Panel stiffness after forming	Good because: HS: Biaxial strains of 3-5%.

5. PROCEDURES

Introduction

Design Procedures (Flow Charts) are provided in [Section 5.1](#) to [Section 5.5](#). These procedures were developed to streamline the design process and to provide for computerized solutions using AISI/CARS.

[Section 5.1](#) contains the Key to CARS Design Procedures that assist in selecting and using the correct procedure from [Section 5.2](#) to [5.5](#).

[Section 5.2](#) contains Design Procedures for [Section 3.1 Straight Linear Members](#).

[Section 5.3](#) contains Design Procedures for [Section 3.2 Curved Members](#).

[Section 5.4](#) contains Design Procedures for [Section 3.3 Surface Elements](#).

[Section 5.5](#) contains Design Procedures for [Section 3.4 Connections](#).

[Table 5-1](#) provides a description of the symbols used in the Design Procedures.

Table 5-1 Design Procedure Symbols

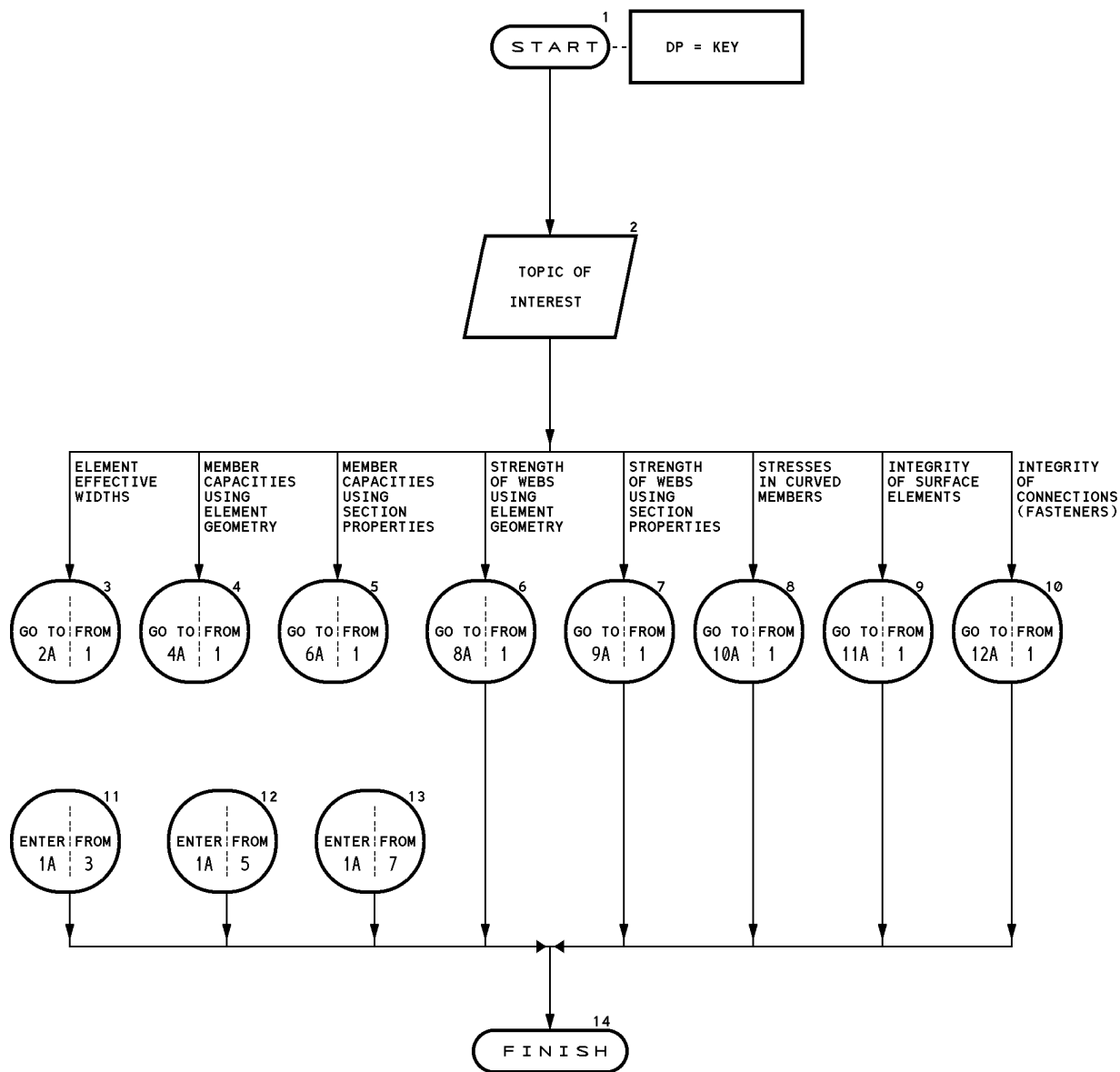
Symbol	Description
	A terminal point in a Design Procedure - start or finish.
	Additional descriptive, clarification, or comment (dotted line extends to symbol, as appropriate).
	A processing function defining an operation(s) causing a change in value, form or location of information.
	Input function - user supplied data.
	Predefined process - steps or operations specified elsewhere.
	A decision or switching type operation that determines which of a number of alternative paths to follow.
	Page connector - exit to or entry from another page of a Design Procedure. For example, specifies going to page 4, entry point A from page 2. Page 4 will show a complementary connector, that specifies entry on page 4 at point A, from page 2.
	Design Procedure connector - exit to or entry from a Design Procedure. For example, specifies going to Design Procedure 3.1-1 at entry point C from Design Procedure 3.1-5. Design Procedure 3.1-1 will have a complementary connector, that specifies entry to Design Procedure 3.1-1 at point C, from Design Procedure 3.1-5. There could be another connector, that specifies exiting Design Procedure 3.1-1, entry point C and return to Design Procedure 3.1-5.

5.1 KEY TO CARS DESIGN PROCEDURES

The following pages contain the Key to CARS Design Procedures for [Section 3.1](#) to [Section 3.4](#). Key is provided to assist the user in selecting and using the correct procedure for the problem at hand.

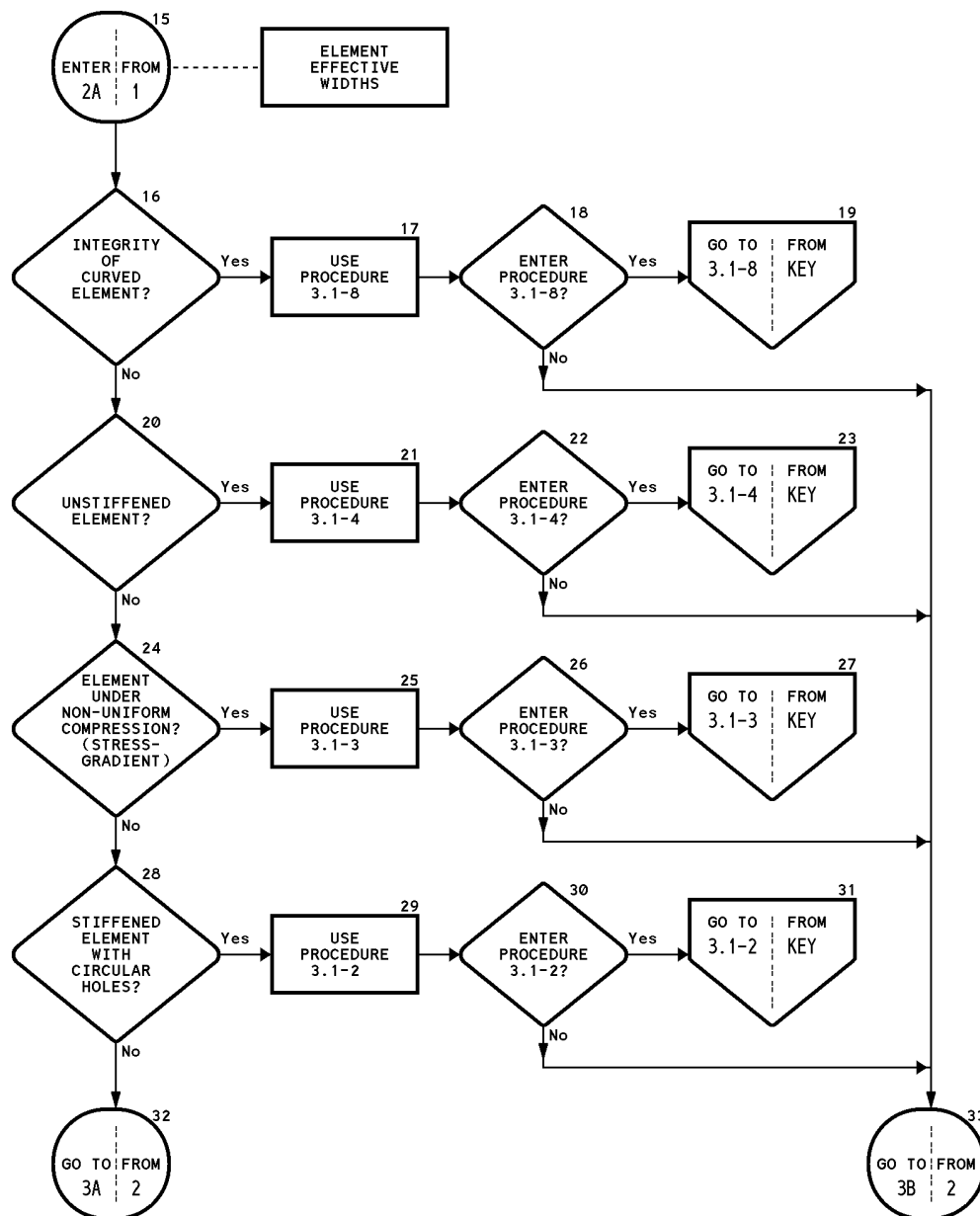
KEY TO CARS DESIGN PROCEDURES (1 of 12)

Reference: Sections 3.1 - 3.4

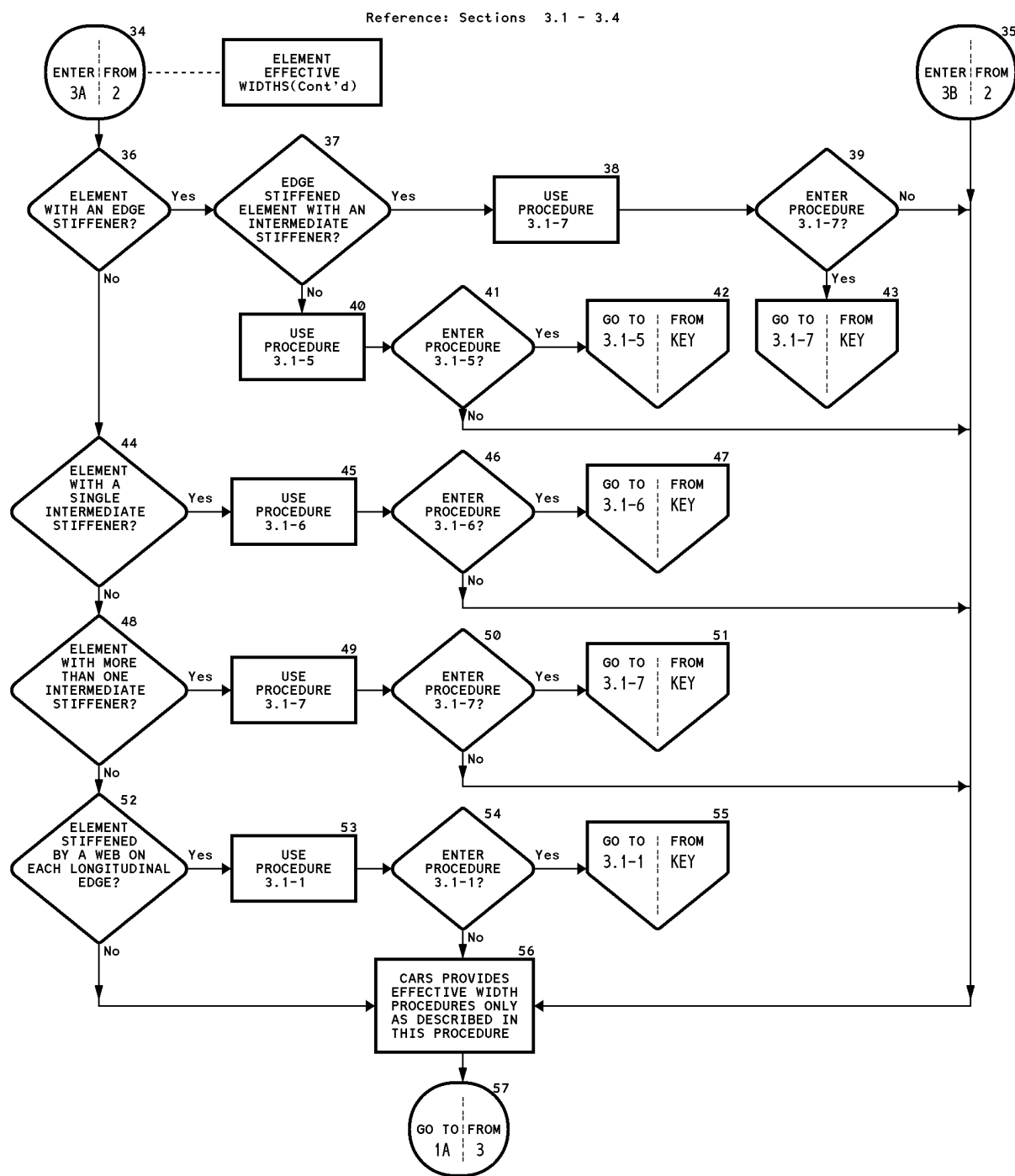


KEY TO CARS DESIGN PROCEDURES (2 of 12)

Reference: Sections 3.1 - 3.4

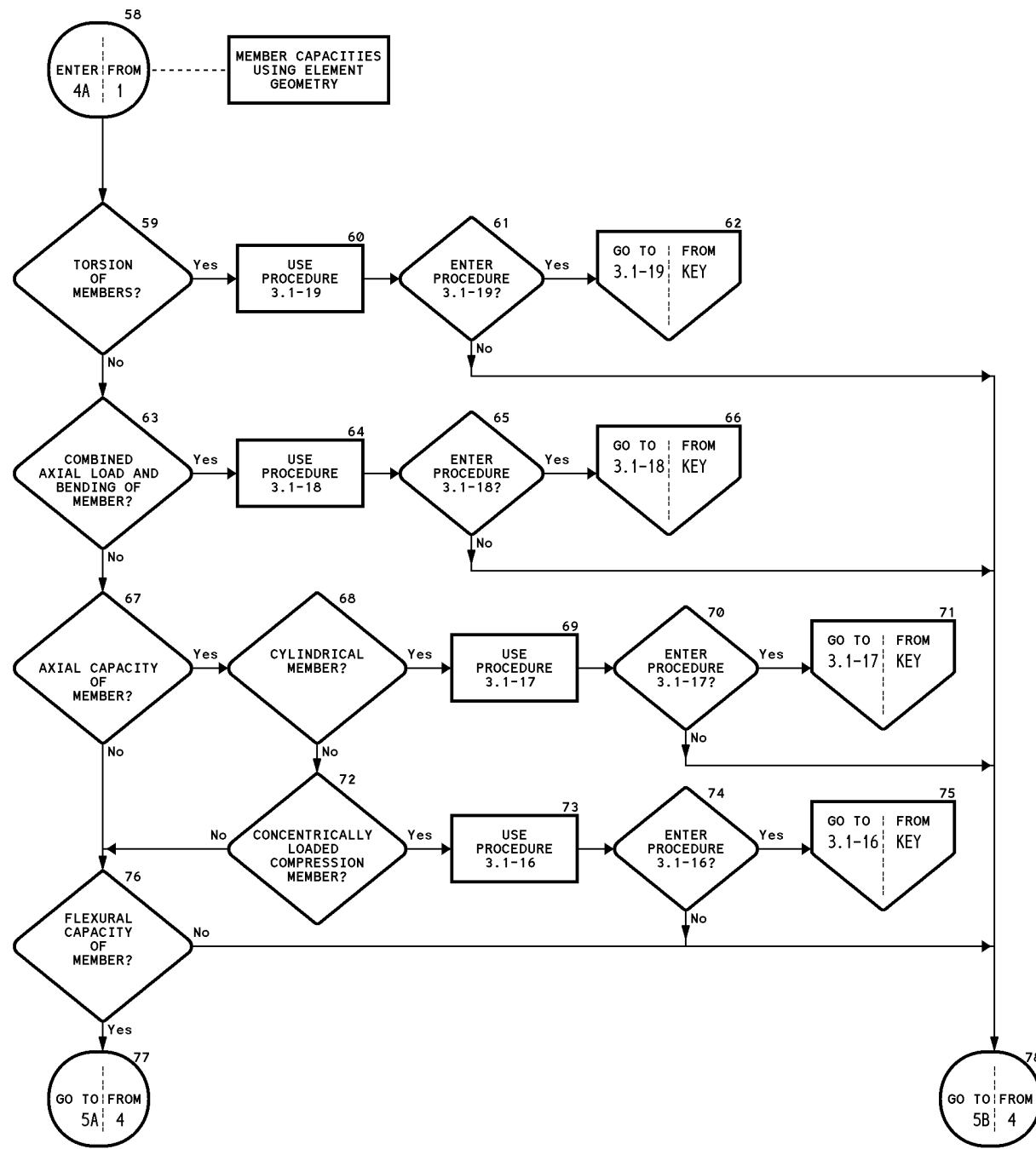


KEY TO CARS DESIGN PROCEDURES (3 of 12)



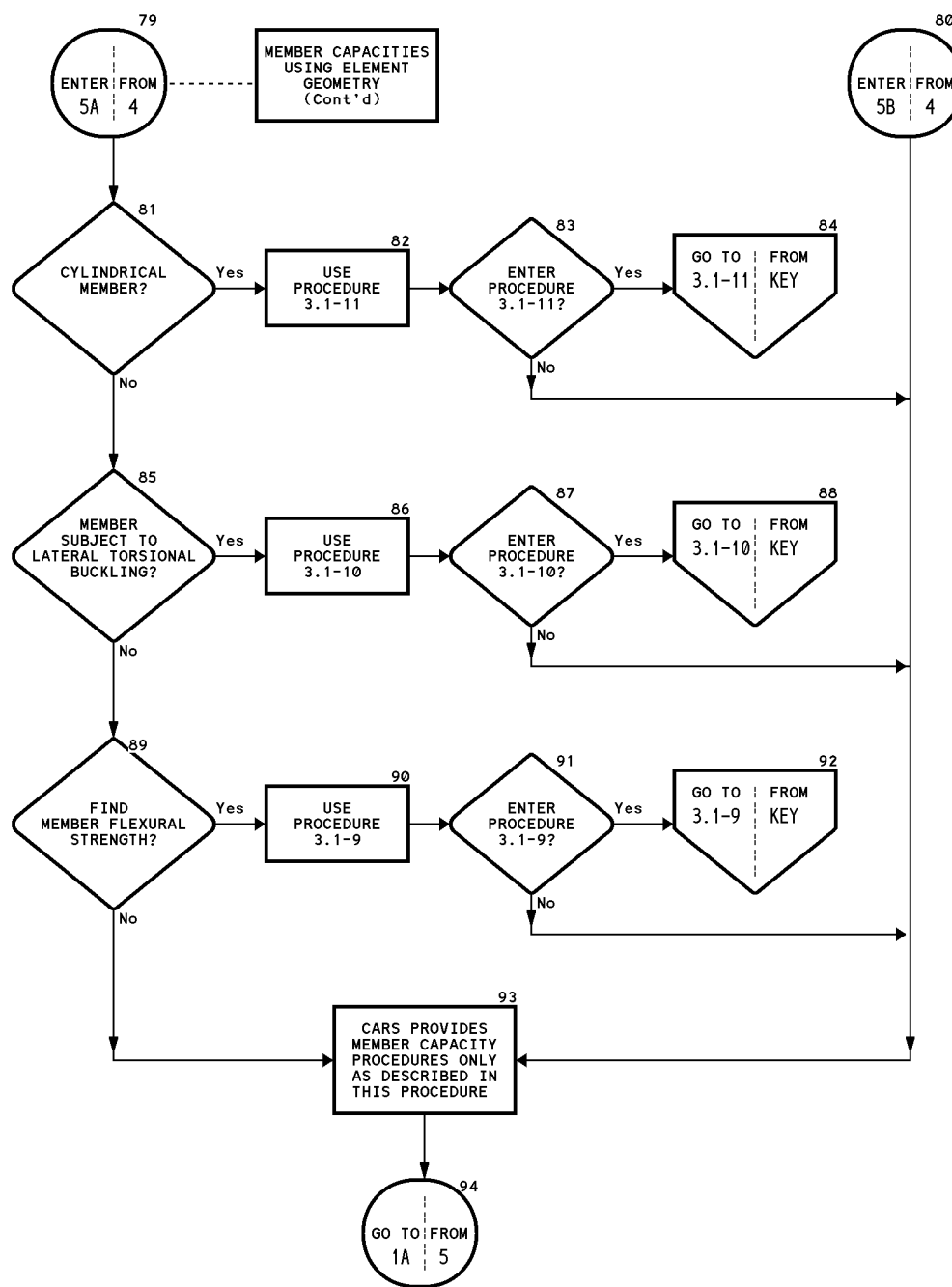
KEY TO CARS DESIGN PROCEDURES (4 of 12)

Reference: Sections 3.1 - 3.4



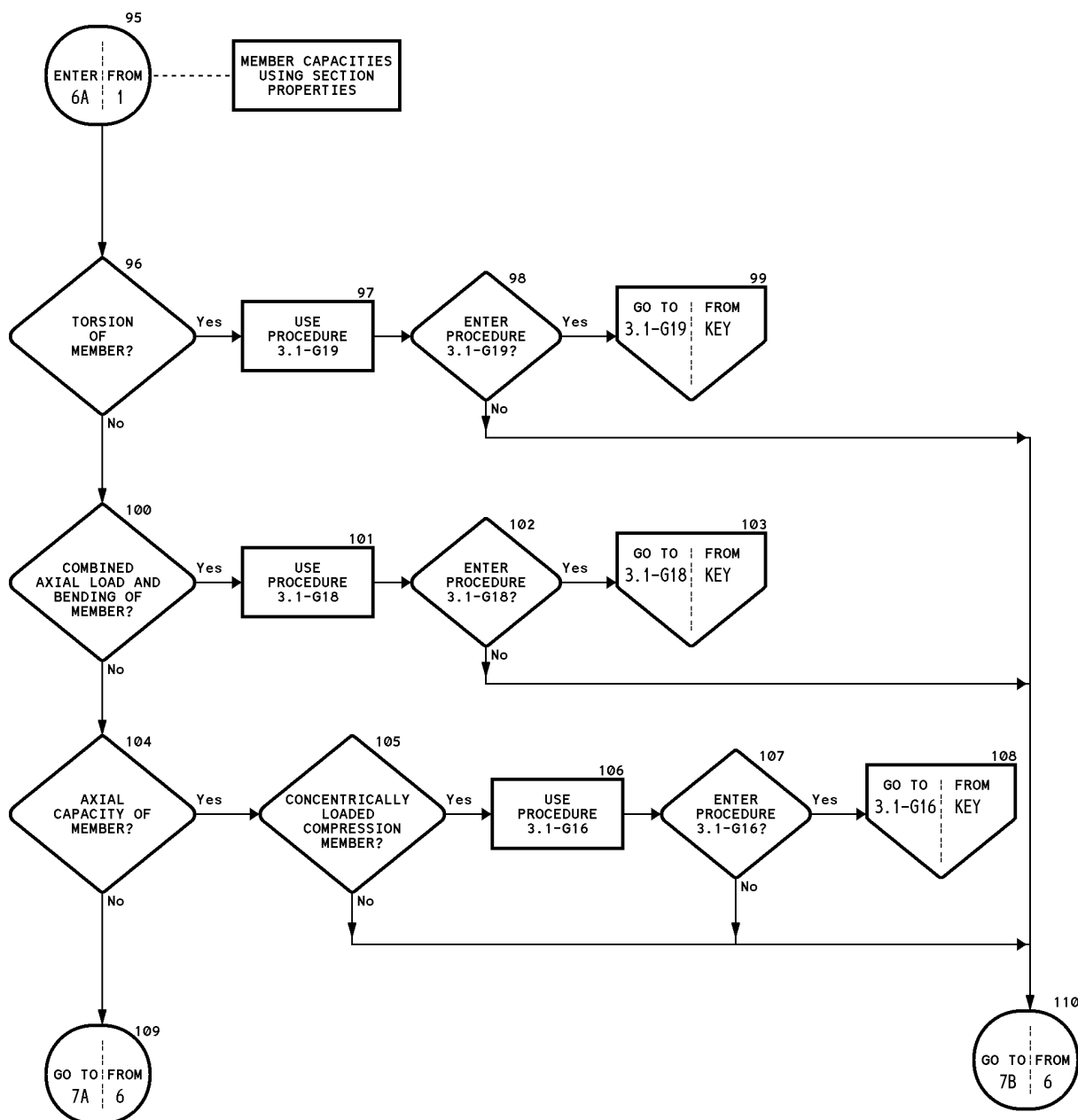
KEY TO CARS DESIGN PROCEDURES (5 of 12)

Reference: Sections 3.1 - 3.4



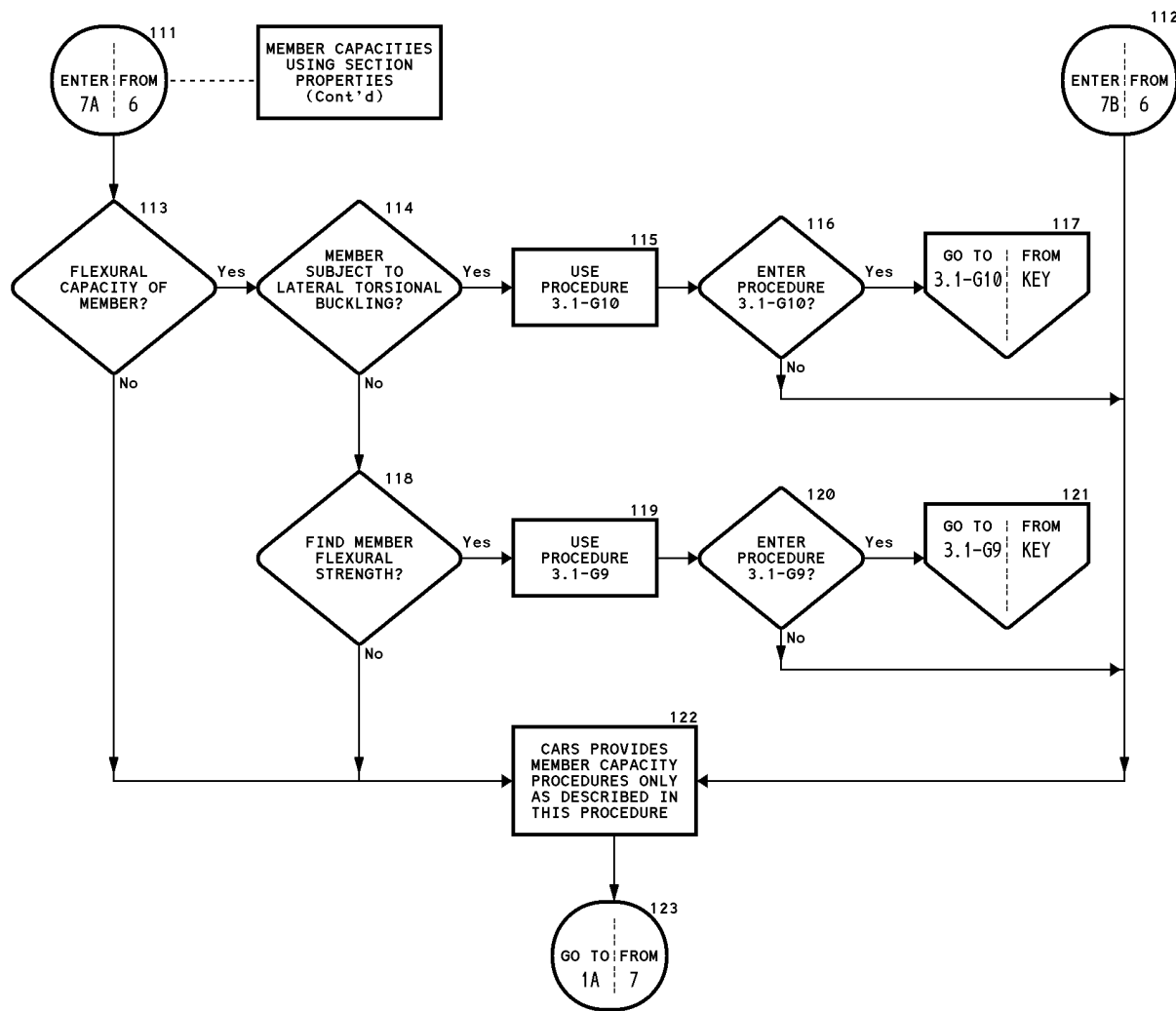
KEY TO CARS DESIGN PROCEDURES (6 of 12)

Reference: Sections 3.1 - 3.4



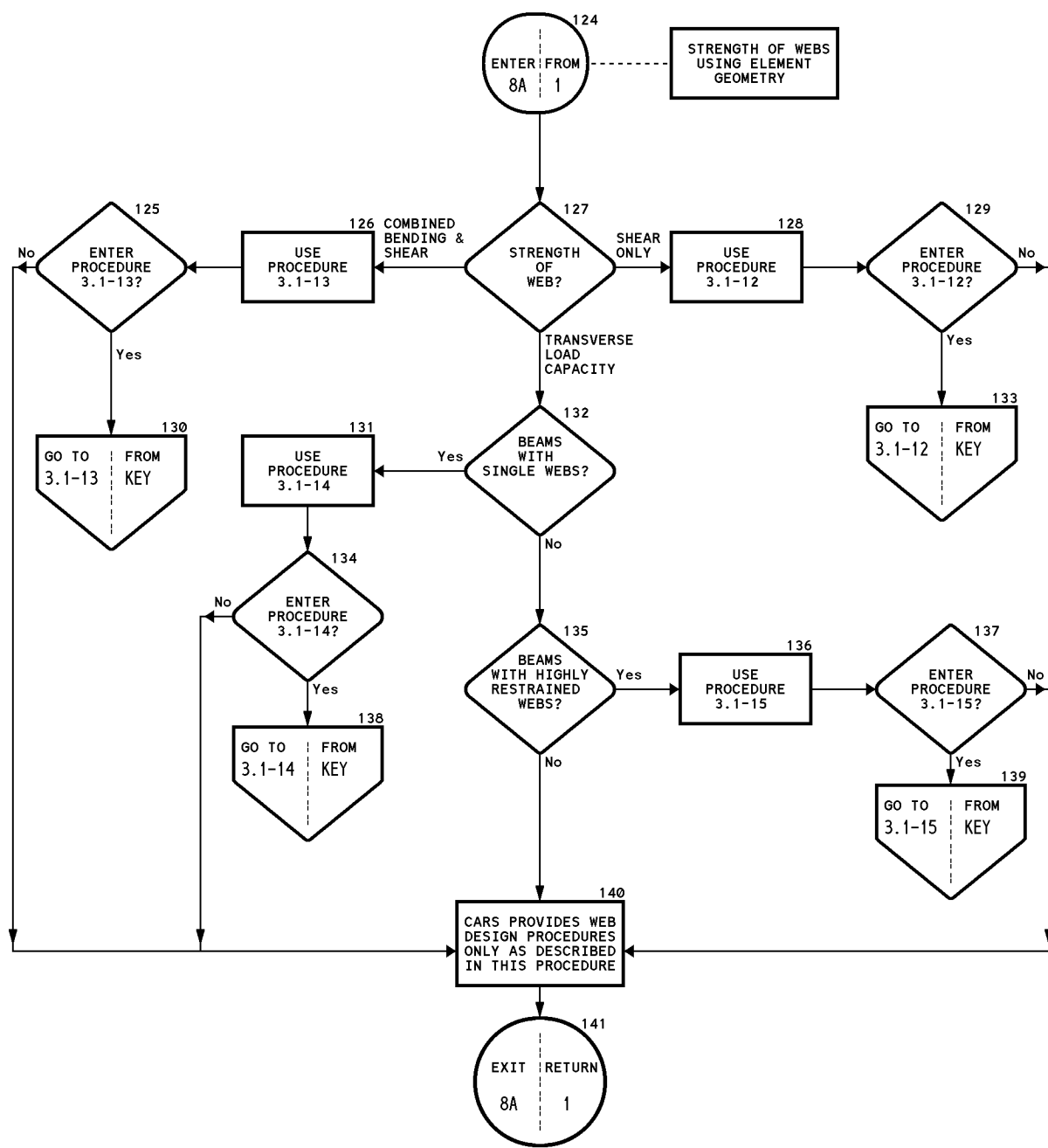
KEY TO CARS DESIGN PROCEDURES (7 of 12)

Reference: Sections 3.1 - 3.4



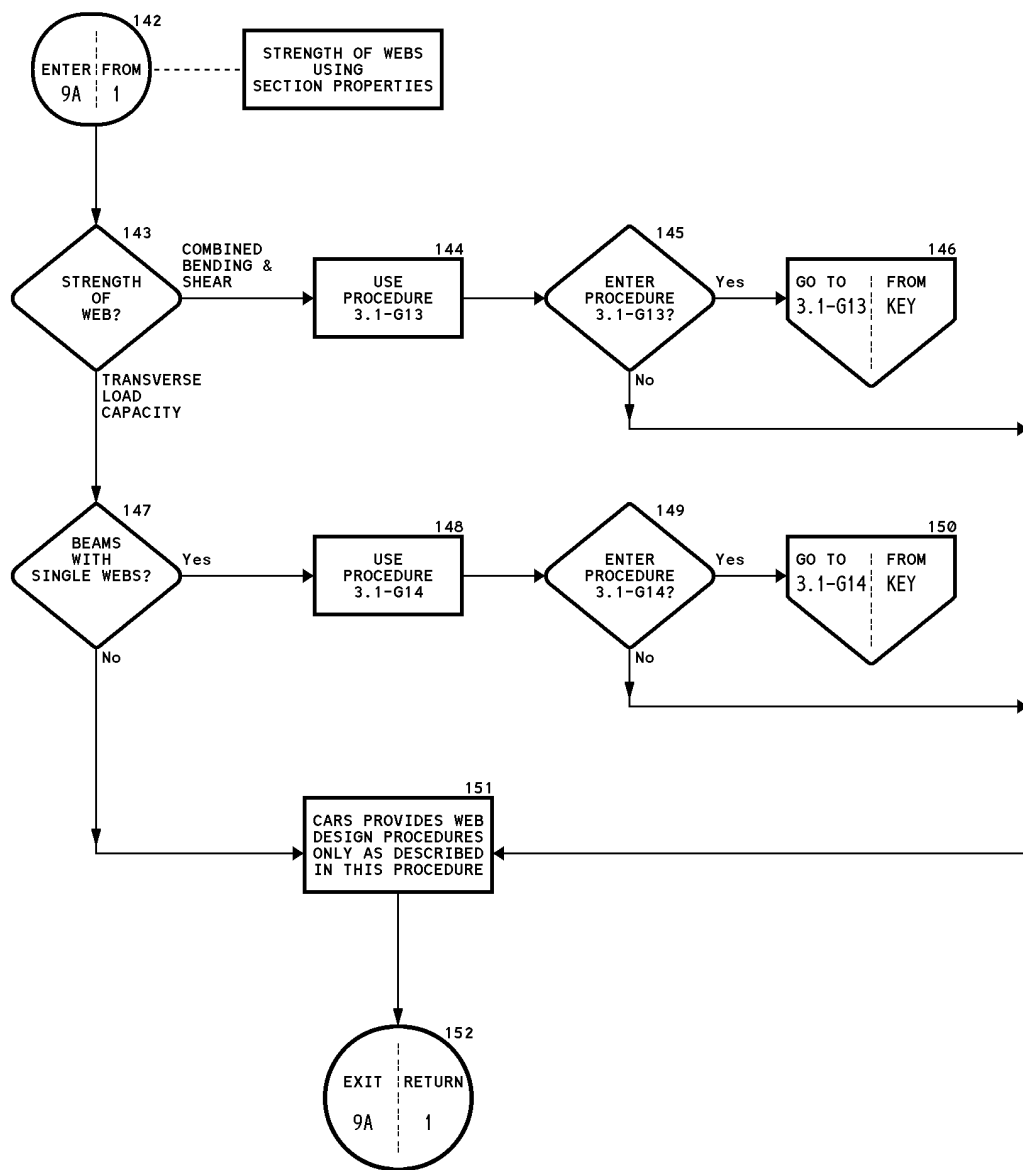
KEY TO CARS DESIGN PROCEDURES (8 of 12)

Reference: Sections 3.1 - 3.4



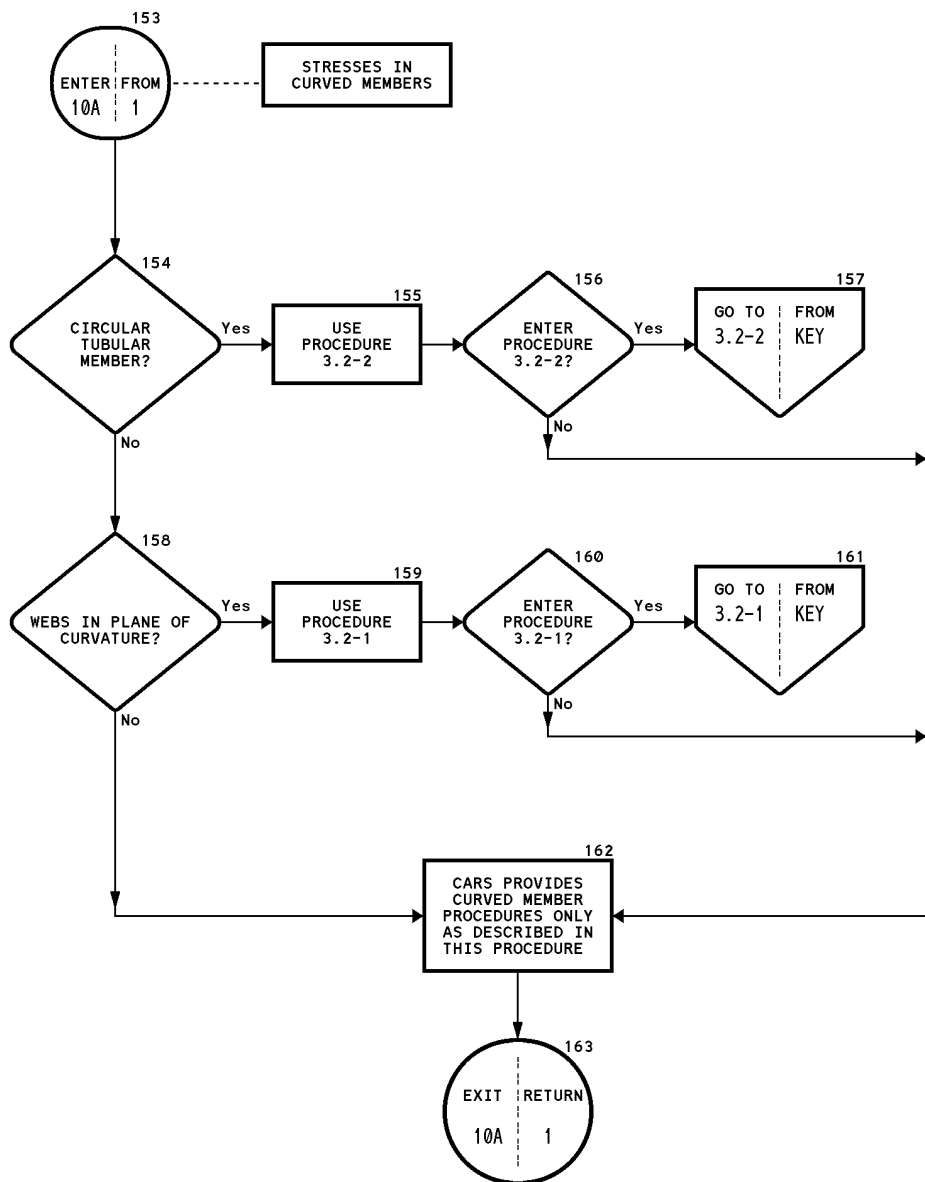
KEY TO CARS DESIGN PROCEDURES (9 of 12)

Reference: Sections 3.1 - 3.4



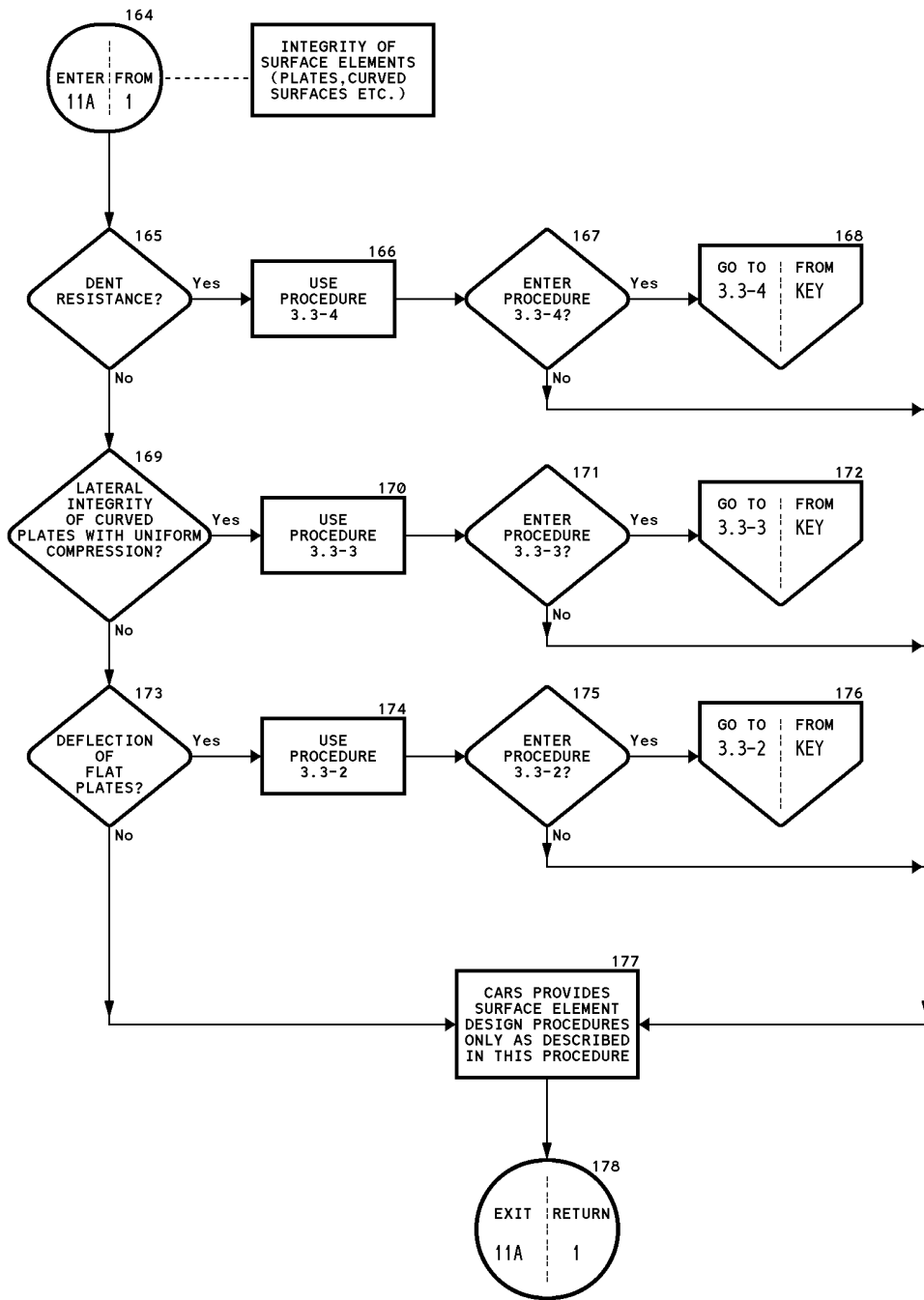
KEY TO CARS DESIGN PROCEDURES (10 of 12)

Reference: Sections 3.1 - 3.4



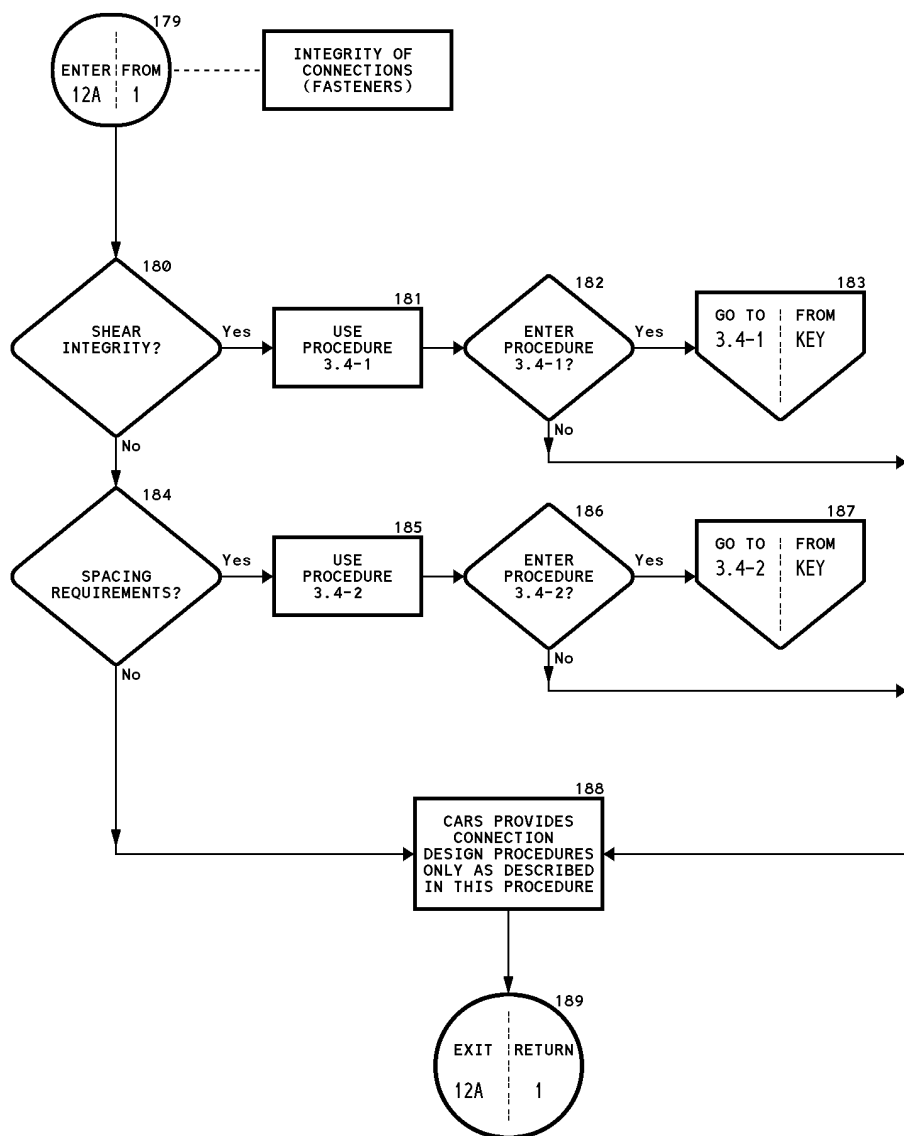
KEY TO CARS DESIGN PROCEDURES (11 of 12)

Reference: Sections 3.1 - 3.4



KEY TO CARS DESIGN PROCEDURES (12 of 12)

Reference: Sections 3.1 - 3.4



5.2 DESIGN PROCEDURES FOR SECTION 3.1

Table 5.2-1 lists the Design Procedures for [Section 3.1 Straight Linear Members](#). Procedures designated with the letter G (e.g., 3.1-G9) provide a faster, more convenient solution by making use of section properties generated by GAS and AISI/CARS. (See [Section 7.1.6](#) for details on the GAS module.)

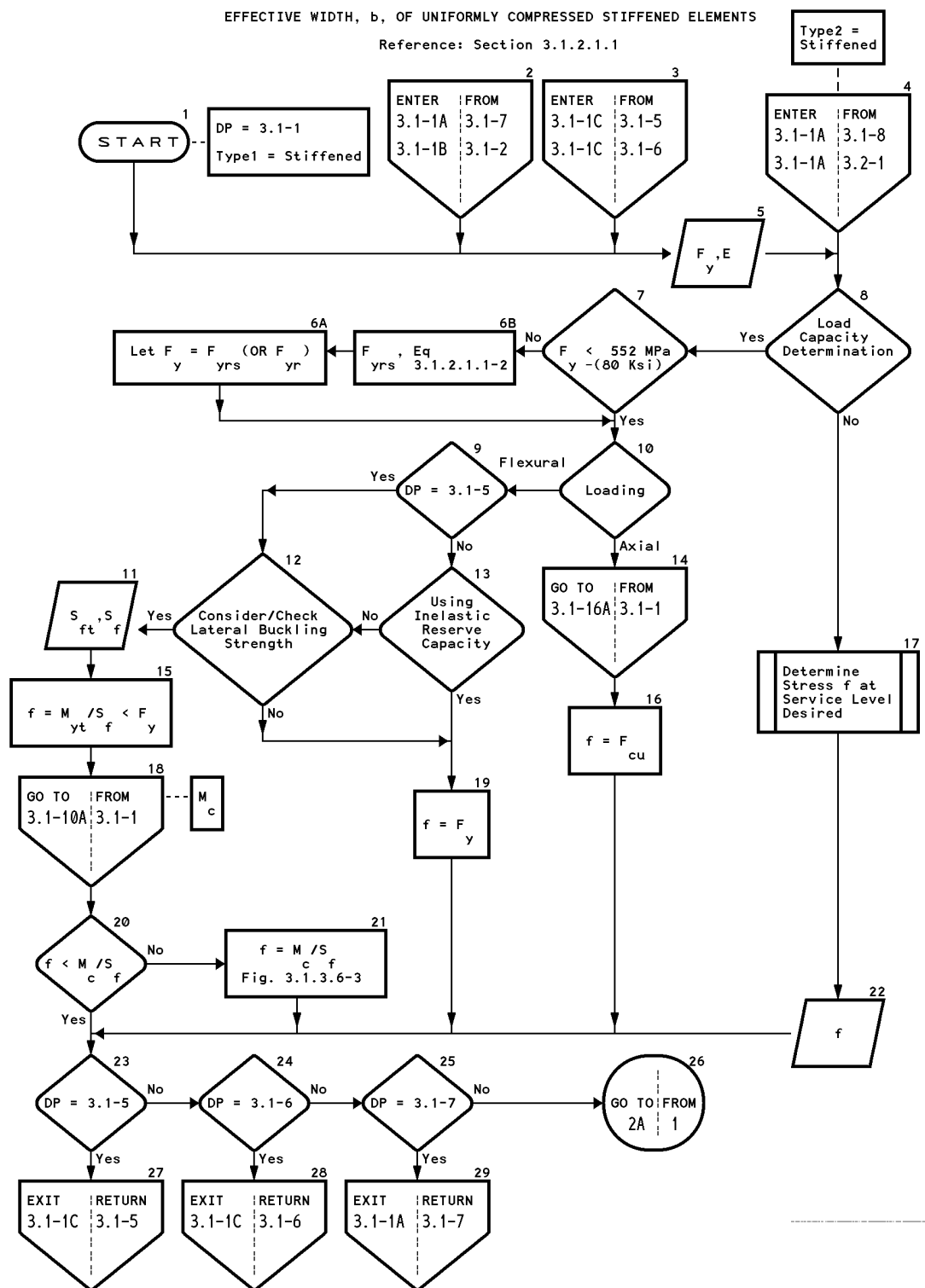
Table 5.2-1 Design Procedures for Section 3.1

Design Procedure	Reference Section	Title	
3.1-1	3.1.2.1.1	Effective Width, b , of Uniformly Compressed Stiffened Elements	
3.1-2	3.1.2.1.1	Effective Width, b , of Uniformly Compressed Stiffened Elements with Circular Holes	
3.1-3	3.1.3.1	Effective width of Webs and Stiffened Elements with Stress Gradient or Limiting Stress, F_{bwu}	
3.1-4	3.1.2.1.2	Effective Width, b , of Unstiffened Elements in Compression	
3.1-5A	3.1.2.1.3	Overview: Effective Width, b , of Uniformly Compressed Elements with an Edge Stiffener	
3.1-5	3.1.2.1.3	Effective Width, b , of Uniformly Compressed Elements with an Edge Stiffener	
3.1-6	3.1.2.1.4	Effective Width, b , of Uniformly Compressed Elements with a Single Intermediate Stiffener	
3.1-7	3.1.2.1.4	Effective Width of Edge Stiffened Elements with Intermediate Stiffeners or Stiffened Elements with More Than One Intermediate Stiffener	
3.1-8	3.1.2.3	Integrity of Curved Element (F_{crp} or b and t_e)	
3.1-G9	3.1.3.1	Member Flexural Strength, M_u (using section properties)	
3.1-9	3.1.3.1	Member Flexural Strength, M_u	
3.1-G10	3.1.3.6	Lateral Buckling Strength in Flexure, M_u (using section properties)	
3.1-10	3.1.3.6	Lateral Buckling Strength in Flexure, M_u	
3.1-11	3.1.3.2	Flexural Capacity, M_u , of Cylindrical Members	
3.1-12	3.1.3.3	Strength of Webs, V_u , for Shear Only	
3.1-G13	3.1.3.4	Strength of Webs for Combined Bending and Shear (using section properties)	
3.1-13	3.1.3.4	Strength of Webs for Combined Bending and Shear	
3.1-G14	3.1.3.5.1	Transverse Load Web Capacity, P_{cu} - Beams with Single Webs (using section properties)	
3.1-14	3.1.3.5.1	Transverse Load Web Capacity, P_{cu} - Beams with Single Webs	
3.1-15	3.1.3.5.2	Transverse Load Web Capacity, P_{cu} - Beams with Highly Restrained Webs	
3.1-G16	3.1.2.5	Axial Capacity, P_u , of Concentrically Loaded Compression Members (using section properties)	
3.1-16	3.1.2.5	Axial Capacity, P_u , of Concentrically Loaded Compression Members	
3.1-17	3.1.2.2 & 3.1.2.5	Axial Capacity, P_u , of Cylindrical Members	
3.1-18A	3.1.3.7	Overview: Combined Axial Load and Bending of Member	
3.1-G18	3.1.3.7	Combined Axial Load and Bending of Member (using section properties)	
3.1-18	3.1.3.7	Combined Axial Load and Bending of Member	
3.1-G19	3.1.4	Torsion of Members (using section properties)	
3.1-19	3.1.4	Torsion of Members	

DESIGN PROCEDURE 3.1-1 (1 of 5)

EFFECTIVE WIDTH, b , OF UNIFORMLY COMPRESSED STIFFENED ELEMENTS

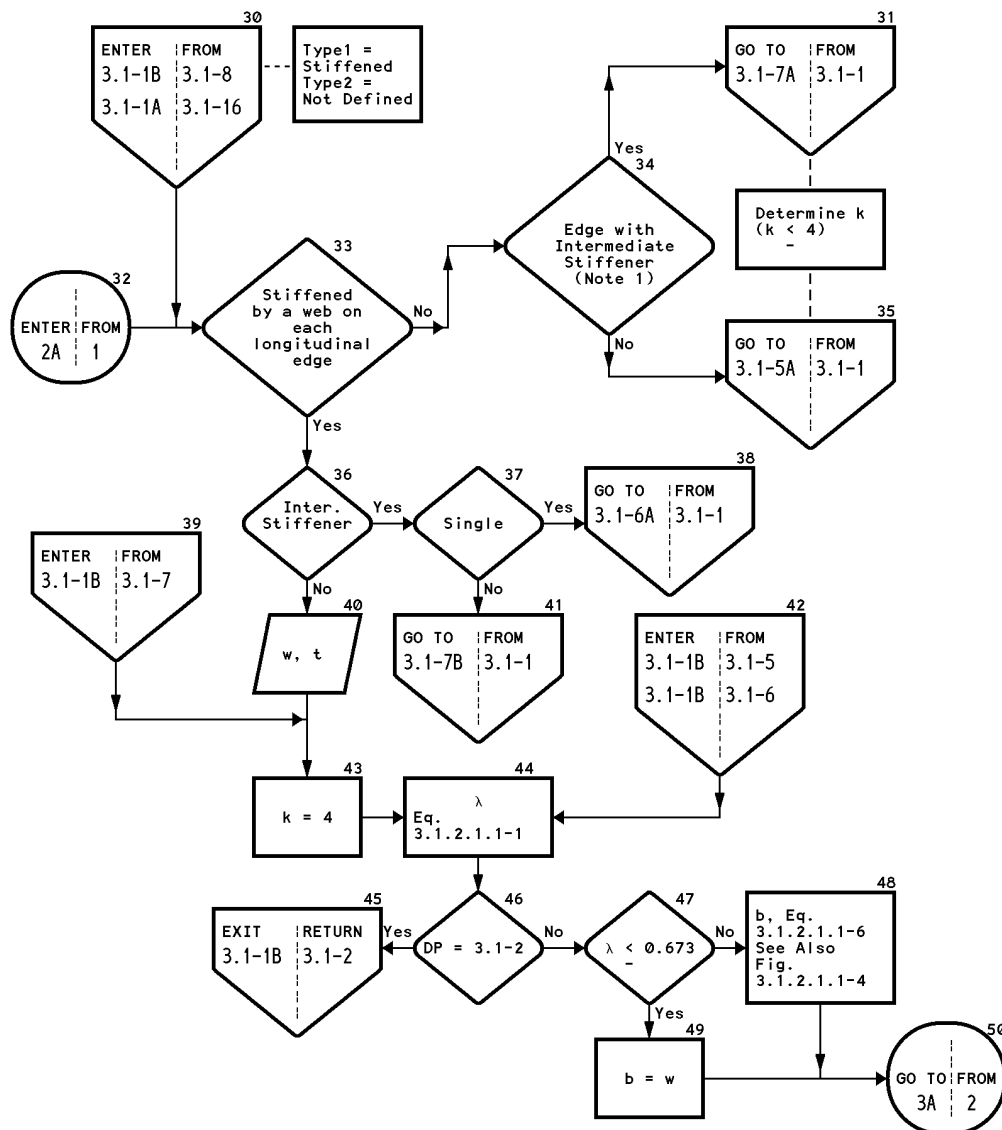
Reference: Section 3.1.2.1.1



DESIGN PROCEDURE 3.1-1 (2 of 5)

EFFECTIVE WIDTH, b , OF UNIFORMLY COMPRESSED STIFFENED ELEMENTS

Reference: Section 3.1.2.1.1

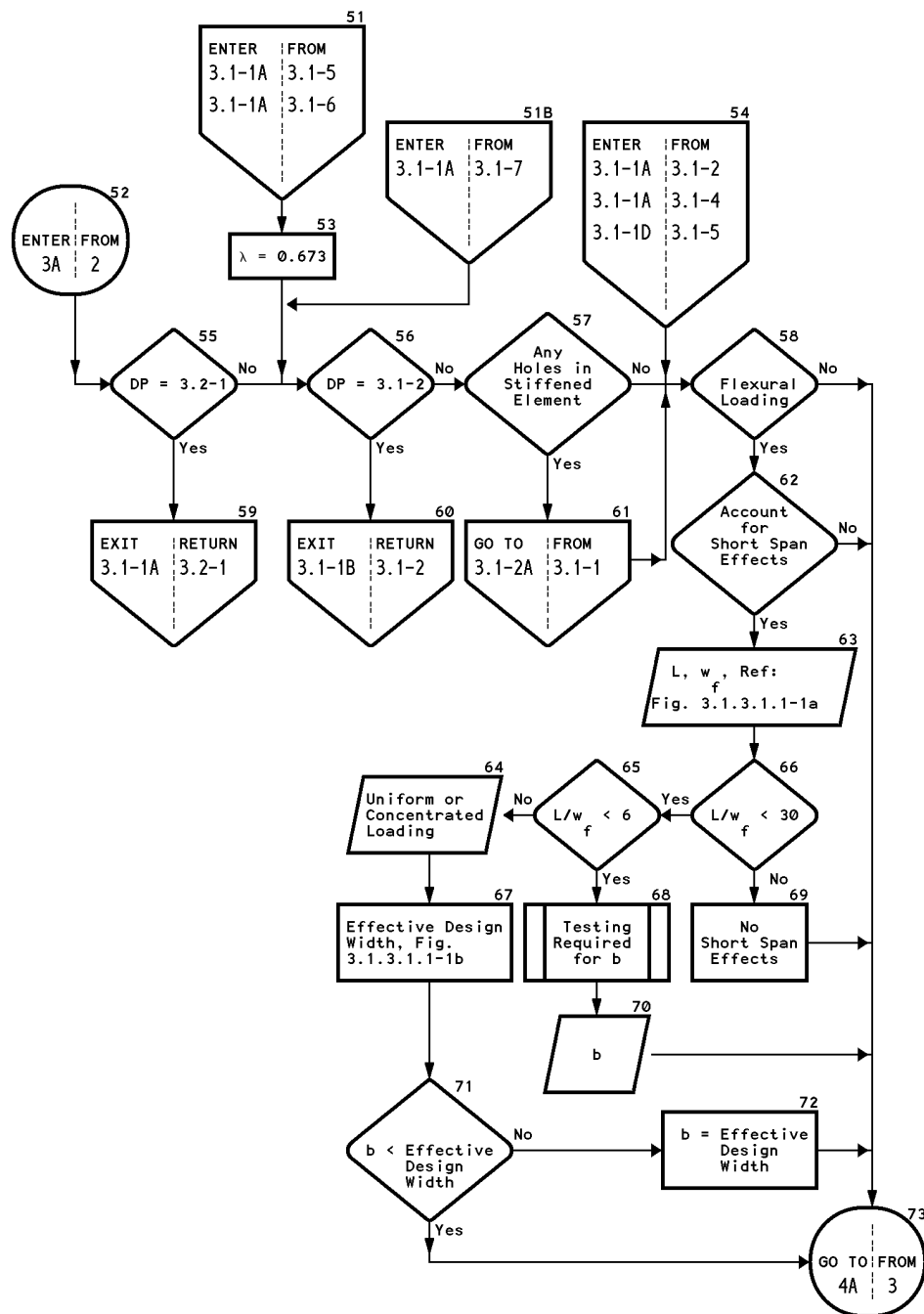


Note 1: If $DP = 3.1-8$, only possibility is edge stiffener (ditto for curved element)

DESIGN PROCEDURE 3.1-1 (3 of 5)

EFFECTIVE WIDTH, b , OF UNIFORMLY COMPRESSED STIFFENED ELEMENTS

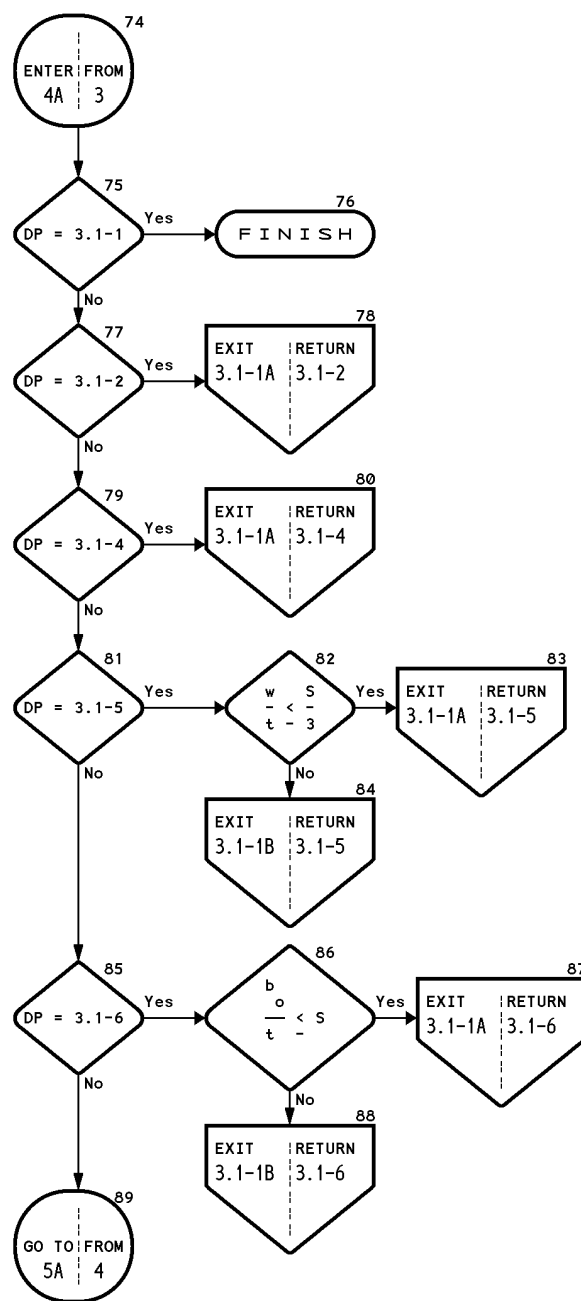
Reference: Section 3.1.2.1.1



DESIGN PROCEDURE 3.1-1 (4 of 5)

EFFECTIVE WIDTH, b , OF UNIFORMLY COMPRESSED STIFFENED ELEMENTS

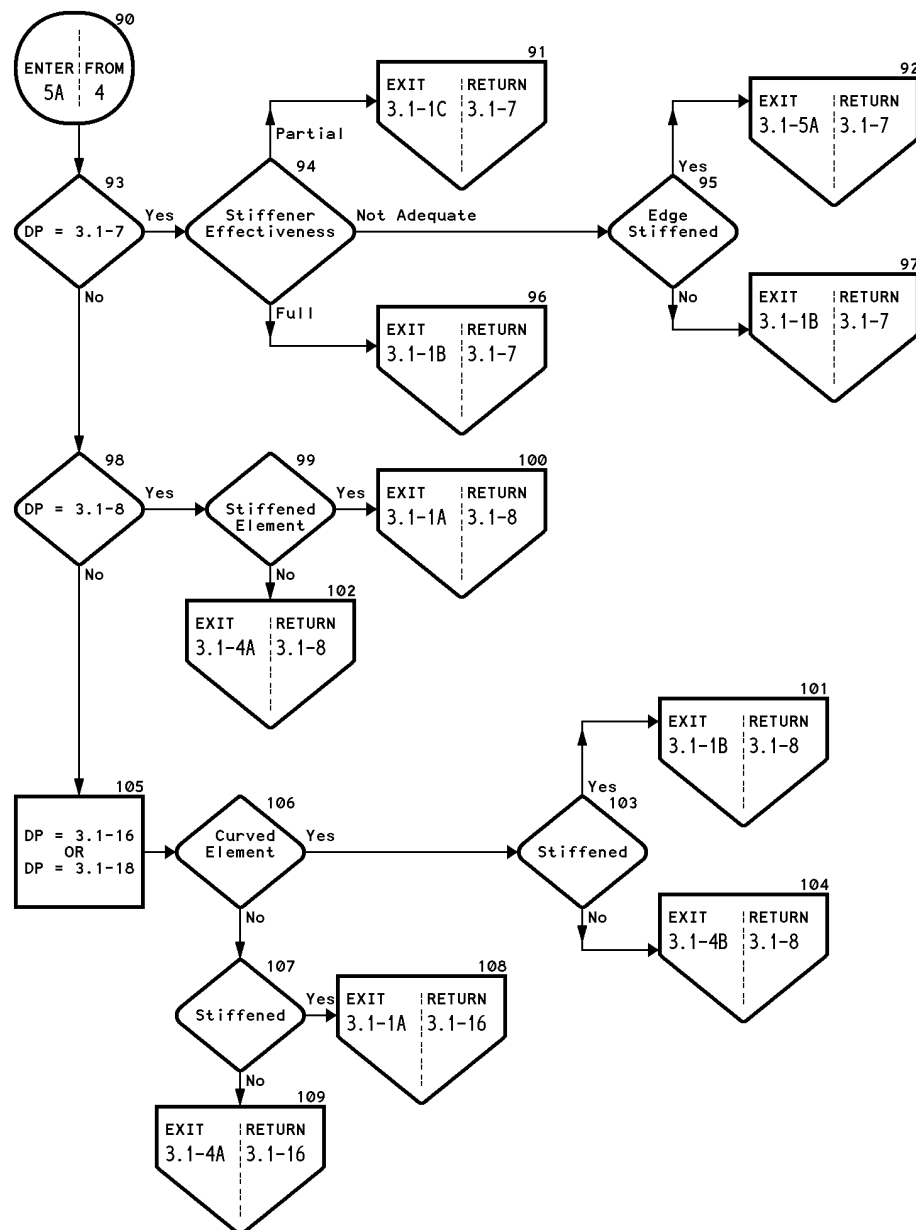
Reference: Section 3.1.2.1.1



DESIGN PROCEDURE 3.1-1 (5 of 5)

EFFECTIVE WIDTH, b , OF UNIFORMLY COMPRESSED STIFFENED ELEMENTS

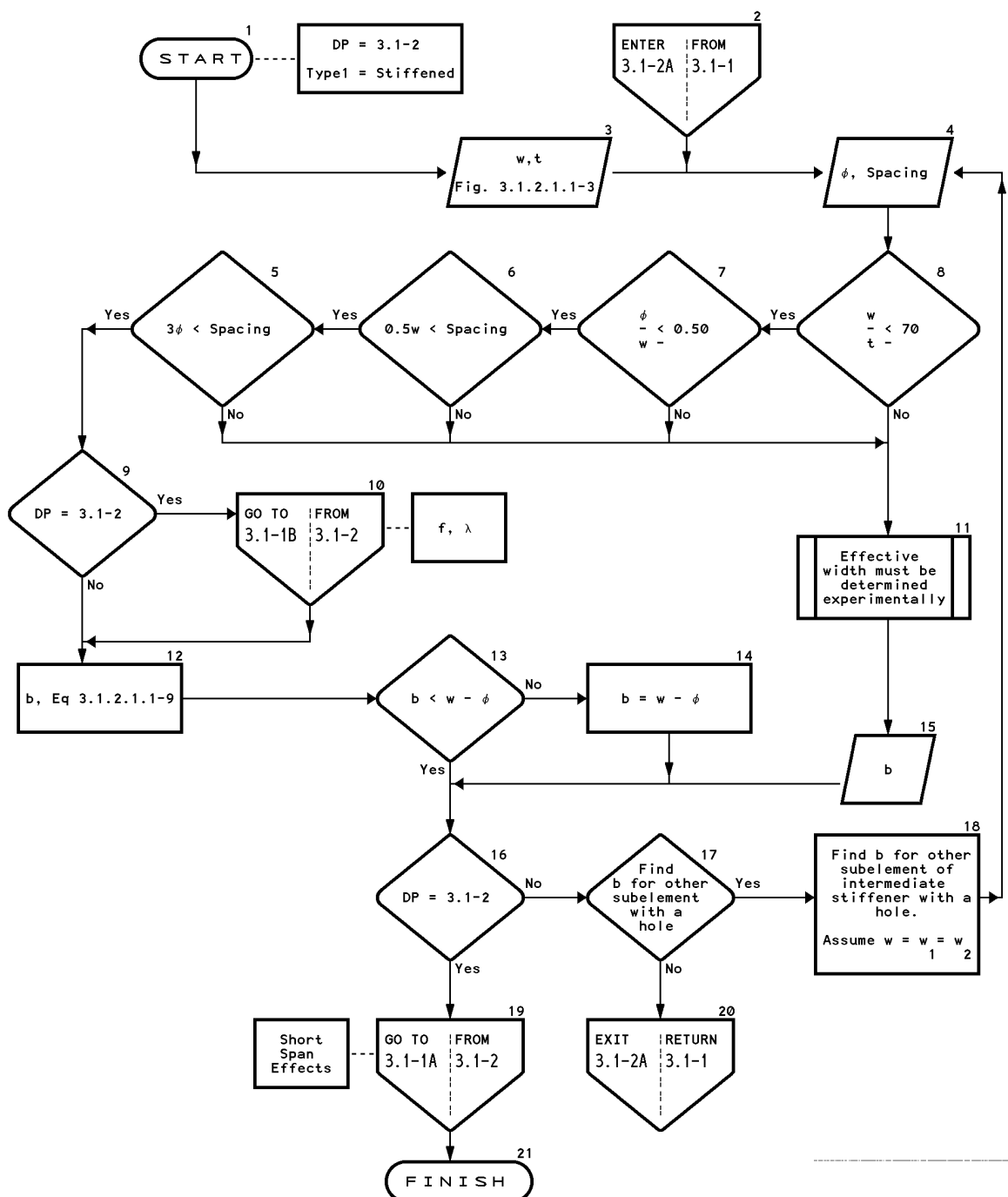
Reference: Section 3.1.2.1.1



DESIGN PROCEDURE 3.1-2

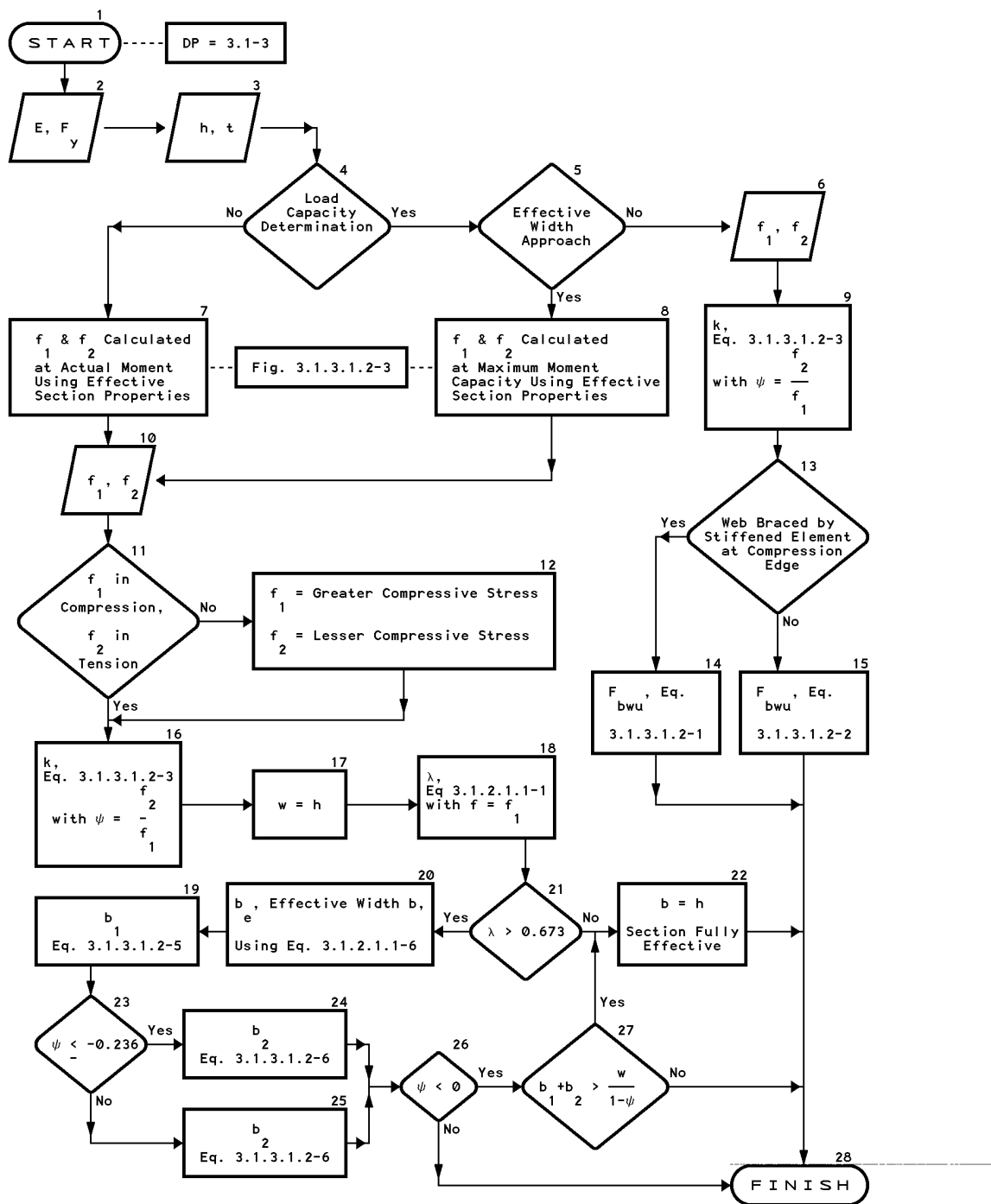
EFFECTIVE WIDTH, b , OF UNIFORMLY COMPRESSED ELEMENTS WITH CIRCULAR HOLES

Reference: Section 3.1.2.1.1



DESIGN PROCEDURE 3.1-3

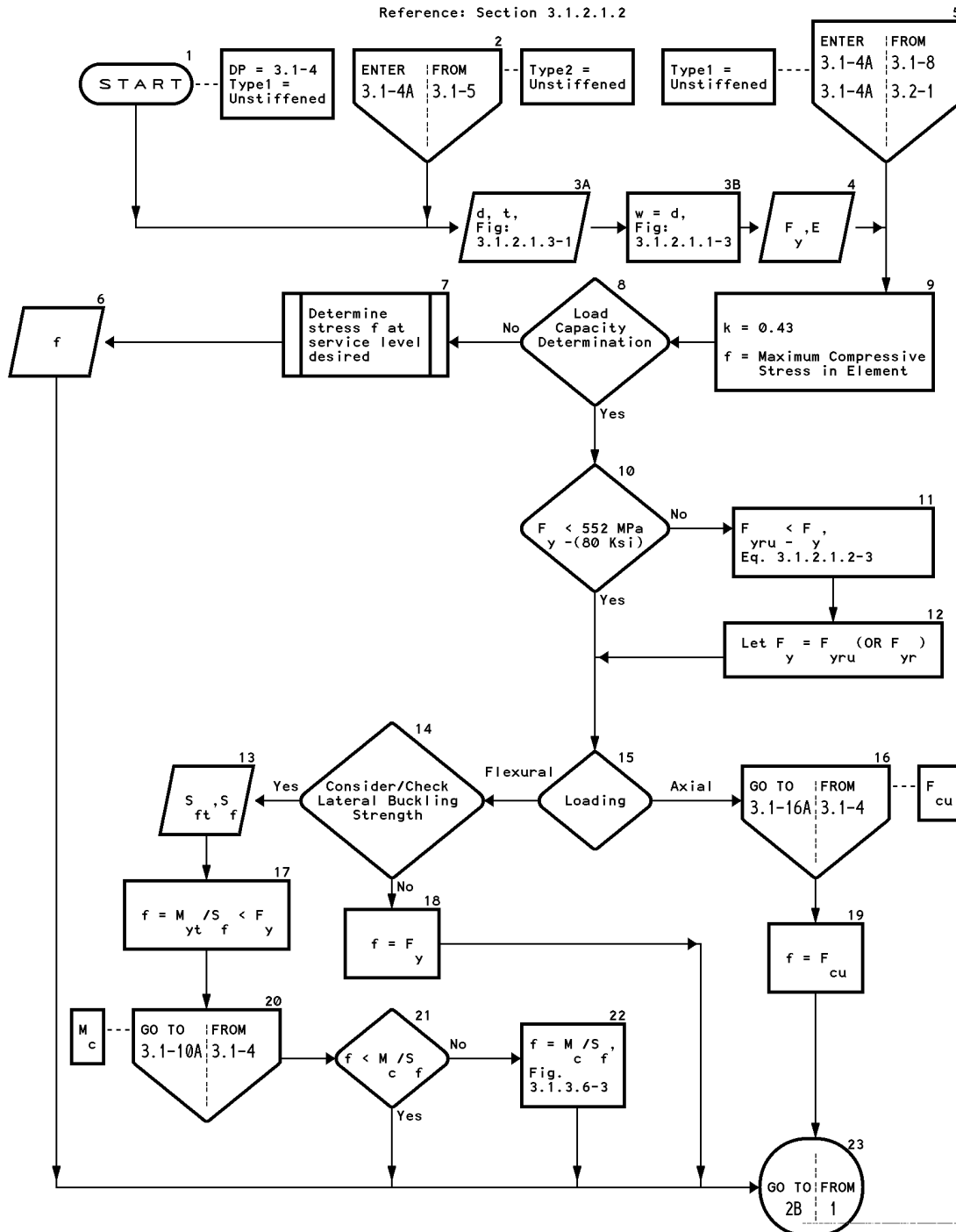
EFFECTIVE WIDTH OF WEBS AND STIFFENED ELEMENTS WITH STRESS GRADIENT OR LIMITING STRESS, F_{bwu}
Reference: Section 3.1.3.1



DESIGN PROCEDURE 3.1-4 (1 of 2)

EFFECTIVE WIDTH, b , OF UNSTIFFENED ELEMENTS IN COMPRESSION

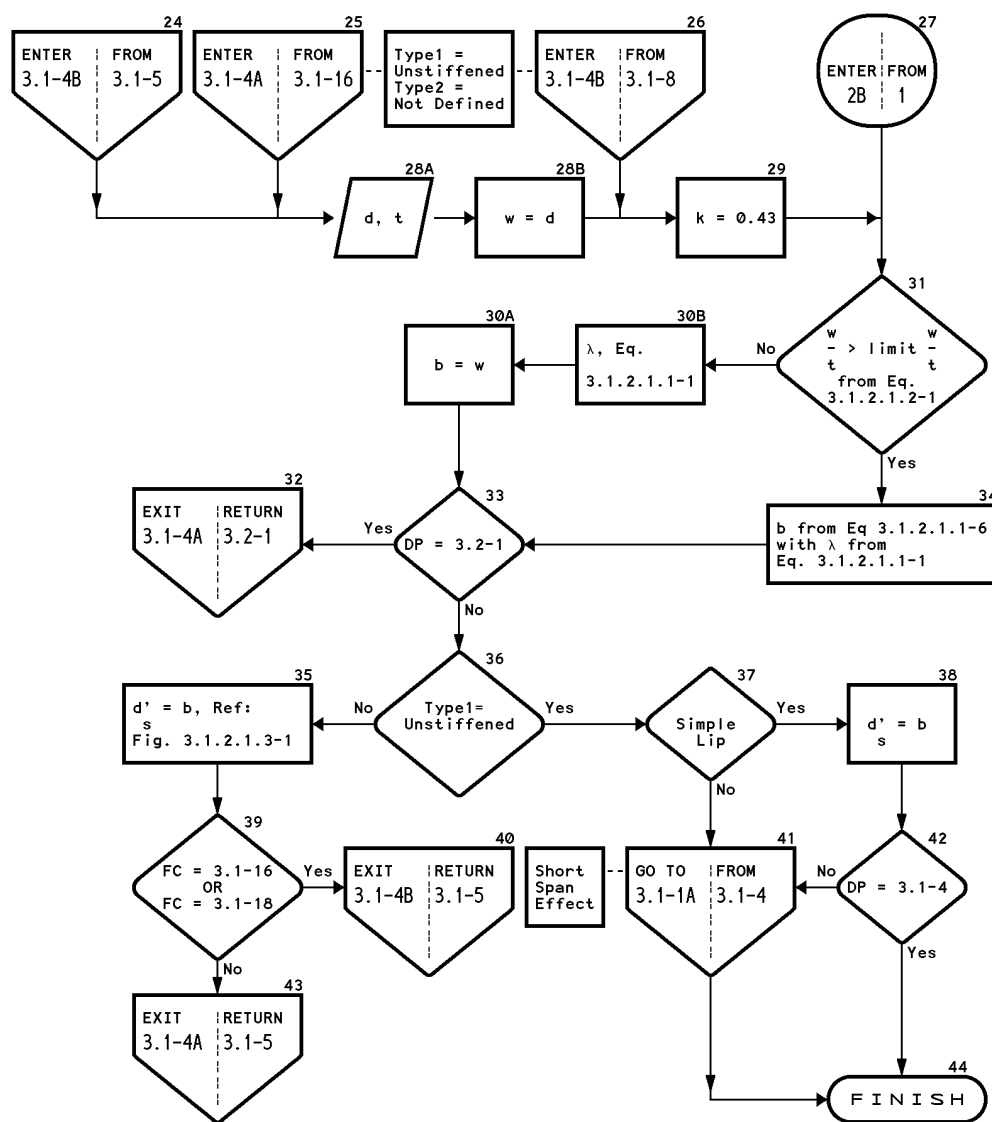
Reference: Section 3.1.2.1.2



DESIGN PROCEDURE 3.1-4 (2 of 2)

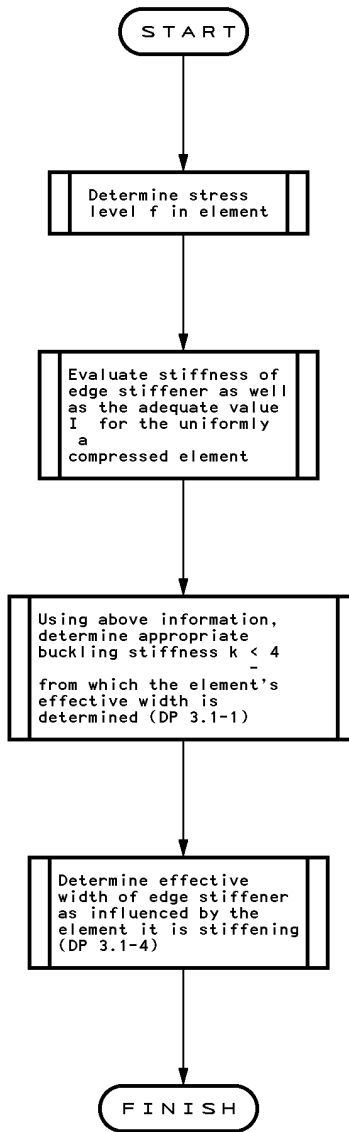
EFFECTIVE WIDTH, b , OF UNSTIFFENED ELEMENTS IN COMPRESSION

Reference: Section 3.1.2.1.2



DESIGN PROCEDURE 3.1-5A

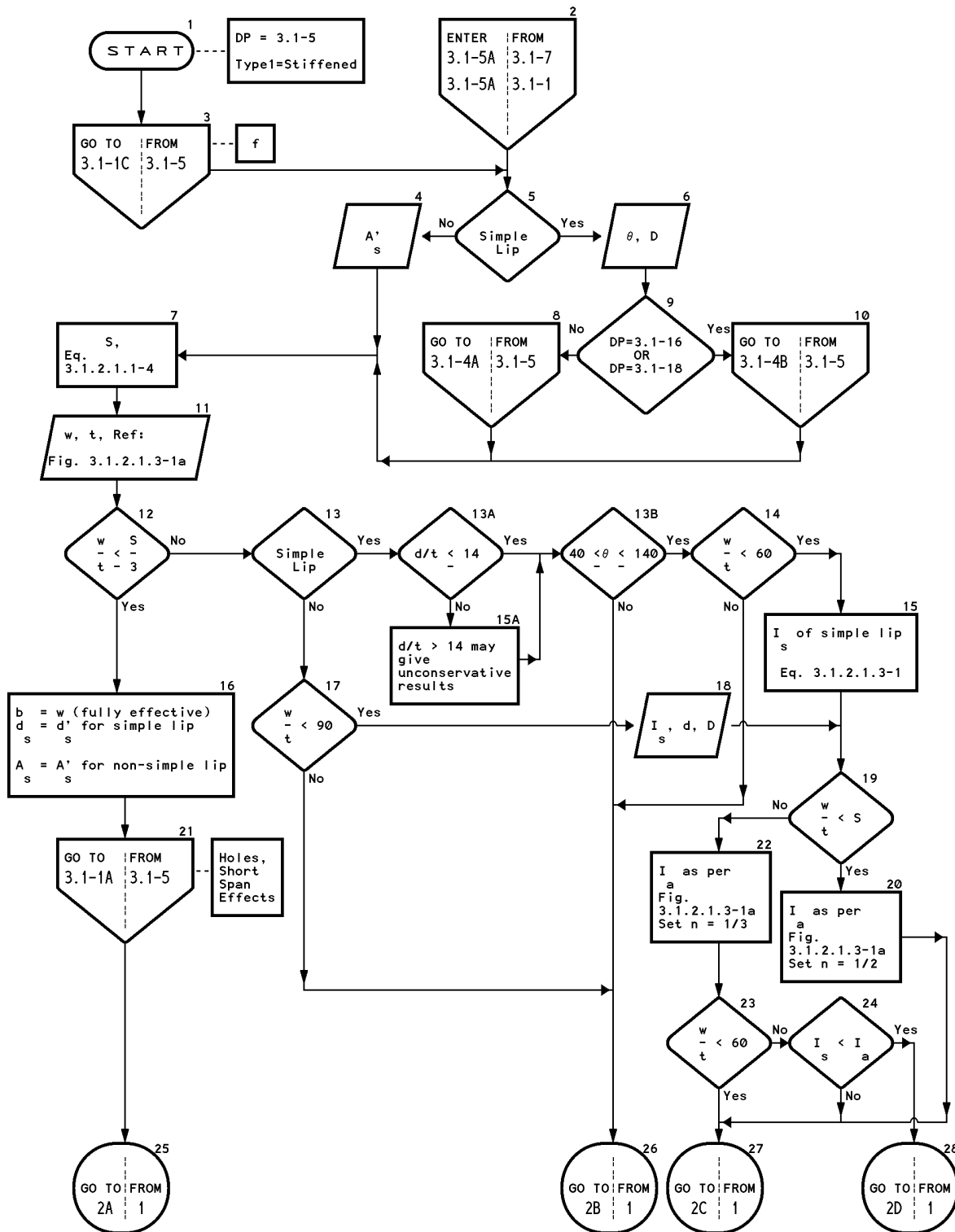
Overview: Effective Width, b , of Uniformly Compressed Elements with an Edge Stiffener
Reference: Section 3.1.2.1.3



DESIGN PROCEDURE 3.1-5 (1 of 2)

EFFECTIVE WIDTH, b , OF UNIFORMLY COMPRESSED ELEMENTS WITH AN EDGE STIFFENER

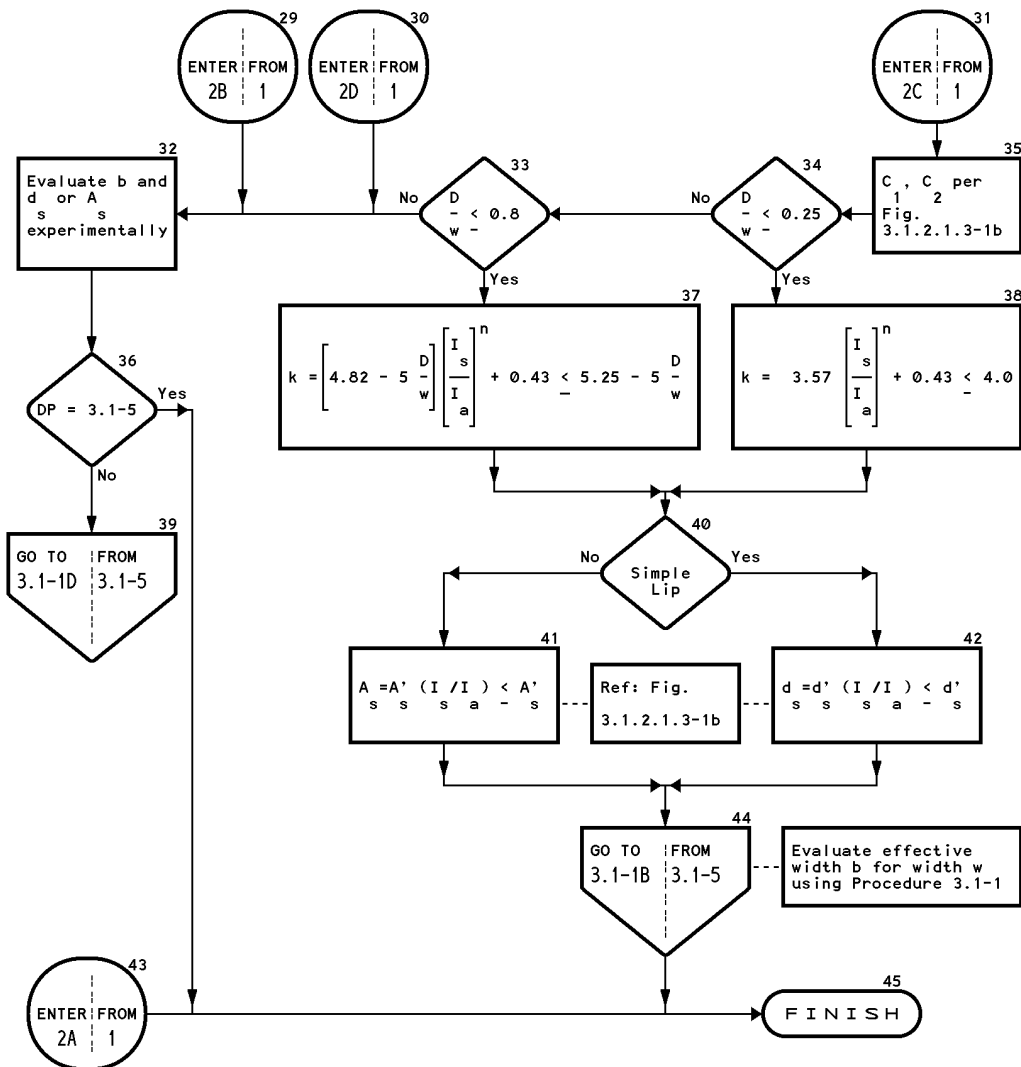
Reference: Section 3.1.2.1.3



DESIGN PROCEDURE 3.1-5 (2 of 2)

EFFECTIVE WIDTH, b , OF UNIFORMLY COMPRESSED ELEMENTS WITH AN EDGE STIFFENER

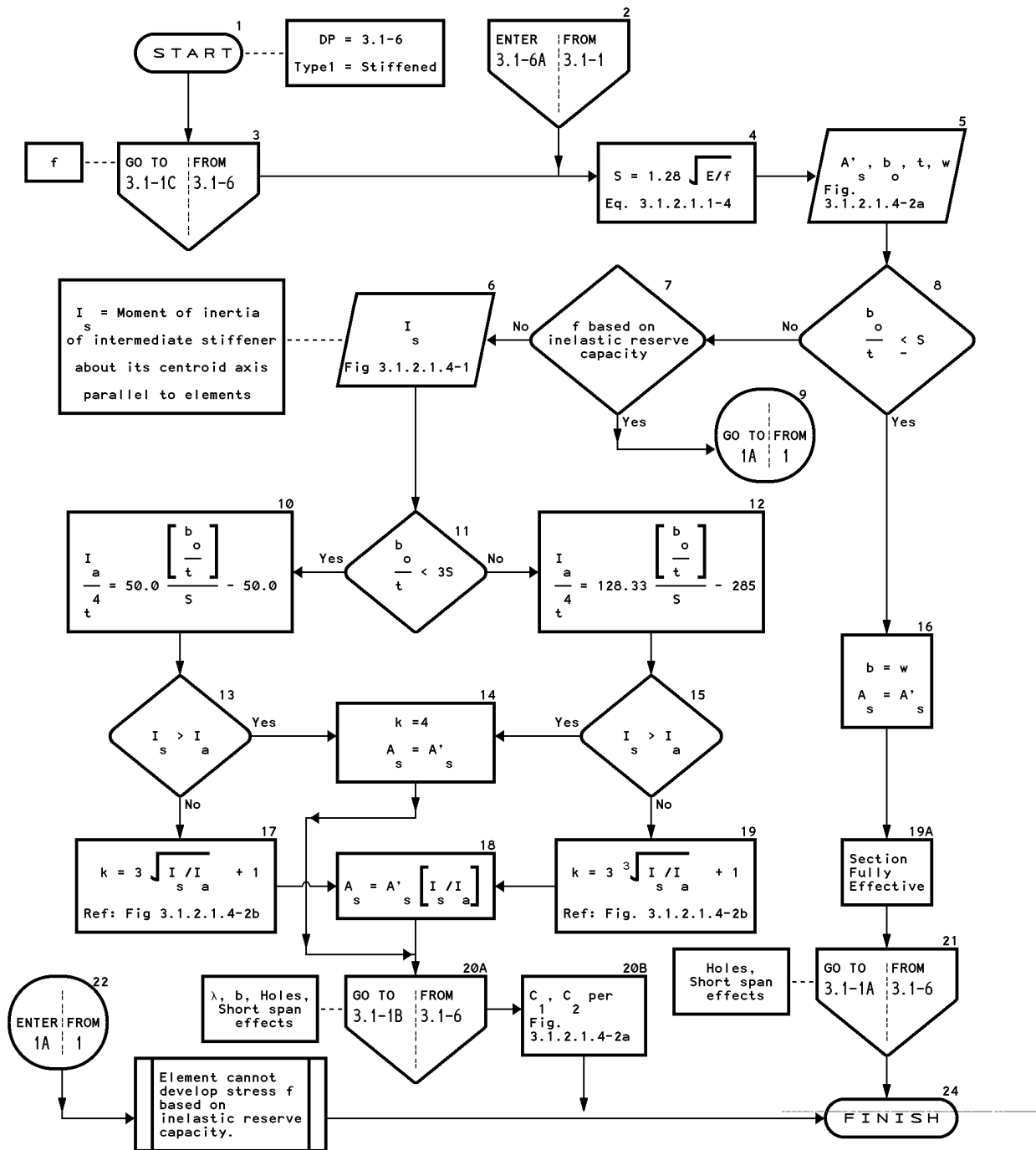
Reference: Section 3.1.2.1.3



DESIGN PROCEDURE 3.1-6

EFFECTIVE WIDTH, b , OF UNIFORMLY COMPRESSED ELEMENTS WITH A SINGLE INTERMEDIATE STIFFENER

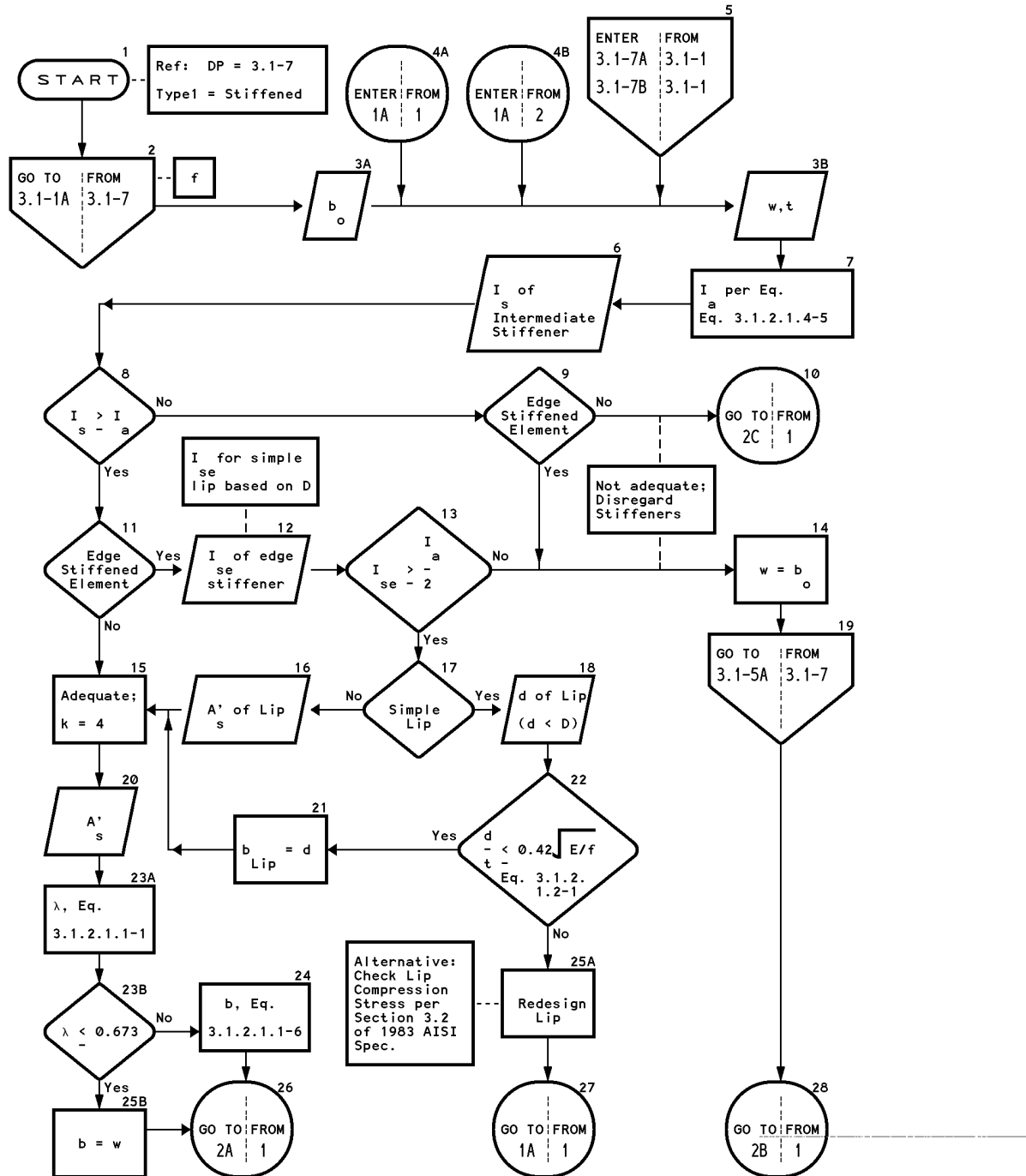
Reference: Section 3.1.2.1.4



DESIGN PROCEDURE 3.1-7 (1 of 2)

EFFECTIVE WIDTH OF EDGE STIFFENED ELEMENTS WITH INTERMEDIATE STIFFENERS OR STIFFENED ELEMENTS WITH MORE THAN ONE INTERMEDIATE STIFFENER

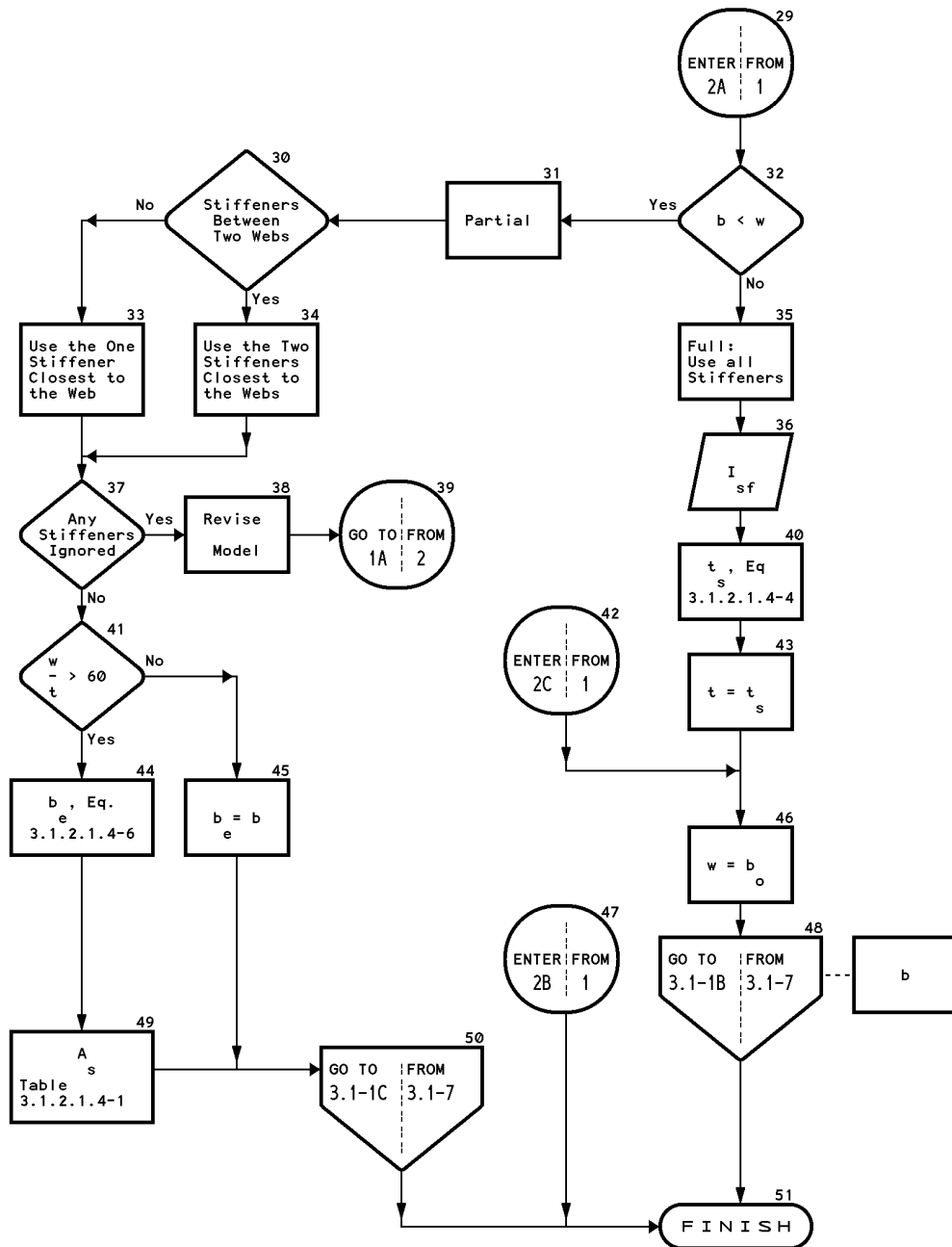
Reference: Section 3.1.2.1.4



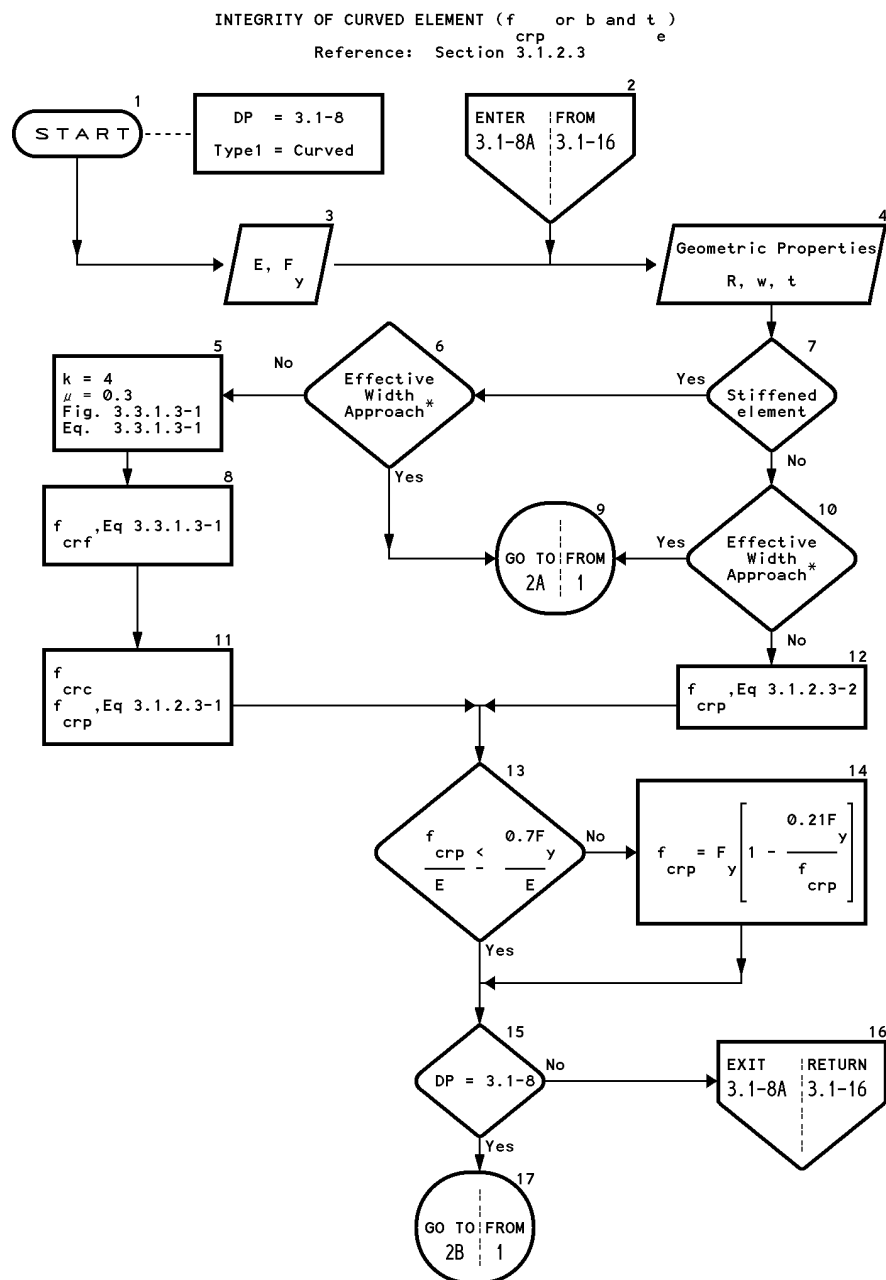
DESIGN PROCEDURE 3.1-7 (2 of 2)

EFFECTIVE WIDTH OF EDGE STIFFENED ELEMENTS WITH INTERMEDIATE STIFFENERS OR
STIFFENED ELEMENTS WITH MORE THAN ONE INTERMEDIATE STIFFENER

Reference: Section 3.1.2.1.4



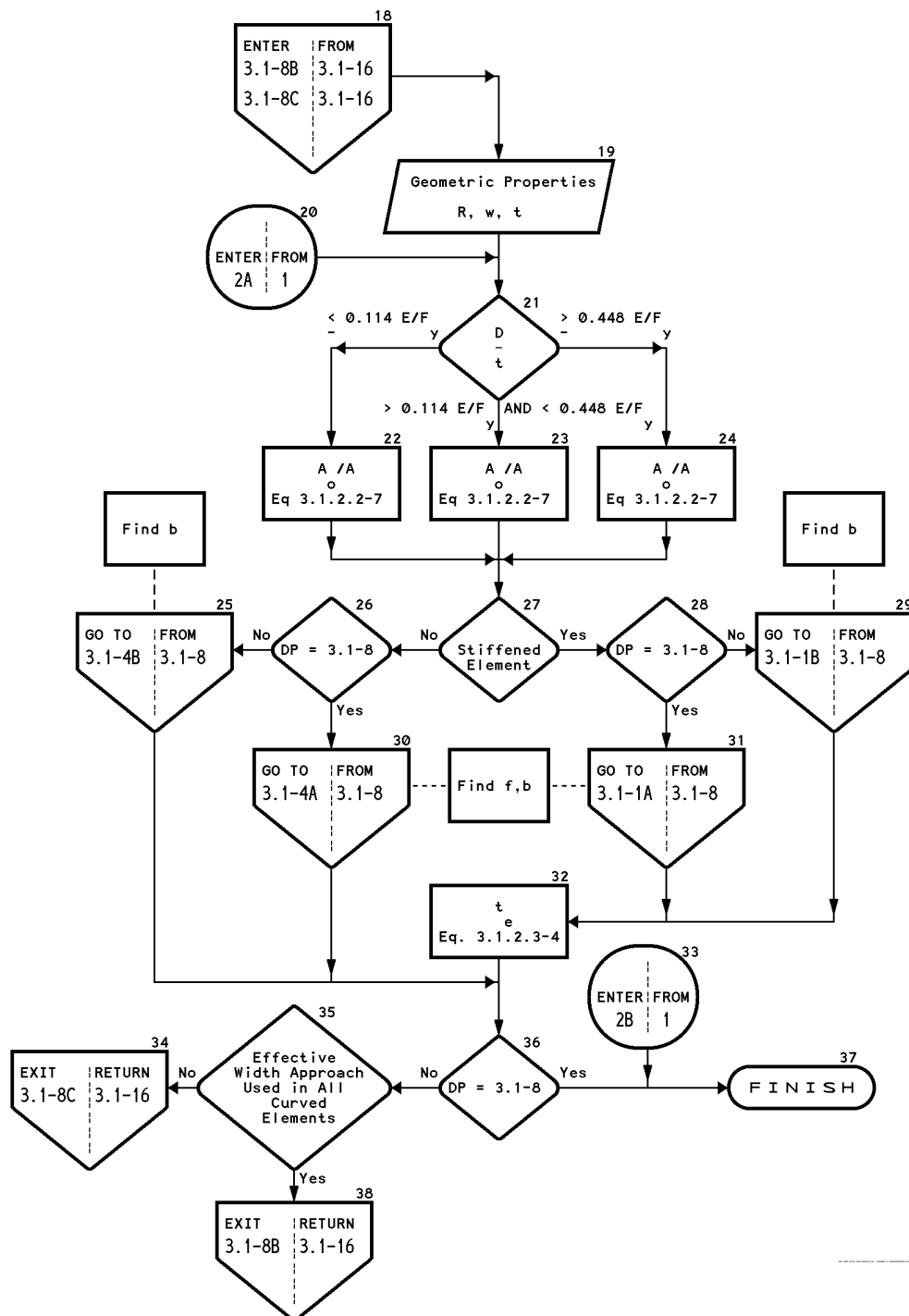
DESIGN PROCEDURE 3.1-8 (1 of 2)



* Element stiffened by bends close to 45^0 required to use effective width approach for post buckling behavior (See Fig 3.1.2.3.1)

DESIGN PROCEDURE 3.1-8 (2 of 2)

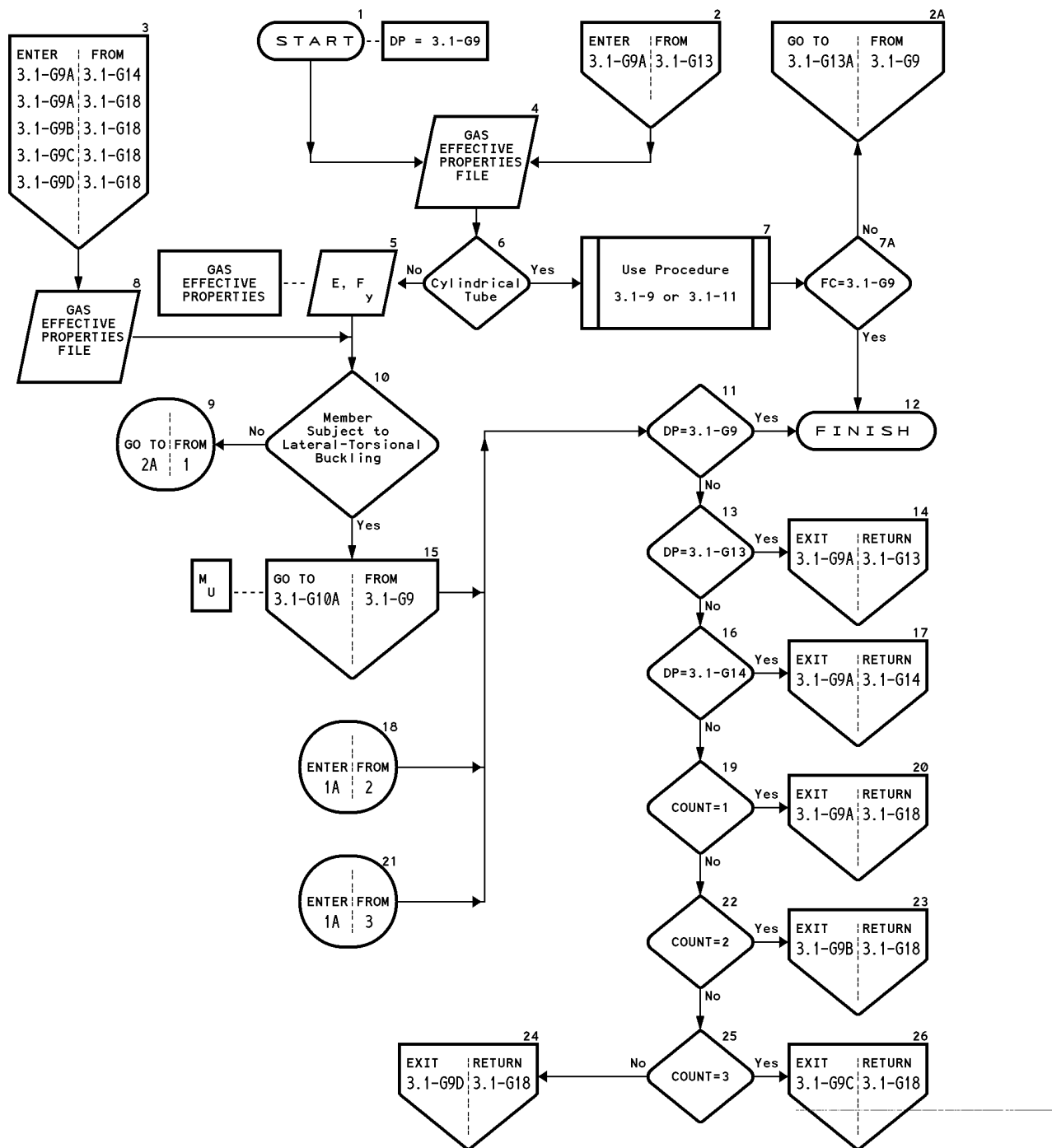
INTEGRITY OF CURVED ELEMENT (f_{crp} or b and t_e)
Reference: Section 3.1.2.3



DESIGN PROCEDURE 3.1-G9 (1 of 3)

MEMBER FLEXURAL STRENGTH, M (USING SECTION PROPERTIES)

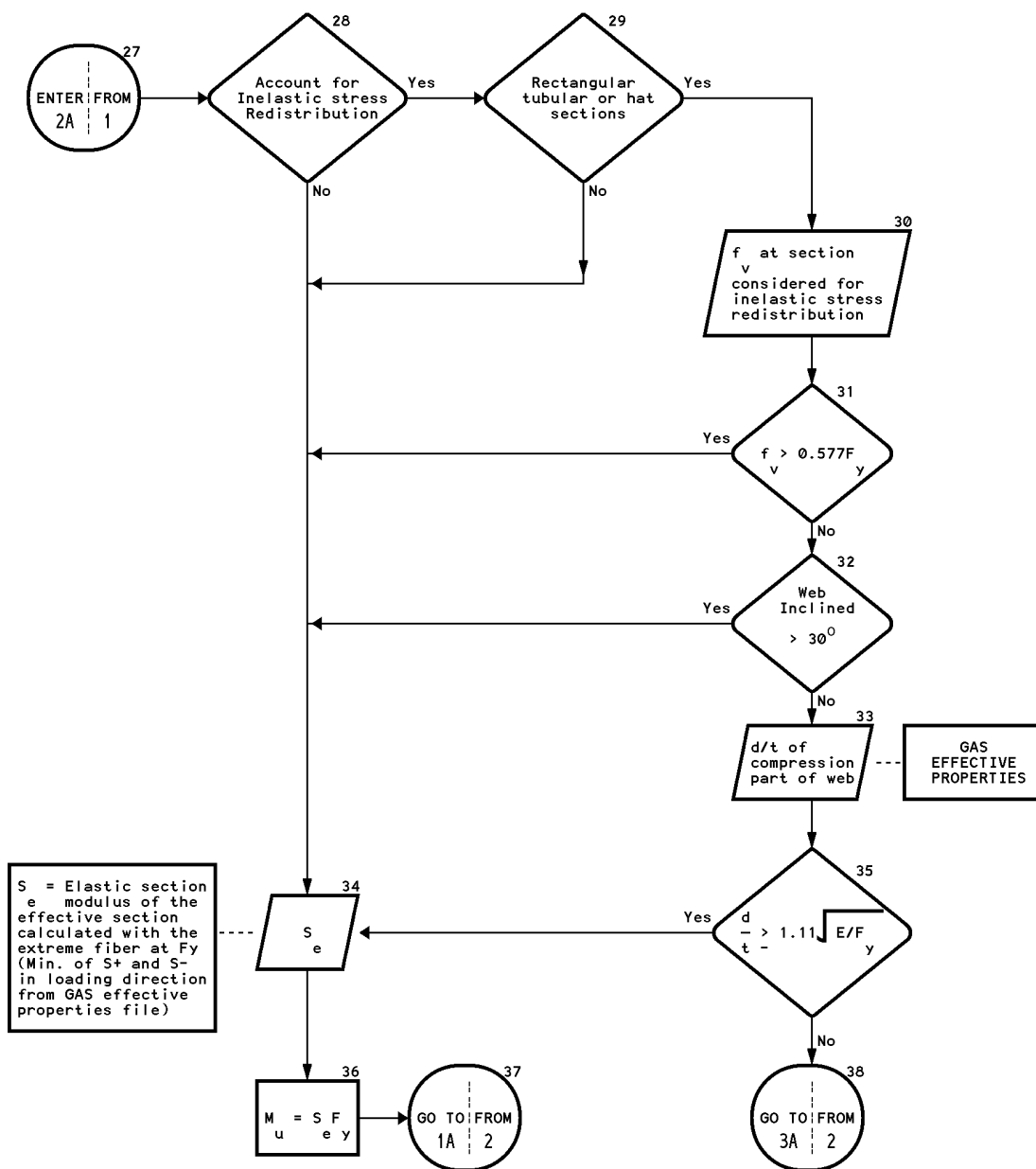
Reference: Section 3.1.3.1



DESIGN PROCEDURE 3.1-G9 (2 of 3)

MEMBER FLEXURAL STRENGTH, M_u (USING SECTION PROPERTIES)

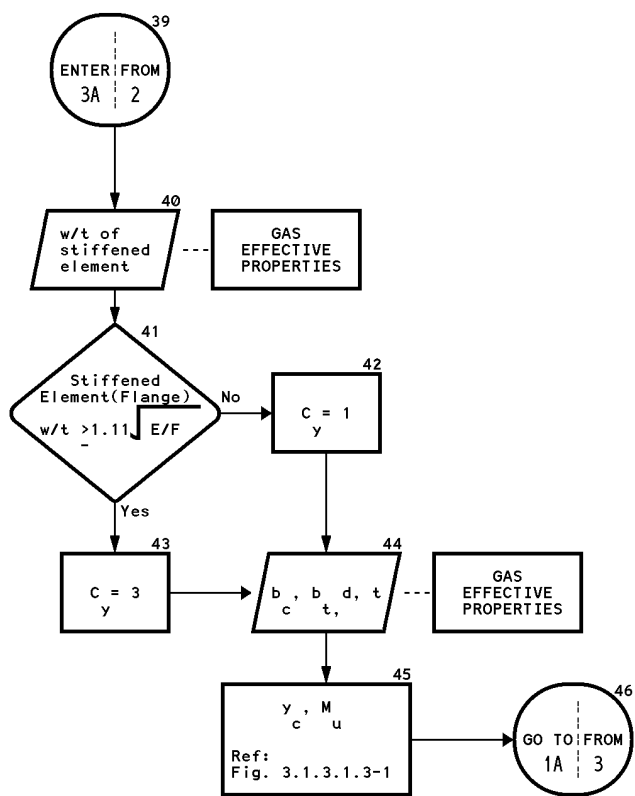
Reference: Section 3.1.3.1



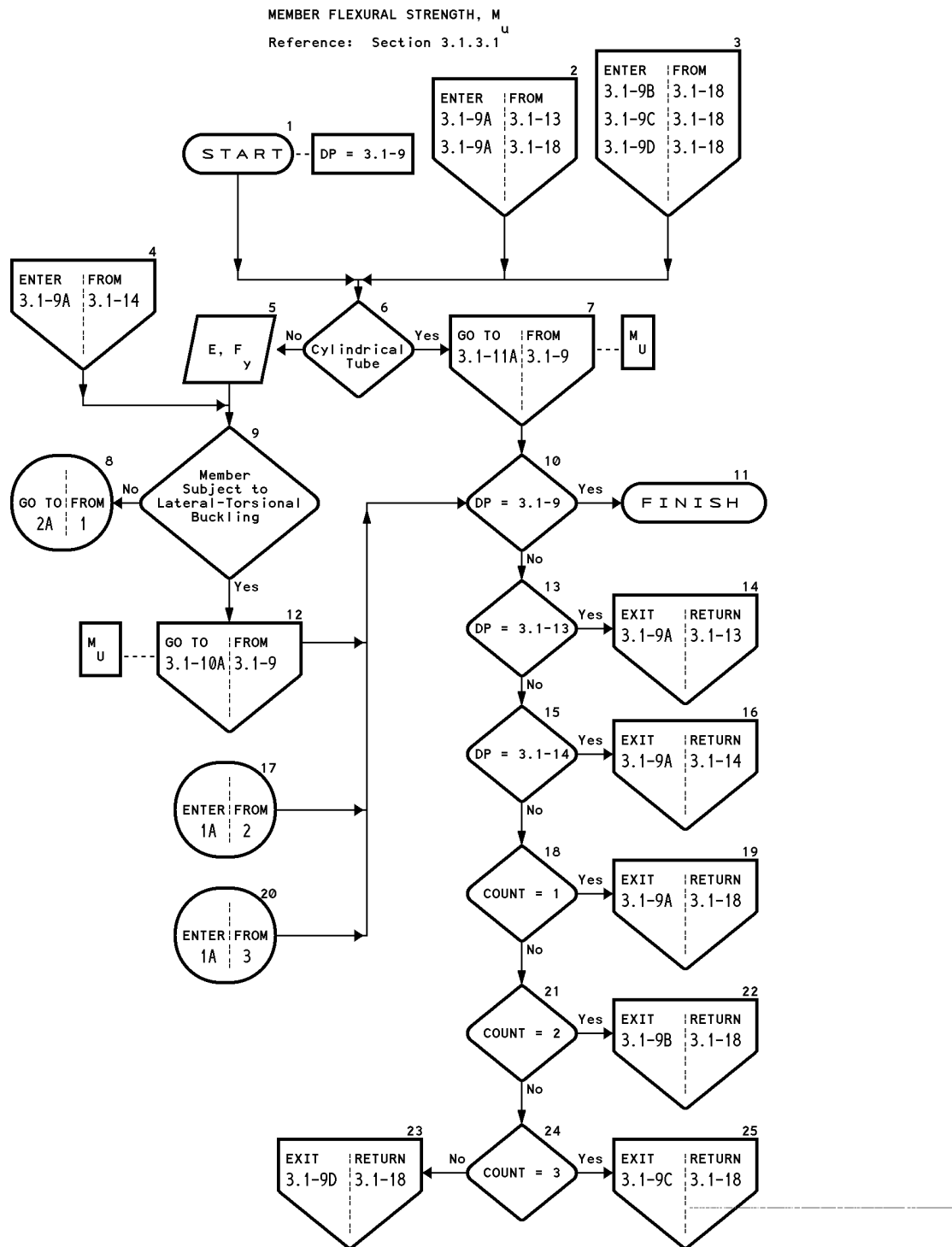
DESIGN PROCEDURE 3.1-G9 (3 of 3)

MEMBER FLEXURAL STRENGTH, M_u (USING SECTION PROPERTIES)

Reference: Section 3.1.3.1

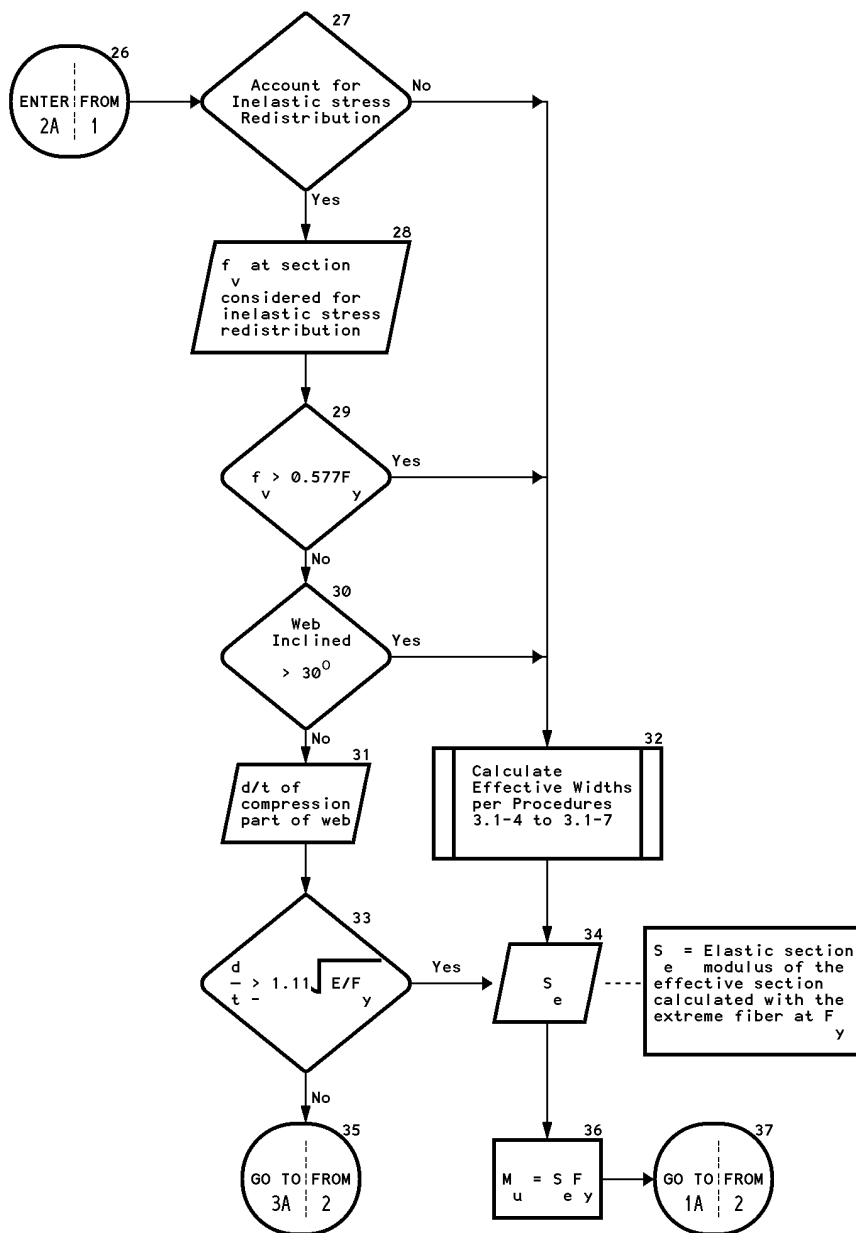


DESIGN PROCEDURE 3.1-9 (1 of 3)

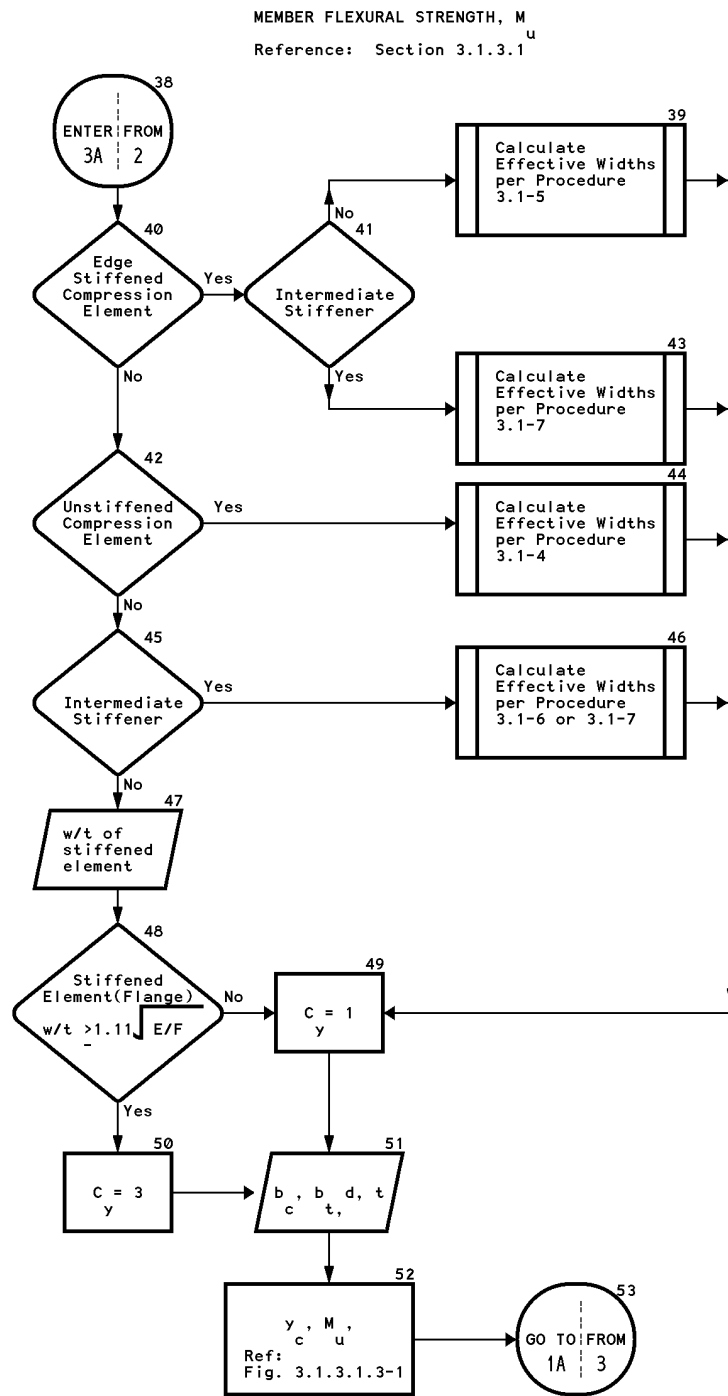


DESIGN PROCEDURE 3.1-9 (2 of 3)

MEMBER FLEXURAL STRENGTH, M_u
Reference: Section 3.1.3.1



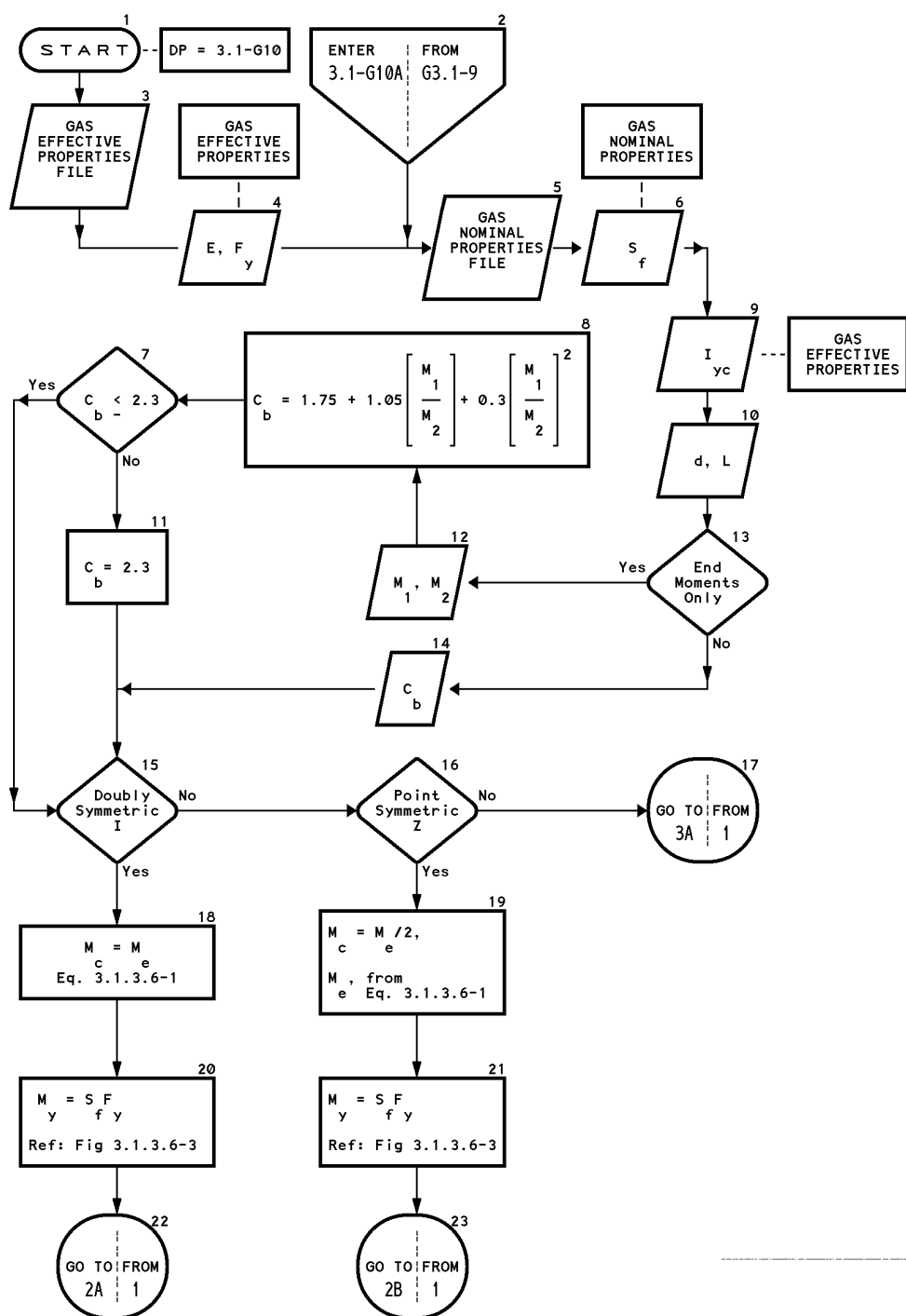
DESIGN PROCEDURE 3.1-9 (3 of 3)



DESIGN PROCEDURE 3.1-G10 (1 of 3)

LATERAL BUCKLING STRENGTH IN FLEXURE, M_u (USING SECTION PROPERTIES)

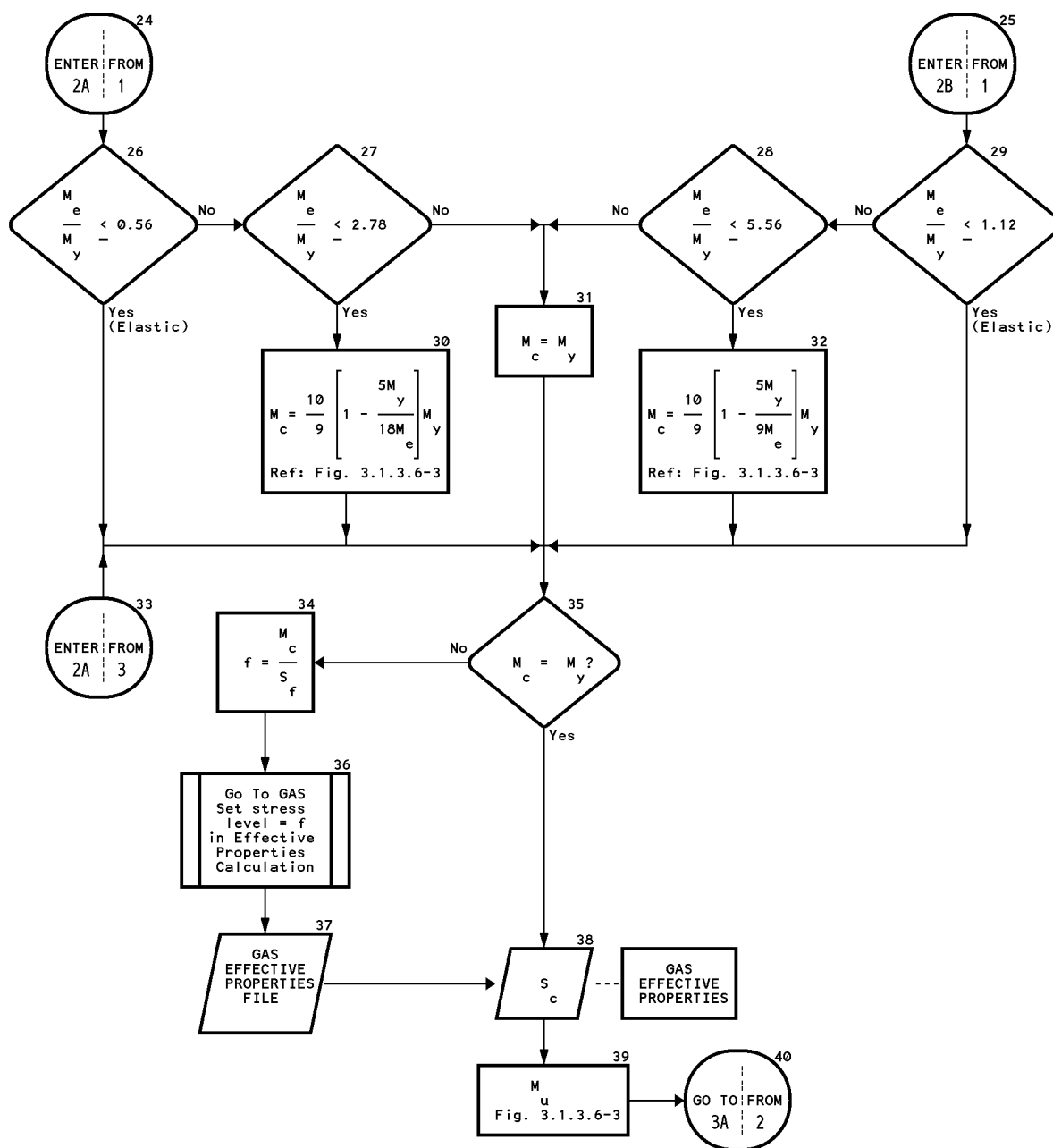
Reference: Section 3.1.3.6, Figure 3.1.3.6-3



DESIGN PROCEDURE 3.1-G10 (2 of 3)

LATERAL BUCKLING STRENGTH IN FLEXURE, M_u (USING SECTION PROPERTIES)

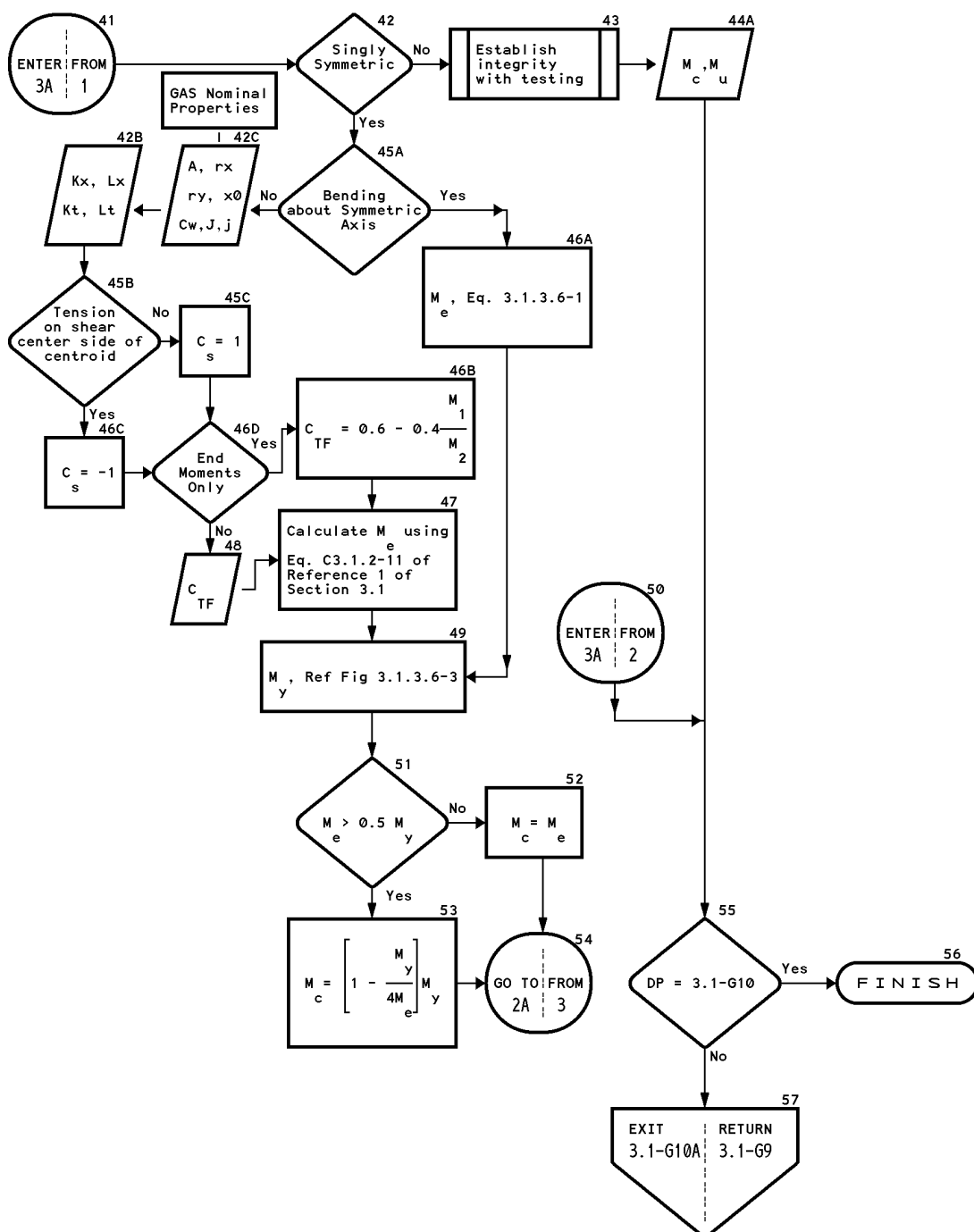
Reference: Section 3.1.3.6, Figure 3.1.3.6-3



DESIGN PROCEDURE 3.1-G10 (3 of 3)

LATERAL BUCKLING STRENGTH IN FLEXURE, M_u (USING SECTION PROPERTIES)

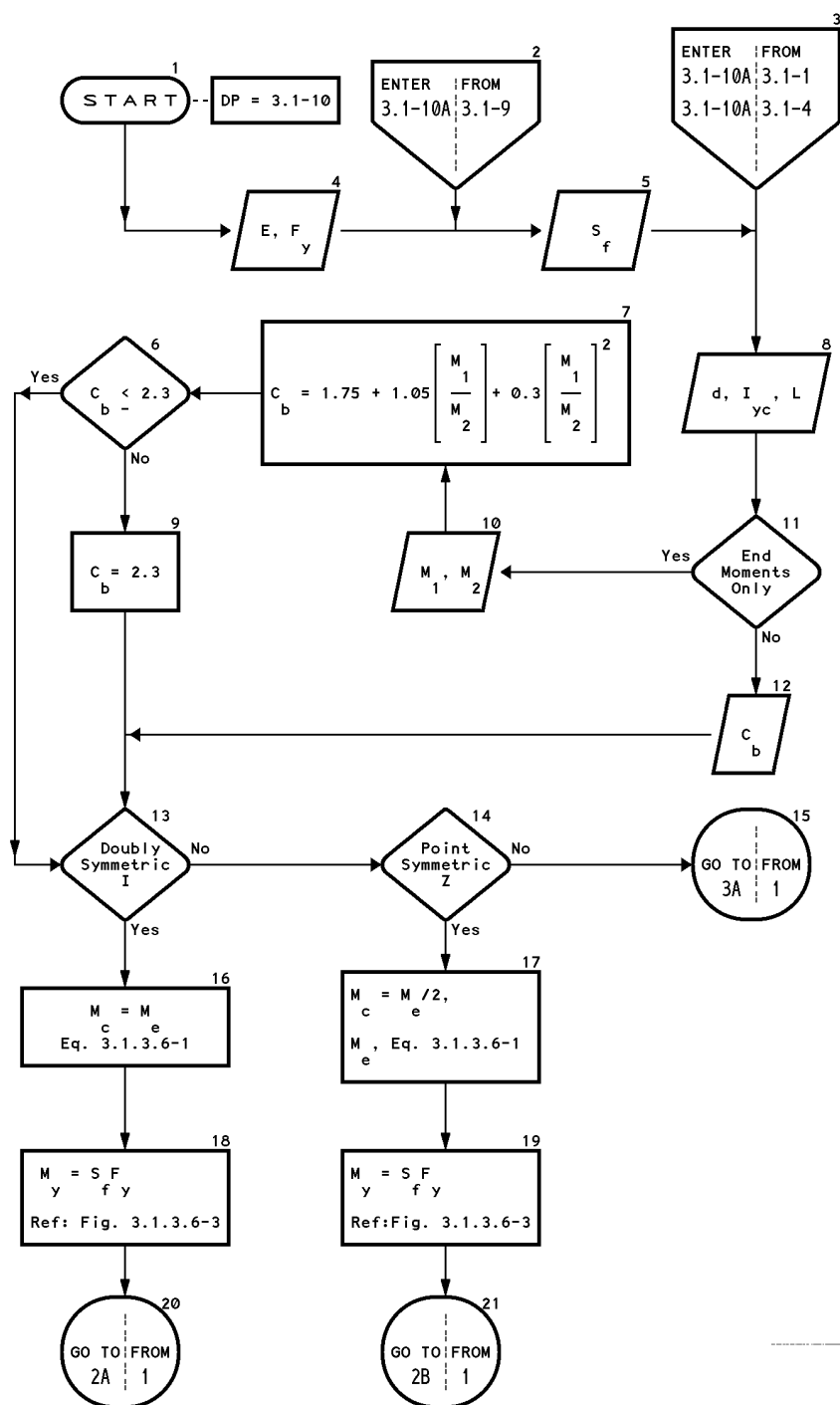
Reference: Section 3.1.3.6, Figure 3.1.3.6-3



DESIGN PROCEDURE 3.1-10 (1 of 3)

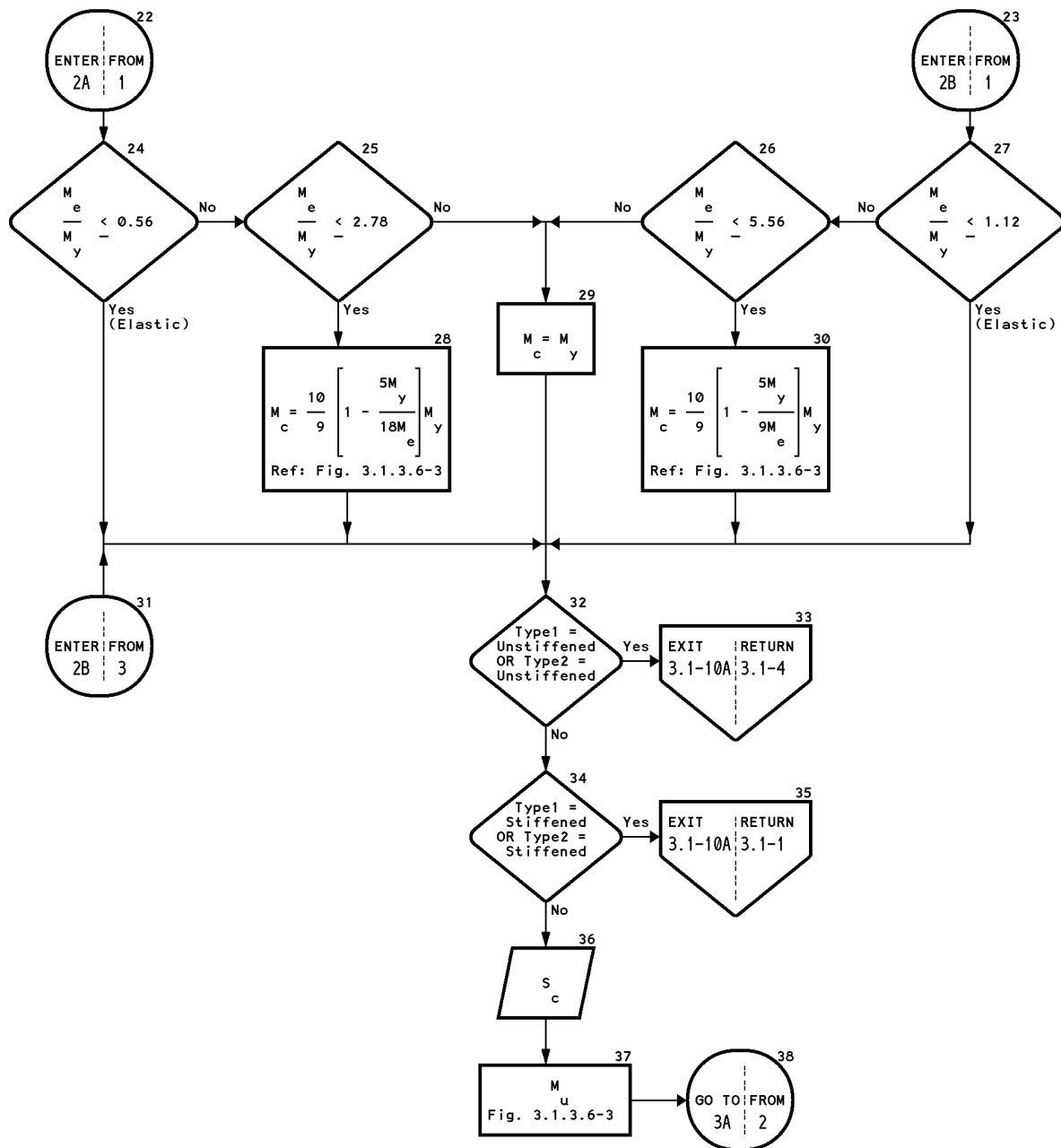
LATERAL BUCKLING STRENGTH IN FLEXURE, M

Reference: Section 3.1.3.6, Figure 3.1.3.6-3



DESIGN PROCEDURE 3.1-10 (2 of 3)

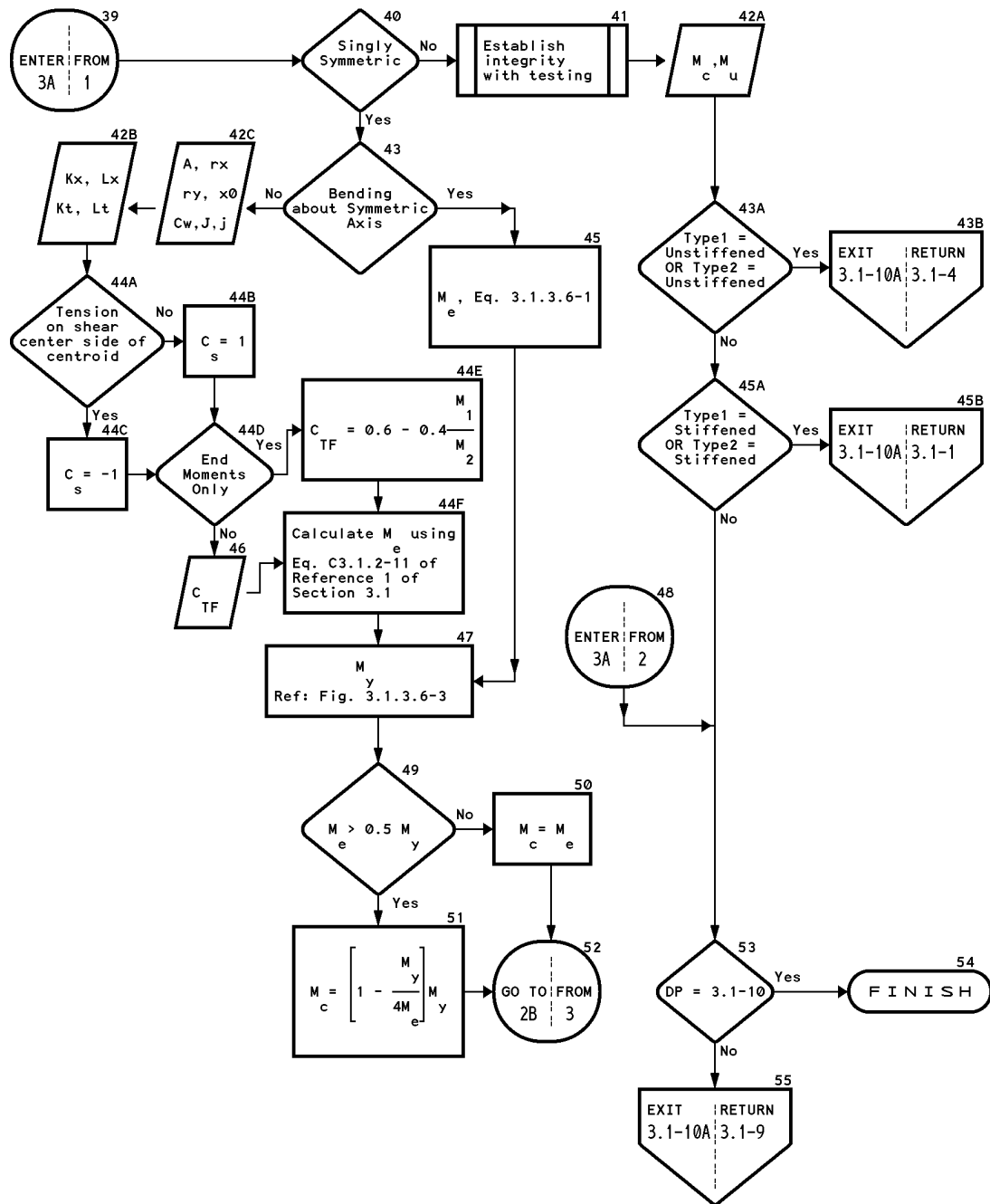
LATERAL BUCKLING STRENGTH IN FLEXURE, M_u
 Reference: Section 3.1.3.6, Figure 3.1.3.6-3



DESIGN PROCEDURE 3.1-10 (3 of 3)

LATERAL BUCKLING STRENGTH IN FLEXURE, M

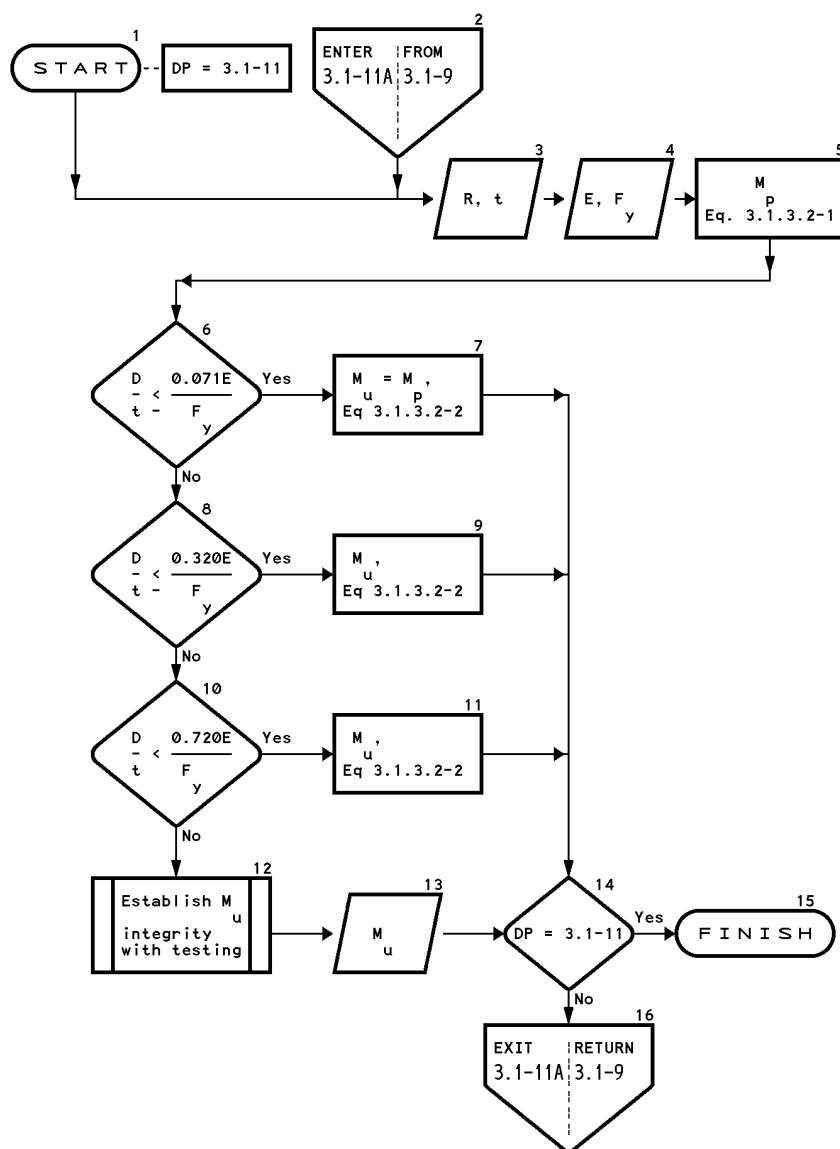
Reference: Section 3.1.3.6, Figure 3.1.3.6-3



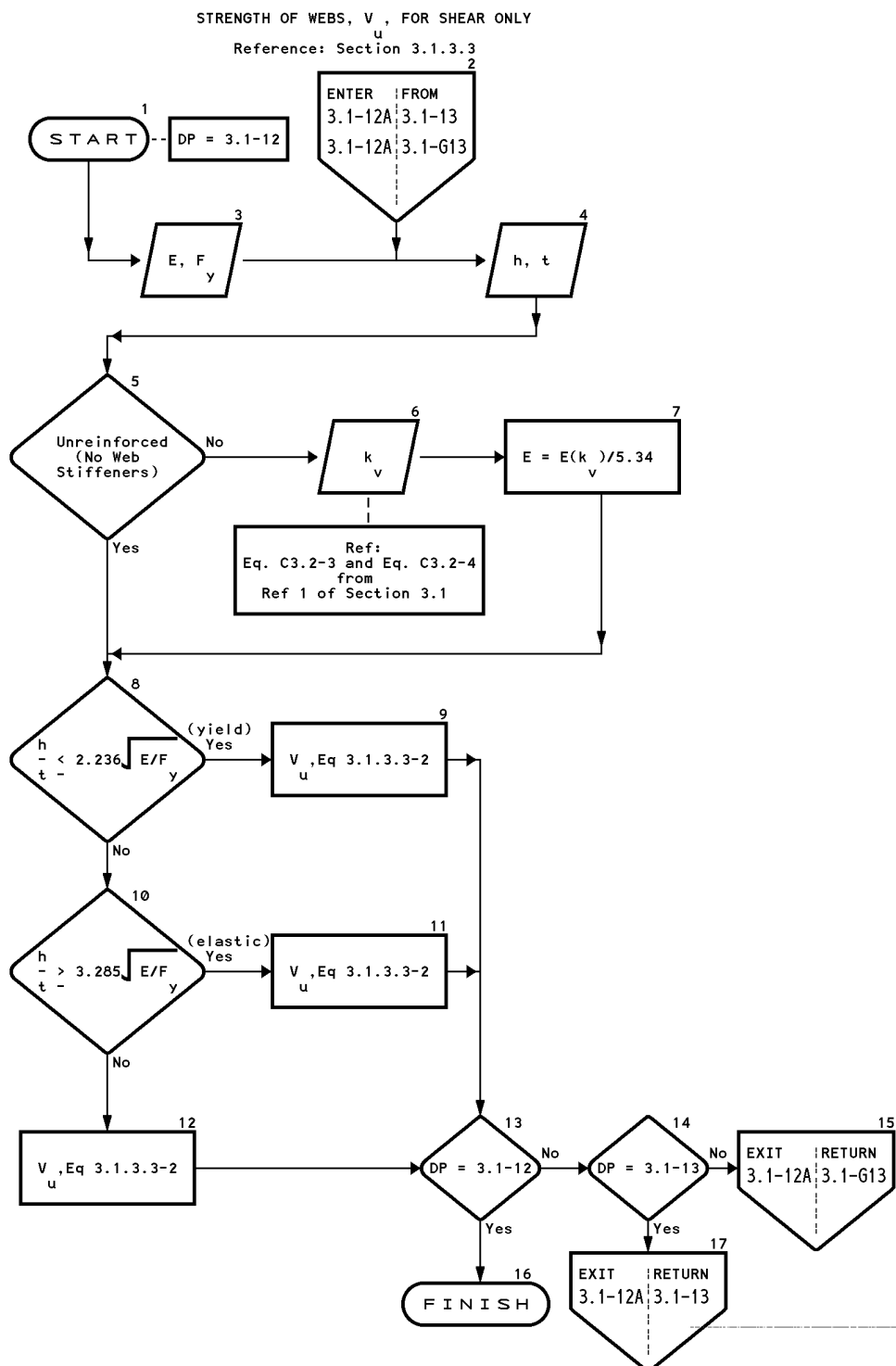
DESIGN PROCEDURE 3.1-11

FLEXURAL CAPACITY, M_u , OF CYLINDRICAL MEMBERS

Reference: Section 3.1.3.2



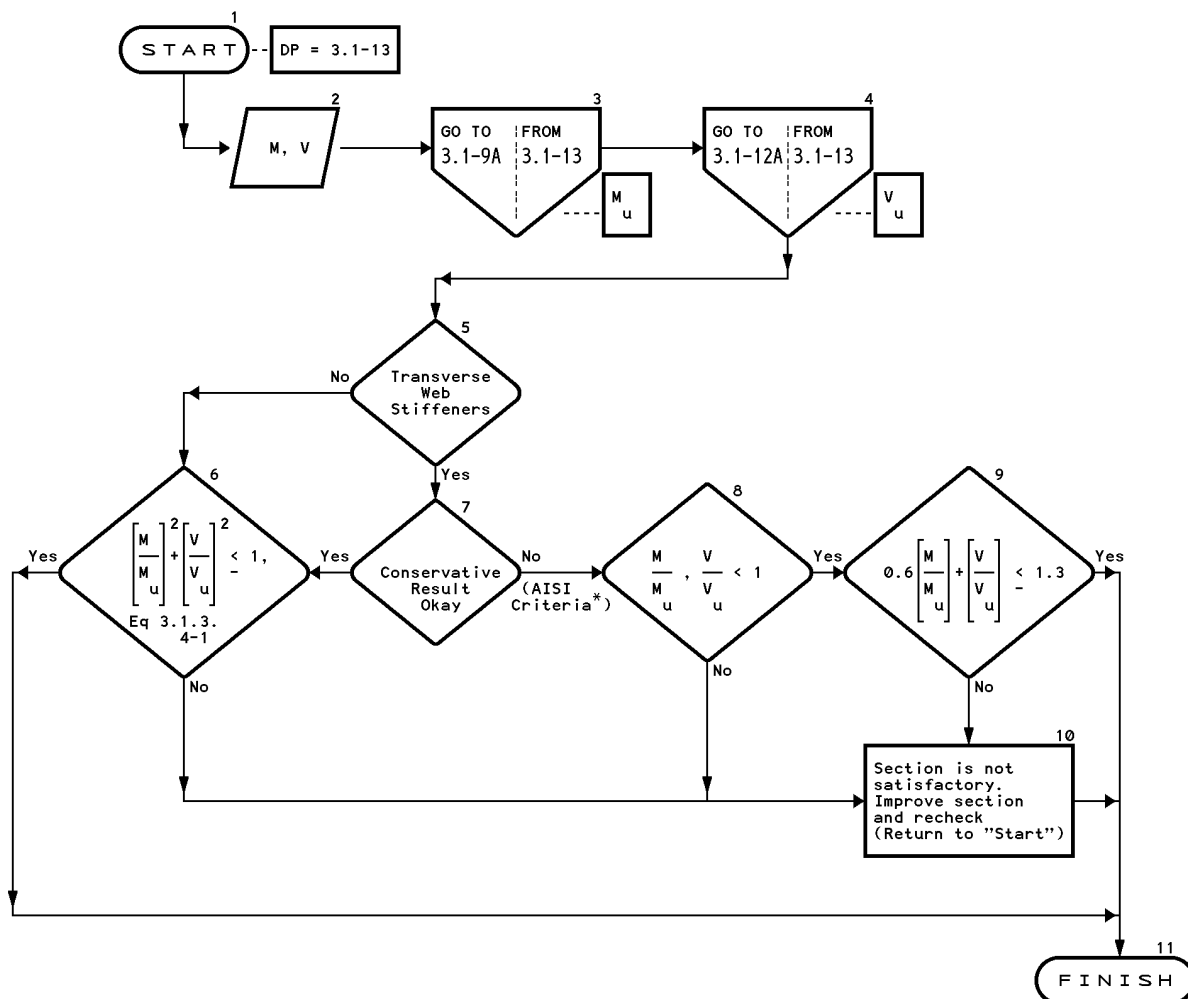
DESIGN PROCEDURE 3.1-12



DESIGN PROCEDURE 3.1-13

STRENGTH OF WEBS FOR COMBINED BENDING AND SHEAR

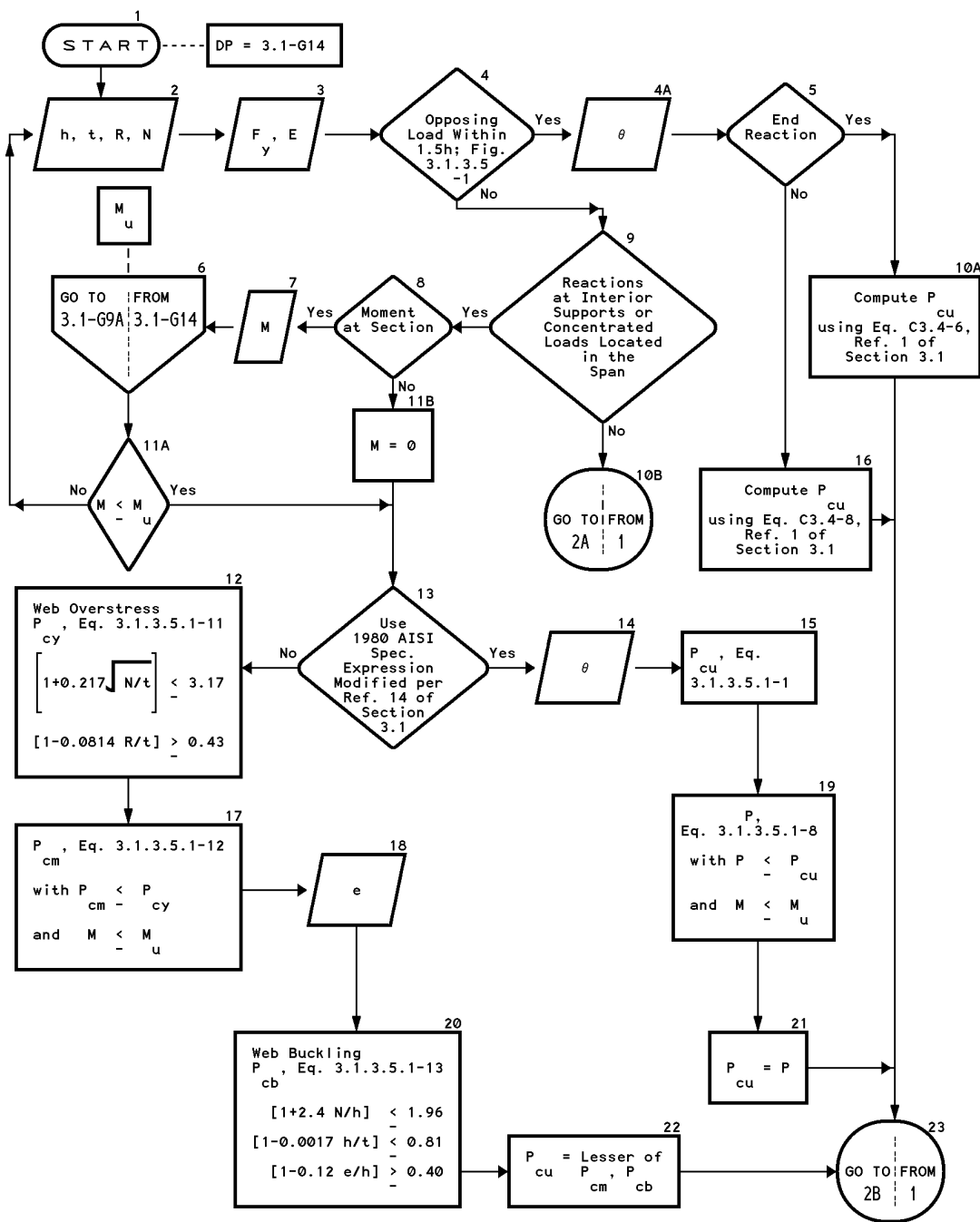
Reference: Section 3.1.3.4



*Reference 1 of Section 3.1

DESIGN PROCEDURE 3.1-G14 (1 of 2)

TRANSVERSE LOAD WEB CAPACITY, P_{cu} , - BEAMS WITH SINGLE WEBS* (USING SECTION PROPERTIES)
 Reference: Section 3.1.3.5.1

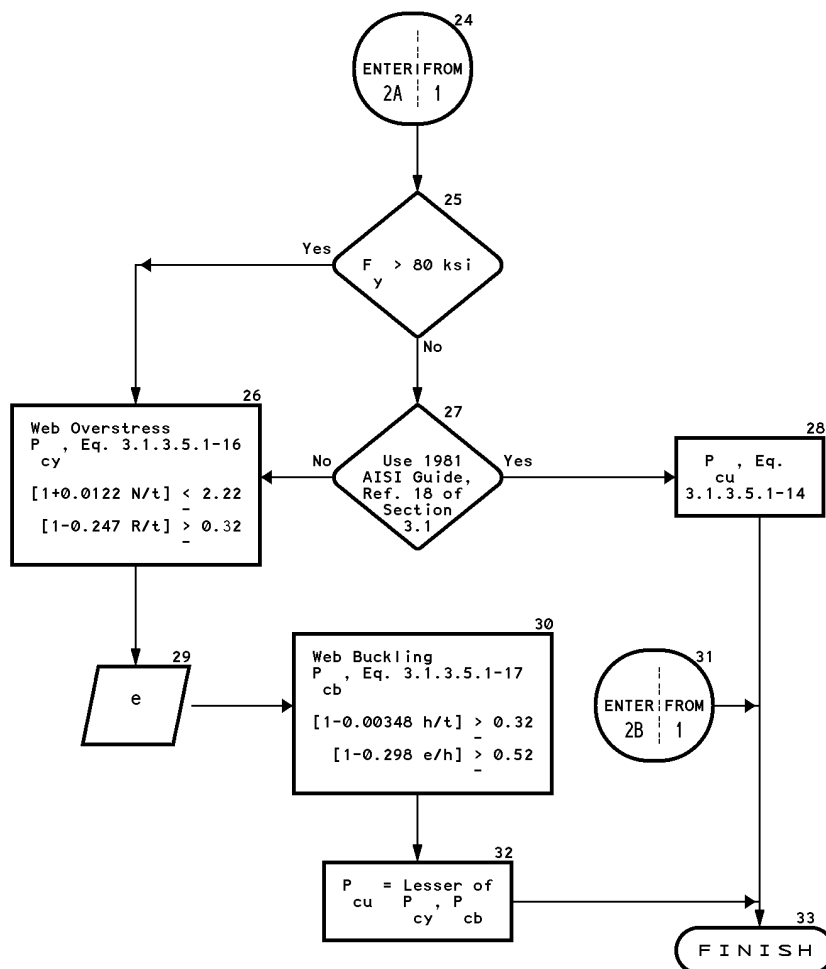


* Webs of hat, zee, channel, or rectangular tubular sections

DESIGN PROCEDURE 3.1-G14 (2 of 2)

TRANSVERSE LOAD WEB CAPACITY, P_{cu} , - BEAMS WITH SINGLE WEBS* (USING SECTION PROPERTIES)

Reference: Section 3.1.3.5.1

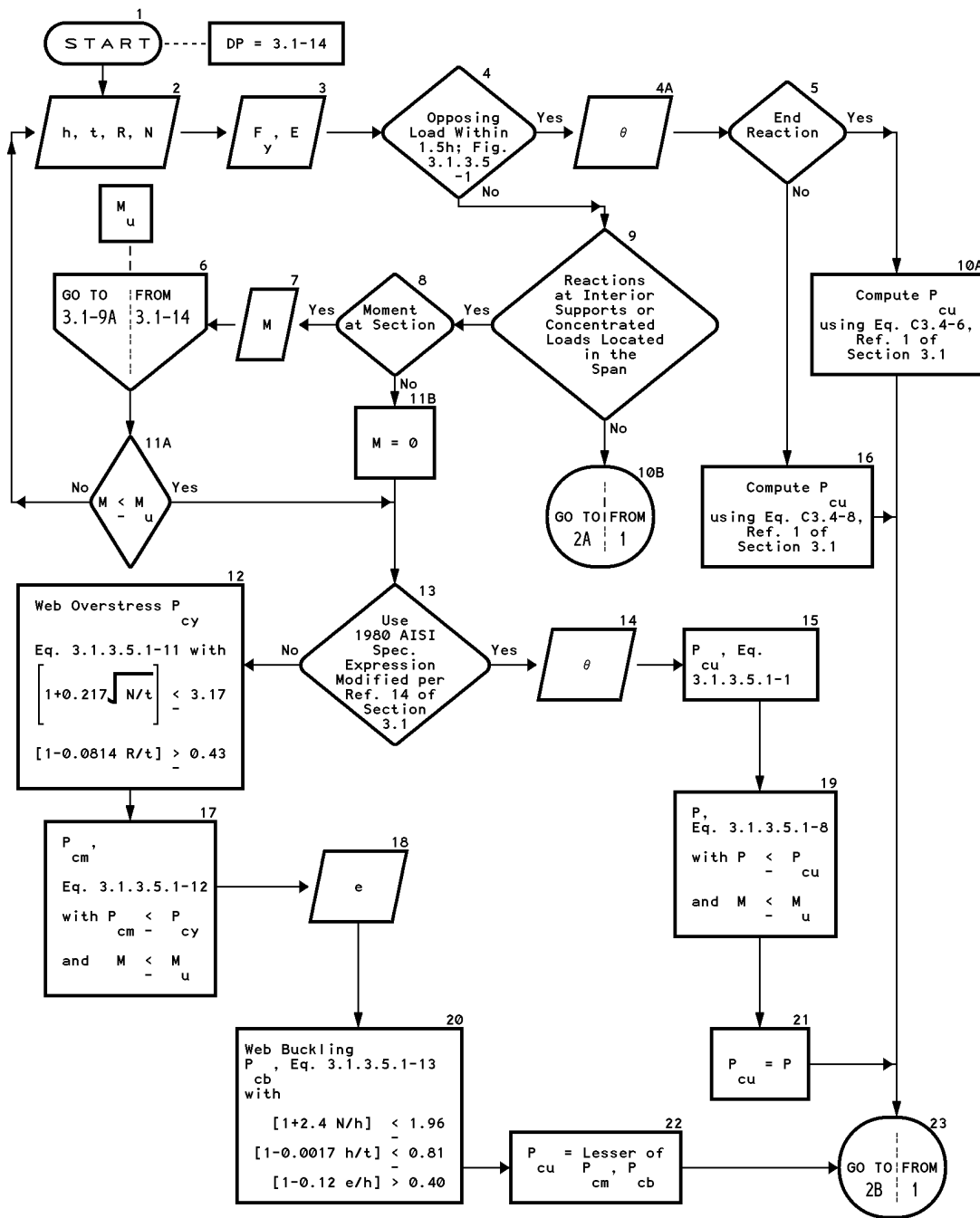


* Webs of hat, zee, channel, or rectangular tubular sections

DESIGN PROCEDURE 3.1-14 (1 of 2)

TRANSVERSE LOAD WEB CAPACITY, P_{cu} , - BEAMS WITH SINGLE WEBS*

Reference: Section 3.1.3.5.1

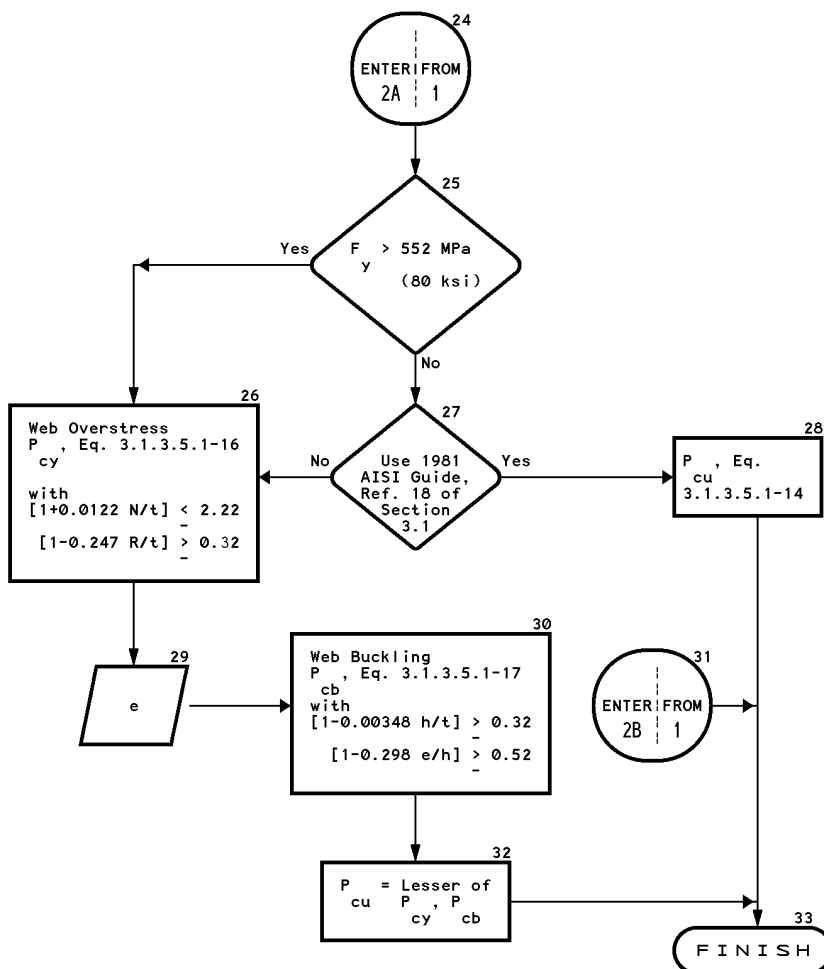


* Webs of hat, zee, channel, or rectangular tubular sections

DESIGN PROCEDURE 3.1-14 (2 of 2)

TRANSVERSE LOAD WEB CAPACITY, P_{cu} , - BEAMS WITH SINGLE WEBS*

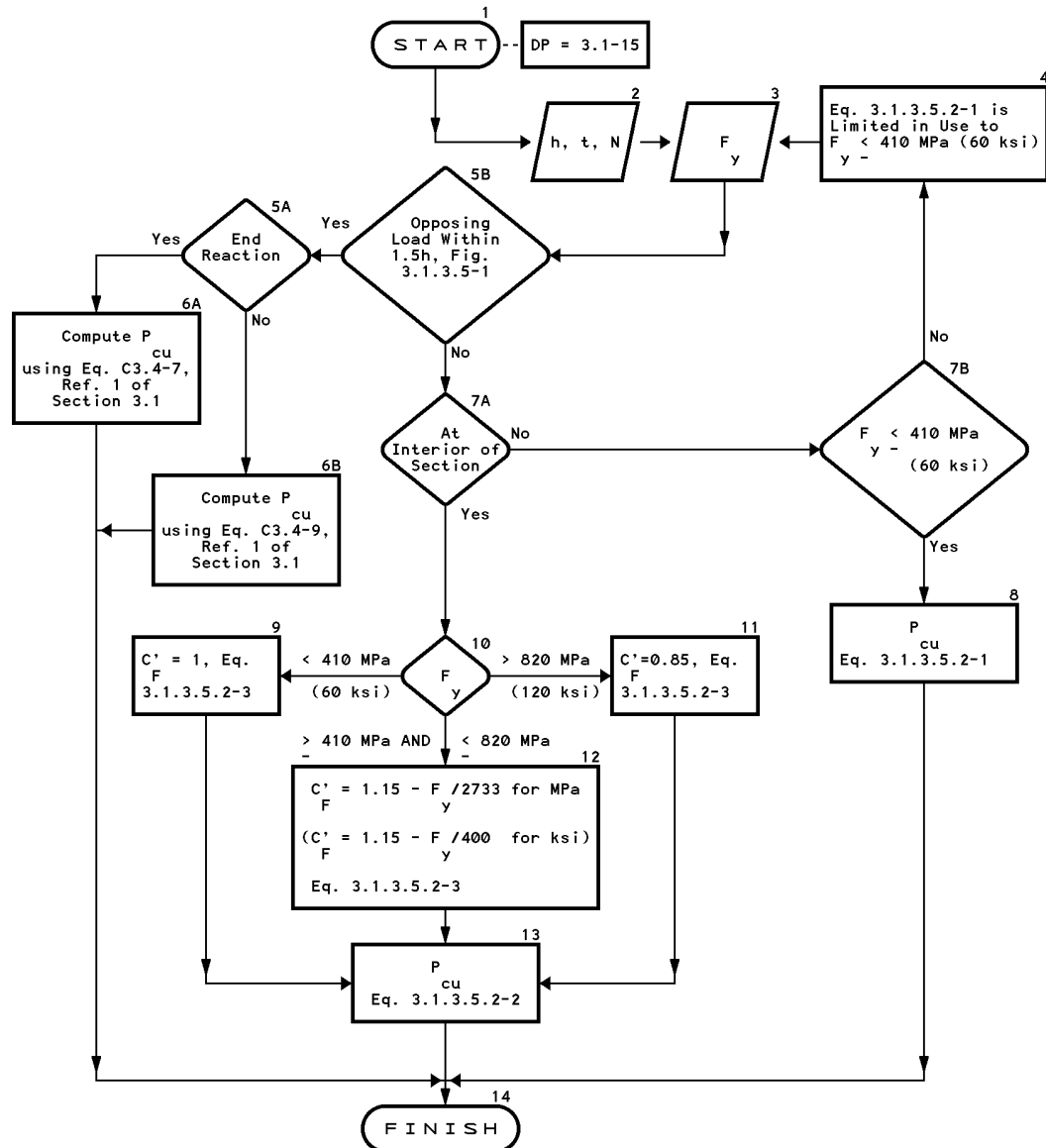
Reference: Section 3.1.3.5.1



* Webs of hat, zee, channel, or rectangular tubular sections

DESIGN PROCEDURE 3.1-15

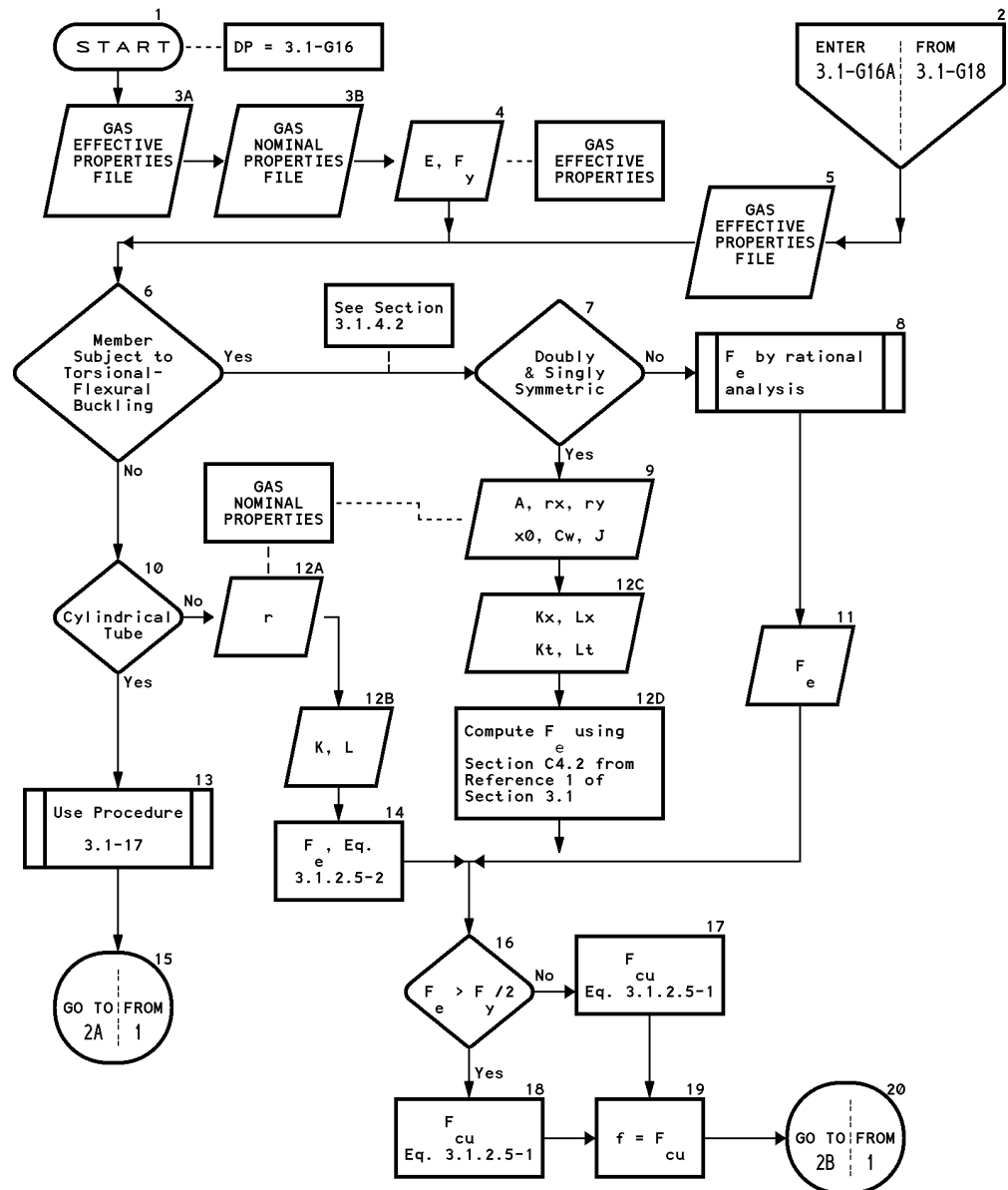
TRANSVERSE LOAD WEB CAPACITY, P_{cu} , - BEAMS WITH HIGHLY RESTRAINED WEBS
 Reference: Section 3.1.3.5.2, Figure 3.1.3.5.2-1



DESIGN PROCEDURE 3.1-G16 (1 of 2)

AXIAL CAPACITY, P_u , OF CONCENTRICALLY LOADED COMPRESSION MEMBERS (USING SECTION PROPERTIES)

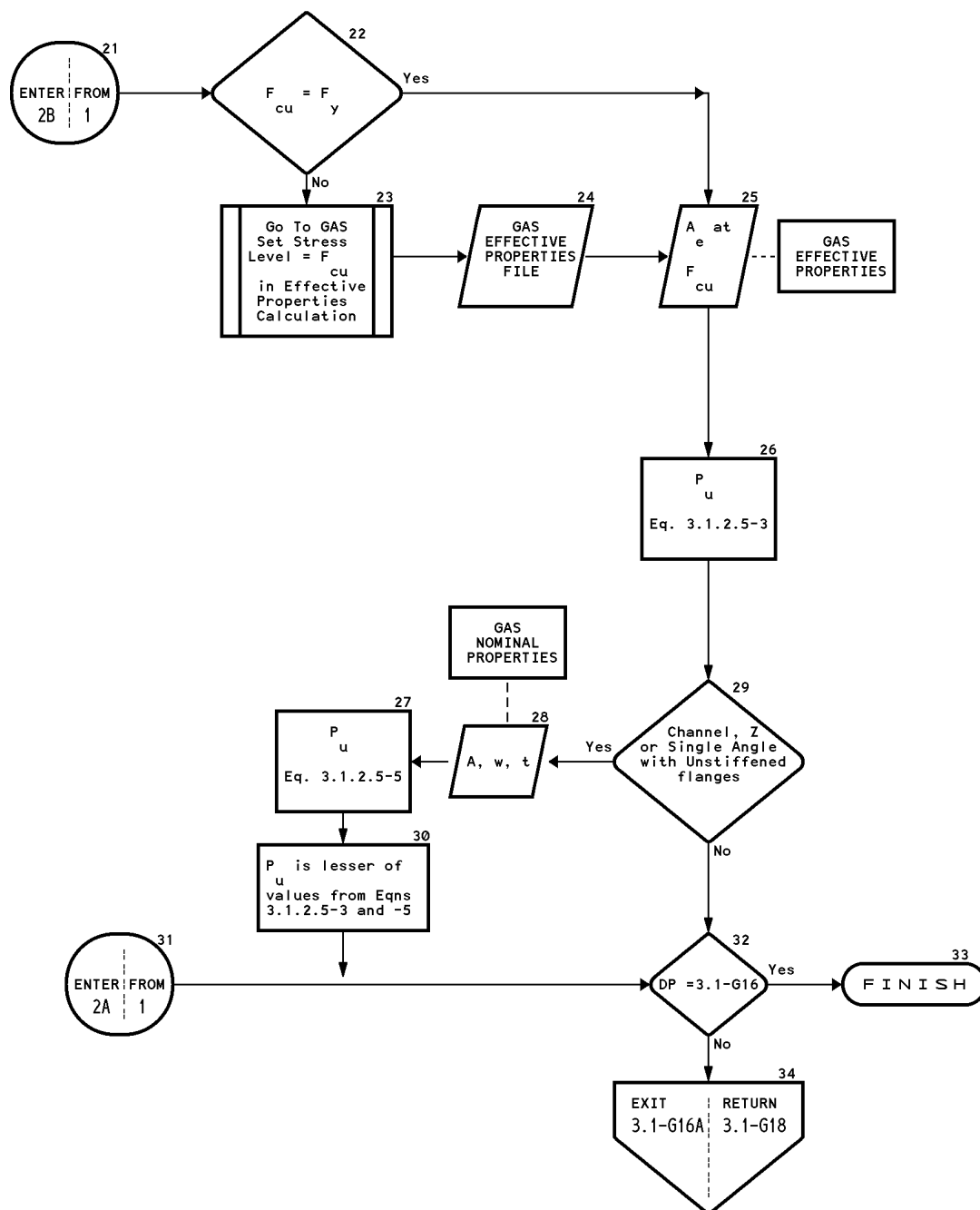
Reference: Section 3.1.2.5



DESIGN PROCEDURE 3.1-G16 (2 of 2)

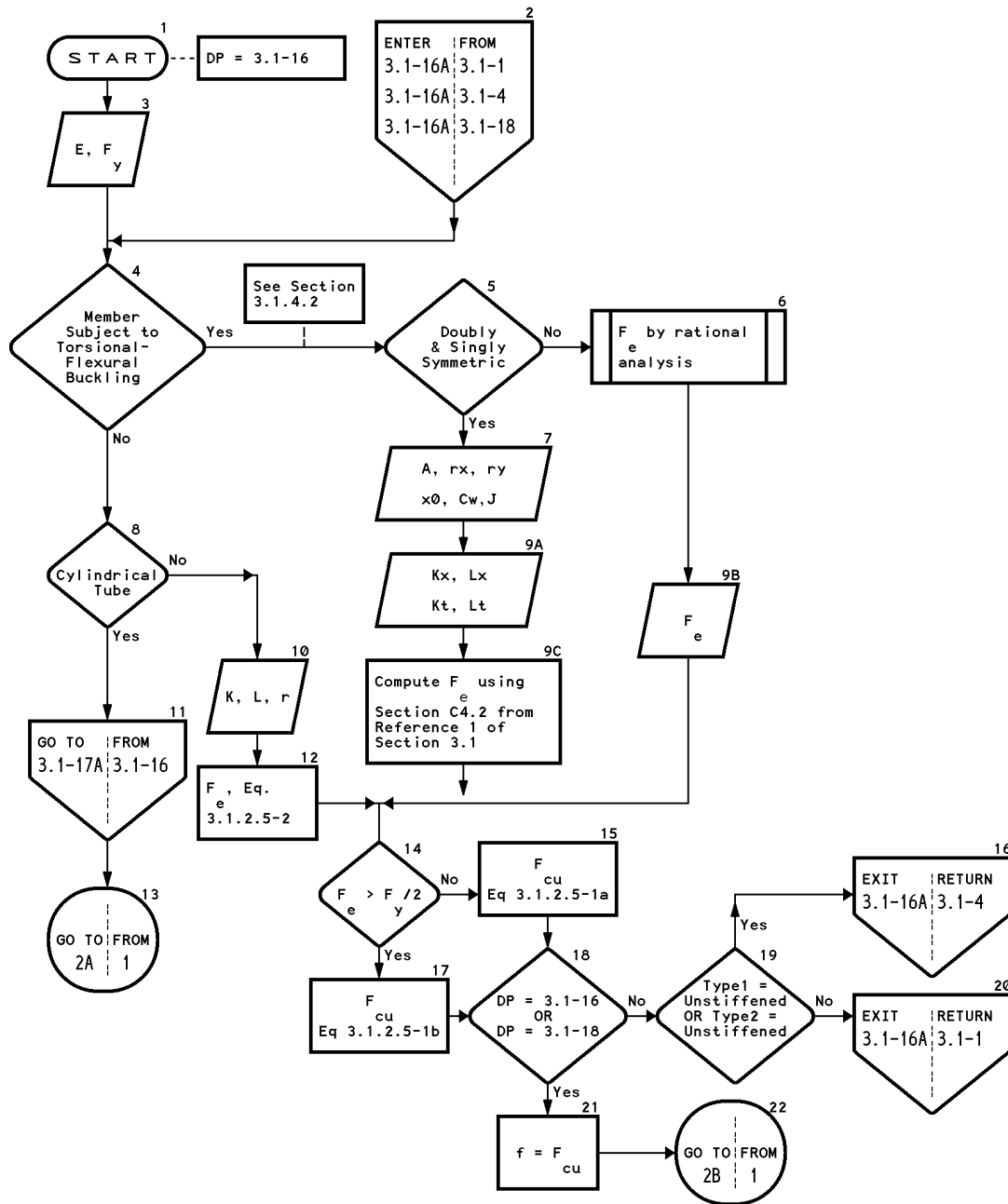
AXIAL CAPACITY, P_u , OF CONCENTRICALLY LOADED COMPRESSION MEMBERS (USING SECTION PROPERTIES)

Reference: Section 3.1.2.5



DESIGN PROCEDURE 3.1-16 (1 of 2)

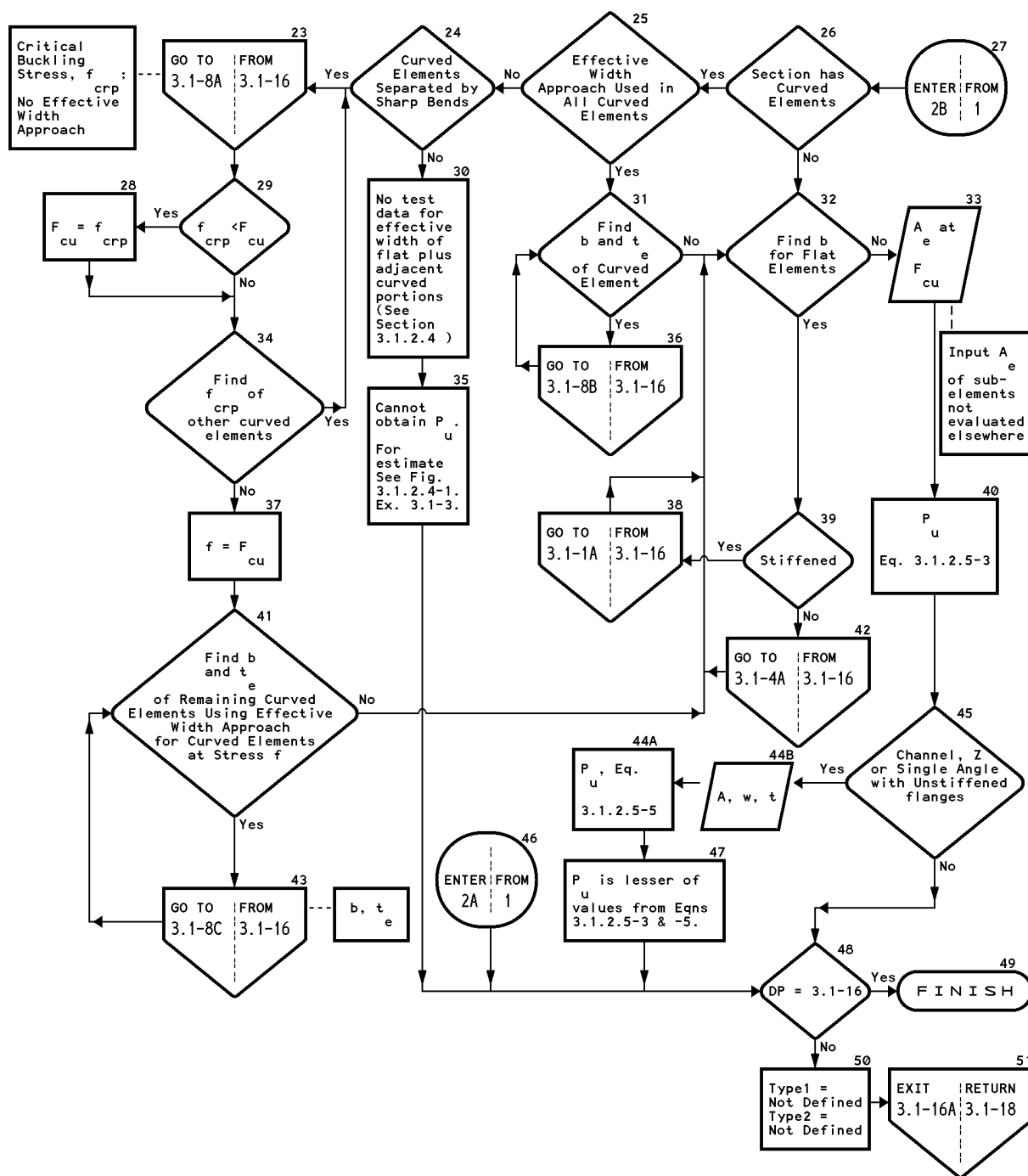
AXIAL CAPACITY, P_u , OF CONCENTRICALLY LOADED COMPRESSION MEMBERS
Reference: Section 3.1.2.5



DESIGN PROCEDURE 3.1-16 (2 of 2)

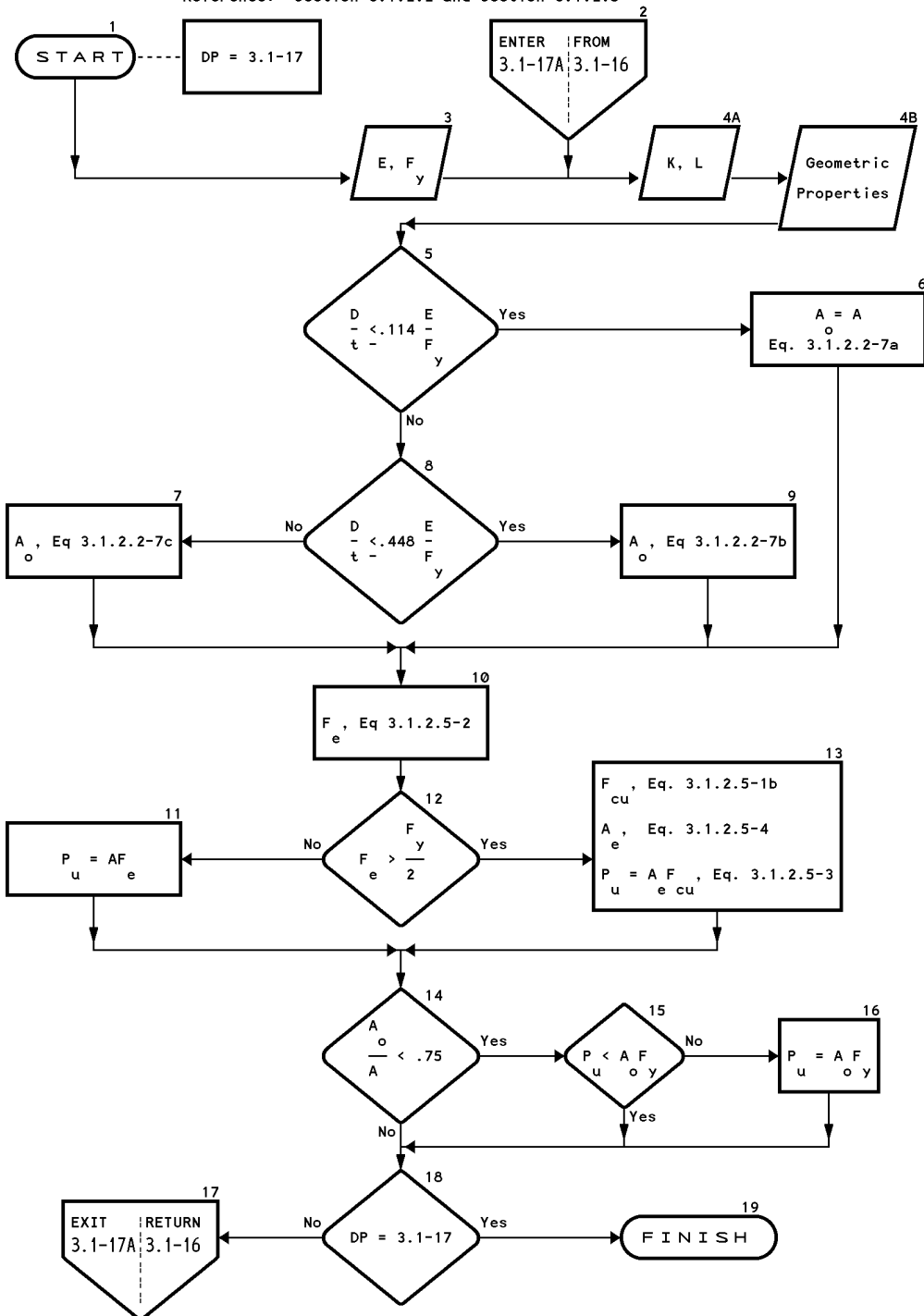
AXIAL CAPACITY, P , OF CONCENTRICALLY LOADED COMPRESSION MEMBERS

Reference: Section 3.1.2.5



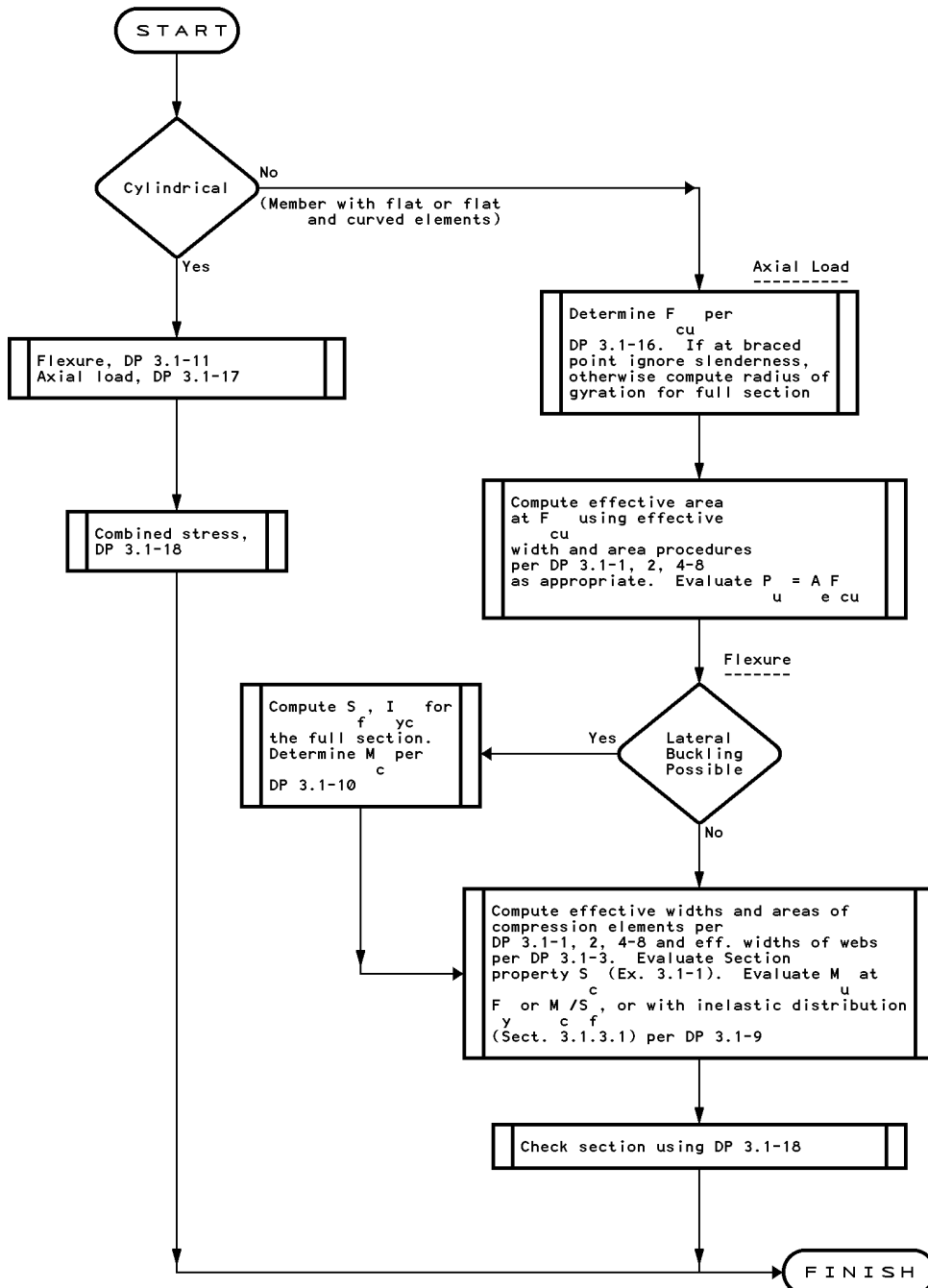
DESIGN PROCEDURE 3.1-17

AXIAL CAPACITY, P_u , OF CYLINDRICAL MEMBERS
Reference: Section 3.1.2.2 and Section 3.1.2.5



DESIGN PROCEDURE 3.1-18A

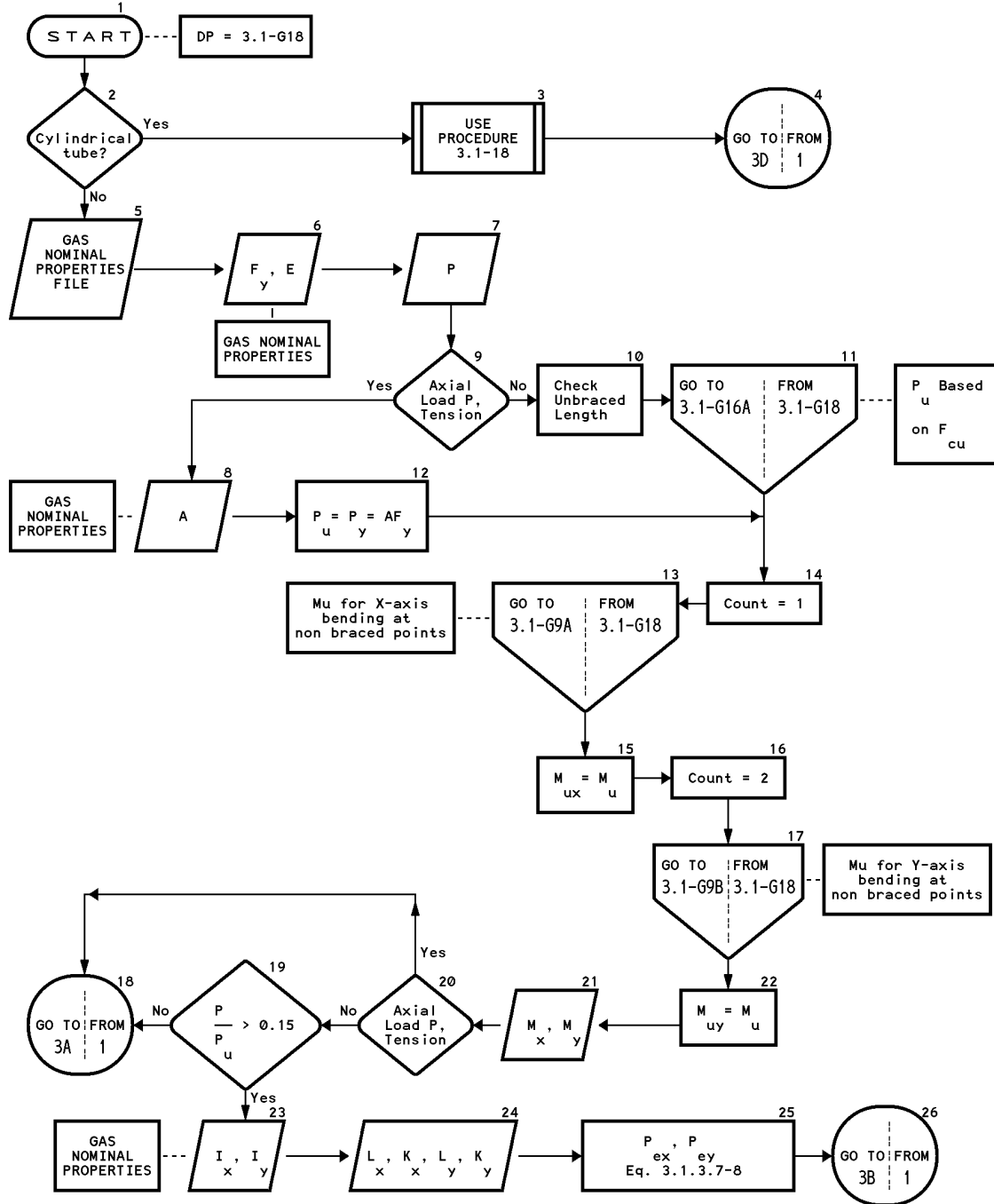
Overview: Combined Axial Load and Bending of Member



DESIGN PROCEDURE 3.1-G18 (1 of 3)

COMBINED AXIAL LOAD AND BENDING OF MEMBER (USING SECTION PROPERTIES)

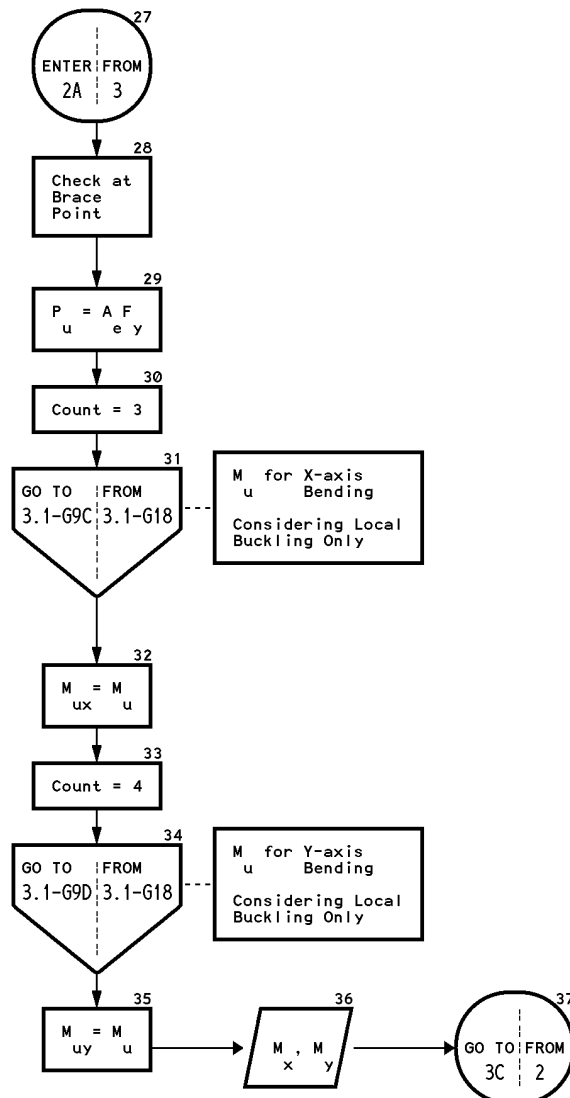
Reference: Section 3.1.3.7



DESIGN PROCEDURE 3.1-G18 (2 of 3)

COMBINED AXIAL LOAD AND BENDING OF MEMBER (USING SECTION PROPERTIES)

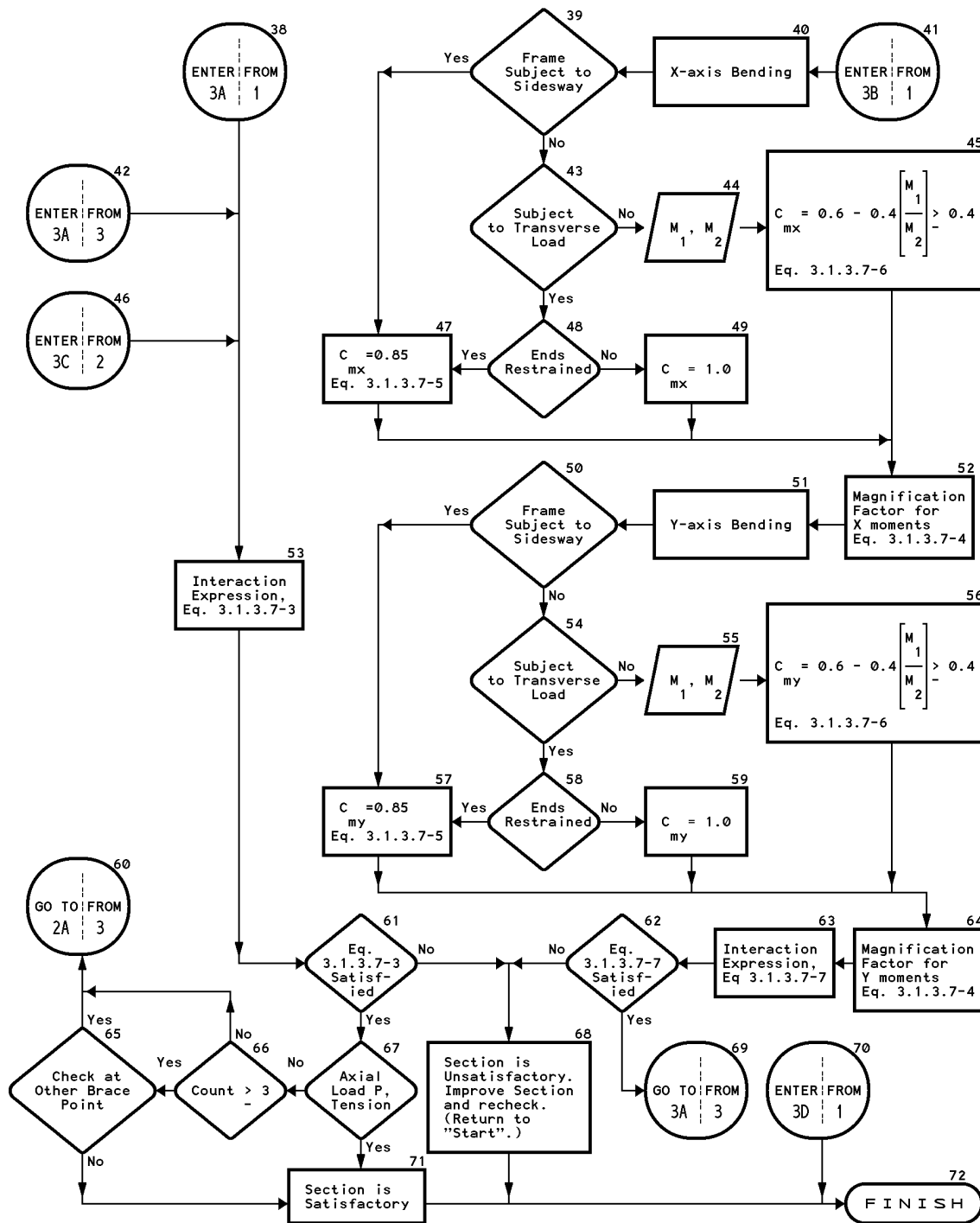
Reference: Section 3.1.3.7



DESIGN PROCEDURE 3.1-G18 (3 of 3)

COMBINED AXIAL LOAD AND BENDING OF MEMBER (USING SECTION PROPERTIES)

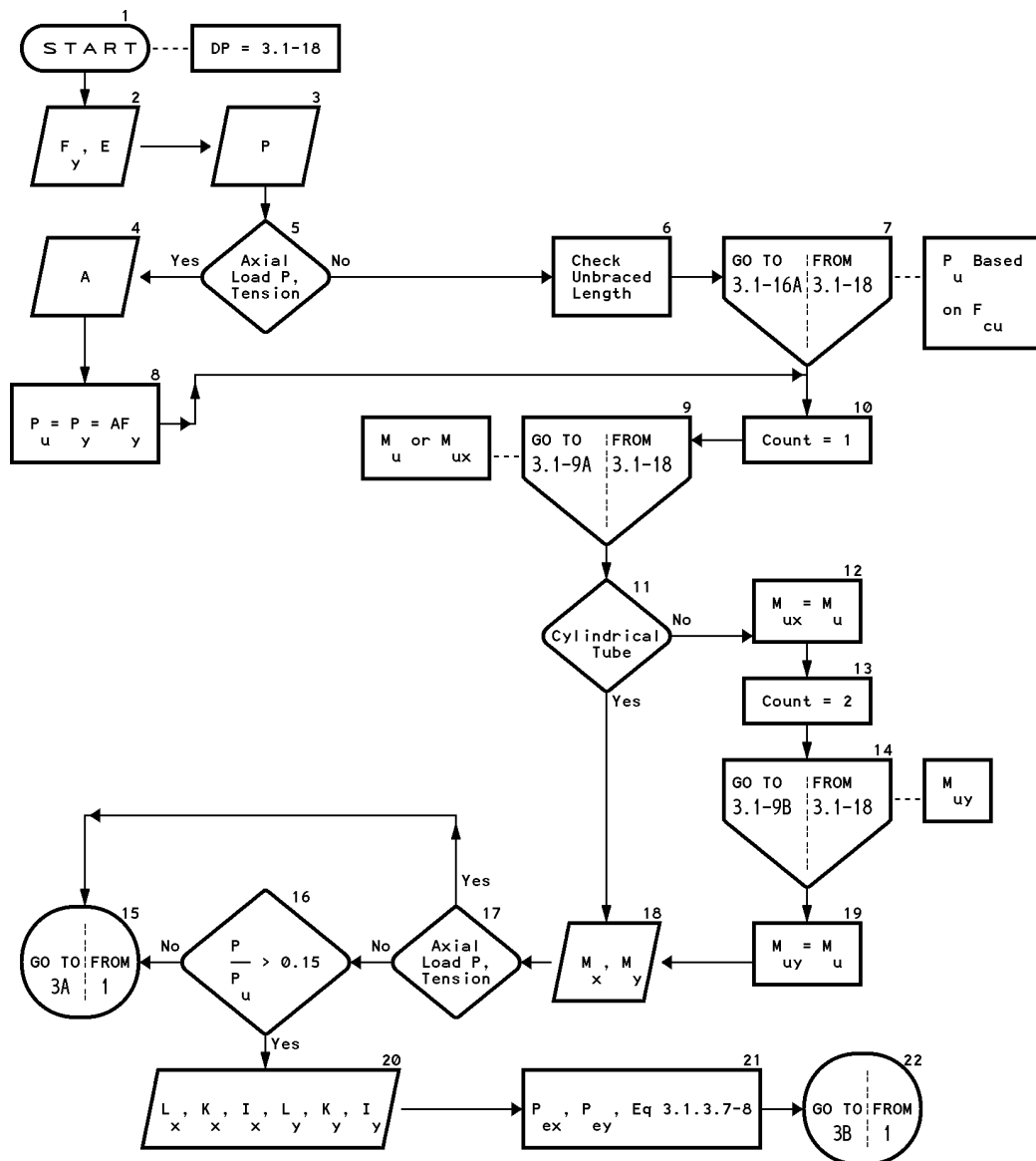
Reference: Section 3.1.3.7



DESIGN PROCEDURE 3.1-18 (1 of 3)

COMBINED AXIAL LOAD AND BENDING OF MEMBER

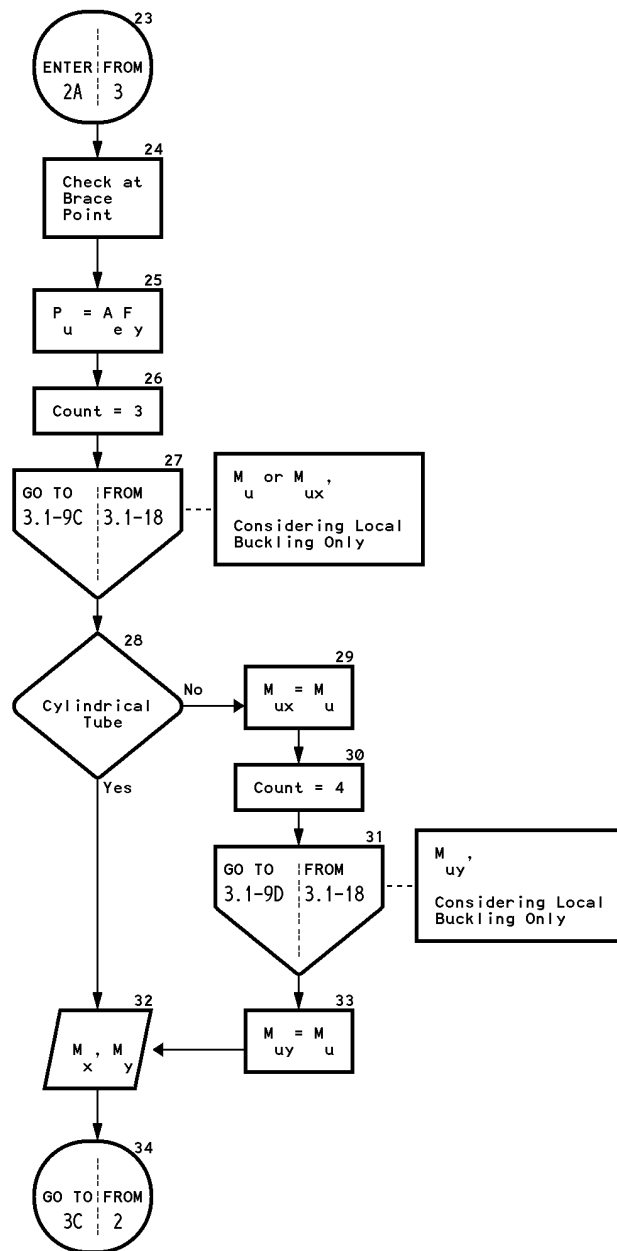
Reference: Section 3.1.3.7



DESIGN PROCEDURE 3.1-18 (2 of 3)

COMBINED AXIAL LOAD AND BENDING OF MEMBER

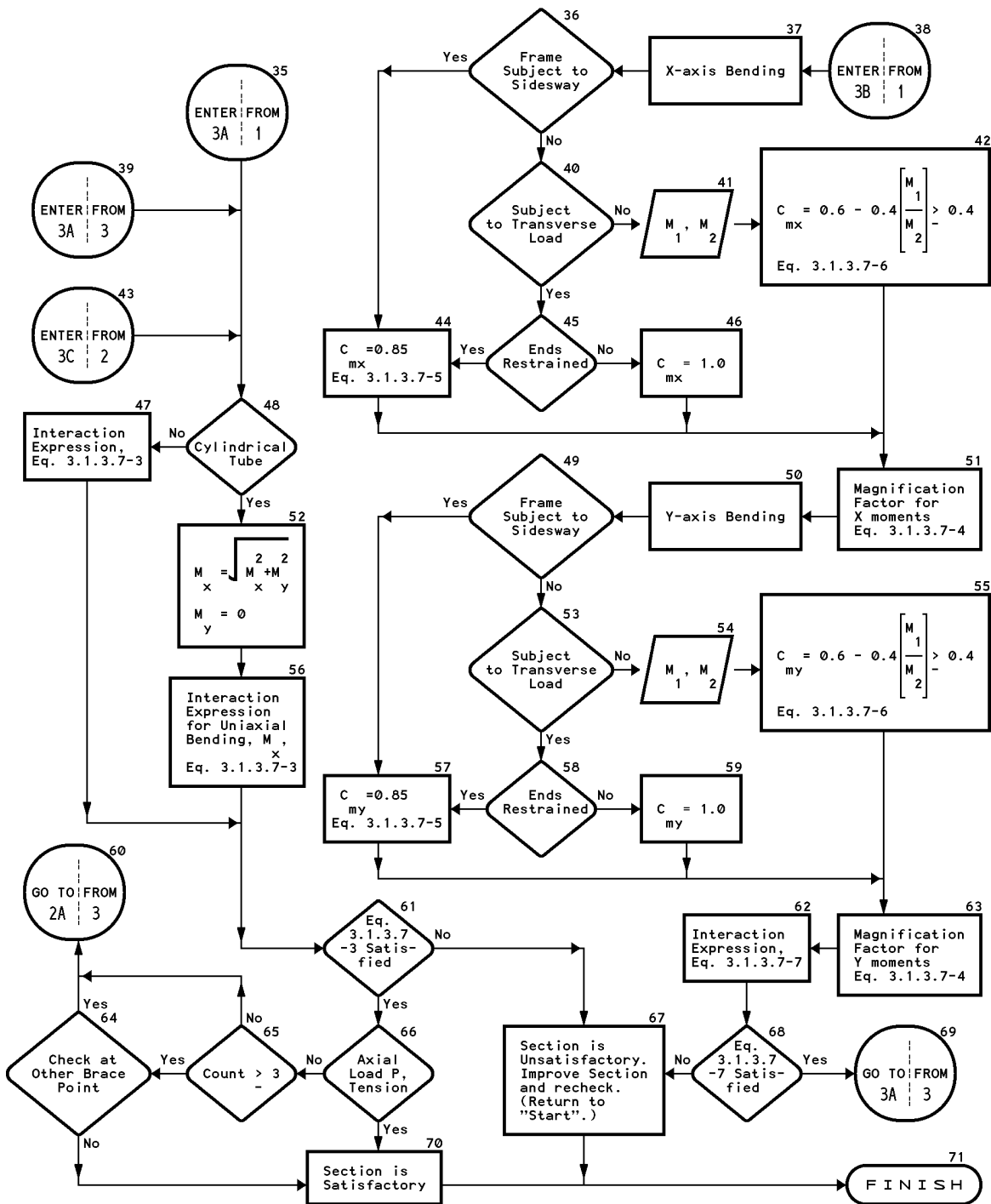
Reference: Section 3.1.3.7



DESIGN PROCEDURE 3.1-18 (3 of 3)

COMBINED AXIAL LOAD AND BENDING OF MEMBER

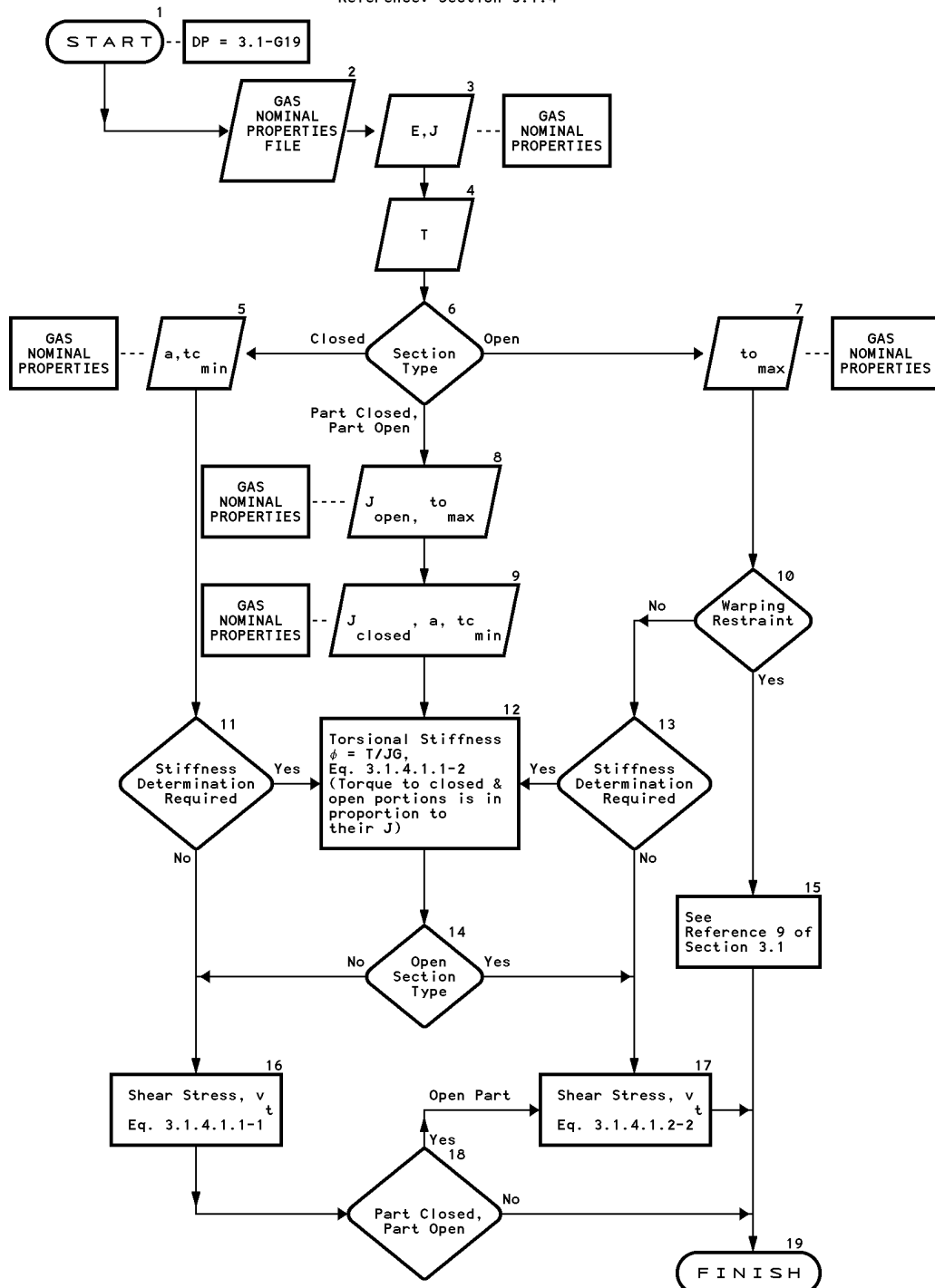
Reference: Section 3.1.3.7



DESIGN PROCEDURE 3.1-G19

TORSION OF MEMBERS (USING SECTION PROPERTIES)

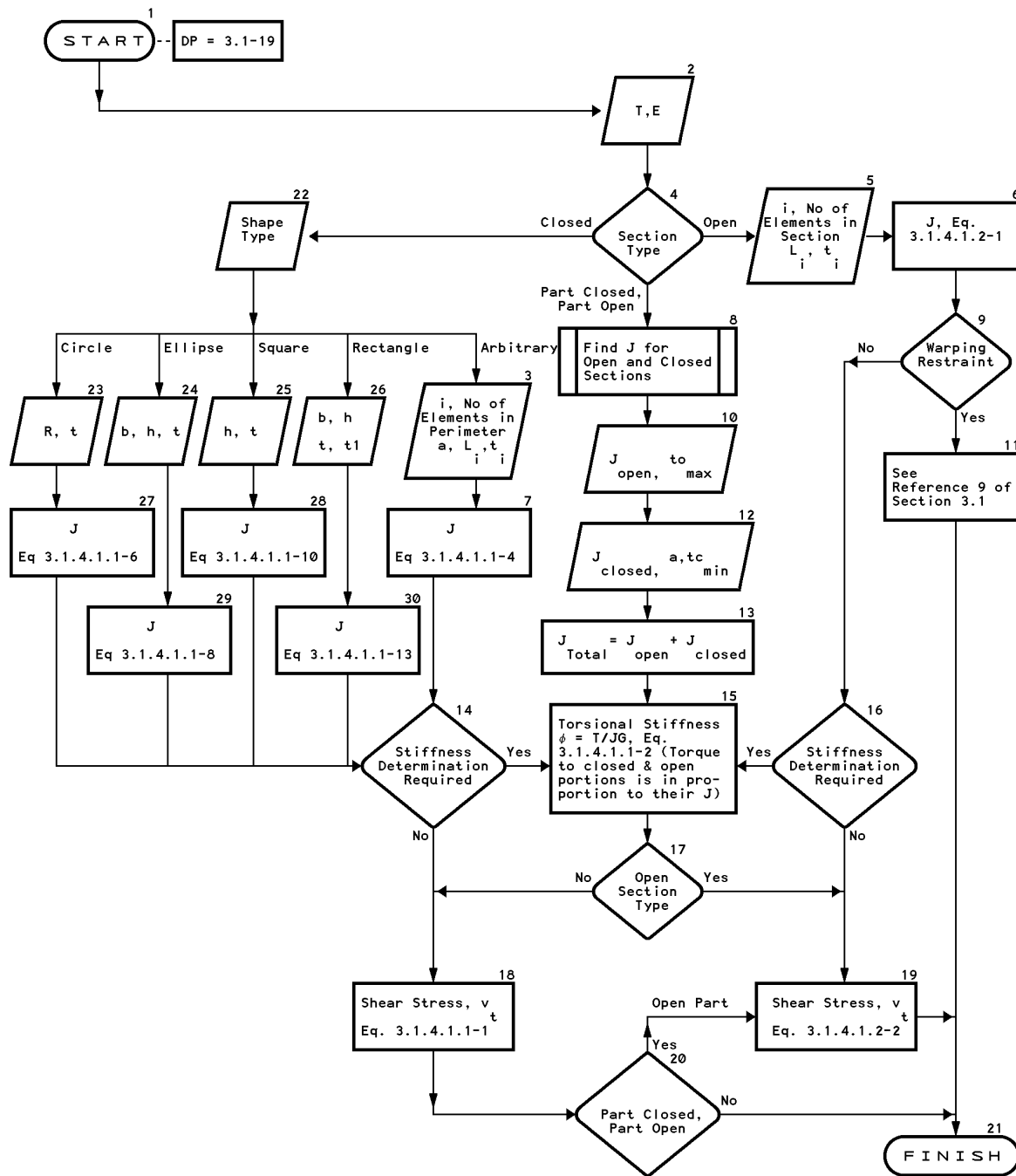
Reference: Section 3.1.4



DESIGN PROCEDURE 3.1-19

TORSION OF MEMBERS

Reference: Section 3.1.4



5.3 DESIGN PROCEDURES FOR SECTION 3.2

[Table 5.3-1](#) lists the Design Procedures for [Section 3.2 Curved Members](#).

Table 5.3-1 Design Procedures for Section 3.2

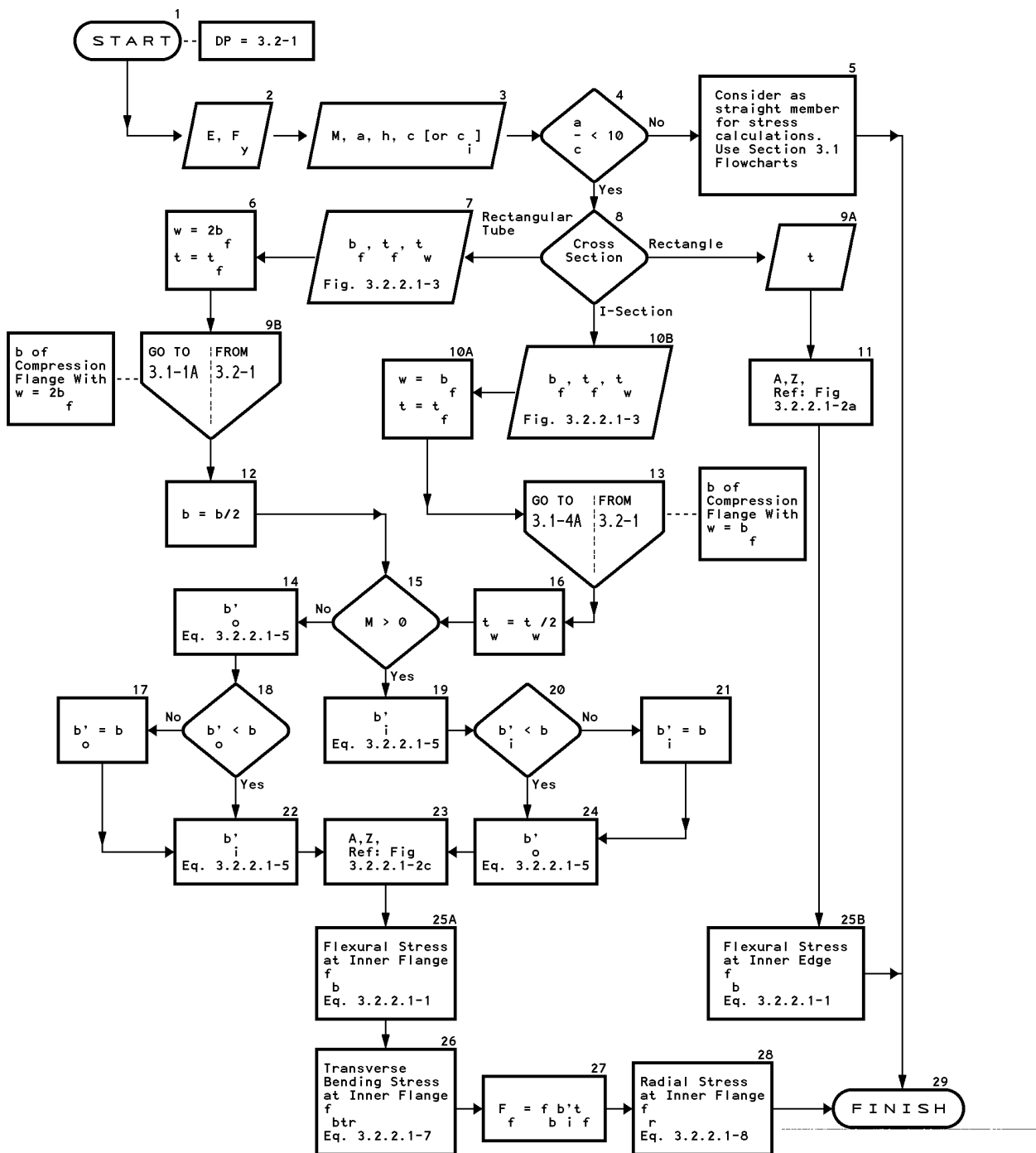
Design Procedure	Reference Section	Title
3.2-1	3.2.2.1	Curved Members - Webs in Plane of Curvature
3.2-2	3.2.2.2	Curved Circular Tubular Members



DESIGN PROCEDURE 3.2-1

CURVED MEMBERS - WEBS IN PLANE OF CURVATURE

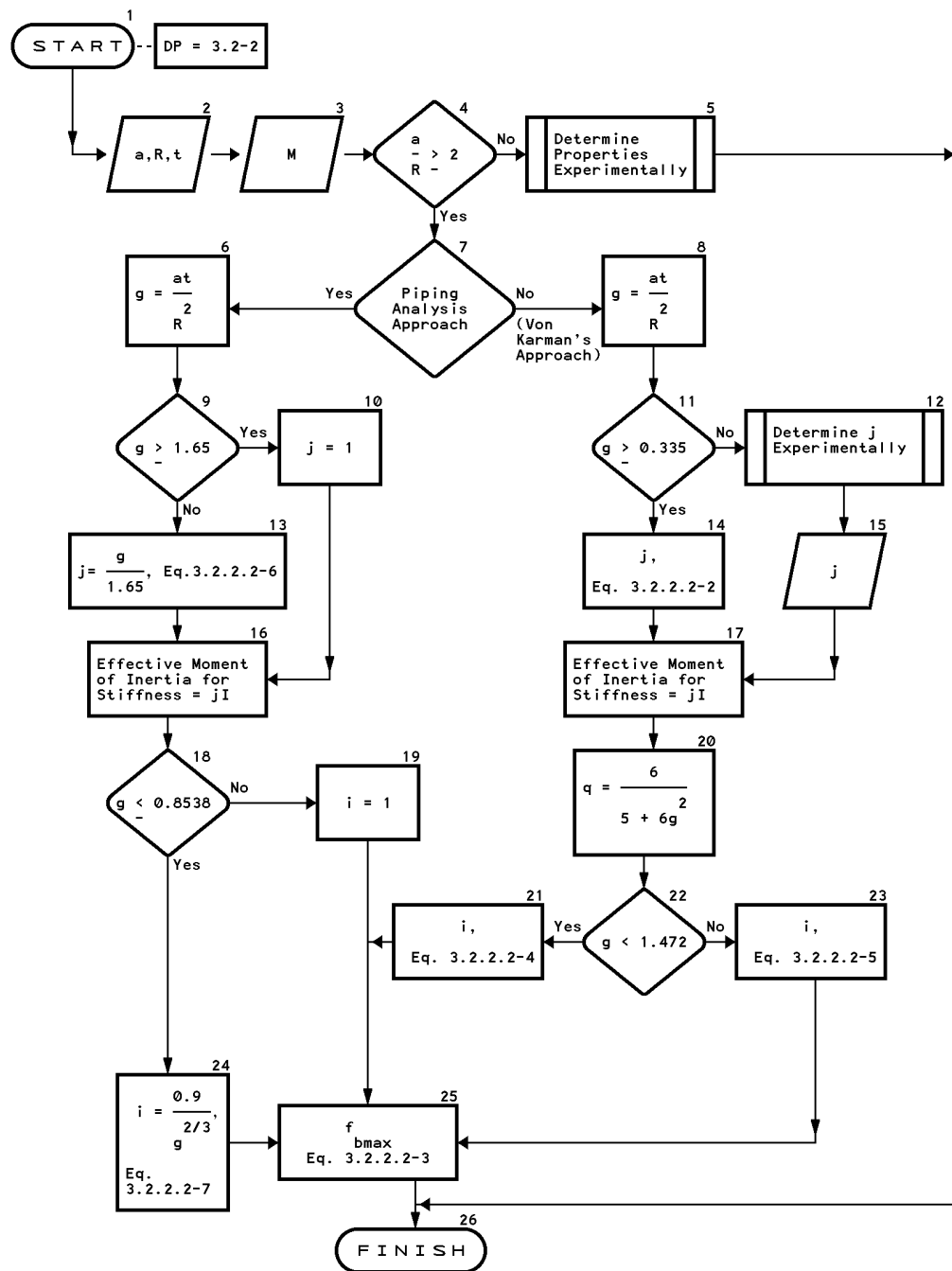
Reference: Section 3.2.2.1



DESIGN PROCEDURE 3.2-2

CURVED CIRCULAR TUBULAR MEMBERS

Reference: Section 3.2.2.2



5.4 DESIGN PROCEDURES FOR SECTION 3.3

[Table 5.4-1](#) lists the Design Procedures for [Section 3.3 Surface Elements](#).

Table 5.4-1 Design Procedures for Section 3.3

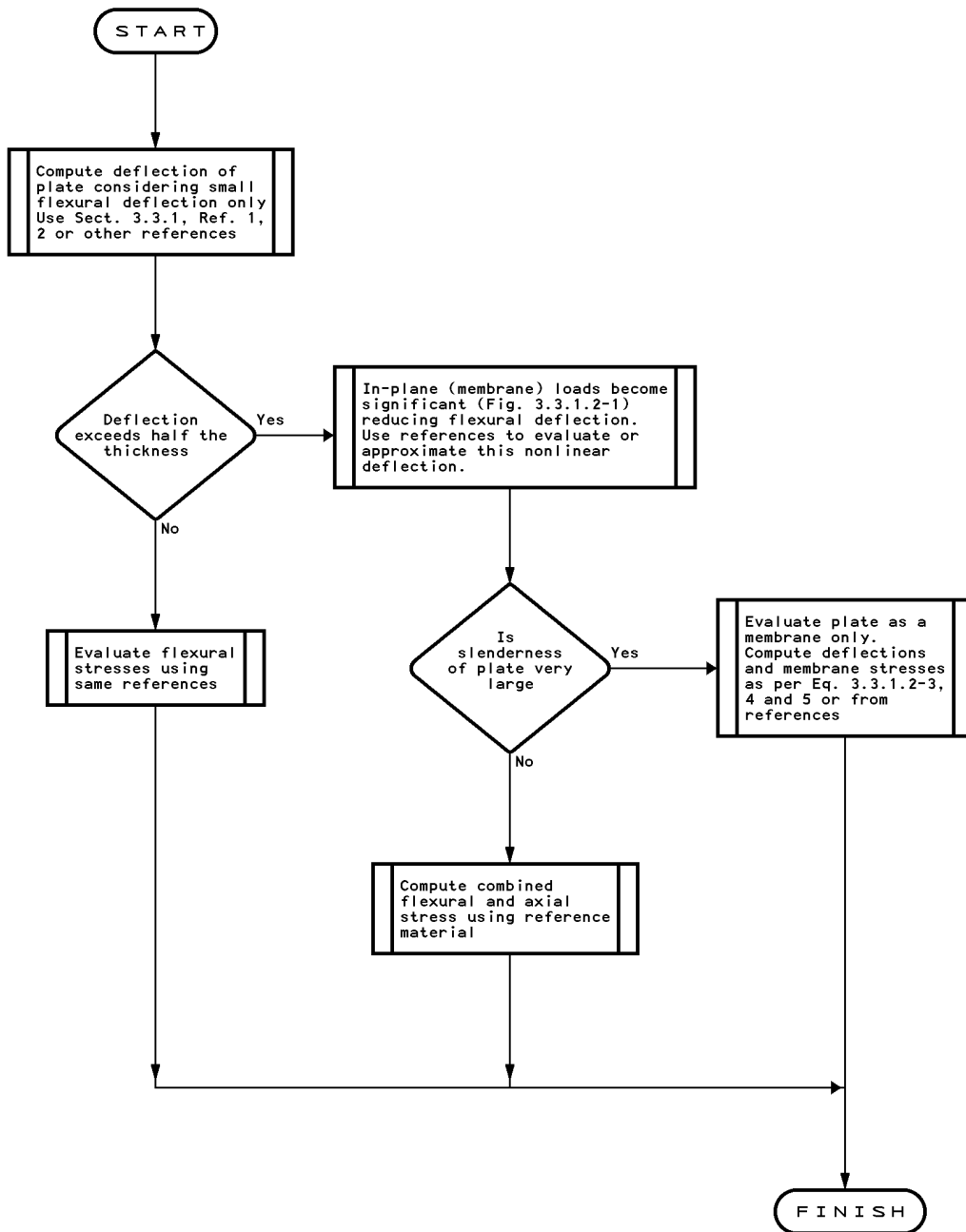
Design Procedures	Reference Section	Title
3.3-1	3.3.1	Overview: Integrity of Flat Plates
3.3-2	3.3.1	Deflection of Flat Plates
3.3-3	3.3.2, 3.3.3	Lateral Integrity of Curved Plates with Uniform Compression
3.3-4	3.3.4	Dent Resistance



DESIGN PROCEDURE 3.3-1

Overview: Integrity of Flat Plates

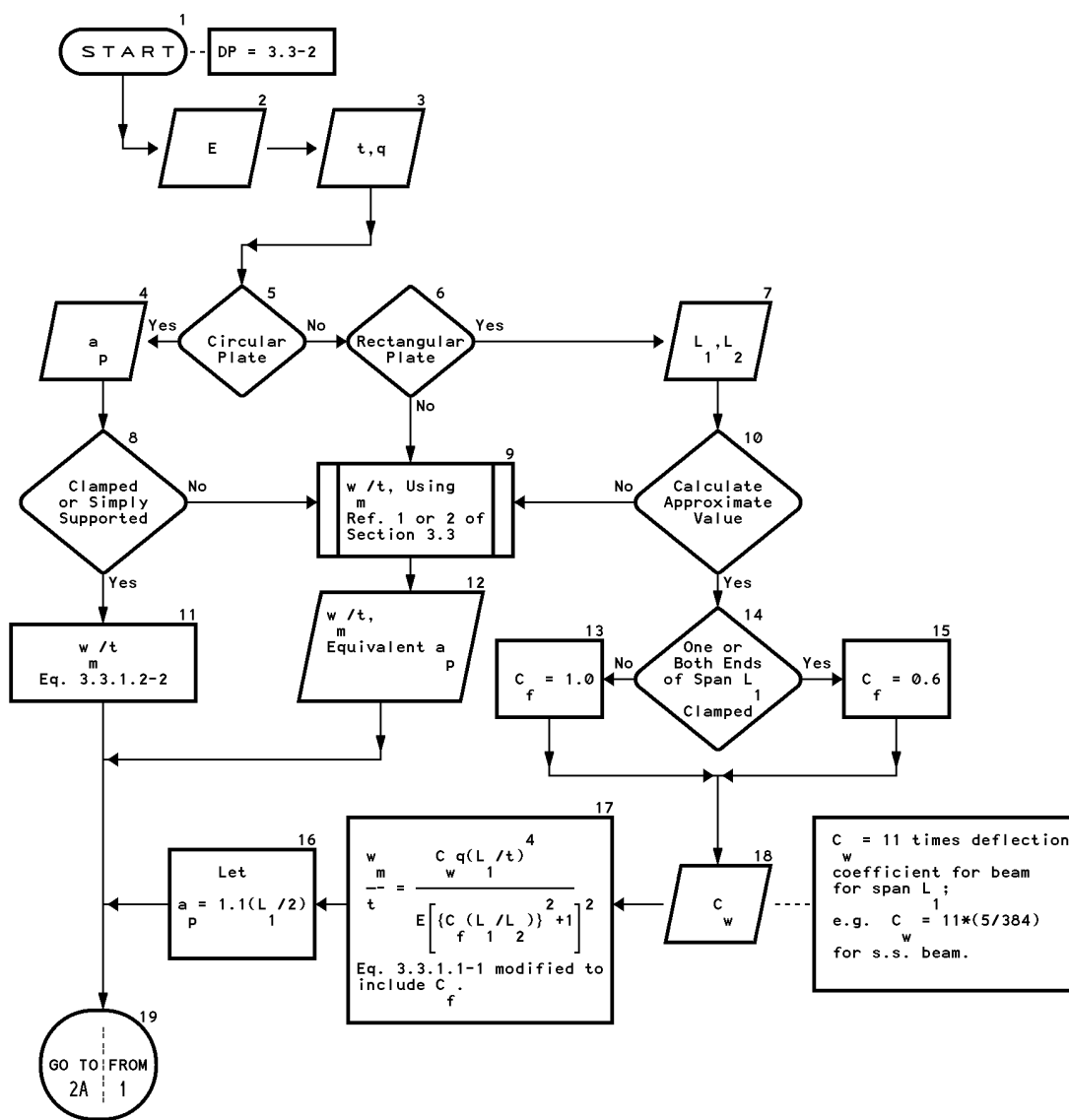
Reference: Section 3.3.1



DESIGN PROCEDURE 3.3-2 (1 of 2)

DEFLECTION OF FLAT PLATES

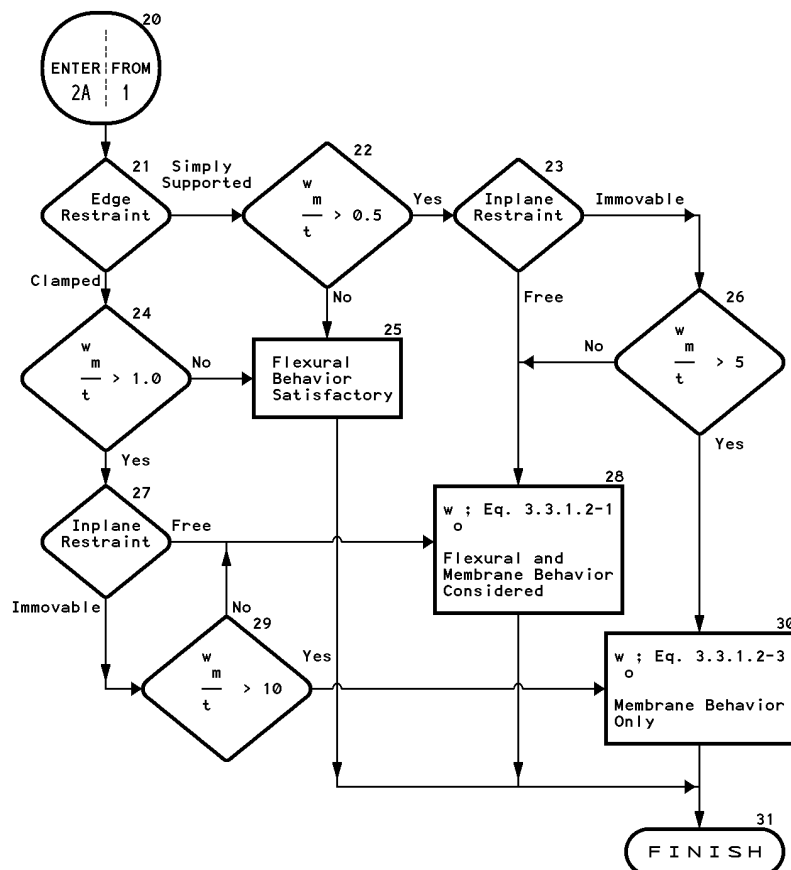
Reference: Section 3.3.1



DESIGN PROCEDURE 3.3-2 (2 of 2)

DEFLECTION OF FLAT PLATES

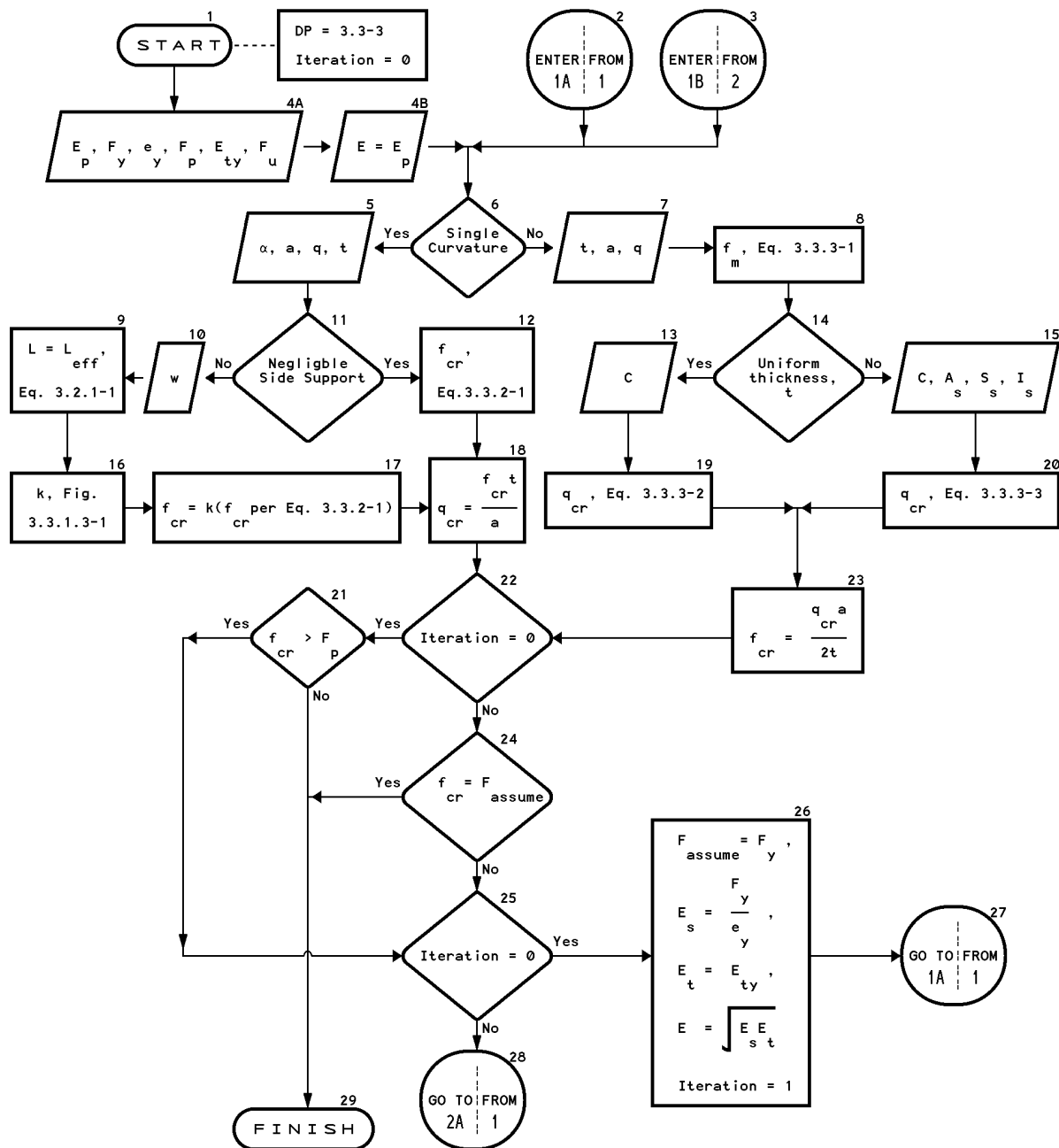
Reference: Section 3.3.1



DESIGN PROCEDURE 3.3-3 (1 of 2)

LATERAL INTEGRITY OF CURVED PLATES WITH UNIFORM COMPRESSION

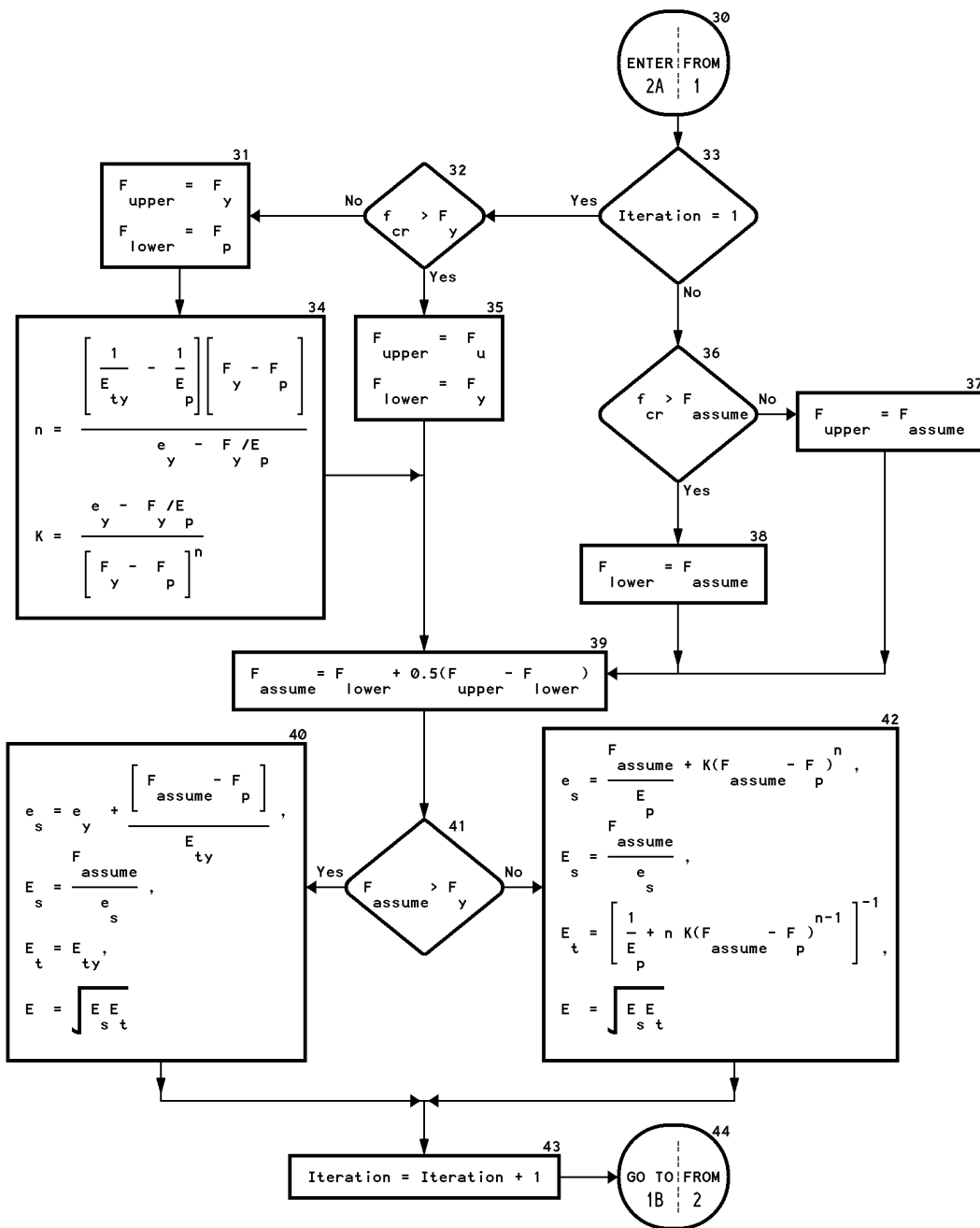
Reference: Section 3.3.2, 3.3.3



DESIGN PROCEDURE 3.3-3 (2 of 2)

LATERAL INTEGRITY OF CURVED PLATES WITH UNIFORM COMPRESSION

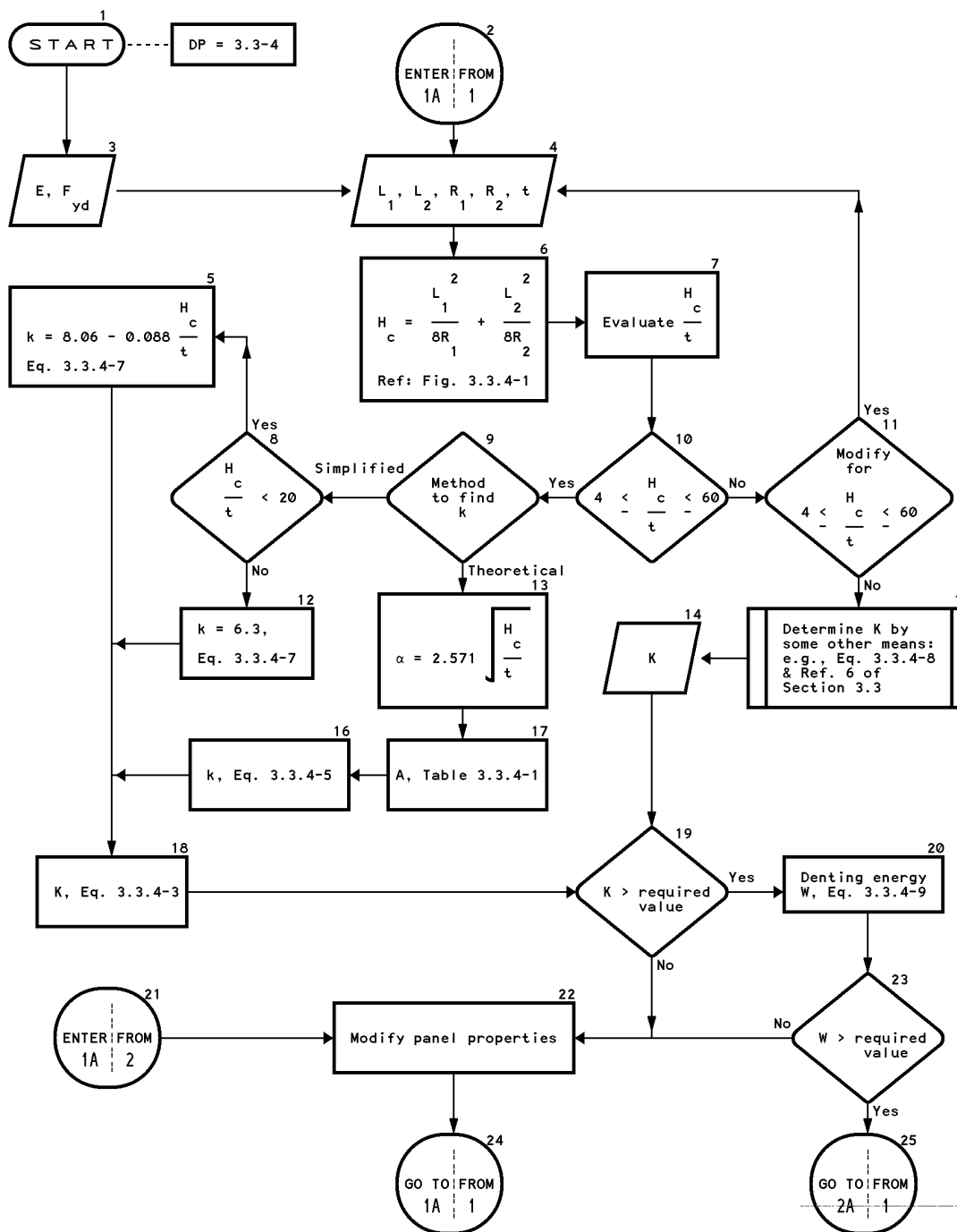
Reference: Section 3.3.2, 3.3.3



DESIGN PROCEDURE 3.3-4 (1 of 2)

DENT RESISTANCE

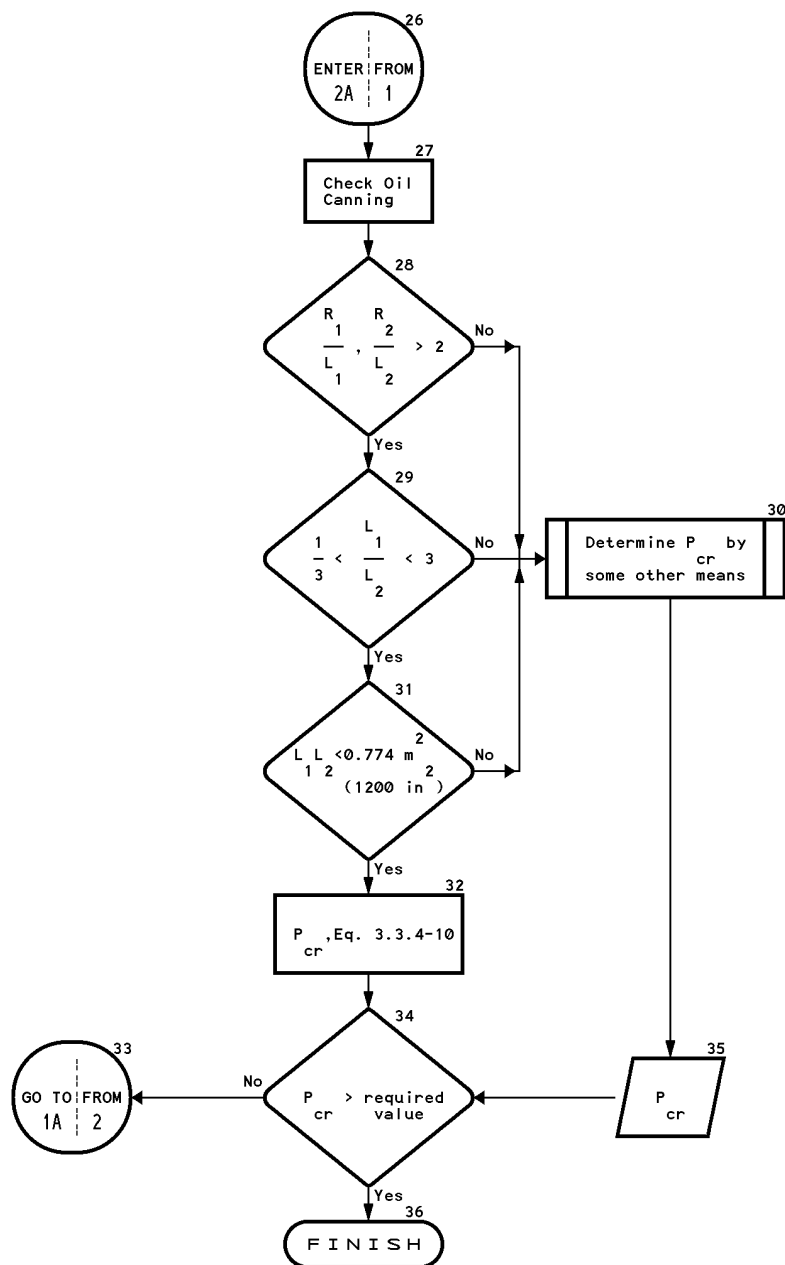
Reference: Section 3.3.4



DESIGN PROCEDURE 3.3-4 (2 of 2)

DENT RESISTANCE

Reference: Section 3.3.4



5.5 DESIGN PROCEDURES FOR SECTION 3.4

[Table 5.5-1](#) lists the Design Procedures for [Section 3.4 Connections](#).

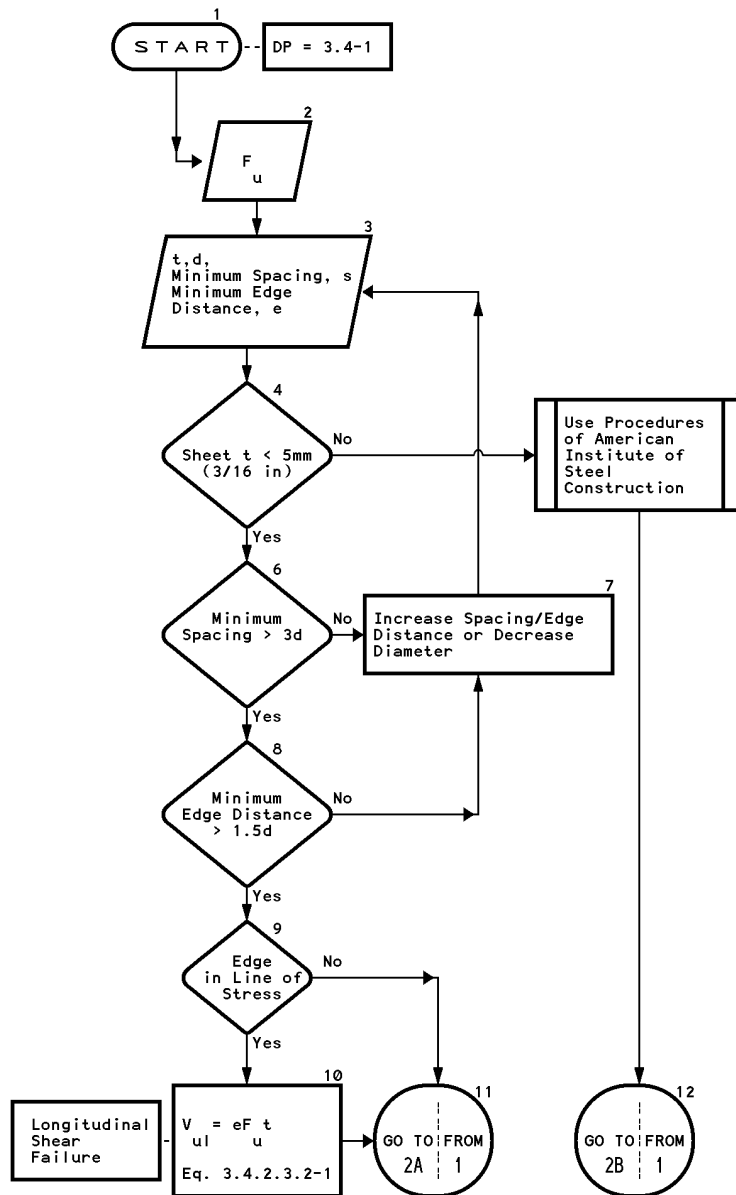
Table 5.5-1 Design Procedures for Section 3.4

Design Procedure	Reference Section	Title	
3.4-1	3.4.2.3	Fastener Shear Integrity Considering Sheet Capacity	
3.4-2	3.4.4	Spacing Requirements of Mechanical Connections	

DESIGN PROCEDURE 3.4-1 (1 of 2)

FASTENER SHEAR INTEGRITY CONSIDERING SHEET CAPACITY

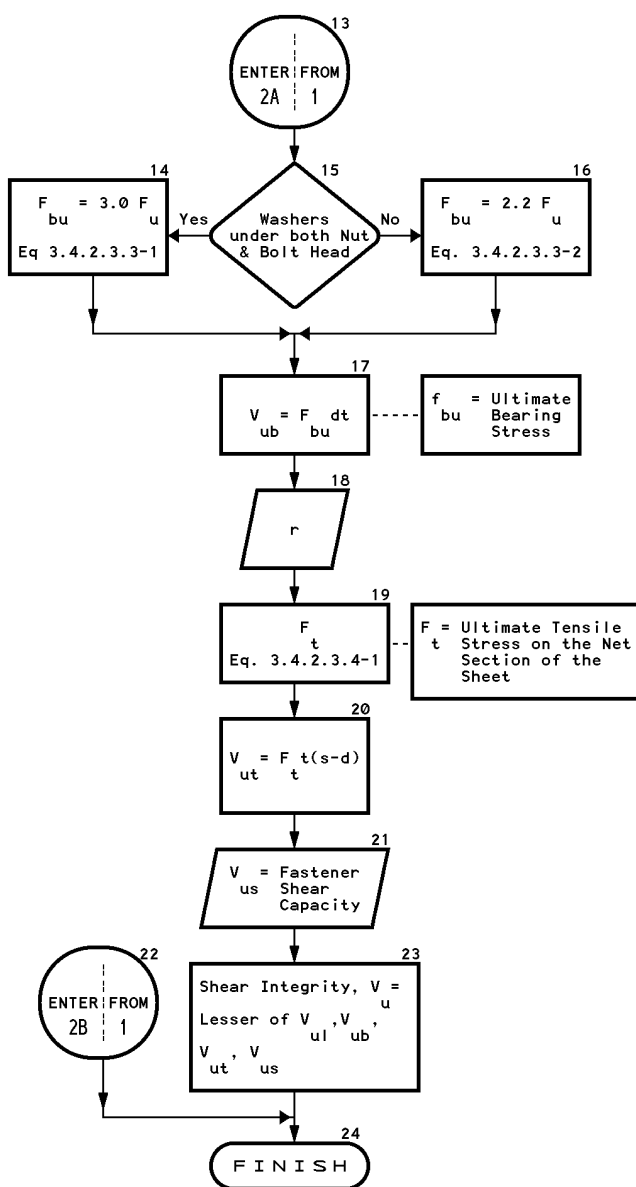
Reference: Section 3.4.2.3



DESIGN PROCEDURE 3.4-1 (2 of 2)

FASTENER SHEAR INTEGRITY CONSIDERING SHEET CAPACITY

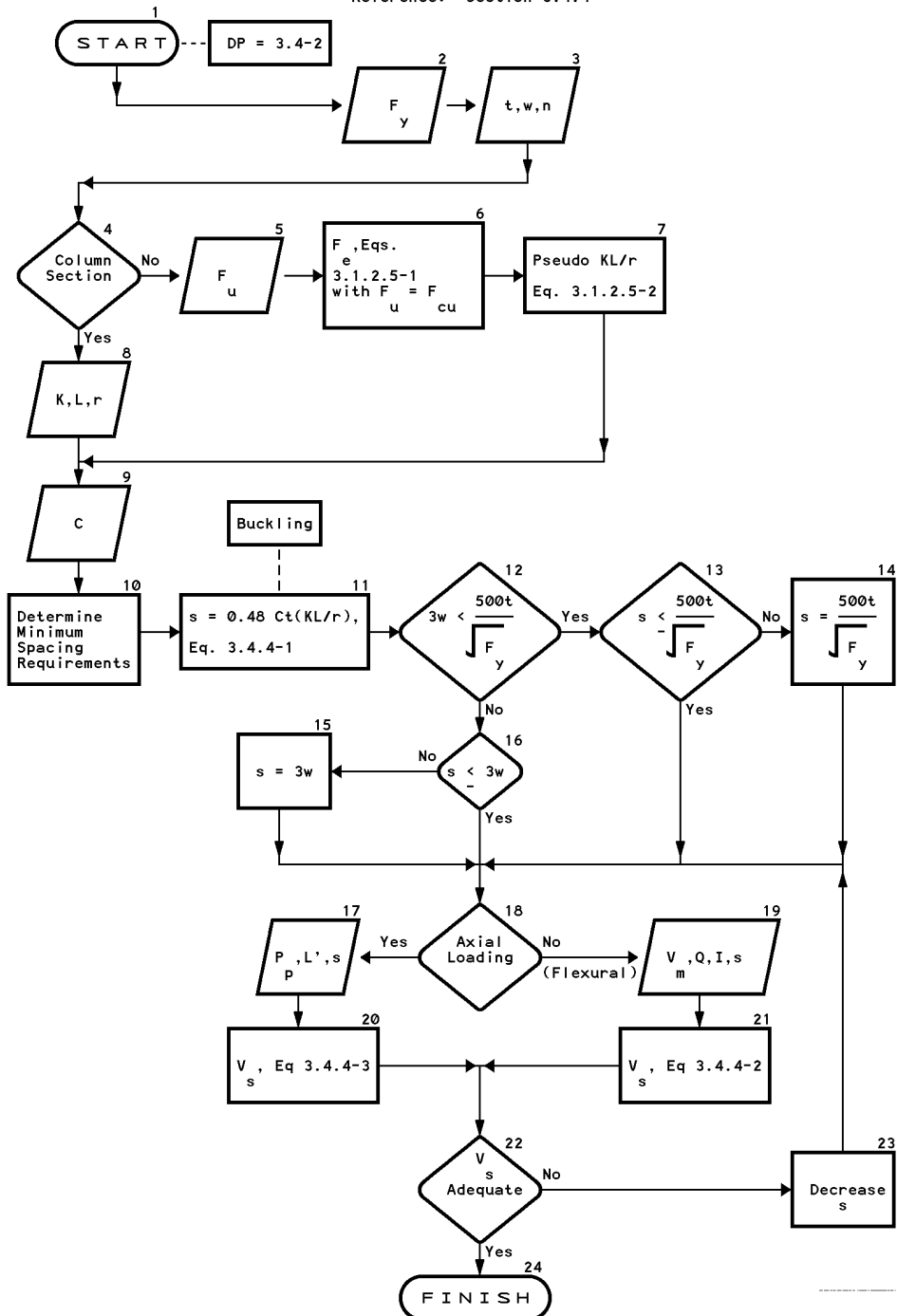
Reference: Section 3.4.2.3



DESIGN PROCEDURE 3.4-2

SPACING REQUIREMENTS OF MECHANICAL CONNECTIONS

Reference: Section 3.4.4



6.1 CASE STUDIES

This section provides case studies that illustrate the application of the principles in [Sections 2, 3](#) and [4](#) to vehicle components. Note that some of the case studies utilize results from CARS 2000. The associated GAS cross section files and KEY Design Procedure files are included with the CARS program for CARS users to review. Some case studies have a corresponding tutorial in [Section 7.2](#). [Table 6.1-1](#) lists the case studies and CARS 2000 program(s), if applicable.

Table 6.1-1 Case Studies

Section	Case Study	CARS Program	Tutorial
6.1.1	Uniside construction		
6.1.2	Front shock tower construction		
6.1.3	Hood inner panel		
6.1.4	Door anti-flutter bar using engineered scrap		
6.1.5	Modular seat support		
6.1.6	Design of an anti-intrusion door beam	GAS	
6.1.7	Design of a front rail	GAS, KEY, MAP	Section 7.2.1

6.1.1 UNISIDE CONSTRUCTION

6.1.1.1 Introduction

The designer frequently finds opportunity to reduce the number of pieces that make up major body assemblies. In many cases, he can assess the alternatives and combine two or three small details, if warranted, with only minor design changes to accommodate tooling. For major assemblies the decision can become quite complex, requiring detailed studies for upper management deliberation.

A typical approach is to establish the design with the greatest number of pieces as a baseline and a set of alternatives. Advantages and disadvantages of each are identified, and dollar values assigned.

The following case study was extracted from an actual design program. It illustrates the approach used to assess the many factors involved in the one-piece versus multi-piece options of a major assembly, the body side. The dollar values generated are unique to the internal circumstances; they have no quantitative significance outside of the environment in which the study was made. They are included in this study to reflect the relative values that were assigned to the various factors involved in the decision.

6.1.1.2 Definition

This case study assesses three design alternatives for the body side assembly: uniside, two-piece and multi-piece. Uniside is a one-piece body side panel that includes the outer A pillar, outer roof rail, rocker panel, outer B pillar, quarter lock pillar, and quarter panel. Two-piece construction incorporates the same components into two major panels, the door opening panel and quarter panels. For the multi-piece, the components listed above are separate details, welded together to form the body side assembly. The three types of construction are shown schematically in [Figure 6.1.1.2-1](#).

A survey of existing cars in the early 80's (see [Table 6.1.1.2-1](#)) shows that there is no clear-cut preference among manufacturers for any of the three alternatives.

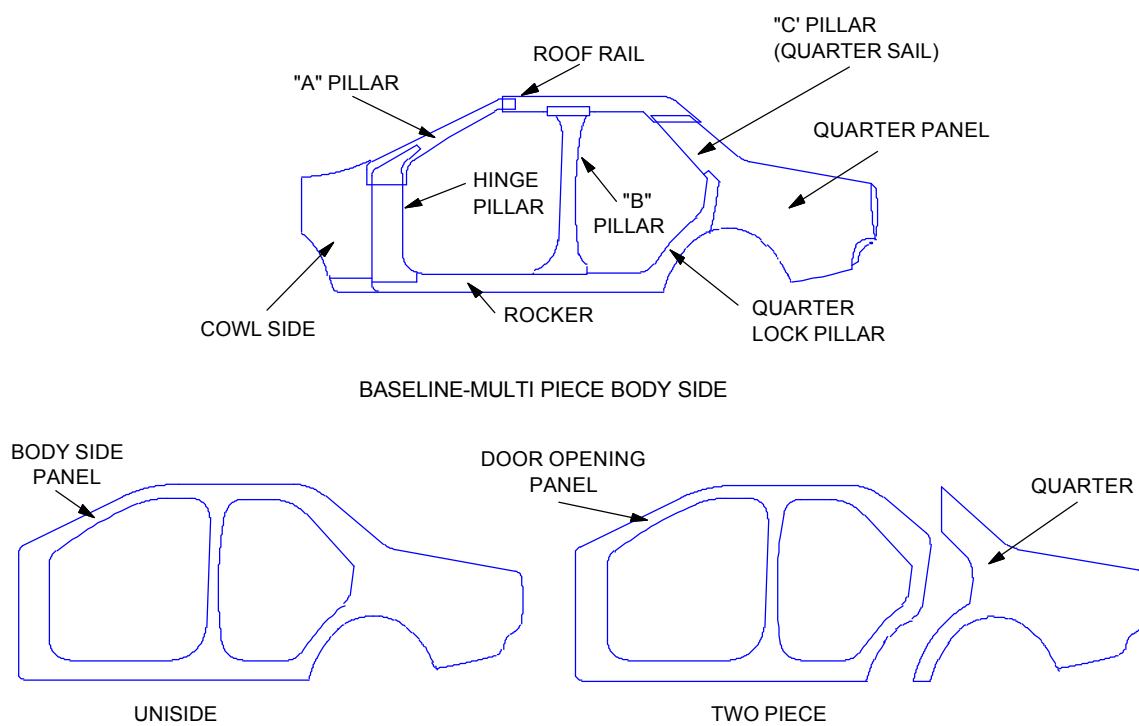


Figure 6.1.1.2-1 Body side construction

Table 6.1.1.2-1 Sample of construction type usage

Uniside	Two Piece	Multi Piece
Opel Kadette	Ford European Scorpio	Audi 100
Fiat UNO	Ford North American DN5 and FN9	Mercedes 190
Chrysler K cars	Toyota Tercel	Nissan Micra
G. M. 4 door J cars	VW Passat	Mitsubishi Galant
Fiat Strada	Opel Rekord	G. M. 2 door J Cars
VW Golf	Renault R5, R9, R11	Toyota (most models)
Honda (most models)		Ford North American (most models)
Ford European (except Scorpio)		Mazda (most models)
Mazda RX7 and BT17		

6.1.1.3 Analysis

Relevant Factors

Many factors must be considered to determine the appropriate type of construction for a particular vehicle. Replacing the several stampings that make up the body side assembly with one or two major panels (uniside or two-piece) will:

1. Require larger press capacity.
2. Increase shipping, handling, and storage costs, depending on the nearness of stamping facility to assembly facility.

3. Limit interchangeability between models.
4. Increase the cost of model-year face lifts.
5. Prohibit the selective use of material gauges, coatings, and strengths, or requires tailor welded blanks.
6. Produce more offal.
7. Limit the depth of draw, die tip angle, and door opening corner radii, reducing styling flexibility.
8. Adversely affect serviceability. Partial service repair panels must be cut from uniform side panels and stocked for collision damage repair.
9. Affect mass, noise, vibration, and harshness due to joint elimination.
10. Tend to reduce mass by eliminating weld joints with overlapping metal. The tendency may be offset by the reduced flexibility in metal gauge.
11. Improve door/body margin control requirements and surface flushness.
12. Improve door/body sealing and reduce wind noise.
13. Increase customer quality appeal due to the clean, no joint appearance.
14. Improve first-run capability at assembly plant.
15. Improve fatigue life expectancy

Concepts and Alternatives

Eighteen (18) design concepts, designated with the letters A through Q and defined in [Table 6.1.1.3-1](#), were weighed (there are two variations of H and L, and no I).

Table 6.1.1.3-1 Concepts A through Q defined

Construction Type	Sedan	Station Wagon		Remarks
		Common Doors	Unique Doors	
Multi Piece	A (Base)	G	K (Base)	
Uniside	B	N	Q	
Two Piece	C	H	L	Quarter assembled to body at assembly plant
Two Piece	D	H	L	Quarter assembled to body at stamping plant
Two piece body opening quarter lock pillar integral w/ quarter panel	E	J	M	
Multi piece upgraded quarter lock pillar integral w/ quarter	F	O	P	

The eighteen concepts can be combined into many alternatives; three that were selected for this study are defined in [Table 6.1.1.3-2](#).

Table 6.1.1.3-2 Definition of alternatives

Number	Construction	Sedan	Wagon	Assembly Plant Receives
1.	Multi piece	A	G	Multi piece construction with common wagon and sedan rear door opening
2.	Uniside	B	N	Uniside construction with common wagon and sedan rear door opening
3.	Two piece	C	H	Two piece construction with common wagon and sedan rear door opening

The cost of facilities, aids, tools, and launch are summarized in [Table 6.1.1.3-3](#), the annual operating costs in [Table 6.1.1.3-4](#), and the estimated reliability, warranty, and owner loyalty variances in [Table 6.1.1.3-5](#).

Table 6.1.1.3-3 One time expenses (\$1,000,000)

	Multi Piece	Uniside	Two Piece
Facilities	6.9	5.8	6.0
Aids	1.4	0.8	1.2
Tools	23.8	19.9	20.4
Launch	<u>0.5</u>	<u>0.5</u>	<u>0.4</u>
Total	32.6	27.0	28.0

Table 6.1.1.3-4 Annual operating costs (\$1000)

	Multi Piece	Uniside	Two Piece
Direct Labor	13,600	11,600	12,300
Direct Material	230	150	190
Indirect Material	650	600	640
Plant Engineering	275	250	250
Quality Control	330	400	400
Material Handling	<u>590</u>	<u>1,000</u>	<u>760</u>
Sub Total	15,675	14,000	14,540
Warehouse Rental	25	150	65
Freight	24,700	38,600	26,100
Inv. Carrying Costs	<u>300</u>	<u>250</u>	<u>295</u>
Total	40,700	53,000	41,000

Table 6.1.1.3-5 Reliability, warranty, and owner loyalty variances

Alternatives	Cost Category	Reliability R/100 Better Than Base	Warranty Cost/Unit Better Than Base	Owner Loyalty Cost/Unit Better Than Base
Multi Piece		Base	Base	Base
Uniside	Structures	8.00	\$1.45	\$1.90
	Paint	0.50	\$0.15	\$0.20
	Trim	4.00	\$1.00	\$0.70
	Total	12.50	\$2.60	\$2.80
Two Piece	Structures	0.80	\$0.15	\$0.20
	Paint	0.30	\$0.10	\$0.15
	Trim	3.80	\$0.95	\$0.70
	Total	4.90	\$1.20	\$1.05

6.1.1.4 Conclusion

In this case, two-piece construction offers a clear choice over the multi-piece alternative. The one-time cost is \$4,600,000 less than multi-piece. This advantage is partially offset by the annual operating cost, which favors multi-piece by \$300,000. Warranty and owner loyalty costs favor two-piece over multi-piece by \$2.25 per vehicle. Two-piece showed improved reliability; rejects were lower by 4.90 per 100 vehicles.

Two-piece construction is also favored over uniside construction. Annual operating costs favor two-piece over uniside by \$12,000,000. This advantage is offset slightly during the first year of production by \$1,000,000 higher one-time costs. However, warranty and owner loyalty costs favor uniside by \$3.15 per vehicle. This per-vehicle advantage would require production volumes of 3.5 million the first year and 3.8 million in subsequent years in order to offset the annual operating costs. Uniside also showed better reliability; rejects were lower by 7.60 per 100 vehicles.

In the actual case, two-piece construction was chosen. It offered essentially the same design advantages as uniside, and it was more profitable to produce than either alternative.

6.1.2 FRONT SHOCK TOWER CONSTRUCTION

6.1.2.1 Introduction

This case study assesses two design alternatives for the front shock absorber tower: one-piece and two-piece. The front shock tower is primarily a structural member that attaches the top of the shock absorber and the upper spring seat. Its location in the vehicle imposes a number of design criteria, beyond the obvious structural requirements. The following case study was extracted from an actual design program. It illustrates the factors involved in the one-piece versus two-piece options, and the impact of the decision on adjacent members.

6.1.2.2 Advantages and Disadvantages

One-piece construction offers the following advantages over two-piece:

1. Reduced stamping and assembly cost, because there are fewer pieces to handle, and welding operations are eliminated.
2. Improved appearance, where under-hood dress-up is a priority.
3. Moisture-proof construction, because the welded joint (and consequently the need to seal it) is eliminated.
4. Higher fatigue life expectancy

The major disadvantage of one-piece construction is the tendency to increased mass, due to the placement of heavier metal gage in the side wall where it is not needed. In the two-piece construction, it was determined that the top of the tower, which directly receives the suspension loads, required 2.64 mm (0.104 in.) minimum metal thickness, while the lower stamping required only 0.84 mm (0.033 in.). The highly loaded top structure of the one-piece tower requires a minimum gage of 1.96 mm (0.077 in.).

6.1.2.3 Preliminary Test Results

A tower was made from 1.96 mm (0.077 in.) thick stock and tested at the proving ground. It failed to meet the requirements of rough roads, because the metal thinned out in the radial transition (top to side wall) area. The gage was increased to 2.59 mm (0.102 in.) to provide adequate strength after thinning; the tower then met the test requirements.

The two constructions are shown in [Figure 6.1.2.3-1](#). The one-piece construction eliminates eighteen (18) spot welds and four (4) 25 mm (1 in.) MIG braze welds per tower. The minimum metal thicknesses and the masses of each piece are also shown.

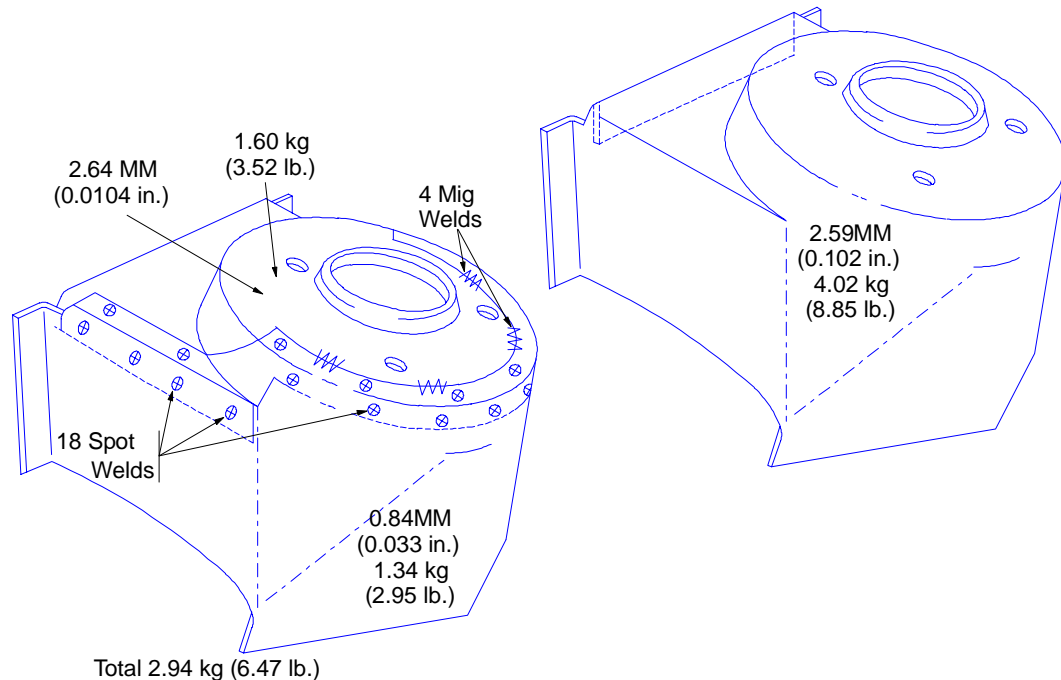


Figure 6.1.2.3-1 Front shock tower construction

6.1.2.4 Design Options

Material selection was governed by the required strength in the radial transition area, which thinned during forming operations. There are three options to achieve the necessary strength in this area:

1. Use 2.59 mm (0.102 in.) thick steel, and allow the metal in the radial transition area to thin.
2. Use 1.96 mm (0.077 in.) thick steel, and adjust manufacturing operations to minimize thinning in the critical area
3. Use a thinner material with offsetting higher strength.

The first option offered less development time and lower development cost, because it had already been proven. However, it imposed a mass penalty of 2.16 kg (4.76 lb) per vehicle ([Table 6.1.2.4-1](#)) exclusive of spin-off effects on other components.

Table 6.1.2.4-1 Comparison of component part mass

	One Piece		Two Piece
	Option 1	Option 2	
Top member			
Thickness, mm (in)	----	----	2.64 (0.104)
Mass, kg (lb)	----	----	1.60 (3.52)
Bottom Member			
Thickness, mm (in)	----	----	0.84 (0.033)
Mass, kg (lb)	----	----	1.34 (2.95)
Total			
Thickness, mm (in)	2.59 (0.102)	1.96 (0.077)	-----
Mass, kg (lb)	4.02 (8.85)	3.04 (6.70)	2.94 (6.47)
Mass increase, kg (lb)			
Per unit	1.08 (2.38)	0.10 (0.22)	-----
Per vehicle	2.16 (4.76)	0.20 (0.44)	-----

The second option can be explored by adjusting manufacturing processes, as described in [Sections 4.1.2.2](#) and [4.1.2.3](#), to control deformation of the sheet steel while it is being formed. It is often possible, with stampings configured like the shock tower, to maintain nearly full stock thickness in the top and radial transition areas, and confine the thinning to the side walls where thinner gage is tolerable. The adjustments, if fully effective, would allow gage reduction to the proven thickness, thus increasing the cost savings, nearly eliminating the mass penalty (see [Table 6.1.2.4-1](#)), and maintaining the other advantages of the one-piece design.

The third option, use of a higher strength material, also affects manufacturing. [Tables 2.5.3.2-1](#), [2.5.3.2-2](#), [2.5.3.3-1](#), [2.5.3.3-2](#), and [2.10-1](#) in [Section 2](#) indicate that higher strength is traded off against lower ductility, which makes the part more difficult to form. Therefore materials personnel as well as the affected manufacturing personnel should participate in the material selection. The higher-strength steel may cost slightly more per pound, but the increase would be

offset, either partially or entirely, by the lower mass from the thinner gage of the higher-strength steel. The other advantages of the one-piece design would be maintained.

6.1.2.5 Spin-Off Effects

A reduction in thickness of the shock tower would allow a reduction in the thickness of the fender shield. The shield, which is welded to the tower, must be at least one third as thick as the tower to maintain a quality weld ratio of 3 to 1. With the shock tower reduced from 2.59 mm (0.102 in.) to the proven thickness of 1.96 mm (0.077 in.), the fender shield could be reduced from 0.86 mm (0.034 in.) to 0.76 mm (0.030 in.).

Section 3.6 indicates that stability of the front longitudinal member is essential to the crash energy absorption capability of the front structure. It should be noted that the shock tower stabilizes the longitudinal member in the vertical direction, and a one-piece tower with heavier side walls can be expected to offer more stability than a two-piece construction with thinner walls. Thus the one-piece shock tower construction may favorably affect crash energy management.

6.1.2.6 Summary

The overall cost and mass comparison for the two design alternatives is summarized in Table 6.1.2.6-1, which is based on design option 1 (utilizing the proven metal gage of 2.59 mm or 0.102 in.).

Table 6.1.2.6-1 Cost and mass summary for one piece tower
based on design option 1 and 1986 economics

	Cost	Mass, kg (lb)
Shock tower (material)	+\$0.95	+1.08 (2.38)
Total manufacturing cost	-4.00	-----
Net, per tower	-3.05	+1.08 (2.38)
Net, per vehicle	-\$6.10	+2.16 (4.76)

Each automotive design center has its own criteria for weighing the actual and potential advantages and disadvantages described above. In this case, the one-piece design was selected because the increase in mass was considered justifiable in view of the reduction in cost and the improved appearance. Of the three available one-piece options, option 1 was selected, rather than attempting to "fine tune" to options 2 or 3. The potentially greater mass and cost savings were not considered to be justified in view of the development cost and time required.

6.1.3 HOOD INNER PANEL

6.1.3.1 Introduction

This case study assesses two design alternatives for a hood inner panel: two-piece laser-welded blank and one-piece blank. It was extracted from an actual design program to illustrate the factors involved in two-piece laser-welded blanks versus one-piece blank options.

The hood inner panel is a structural member that stiffens the hood assembly to reduce flutter and give the hood a solid feel when it is raised. Design analysis and test indicated that the hood

assembly could develop the required stiffness with an inner panel made from 0.022 in. (0.56 mm) stock. However, the application requires 72 in. (1830 mm) wide blanks, and the thinnest gauge available in the required width when the study was begun was 0.028 in. (0.71 mm). Corrosion protection dictates the use of two-side galvanized steel. Three options, illustrated in [Figure 6.1.3.1-1](#), were considered:

1. Use the 0.028 in. stock at 72 in. width and accept the increased mass.
2. Cut half blanks from 48 in. (1220 mm) wide stock, which was available in the 0.022 in. thickness, and laser weld to make 72 in. wide blanks.
3. Cut half blanks identical to option 2 from 36.5 in. (925 mm) wide stock and laser weld as in option 2.

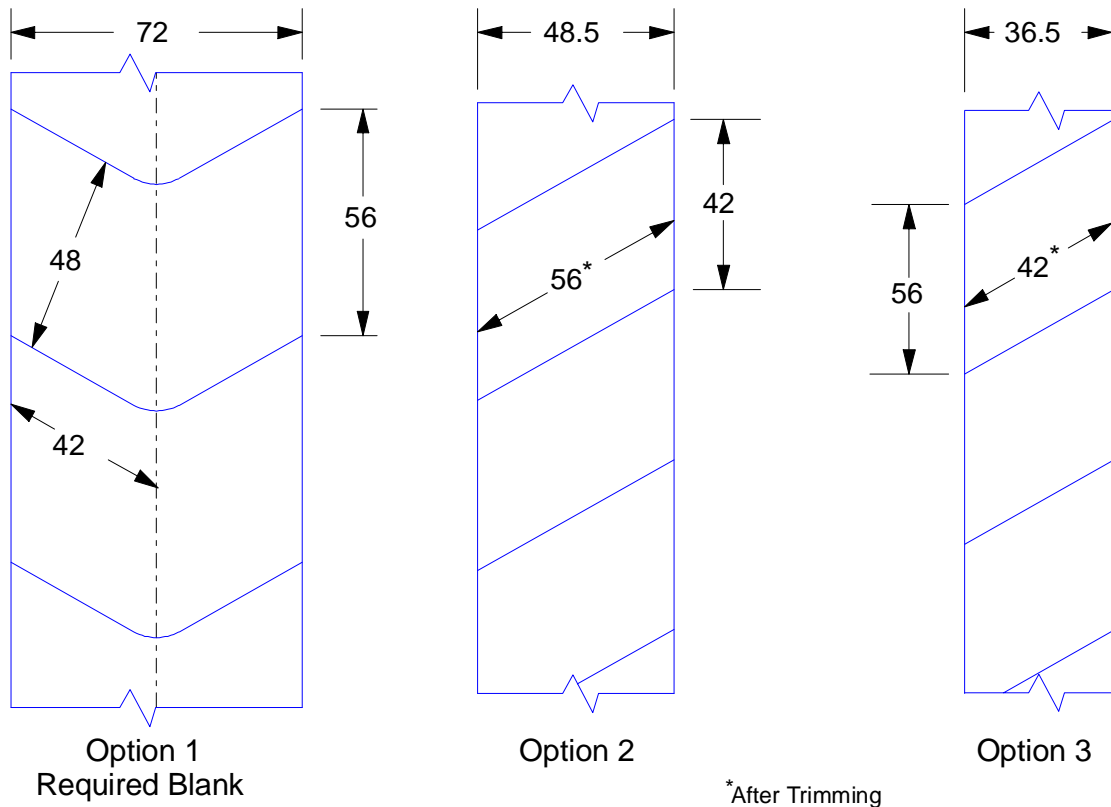


Figure 6.1.3.1-1 Hood inner panel blank options

6.1.3.2 Requirements For Laser-Welded Blanks

Laser welding requires a precision cut so that the gap at the weld line does not exceed 10% of the sheet thickness, or 0.002 in. (0.08 mm). This precision in general can only be achieved by a retrim of 1/4 to 1/2 in. (6.5 to 13 mm) from the blank along the edge to be welded, using a special precision cutoff shear or laser cutter. The two major factors that make retrim necessary, especially for long welds, are coil-edge variation and release of coil residual stresses during blanking. Thus, options 2 and 3 generate a small amount of engineered scrap as the weld edge is retrimmed.

6.1.3.3 Tradeoffs

Option 1 offers lower cost than Options 2 and 3, but it incurs a higher mass. Only one blank is required per piece, and blanks are formed with a simple V-shaped die in a process that develops essentially no engineered scrap. Options 2 and 3 offer a lower material cost than 1, but that cost is more than offset by the cost of the laser-welding operation. Options 2 and 3 weigh and cost the same.

After the blanks are formed, the piece price and tooling cost for further processing (stamping and trimming) are essentially equal for all three options.

The effects of the above variables on cost and mass are shown in [Table 6.1.3.3-1](#).

Table 6.1.3.3-1 Laser welded vs. single piece blanks

	Option 1	Option 2	Option 3
Coil Width in. (mm)	72 (1829)	48 (1219)	36.5 (927)
Minimum Thickness in. (mm)	0.028 (0.71)	0.022 (0.56)	0.022 (0.56)
Raw Matl. Mass* lb (kg)	33.7 (15.3)	13.6 (6.2)	13.6 (6.2)
No. Blanks Required	1	2	2
Total Raw Matl Mass lb (kg)	33.7 (15.3)	27.2 (12.3)	27.2 (12.3)
Finished Panel Mass lb (kg)	28.6 (13.0)	22.8 (10.3)	22.8 (10.3)
Material Cost (\$)	11.31	9.71	9.71
Laser Welding Cost (\$)	0.00	5.00	5.00
Blanking Die Cost (\$)	44,000	---	---
Blanking Die Amortization** (\$)	0.07		
Cost Differential (\$)	Base	3.33	3.33
Mass Reduction lb (kg)	Base	5.8 (2.7)	5.8 (2.7)
Cost Per Mass Reduction \$/lb (\$/kg)	Base	0.57 (1.27)	0.57 (1.27)

* All masses are based on maximum thickness for quarter tolerance stock,
i.e. minimum thickness + 0.0015 in.

** Based on a projected product life of 600,000 units

The choice of option 1 versus options 2 or 3 will vary among profit centers, depending on the value ascribed to mass reduction.

In some applications for laser-welded blanks requiring developed blanks, one side of the stamping requires a different level of surface finish or a different coating from the other, such as one-side galvanized or differential-galvanized steel. Those applications require either two sets of blanks, left-hand and right-hand, or the use of material with surface treatment on both sides that meets the higher requirements. In those cases, material purchase price and the extra cost of set-up plus in-plant handling would have to be factored into the cost of the options.

It should be noted that all comparisons are based on available coil widths at the time the study was initiated. As thinner gauges become available in wide coil widths, the mass advantage offered by the laser-welded blanks will diminish.

6.1.4 DOOR ANTI-FLUTTER BAR USING ENGINEERED SCRAP

6.1.4.1 Introduction

Anti-flutter bars are welded inside the doors of some vehicles just below belt line to stiffen the door structure against vibration or flutter when driving on rough roads and at highway speeds. Two-side galvanized steel is used because of the possibility for corrosion. There are no cosmetic requirements because the bar is not visible.

The flutter bar in this application ([Figure 6.1.4.1-1](#)) illustrates the use of engineered scrap, or offal, by laser welding blanks.

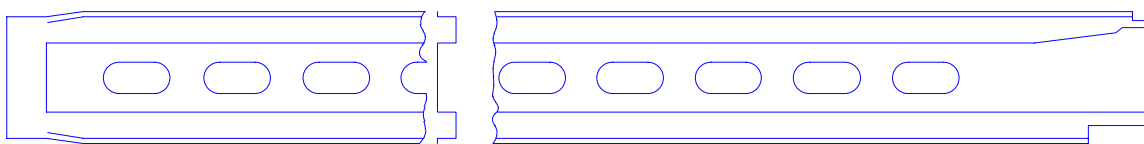


Figure 6.1.4.1-1 Anti-flutter bar

The engineered scrap, approximately 710 mm × 380 mm (28 in. × 15 in.) is generated when the window opening is trimmed from the door inner panel, which is stamped from 0.75 mm (0.030 in.) two-side galvanized steel. The required 1270 mm × 230 mm (50 in. × 9 in.) blank is generated by laser welding two pieces.

Since each piece of engineered scrap produces only one half-blank, the engineered scrap supplies blanks for only one half of the required production. The remaining blanks are fabricated from purchased coil stock of the same specification.

6.1.4.2 Requirements For Laser Welded Blanks

The laser welded full blanks are made dimensionally identical with the blanks made from purchased coil stock so that they can be processed interchangeably. The half-blanks are cut approximately 635 mm × 230 mm (25 in. × 9 in.) in an operation that gives the required precision on the edge that is to be welded (0.075 mm or 0.003 in. maximum gap).

6.1.4.3 Tradeoffs

The savings in material purchase price for the laser welded blanks is gained at the cost of handling blanking and welding the scrap. Since both types of blank have identical dimensions, there is no difference in the masses of the finished bars.

The effects of the above factors on cost is shown in [Table 6.1.4.3-1](#). The cost differential will vary among profit centers, depending on manufacturing cost variables such as material handling methods and availability of equipment. The projected product life, which affects tool amortization, is a minor factor.

In some potential applications for blanks laser welded from engineered scrap, the scrap may be thicker than required for the application. In those cases, the mass penalty for upgauging will be a factor in the analysis.

Table 6.1.4.3-1 Laser welded vs. single piece blanks

	Option 1	Option 2
Type of blank	One piece	Two piece laser welded
Purchased Raw Material Mass kg (lb)	1.63 (3.6)	---
Finished Part Mass kg (lb)	1.3 (2.9)	1.3 (2.9)
Material Handling and Blanking Cost	Base	0.30
Blanking Die Cost	---	40,000
Blanking Die Amort.*	---	0.03
Welding Cost	---	0.90
Material Cost	1.30	---
Cost Reduction	Base	0.07

* Based on a projected product life of 1,500,000 units

6.1.5 MODULAR SEAT SUPPORT

The modular seat support is a two-piece assembly that attaches a pair of bucket seats and a center console to the floor pan of a light truck utilizing the same attachment holes as the standard bench seat. Since the support transmits loads from the seat to the vehicle structure, it must pass all Federal Motor Vehicle Safety Standards (FMVSS) for crashworthiness, as well as the manufacturer's durability requirements.

Several material and process options were considered, including fiber-reinforced composites, aluminum and magnesium permanent mold castings, and aluminum and magnesium die castings. The stamped cold-rolled steel design was chosen for its cost advantage and its ability to meet the design requirements, particularly FMVSS crash testing and durability. Preliminary cost analyses also indicated that the piece costs for the steel unit were approximately one half that for an alternate aluminum casting, and the mass was equal.

The support, shown in [Figure 6.1.5-1](#), is a two piece assembly consisting of a base and a leg. Both pieces are made from a $1475 \times 560 \times 1.5$ mm (58 × 22 × 0.060 in.) AISI 1010 cold-rolled sheet. The base is made in a five-step blank, draw, trim, flange, and finish flanging process. The leg is made in a nine-stage progressive die. The parts are assembled by conventional spot welding. The finished assembly is 1370 mm (54 in.) long by 455 mm (18 in.) wide by 125 mm (5 in.) high and weighs approximately 6.35 kg (14 lb). The assembly is painted for both appearance and corrosion protection.

The modular support is completely interchangeable with the standard bench seat, and it uses the same mounting holes. This arrangement gives a bucket seat option that required no changes to the floor pan assembly or the assembly plant tooling. The use of carryover seats reduced product development cost compared with a new seating program. The development time was also reduced by approximately 80%.

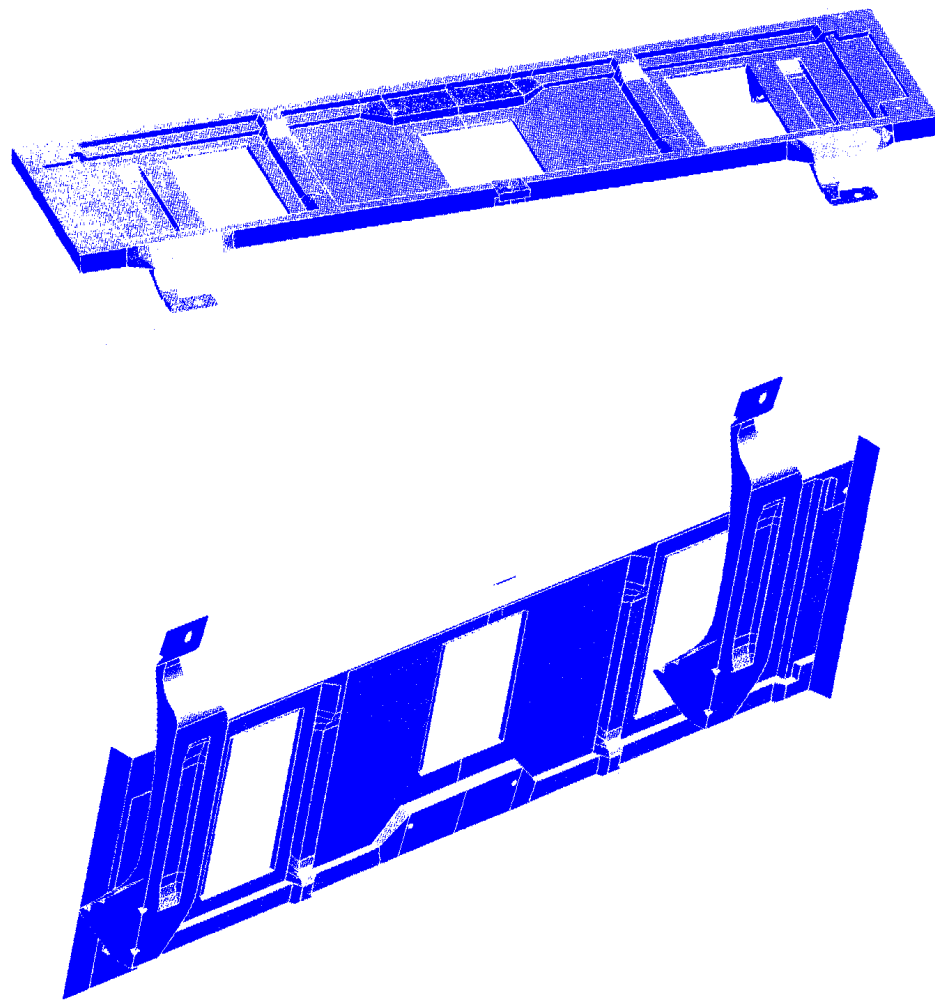


Figure 6.1.5-1 Modular seat support

6.1.6 DESIGN OF AN ANTI-INTRUSION DOOR BEAM

6.1.6.1 Introduction

As a result of increases in the exchange rate, an automotive parts producer supplying anti-intrusion door beams experienced escalating imported steel costs. The part was manufactured from hot rolled high strength steel with a minimum 965 MPa (140 ksi) yield strength. It was felt that, by sourcing the steel supply from a domestic supplier, the material cost could be reduced and the material cost volatility stemming from fluctuating exchange rates could be eliminated. In addition, it became evident that manufacturing costs had to be reduced to remain competitive with other automotive parts producers after the contract expiration date.

The original beam was composed of four components as shown in [Figure 6.1.6.1-1](#).

1. A hat section which runs the full length of the beam, with the top of the hat oriented toward the car interior.
2. A flat plate with stiffener lipped edges running the full length of the beam located toward the car exterior.

3. A short length smaller hat section located in the interior of the larger hat.
4. A short length flat plate located above the smaller hat.

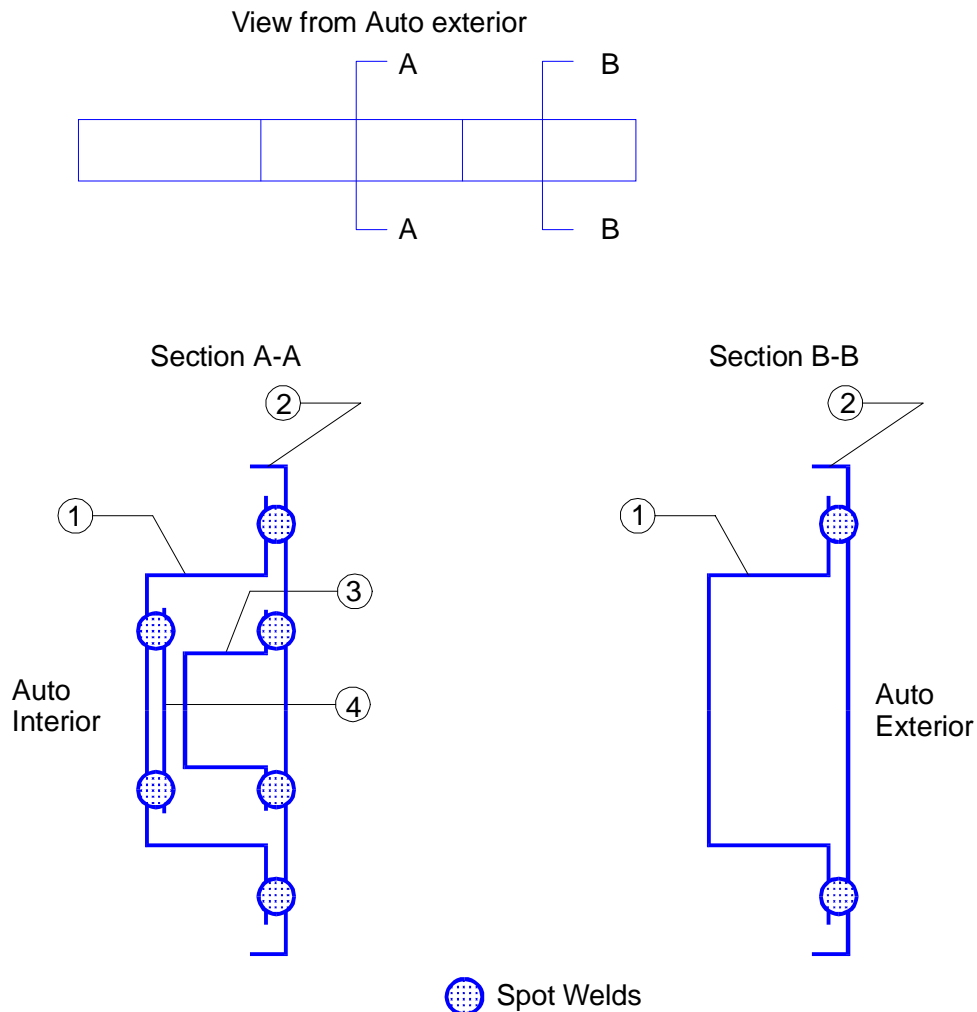


Figure 6.1.6.1-1 Schematic of the original anti-intrusion door beam

The flat plate with lipped edges is welded to the full length hat section to form a closed section. The other two shorter components are welded inside the closed section at the center of the beam to provide additional support. Ten holes are punched at the ends of the beam to reduce mass.

Each component was roll formed, then assembled using 84 spot welds. Fabrication of the beam involved many manufacturing steps, which contributed to the overall cost. Therefore, the production cost could be substantially reduced if the beam could be made with fewer parts.

6.1.6.2 Design Considerations

The alternative of using aluminum was not acceptable. The advantage of lower material density was more than offset by the lower yield strength and higher material cost. Its use would also have required costly changes to the existing manufacturing process and equipment, which could not be passed on to the automotive company.

Domestically available high strength galvanized steel with a minimum yield strength of 830 MPa (120 ksi) was chosen as a substitute for hot rolled high strength steel. Although this chosen yield strength was lower than that of the existing beam, it was believed that the design could be improved to offset this disadvantage.

Space within the door was limited due to the presence of the window mechanism and other door components, restricting the maximum design height of the beam to 32 mm (1.25 in.) and the width to 205 mm (8 in.).

The static load capacity of the existing beam, based on tests conducted by the manufacturer, was:

- Yield load of 22,700 N (5100 lb) applied at the center of the beam.
- Simply supported beam.
- Distance between supports 900 mm (35.4 in.).

The static load capacity of the redesigned beam would be required to meet or exceed this value.

6.1.6.3 Analysis And Results

The Geometric Analysis of Sections (GAS) portion of the American Iron and Steel Institute's Computerized Application and Reference System (AISI/CARS) computer program was used to input the section geometry and to calculate section properties of four proposed designs. (For information on the AISI/CARS computer program, refer to [Section 7 AISI/CARS](#).) [Figure 6.1.6.3-1](#) shows the cross section shapes of the designs considered.

Design A featured a one piece hat section suggested by the manufacturer because of its very low production cost. After the cross section geometry was entered into the CARS program, calculations were performed showing the section modulus (S_x) to be 1224 mm^3 (0.0747 in.^3) at the proposed steel thickness. The yield load was calculated as follows:

$$\begin{aligned}\text{Yield Load} &= 4 * S_x * \text{yield stress} / (\text{span length}) \\ &= 4 * 1224 * 830 / 900 \\ &= 4515 \text{ N (1,012 lb)} \text{ versus } 22,700 \text{ N (5100 lb) required.}\end{aligned}$$

The design was not acceptable because the yield load was only 20% of the required value. Additional iterations were performed with increasing metal thickness until the yield load of the beam exceeded the required peak load requirement. However, the required steel thickness exceeded the manufacturing capabilities of the supplier.

Design B was a one piece W shaped section. A number of W shaped cross sectional beams with slightly different dimensional characteristics were analyzed, using the CARS program. This effort produced a beam with the required load carrying capacity, but the calculated mass was 5.2 kg (11.5 lb), or 0.68 kg (1.5 lb) heavier than the existing unit. This was unacceptable, due the trend towards lighter mass vehicles.

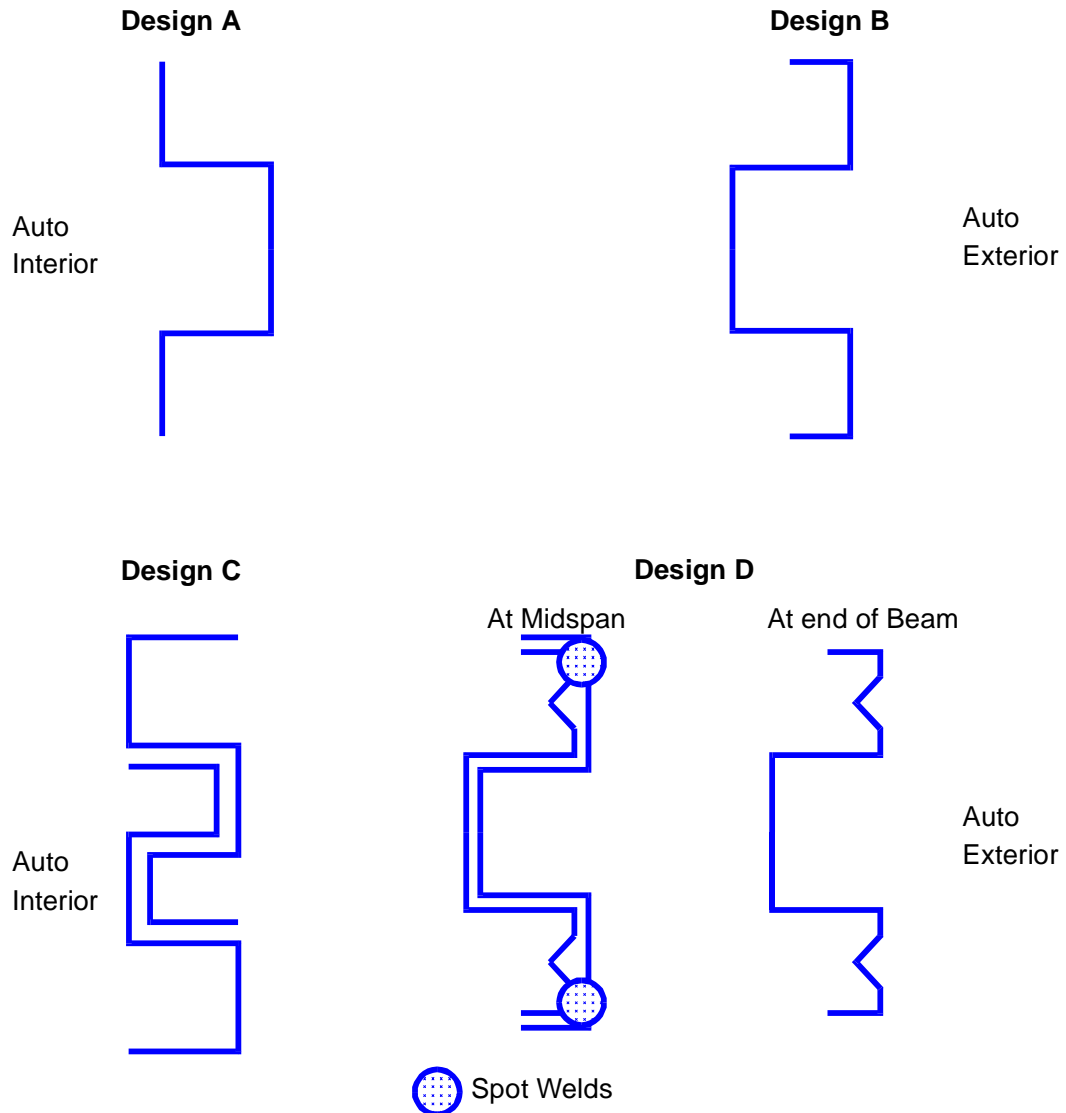


Figure 6.1.6.3-1 Cross sectional shapes of door beam designs considered

Design C consisted of two full length W shaped sections, which were designed to interlock when one is inverted over the other. Two lengths of the same cross section could be produced with only a slight marginal cost penalty over a one piece beam. The resulting beam design was also heavier than the present beam, and therefore unacceptable.

Design D, shown in [Figure 6.1.6.3-2](#), consists of two interlocking W shapes, one full length and one shorter length at midspan. This concept was suggested by calculations performed on previously considered designs, which indicated the need to remove steel from areas of the beam where bending moments are lower, such as the ends, to reduce the beam mass without reducing its strength. Placing a short reinforcement over the central portion of the beam where the bending moment is highest provides strength where required.

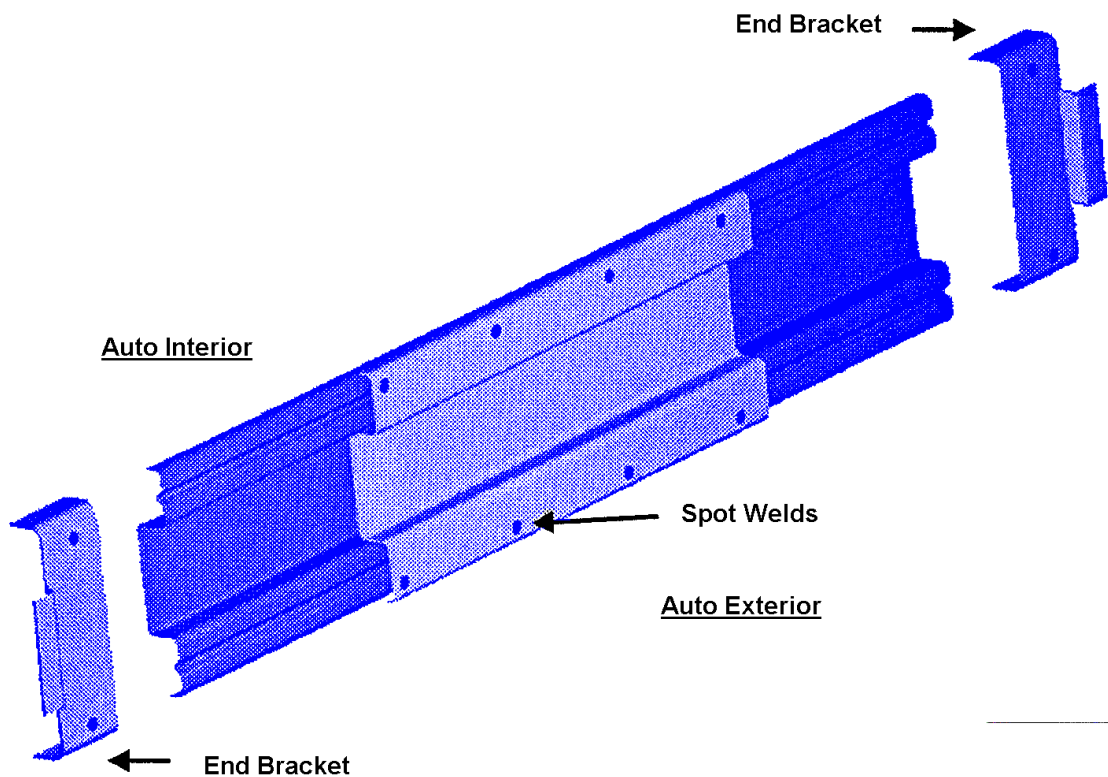


Figure 6.1.6.3-2

Figure 6.1.6.3-3 shows the beam bending moment diagram. Note that, for this arrangement and the indicated loading direction, the two members act in unison but independently, and there is no need for shear transfer between members. Hence, fewer spot welds are required. The beam weighs 4.25 kg (9.4 lb), or 6% less than the original beam. The yield load was 26,564 N (5977 lb), or 17% higher.

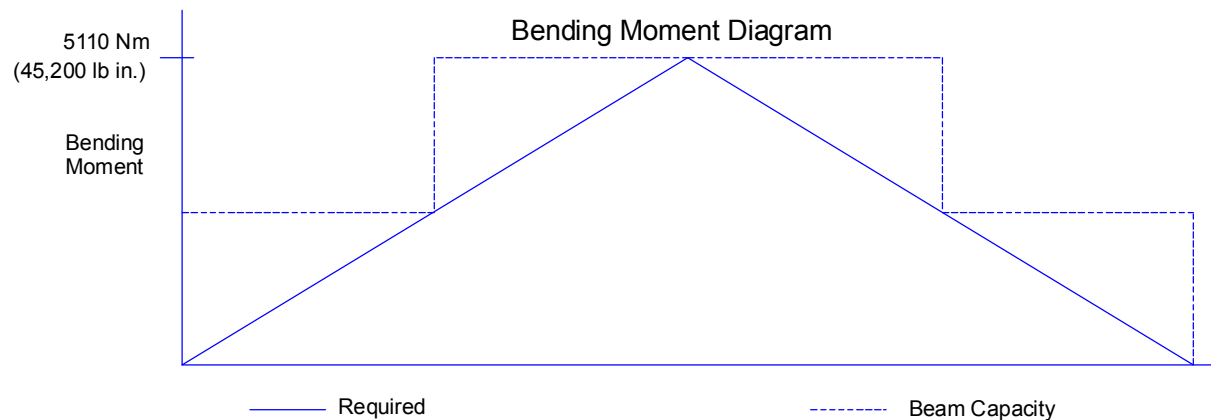


Figure 6.1.6.3-3 Beam moment diagram

Results of the GAS analysis for design D, section A-A (at the center of the beam) and section B-B (at the ends of the beam) are shown in [Table 6.1.6.3-1](#).

Table 6.1.6.3-1 Results from the CARS computer program (GAS analysis) for Design D

Property	Effective Properties	
	Section A-A (center of beam)	Section B-B (at ends of beam)
Area	1.112	.049783
cx	-.00061049	-1.4575E-07
cy	0.49573	0.5309
Ixx	0.27544	0.11859
Iyy	6.3078	2.8346
Ixy	0.0061607	0.0024984
Sx+	0.42403	0.19301
Sy+	1.5759	0.71945
Sx-	-0.4743	-0.21411
Sy-	-1.5764	-0.71945
Theta	0.058515	0.052705
Iuu	0.27543	0.11859
Ivv	6.3078	2.8346
Su+	0.42288	0.19251
Sv+	1.5759	0.71945
Su-	-0.47125	-0.21283
Sv-	-1.5763	-0.71941
rx	0.4977	0.48807
ry	2.3817	2.3862
Iyc	5.5548	2.4499

The iterative process allowed refinements to be made to subsequent designs. Design D was chosen.

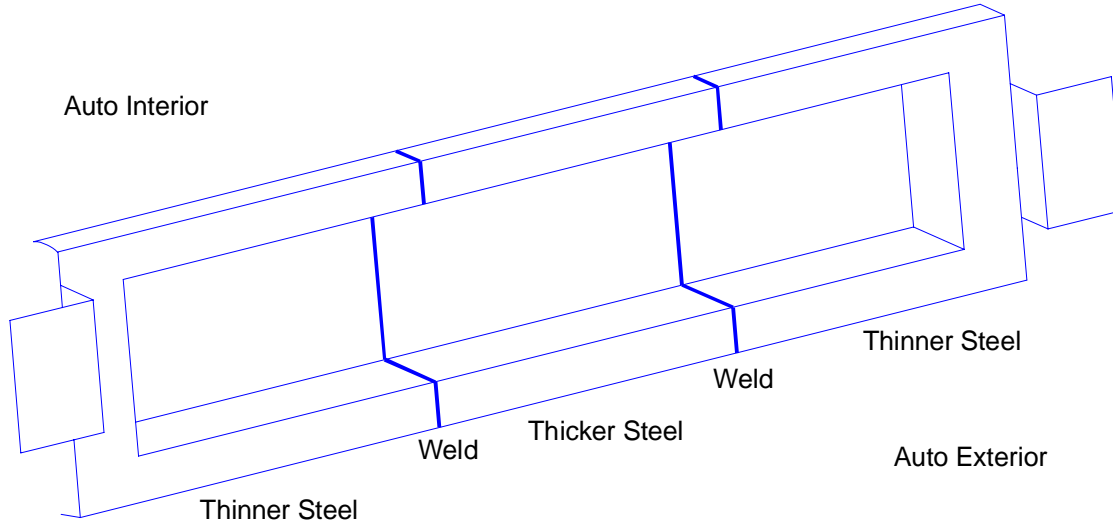
6.1.6.4 Benefits Of The Newly Designed Anti-Intrusion Beam

The redesigned anti-intrusion door beam offered the following advantages over the original beam:

- 6% lower mass, which contributes to improved fuel economy.
- 17% Higher beam capacity in static bending.
- Spot welds reduced from 84 to 8, which contributes to lower manufacturing cost.
- Material cost reduced by sourcing the steel from a domestic supplier.
- Parts count reduced from four to two, resulting in fewer manufacturing steps (utilizing existing equipment) and lower cost.

After prototype testing, the beam design could be refined to further reduce the beam mass and reduce costs. Design strategies to be considered include:

- Selectively inserting lightening holes in the beam.
- Reducing steel thickness.
- Using tailor welded blanks to reduce assembly costs (see [Figure 6.1.6.4-1](#)).



Note: Thicker steel is utilized in the central portion of beam where more strength is required. The ends of the beam are fabricated with thinner steel to reduce beam mass.

Figure 6.1.6.4-1 Concept for door beam utilizing tailor welded blank

6.1.7 DESIGN OF A FRONT RAIL

This case study evaluates options for weight reduction of a front rail. The front rail and its connection to the body have a great influence on load transfer. The following case study was extracted from the research conducted by the UltraLight Steel Auto Body (ULSAB) Consortium. In this project, a new UltraLight front rail as shown in [Figure 6.1.7-1](#) was created to improve the load transfer by distributing the load along three paths. The front rail is joined directly to the rocker. The dash cross member transfers loads cross-car. The front rail extension carries some of the load directly to the front floor cross member.

Traditionally, hat sections, as shown in [Figure 6.1.7-2](#), are used for the front rail. The large w/t ratios of the top and bottom flanges result in their partial effectiveness under axial loads. The effectiveness of the top and bottom flanges under axial loads can be increased by using a hexagonal section as shown in [Figure 6.1.7-3](#). The question is: can the hat section be replaced by a hexagonal section while achieving mass reduction and maintaining strength? The GAS and Design Key applications of the AISI/CARS 2000 program was used to investigate this question. [Section 7.2.1](#) presents the entire process in the form of a tutorial. The results of the

investigation are shown in [Section 7.2.1.6](#), and indicates that the hexagonal section can effectively replace the hat section while achieving a mass reduction of eight percent.

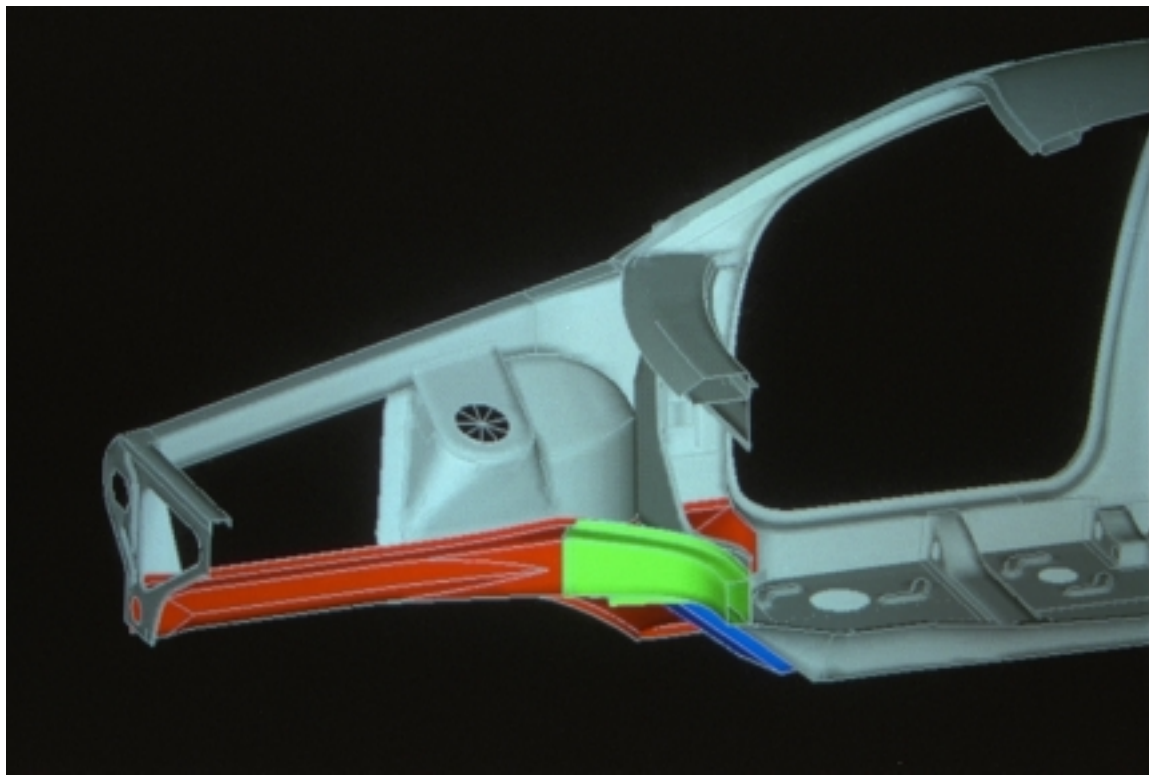


Figure 6.1.7-1 Concept for door beam utilizing tailor welded blank

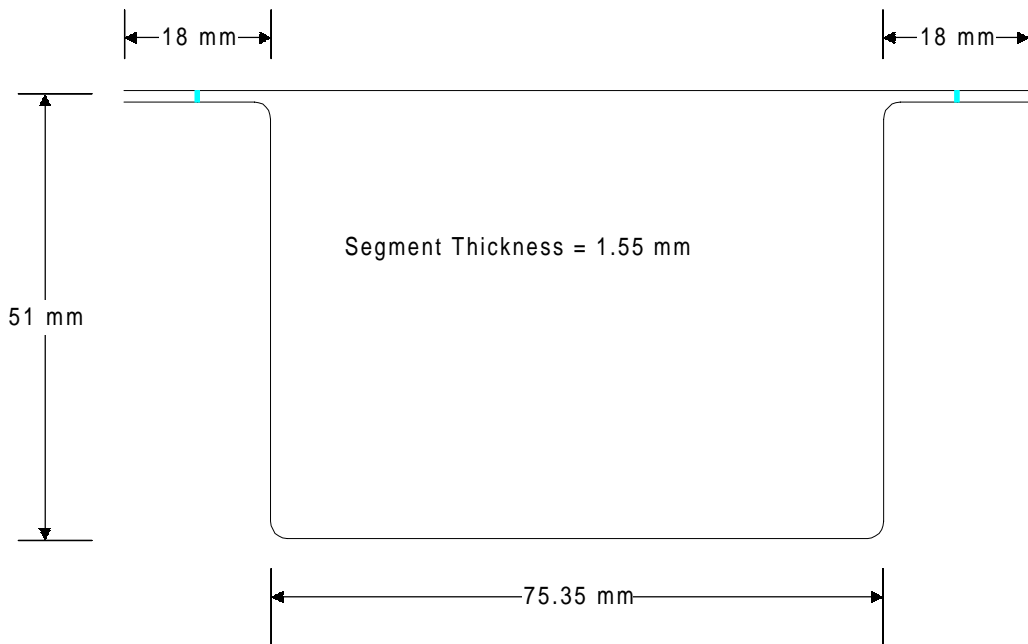


Figure 6.1.7-2 Typical hat section of a front rail

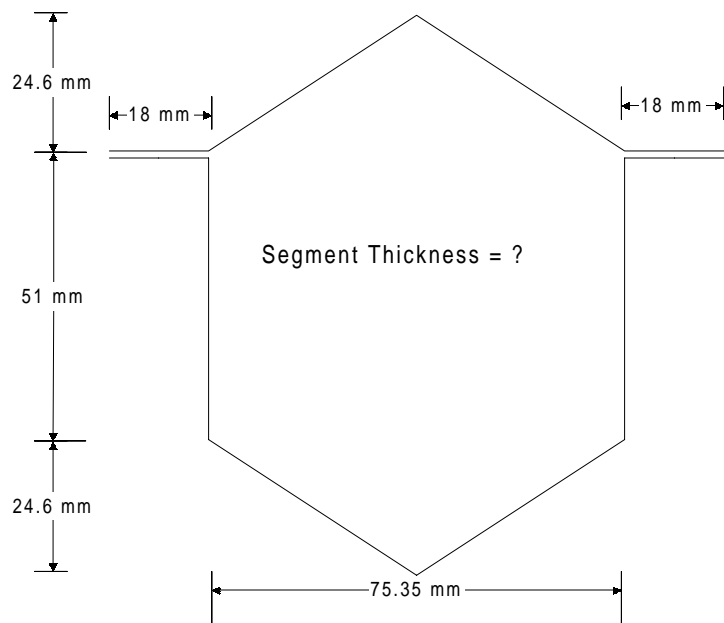


Figure 6.1.7-3 Proposed hexagonal section for a front rail

6.2 EXAMPLES

This section provides examples that illustrate the application of the design concepts that are presented in [Section 3](#). Note that many of the examples could be solved faster and with greater accuracy using CARS 2000. GAS cross section files and KEY Design Procedure files are included with the CARS program for CARS users to review. [Table 6.2-1](#) lists the example problems, reference section, and CARS 2000 program(s), if applicable.

Table 6.2-1 Example problems

Section	Example	Reference Section	CARS Program
6.2.1.1	3.1-1, Effective Area for Channel Section	3.1	GAS
6.2.1.2	3.1-2, Effective Width Concept for a Curved Element with Stiffened Edges	3.1	GAS
6.2.1.3	3.1-3, Evaluating Effective Properties of a Flat Width with a Large Tangent Radius	3.1	
6.2.1.4	3.1-4, Column Equations for a Lipped Channel	3.1	
6.2.1.5	3.1-5, Effective Web Area	3.1	
6.2.1.6	3.1-6, Web Crippling	3.1	KEY
6.2.1.7	3.1-7, Moment Capacity Controlled by Lateral Buckling	3.1	KEY
6.2.1.8	3.1-8, Torsional Stiffness of Open and Closed Sections	3.1	GAS, KEY
6.2.2.1	3.2-1, Section Properties and Stresses in a Curved Member with Web(s) in the Plane of Curvature	3.2	GAS, KEY
6.2.2.2	3.2-2, Properties and Stresses in a Curved Tubular Section	3.2	GAS, KEY
6.2.3.1	3.3-1, Stiffness, Denting, and Oil Canning	3.3	KEY
6.2.4.1	3.4-1, Spacing Criteria for Connection of a Flat Plate	3.4	KEY
6.2.5.1	3.5-1, Strain Life Estimated for Two Steels of Different Strength Levels	3.5	
6.2.5.2	3.5-2, Fatigue Life Estimate of a Tensile-Shear Spot Welded Specimen	3.5	
6.2.5.3	3.5-3, Fatigue Properties Using the Load-Life (P-N) Method	3.5	
6.2.5.4	3.5-4, Fatigue Properties Using the Stress-Life (S-N) Method	3.5	
6.2.5.5	3.5-5, Fatigue Properties Using the Plastic Strain-Life Method	3.5	
6.2.5.6	3.5-6, Fatigue Properties Using the Statistical Cyclic Stress-Strain Curve	3.5	

6.2.1 EXAMPLES FOR SECTION 3.1

6.2.1.1 Example 3.1-1, Effective Area for Channel Section

This example illustrates how to evaluate the effective area for a channel section using the procedures of [Section 3.1.2.1](#). The advantage of intermediate stiffeners is illustrated in the second half of the example.

- Evaluate A_e , the effective area of the lipped channel in compression (see [Figure 6.2.1.1-1](#)) if

$$\begin{aligned} t &= 1.2 \text{ mm} \\ w_2 &= 180 \text{ mm} \\ D &= 24.6 \text{ mm} \\ \text{stress } f &= 300 \text{ MPa} \end{aligned}$$

$$\begin{aligned} w_1 &= 48 \text{ mm} \\ d &= 21 \text{ mm} \\ \text{sheet width} &= 336.8 \text{ mm} \end{aligned}$$

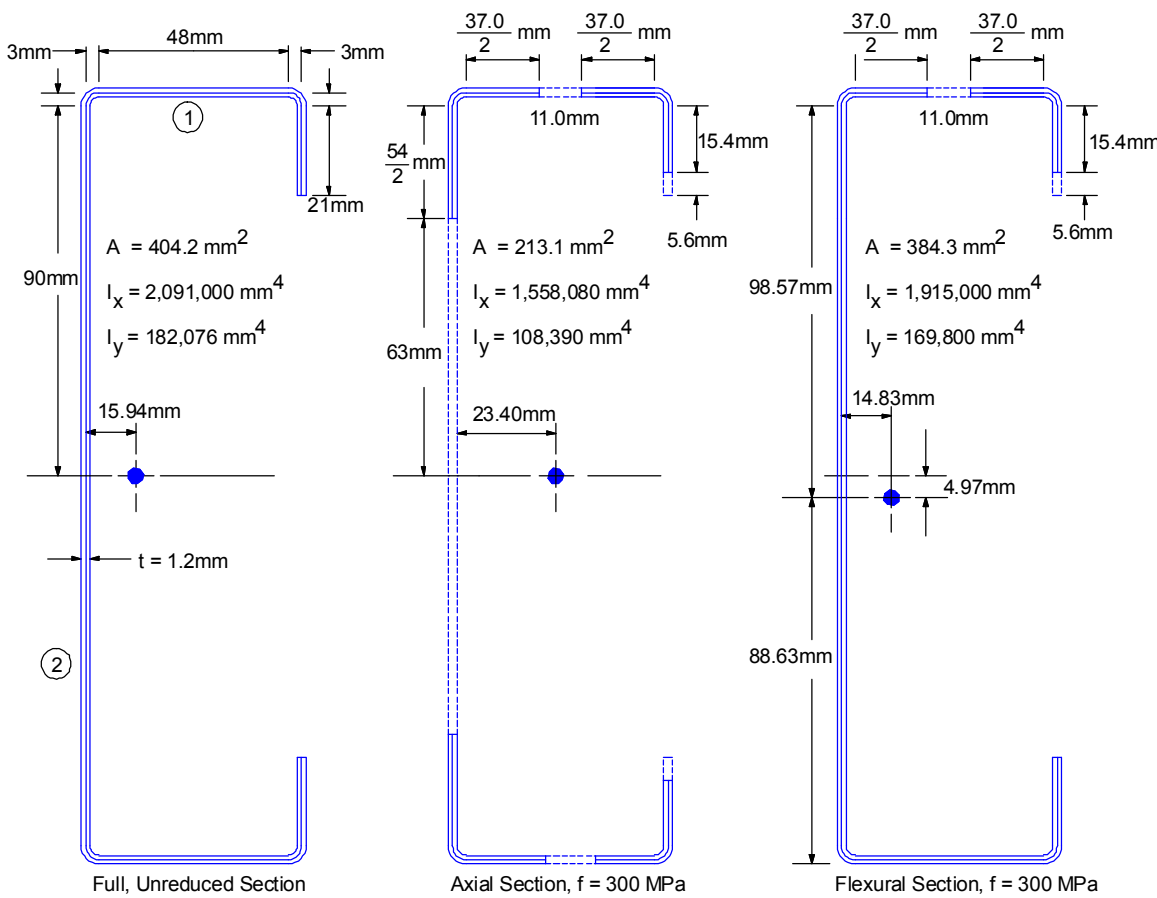


Figure 6.2.1.1-1 Nominal and effective properties of a channel section

For element 2:

$$\frac{w_2}{t} = 150$$

From [Figure 3.1.2.1.1-5](#)

$$\frac{\lambda}{\left(\frac{w}{t}\right)} = 0.0205 \quad \text{for } f = 300 \text{ and } k = 4$$

$$\lambda = 0.0205(150) = 3.075$$

From [Figure 3.1.2.1.1-4](#)

$$b_2 = 0.3w = 54 \text{ mm}$$

For the simple lip:

$$\frac{d}{t} = \frac{21}{1.2} = 17.5$$

From [Figure 3.1.2.1.1-5](#)

$$\frac{\lambda}{\left(\frac{w}{t}\right)} = 0.062 \quad \text{for } f = 300 \text{ and } k = 0.43$$

$$\lambda = 0.062(17.5) = 1.085$$

From [Figure 3.1.2.1.1-4](#)

$$d'_s = 0.735(21) = 15.4 \text{ mm}$$

For element 1:

$$\frac{w_1}{t} = 40$$

From [Equation 3.1.2.1.1-4](#) $S = \frac{572}{\sqrt{300}} = 33.0 ; \quad \frac{w_1}{t} = 1.21S$

$$\frac{I_s}{t^4} = \left(\frac{d}{t}\right)^3 \frac{\sin^2 \theta}{12} = 446.6$$

From [Figure 3.1.2.1.3-1 \(a\)](#) $\frac{I_a}{t^4} = 144.2 \quad \text{at } \frac{w}{t} = 1.21S$

From [Equation 3.1.2.1.3-4](#) $d_s = d'_s$

From [Figure 3.1.2.1.3-1\(b\)](#) $k = 2.7 \quad \text{since } \frac{D}{w} = \frac{24.6}{48} = 0.512$

From [Figure 3.1.2.1.1-5](#) $\frac{\lambda}{\left(\frac{w}{t}\right)} = 0.025$

$$\lambda = 0.025(40) = 1.00$$

From [Figure 3.1.2.1.1-4](#) $b_1 = 0.770(48) = 37.0 \text{ mm}$

Therefore, $A_e = 1.2 \text{ mm} [336.8 - (180 - 54) - 2(21 - 15.4) - 2(48 - 37.0)]$
 $= 1.2 (336.8 - 159.2)$
 $= 213.12 \text{ mm}^2$

whereas the gross area is 404.16 mm^2 .

2. To improve A_e , consider the effect of adding a single intermediate stiffener at the center of the web. This stiffener has:

an $I_s = 500 \text{ mm}^4$, a width of 12 mm, and an area of $30(1.2) = 36 \text{ mm}^2 = A'_s$.

Thus $b_o = 180 \text{ mm}$, and $w = \frac{(180 - 12)}{2} = 84 \text{ mm}$

Since $S = 33$ $\frac{b_o}{t} = 150 = 4.55S \quad \text{and} \quad \frac{I_s}{t^4} = \frac{500}{(12)^4} = 241$

From [Figure 3.1.2.1.4-2\(a\)](#) $\frac{I_a}{t^4} = 300 \quad \text{at } 4.55S$

Since $\frac{I_s}{I_a} = 0.80$ $k = 3.8$ from [Figure 3.1.2.1.4-2\(b\)](#)

From [Figure 3.1.2.1.1-5](#) $\frac{\lambda}{\left(\frac{w}{t}\right)} = 0.021$

Since $\frac{w}{t} = \frac{84}{1.2} = 70$ $\lambda = 1.47$

From [Figure 3.1.2.1.1-4](#) $b = 0.575(84) = 48.3 \text{ mm}$
 $A_s = 36(0.80) = 28.8 \text{ mm}^2$

Therefore, $A_e = 1.2[336.8 - 12 - 2(84 - 48.3) - 2(21 - 15.4) - 2(48 - 37.0)] + 28.8 = 293.04 \text{ mm}^2$
from a gross area of $1.2(336.8 - 12 + 30) = 425.76 \text{ mm}^2$

3. Consider the addition of two intermediate stiffeners with $A'_s = 36 \text{ mm}^2$ and $I_s = 500 \text{ mm}^4$

$$w = \frac{[180 - 12(2)]}{3} = 52 \text{ mm}$$

$$\frac{w}{t} = \frac{52}{1.2} = 43.3; S = 33 \quad \text{from } \text{Equation 3.1.2.1.4-5} \text{ so the stiffeners can be considered.}$$

$$\frac{I_s}{t^4} = 241 \geq \frac{I_a}{t^4} = 155$$

Since $\frac{w}{t} < 60$, compute b using [Figures 3.1.2.1.1-4](#) and [3.1.2.1.1-5](#) and $k = 4$.

$$\lambda = 0.205(43.3) = 0.888$$

$$b = 0.85 (52) = 44.2 \text{ mm}$$

Therefore $A_s = A'_s$ from [Table 3.1.2.1.4-1](#).

6.2.1.2 Example 3.1-2, Effective Width Concept for a Curved Element with Stiffened Edges

This example illustrates use of the effective width concept for a curved element with stiffened edges. Consider the top shape in [Figure 3.1.2.3-1](#) having

$$t = 0.6477 \text{ mm} \quad w = 75 \text{ mm} \quad R = 300 \text{ mm} \quad F_y = 345 \text{ MPa}$$

$$\frac{w}{t} = 115.8 \quad \frac{R}{t} = 463 \quad \frac{D}{t} = 926$$

$$\frac{A_o}{A} = \frac{0.336(200,000)}{345 \times 926} = 0.21 \text{ from } \text{Equation 3.1.2.2-7}$$

$$t_e = 0.21(0.6477) = 0.136 \text{ mm}$$

$$\lambda = 0.022(115.8) = 2.547 \text{ (Figure 3.1.2.1.1-5 with } k = 4)$$

$$b = 0.355(75) = 26.6 \text{ mm (Figure 3.1.2.1.1-4)}$$

The effective section at yield will look as shown in [Figure 6.2.1.2-1](#).

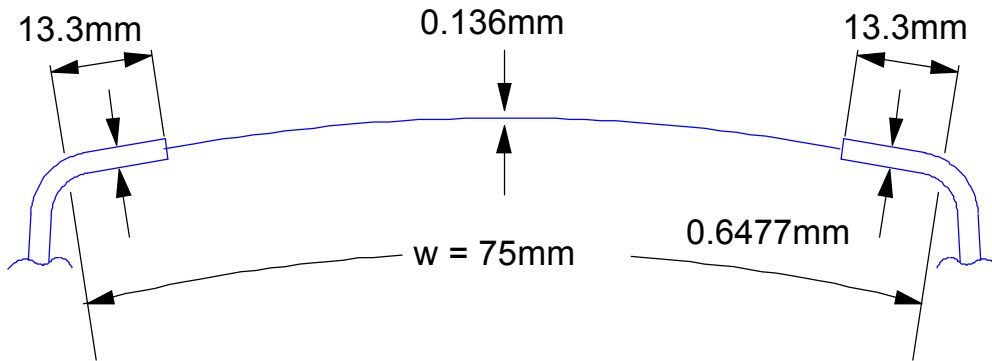


[Figure 6.2.1.2-1 Effective section at yield](#)

If the section were to be examined at a stress of $f = 200 \text{ MPa}$ rather than at yield, the effective thickness would increase to

$$0.21 \left(\frac{345}{200} \right) 0.6477 = 0.235 \text{ mm}$$

The element would be fully effective when the f/F_y ratio is just equal to A_o/A .

6.2.1.3 Example 3.1-3, Evaluating Effective Properties of a Flat Width with a Large Tangent Radius

This example illustrates a possible procedure for evaluating effective properties of a flat width with a large tangent radius. Test backup for this procedure has not been established.

Consider first an element similar to [Figure 3.1.2.4-1](#) in which

$$\frac{R}{t} > 7, \text{ but less than } 0.057 \frac{E}{F_y}, \text{ such that the radius portion will reach yield.}$$

Take the actual flat width to be 90 mm, and the radius to be 36 mm with $t = 1.8$ mm. Arbitrarily establish a new w larger than 90 mm by estimating an amount of the arc to add, e.g.,

$$\frac{\pi}{4}t \left(\frac{R}{t} - 7 \right)$$

to 90 mm when the arc is 90° or more. Thus,

$$w = \frac{\pi}{4}1.8 \left(\frac{36}{1.8} - 7 \right) + 90 = 108.4 \text{ mm}$$

Calculate b using the procedure in [Section 3.1.2.1.1](#) with $k = 4$. If b is calculated to be 80 mm, then 40 mm would be considered effective adjacent to the sharp bend in [Figure 3.1.2.4-1\(b\)](#), while $40 - 18.4 = 21.6$ mm of the flat portion adjacent to the large radius corner would be considered effective.

Consider next an element similar to [Figure 3.1.2.4-1\(c\)](#) in which R/t is large enough so that the equivalent area A_o of the radius is less than the actual area. This means that the effective region near the sharp radius corner can achieve a higher stress than the large radius portion. Change the radius in the first part of the example to 84 mm. Using the same relationship for amount of arc:

$$w = \frac{\pi}{4}1.8 \left(\frac{84}{1.8} - 7 \right) + 90 = 146.1 \text{ mm}$$

Consider the A_o/A value from [Figure 3.1.2.2-1](#) to be equivalent to the A_s/A_s' ratio for intermediate stiffeners. Thus, [Figure 3.1.2.1.4-2](#) for intermediate stiffeners can be used as a means to obtain b . Use $I_s/I_a = A_o/A$ and obtain C_1, C_2, k from [Figure 3.1.2.1.4-2](#) and then find b from [Equation 3.1.2.1.1-6](#). The $C_2 b/2$ width is likely to be entirely in the radius portion. The stress on the section is likely to be governed by the limiting stress on the radius portion, $(A_o/A)F_y$.

6.2.1.4 Example 3.1-4, Column Equations for a Lipped Channel

This example illustrates the use of column [Equation 3.1.2.5-1](#) for the lipped channel in [Figure 3.1.2.1.1-2](#) (for which the effective flat widths were evaluated in [Example 3.1-1](#)). Determine the effective length KL at which $F_{cu} = 300$ MPa, if $F_y = 345$ MPa, presuming that flexural buckling controls (see [Section 3.1.2.5](#)).

Since $F_{cu} > \frac{F_y}{2}$, from [Equation 3.1.2.5-1](#)

$$300 = 345 \left(1 - \frac{345}{4F_e} \right)$$

$$F_e = 661.25 \text{ MPa} = \frac{1,974,000}{\left(\frac{KL}{r} \right)^2}$$

$$\text{Therefore } \frac{KL}{r} = 54.6$$

The full, unreduced section properties are

$$I_x = 2,091,000 \text{ mm}^4 \quad I_y = 182,076 \text{ mm}^4 \quad A = 404 \text{ mm}^2$$

$$r_x = 71.92 \text{ mm} \quad r_y = 21.22 \text{ mm}$$

With r_y controlling,

$$KL = 54.6 (21.22) = 1,159 \text{ mm} = 1.16 \text{ m}$$

6.2.1.5 Example 3.1-5, Effective Web Area

This example illustrates how to evaluate the effective web area and compares the results with the reduced stress approach from [Figure 3.1.3.1.2-2](#). At the web limit $h/t = 200$, with a value of w/t equal to 195, determine what fraction of the web is ineffective at 345 MPa (50 ksi) under pure flexural stress.

With $\psi = -1$ and $k = 24$

From [Equation 3.1.2.1.1-1](#)

$$\lambda = \frac{(1.052)(195)\sqrt{\frac{345}{200,000}}}{\sqrt{24}} = 1.739$$

From [Figure 3.1.2.1.1-4](#)

$$b_e = 0.5 w \text{ at } \psi = -1 \text{ and}$$

$$b_1 = \frac{b_e}{(3+1)} = 0.125w \text{ per } \text{Equation 3.1.3.1.2-5}$$

$$b_2 = \frac{b_e}{2} = 0.25w \text{ per } \text{Equation 3.1.3.1.2-6}$$

The ineffective portion of the compression portion of the flat width is

$$\frac{w}{2} - b_1 - b_2 = 0.125w$$

From the 1980 AISI provisions, the maximum web stress would be limited to no more than 270 MPa (39 ksi) per [Figure 3.1.3.1.2-2](#). Since with the new procedure, the stress remains at 345 MPa with only an eighth of the web removed, it is obvious that the reduced stress approach is more conservative than the effective width approach.

6.2.1.6 Example 3.1-6, Web Crippling

This example illustrates the application of the web crippling expressions and compares the various results using 345 MPa (50 ksi) and 552 MPa (80 ksi) yield steel. Consider the beam in [Figure 6.2.1.6-1](#) with $t = 1.27\text{ mm (.05")}$, $\theta = 90^\circ$, and $R = 1.5t$

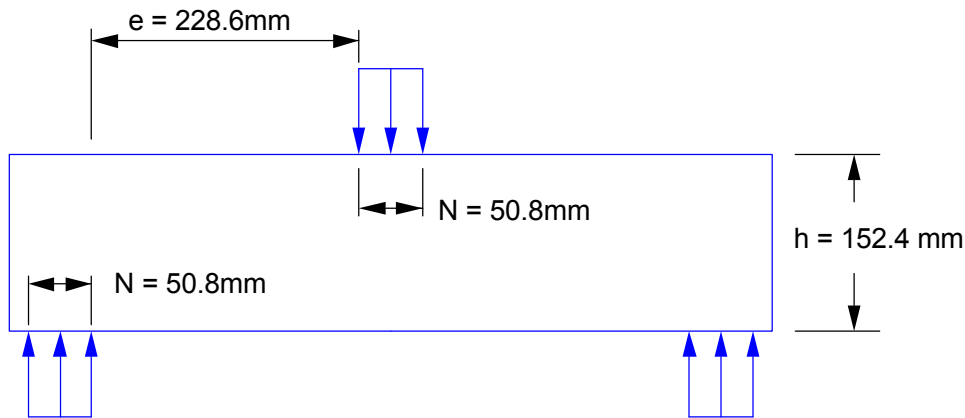


Figure 6.2.1.6-1 Web crippling investigation at interior and exterior supports

Interior Support

Using [Equation 3.1.3.5.1-1](#) with:

$$\frac{h}{t} = 120$$

$$\frac{N}{t} = 40$$

$$\frac{R}{t} = 1.5$$

$$C_t = 0.0276 \text{ kN (0.00621 kips)}$$

$$C_h = 243$$

$$C_R = 0.97$$

$$C_N = 1.28$$

$$C_\theta = 1$$

$$\begin{aligned} P_{cu} &= (0.0276)(243)(0.97)(1.28)(1)C_F \text{ kN} \\ &= (0.00621)(243)(0.97)(1.28)(1)C_F \text{ kips} \end{aligned}$$

$$\begin{aligned} &= 8.335 \left(1.375 - 0.375 \frac{F_y}{F_o} \right) \frac{F_y}{F_o} \text{ kN} \\ &= 1.874 \left(1.375 - 0.375 \frac{F_y}{F_o} \right) \frac{F_y}{F_o} \text{ kips} \end{aligned}$$

$$\text{For } F_y = F_o$$

$$\begin{aligned} P_{cu} &= 8.335 \text{ kN} \\ &= 1.874 \text{ kips} \end{aligned}$$

$$\begin{aligned} \text{For } F_y &= 552 \text{ MPa} \\ &= 80 \text{ ksi} \end{aligned}$$

$$\begin{aligned} P_{cu} &= 10.33 \text{ kN} \\ &= 2.323 \text{ kips} \end{aligned}$$

Using [Equation 3.1.3.5.1-11](#) and [Equation 3.1.3.5.1-13](#)

$$\begin{aligned} P_{cy} &= 0.0078(1.27)^2 345 \left[1 + 0.217\sqrt{40}\right] \left[1 - 0.0814(1.5)\right] = 9.04 \text{ kN} \\ &= 7.8 (0.05)^2 50 \left[1 + 0.217\sqrt{40}\right] \left[1 - 0.0814(1.5)\right] = 2.03 \text{ kips} \end{aligned}$$

$$\begin{aligned} P_{cb} &= 5.65(1.27)^2 \underbrace{\left[1 + 2.4(0.333)\right]}_{<1.96} \underbrace{\left[1 - 0.0017(120)\right]}_{<.081} \underbrace{\left[1 - 0.12(1.5)\right]}_{>0.40} = 10.70 \text{ kN} \\ &= 820(0.05)^2 \underbrace{\left[1 + 2.4(0.333)\right]}_{<1.96} \underbrace{\left[1 - 0.0017(120)\right]}_{<.081} \underbrace{\left[1 - 0.12(1.5)\right]}_{>0.40} = 2.41 \text{ kips} \end{aligned}$$

Web overstress controls. The moment at the section may lead to a lower P_{cm} value per [Equation 3.1.3.5.1-12](#). Based on P_{cb} from [Equation 3.1.3.5.1-13](#), there would be a small benefit to using an 80 ksi yield steel to increase P_{cy} and P_{cm} .

If the webs were restrained against rotation, [Equation 3.1.3.5.2-2](#) gives:

$$\begin{aligned} P_{cu} &= 0.001(1.27)^2 (345) (15 + 3.25\sqrt{40}) = 19.78 \text{ kN} @ 345 \text{ MPa} \\ &= (1.0) (0.05)^2 (50) (15 + 3.25\sqrt{40}) = 4.44 \text{ kips} @ 50 \text{ ksi} \end{aligned}$$

$$\begin{aligned} P_{cu} &= 0.001(1.27)^2 (552) (15 + 3.25\sqrt{40}) = \left(1.15 - \frac{552}{2733}\right) = 30.0 \text{ kN} @ 552 \text{ MPa} \\ &= (1.0) (0.05)^2 (80) (15 + 3.25\sqrt{40}) = \left(1.15 - \frac{80}{400}\right) = 6.75 \text{ kips} @ 80 \text{ ksi} \end{aligned}$$

The restraint of web rotation more than doubles the concentrated load capacity per web, with increased capacity for higher yield steel.

Exterior Support

Using [Equation 3.1.3.5.1-14](#) with

$$\frac{h}{t} = 120 \quad \frac{N}{t} = 40 \quad \frac{R}{t} = 1.5$$

$$\begin{aligned} P_{cu} &= 0.01606(1.27)^2 [1.15 - 0.15(1.5)] [98 + 4.2(40) - 0.022(40)(120)] C'_f \text{ kN} \\ &= 2.33 (0.05)^2 [1.15 - 0.15(1.5)] [98 + 4.2(40) - 0.022(40)(120)] C'_f \text{ kips} \\ &= 3.843 C'_f \text{ kN} \\ &= 0.864 C'_f \text{ kips} \end{aligned}$$

For $F_y = 345 \text{ MPa}$ (50 ksi), $P_{cu} = 3.843 \text{ kN}$ (0.864 kips)

For $F_y = 552 \text{ MPa}$ (80 ksi), $P_{cu} = 4.11 \text{ kN}$ (0.924 kips)

Using [Equation 3.1.3.5.1-16](#) and [Equation 3.1.3.5.1-17](#)

$$P_{cy} = 0.0099(1.27)^2(345) \left[1 + 0.0122(40) \right] \overbrace{\left[1 - 0.247(1.5) \right]}^{>0.32} = 5.16 \text{ kN}$$

$$9.90 (0.05)^2 (50) \left[1 + 0.0122(40) \right] \overbrace{\left[1 - 0.247(1.5) \right]}^{>0.32} = 1.159 \text{ kips}$$

$$P_{cb} = 9.55(1.27)^2 \left[1 - 0.00348(120) \right] \overbrace{\left[1 - 0.298(1.5) \right]}^{>0.52} = 4.96 \text{ kN}$$

$$1385(0.05)^2 \left[1 - 0.00348(120) \right] \overbrace{\left[1 - 0.298(1.5) \right]}^{>0.52} = 11.15 \text{ kips}$$

Therefore

$$P_{cu} = 4.96 \text{ kN (1.115 kips) for } 345 \text{ and } 552 \text{ MPa (50 and 80 ksi) yield stress.}$$

In this case, the first set of equations governs. It is observed that the use of 552 MPa (80 ksi) yield stress is of little value in this case.

If the web is well restrained, [Equation 3.1.3.5.2-1](#) gives for each web

$$P_{cu} = 0.001(1.27)^2(345)(10 + 1.25\sqrt{40}) = 9.96 \text{ kN @ 345 MPa}$$

$$= (1.0)(0.05)^2 (50) (10 + 1.25\sqrt{40}) = 2.24 \text{ kips @ 50 ksi}$$

$$\text{and } P_{cu} = 0.001(1.27)^2 (410)(10 + 1.25\sqrt{40}) = 11.92 \text{ kN @ 552 MPa}$$

$$(1.0)(0.05)^2 (60) (10 + 1.25\sqrt{40}) = 2.68 \text{ kips @ 80 ksi}$$

6.2.1.7 Example 3.1-7, Moment Capacity Controlled by Lateral Buckling

This example illustrates the evaluation of moment capacity controlled by lateral buckling. Evaluate the moment capacity of the section in [Example 3.1-1](#) if

$$F_y = 345 \text{ MPa}$$

L, the effective lateral unbraced length, equals 1.5 meters

$$C_b = 1.$$

From the full, unreduced section

$$S_f = \frac{2,091,000}{93.6} = 22,340 \text{ mm}^3$$

$$\text{Thus } M_y = 345 (22,340) = 7.707 \times 10^6 \text{ N-mm} = 7.707 \text{ kN-m}$$

$$M_e = \pi^2 E C_b d \frac{I_{yc}}{L^2} = (1,974,000)(1)(186) \left(\frac{\frac{182,076}{2}}{1500^2} \right)$$

$$= 14.77 \times 10^6 \text{ N-mm} = 14.77 \text{ kN-m}$$

Using $\frac{M_e}{M_y} = \frac{14.77}{7.707} = 1.928$ in [Figure 3.1.3.6-3](#),

find $\frac{M_c}{M_y} = 0.87$ for channels.

Therefore

$$M_c = 0.87 (7.707) = 6.705 \text{ kN-m}$$

$$\text{and } \frac{M_c}{S_f} = \frac{6.705 \times 10^6}{22,340} = 300 \text{ MPa}$$

If the stress gradient in the simple lip is ignored, the effective widths of the lip on the compression flange will be the same as the values calculated in [Example 3.1-1](#) at 300 MPa. Calculate the effective width for the web assuming the neutral axis to be at the center of the web.

$$\text{With web } \frac{w}{t} = 150 \quad \text{and } S = \frac{572}{\sqrt{300}} = 33$$

$$\frac{w}{t} = 4.55S$$

From [Figure 3.1.3.1.2-4](#) at $\psi = -1$ and $\frac{w}{t} = 4.55S$, the section is just at the fully effective line.

With the neutral axis lower than assumed so that $\psi > -1$, a small portion of the web will actually be ineffective. Ignore this small ineffective area in this problem for simplicity. The section and its properties in flexure are then as shown in the [Figure 6.2.1.1-1](#) for [Example 3.1-1](#).

The section modulus at the critical moment is

$$S_c = \frac{1,915,000}{98.57} - 19,428 \text{ mm}^3$$

The moment capacity

$$M_u = \left(\frac{M_c}{S_f} \right) S_c = 300(19,428) = 5.83 \times 10^6 \text{ N-mm} = 5.83 \text{ kN-m}$$

6.2.1.8 Example 3.1-8, Torsional Stiffness of Open and Closed Sections

This example illustrates the difference in relative torsional stiffness of open and closed sections. Apply a torque T to each of the sections in [Figure 6.2.1.8-1](#) and compare stress and rotation for members cantilevered 750 mm.

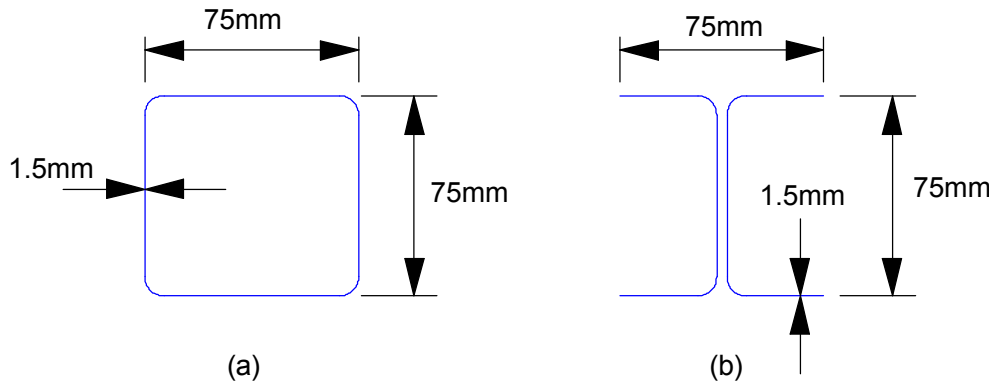


Figure 6.2.1.8-1 Open and closed sections

$$\text{For (a), } v_{tc} = \frac{T}{2 \times 75^2 \times 1.5} = \frac{T}{16,875}$$

$$J = \frac{4(75^2)^2}{4\left(\frac{75}{1.5}\right)} = 632,810 \text{ mm}^4$$

$$\phi_c = \frac{T}{632,810G}$$

$$\text{For (b), } J = \frac{1}{3}(4 \times 75)(1.5)^3 = 337.5 \text{ mm}^4$$

$$v_{to} = \frac{T(1.5)}{337.5} = \frac{T}{225}$$

$$\phi_o = 0.00296 \frac{T}{G}$$

$$\text{Comparing } \frac{v_{to}}{v_{tc}} = 75 \quad \frac{\phi_o}{\phi_c} = 1875$$

Consider flange bending (from warping restraint) to take the torque in (b).

$$\delta = \frac{PL^3}{3EI}$$

$$P = \frac{T}{75}$$

$$L = 750 \text{ mm}$$

$$I = \frac{1.5(75)^3}{12}$$

$$E = 2.5G$$

$$\delta = \frac{\left(\frac{T}{75}\right)(75)^3}{3(2.5G)(52,734)} = 14.22 \frac{T}{G}$$

The rotation is twice this deflection divided by 75 mm. This rotation divided by 750 mm represents an average ϕ_w .

Therefore:

$$\text{ave. } \phi_w = \frac{2\delta}{75 \times 750} = 0.000506 \frac{T}{G} = 0.171\phi_o$$

The rotational stiffness of the open section is often highly dependent on the flange bending rather than St. Venant's torsion. An enormous increase in rotational stiffness can be achieved by using the same material to produce a closed section.

6.2.2 EXAMPLES FOR SECTION 3.2

6.2.2.1 Example 3.2-1, Section Properties and Stresses in a Curved Member With Web(s) in the Plane of Curvature

This example illustrates the evaluation of section properties and stresses in a curved member with web(s) in the plane of curvature. Consider the square tubular section 90 mm x 90 mm with 1.2 mm wall that has a 120 mm radius of curvature, a. Determine its flexural properties and compute the maximum stresses developed from a moment of 1500 kN-mm.

Properties: Refer to [Figure 3.2.2.1-2\(c\)](#) for definitions of variables used for the half section.

$$a_i = 120 - 45 = 75 \text{ mm}$$

$$b'_i = 0.7\sqrt{75(1.2)} = 6.64 \text{ mm}$$

$$a_o = 120 + 45 = 165 \text{ mm}$$

$$b'_o = 0.7\sqrt{165(1.2)} = 9.85 \text{ mm}$$

$$\text{half area } A = (90 + 6.64 + 9.85)(1.2) = 127.8 \text{ mm}^2$$

$$Z = -1 + \frac{120}{127.8} [(9.85 + 1.2) \ln 165 - (6.64 + 1.2) \ln 75 - 9.85 \ln(165 - 1.2) + 6.64 \ln(75 + 1.2)] \\ = 0.05488$$

Stresses:

$$\text{Maximum } f_b = \frac{M}{aA} \left(1 - \frac{c}{(a-c) \times Z} \right)$$

where $c = 45 \text{ mm}$

$$A = 255.6 \text{ mm}^2$$

$$Z = 0.05488$$

$$f_{b\max} = \left(\frac{1500 \times 10^3}{120 \times 255.6} \right) \left(1 - \frac{45}{(120-45)0.05488} \right) = -485.8 \text{ MPa}$$

Had the full section been used and the stress calculated from the common expression for flexural stress

$$I = \frac{2(1.2)(90)^3}{12} + 2(1.2)(90)(45)^2 = 583,200 \text{ mm}^4$$

$$f_b = -\frac{1500 \times 10^3 (45)}{583,200} = -115.7 \text{ MPa}$$

which is about one quarter the actual maximum stress. (The negative sign is applied because the stress is known to be compression).

Calculate f_{btr} from [Equation 3.2.2.1-6](#) when

$$B = \frac{1.7(90 / 2 - 1.2)}{\sqrt{75(1.2)}} = 7.85 > 17; \quad \text{Use } B = 1.7$$

Therefore $f_{btr} = 1.7 (485.8) = 826 \text{ MPa}$ at inside flange.

Calculate f_r from [Equation 3.2.2.1-8](#)

$$f_r = \frac{485.8(6.64 \times 1.2)}{75 \times 1.2} = 43.0 \text{ MPa}$$

6.2.2.2 Example 3.2-2, Properties and Stresses in a Curved Tubular Section

This example illustrates the evaluation of properties and stresses in a curved tubular section. Consider a circular tubular section with a diameter of 40 mm, a wall thickness of 1.2 mm, and longitudinal radius of curvature of 120 mm. Evaluate the flexural properties and the stress developed from a moment of 200 kN-mm using the expressions in the preceding section.

$$I = \pi R^3 t = \pi (20)^3 (1.2) = 30,160 \text{ mm}^4$$

$$g = \frac{120(1.2)}{20} = 0.36 > 0.335$$

Using the von Karman approach for $a = 120$ mm

$$j = 1 - \frac{9}{10 + 12(0.36)^2} = 0.221$$

$$q = \frac{6}{5 + 6(0.36)^2} = 1.038$$

Since $g < 1.472$,

$$i = \frac{2}{3(0.221)\sqrt{3(1.038)}} = 1.709$$

Using the pipe stress analysis approach for $a = 120$ mm

$$j = \frac{0.36}{1.65} = 0.218$$

$$i = \frac{0.9}{g^{2/3}} = 1.778$$

Using the pipe stress analysis values, the effective moment of inertia for stiffness would be

$$0.218(30,160) = 6575 \text{ mm}^4$$

The stress from the 200 kN-mm moment using [Equation 3.2.2.2-3](#) is

$$(1.778) \frac{200 \times 10^3 (20)}{30,160} = 236 \text{ MPa}$$

6.2.3 EXAMPLE FOR SECTION 3.3

6.2.3.1 Example 3.3-1, Stiffness, Denting, and Oil Canning

This example illustrates the use of the equations for stiffness, denting, and oil canning in the design of a body panel where

$$L_1 = 26" (660 \text{ mm}) \quad L_2 = 30" (762 \text{ mm})$$

1. Begin with:

$$R_1 = 225" (5,715 \text{ mm})$$

$$t = 0.028" (0.71 \text{ mm})$$

$$R_2 = 620" (15,748 \text{ mm})$$

$$F_y = 27,000 \text{ psi (186 MPa)}$$

Calculate stiffness first:

$$H_c = \frac{26^2}{8(225)} + \frac{30^2}{8(620)} = 0.557" (14.15 \text{ mm})$$

$$\alpha = 2.571 \sqrt{\frac{0.557}{0.028}} = 11.47$$

From [Table 3.3.4-1](#), using α and $A = 0.049$

$$k = A\alpha^2 = 6.44 \quad (k = 6.31 \text{ using the simplified approach}) \quad (\text{Equation 3.3.4-7})$$

$$K = \frac{9.237(29.5 \times 10^6)(0.028)^2(0.557)\pi^2}{(6.44)(26)(30)\sqrt{0.91}} = 245.1 \text{ lb/in} (42.9 \text{ N/mm})$$

or $K = 250.1 \text{ lb/in} (43.8 \text{ N/mm})$ using the simplified approach for k .

Denting energy:

From [Figure 3.3.4-3](#), F_{yd}/F_y is approximately equal to 1.6. The energy

$$W = \frac{56.8 \left[1.6 \times 27,000(0.028)^2 \right]^2}{245.1} = 265.8 \text{ in-lb} (30,040 \text{ N-mm})$$

or $W = 260.5 \text{ in-lb} (29,400 \text{ N-mm})$ using the simplified approach for k .

Critical oil canning load:

Check that R_1/L_1 , R_2/L_2 , L_1/L_2 are within the limits stated by inspection and $L_1L_2 = 780 < 1200$.

$$C = 0.645 - 0.0005(780) = 0.255$$

$$\lambda = 0.5 \sqrt{\left(\frac{780}{0.028}\right) \sqrt{\frac{12(0.91)}{225 \times 620}}} = 7.85$$

$$R_{cr} = 45.929 - 34.183(7.85) + 6.397(7.85)^2 = 171.77$$

$$P_{cr} = \frac{(0.255)(171.77)\pi^2(29.5 \times 10^6)(0.028)^4}{780(0.91)} = 11.04 \text{ lb} (49.1 \text{ N})$$

2. One means of increasing K , W , and P_{cr} would be to increase the thickness.

If $t = 0.030"$ (0.762 mm),

$$\alpha = 11.08$$

$$A = 0.052$$

$$k = 6.38 \quad (k = 6.43 \text{ using the simplified approach})$$

$$K = \frac{9.237(29.5 \times 10^6)(0.030)^2(0.557)\pi^2}{(6.38)(26)(30)\sqrt{0.91}} = 283.9 \text{ lb/in}$$

or $K = 281.8 \text{ lb/in}$ using the simplified approach for K .

$$W = \frac{56.8 \left[1.6 \times 27,000(0.030)^2 \right]^2}{283.9} = 302.4 \text{ in-lb}$$

or $W = 304.7 \text{ in-lb}$ using the simplified approach

$$\lambda = 0.5 \sqrt{\left(\frac{780}{0.030}\right)} \sqrt{\frac{12(0.91)}{225 \times 620}} = 7.58$$

$$R_{cr} = 154.59$$

$$P_{cr} = \frac{(0.255)(154.59)\pi^2(29.5 \times 10^6)(0.030)^4}{780(0.91)} = 13.1 \text{ lb}$$

3. Alternatively, the thickness can be retained at 0.028 in (0.71 mm) and the radii of curvature decreased. If R_2 is changed to 480 in (12.192 mm).

$$H_c = 0.610$$

$$\alpha = 12$$

$$k = 6.335$$

and $K = 272.8 \text{ lb/in}$ (274.4 lb/in using the simplified approach)

Then $W = 238.8 \text{ in-lb}$ (237.5 in-lb using the simplified approach)

$$\lambda = 8.37$$

$$R_{cr} = 207.8$$

$$P_{cr} = 13.36 \text{ lb}$$

6.2.4 EXAMPLE FOR SECTION 3.4

6.2.4.1 Example 3.4-1, Spacing Criteria for Connection of a Flat Plate

This example illustrates the evaluation of the spacing criteria for connection of a flat plate. Design the spacing for connecting the flat plate to the hat section shown in [Figure 6.2.4.1-1](#).

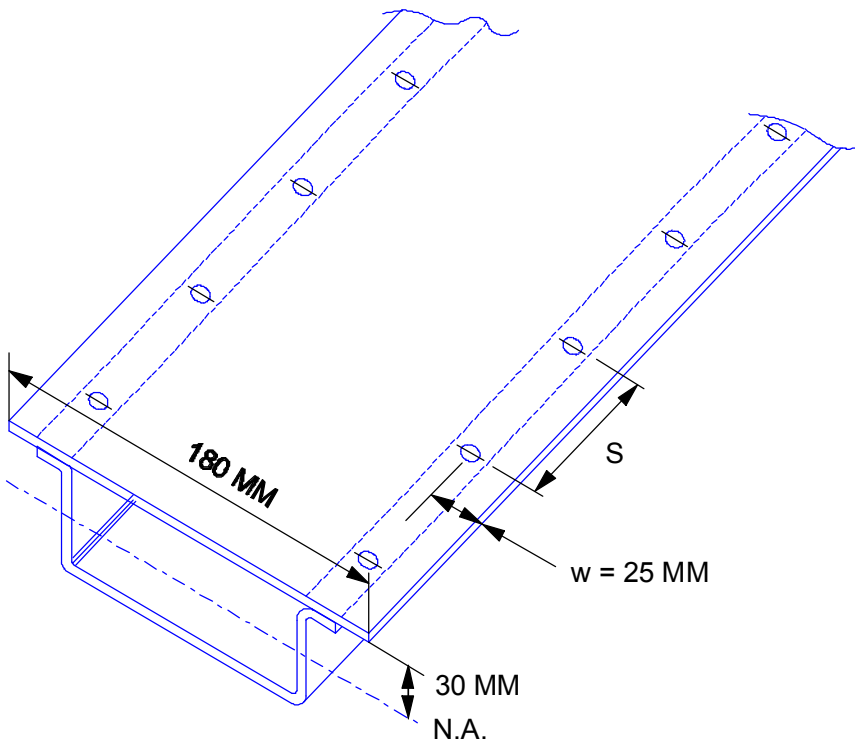


Figure 6.2.4.1-1 Spacing for a connection of a flat plate

The maximum or critical compression stress in the plate is 300 MPa. $F_y = 345 \text{ MPa}(50 \text{ ksi})$ and $t = 2.5 \text{ mm}$.

$$\text{At } F_u = 300 \text{ MPa} = 345 \left(1 - \frac{345}{4F_e}\right) \quad (\text{From } \text{Equation 3.1.2.5-1})$$

$$F_e = 661.25 \text{ MPa}$$

$$\frac{KL}{r} = \sqrt{\frac{1,974,000}{661.25}} = 54.6$$

Therefore $s \leq (0.48)(1)(2.5)(54.6) = 65.5 \text{ mm}$ from [Equation 3.4.2.3.4-1](#) using factor $C = 1$.

With an edge distance of 25 mm,

$$s \leq 3(25) = 75 \text{ mm}$$

which does not govern in this case. If the edge distance w is changed to 15 mm, then

$$3(15) = 45 \text{ mm.}$$

The 45 mm, however, is less than $500(2.5)\sqrt{345} = 67.3 \text{ mm}$ (the least required) so that the 67.3 mm should be compared with the 65.5 mm value.

At this point, the shear force per spot can be evaluated using either [Equation 3.4.4-2](#) or [3.4.4-3](#) with $s \leq 65.5$ mm and $n = 2$.

Thus, if it is desired to transfer a shear force V_m of 50 kN to the section with $I = 10^6$ mm at a 60 mm connection spacing, from [Equation 3.4.4-2](#),

$$V_s = \left(\frac{60}{2} \right) \frac{50 \text{ kN} (2.5 \times 180 \times 30)}{10^6} = 20.25 \text{ kN / spot}$$

$$= 4.55 \text{ kips / spot}$$

A spot weld is satisfactory per [Table 3.4.1.6-1](#).

6.2.5 EXAMPLES FOR SECTION 3.5

6.2.5.1 Example 3.5-1, Strain Life Estimated for Two Steels of Different Strength Levels

Determine the difference in fatigue strength for two steels being considered for use in a double edge notch tensile strip shown in [Figure 6.2.5.1-1](#). Assume the part will be loaded under a completely reversed ($R = -1$) axial loading. Compare the fatigue strength for initiating a crack in 500,000 cycles, for a hot rolled 1005 carbon steel and a HF80 steel. The properties for the steels are shown in [Table 6.2.5.1-1](#) (taken from [Table 3.5.6.1-1](#)).

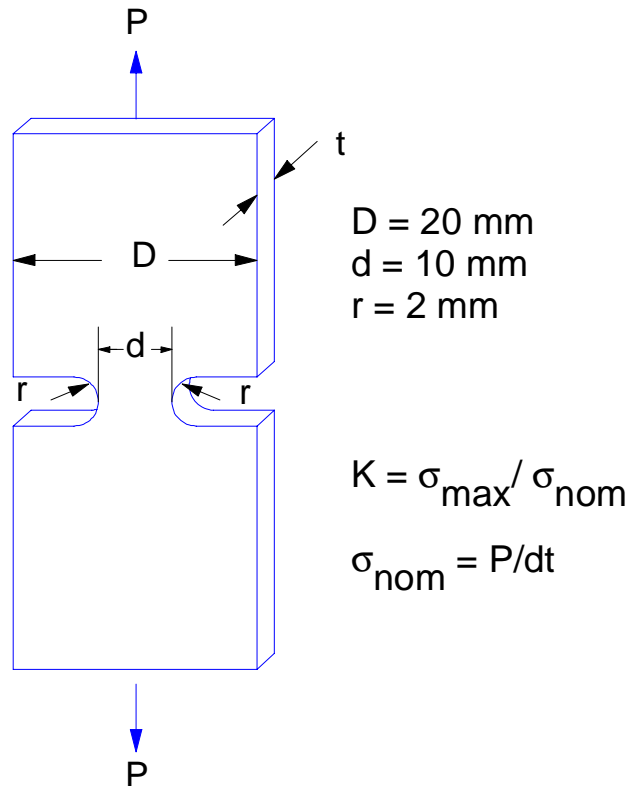


Figure 6.2.5.1-1 Double notched tensile strip

Table 6.2.5.1-1 Steel properties
(Values are taken from [Table 3.5.6.1-1](#))

Property	1005 Hot Rolled	HF80
Monotonic		
Tensile strength, S_t , MPa	356	657
Yield strength, S_y , MPa	234	596
Modulus of elasticity, E , MPa	2.07×10^5	2.07×10^5
Cyclic stress strain		
Strain hardening exponent, n'	0.200	0.096
Strength coefficient, K' , MPa	834	981
Cyclic stress life		
Fatigue strength coefficient σ'_f , MPa	878	1512
Fatigue strength exponent, b	-0.129	-0.119
Fatigue ductility coefficient, ϵ'_f	0.46	2.214
Fatigue ductility exponent, c	-0.536	-0.826

The calculations are made as follows:

The material constant a used to calculate K_f is determined as¹

$$a \text{ (in inches)} = 10^{-3} \left(\frac{300,000}{S_t} \right)^{1.8}$$

Equation 6.2.5.1-1



where S_t = Tensile Strength (in psi)

1005	HF80
$a = 10^{-3} \left[\frac{300,000}{356 \times 145} \right]^{1.8}$ $= 0.0238 \text{ inches}$ $= 0.603 \text{ mm}$	$a = 10^{-3} \left[\frac{300,000}{657 \times 145} \right]^{1.8}$ $= 0.00788 \text{ inches}$ $= 0.200 \text{ mm}$

The theoretical stress concentration factor K_t is found in [Reference 2](#) as $K_t = 2.3$ ([Figure 6.2.5.1-2](#)). From [Equation 3.5.3.3-2](#):

$$K_f = 1 + \frac{K_t - 1}{1 + \frac{a}{r}}$$

1005	HF80
$K_f = 1 + \frac{2.3 - 1}{1 + \frac{0.603}{2}}$ $= 2.0$	$K_f = 1 + \frac{2.3 - 1}{1 + \frac{0.200}{2}}$ $= 2.18$

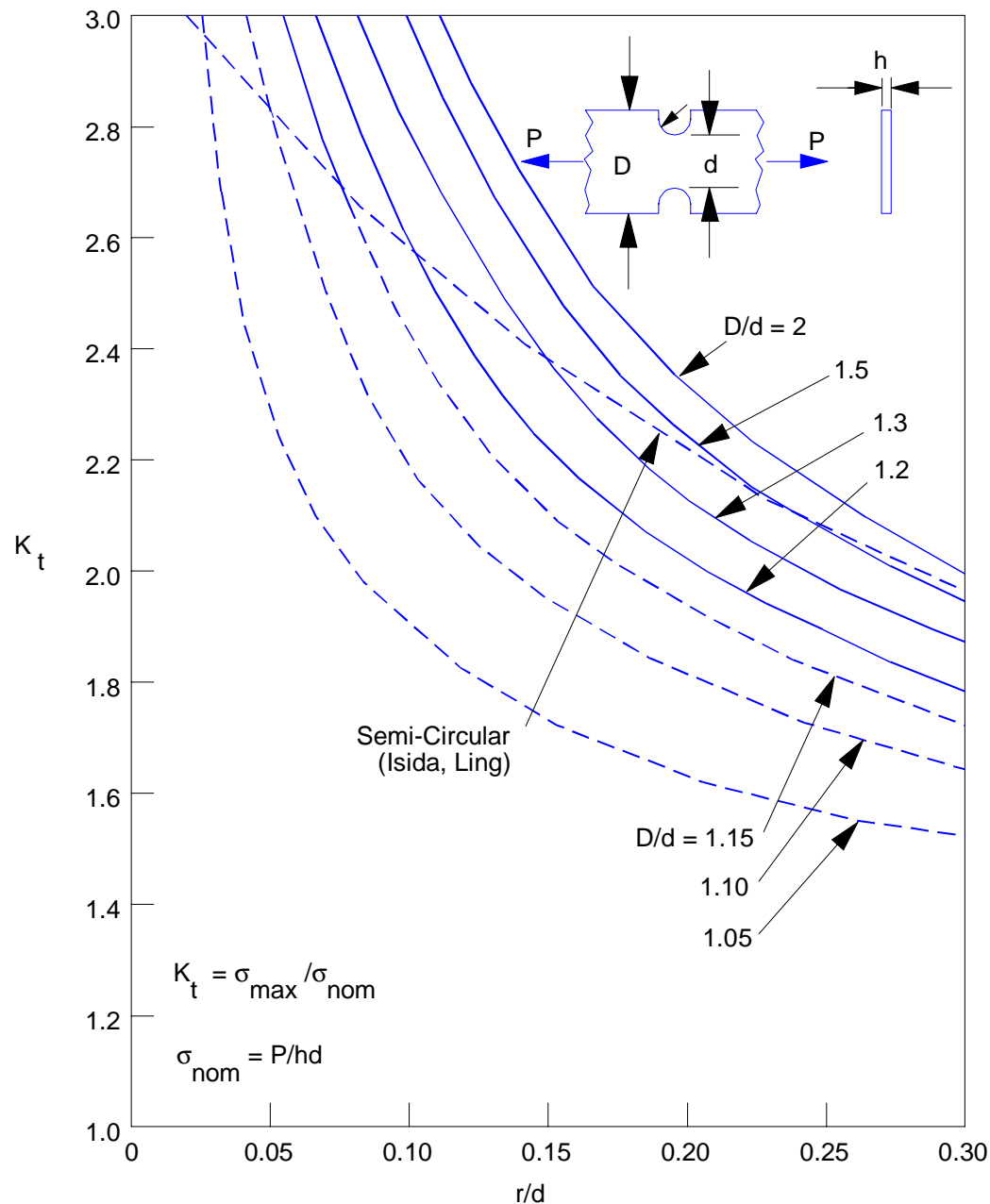


Figure 6.2.5.1-2 Stress concentration factor K_t for a flat tension bar with opposite U notches ([Reference 2](#))

The cyclic stress range is calculated from [Equation 3.5.4.1-3](#):

$$\Delta\sigma = 2\sigma'_f (2N_f)^b$$

1005	HF80
$\Delta\sigma = 2(878)(10^6)^{-0.129}$ $= 291 \text{ MPa}$	$\Delta\sigma = 2(1512)(10^6)^{-0.119}$ $= 576 \text{ MPa}$

The total strain range is the sum of the elastic and plastic ranges according to [Equation 3.5.4.1-5](#):

$$\Delta\varepsilon = \left[\frac{2\sigma'_f}{E} \right] (2N_f)^b + 2\varepsilon'_f (2N_f)^c$$

1005	HF80
$\Delta\varepsilon = \frac{2(878)(10^6)^{-0.129}}{2.07 \times 10^5} + 2(0.46)(10^6)^{-0.536}$ $= 0.0014 + 0.00053$ $= 0.00193$	$\Delta\varepsilon = \frac{2(1512)(10^6)^{-0.119}}{2.07 \times 10^5} + 2(2.214)(10^6)^{-0.826}$ $= 0.00278 + 0.000049$ $= 0.00283$

The nominal cyclic stress range is obtained from [Equation 3.5.4.2-4](#):

$$\Delta S = \frac{\sqrt{\Delta\sigma \Delta\varepsilon E}}{K_f}$$

1005	HF80
$\Delta S = \frac{\sqrt{291 \times 0.00193 \times 2.07 \times 10^5}}{2}$ $= 170 \text{ MPa}$	$\Delta S = \frac{\sqrt{576 \times 0.00283 \times 2.07 \times 10^5}}{2.18}$ $= 266 \text{ MPa}$

The calculations demonstrate that the high strength steel, HF80, provides a significantly higher fatigue strength than the 1005 steel for initiation of a crack after 500,000 cycles. However, the

increase in fatigue strength is not in proportion to the increase in monotonic yield strength or monotonic tensile strength:

$$\frac{S_y(\text{HF80})}{S_y(1005)} = \frac{596}{234} = 2.55 \quad \text{monotonic properties}$$

$$\frac{S_t(\text{HF80})}{S_t(1005)} = \frac{657}{356} = 1.85 \quad \text{monotonic properties}$$

$$\frac{\Delta S(\text{HF80})}{\Delta S(1005)} = \frac{266}{170} = 1.56 \quad \text{fatigue properties}$$

The appropriateness of using a higher strength steel for a particular application would have to be based upon additional considerations such as material costs, formability, and weldability. The reader is reminded, as discussed in [Section 3.5.7](#), that the increase in fatigue strength of sheet steels with increasing yield strength may not be realized in welds of those same steels.

6.2.5.2 Example 3.5-2, Fatigue Life Estimate of a Tensile-Shear Spot Welded Specimen

Estimate the fatigue life of a tensile-shear spot welded specimen subjected to the maximum cyclic force of 2,500 N with $R=0$. The spot weld specimen made of low carbon steel ($\beta=2.0$) has a thickness of 1.4 mm, a width of 38.0 mm, and a nugget diameter of 6.0 mm.

The calculations are as follows:

From [Equation 3.5.7.3.1-4](#)

$$K_i = \frac{F}{2t\sqrt{\pi W(36t^2 + D^2)}} \sqrt{36t^2 + \beta \times D^2} = \frac{2500}{2(1.4)\sqrt{\pi(38)(36 \times 1.4^2 + 6.0^2)}} \sqrt{36 \times 1.4^2 + 2.0 \times 6.0^2} = 94.5 \quad \text{MPa}\sqrt{\text{mm}}$$

The fatigue life of the spot welded specimen with 50% reliability is calculated via [Equation 3.5.7.3.1-8](#) follows:

$$N_f = \left(\frac{K_i}{1223} \right)^{1/(-0.187)} = \left(\frac{94.5}{1223} \right)^{1/(-0.187)} = 884,000 \quad \text{cycles}$$

The fatigue life of the spot welded specimen with 99.7% reliability is calculated via [Equation 3.5.7.3.1-9](#) as follows:

$$N_f = \left(\frac{K_i}{433} \right)^{1/(-0.187)} = \left(\frac{94.5}{433} \right)^{1/(-0.187)} = 3,430 \quad \text{cycles}$$

6.2.5.3 Example 3.5-3, Fatigue Properties Using the Load-Life (P-N) Method

The fatigue data (load amplitude vs. life) for the SAE key-hole specimen made of RQC-100³ are given in [Table 6.2.5.3-1](#). Failure is defined as a crack of 2.54 mm (0.1 in). Load-control tests were performed on the SAE keyhole samples. Determine statistics of the fatigue properties of the P-N equation.

Table 6.2.5.3-1 Load amplitude versus life data for the SAE key-hole specimen made of RQC-100

Load Amplitude (kN) P_a	Cycles To Failure N_f
88.9	60
66.7	194
62.3	290
53.4	650
35.6	3,600
17.8	55,000
17.8	107,500
17.8	140,000
15.6	200,000
13.3	605,000

The calculations are as follows:

Results of the least squares analysis ($n=10$) are shown below

$$\hat{A} = 25.171; \quad \hat{B} = -4.721; \quad s = 0.292; \quad r^2 = 0.993; \quad s_A^2 = 0.226; \quad s_B^2 = 0.0185$$

Thus,

$$m = -0.212$$

From [Equations 3.5.9.1-6](#) and [3.5.9.1-8](#),

$$\hat{C}_{Pf} = 0.0620; \quad \hat{\mu}_{Pf} = 206.791$$

From [Equation 3.5.9.1-10](#),

$$\hat{C}_{Nf} = 0.298$$

The P-N curve is illustrated in [Figure 6.2.5.3-3](#).

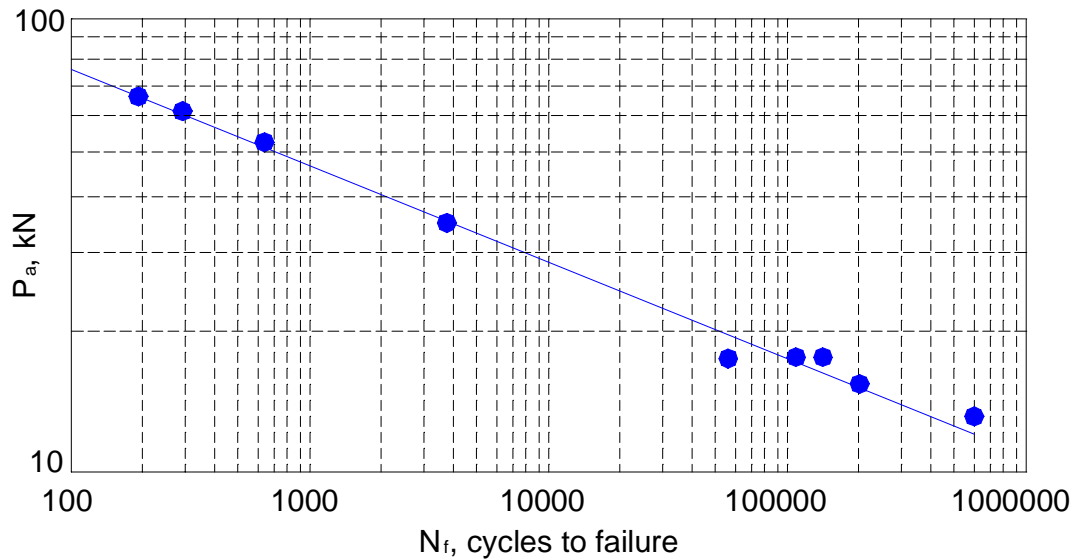


Figure 6.2.5.3-3 Load versus life (P-N) curve for the SAE key-hole specimen made of RQC-100

6.2.5.4 Example 3.5-4, Fatigue Properties Using the Stress-Life (S-N) Method

The fatigue data (stress amplitude vs. life) for the smooth specimens made of RQC-100 are given in [Table 6.2.5.4-1](#). Crack initiation is defined as an average crack of 2.54 mm (0.1 in). Determine statistics of the fatigue properties of the $\sigma_a - 2N_f$ equation.

The calculations are as follows:

Results of the least squares analysis ($n=15$) are shown below

$$\hat{A} = 70.956; \hat{B} = -9.732; s = 1.397; r^2 = 0.690; s_A^2 = 133.606; s_B^2 = 3.270$$

Therefore,

$$b = -0.103$$

From [Equations 3.5.9.2-4](#) and [3.5.9.2-5](#),

$$\hat{\mu}_{\sigma'_f} = 1467.035; \hat{C}_{\sigma'_f} = 0.145$$

From [Equations 3.5.9.2-3](#),

$$\hat{C}_{2N_f} = 2.458$$

The S-N curve is shown in [Figure 6.2.5.4-4](#).

Table 6.2.5.4-1 Stress Amplitude Versus Life Data for the Smooth Specimens Made of RQC-100

Stress Amplitude (MPa) σ_a	Reversals to Failure $2N_i$
870	228
785	390
625	880
605	978
745	1,320
580	1,900
705	2,330
545	4,240
560	4,400
565	4,460
620	54,900
495	38,300
525	167,000
505	185,000
380	580,000

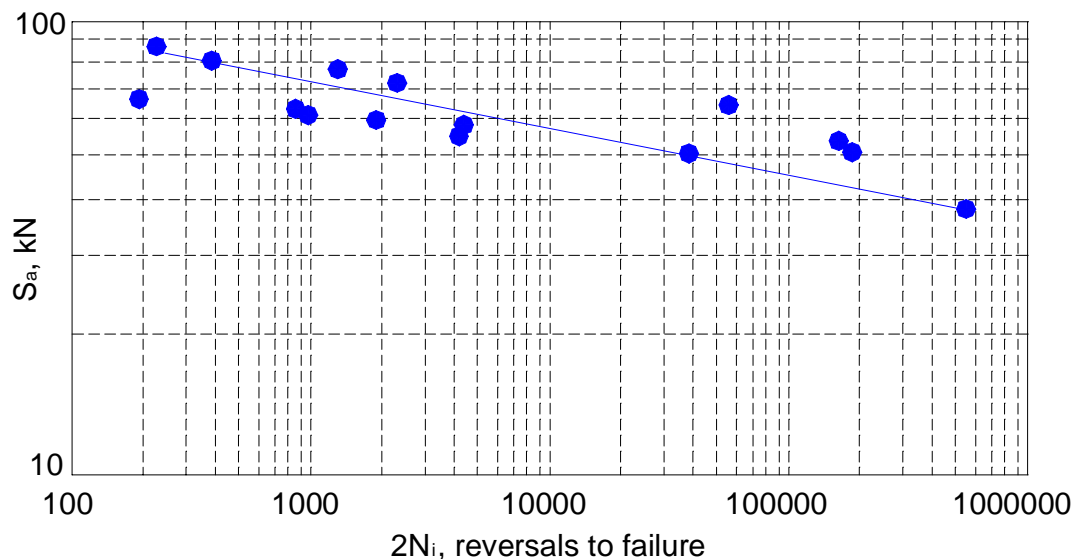


Figure 6.2.5.4-4 Stress versus life curve for the SAE key-hole specimen made of RQC-100

6.2.5.5 Example 3.5-5 Fatigue Properties Using the Plastic Strain-Life Method

The fatigue data (plastic strain amplitude vs. life) for the smooth specimens made of RQC-100 (Reference 5) are given in [Table 6.2.5.5-1](#). Crack initiation is defined as an average crack of 2.54 mm (0.1 in). Note that any plastic strain amplitude less than 0.001 are ignored because of the experimental error in measuring and determining plastic strains at long lives. Determine statistics of the fatigue properties of the ϵ_a - $2N_f$ equation.

Table 6.2.5.5-1 Plastic strain amplitude versus life data for the smooth specimens made of RQC-100

Plastic Strain Amplitude ϵ_a^p	Reversals to Failure $2N_i$
0.015597	228
0.011208	390
0.006981	880
0.007077	978
0.006401	1,320
0.003398	1,900
0.002594	2,330
0.002667	4,240
0.002295	4,400
0.002271	4,460

The calculations are as follows:

Results of the least squares analysis ($n=10$) are shown below

$$\hat{A} = -0.361 \quad \hat{B} = -1.430 \quad s = 0.234 \quad r^2 = 0.954 \quad s_A^2 = 0.236 \quad s_B^2 = 0.00811$$

Statistical fatigue properties are determined as follows:

$$c = -0.103$$

From [Equations 3.5.9.3-4](#) and [3.5.9.3-5](#),

$$\hat{\mu}_{\epsilon_f} = 0.237 \quad \hat{C}_{\epsilon_f} = 0.165$$

From [Equations 3.5.9.3-1](#),

$$\hat{C}_{2N_f} = 0.237$$

The plastic strain amplitude-life curve is presented in [Figure 6.2.5.5-5](#).

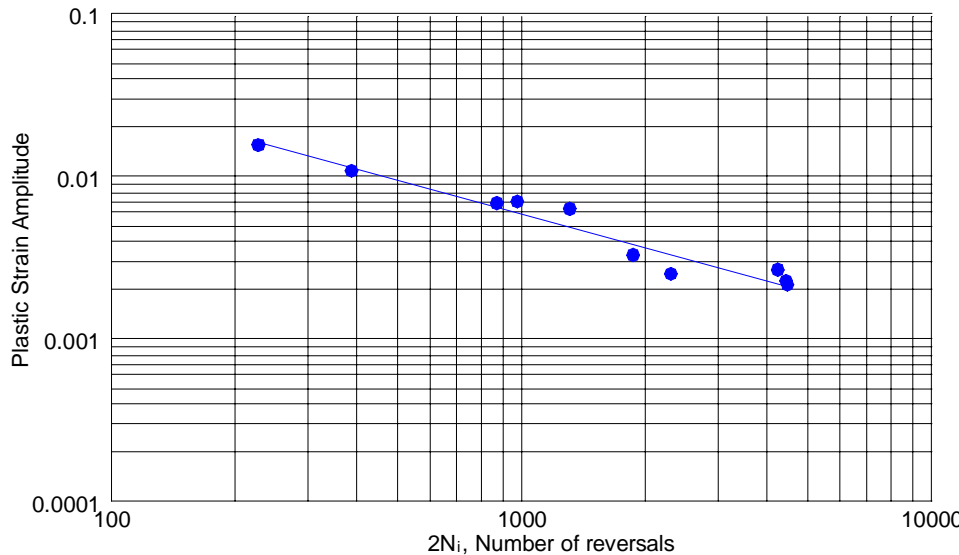


Figure 6.2.5.5-5 Plastic strain amplitude versus life curve for the SAE key-hole specimen made of RQC-100

6.2.5.6 Example 3.5-6 Statistical Cyclic Stress-Strain Curve

For the RQC-100 material, the statistical cyclic stress-strain properties can be determined

$$n' = \frac{b}{c} = \frac{0.103}{0.699} = 0.147$$

$$\hat{\mu}_{K'} = \frac{\mu_{\sigma'_f}}{(\mu_{\epsilon'_f})^{n'}} = \frac{1467}{0.777^{0.147}} = 1522.4 \quad MPa$$

Because σ'_f and ϵ'_f are log-normally distributed, K' will follow the lognormal distribution.

Hence,

$$\hat{C}_{K'} = \sqrt{(1 + \hat{C}_{\sigma'_f}^2)(1 + \hat{C}_{\epsilon'_f}^2)^{(n')^2} - 1} = 0.15$$

REFERENCES FOR SECTION 6.2

1. *Fatigue Design Handbook*, Advances in Engineering, Volume 4, Society of Automotive Engineers, Edited by J.A. Graham, J.F. Millan, and F. J. Appl, 1966.
2. Peterson, R.E., Stress Concentration Factors, John Wiley and Sons, 1974.
3. Tucker, L. and Bussa, S., "The SAE Cumulative Fatigue Damage Test Program," SAE 750038, 1975.

7.1 AISI/CARS USER'S MANUAL

The Computerized Application and Reference System (CARS) is a computerized version of the Automotive Steel Design Manual. This section contains the User's Manual for CARS. Most of the contents of this section are also available through the CARS on-line help system.

[Table 7.1-1](#) lists the main sections of the User's Manual.

Table 7.1-1 AISI/CARS User's Manual contents

Section	Description
<u>7.1.1</u>	CARS installation, startup, and uninstallation instructions
<u>7.1.2</u>	CARS operating environment
<u>7.1.3</u>	Overview of the CARS applications
<u>7.1.4</u>	CARS Instrument Panel
<u>7.1.5</u>	CARS Design Key
<u>7.1.6</u>	CARS GAS
<u>7.1.7</u>	CARS MAP
<u>7.1.8</u>	CARS ASDM
<u>7.1.9</u>	CARS Test Drive
<u>7.1.10</u>	Technical Support
<u>7.1.11</u>	Copyrights, notices and license agreements

7.1.1 INSTALLATION, STARTUP, AND UNINSTALLATION INSTRUCTIONS

7.1.1.1 System Requirements

The minimum system requirements for CARS include the following:

- IBM PC or compatible
- CPU (486 or higher recommended)
- Windows 95, 98, 2000, or NT
- Hard disk with at least 60 Mbytes of free space
- 16Mbytes of physical RAM (32Mbytes recommended)
- SVGA monitor (800 x 600 resolution and 256 colors recommended)
- Microsoft compatible mouse

Optional system requirements include a digitizing tablet compatible with the Wintab tablet driver for Microsoft Windows.

7.1.1.2 Installation

To install CARS:

- Close all other Windows programs, including Microsoft Office.
- Use the Start Menu to run SETUP for CARS. If you are installing from drive D:
 - Use the Start Menu and select Run.
 - In the Run dialog box, type D:\SETUP and choose OK.
 - Follow the installation instructions provided by the setup program.
 - CARS requires Adobe Acrobat 5.0 or later to display the Automotive Steel Design Manual contents which are stored in Acrobat PDF format. If you instruct SETUP to install Acrobat 5.0 onto your system, please run SETUP again after Acrobat is installed to complete the CARS installation. If you are not sure whether you have Acrobat 5.0 on your system Setup can search your local drives to find Acrobat 5.0.
- If Acrobat is already installed on your system, SETUP will proceed to install the CARS program files, data files and security files. After all files are copied to the hard drive, the "AISI CARS 2002" program group and contents are created.
- For Windows 95 and Windows 98 systems, the installation program will display the registration screen. Follow the instruction to install authorization. For Windows NT systems, the installation program will install the Windows NT drivers for the security system. Restart Windows NT to load the drivers and run the registration program in the program group "AISI CARS 2002".

7.1.1.3 Authorization

The CARS program is copy protected to ensure the latest CARS version utilization, to facilitate user registration, and to prevent unauthorized use.

Two types of authorization is available - temporary and permanent. Temporary authorization is valid for 7 days and permanent authorization is valid for approximately two (2) years. Updates will be sent more frequently to ensure that only the latest version of CARS is utilized.

The CARS security system creates six files (of which four are hidden) in the WINDOWS\DEI\CARS.L1 directory. If these files are deleted or moved (i.e., during disk optimization), access to the CARS program will be denied.

7.1.1.4 AISI CARS **2002** Folder

The CARS Installation program creates a folder, AISI CARS 2002, on the Start Menu. The AISI CARS 2002 Folder contains the following icons and shortcuts:



CARS Registration



CARS Design Key



CARS Geometric Analysis of Sections (GAS)



CARS Material Archive Program (MAP)



CARS Automotive Steel Design Manual



Unit Conversion



Read Me



Help



Uninstall CARS

To start a CARS application , click the shortcut of the CARS application you want to run or click the Instrument Panel shortcut to display . Refer to the appropriate section for details on the available options in the selected application.

7.1.1.5 Uninstalling CARS

Use the CARS uninstall utility that is located in the AISI CARS 2002 folder. Click on the Uninstall CARS 2002 shortcut. Click on the desired uninstall option, Automatic or Custom.

7.1.2 OPERATING ENVIRONMENT

CARS operates interactively and is controlled by a series of menus and popup windows. Screen specific features provide additional controls with help screens only a keystroke away. Error checking of keyboard entries eliminates erroneous input entries from reaching the equation solving stage.

See [Section 7.1.2.1](#) for CARS General Input Rules.

See [Section 7.1.2.2](#) for CARS Function Key Shortcuts.

See [Section 7.1.2.3](#) for CARS Mouse Usage.

See [Section 7.1.2.4](#) for CARS Tablet Usage.

7.1.2.1 General Input Rules

CARS identifies valid input entries quickly and rejects invalid key entries. A "message" is provided to indicate the input specification attempt is either illegal or invalid. Reenter the input

in an acceptable format or within the specified limits. This procedure eliminates erroneous input entries from reaching the equation solving stage. A warning message indicates the input specification attempt is valid but not recommended.

CARS accepts integer and decimal notation.

"Illegal" input entries are classified as inappropriate characters or function keys during a menu selection or input entry. (For example, a letter or an inactive function key cannot be accepted when an input prompt requests a number from 1 to 4.)

"Invalid" input entries are classified as one of the following types of entries:

- Numerical overflow or underflow:
Overflow: Input > 9.99999E+11
Underflow: Input < 9.99999E-11
- Illegal numerical format:
(two decimal points, a decimal point following an exponential "E" character, etc.)
- Inappropriate negative values:
(for dimensions, Poisson's ratio, etc.)
- Entries that do not satisfy the problem's constraints:
(inner radius > outer radius, etc.)
- Input variables that exceed the maximum number of characters available as displayed during input entry.
- "Not Recommended" input entries are classified as inappropriate values for procedures developed exclusively for steel. (These procedures are not recommended for non-steel materials.) CARS screens non-steel materials by uniting the values of E, Modulus of Elasticity, to:

203,000 MPa (\pm 3000 MPa)
29,500 ksi (\pm 500 ksi)

Enter the BACKSPACE key to clear characters entered, thus permitting corrections before clicking the left mouse button or entering the RETURN key. These actions commence CARS input entry checking and advance to the next prompt, if CARS finds the input acceptable in terms of format and numerical limits.

In general, input entries can occur at three locations:

1. Menu level
2. Pulldown or popup window level
3. Input request display prompts

Menu Level:

At the menu level either pull down a window menu or enter activated function keys. Any other character is rejected and CARS may "beep" to notify that the entry is illegal and a new entry is needed.

Pulldown or popup window level:

At the pulldown or popup window level several options are available. A selection is made by entering the keystroke identifying the corresponding selection. If any character other than highlighted keystrokes is entered, CARS "beeps" to notify that the entry is illegal and a new entry is needed.

Input Request Display Level Prompting:

At the input request display level, several multi-character input entries are made. Each entry is made by typing the appropriate numerical values in integer or decimal format using as many characters as required. The maximum number of characters for an input entry is displayed by a series of "blank" characters. Invalid characters are rejected as previously described and the cursor is repositioned such that rejected input can be reentered.

These input restrictions implemented by CARS act to minimize the potential for error when entering input data. Time is saved since the equation solving routines are not initiated with illegal or invalid input variables that are known to give inaccurate results. These restrictions serve to minimize the time necessary to obtain correct solutions within CARS.

7.1.2.2 Function Key Shortcuts

Function key shortcuts are provided within CARS for program control and operation as follows:

Function Key	SHIFT	CTRL	CTRL+SHIFT	ALT	ALT+SHIFT
F1					
F2					
F3					
F4		Close the window		Exit	
F5					
F6		Go to the next window	Go to the previous window		
F7					
F8					
F9					
F10	Activate the menu bar				
F11					
F12					

7.1.2.3 Mouse Usage

A CARS session can be controlled more easily when using a mouse/cursor tracking device. CARS supports mouse tracking operations with the Microsoft Mouse.

The Microsoft Mouse has a serial and bus version. The serial version connects to a standard serial card. The bus version uses its own special interface card.

The movement of the mouse replaces the UP, DOWN, LEFT, and RIGHT arrow keys in the keyboard mode. The left key of the mouse replaces the RETURN in the keyboard mode. In most cases, the right key of the mouse replaces the ESC key in the keyboard mode.

To pull down a submenu, merely "click" (the equivalent of a keyboard's RETURN) on the desired submenu. Moving the mouse within the submenu will change the current active submenu option. Select the desired submenu option by moving the cursor to highlight the option and click.

Some popup windows may contain more listings than can be displayed on the screen at one time. The status bar to the right of the popup window indicates the relative location of the information that is currently displayed in the popup. Merely scroll down to the desired option and select as usual. When using a mouse, move to the up or down arrow in the status bar and click to begin scrolling.

Popup windows can be moved or resized with a mouse except for those windows that contain more listings than can be displayed on the screen at one time. This feature is useful when the popup window covers important information that should be viewed concurrently with the popup window.

To move a popup window, click with the left button on any part of the popup window border except the corners and, while keeping the button pressed, drag the mouse until the popup window is where you want it to be. Releasing the left button sets the popup window to the new position.

To resize a popup window, click with the left button on any corner of the popup window border and, while keeping the button pressed, drag the mouse until the window attains the desired size. Releasing the left button sets the popup window to the new size.

To exit a popup window without selecting any option, enter the ESC key or mouse equivalent to "back up" one window or to return to the active pulldown submenu.

To install the mouse, see the manual that came with the mouse/cursor tracking device.

7.1.2.4 Tablet Usage

GAS is a Wintab-compliant application, which means it can support all the Wintab-aware pointing devices. Wintab is an industry standard tablet driver for Microsoft Windows. Refer to your tablet user's manual for the installation of the Wintab driver.

If GAS detects the tablet, all the tablet-related menu options will become active.

7.1.3 OVERVIEW

CARS consists of the following applications:

- CARS Instrument Panel
- CARS Design Key
- CARS ASDM (Automotive Steel Design Manual)
- CARS GAS (Geometric Analysis of Sections)
- CARS MAP (Material Archive Program)
- Unit Conversion
- CARS Help

The CARS Instrument Panel is a toolbar program from which any of the other CARS applications can be started. The CARS Instrument Panel can also be used to switch from one CARS application to another. See [Section 7.1.4](#) for details.

CARS Design Key provides numerical and graphical solutions to the equations and algorithms found in the Automotive Steel Design Manual. Interactive design procedures (flowcharts) automatically lead users through the design process while permitting them to pause to perform parametric studies and trend analyses and then continue with selectively overridden values, if desired. See [Section 7.1.5](#) for details.

CARS GAS calculates geometric section properties (nominal and effective) for arbitrary thin walled sections and interfaces with the CARS Design Key to determine member capacities. See [Section 7.1.6](#) for details.

CARS MAP is used to locate, view, create and edit material properties. See [Section 7.1.7](#) for details.

CARS ASDM quickly and selectively accesses Material, Design, Manufacturing and related information found in the Automotive Steel Design Manual. Design guidelines, tables, equations, figures and other reference information can be located and viewed quickly and easily. Hyperlinks and keyword searches permit rapid identification of desired information. Printed reports of any reference information can be obtained. See [Section 7.1.8](#) for details.

CARS Unit Conversion converts entered value of selected units of measure from one system of units to other systems of units. There are ten categories of units of measure available for unit conversion. The ten categories are angular, area, force, inertia, length, mass, moment, stress, temperature and mass density.

The CARS Help system provides index and context sensitive help features. All the contents of this section of the Manual are included in the Help system.

7.1.4 CARS INSTRUMENT PANEL

The CARS Instrument Panel is a toolbar that lets you start a CARS application or switch from one CARS application to another. To start the CARS Instrument Panel, double-click the CARS Instrument Panel icon in the program group where your CARS applications are installed. The CARS Instrument Panel toolbar is then displayed.



The icons in the CARS Instrument Panel toolbar are for applications as follows:



CARS Design Key



CARS Geometric Analysis of Sections (GAS)



CARS Material Archive Program (MAP)



CARS Automotive Steel Design Manual (ASDM)



Unit Conversion



CARS Test Drive



Help

To start a CARS application using the CARS Instrument Panel toolbar, click the button of the CARS application you want to run. Refer to the appropriate section for details on the available options in the selected application.

To make the CARS Instrument Panel visible from any CARS application, select the ‘Always on Top’ option in the Application Control Menu.

To display the CARS Instrument Panel toolbar whenever you start Windows, copy the CARS Instrument Panel into the Windows Startup group as follows:

- From the CARS 2002 program group, select the CARS Instrument Panel icon.
- In the Program Manager window, choose Copy from the File menu.
- In the To Group box, select Startup.
- Choose the OK button.

To close the CARS Instrument Panel toolbar, do one of the following:

- Open the Application Control Menu using the mouse, or press ALT+SPACEBAR, and then choose Close.
- Double-click on the Application Control box.

7.1.5 CARS DESIGN KEY

7.1.5.1 CARS Design Key Overview

The CARS Design Key provides numerical and graphical solutions to the equations and algorithms found in the Automotive Steel Design Manual. Interactive design procedure automatically lead users through the design process while permitting them to pause to perform parametric studies and trend analyses.

7.1.5.1.1 Operating Environment

7.1.5.1.1.1 Tree-Type Selection

CARS Design Key uses a tree-type selection box for the selection of a design procedure, an equation, a figure, or a table. In this type of list box, the items are listed in the format of a collapsible/expandable tree. A “+” sign in front of a list item means that item is expandable. A “-” indicates that the item is collapsible. A check mark (✓) indicates that the item is a selectable item. Press the + key to expand a branch. Press the - key to collapse a branch. Double click an item to expand or collapse the branch. Select a design procedure and click OK or double click the design procedure to select it. If the View button is active, the selected equation or figure can be viewed in a separate window.

Use the Folder List button to modify the tree structure display. Click on Folder List button to bring up the popup menu with two options - Expand All and Collapse All. Expand All expands all the branches in the tree structure and Collapse All collapses all the branches in the tree structure. The View Subsections option permits changing the format of the collapsible/expandable tree in the Tree-Type Selection Box. If the View Subsection option is ON, the tree structure will contain the titles of all levels of subsections. If View Subsections option is OFF, only the titles of the chapters and sections will be in the tree structure. For example, if you expand Section 3.1 with View Subsections option OFF, all the equations in Section 3.1 will be listed for subsequent selection.

7.1.5.1.1.2 Copy Graphics onto Clipboard

To copy graphics in the Design Key window to the Clipboard

- Press the Print Scrn key if you want to copy the whole screen or press ALT and Print Scrn keys simultaneously to copy the active window.
- Start Paint.
- Paste the copied graphics in Paint using the Edit/Paste command or by pressing the CTRL and V Keys simultaneously.
- Save the image using File/Save.

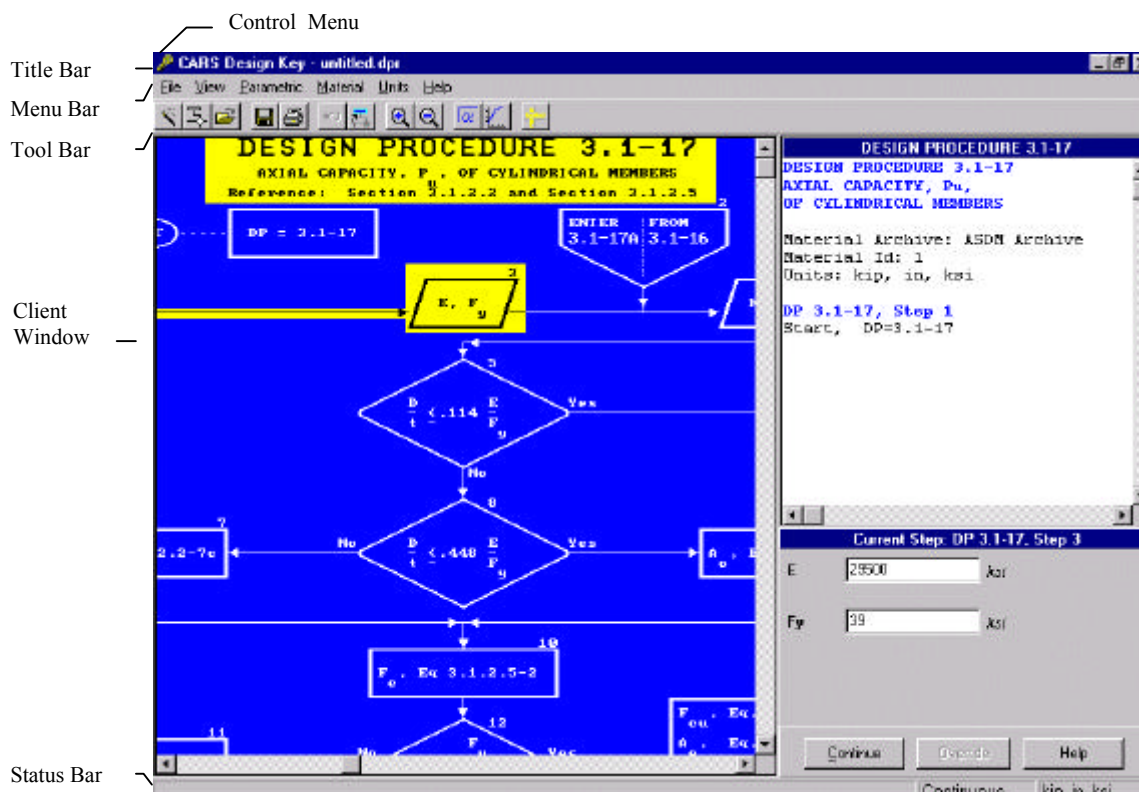
7.1.5.1.1.3 Copy Results onto Clipboard

To copy numerical results in Design Key onto the Clipboard:

- Use mouse to highlight a portion of the results
- Press the CRTL and C keys simultaneously
- Paste the copied results into the desired application using the Edit/Paste command or by pressing the CTRL and V Keys simultaneously.

7.1.5.2 CARS Design Key Screen

The CARS Design Key screen contains a title bar, a menu bar, a toolbar, a status bar and a client window.



7.1.5.2.1 Design Key Title Bar

The Title Bar displays at the top of screen the name of the active application (CARS Design Key), and the current design file name.

7.1.5.2.2 Design Key Menu Bar

The Menu Bar displays all CARS Design Key menus across the top of the CARS Design Key screen, below the title bar.

7.1.5.2.3 Design Key Toolbar

The Toolbar contains buttons that give you quick mouse access to many commands and features in CARS Design Key. The following buttons are available on the toolbar:

- Design Expert
- New Design
- Open Design
- Undo Button
- Restart Design
- Save
- Print



Zoom In



Zoom Out



Equation/Single Calculation



Equation/Trend Analysis



Unit Conversion

7.1.5.2.4 Design Key Client Window

The Client window is the area that shows the current viewing contents. The client window is used to show one of the following:

- Design Procedure and Results
- Data Input for the Design Procedure
- Data Input for a Parametric Study
- Trend Analysis Results (XY Plot and Numerical Results)

7.1.5.2.5 Design Key Status Bar

The Status Bar shows information and messages at the bottom of the CARS Design Key Screen that help you use CARS Design Key. When a menu option is highlighted or when the cursor is pointing to a button on the toolbar, the status bar shows the associated help message. Otherwise, the status bar consists of two areas:

- Design Control: Shows whether the control of the Design Procedure is Continuous or Single Step.
- Current System of Units: Shows the current system of units as kip,in,ksi or N,mm,MPa

7.1.5.3 Design Key File Menu

Provides commands for file operations. The file menu includes Design Expert, New Design, Open Design, Restart Design, Close, Save, Save As, Print and Exit.

7.1.5.3.1 Design Expert (Design Key File Menu)

Permits selecting the design procedure by answering interactive questions presented in flowchart fashion.

To start the Design Expert, click on the Design Expert button on the toolbar:



Design Expert

7.1.5.3.2 New Design (Design Key File Menu)

Permits starting a new design by identifying the design procedure to be analyzed from a list of design procedures available in CARS . Design procedures are numbered for easy reference as A.B-CYZ where A.B refers to the section in Automotive Steel Design Manual (ASDM) that the

design procedure originates (e.g., 3.1 for Section 3.1 Straight Linear Members), YZ is a numerical identifier (e.g., 19 for Design Procedure 3.1-19 Torsion of Members) and C is either blank (in most cases) or a "G" to signify that a GAS results file is required to provide default section properties when solving a design procedure (e.g., Design Procedure 3.1-G19 Torsion of Members using section properties).

The design procedures are listed in the format of a collapsible/expandable tree. See [Section 7.5.1.1.1](#) for details.

To quickly start a new design, click on the New Design button on the toolbar.



New Design

7.1.5.3.3 Open Design (Design Key File Menu)

Permits opening a previously saved CARS Design file (.DPR) and returning to a specific point in a previous CARS session. CARS prompts for the file name to open.

To quickly open a previous saved design, click on the Open Design button on the toolbar.

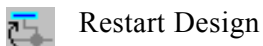


Open Design

7.1.5.3.4 Restart Design (Design Key File Menu)

Permits restarting the current design procedure. CARS will go back to the beginning of the current design procedure. All the previously entered values in the current session will be retained as the default values in the new session.

To quickly restart the design, click on the Restart Design button on the toolbar.



Restart Design

7.1.5.3.5 Close (Design Key File Menu)

Permits closing the current design procedure. If the design has not yet been saved, CARS will prompt to save the design before closing.

7.1.5.3.6 Save (Design Key File Menu)

Permits saving the design results to the currently specified file. Note that if the file name has not yet been specified, the file name UNTITLED.DPR is displayed in the title bar.

To quickly save the design, click the Save button on the toolbar.



Save

7.1.5.3.7 Save As (Design Key File Menu)

Permits saving the design to a different file. CARS prompts for a file name.

7.1.5.3.8 Print (Design Key File Menu)

Displays the Print dialog box to print the contents in the active window. Before using this command, you must have installed and selected a default printer. To install a printer, see your Windows documentation.

CARS provides the option to print the design flowpath along with the results.

To quickly print contents in the active window, click on the Print button on the toolbar.



7.1.5.3.9 Exit (Design Key File Menu)

Ends the CARS Design Key session. CARS prompts to save any unsaved design. Other ways to exit CARS Design Key are as follows:

- Open the Application Control Menu using the mouse, or press ALT+SPACEBAR, and then choose Close.
- Double-click on the application Control box.

7.1.5.4 Design Key View Menu

Provides commands to view the design procedure and to change the program control.

7.1.5.4.1 Zoom In (Design Key View Menu)

Permits magnifying the design procedure image by 20%. Successive use of this command will continue to zoom in on the design procedure by 20%.

To quickly magnify the design procedure, click on the Zoom In button on the toolbar.



7.1.5.4.2 Zoom Out (Design Key View Menu)

Permits shrinking the design procedure image by 20%. Successive use of this command will continue to zoom out on the design procedure by 20%.

To quickly shrink the design procedure image, click the Zoom Out button on the toolbar.



7.1.5.4.3 Full Screen (Design Key View Menu)

CARS will display the flowchart using the whole window. The results and instruction box will be covered.

If Full Screen is active, a check mark (✓) will appear in front of the menu option.

7.1.5.4.4 Single Step (Design Key View Menu)

CARS will pause after displaying the results of each step. A dialog box with two buttons, Continue and Override, will appear. Choose Continue to continue with the procedure and proceed to the next flowbox. If the current step calculation involves an equation, figure or table, the Override button will be active. Otherwise, the Override button will be inactive. A click on the Override button permits overriding the current result by inputting the desired value. The analysis will then continue using the new value.

If Single Step is active, a check mark (✓) will appear in front of the menu option.

7.1.5.4.5 Continuous (Design Key View Menu)

CARS shows the result of each step and proceeds directly to the next step. CARS will pause only when data input is necessary. This option should be used when the desired result is of primary interest. Continuous should not be used when the resulting flowpaths are of interest in addition to the desired results.

If Continuous is active, a check mark (✓) will appear in front of the menu option.

7.1.5.4.6 Undo (Design Key View Menu)

Permits undo the previous action and restore the design to the status before the action. This command is available only if there is something to undo.

To quickly undo the design, click on the Undo button on the toolbar.



Undo Button

7.1.5.5 Design Key Parametric Menu

Provides commands to initiate a parametric study of an equation or figure. The equation or figure desired for parametric study is selected using a collapsible/expandable tree. See [Section 7.1.5.1.1.1](#) for how to use a collapsible/expandable tree.

7.1.5.5.1 Equation (Design Key Parametric Menu)

Two types of parametric studies are available for equation - Single Calculation and Trend Analysis.

7.1.5.5.1.1 Single Calculation (Design Key Parametric/Equation Menu)

Provides one numerical result based on a set of input data. CARS identifies the necessary input variables to solve the equation in the Input Tab. The Reference Tab contains the equation image. Enter the appropriate input values in the data fields. Click the Solve button to initiate the calculation. After displaying the results, the input fields become inactive. Click the Redo button to clear the current result and new input data can be entered to perform another calculation. Click the Close button to finish Single Calculation.

To quickly perform a single calculation of an equation, click the Equation/Single Calculation Button on the toolbar.



Equation/Single Calculation Button

7.1.5.5.1.2 Trend Analysis (Design Key Parametric/Equation Menu)

Calculates results for 101 sets of input data for a specified equation. For Trend analysis, the Input Tab window is similar to that described for single calculation. In addition, a varying parameter from the equation must be identified using the option button in front of the parameter to define the varying parameter. Only one varying parameter can be defined. Only the varying parameter can have a value in the "To" column. The Reference Tab contains the equation image.

Click the Solve button to initiate the calculation. Trend Analysis results are shown in two tabs - Numerical Results Tab in tabular form and Graphical Results Tab in XY Plot form. In XY Plot form, the varying parameter value is used for X-axis values and the calculated result is used for Y-axis values. Grid lines are displayed to assist data lookup. In tabular form the trend analysis results are represented in two columns, one for the varying parameter and another for the calculated result.

After the results are displayed, the input fields in the data input window become inactive. Click the Redo button to close two result tabs and new input data can be entered to perform another calculation. Click the Close button to finish Trend Analysis.

Click the Export button to export the results to a file. There are three export options - As Text File, As Excel File and As Metafile. Export As Text File option will save the numerical results in ASCII text format. Export as Excel File option will save the numerical results in Excel file format. Export as Metafile option will export the XY-plot in metafile format.

Click the Print button to print the results. The printed output will contain the input parameters, numerical results and graphical results.

To quickly perform a trend analysis of an equation, click the Equation/Trend Analysis Button on the toolbar.



Equation/Trend Analysis Button

7.1.5.5.2 Figure (Design Key Parametric Menu)

CARS identifies the necessary input variables to solve the equations found in the selected figure. Enter the appropriate input values in the data fields. Click the Solve button to initiate the calculation. After displaying the results, the input fields become inactive, Click the Redo button to clear the current result and new input data can be entered to perform another calculation. Click the Close button to finish.

7.1.5.6 Design Key Material Menu

Provides commands related to the current material. The Material menu includes Show Current Material and Set Current Material.

7.1.5.6.1 Show Current Material (Design Key Material Menu)

Lists the properties of the current material in a dialog box. Included in the box are constants for five steel properties: Modulus of Elasticity, Shear Modulus, mass density, Poisson's Ratio and coefficient of thermal expansion. Click OK to close the dialog box.

7.1.5.6.2 Set Current Material (Design Key Material Menu)

Permits changing the current material. CARS Design Key displays a submenu from which to choose the current material. The submenu includes CARS Default, ASDM Archive, Steel Company Archive, and User Defined Archive.

7.1.5.6.2.1 CARS Default (Design Key Material/Set Current Material Menu)

Sets the current material to the CARS default material set in Material Archive Program (MAP).

7.1.5.6.2.2 ASDM Archive (Design Key Material/Set Current Material Menu)

Selects the current material from the ASDM Archive.

7.1.5.6.2.3 Steel Company Archive (Design Key Material/Set Current Material Menu)

Selects the current material from a Steel Company Archive.

7.1.5.6.2.4 User Defined Archive (Design Key Material/Set Current Material Menu)

Selects the current material from a User Defined Archive.

7.1.5.7 Design Key Units Menu

Provides commands related to current system of units and unit conversion. The Units menu includes kip,in,ksi (kilopounds, inches, kilopounds per square inch), N,mm,MPa (Newton, millimeter, MegaPascal), and Unit Conversion.

7.1.5.7.1 kip,in,ksi (Design Key Units Menu)

Permits changing the active system of units to kip,in,ksi. If set, a check mark (✓) will appear before this option.

7.1.5.7.2 N,mm,MPa (Design Key Units Menu)

Permits changing the active system of units to N,mm,MPa. If set, a check mark (✓) will appear before this option.

7.1.5.7.3 Unit Conversion (Design Key Units Menu)

Converts entered value of selected units of measure from one system of units to other systems of units. There are ten categories of units of measure available for unit conversion: angular, area, force, inertia, length, mass, moment, stress, temperature, and mass density.

To quickly access the unit conversion tool, click the Unit Conversion button on the toolbar.



Unit Conversion

7.1.5.8 Design Key Help Menu

Provides commands for accessing online help. The Help menu includes Contents, Search for Help on, and About.

7.1.5.8.1 Contents (Design Key Help Menu)

Displays the CARS Design Key online Help contents. It provides a comprehensive list that summarizes the organization of topics in the Help system.

7.1.5.8.2 Search for Help on (Design Key Help Menu)

Opens the Search dialog box for Help to find information related to topics on which you want more information.

To use the Search For Help On command, type the topic or select it from the list in the Search dialog box, and then choose the Show Topics button to see related topics. To display a particular topic from the list of topics, select it and then choose the Go To button.

7.1.5.8.3 Obtaining Technical Support (Design Key Help Menu)

Displays the help information regarding how to obtain the technical support.

7.1.5.8.4 About (Design Key Help Menu)

Displays information on the development and sponsors of the CARS program.

7.1.5.9 CARS Design Key Error Messages

Error messages are provided within CARS Design Key showing an error identification number and associated message. Refer to this section to correlate the error identification number with a brief error message description. These descriptions define each error and provide suggestions for correction of the problem.

Error 2: Invalid input combinations:

This combination of input variables is not reasonable, i.e., Poisson's ratio is larger than 1.

Remedy: Review input variables as defined. Pay attention to the relationship between variables and the physical meaning of each variable.

Error 21: The file is not generated by the current version of CARS.

Remedy: Review file name entered and ensure it is generated by the current version of CARS.

Error 24: Unmatched cross section name

The cross section name in the nominal property file and the cross section name in the effective property file is different.

Remedy: Review the nominal property file and the effective property file to make sure the cross section names in the files are the same.

Error 25: Incorrect loading direction

The loading direction in the effective property file is not the desired loading direction.

Remedy: Review the loading direction in the effective property file. For example, Design Procedure 3.1-G16 requires axial loading and Design Procedures 3.1-G9 and 3.1-G10 need moment loading.

Error 26: No torsional constant in the result file

The nominal property file does not contain torsional constant. GAS does not calculate torsional constant for a composite section (consisting of materials with differing Modulus of Elasticities).

Remedy: Choose a nominal property file for a homogeneous cross section.

7.1.6 CARS GAS (GEOMETRIC ANALYSIS OF SECTIONS)

7.1.6.1 CARS GAS Overview

The Geometric Analysis of Sections (GAS) calculates geometric section properties for arbitrary two-dimensional thin-walled sections. GAS calculates nominal section properties and effective section properties. The effective section property calculation can be based on one of the four following stress levels:

- Yield
- User specified
- Load associated
- First onset of local buckling.

Trend analyses permit parametric studies by varying section dimensions. Cross sections and their nominal properties can be saved to a geometric database. Databases can be searched by a user-specified criterion..

7.1.6.1.1 Cross Section Modeling In GAS

In general, GAS utilizes the “linear” or “midline” method for section modeling and analysis. In this method the material of the section is considered to be concentrated along the centerline or midline of straight or curved line elements. Therefore, a cross section in GAS can consist of three kinds of entities: lines, arcs and welds.

When a line or an arc is created, the default material and physical properties automatically are assigned to that entity. Line properties include material, thickness and line type. Arc properties include material, thickness and arc type. No property is needed for welds.

7.1.6.1.1.1 Line Type

Line type is used in the effective property analysis. The line type specified determines which procedure will be used to compute the effective width of that line. Four line types can be assigned to a line:

- Segment
- Intermediate Stiffener
- Edge Stiffener
- Unstiffened

GAS is shipped with the default line type set to Segment.

When a new line is created, the default line type is assigned to the new line. Use Edit Menu to modify line type of one line or a group of lines. To change the Default line type, Use Physical/Set Default Physical Properties Menu.

An Edge Stiffener is used to provide a continuous support along a longitudinal edge of the compression flange to improve the buckling stress. In other words, an Edge Stiffener is used to stiffen the compression flange. An Intermediate Stiffener Line is a line associated with an intermediate stiffener in the compression flange. An Unstiffened compression element is a flat compression element that is stiffened at only one edge parallel to the direction of stress. The Unstiffened compression element is illustrated in [Figure 3.1.2.1-1](#). If a line is a “Segment”, GAS will determine the line type according to [Section 3.11.5.5](#).

The line type specified and line type used in analysis are shown in the effective property calculation numerical results.

7.1.6.1.1.2 Arc Type

Arc type is used in the effective properties analysis. The arc type specified determines which procedure will be used to compute the effective width of that arc. Four arc types can be assigned to an arc:

- Segment
- Intermediate Stiffener
- Fully Effective
- Unstiffened

GAS is shipped with the default arc type set to Fully Effective.

When a new arc is created, the default arc type is assigned to the new arc. Use Edit Menu to modify arc type of one arc or a group of arcs. To change the default arc type, Use Physical/Set Default Physical Properties Menu.

The Fully Effective arc is assumed to be fully effective in the calculation and no effective width calculation will be done for that arc. Therefore, the Fully Effective arc should only be used for an arc which the user believes to be fully effective such as a fillet. An Intermediate Stiffener arc is an arc associated with an Intermediate Stiffener. An Unstiffened compression curved element is a curved element that is stiffened at only one edge parallel to the direction of stress. The Unstiffened curved element is illustrated in [Figure 3.1.2.3-1](#). If an arc is a “Segment”, GAS will determine the arc type according to [Section 3.11.5.5](#).

The arc type specified and the arc type used in analysis are shown in the effective property calculation numerical results.

7.1.6.1.1.3 Graphical Entity Selection

In model creation screen, entities can be selected graphically using the cursor. To select an entity, move the cursor around it and click the left button of the mouse. To select multiple entities, hold down the CTRL key, and then click each entity you want to select.

To select all the entities in a rectangular box:

- Move the cursor to one corner of the rectangular box and press left button of the mouse.
- Hold down the left button and move the cursor to the opposite corner.
- Release the left button.

Once an entity is selected, the color of the entity will be changed. To delete the selected entities, press "Delete" key or "Del" key.

The Shortcut menu will be available once any entity is selected. To activate the shortcut menu, point the cursor anywhere inside the client window and click right button of the mouse. The shortcut menu options vary depending on the selected entities.

7.1.6.1.2 GAS Database

Each GAS database contains four files as described as follows:

File Contents	File Extension	Backup File Extension
Index of Sections in Database	.IDX	.BAK
Cross Section Geometric Data	.MOD	.OLD
Nominal Properties	.NOM	.OLM
Material Archive Locations	.LOC	.LOB

Whenever a database is updated, backup files are created. Backup files are useful when a file is corrupted or accidentally deleted. Database files can be corrupted if an abnormal condition happens during an update operation, such as a power outage, no space on the hard disk, or too many files in the directory. Use the File Menu to create, open, and delete databases.

7.1.6.1.3 GAS Analysis

A GAS analysis can be a single calculation or a trend analysis. Two types of cross section properties can be calculated - nominal property and effective property. In addition, GAS can be used to compute the Axial Capacity, Flexural Capacity or Combined Axial and Flexural Stability of a member with the current cross section. Until saved using the File/Save As command, the analysis results are stored in temporary files described as follows:

Analysis Type	Temporary File Name
Single Calculation, Nominal Properties	GSN.TMP
Single Calculation, Effective Properties	GSE.TMP
Single Calculation, Axial Capacity	GSA.TMP
Single Calculation, Flexural Capacity	GSF.TMP
Single Calculation, Combined Axial and Flexural Stability	GSC.TMP
Axial Force Deflection of Stub Column	GFD.TMP
Trend Analysis, Nominal Properties	GTN.TMP
Trend Analysis, Effective Properties	GTE.TMP
Trend Analysis, Axial Capacity	GTA.TMP
Trend Analysis, Flexural Capacity	GTF.TMP
Trend Analysis, Combined Axial and Flexural Stability	GTC.TMP

7.1.6.1.3.1 Nominal Properties Calculation

GAS calculates the nominal properties of the cross section. GAS calculates 32 properties for a section without a discontinuity. If a discontinuity is found in the cross section, GAS calculates 19 properties. See [Section 3.11.3](#) for the theory of nominal properties calculation in GAS.

The nominal properties GAS calculates are as follows:

Area	Area of the section
cx	X coordinate of the centroid
cy	Y coordinate of the centroid
Ixx	Moment of inertia about X axis
Iyy	Moment of inertia about Y axis
Ixy	Product of inertia
Sx+	Section modulus about X axis in positive Y direction
Sy+	Section modulus about Y axis in positive X direction
Sx-	Section modulus about X axis in negative Y direction
Sy-	Section modulus about Y axis in negative X direction
Theta	Reference angle
Iuu	Moment of inertia about major principal axis, u axis
Ivv	Moment of inertia about minor principal axis, v axis
Su+	Section modulus about u axis at positive v direction
Sv+	Section modulus about v axis at positive u direction
Su-	Section modulus about u axis at negative v direction
Sv-	Section modulus about v axis at negative u direction
rx	Radius of gyration about X axis
ry	Radius of gyration about Y axis
J	Torsional Constant
Cw	Warping Constant
ex	X coordinate of the shear center
ey	Y coordinate of the shear center
Cuu	Shear coefficient about u axis
Cvv	Shear coefficient about v axis
Jopen	Torsional constant of the open portion
Jc	Torsional constant of the closed portion
tomax	Maximum thickness in the open portion
tmin	Minimum thickness in the closed portion
Ao	Enclosed Area
j	Section property for torsional-flexural buckling
w	Flat strip width

7.1.6.1.3.2 Effective Properties Calculation

Calculates the effective cross section and 21 properties of the effective cross section under a specified stress level:

- Yield Stress
- Specified Stress
- Stress from Loads
- At First Onset Of Local Buckling

Under the stress level of Yield Stress, GAS will calculate the effective properties of the cross section when the maximum stress in the cross section reaches the material's yield stress. Select

the load direction from among Axial, M_{x+} , M_{x-} , M_{y+} or M_{y-} . For example, for a stress level of Yield Stress and M_{x+} , GAS calculates the effective properties of the cross section when the stress at the extreme fiber reaches yield stress under positive moment about the X axis. The direction of the moment loading such as M_{x+} is defined by right-hand rule.

Under the stress level of Specified Stress, GAS will calculate the effective properties of the cross section when the maximum stress in the cross section reaches the specified stress. Select the load direction from among Axial, M_{x+} , M_{x-} , M_{y+} or M_{y-} and specify the value of the specified stress.

Under the stress level of Stress from Loads, GAS will calculate the effective properties of the cross section under the user specified loads. Specify the values of the loads - axial load, moment about X axis (M_x) and moment about Y axis (M_y).

Under the stress level of At First Onset Of Local Buckling, GAS will find the stress distribution when the first onset of local buckling occurs and calculate the effective properties of the cross section under that stress distribution.

See [Section 3.11.5](#) for the theory of effective cross section properties calculation in GAS.

The effective properties GAS calculates are as follows:

Area	Area of the section
c_x	X coordinate of the centroid
c_y	Y coordinate of the centroid
I_{xx}	Moment of inertia about X axis
I_{yy}	Moment of inertia about Y axis
I_{xy}	Product of inertia
S_{x+}	Section modulus about X axis in positive Y direction
S_{y+}	Section modulus about Y axis in positive X direction
S_{x-}	Section modulus about X axis in negative Y direction
S_{y-}	Section modulus about Y axis in negative X direction
Theta	Reference angle
I_{uu}	Moment of inertia about major principal axis, u axis
I_{vv}	Moment of inertia about minor principal axis, v axis
S_{u+}	Section modulus about u axis at positive v direction
S_{v+}	Section modulus about v axis at positive u direction
S_{u-}	Section modulus about u axis at negative v direction
S_{v-}	Section modulus about v axis at negative u direction
r_x	Radius of gyration about X axis
r_y	Radius of gyration about Y axis
I_{yc}	Moment of inertia of the compression portion about the neutral axis using the full unreduced section.
P M_{x+} M_{x-} M_{y+} M_{y-}	Reference Loads

7.1.6.1.3.3 Single Calculation

GAS calculates the cross section properties of the current cross section.

7.1.6.1.3.4 Trend Analysis

Gas calculates the cross section properties of a series of cross sections which are variations of the current cross section and are based on a user specified parameter. The parameter can be the thickness of one or a group of entities or the length of a line. GAS prompts for the parameter identification name, the parameter type (thickness of all entities, line thickness, arc thickness or line length), the range of entities (for line thickness and arc thickness), and the parameter value. An arc length can not be used as a parameter. During a trend analysis, GAS will show the current status of the analysis.

7.1.6.1.3.5 Coincident Points Merge

Before GAS starts the analysis, it will check to see if any coincident points, points with the same coordinates, exist in the model. If coincident points are detected, GAS prompts the user to merge them.

7.1.6.1.4 GAS Results Files

GAS stores the results of analyses in one of four kinds of result files. The default file extensions for GAS result files are:

Analysis Type	File Extension
Single Calculation, Nominal Properties	GSN
Single Calculation, Effective Properties	GSE
Single Calculation, Axial Capacity	GSA
Single Calculation, Flexural Capacity	GSM
Single Calculation, Combined Axial and Flexural Stability	GSC
Axial Force Deflection of Stub Column	GFD
Trend Analysis, Nominal Properties	GTN
Trend Analysis, Effective Properties	GTE
Trend Analysis, Axial Capacity	GTA
Trend Analysis, Flexural Capacity	GTM
Trend Analysis, Combined Axial and Flexural Stability	GTC

Use the View/Results command to view a GAS results file.

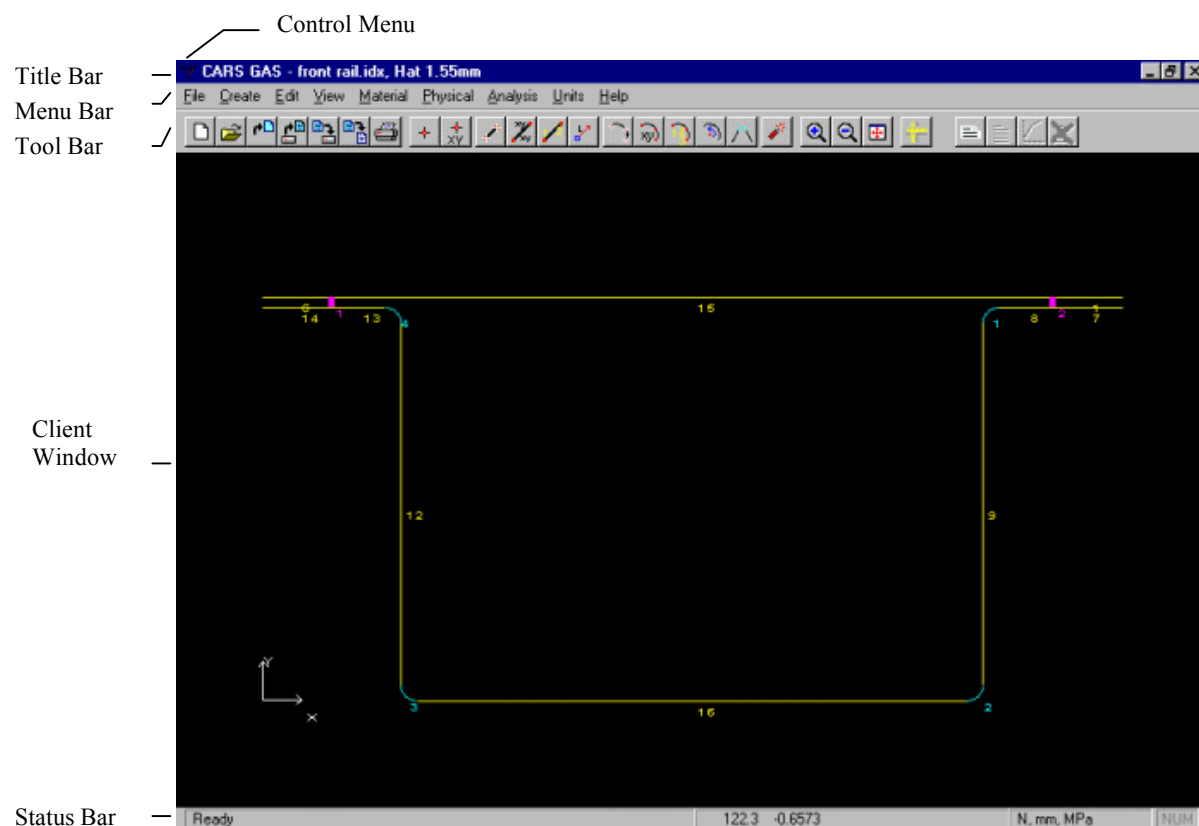
7.1.6.1.5 Tablet Usage

GAS is a Wintab-compliant application which means it can support all the Wintab-aware pointing devices. Wintab is an industry standard tablet driver for Microsoft Windows. Refer to your tablet user's manual for the installation of the Wintab driver.

If GAS detects the tablet, all the tablet-related menu options will become active.

7.1.6.2 GAS Screen

The GAS screen contains a title bar, a menu bar, a toolbar , a client window, and a status bar.



7.1.6.2.1 GAS Title Bar

The Title Bar displays at the top of the GAS screen the name of the active application (GAS or GAS Results), the database name, and the cross section name.

7.1.6.2.2 GAS Menu Bar

The Menu Bar displays all the GAS menus across the top of the GAS screen, just below the title bar.

7.1.6.2.3 GAS Toolbar

The Toolbar contains buttons that give you quick mouse access to many commands and features in GAS. The GAS toolbar is movable and dockable. To move the toolbar:

- Point between buttons on the toolbar, or point to the toolbar title bar if it is floating.
- Drag the toolbar to a new location. If the toolbar is dragged to the edge of the application window, it will dock to the edge of the window automatically.

When the toolbar is floating, it can be resized.

The following buttons are available on the toolbar:

-  New Database
-  Open Database
-  New Section
-  Get Section
-  Save Section
-  Save Section As
-  Print
-  Create Points using Cursor
-  Create Points by Specifying Coordinates
-  Create Lines using Cursor
-  Create Lines by Specifying End Point Coordinates
-  Create Lines by Specifying End Point Numbers
-  Create Lines by Specifying End Point, Length and Angle
-  Create Arcs using Cursor
-  Create Arcs by Specifying 3-point Coordinates
-  Create Arcs by Specifying Three Existing Points
-  Create Arcs by Specifying Center Point, Angle and Radius
-  Create Arcs using Tangent Lines
-  Create Welds
-  Zoom In
-  Zoom Out
-  Pan
-  Unit Conversion

7.1.6.2.4 GAS Client Window

The Client window is the area that shows the current viewing contents. The client window is used to show one of the following:

- Cross section geometry
- Graphical results of the computed nominal properties
- Graphical results of the computed effective properties

Use the View Menu to change the client window contents.

7.1.6.2.5 GAS Status Bar

The Status Bar shows information and messages at the bottom of the GAS Screen that help you use GAS. When a menu option is highlighted or when the cursor is pointing to a button on the toolbar, the status bar shows the associated help message. Otherwise, the status bar consists of four areas:

- Cursor Mode: Shows the operation mode of the cursor. The operation modes of cursor are Ready, Zoom In and Pan.
- Cursor Location: Shows the X and Y coordinates of the cursor location.
- Current System of Units: Shows the current system of units as kip,in,ksi or N,mm,MPa.
- Num Lock status: Shows whether the Num Lock key is active on the keyboard.

7.1.6.3 GAS File Menu

Provides commands for file operations including New Database, Open Database, Open, Delete Database, New Section, Get Section, Save Section, Save Section As, Delete Section, Open, Save As, Close, Save Section w/Nominal Properties, Search Database, DXF Import, DXF Export, IGES Import, NASTRAN Grid Points Import, Export to The Desktop Engineer, Export to NASTRAN PBEAM, Print Graphics and Entity List, Print Graphics and Numerical Results, Print Window, and Exit.

7.1.6.3.1 New Database (GAS File Menu)

Creates a new database. GAS displays the Select Database dialog box, in which you specify a name and location for the database. You can type the name of the database you want to create. If the database already exists, GAS will display an error message. A database name can consist of up to eight characters but can't contain spaces.

To quickly create a new database, click the New Database button on the toolbar.



7.1.6.3.2 Open Database (GAS File Menu)

Selects an existing database to be the current database. GAS displays the Database Selection dialog box, in which you specify a name and location for the database. You can type the name of the database you want to open, or select a name from the list. You can use wildcard characters to specify the type of files you want to display in the list. Once a database is selected, use the Section related commands to create, get or save cross section information. Selecting a different database does not change the current cross section even if the current cross section is from another database. If you want to copy a section from one database to another, select the target database while the section is loaded and save the section to the target database.

To quickly open an existing database, click the Open Database button on the toolbar.



7.1.6.3.3 Delete Database (GAS File Menu)

Deletes an existing database. GAS displays the Database Selection dialog box, in which to select the database you want to delete. GAS will delete all the associated files related to the selected database such as .IDX, .MOD, .NOM, .LOC, BAK, .OLD, OLM, and .OLB. See the GAS Database for descriptions of database files.

7.1.6.3.4 New Section (GAS File Menu)

Creates a new cross section. If the current section is modified, GAS will ask you to save the current cross section. You can define the section name and description in the Cross Section Definition dialog box. GAS allows up to 14 characters for a section name and up to 45 characters for the description of a section. Blank spaces are allowed in the case sensitive section name.

To quickly create a new cross section, click the New Section button on the toolbar.



New Section

7.1.6.3.5 Get Section (GAS File Menu)

Loads an existing cross section from the current database. If you have not created or selected the database, GAS first displays the Database Selection dialog box. If the database is selected, GAS displays the section names and their descriptions in the database in the Cross Section Selection dialog box from which to choose a cross section. An asterisk (*) in front of the section name indicates nominal properties of that section have been calculated and are stored in the database.

To quickly load an existing cross section from the current database, click the Get Section button on the toolbar.

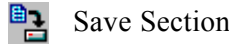


Get Section

7.1.6.3.6 Save Section (GAS File Menu)

Saves the current cross section into the current database using its existing name and description. If the current database is not specified, GAS displays the Database Selection dialog box in which to specify the current database. If the section name is not defined, GAS displays the Cross Section Definition dialog box in which to define the name and the description of the section. If GAS finds the same cross section name in the current database, GAS will prompt for confirmation before replacing the existing section in the database with the current section.

To quickly save the current cross section, click the Save Section button on the toolbar.



Save Section

7.1.6.3.7 Save Section As (GAS File Menu)

Displays the Cross Section Definition dialog box in which to define the name and the description of the section. If GAS finds the same cross section name in the current database, GAS will prompt for confirmation before replacing the existing section in the database with the current section.

To quickly save a cross section with its existing name and description use the Save Section Command or click the Save Section button on the toolbar.

To quickly save a cross section as a different name, click the Save Section As button on the toolbar.



7.1.6.3.8 Delete Section (GAS File Menu)

Displays the Section Selection dialog box, from which to select the cross section you want to delete. If the database is empty, GAS will issue an error message. If a section is accidentally deleted, use the backup files of the database to restore the cross section.

7.1.6.3.9 Open Results (GAS File Menu)

Displays the Results File Selection dialog box. You can select any previously stored GAS results file. See the GAS Results for the descriptions of GAS results files.

7.1.6.3.10 Save Results As (GAS File Menu)

Displays the Save Results File dialog box. The default file extension is shown in the dialog box according to the analysis type associated with the results file. Use the default file extension to store the results file. To use the default file extension, just type the file name without the file extension.

7.1.6.3.11 Close Results (GAS File Menu)

Closes the results viewing window and goes back to the cross section viewing window. GAS prompts to save any unsaved analysis results.

To quickly close the results, click the Close Results button on the toolbar.



7.1.6.3.12 Save Section w/Nominal Properties (GAS File Menu)

Saves the current cross section and its nominal properties, calculated by GAS, to the current database. This is useful for performing a subsequent CARS Design or a database search of sections having nominal properties. A single calculation of nominal properties for the current cross section should be performed before selecting this command.

7.1.6.3.13 Search Database (GAS File Menu)

Searches cross sections in the current database according to a user specified criterion. The search criteria are defined in the Define Database Search Criteria dialog box. The search criteria

can be a lower bound, an upper bound or a range of a selected nominal property (as calculated by GAS):

- Lower Bound: Searches for all the cross sections in the current database having a value of the user selected nominal property larger than the user specified lower bound.
- Upper Bound: Searches for all the cross sections in the current database having a value of the user selected nominal property smaller than the user specified upper bound.
- Range: Searches for all the cross sections in the current database having value of the user selected nominal property within the user specified range.

The search results are displayed in the Database Search Results dialog box. The dialog box has two display windows: search description and search results. Search description shows the database name, search property, search criteria, units system and criteria values. Search results shows the section names having nominal properties that match the search criteria and their property values in two columns. Click the New Search button to go back to the Define Database Search Criteria dialog box for another search.

7.1.6.3.14 DXF Import (GAS File Menu)

Imports the entities in a DXF file into the current cross section. A DXF file is the Data Exchange File of AutoCAD. GAS only imports two-dimensional entities such as points, lines, arcs, and polylines. The material and physical properties of the new entities imported from the DXF are assigned as the current default material and physical properties of GAS at the time when DXF file is imported. GAS cannot import DXF file generated by AutoCAD release 14 and 2000. For AutoCAD release 14 and 2000 users, please generate IGES file using AutoCAD and choose File/IGES import option.

7.1.6.3.15 DXF Export (GAS File Menu)

Exports the entities in the current cross section to a DXF file. A DXF file is the Data Exchange File of AutoCAD. GAS only exports the geometry information of the entities. The material and physical properties of the entities are not exported. Welds are exported as lines. The DXF file GAS generates is in compliance with AutoCAD release 13 DXF file format.

7.1.6.3.16 IGES Import (GAS File Menu)

Import geometry information of a cross section from an IGES file generated by CATIA using IGES 5.1file format. The Initial Graphics Exchange Specification (IGES) is an American national standard (ANSI Y14.26M) defining a neutral representation for exchange of mechanical product drawings between dissimilar Computer Aided Design (CAD) systems.

There are three types of IGES file format:

- Fixed ASCII format
- Compressed ASCII format
- Binary format

GAS only reads Fixed ASCII format.

Since a cross section in GAS is composed of lines and arcs, the following entity types are recommended to be imported into GAS from an IGES file:

- Circular Arc (Entity Type 100)
- Conic Arc (Entity Type 104)
- Polyline (Entity Type 106)
- Line (Entity Type 110)
- Rational B-Spline (Entity Type 126)

Conic Arcs and Rational B-Spline are converted into lines. If the specified IGES file contains conic arcs or rational B-Splines, GAS will prompt for number of segments for the curve conversion.

Since the entities in IGES are defined in 3D space and GAS can handle only 2D entity, the user needs to specify the projection plane to convert 3D objects to 2D objects. Three choices of the projection plane are available - XY plane, YZ plane or XZ plane.

7.1.6.3.17 NASTRAN Grid Points Import (GAS File Menu)

Imports the grid points in a NASTRAN bulk data deck file. The default type for the NASTRAN grid point files is .PTS. Since the NASTRAN grid points contain x, y and z coordinates and GAS can handle only 2D points, the user needs to specify the projection plane to convert the 3D object to a 2D object. Three choices of the projection plan are available - XY plane, YZ plane or XZ plane.

A sample NASTRAN bulk data deck file is shown as follows:

```
BEGIN BULK
GRID      6423      300.14 499.963-6.34-13
GRID      6424      306.88 498.156-1.07-12
GRID      6425      313.62 496.349-1.56-12
GRID      6426      317.45  493.2-1.81-12
ENDDATA
```

7.1.6.3.18 Export to The Desktop Engineer (GAS File Menu)

Exports the nominal properties to a Desktop Engineer compatible file.

7.1.6.3.19 Export NASTRAN PBEAM (GAS File Menu)

Export the nominal properties to a file in the format of NASTRAN PBEAM card.

7.1.6.3.20 Print Graphics and Entity List (GAS File Menu)

Displays the Print dialog box to print the graphics and the entity list in a report. Before using this command, you must have installed and selected a default printer. To install a printer, see your Windows documentation.

7.1.6.3.21 Print Graphics and Numerical Results (GAS File Menu)

Displays the Print dialog box to print the graphics and the numerical results in a report. Before using this command, you must have installed and selected a default printer. To install a printer, see your Windows documentation.

7.1.6.3.22 Print Window (GAS File Menu)

Displays the Print dialog box to print the contents in the active window. Before using this command, you must have installed and selected a default printer. To install a printer, see your Windows documentation.

To quickly print the graphics in the viewing window, click on the Print button on the toolbar.

7.1.6.3.23 Exit (GAS File Menu)

Ends the GAS session. GAS prompts to save any unsaved changes in a cross section or unsaved analysis results. Other ways to exit GAS are as follows:

- Open the Application Control Menu using the mouse, or press ALT+SPACEBAR, and then choose Close.
- Double-click the application Control box.

7.1.6.4 GAS Create Menu

Provides commands for creating entities of a cross section. Entities can be points, lines, arcs or welds. The Create menu includes Points, Lines, Arcs, Welds and Digitizing Tablet Setup.

7.1.6.4.1 Points (GAS Create Menu)

Creates new points. GAS displays a submenu from which to choose the method for point creation. The Create Point menu includes Cursor, Coordinate, and Tablet.

7.1.6.4.1.1 Cursor (GAS Create/Points Menu)

Uses cursor on the screen to define the location of new points. Use the pointing device to move the screen cursor. The current coordinate of the screen cursor is shown on the status bar and it is updated whenever you move the pointing device. Click the left button of the pointing device to create a point. When done, press ESC, click the right button or choose other commands.

To quickly create points using cursor, click on the Create Points using Cursor button on the toolbar.



Create Points using Cursor

7.1.6.4.1.2 Coordinate (GAS Create/Points Menu)

Permits creating points by inputting the coordinates. GAS displays a submenu of two options: Single Point and Group Points.

7.1.6.4.1.2.1 Single Point (GAS Create/Points/CoordinateMenu)

Creates a point by inputting its X and Y coordinates in a dialog box. Choose the More button to define the next new point. Choose OK to take the current input and finish Point Creation. Choose Cancel to ignore current input and finish Point Creation.

To quickly create points by specifying coordinates, click on the Create Points by Specifying Coordinates button on the toolbar.



Create Points by Specifying Coordinates

7.1.6.4.1.2.2 Group Points (GAS Create/Points/Coordinate Menu)

Creates a group of points by inputting their X and Y coordinates in a dialog box. Use arrow key to move between input fields. Choose OK to take the current input and finish Point Creation. Choose Cancel to ignore current input and finish Point Creation.

7.1.6.4.1.3 Tablet (GAS Create/Points Menu)

Define new points using the digitizing tablet. Once this command is selected, the screen cursor will disappear. The current coordinate of the tablet pointing device is shown on the status bar. Click the pointing device to define a point. Press ESC when done.

7.1.6.4.2 Lines (GAS Create Menu)

Creates new lines. GAS displays a submenu from which to choose the method for line creation. The submenu includes Cursor, End Points Coordinates, Existing Points, Pt/Length/Angle, and Tablet.

7.1.6.4.2.1 Cursor (GAS Create/Lines Menu)

Uses cursor on the screen to define the locations of the end points of new lines. Use the pointing device to move the screen cursor. The current coordinate of the screen cursor is shown on the status bar and it is updated whenever you move the pointing device. Click the left button of the pointing device to define an endpoint. After the first endpoint is created, GAS will display a tentative line from that endpoint to the current cursor location. After the first line is created, a new line can be connected to the previously defined line by defining a new end point. When done, press ESC, click the right button or choose other commands.

To quickly create lines using cursor, click on the Create Lines using Cursor button on the toolbar.



Create Lines using Cursor

7.1.6.4.2.2 End Points Coordinates (GAS Create/Lines Menu)

Creates a new line by inputting the X and Y coordinates of its endpoints in a dialog box. Choose the More button to define the next new line. Choose OK to accept current input and finish Line Creation. Choose Cancel to ignore current input and finish Line Creation.

To quickly create lines by specifying end point coordinates, click on the Create Lines by Specifying End Point Coordinates button on the toolbar.



Create Lines by Specifying End Point Coordinates

7.1.6.4.2.3 Existing Points (GAS Create/Lines Menu)

Create lines using the existing points. GAS displays a submenu with two options: Single Line and Group Lines.

7.1.6.4.2.3.1 Single Line (GAS Create/Lines/Existing Points Menu)

Creates a line using the existing points as its endpoints. The starting point number and ending point number of the new line are input in a dialog box. Choose the More button to define the next new line. Choose OK to accept current input and finish Line Creation. Choose Cancel to ignore current input and finish Line Creation.

To quickly create lines by specifying end point numbers, click on the Create Lines by Specifying End Point Numbers button on the toolbar.



Create Lines by Specifying End Point Numbers

7.1.6.4.2.3.2 Group Lines (GAS Create/Lines/Existing Points Menu)

Creates a group of lines by specifying their end point numbers in a dialog box. Use arrow key to move between input fields. Choose OK to accept current inputs and finish Line Creation. Choose Cancel to ignore current input and finish Line Creation.

7.1.6.4.2.4 Pt/Length/Angle (GAS Create/Lines Menu)

Creates a line by defining its starting point number, the line length and an angle. The angle, defined in degrees with positive being counter-clockwise, is the angle between the positive X axis and the line.

To quickly create lines by specifying end point, length and angle, click on the following button on the toolbar.



Create Lines by Specifying End Point, Length and Angle

7.1.6.4.2.5 Tablet (GAS Create/Lines Menu)

Create lines using a digitizing tablet. Once this command is selected, the screen cursor will disappear. The current coordinate of the tablet pointing device is shown on the status bar. Click the pointing device to define the endpoints of a line. After the first line is created, a new line can be connected to the previously defined line by defining a new end point. Press ESC when done.

7.1.6.4.3 Arcs (GAS Create Menu)

Creates new arcs. GAS displays a submenu from which to choose the method for arc creation. The submenu includes Cursor, 3-point Coordinates, 3 Existing Points, Center Pt/ Angle/Radius, Tangent Lines, and Tablet.

7.1.6.4.3.1 Cursor (GAS Create/Arcs Menu)

Uses the cursor on the screen to define the locations of points on new arcs. Use the pointing device to move the screen cursor. The current coordinate of the screen cursor is shown on the status bar and it is updated whenever you move the pointing device. Click the left button of the pointing device to define a point on the arc. After three new points are defined, GAS creates an

arc which passes through the three points. To cancel the arc creation operation, press ESC, click the right button or choose other commands.

To quickly create arcs using cursor, click on the following button on the toolbar.



Create Arcs using Cursor

7.1.6.4.3.2 3-point Coordinates (GAS Create/Arcs Menu)

Creates a new arc by inputting the X and Y coordinates of three points on the arc in a dialog box. Choose the More button to define the next new arc. Choose OK to accept current input and finish Arc Creation. Choose Cancel to ignore current input and finish Arc Creation.

To quickly create arcs by specifying 3-point coordinates, click on the following button on the toolbar



Create Arcs by Specifying 3-point Coordinates

7.1.6.4.3.3 3 Existing Points (GAS Create/Arcs Menu)

Creates an arc by identifying three existing points, which lie on the arc. An arc is created which passes through the three points in the same sequence as how they are defined. The point numbers of those three points are input in a dialog box.

To quickly create arcs by specifying three existing points, click on the following button on the toolbar



Create Arcs by Specifying Three Existing Points

7.1.6.4.3.4 Center Pt/ Angle/Radius (GAS Create/Arcs Menu)

Creates an arc by identifying its center point, the starting angle, the ending angle and the radius. The angles, defined in degrees with positive being counter-clockwise, are the angles between the positive X axis and the tangent lines. GAS will create two new points as the end points of the arc. Do not use this command to create an arc to connect to existing entities. Otherwise, connectivity between entities will not be created.

To quickly create arcs by specifying center point, angle and radius, click on the following button on the toolbar



Create Arcs by Specifying Center Point, Angle and Radius

7.1.6.4.3.5 Tangent Lines (GAS Create/Arcs Menu)

Creates an arc by identifying two lines which are tangent to the new arc. This command is ideal for arc creation between two line segments. Depending on the orientation of the line segments, there can be two or more arc generation possibilities. The arc possibilities are displayed in a different color than the normal arc color. (For two crossed lines, there are 8 possible arcs. For two lines whose intersection point lies on one of the lines, there are 4 possible arcs. For two

lines whose intersection point lies on neither of the lines, there are 2 possible arcs). If the arc displayed is not the desired arc, do not accept it. GAS will show the next possible arc and prompt for confirmation. This continues until all the possibilities have been displayed. If confirmed, a new arc will be added and the two tangent lines will be modified. For the line modification, GAS keeps the end point that is farther from the intersection point of the two lines and computes the intersection point of the line and the new arc. Thus, the modified tangent line will be from the original end point to the computed intersection point. The intersection points are automatically added to the cross section.

To quickly create arcs using tangent lines, click on the following button on the toolbar



Create Arcs using Tangent Lines

7.1.6.4.3.6 Tablet (GAS Create/Arcs Menu)

Creates arcs using a digitizing tablet. Once this command is selected, the screen cursor will disappear. The current coordinate of the tablet pointing device is shown on the status bar. Click the pointing device to define points on an arc. After three new points are defined, GAS creates an arc which passes through the three points. Press ESC when done.

7.1.6.4.4 Welds (GAS Create Menu)

Creates welds by specifying two end points of the welds. GAS prompts for the end points numbers.

7.1.6.4.5 Digitizing Tablet Setup (GAS Create Menu)

Defines the tablet coordinate system by digitizing the origin and another point on the X axis. GAS prompts for the distance between those two digitized points.

7.1.6.5 GAS Edit Menu

Provides commands for editing entities of a cross section. The Edit menu includes Undo, Redo, Coordinate System, Scale, Point Coordinates, Line End Points, Line Length, Weld End Points, Entity Renumber, Merge Coincident Points, Properties of Single Entity, Material of Group Entities, Thickness of Group Entities, Line Type of Group Lines, Arc Type of Group Arcs, Delete Entity, and Undelete Entity.

7.1.6.5.1 Undo (GAS Edit Menu)

Permits undo the previous action and restore the model to the status before the action. This command is available only if there is something to undo.

7.1.6.5.2 Redo (GAS Edit Menu)

This command reverses the effect of the most recent Undo command. Redo only has an effect immediately after an Undo command or another Redo command. A series of Redo commands reverses the effects of a series of Undo commands. This command is available only if there is something to redo.

7.1.6.5.3 Coordinate System (GAS Edit Menu)

Defines a new coordinate system for the cross section by specifying a new origin and a rotation angle about the current coordinate system. The angle, with positive being counter-clockwise, is defined in degrees.

7.1.6.5.4 Scale (GAS Edit Menu)

Increases or decreases the cross section size. GAS prompts for scaling factors in the X and Y directions. Scaling is achieved by modifying the point coordinates of a section. Thus, if the scaling factor is larger than 1, the cross section will be enlarged and all the entities will be shifted away from the origin. If the scaling factor is between 0 and 1, the cross section will be shrunk and all the entities will be shifted toward the origin. If the X or Y scaling factor is negative, the cross section will be flipped about the associated axis. When arcs exist, the X and Y scaling factors must be equal.

7.1.6.5.5 Point Coordinates (GAS Edit Menu)

Permits changing the X and Y coordinates of a point. GAS prompts for point number, X coordinate and Y coordinate in a dialog box. Once the Point Number input field is modified, GAS displays the current X and Y coordinates of the specified point as the default values in the associated input fields.

7.1.6.5.6 Line End Points (GAS Edit Menu)

Permits changing the end points of a line. GAS prompts for line number, starting point number and ending point number in a dialog box. Once the Line Number input field is modified, GAS displays the current starting and ending point numbers of the specified line as the default values in the associated input fields.

7.1.6.5.7 Line Length (GAS Edit Menu)

Permits changing the length of a line. GAS prompts for line number and line length in a dialog box. Once the Line Number input field in the dialog box is modified, GAS displays the current line length of the specified line as the default value in the associated input field.

The line is modified at the end with the larger point number. In addition to the specified line length change, the position of all the connected entities will be modified accordingly.

7.1.6.5.8 Weld End Points (GAS Edit Menu)

Permits changing the end points of a weld. GAS prompts for weld number, starting point number and ending point number in a dialog box. Once the Line Number input field is modified, GAS displays the current starting and ending point numbers of the specified line as the default values in the associated input fields.

7.1.6.5.9 Entity Renumber (GAS Edit Menu)

Renumbers the entity numbers and reuses the entity numbers of the deleted entities. This feature is most useful when a user has reached the numbering limitation of the GAS program (1000 points, 700 lines, 70 arcs, and 50 welds) and has previously deleted entities that can now be reused. An example of the renumbering action for points is as follows: Assume a GAS model contains points 1, 2, 3, and 4. If the user deletes points 2 and 3, those numbers can not be reused. After activating the Entity Renumber feature, point number 4 would be changed to number 2 and points 3 and 4 would be available to be defined with new coordinate values. A similar process would apply to renumbering lines, arcs, and welds.

7.1.6.5.10 Merge Coincident Points (GAS Edit Menu)

Merge points with the same coordinates. GAS prompts for tolerance. If the X and Y coordinates differences of two points are within the specified tolerance, they are considered as Coincident points. If Coincident points are found, GAS will use the smaller point number for the Coincident points and change the connectivity of all the associated lines, arcs and welds.

7.1.6.5.11 Properties of Single Entity (GAS Edit Menu)

Permits modifying the properties of a specified entity. GAS displays a submenu from which you choose the entity type for modification. The submenu includes Line and Arc.

7.1.6.5.11.1 Line (GAS Edit/Properties of Single Entity Menu)

Changes the properties of a specified line. Line properties include material, thickness and line type.

7.1.6.5.11.2 Arc (GAS Edit/Properties of Single Entity Menu)

Changes the properties of a specified arc. Arc properties include material, thickness and arc type.

7.1.6.5.12 Material of Group Entities (GAS Edit Menu)

Permits changing the material property of a specified group of entities. GAS displays a submenu from which to choose the entity type for modification. The submenu includes All Entities, Lines and Arcs.

To change the material shown in the dialog, Click the Change button and GAS will bring up the Select Material dialog with the list of materials in the archive. Point and click to choose the desired material. To change to a different archive, Click the ASDM Archive or Other Archive button on the toolbar.

7.1.6.5.12.1 All Entities (GAS Edit/Material of Group Entities Menu)

Changes the materials of all the entities.

7.1.6.5.12.2 Lines (GAS Edit/Material of Group Entities Menu)

Changes the material of a group of lines.

7.1.6.5.12.3 Arcs (GAS Edit/Material of Group Entities Menu)

Changes the material of a group of arcs.

7.1.6.5.13 Thickness of Group Entities (GAS Edit Menu)

Permits changing the thickness of a specified group of entities. GAS displays a submenu from which you choose the entity type for modification. The submenu includes All Entities, Lines and Arcs.

7.1.6.5.13.1 All Entities (GAS Edit/Thickness of Group Entities Menu)

Changes the thickness of all the entities. GAS prompts for new thickness.

7.1.6.5.13.2 Lines (GAS Edit/Thickness of Group Entities Menu)

Changes the thickness of a group of lines. GAS prompts for line number range and new thickness.

7.1.6.5.13.3 Arcs (GAS Edit/Thickness of Group Entities Menu)

Changes the thickness of a group of arcs. GAS prompts for arc number range and new thickness.

7.1.6.5.14 Line Type of Group Lines (GAS Edit Menu)

Permits changing the line type of a specified group of lines. The line type can be a Segment, an Intermediate Stiffener, or an Edge Stiffener. Line type is used in the effective properties analysis. An Edge Stiffener is used to provide a continuous support along a longitudinal edge of the compression flange to improve the buckling stress. An Intermediate Stiffener Line is a line associated with an intermediate stiffener in the compression flange. If the line is not an Intermediate Stiffener or an Edge Stiffener, it should be assigned as a Segment.

7.1.6.5.15 Arc Type of Group Arcs (GAS Edit Menu)

Permits changing the arc type of a specified group of arcs. The arc type can be Segment, Intermediate Stiffener, or Fully Effective. The arc type is used in the effective properties analysis. The Fully Effective arc is assumed to be fully effective. Therefore, the Fully Effective arc should only be used for an arc which the user believes to be fully effective. An Intermediate Stiffener arc is an arc associated with an Intermediate Stiffener. Arcs that are not Fully Effective or associated with an Intermediate Stiffener should be assigned as an Arc Segment.

7.1.6.5.16 Delete Entity (GAS Edit Menu)

Provides commands to delete unnecessary entities from the cross section. GAS displays a submenu from which you choose the entity type for deletion. The submenu includes Delete Point, Delete Line, Delete Arc, Delete Weld and Delete All.

7.1.6.5.16.1 Delete Point (GAS Edit/Delete Entity Menu)

Deletes unnecessary points from the cross section. GAS prompts for a point number. Points connected to lines, arcs, or welds cannot be deleted until those lines, arcs, or welds are deleted.

7.1.6.5.16.2 Delete Line (GAS Edit/Delete Entity Menu)

Deletes unnecessary lines from the cross section. GAS prompts for a line number.

7.1.6.5.16.3 Delete Arc (GAS Edit/Delete Entity Menu)

Deletes unnecessary arcs from the cross section. GAS prompts for an arc number.

7.1.6.5.16.4 Delete Weld (GAS Edit/Delete Entity Menu)

Deletes unnecessary welds from the cross section. GAS prompts for a weld number.

7.1.6.5.16.5 Delete All (GAS Edit/Delete Entity Menu)

Deletes all the entities in the cross section. Caution!! Unlike the Delete commands for a specific entity which can be “undone” using the Undelete commands, the Delete All command can not be “undone”.

7.1.6.5.17 Undelete Entity (GAS Edit Menu)

Provides commands to undelete previously deleted entities. GAS displays a submenu from which to choose the entity type for undeletion. The submenu includes Undelete Point, Undelete Line, Undelete Arc, and Undelete Weld.

7.1.6.5.17.1 Undelete Point (GAS Edit/Undelete Entity Menu)

Undeletes previously deleted points. GAS prompts for a point number.

7.1.6.5.17.2 Undelete Line (GAS Edit/Undelete Entity Menu)

Undeletes previously deleted lines. GAS prompts for a line number.

7.1.6.5.17.3 Undelete Arc (GAS Edit/Undelete Entity Menu)

Undeletes previously deleted lines. GAS prompts for an arc number.

7.1.6.5.17.4 Undelete Weld (GAS Edit/Undelete Entity Menu)

Undeletes previously deleted welds. GAS prompts for a weld number.

7.1.6.6 GAS View Menu

Provides commands for changing viewing window contents and graphical display controls of the viewing window. The View menu includes Results, Entity List, Step, Results Summary, Graphical Results, Numerical Results, XY Plot, Set View Window, Zoom In, Zoom Out, Zoom Out Excluding Arc Centers, Pan, Redraw, Labels, Point Marker, Thickness, Ruler, Grid, and Snap.

7.1.6.6.1 Results (GAS View Menu)

Activates the postprocessor. The default result file is the results file of the last analysis performed or the last results file you chose in the postprocessor in the current session. If no analysis is performed, GAS prompts for the results file.

For nominal property results, GAS plots the cross section, the centroid, the reference axes, the principal axes, and the shear center, if available. For effective property results, GAS plots the original cross section, the effective cross section, the reference axes, the principal axes of the effective cross section, and the centroid of the effective cross section.

7.1.6.6.2 Entity List (GAS View Menu)

Displays numerical entity information in a dialog box. When finished viewing, click the Close command to return to the cross section display window. Use the Print button in the dialog box to print the list.

To copy the whole entity list to clipboard:

- Point the cursor inside the list display area
- Right-click to popup the menu and choose Select All

- Right-click again and choose Copy

To copy a portion of the entity list to clipboard:

- Use mouse to highlight a portion of the list
- Right-click to popup the menu and choose Copy

7.1.6.6.3 Step (GAS View Menu)

Permits changing the analysis step in the trend analysis results for viewing.

7.1.6.6.4 Results Summary (GAS View Menu)

Displays the summary of the current results file in a dialog box.

7.1.6.6.5 Numerical Results (GAS View Menu)

Displays output from the current result file in a dialog box. When finished viewing, click the Close button. Use the Print button in the dialog box to print the numerical results.

To copy everything to clipboard:

- Point the cursor inside the list display area
- Right-click to popup the menu and choose Select All
- Right-click again and choose Copy

To copy a portion of the results to clipboard:

- Use mouse to highlight a portion of the list
- Right-click to popup the menu and choose Copy

7.1.6.6.6 XY Plot (GAS View Menu)

Displays trend analysis results in XY Plot form. One property at a time should be selected for the XY Plot. The varying parameter value is used for the X-axis and the selected property is used for the Y-axis. The summary of the XY plot data is shown in the Summary Tab. Use the Print Plot button to print the plot.

7.1.6.6.7 Set View Window (GAS View Menu)

Sets the display window by specifying the coordinates of the lower left and upper right corners of the desired window. The desired window can be any rectangular area. Since GAS maintains the aspect ratio of the display window, it calculates a proper display window to cover the user specified area.

7.1.6.6.8 Zoom In (GAS View Menu)

Expands a portion of the current display using a zoom-in window. The zoom-in window, any rectangular area in the current display, is defined by specifying two opposite corner points using the input device.

To quickly expand a portion of the current display, click the Zoom In button on the toolbar.



7.1.6.6.9 Zoom Out (GAS View Menu)

Instructs GAS to calculate a proper display window to best accommodate all the entities defined thus far.

To quickly show the whole cross section, click the Zoom Out button on the toolbar.



7.1.6.6.10 Zoom Out Excluding Arc Centers (GAS View Menu)

Instructs GAS to calculate a proper display window to best accommodate all the entities excluding the arc centers. If the curvature of an arc is small, the center of the arc may be far away from the model. Zooming out including the arc center will make the model very small in the display window.

7.1.6.6.11 Pan (GAS View Menu)

Moves the display viewport by specifying the moving distance. The moving distance is specified by defining two points on the screen using the pointing device.

To quickly move the display viewport, click the Pan button on the toolbar.



7.1.6.6.12 Redraw (GAS View Menu)

Redraws the cross section. This command is used only when the display has not been properly refreshed.

7.1.6.6.13 Labels (GAS View Menu)

Sets label display options. The label display options control the display of the identification numbers for points, lines, arcs and welds. GAS displays a dialog box from which to set the label display option: The current status of this option is indicated by a check mark (✓).

Labels	Description
Points	Toggles the points labels display option.
Lines	Toggles the line label display option.
Arcs	Toggles the arc label display option.
Welds	Toggles the weld label display option.

7.1.6.6.14 Point Marker (GAS View Menu)

Toggles point marker display option. The point marker display option controls the display of the identification markers (+) and numbers for points. The current status of this option is indicated by the appearance of a check mark (✓) in front of the menu option.

7.1.6.6.15 Thickness (GAS View Menu)

Toggles thickness display option. The thickness display option controls the display of the thickness of lines and arcs. The current status of this option is indicated by the appearance of a check mark (✓) in front of the menu option. View Thickness option is not available when viewing effective property results.

If the thickness display option is “ON”, the entity thickness will be shown to scale but not less than 1 pixel. Otherwise, the lines and arcs will be shown as 1 pixel thick.

7.1.6.6.16 Ruler (GAS View Menu)

Toggles ruler display option. The ruler display option controls the display of the rulers at left and bottom borders of the client window. The current status of this option is indicated by the appearance of a check mark (✓) in front of the menu option.

7.1.6.6.17 Grid (GAS View Menu)

Provides commands for creating grids - a frame of reference or a series of construction points that are not part of the cross section. The grids help locate points and visualize distances on the screen. GAS displays a submenu from which you choose the command. The submenu includes Grid On, Grid Off, and Grid Spacing.

7.1.6.6.17.1 Grid On (GAS View/Grid Menu)

Displays the grid according to the specified spacing. If the grid spacing is not defined, the default value is 5 units in the X and Y direction. If set, a check mark will appear before this option.

7.1.6.6.17.2 Grid Off (GAS View/Grid Menu)

Turns off the grid. If set, a check mark will appear before this option.

7.1.6.6.17.3 Grid Spacing (GAS View/Grid Menu)

Specifies the grid spacing in the X and Y directions. The grid spacing should be larger than the distance represented by one pixel of the screen display. The grid will not be displayed if the grid spacing is too small to be useful.

If the grid spacing is different than the snap spacing, GAS prompts the question to see whether you want to change the snap spacing to be the same as the grid spacing.

7.1.6.6.18 Snap (GAS View Menu)

Restricts cursor movement to specified intervals. The points you enter with a pointing device can be locked into alignment by the snap mechanism. The snap grid is invisible. Use SNAP with the GRID command to display a separate visible grid. Set the spacing of the two grids to

equal or related values. GAS displays a submenu from which you choose the command. The submenu includes Snap On, Snap Off, and Snap Spacing.

7.1.6.6.18.1 Snap On (GAS View/Snap Menu)

Turns on the snap with the specified spacing. If the snap spacing is not defined, the default value is 5 units in the X and Y direction. If set, a check mark will appear before this option.

7.1.6.6.18.2 Snap Off (GAS View/Snap Menu)

Turns off the snap. If set, a check mark will appear before this option.

7.1.6.6.18.3 Snap Spacing (GAS View/Snap Menu)

Specifies the snap grid spacing in the X and Y directions. The snap grid spacing should be larger than the distance represented by one pixel of the screen display.

If the grid spacing is different than the snap spacing, GAS prompts the question to see whether you want to change the snap spacing to be the same as the grid spacing.

7.1.6.7 GAS Material Menu

Provides commands related to the current material used for new entity creation. The Material menu includes Show Current Material and Set Current Material.

7.1.6.7.1 Show Current Material (GAS Material Menu)

Lists the properties of the current material in a dialog box. Included in the box are constants for five steel properties: Modulus of Elasticity, Shear Modulus, mass density, Poisson's Ratio and coefficient of thermal expansion. Click OK to close the dialog box.

7.1.6.7.2 Set Current Material (GAS Material Menu)

Permits changing the current material. GAS displays a submenu from which to choose the current material. The submenu includes CARS Default, ASDM Archive, Steel Company Archive, and User Defined Archive.

7.1.6.7.2.1 CARS Default (GAS Material/Set Current Material Menu)

Sets the current material to the CARS default material set in Material Archive Program (MAP).

7.1.6.7.2.2 ASDM Archive (GAS Material/Set Current Material Menu)

Selects the current material from the ASDM Archive.

7.1.6.7.2.3 Steel Company Archive (GAS Material/Set Current Material Menu)

Selects the current material from a Steel Company Archive.

7.1.6.7.2.4 User Defined Archive (GAS Material/Set Current Material Menu)

Select the current material from a User Defined Archive.

7.1.6.8 GAS Physical Menu

Provides commands related to the default physical properties used for new entity creation. Default physical properties include thickness, line type, and arc type. The Physical menu includes Show Default Physical Properties and Set Default Physical Properties.

7.1.6.8.1 Show Default Physical Properties (GAS Physical Menu)

Lists the default physical properties in a dialog box. Included in the box are default Thickness, the default Line Type, and the default Arc Type. Click OK to close the dialog box.

7.1.6.8.2 Set Default Physical Properties (GAS Physical Menu)

Permits changing the default thickness, the default line type, and the default arc type.

7.1.6.9 GAS Analysis Menu

Performs cross section property calculations. The analysis can be a Single calculation or a Trend Analysis. Two types of cross section properties can be calculated - Nominal Property and Effective Property.

7.1.6.9.1 Nominal Properties (GAS Analysis Menu)

Calculates the nominal properties of the cross section. The analysis can be a Single calculation or a Trend Analysis.

7.1.6.9.1.1 Single Calculation (GAS Analysis/ Nominal Properties Menu)

Calculates the nominal properties of the cross section.

7.1.6.9.1.2 Trend Analysis (GAS Analysis/ Nominal Properties Menu)

Calculates the nominal properties of a series of cross sections which are variations of the current cross section and are based on a user specified parameter.

7.1.6.9.2 Effective Properties (GAS Analysis Menu)

Calculates the effective cross section and 21 effective properties of the effective cross section under a specified stress level. The analysis can be a Single calculation or a Trend Analysis.

7.1.6.9.2.1 Single Calculation (GAS Analysis/Effective Properties Menu)

Calculates the effective properties of the cross section.

7.1.6.9.2.2 Trend Analysis (GAS Analysis/Effective Properties Menu)

Calculates the effective properties of a series of cross sections which are variations of the current cross section and are based on a user specified parameter.

7.1.6.9.3 Axial Capacity (Gas Analysis Menu)

Calculates the axial capacity of a member with the current cross section. The analysis can be a Single calculation or a Trend Analysis.

7.1.6.9.3.1 Single Calculation (GAS Analysis/Axial Capacity Menu)

Calculates the axial capacity of a member with the current cross section.

7.1.6.9.3.2 Trend Analysis (GAS Analysis/Axial Capacity Menu)

Calculates the axial capacity of a series of members with the cross sections which are variations of the current cross section and are based on a user specified parameter.

7.1.6.9.4 Flexural Capacity (Gas Analysis Menu)

Calculates the flexural capacity of a member with the current cross section. The analysis can be a Single Calculation or a Trend Analysis.

7.1.6.9.4.1 Single Calculation (GAS Analysis/Flexural Capacity Menu)

Calculates the flexural capacity of a member with the current cross section.

7.1.6.9.4.2 Trend Analysis (GAS Analysis/Flexural Capacity Menu)

Calculates the flexural capacity of a series of members with the cross sections which are variations of the current cross section and are based on a user specified parameter.

7.1.6.9.5 Combined Axial and Flexural Stability (GAS Analysis Menu)

Calculates the interaction ratio under axial and flexural loading of a member with the current cross section. The analysis can be a Single Calculation or a Trend Analysis.

7.1.6.9.5.1 Single Calculation (GAS Analysis/Combined Axial and Flexural Stability Menu)

Calculates the interaction ratio under axial and flexural loading of a member with the current cross section.

7.1.6.9.5.2 Trend Analysis (GAS Analysis/Combined Axial and Flexural Stability Menu)

Calculates the interaction ratio under axial and flexural loading of a series of members with the cross sections which are variations of the current cross section and are based on a user specified parameter.

7.1.6.9.6 Axial Force Deflection Properties of Stub Column

Calculates the axial force deflection properties of a stub column with the current cross section.

7.1.6.10 GAS Units Menu

Provides commands related to current system of units and unit conversion. The Units menu includes kip,in,ksi (kilopounds, inches, kilopounds per square inch), N,mm,MPa (Newton, millimeter, MegaPascal), and Unit Conversion.

7.1.6.10.1 kip,in,ksi (GAS Units Menu)

Permits changing the active system of units to kip,in,ksi. If set, a check mark (✓) will appear before this option.

7.1.6.10.2 N,mm,MPa (GAS Units Menu)

Permits changing the active system of units to N,mm,MPa. If set, a check mark (✓) will appear before this option.

7.1.6.10.3 Unit Conversion (GAS Units Menu)

Converts entered value of selected units of measure from one system of units to other systems of units. There are ten categories of units of measure available for unit conversion. The ten categories are angular, area, force, inertia, length, mass, moment, stress, temperature and mass density.

To quickly access unit conversion tool, click the Unit Conversion button on the toolbar.



Unit Conversion

7.1.6.11 GAS Help Menu

Provides commands for accessing online help. The Help menu includes Contents, Search for Help on, GAS Hints, Examples and Tutorials, Obtaining Technical Support, and About.

7.1.6.11.1 Contents (GAS Help Menu)

Displays the GAS online Help contents. It provides a comprehensive list that summarizes the organization of topics in the Help system.

7.1.6.11.2 Search for Help on (GAS Help Menu)

Opens the Search dialog box for Help to find information related to topics on which you want more information.

To use the Search For Help On command, type the topic or select it from the list in the Search dialog box, and then choose the Show Topics button to see related topics. To display a particular topic from the list of topics, select it and then choose the Go To button.

7.1.6.11.3 GAS Hints, Examples and Tutorials (GAS Help Menu)

Displays the help information regarding how to find GAS hints, examples and tutorials in ASDM.

7.1.6.11.4 Obtaining Technical Support (GAS Help Menu)

Displays the help information regarding how to obtain the technical support.

7.1.6.11.5 About (GAS Help Menu)

Displays information on the development and sponsors of the CARS program.

7.1.6.12 Gas Shortcut Menus

Shortcut menus are available in entity list dialog box, numerical results dialog box and model creation screen after entities are selected. The menu can be shown by clicking the right button of the mouse. The menu options vary depending on location of the cursor and selected entities.

7.1.6.12.1 Shortcut Menu For Single Line

If only one line is selected, the following menu options are available in the shortcut menu:

- View Selected Line: Shows the information about the selected line in a dialog box.
- Delete Selected Line: Deletes the selected line.
- Edit Line End Points: Permits changing the end points of the selected line.
- Edit Line Length: Permits changing the length of the selected line.
- Edit Line Properties: Permits modifying the properties of the selected line.

7.1.6.12.2 Shortcut Menu For Single Arc

If only one arc is selected, the following menu options are available in the shortcut menu:

- View Selected Arc: Shows the information about the selected arc in a dialog box.
- Delete Selected Arc: Deletes the selected arc.
- Edit Arc Properties: Permits modifying the properties of the selected arc.

7.1.6.12.3 Shortcut Menu For Single Weld

If only one weld is selected, the following menu options are available in the shortcut menu:

- View Selected Weld: Shows the information about the selected arc in a dialog box.
- Delete Selected Weld: Deletes the selected arc.
- Edit Weld End Points: Permits changing the end points of the selected weld.

7.1.6.12.4 Shortcut Menu For A Group Of Lines

If a group of lines are selected, the following menu options are available in the shortcut menu:

- View Selected Lines: Shows the information about the selected lines in a dialog box.
- Delete Selected Lines: Deletes the selected lines.
- Edit Material: Permits modifying the material of the selected lines.
- Edit Thickness: Permits modifying the thickness of the selected lines.
- Edit Line Type: Permits modifying the Line Type of the selected lines.

7.1.6.12.5 Shortcut Menu For A Group Of Arcs

If a group of arcs are selected, the following menu options are available in the shortcut menu:

- View Selected Arcs: Shows the information about the selected arcs in a dialog box.
- Delete Selected Arcs: Deletes the selected arcs.
- Edit Material: Permits modifying the material of the selected arcs.
- Edit Thickness: Permits modifying the thickness of the selected arcs.
- Edit Arc Type: Permits modifying the Arc Type of the selected lines.

7.1.6.12.6 Shortcut Menu For A Group Of Lines And Arcs

If the selected entities contain only lines and arcs, the following menu options are available in the shortcut menu:

- View Selected Entities: Shows the information about the selected entities in a dialog box.
- Delete Selected Entities: Deletes the selected entities.
- Edit Material: Permits modifying the material of the selected entities.

- Edit Thickness: Permits modifying the thickness of the selected entities.

7.1.6.12.7 Shortcut Menu For Miscellaneous Entities

If the selected entities contain unused points or welds with lines and arcs, the following menu options are available in the shortcut menu:

- View Selected Entities: Shows the information about the selected entities in a dialog box.
- Delete Selected Entities: Deletes the selected entities.

7.1.6.12.8 Shortcut Menu For Entity List And Numerical Results Dialog Boxes

When the cursor is in Entity List or Numerical dialog boxes, the following menu options are available in the shortcut menu:

- Copy: Copy the selected text to the Clipboard.
- Select All: Select all the text in the dialog box.

7.1.6.13 Hints on Using GAS

Like all engineering analysis computer programs, the correctness of the results relies largely on the correctness of the input data. The input data for GAS is the user created cross section. To prevent “Garbage In, Garbage Out”, this section presents some hints when using GAS.

7.1.6.13.1 Entity Connectivity

Connectivity is very important in the properties calculation, especially for torsional properties. Entities that appear connected on the screen do not necessarily guarantee that they are connected since different end points can have the same coordinates. Use Edit/Coincident Points Merge to merge points with the same coordinates. Use the View/Entity List command to make sure connected entities share the same end point identification number. One possible pitfall is when using the Point/Angles/Radius command to create an arc. This command creates two new points as the end points of the arc and does not create any connectivity with other entities.

7.1.6.13.2 Line Types And Arc Types

Line types and arc types are utilized for effective properties calculations. The type specified determines which procedure will be used to compute the effective width of that entity. Be sure to check all the line types and arc types before performing an effective properties calculation. Line types and arc types are ignored when performing nominal calculations. See [Section 3.11](#) for Segment Type Determination in GAS.

7.1.6.13.3 Arc Generation Using Two Parallel Lines

Currently, an arc cannot be automatically inserted between parallel lines. However, an arc can be defined using the 3 Existing Points option if two of the points are on the parallel lines and the third point is correctly positioned between the two lines.

7.1.6.13.4 Arc Segments Under A Stress Gradient

Currently, there are no procedures available in CARS to calculate the effective width of an arc segment under a stress gradient (due to moment loading). In order to get an approximation for the effective width of other entities under a moment loading, the user can assign Fully Effective

to all the arc elements knowing that a Fully Effective arc is assumed to be fully effective. This bypasses effective width calculations of arcs with a stress gradient. AISI is monitoring ongoing research on the effectiveness of arc segments under a stress gradient and will implement new procedures when appropriate.

7.1.6.13.5 Circular Elements

Circular elements are not permitted in GAS. However, a circular section can be modeled by defining an arc using the Point/Angles/Radius option. Set the starting and ending angles to 0.0 and 359.99, respectively. Then, define a weld at the two points to close the circle. While GAS can calculate nominal properties for this section, it does not calculate effective properties. Use Design Procedures 3.1-11 and 3.1-17 for evaluating the effectiveness of a circular, tubular section under moment and axial loading, respectively.

7.1.6.13.6 Colinear Line Elements

Do not use colinear line elements to model a line in a section when determining effective properties. In the effective properties calculation, GAS assumes a line element is supported if the end point is connected to other entities. The element length is based on the distance between support points. If a line is modeled using two line segments, the capacity of the line will be overestimated since the length/thickness (w/t) ratio will be smaller than it should be. If colinear line elements are found during an effective properties calculation, GAS prompts the question to merge the colinear element. The analysis will be terminated if you choose not to merge the colinear elements. After the merge operation, GAS prompts the question to save the revised cross section. If it is not saved, the revised cross section will be used for this analysis only.

7.1.6.13.7 Default Settings For Physical And Material Properties

GAS utilizes default settings for physical and material properties. If your cross sections can utilize the same default settings, you should create an empty cross section with the proper default settings and save the section into the database. This empty cross section can then be used as a template for a new section. This avoids re-entering defaults at the start of each session. Remember to save the finished cross section using a different name.

7.1.6.13.8 Cross Section With Discontinuity

GAS does not calculate torsional properties of a “non-integrated” section (a section containing non-connected elements) since the theoretical formulas are derived under the assumption that the member is a prismatic integrated member. When a discontinuity is found in the cross section, GAS will issue a warning message stating that torsional properties will not be computed for this cross section and flexural properties will be calculated based on the assumption that somewhere along the member length welds, fasteners or other types of connections are provided. For a non-integrated prismatic member each “integrated” portion should be considered as one cross section and analyzed separately.

7.1.6.13.9 Net Sections

For net sections, a cross section of the member where holes reside, do not use the results of the following nominal properties - torsional constant, shear center location, warping constant, and shear coefficients. Also, effective properties for a net section are conservative since the calculations are based on the assumption that the cross section is representative of the entire

member. For more information on GAS analysis methods and approximations, refer to [Section 3.11](#) of the ASDM.

7.1.6.13.10 Cross Section Copy Between Databases

To copy one section to another database:

- Use File/Get Section to retrieve the section to be copied.
- Use File/Open Database to open the target database.
- Use File/Save Section or File/Save Section As to save the section into the target database.

7.1.6.13.11 Copy Graphics onto Clipboard

To copy graphics in GAS window:

- Press Print Scrn key if you want to copy the whole screen or press ALT and Print Scrn simultaneously to copy the active window.
- Start Paint.
- Paste the copied graphics in Paint using Edit/Paste.
- Save the image using File/Save.

7.1.6.14 Error Messages

Error messages are provided within GAS showing an error identification number and associated message. Refer to this section to correlate the error identification number with a brief error message description. These descriptions define each error and provide suggestions for correction of the problem.

The types of error messages issued by GAS are:

- GAS Preprocessor Errors (Errors 300-321)
- GAS Solution Errors (Errors 351 - 364)
- GAS Postprocessor Errors (Errors 381 -383)

7.1.6.14.1 GAS Preprocessor Errors (Errors 300-321)

Error 300: Invalid point number

The specified point number is either deleted or not defined.

Remedy: Use the View/Entity List to view available active points. Make sure the input point number is active.

Error 301: Invalid line number

The specified line number is either deleted or not defined.

Remedy: Use View/Entity List to view active lines. Make sure the input line number is active.

Error 302: Invalid arc number

The specified arc number is either deleted or not defined.

Remedy: Use View/Entity List to view active arcs. Make sure the input arc number is active.

Error 303: Invalid weld number

The specified weld number is either deleted or not defined.

Remedy: Use View/Entity List to view active welds. Make sure the input weld number is active.

Error 304: Unable to delete the point

A point cannot be deleted if it is used by other active entities.

Remedy: Delete all the connected entities (lines, arcs, or welds) before deleting a point.

Error 305: Invalid Material ID

The specified material ID number cannot be found in the specified material archive.

Remedy: Use MAP to view the specified archive and choose the proper material ID.

Error 306: No more room for additional points

Due to memory constraint, the current version of GAS allows only 1000 points.

Remedy: Reuse the deleted point numbers by using Edit/Entity Renumber or by undeleting them first then use Edit/Point Coordinate to change their coordinates to the desired coordinates.

Error 307: No more room for additional lines

Due to memory constraints, the current version of GAS allows only 700 lines.

Remedy: Reuse the deleted line numbers by using Edit/Entity Renumber or by undeleting them first then use Edit/Line End Points to change their end points to the desired end points.

Error 308: No more room for additional arcs

Due to memory constraints, the current version of GAS allows only 70 arcs.

Remedy: Reuse the deleted point numbers by using Edit/Entity Renumber or by undeleting them first then use Edit/Point Coordinate to change their coordinates to the desired coordinates.

Error 309: No more room for additional welds

Due to memory constraints, the current version of GAS allows only 50 welds.

Remedy: Reuse the deleted weld numbers by using Edit/Entity Renumber by undeleting them first then use Edit/Weld End Points to change their end points to the desired end points.

Error 310: No section in the database

The current database is empty.

Remedy: Use File/New Section to create a section and use Section/Save to save it into the current database.

Error 311: No nominal properties are available in the database

All the sections in the current database were saved using the File/Save Section command rather than using File/Save Section w/Nominal command. Since there are no nominal properties associated with the sections, the search operation cannot be performed.

Remedy: Perform a Single Calculation/Nominal Property analysis and use the File/Save Section w/Nominal command to save the results into the current database for all the sections you want to include in the search operation.

Error 312: Property title file is missing

GAS cannot find the file PROP.TIL.

Remedy: The PROP.TIL file must reside in the CARS directory. Reinstall if necessary.

Error 313: Perform a single calculation for nominal properties

This error message occurs when the user attempts to use the File/Save Section w/Nominal command without performing a Single Calculation/Nominal Property analysis beforehand.

Remedy: Use the Analysis command to perform a Single Calculation/Nominal Property analysis.

Error 314: Section has been changed since last analysis

This error message occurs when the user tries to use the command File/Save Section w/Nominal to save the section and its nominal properties into the database but the current section has been modified after the last Single Calculation/Nominal property analysis.

Remedy: Use the Analysis command to perform another Single Calculation/Nominal Property analysis.

Error 315: Parallel tangent lines

The two tangent lines specified for arc creation are parallel lines. GAS cannot create an arc using parallel lines as the tangent lines.

Remedy: Specify two lines that are not parallel as the tangent lines or use 3 Existing Points.

Error 316: X, Y scaling factors must be the same for a section with arcs

GAS only supports circular arcs. If the scaling factors specified for the Geometry/Scale command are different in X and Y directions, GAS will scale a circular arc into a non-circular arc.

Remedy: Specify the same value for X and Y scaling factors.

Error 317: Grid too dense to display

The specified grid spacing is too small for the current display window.

Remedy: Use View/Grid/Grid Spacing to specify a reasonable grid size.

Error 318: Digitize two different points on the tablet

GAS requires two different points on the tablet to define the X axis.

Remedy: Digitize a point on the X axis other than the origin.

Error 319: Segment length of a closed section cannot be changed

The line specified for the command Edit/Line Length or the line specified in the trend analysis parameter, with the type of Length, is part of a closed section. Since GAS maintains the angles between entities during line length modification, line length change of any segment of a closed section cannot be done.

Remedy: Do not attempt to change the length of any line that is part of a closed section.

Error 320: A cross section cannot use more than 10 material archives

GAS keeps track of the material archives used in the current section. The limit is 10.

Remedy: Add the additional materials into current used material archives by using MAP.

Error 321: Invalid Parameter

The parameter defined for trend analysis is not reasonable.

Remedy: Review the defined parameter.

7.1.6.14.2 GAS Solution Errors (Errors 351 - 374)

Error 351: Currently the ASDM does not address effective width of curved elements with stress gradient.

Remedy: Consider changing arc segments to fully effective arcs to get an approximate answer.

Error 352: Currently the ASDM does not address effective width of an unstiffened element with intermediate stiffener

Remedy: Revise the section geometry.

Error 353: Invalid cross section

The current cross section is not completed for analysis. For example, the section is empty or there are no lines or arcs.

Remedy: Check the current section before performing any analysis.

Error 354: Stresses in some elements are larger than the yield stress of the material

Remedy: Reduce the stress value for the Specified Stress option or reduce the loads for the Stress From Loads option.

Error 355: Inappropriate segment type assignment

This error message occurs when GAS detects illogical segment type assignment during analysis. For example, a both-ends-connected segment is assigned as an edge stiffener or an intermediate stiffener is attached to an edge stiffener.

Remedy: Use View/Entity List to review segment type assignments.

Error 356: No more than 10 intermediate stiffeners can be defined for a segment

Remedy: Revise the design

Error 357: Element length must be the same (within 5%) for elements stiffened by intermediate stiffeners:

Currently the ASDM does not address effective width of unequal length elements stiffened by intermediate stiffeners.

Remedy: Revise the design

Error 358: Curved element must be stiffened by bends larger than 45 degrees

Remedy: Revise the design or assign Fillet as the arc type of that curved element to avoid effective width evaluation for that segment.

Error 359: w/t or D/w of an entity stiffened by edge stiffener exceeds the upper bound covered by ASDM. Effective properties have to be evaluated experimentally

Remedy: Review all the elements with one end free. If the line type assignment of the element is "Segment", it is possible GAS assigns the line type of "Edge Stiffener" during analysis. See [Section 3.11](#) for Segment Type Determination in GAS. If any element with one end free should be considered as unstiffened element, use Edit menu option to change the line type. Or revise the design by reducing w/t or D/w of the entity stiffened by an edge stiffener.

Error 360: Redesign the lip

GAS requires the simple lip in an edge stiffened element with intermediate stiffeners to be fully effective.

Remedy: Revise the design by reducing the length/thickness ratio of the simple lip.

Error 361: Intermediate stiffener ignored, please revise the cross section

Remedy: Revise the design

Error 362: Unable to find cell cut locations

To calculate shear center location for closed sections, GAS will try to find cut locations first. This message appears if GAS fails to find the locations.

Remedy: Try different element number assignment.

Error 363: Small Pivot, Matrix may be singular

This error message can be caused by very small material G value or very small segment thickness.

Remedy: Review the current section and make sure proper value of G and proper segment thickness are used.

Error 364: Intersecting entities are found in the cross section

Remedy: Delete the intersecting entities. Introduce a new point at the intersection point and recreate the entities.

Error 365: Computation overflow due to a closed section with zero enclosed area. Check for duplicate lines/arcs.

Remedy: Use Edit/Merge Coincident Point menu option to merge points with the same coordinate. Use View/Entity List menu option to check lines or arc with the same end point number.

Error 366: Co-linear segments with different thickness can not be merged.

This error message occurs when GAS tries to merge two co-linear segments with different thickness.

Remedy: Use Edit/Properties of Single Entity or Edit/Thickness of Group Entities to modify the thickness of those lines.

Error 367: Co-linear segments with different material can not be merged.

This error message occurs when GAS tries to merge two co-linear segments with different material.

Remedy: Use Edit/Properties of Single Entity or Edit/Material of Group Entities to modify the material of those lines.

Error 368: Co-linear segments with different segment type can not be merged.

This error message occurs when GAS tries to merge two co-linear segments with different segment type.

Remedy: Use Edit/Properties of Single Entity or Edit/Line Type of Group Entities to modify the line type of those lines.

Error 369: Analysis was terminated due to the co-linear segments in the section.

This error message occurs when GAS finds co-linear segments and user does not want to merge them.

Remedy: If you do not want the cross section to be modified, save the cross section before the analysis and retrieve the “pre-merge” cross section after reviewing the analysis results.

Error 370: A weld must connect two entities.

This error message occurs when GAS finds a weld does not connect two entities.

Remedy: Modify the cross section.

Error 371: Invalid IGES file

Remedy: Check the specified IGES file.

Error 373: ASDM requires the angle between the edge stiffener and the stiffened element to be between 40 and 140 degrees.

Remedy: Modify the cross section.

Error 374: Current research results for hybrid cross sections are limited to the stress level of "Yield Stress".

Please choose "Yield Stress" in the Effective Properties Analysis Option Dialog Box.

Remedy: Choose "Yield Stress" in the Effective Properties Analysis Option Dialog Box.

7.1.6.14.3 GAS Postprocessor Errors (Errors 381 -383)

Error 381: Invalid GAS output file

Remedy: Review file name entered for Result/Get and ensure it contains GAS analysis results.

Error 382: Invalid trend analysis output file

GAS needs a trend analysis result file to produce an XY Plot.

Remedy: Make sure the result file contains results of a trend analysis.

Error 383: Incomplete trend analysis result

Remedy: Rerun the trend analysis with correct model.

7.1.7 MATERIAL ARCHIVE PROGRAM (MAP)

7.1.7.1 MAP Overview

The Material Archive Program is used to locate, view, create and edit material properties for use in CARS Design Key and GAS. Three types of Material Archives are available in MAP - ASDM, Steel Company and User Defined.

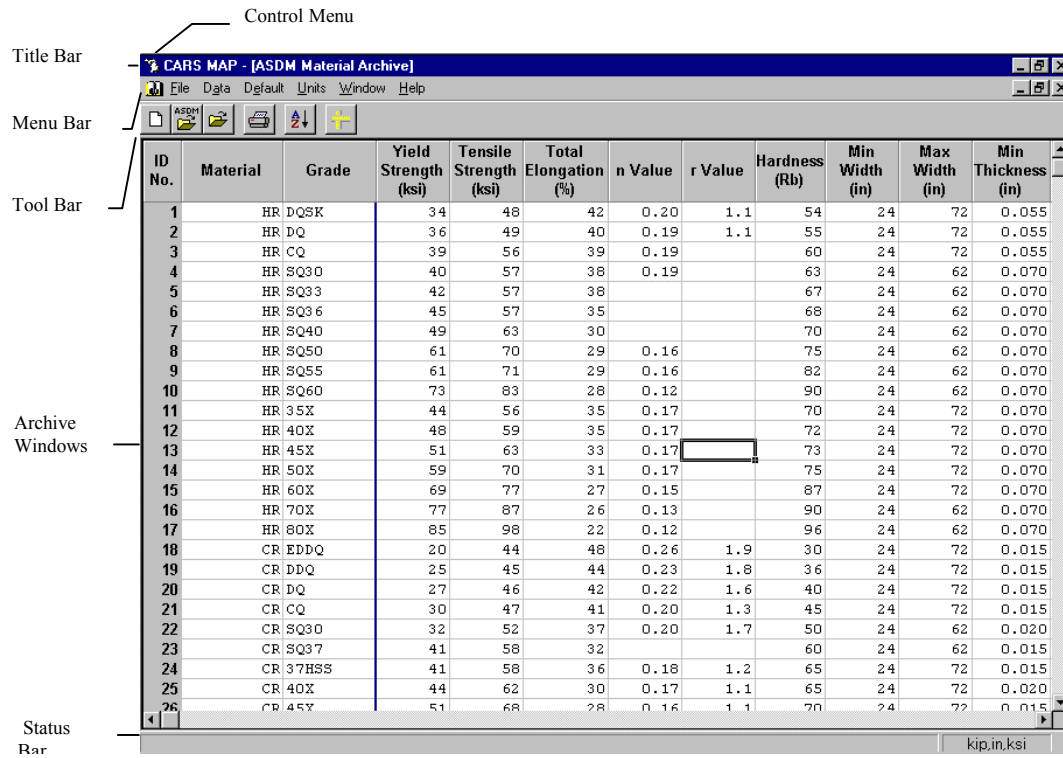
The ASDM archive contains data on the mechanical properties of many different grades of sheet steels, as shown in ASDM [Table 2.4.4-1](#). The values are based on thousands of tests made by steel producers and the Materials Uniformity Task Force of the Auto/Steel Partnership and are typical for the steels produced by AISI member companies. The ASDM archives are protected and cannot be edited. Steel Company Archives permit access to Steel Company archives. Steel Company archives are protected and cannot be edited. Consult your steel company to obtain an archive for CARS usage. User Defined archives can be created and edited. User Defined properties can be input one at a time using the edit feature or in mass using the import feature.

All archives consist of columns of properties for each material. Material properties are entered and saved in either N, mm, MPa or kip, in, ksi units. Each system of units has a different allowable range of material property values. Accordingly, there may be some loss of precision in material property values when converting from one system of units to another. Refer to [Section 7.1.7.4.2](#) for details.

Data not currently available in the ASDM and Steel Company archives is displayed as a blank in the appropriate field. The ASDM and Steel Company archives are stored in the CARS directory. User Defined archives can be stored in any directory.

7.1.7.2 Map Screen

The MAP screen contains a title bar, a menu bar, a toolbar, a status bar and one or more archive viewing windows.



7.1.7.2.1 MAP Title Bar

The Title Bar displays the name of the active application (CARS Material Archive Program).

7.1.7.2.2 MAP Menu Bar

The Menu Bar displays all MAP menus across the top of the CARS MAP screen, just below the title bar.

7.1.7.2.3 MAP Toolbar

The Toolbar contains buttons that give you quick mouse access to many commands and features in MAP. The following buttons are available on the toolbar:



New Archive



Open ASDM Material Archive



Open User Defined Archive



Print



Sort



Unit Conversion

7.1.7.2.4 MAP Status Bar

The Status bar shows information and messages at the bottom of the MAP Screen that help you use MAP. When a menu option is highlighted or when the cursor is pointing to a button on the toolbar, the status bar shows the associated help message. Otherwise, the status bar consists of two areas:

- Program status: Shows the action the program is currently engaging
- Current System of Units: Shows the current system of units as kip,in,ksi or N,mm,MPa
- Num Lock status: Shows whether the Num Lock key is active on the keyboard.

7.1.7.2.5 MAP Archive Windows

Archive window is the area to show the current viewing archive.

7.1.7.3 MAP File Menu

Provides commands for file operations. The file extension for a material archive is .MAT. The file menu includes New, Open, Close, Print, Export, and Exit.

7.1.7.3.1 New (MAP File Menu)

Permits creating a new archive. A new archive can be created by first inputting the titles for 3 user defined columns in the archive. Each column title contains two fields - Description and Units. The units in the user defined column will be the same regardless the system of units.

To quickly create a new archive, click New Archive button on the toolbar.



New Archive

7.1.7.3.2 Open (MAP File Menu)

Permits opening a previously saved archive. Four types of archives are available: ASDM Material Archive, Steel Company Archive, User Defined Archive, and ASDM Historical Archive - 1998.

7.1.7.3.2.1 ASDM Material Archive (MAP File/Open Menu)

Opens the ASDM Material Archive.

To quickly open the ASDM Material Archive, click Open ASDM Material Archive button on the toolbar.



Open ASDM Material Archive

7.1.7.3.2.2 Steel Company Archive (MAP File/Open Menu)

Permits opening a Steel Company Archive.

Material Archives from the following steel companies can be accessed:

- AK Steel Corporation
- Bethlehem Steel Corporation
- Dofasco Inc.
- Ispat Inland Inc.
- National Steel Corporation
- Rouge Steel Company
- Stelco Inc.
- US Steel Group, A Unit of USX Corporation
- WCI Steel, Inc.
- Weirton Steel Corporation

7.1.7.3.2.3 User Defined Archive (MAP File/Open Menu)

Permits opening an existing user defined archive. MAP prompts for the file name.

To quickly open an existing user defined archive, click the Open User Defined Archive button on the toolbar.



Open User Defined Archive

7.1.7.3.2.4 ASDM Historical Archive - 1998 (MAP File/Open Menu)

Opens the material archive used in CARS '98. This archive is used for reference purposes only. The material from the historical archive can not be used as the default material. The Set CARS Default Material menu option will be disabled when viewing the historical archive.

7.1.7.3.3 Close (MAP File Menu)

Close the active archive.

7.1.7.3.4 Print (MAP File Menu)

Permits printing a summary report of one material from the active viewing archive. The report will show the steel constants and material data in the current system of units. The highlighted material or the material where the cursor locates will be printed.

7.1.7.3.5 Export (MAP File Menu)

Permits the export of some or all the materials of an archive to a file. Two types of file format are available: Text File and Excel File.

7.1.7.3.5.1 As Text File (MAP File/Export Menu)

Export some or all the materials of an archive to a tab delimited ASCII text file. You can choose the materials you want to export by highlighting them. Properties for each material are separated by tabs. The default file extension for the exported file is .TXT.

7.1.7.3.5.2 As Excel File (MAP File/Export Menu)

Export some or all the materials of an archive to an Excel file. You can choose the materials you want to export by highlighting them. Properties for each material are stored in a row in the spreadsheet. The default file extension for the exported file is .XLS.

7.1.7.3.6 Exit (MAP File Menu)

Ends the MAP session. MAP prompts you to save any unsaved material archive. Other ways to exit MAP are as follows:

- Open the Application Control Menu using the mouse, or press ALT+SPACEBAR, and then choose Close.
- Double-click on the application Control box.

7.1.7.4 MAP Data Menu

Provides commands to modify and sort material properties in the active viewing archive. The Data menu includes Edit, Add and Sort.

7.1.7.4.1 Edit (MAP Data Menu)

Permits editing an existing material record in the current viewing archive. MAP displays the current properties of the specified material. Move to any field and type in the new property value. Click on OK when done or click on Cancel to discard the changes.

7.1.7.4.2 Add (MAP Data Menu)

Adds a new record at the end of the current viewing archive. The ID number for the new material will be the current maximum ID number, plus one. The data input dialog box for adding a new material is the same as that for editing an existing record. Click on OK when done or click on Cancel to discard the changes.

The allowable ranges for the different properties are as follows:

Property	SI Units Min	SI Units Max	English Units Min	English Units Max
Material	-	-	-	-
Grade	-	-	-	-
Yield Strength	1	6894	0.1	999.9
Tensile Strength	1	6894	0.1	999.9
Total Elongation	1	99	1	99
n Value	0.01	9.99	0.01	9.99
r Value	0.1	9.9	0.1	9.9
Hardness	1	999	1	999
Min Width	25.4	3048	1	120
Max Width	25.4	3048	1	120
Min Thickness	0.03	99.99	0.001	3.936
Max Thickness	0.03	99.99	0.001	3.936
User Defined-1	-	-	-	-
User Defined-2	-	-	-	-
User Defined-3	-	-	-	-
Comments	-	-	-	-

7.1.7.4.3 Sort (MAP Data Menu)

Permits arranging material records in the active viewing archive according to the particular material properties. MAP displays the Sort Dialog Box in which you can choose the material properties you want to sort by and to select either ascending or descending sort order.

Select the Ascending option button to put the lowest number or beginning of the alphabet first in the list of sorted items. Select the Descending option button to put the highest number or end of the alphabet first in the list of sorted items.

The sort property defined in the Sort By box is used as the primary sorting key. Two additional boxes, Then By, in the Sort Dialog Box enable you to specify the order in which to sort if there are duplicate items in the previous material property you specified. Select the Ascending or Descending option button for each box to determine the arrangement of the data.

7.1.7.5 MAP Default Menu

Provides commands to show or set CARS default material. The Default menu includes Show CARS Default and Set CARS Default.

7.1.7.5.1 Show CARS Default (MAP Default Menu)

Lists the properties of the current CARS default material in a dialog box. Included in the box are constants for five steel properties: Modulus of Elasticity, Shear Modulus, mass density, Poisson's Ratio and coefficient of thermal expansion. Click on OK to close the dialog box.

7.1.7.5.2 Set CARS Default (MAP Default Menu)

Permits changing CARS default material using a material in the active viewing archive. CARS prompts for a new default ID number. Enter a number and click on OK to change the default material. Click Cancel to cancel the change operation.

7.1.7.6 MAP Units Menu

Provides commands related to current system of units and unit conversion. The Units menu includes kip,in,ksi (kilopounds, inches, kilopounds per square inch), N,mm,MPa (Newton, millimeter, MegaPascal), and Unit Conversion.

7.1.7.6.1 kip,in,ksi (MAP Units Menu)

Permits changing the active system of units to kip,in,ksi. If set, a check mark (✓) will appear before this option.

7.1.7.6.2 N,mm,MPa (MAP Units Menu)

Permits changing the active system of units to N,mm,MPa. If set, a check mark (✓) will appear before this option.

7.1.7.6.3 Unit Conversion (MAP Units Menu)

Converts entered value of selected units of measure from one system of units to other systems of units. There are ten categories of units of measure available for unit conversion. The ten categories are angular, area, force, inertia, length, mass, moment, stress, temperature and mass density.

To quickly access unit conversion tool, click the Unit Conversion button on the toolbar.



Unit Conversion

7.1.7.7 MAP Window Menu

Provides window management commands. The Window menu includes Tile, Cascade, Arrange Icons, Freeze Columns, and Unfreeze Columns.

7.1.7.7.1 Tile (MAP Window Menu)

Arranges the windows from top to bottom so that they cover the entire width of the desktop without overlapping one another. If there are more than three windows, CARS arranges them in a manner that allows more width than height.

7.1.7.7.2 Cascade (MAP Window Menu)

Stacks all windows and overlaps them so that each is the same size as all others and only part of each underlying window is visible.

7.1.7.7.3 Arrange Icons (MAP Window Menu)

Rearranges any icons on the desktop. The rearranged icons are evenly spaced, beginning at the lower left corner of the desktop. This command is useful when you resize your desktop that has minimized windows. It is unavailable when no windows are minimized.

7.1.7.7.4 Freeze Column (Map Window Menu)

Freezes one or more columns so that they become the leftmost columns and are visible at all times. Select the column to the right of the column where you want the split to appear and choose this menu option.

When an archive is open, the first two columns are frozen.

7.1.7.7.5 Unfreeze Column (Map Window Menu)

Unfreeze the frozen columns.

7.1.7.8 MAP Help Menu

Provides commands for accessing online help. The Help menu includes Contents, Search for Help on, Obtaining Technical Support, and About.

7.1.7.8.1 Contents (MAP Help Menu)

Displays the MAP online Help contents. It provides a comprehensive list that summarizes the organization of topics in the Help system.

7.1.7.8.2 Search for Help on (MAP Help Menu)

Opens the Search dialog box for Help to find information related to topics on which you want more information.

To use the Search For Help On command, type the topic or select it from the list in the Search dialog box, and then choose the Show Topics button to see related topics. To display a particular topic from the list of topics, select it and then choose the Go To button.

7.1.7.8.3 Obtaining Technical Support (MAP Help Menu)

Displays the help information regarding how to obtain the technical support.

7.1.7.8.4 About (MAP Help Menu)

Displays information on the development and sponsors of the CARS program.

7.1.7.9 MAP Shortcut Menu

A shortcut menu is a floating menu displayed over an archive viewing window, independent of the menu bar. The available menu options on the shortcut menu depend on where the pointer was located when the right mouse button was pressed. The Shortcut Menu contains the following options: Set as Default, View, Edit, Add, Print, Quick Sort Ascending, Quick Sort Descending, Sort by Material ID and Sort.

7.1.7.9.1 Set as Default (MAP Shortcut Menu)

Permits changing the default material using the highlighted material in the active viewing database. MAP prompts for a new default ID number in the Set Default Material dialog box. Enter a number and click on OK to change the default material. Click Cancel to cancel the change operation.

7.1.7.9.2 Edit (MAP Shortcut Menu)

Permits editing an existing material record in the current viewing database. Material Manager displays the current properties of the specified material in the Edit dialog box. Click on OK when done or click on Cancel to discard the changes.

7.1.7.9.3 Add (MAP Shortcut Menu)

Adds a new record at the end of the current viewing database. The ID number for the new material will be the current maximum ID number, plus one. The data input dialog box for adding a new material is the same as that for editing an existing record. Click on OK when done or click on Cancel to discard the changes.

7.1.7.9.4 Print (MAP Shortcut Menu)

Displays the Print Setup dialog box to print the currently highlighted material.

To quickly print the highlighted material, click on the Print button  on the toolbar.

7.1.7.9.5 Quick Sort Ascending (MAP Shortcut Menu)

Sorts the material records in the active viewing archive according to the highlighted material property in the ascending order.

7.1.7.9.6 Quick Sort Descending (MAP Shortcut Menu)

Sorts the material records in the active viewing archive according to the highlighted material property in the descending order.

7.1.7.9.7 Sort by Material ID (MAP Shortcut Menu)

Sorts the material records in the active viewing archive according to the material ID in the ascending order.

7.1.7.9.8 Sort (MAP Shortcut Menu)

Permits arranging material records in the active viewing archive according to the particular material properties. MAP displays the Sort Dialog Box in which you can choose the material properties you want to sort by and to select either ascending or descending sort order.

Select the Ascending option button to put the lowest number or beginning of the alphabet first in the list of sorted items. Select the Descending option button to put the highest number or end of the alphabet first in the list of sorted items.

The sort property defined in the Sort By box is used as the primary sorting key. Two additional boxes, Then By, in the Sort Dialog Box enable you to specify the order in which to sort if there are duplicate items in the previous material property you specified. Select the Ascending or Descending option button for each box to determine the arrangement of the data.

7.1.7.10 MAP Error Messages

Error messages are provided within MAP showing an error identification number and associated message. Refer to this section to correlate the error identification number with a brief error message description. These descriptions define each error and provide suggestions for correction of the problem.

Error 201: Unexpected Data in Archive:

The archive has information that MAP does not expect to find. The archive may have been corrupted.

Remedy: Check if there are other files in the same directory with the same filename as the current archive.

7.1.8 CARS ASDM

CARS ASDM is used to quickly and selectively access the contents of the Automotive Steel Design Manual (ASDM). Design guidelines, tables, equations, figures and other reference information can be viewed quickly and easily. Keyword searches and hyperlinks permit rapid identification of desired information.

CARS uses the Acrobat portable document format (PDF) program to display and access the ASDM contents. Refer to the on-line help supplied by Acrobat for details on the use of this versatile program. Refer to Acrobat's Plug-In Help for details on using Acrobat Search, a full-text indexed search utility that provides word stemming, thesaurus, proximity and Boolean operator search options.

When viewing the ASDM using the full screen option in Acrobat Reader, the Instrument Panel might be replaced with a black area on the screen. To correct this, please minimize the Instrument Panel then restore it.

7.1.9 CARS TEST DRIVE

CARS Test Drive is a slide show demo which provides an overview of CARS .

7.1.10 TECHNICAL SUPPORT

AISI/CARS was developed and is supported and distributed by Desktop Engineering Int'l Inc., Woodcliff Lake, New Jersey. For further information or technical support, contact:

AISI/CARS
Desktop Engineering Int'l Inc.
172 Broadway
Woodcliff Lake, NJ 07677 USA

Hotline: (800) 888-8680
Tel: (201) 505-9200
Fax: (201) 505-1566
e-mail: techsupport@deiusa.com
Internet: www.deiusa.com

Engineering consultation will also be available upon request to assist in solving complex problems and to develop customized user-defined modules.

7.1.11 AISI/CARS COPYRIGHTS, NOTICES AND LICENSE AGREEMENTS

7.1.11.1 Copyright

This software product is copyrighted and all rights are reserved by American Iron and Steel Institute and Desktop Engineering Int'l Inc. The distribution and sale of this product are intended for the use of the original purchaser only and for use only on the computer system specified. The software product may be used only under the provisions of the License Agreement that is included with this package.

The manual is copyrighted and all rights are reserved. This document may not be copied, photocopied, reproduced, translated, or reduced to any electronic medium or machine readable form, in whole or in part, without prior consent, in writing, from American Iron and Steel Institute or Desktop Engineering Int'l Inc.

The equations displayed in this manual were created using Mathtype from Design Science, Inc., Long Beach, CA 90803

Desktop Engineering Int'l Inc. is a subsidiary of D. V. Schiavello Enterprises Inc.

AISI/CARS is a trademark of American Iron and Steel Institute.

THE DESKTOP ENGINEER and DE/CAASE are trademarks of Desktop Engineering Int'l Inc.

Microsoft, MS, Windows and Windows NT are trademarks of Microsoft Corporation.

Copyright © 1991, 1998, 2000, 2002 American Iron and Steel Institute, Washington D. C., 20005.

Acrobat ® Reader copyright © 1987 - 1999 Adobe Systems Incorporated. Adobe and Acrobat are trademarks of Adobe Systems Incorporated.

Portions of this product were created using LEADTOOLS ©1991-2000, LEAD Technologies, Inc. ALL RIGHTS RESERVED.

Portions Copyright © 1985-2002 Desktop Engineering Int'l Inc., Woodcliff Lake, NJ 07677. All rights reserved.

7.1.11.2 Notice

The CARS program is for general information only. The information in it should not be used without first securing competent advice with respect to its suitability for any given application. The use of information contained in this program is not warranted to be applicable or suitable for any particular purpose. Any liability, including infringement of trademarks, copyrights or patents arising from the use of these materials is the sole responsibility of the user.

Section 3.1 of this manual contains equations and procedures that have been developed exclusively for steel. Use of these equations or procedures for non-steel material is not recommended.

7.1.11.3 License Agreement

CAREFULLY READ ALL THE TERMS AND CONDITIONS OF THIS AGREEMENT PRIOR TO OPENING THIS PACKAGE. OPENING THIS PACKAGE INDICATES YOUR ACCEPTANCE OF THESE TERMS AND CONDITIONS.

IF YOU DO NOT AGREE TO THESE TERMS AND CONDITIONS, RETURN THE UNOPENED DISKETTE PACKAGE AND THE OTHER COMPONENTS OF THIS PRODUCT TO THE PLACE OF PURCHASE AND YOUR MONEY WILL BE REFUNDED. NO REFUNDS WILL BE GIVEN FOR PRODUCTS WHICH HAVE OPENED DISKETTE PACKAGES OR MISSING COMPONENTS.

1. LICENSE

You have the non-exclusive right to use the enclosed package. This program can only be used on a single computer. You may physically transfer the program from one computer to another, provided that the program is used on only one computer at a time. You may not electronically transfer the program from one computer to another over a network. You may not distribute copies of the program or documentation to others. You may not modify or translate the program or related documentation without the prior written consent of American Iron and Steel Institute (hereinafter referred to as "AISI").

YOU MAY NOT USE, COPY, MODIFY, REVERSE ASSEMBLE, REVERSE COMPILE, OR TRANSFER THE PROGRAM OR DOCUMENTATION, OR ANY COPY EXCEPT AS EXPRESSLY PROVIDED IN THIS AGREEMENT.

2. BACK-UP AND TRANSFER

You may make one (1) copy of the program solely for back-up purposes. You must reproduce and include the copyright notice on the back-up copy. You may transfer the license and the product to another party if the other party agrees to the terms and conditions of this Agreement. If you transfer the program you must at the same time transfer the documentation and back-up copy or transfer the documentation and destroy the back-up copy.

3. COPYRIGHT

The program and its related documentation are copyrighted. You may not copy the program or its documentation except for back-up purposes and to load the program into the computer as part of executing the program. All other copies of the program and its documentation are in violation of this Agreement.

4. TERM

This license is effective until terminated. You may terminate it by destroying the program and documentation and all copies thereof. This license will also terminate if you fail to comply with any term or condition of this Agreement. You agree upon such termination to destroy all copies of the program and documentation.

5. LIMITED WARRANTY

THE PROGRAM IS PROVIDED "AS IS" WITHOUT WARRANTY OF ANY KIND. THE ENTIRE RISK AS TO THE RESULTS AND PERFORMANCE OF THE PROGRAM IS ASSUMED BY YOU. SHOULD THE PROGRAM PROVE DEFECTIVE, YOU (AND NOT AISI OR ITS DISTRIBUTOR AND DEALERS) ASSUME THE ENTIRE COST OF ALL NECESSARY SERVICING, REPAIR, OR CORRECTION. FURTHER, AISI DOES NOT WARRANT, GUARANTEE, OR MAKE ANY REPRESENTATIONS REGARDING THE USE OF, OR THE RESULTS OF THE USE OF, THE PROGRAM IN TERMS OF CORRECTNESS, ACCURACY, RELIABILITY, CURRENTNESS, OR OTHERWISE, AND YOU RELY ON THE PROGRAM AND RESULTS SOLELY AT YOUR OWN RISK.

AISI does warrant to the original licensee that the diskette(s) on which the program is recorded be free from defects in materials and workmanship under normal use and service for a period ninety (90) days from the date of delivery as evidenced by a copy of your receipt. AISI's and its distributors' and dealers' entire liability and your exclusive remedy shall be replacement, or at AISI's sole discretion, refund of purchase price, of the diskette not meeting AISI's limited warranty and which is returned to AISI with a copy of your receipt. If failure of the diskette has resulted from accident, abuse, or misapplication of the product, then AISI shall have no responsibility to replace the diskette under this Limited Warranty.

THE ABOVE IS THE ONLY WARRANTY OF ANY KIND, EITHER EXPRESSED OR IMPLIED, INCLUDING, BUT NOT LIMITED TO, THE IMPLIED WARRANTIES OF MERCHANTABILITY AND FITNESS FOR A PARTICULAR PURPOSE THAT IS MADE BY AISI ON THIS AISI PRODUCT. THIS WARRANTY GIVES YOU SPECIFIC LEGAL RIGHTS AND YOU MAY ALSO HAVE OTHER RIGHTS WHICH VARY FROM STATE TO STATE.

NEITHER AISI NOR ANYONE ELSE WHO HAS BEEN INVOLVED IN THE CREATION, PRODUCTION, OR DELIVERY OF THIS PROGRAM SHALL BE LIABLE FOR ANY DIRECT, INDIRECT, CONSEQUENTIAL, OR INCIDENTAL DAMAGES ARISING OUT OF THE USE, THE RESULTS OF USE, OR INABILITY TO USE SUCH

PRODUCT EVEN IF AISI HAS BEEN ADVISED OF THE POSSIBILITY OF SUCH DAMAGES OR CLAIM.

6. MISCELLANEOUS

This license agreement shall be governed by the laws of the State of Michigan.

7. ACKNOWLEDGMENT

YOU ACKNOWLEDGE THAT YOU HAVE READ THIS AGREEMENT, UNDERSTAND IT, AND AGREE TO BE BOUND BY ITS TERMS AND CONDITIONS. YOU ALSO AGREE THAT THIS AGREEMENT IS THE COMPLETE AND EXCLUSIVE STATEMENT OF AGREEMENT BETWEEN THE PARTIES AND SUPERSEDES ALL PROPOSALS OR PRIOR AGREEMENTS, VERBAL OR WRITTEN, AND ANY OTHER COMMUNICATIONS BETWEEN THE PARTIES RELATING TO THE SUBJECT MATTER OF THIS AGREEMENT.

Should you have any questions concerning this Agreement, please contact in writing American Iron and Steel Institute, 1101 17th Street, NW, Washington, D.C. 20005.

REFERENCES FOR SECTION 7.1

1. Automotive Steel Design Manual, Revision 6, American Iron and Steel Institute, Washington D.C., April 2000.
2. Cold Formed Steel Design Manual, American Iron and Steel Institute, Washington D.C., 1996 Edition .
3. The Desktop Engineer 2000, Version 6.0, February 2000, Desktop Engineering Int'l Inc., Woodcliff Lake, New Jersey.

7.2 AISI/CARS TUTORIALS

This section provides tutorials that illustrate the use of AISI/CARS for the design of vehicle components. Note that some of these tutorials have a corresponding case study in [Section 6.1](#). [Table 7.2-1](#) lists the tutorials and the CARS program(s) used in the tutorial. The associated GAS cross section files and KEY Design Procedure files are included with the CARS program for CARS users to review.

Table 7.2-1 Tutorials

Section	Tutorial	CARS Program	Case Study
7.2.1	Front Rail Design	GAS, KEY, MAP	Section 6.1.7
7.2.2	Hybrid Section Analysis	GAS, KEY, MAP	

7.2.1 FRONT RAIL DESIGN

7.2.1.1 Problem Description

To help demonstrate CARS capability, a front rail design example is considered. The front rail and its connection to the body have a great influence on load transfer in the automotive body. The cross section for the front rail used in this tutorial is a hat section with segment thickness of 1.55 mm as shown in [Figure 7.2.1.1-1](#). The length of the front rail is 300 mm and the yield strength of the material is 365 MPa. The challenge in this study is to reduce the mass of the front rail and maintain the axial capacity. This study is divided into four parts:

1. Axial Capacity Calculation for the Front Rail with Hat Section
2. Front Rail Mass Reduction Study Using CARS Results
3. Trend Analysis in GAS to Find Optimal Segment Thickness for the Hexagonal Section
4. Axial Capacity Calculation for the Front Rail With Hexagonal Section

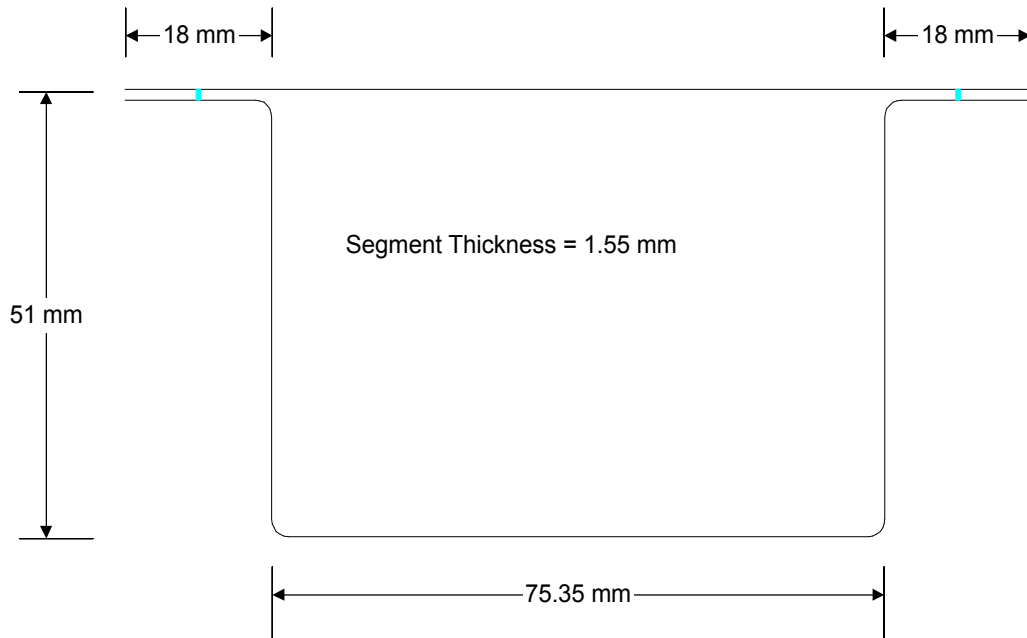


Figure 7.2.1.1-1 Hat section of the front rail

7.2.1.2 Axial Capacity Calculation for the Front Rail with Hat Section

To explore possible mass reduction means, we need to compute the axial capacity of the front rail with the hat section and study the results. The following steps outline the process of calculating the axial capacity of the front rail with the hat section using CARS:

- Define the default material in MAP.
- Construct the hat section in GAS.
- Compute nominal cross section properties using GAS.
- Compute effective cross section properties using GAS.
- Compute axial capacity using Design Procedure 3.1-G16 and GAS.

7.2.1.2.1 Define The Default Material In MAP

CARS provides an ASDM material archive with the most frequently used automotive steels. In addition, CARS offers the capability of default material assignment. Once a default material is defined, the material properties associated with that material will be used in Design Key and GAS automatically.

The following steps outline the process of setting the default material:

1. Start MAP (Material Archive Program) in the CARS program group.
2. Select File/Open/ASDM Material Archive from the pull-down menu.
3. Select Default/Set CARS Default from the pull-down menu.
4. Select material CR SAE J2340 Grade 340X by entering 25 in the input box as the new default material ID and click OK.

7.2.1.2.2 Construct the Hat Section in GAS

The following steps outline the process of constructing the hat section in GAS:

1. Start GAS (Geometric Analysis of Section) in the CARS program group
2. Change the units system to the metric system by choosing Units/N, mm, MPa from the pull-down menu.
3. Select Physical/Set Default Physical Properties from the pull-down menu and enter 1.55 into the "Thickness" input box. This ensures the lines and arcs created afterward will have 1.55 mm thickness.
4. Create the points by using Create/Points/Coordinate menu option.
5. Create the lines by using Create/Lines/Existing Points menu option. For each line, enter the starting point number and the ending point number.
6. Create arcs using Create/Arcs/Tangent Lines menu option. Specify the line numbers of two tangent lines of the arc and the radius of the arc.
7. Create the welds using Create/Welds menu option. Specify the end point numbers of the weld.
8. Select File/Save Section menu option. Specify the database name and the section name.

7.2.1.2.3 Compute Nominal Cross Section Properties

In GAS, the following steps can be used to compute the nominal cross section properties and to save the results to a file:

1. Select Analysis/Nominal Properties/Single Calculation from the pull-down menu.
2. When the analysis is successfully done, a dialog box with the message “Analysis complete. View Results?” will appear. Click Yes to view the results.
3. Select File/Save Results As from the pull-down menu and specify a file name to save the results to a file.

7.2.1.2.4 Compute Effective Cross Section Properties

In GAS, the following steps can be used to compute the effective cross section properties for axial capacity calculation and to save the results to a file:

1. Select Analysis/Effective Properties/Single Calculation from the pull-down menu.
2. In the Effective Properties Analysis Option dialog box, select Yield Stress as the stress level and Axial in the direction selection box.
3. Click OK for the warning message about edge stiffener.
4. When the analysis is successfully done, a dialog box with the message “Analysis complete. View Results?” will appear. Click Yes to view the results.
5. Select File/Save Results As from the pull-down menu and specify a file name to save the results to a file.

7.2.1.2.5 Compute Axial Capacity Using Design Procedure 3.1-G16 and GAS

Design Procedure 3.1-G16 in Design Key automates the process of calculating member axial capacity. It reads the cross section properties required in the process from the specified GAS nominal and effective property result files. The process of using Design 3.1-G16 and GAS for the front rail axial capacity calculation is shown as follows:

1. Start Design Key in the CARS program group.
2. Make sure the units system is the metric system. If not, choose Units/N, mm, MPa menu option.
3. Select File/New Design from the pull-down menu.
4. Highlight 3.1-G16 in the Select Design Procedure dialog box and click OK.
5. Click OK in the dialog box with the message “ASDM design procedures should be reviewed prior to performing an analysis”.
6. At Step 3A of DP 3.1-G16, select the effective property file saved in [Section 7.2.1.2.4](#).
7. At Step 3B of DP 3.1-G16, select the nominal property file saved in [Section 7.2.1.2.3](#).
8. At Step 4 of DP 3.1-G16, click OK in the Data Input dialog box to take the default E and Fy values read from the effective property file.
9. At Step 6 of DP 3.1-G16, select No as the answer to the question “Member subject to torsional-flexural buckling?” and click OK.
10. At Step 10 of DP 3.1-G16, select No as the answer to the question “Cylindrical tube?” and click OK.
11. At Step 12A of DP 3.1-G16, click OK in the Data Input dialog box to take the default “r value” read from the nominal property file.
12. At Step 12B of DP 3.1-G16, Enter 1 as K and 300 as L. Click OK to continue.

13. At Step 23 of DP 3.1-G16, A message box will appear that states “Go to GAS. Set stress level = F_{cu} in Effective Property Calculation”. This indicates the ultimate stress, F_{cu} , computed from the global buckling is less than the yield stress. Since the effective properties calculated in [Section 7.2.1.2.4](#) were based on the assumption that the member will reach yield stress, the effective properties should be recalculated using the computed F_{cu} . From the results at Step 18 of DP 3.1-G16, $F_{cu} = 363.7$ MPa.
14. Start GAS in the CARS program group.
15. Select File/Get Section from the pull-down menu to retrieve the saved cross section.
16. Follow [Section 7.2.1.2.4](#) to redo the effective property calculation. However, in the Effective Properties Analysis Option dialog box, select Specified Stress as the stress level as well as Axial in the direction selection box and type 363.7 in the “Stress” input box. The graphical results of this effective property calculation are shown in [Figure 7.2.1.2-1](#). Save the results to a file by selecting File/Save Results As from the pull-down menu.
17. Go back to Design Key and click OK in the message box.
18. At Step 24 of DP 3.1-G16, select the effective property result file using the analysis option of stress level of 364.1 MPa.
19. At Step 25 of DP 3.1-G16, click OK in the Data Input dialog box to take the default A_e value read from the effective property file.
20. The final results from Design Key are shown in [Figure 7.2.1.2-2](#). P_u is 151800 Newtons (Step 26 of DP 3.1-G16).

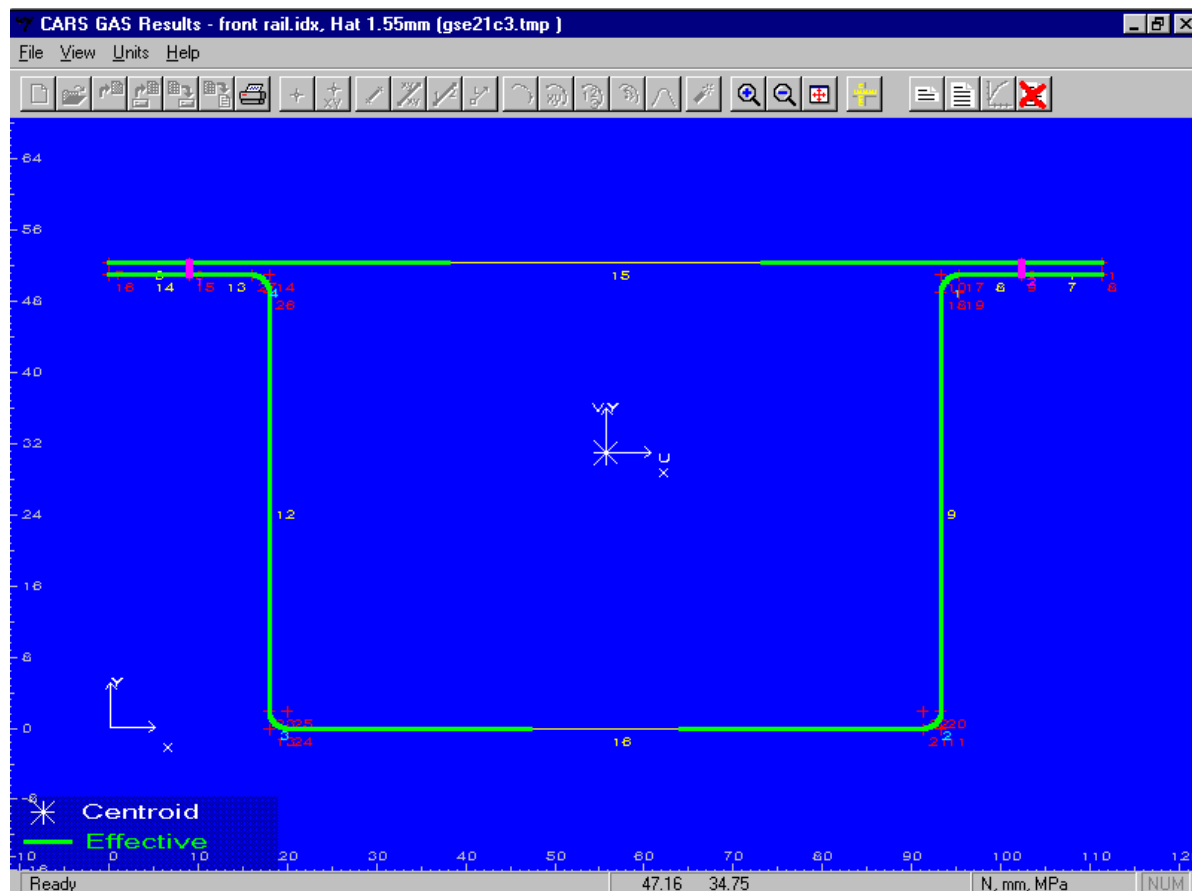


Figure 7.2.1.2-1 Graphical results of effective property calculation for hat section

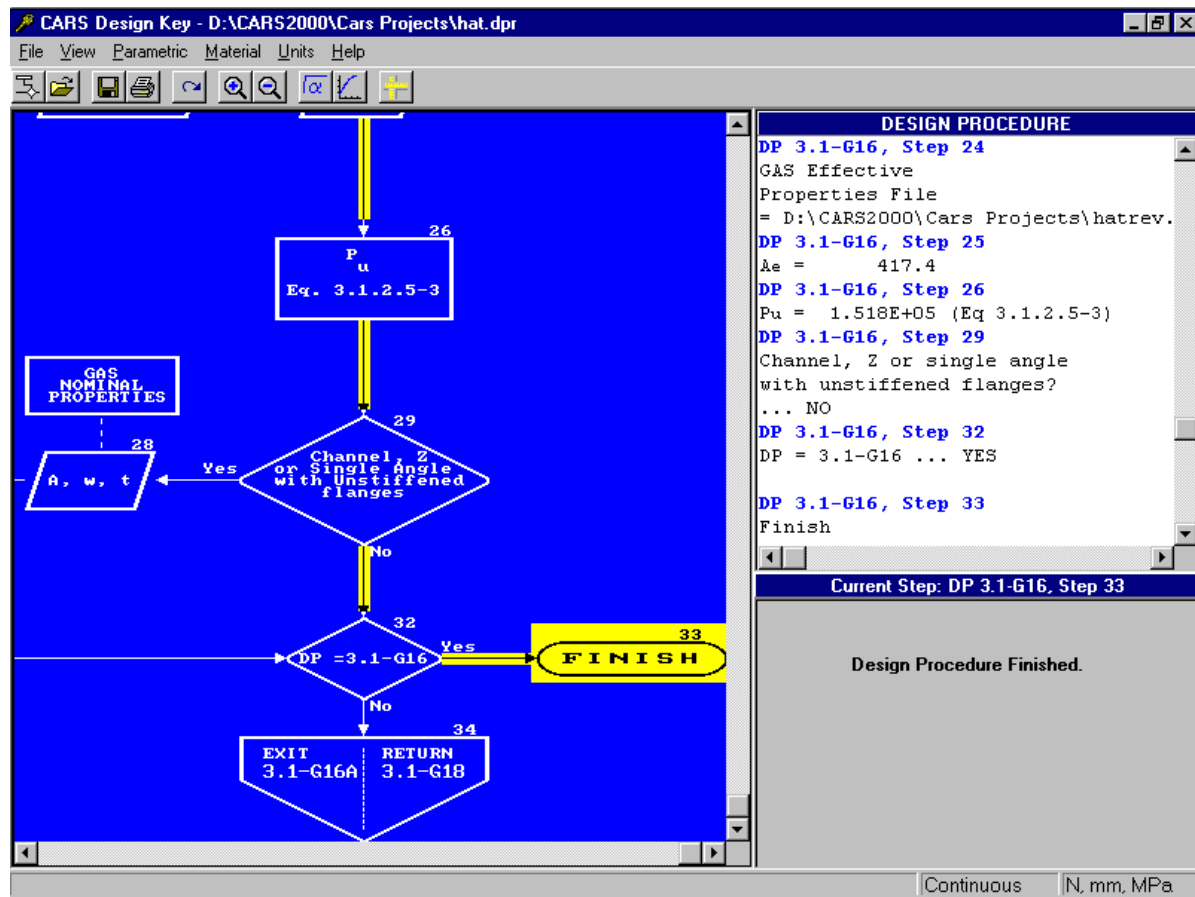


Figure 7.2.1.2-2 Axial capacity calculation results for front rail with hat section

7.2.1.3 Front Rail Mass Reduction Study Using CARS Results

From the analysis results ([Figure 7.2.1.2-2](#)), the axial capacity is computed using [Equation 3.1.2.5-3](#) of the ASDM.

$$P_u = A_e * F_{cu}$$

where P_u = axial load capacity

A_e = the effective area at the stress F_{cu}

F_{cu} = ultimate compression stress under concentric loading

From the above equation, it is shown that the axial capacity is a function of F_{cu} and the effective area at stress F_{cu} . The effective area is the sum of the product of effective width and thickness of all the segments. [Figure 7.2.1.2-1](#) shows the graphical results of the effective property calculation. The thick lines indicate the effective width of segments. The effective width gives an indication of how much of the segment is effective at the specified stress level. It was observed that the top and bottom flanges were not fully effective.

To improve the effectiveness of the top and bottom flanges, a hexagonal shape shown in [Figure 7.2.1.3-1](#) was proposed. The idea is to increase the effective width of the flanges by breaking the partially effective segments into two. This can lead to a smaller width/thickness ratio, w/t , thus resulting in a larger effective width. If we can increase the effective width, the required segment thickness might be reduced.

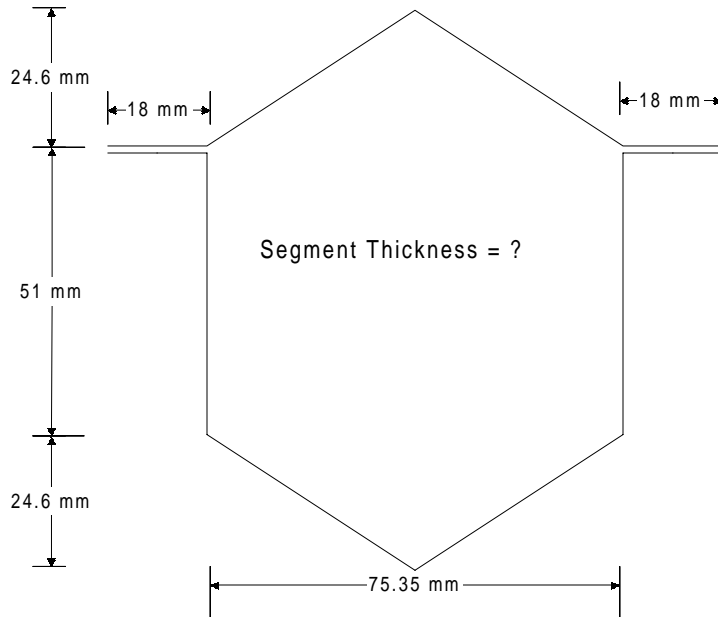


Figure 7.2.1.3-1 Proposed hexagonal section

7.2.1.4 Trend Analysis in GAS to Find Optimal Segment Thickness for the Hexagonal Section

The next step is to find the thickness of the proposed hexagonal section that can provide the same axial capacity of the original design. As discussed in [Section 7.2.1.3](#), the axial capacity is a function of the effective area. The effective area of the hat section was 417.4 mm^2 . The effective area of the hexagonal section should be at least 417.4 mm^2 . GAS can be used for this task as follows:

1. Construct the hexagonal section in GAS.
2. Select **Analysis/Effective Properties/Trend Analysis** from the pull-down menu.
3. Select **Specified Stress** as the stress level as well as **Axial** in the Direction selection box and type **363.7** in the "Stress" input field.
4. In Define Trend Analysis Parameter dialog box, enter **Thickness** as the parameter name, select **Thickness of All Entities** as the parameter type, as well as enter **1.2** in the "From" input box, **1.55** in the "To" input box and **0.05** in the "Interval" input box. GAS will compute the effective properties of 8 cross sections with the thickness varying from 1.2 mm to 1.55 mm with the interval of 0.05 mm.
5. Click **OK** for the warning message about edge stiffener.
6. When the analysis is successfully done, a dialog box with the message "Analysis complete. View Results?" will appear. Click **Yes** to view the results.

7. Select **Step 1: Thickness = 1.2** in the Select Parametric Study Results dialog box and click **OK**.
8. GAS will show the effective cross section of the hexagonal section with thickness of 1.2 mm.
9. Select **View/XY Plot** menu option and GAS will show a plot of Effective Area vs. Thickness as shown in [Figure 7.2.1.4-1](#).
10. The effective area of the hexagonal section with a thickness of 1.3 mm is 424.13 mm^2 which is greater than 417.3 mm^2 . Use 1.3 mm as the thickness of the hexagonal section.

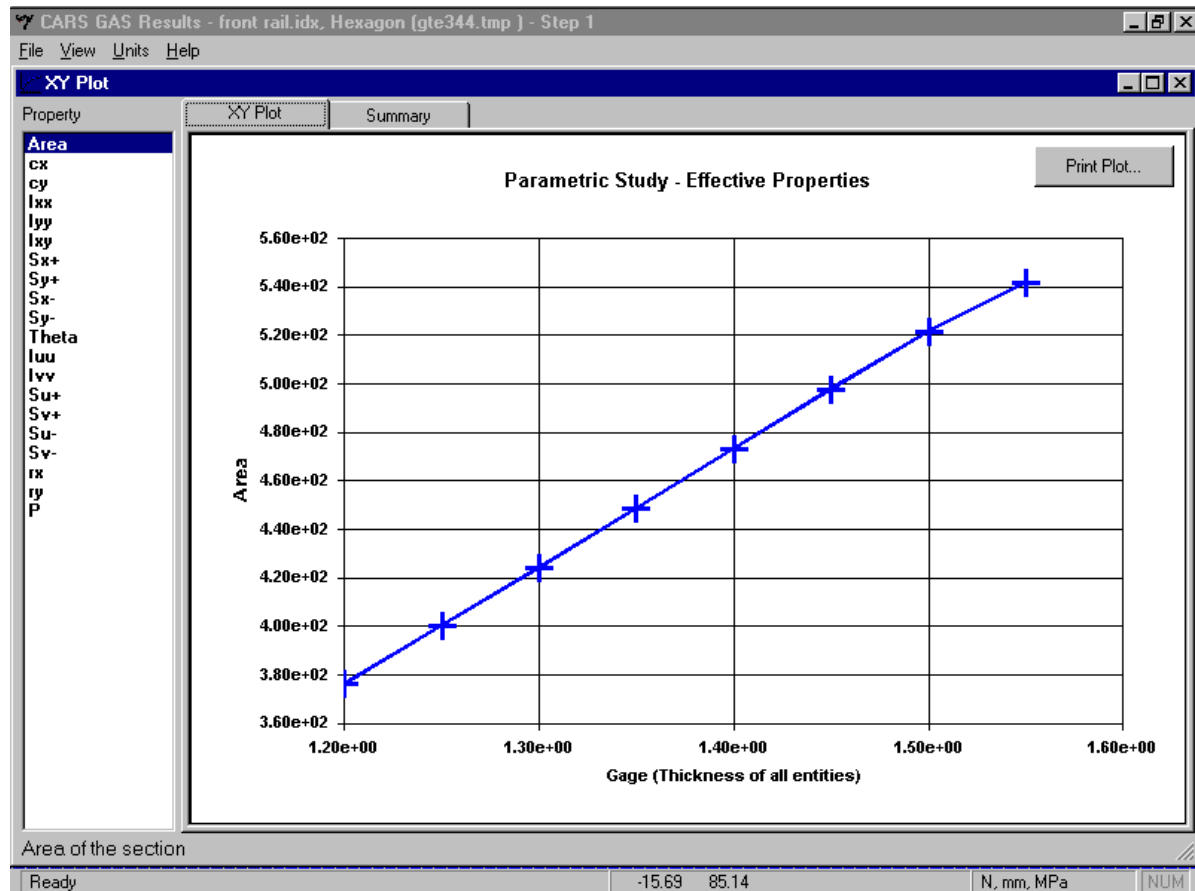


Figure 7.2.1.4-1 Plot of effective area vs. thickness from the Trend Analysis results in GAS

7.2.1.5 Axial Capacity Calculation for the Front Rail With Hexagonal Section

Follow the procedure outlined in [Section 7.2.1.2.5](#) to compute the axial capacity of the front rail with hexagonal section. The results are shown in [Figure 7.2.1.5-1](#). The computed axial capacity, P_u , is 154,400 Newtons.

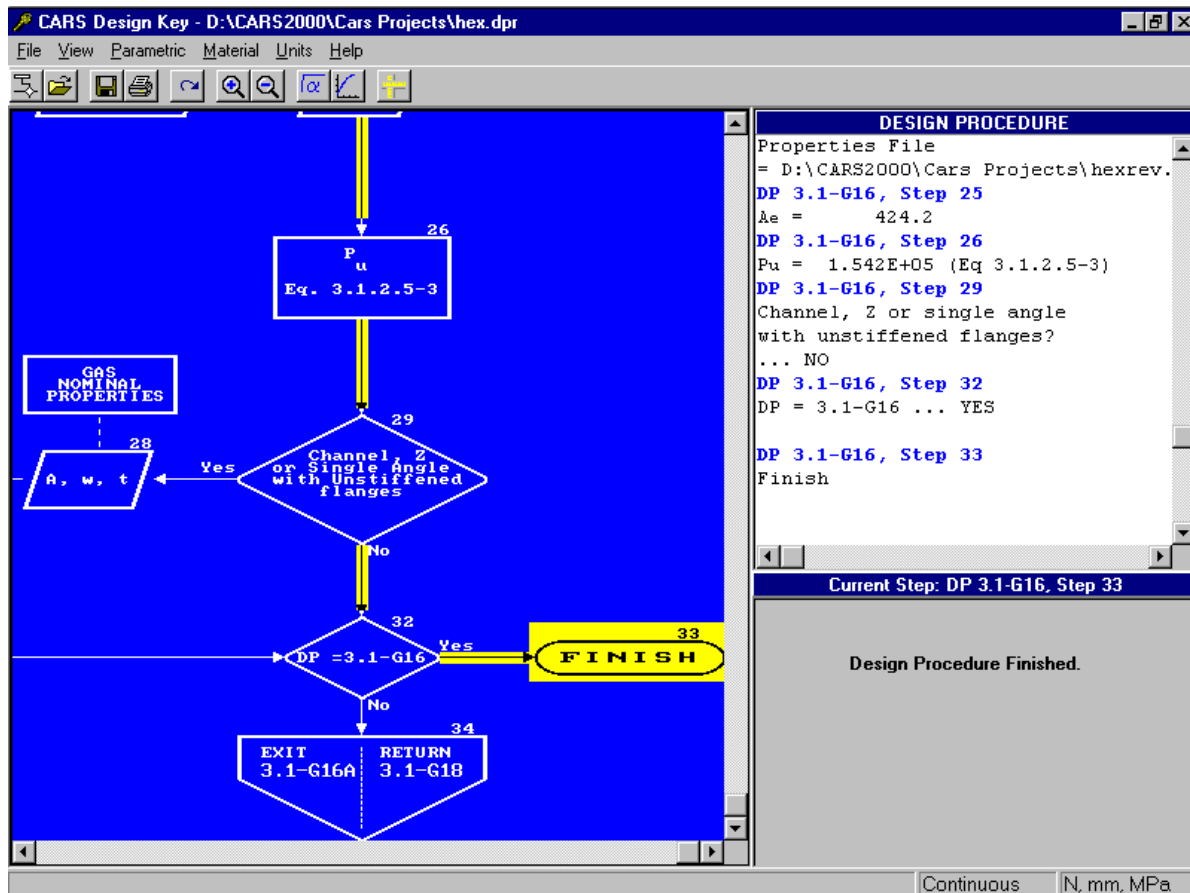


Figure 7.2.1.5-1 Axial capacity results for front rail with hexagonal section

7.2.1.6 Conclusions

Table 7.2.1.6-1 summarizes the results. By using CARS , we found that the hexagonal section can effectively replace the hat section. In addition, we have achieved a mass reduction of eight percent.

Table 7.2.1.6-1 Results Summary

Description	Front Rail w/ Hat Section	Front Rail w/ Hexagonal Section
Thickness	1.55 mm	1.3 mm
Axial Capacity	151,800 Newtons	154,200 Newtons
Mass	1.16 kg	1.07 kg

7.2.2 HYBRID SECTION ANALYSIS

7.2.2.1 Problem Description

Two new features in GAS are:

- Calculation of the effective properties of a hybrid section
- Calculation of the Reference Load

A hybrid section is defined as a section that consists of more than one material. The Reference Load is the load corresponding to the computed stress distribution for the effective cross section properties calculation. To illustrate how to use these two new features, this tutorial uses a test specimen from the University of Missouri-Rolla. The task is to compute the axial capacity of a stub column with a hybrid section using GAS and compare the results with the test results.

The box-shaped specimen was assembled by using two hat sections fabricated from two different materials (50SK and 25AK). The configuration of the specimen is shown in [Figure 7.2.2-1](#). The specimen is tested under a strain rate of 0.01.

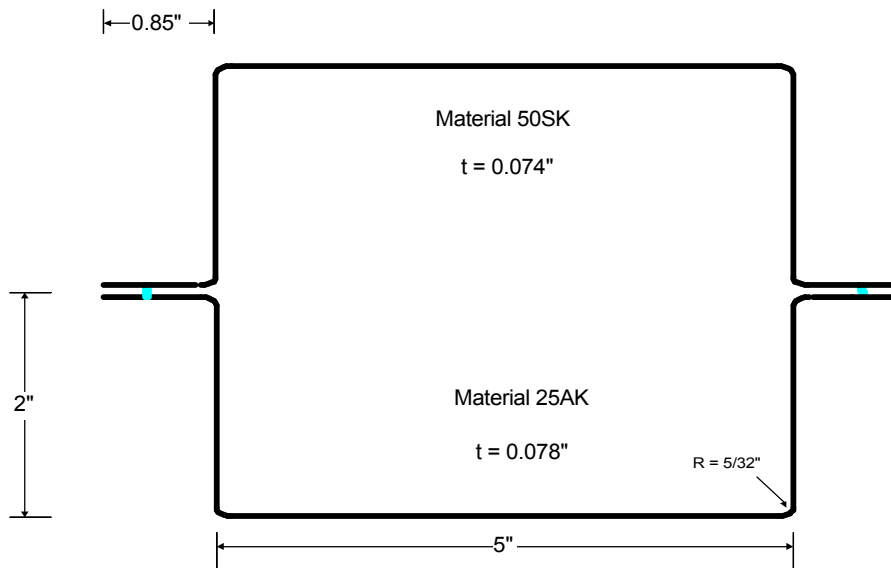


Figure 7.2.2-1 Hybrid Box-Shaped Stub Column

This tutorial is divided into four parts:

1. User Defined Archive Creation
2. Cross Section Creation
3. Effective Properties Calculation
4. Results Comparison

7.2.2.2 User Defined Archive Creation

The material properties presented in the ASDM archive are typical values. Since the purpose of this study is to verify the test results, the exact material property values from the material test should be used. From Tables 3.7 and 3.8 in [Reference 1](#), the dynamic yield strength under the strain rate of 0.01 is 27.86 ksi for 25AK sheet steel and 56.83 ksi for 50SK sheet steel.

The following steps outline the process of creating a user defined archive containing two materials mentioned above:

1. Start MAP (Material Archive Program) in the CARS program group.
2. Select Units/kip, in ksi from the pull-down menu.
3. Select File/New from the pull-down menu and define the archive name - Hybrid.
4. Click OK in the dialog box for the user defined column titles.
5. The Add Material dialog box will appear. Enter 25AK in the Material input field and 27.86 in the Yield Strength input field. ([Figure 7.2.2.2-1](#)).
6. Select Data/Add from the pull-down menu. Enter 50SK in the Material input field and 56.83 in the Yield Strength input field.
7. Select Default/Set CARS Default from the pull-down menu.
8. Select material 50SK by entering 2 in the input box as the new default material ID and click OK.
9. Select File/Exit from the pull-down menu to close MAP and the archive.

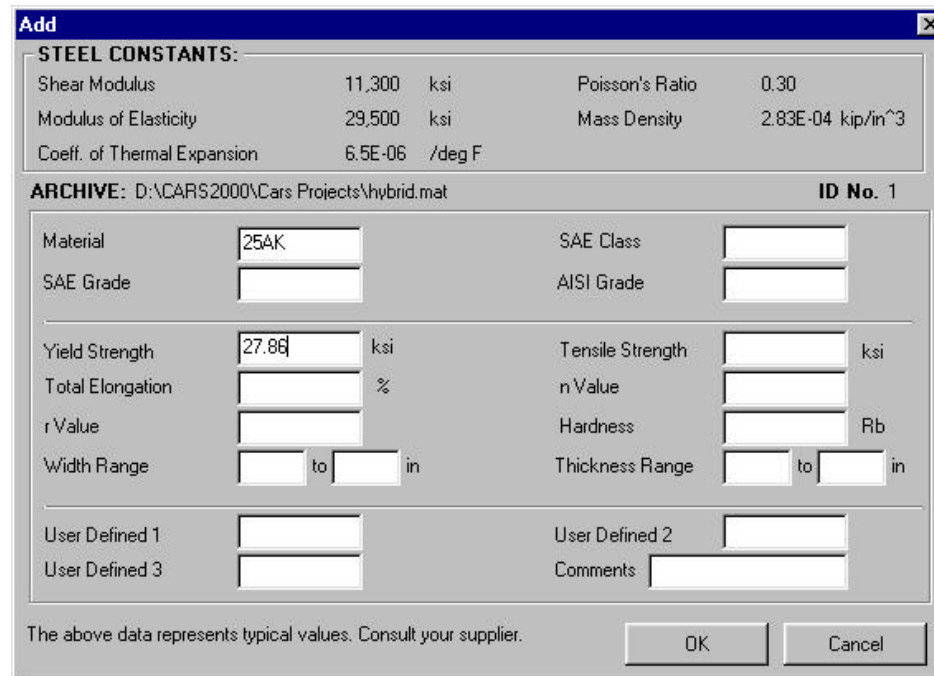


Figure 7.2.2.2-1 Add Material Dialog Box in MAP

7.2.2.3 Cross Section Construction

The following steps outline the process of constructing the section in GAS:

1. Start GAS (Geometric Analysis of Section) in the CARS program group.
2. Set the units system to the English system by choosing Units/kip, in, ksi from the pull-down menu.
3. Select Physical/Set Default Physical Properties from the pull-down menu and enter 0.074 into the "Thickness" input box. This ensures the lines and arcs created afterward will have 0.074" thickness.
4. Follow steps presented in [Section 7.2.2.3.1](#) for points creation.
5. Follow steps presented in [Section 7.2.2.3.2](#) for lines creation.
6. Follow steps presented in [Section 7.2.2.3.3](#) for arcs creation.
7. Follow steps presented in [Section 7.2.2.3.4](#) for welds creation.
8. Follow steps presented in [Section 7.2.2.3.5](#) for entities properties modification.
9. Use View/Entity List menu option to check the description of all the entities.
10. Use File/Save Section menu option to save the created section into a database.

7.2.2.3.1 Points Creation

The first step of cross section construction is to define the construction points. We need to input 16 construction points, 8 points for each hat section. The point coordinates are shown in [Table 7.2.2.3.1-1](#). The following steps outline the process of creating the construction points:

1. Select Create/Points/Coordinate from the pull-down menu or click the  icon on the tool bar.
2. Enter the coordinates of point 1 and click Next Button. ([Figure 7.2.2.3.1-1](#))
3. Enter the coordinates of each point and click Next Button. When entering the coordinate of the last point, point 16, click Finish Button.

Table 7.2.2.3.1-1 Coordinates of the construction points

Point No.	X	Y	Point No.	X	Y
1	-0.85	0	9	-0.85	-0.074
2	-0.425	0	10	-0.425	-0.074
3	0	0	11	0	-0.074
4	0	2	12	0	-2.074
5	5	2	13	5	-2.074
6	5	0	14	5	-0.074
7	5.425	0	15	5.425	-0.074
8	5.85	0	16	5.85	-0.074

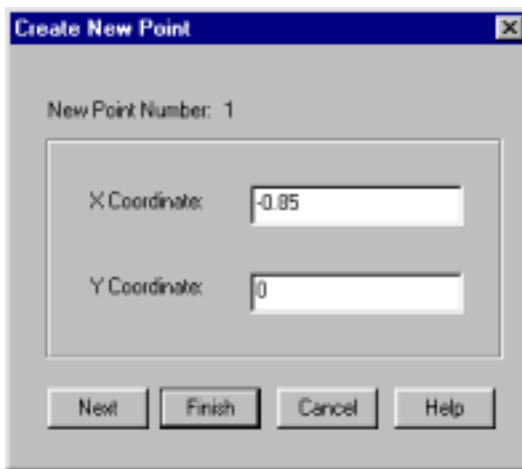


Figure 7.2.2.3.1-1 Point Creation Dialog Box

7.2.2.3.2 Line Creation

The cross section contains 14 lines. The connectivity of the 14 lines are shown in [Table 7.2.2.3.2-1](#). The following steps outline the process of constructing the lines:

1. Select **Create/Lines/Existing Points** from the pull-down menu or click the  icon on the tool bar.
2. Enter the starting point number and ending point number of line 1 and click **Next** Button. ([Figure 7.2.2.3.2-1](#))
3. Enter the starting point number and ending point number of each line and click **Next** Button. When entering the connectivity of the last line, line 14, click **Finish** Button.

Table 7.2.2.3.2-1 Connectivity of Lines

Line No.	Starting Point No.	Ending Point No.	Line No.	Starting Point No.	Ending Point No.
1	1	2	8	9	10
2	2	3	9	10	11
3	3	4	10	11	12
4	4	5	11	12	13
5	5	6	12	13	14
6	6	7	13	14	15
7	7	8	14	15	16

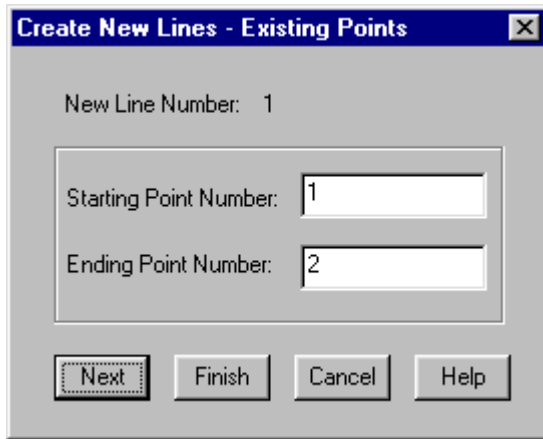


Figure 7.2.2.3.2-1 Line Creation Dialog Box

7.2.2.3.3 Arcs Creation

The cross section contains 8 arcs with a radius of 5/32" or 0.15625". The tangent lines used for arcs creation are shown in [Table 7.2.2.3.3-1](#). The following steps outline the process of constructing the arcs:

1. Select **Create/Arcs/Tangent Lines** from the pull-down menu or click the  icon on the tool bar.
2. Enter the line numbers of the tangent lines, which are lines 2 and 3, of arc 1 and click **OK Button**. ([Figure 7.2.2.3.3-1](#))
3. GAS will show the arc and ask for confirmation. Click Yes to accept the arc.
4. Repeat Steps 1 to 3 for each arc.

Table 7.2.2.3.3-1 Tangent Lines for Arcs Creation

Arc No.	First Tangent Line No.	Second Tangent Line No.	Arc No.	First Tangent Line No.	Second Tangent Line No.
1	2	3	5	9	10
2	3	4	6	10	11
3	4	5	7	11	12
4	5	6	8	12	13

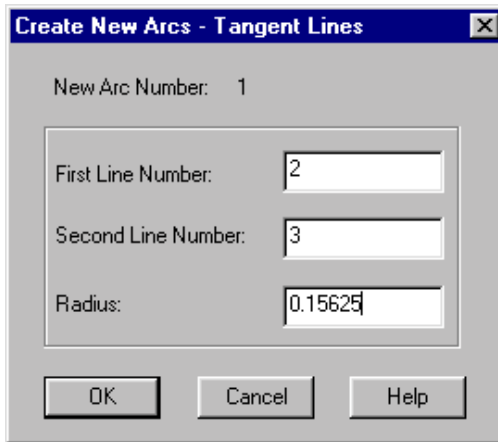


Figure 7.2.2.3.3-1 Arc Creation Dialog

7.2.2.3.4 Welds Creation

The cross section contains 2 welds. The following steps outline the process of constructing the welds:

1. Select **Create/Welds** from the pull-down menu or click the  icon on the tool bar.
2. Enter the starting point number and ending point number, which are points 2 and 10, of weld 1 and click **Next** Button. ([Figure 7.2.2.3.4-1](#))
3. Enter the starting point number and ending point number, which are points 7 and 15, of weld 2 and click **Finish** Button.

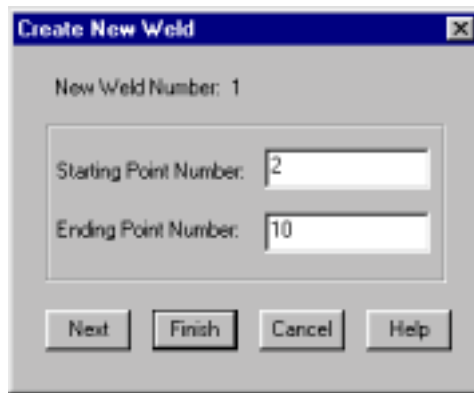


Figure 7.2.2.3.4-1 Weld Creation Dialog Box

7.2.2.3.5 Entities Properties Modification

All the entities created so far were assigned the default thickness 0.074" and the default material 50SK. Since the bottom hat section has different thickness and material, entities properties modification is necessary. To edit the bottom hat section, follow the following steps:

1. Define a rectangular box on the screen which include the bottom hat section by:
 - Move the cursor to one corner of the rectangular box and press left button of the mouse.
 - Hold down the left button and move the cursor to the opposite corner
 - Release the left button

2. Click right button of the mouse to activate the shortcut menu.
3. Select **Edit Material** from the shortcut menu and click **Modify** button.
4. Select **25AK** and click **OK**.
5. Click right button of the mouse to activate the shortcut menu.
6. Select **Edit Thickness** from the shortcut menu and enter **0.078** in the dialog box.

7.2.2.4 Compute Effective Cross Section Properties

The following steps can be used to compute the effective cross section properties for axial capacity calculation and to save the results to a file:

1. Select **Analysis/Effective Properties/Single Calculation** from the pull-down menu.
2. In the Effective Properties Analysis Option dialog box, select **Yield Stress** as the stress level and **Axial** in the direction selection box.
3. When the analysis is successfully done, a dialog box with the message “Analysis complete. View Results?” will appear. Click **Yes** to view the results.
4. Select **View/Results Summary** from the pull-down menu.
5. From the Results Summary dialog box ([Figure 7.2.2.4-1](#)), find the Reference Load P which is 56.203 kips.
6. Select **File/Save Results As** from the pull-down menu and specify a file name to save the results to a file.

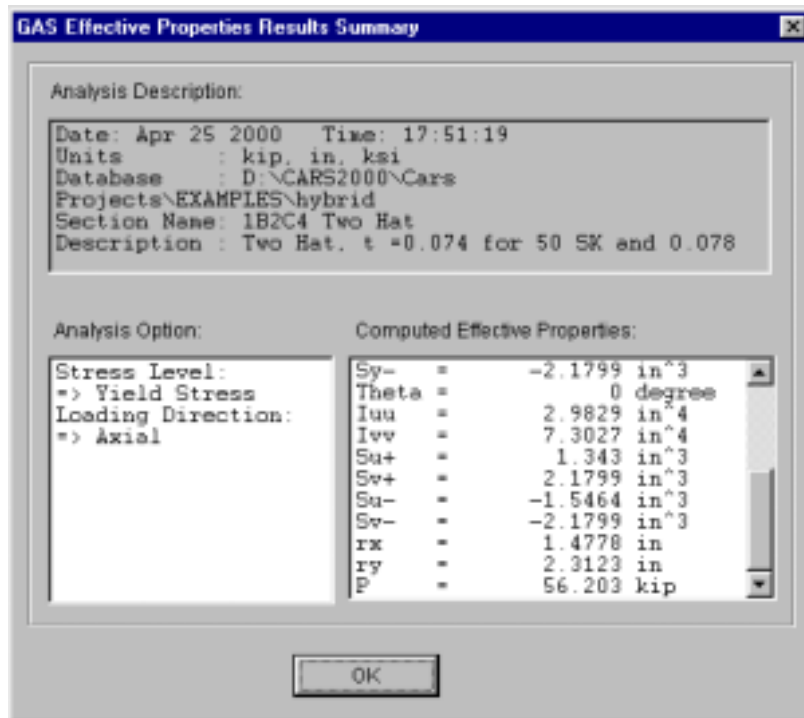


Figure 7.2.2.4-1 Results Summary of the Effective Cross Section Properties Calculation

7.2.2.5 Results Comparison

The slenderness ratio of the test stub column was small to avoid overall buckling of the member. Therefore, the reference load computed by GAS can be used to compare with the ultimate load obtained from the test results. Comparisons of the test and GAS computed ultimate loads are presented in [Table 7.2.2.5-1](#). The difference is about 1.3 percent.

Table 7.2.2.5-1 Results Comparison

Test Ultimate Load	GAS Computed Ultimate Load	Difference
55.5 kips	56.203 kips	1.3 %

REFERENCES FOR SECTION 7.2

1. Pan, Chi-Ling and Yu, Wei-Wen "Effect of Strain Rate on the Structural Strength and Crushing Behavior of Cold-Formed Steel Stub Columns", Nineteenth Progress Report, Civil Engineering Study, 93-1, University of Missouri-Rolla, July 1993.

APPENDIX A SYMBOLS AND DEFINITIONS

[Table A-1](#) lists the symbols and definitions used in the Manual.

Table A-1 Symbols and Definitions

Symbol	Definition	Section
$2N_f$	Reversals to failure	3.5.3.2
$2N_f$	Reversals to failure	3.5.3.4
$2N_f$	Reversals to failure	3.5.4.1
$2N_f$	Reversals to failure	3.5.4.2
$2N_f$	Reversals to failure	3.5.5.3
$2N_f$	Reversals to failure	3.5.9.2
$2N_f$	Reversals to failure	3.5.9.3
$2N_f$	Reversals to failure	3.5.9.4
$2N_t$	Transition fatigue life	3.5.4.1
α	Reduction factor for area of stiffeners	3.1.2.1.4
α	Angle of arc (in deg.)	3.2.1
α	Angle of arc (in deg.)	3.3.2
β	Material constant	3.5.7.3.1
β	Material constant	3.5.7.3.3.1
δ_l	Change in gage length	3.5.2
Δe	Change in engineering strain	3.5.2
Δe	Nominal strain range remote from notch	3.5.4.2
ΔK_{eq}	Equivalent stress intensity factor range	3.5.7.3.2
ΔS	Change in engineering stress	3.5.2
ΔS	Nominal stress range remote from notch	3.5.4.2
$\Delta \epsilon$	Local true strain range at the notch root	3.5.4.2
$\Delta \epsilon/2$	Total strain amplitude	3.5.4.1
$\Delta \epsilon/2$	Morrow model (total strain amplitude)	3.5.5.3
$\Delta \epsilon_e/2$	True elastic strain amplitude	3.5.4.1
$\Delta \epsilon_p/2$	Stable plastic strain amplitude	3.5.4.1
$\Delta \sigma$	Total stress range	3.5.4.1
$\Delta \sigma$	Local true stress range at the notch root	3.5.4.2
$\Delta \sigma/2$	Stable stress amplitude	3.5.4.1
$\Delta \sigma_{t,max}$	Maximum local notch stress range	3.5.7.3.2
φ	Hole diameter	3.1.2.1.1
φ	Angle of twist per unit length	3.1.4.1.1
ϵ	Strain rate	2.11
ϵ	True strain	3.5.2
ϵ	Total true strain	3.5.2
ϵ_a	Normal strain amplitude	3.5.8.2
ϵ_a	Strain amplitude	3.5.4.1

Table A-1 (Continued)

Symbol	Definition	Section
ε_a	Strain amplitude	3.5.9.4
ε_a^e	Elastic strain amplitude	3.5.9.4
ε_a^p	Plastic strain amplitude	3.5.9.3
$\varepsilon_a^{p'}$	Plastic strain amplitude	3.5.9.4
ε_{cu}	Parameter	3.1.3.1.3
ε_f	True fracture ductility	3.5.2
ε'_f	Fatigue ductility coefficient	3.5.4.1
ε''_f	Fatigue ductility coefficient	3.5.4.2
ε'''_f	Fatigue ductility coefficient	3.5.5.3
ε''''_f	Fatigue ductility coefficient	3.5.9.3
ε'''_f	Fatigue ductility coefficient	3.5.9.4
ε''_f	Fatigue ductility coefficient	3.5.9.5
ε_p	True plastic strain	3.5.2
ε_y	Parameter	3.1.3.1.3
γ_a	Shear strain amplitude	3.5.8.2
γ	Parameter	3.3.3
λ	Slenderness factor	3.1.2.1.1
λ	Oil canning buckling parameter	3.3.4
μ_{P_f}	Mean of P_f	3.5.9.1
$\mu_{\varepsilon'_f}$	Mean of ε'_f	3.5.9.3
$\mu_{\sigma'_f}$	Mean of σ'_f	3.5.9.2
ν	Poisson's ratio	3.1.2.2
ν	Poisson's ratio	3.1.4.1.1
ν	Poisson's ratio	3.3.1.3
ν	Poisson's ratio	3.3.2
ν	Poisson's ratio	3.3.4
%elong.	Percent Elongation	3.5.2
%RA	Percent reduction in area	3.5.2
ρ	Curvature radius of the spot welded notch	3.5.7.3.2
ρ	Reduction factor	3.11.5.4.1
σ	Normal stress	3.5.7.3.3.2
σ	True stress	3.5.2
σ	True stress	3.5.2
$\sigma_{1,3}$	Maximum in-plane principal stress at pt 3	3.5.7.3.3.2
σ_a	True stress amplitude	3.5.3.2
σ_a	True stress amplitude	3.5.3.4
σ_a	Stress amplitude	3.5.7.3.3.3
σ_A	Standard deviation of A	3.5.9.1
σ_a	True stress amplitude	3.5.9.2
$\sigma_a R=0$	Stress amplitude at R=0	3.5.7.3.3.3
σ_{eq}	Von Mises' equivalent stress	3.5.8.2
σ_f	True fracture strength	3.5.2
σ'_f	Fatigue strength coefficient	3.5.3.2
σ''_f	Fatigue strength coefficient	3.5.3.4
σ'''_f	Fatigue strength coefficient	3.5.4.1
σ''''_f	Fatigue strength coefficient	3.5.4.2

Table A-1 (Continued)

Symbol	Definition	Section
σ'_f	Fatigue strength coefficient	3.5.5.3
σ'_f	Fatigue strength coefficient	3.5.9.2
σ'_f	Fatigue strength coefficient	3.5.9.4
σ'_f	Fatigue strength coefficient	3.5.9.5
$\sigma'_{fR=0}$	Intercepting stress amplitude at one reversal	3.5.7.3.3.3
$\sigma_{\ln(N_f)}$	Standard deviation of $\ln(N_f)$	3.5.9.1
$\sigma_{\ln(P_f')}$	Standard deviation of $\ln(P_f')$	3.5.9.1
σ_m	Mean stress	3.5.3.4
σ_m	Mean stress	3.5.5.3
σ_m	Mean stress	3.5.7.3.3.3
$\sigma_{max\varepsilon_a}$	Uniaxial Smith-Watson-Topper parameter	3.5.8.2
σ_{Mx3}	Normal stress due to moment $Mx3$	3.5.7.3.3.2
σ_{My3}	Normal stress due to moment $My3$	3.5.7.3.3.2
σ_{Nz3}	Normal stress due to normal force	3.5.7.3.3.2
σ_r	Radial stress	3.5.7.3.3.1
$\sigma_{r,Mx1}$	Radial stress due to moment $Mx1$	3.5.7.3.3.1
$\sigma_{r,Mx2}$	Radial stress due to moment $Mx2$	3.5.7.3.3.1
$\sigma_{r,Mxi}$	Radial stress due to moment Mxi	3.5.7.3.3.1
$\sigma_{r,My1}$	Radial stress due to moment $My1$	3.5.7.3.3.1
$\sigma_{r,My2}$	Radial stress due to moment $My2$	3.5.7.3.3.1
$\sigma_{r,Myi}$	Radial stress due to moment Myi	3.5.7.3.3.1
$\sigma_{r,Nz1}$	Radial stress due to normal force $Nz1$	3.5.7.3.3.1
$\sigma_{r,Nz2}$	Radial stress due to normal force $Nz2$	3.5.7.3.3.1
$\sigma_{r,Nzi}$	Radial stress due to normal force Nzi	3.5.7.3.3.1
$\sigma_{r,Vx1}$	Radial stress due to lateral force $Vx1$	3.5.7.3.3.1
$\sigma_{r,Vx2}$	Radial stress due to lateral force $Vx2$	3.5.7.3.3.1
$\sigma_{r,Vxi}$	Radial stress due to lateral force Vxi	3.5.7.3.3.1
$\sigma_{r,Vy1}$	Radial stress due to lateral force $Vy1$	3.5.7.3.3.1
$\sigma_{r,Vy2}$	Radial stress due to lateral force $Vy2$	3.5.7.3.3.1
$\sigma_{r,Vyi}$	Radial stress due to lateral force Vyi	3.5.7.3.3.1
σ_{r1}	Radial stress at point 1	3.5.7.3.3.1
σ_{r2}	Radial stress at point 2	3.5.7.3.3.1
σ_{tmax}	Maximum tangential stress	3.5.7.3.2
σ_1	Principal stress	3.5.8.2
σ_2	Principal stress	3.5.8.2
σ_3	Principal stress	3.5.8.2
θ	Angle	3.1.2.1.3
θ	Angle	3.5.7.3.3.2
θ	Angle around circumference of spot weld	3.5.7.3.3.1
τ	Shear stress	3.5.7.3.3.2
τ_{max}	Maximum shear stress	3.5.8.2
τ_{Vx3}	Shear stress due to lateral force $Vx3$	3.5.7.3.3.2
τ_{Vy3}	Shear stress due to lateral force $Vy3$	3.5.7.3.3.2
θ	Angle of load relative to a line \perp to web	3.1.3.5.1
ψ	Reduction factor	3.1.3.1.2
ψ	Tensile/Compressive stress ratio	3.1.3.1.2

Table A-1 (Continued)

Symbol	Definition	Section
A	Coefficient	2.11
A	Estimated A	3.5.9.1
A	Estimated A	3.5.9.2
A	Estimated A	3.5.9.3
A	Fatigue property of spot welded specimen	3.5.7.3.2
A	Full unreduced xsection area	3.1.2.3
A	Full unreduced xsection area	3.1.2.5
A	Full unreduced xsection area	3.2.1
A	Full unreduced xsection area	3.2.2.1
A	Material constant based on strength	3.5.3.3
A	Material constant based on strength	3.5.3.3
A	Parameter	3.3.4
A	Parameter to determine (Fy)pred	2.11
A	Total area of cylindrical tube	3.1.2.2
A _s	Actual area of lip for a non-simple lip	3.1.2.1.3
A _s	Actual area of lip for a non-simple lip	3.1.2.1.4
A _e	Effective area	3.1.2.5
A _e	Effective area	3.2.1
A _{ey}	A _e evaluated at stress F _y	3.1.2.5
(A _e) ₁	Effective cross sectional area, 1	3.6.8
(A _e) ₂	Effective cross sectional area, 2	3.6.8
A _f	Minimum cross sectional area at fracture	3.5.2
A _{inst}	Instantaneous min. cross sectional area	3.5.2
A _o	Equivalent area	3.1.2.2
A _o	Equivalent area	3.1.2.3
A _o	Equivalent area	3.1.2.5
A ₀	Original minimum cross sectional area	3.5.2
A _s	Reduced area of lip	3.1.2.1.3
A _s	Reduced area of lip	3.1.2.1.4
A _s	Stiffener area	3.3.3
a	Area inside tube perimeter	3.1.4.1.1
a	Aspect Ratio (d'/b')	3.6.8
a	Parameter	3.3.4
a	Radius of curvature	3.2.1
a	Radius of curvature	3.2.2.1
a	Radius of curvature of cylindrical plate	3.3.2
a	Radius of curved member	3.2.2.1
a	Spherical radius	3.3.3
a	Spherical radius	3.3.4
a _f	Radius of curvature at flange	3.2.2.1
a _h	Horizontal radius (spherical shell)	3.3.3
a _p	Radius (circular plate)	3.3.1.2
B	Coefficient	2.11
B	Coefficient	3.2.2.1
B	Estimated B	3.5.9.1
B	Estimated B	3.5.9.2

Table A-1 (Continued)

Symbol	Definition	Section
B	Estimated B	3.5.9.3
B	Fatigue property of spot welded specimen	3.5.7.3.2
B	Fatigue strength exponent	3.5.3.2
B	Fatigue strength exponent	3.5.3.4
B	Fatigue strength exponent	3.5.4.1
B	Parameter to determine (Fy)pred	2.11
b	Effective width	3.1.2.1.1
b	Effective width	3.1.2.1.2
b	Effective width	3.1.2.1.4
b	Fatigue strength exponent	3.5.4.2
b	Fatigue strength exponent	3.5.5.3
b	Fatigue strength exponent	3.5.7.3.3.3
b	Fatigue strength exponent	3.5.9.2
b	Fatigue strength exponent	3.5.9.4
b	Fatigue strength exponent	3.5.9.5
b	Width	3.1.4.1.1
b	Width of member	3.2.2.1
b'	Effective flange width	3.2.2.1
b ₁	Eff. width near max. comp. stress	3.1.3.1.2
b ₂	Effective width near minimum stress	3.1.3.1.2
b _c	Comp. flange width	3.1.3.1.3
b _c	Comp. flange width (Fig. 3.1.3.1.3-1)	3.1.3.1.3
b _e	Reduced effective width	3.1.2.1.4
b _e	Reduced effective width	3.1.3.1.2
b _f	Flange width beyond web	3.2.2.1
b _i '	Eff. flange width (inner)(Fig. 3.2.2.1-2)	3.2.2.1
b _o	Entire width between webs	3.1.2.1.4
b _o '	Eff. flange width (outer)(Fig. 3.2.2.1-2)	3.2.2.1
b _t	Ten. flange width	3.1.3.1.3
b _t	Ten. flange width (Fig. 3.1.3.1.3-1)	3.1.3.1.3
C	Coefficient	3.3.4
C	Critical loading coefficient	3.3.3
C	Critical slenderness coefficient	3.4.4
C	Fatigue property of spot welded specimen	3.5.7.3.2
C'	Constant	3.3.4
C' _F	High Yield Strength Modifier	3.1.3.5.2
C' _f	Yield Strength Factor	3.1.3.5.1
C' _w	Deflection coeff.(circular plate)	3.3.1.2
C _θ	Parameter	3.1.3.5.1
C ₂	Function of panel geometry	3.3.4
C _{2Nf}	Estimated COV of 2N _f	3.5.9.2
C _{2Nf}	Estimated COV of 2N _f	3.5.9.3
C _b	Bending coefficient	3.1.3.6
C _{e'f}	Estimated COV of e' _f	3.5.9.3
C _F	Parameter	3.1.3.5.1
C _f	Stress coefficient	3.3.1.1

Table A-1 (Continued)

Symbol	Definition	Section
C_h	Parameter	3.1.3.5.1
C_m	Coefficient to modify max. moment	3.1.3.7
C_{mx}	Modifying coefficient along X	3.1.3.7
C_{my}	Modifying coefficient along Y	3.1.3.7
C_{Nf}	Estimated COV of N_f	3.5.9.1
$C_{Nf'}$	Coefficient of variation for N_f	3.5.9.1
C_o	Deflection coefficient-flat plate	3.3.1.2
Cost	Expenditures or resource	3.9.2.4
$C_{Pf'}$	Estimated COV of P_f	3.5.9.1
$C_{Pf''}$	Coefficient of variation for P_f	3.5.9.1
C_R	Parameter	3.1.3.5.1
$C_{s'f}$	Estimated COV of s'_f	3.5.9.2
C_t	Parameter	3.1.3.5.1
C_y	Max. comp. strain permitted/yield strain	3.1.3.1.3
C_w	Deflection coefficient	3.3.1.1
c	Distance to extreme fiber	3.2.1
c	Fatigue ductility exponent	3.5.4.1
c	Fatigue ductility exponent	3.5.4.2
c	Fatigue ductility exponent	3.5.5.3
c	Fatigue ductility exponent	3.5.9.3
c	Fatigue ductility exponent	3.5.9.4
c	Fatigue ductility exponent	3.5.9.5
c_i	Distance from N.A. to inner fiber	3.2.2.1
c_o	Distance from N.A. to outer fiber	3.2.2.1
D	Depth of simple lip	3.1.2.1.3
D	Diameter of largest blank	4.1.6.7
D	Diameter of small rigid circular plate	3.5.7.3.3.1
D	Diameter of small rigid circular plate	3.5.7.3.3.2
D	Diameter of the spot weld nugget	3.5.7.3.2
D	Fatigue property of spot welded specimen	3.5.7.3.2
D	Logarithmic ductility of material	3.5.4.1
D	Outside diameter	3.1.2.2
D	Outside diameter	3.1.3.2
D	Weld nugget diameter	3.5.7.3.1
d	Cup diameter	4.1.6.7
d	Depth along the web	3.1.3.1.3
d	Depth along the web	3.1.3.6
d	Depth of simple lip (flat part)	3.1.2.1.3
d	Nominal dia. of fastener	3.4.2.3.4
d	Nominal diameter	3.4.2.1.1
d	Out-of-straightness after load	3.2.1
d'_s	Actual effective width of lip	3.1.2.1.3
dA	Reduction in area	3.5.4.1
d_o	Original out-of-straightness	3.2.1
D_p	Diameter of larger flexible circular plate	3.5.7.3.3.1
d_s	Effective width of lip	3.1.2.1.3

Table A-1 (Continued)

Symbol	Definition	Section
E	Modulus of elasticity	3.1.2.1.1
E	Modulus of elasticity	3.1.2.1.2
E	Modulus of elasticity	3.1.2.2
E	Modulus of elasticity	3.1.2.3
E	Modulus of elasticity	3.1.2.5
E	Modulus of elasticity	3.1.3.1.2
E	Modulus of elasticity	3.1.3.2
E	Modulus of elasticity	3.1.3.3
E	Modulus of elasticity	3.1.3.6
E	Modulus of elasticity	3.1.3.7
E	Modulus of elasticity	3.1.4.1.1
E	Modulus of elasticity	3.2.1
E	Modulus of elasticity	3.3.1.1
E	Modulus of elasticity	3.3.1.2
E	Modulus of elasticity	3.3.1.3
E	Modulus of elasticity	3.3.2
E	Modulus of elasticity	3.3.3
E	Modulus of elasticity	3.3.4
E	Modulus of elasticity	3.5.2
E	Modulus of elasticity	3.5.4.1
E	Modulus of elasticity	3.5.4.2
E	Modulus of elasticity	3.5.5.3
E	Modulus of elasticity	3.5.9.4
E_t	Tangent modulus of elasticity	3.1.2.3
e	% Strain	4.1.5.3
e	Clear dist. to closest opposite bearing point	3.1.3.5.1
e	Engineering strain	3.5.2
e	Length of moment arm	3.5.7.3.1
e	Length of moment arm	3.5.7.3.2
e_{min}	Minimum distance (hole to part)	3.4.2.3.2
F	Applied force	3.5.7.3.1
F	Applied force	3.5.7.3.2
F	Stress limit	3.1.3.7
F_a	Limiting axial stress	3.1.3.7
F_b	Limiting flexural stress	3.1.3.7
F_{bu}	Ultimate bearing stress	3.4.2.3.3
F_{bwu}	Max. web comp. stress at buckling	3.1.3.1.2
F_{cr}	Critical stress	3.1.2.2
F_{cu}	Ultimate compressive stress	3.1.2.5
F_e	Euler buckling stress	3.1.2.5
F_f	Flange force	3.2.2.1
F_t	UTS at net section	3.4.2.3.4
F_u	Tensile strength of steel	3.1.1
F_u	Tensile strength of steel	3.1.4.2
F_u	Tensile strength of thinnest part	3.4.2.3.2
F_u	Tensile strength of thinnest part	3.4.2.3.3

Table A-1 (Continued)

Symbol	Definition	Section
F_u	Tensile strength of thinnest part	3.4.2.3.4
Function	Function of product, process, etc.	3.9.2.4
F_y	Yield strength	2.11
F_y	Yield strength	3.1.2.1.1
F_y	Yield strength	3.1.2.1.2
F_y	Yield strength	3.1.2.2
F_y	Yield strength	3.1.2.3
F_y	Yield strength	3.1.2.5
F_y	Yield strength	3.1.3.1.2
F_y	Yield strength	3.1.3.1.3
F_y	Yield strength	3.1.3.2
F_y	Yield strength	3.1.3.3
F_y	Yield strength	3.1.3.5.1
F_y	Yield strength	3.1.3.5.2
F_{yd}	Dynamic yield strength	3.3.4
F_{yrs}	Reduced yield strength	3.1.2.1.1
F_{yru}	Reduced yield strength	3.1.2.1.2
$(F_y)_1$	Dynamic Tensile Stress, 1	3.6.8
$(F_y)_2$	Dynamic Tensile Stress, 2	3.6.8
$(F_y)_{pred}$	Predicted dynamic yield strength	2.11
$(F_y)s$	Static yield strength	2.11
f	Stress in the element	3.1.2.1.1
f	Stress in the element	3.1.2.1.2
f	Stress in the element	3.1.2.3
f_1	Compressive stress	3.1.3.1.2
f_2	Tensile stress	3.1.3.1.2
f_a	Axial stress	3.1.3.7
f_b	Flexural stress	3.1.3.7
f_b	Flexural stress	3.2.2.1
f_{bm}	Maximum stress	3.3.1.1
f_{bmax}	Maximum flexural stress	3.2.2.2
f_{btr}	Transverse bending stress	3.2.2.1
f_{cr}	Critical stress at buckling	3.1.2.2
f_{cr}	Critical stress at buckling	3.3.1.3
f_{cr}	Critical stress at buckling	3.3.2
f_{crc}	Buckling stress of full cylinder	3.1.2.3
f_{crf}	Buckling stress of flat plate	3.1.2.3
f_{crp}	Buckling stress of panel	3.1.2.3
f_m	Membrane stress	3.3.3
f_{max}	Maximum stress	3.2.1
f_r	Radial stress	3.2.2.1
$(f_r)r=0$	Tensile membrane stress($r=0$)	3.3.1.2
$(f_r)r=a$	Tensile membrane stress($r=a$)	3.3.1.2
f_v	Nominal shear stress	3.1.3.3
G	Geometric correction factor	3.5.7.3.3.1
G	Shear modulus of elasticity	3.1.4.1.1

Table A-1 (Continued)

Symbol	Definition	Section
G_i	Geometric correction factor	3.5.7.3.3.1
g	Distortion parameter	3.2.2.2
g	Parameter	3.3.3
H_c	Crown Height	3.3.4
h	Height	3.1.4.1.1
h	Height of member	3.2.2.1
h	Overall height of web	3.1.3.1.2
h	Overall height of web	3.1.3.3
h	Overall height of web	3.1.3.5.1
I	Effective section moment of inertia	3.2.2.2
I	Section moment of inertia	3.2.2.2
I	Section moment of inertia	3.4.4
I_a	I required for full stiffening	3.1.2.1.2
I_a	I required for full stiffening	3.1.2.1.3
I_a	I required for full stiffening	3.1.2.1.4
Ir	Interaction Ratio	3.1.3.4
Ir	Interaction Ratio	3.1.3.5.1
Ir	Interaction Ratio	3.1.3.7
Ir	Interaction Ratio	3.4.4
I_s	I of stiffener	3.1.2.1.3
I_s	Stiffener moment of inertia	3.3.3
I_s/I_a	Ratio of I_s to I_a	3.1.2.1.3
I_s/I_a	Ratio of I_s to I_a	3.1.2.1.4
I_{sf}	I of full area of stiffened element	3.1.2.1.4
I_x	Moment of inertia about X-axis	3.1.3.7
I_{yc}	I of compression portion	3.1.3.6
i	Stress in curved tube/straight tube	3.2.2.2
J	Torsional stiffness constant	3.1.4.1.1
J	Torsional stiffness constant	3.1.4.1.2
j	(Eff. I)/(Full I) of curved tube	3.2.2.2
K	Effective length factor	3.1.2.5
K	Effective length factor	3.4.4
K	Material constant	3.5.8.2
K	Monotonic strength coefficient	3.5.2
K	Theoretical stiffness	3.3.4
K'	Cyclic strength coefficient	3.5.9.5
K_e	Elastic strain concentration factor	3.5.4.2
K_{eq}	Equivalent stress intensity factor	3.5.7.3.2
K_f	Fatigue notch concentration factor	3.5.3.3
K_f	Fatigue stress concentration factor	3.5.4.2
K_f^*dS	K_f^*dS	3.5.4.2
K_i	Stress index	3.5.7.3.1
K_I	Stress index	3.5.7.3.1
K_I	Stress index	3.5.7.3.2
$K_{I,max}$	Maximum stress index	3.5.7.3.1
K_{II}	Stress index	3.5.7.3.1

Table A-1 (Continued)

Symbol	Definition	Section
K_{II}	Stress index	3.5.7.3.2
$K_{II,max}$	Maximum stress index	3.5.7.3.1
K_{III}	Stress index	3.5.7.3.2
K_s	Elastic stress concentration factor	3.5.4.2
K_t	Theoretical stress concentration factor	3.5.3.3
K_t'	Theoretical stress concentration factor	3.5.4.2
K_x	Effective length factor	3.1.3.7
k	Buckling coefficient	3.1.2.1.1
k	Buckling coefficient	3.1.2.1.3
k	Buckling coefficient	3.1.2.1.4
k	Buckling coefficient	3.1.3.1.2
k	Buckling coefficient	3.3.1.3
k	Constant - see table 3.4.2.1.1-1	3.4.2.1.1
k	Spherical shell factor	3.3.4
L	Eff. unbraced length of comp. flange	3.1.3.6
L	Unbraced length of member	3.1.2.2
L	Unbraced length of member	3.1.2.5
L	Unbraced length of member	3.4.4
L'	Load transmission length	3.4.4
L_1	Shorter plate dimension	3.3.1.1
L_1	Shorter plate dimension	3.3.4
L_1	Smaller rectangular panel dimension	3.3.4
L_2	Larger plate dimension	3.3.1.1
L_2	Larger plate dimension	3.3.4
L_2	Larger rectangular panel dimension	3.3.4
LDR	Limiting drawing ratio	4.1.6.7
L_{eff}	Effective unbraced length	3.2.1
L_x	Actual unbraced L (y-plane bending)	3.1.3.7
l	Length of an element of the cross section	3.1.2.2
l/a	Curvature	3.3.4
l_0	Original gage length	3.5.2
l_1	Initial circle diameter	4.1.5.3
l_2	Final major or minor ellipse diameter	4.1.5.3
l_f	Gage length at fracture	3.5.2
l_{inst}	Instantaneous gage length	3.5.2
limit w/t	Upper bound of w/t ratio	3.1.2.1.1
limit w/t	Upper bound of w/t ratio	3.1.2.1.2
$\ln(2N_f)$	Natural log of $2N_f$	3.5.9.2
$\ln(N_f)$	Natural log of N_f	3.5.9.1
M	Applied bending moment	3.5.7.3.3.1
M	Bending force applied to the weld nugget	3.5.7.3.1
M	Flexural moment	3.1.3.4
M	Flexural moment	3.1.3.5.1
M	Flexural moment	3.2.2.1
M	Flexural moment	3.2.2.2
M	Mean stress sensitivity factor	3.5.7.3.3.3

Table A-1 (Continued)

Symbol	Definition	Section
M_c	Elastic critical moment	3.1.3.6
M_1	Smaller moment at beam end	3.1.3.6
M_1	Smaller moment at beam end	3.1.3.7
M_2	Larger moment at beam end	3.1.3.6
M_2	Larger moment at beam end	3.1.3.7
M_e	Elastic buckling moment	3.1.3.6
M_f	Magnification factor	3.1.3.7
M_p	Plastic moment	3.1.3.2
M_u	Ultimate moment	3.1.3.1.3
M_u	Ultimate moment	3.1.3.2
M_u	Ultimate moment capacity	3.1.3.4
M_u	Ultimate moment capacity	3.1.3.5.1
M_{ux}	Ultimate bending moment along X	3.1.3.7
M_{uy}	Ultimate bending moment along Y	3.1.3.7
M_x	Flexural moment in X-direction	3.1.3.7
M_x	Moment acting on the nugget	3.5.7.3.2
M_{x3}	Applied bending moment at point 3	3.5.7.3.3.2
M_{xi}	Applied bending moment	3.5.7.3.3.1
M_y	Moment acting on the nugget	3.5.7.3.2
M_y	Flexural moment in Y-direction	3.1.3.7
M_y	Yield moment, at first compression yield	3.1.3.6
M_{y3}	Applied bending moment at point 3	3.5.7.3.3.2
M_{yi}	Applied bending moment	3.5.7.3.3.1
M_{yt}	Yield moment, at first tensile yield	3.1.3.6
M_z	Moment acting on the nugget	3.5.7.3.2
m	Fatigue strength exponent	3.5.9.1
N	Applied normal force	3.5.7.3.3.1
N	Bearing length of load or reaction	3.1.3.5.1
N	Bearing length of load or reaction	3.1.3.5.2
N	Monotonic strain hardening exponent	3.5.2
N	Normal force applied to the weld nugget	3.5.7.3.1
N_f	Cycles to failure	3.5.9.1
N_f	Total fatigue life	3.5.7.3.1
N_f	Total fatigue life	3.5.7.3.2
N_f	Total fatigue life	3.5.7.3.3.3
N_z	Out-of-plane normal force on the nugget	3.5.7.3.2
N_{z3}	Applied normal force at point 3	3.5.7.3.3.2
N_{zi}	Applied normal force	3.5.7.3.3.1
n	Number of attachment points	3.4.4
n'	Cyclic strain hardening exponent	3.5.9.5
P	Applied load (tension positive)	3.2.1
P	Axial load	3.1.3.7
P	Applied load	3.5.2
P	Axial load on bolt or stud	3.4.2.1.1
P	Concentrated load on web	3.1.3.5.1
P_a	Load amplitude	3.5.9.1

Table A-1 (Continued)

Symbol	Definition	Section
P_{cb}	Max. concentrated buckling load	3.1.3.5.1
P_{cm}	Reduced value of P_{cy}	3.1.3.5.1
P_{cr}	Critical loading for shell	3.3.3
P_{cr}	Critical oil canning load	3.3.4
P_{cu}	Max. concentrated crippling load	3.1.3.5.1
P_{cu}	Max. concentrated crippling load	3.1.3.5.2
P_{cy}	Max. concentrated load on web	3.1.3.5.1
P_e	Euler buckling load	3.1.3.7
P_e	Euler buckling load	3.2.1
P_{ex}	Euler buckling load along X	3.1.3.7
P_{ex}	X-axis Euler buckling load	3.1.3.7
P_{ey}	Euler buckling load along Y	3.1.3.7
P_f	Applied load at the fracture	3.5.2
P_f'	Fatigue strength coefficient	3.5.9.1
P_{max}	Maximum applied load	3.5.2
P_{mean}	Mean crushing load	3.6.8
P_p	Axial force in cover plate	3.4.4
P_u	Axial load capacity	3.1.2.5
P_u	Axial load capacity	3.1.3.7
P_u	Computed ultimate load	3.6.8
P_u	Ultimate strength of stub column	3.6.8
P_y	Axial load at yield strength	3.1.3.6
parameter	Brown and Miller's parameter	3.5.8.2
parameter	Modified Smith-Watson-Topper parameter	3.5.8.2
Q	Moment about section neutral axis	3.4.4
q	Coefficient	3.2.2.2
q	Fatigue notch sensitivity	3.5.3.3
q	Uniform load per unit area	3.3.1.1
q	Uniform load per unit area	3.3.1.2
q	Uniform load per unit area	3.3.3
q_{cr}	Critical loading per unit area	3.3.3
R	Corner bend radius	3.1.3.5.1
R	Radius	3.1.4.1.1
R	Radius of curvature	3.1.2.3
R	Radius of tubular section	3.1.2.2
R	Radius of tubular section	3.1.3.2
R	Radius of tubular section	3.2.2.2
R	Stress ratio	3.5.3.1
R	Stress ratio	3.5.7.3.1
R_1	Radius of curvature - R1	3.3.4
R_2	Radius of curvature - R2	3.3.4
Ratio	Engineered scrap	4.1.8
R_{cr}	Coefficient	3.3.4
r	Curvature radius of the spot welded notch	3.5.7.3.2
r	Force transmitted/tension force	3.4.2.3.4
r	Notch root radius	3.5.3.3

Table A-1 (Continued)

Symbol	Definition	Section
r	Radius of gyration of xsection	3.1.2.5
r	Radius of gyration of xsection	3.2.1
r	Radius of gyration of xsection	3.2.1
r	Radius of gyration of xsection	3.4.4
S	Engineering stress	3.5.2
S	w/t value at which buckling begins	3.1.2.1.1
S	w/t value at which buckling begins	3.1.2.1.2
S	w/t value at which buckling begins	3.1.2.1.3
S	w/t value at which buckling begins	3.1.2.1.4
S_a	Stress amplitude	3.5.3.1
S_a	Stress amplitude for same life as S_{cr}	3.5.3.4
S_a	Stress amplitude at 2×10^6 cycles	3.5.7.3.3.3
$S_{a,R=0}$	Stress amplitude at $R=0$ and 2×10^6 cycles	3.5.7.3.3.3
S_c	Effective section modulus	3.1.3.6
S_{cr}	Stress amplitude for $R=-1$	3.5.3.4
S_f	Section modulus for compressive fiber	3.1.3.6
S_{ft}	Section modulus for tension fiber	3.1.3.6
S_m	Mean stress	3.5.3.1
S_m	Mean stress	3.5.3.4
S_m	Mean stress at 2×10^6 cycles	3.5.7.3.3.3
$S_{m,R=0}$	Mean stress at $R=0$ and 2×10^6 cycles	3.5.7.3.3.3
S_{max}	Maximum stress	3.5.3.1
S_{min}	Minimum stress	3.5.3.1
S_r	Stress range	3.5.3.1
S_s	Stiffener spacing	3.3.3
S_u	Ultimate tensile strength	3.5.2
S_u	Ultimate tensile strength	3.5.3.3
S_u	Ultimate tensile strength	3.5.3.4
s	Measured deviation about Y on X	3.5.9.1
s	Measured deviation about Y on X	3.5.9.2
s	Measured deviation about Y on X	3.5.9.3
s	Spacing of attachment points	3.4.4
s	Spacing of bolts	3.4.2.3.4
T	Applied torque	3.1.4.1.1
T	Applied torque	3.1.4.1.2
T	Torque applied to nut	3.4.2.1.1
t	Metal sheet thickness	3.5.7.3.1
t	Thickness of flange or member	3.2.2.1
t	Thickness of flat or curved element	3.1.2.1.1
t	Thickness of flat or curved element	3.1.2.1.2
t	Thickness of flat or curved element	3.1.2.1.3
t	Thickness of flat or curved element	3.1.2.1.4
t	Thickness of flat or curved element	3.1.2.3
t	Thickness of flat or curved element	3.1.2.5
t	Thickness of flat or curved element	3.1.3.1.2
t	Thickness of flat or curved plate	3.1.2.1.3

Table A-1 (Continued)

Symbol	Definition	Section
t	Thickness of flat or curved plate	3.1.3.1.3
t	Thickness of flat or curved plate	3.1.4.1.2
t	Thickness of flat or curved plate	3.3.1.1
t	Thickness of flat or curved plate	3.3.1.2
t	Thickness of flat or curved plate	3.3.1.3
t	Thickness of flat or curved plate	3.3.2
t	Thickness of flat or curved plate	3.3.3
t	Thickness of flat or curved plate	3.3.4
t	Thickness of flat or curved plate	3.4.4
t	Thickness of thinnest part	3.4.2.3.2
t	Thickness of the metal sheet	3.5.7.3.2
t	Thickness of the circular plate	3.5.7.3.3.1
t	Thickness of web	3.1.3.3
t	Thickness of web	3.1.3.5.1
t	Thickness of web	3.1.3.5.2
t	Tube wall thickness	3.1.2.2
t	Tube wall thickness	3.1.3.2
t	Tube wall thickness	3.1.4.1.1
t ₁	Thickness	3.1.4.1.1
t _B	Equivalent bending thickness	3.3.3
t _e	Effective thickness	3.1.2.3
t _f	Flange thickness	3.2.2.1
t _i	Thickness of the circular plate	3.5.7.3.3.1
t _m	Equivalent membrane thickness	3.3.3
t _s	Equivalent thickness	3.1.2.1.4
t _w	Thickness of web	3.2.2.1
t _w	Thickness-see Fig 3.2.2.1-4	3.2.2.1
V	Applied lateral force	3.5.7.3.3.1
V	Shear force applied to the weld nugget	3.5.7.3.1
V	Transverse shear force	3.1.3.3
V	Transverse shear force	3.1.3.4
Value	Function-cost relationship	3.9.2.4
V _m	Max. shear force in beam	3.4.4
V _s	Shear force per attachment point	3.4.4
V _u	Shear force transmitted by bolt	3.4.2.3.2
V _u	Ultimate shear force of web	3.1.3.3
V _u	Ultimate shear force of web	3.1.3.4
V _u	Ultimate shear force of web	3.1.3.5.1
V _x	In-plane shear force acting on the nugget	3.5.7.3.2
V _{x3}	Applied lateral force at point 3	3.5.7.3.3.2
V _{xi}	Lateral force	3.5.7.3.3.1
V _y	In-plane shear force acting on the nugget	3.5.7.3.2
V _{y3}	Applied lateral force at point 3	3.5.7.3.3.2
V _{yi}	Lateral force	3.5.7.3.3.1
v _t	Torsional shear stress	3.1.4.1.1
v _t	Torsional shear stress	3.1.4.1.2

Table A-1 (Continued)

Symbol	Definition	Section
v_{t1}	Torsional shear stress	3.1.4.1.1
W	Denting energy	3.3.4
w	Metal sheet width	3.5.7.3.1
w	Width of flat or curved element	3.1.2.1.1
w	Width of flat or curved element	3.1.2.1.2
w	Width of flat or curved element	3.1.2.1.3
w	Width of flat or curved element	3.1.2.1.4
w	Width of flat or curved element	3.1.2.3
w	Width of flat or curved element	3.1.2.5
w	Width of flat or curved element	3.1.3.1.2
w	Width of flat or curved element	3.3.1.3
w_f	Flange projection of I or C section	3.1.3.1.1
w_f	Half the distance between webs	3.1.3.1.1
w_1	Mass of metal consumed	4.1.8
w_2	Mass of parts produced	4.1.8
w_m	Max. plate deflection	3.3.1.1
w_m	Max. plate deflection	3.3.1.2
w_o	Center deflection	3.3.1.2
y	Distance from centroidal axes	3.2.2.1
y_c	Parameter	3.1.3.1.3
y_{cp}	Parameter	3.1.3.1.3
y_p	Parameter	3.1.3.1.3
y_t	Parameter	3.1.3.1.3
y_{tp}	Parameter	3.1.3.1.3
Z	Sectional property	3.2.2.1

APPENDIX B STEEL CONSTANTS AND CONVERSION FACTORS

[Table B-1](#) lists the constants recommended for steel. These values are used throughout the Manual and in the CARS '98 program.

Table B-1 Recommended constants for steel

Constants	SI Units	U.S. Customary Units
Average Mass Density	7.85E-06 kg/mm ³	0.284 lbm/in ³
Modulus of Elasticity	203,000 MPa	29,500 ksi
Shear Modulus	78,000 MPa	11,300 ksi
Poisson's Ratio	0.3	0.3

[Table B-2](#) lists conversion factors recommended when using the Manual or the CARS '98 program.

Table B-2 Recommended conversion factors

	SI Units	Conversion Units		U.S. Customary Units
		SI to U.S. Customary, Multiply by	U.S. Customary to SI, Multiply by	
Length	mm (millimeter)	39.37E-03	25.4	inch (in.)
Area	mm ²	1.550E-03	645.2	in. ²
Volume	mm ³	61.02E-06	16.39E+03	in. ³
Area Moment of Inertia	mm ⁴	2.403E-06	416.2E+03	in. ⁴
Strain	mm/mm	1	1	in./in.
Mass Density	kg/mm ³	36.1E+03	27.7E.06	lbm/in. ³
Mass Per Unit Area	kg/mm ²	1.422E+03	703E-06	lbm/in. ²
Mass per Unit Length	kg/mm	56.0	17.9E-03	lbm/in.
Mass	kg (kilogram)	2.205	454E-03	lbm
Force	Newtons (N or kn)	225E-03 225E-03	4.45 4.45	pound-force (lbf) or kilo-lbf (kip)
Moment	N-mm	8.85E-06	113E+03	kip-in.
Stress	MPa	145E-03	6.89	ksi

Notes:

k = kilo or 10³

M = mega or 10⁶

1 Newton (N) = 0.225 lbf

1 Pascal (Pa) = 1 Newton/meter²

1 Mpa = 1 Newton/mm²

